

# The 14<sup>th</sup> Asia Lighting Conference

# Innovation of Lighting

August 17-18, 2023  
The University of Tokyo  
Tokyo, Japan

## Proceedings



Asia Lighting Conference



中国照明学会  
CHINA ILLUMINATING ENGINEERING SOCIETY



一般社団法人 照明学会  
THE ILLUMINATING ENGINEERING INSTITUTE OF JAPAN



대한민국조명·전기설비학회  
THE KOREAN INSTITUTE OF ILLUMINATING AND ELECTRICAL INSTALLATION ENGINEERS



ALC Web Page



Furusho Masao  
The President of the Illuminating Engineering Institute  
of Japan

Dear, all distinguished participants of Asia Lighting Conference 2023. On behalf of the IEIJ, it's my great pleasure to extend my sincere greetings and gratitude to all of you.

As the effects of covid-19 infections are still lingering, the ALC2023 is being held in both a face-to-face and online environment after careful consideration by the committee members. I am very pleased to be able to resume face-to-face meetings, even if it is limited for some of the participants. I hope that academic exchanges in a face-to-face environment will have a strong and constructive impact on young participants. In ALC2023, academic exchanges in an online environment complement face-to-face exchanges. As for academic exchange in an online environment, we have had two successful online conferences, 'ALC2021 Forum' and ALC2022, organized by the Chinese ALC committee. I would like to express my deep gratitude to the Chinese ALC committee for successfully organizing the two conferences under difficult circumstances.

Let me briefly introduce ourselves. The IEIJ is based on the tradition of 107 years since its foundation in 1916. Now we have positioned the following three points as the most significant principles for our activities.

1. Promoting the presentation of academic research and revitalizing academic activities through human exchanges among researchers, engineers, and practitioners.
2. Promoting the use of digital technology.
3. Stabilization of the financial balance on the basis of an appropriate budget plan.

The activities of the ALC are in accordance with these principles.

We are connected to each other on a single earth. With everyone here, I'd like to contribute to the growth of the lighting industry in Asia as well as academic activities.

Finally, I'd like to express my sincere appreciation to all the participants, the members of the International Organizing Committee, the Local Organizing Committee, and the supporting staff of IEIJ for their outstanding efforts to support this wonderful ALC2023.





Hirotaka Suzuki  
The Chair of ALC2023

Dear ALC colleagues, who love lighting design and engineering.

It has been four years since the 12th Asia Lighting Conference (ALC2019) was held in Daegu. After the conference, we were attacked by the Covid-19 pandemic, which severely restricted our academic activities and daily lives.

ALC2020, which was to be held in Beijing, was postponed due to the effects of the pandemic. Although we were unable to hold the formal conference in the year 2021, the warm-up activity, 'ALC2021 Forum', was held in an online environment and we were able to restart academic exchanges thanks to the excellent efforts of Chinese colleagues. And in the year 2022, with the strong will and dedication of Chinese colleagues, the official ALC, the 13th Asia Lighting Conference, was resumed in an online environment.

The ALC committee in Japan had a long and deep discussion about how to organize the conference. The decision to include face-to-face participation was a bit of a gamble. Fortunately, we won our bet and much more people than expected will be able to join ALC2023 in person.

When we held ALC2018 in Kobe, despite the accident at Kansai airport, Chinese and Korean colleagues overcame difficulties to participate in the conference. The first face-to-face participation after the Covid-19 pandemic will also be a participation in the midst of many difficulties and anxieties. We are deeply grateful to those who will be attending in person under these circumstances, and to those who will be contributing academically to the ALC even if they will participate in an online environment.

I am looking forward to seeing you in Tokyo.

# Contents

## Keynote Speech P.1-

- K-01 VISUALIZATION OF IMAGE CNNs AS EXPLAINABLE AI**  
Prof. Yasushi Yamaguchi

## Invited Lecture P.3-

- I-01 THE ALTERNATIVE USE OF LIGHTING SIMULATION**  
Prof. Miki Kozaki
- I-02 DAYLIGHTING PROTECTION IN TRADITIONAL CHINESE BUILDINGS BASED ON PAPER WINDOWS.**  
Prof. Xin Zhang
- I-03 THE EFFECT OF COLOR TEMPERATURE ON IMAGE QUALITY FOR DISPLAY APPLICATIONS**  
Prof. YungKyung Park

## Research Oral Session P.15-

### Oral Session-1

- O-1 THE EFFECTS OF DAYLIGHT CHANGES IN APARTMENT BUILDING ON PSYCHOPHYSIOLOGICAL ASPECTS OF RESIDENTS**  
Emi Murayama, Jaeyoung Heo, Hiroko Kubo and Shinji Yoshida
- O-2 RESEARCH ON IMPROVED YOLOV5 GESTURE RECOGNITION ALGORITHM FOR LOW-LIGHT ENVIRONMENT**  
Yuan Fang, Jia-Huan Wu and Nian-Yu Zou
- O-3 3D VISIBLE LIGHT POSITIONING METHOD FOR DRONES WITH TILT CONSIDERATION**  
Ryunosuke Inoshita and Saeko Oshiba
- O-4 SUBJECTIVE INVESTIGATION ON SLEEP AND MOOD OF CHINESE ANTARCTIC RESEARCH EXPEDITION DURING VOYAGE**  
Yanni Wang, Rongdi Shao, Li Wei and Luoxi Hao
- O-5 PUPIL SIZE AND SUBJECTIVE LIGHT EVALUATION DIFFERENCE OF ELDERLY PEOPLE BETWEEN DARK AND LIGHT CONDITIONS**  
Noriko Umemiya, Saki Tahara and Tomoyuki Minami
- O-6 A COMPARATIVE STUDY OF THE LIVING ROOM LIGHTING PREFERENCES OF THE ELDERLY VS. THOSE OF THE YOUNG AND MIDDLE-AGED**  
Xinyi Hao, Lishu Hong, Bo Tang and Xin Zhang



# Contents

## Oral Session-2

- O-7**      **COMPARATIVE ANALYSIS OF ILLUMINANCE DISTRIBUTION IN INDOOR ENVIRONMENTS USING ILLUMINANCE SENSORS AND SIMULATION MODELS**  
Seo Jiyoung and Anseop Choi
- O-8**      **HIGH CIRCADIAN LIGHT THERAPY FOR DEPRESSED YOUTH: A SYSTEMATIC REVIEW AND META-ANALYSIS**  
Ranpeng Chen
- O-9**      **STUDY ON SUITABILITY REVIEW OF ROAD LIGHTING CLASS SELECTION PARAMETERS AND DOMESTIC APPLICATION PLAN**  
Seongsik Yoo, JinSoo Shin and Jong-Min Lim
- O-10**     **A MODIFIED CLIMATE-BASED DAYLIGHT MODELING METHOD FOR BUILDINGS**  
Yongqing Zhao and Zhen Tian
- O-11**     **ILLUMINATING WELLBEING: A SIMULATION-BASED ANALYSIS OF HUMAN-CENTRIC LIGHTING IN TROPICAL HOSPITALS**  
Chong Lin Venjamin Quek, Szu-Cheng Chien, Kai Ting Foo, Nicholas Wei Kiat Tan, Kevin Chong, Ann Mei Wong and Luke Sher Guan Low
- O-12**     **DECOMPOSING LIGHT POLLUTION IN XICHONG INTERNATIONAL DARK SKY COMMUNITY USING ENCIRCLED AERIAL PHOTOS**  
Siyi Zhao, Junda Ma, Shengzhi Zou, Yan Zhang and Biao Yang

# Contents

## Oral Session-3

- O-13      EFFECTS OF LIGHTING DIFFUSENESS AND OBJECT SHAPE ON SURFACE APPEARANCE**  
Akira Kudo, Yoshinori Dobashi, Hiromi.Y Sato and Yoko Mizokami
- O-14      BIRD RISK ASSESSMENT UNDER LIGHT POLLUTION IN URBAN ECOLOGICAL PATCH**  
Qingli Hao, Lixiong Wang, Gang Liu and Juan Yu
- O-15      COLOR MATCHING AND HUE ESTIMATION EXPERIMENTS USING RGB LEDS**  
Minjeong Ko and Youngshin Kwak
- O-16      A STUDY OF DAYLIGHT UTILIZATION IN OFFICE SPACES CONSIDERING OCCUPANTS' ADAPTATION TO CHANGES IN GLARE PERCEPTION DEPENDING ON THEIR BEHAVIOR AND LIGHT COLOR**  
Akari Kawaguchi, Yuji Zhu and Hikaru Kobayashi
- O-17      ARCHIVING THE PERSONAL MEMORIES OF ATTRACTIVE LIGHT: DATABASE BUILDING AND APPLICATIONS**  
Byeongjin Kim, Giyun Lee and Hyeon-Jeong Suk
- O-18      VISIBLE LIGHT ID TRANSMITTER USING HIGH CIRCADIAN AND VISIBLE PERFORMANCES LED LIGHTING**  
Shogo Sakane and Sakeko Oshiba



# Contents

## Oral Session-4

- O-19      RESEARCH ON NOTICEABILITY OF DIGITAL BILLBOARDS FOCUSING ON VISUAL INFORMATION CHANGES**  
Yihan Wang and Miki Kozaki
- O-20      TUNNEL LIGHTING SYSTEM FOR ENHANCED MAINTENANCE**  
Shigeru Muramatsu
- O-21      PROMOTING AFTERNOON REST IN THE CAR: THE EFFECT OF ILLUMINANCE AND COLOR TEMPERATURE OF AUTOMOTIVE INTERIOR LIGHTING ON AFTERNOON SLEEPINESS, FATIGUE, AND MOOD**  
Nuoyi Li, Wenqing Miao, Christopher Weirich and Yandan Lin
- O-22      A STUDY ON THE VISIBLE LIGHT CONVERSION STRUCTURE TO IMPROVE MELANOPIC-LUX HCL LED LIGHTING FIXTURE**  
Jeremy Gahee Yoon
- O-23      MINI LED APPLICATION FOR SMART HEAD LAMP**  
Jae Young Joo
- O-24      OBJECTIVE AND SUBJECTIVE EVALUATION FOR AUTOMOTIVE AMBIENT LIGHTS**  
Seo Young Choi, Jae Kyu Ko and Mi So Noh
- O-25      EXPLORATION OF INTERIOR LIGHTING PREFERENCE CONDITIONS IN DIFFERENT SCENARIOS FOR AUTONOMOUS VEHICLES**  
Hyeran Kang, Hyensou Pak, Jemok Lee, Donguk Shin and Chan-Su Lee

# Contents

## Short Oral Session

P.198-260 P.502-534

- SO-1  
PT-1     **THE APPROPRIATE LIGHTING TECHNIQUES CONSIDERING DAILY  
ACTIVITIES IN WORKING ENVIRONMENT**  
Ayano Nakamura, Jaeyoung Heo and Youko Inoue
- SO-2  
PT-2     **STUDY ON OUTDOOR URBAN FARMING PLANTERS THROUGH DAYLIGHT  
SIMULATIONS: A FULL-SCALE EXPERIMENT IN SINGAPORE**  
Chew Beng Soh, R Haridarshan, Szu-Cheng Chien, Hui An, Arijit Saha and Mei  
Ting Teoh
- SO-3  
PT-3     **EVIDENCE-BASED RESEARCH AND APPLICATIONS FOR HEALTH LIGHTING  
DESIGN IN UNIVERSITY CLASSROOMS**  
Tongyue Wang, Rongdi Shao and Luoxi Hao
- SO-4  
PT-4     **THE EFFECT OF CEILING LAMPS' CONTRIBUTION TO HOME NIGHT  
READING ON VISUAL HEALTH**  
Yuanyi Luo, Bing Cheng, Yixiang Zhao, Xin Zhang, Hongxing Xia and Wei Wang
- SO-5  
PT-5     **RESEARCH ON APPROPRIATE LIGHTING METHODS THAT TAKE INTO  
ACCOUNT THE PSYCHOLOGICAL CHANGES DUE TO THE SEASONS**  
Minami Hagio, Jeayoung Heo and Youko Inoue
- SO-6  
PT-6     **VERIFICATION OF THE EVALUATION METHOD FOR THE SENSITIVITY TO  
LIGHT EXPOSURE**  
Taiki Saito, Yuki Kawashima, Kazuaki Ohkubo and Yasuki Yamauchi
- SO-7  
PT-7     **COLOR APPEARANCE OF COLORED LIGHTING**  
Soonhyeng An and Youngshin Kwak
- SO-8  
PT-8     **HARNESSING SUNLIGHT FOR SUSTAINABLE URBAN FARMING: OPTIMIZING  
PHOTOVOLTAICS IN TROPICAL CONTAINER-BASED AQUAPONICS  
SYSTEMS**  
Rui Xuan Teng, Szu-Cheng Chien and Andrew Keong Ng



# Contents

- SO-9  
PT-9      **BASIC RESEARCH ON THE DEVELOPMENT OF LED LAMPS TO SECURE THE VISIBILITY OF ROAD LIGHTING IN THE EVENT OF FOG**  
Ji-Myung Kim, Sung-Gi Chae, Young-Ju Cho, Meeryoung Cho and An-Seop Choi
- SO-10  
PT-10      **EXPERIMENT OF HEALING LIGHT FOR SLEEP AND MOODS RELIEVEMENT DURING POLAR NIGHT IN SOUTH POLE EXPEDITON STATION**  
Shao Rongdi, Li Wei and Hao Luoxi
- SO-11  
PT-46      **AN ANALYSIS OF ENERGY SAVINGS IN PUBLIC BUILDINGS THROUGH THE EMPIRICAL STUDY BY THE APPLYING DAYLIGHTING RESPONSIVE DIMMING SYSTEM LINKED TO AN INDOOR SHADE AUTOMATED CONTROL SYSTEM**  
Kim Yu-Sin, Intae Kim, Ki-Chan Woo, Kyungho Shin, Meeryoung Cho and Sang-Bin Song
- SO-12  
PT-47      **OPTIMAL CONTROL METHOD OF THE PV-OLED BLIND SYSTEM FOR IMPROVING THE INDOOR ILLUMINANCE DISTRIBUTION**  
Su-In Yun and Anseop Choi
- SO-13  
PT-48      **THE COMPARISON AND ACCURACY EVALUATIONS OF CIRCADIAN SENSITIVITY MODELS FOR LIGHT INDUCED CIRCADIAN RESPONSE**  
Yingying Huang and Qi Dai
- SO-14  
PT-49      **EFFECT OF CORRELATED COLOR TEMPERATURE AND ILLUMINANCE OF LIGHT ON VISUAL PERCEPTION AND MOOD IN SUBMARINE CABIN OF DIFFERENT ENVIRONMENT COLOR**  
Chenyao Zhao, Yandan Lin and Yixuan Zhao
- SO-15  
PT-50      **TEST METHODE(GUIDANCE) FOR U ZERO CLASIFFICATION OF OUTDOOR LUMINAIRE ACCORDING TO IES LM-75-19**  
Junseok Oh, Hee-Suk Jeong, Eun-cheol Jung, Minkyu Kang and HyoSeok Oh

Poster Session-1

- PT-11     **EVALUATION OF THE EFFECTIVENESS OF YELLOW AND BLURRED LENSES IN REDUCING HEADLIGHT GLARE**  
Tatsuya Iizuka, Shuya Suzuki, Takushi Kawamorita and Hitoshi Ishikawa
- PT-12     **APPLICATION OF VISIBLE LIGHT COMMUNICATION TECHNOLOGY IN DIGITAL OPERATING ROOM**  
Xiaofei Wang, Huafeng Yan and Jian Song
- PT-13     **BRIGHTNESS PERCEPTION THRESHOLDS OF LIGHT-EMITTING UNITS IN DIFFERENT FORMS: COMPARISON OF VIRTUAL REALITY AND REAL ENVIRONMENTS**  
Guangyan Kong, Lixiong Wang, Juan Yu and Shuo Chen
- PT-14     **STUDY ON THE EFFECT OF ALERT ZONE IN LONG TUNNEL ON REDUCING DRIVER FATIGUE**  
Li Peng, Lu Gao, Ji Weng and Yiran Lv
- PT-15     **RESEARCH ON LED ADVERTISING SCREEN TRESPASS BASED ON URBAN LIGHT ENVIRONMENT ZONING AND SCENE SETTINGS**  
Qing Fan, Mingyu Zhang and Chenge Lv
- PT-16     **THE INTERVENTION EXPERIMENT OF LIGHTING IN WORKING SPACES ON HUMAN EMOTIONS**  
Weiwei Chen, Yi Su and Yaowu Yang
- PT-17     **EFFICIENT AND PERSONALIZED HUMAN-CENTRIC LIGHTING DESIGN WITH MEDI AND AI: A CLOUD-BASED SOLUTION FOR CIRCADIAN RHYTHMS OPTIMIZATION**  
Shaokun Chen, Shu Yi, Heng Li and Huaming Chen
- PT-18     **LIGHT&SPACE: RULE-BASED SOFTWARE FOR EFFICIENT AND CODE-COMPLIANT OFFICE LIGHTING DESIGN**  
Shu Yi, Shaokun Chen, Heng Li and Huaming Chen
- PT-19     **BASIC RESEARCH ON THE DEVELOPMENT OF LED LAMPS TO SECURE THE VISIBILITY OF ROAD LIGHTING IN THE EVENT OF FOG - POSTER**  
Young-Ju Cho, Kim Jimyung, Sung-Gi Chae, Meeryoung Cho and An-Seop Choi
- PT-20     **ANALYSIS OF CLASSROOM LIGHTING RENOVATION PROJECT FOR SCHOOLS AND KINDERGARTENS IN THE YANGTZE RIVER DELTA REGION**  
Yuting Tong, Weijia Jiang, Jun Zhao, Lihua Chen, Nianyu Zou and Pengpeng Guo



# Contents

- PT-21     **A STUDY ON THE EFFECT OF SOUND AND LIGHT INTERFERENCE ON HUMAN COMFORT IN URBAN NIGHTSCAPES**  
Yifei Li and Xiaoxi Liu
- PT-22     **DISCUSSION OF THE INFLUENCE OF LIGHT ENVIRONMENT BEFORE BEDTIME ON SLEEP QUALITY BASED ON MULTI-LEVEL POPULATION SURVEY**  
Kehui Zhao, Ming Liu, Baogang Zhang, Lie Feng and Jiamin Li
- PT-23     **DEVELOPMENT OF A LIGHTING CONTROL AND CONDITION MONITORING SYSTEM**  
Yumi Hayashi, Tatsuya Nagai, Hiroki Okamoto and Kazuki Fujimoto
- PT-24     **RESEARCH ON THE EFFECTS OF LIGHTING ENVIRONMENTS ON HUMAN PERFORMANCE AND BIOLOGICAL RESPONSES.**  
Toru Kitano and Kunio Kanemaru
- PT-25     **A SEQ2SEQ MODEL BASED ON CLUSTERING AND GENETIC ALGORITHM CO-OPTIMIZATION FOR LIGHTING LOAD PREDICTION**  
Haozhe Zhu, Qingcheng Lin, Xuefeng Li and Hui Xiao
- PT-26     **RESEARCH AND ANALYSIS OF LIGHTING ENVIRONMENT AND COLOR OF MOTHER AND BABY ROOM IN COMMERCIAL SPACE IN SHANGHAI**  
Shujian Dai, Lei Shi and Luoxi Hao
- PT-27     **EFFECTS OF CHROMATIC LIGHT WITH DIFFERENT SPECTRAL DISTRIBUTION ON EEG DURING EYES CLOSED CONDITION**  
Jun Mukondo and Hiroshi Takahashi
- PT-28     **POSSIBLE IMPACT ON SLEEP QUALITY CAUSED BY EXTERIOR LIGHTING IN COMMERCIAL BUSINESS DISTRICTS AT NIGHT**  
Shenfei Chen, Yi Lin, Xianxian Zeng and Bing Zhang
- PT-29     **MULTI-OBJECTIVE OPTIMIZATION OF VISUAL AND ENERGY PERFORMANCE OF ADAPTIVE FAÇADES OF OFFICE BUILDINGS IN SHANGHAI, CHINA**  
Yuyan Wang, Tongyue Wang, Lixing Yang and Luoxi Hao
- PT-30     **AN FIELD STUDY ON ENERGY USAGE AND HUMAN COMFORT IN A SMART LIGHTING OFFICE**  
Songbo Zhang, Hang Su and Biao Yang

# Contents

- PT-31      **HOW CAMPUS LANDSCAPE LIGHT INFLUENCES VISUAL ATTENTION AND RESTORATIVE PERCEPTION: A SPATIAL MEASUREMENT STUDY EMPLOYING EYE TRACKING**  
Xianxian Zeng, Yi Lin, Bing Zhang and Shenfei Chen
- PT-32      **INVESTIGATION AND SIMULATION ABOUT LIGHT EXPOSURE AND ACTIVITIES ON THE ELDERLY: A CASE STUDY OF THE THIRD TYPE OF DAYLIGHT CLIMATIC ZONE OF UFRUMQI**  
Juanjie Li, Luoxi Hao, Rongdi Shao and Chuang Yu
- PT-33      **A META-ANALYSIS OF THE INDOOR LIGHTING PARAMETERS FOR PROMOTING SLEEP HEALTH ACROSS THE AGE SPECTRUM**  
Yixiao Cao, Luoxi Hao and Rongdi Shao
- PT-34      **A BASIC STUDY ON THE EFFECTS OF INTERACTION BETWEEN PURE TONE FREQUENCIES AND LIGHTING LUMINANCE ON THE PSYCHOLOGICAL STATE**  
Yuki Kato, Hanui Yu, Takeshi Akita, Naoko Sano and Kotaroh Hirate
- PT-35      **INVESTIGATION OF ERRORS DUE TO SELF-ABSORPTION CORRECTION IN INTEGRATING SPHERE MEASUREMENTS.**  
Kazuma Matsumoto, Kazuaki Ohkubo and Yasuki Yamauchi
- PT-36      **AESTHETIC EVALUATION STANDARD OF ARCHITECTURE LIGHTING EXTERIOR**  
Xing Zhang and Qian Liu
- PT-37      **CHARACTERISTICS OF BRIGHTNESS SENSITIVITY BY TWO LIGHT SOURCES PRESENTED TO PERIPHERAL VISION**  
Kouya Yamamoto and Hiroshi Takahashi
- PT-38      **EXPLORING KEY METRICS FOR HUMAN CENTRIC LIGHTING DESIGN IN MULTI-APPLICATION SCENARIOS: A COMPREHENSIVE STUDY**  
Luya Luo and Huaming Chen
- PT-39      **EMOTIONAL EFFECTS OF VIRTUAL REALITY-BASED IMMERSIVE EXHIBITION: A COMPARATIVE EXPERIMENT**  
Haoyu Wu and Xin Zhang
- PT-40      **REFLECTIONS ON OPTICAL LINGUISTICS FROM THE PERSPECTIVE OF EASTERN PHILOSOPHY**  
Hao Shen

# Contents

- PT-41     **COMPARISON OF LUMINANCE MEASUREMENT BETWEEN SPOT LUMINANCE METER AND ILMD**  
Xiaobo Zhuang, Xilong Yu and Xin He
- PT-42     **STUDY ON THE OPTIMIZATION OF THE CURVES THAT COMPOSE THE REFLECTOR OF A REGULAR-REFLECTION LIGHT SHELF**  
Ryota Higashino and Hirotaka Suzuki
- PT-43     **A STUDY ON THE CRYSTAL LIGHTING OF TRANSPARENT DISPLAY USING PET FILM**  
Yeonho Yang and Sanghun Lee
- PT-44     **MANUFACTURING AND EVALUATION OF POLYTOPE TENSEGRITY LAMPSHADES**  
Anqi Duan and Hirotaka Suzuki
- PT-45     **EFFECTS OF TASTE-ASSOCIATED COLORS ON TASTE THRESHOLDS**  
Takuma Hashimoto and Hiroshi Takahashi

# Contents

## Poster Session-2

- PT-51     **HOW TO LIGHT UP A PLANE UNIFORMLY USING TWO ROWS OF LUMINAIRES**  
Xingwu Chu
- PT-52     **THE EFFECT OF ILLUMINATION COLOR TEMPERATURE ON VISUAL FATIGUE IN VDT WORKING ENVIRONMENT**  
Zhengdong Li
- PT-53     **OPTIMIZING CLASSROOM LIGHTING AND VIEW CLARITY WITH A NOVEL SWITCHABLE BLIND WINDOW SYSTEM**  
Yanan Chen and Yu Bian
- PT-54     **A LABORATORY STUDY ON DYNAMIC DURATION PREFERENCE IN SHADING LIGHTING: BASED ON VISUAL COMFORT EVALUATION AND AOI OF EYE MOVEMENT**  
Luoxi Hao and Kai Feng
- PT-55     **APPLICATION OF CARBON NANOSCALE VESICLES IN ELECTROLUMINESCENT DIODES**  
Wei Yang, Li-Li Jiang and Zai-Dao Yu
- PT-56     **A CROSS-CAMERAS COLOR CONSISTENCY APPROACH IN RAW DOMAIN FOR ARBITRARY LIGHTING SCENES**  
Minhang Yang, Haisong Xu and Yiming Huang
- PT-57     **RESEARCH ON COLOR QUALITY MANAGEMENT TECHNOLOGY IN LIGHTING FOR CULTURAL TOURISM**  
Xian Tang, Xiong Yang, Qian Li and Jiangen Pan
- PT-58     **RESEARCH ON LUMINANCE PAIR RATIO AND LIGHTING CONTROL IN MULTIMEDIA CLASSROOM**  
He Wei, Yang Chunyu, Liu Yuwen and Xiao Qingyang
- PT-59     **RESEARCH PROGRESS OF BUILDING NATURAL LIGHT ENVIRONMENT BASED ON CLIMATE-BASED DAYLIGHT MODELING**  
Shuying Liang and Yi Yang
- PT-60     **THE DIFFERENCE OF PERFORMANCE IN THE COMPLEX LIGHT ENVIRONMENT OF METAMERISM**  
Yan Li, Junxian Chen, Xiong Zhou, Daqing Zhu, Xiaohan Zhou and Wu Song



# Contents

- PT-61     **A STUDY ON THE SELECTION AND OPTIMIZATION METHODOLOGY OF MACHINE LEARNING ALGORITHMS FOR DAYLIGHT PREDICTION**  
Qiuping Liu, Yaodong Chen, Yang Liu and Yuanfang Lei
- PT-62     **EFFECT OF DESKTOP TO BLACKBOARD ILLUMINATION RATIO ON STUDENTS' VISUAL FATIGUE IN A MULTIMEDIA CLASSROOM LIGHT ENVIRONMENT**  
Ji Weng, Wenshu Bai, Siyi Ke and Jiayi Tang
- PT-63     **GRAYSCALE-LUMINANCE CONVERTING POLYNOMIAL FUNCTION FOR EVALUATING INDICATORS OF SPATIAL LUMINANCE DISTRIBUTION VIA DIGITAL IMAGES: A PILOT STUDY IN LOW-CONTRAST LIT SPACE**  
Peng Chen, Lixiong Wang, Aiyang Wang, Juan Yu and Yuting Wu
- PT-64     **STUDY ON THE IMPROVEMENT STRATEGY OF PEDESTRIAN SPACE LIGHT ENVIRONMENT IN THE OLD MOUNTAIN COMMUNITY: A CASE STUDY OF CHONGQING WHITE ELEPHANT COMMUNITY**  
Yulin Shi
- PT-65     **INTELLIGENT STREET LIGHTING CONTROL SYSTEM WITH VISIBILITY PREDICTION FUNCTION**  
Xizhe Li, Nianyv Zou and Zhisheng Wang
- PT-66     **COMPARATIVE ANALYSIS OF MENTAL HEALTH EVALUATION UNDER NATURAL LIGHT AND ARTIFICIAL LIGHT ENVIRONMENT**  
Shouyi Wang, Fanpu Meng and Hua Feng
- PT-67     **RESEARCH ON CROSS-MEDIA PERCEPTION OF CITY NIGHT IMAGE THROUGH A COGNITIVE MODEL**  
Xiaoxi Liu, Tianke He, Bowen Yang and Yifei Li
- PT-68     **DEVELOPMENT AND RESEARCH OF HIGH-POWER COB PHASE CHANGE HEAT SINK WITH HIGH THERMAL CONDUCTIVITY**  
Chaoyue Liu, Long Sun, Cheng Ruan, Yaowei Huang, Yang Wang and Yu Cui
- PT-69     **IMPACT OF URBAN AIR POLLUTANTS ON THE NIGHT SKY BRIGHTNESS AND COLOR IN HOHHOT**  
Xuran Guo, Yongqing Zhao, Zhen Tian and Xiaoming Su
- PT-70     **STUDY OF LIGHTING METHOD CONSIDERING RESIDENTS' CIRCADIAN RHYTHMS**  
Jingru Shen, Jaeyoung Heo and Youko Inoue

# Contents

- PT-71      **RESEARCH OF CURRENT BEDROOM LIGHTING SITUATION FOR THE ELDERLY RISING AT NIGHT IN CHINA**  
Junliang Li, Tongyue Wang, Rongdi Shao and Luoxi Hao
- PT-72      **ANALYSIS OF NIGHT LIGHT POLLUTION DETECTION METHODS AND OPTIMIZATION MEASURES BASED ON (ULTRA) LOW ALTITUDE PERSPECTIVE**  
Yezhen Cai, Rongdi Shao, Tongyue Wang and Luoxi Hao
- PT-73      **ASSESSMENT OF SPATIAL BRIGHTNESS FOR A VISUAL FIELD IN INTERIOR SPACES BASED ON INDIRECT CORNEAL ILLUMINANCE**  
Zhiguo Hu and Qi Dai
- PT-74      **THE CONTROL OF DAYLIGHT AND ELECTRIC LIGHT COMBINATION MODES IN CLASSROOMS FOR ADOLESCENTS' NON-VISUAL HEALTH: A SIMULATION-BASED APPROACH**  
Diehong Tong and Junli Xu
- PT-75      **RESEARCH ON GUIDING FACTORS OF LIGHTING IN COMPLEX SPACE OF UNDERGROUND RAIL TRANSIT STATION**  
Lixiong Wang, Bochao Huang, Juan Yu and Chuyao Wang
- PT-76      **ULTRAVIOLET LAMP BASED ON MICROWAVE STIMULATED AND APPLICATION IN PHOTOLYZING VOLATILE ORGANIC COMPOUNDS (VOCS)**  
Zhu Shenghe and Lyu Jiadong
- PT-77      **RESEARCH ON THE LIGHTING DESIGN STRATEGY OF SCHOOL FIELD BASED ON VISUAL COMFORT**  
Yushan Liu, Yue Liu and Zheng Liang
- PT-78      **THE IMPACT AND PREDICTION OF CLASSROOM LIGHTING ENVIRONMENT AND EDUCATIONAL PRESSURE ON THE DEVELOPMENT OF MYOPIA**  
Yang Wang and Yandan Lin
- PT-79      **INNOVATION AND PRACTICE OF DARK SKY PROTECTION IN URBAN LIGHTING CONSTRUCTION -- TAKING SHENZHEN XICONG INTERNATIONAL DARK SKY COMMUNITY DECLARATION AS AN EXAMPLE**  
Yushan Liu, Guanhua Zhang, Yue Liu, Ziyang Song, Zhenchao Xu and Zheng Liang
- PT-80      **A LAB EXPERIMENT OF THE LIGHT ENVIRONMENT COMPROMISING READING INTERACTIVELY ON PAPER AND VDT**  
Xiaobo Miao, Hang Su and Biao Yang

# Contents

- PT-81     **WHITE LEDS FOR ILLUMINATION OF POLARIZING MICROSCOPE**  
Man Li, Yahong Li and Nianyu Zou
- PT-82     **AN ANALISYS OF VERTIPOINTS LIGHTING TREND IN THE URBAN AIR MOBILITY**  
Hyunyoung Lee, Jongbin Park, Kyeongsik Kim, Jonghyun Han and Hojune Bae
- PT-83     **A STUDY ON THE STANDARDS FOR INSTALLATION SITES OF STREET LIGHTING ON EXPRESSWAYS**  
Gi-Hoon Kim
- PT-84     **ANALYSIS OF THE CAUSES AND FACILITIES OF HIGHWAY TRAFFIC ACCIDENT MULTIPLE OCCURRENCE SECTION**  
Gi-Hoon Kim
- PT-85     **COMPARATIVE STUDY ON THE LIGHTING EFFECT OF TUNNEL INTERIOR MATERIALS CONDITIONS**  
Gi-Hoon Kim
- PT-86     **INVESTIGATION OF THE DRIVING ENVIRONMENT IN THE SECTION WITH FREQUENT ACCIDENTS AT NIGHT ON HIGHWAYS**  
Gi-Hoon Kim
- PT-87     **RESEARCH ON INDOOR WORKING FACE LIGHTING CONTROL BASED ON MOTION AMPLITUDE DETECTION**  
Zhide Wang, Mingyu Zhang, Mengyuan Zhang and Shengdong Li

# Contents

## Design Oral Session

P172-

- DO-1     **A PRELIMINARY STUDY ON THE LIGHTING DESIGN OF COMMUNITY NURSING HOMES**  
Kehang Chen
- DO-2     **HEALTH-ORIENTED WARD LIGHTING DESIGN: TAKING THE DESIGN OF THE SMART HOSPITAL IN CHONGQING WESTERN SCIENCE CITY AS AN EXAMPLE**  
Guangzhi Hu and Tongyue Wang
- DO-3     **A STUDY ON THE APPLICATION OF LED EDGE LINEAR LIGHT TO PASSGEWAY OF LNG CARRIER**  
Minjeong Yoo, Jin Kim and Anseop Choi
- DO-4     **LIGHTING DESIGN AT THE MAIN LOBBY OF HIGH-RISE TOWER AS A BASE OF THE SCULPTURAL FACADE**  
Eunjeong Wang

## Workshop1

P.8-

- W-01     **QUANTIFYING THE LIGHT POLLUTION IN THE URBAN AREA: BEYOND STATIC AND GROUND**  
Prof. Biao Yang
- W-02     **ECOLOGICAL IMPACTS OF NIGHT-TIME LIGHTING ON TERRESTRIAL INSECTS AND FIELD SURVEY GUIDELINES FOR ENVIRONMENTAL IMPACT ASSESSMENT**  
Dr. Sangbum Lee
- W-03     **LIGHT POLLUTION CAUSED BY URBANIZATION IN JAPAN: TOWARD THE DEVELOPMENT OF INDICATOR OF DEGREE OF URBANIZATION**  
Prof. Etsuko Mochizuki

## Workshop2

P.11-

- W-04     **RECENT TREND IN AUTOMOTIVE LIGHTING AND RESEARCH OPPORTUNITY**  
Prof. Yandan Lin
- W-05     **RECENT TREND IN AUTOMOTIVE LIGHTING AND RESEARCH OPPORTUNITY**  
Dr. Kazuyuki Yamae

# The 14<sup>th</sup> Asia Lighting Conference

# Innovation of Lighting

August 17-18, 2023  
The University of Tokyo  
Tokyo, Japan

## Keynote Speech



Asia Lighting Conference



中国照明学会  
CHINA ILLUMINATING ENGINEERING SOCIETY



一般社団法人 照明学会  
THE ILLUMINATING ENGINEERING INSTITUTE OF JAPAN



대한민국조명·전기설비학회  
THE KOREAN INSTITUTE OF ILLUMINATING AND ELECTRICAL INSTALLATION ENGINEERS



ALC Web Page



# Keynote Speech



Prof. Yasushi Yamaguchi

## Affiliation

Graduate School of Arts and Sciences, The University of Tokyo

## Title of the presentation

Visualization of Image CNNs as Explainable AI

## Biography

- Mar. 1988 The University of Tokyo, Graduate School of Engineering, Doctor of Engineering
- Apr. 1988 The University of Tokyo, College of Arts and Sciences, Research Associate
- Oct. 1989 Tokyo Denki University, Faculty of Engineering, Lecturer
- Oct. 1993 The University of Tokyo, Graduate School of Arts and Sciences, Assistant Professor
- Apr. 2002 The University of Tokyo, Graduate School of Arts and Sciences, Professor (To present)

## Meanwhile

- Apr. 2003 - Mar. 2007 The University of Tokyo, Interfaculty Initiative in Information Studies, Professor
- Apr. 2020 - Mar. 2021 The University of Tokyo, Graduate School of Arts and Sciences, Associate Dean

The 14<sup>th</sup> Asia Lighting Conference

# Innovation of Lighting

August 17-18, 2023  
The University of Tokyo  
Tokyo, Japan

## Invited Lecture



Asia Lighting Conference



中国照明学会

CHINA ILLUMINATING ENGINEERING SOCIETY



一般社団法人 照明学会

THE ILLUMINATING ENGINEERING INSTITUTE OF JAPAN



대한민국조명·전기설비학회

THE KOREAN INSTITUTE OF ILLUMINATING AND ELECTRICAL INSTALLATION ENGINEERS



ALC Web Page



# Invited Lecture (Japan)



Prof. Miki Kozaki

Photographer: KAN

## Affiliation

Graduate School of Frontier Sciences, The University of Tokyo

## Title of the presentation

The Alternative Use of Lighting Simulation

## Biography

- Mar. 2014 The University of Tokyo, Graduate School of Engineering, Doctor of Engineering
- Mar. 2015 Ochanomizu University, Faculty of Core Research Natural Science Division, Assistant Professor
- Apr. 2020 Ochanomizu University, Faculty of Core Research Natural Science Division, Associate Professor
- June. 2020 The University of Tokyo, Graduate School of Frontier Sciences, Associate Professor (To present)

## Meanwhile

- Apr. 2014 - Feb. 2015 Tokyo Denki University, Researcher
- May. 2014 - Mar. 2015 Building Research Institute, Special Researcher
- Part-time lecturer experiences at Tokyo Denki University, Shibaura Institute of Technology, Meiji University, Ochanomizu University, Jissen Women's University

# Invited Lecture (China)



Prof. Xin Zhang

## Affiliation

Tsinghua University

## Title of the presentation

Daylighting protection in traditional Chinese buildings based on paper windows

## Biography

Tenure Associate Professor of School of Architecture, Tsinghua University

Director of interior lighting Committee of China Illuminating Engineering Society (CIES)

Professional member of International Association of Lighting Designer (IALD)

Representative works:

Schematic design and general consultant of Beijing 2022 Olympic Winter Game Yanqing Zone,  
Beijing 2022 Venue Big Air Shougang and its surroundings General planning of night scape lighting  
in Chongli Winter Olympic core area, Zhangjiakou,

China Jokhang Temple, Lhasa,

China Shougang 3# Blast Furnace Museum and its affiliated structures, Beijing,

China Lounge Bridge in Shimen Village, Songyang,

China Exhibition Halls and Workshops of Rice Barns, Wuzhen, China

The Palace Museum Sculpture Gallery, Beijing, China

Imperial Examination Museum of China, Nanjing,

China National Exhibition and Convention Center (Shanghai), Shanghai, China

China Pavilion for the 14th Venice Architecture Biennale, Venice, Italy

# Invited Lecture (Korea)



Prof. YungKyung Park

## **Affiliation**

Ewha Womans University

## **Title of the presentation**

The effect of color temperature on image quality for display applications

## **Biography**

YungKyung Park, Ph.D. has been Professor at Ewha Womans University since 2012 with researching in color science field.

Prior to joining Ewha Womans University, Park was senior engineer for Samsung Electronics (LCD division).

During her 2 years at Samsung electronics, Park spent time doing research on Image quality and color appearance.

Park received a Ph.D. in color science field from Leeds University, UK and a master degree in color imaging science from the Derby University, UK.

Park received her BA and Master Degree in physics from Ewha Womans University, Korea.

# The 14<sup>th</sup> Asia Lighting Conference

# Innovation of Lighting

August 17-18, 2023  
The University of Tokyo  
Tokyo, Japan

## Workshop



Asia Lighting Conference



中国照明学会  
CHINA ILLUMINATING ENGINEERING SOCIETY



一般社団法人 照明学会  
THE ILLUMINATING ENGINEERING INSTITUTE OF JAPAN



대한민국조명·전기설비학회  
THE KOREAN INSTITUTE OF ILLUMINATING AND ELECTRICAL INSTALLATION ENGINEERS



ALC Web Page





Prof. Biao Yang

**Affiliation**

Harbin Institute of Technology (Shenzhen)

**Title of the presentation**

Quantifying the light pollution in the urban area: beyond static and ground

**Biography**

Dr. Biao Yang is now an associate professor at Harbin Institute of Technology and the director of Lab. He worked in University College London as research associate from 2014-2016. He received his PhD degree from the University of Sheffield in 2014 and MSc degree from Fudan University in 2011. His current research interests focus on intelligent and integrative lighting.

# Workshop1 (Korea)



Dr. Sangbum Lee

## **Affiliation**

Korea Environment Institute

## **Title of the presentation**

Ecological Impacts of Night-time Lighting on Terrestrial Insects and Field Survey Guidelines for Environmental Impact Assessment

## **Biography**

Chief Research Fellow

Environmental Assessment Group,

Korea Research Institute

Ph.D: Rutgers University, Geography

Research Interests: Environment Impact Assessment, Landscape Ecology, Remote Sensing

# Workshop1 (Japan)



Prof. Etsuko Mochizuki

## **Affiliation**

Chiba Institute of Technology

## **Title of the presentation**

Light pollution caused by urbanization in Japan: Toward the development of indicator of degree of urbanization

## **Biography**

Dr. Etsuko MOCHIZUKI is the professor of Department of Architecture at Chiba Institute of Technology, Japan. Her research topic is mainly concerned about visually comfortable and healthy lighting environment with low energy use.

She is the National representative of CIE Division 3 from Japan, and she is also a member of the national committee of CIE Division 4.

She was also involved in the revision of the light pollution control guidelines issued by the Japanese Ministry of the Environment.





Dr. Seo Young Choi

## **Affiliation**

Korea Institute of Lighting & ICT

## **Biography**

Korea Institute of Lighting & ICT (2013~present)

Samsung Electronics / SAIT (2008~2013)

Samsung SID / PDP Division (1996~2008)

# Workshop2 (China)



Prof. Yandan Lin

## **Affiliation**

Fudan University

## **Title of the presentation**

Recent trend in automotive lighting and research opportunity

## **Biography**

Yandan Lin received B.S. and Ph.D. degrees in the Department of Light Sources & Illuminating Engineering, Fudan University in 1999 and 2005, respectively. She is now a full professor at the Department of Light Sources & Illuminating Engineering, Fudan University. Her research interests include visual comfort, color vision, and human centric lighting. She has been awarded more than 30 funding projects, including the National Natural Science Foundation of China, and the Special Project for China Commercial Aircraft. She has published more than 100 academic articles. She is the Chair of CIE TC 1-91 (Color Quality of White Light) and is active in the field of color and vision.

# Workshop2 (Japan)



Dr. Kazuyuki Yamae

## **Affiliation**

Electric Works Company, Panasonic Corporation

## **Title of the presentation**

Recent trend in automotive lighting and research opportunity

## **Biography**

Kazuyuki Yamae received the BS and MS in Electronic Science and Engineering from Kyoto University, Kyoto, Japan in 2001 and 2003, respectively. He also received the Ph.D. in Material and Manufacturing Science from Osaka University, Osaka, Japan in 2019.

In 2003, he joined Panasonic Electric Works Co. Ltd. (PEW: now Panasonic Corporation) and since then has been involved in the development of highly efficient solid-state lighting devices. In 2023, he joined Panasonic R&D Center Singapore and since then has been leading research and development of technology regarding data-driven platform system including lighting control.

The 14<sup>th</sup> Asia Lighting Conference

# Innovation of Lighting

August 17-18, 2023  
The University of Tokyo  
Tokyo, Japan

## Papers



Asia Lighting Conference



中国照明学会

CHINA ILLUMINATING ENGINEERING SOCIETY



一般社団法人 照明学会

THE ILLUMINATING ENGINEERING INSTITUTE OF JAPAN



대한민국 조명·전기설비학회  
THE KOREAN INSTITUTE OF ILLUMINATING AND ELECTRICAL INSTALLATION ENGINEERS



ALC Web Page



The 14<sup>th</sup> Asia Lighting Conference

# Innovation of Lighting

August 17-18, 2023  
The University of Tokyo  
Tokyo, Japan

## Research Oral Session



Asia Lighting Conference



中国照明学会

CHINA ILLUMINATING ENGINEERING SOCIETY



一般社団法人 照明学会

THE ILLUMINATING ENGINEERING INSTITUTE OF JAPAN



대한민국조명·전기설비학회

THE KOREAN INSTITUTE OF ILLUMINATING AND ELECTRICAL INSTALLATION ENGINEERS



ALC Web Page

# THE EFFECTS OF DAYLIGHT CHANGES IN APARTMENT BUILDING ON PSYCHOPHYSIOLOGICAL ASPECTS OF RESIDENTS

Emi Murayama<sup>1</sup>, Jaeyoung Heo<sup>1</sup>, Hiroko Kubo<sup>2</sup>, Shinji Yoshida<sup>1</sup>

(Residential Architecture and Environmental Science, Nara Women's University, Nara, Japan<sup>1</sup>  
Faculty of Engineering, Nara Women's University, Nara, Japan<sup>2</sup>)

## ABSTRACT

It has been pointed out that, despite the fact that the amount of sunlight is secured by the Building Standards Law in Japan, sufficient sunlight is not ensured. In addition, in commercial areas, where no regulations are established to ensure the amount of sunlight, residential construction is permitted, and because of the convenience of that districts, residential buildings are often built, resulting in a situation where residential buildings are intermingled with commercial facilities. However, as a result, there are many voices pointing out the sunlight blockage even in unregulated districts, and it can be said that the sunlight problem is often pointed out from a composite perspective. However, the impact of sunlight blockage has not been clarified from several perspectives. Therefore, this study conducted experiments to analyze the changes in the residential environment caused by sunlight blockage from an apartment building on the land to the south and its effects on residents from the subject apartment building in terms of psychological, physiological, and physical quantities. As the result of the experiment, it is clarified that blockage of sunlight caused by a proximate building led the significant decrease in illuminance. In addition, the results of impression evaluation showed that the impressions of the residential environment decreased, confirming that the change in the residential environment has a significant impact on the psychological aspects of the residents.

Keywords: Daylight, Apartment Building, Impression Evaluation, Illuminance, Commercial District

## 1. INTRODUCTION

In Japan, buildings are regulated by the Building Standards Law to ensure sunlight. However, the fact that buildings are built within the scope of the law does not necessarily mean that the surrounding residential environment and residents are unaffected, and this has been long discussed [1]. Even more, there are some districts from which these regulations ensuring sunlight are exempted. One of them is commercial districts. Commercial districts are the districts designated to promote the convenience of commerce and other businesses. However, there are no restrictions on the construction of residences, and houses and apartment houses can be built in commercial districts. Because of the convenience of the commercial districts, houses and apartment houses are often mixed in with commercial facilities, etc. [2] As a result, sunlight problems have long been pointed out from various aspects.

Ensuring the amount of sunlight is considered to have an indirect effect on improving the residential environment in terms of lighting, ventilation, privacy, etc., and sunlight is regarded as a comprehensive indicator [3]. On the other hand, the impact on the psychological and physiological aspects and lifestyles associated with changes in the residential environment caused by surrounding buildings blocking sunlight has not been fully clarified. In this study, we investigate the effects of daylight changes on residents and residential environment from the combined perspectives of psychological, physiological, and physical quantities.

## 2. METHOD

The experiment in this study was conducted on a seven-story apartment building. An eight-story apartment building was under construction on the adjacent land to the south side of the subject apartment building, and this study was conducted in parallel for one year from the early stage of its construction in spring (April-May), summer (July-August), and winter (December) of 2022, and in spring (March) of 2023. The duration of each experiment was one week, and twenty



residents from subject apartment building participated in this experiment. They were divided into groups of ten participants for one week each. The schedule is shown in Table 1.

In the experiment, twenty participants were asked to complete seven questionnaires and a Stroop test to measure psychological quantities. Moreover, they were asked to wear activity meters and record their heart rate to measure physiological quantities, such as sleep variability and blood pressure. In addition to that, illuminance, temperature, and humidity were measured in the rooms of participants' apartments and recorded at two-minute intervals for each one week. Besides, noise of the construction was measured during Stroop test. Psychological quantities were measured through two questionnaires with all sixty-nine apartments as well.

We report results of the impression evaluation of residential environment, and the illuminance measurement in this paper.

Table 1. Schedule of the Experiment

	1st (Spring)	2nd (Summer)	3rd (Winter)	4th (Spring)
date	2022/4/14~4/21, 4/24~5/1	2022/7/23~30, 8/2~9	2022/12/9~16, 12/18~23	2023/3/9~16, 3/18~25

## 2.1 Impression Evaluation

The impression evaluation of the residential environment was conducted to all sixty-nine apartments (response rate: 75%). The residents were asked to evaluate impressions of their residential environment using the semantic differential method on a scale of one-five based on pairs of opposing adjectives consisting of 20 items (Table 2).

Table 2. Items of the Impression Evaluation

Evaluation Scale		
Dark :1	⇔	5: Bright
Unpleasant :1	⇔	5: Pleasant
Anxious :1	⇔	5: Safety
Closed :1	⇔	5: Opened
Stiff :1	⇔	5: Soft
Chilly :1	⇔	5: Mild
Listless :1	⇔	5: Energetic
Unusual :1	⇔	5: Usual
Tense :1	⇔	5: Relaxing
Gloomy :1	⇔	5: Cheerful
Unrefined :1	⇔	5: Refined
Dewy :1	⇔	5: Lively
Cool :1	⇔	5: Warm
Plain :1	⇔	5: Colorful
Unclear :1	⇔	5: Refreshing
Boring :1	⇔	5: Delightful
Unfamiliar :1	⇔	5: Familiar
Unshowy :1	⇔	5: Showy
Glare :1	⇔	5: Low Glare
Dislike :1	⇔	5: Like



## 2.2 Illuminance Measurement

Illuminance meters (RS-13L, Espec Mic Corp.) were set up in the one of the two rooms facing the balconies that were used most frequently in the apartments of twenty participants, and the illuminance was measured and recorded at two-minute intervals for each one week.

## 3. RESULTS



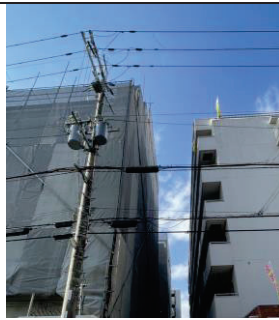

### 3.1 Impression Evaluation

The results of the impression evaluation were analysed for each direction of apartments classified as south, east, and west, and for each floor level. Of the sixty-nine apartments in this apartment building, forty-five apartments face south, twelve apartments each face east and west. As the results of evaluation in each direction, the evaluation of south side showed a tendency to decline with each passing experiment. On the other hand, no significant changes were observed on the east and west sides throughout the whole experiments (Figure 1). Although the changes in evaluation could be due to seasonal and weather effects, the fact that the evaluation of the east and west sides, which are not affected by the construction, did not change suggests that the changes in evaluation of the south side is due to the environmental changes caused by the construction. The process of the construction is show in Table 3.

In addition, in the evaluation by floor level, there was a tendency for the evaluation of each floor on the south side to decline as the construction progressed. The evaluation on the lower floor (first-second floor) declined significantly from summer (Figure2), while middle floor (third-fifth floors) declined significantly from winter (Figure 3). On the other hand, there were no significant changes on east and west sides. The fact that the evaluation significantly declined when the eight-story apartment building was constructed up to the height of each floor on the south side suggests that environmental changes may have influenced the decrease in evaluation on the south side. In addition, the evaluations on the upper floor (fifth-sixth floors) on the south side declined at regular intervals as the experiments progressed unlike the tendency observed in the lower and middle floors (Figure 4).

The gradual decrease in the evaluation from the upper floor on the south side suggests that not only environmental changes caused by the apartment building blocking sunlight, but also other environmental changes including noise and dust from the construction work affected the evaluation. The second spring results showed slightly higher ratings than winter on all floor levels only on the south side, but no significant changes on both the west and east sides were observed. Although second spring results showed slightly higher ratings than in winter on the south side, the second spring ratings did not exceed those of the first spring. Thus, it is indicated that the changes in evaluations were less influenced by the seasons and more by the environmental change caused by the new apartment building built on the south side.

Table 3. Process of the Construction

			
2022/4/14~4/21, 4/24~5/1	2022/7/23~30, 8/2~9	2022/12/9~16, 12/18~23	2023/3/9~16, 3/18~25

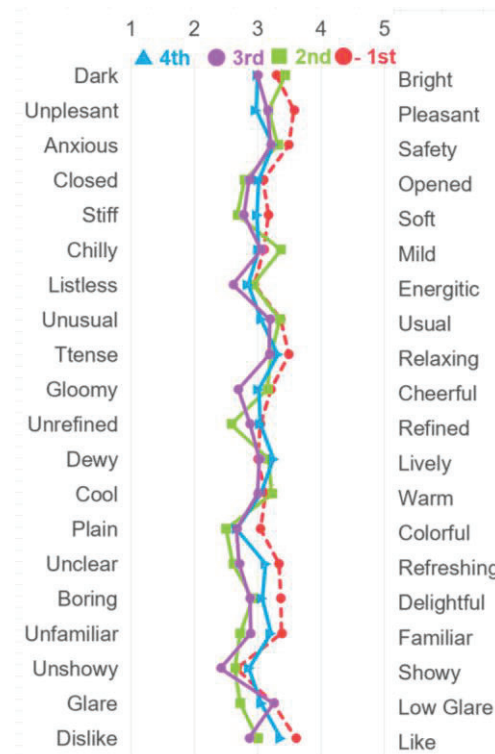


Figure 1. Average Scores of the Impression Evaluation on the East and West Sides Compared by the Each Experiment (Whole Floor)

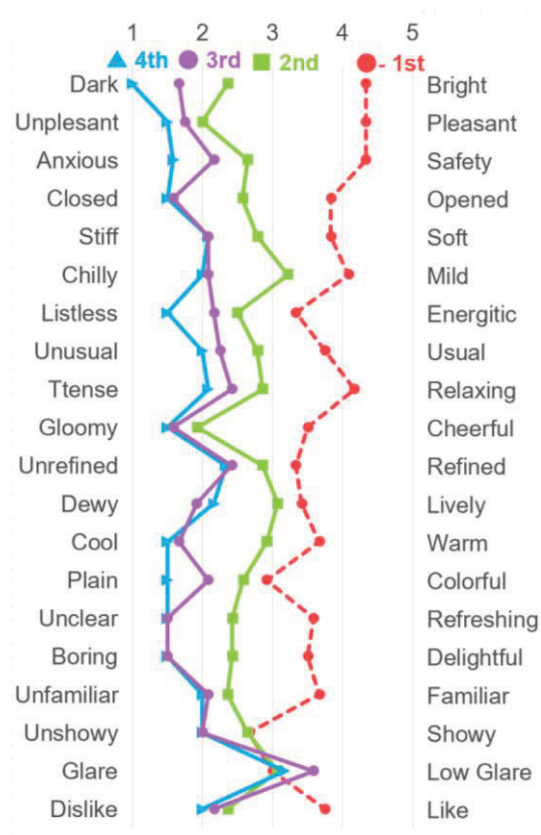


Figure 2. Average Scores of the Impression Evaluation on the South Side Compared by the Each Experiment (Lower Floor)

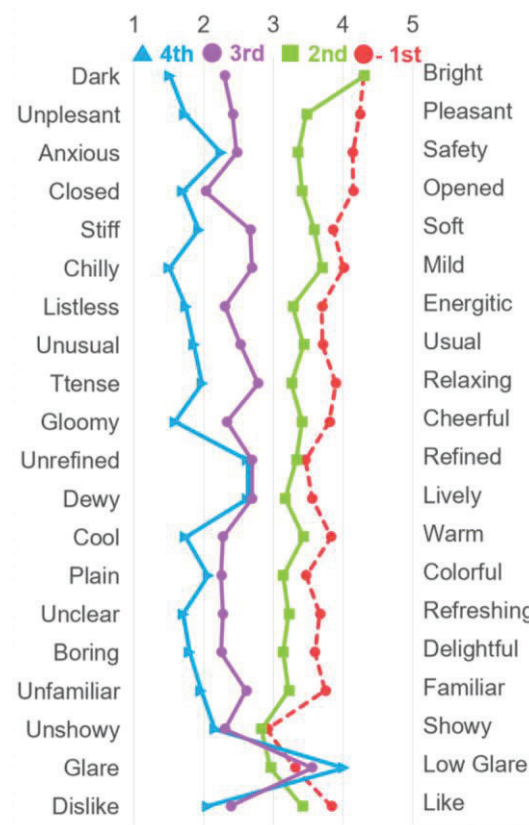


Figure 3. Average Scores of the Impression Evaluation on the South Side Compared by the Each Experiment (Middle Floor)

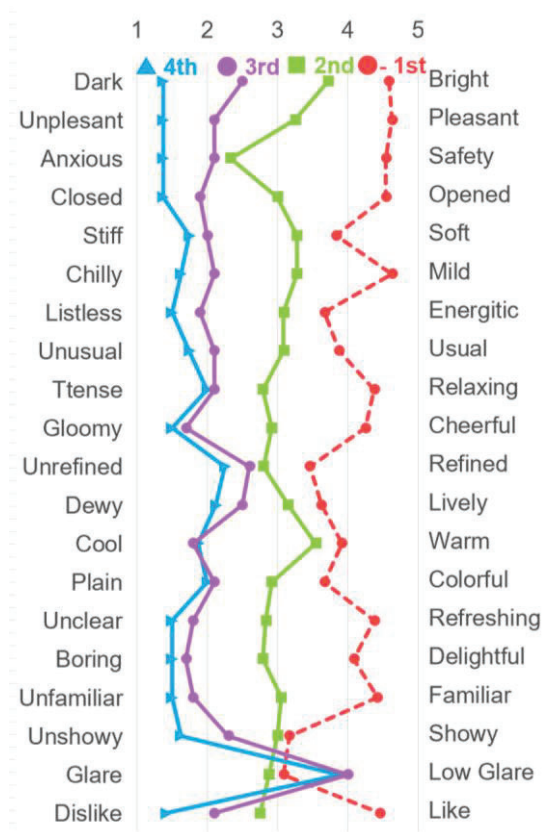


Figure 4. Average Scores of the Impression Evaluation on the South Side Compared by the Each Experiment (Upper Floor)

### 3.2 Illuminance Measurement

As for the result of illuminance measurement, illuminance may be affected by lighting equipment, seasons, and weather, but decreases in illuminance were observed in rooms facing south with each successive experiment, even though the south side usually receives the greatest amount of solar radiation in the winter and has longer daylight hours than in the summer. It was obvious that the illuminance of the rooms facing south tended to decrease with the construction of the apartment building. When the participants' apartments facing south were classified into lower floor (first-second floors), middle floor (third-fifth floors), and upper floor (sixth-seventh floors), the illuminance on the lower floor decreased after first spring, and that on the middle floor and upper floor decreased after summer, at different times, and significantly decreased when the construction of the apartment building reached each floor. The same significant decreases in illuminance were observed regardless of the length of room stay time. The illuminance changes for each floor level on the south side are shown in Figures 5, 6, and 7, using one room each as an example.

In addition, even there were only two apartments facing east, and west sides, lowest illuminance was observed in winter. This was because of the amount of all-day solar radiation and daylight hours due to the direction of the apartments. Therefore, the results of this experiment suggest that the influence of lighting equipment was relatively small and the changes in illuminance was large due to changes in brightness caused by the apartment building blocking sunlight. In addition, some rooms showed a slight increase in illuminance in the second spring. This may be due to the removal of the scaffold sheeting and the dismantling of scaffolding, which widened the distance between adjacent apartment buildings and allowed sunlight to shine in. However, the illuminance did not exceed that of the first spring, and the comparison of the illuminance in the same season showed a significant decrease, suggesting that the significant decrease and tendency in illuminance was caused by the presence of the adjacent apartment building blocking the sunlight.

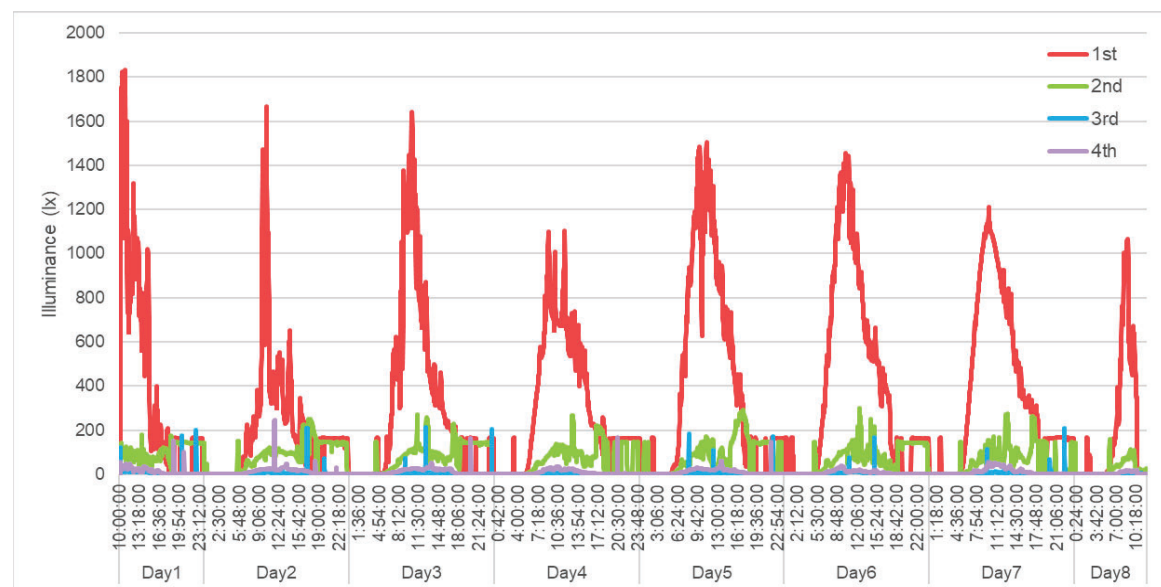


Figure 5. Illuminance on the South Side (Lower Floor)



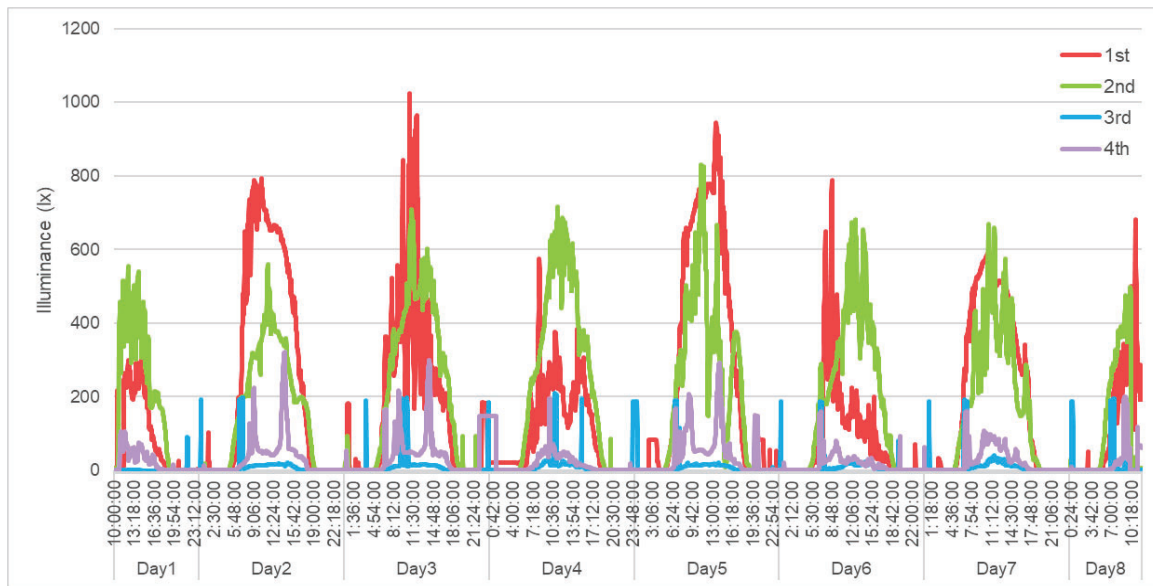


Figure 6. Illuminance on the South Side (Middle Floor)

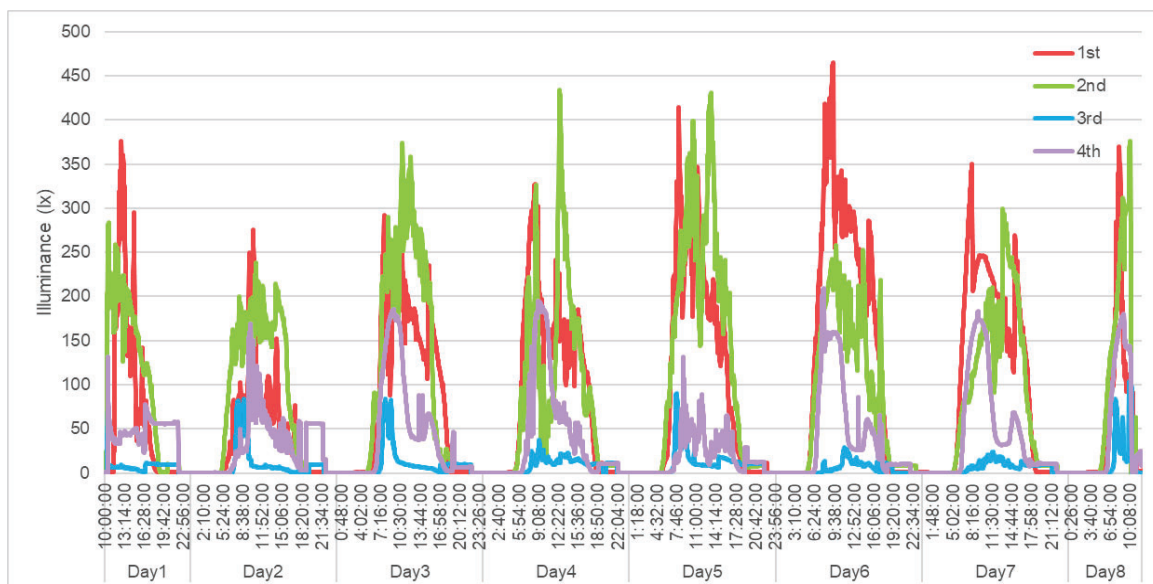


Figure 7. Illuminance on the South Side (Upper Floor)

#### 4. CONCLUSION

Although the impact of the changes in the duration of sunlight on residential environment and residents in surrounding areas have been unclear, the impression evaluation of the residential environment revealed that changes in the environment caused by the changes in the duration of sunlight have a significant impact on the psychological aspects of residents. The results of the illuminance measurements also revealed that the illuminance decreased on the south side where apartment is blocking sunlight. The results obtained in this study suggest that environmental changes such as shortened hours of sunlight associated with the proximate apartment building have impact on not only physical impact on the residential environment, but also affects the psychological aspects of residents. As a future issue, in addition to the psychological and physical quantities affected by changes in the residential environment, it is necessary to analyse how psychological quantities such as circadian rhythm was affected, and correlation between them. Moreover, it is necessary to further understand the changes in the amount of sunlight during the year and the heating and cooling load using simulation.

## REFERENCE

- [1] Hitoshi, K., Hitomi, K., Masahiko, N., Sanae, S., Akihiko, O. Enact process and operational change of shadow regulations: contemporary significance and issues as urban form regulations. Journal of the city planning institute of Japan, Vol. 49 No. 3, October, 2014.
- [2] Tetsu, K., Masao, M. A field survey on sunshine and residents' consciousness in commercial district: A study to residents in mid-to-high-rise apartment houses in the commercial district near Kawaguchi station. J. Archit. Plann. Environ. Eng., AIJ, No. 562, 89-96, Dec., 2002.
- [3] Moriaki, H., Nobuaki, M., Akiko, O., Joji, A. Studies on sunshiny conditions of dwelling places in urban district (Part1): Effects of sunshine on life. Architectural Institute of Japan, No. 178, Dec., 1970

## ACKNOWLEDGEMENTS

We would like to thank the people who provided guidance and encouragement in this research. We would like to express our deepest gratitude to them. We would also like to thank the people involved in the apartment building who willingly cooperated with the survey despite their busy schedules in carrying out this study.

Corresponding Author Name: Jaeyoung Heo

Affiliation: Residential Architecture and Environmental Science, Nara Women's University, Nara, Japan

e-mail: heo@cc.nara-wu.ac.jp

# Research on Improved YOLOv5 Gesture Recognition Algorithm for Low-light Environment

Yuan FANG<sup>1</sup>, Jia-huan Wu<sup>2</sup>, Nian-yu Zou<sup>2</sup>

(1: School of Engineering Practice and Innovation-Entrepreneurship Education, Dalian Polytechnic University, China

2: School of Information Science and Engineering, Dalian Polytechnic University, China)

## ABSTRACT

Design a gesture recognition system using the improved YOLOv5 model. The YOLOv5 model is improved to address the problem of low gesture recognition rate in low-light environments. The spatial pyramid pooling structure is improved. A dense network (DenseNet) is added into the YOLOv5 model to alleviate the gradient disappearance problem brought by the training process and enhance the feature transfer. A decoupled head structure is used in YOLOv5 for solving the bias problem caused by classification and prediction differences. The experimental results show that the improved YOLOv5 model is used for gesture recognition in low-light complex backgrounds. The average accuracy mean value reaches 95.33%, which is effectively improved on the basis of the original model, and better detection effects and stronger robustness are obtained.

Keywords: YOLOv5; Low light; Gesture recognition; DenseNet; Decoupling head;

## 1. INTRODUCTION

Gesture recognition is defined as human-computer interaction through gesture information. Gesture recognition is mainly the process of acquiring gesture information through wearable devices and computer vision technology, extracting gesture features and realizing interaction. Wearable devices have been used for gesture recognition since the 1980s. In 1983, Grimes[1] used the method of wearing data gloves to achieve the collection of gesture information, completing simple gesture recognition. Gesture recognition based on this method has been continuously optimized, but limited by the data glove to collect information, requires a large number of sensor support, high cost, and cumbersome wearing, resulting in fewer follow-up studies. With the development of computer vision, the collection of gesture information is gradually changing from wearable device acquisition to image acquisition. Gesture recognition based on computer vision only needs to use ordinary camera devices for information collection, which is convenient to operate and has few restrictions, and the application scenarios are very broad. Gesture recognition is classified into detection and segmentation of gestures. Mathematical statistics, template matching, and neural networks have been applied to vision-based gesture recognition. Mathematical statistics-based recognition methods include Hidden Markov (HMM) models. Ma et al.[2] applied the HMM to gesture recognition in 2001, and the input gesture was matched with the gesture in the database, and the starting position of the gesture was determined according to the input image, which obtained strong accuracy and robustness. The recognition method based on template matching usually adopts dynamic time regularization (DTW) algorithm, CL[3] et al. use DTW algorithm for dynamic gesture recognition. DTW algorithm is improved, by reducing the calculation time, improving the recognition speed of gesture recognition. Neural network-based gesture recognition typically employs RCNN and YOLO. Alberto[4] et al. designed a gesture recognition system based on convolutional neural network and color image by using RCNNs for human-computer interaction, with an average recognition rate of 96.92%, which is robust to changes in the light environment while ensuring real-time gesture recognition. As a first-stage network, YOLO has greatly improved the recognition speed compared with RCNN, and it can directly detect and identify objects in the network to achieve the effect of real-time detection. The YOLO algorithm, proposed by Joseph Redmon[5] in 2015, has attracted much attention due to its detection speed of up to 45 frames. In 2019, Mujahid[6] et al. used YOLOv3 combined with DarkNet-53 lightweight network for gesture recognition, and was able to successfully detect gestures in complex environments and low-resolution image situations, obtaining an accuracy of 94.88%, and can be used for real-time monitoring. In 2020, Zhan, JF[7] improved the problem of low accuracy of multi-gesture scenes on YOLOv3, used K-means++ algorithm to cluster the training set, and improved the non-maximum suppression to improve the

recognition accuracy. The accuracy and real-time performance are gradually getting higher to meet the needs of human-computer interaction, and gesture recognition based on computer vision can reduce the limitations of human-computer interaction. However, few studies have been conducted on gesture recognition systems that meet high real-time performance in low-light environments and complex backgrounds. An improved YOLOv5 model is used, a gesture recognition system is designed in low-light environment and complex background, SPPF-C is applied to the spatial pyramid pooling (SPP) structure, SIOU is selected as the bounding box regression loss function, a decoupling head is added to the YOLOv5 model to improve the network detection accuracy, and the feature transmission of the DenseNet dense network YOLOv5 network model is adopted.

## 2. ABOUT YOLO

### 2.1 YOLOv5

The classification problem is transformed into a regression problem in the YOLO network. The first release of the series is YOLOv1, which the entire image is input, the class and position of the detection frame are output. Each image is partitioned into  $S \times S$  grids, and in each grid the respective prediction tasks are completed, including the normalized bounding box parameters  $(x, y, w, h)$ , object categories, and confidence levels. If the number of bounding boxes in each grid is  $B$  and the number of prediction classes is  $M$ , then the tensor  $S \times S \times (B \times C + M)$  is finally output, where  $C$  is the parameters of the bounding boxes and the confidence level. In YOLOv2, a high-resolution image classifier is employed to train the samples and improve the mAP of the model. as the third-generation version of YOLO, YOLOv3 improves the detection accuracy of small targets with guaranteed detection speed.

In YOLOv2, a high-resolution image classifier is employed to train the samples and improve the mAP of the model. as the third generation version of YOLO, YOLOv3 improves the detection accuracy of small targets with guaranteed detection speed. YOLOv5 is the more advanced algorithm. Four models are included in this algorithm, including YOLOv5s, YOLOv5m, YOLOv5l, and YOLOv5x [8]. The network framework of YOLOv5s is shown in Figure 1, which includes four parts: Input, Backbone, Neck, and Head. Mosaic image enhancement [9] is applied to the Input to achieve data preprocessing. Focus down-sampling [10], CSP [11], and SPP pooling methods are applied to the Backbone layer to achieve the extraction of image feature information. FPN+PAN [12] is applied to the Neck part to achieve the transfer of target information of different sizes. Three loss functions are applied to Head for the computation, localization, and confidence prediction tasks, the non-maximum suppression (NMS) [13] is employed in order to achieve the best prediction frame selection.

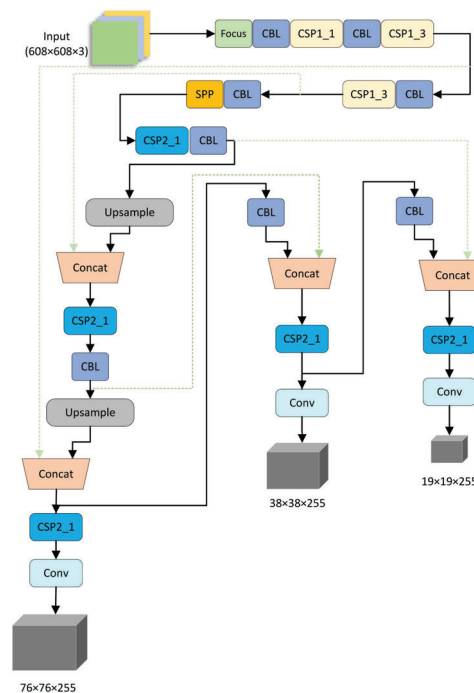


Figure 1. YOLOv5s Network Framework



## 2.2 Improved YOLOv5

### 2.2.1 Spatial Pyramid Pooling (SPP) Structure Improvement

SPP is an algorithm proposed by He Kaiming[14] to solve the problem of input image size in RCNN. The feature map of the candidate region is divided into multiple grids of different sizes, and each grid is pooled so that the image meets the requirements of fully connected layer input. The SPP diagram is shown as shown in Figure 2, and the feature map obtained by convolution is divided into three sizes, which effectively avoids the distortion problem caused by the image transformation process, and solves the problem of repeated extraction of features by the network, saving the calculation cost.

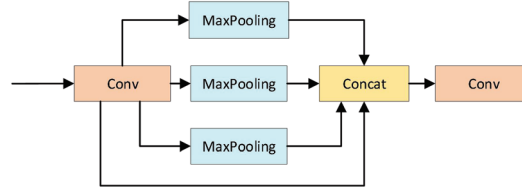


Figure 2. SPP Structure Diagram

In gesture recognition, the scale of gestures in each image is different, and different pooling layers are more conducive to the differentiation of gesture targets. The SPP in YOLOv5 is adjusted to add an improved pyramid pooling structure, which is named SPPF-C in this paper, and its structure diagram is shown in Figure 3 below. 4 pooling layer branches are included, meaning it has 4 receptive fields and the ability to handle different targets.

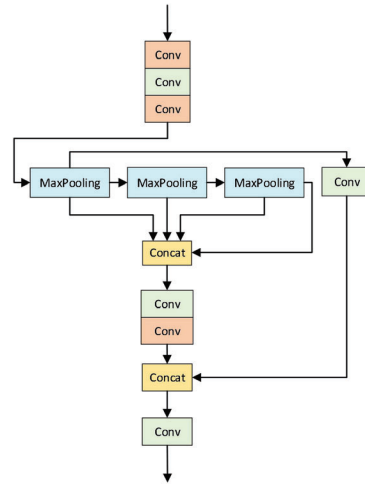


Figure 3. SPP Structure Diagram

### 2.2.2 Introduction of Decoupling Heads

In object detection, classification conflicts with regression. Classification and regression are decoupled in YOLOX to improve the detection efficiency. However, The detection head in YOLOv5 is designed as a coupling structure, which will cause spatial offset problems and affect the detection accuracy, as shown in Figure 4.

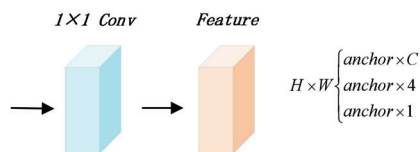


Figure 4. SPPF-C Structure Diagram

By decoupling the YOLOv5 header[15], the convergence speed can be improved. As shown in Figure 5, a  $1 \times 1$  Conv layer is employed to reduce the characteristic channel to 256, and two  $3 \times 3$  convolutions and one  $1 \times 1$  convolution are used for output during classification. Two  $3 \times 3$  convolutions are used in the positioning process, and  $1 \times 1$  convolution are performed respectively. The deviation problem caused by the difference of tasks in the classification and prediction process is solved, and the accuracy of the model is improved.

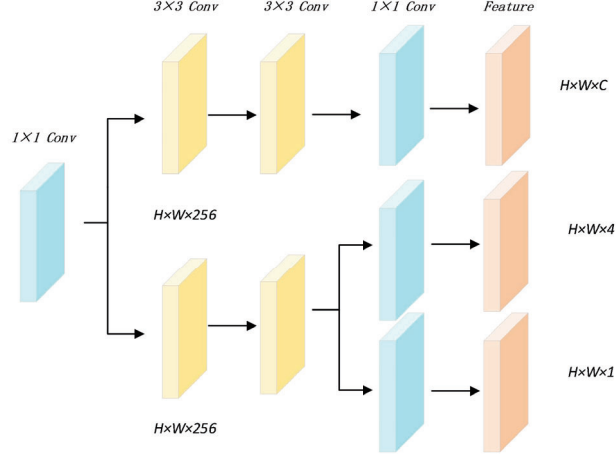


Figure 5. YOLOv5 Coupling Head Structure

### 2.2.3 DenseNet

DenseNet [16] is an efficient network that has the advantages of mitigating gradient vanishing, enhancing feature transfer, and reducing parameters. The core of the network is a dense, which adopts the method of hierarchical multiplexing, any layer obtains input from all previous layers, and maps the characteristics to all subsequent layers, while reducing the width of each layer to achieve the purpose of reducing redundancy. The network is applied to the C3 module of the YOLOv5 model, and the number of parameters is slightly increased due to the use of many residual branches, but it is proved that the network can effectively improve the accuracy.

## 3. EXPERIMENTAL

### 3.1 Experimental Environment Configuration

The experimental environment configuration is shown in Table 1 below, the operating system adopts Windows 11, and the memory is 16GB; NVIDIA GeForce RTX 3060, The GPU is Deep Learning Framework for Pytorch, and CUDA version 11.6.

Table 1. Experimental Environment

Parameter	Experimental Environment
System	Windows11 x64
RAM	16GB
CPU	12th Gen Intel(R) Core(TM) i9-12900H 2.50 GHz
GPU	NVIDIA GeForce RTX 3060
framework	Pytorch1.16、CUDA11.6

### 3.2 Datasets

5569 images of 18 gestures in HaGRID are randomly sampled, as shown in Figure 6. Gamma transforms are used to reduce image contrast and create a low-light environment. 552992 samples with a total of eighteen gestures are included in the Ha-GRID. The dataset includes mainly indoor collections, the lighting environment includes natural and artificial light, subjects are asked to shoot within 0.5m to 4m of the camera. The processed dataset is named

the L-HaGRID dataset, and the dataset is divided into training and test sets in an 8:2, of which 4374 are used for training and 1195 for testing.



Figure 6. Gestures in the HaGRID Dataset

#### 4. RESULTS

Based on the L-HaGRID dataset, experiments are performed sequentially for each added or improved module. YOLOv5s accounted for a small proportion and fast detection speed, and the model tended to be lightweight, so YOLOv5s is selected as the original model. The experimental results are shown in Table 2, and a total of 5 sets of experiments are designed, in which SPPF-C is the improved feature pyramid structure, DenseNet is the dense network, and Decoupled is a decoupling head. The YOLOv5s model that integrates SPPF-C, decoupling heads, and dense networks in this paper is named YOLOv5s-T.

Table 2. Experimental results

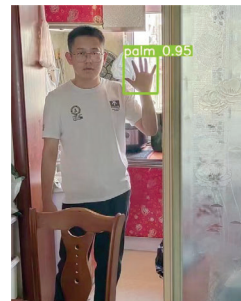
Number	Model	mAP@0.5(%)
1	YOLOv5s	94.77
2	YOLOv5s+SPPF-C	95.19
3	YOLOv5s+Decoupled	95.14
4	YOLOv5s+DenseNet	95.15
5	YOLOv5s-T	<b>95.33</b>

As shown in Table 2, the mAP of the basic model is 94.77% in the L-HaGRID dataset, the improved feature pyramid structure is improved by 0.32% on the original model, the dense network algorithm is increased by 0.28%, the accuracy of the improved feature pyramid structure, dense network and decoupling method is increased by 0.56%, and the mAP is improved to a certain extent by using the improved feature pyramid layer structure, dense network algorithm and decoupling head structure. The YOLOv5s-T model performs gesture recognition with the highest mAP.

In order to verify the gesture recognition effect of the model, gesture images in different light environments and background environments are collected, and YOLOv5 and YOLOv5-T are used to carry out gesture recognition experiments.

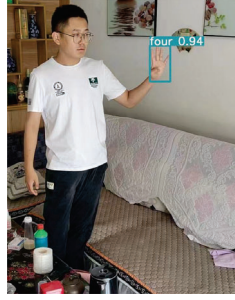


(a) YOLOv5 recognizes Palm gestures

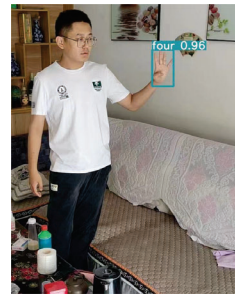


(b) YOLOv5-T recognizes Palm gestures

Figure 7. Gesture Recognition in Complex Environments under Two Algorithms



(a) YOLOv5 recognizes Four gestures

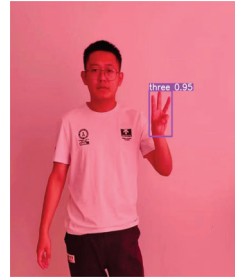


(b) YOLOv5-T recognizes Four gestures

Figure 8. Gesture Recognition in General Environments under Two Algorithms

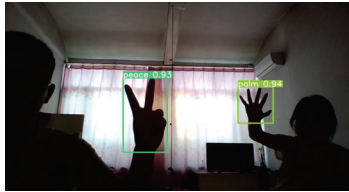


(a) YOLOv5 recognizes Three gestures



(b) YOLOv5-T recognizes Three gestures

Figure 9. Gesture Recognition in Single Environments under Two Algorithms



(a) YOLOv5 recognizes Peace and Palm



(b) YOLOv5-T recognizes Peace and Palm

Figure 10. Gesture Recognition in low-light Environments under Two Algorithms



(a) YOLOv5 recognizes Peace and Mute



(b) YOLOv5-T recognizes Peace and Mute

Figure 11. Gesture Recognition in Unevenly Lit Environments under Two Algorithms

The gesture recognition effect under strong lighting conditions is shown in Figure 7. The two models recognize the Palm gesture, both models have basically the same recognition effect for gestures. Figure 8 shows the recognition effect of gesture Four in the general environment, the algorithm recognition effect described is higher than that of YOLOv5, Figure 9 shows the recognition effect of gesture Three in a single background, YOLOv5-T has a certain improvement compared with YOLOv5. Figure 10 shows the gesture recognition effect in a low-light environment, and the YOLOv5-T has better recognition performance. Figure 11 shows the recognition effect of YOLOv5 and YOLOv5-T for gesture Peace and gesture Mute under uneven illumination, when using YOLOv5 for gesture recognition, Peace is mistakenly recognized as Peace\_inverted, and the Mute gesture is not recognized after setting the recognition threshold, while YOLOv5-T can effectively recognize peace and mute gestures, and achieve an accuracy of 0.94 and 0.85. In summary, compared with the improved model, the recognition performance is better, and the accuracy of gesture recognition under uneven illumination is greatly improved, and the gesture recognition accuracy is not lower than that of the YOLOv5 model in most cases.

## 5. CONCLUSION

The YOLOv5 is used to build a gesture recognition model, aiming to improve the detection and recognition effect of gestures in low-illumination complex environments. DenseNet is added into the original model, and the decoupling head is adopted, and the SPPF-C is added into the original pyramid pooling layer. The experimental results show that the detection accuracy of the proposed method is improved by 0.56% compared with the YOLOv5 model on the L-HaGRID dataset. In further research, operations such as pruning and distilling the network will be carried out to facilitate the deployment of gesture recognition models.

## REFERENCES

- [1] GRIMES G J. Digital data entry glove interface device: US, US4414537 A[P].
- [2] Ma G, Lin X. HMM-based operational gesture recognition method[C]//Image Matching & Analysis. International Society for Optics and Photonics, 2001.
- [3] Cheng, Chunling et al. "Real-Time Dynamic Gesture Recognition based on Boundary-Constraint Dynamic Time Warping." 2019 IEEE National Aerospace and Electronics Conference (NAECON) (2019): 545-551.
- [4] Tellaeche Iglesias, A.; Fidalgo Astorquia, I.; Vázquez Gómez, J.I.; Saikia, S. Gesture-Based Human Machine Interaction Using RCNNs in Limited Computation Power Devices. *Sensors* 2021, 21, 8202.
- [5] REDMON J, DIVVALA S, GIRSHICK R, et al. You Only Look Once: Unified, Real-Time Object Detection[C]//Computer Vision & Pattern Recognition. IEEE, 2016.
- [6] Mujahid, A.; Awan, M.J.; Yasin, A.; Mohammed, M.A.; Damaševičius, R.; Maskeliūnas, R.; Abdulkareem, K.H. Real-Time Hand Gesture Recognition Based on Deep Learning YOLOv3 Model. *Appl. Sci.* 2021, 11, 4164.
- [7] J. Zhan, W. Liu and W. Yang, "Improved gesture detection algorithm based on YOLOv3," 2021 40th Chinese Control Conference (CCC), Shanghai, China, 2021, pp. 7068-7073.
- [8] Ahmad, I.; Yang, Y.; Yue, Y.; Ye, C.; Hassan, M.; Cheng, X.; Wu, Y.; Zhang, Y. Deep Learning Based Detector YOLOv5 for Identifying Insect Pests. *Appl. Sci.* 2022, 12, 10167.
- [9] F. Dadboud, V. Patel, V. Mehta, M. Bolic and I. Mantegh, "Single-Stage UAV Detection and Classification with YOLOV5: Mosaic Data Augmentation and PANet," 2021 17th IEEE International Conference on Advanced Video and Signal Based Surveillance (AVSS), Washington, DC, USA, 2021, pp. 1-8.
- [10] S. Gao, Z. Liu and X. Li, "Study of Improved Yolov5 Algorithms for Gesture Recognition," 2022 IEEE 6th Advanced Information Technology, Electronic and Automation Control Conference (IAEAC), Beijing, China, 2022, pp. 378-384.
- [11] N. Mamat, M. F. Othman and F. Yakub, "Animal Intrusion Detection in Farming Area using YOLOv5 Approach," 2022 22nd International Conference on Control, Automation and Systems (ICCAS), Jeju, Korea, Republic of, 2022, pp. 1-5.
- [12] Jiang, T., Cheng, L., Yang, M., & Wang, Z. (2022). An improved YOLOv5s algorithm for object detection with an attention mechanism. *Electronics*, 11(16), 2494.
- [13] Y. Feng, Y. Wei, K. Li, Y. Feng and Z. Gan, "Improved Pedestrian Fall Detection Model Based on YOLOv5," 2022 IEEE 6th Advanced Information Technology, Electronic and Automation Control Conference (IAEAC), Beijing, China, 2022, pp. 410-413.
- [14] K. He, X. Zhang, S. Ren and J. Sun, "Spatial Pyramid Pooling in Deep Convolutional Networks for Visual Recognition," in *IEEE Transactions on Pattern Analysis and Machine Intelligence*, vol. 37, no. 9, pp. 1904-1916, 1 Sept. 2015.
- [15] Ge Z, Liu S, Wang F, et al. YOLOX: Exceeding YOLO Series in 2021[J]. 2021.
- [16] Xu, D.; Wu, Y. Improved YOLO-V3 with DenseNet for Multi-Scale Remote Sensing Target Detection. *Sensors* 2020, 20, 4276.

## **ACKNOWLEDGEMENTS**

This research was funded in part by Liaoning Natural Science Foundation, China (2022-BS-263); Liaoning Education Science Project(JG21DB054 ); Key Scientific Research Projects (LJKZZ20220069); Dalian Polytechnic University Reform of Education Project Foundation (JGLX2023028); Humanity and Social Science Foundation of Ministry of Education of China(21YJAZH088); University-Industry Collaborative Education Program(202102092001); Liaoning Provincial Department of Education Project(1010152); China National Textile And Apparel Council(2021BKJGLX321). We would like to express our heartfelt thanks.

Corresponding Author: Yuan Fang

Affiliation: School of Engineering Practice and Innovation-Entrepreneurship Education, Dalian Polytechnic University

e-mail : fangy@dpu.edu.cn



# 3D VISIBLE LIGHT POSITIONING METHOD FOR DRONES WITH TILT CONSIDERATION

Ryunosuke Inoshita, Saeko Oshiba

Graduate School of Science and Technology, Kyoto Institute of Technology

## ABSTRACT

In recent years, drone cameras have attracted attention for crime prevention and indoor facility inspection. Waypoint flight, in which a target location called a waypoint is specified in advance along a desired flight route, is widely used for autonomous drone flight. The drone passes through the waypoints in succession based on its own position information acquired from its onboard global positioning system. However, in indoor locations such as inside buildings or underground, radio waves are blocked and accurate positioning is not possible.

In this study, we focused on light-emitting diode (LED) lighting, which is rapidly gaining popularity, and investigated an indoor visible light positioning method that uses light from LED lighting and image sensors. Previously, we demonstrated that three-dimensional (3D) visible-light positioning with an error of approximately 10 cm is possible when an image sensor is placed horizontally with respect to the ground. However, horizontal positioning is essential and tilted image sensors lead to errors. We used information from the angle sensor to demonstrate that 3D visible light positioning with the same level of accuracy is possible with only two reference points, even when the image sensor is tilted.

**Keywords:** 3D self-position estimation, visible-light identification, image sensors, indoor autonomous drone navigation

## 1. INTRODUCTION

In recent years, drone cameras have attracted considerable attention for crime prevention and indoor facility inspection [1]. Conventionally, security based on video analysis using fixed security cameras has been widely adopted. However, fixed-position security cameras have disadvantages such as the inability to clearly capture distant objects and the existence of blind spots. In contrast, freely moving drones can capture images of distant objects and blind spots using security cameras.

A waypoint flight, in which a target position called a waypoint is specified in advance on a desired flight route, is widely used for autonomous drone flight. The drone passes through the waypoints consecutively based on its own position information acquired from its onboard global positioning system (GPS) [2]. However, accurate position estimation is not possible indoors, such as inside buildings or underground, because the GPS radar waves are blocked.

In indoor locations, where GPS signals are insufficient because of shielding by buildings, simultaneous localization and mapping (SLAM) based on feature points in images obtained by monocular, stereo, and RGB-D cameras that can simultaneously acquire RGB and depth images, may be used. Despite the popularization of SLAM technology [3], obtaining sufficiently fast and reliable results for small drones remains challenging owing to the limited computational power of onboard-embedded computers.

We focused on light-emitting diode (LED) lighting, which is rapidly gaining popularity as an alternative to GPS, and investigated an indoor visible light positioning method using light from LED lighting and an image sensor. We showed that three-dimensional (3D) visible light positioning with an error of approximately 10 cm is possible when the image sensor is placed horizontally to the ground [4]. However, an error occurred when the image sensor was tilted because the method was examined and verified under the constraint that the image sensor was installed horizontally with respect to the ground. Therefore, we used the information from the angle sensor to verify whether 3D visible light positioning with the same level of accuracy as horizontal positioning with only two reference points was possible even when the image sensor was tilted.



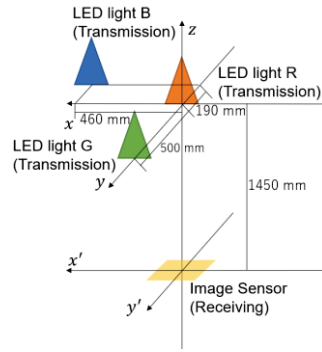


Figure 1. Schematic of the system configuration

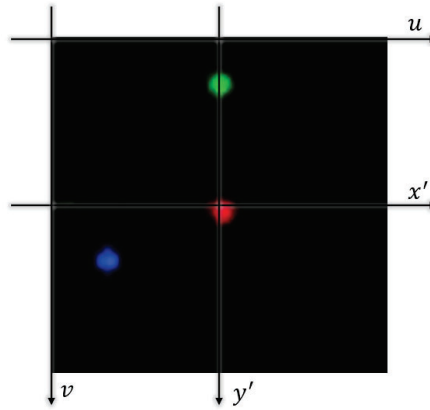


Figure 2. Image captured by image sensor

## 2. PROPOSED METHOD

In this section, we describe the proposed location estimation method. In the proposed method, the positions of the LED lights were obtained by visible light identification (ID) [5] and the receiver side estimated the position by image processing using two or more LED lights and image sensors. Figure 1 and Figure 2 illustrate the system configuration and images captured by the image sensors, respectively. Three LED lights were placed at a height of 1450 mm in the z-direction from the plane where the image sensor, which was the target for position estimation, was placed. The image sensor was illuminated by the images from each LED light. The coordinates of the LED lights and the pixels of the image sensor that represent the center of the LED light were  $(x, y, z)$ , and  $(u, v)$ , respectively. At this position, the intensity of the LED light was at its maximum value. The intensity was determined using the RGB values output from the image sensor, where R, G, and B denote red, green, and blue LED light, respectively. The positional relationship between these values is represented by equations (1)–(6) using a perspective projection transformation [6].

$$s \begin{bmatrix} u \\ v \\ 1 \end{bmatrix} = \begin{bmatrix} P_{11} & P_{12} & P_{13} & P_{14} \\ P_{21} & P_{22} & P_{23} & P_{24} \\ P_{31} & P_{32} & P_{33} & P_{34} \end{bmatrix} \begin{bmatrix} x \\ y \\ z \\ 1 \end{bmatrix} \quad (1)$$

$$\begin{bmatrix} P_{11} & P_{12} & P_{13} & P_{14} \\ P_{21} & P_{22} & P_{23} & P_{24} \\ P_{31} & P_{32} & P_{33} & P_{34} \end{bmatrix} = \begin{bmatrix} f_x & 0 & c_x \\ 0 & f_y & c_y \\ 0 & 0 & 1 \end{bmatrix} \begin{bmatrix} r_{11} & r_{12} & r_{13} & t_x \\ r_{21} & r_{22} & r_{23} & t_y \\ r_{31} & r_{32} & r_{33} & t_z \end{bmatrix} \quad (2)$$

$$\begin{bmatrix} r_{11} & r_{12} & r_{13} \\ r_{21} & r_{22} & r_{23} \\ r_{31} & r_{32} & r_{33} \end{bmatrix} = \mathbf{R}_x \mathbf{R}_y \mathbf{R}_z \quad (3)$$

$$\mathbf{R}_x = \begin{bmatrix} 1 & 0 & 0 \\ 0 & \cos \theta_x & -\sin \theta_x \\ 0 & \sin \theta_x & \cos \theta_x \end{bmatrix} \quad (4)$$

$$\mathbf{R}_y = \begin{bmatrix} \cos \theta_y & 0 & \sin \theta_y \\ 0 & 1 & 0 \\ -\sin \theta_y & 0 & \cos \theta_y \end{bmatrix} \quad (5)$$

$$\mathbf{R}_z = \begin{bmatrix} \cos \theta_z & -\sin \theta_z & 0 \\ \sin \theta_z & \cos \theta_z & 0 \\ 0 & 0 & 1 \end{bmatrix} \quad (6)$$

Here,  $s$  is an arbitrary constant;  $P_{11}$ – $P_{34}$  are the perspective camera matrices;  $f_x$  and  $f_y$  are the focal lengths;  $c_x$  and  $c_y$  are the center pixels of the image sensor;  $t_x, t_y$  and  $t_z$  are the image sensor coordinates; and  $\theta_x, \theta_y$  and  $\theta_z$  are the rotation angles of the  $x, y, z$  axes.

Next, equations (7) and (8) were obtained by expanding and rearranging Equation (1).  $P_{14}, P_{24}$ , and  $P_{34}$ , which included the coordinates of the image sensor, were used to estimate the position of the image sensor.

$$u = \frac{P_{11}x + P_{12}y + P_{13}z + P_{14}}{P_{31}x + P_{32}y + P_{33}z + P_{34}} \quad (7)$$

$$v = \frac{P_{21}x + P_{22}y + P_{23}z + P_{24}}{P_{31}x + P_{32}y + P_{33}z + P_{34}} \quad (8)$$

Minimum two LEDs with known coordinates are required to obtain  $P_{14}, P_{24}$ , and  $P_{34}$ . In this study, the LED lights R ( $x, y, z$ ) = (0,0,0), G( $x, y, z$ ) = (0,500,0), and B ( $x, y, z$ ) = (460, –190,0) (all units are in mm) were used to estimate the position with three sets of LED lights: R and B, R and G, and B and G.

### 3. CONFIGURATION OF THE EXPERIMENTAL SYSTEM

We constructed the experimental system shown in Figure 1 and conducted position-estimation experiments based on the proposed method using LED light and image sensors. The experimental system comprised an LED light and image sensor as a transmitter and receiver, respectively. These are described in sections 3.1 and 3.2.

#### 3.1 Transmitter

In this experiment, a smart light (PHILIPS Hue, full-color single-lamp E26) with variable color and brightness, using a mixture of three RGB LED colors, was used for lighting. The smart light was connected to a power supply (AC 100 V, 60 Hz), and the light intensity and color were controlled using the PHILIPS Hue app.

#### 3.2 Receiver

A Raspberry Pi camera module (Raspberry Pi Camera Module V2.1) from RS was used as the image sensor for the receiver. Its output signal was connected to a Raspberry Pi 4 Model B / 8GB from SWITCH SCIENCE for image signal processing. Subsequently, image signal processing was performed using Python as the programming environment, and the RGB values were obtained using the OpenCV library.

##### 3.2.1 Sensitivity settings of the image sensor

When the smart light was set to red, the output was 100%. The sensitivity setting of the image sensor was set to automatic and the center of the captured light was white, as shown in Figure 3(a). In this case, the RGB values were R = 255, G = 255, and B = 255. Therefore, the receiving sensitivity of the image sensor is saturated, and the G and B values that do not emit light are high. Table 1 lists the conditions under which only the value of R can be correctly received by changing the output of the smart light, ISO sensitivity of the image sensor, shutter speed, and other settings to reduce the amount of light received by the image sensor.

The RGB values of the images captured with these settings were R = 241, G = 11, and B = 37, with the value of R being twice as high as the other B and G values. Figure 3(b) shows the photographs obtained. The B and G values are non-zero because of the built-in filter of the image

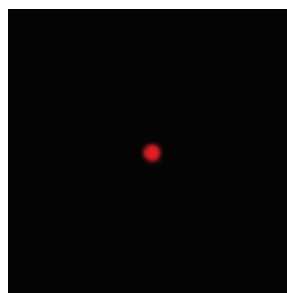
sensor. However, because these values are sufficiently suppressed and the values of R are unsaturated, the proposed method is suitable for color discrimination.

Table 1. Image sensor sensitivity settings

Smart light output	Lighting R: 3%, Lighting G: 8%, Lighting B: 1%
ISO sensitivity (0~1600, 0 is auto)	camera.ISO = 100
Shutter speed (unit: microseconds, 0: automatic)	camera.shutter_speed = 50000
Exposure compensation (-25 to 25)	camera.exposure_compensation = 0
Metering mode	camera.meter_mode = 'average'
White balance mode	camera.awb_mode = 'off'
Manual white balance adjustment (0.0-8.0)	camera.awb_gains = (1.6, 1.6)

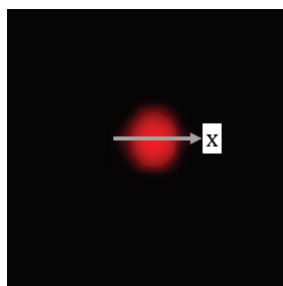


(a) Image before sensitivity adjustment  
(R=255, G=255, B=255)

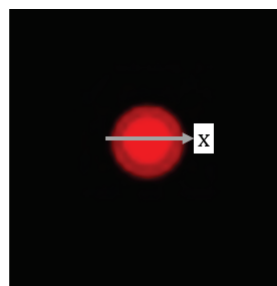


(b) Image after sensitivity adjustment.  
(R=241, G=11, B=37)

Figure 3. Image taken with an image sensor

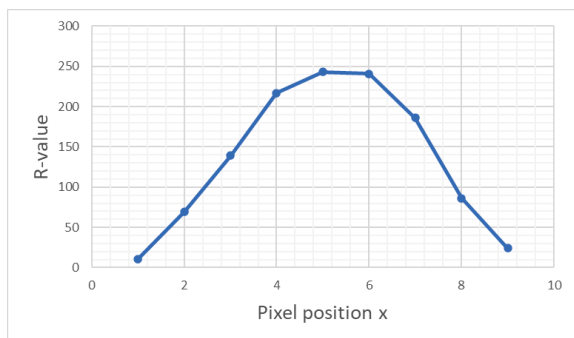


(a) 90 x 90 pixel resolution

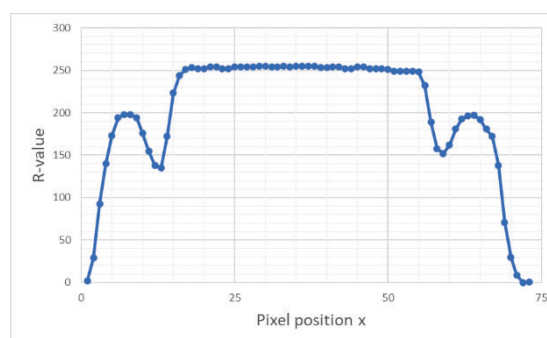


(b) 1000 x 1000 pixel resolution

Figure 4. Images of red LED light by resolution



(a) 90 x 90 pixel resolution



(b) 1000 x 1000 pixel resolution

Figure 5. R-value of red LED light by resolution

### 3.2.2 Optimization of image sensor resolution

The RGB values measured by the image sensor were used to determine the position of the LED light on the image sensor. For the red LED, the pixel with the largest value of R measured by the image sensor was used as the position of the LED light. As shown in Figure 4(a) and Figure 5(a), many pixels show the maximum value of R in the case of a  $1000 \times 1000$  pixel high-quality image. Therefore, the resolution of the image sensor was set such that only one pixel showed the maximum value at a resolution of  $90 \times 90$  pixels, as shown in Figure 4(b) and Figure 5(b). Furthermore, measurements of low quality images reduce the amount of computation required.

## 4. EXPERIMENTAL MEASUREMENTS

In the experimental system shown in Figure 1, the height  $z$  of the image sensor and LED light was fixed at -1450 mm and the image sensor was moved to 9 points on the  $x'y'$  plane at  $(x, y) = (0,0), (0,150), (0,300), (150,0), (150,150), (150,300), (300,0), (300,150),$  and  $(300,300)$  (all units are in mm). In this study, to verify the position estimation accuracy when the image sensor was installed in an inclined manner, we rotated  $\theta_x$  and  $\theta_y$  around the  $x$ -axis and  $y$ -axis in four steps of  $5^\circ$  each, as shown in Figure 6. The position estimation results in the  $x$ - $y$  plane are shown in Figure 7. The vertical and horizontal axes represent the measured positions on the  $x'y'$  plane. Bg, rb, and rg denote the results of position estimation with the LED lights B and G, R and B, and R and G, respectively. However, most of the estimated points did not accurately estimate the position. In particular, there was a point where the solution was not uniquely determined when the position was estimated using LED lights R and G because these LED lights were not used during position estimation. This may be attributed to the fact that these LED lights were installed parallel to the  $y$ -axis.

In the experimental results shown in Figure 7, we consider the correction of the position estimation results in the  $x'y'$  plane. Because the position cannot be estimated using LED lights R and G, we consider only the results of position estimation with LED lights B and G, and R and B.

Figure 8 illustrates the position estimation errors in the  $x$ -direction for rotations around the  $y$ -axis without changing the rotation angle  $\theta_x$  around the  $x$ -axis. Figure 9 presents the position estimation errors in the  $y$ -direction when for rotations around the  $x$ -axis without changing the rotation angle  $\theta_y$  around the  $y$ -axis. The position estimations in the  $x$ - and  $y$ -directions exhibit angular correlations with the  $y$ -axis and  $x$ -axis rotations, respectively. Analysis of this correlation showed that the error could be approximated by the product of the height  $z$  and  $\tan \theta$ . Therefore, the correction equations ((9) and ((10) are used to correct the estimation results shown in Figure 7. The corrected results  $(x_c, y_c)$  are shown in Figure 10.

$$x_c = x - z \tan \theta_y \quad (9)$$

$$y_c = y + z \tan \theta_x \quad (10)$$

As shown in the figure, the error between the estimated and measured values is less than  $\pm 10$  cm at all the measurement points. The error means and standard deviations are listed in Table 2.

Table 3 lists the mean and standard deviation of the errors in height estimation for the cases where the position is estimated by LED lights B and G, and by R and B.

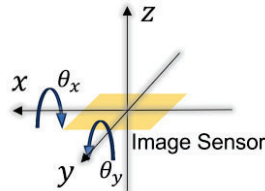


Figure 6. Example of angular change of an image sensor

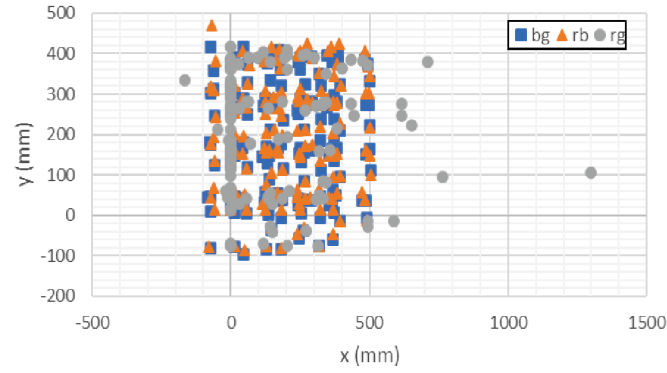
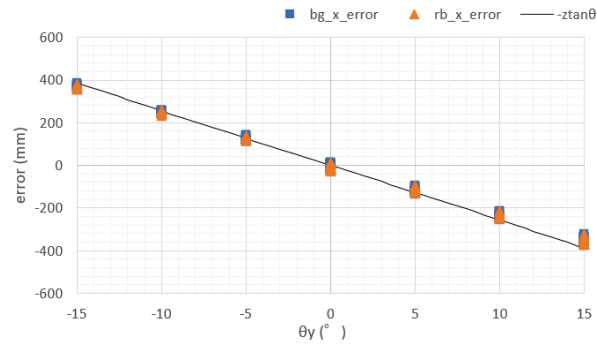
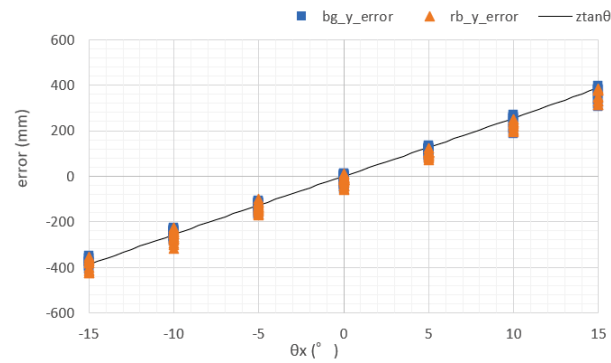

Figure 7. Estimation results for  $x'y'$  plane

Table 2. Results for position estimation in the  $x'y'$  plane

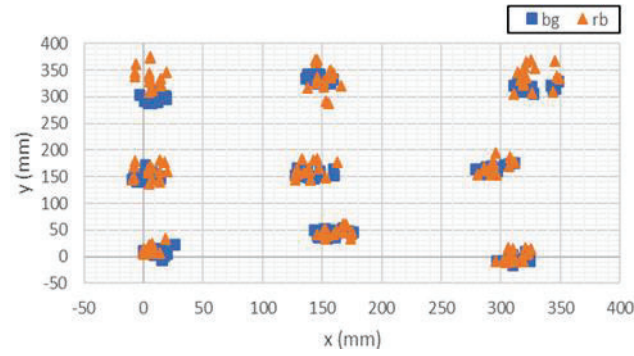
		Error average (mm)	Standard deviations (mm)
bg	x	-4.9	13.5
	y	-13.5	17.3
rb	x	-6.8	13.8
	y	-23.0	21.7

Table 3. Results of height estimation

		Error average (mm)	Standard deviations (mm)
bg	z	63.7	69.3
rb	z	42.4	81.9


Figure 8. Position estimation errors in the  $x$  direction

Figure 9. Position estimation errors in the  $y$  direction



Figure 10. Corrected results for the  $x'y'$  plane

## 5. EVALUATION OF THE ACCURACY

We evaluate the accuracy of the proposed method based on the experimental results presented in Section 4.

The measured results were used as the sample and the interval estimation of the population mean  $\mu$  was used to obtain the probability  $P$  that the error was higher than 10 cm. The sample and population were assumed to be normally distributed because the sample error was not dominant.

When the mean  $\bar{x}$  and unbiased variance  $u^2$  are obtained for the sample values, the confidence interval at the confidence level of  $1 - \alpha$  for the population mean  $\mu$  is expressed by Equation (11) [7]. Here,  $n$  is the number of degrees-of-freedom (number of measurement points).

$$\left[ \bar{x} - t_{n-1} \left( \frac{\alpha}{2} \right) \frac{u}{\sqrt{n}}, \bar{x} + t_{n-1} \left( \frac{\alpha}{2} \right) \frac{u}{\sqrt{n}} \right] \quad (11)$$

From this interval estimate of the population mean  $\mu$ , the probability  $P$  of the error being 10 cm or more was calculated using the mean value  $\mu_m$ , that had the largest probability of being 10 cm or greater. The calculation method is based on Equation (12).

$$P = 1 - \int_{-10}^{10} \frac{1}{\sqrt{2\pi}u} e^{-\frac{(x-\mu_m)^2}{2u^2}} dx \quad (12)$$

Using Equation (12), Table 4 and Table 5 list the mean value  $\mu_m$  and the unbiased variance  $u^2$  that maximize the probability of the error being greater than 10 cm, based on the error means and standard deviations in Table 2 and Table 3 for the 95% confidence level. Additionally, the provided information includes the depiction of the degrees of freedom  $n$  and the probability  $P$  indicating that the error is higher than 10 cm.

Table 4. Accuracy of the estimation of the  $x'y'$  plane location

		x	y
bg	Degrees of freedom $n$	144	144
	Mean $\mu_m$ (cm)	-7.16	-16.40
	Unbiased variance $u^2$ (cm <sup>2</sup> )	82.44	0.00
	Probability $P$	$3.9 \times 10^{-12}$	$8.3 \times 10^{-7}$
rb	Degrees of freedom $n$	144	144
	Mean $\mu_m$ (cm)	-9.04	-26.56
	Unbiased variance $u^2$ (cm <sup>2</sup> )	13.90	21.84
	Probability $P$	$3.0 \times 10^{-11}$	$3.9 \times 10^{-4}$

Table 5. Accuracy of the height estimation

	bg	rb
Degrees of freedom $n$	144	144
Mean $\mu_m$ (cm)	75.17	56.01
Unbiased variance $u^2$ (cm <sup>2</sup> )	69.78	82.44
Probability $P$	$3.6 \times 10^{-1}$	$3.2 \times 10^{-1}$

Table 4 shows that for position estimation in the  $x'y'$  plane, the probability  $P$  of obtaining errors that exceed 10 cm is less than 1% at a 95% confidence level. The objective of this study is the autonomous flight of the drone, and if a 60 fps camera is used for estimation, the highest probability of error is 10 cm or more once every 42.7 s for the plane direction estimation. Further, the  $x'y'$  plane is sufficient to achieve the goal in terms of navigation. However, Table 5 shows that height estimation is insufficient for achieving the target.

Table 5 shows that the probability  $P$  of an error of 10 cm or more exceeds 30% at a 95% confidence level for height estimation. In the case of an error probability of 25 cm or more, it is less than 1%, and the accuracy is approximately 25 cm.

Thus, the position estimation method using the two lights and an image sensor can estimate the 3D position with accuracies of 10 cm and 25 cm in the  $x'y'$  plane and height direction, respectively.

Further studies are required to improve the accuracy of the position estimated in the height direction.

## 6. CONCLUSION

In this study, we focused on LED lighting to obtain indoor location information where GPS is unavailable, proposed an indoor location estimation method using optical ID from LED lighting and an image sensor, and discussed its location estimation accuracy. In particular, by using LED lighting as a reference point and an image sensor as a receiver, we experimentally demonstrated that 3D position estimation is possible using only two reference points, with accuracies of 10 cm and 25 cm in the  $x'y'$  plane and height direction, respectively.

## REFERENCES

- [1] Hayat,S., Yanmaz,E., and Muzaffar,R. : Survey on unmanned aerial vehicle networks for civil applications: A communications viewpoint, IEEE Commun. Surveys Tuts., 18-4, pp. 2624-2661, (2016).
- [2] Shimonomura,K. : Technical Aspects of Drones: Current Situation, Unsolved Issues and Prospects. IATSS Review, 44-2, pp.100-107 (2019). (in Japanese)
- [3] Mur-Artal,R., Montiel,J.M.M., and Tardos,J.D. : ORB-SLAM: A Versatile and Accurate Monocular SLAM System, IEEE Trans. Robotics, 31-5, pp.1147-1163 (2015).
- [4] Ryunosuke Inoshita, Saeko Oshiba, "3D Self-position Estimation Using Illumination and Image Sensors," Proceedings of the 13th Asia Lighting Conference, pp. 37-44, China, 2022.
- [5] Xie,C., Guan,W., Wu,Y., Fang,L., and Cai,Y. : The LED-ID detection and recognition method based on visible light positioning using proximity method, IEEE Photon. J., 10-2, pp.1-16, (2018).
- [6] Kim,N., Baek,S., and Kim,G. : Absolute IOP/EOP Estimation Models without Initial Information of Various Smart City Sensors, Sensors, 23-2, 742, (2023).
- [7] Tadashi Kurisu, Toshio Hamada, and Nobuo Inagaki, "Interval Estimation," Fundamentals of Statistics, pp.101-112, Shokabo, Tokyo, (2001). (in Japanese)

## ACKNOWLEDGMENT

We thank Dr. Takanori Iwamatsu of Life Laboratory, Inc. for his useful advice in conducting this study. This study was also supported by a JSPS Grant-in-Aid for Scientific Research (JP 19K04375). We would like to thank Editage (www.editage.com) for English language editing.

Corresponding Author: Ryunosuke Inoshita

Affiliation: Graduate School of Science and Technology, Kyoto Institute of Technology

e-mail: ryu10p104t@gmail.com

# SUBJECTIVE INVESTIGATION ON SLEEP AND MOOD OF CHINESE ANTARCTIC RESEARCH EXPEDITION DURING VOYAGE

Yanni Wang<sup>1,2</sup>, Rongdi Shao<sup>1,2</sup>, Li Wei<sup>1,3</sup>, Tongyue Wang<sup>1,4</sup>, Luoxi Hao<sup>1,2</sup>

- (1. College of Architecture and Urban Planning, Tongji University, Shanghai, China, 200092;
2. Key Laboratory of Ecology and Energy-saving Study of Dense Habitat (Tongji University), Ministry of Education, Shanghai, China, 200092;
3. Polar Research Institute of China, Shanghai, China, 200092;
4. Shanghai Yangzhi Rehabilitation Hospital (Shanghai Sunshine Rehabilitation Center), School of Medicine, Tongji University, Shanghai, China, 201619)

## ABSTRACT

The Chinese Antarctic Research Expedition arrived in Antarctica after dozens of days at sea, crossing different climatic zones and departing from Shanghai. The sudden changes in light, temperature, humidity and wind speed from subtropical to cold polar climates force the body to undergo multiple adaptation processes, and the extreme environmental stimuli have both physiological and psychological effects. A subjective questionnaire survey was conducted on the sleep, mood and physical health of the expedition members during the voyage, and data was collected at various time points during the voyage to analyze the overall changes in the physical and mental state of the crew during the voyage. At the same time, further analysis was conducted on the quality and color of the lighting environment in different spaces of the research vessels, and the preference of personal colors and media interface content, in order to provide reference data for improving the indoor environment quality of the research vessels. The results show that there were significant differences in the feedback data obtained between the Xuelong and Xuelong2 in terms of physical health status and moods. During the voyage, the Xuelong crew were most likely to suffer from sleep quality, while the Xuelong2 were most likely to suffer from maladaptive illnesses such as motion sickness; the Xuelong crew mainly showed negative emotions of helplessness and irritability, while the Xuelong2 were more nervous and lonely. The trend in sleep and mood states was the same for both research vessels, with both reaching their lowest point at the latter part of the voyage. The focus of lighting environment quality and color in different spaces of the research vessels interior is on the lack of natural light and the lack of vivid colors. 83% of the expedition members would like to add colored lighting to the room as appropriate, especially in the multi-function hall, and 72% preferred to focus on natural scenery for indoor lighting art media interface content.

**Keywords:** Chinese Antarctic Research Expedition, Research vessels, Subjective investigation, Physical state of health, Sleep and mood changes, Preference of indoor lighting environment

## 1. INTRODUCTION

During long-distance ocean voyages, the complex living environment and harsh sea conditions put a variety of stresses on crew members, leading to chronic health problems such as abnormal bowel movements, insomnia, poor sleep quality, nausea and overeating, known as 'seafaring syndrome' [1]. Regular physical activities and sleep patterns are restricted during the voyage, the intensity of physical activities and sleep duration are lower than usual, the number of night awakenings increase and sleep becomes more restless [2]. Nighttime awakenings, daytime sleepiness, difficulty concentrating and inconsistent sleep schedules, resulting in slower reaction times, impaired reasoning, emotional instability, persistent fatigue, migraines and inability to sleep. Longer sleep duration and healthy mental state can directly and indirectly alleviate these symptoms [3]. Voyage data from the UK to Antarctica show that the primary sleep duration of vessel duty personnel (fixed and shift) is shorter than that of day shift workers, while shift workers suffer from a significant reduction in sleep quality, inefficient and fragmented sleep and delayed circadian rhythms due to the inability of their internal clocks to adapt quickly to sudden changes in schedules [4]. The early warning system, the special environment at sea, and stress during navigation in the navy can also contribute to the occurrence of circadian rhythm disorders, causing sleep disturbances, fatigue and health problems [5]. Sleep deprivation is also closely

related to moods such as anxiety and depression, with poor sleep quality triggering more frequent depression and anxiety [6]. However, depression and motion sickness are prevalent among crew members, and depression is associated with poor adaptation to sea sickness [7].

Maritime navigation makes crew members to spend long periods of time in the same confined environment for both work and leisure time, with prolonged exposure to noise, vibration and heat-induced stressors, many of which can be considered chronic. Length of time spent at sea and seafaring experience all have an impact on crew members' sleep quality and fatigue [8-10]. The impact of fatigue on their health and safety has attracted attention, and in addition to acute effects (e.g. cognitive impairment, accidents), fatigue contributes to the development of chronic diseases that are particularly prevalent among them through autonomic, immune and metabolic pathways [11]. Crew members' complaints about fatigue are much higher than in general occupational environment, with factors such as "boredom toward work" and "quality of sleep", and physical fatigue, between the "anxiety over disease" and mental fatigue and "anxiety over disease" [12]. Sleep abnormalities, generalized anxiety disorder, depression, perceived health status, lack of social communication, unavoidable stressors (nature of the occupation and psychosocial work environment) and current mental health status can also directly or indirectly affect crew members' life satisfaction [13-14]. A questionnaire survey of 917 Chinese crew members was conducted on social support, mental distress, perceived occupational stress and health-related quality of life. The results showed that 40.7% felt that the level of social support was high and 39.1% were very satisfied with their overall quality of life. Depression, occupational stress, occupational activity and sleep duration were all determinants of the poor health-related quality of life of them compared to the general population, but social support had a significant positive impact. Crew members with high levels of social support scored higher on physical health, mental health, social relationships and quality of life [15]. 12 Australian crew members were divided into 2 groups for a 100-day voyage around the Lambert Glacier Basin in Antarctica to study psychological adaptation in extreme environments and to analyze the effects of personality traits, environmental factors and interpersonal factors on group tensions, individual morale and emotional state, but the data showed that most of the psychological discomfort and problems that occurred appeared to occur within or between individuals [16].

## 2. METHODS

This investigation was conducted for the 37th and 38th Chinese Antarctic Research Expedition, using a subjective evaluation questionnaire for some members of the Xuelong and Xuelong2 crew. The questionnaire was designed in sections, with the research vessels departing from Shanghai, China to the Antarctic research stations. A multi-dimensional study was conducted on the sleep quality, mood state, physical health, the current state of the lighting environment in the cabin and the color preference of the research members under different sections of the voyage.

A total of 15 crew members of the Xuelong participated in the investigation, with positions involving navigation, engine maintenance, scientific research, logistics and other types of work, mainly crew members sailing with the ship, with more than three times experience on board the Xuelong. A total of 13 crew members of the Xuelong2 participated in the investigation, with positions involving station management, meteorological observation, engine maintenance, logistics and other types of work, mainly wintering research members of the Great Wall Station, for the first time on board the Xuelong2.

The Xuelong and Xuelong2 departed from Shanghai, China, and sailed through subtropical and tropical regions for dozens of days before finally arriving in Antarctica. Figure 1 shows the schematic diagram of the route of the Xuelong and Xuelong2 [17]. During the voyage, the research vessels were exposed to severe sea weather such as wind, waves and thunderstorms, as well as complex sea conditions such as swells, tides and sea ice, and the light, temperature and humidity, wind speed and so on also changed from time to time, which differed greatly from the crew's usual place of residence. The voyage across time zones disrupts the body's normal sleep and rhythms, and the body needs to adjust to extreme environmental changes at all times. During the voyage, the only thing in view is the infinite ocean, which prevents communication with the outside world and limits normal social activities and exercise. The overall state of isolation can lead to negative moods such as depression, agitation and boredom.



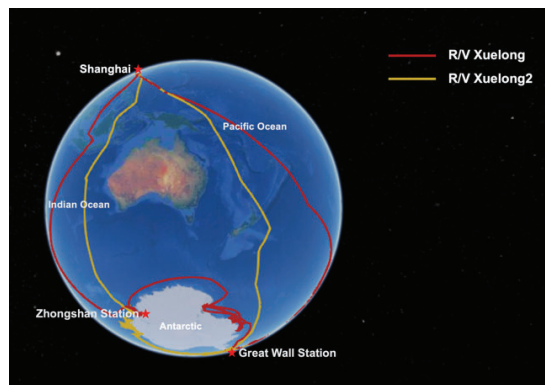


Figure 1. The schematic diagram of the route of the Xuelong and Xuelong2

The Xuelong was built in 1993 and has been upgraded several times since then [18]. According to field research, the cabin of the Xuelong has small windows, mainly artificial lighting, and the overall lighting facilities are relatively old, mainly using round recessed downlights and square flat-panel lights. The main lights in the accommodation are square flat-panel lights, and each bunk is equipped with a small wall light for the crew to use independently in accordance with their own work and rest patterns; the dining room and gymnasium use strip flat-panel lights, and the function room uses round recessed downlights (Figure 2).



Figure 2. Current situation of indoor lighting environment of Xuelong

Delivered in July 2019, Xuelong2 is China's first indigenously built icebreaker for polar scientific expedition [19]. The cabins are also dominated by artificial lighting, with less natural light introduced. The overall lighting is based on round recessed downlights, with the main lights in the accommodation being strip flat-panel lights, partially assisted by round downlights, plus desk lights and bedside wall lights. The dining room is equipped with a luminous ceiling, which provides a high level of brightness and creates a pleasant and tidy dining environment; the function room, in addition to the top downlights, is evenly decorated with connected strip lights on both sides of the wall and on top, making the overall space spacious and bright, with a high degree of uniformity and a sense of modern technology (Figure 3).





Figure 3. Current situation of indoor lighting environment of Xuelong2

### 3. CONCLUSION

The questionnaire was designed according to the work of the research members on vessels. The Xuelong was mainly a crew member sailing with the ship, and the questionnaire was designed to focus on the impact of sea conditions on the team members, dividing the entire voyage into three periods: the early days of voyage, the westerlies sailing period and the polar ice navigation period. The Xuelong2 was mainly a crew member wintering at the Great Wall Station, and the questionnaire was designed to focus on the impact of the voyage time on the team members, dividing the entire voyage into three periods: the early days of voyage, the arrival at Zhongshan Station and Zhongshan Station to Great Wall Station.

#### 3.1 Sleep quality and mood state

The subjective evaluation of sleep quality and mood state is on a scale of 0-10, with 0 indicating very poor sleep quality or very poor mood state and 10 indicating very good sleep quality or very good mood state. The results show that the sleep quality and mood state of the Xuelong crew members who participated in the investigation showed a decreasing trend throughout the voyage. The members' sleep quality was best at the early days of the voyage and worst during the polar ice navigation period, with a clear trend of gradual decline over the three periods, but not significant. Mood state was best at the early days of the voyage and worst during the polar ice navigation period, but the difference between the westerlies sailing period voyage and the polar ice navigation period was weaker, with an overall trend of decreasing and then remaining a steady trend.

The sleep quality and mood state of the Xuelong2 crew members who participated in the investigation decreased first and then increased during the whole voyage. The sleep quality of the crew members was best during the voyage from Zhongshan Station to Great Wall Station, even better than at the early days of the voyage, and worst during the period before arriving at Zhongshan Station, with a clear trend of decreasing and then increasing during the three periods, but not significant. Mood state was best at the early days of the voyage and worst in the period before arriving at Zhongshan Station, after which there was a slight rebound, showing a trend of declining first and then basically maintaining a steady state.

Overall, the Xuelong and Xuelong2 crew members' sleep quality was more likely to be affected, and the trend was more pronounced, with mood states being more susceptible in the early days of the voyage, and then changing slightly and remaining flat.

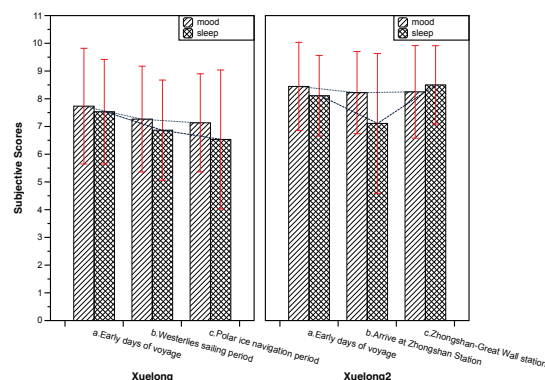


Figure 4. Current situation of indoor lighting environment of Xuelong2

#### 3.2 Physical state of health

Health problems such as sleep disturbance and fatigue can occur during long sea voyages. The physical health states section of the questionnaire focuses on poor sleep quality, fatigue, loss of appetite, maladaptive disorders such as motion sickness and impairment of body functions. The members chose the health problems they experienced during different periods of the voyage in relation to their own feelings.

The results show that the physical health problems of the Xuelong crew during different periods of the voyage were reflected in different aspects (Figure 5). At the early days of the voyage, poor sleep quality was the most serious problem, and maladaptive illnesses such as

motion sickness were also evident; during the westerlies sailing period, in addition to poor sleep quality, loss of appetite was the most frequently proposed influence; during the polar ice navigation period, the body was most likely to experience poor sleep quality, and to the highest degree among the three periods. Overall, poor sleep quality was a concentrated health problem during the Xuelong voyage.

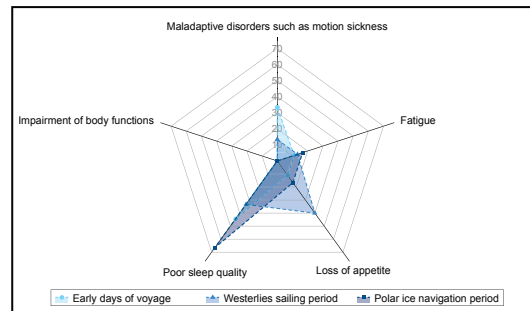


Figure 5. Physical state of health of Xuelong

The physical health problems on Xuelong2 differed significantly from those on Xuelong, with different focal points on the three periods (Figure 6). The results show that maladaptive illnesses such as motion sickness were the main influencing factor at the early days of the voyage; loss of appetite was most evident in the period before arriving at Zhongshan Station; and maladaptive illnesses such as motion sickness and fatigue were concentrated among the crew in the period from Zhongshan Station to Great Wall Station. Overall, maladaptive illnesses such as motion sickness and loss of appetite were more frequent during the Xuelong2 voyage, and the difference in physical state of health between the two voyages before reaching the Antarctic and the post-Antarctic diversions was significant, with the latter showing a significant increase in fatigue, in line with the psychological 'three-quarters' phenomenon, where physical fatigue peaks before reaching the destination.

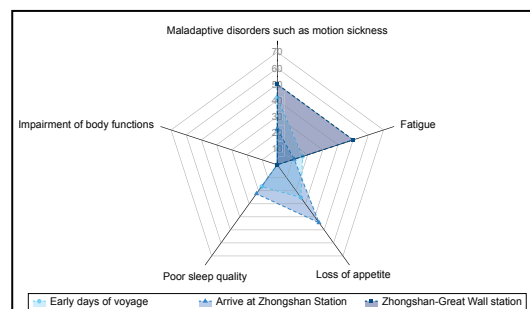


Figure 6. Physical state of health of Xuelong2

### 3.3 Negative moods state

The extreme environment of the sea and multiple stressors have a negative impact on the psychological well-being of the crew members. It is important to explore the negative moods that are likely to occur during the voyage and to subsequently propose targeted strategies to improve the physical and psychological health of the crew members. The questionnaire was designed to include the negative moods of depression, irritability, loneliness, tension, obsessive-compulsive, anxiety and helplessness, and the crew members selected the most likely negative moods to occur during different voyage periods.

The results showed that the negative moods were relatively similar between the different periods of the Xuelong (Figure 7). Feelings of helplessness, irritability and loneliness were most predominant at the early days of the voyage; helplessness and irritability were most pronounced during the westerlies sailing period; and irritability most affected one's stable mood during the polar ice navigation period. Overall, helplessness and irritability caused the most mood disturbance to the crew throughout the voyage, followed by loneliness and anxiety.

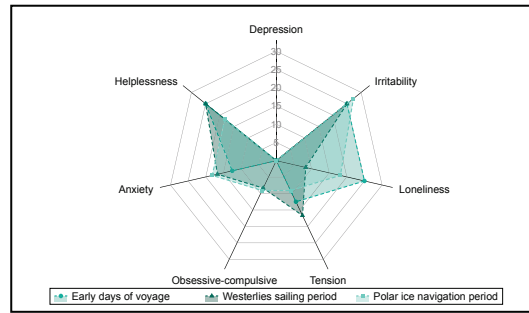


Figure 7. Negative moods state of Xuelong

The negative mood feedback on Xuelong2 differed significantly from that of Xuelong, with only helplessness, tension, loneliness and anxiety being present throughout the voyage, and not otherwise represented (Figure 8). Helplessness, loneliness and tension were raised by the crew during the early days of the voyage; loneliness peaked in the period before arriving at Zhongshan Station, accompanied by helplessness and anxiety; tension and anxiety both peaked in the period from Zhongshan Station to Great Wall Station, where they were about to live and work for a long time.

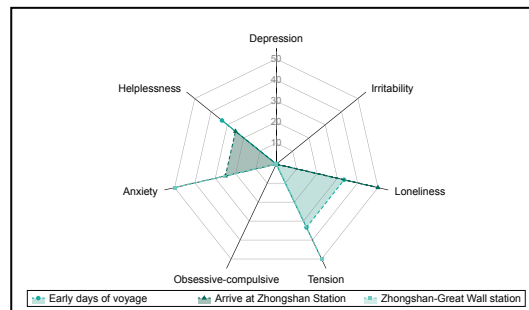


Figure 8. Negative moods state of Xuelong2

### 3.4 Colored lighting preference

The artificial lighting in the Xuelong and Xuelong2 is warm white, and the introduction of colored lighting and lighting art installations can have a soothing effect on the negative moods of the crew members. The questionnaire investigated the preference for colored lighting and the interface elements of the lighting art installations. The use of colored lighting was categorized as no colored lighting, partial single color, partial multi-color, overall spatial single color and overall colorful. There are five different interface elements styles of lighting art installations: natural scenery, cute animals, urban imagery, abstract paintings and blurred color blocks. Each option of colored lighting and interface elements is equipped with the rendering, which are visually more intuitive and judged by the crew members according to their own preferences and usage habits. The results showed that 83% of the them wanted to add colored lighting to the interior, with 29% of them choosing partial single color. 72% of their preference for the interface elements of the lighting art installation was focused on natural landscapes.

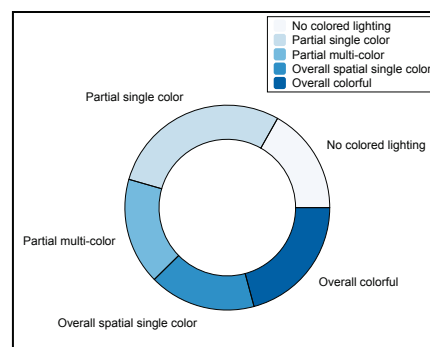


Figure 9. Colored lighting preference of Xuelong2

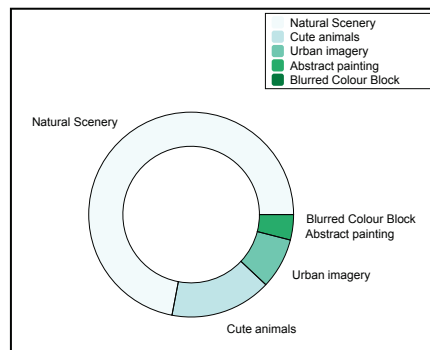


Figure 10. Interface elements of lighting art installations preference of Xuelong2

#### 4. CONCLUSIONS

The Antarctic research expedition face not only social isolation, fatigue, limited recreational activities and sleep deprivation during their voyage, but also the inevitable work-related stresses that can have an impact on physical and psychological health. Research data shows that the changes of the quality of sleep and mood state during the voyage are not the same between crew members with different sailing experience, and that the focus of negative moods is also different. Information on known stressors during voyage can be provided to help reduce their perception of stress. Strategies for coping with stress can also be researched and developed to enhance the resilience of crew members based on their sailing experience, type of work and working environment [20-23]. In terms of the design of the lighting environment in the cabin, providing healthy lighting that can regulate circadian rhythms and improve the quality of sleep of the crew members. Social isolation seriously affects psychological health and it is important to include it in the accident prevention programs and to develop policies to promote psychological health [24-25]. Appropriate introduction of colored lighting and lighting art installations in the public space can break the single and boring characteristics of indoor space, alleviate the negative moods such as helplessness, irritability and loneliness, and actively guide the communication and exchange among crew members. It is of great significance to provide the crew members with good scientific research facilities and improve the working and living environment quality during the voyage.

#### REFERENCE

- [1] Sun Z, Zhang M, Li M, Bhaskar Y, Zhao J, Ji Y, Cui H, Zhang H, Sun Z. Interactions between Human Gut Microbiome Dynamics and Sub-Optimal Health Symptoms during Seafaring Expeditions. *Microbiol Spectr.* 2022 Feb 23;10(1): e0092521.
- [2] Youn IH, Lee JM. Seafarers' Physical Activity and Sleep Patterns: Results from Asia-Pacific Sea Routes. *Int J Environ Res Public Health.* 2020 Oct 5;17(19):7266.
- [3] Galić M, Sić L, Slišković A. "I Constantly Feel Worn Out": Mixed-methodology Approach to Seafarers' Sleep on Board. *Inquiry.* 2023 Jan-Dec;60: 469580231159746.
- [4] Arendt, J., et al., Sleep and circadian phase in a ship's crew. *JOURNAL OF BIOLOGICAL RHYTHMS*, 2006. 21(3): p. 214-221.
- [5] Li H, Liu Y. Navy Sailors Health Behavior: A Multi-Factor Analysis of Circadian Rhythm on Naval Operational Capability. *Am J Health Behav.* 2023 Apr 30;47(2):349-359.
- [6] Andruskiene J, Barseviciene S, Varoneckas G. Poor sleep, anxiety, depression and other occupational health risks in seafaring population. *TransNav: International Journal on Marine Navigation and Safety of Sea Transportation.* 2016;10(1):19–26.
- [7] Park CY, Park S, Han SG, Sung T, Kim DY. Association of Depression With Susceptibility and Adaptation to Seasickness in the Military Seafarers. *J Korean Med Sci.* 2022 Jul 25;37(29): e231.
- [8] Hystad SW, Eid J. Sleep and Fatigue Among Seafarers: The Role of Environmental Stressors, Duration at Sea and Psychological Capital. *Saf Health Work.* 2016 Dec;7(4):363-371.

- [9] Oldenburg M, Felten C, Hedtmann J, Jensen HJ. Physical influences on seafarers are different during their voyage episodes of port stay, river passage and sea passage: A maritime field study. *PLoS One*. 2020 Apr 8;15(4): e0231309.
- [10] Forsell K, Eriksson H, Järholm B, Lundh M, Andersson E, Nilsson R. Work environment and safety climate in the Swedish merchant fleet. *Int Arch Occup Environ Health*. 2017 Feb;90(2):161-168.
- [11] Jepsen JR, Zhao Z, van Leeuwen WM. Seafarer fatigue: a review of risk factors, consequences for seafarers' health and safety and options for mitigation. *Int Marit Health*. 2015;66(2):106-17.
- [12] Kamada T, Iwata N, Kojima Y. [Analyses of neurotic symptoms and subjective symptoms of fatigue in seamen during a long voyage]. *Sangyo Igaku*. 1990 Nov;32(6):461-9. Japanese.
- [13] Baygi F, Smith A, Mohammadian Khonsari N, Mohammadi-Nasrabadi F, Mahmoodi Z, Mahdavi-Gorabi A, Qorbani M. Seafarers' mental health status and life satisfaction: Structural equation model. *Front Public Health*. 2022 Nov 30;10: 969231.
- [14] Baygi F, Shidfar F, Sheidaei A, Farshad A, Mansourian M, Blome C. Psychosocial issues and sleep quality among seafarers: a mixed methods study. *BMC Public Health*. 2022 Apr 9;22(1):695.
- [15] Xiao J, Huang B, Shen H, Liu X, Zhang J, Zhong Y, Wu C, Hua T, Gao Y. Association between social support and health-related quality of life among Chinese seafarers: A cross-sectional study. *PLoS One*. 2017 Nov 27;12(11): e0187275.
- [16] Wood, J., et al., Psychological Changes in Hundred-Day Remote Antarctic Field Groups. *Environment and Behavior*, 1999. 31(3): p. 299-337.
- [17] <http://x.hbaa.cn/Long/>
- [18] [https://baike.baidu.com/item/%E9%9B%AA%E9%BE%99%E5%8F%B7%E6%9E%81%E5%9C%B0%E8%80%83%E5%AF%9F%E8%88%B9/2868622?fr=ge\\_al](https://baike.baidu.com/item/%E9%9B%AA%E9%BE%99%E5%8F%B7%E6%9E%81%E5%9C%B0%E8%80%83%E5%AF%9F%E8%88%B9/2868622?fr=ge_al)
- [19] [https://baike.baidu.com/item/%E9%9B%AA%E9%BE%99%E5%8F%B7%E6%9E%81%E5%9C%B0%E8%80%83%E5%AF%9F%E8%88%B9/22143505?fr=ge\\_al](https://baike.baidu.com/item/%E9%9B%AA%E9%BE%99%E5%8F%B7%E6%9E%81%E5%9C%B0%E8%80%83%E5%AF%9F%E8%88%B9/22143505?fr=ge_al)
- [20] Oldenburg M, Baur X, Schlaich C. Occupational risks and challenges of seafaring. *J Occup Health*. 2010;52(5):249-56.
- [21] Carotenuto A, Molino I, Fasanaro AM, Amenta F. Psychological stress in seafarers: a review. *Int Marit Health*. 2012;63(4):188-94.
- [22] Ali SNM, Cioca LI, Kayati RS, Saputra J, Adam M, Plesa R, Ibrahim RZAR. A Study of Psychometric Instruments and Constructs of Work-Related Stress among Seafarers: A Qualitative Approach. *Int J Environ Res Public Health*. 2023 Feb 6;20(4):2866.
- [23] Doyle N, MacLachlan M, Fraser A, Stilz R, Lismont K, Cox H, McVeigh J. Resilience and well-being amongst seafarers: cross-sectional study of crew across 51 ships. *Int Arch Occup Environ Health*. 2016 Feb;89(2):199-209.
- [24] Sampson H, Thomas M. The social isolation of seafarers: causes, effects, and remedies. *Int Marit Health*. 2003;54(1-4):58-67.
- [25] Abila, S. and I. Acejo, Mental health of Filipino seafarers and its implications for seafarers' education. *International Maritime Health*, 2021. 72(3): p. 183-192.

## ACKNOWLEDGEMENT

The research was financially supported by the Science and Technology Commission of Shanghai Municipality (Grant No.20dz1207204).

Corresponding Author Name: Luoxi Hao  
 Affiliation: College of Architecture and Urban Planning, Tongji University  
 e-mail: haoluoxi@tongji.edu.cn  
 Corresponding Author: Yanni Wang  
 Affiliation: College of Architecture and Urban Planning, Tongji University  
 e-mail: 1484249250@qq.com



# PUPIL SIZE AND SUBJECTIVE LIGHT EVALUATION DIFFERENCE OF ELDERLY PEOPLE BETWEEN DARK AND LIGHT CONDITIONS

Noriko Umemiya, Saki Tahara, Tomoyuki Minami  
Osaka City University

## ABSTRACT

Pupil size and subjective light environment evaluation were measured for elderly and young people in experiment chamber where illuminance was set two levels of about 2800 lx and about 450 lx on the center of the desk. Brightness, brightness for writing, glare, comfort, preference and performance of the environment were evaluated.

Pupil size was larger for young participants than for elderly participants under both dark and light conditions. Larger difference in light evaluation between light and dark conditions were found in elderly participants than in young participants. Significant differences were found in all light evaluations between dark and light conditions for elderly participants. No difference was found in glare evaluation between elderly and young participants under light condition. No difference was found in performance evaluation between young and elderly participants under both dark and light conditions.

Pupils under light condition were smaller for elderly participants with better eyesight than for elderly participants with worse eyesight. Pupils under light conditions were larger for elderly participants who had reported 'difficulty seeing in a dark environment' or 'easy to be tired in eyes' than those of elderly participants without these characteristics. Pupils under dark conditions were larger for elderly participants who 'prefer a uniformly lit environment' than for elderly participants without these characteristics. There found no difference in pupil diameter by vision awareness for young participants in light condition.

Pupil size was found to be related to the subjective evaluation of brightness, brightness for writing, glare, comfort, preference and performance for young participants, whereas it was found to be related only to the evaluation of brightness for writing and performance for elderly participants.

Pupils were smaller for elderly participants who evaluated dark condition as brighter and as more preferable than those of elderly participants who evaluated dark conditions as darker and less preferable.

Keywords: Pupil size, Light evaluation, Elderly people

## 1. INTRODUCTION

Recently, increasingly elderly workers are expected to be employed in highly aging societies with lower birth rates. The rate of retirees under the age of 59 was 60.3% in 1980 in Japanese enterprises. The rate decreased to 0.8% in 2000, where of the rate of retirees under 65 was 2.7% in 1990. It increased to 12.8% in 2010. The Law of Employment Stability of Senior Workers, which was enforced in 2013, obligates job security until 65 years old to employees working before April 2025. Despite these protections for older workers, the physical environment of the workplace is not necessarily prepared for elderly workers. This study was conducted to improve the light environment for elderly workers. Pupil size and subjective light environment evaluation were measured in dark and light conditions for elderly and young people. Then they were compared.

## 2. METHODS

In these experiments, 132 elderly people over 65 years old and 85 university students participated. Pupil sizes were measured at intervals of 30 Hz using a view tracking device fixed by a belt on the head. Figure 1 shows the experiment chamber and

experiment room. Participants began to fill in questionnaire sheets about the light environment about ten minutes after entering the experiment chamber. Brightness, brightness for writing, glare, comfort, preference and performance of light environment were evaluated. Two conditions of the illuminance were examined. Illuminance of the questionnaire sheets on the table in the experiment chamber was set as about 2800 lx for the LIGHT condition and about 450 lx for the DARK condition.

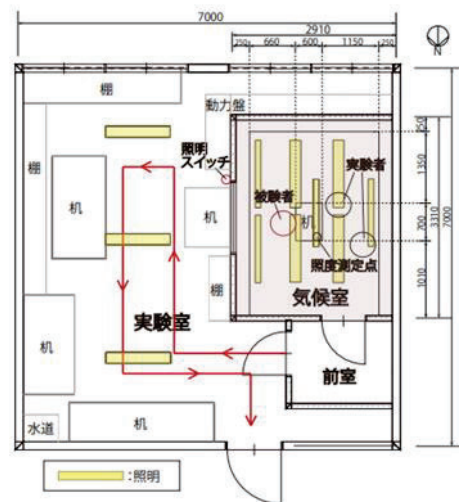


Figure 1. Plan of the experiment chamber and the experiment room

After the evaluation, participants stood up and walked out of the chamber to the experiment room and into the corridor. After walking in the corridor about four minutes, they returned to the experiment room and into the chamber. This procedure was repeated three times for each participant in the order of LIGHT, DARK, and LIGHT conditions. Pupil sizes were investigated in the chamber and experiment room.

### 3. RESULTS AND DISCUSSION

#### 3.1 Pupil diameter comparison between elderly and young participants under LIGHT and DARK conditions

Figure 2 shows the frequency distribution of pupil diameter. Mean and standard deviation of pupil diameter were  $54.3 \pm 8.3$  mm under the DARK condition and  $47.4 \pm 8.1$  mm under the LIGHT condition for elderly participants, and  $60.9 \pm 7.7$  mm under the DARK condition and  $53.8 \pm 7.47$  mm under the LIGHT condition for young participants. Pupils of young participants were larger than those of elderly participants both under LIGHT and DARK conditions. No significant difference was found between young and elderly participants for individual pupil sizes between the first LIGHT and DARK condition ( $p=0.0693$ ), but the difference between the DARK and second LIGHT conditions was greater for young participants than for elderly participants ( $p=0.0335$ ).

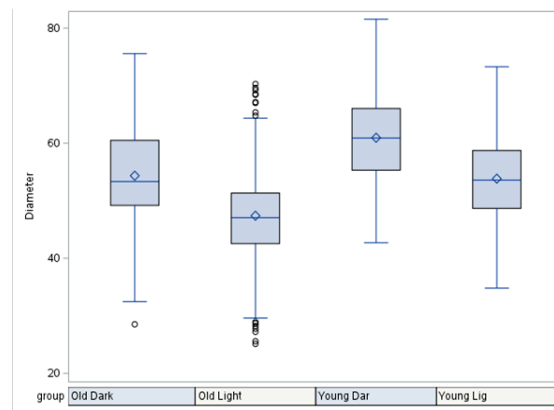


Figure 2. Distribution of pupil diameter under dark and light conditions for elderly and young participants

### 3.2 Frequency distribution of subjective light evaluation

Figure 3 shows frequency distribution of light evaluation of young participants under LIGHT condition, young participants under DARK condition, elderly participants under LIGHT condition and elderly participants under DARK condition. Table 1 compares subjective light evaluations between young and elderly participants under DARK and LIGHT conditions. Subjective light evaluations under DARK and LIGHT conditions are also compared between young and elderly participants.

Significant differences were found in light evaluation between young and elderly participants except in performance evaluation under DARK condition. Significant differences were found in light evaluation between young and elderly participants except in glare and performance evaluation under LIGHT condition. Significant differences were found in light evaluations between under DARK and LIGHT conditions for young participants except in preference evaluation. Significant differences were found in all light evaluations between DARK and LIGHT conditions for elderly participants.

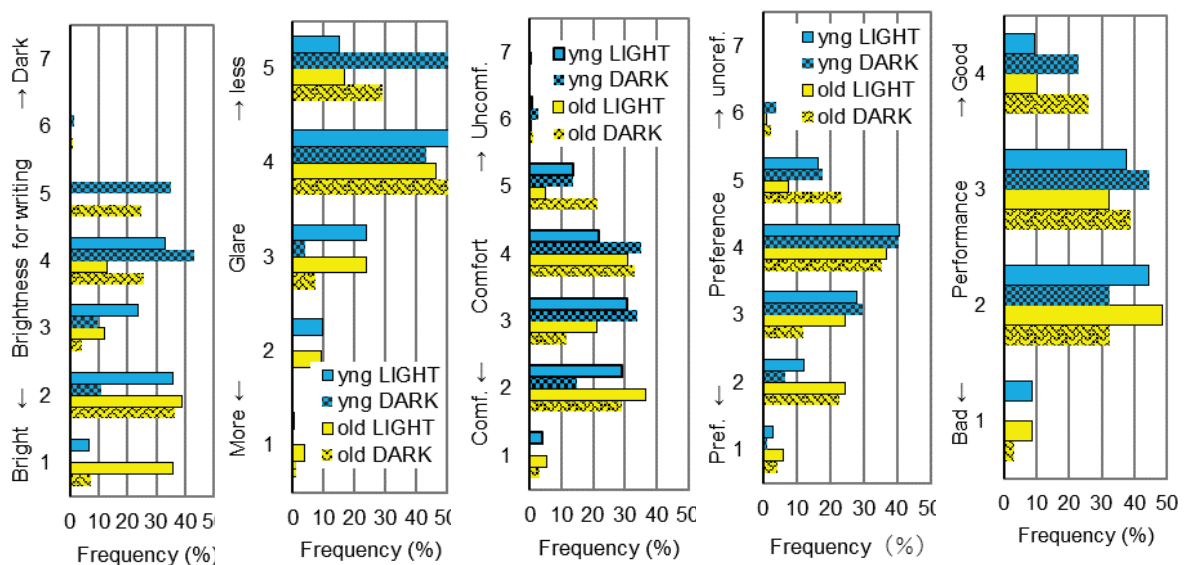


Figure 3. Frequency Distribution of subjective light evaluation

Table 1. P values of the uniformity test between young and old and between dark and light

	DARK	LIGHT	Young	Elderly
	Young vs Elderly	Young vs Elderly	DARK vs LIGHT	DARK vs LIGHT
Brightness	1%	1%	1%	1%
Brightness for writing	1%	1%	1%	1%
Glare	2%	N	1%	1%
Comfort	1%	2	5%	1%
Preference	1%	1%	N	1%
Performance	N	N	1%	1%

### 3.3 Personal attributes and pupil diameter

Table 2 shows the results of t-test of diameter difference by eyesight, grip and two step value under LIGHT condition. Two step value is an index of falling risk, which is the ratio of full stride length of two steps to the height. Pupils under the LIGHT condition were smaller for elderly participants with better eyesight than for elderly participants with worse eyesight ( $p=0.0087$ ). Diameter difference between elderly under and over 75 years old but no difference was found. No difference by personal attributes were found in pupil diameter under DARK condition.

Table 2. Diameter difference between personal attributes for elderly and young people in light condition

LIGHT COND.		elderly					young					
		n	dia.	difference	dia.	n	n	dia.	difference	dia.	n	
				p(%)					p(%)			
man		154	47.0	≐	47.7	180	157	54.5	≐	54	88	w oman
age	65-74	160	48.0	≐	46.9	174	-	-	-	-	-	75-
eyesight	w orse	162	48.5	<div>&gt; 0.87</div>	46.1	162	57	57.5	≐	56	64	better
grip	w eaker	168	48.5	<div>&gt; 0.9</div>	46.2	166	70	54.4	<div>&lt; 0.07</div>	59	68	stronger
2-step value	smaller	152	48.2	≐	46.7	174	68	56.1	≐	54	67	larger

### 3.4 Vision awareness and pupil diameter

Table 3 shows the relation of vision awareness and pupil diameter under LIGHT and DARK conditions. Pupils under LIGHT conditions were larger for elderly participants who had reported 'difficulty seeing in a dark environment' or 'easy to be tired in eyes' than those of elderly participants without these characteristics (respectively,  $p=0.0182$  and  $p=0.0086$ ). Pupils under DARK conditions were larger for elderly participants who 'prefer a uniformly lit environment' than for elderly participants without these characteristics ( $p=0.0395$ ).

There found no difference in pupil diameter by vision awareness for young participants in LIGHT condition. Pupils under DARK conditions were smaller for young participants who 'prefer a uniformly lit environment' than for elderly participants without these characteristics ( $p=0.0016$ ).

Table 3. Diameter difference between vision awareness for elderly and young people

LIGHT COND.		elderly					young				
		n	diam eter	difference p(%)	diam eter	n	n	diam eter	difference p(%)	diam eter	n
prefer to uniformly light environment	yes	124	48.1	$\div$	47.0	206	94	54.7	$\div$	54.2	97
hard to see in dark environment	yes	180	48.2	$>$ 1.82	46.1	146	82	54.6	$\div$	54.1	113
easy to be tired in eyes	yes	160	48.5	$>$ 0.86	46.2	170	126	54.7	$\div$	53.6	69

DARK COND.		elderly					young				
		n	diam eter	difference p(%)	diam eter	n	n	diam eter	difference p(%)	diam eter	n
prefer to uniformly light environment	yes	60	56.1	$>$ 3.95	53.3	106	43	59.6	$<$ 0.16	63.9	51
hard to see in dark environment	yes	92	54.7	$\div$	53.7	72	40	60.6	$\div$	62.9	56
easy to be tired in eyes	yes	80	55.0	$\div$	53.4	86	61	61.2	$\div$	63.2	35

### 3.5 Subjective light evaluation and pupil diameter

Figure 4 shows mean pupil diameter for each light evaluation category. Pupil size was found to be related to the evaluation of brightness, brightness for writing, glare, preference and performance for young participants, whereas it was found to be related only to the evaluation of brightness for writing and performance for elderly participants.

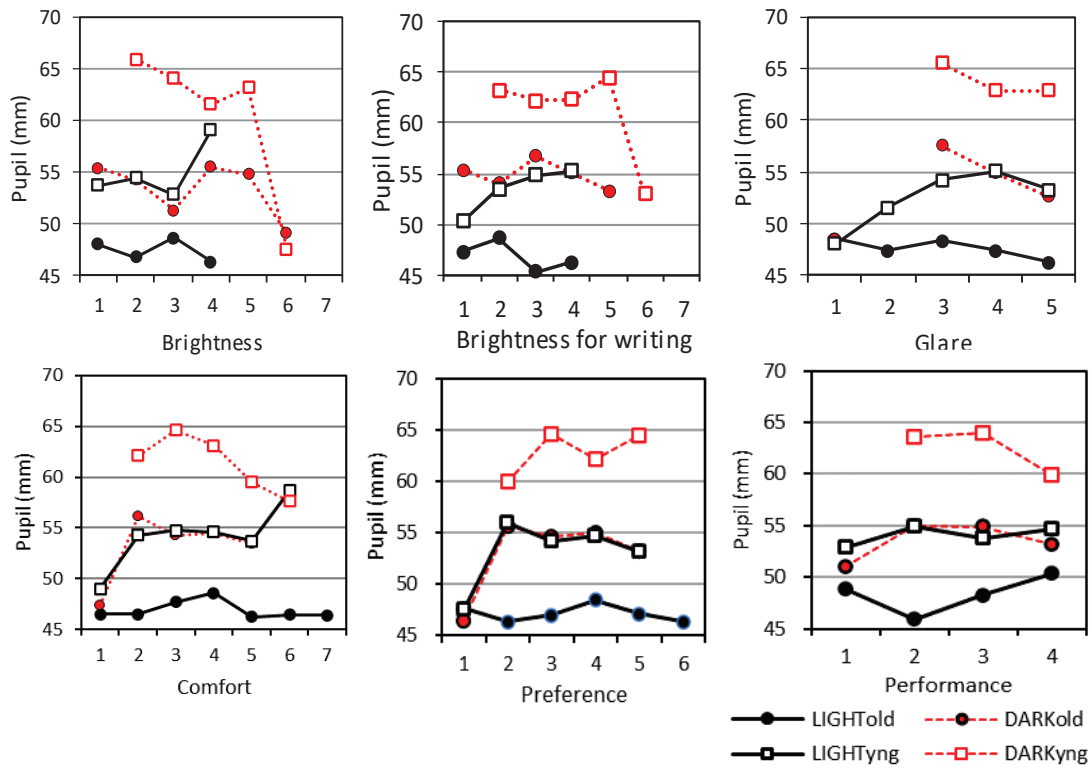


Figure 4. Mean pupil diameter for each light evaluation category



Table 4 shows the pupil diameter difference between Pupils were smaller for elderly participants who evaluated Dark condition as brighter and as more preferable than those of elderly participants who evaluated Dark conditions as darker and less preferable (respectively,  $p=0.0126$ ,  $p<0.0001$ ).

Table 4. Pupil diameter difference in light evaluation of DARK condition for elderly people of smaller pupil diameter

DARK COND.		elderly					
		n	diameter	difference p(%)	diameter	n	
brightness	brighter	12	36.4	$\approx$	39.5	10	darker
brightness for writing	brighter	10	35.6	$<$ 1.26	39.7	12	darker
glare	more sens.	10	38.7	$\approx$	37.1	12	less sens.
comfort	more comf.	12	36.5	$\approx$	39.4	10	less comf.
preference	more pref.	6	32.9	$<$ $<0.01$	39.7	16	less pref.
performance	higher	12	36.5	$\approx$	39.4	10	lower

#### 4. CONCLUSIONS

Larger difference in light evaluation between light and dark conditions were found in elderly participants than in young participants. No difference was found in glare evaluation between elderly and young participants under light condition. No difference was found in performance evaluation between young and elderly participants under both dark and light conditions. Pupils under light conditions were larger for elderly participants with difficulty seeing in a dark environment or fatigue ease in eyes. Pupils under dark conditions were larger for elderly participants who prefer a uniformly lighting. There found no difference in pupil diameter by vision awareness for young participants in light condition. Pupil size was found to be related only to the evaluation of brightness for writing and performance for elderly participants.

#### REFERENCE

- [1] Statistics Bureau, Ministry of Internal Affairs and Communications of Japan. National census, 2020. <https://www.stat.go.jp/data/kokusei/2020/kekka.html>.
- [2] N. Umamiya and W. Quiao. Difference of light environment evaluation between elderly and young people. Proceedings of the 29th Session of the CIE, 2019:745-750.
- [3] S. Ohno, Pupil and its Disorders, Practical Ophthalmology, 3(5), 2000:2-13.
- [4] I.E. Lowenfeld, Pupillary changes related to age. Topics in neuro-ophthalmology. S. Thomson ed, Williams and Wilkins, Baltimore, London, 1979:130.
- [5] C.H. Philip and R.M. Neer, Lighting for the elderly: A psychobiological approach to lighting. Human Factors, 23(1), 1981:65-85.

#### ACKNOWLEDGEMENT

This study was funded by a JSPS Grant-in-Aid for Scientific Research (C) 17K06676 and Foundation of Wellness Open Living Laboratory.

Corresponding Author: Noriko Umamiya  
Affiliation: School of Architecture, Osaka City University  
e-mail: [umamiyanor@omu.ac.jp](mailto:umamiyanor@omu.ac.jp)

# A COMPARATIVE STUDY OF THE LIVING ROOM LIGHTING PREFERENCES OF THE ELDERLY VS. THOSE OF THE YOUNG AND MIDDLE-AGED

Xinyi Hao, Lishu Hong, Bo Tang, Xin Zhang\*

School of Architecture, Tsinghua University, Beijing, China

## ABSTRACT

People's preferences for correlated color temperature (CCT) and illuminance have always been the focus in the field of lighting. Research advances in rhythmic lighting and light therapy point to the existence of varied CCT and illuminance needs at different times of the day for people of all ages in a residence. However, when Light Emitting Diode (LED) technology advances to the point where CCT and illuminance can be adjusted independently, people are more likely to adjust based on their own preferences rather than the preset parameters according to standards. This study aims to explore the preferences of elderly, young, and middle-aged people for CCT and illuminance in the context of independent adjustment in the living room.

In a Beijing living room, 45 elderly and 50 middle-aged and young adults were asked to independently adjust the lighting and choose their preference for two visual activities: watching TV and reading. The experimental results were analyzed using descriptive statistics, analysis of variance, and nonparametric tests. The study showed that participants' lighting preferences differed between the two behaviors. The association between CCT and illuminance preference was not confined to the Kruithof curve's range, but rather indicated a wider range. Age and gender had an effect on illuminance preference but no significant effect on CCT preference, and they showed distinct main effects and interactions in different behaviors. Participants' preferences of different ages and genders showed various degrees of dispersion. The results can provide a concrete basis for the development of residential lighting standards, suggestions for the use of adjustable intelligent lighting for the elderly, young, and middle-aged people, and valuable references for residential lighting control and luminaire design.

**Keywords:** Illuminance and CCT preferences; Residential lighting; Intelligent lighting control; Elderly; Young and middle-aged people

## 1. INTRODUCTION

People's preferences for color temperature and illuminance have always been the focus in the field of lighting. In 1941, Kruithof proposed the illuminance range of light sources suitable for specific color temperatures, that is, the viewpoint of "high illuminance and high color temperature and low illuminance and low color temperature" [1]. However, his study lacks details on experimental methods, procedures, and data analysis. Since then, scholars have explored the participants' preference for correlated color temperature (CCT) and illuminance by setting different combinations, using various methods such as task performance and subjective evaluation. Fotios used a meta-analysis of previous works and demonstrated the Kruithof curve was not always confirmed [2]. The participants' preferences varied depending on the experimental conditions, such as experimental environment, time, participants, and lighting parameters.

Established studies have shown that using people's preferred lighting conditions can have a healing effect by generating positive emotions and increasing satisfaction with the environment [3-5]. A low color temperature and illuminance lighting is more emotionally friendly, making people feel emotionally relaxed and warm [6], while a high color temperature makes participants feel awake and focused [7-8]. However, too high a color temperature can also increase visual and brain fatigue. These findings are from laboratory and office, not in residential environments.

Nowadays, LED technology can achieve separate adjustments for illuminance and color temperature and more diverse combinations under behavioral patterns [9-11]. People are more likely to adjust based on preferences rather than the preset parameters according to standards. Lighting in real-life residential environments tends to be more finely designed, distinguishing between general and task lighting. The differences in task and ambient lighting preferences of different ages in various behavioral patterns have yet to be refined and studied. It remains to be explored whether the user's preferences match the reasonable interval specified in the standards.

In China, the luminaire selection determined by the lighting design habits and factory parameters of the existing non-dimmable luminaires are not necessarily applicable to the new needs. While studies have shown that warm-tone lighting is more comfortable and more in line with residents' preferences overall, cool-tone lighting is actually used more often [12]. The residential behavioral lighting preferences of Chinese residents, as well as the direction of lighting design improvement and luminaire development to meet their preferences, are yet to be studied.

Current human factors research should take into account the visual and non-visual effects of light. There are differences in visual ability of the elderly, young and middle-aged people. The physiological changes in the eyes of the elderly lead to decreased light intake and yellowing, resulting in reduced vision and color discrimination [13]. This will lead to different judgments of the same environment by people of different ages, and it is of practical importance to reveal the differences in their preferences for a multigenerational shared space such as a living room. The human body achieves light synchronization of circadian rhythm through light perception, according to non-visual effects [14-16]. The use of living room lighting is mainly at night. Inappropriate lighting can disrupt the stability of the circadian rhythm and cause negative health effects, such as diabetes, obesity, depression, metabolic disorders, and sleep disorders [17-24]. The established studies on lighting preferences have limitations in setting experimental conditions, such as time and exposure history, so the experiment of this study were conducted at night.

In this study, 45 elderly and 50 young and middle-aged people were invited to participate in an experiment in a real-life living room located in Beijing. Participants independently performed adjustments of task illuminance, ambient illuminance, task color temperature, and ambient color temperature to select lighting preferences under different visual tasks. The lighting preferences chosen by participants of different ages and genders provide a specific basis for the development of residential lighting standards. The findings can also serve as a reference for the use of intelligent lighting controls for the elderly, the young, and the middle-aged to ensure that people use more reasonable residential lighting that is not entirely determined by preferences or pre-set options. The results can help guide the design of lighting control modes and provide a refined reference for future directions in interior lighting design improvement and luminaire development.

## 2. RESEARCH METHODS

### 2.1 Experimental environment

A real living room environment was selected for the experiment. Adjustable lighting variables in the living room included ambient lighting provided by two ceiling light strips with independently adjustable illuminance and color temperatures ranging from 2000–5000 K and 0–100 lx, and the task lighting was provided by table lamps with independently adjustable illuminance and color temperatures ranging from 2500–6500 K and 0–1500 lx. In the living room, the measurement points was set, including six for ambient lighting and two for the task lighting (horizontal measurement points of the work surface and vertical measurement points of the participant's eye).

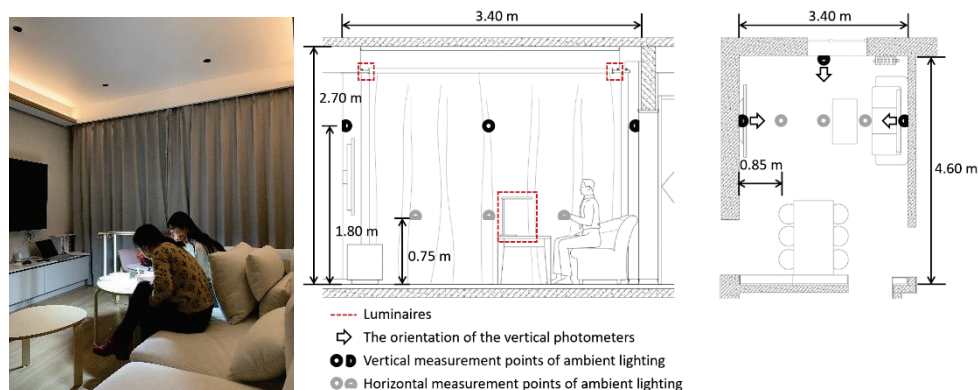


Figure 1. Experimental environment in the living room (photographed and drawn by the author)

### 2.2 Participants and visual tasks

Forty-five elderly people (62–77 years old) and 50 young and middle-aged people (20–58 years old) were invited to participate in this experiment, including a total of 32 men and 63 women. Each participant was required to complete two typical visual tasks in the living room: watching TV and

reading, using the same visual materials. The participant completed the lighting adjustments independently, and the ambient and task lighting selected by the participants were measured.

### 2.3 Experimental procedure

The experiment lasted for 16 days, and each day after dark, the participants entered the living room and were shown the lighting control methods of the smart lighting control app. Five minutes were set aside for familiarization, after which the ambient light was adjusted to the initial lighting (color temperature 2624 K, illuminance 46 lx), and the formal experiment was conducted. During the experiment, the room temperature (23°C), humidity (57%) were kept constant.

#### 2.3.1 Watching TV

The participant watched TV for 1 min in the initial lighting state. Then the participant adjusted the ambient lighting to a comfortable and preferred illuminance and color temperature and continued watching TV for 1 min. If the participant did not feel comfortable enough, he could continue to adjust. After the participant determined, the TV was turned off, and the experimenter measured the illuminance and color temperature of the ambient light and the participant's eyes.

#### 2.3.2 Reading

The experimenter adjusted the lamp so that the work surface met 500 lx, 4000 K. The participant was asked to read for 1 min, and only adjust the color temperature of the lamp and chose a preferred one. The experimenter checked the lamp to keep the illuminance unchanged. After the adjustment, the participant continued reading for 1 min. If the participant did not feel comfortable enough, he could continue to adjust. After the participant determined, the experimenter measured the ambient light. Then the participant was asked to take a break, during which the experimenter kept the lamp at the color temperature the participant had just chosen and adjusted the illuminance to the darkest state. Keeping the color temperature unchanged, the participant adjusted the illuminance of the lamp and chose a preferred one, and then continued reading for 1 min. If the participant did not feel comfortable enough, he could continue to adjust. After the participant determined, the experimenter measured the ambient light and the reading surface.

### 2.4 Data analysis

In this study, a between-subjects experimental design was used, and the independent variables included two between-subjects factors (age group and gender), and the dependent variables included the illuminance and color temperature chosen by the participants independently. The statistical methods mainly included descriptive statistical analysis and two-way ANOVA. If the normality or equal variance was not satisfactory, nonparametric tests were conducted.

## 3. RESULTS

### 3.1 Lighting preferences for watching TV

Descriptive statistics were analyzed for the lighting preferences with TV-watching, and a two-way ANOVA was used to analyze the effects of age group and gender on the choice of ambient lighting. Participants' overall preference tended to be the ambient lighting with a color temperature of approximately 2890 K and an illuminance of approximately 20 lx (Table 1).

Table 1. Descriptive statistics of ambient lighting preferences for watching TV

Age group	Gender	Ambient color temperature/K		Ambient illuminance/lx		N
		Mean	Std. Deviation	Mean	Std. Deviation	
Elderly	Male	2979.29	439.697	26.43	11.863	14
	Female	2845.55	515.271	21.71	13.484	31
	Total	2887.16	492.003	23.18	13.055	45
Young and middle-aged	Male	2899.72	538.676	12.39	6.344	18
	Female	2889.22	577.678	20.25	12.736	32
	Total	2893.00	558.410	17.42	11.450	50
Total	Male	2934.53	491.742	18.53	11.453	32
	Female	2867.73	543.884	20.97	13.024	63
	Total	2890.23	525.226	20.15	12.509	95

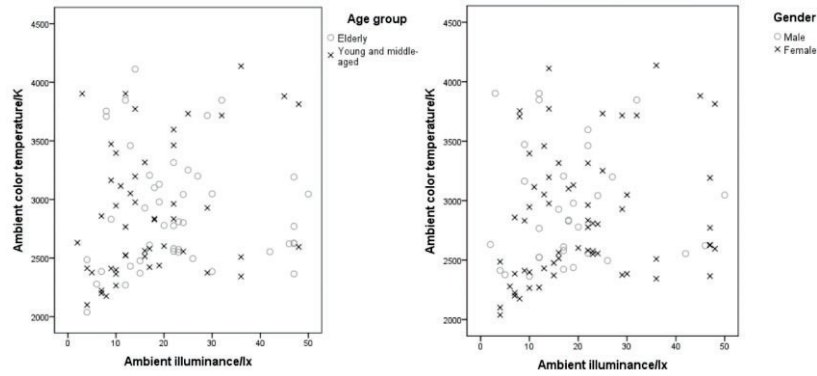


Figure 2. Scatter plots of ambient lighting preferences for watching TV

Analysis of the ambient light color temperature preference showed that there was no interaction between the age group and gender ( $F = 0.282$ ,  $P = 0.597$ ). The main effects analysis suggested that the effect of the age group was not statistically significant ( $F = 0.024$ ,  $P = 0.877$ ). The effect of gender was also not statistically significant ( $F = 0.386$ ,  $P = 0.536$ ).

The results showed that there was an interaction between age group and gender on the effect of the preference for ambient illuminance ( $F = 5.817$ ,  $P = 0.018$ ). Simple effects analysis suggested that among young and middle-aged people, illuminance preference differed by participants' gender, with men having a lower illuminance preference than women by 7.861 lx (95% CI: 0.867–14.855),  $P = 0.028$ . Among males, illumination preference differed by participants' age, with older people having a higher illuminance preference of 14.04 lx (95% CI: 5.581–22.499) than the young and the middle-aged,  $P = 0.001$ .

### 3.2 Lighting preferences for reading

Lighting preferences for reading behavior are jointly influenced by task lighting and ambient lighting. Participants' overall preference was for task lighting with a color temperature of approximately 3930 K and an illuminance of approximately 600 lx (Table 2).

Table 2. Descriptive statistics of task lighting preferences for reading

Age group	Gender	Work surface color temperature/K		Work surface illuminance/lx		N
		Mean	Std. Deviation	Mean	Std. Deviation	
Elderly	Male	3943.14	846.918	648.36	140.931	14
	Female	3976.35	949.600	644.61	125.361	31
	Total	3966.02	909.387	645.78	128.788	45
Young and middle-aged	Male	3814.22	748.949	596.00	222.761	18
	Female	3944.06	818.055	536.91	123.761	32
	Total	3897.32	788.638	558.18	166.515	50
Total	Male	3870.62	782.698	618.91	190.362	32
	Female	3959.95	878.179	589.90	134.940	63
	Total	3929.86	844.095	599.67	155.405	95

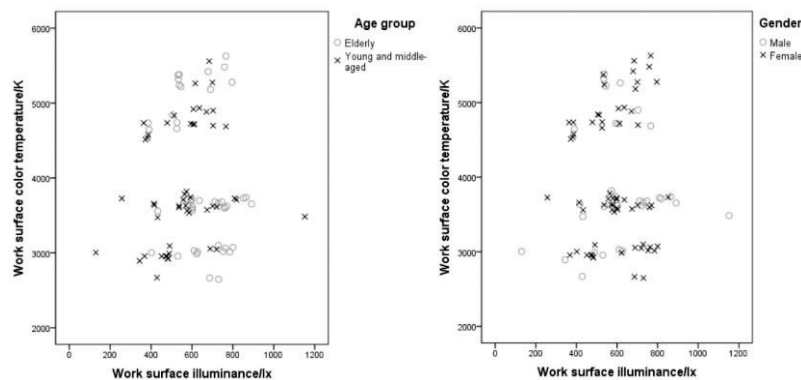


Figure 3. Scatter plots of task lighting preferences for reading



The scatter plots indicate that the participants' preferences for the work surface color temperature tend to be around the three values of 3000 K, 3700 K, and 5000 K, while no significant clustering is observed for the illuminance preference (Figure 3).

The results showed that there was no interaction between the age group and gender on the effect of the work surface color temperature preference ( $F = 0.067$ ,  $P = 0.796$ ). The main effects analysis suggested that the effect of the age group was not statistically significant ( $F = 0.186$ ,  $P = 0.667$ ). The influence of gender was also not statistically significant ( $F = 0.191$ ,  $P = 0.664$ ).

Analysis showed that there was no interaction between the age groups and gender on the effect of the work surface illuminance preference ( $F = 0.715$ ,  $P = 0.400$ ). The main effects analysis suggested that the effect of the age group on the work surface illuminance preference was statistically significant. The work surface illuminance preferences of the elderly were 80.032 lx (95% CI: 15.001–145.063) higher than those of the young and the middle-aged ( $F = 5.976$ ,  $P = 0.016$ ). The effect of gender was not statistically significant ( $F = 0.921$ ,  $P = 0.340$ ).

While reading, the participants' overall preference for ambient lighting was with a color temperature of approximately 2908 K and an illuminance of approximately 44 lx (Table 3).

Table 3. Descriptive statistics of ambient lighting preferences for reading

Age group	Gender	Ambient color temperature/K		Ambient illuminance/lx		N
		Mean	Std. Deviation	Mean	Std. Deviation	
Elderly	Male	2668.36	95.068	42.07	11.479	14
	Female	2918.52	470.364	47.42	6.480	31
	Total	2840.69	408.943	45.76	8.592	45
Young and middle-aged	Male	2885.83	505.348	40.00	12.570	18
	Female	3014.37	654.156	42.37	8.867	32
	Total	2968.10	602.668	41.52	10.290	50
Total	Male	2790.69	394.778	40.91	11.958	32
	Female	2967.21	568.635	44.86	8.130	63
	Total	2907.75	521.251	43.53	9.709	95

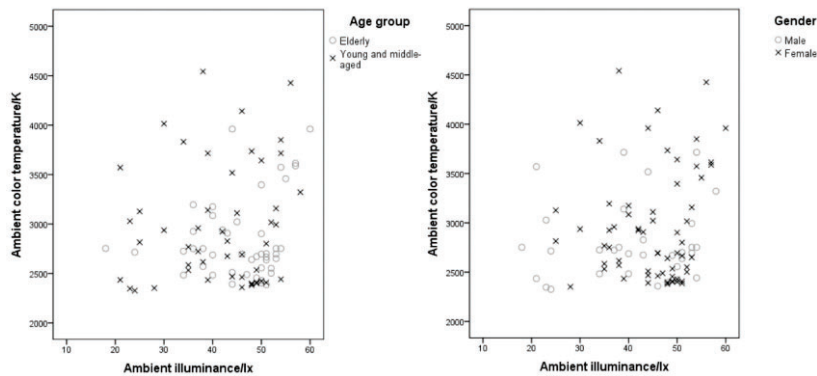


Figure 4. Scatter plots of ambient lighting preferences for reading

The results of the analysis of ambient color temperature preference showed that there was no interaction between the age group and gender on the effect of ambient color temperature preference ( $F = 0.290$ ,  $P = 0.592$ ). And there was no interaction between the age group and gender on the effect of ambient illuminance preference ( $F = 0.522$ ,  $P = 0.472$ ).

Due to uneven variance, the non-parametric test showed a significant difference in the effect of the age group on the ambient illuminance preference,  $P=0.039$ , with  $45.76 \text{ lx} \pm 8.592$  for the elderly and  $41.52 \text{ lx} \pm 10.290$  for the young and the middle-aged, with the elderly preferring higher illuminance. There was no significant difference in the effect of age and gender ( $P > 0.05$ ).

### 3.3 Comparative analysis

For watching TV, participants preferred ambient lighting with a low-to-medium color temperature of approximately 2890 K and a low illuminance of approximately 20 lx. For reading, participants preferred the task lighting of about 3930 K, 600 lx, and ambient lighting of about 2908 K, 44 lx.

The box plots indicate that participants' lighting preferences of different age and gender show various degrees of dispersion and preference under different behaviors. Elderly males had the lowest dispersion of ambient light color temperature preferences. Young and middle-aged males had the lowest dispersion of ambient illuminance preference for TV watching, while elderly females had the lowest dispersion of ambient illuminance preference for reading.

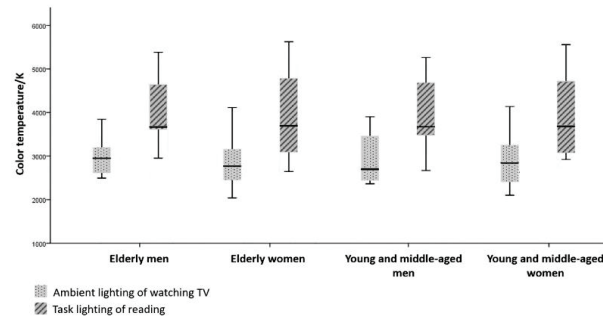


Figure 5. Box plots of the color temperature preferences under different behaviors

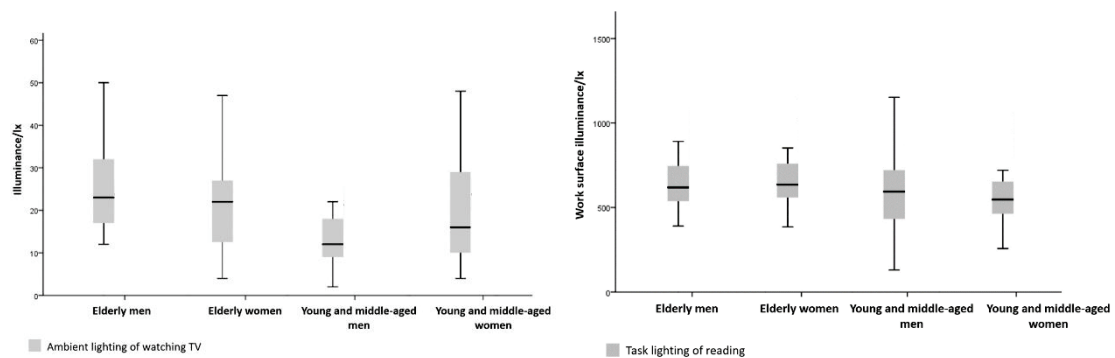


Figure 6. Box plots of the illuminance preferences of watching TV and reading

#### 4. DISCUSSION AND CONCLUSION

This study used a real residential environment and conducted the experiment at night. Compared with simulations in the laboratory, the results were closer to the real situation of human rhythm and cognition. The results showed that the age group and gender did not always have a significant effect on the choice of color temperature and illuminance. The relationship between the color temperature preference and illuminance preference was not limited to the Kruithof curve, but reflects a wider distribution of choices. There was no significant difference in the preference for the color temperature among the participants of different age groups and genders. However, there was an interaction between the age group and gender on the preference of ambient illuminance under the TV watching behavior. There were significant differences in the preferences of different age groups for the ambient and task illuminance under reading.

Table 4. Comparison of the residential indoor lighting design standards and experimental results

Living room lighting	Experimental results of this study		Architectural Lighting Design Standard GB50034-2022, China [25]		ANSI/IES RP-28-16, USA [26]	ANSI IESNA RP-11-17, USA [27]		Lighting Manual 2003, Japan [28]	JISZ 9110-2010, Japan [29]
	Elderly	Young and middle-aged	Elderly	Young and middle-aged	Elderly	Elderly	Young and middle-aged	Elderly	Young and middle-aged
General lighting	46 lx 2841 K	42 lx 2968 K	200 lx < 3300 K	100 lx < 3300 K	200 lx 2700–3000 K	60 lx -	30 lx -	50–150 lx -	50 lx -
Writing and reading	646 lx 3966 K	558 lx 3897 K	500 lx 3300–5300 K	300 lx 3300–5300 K	750 lx 2700–3000 K	800 lx -	400 lx -	600–1500 lx -	500 lx -

According to the residential lighting standards, for young and middle-aged people, the standards are close to the preferences, and adjustable task lighting is recommended to refer to the preferences, with a higher range of illuminance and diverse color temperature options. The elderly prefer warm color temperature lighting, but due to their sensitivity to color temperature changes declining, the adjustment can have a certain degree of flexibility [13]. For the elderly, the preference for general lighting is much lower than the standard value. In order to ensure the safety, it is not recommended that the ambient lighting is adjusted according to preference. Changes in the visual system can be compensated for by appropriately increasing the illuminance or increasing the brightness ratio between the target and the background [30].

According to the rhythmic demands, high illuminance and color temperature lighting should be provided during the day and lower illuminance and color temperature lighting at night [31-32]. This study focused on nighttime lighting, the eye exposure for watching TV met the rhythmic demands. The eye exposure of reading is higher, and the elderly have a higher preference than the young and middle-aged, which does not meet the rhythmic needs. It is recommended that the elderly not do such tasks before bedtime. Combining the residential lighting standards with the results of this paper can help elderly, young, and middle-aged people control living room lighting in a comfortable and healthy way. It provides a valuable reference for the improvement of behavioral lighting, luminaire products, and adjustable intelligent lighting control design in residential houses.

This study used a method in which the participants adjusted the lighting independently, and the adjustment range was limited by the luminaire parameters. Although it has been noted that self-adjustment causes participants' preferences to be close to the middle of the adjustment range [33], in this experiment, the results of preferences for task lighting and ambient color temperature were not affected by range bias. Also, for the same adjustment range, participants' preferences differed significantly by visual tasks. This may be due to the fact that participants were given sufficient time to adapt and adjust, and that participants' adjustments to the lighting parameters were continuously variable rather than graded. The evaluation methods (such as interviews and physiological data monitoring) can be used to refine the assessment of the lighting preferences.

## REFERENCES

- [1] Kruithof, A. A. Tubular luminescence lamps for general illumination. *Philips Technical Review*, 1941, 6, 65-96.
- [2] Fotios, S. A revised Kruithof graph based on empirical data. *Leukos*, 2017, 13, 1, 3-17.
- [3] Newsham, G. R., Veitch, J. A. Lighting quality recommendations for VDT offices: A new method of derivation. *Lighting Research & Technology*, 2001, 33, 97-113.
- [4] Newsham, G. R., Veitch, J., Arsenault, C., et al. Effect of dimming control on office worker satisfaction and performance. *Proceedings of the IESNA annual conference*. New York, NY, USA: IESNA, 2004, 19-41.
- [5] Veitch, J. A., Newsham, G. R., Boyce, P. R., et al. Lighting appraisal, well-being and performance in open-plan offices: A linked mechanisms approach. *Lighting Research & Technology*, 2008, 40, 2, 133-151.
- [6] Hao, L., Cao, Y., Cui, Z., et al. Research Trends and Application Prospects on Light and Health. *China Illuminating Engineering Journal*, 2017.
- [7] Shimomura, Y., Iwanaga, K., Harada, H., et al. I-3 Effects of the Color Temperature of Illumination on Arousal Level in Working. *Journal of Physiological Anthropology & Applied Human Science*, 2001, 20.
- [8] Kim, I. T., Choi, A. S., Sung, M. K. Development of a Colour Quality Assessment Tool for indoor luminous environments affecting the circadian rhythm of occupants. *Building and Environment*, 2017, 126, 252-265.
- [9] Osorio, R., Alonso, J. M., Vázquez, N., et al. Fuzzy logic control with an improved algorithm for integrated LED drivers. *IEEE Transactions on Industrial Electronics*, 2018, 65, 9, 6994-7003.
- [10] Malik, R., Ray, K. K., Mazumdar, S. Wide-range, open-loop, CCT and illuminance control of an LED lamp using two-component color blending. *IEEE Transactions on Power Electronics*, 2017, 33, 11, 9803-9818.
- [11] Chi, S. W., Loo, K. H., Lu, H. C., et al. Independent control of multicolour-multistring LED lighting systems with fully switched-capacitor-controlled LCC resonant network. *IEEE Transactions on Power Electronics*, 2017, 15, 2, 115.
- [12] Sun, M. M., He, X. Y., Zou, N. Y., et al. The contrast and analysis on the residential lighting in China and Japan. *China Illuminating Engineering Journal*, 2012, 23, 06, 24-29.

- [13] Cui, Z., Chen, Y. D., Hao, L.X. Research trends on elderly healthy lighting in human habitat based on their optic characteristics. *China Illuminating Engineering Journal*, 2016, 27, 05, 21-26+86.
- [14] Brainard, G. C., Hanifin, J. P., Greeson, J. M., et al. Action spectrum for melatonin regulation in humans: evidence for a novel circadian photoreceptor. *Journal of Neuroscience*, 2001, 21,16, 6405-6412.
- [15] Rea, M. S., Figueiro, M. G., Bierman, A., et al. Modelling the spectral sensitivity of the human circadian system. *Lighting Research & Technology*, 2012, 44, 4, 386-396.
- [16] Hattar, S., Liao, H. W., Takao, M. Melanopsin-containing retinal ganglion cells: architecture, projections, and intrinsic photosensitivity. *Science*, 2002, 295, 5557, 1065-1070.
- [17] Cho, Y. M., Ryu, S. H., Lee, B. R., et al. Effects of artificial light at night on human health: A literature review of observational and experimental studies applied to exposure assessment. *Chronobiology international*, 2015, 32, 9, 1294-1310.
- [18] Grosbellet, E., Challet, E. *Circadian Rhythms and Metabolism*. Springer International Publishing, 2016.
- [19] Plano, S. A., Casiraghi, L. P., Paula, G. M., et al. Circadian and Metabolic Effects of Light: Implications in Weight Homeostasis and Health. *Frontiers in Neurology*, 2017, 8, 558.
- [20] Fonken, L. K., Nelson, R. J. The effects of light at night on circadian clocks and metabolism. *Endocrine reviews*, 2014, 35, 4, 648-670.
- [21] Boyce, P., Barriball, E. Circadian rhythms and depression. *Australian Family Physician*, 2010, 39, 5, 307-10.
- [22] Germain, A., Kupfer, D. J. Circadian rhythm disturbances in depression. *Human Psychopharmacology: Clinical and Experimental*, 2008, 23, 7, 571-585.
- [23] Hurley, S., Goldberg, D., Nelson, D., et al. Light at night and breast cancer risk among California teachers. *Epidemiology (Cambridge, Mass.)*, 2014, 25, 5, 697.
- [24] Li, Q., Zheng, T., Holford, T. R., et al. Light at night and breast cancer risk: results from a population-based case-control study in Connecticut, USA. *Cancer Causes & Control*, 2010, 21, 12, 2281-2285.
- [25] Ministry of Housing and Urban-rural Development of the People's Republic of China. Standard for Lighting Design of Buildings. GB50034-2022. Ministry of Housing and Urban-rural Development of the People's Republic of China, 2022.
- [26] Illuminating Engineering Society of North America. Recommended Practice for Lighting and the Visual Environment for Senior Living. ANSI, IES RP-28-16. IESNA, 2016.
- [27] Illuminating Engineering Society of North America. Recommended Practice for Lighting for Interior and Exterior Residential Environments. ANSI, IES RP-11-17. IESNA, 2017.
- [28] Illuminating Engineering Institute of Japan. Japan Lighting Handbook. IEIJ, 2003.
- [29] Illuminating Engineering Institute of Japan. General Rules of Recommended Lighting Levels. JIS Z 9110-2010. IEIJ/JSA, 2010.
- [30] Hengstberger, F., Pollard, N., Sagawa, K., et al. CIE guide to increasing accessibility in light and lighting. CIE, 2011.
- [31] Zhou, J. N., Liu, R. Y., Kamphorst W, et al. Early neuropathological Alzheimer's changes in aged individuals are accompanied by decreased cerebrospinal fluid melatonin levels. *Journal of pineal research*, 2003, 35, 2, 125-130.
- [32] Wulff, K., Gatti, S., Wettstein, J. G., et al. Sleep and circadian rhythm disruption in psychiatric and neurodegenerative disease. *Nature Reviews Neuroscience*, 2010, 11, 8, 589-599.
- [33] Fotios, S. A., Cheal, C. Stimulus range bias explains the outcome of preferred-illuminance adjustments. *Lighting Research & Technology*, 2010, 42, 4, 433-447.

## ACKNOWLEDGEMENTS

The Research Centre for Sustainable Community School of Architecture Tsinghua University is appreciated for its support. Bentian Niu is thanked for their support in the experiment. This work was supported by a grant from the Tsinghua University Initiative Scientific Research Program (grant number 20211080095) and the National Natural Science Foundation of China (grant number 52078266).

Corresponding Author Name: Xin Zhang

Affiliation: School of Architecture, Tsinghua University, Beijing, China

e-mail: zhx@mail.tsinghua.edu.cn

# COMPARATIVE ANALYSIS OF ILLUMINANCE DISTRIBUTION IN INDOOR ENVIRONMENTS USING ILLUMINANCE SENSORS AND SIMULATION MODELS

Jiyoung Seo, Anseop Choi\*

Department of Architectural Engineering, Sejong University  
Seoul, Korea

## ABSTRACT

The development of multiple IoT sensors has facilitated data acquisition in smart buildings or offices, allowing various types of sensors to be attached to a single IoT sensor. However, accurately measuring illuminance on the work plane with multiple IoT sensors attached to walls or ceilings poses challenges. This study addresses this issue by installing photo sensors at various locations in a room and comparing them with simulation values. The photo sensors include tri-directional sensors, bi-directional sensors, and wall sensors, along with built-in photo sensors in three lighting fixtures. The study compares the illuminance values measured by the photo sensors at different locations in the room with the illuminance values on the work plane and infers values that would be measured in different conditions and locations through simulation. The results demonstrate a strong agreement between the measured illuminance values and the simulated values, validating the effectiveness of the proposed method. The findings contribute to the development of more accurate and efficient lighting control systems in indoor environments.

Keywords: photo sensor, illuminance, indoor environments

## 1. INTRODUCTION

With the advancement of IoT (Internet of Things) sensors, there has been an increasing trend in the application of multiple IoT sensors in buildings to collect various real-time information. These sensors enable the collection, transmission, and analysis of large volumes of data through internet and cloud platforms. By installing a single sensor, it becomes possible to gather diverse information such as light intensity, indoor air quality, occupancy detection, and fire detection. Furthermore, the utilization of this collected data allows for the control of building environments, reduction of energy consumption, and provision of suitable conditions for occupants.

However, the installation of IoT sensors primarily occurs on ceilings or walls in locations that minimize inconvenience to occupants, resulting in variations in measured values (1). In particular, when IoT sensors are installed on ceilings or walls, the values of the built-in photo sensor differ depending on the location, direction, and angle of measurement, deviating from the illuminance values measured at the working plane. This poses challenges in maintaining the desired illuminance level on the working plane, especially for tasks such as lighting dimming and control, as well as shading device control.

To address these challenges, this study placed photo sensors in various locations and analyzed the relationship between the measured data and simulated data to understand their correlation with the illuminance at the working plane. The deployed photo sensors were classified as three-directional sensors, two-directional sensors, wall sensors, working plane illuminance sensors, and built-in light photo sensors within lighting fixtures.

## 2. FURTHER CLAUSE

### 2.1 Mock up



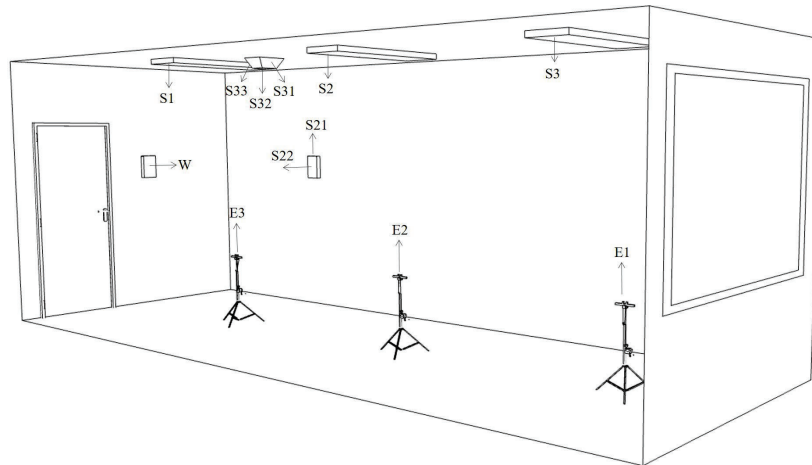


Figure 1. Sensor position

The installed sensors and their respective placements are illustrated in [Figure 1]. The illuminance measurement was conducted using the KONICA MINOLTA T-10A series meter at three specific points on the working plane: near the window (E1), at the center (E2), and near the entrance (E3). The three-directional sensors were capable of measuring illuminance from three different directions, with their values designated as near the window (S31), at the center (S32), and near the entrance (S33). The wall-mounted sensors were represented by the symbol "W" for their corresponding illuminance values. As for the photo sensors integrated within the lighting fixtures, they were denoted as near the window (S1), at the center (S2), and near the entrance (S3). Roller blinds were installed as the shading devices in the experimental setup.

## 2.2 Simulation

DIALux evo (2), a lighting simulation program known for its capabilities in indoor and outdoor lighting planning, calculations, and visualization, was employed in this study to compare and analyze the measured photo sensor values with simulation data. DIALux evo offers four distinct categories for sky conditions, namely no daylight, clear sky, average sky, and overcast. To align with the data obtained from meteorological agencies, which is based on cloud cover, the following classifications were used: clear (1) for clear sky, partly cloudy (2) for average sky, mostly cloudy (3), and overcast (4) for overcast sky conditions. The simulation was conducted with direct sunlight taken into account.

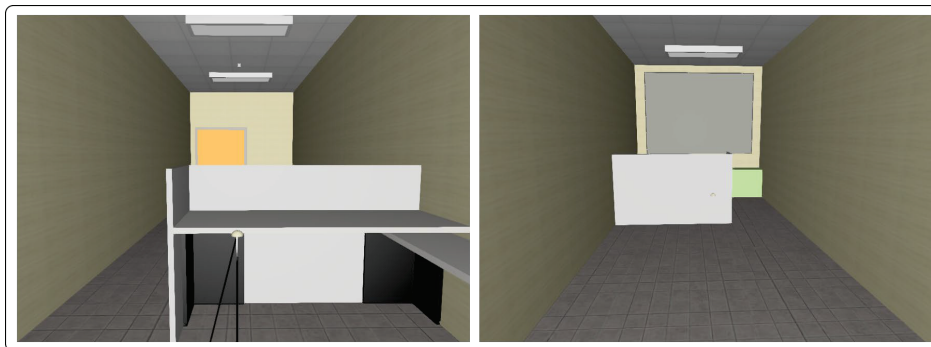


Figure 2. Simulation modeling

Figure 2 represents the DIALux evo simulation model. The modeling was conducted at the same location (127.07, 37.55) and direction (238° southwest) as the office, with the dimensions of the room being  $7.9 \times 2.8 \times 3.1$  cubic meters and the elevation set at 40 meters. The study compared and analyzed data for one clear day, two partly cloudy days, and one overcast day from February 14th to February 19th. The simulation was conducted from 8:00 AM to 6:00 PM, and the same time frame was used for the experimental measurements in the actual room.

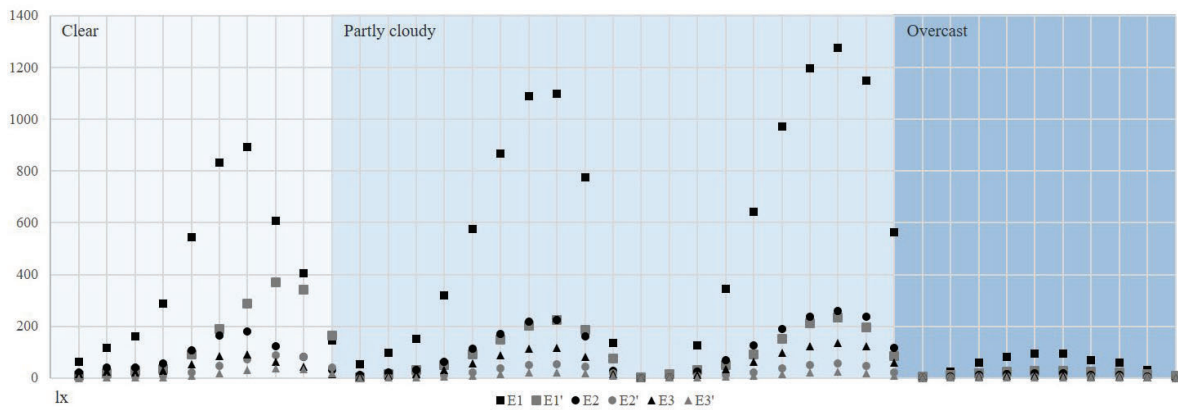


Figure 3. Illuminance by sky condition

Figure 3 depicts the comparison between the measured and simulated data for sky conditions at E1, E2, and E3. The values for E1, E2, and E3 at 8:00 AM represent the average of E1 values from 8:00 AM to 9:00 AM, and the measurements were taken at 1-minute intervals. The maximum average value of the working plane illuminance from the measurements is observed when the sky condition is "partly cloudy," and similar patterns can be seen on February 15th and February 19th. Additionally, it is evident that the average maximum value of the working plane illuminance is lower (94.83 lx) during "overcast" sky conditions. Overall, there is a notable similarity between the simulation and measured values.

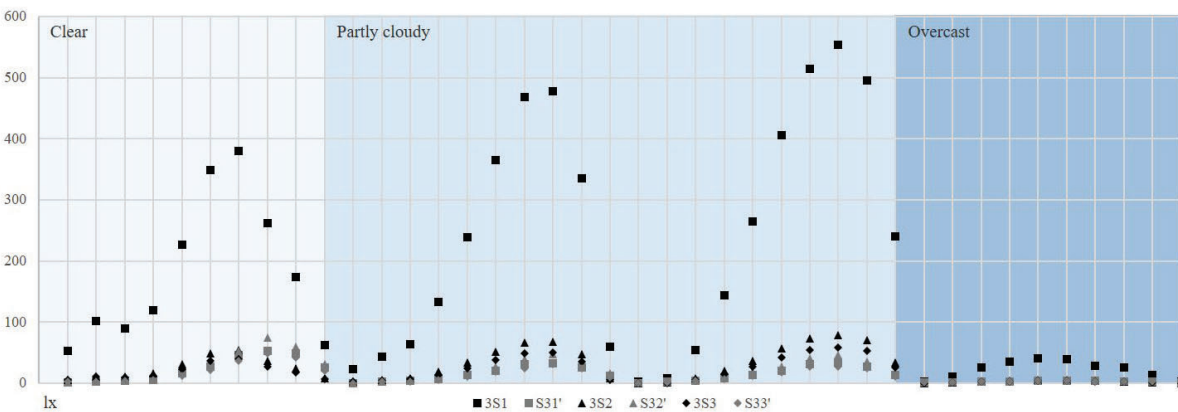


Figure 4. Three-way sensor by sky condition

Figure 4 presents the comparison between the measured and simulated values for the three-way sensor. Similar to E1, E2, and E3, the measured values show the highest illuminance when the sky condition is "partly cloudy." It is evident that the patterns of the measured values and simulated values exhibit a similarity.

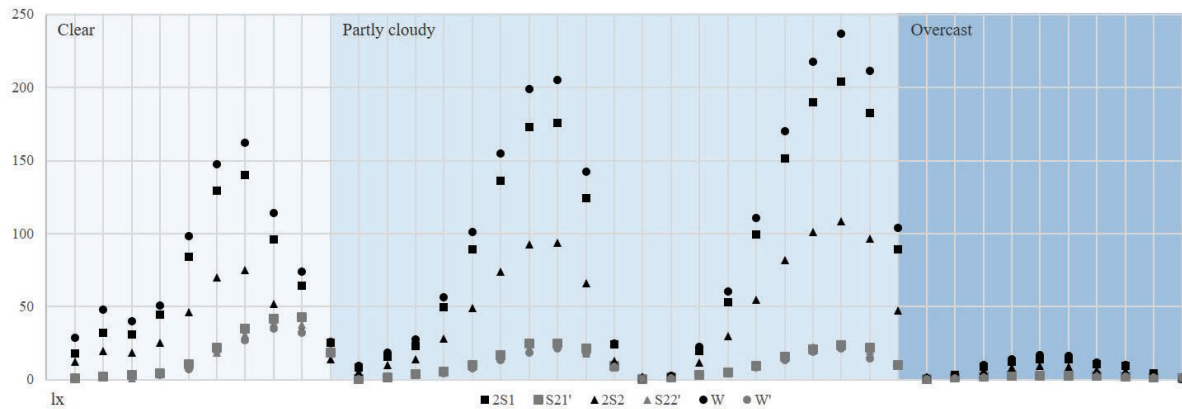


Figure 5. Two-way sensor and wall sensor by sky condition

Figure 5 represents the comparison between the measured and simulated values for the two-way sensor and wall sensor. By examining Figures 3, 4, and 5, it is evident that the simulated values closely resemble the measured values. This indicates that simulation can be a valuable tool for predicting the working plane illuminance based on the values obtained from IoT sensors installed at various locations within the space. Collecting data in diverse environments and comparing them with simulations can provide further insights for accurately estimating the working plane illuminance.

### 3. CONCLUSION

This study aimed to investigate the correlation between illuminance values obtained from IoT sensors installed at various locations and angles and the working plane illuminance. To achieve this, IoT sensors were installed at different positions, including three-directional sensors, two-directional sensors, and wall sensors. The simulation was also conducted by placing photo sensors in the same positions as the installations. The results demonstrated a similar pattern between the measured data and simulation data for different sky conditions. It suggests that simulation can be utilized to estimate the working plane illuminance based on IoT sensor values. Further comparisons and analyses using a wider range of locations and dates could enhance the ability to predict the working plane illuminance through simulation.

### REFERENCES

- (1) Vladimir Tanasiev, George Cristian Pătru, Daniel Rosner, Gabriela Sava, Horia Necula, Adrian Badea,, Enhancing environmental and energy monitoring of residential buildings through IoT, Automation in Construction, 126(2021), 103662
- (2) DIALux evo, accessed July 05, 2023, <https://www.dialux.com/en-GB/dialux>

### ACKNOWLEDGEMENTS

This work was supported by the Korea Institute of Energy Technology Evaluation and Planning (KETEP) grant funded by the Korean government (MOTIE) (No. 20212020800120).

Corresponding Author Name: Anseop Choi

Affiliation: Department of Architectural Engineering, Sejong University

E-mail: aschoi@sejong.ac.kr

# CIRCADIAN LIGHT THERAPY FOR DEPRESSED YOUTH: A SYSTEMATIC REVIEW AND META-ANALYSIS

Ranpeng Chen

(School of Architecture and Urban planning, Chongqing University, Chongqing, China)

## ABSTRACT

The efficacy for youth depression targeted light therapy was explored. Articles through Web of Science, Cochrane Library, Medline, PubMed, CINAHL, APA PsycInfo, Embase were retrieved. Meta-regression and subgroup meta-analysis were performed for light therapy efficacy. Up to 2100 accumulative minutes of exposure has proved efficacious for youth groups (SMD=-1.39, 95%CI=-1.65 to -1.13,  $I^2=91.5\%$ ). There was significant greater effect size in 1000-1500mins subgroups, indicating threshold for practical guidance. The results may support depression treatment and LT device application in the post-pandemic era.

Keywords: light therapy, youth, circadian light, meta-analysis

## 1. INTRODUCTION

High circadian light therapy has proved efficacious for adults [1], but the antidepressant effect of circadian light therapy for depressed youth remains less known. Circadian light therapy mainly bases on circadian phototransduction mechanism, which help circadian rhythm adjustment for SAD, NAD, BD (bipolar disorder), MDD and even ADHD, Parkinson, Alzheimer disease, DSPS related circadian rhythm disturbances, depression and sleeping problems. Human circadian phototransduction that tightly related to non-visual effects of light mostly bases on photoreceptor like intrinsically photosensitive retinal ganglion cells (ipRGCs) that send light information to the biological clock in the hypothalamic suprachiasmatic nucleus (SCN), who then synchronize biological rhythms and project signals to ventrolateral preoptic (VLPO) nucleus, dorsal raphe-, as well as pineal body, etc. Meanwhile, as the ipRGCs photoreceptor and correspond photopigment melanopsin more sensitive to “blue” wavelength at around 480nm [2], light therapy devices have mainly adopted blue-enriched light sources. The study aims at verifying efficacy and vital parameters of circadian light therapy for youth group.

## 2. METHOD

### 2.1 Literature research

This systematic review was registered with PROSPERO under code number CRD42022375211 and was conducted following Preferred Reporting Items for Systematic Reviews and Meta-Analysis (PRISMA) guidelines [3]. Articles were searched through Web of Science, PubMed, Embase, ProQuest, CINAHL, Cochrane Library, Medline, APA PsycInfo databases, as well as websites of National Library of Medicine, ClinicalTrials.gov and Scholars. Advanced searches with MeSH (medical subject heading) terms were included when available. Full text was required.

### 2.2 Inclusion criteria

Studies met the following criteria were included: (A) The subjects are youth/young adults, (B) Must have bright light therapy as primary independent intervention, (C) Details of BLT included (e.g specific device model, light sources, illumination, CCT); (D) Outcomes reported in standardized depression scales, e.g. HAM-D, HIGH-SAD, BDI-II, MADRS, CES-D or other scales with similar structures as reliable, quantified results.

Studies met the following criteria were excluded: (1) Older aged groups; (2) LLLT (low level laser therapy) treatment studies; (3) Mere abstracts, cases reports, case series, or literature reviews excluded.

### 2.3 Data extraction

Among the 599 articles after excluding duplication, the research team reviewed the titles and abstracts of all downloaded literature for initial screening. The research team reviewed the titles

and abstracts of all downloaded literature for initial screening. The articles were further filtered based on the relevancy of their contents. After thorough screening for relevancy and suitability through a full-text review, two dependent reviewers extracted required information such as subjects' information, experimental design, BLT device details, sample size of experiment group and quantitative outcomes of measurement scales before and after intervention.

### 3. RESULTS

#### 3.1 Study characteristics

The selected articles were mainly small-sample clinical trials, among which most were RCTs. The subjects were mainly SAD or non-seasonal depressed patients. Depressed youth with anorexia nervosa, cystic fibrosis, mild traumatic brain injury, cancer-related fatigue (CRF), Tourette's disorder, bulimia nervosa, borderline personality disorder (BPD) as well as healthy individuals were all involved for validation. In a few studies, BLT intervention were accompanied by antidepressant drugs or other treatments, but it can be guaranteed that BLT was the only variable. In terms of intervention time, 1 study carried out both morning and night BLT, 2 studies carried out BLT at early evening and 2 experimented in late night, and the rest BLT were all morning intervention.

#### 3.2 Risk-of-bias assessment

For randomized controlled trials (RCT), the quality of evidence was evaluated with revised Cochrane Risk of Bias Tool [4]. Those adopted randomizer-box and computer software were regarded at low risk for selection bias. For quasi-experiment/non-randomized controlled studies, the quality of evidence was evaluated with Joanna Briggs Institute (JBI) Critical Appraisal Checklist for Quasi-Experimental studies. On the whole, the quality of evidence met the criteria and were included in meta-analysis.

#### 3.3 Clinical efficacy of Circadian lighting

The overall heterogeneity of the included studies was too high ( $I^2=91.5\%$ ) so the combined effects showing efficacy ( $SMD=-1.39$ ,  $95\%CI=-1.65$  to  $-1.13$ ) required validation. Most studies indicated at least small to huge change of effect size, indicating that when exerting circadian light exposure, up to 2100 minutes of accumulative time has proved efficacious. Besides, the correlation between therapeutic effect size and accumulative exposure time had indicated 1000-1500mins of accumulative exposure time as threshold.

#### 3.4 Publication Bias

We found there existed publication bias and small study effects by Egger's linear regression method within included studies (intercept=  $-4.30$ ,  $95\% CI=-6.462$  to  $-2.138$ ,  $t=-3.96$ ,  $p=0.000 < 0.05$ ). However, as the study aims for efficacy validation, as much data included as better.

### 4. CONCLUSION

To our knowledge, the study may not be the first systematic review of BLT on youth, but is the first meta-analysis of circadian lighting therapy and correspond lighting dose carried out for young people. Despite high value of  $I^2$  ( $I^2=91.5\%$ ) indicating degree of heterogeneity, it can be conservatively concluded that up to 2100 minutes of accumulative time (roughly within 8 weeks) has proved efficacious. The therapeutic effect has shown positive relationship with increasing light dose and 1000-1500mins of accumulative exposure time may lead to saturation. The conclusion has overlapped with and expanded previous conclusions suggesting 2-5 weeks of therapy [5]. On the other hand, circadian lighting with probable similar therapeutic mechanism for broader range of depression pathologic features may enlighten further clinical trials.

### REFERENCE

- [1] Zhou L, Hou D, Wang Y, Zhou S, Lin Y. High circadian stimulus lighting therapy for depression: Meta-analysis of clinical trials. *Frontiers in Neuroscience*. 2022;16.



- [2] Cie S. 026/E: 2018 CIE System for Metrology of Optical Radiation for ipRGC-Influenced Responses to Light. *Color Res Appl.* 2018;44: 316–316.
- [3] Liberati A, Altman DG, Tetzlaff J, Mulrow C, Gøtzsche PC, Ioannidis JP, et al. The PRISMA statement for reporting systematic reviews and meta-analyses of studies that evaluate health care interventions: explanation and elaboration. *Annals of internal medicine.* 2009;151(4): W–65.
- [4] Higgins JP, Savović J, Page MJ, Elbers RG, Sterne JA. Assessing risk of bias in a randomized trial. *Cochrane handbook for systematic reviews of interventions.* 2019; p. 205–228.
- [5] Al-Karawi D, Jubair L. Bright light therapy for nonseasonal depression: meta-analysis of clinical trials. *Journal of affective disorders.* 2016; 198:64–71.

## ACKNOWLEDGEMENTS

The author would like to thank Huifang Zhai and Xiang Cheng for the data collecting process, as well as the advice on writing given by Professor Yonghong Yan.

Corresponding Author Name: Ranpeng Chen

Affiliation: School of Architecture and Urban planning, Chongqing University, Chongqing, China

e-mail: 872848644@qq.com

# STUDY ON SUITABILITY REVIEW OF ROAD LIGHTING CLASS SELECTION PARAMETERS AND DOMESTIC APPLICATION PLAN

Seongsik Yoo, Jinsoo Shin, Jong-Min Lim  
KIEL Institute, Korea

## ABSTRACT

The Road Lighting Guidelines of the Ministry of Land, Infrastructure and Transport were revised in 2016 to determine the lighting level by considering various road factors. An attempt was made to apply the revised guidelines, but it is difficult to select a lighting grade because it is not suitable for application to actual roads.

In this paper, problems that occur when the lighting level selection parameters are applied to actual roads are found, and some of the parameters are modified and presented. In addition, by applying the modified parameters to the road routes in Jeju Island, the road lighting level suitable for the characteristics of the road was presented.

Keywords: Road lighting level, Luminance level, Luminance uniformity, Road and street, Korea

## 1. INTRODUCTION

The lighting class for roads where lighting is installed shall be determined in accordance with the "Continuous Lighting Standards for Automobile Traffic" of Chapter 4 of the Road Safety Facility Installation and Management Guidelines - Lighting Facilities.

The continuous lighting standards of the Ministry of Land, Infrastructure and Transport's guidelines were revised in 2016 to reflect the Commission internationale de l'éclairage recommendations (CIE115:2010) that determine lighting levels by judging parameters that consider traffic and surrounding environmental factors. Although the guidelines have been revised, it is difficult to select the lighting grade using the guidelines due to the lack of determining the parameters of the actual Korean roads.

In this paper, the guidelines of the Ministry of Land, Infrastructure and Transport were reviewed to supplement the parameter determination method and select the lighting class for the actual one road route on Jeju Island.

## 2. METHODS

### 2.1 Method of determining road lighting level

According to the Ministry of Land, Infrastructure and Transport's guidelines, eight parameters that affect automobile traffic are reviewed and weights are selected according to options to select lighting classes. The continuous lighting rating is determined by calculating the difference between the calculated total weight ( $V_{ws}$ ) and constant 6 by adding the weight for each parameter shown in Table 1.

Table 1. Lighting Class Selection Parameters

Parameter	Option	Detail Option		Weighting Value	Description
Speed	Very high	90(km/h)~		1	Select the lower of the design speed or the limit speed
	High	70~80(km/h)		0.5	
	Moderate	~60(km/h)		0	
Traffic volume (Service level)	Very high	E or higher		1	Estimate the level of traffic service by analyzing the design traffic volume per hour
	High	D		0.5	
	Moderate	C		0	
	Low	B		-0.5	Attach operation plan by time zone
	Very low	A		-1	
Traffic composition	Mixed with high percentage of non-motorized	High percentage of pedestrians		2	Mixed traffic composition using roads
	Mixed	a mix of cars, bicycles, and pedestrians		1	
	Motorized only	motorway		0	
Separation of lanes	No	plane intersection		1	Separation of lanes and intersections
	Yes	Overpass or interchange		0	
Intersection density	High	3 places or more/km		1	
	Low	Less than 3 places/km		0	
Parking the vehicle	Present	On-street parking permit area		0.5	Availability of on-street parking
	Not present	no parking area		0	※ It is assumed that there is no illegal parking
Ambient brightness	High	Zone 4	commercial area	1	Divided into lighting environment management zones
	Moderate	Zone 3	residential area	0	
	Low	Zone 1, 2	Agriculture, production, and natural environment conservation area	-1	
Traffic control facilities	Poor			0.5	Pedestrian crossing / traffic lights / traffic information signs, fence/crossing ban facility, etc.
	Moderate or Good			0	
Sum of Weighting Values (V <sub>ws</sub> )					
Lighting Class(M) = 6 - V <sub>ws</sub>					

## 2.2 Complementary to the weighting method

Among the parameters applied in the current directive, traffic volume and lane separation are not suitable for actual road applications and require some modification. Other weights will be applied as they are in accordance with the criteria in the current guidelines.

Currently, the Ministry of Land, Infrastructure and Transport's guidelines suggest "traffic service level" as an option for traffic volume, which explains the driving status of roads such as traffic speed, travel time, freedom of passage, comfort, and traffic safety. Service levels can be divided into six grades, from "A" to "F", with "A" levels representing the best conditions, "F" levels representing the worst conditions, and "E" levels and "F" levels generally represent capacity. This service level changes to indicate how congested the road is at a particular time and is not a

suitable parameter for use in the lighting level selection stage because the traffic capacity of the road needs to be known.

To replace this, it is appropriate to determine the traffic level based on the value of [traffic level-local road] of "6.13 appropriate traffic volume by road" in 『Manual of road operations (2022)』 of the Ministry of Land, Infrastructure and Transport. Traffic volume on the road was collected at the occasional traffic survey point of the traffic volume information provision system.

Roads on Jeju Island do not have highways, and most of them apply the plane intersection method, so a weight of 1 is given for the explanation of the guidelines, which makes the lighting level high. However, in CIE115:2010 guidelines cited by the guidelines, lane separation means whether lanes in the same direction are separated. The weight of lane separation means whether there is a traffic risk because vehicles driving in the opposite direction can cross the centre line, which can be seen as somewhat different from the contents of the current guidelines.

Accordingly, the parameter option was changed with the presence or absence of a road central separation facility to apply the weighting value. The presence or absence of central separation was confirmed using a load view.

### 3.2 Application Results for Actual Roads

To confirm the actual results of the application method, weights were applied to some illumination of Jeju Island. Il-ju Road is a four-lane road that passes around the coastal area of Jeju Island. The weight excluding the traffic volume was selected as shown in Table 4 and shown in 2. The final weight applied to the traffic volume is shown in Table 3.

Finally, the lighting classes selected for all sections of the Il-ju road are shown in Figure 1.

Table 2. Basic weighting value selection for Il-ju road

Parameter	Option	Detail Option	Weighting Value	selection
Speed	Very high	90(km/h)~	1	
	High	70~80(km/h)	0.5	
	Moderate	~60(km/h)	0	0
Traffic volume (Service level)	Very high	Apply Table 3	1	Apply Table 3
	High		0.5	
	Moderate		0	
	Low		-0.5	
	Very low		-1	
Traffic composition	Mixed with high percentage of non-motorized	High percentage of pedestrians	2	
	Mixed	a mix of cars, bicycles, and pedestrians	1	1
	Motorized only	motorway	0	
Separation of lanes	No	absence of road central separation facility	1	
	Yes	presence of road central separation facility	0	0
Intersection	High	3 places or more/km	1	1

density	Low	Less than 3 places/km		0	
Parking the vehicle	Present	On-street parking permit area		0.5	
	Not present	no parking area		0	0
Ambient brightness	High	Zone 4	commercial area	1	Applied by section
	Moderate	Zone 3	residential area	0	
	Low	Zone 1, 2	Agriculture, production, and natural environment conservation area	-1	
Traffic control facilities	Poor			0.5	
	Moderate or Good			0	0
Sum of Weighting Values ( $V_{ws}$ )					2
Lighting Class(M) = 6 - $V_{ws}$					Applied by section

Table 3. Final weighting value selection for Il-ju road

Traffic Survey Point No.	The number of lanes	Traffic volume	Traffic volume rating	Weighting value	commercial area	Residential area	Other areas
1132-01	6	15,582	A	-1	M4	M5	M5
1132-23	4	33,240	D	0.5	M2	M3	M4
1132-02	4	19,059	B	-0.5	M3	M4	M5
1132-05	4	14,259	B	-0.5	M3	M4	M5
1132-07	4	10,223	A	-1	M4	M5	M5
1132-09	4	6,012	A	-1	M4	M5	M5
1132-10	4	10,700	A	-1	M4	M5	M5
1132-21	4	32,834	D	0.5	M2	M3	M4
1132-12	6	21,756	B	-0.5	M3	M4	M5
1132-13	4	16,461	B	-0.5	M3	M4	M5
1132-15	4	15,931	B	-0.5	M3	M4	M5
1132-17	4	3,585	A	-1	M4	M5	M5
1132-18	4	10,353	A	-1	M4	M5	M5
1132-19	4	23,538	C	0	M3	M4	M5
1132-22	4	36,173	D	0.5	M2	M3	M4
1132-20	4	42,275	E	1	M2	M3	M4



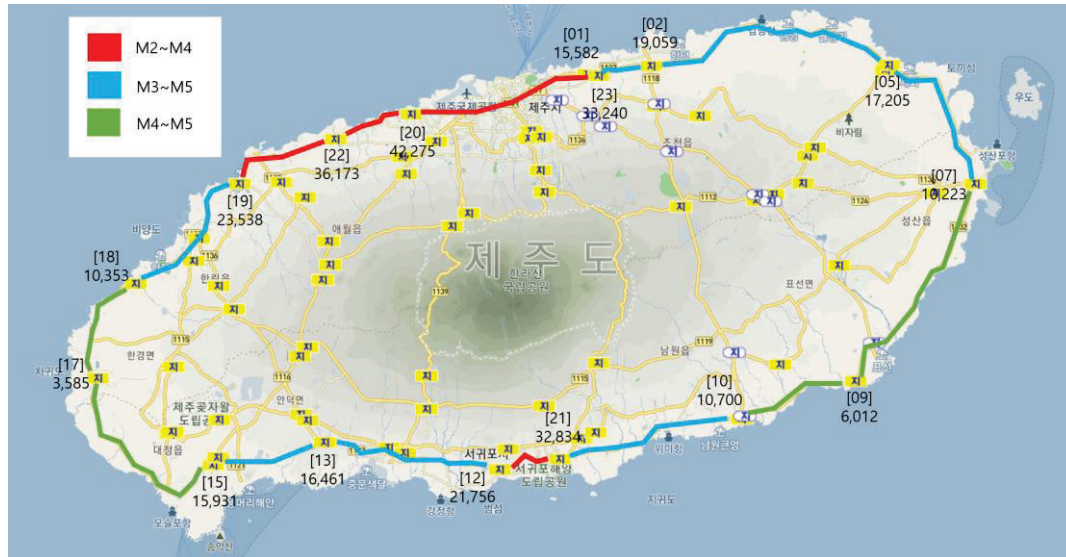


Figure 1. Lighting class by section of the Il-ju road

#### 4. Conclusion

As a result of partially revising the weight application to traffic volume and lane separation among the lighting class selection parameters in the Ministry of Land, Infrastructure and Transport guidelines and applying it to Jeju Island's Il-ju road, it was confirmed that lighting classes could be selected without problems. However, the traffic volume survey is conducted on roads above local roads, but there is no information on detailed roads such as cities and provinces. In addition, it is expected to be more helpful in optimizing the lighting level if it is possible to collect traffic information over time in the future, given that the actual road lighting is used at night.

#### REFERENCE

- [1] Ministry of Land Infrastructure and Transport, the Road Safety Facility Installation and Management Guidelines - Lighting Facilities, 2016.
- [2] Ministry of Land Infrastructure and Transport, Manual of road operations, 2022.

Corresponding Author: Seongsik Yoo  
 Affiliation: KIEL Institute  
 e-mail: yoo0139@kiel.re.kr

# MODIFIED CLIMATE-BASED DAYLIGHT MODELING METHODS FOR BUILDINGS

Yongqing Zhao, Zhen Tian

(School of architecture and planning, Hunan University, Changsha, China)

## ABSTRACT

This study proposes a method for calculating direct sunlight contribution, which can replace the sun-coefficient method and obtain a modified five-phase methods for dynamic building daylight modeling. Compared with the 5-PM with MF:3, the M5-PM can reduce computation time by 67% for modeling the specular blind systems, and the M5-PM can save 94.9% of the calculation time compared with the 5-PM with MF:6, using Shanghai as the test location. The results also indicate that the simulation accuracy of M5-PM is slightly improved in contrast to 5-PM for modeling the specular blind. Compared with the 5-PM, the M5-PM can use exact sun positions instead of placing suns at the centers of Reinhart patches. This overcomes the limitation of the 5-PM, where the sun or specular light reflected by blinds may not be predicted accurately in the field of view when modeling fenestration systems sensitive to solar positions and sunlight reflection. This is particularly important for applications such as model-based control for blind systems. However, the time benefits of M5-PM are influenced by the climate and not fit for parametric analysis.

Keywords: Climate-based daylight modeling; Radiance; Modified five-phase methods; Luminance and glare evaluation; Validation

## 1. INTRODUCTION

Daylight, as a primary renewable light source for buildings, not only can provide natural lighting for occupants but also reduce artificial lighting energy demand [1], and associated cooling energy use. However, it may also bring discomfort, and glare problems, as well as excess solar heat gains [2–6]. Taking full advantages of daylight and minimizing the discomfort glare, and the negative impacts from solar heat gain are the main goals that researchers focused on and worked towards. To achieve this target, more and more innovative daylighting and shading integration products are developed, such as prism daylight redirection fenestration (PDRF) [7,8], venetian blinds, woven fabric shading, dynamic building facades, and so on. These products are categorized as complex fenestration systems (CFS). However, the design, development and evaluation of complex fenestration systems rely on accurate and time-efficient tools that promote the development of new, innovative daylight and solar control technologies. Traditional daylight evaluation methods based on point-in-time simulation cannot meet these innovative CFS requirements since daylight varies with time and sky conditions. Thus, it is necessary to develop tools that conduct climate-based dynamic daylight and solar heat gains simulation efficiently and accurately, and numerous researchers were devoted to this effort [9–16].

In 1995, Mardaljevic [10] used the Daylight Coefficient Method to predict time-varying illuminances and implement it in Radiance, which utilized matrix multiplication of precalculated daylight coefficient matrix and sky matrix stacked by time-varied sky vectors to obtain indoor illuminances. In 2011, Ward [11] introduced the Three-phase method (3-PM) to simulate the annual daylight performance of Complex Fenestration Systems using the Bidirectional Scattering Distribution Functions (BSDF), which split the light transmission path into three phases. The View matrix (V), Transmission matrix (T), and Daylight matrix (D) were employed to describe the transmission flux matrices of three phases, respectively. Then the Daylight Coefficient can be derived by the matrix multiplication of these three matrices.

The 3-PM can model annual daylight performance efficiently through matrix calculation. Another benefit of this method lies in that the individual phases in the 3-PM are calculated independently, which helps to implement parametric simulation. For example, when evaluating different fenestration systems' impact on indoor daylight luminous environments, once one simulation was completed, the V, D, and s matrices can be reused. Only the T matrix needs to be replaced. However, the 3-PM method has the following shortcomings [11,12]:

- 1) Inaccuracy prediction of direct sunlight since the Reinhart discretization of sky model leads to sun size and position deviation.
- 2) The T matrix is characterized by a low-resolution BSDF (10-15° angular resolution), making it challenging to predict the spatial distribution of transmitted and reflected irradiance or illuminance

from the sun ( $0.5^\circ$  resolution). Further, this method is unable to meet the requirements of modeling some metrics such as discomfort glare, annual sunlight exposure, and thermal discomfort [13].

McNeil *et al.* [12] validate the 3-PM by comparing simulated with measured illuminance values for a daylight-redirecting optical louver system. The results showed that the absolute mean bias error was below 13%, and the root mean square error was below 23%. The 3-PM was employed to evaluate and optimize external blind designs [17–19], conduct the daylight performance evaluation of CFS [23–25], and perform annual daylight metrics calculations [23].

To address the above problems, McNeil *et al.* [14] proposed an annual daylight simulation method that can accurately model direct sunlight, the well-known Five-phase method (5-PM). The 5-PM is an improvement of the 3-PM, where the direct sun and diffuse sky's contribution are calculated separately. The diffuse sky's contribution is calculated with the Reinhart sky model using the 3-PM. The direct sun's contribution is derived by using the sun-coefficient method, which uses the intensity of the sun with its actual solid angle to avoid the oversized solid angle in the Reinhart sky model. Also, high-resolution BSDF or accurate geometry can be employed in the sun coefficient method, which helps to improve the accuracy of direct sun contribution calculation. The 5-PM was divided into three parts: 1) the 3-PM considering direct sun and diffuse sky's contribution, 2) the 3-PM considering only direct sun contribution, and 3) the sun-coefficient method. Finally, results are obtained through part 1) minus part 2) plus part 3).

Geisler-Moroder *et al.* [15] validated the 5-PM through comparing field-measured data with the simulated results derived by the 5-PM, revealing that 5-PM outperforms 3-PM for predicting horizontal and vertical illuminance values, as well as calculated glare metrics. The relative error of Daylight Glare Probability (DGP) predicted with the 5-PM was within 10% for most of the conditions. Additionally, Geisler-Moroder *et al.* [15] proposed a refined imaged-based five-phase method, which split the direct-sun aspect of the simulation into two different matrices. These two matrices address the interior of spaces and the overall scene separately.

However, in the 5-PM or any matrix-based methods using the separation method of direct sunlight and diffuse sky contributions, the sun-coefficient method was employed to calculate direct solar contribution, which has two shortcomings [24]: 1) the high Reinhart subdivision for sun patches can keep high accuracy, but it also causes a long computation time for the image-based simulation. In contrast, a low Reinhart subdivision can reduce computation time but it sacrifices the level of accuracy; and 2) even if the maximum number of patches for sun-coefficient calculation was used, the error may still occur due to the angular separation between the actual position and that of the assigned patch still exist.

## 2. METHODS

In this study, a modified method for computing the direct sunlight contribution were proposed. It allows for the use of exact solar positions and is more time-efficient. This method also enables the specification of the accuracy of sun positions using a tolerance of solar direction deviation, which was named as the modified five-phase method. The modified direct solar computation method proposed in this study were employed to replace the sun-coefficient method in the 5-PM, as illustrated in Fig. 1.

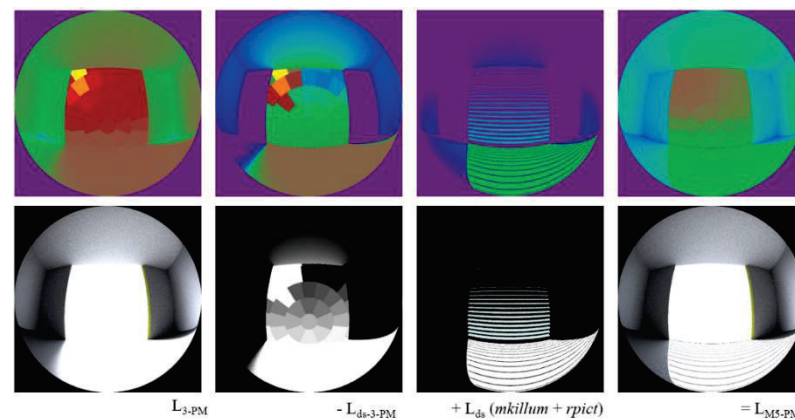


Fig. 1 The process of the rendering of the modified Five-phase methods

## 2.1 The core optimization mechanism

In the 5-PM, rcontrib was employed to calculate the contribution coefficient, which is the core of the matrix-based daylight modeling methods, however, the ambient cache is disabled in rcontrib. This mechanism is a crucial tool for diffuse reflection in Radiance, which can accelerate the rendering process and reduce the artifacts. Rcontrib uses the standard Monte Carlo methods to evaluate the rendering equation, which needs to sample random directions over the hemisphere at each pixel for diffuse reflection calculation. This would lead to a huge computation cost since it takes 100-1000 rays to adequately sample the hemisphere at a given point and even more if multiple interreflections are considered. To reduce the calculation cost, only several points over the hemisphere are sampled and cached, and interpolation is done between these values. This is feasible because the diffuse indirect components change slowly over surfaces [25]. This mechanism is called ambient cache and is used in rtrace/rpict. However, the ambient cache is disabled in rcontrib because the computation of the contribution coefficient needs to cache all the rays' contribution on final values, which causes the entire ray tree associated with each cached value to be stored, quickly consuming all the available memory. Thus, it is necessary to conduct the hemisphere sample at each pixel in rcontrib. This pixel-by-pixel approach will produce pixel noise and take a long time. In sun-coefficient method, the illuminance images should be first calculated, and then the material map should be used to convert them to luminance images to obtain direct sunlight's contribution on indoor surfaces. Any surfaces in the field of view would be replaced by a Lambertian surface when conducting illuminance calculation. Thus, it will lead to the indirect calculation without the ambient cache.

In this study, the core optimization mechanism is using the ambient cache to accelerate the dynamic daylight simulation, which is implemented by the program rpict, rather than rcontrib. To fully take advantage of the ambient cache, the overture calculation was employed to further optimize computation efficiency. The overture calculation pre-generates an ambient file for a small picture size (64 pixels × 64 pixels) and then reuses this ambient file to render a larger picture.

To eliminate artifacts caused by the indirect calculation of rpict, mkillum was used with an ambient bounce of zero to generate a secondary light source (illum type). The secondary light source was then incorporated into the model for ray-tracing calculations. The benefits of using mkillum include not only eliminating artifacts but also accelerating rendering for the case incorporating BSDF.

## 2.2 The Modified Five-phase Method

The core optimization mechanism of this method is presented in section 2.1, which uses ambient cache to accelerate the calculation, and mkillum to improve the image quality. In addition to this, the M5-PM uses the rpict to conduct rendering at each timestep for the specific location, thus it does not need to simulate the tons of sun patches to achieve an accuracy enough like what is doing in the 5-PM. Another advantage is it can use the exact sun positions to calculate the direct sunlight contribution. This method also enables the specification of the accuracy of sun positions using a tolerance of solar direction deviation. If the deviation of the solar position at the current timestep and the previous timestep is within the specified tolerance, the previously calculated HDR image can be used to derive the HDR image of the current timestep. The deviation between sun vectors at timestep  $i$  and  $j$  can be calculated as formula (1):

$$\theta = \arccos \frac{\vec{S}_i \cdot \vec{S}_j}{|\vec{S}_i| |\vec{S}_j|} \quad (1)$$

where:

$\vec{S}_i$  are the sun vector at timestep  $i$ ;

$\vec{S}_j$  are the sun vector at timestep  $j$ ;

$\theta$  are the angle between  $\vec{S}_i$  and  $\vec{S}_j$ .

To further reduce computation time, the ray-tracing procedure was executed only when the direct irradiance from the sky was greater than zero. If the direct irradiance from the sky was zero, pcomb was used to generate a black HDR image to represent no direct light contribution. The computation procedure is shown in Fig. 2. A Python program was developed following the procedures, in which the parallel computing technology based on a thread pool was used to accelerate the run. Additionally, the exact solar position was employed to conduct the glare metrics calculation.

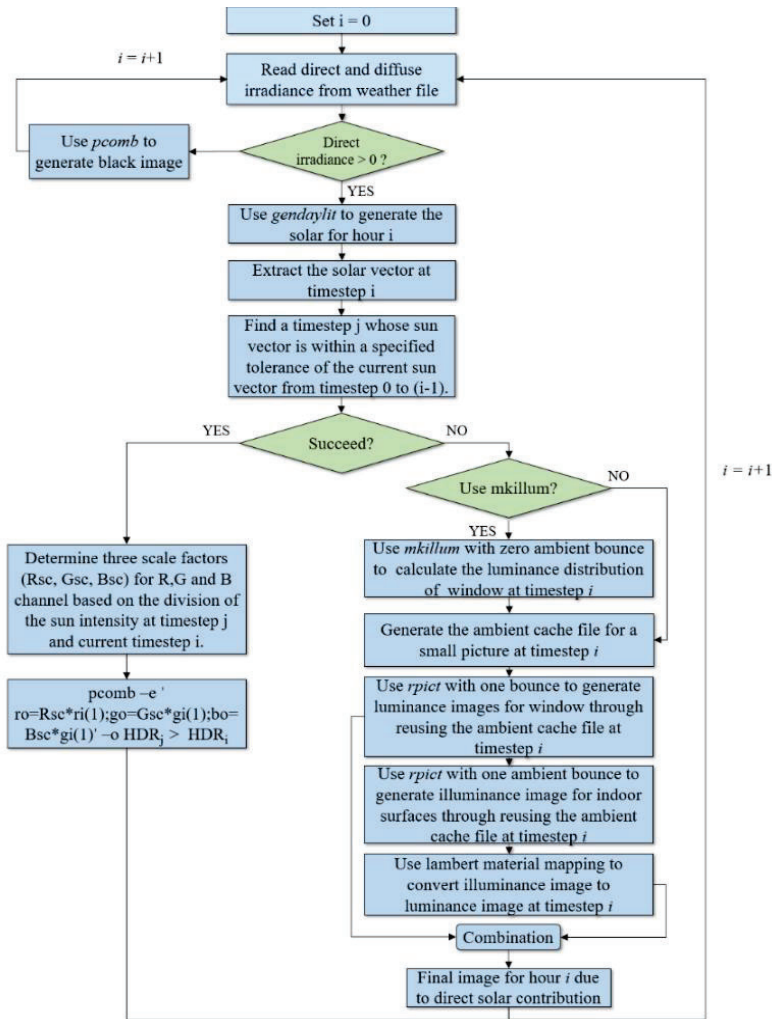


Fig. 2 Computation procedures of direct sunlight calculation

### 2.3 Test Models

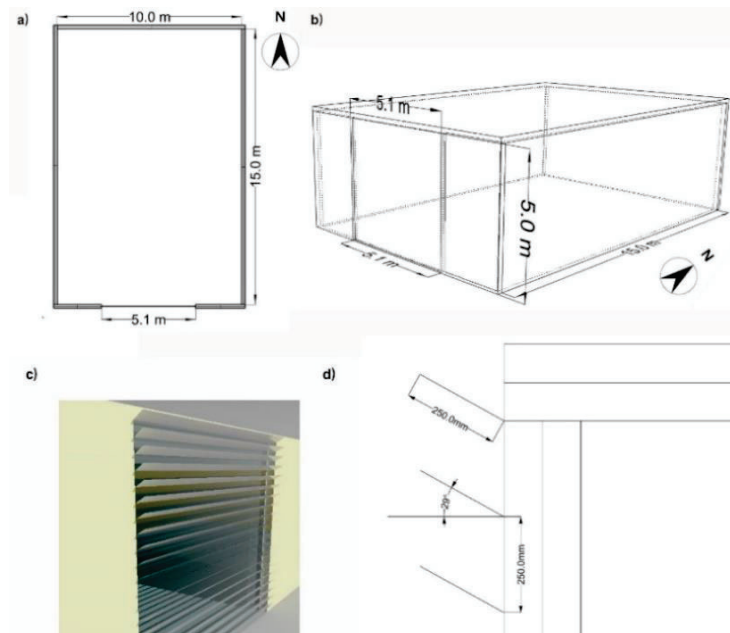


Fig. 3 a) Floor plan of the research model  
 b) 3D dimension of the research model  
 c) Model façade with blinds  
 d) Dimension and tilt angle of the blind slats



This study modeled an open office facing south in Shanghai (120.6°E, 31.3°N) with a dimension of 10.0 m in width, 15.0 m in depth, and 5.0 m in height, as shown in Fig. 4 a) and b). The window dimension is 5.1m in height and 5m in width. The reflectance values of the ceiling, wall, and floor were set to 0.75, 0.55, and 0.20, respectively. To model the reflection of outdoor ground, a ground plane was added with a reflectance value of 0.20.

A horizontal specular blind system was applied in the building. The accurate geometry of the horizontal blinds was necessary for modeling as it allowed for a more realistic representation of the system. The specular blind had a reflectance value of 0.70 and a specular ratio of 0.02. A Klems format BSDF, generated using genBSDF, was used to model the horizontal blinds in the 3-PM calculation.

## 2.4 Comparison and validation

To evaluate the performance improvement of the new method, the results obtained by the modified Five-phase method were compared with those obtained using the 5-PM and the conventional ray-tracing method (RT). The accuracy of the modified Five-phase methods and 5-PM methods were evaluated based on a benchmark provided by the RT method. Mean bias errors (MBE) and relative root mean squared errors (RMSE) were used to describe the errors in this study.

## 3. RESULTS

### 3.1 Comparison of Glare Metrics

Table 1 presents the errors for the 5-PM with proxy geometry under various sun patches and the modified Five-phase methods with geometry. It shows that 5-PM with 145 sun patches (MF:1) has significant errors for DGP, Ev, and DGI. This is due to the significant deviation in solar positions when used 145 sun patches. However, once the sun patches are increased to 577 (MF:2), the errors of glare metrics values in imperceptible, perceptible, and disturbing levels drop sharply and become stable when the sun patches grow to above 1297 (MF:3). This suggests that increasing the number of sun patches can greatly improve the accuracy of the 5-PM with proxy geometry. Meanwhile, Table1 indicates that the RMSEs of glare metric values at imperceptible, perceptible, and disturbing levels calculated with the M5-PM are similar to those calculated with the 5-PM using 1297 or above sun patches. However, the RMSEs for glare metrics values at intolerable level calculated with the M5-PM are smaller, and so are the overall RMSEs. Meanwhile, it was shown that even when the MF value was increased to 6, the RMSEs of the 5-PM derived DGP values remained above 0.05. This was due to the inaccuracy of the employed sun positions, resulting in the inability to precisely predict the moments when the sun appears in the field of view through the gap between the blind slats and when the light reflected on the blind slats enters the eyes.

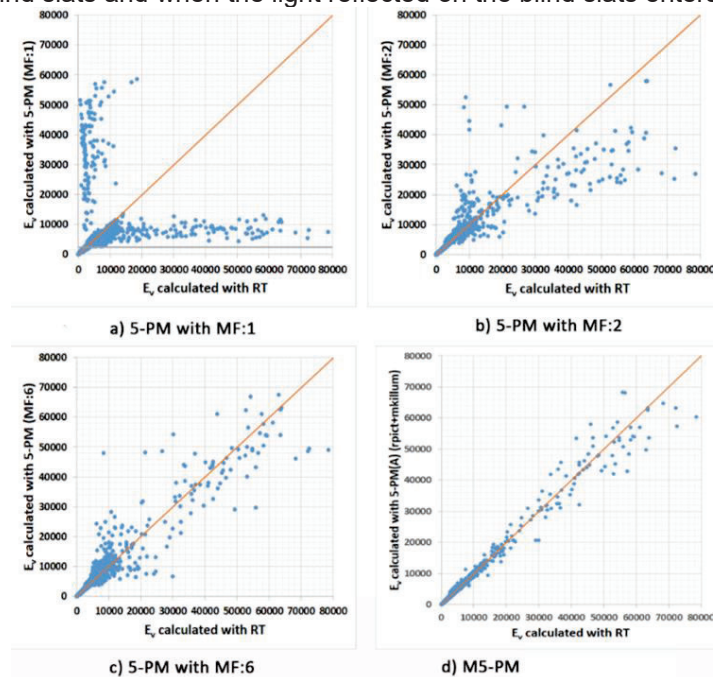


Fig. 4  $E_v$  values derived by the 5-PM with proxy geometry and the M5-PM

Figs. 4 and 5 show the relationship between the DGP and Ev values calculated by the 5-PM and M5-PM and the values calculated by RT. As the number of sun patches increases for the 5-PM, the agreement between the 5-PM derived glare metrics values and the RT calculated values improves. However, there are more outliers for the 5-PM derived DGP and Ev values compared to the M5-PM derived values, which significantly deviate from the RT calculated values. Despite this, most of these outliers are in the same glare level range as the RT derived values and do not affect the overall glare evaluation.

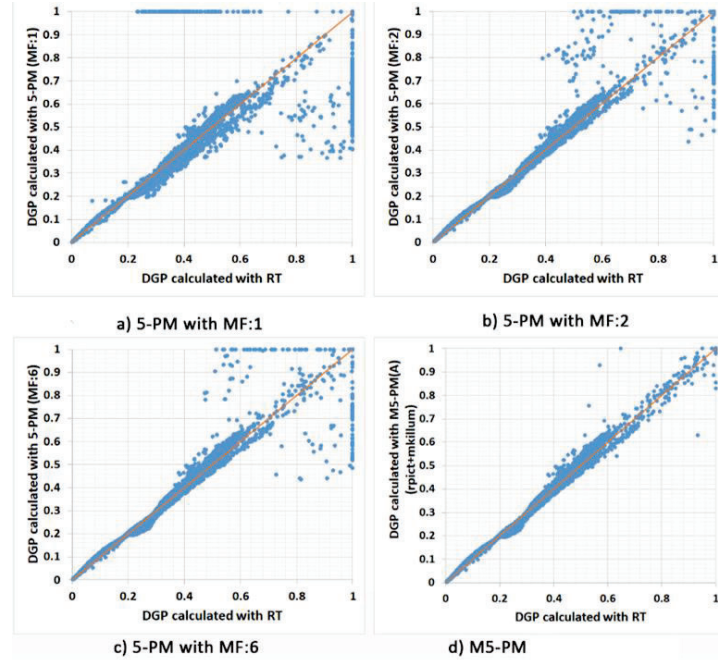


Fig. 5 DGP values derived by the 5-PM with proxy geometry and the M5-PM

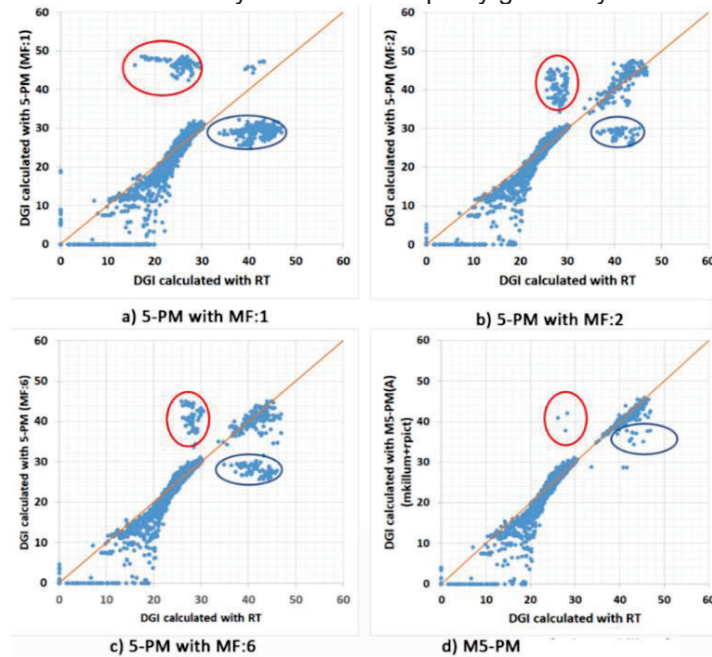


Fig. 6 DGI values calculated with the 5-PM and the M5-PM

Table 1 Error comparison between the 5-PM and M5-PM with geometry for specular blinds

Glare Metrics			5-PM MF:1	5-PM MF:2	5-PM MF:3	5-PM MF:4	5-PM MF:5	5-PM MF:6	M5-PM
DGP	<0.35	RMSE	0.100	0.013	0.013	0.013	0.013	0.012	0.012
		MBE	-0.015	0.001	0.001	0.001	0.001	0.001	0.001

	0.35-0.40	RMSE	0.135	0.026	0.018	0.018	0.018	0.018	0.018
		MBE	-0.008	-0.002	-0.002	-0.002	-0.002	-0.002	-0.002
	0.40-0.45	RMSE	0.123	0.045	0.024	0.024	0.024	0.024	0.024
		MBE	-0.009	-0.005	-0.004	-0.004	-0.004	-0.004	-0.004
	≥0.45	RMSE	0.193	0.12	0.140	0.134	0.120	0.120	0.03
		MBE	0.068	-0.017	-0.010	0.002	-0.011	-0.002	-0.007
	Overall	RMSE	0.138	0.123	0.070	0.068	0.060	0.059	0.021
		MBE	0.002	-0.006	-0.003	-0.001	-0.004	-0.002	-0.003
Frequency (DGP > 0.40)			36.4%	36.3%	36.4%	36.4%	36.4%	36.5%	36.4%
E <sub>v</sub>	Overall	RMSE	8079	3202	3023.0	3275	2223	2071	928
		MBE	-161.6	95.8	-221.5	168.3	17.4	19.8	-65.8
DGI	<18	RMSE	6.3	4.5	4.7	4.5	4.5	4.3	4.8
		MBE	1.80	1.49	1.55	1.50	1.50	1.52	1.56
	18-24	RMSE	7.1	4.9	5.0	5.0	5.1	5.2	5.1
		MBE	0.45	0.68	0.69	0.68	0.68	0.69	0.68
	24-31	RMSE	4.6	3.0	2.9	2.4	2.7	2.5	1.1
		MBE	-1.38	-1.06	-1.01	-0.88	-0.94	-0.86	-0.55
	>31	RMSE	12.3	6.4	8.1	5.47	7.0	6.3	2.3
		MBE	11.55	2.40	5.08	4.47	3.56	5.9	0.90
	Overall	RMSE	6.26	4.11	4.18	4.18	4.10	4.46	3.48
		MBE	0.79	0.50	0.77	0.77	0.63	0.74	0.70
Frequency (DGI > 24)			52.2%	52.1%	52.1%	52.2%	52.2%	52.1%	52.2%

Fig. 6 presents the 5-PM and M5-PM derived DGI values against RT derived values. It illustrates that there are many outliers that affect the glare evaluation in 5-PM derived values. For example, the outliers marked with a red circle should belong to a glare level below disturbing, but were predicted to fall into the intolerable level. However, the outliers marked with a blue circle should belong to the intolerable level but were predicted to fall into the disturbing level. This indicates that errors in DGI values may lead to unreliable glare ratings. However, when calculating the percentage of annual discomfort occurrence, the presence of outliers would not significantly impact the results.

### 3.2 Computation time

A Laptop with an eight-core/16-thread CPU (AMD Radeon, eight physical cores and 16 virtual cores, 3.2 MHz), 24G RAM (8G Samsung and 16G Kingston), and 1T SSD hard disk was used to test the computation performance of the 5-PM and M5-PM, and Windows Subsystem Linux (Ubuntu 20.04 LTS) was used as the test platform. For the M5-PM, 1996 timesteps were conducted for the rpict running. The average computation time per timestep is approximately 11s. The computation time for the M5-PM includes all the procedures required in the M5-PM, such as constructing sky and octree files, as well as the rpict running. For a fair comparison, all simulations were performed using 16 CPU cores for parallel computing in this investigation.

The computation times for the 5-PM and M5-PM are presented in Table 2. The results show that the M5-PM outperforms 5-PM with MF:6 for specular blinds, the M5-PM can reduce the computation time by up to 94.9% and 81.1% for the direct sunlight calculation and entire computation, respectively, compared to 5-PM with MF:6. Moreover, as demonstrated in Section 3.2, the results indicate that the 5-PM with MF:3 may be sufficient to predict the glare metrics but need to be further validated. Therefore, when compared to the 5-PM with MF:3, the M5-PM can reduce the computation time by up to 67% and 33% for the direct sunlight calculation and entire computation, respectively when modeling specular blinds.

Table 2 Computation time of the 5-PM and M5-PM

Procedure	5-PM						M5-PM
MF	1	2	3	4	5	6	/
3-PM	2.61	2.61	2.61	2.61	2.61	2.61	2.61
Direct 3-PM	1.01	1.01	1.01	1.01	1.01	1.01	1.01
Direct sunlight	0.43	1.54	3.92	7.03	11.7	19.8	1.1
Combine	0.56	0.56	0.56	0.56	0.56	0.56	0.56
Total	4.61	5.72	8.1	11.2	15.9	24	5.3

## 4 Conclusions

This study proposed two optimized direct solar computation methods and they were used to replace the sun coefficient method in the 5-PM simulation, thus obtaining two modified Five-phase methods. Results derived by the 5-PM and the modified Five-phase methods are compared, and the key findings are that for fenestration systems that are sensitive to solar position or specular reflect sunlight, the M5-PM can obtain more reliable values for contrast-based glare metrics compared with the 5-PM, even if the maximum sun patches (5185 sun patches) are applied in the sun coefficient method. Additionally, for the calculation of saturation-based glare metrics or glare metrics based on both contrast and saturation, the M5-PM can reduce outliers and obtain more accurate glare metric values. This is essential for some application scenarios such as model-based control blinds.

## REFERENCES

- [1] Boyce P.R., Hunter CM. The benefits of daylight through windows. Lighting Research Center Rensselaer, Polytechnic Institute, 2003.
- [2] E.J. Gago, T. Muneer, M. Knez, H. Köster, Natural light controls and guides in buildings. Energy saving for electrical lighting, reduction of cooling load, Renewable and Sustainable Energy Reviews. 41 (2015) 1–13. <https://doi.org/10.1016/J.RSER.2014.08.002>.
- [3] X. Yu, Y. Su, Daylight availability assessment and its potential energy saving estimation –A literature review, Renewable and Sustainable Energy Reviews. 52 (2015) 494–503. <https://doi.org/10.1016/J.RSER.2015.07.142>.
- [4] M.B. Hirning, G.L. Isoardi, I. Cowling, Discomfort glare in open plan green buildings, Energy Build. 70 (2014) 427–440. <https://doi.org/10.1016/J.ENBUILD.2013.11.053>.
- [5] M.B. Hirning, G.L. Isoardi, S. Coyne, V.R. Garcia Hansen, I. Cowling, Post occupancy evaluations relating to discomfort glare: A study of green buildings in Brisbane, Building and Environment. 59 (2013) 349–357. <https://doi.org/10.1016/J.BUILDENV.2012.08.032>.
- [6] K. Konis, Predicting visual comfort in side-lit open-plan core zones: Results of a field study pairing high dynamic range images with subjective responses, Energy and Buildings. 77 (2014) 67–79. <https://doi.org/10.1016/J.ENBUILD.2014.03.035>.
- [7] J. Fang, Y. Zhao, Z. Tian, P. Lin, Analysis of dynamic louver control with prism redirecting fenestrations for office daylighting optimization, Energy and Buildings. 262 (2022) 112019. <https://doi.org/10.1016/j.enbuild.2022.112019>.
- [8] P. Lin, Z. Tian, J.C. Jonsson, Analysis of the performance of prism daylight redirecting systems with bi-directional scattering distribution functions, Building Simulation. 13 (2020) 305–316. <https://doi.org/10.1007/s12273-020-0607-4>.
- [9] P.R. Tregenza, I.M. Waters, Daylight coefficients, Lighting Research & Technology. 15 (1983) 65–71. <https://doi.org/10.1177/096032718301500201>.
- [10] John Mardaljevic, Daylight simulation: validation, sky models and daylight coefficients, DeMontfort University, Leicester, 2000.
- [11] G. Ward, R. Mistrick, E.S. Lee, A. McNeil, J. Jonsson, Simulating the daylight performance of complex fenestration systems using bidirectional scattering distribution functions within radiance, Journal of Illuminating Engineering Society of North America. 7 (2011) 241–261. <https://doi.org/10.1080/15502724.2011.10732150>.
- [12] A. McNeil, E.S. Lee, A validation of the Radiance three-phase simulation method for modelling annual daylight performance of optically complex fenestration systems, Journal of Building Performance Simulation. 6 (2012) 24–37. <https://doi.org/10.1080/19401493.2012.671852>.
- [13] G.J. Ward, B. Bueno, D. Geisler-Moroder, L.O. Grobe, J.C. Jonsson, E.S. Lee, T. Wang, H. Rose Wilson, Daylight simulation workflows incorporating measured bidirectional scattering distribution functions, Energy and Buildings. 259 (2022) 111890. <https://doi.org/10.1016/J.ENBUILD.2022.111890>.
- [14] A. Mcneil, The Five-Phase method for simulating complex fenestration with Radiance, Lawrence Berkeley National Laboratory, 2013.
- [15] D. Geisler-Moroder, E.S. Lee, G.J. Ward, Validation of the five-phase method for simulating complex fenestration systems with radiance against field measurements, in: Building Simulation Conference Proceedings, International Building Performance Simulation Association, 2017: pp. 927–935. <https://doi.org/10.26868/25222708.2017.401>.
- [16] D. Bourgeois, C.F. Reinhart, G. Ward, Standard daylight coefficient model for dynamic daylighting simulations, Building Research and Information. 36 (2008) 68–82. <https://doi.org/10.1080/09613210701446325>.
- [17] S. Hoffmann, E.S. Lee, A. McNeil, L. Fernandes, D. Vidanovic, A. Thanachareonkit, Balancing



- daylight, glare, and energy-efficiency goals: an evaluation of exterior coplanar shading systems using complex fenestration modeling tools, *Energy and Buildings*. 112 (2016) 279–298. <https://doi.org/10.1016/J.ENBUILD.2015.12.009>.
- [18] S. Vera, D. Uribe, W. Bustamante, G. Molina, Optimization of a fixed exterior complex fenestration system considering visual comfort and energy performance criteria, *Building and Environment*. 113 (2017) 163–174. <https://doi.org/10.1016/J.BUILDENV.2016.07.027>.
  - [19] L. Santos, A. Leitão, L. Caldas, A comparison of two light-redirecting fenestration systems using a modified modeling technique for Radiance 3-phase method simulations, *Solar Energy*. 161 (2018) 47–63. <https://doi.org/10.1016/j.solener.2017.12.020>.
  - [20] Y. Sun, Y. Wu, R. Wilson, Analysis of the daylight performance of a glazing system with Parallel Slat Transparent Insulation Material (PS-TIM), *Energy and Buildings*. 139 (2017) 616–633. <https://doi.org/10.1016/J.ENBUILD.2017.01.001>.
  - [21] A. McNeil, E.S. Lee, J.C. Jonsson, Daylight performance of a microstructured prismatic window film in deep open plan offices, *Building and Environment*. 113 (2017) 280–297. <https://doi.org/10.1016/J.BUILDENV.2016.07.019>.
  - [22] J. Gong, A. Kostro, A. Motamed, A. Schueler, Potential advantages of a multifunctional complex fenestration system with embedded micro-mirrors in daylighting, *Solar Energy*. 139 (2016) 412–425. <https://doi.org/10.1016/J.SOLENER.2016.10.012>.
  - [23] A. Nezamdoost, K. van den Wymelenberg, A daylighting field study using human feedback and simulations to test and improve recently adopted annual daylight performance metrics, *Journal of Building Performance Simulation*. 10 (2017) 471–483.
  - [24] S. Subramaniam, Daylighting simulations with Radiance using matrix-based methods, Lawrence Berkeley National Laboratory, 2017.
  - [25] Greg Ward Larson, Rob Shakespeare, *Rendering with Radiance*, 2021.

## ACKNOWLEDGEMENTS

The research is funded by the National Natural Science Foundation of China (Grant No. 51978429), Hunan provincial Natural Science Foundation (2023JJ30151), Hunan Key Laboratory of Science of Urban and Rural Human Settlements at Hilly Areas (2020TP1009). Many thanks to Mr. Greg Ward for providing very useful suggestion in the discussion of exploring new daylighting modeling methods.

Corresponding Author Name: Zhen Tian

Affiliation: School of architecture and planning, Hunan University

e-mail: zhentian@hnu.edu.cn



# ILLUMINATING WELL-BEING: A SIMULATION-BASED LIGHTING EVALUATION AND TOOL DEVELOPMENT FOR A TROPICAL HOSPITAL

Quek Chong LIN Venjamin<sup>1</sup>, Szu-Cheng CHIEN<sup>1</sup>, Kai Ting FOO<sup>1</sup>, Nicholas Wei Kiat TAN<sup>2</sup>, Kevin CHONG<sup>2</sup>, Ann Mei WONG<sup>2</sup>, Luke Sher Guan LOW<sup>2</sup>

<sup>1</sup> Engineering Cluster, Singapore Institute of Technology, Singapore

<sup>2</sup> SingHealth Community Hospitals

## ABSTRACT

The increasing awareness of the vital role lighting plays in promoting health and wellbeing has led to a growing interest in lighting performance, particularly within healthcare facilities. In tropical regions, the unique micro-climatic conditions and distinct daylight characteristics present additional challenges in optimizing lighting for the benefit of patients and staff. However, conducting a thorough lighting performance simulation that considers cost effectiveness and time constraints can be challenging. To address this, this study aims to thoroughly investigate the lighting performance within a tropical hospital ward setting through a simulation-based evaluation. The simulations were carried out using Rhino 7 in conjunction with the ClimateStudio plugin, providing a temporal, environmental (considering weather conditions), and spatial analysis of human-centric lighting performance. Furthermore, to enhance the lighting performance evaluation and decision-making process, an agile multi-objective optimization tool was developed using Grasshopper, Ladybug, and Honeybee plugins. This tool allows for agile multi-objective optimization, enabling the exploration of various lighting scenarios and facilitating informed decision-making. The findings of this study contribute not only to the existing knowledge on lighting performance in healthcare facilities but also provide a strong basis for the development of effective lighting control strategies tailored to tropical hospital settings. By enhancing our understanding of the role of lighting in promoting health and wellbeing, the outcomes of this research effort are expected to improve the overall experience and outcomes for patients and staff in tropical healthcare environments.

**Keywords :** Lighting performance, Healthcare facilities, Tropical regions, Simulation-based evaluation, Agile multi-objective optimisation

## 1. INTRODUCTION

Lighting is a multifaceted concept that has profound effects on human health and well-being. It pertains to both positive and negative effects, biologically and physically. Biologically, proper lighting plays an essential role in regulating human circadian rhythms, fostering positive mood, and improving sleep quality. From a psychological viewpoint, adequate lighting can mitigate the risk of mental health issues and boost cognitive abilities. Research has consistently shown that having adequate lighting, especially natural light, can aid in patients' recovery and create positive emotions [1]. On the contrary, insufficient or inadequate lighting in healthcare facilities can result in sleep deprivation, amplify negative emotions, and hinder healing. In certain instances, inappropriate lighting in hospital settings has been associated with adverse outcomes like falls or medical errors. The experience of being admitted into a hospital can be inherently stressful and anxiety-inducing due to the unfamiliar environment, medical procedures, and intimidating medical apparatus. Hospitalization can exacerbate negative emotions and contribute to the development of depression and anxiety [2]. Furthermore, studies have demonstrated a significant correlation between sleep deprivation and the occurrence of mental health disorders among hospitalized patients [3]. Despite the critical role of lighting in healthcare environments, the lighting performance in tropical hospitals is rarely evaluated systematically and reliably. Given the challenges involved in conducting thorough lighting performance simulations that are both cost-effective and time-efficient, it becomes even more imperative to address this gap in evaluating and optimising lighting conditions in tropical hospital settings.

Thereby, this study aims to investigate the lighting performance within a tropical hospital ward setting through a simulation-based evaluation. The simulations were carried out using Rhino 7

and the ClimateStudio plugin, providing a temporal, environmental (considering weather conditions), and spatial analysis of the performance of healthcare lighting. Furthermore, to enhance the lighting performance evaluation and decision-making process, an agile multi-objective optimisation tool was developed using Grasshopper, Ladybug, and Honeybee plugins. This tool allows for multi-objective optimisation, enabling the exploration of various lighting scenarios and facilitating informed decision-making. The findings of this study contribute not only to the existing knowledge on lighting performance in healthcare facilities but also provide a strong basis for the development of effective lighting control strategies tailored to tropical hospital ward settings. By enhancing our understanding of the role of healthcare lighting, the outcomes of this research effort are expected to improve the overall visual experience, health and well-being of patients and staff in tropical healthcare environments.

## 2. METHODOLOGY

Firstly, literature review was conducted to gain a comprehensive understanding of the current state of healthcare lighting research and to identify relevant lighting performance metrics. Subsequently, a detailed 3D model of a selected ward area in a tropical hospital was created using Rhino 7 Modeling software. The simulations were carried out using rhino 7 and the ClimateStudio plugin, providing a temporal, environmental (considering weather conditions), and spatial analysis of the performance of healthcare lighting. Finally, an agile multi-objective optimization tool was developed.

### 2.1 Lighting Performance Metrics

Based on the Singapore Standard SS531 [4], ward spaces have specific illuminance requirements based on the occupants' needs. These requirements include general lighting at 100 lx (at floor level), reading lighting at 300 lx, simple examination lighting at 300 lx, examination and treatment lighting at 1000 lx, and night light and observation lighting at 5 lx. Another important parameter to consider is glare control, as it can negatively impact visual performance and cause discomfort [5]. In the ward, the Uniform Glare Rating (UGR) should be kept at 19 or below. To assess discomfort glare, the Daylight Glare Probability (DGP) metric is also considered. DGP quantifies the probability of users experiencing glare, especially from the sun, at specific positions and orientations. Table 1 outlines four distinct bands of DGP glare values, ranging from 0% to 100%.

Table 1. DGP Glare Band

Glare	DGP Range	Reference
Unnoticeable Glare	$DGP \leq 34\%$	[6]
Noticeable Glare	$34\% < DGP \leq 38\%$	
Unpleasant Glare	$38\% < DGP \leq 45\%$	
Unbearable Glare	$45\% < DGP$	

### 2.2 Computational Lighting simulations

#### 2.2.1 Description of the Ward Model

For the case study of the performance evaluation of healthcare lighting, a specific tropical hospital ward with five beds, located on level 6 and facing north, was selected. This ward is part of a selected tropical hospital that provides long-term care for the management of chronic diseases and encompasses various specialist clinics. To visualise the ward and aid in the evaluation process, Figure 1 illustrates the ward's floor plan, while Figure 2 presents a rendered 360° View of the selected hospital ward.

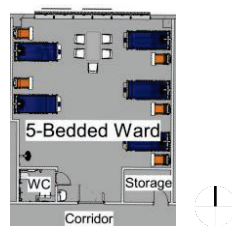


Figure 1. Tropical Hospital Ward plan



Figure 2. Rendered 360° View of the Ward

### 2.2.2 Simulation Parameters

To ensure a realistic and accurate simulation of illuminance, simulation parameters were carefully defined and discussed. The simulations were conducted based on the Autumnal Equinox Day (21<sup>st</sup> September) was selected specifically to represent the worst-case scenario for daylighting performance, allowing for a thorough evaluation of the lighting performance under challenging lighting conditions, ensuring that the simulation captures the potential limitations and areas for improvement in the ward's daylighting design. Also, two sky conditions are considered, namely clear and overcast sky conditions. A set of single point-in-time daylight simulations with intervals of 3 hours were conducted to account for different lighting conditions experienced throughout the day. The specific time steps selected were 8am, 11am, 2pm, 5pm, 7pm, 10pm, 12mn (midnight), and 3am. The workplane offsets for both daylight and artificial lighting were set at 850mm (Lying), 1200mm (Sitting) and 1600mm (Standing), while night light simulation specifically focused on 850mm (Lying). For the adopted lighting utilised for the simulation, it adheres to the lighting specifications provided by the hospital. The measurement area for both illuminance and glare simulations was established based on Figure 3. The ward was divided into left and right areas, and within each area, three segments were defined. Segment 1 spanned from 0-3m from the window, segment 2 covered the distance from 3m to 5.5m from the window, and segment 3 extended from 5.5m to 7.5m from the window. Each segment was further evaluated by identifying seven measurement points: W1, W2, B1, B2, B3, B4, and B5. Similarly, for the glare simulation, the measurement area was divided into two segments: the 1st half and the 2nd half, as shown in Figure 4. In addition to the previous information, a total of 224 sensors were strategically placed within the ward model, with a spacing of 609.6mm between each sensor to obtain a detailed understanding of the illuminance distribution within the space. Furthermore, the reflectance magnitudes of the ward spaces (including wall, floor, ceiling, furnitures) were determined based on on-site measurement via a luminance meter (Gossen MAVO SPOT 2) and a homogenized grey card with a reflectance level of 18%. This is to ensure accurate representation in the lighting simulations.

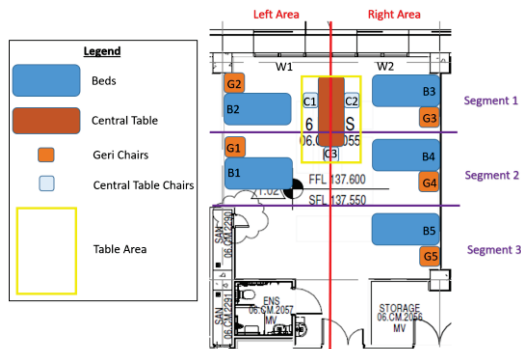


Figure 3. Measurement Area for Illuminance Simulation

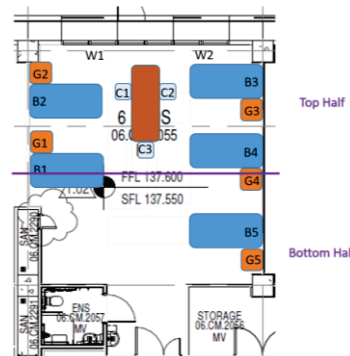


Figure 4. Measurement Area for Glare Simulation

## 2.3 Multi-objective tool

Previous simulation processes involve tedious simulation processes with the potentials of the human errors. To enhance the lighting performance evaluation and decision-making process, an agile multi-objective optimization tool was developed using Grasshopper, Ladybug, and Honeybee plugins. This tool allows for agile multi-objective optimization, enabling the exploration of various lighting scenarios and facilitating informed decision-making.

## 3. RESULTS

### 3.1 Illuminance Evaluation

Figures 5-8 show the average illuminance level for 8am, 11am, 2pm and 5pm for different segmented areas under various sky conditions, both with and without artificial lighting. Without artificial lighting, there is noticeable variation in average illumination levels across different eye-level positions within the segmented areas. Additionally, as the distance from the window increases, the average illuminance level decreases. However, when artificial lighting is introduced, the average illuminance level fluctuates across the segmented area for different eye-

level positions. When analysing the results in terms of 3 eye-level positions, the lying eye-level experiences a decrease in average illuminance with increasing distance from the window, regardless of artificial lighting. Similarly, sitting and standing eye-level positions also show a decrease in average illuminance without artificial lighting, but with artificial lighting, the average illuminance fluctuates. Figures 9-10 depict the average illuminance levels at 7pm and 8pm with the presence of artificial light under a single sky condition. Generally, the average illuminance levels exhibit fluctuations across the segmented areas, even as the distance from the window increases. When considering each distinct eye-level point, it can be observed that for the lying position, the average illuminance level fluctuates despite the increase in distance from window. Lastly, Figures 11-12 demonstrate the average illuminance levels at 12am and 3am with the sole presence of night light under a single sky condition. Generally, the average illuminance levels remain relatively stable, ranging from approximately 18 – 28 lx, at the lying position.

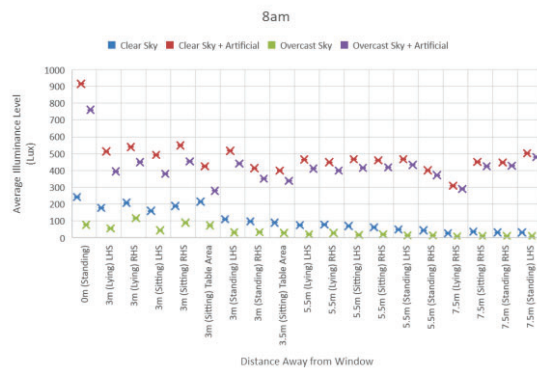


Figure 5. Illuminance Evaluation at 8am

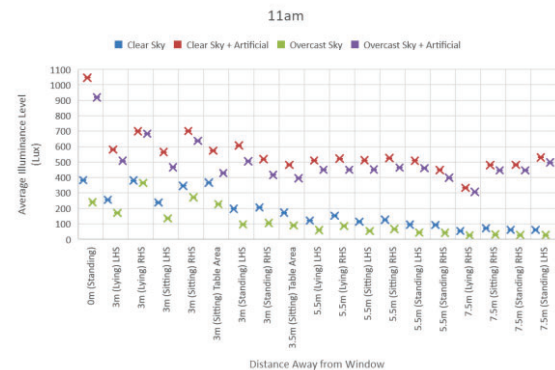


Figure 6. Illuminance Evaluation at 11am

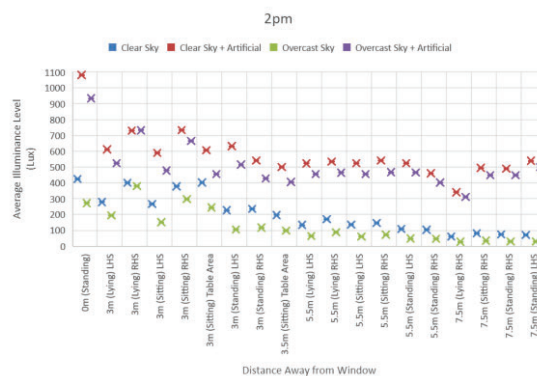


Figure 7. Illuminance Evaluation at 2pm

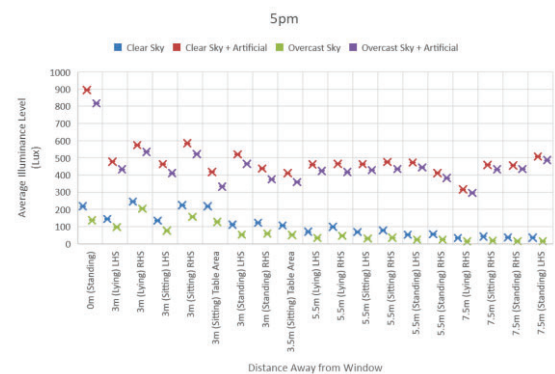


Figure 8. Illuminance Evaluation at 5pm

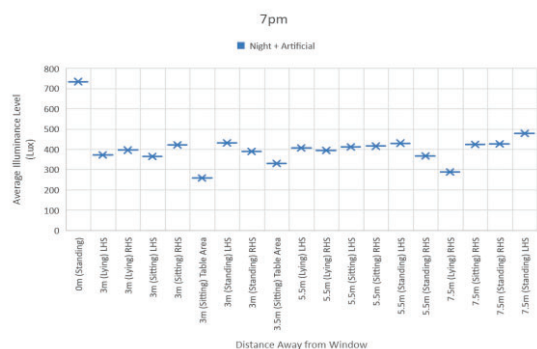


Figure 9. Illuminance Evaluation at 7pm

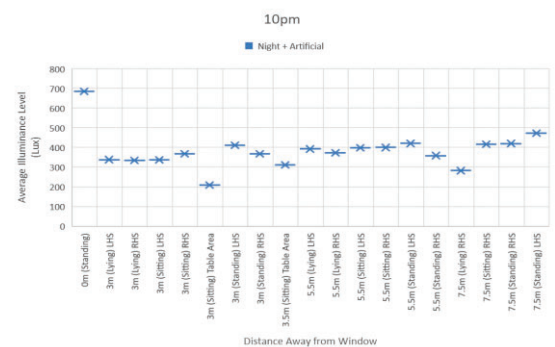


Figure 10. Illuminance Evaluation at 8pm



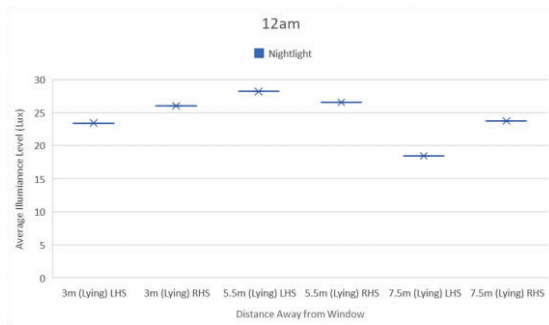


Figure 11. Illuminance Evaluation at 12am

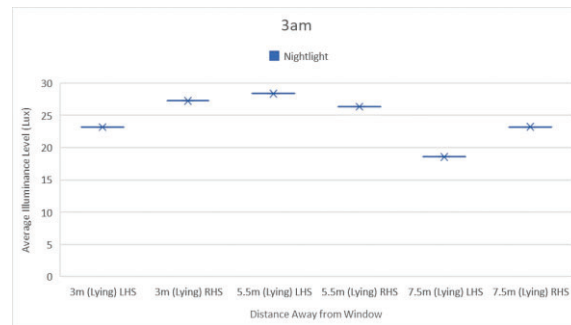


Figure 12. Illuminance Evaluation at 3am

### 3.2 Glare Evaluation

Figure 13 presents the mean annual daylight glare levels at an eye-level of 850mm. It shows approximately 2.2% of views are with disturbing glare for more than 5% of the year. Also, the results indicate that the top 3 rows the ward encounter intolerable glare (in red) ranging from 3% to 19% and disturbing glare (in orange) ranging from 3% to 24%. Figure 14 showcases the mean annual daylight glare at an eye-level of 1200mm. Based on the simulation results, it shows approximately 1.8% of views are with disturbing glare for more than 5% of the year. Also, the top 2 rows of the ward encounter intolerable glare (in red) ranging from 1% to 14% and disturbing glare (in orange) ranging from 1% to 3%. Figure 15 illustrates the mean annual daylight disturbing glare at an eye-level of 1600mm. The simulation results indicate that approximately 0.7% of views are with disturbing glare for more than 5% of the year. Similarly, the top 2 rows of the upper part of the ward encounter an intolerable glare (in red) ranging from 1% to 12% and disturbing glare (in orange) ranging from 1% to 2%.

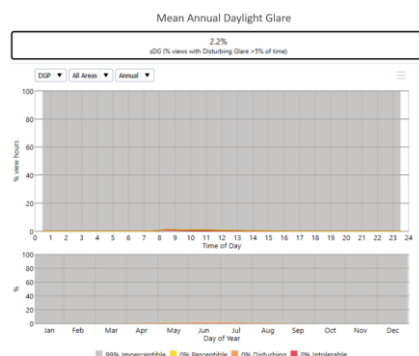


Figure 13. Glare Simulation Results (850mm)

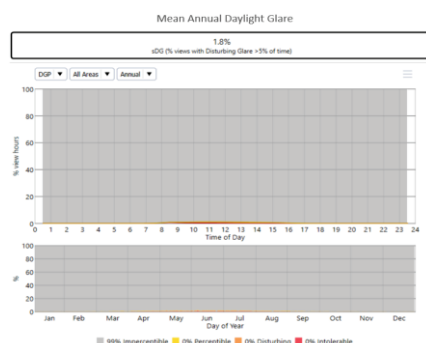
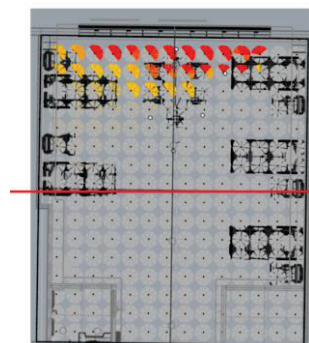
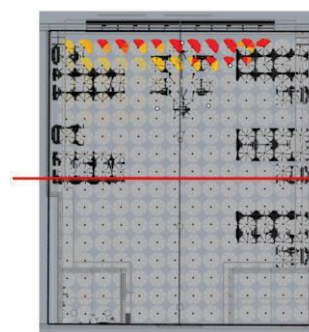


Figure 14. Glare Simulation Results (1200mm)





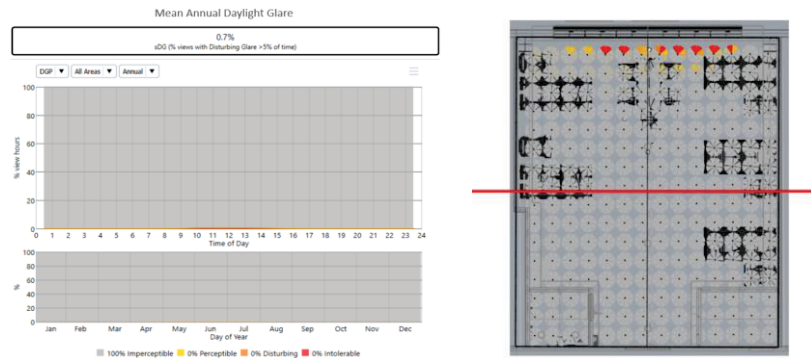


Figure 15. Glare Simulation Results (1600mm)

### 3.3 Agile multi-objective optimization tool

Figure 16 provides an overview of the agile multi-objective optimization tool for illuminance simulation using Grasshopper, Ladybug and Honeybee. As shown, some of the segment is not highlighted because it functions the same way as the yellow segment. Beginning with the red segmented section shown in Figure 17, this section is to define the furniture reflectance level, as well as, the simulation month, date and hours. All these information is to be connected to the yellow segmented section from “HBSurface” to “HBObjets”. Moving on to the orange segmented section depicted in Figure 18, the grid sensor point are defined. To accomplish this, the test geometry (in this case, the floor) is selected first. Then, the sensor grid size and eye-level position are determined. Additionally, the sky condition for the simulation is specified based on user requirements. Once these variables are defined, they are connected to the yellow segmented section under "analysisReceipe". Lastly, the yellow segment shown in Figure 19, integrates the information from red and orange segmented areas into “HBObjets” and “analysisReceipe”. Once the integration is completed, a toggle is included in this segment to run or stop the simulation. For the illuminance value, which is the desired result in this tool, a colour mesh can be shown on the model for visualisation purposes by linking the “illuminance\_values” to “\_analysisResult”.

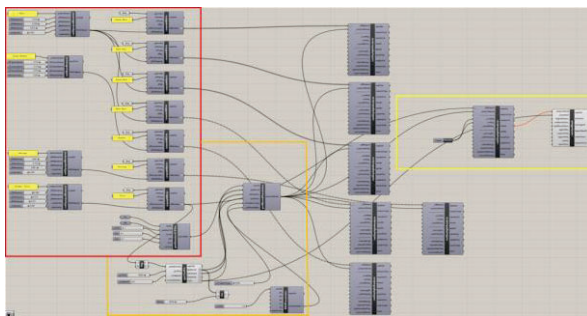


Figure 16. Overview of the agile multi-objective optimization tool

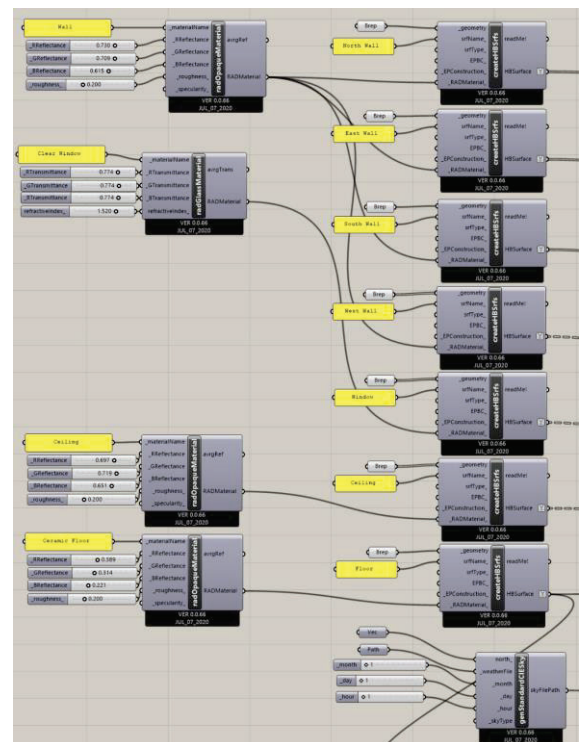


Figure 17 Red Segment of the tool

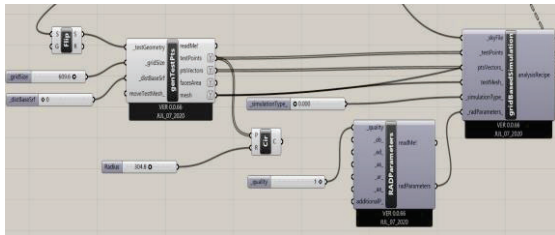


Figure 18 Orange Segment of the tool

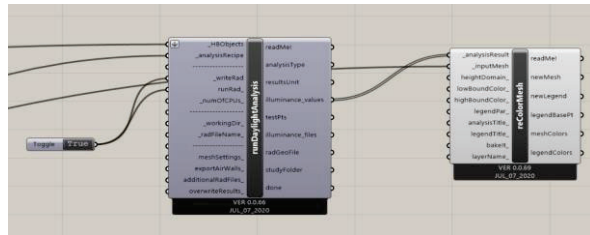


Figure 19 Yellow Segment of the tool

## 4. DISCUSSION

### 4.1 Comparison with Standards

With reference to Singapore Standards SS531, the daylight simulation results show that the average illuminance of the ward does not meet the requirement of 300 lx. However, without the provision of artificial light, the ward appears to be generally dim, which would affect the circadian rhythm of the patients. On the other hand, when considering daylight with the inclusion of artificial lights, the average illuminance throughout the entire ward falls within the range of 400 to 500 lx. Even though the illuminance values exceed the SS531 requirement, the occupants with special needs (e.g. the elderly) do require higher illuminance levels, about 50% more [7-8]. As such, the illuminance requirement for the elderly is approximately about 450 lx. However, it was noted that for points B2 and B1, some of the illuminance level does not meet the illuminance requirement for the elderly of 450 lx at 1200mm eye-level and 1600mm eye-level, especially during overcast sky situation. Contrastingly, for the rest of the 5 points; W1, W2, B3, B4, and B5, most of the illuminance levels exceed steeply, ranging from a minimum of 861 lx to a maximum of 2265 lx.

According to SLL night light standard, the average maintained illuminance level should not surpass 5 lux. In addition, the maximum permitted illuminance level measured within any points at the pillow area should be 0.5 lux, and the highest tolerated illumination level should not be higher than 10 lux. However, the ward night light result at 850mm (lying position) is around 20 lux which exceeds the standard requirement, which might result in discomfort to the patients and affect the patient's circadian rhythm.

### 4.2 Limitations and Ongoing Work

The study recognises that, due to the absence of better alternatives, the current study is compelled to compare the lighting conditions against existing standards, such as SS531 and SLL night light standards, despite their limitations. These standards specify the lighting requirements for healthcare workers to work comfortably but do not provide guidance on designing genuine human-centric lighting (HCL) systems. The concept of human-centric lighting encompasses both credible potential and unsubstantiated marketing claims, posing a challenge for designers to navigate. While environmental lighting is known to impact human health, there is a need for practical guidance in implementing human-centric lighting, which is currently lacking [9]. Moreover, this study suggests further discussion on the impact of lighting conditions on older adults and individuals with clinical conditions, aspects not adequately addressed by the existing standards. Additionally, collaborative efforts between academia, designers and hospital clinicians are required to identify design best practices and fill the gaps outlined by SS531.

## 5. CONCLUSION

In this research, a framework was constructed for evaluating the performance of healthcare lighting. Also, a set of simulation tools have been employed, including Rhino 7 and associated plugins such as ClimateStudio, grasshopper, ladybug, and honeybee. ClimateStudio served as the primary simulation tool, enabling a comprehensive assessment of the healthcare lighting performance. Based on the results, it can be summarised into 3 situations. Firstly, irrespective of the weather conditions, the illuminance situation in the ward lacks sufficient brightness. Secondly, when the artificial lights are activated, irrespective of the weather conditions, the average illuminance levels of the entire ward met the required level of 450 lx for the elderly. However, the various points indicate that the illuminance levels are excessively high, leading to glare, while others had illuminance levels that were too low. Lastly, the presence of

night lights was identified as a potential hindrance to achieving better sleep for the patients. This suggests that further attention should be given to the design and implementation of night lighting in order to create a more conducive and restful environment for patients during nighttime hours.

The agile multi-objective optimisation tool was employed to conduct simulations that aimed to replicate the results obtained from ClimateStudio. The focus was on developing computational codes to perform illuminance simulations using the tool. Additionally, other environmental analysis simulations, such as Sun Path Modeling and Direct Sun Analysis, were conducted to complement the results obtained from ClimateStudio. However, in order to further improve the program coding for illuminance simulation, additional studies on the software and its coding sequence are necessarily required. The complexity of the program coding sequence necessitates further investigation, refinement, and validation to enhance the present program coding. By continuously refining the computational codes, the accuracy and efficiency of the illuminance simulations could be improved, leading to more reliable and robust results for evaluating the performance of healthcare lighting in the tropical hospital ward. Furthermore, it is with the potentials to enable the identification of optimal lighting solutions balancing illuminance levels, glare control, and energy efficiency. By leveraging this tool, informed decision-making can be facilitated, supporting designers to consider data-driven scenarios for enhancing the lighting performance in the tropical hospital ward.

## REFERENCES

- [1] Strong, DTG., & Phil, D. "Daylight Benefits in Healthcare buildings." [designingbuildings.co.uk. https://www.designingbuildings.co.uk/w/images/2/22/David\\_Strong\\_%282of2%29Daylight\\_Benefits\\_in\\_Healthcare\\_buildings\\_TSB-BRE\\_v\\_1.pdf](https://www.designingbuildings.co.uk/w/images/2/22/David_Strong_%282of2%29Daylight_Benefits_in_Healthcare_buildings_TSB-BRE_v_1.pdf) (accessed Sep 16, 2022)
- [2] Naif, A. "The effect of hospitalization on patient's emotional and psychological well-being among adult patients: An integrative review." [pubmed.ncbi.nlm.nih.gov. https://pubmed.ncbi.nlm.nih.gov/34544571/](https://pubmed.ncbi.nlm.nih.gov/34544571/). (accessed Aug 15, 2022)
- [3] Columbia University. "How Sleep Deprivation Impacts Mental Health." [columbiapsychiatry.org. https://www.columbiapsychiatry.org/news/how-sleep-deprivation-affects-your-mental-health#:~:text=While%20insomnia%20can%20be%20a,anxiety%2C%20and%20even%20suicidal%20ideation.](https://www.columbiapsychiatry.org/news/how-sleep-deprivation-affects-your-mental-health#:~:text=While%20insomnia%20can%20be%20a,anxiety%2C%20and%20even%20suicidal%20ideation.) (accessed Sep 16, 2022)
- [4] Singapore Standard. "SS 531 – 1 : 2006 (2019) Code of practice for lighting of work places – Indoor." [singaporestandardseshop.sg. http://www.singaporestandardseshop.sg](http://www.singaporestandardseshop.sg). <http://www.singaporestandardseshop.sg.singaporetech.remotexts.co/Subscription/Product/Viewer> (accessed Sep 19, 2022)
- [5] Versant Health. "What Glare Is and How It Can Hurt Your Vision." [versanthealth.com. https://versanthealth.com/blog/understanding-glare-effect-on-your-vision/](https://versanthealth.com/blog/understanding-glare-effect-on-your-vision/) (accessed Oct 22, 2022)
- [6] ClimateStudio. "Annual Glare." ClimateStudio. <https://climatestudiodocs.com/docs/annualGlare.html> (accessed Oct 22, 2022).
- [7] Figueiro, M. G. (2001). *Lighting the Way, a Key to Independence*. Lighting Research Center, Rensselaer Polytechnic Institute. Retrieved from <https://www.lrc.rpi.edu/programs/lighthealth/aarp/pdf/aarpbook2.pdf>
- [8] Falkenberg, H. K., Kvikstad, T. M., & Eilertsen, G. (2019). Improved indoor lighting improved healthy aging at home - an intervention study in 77-year-old Norwegians. *Journal of Multidisciplinary Healthcare*, 12, 315-324. doi: 10.2147/JMDH.S198763.
- [9] Houser KW and Esposito T (2021) Human-Centric Lighting: Foundational Considerations and a Five-Step Design Process. *Front. Neurol.* 12:630553. doi: 10.3389/fneur.2021.630553

## ACKNOWLEDGEMENTS

This research is supported by the Singapore Ministry of Health's National Medical Research Council under its Clinician Innovator Development Award (MOH-000663-00).

Corresponding Author Name: Szu-Cheng CHIEN  
Affiliation: Singapore Institute of Technology  
e-mail: [SzuCheng.Chien@Singaporetech.edu.sg](mailto:SzuCheng.Chien@Singaporetech.edu.sg)

# DECOMPOSING LIGHT POLLUTION IN XICHONG INTERNATIONAL DARK SKY COMMUNITY USING ENCIRCLED AERIAL PHOTOS

Siyi Zhao, Junda Ma, Shengzhi Zou, Yan Zhang, Biao Yang

School of Architecture, Harbin Institute of Technology, Shenzhen, Guangdong, China

## ABSTRACT

As urbanization develops, the abuse of lighting occurs from time to time, causing serious light pollution. Promoting dark sky protection is an important way to prevent light pollution. Assessment of status light pollution in the community is essential in building a dark sky community. The aim of this paper is to quantify the extend of light pollution in the Xichong community and the impact of its various components on sky glow. There are eight villages in the Xichong International Dark Sky Community. One of them, Xinwu Village, which is closest to the Shenzhen Observatory, was selected as case. An unmanned aircraft sky quality meter was used to measure and record the nighttime light environment data of Xinwu Village. The processed luminance values of the light in each functional area and the sky luminance values were correlated to calculate the composition of sky glow. The results show that light sources with different emission angles produce different degrees of light pollution in different areas of the sky. The contribution of light from different functional areas to sky glow is also different. The order of contribution to the brightness of the sky is street lights, decorative lights, residential lights, commercial sign lights, and basketball court lights. With the change of time, the amount of light released by different functional areas of artificial light sources at different times will also change. The results of this paper are to be beneficial for the building of dark sky communities and dark sky protection in the future.

Key words: light pollution, dark sky community, sky quality meter, unmanned aircraft

## 1. INTRODUCTION

With the continuous improvement of people's living quality, people's requirements for the urban night environment are becoming higher and higher. There is a lot of light abuse in the city. There is a large amount of artificial light reflected to the sky in the urban nighttime light environment resulting in sky glow [1]. About 80% of the world's population now lives in a lightly polluted night sky [2]. The continuous disappearance of darkness not only has an impact on flora and fauna, but also alters the delicate balance of the environment with implications for the climate and for humans themselves [3]. Therefore, it is important to focus on the conservation of darkness and to plan and designate darkness reserves [4]. The American non-governmental organisation International Dark Sky Association (IDA) has proposed the International Dark Sky Places (IDSP) scheme to certify and delineate dark sky protected areas. Dark Sky Protected Areas include: International Dark Sky Sanctuaries, International Dark Sky Parks, International Dark Sky Reserves, Urban Night Sky Places and International Dark Sky Communities[5].

Unlike the other four categories, International Dark Sky Communities are usually located in towns and cities and also involve a much larger population. Therefore, the transformation into an International Dark Sky Community requires not only consultation with multiple parties, but also long-term supervision. There is also a greater variety of businesses and a more complex lighting environment than in other locations. The renovation and certification of the International Dark Sky Community will be influenced by its complex light environment.

The Xichong International Dark Sky Community, located in the first-tier city of Shenzhen, is the only international dark community in China, which can represent the current situation in the construction of dark communities in economically developed cities in China. The aim of this paper was therefore to investigate how to quantify the extent of light pollution in community and the impact of its various components on the glow of the sky, using the Xichong International Dark



Sky Community as an example. We anticipate that this knowledge will be helpful in making decisions about the priority of various light sources for treatment.

## 2. METHODS

### 2.1 Data measurement

The Xichong International Dark Sky Community consists of eight villages. The eight villages were visited and compared, and Xinwu Village was selected for the follow-up experiment. A drone was used to take aerial photographs of Xinwu village and a sky quality meter[6] was used to record the changes in night sky brightness throughout the night. The data collected during this experiment can be divided into aerial photography data from the UAV, sky brightness data from the SQM, sky image data from the imaging luminance meter, and data from the determination of the baseline road brightness value.

(1) UAV aerial image data: two sets of image data per hour, one set of overhead image data from multiple fixed points directly above Xinwu Village, and the other set of side overhead images from eight directions around Xinwu Village. Total 22 groups, 627 images.

The location of the first set of UAV overhead photography points is shown in Figure 1a. From 19:00 onwards, the drones set off once an hour at a uniform height of 150m to take overhead photographs of all parts of Xinwu Village. In order to ensure the quality of the subsequent image stitching, the overlap rate of the heading was not less than 65% and the overlap rate of the side direction was not less than 60%. The images obtained are shown in Figure 1b.

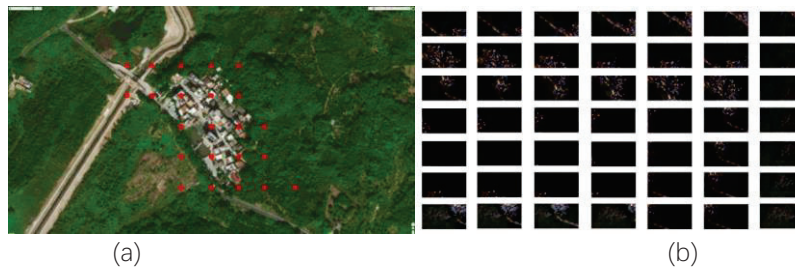


Figure 1 Aerial photography  
(a) fixed-point map, (b) Example of overhead view photo group

The locations of the second set of eight directional UAV side swoop photo points are shown in Figure 2a. In the eight directions of Xinwu village, east, southeast, west, southwest, south, northeast, north and northwest, about 150m from the centre of Xinwu village, at an altitude of 150m, with a pitch angle of 53°, facing Xinwu village to take pictures of the village, the images obtained are shown in Figure 2b.

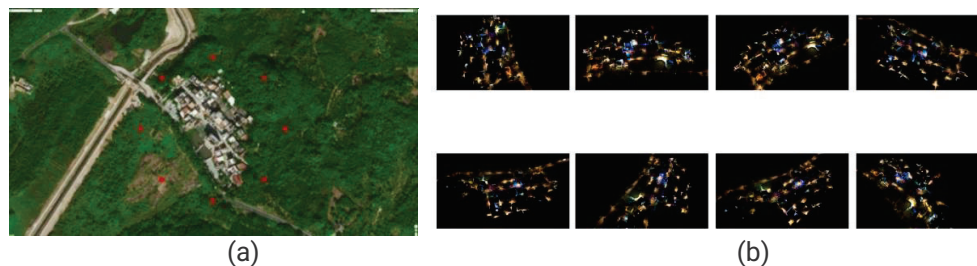


Figure 2 Aerial photography  
(a) fixed-point map in eight directions, (b) Example of photo group in eight directions

(2) SQM sky brightness data: SQM automatically measured the sky brightness conditions every five minutes from 19:00 until 5:00 the following day, for a total of 126 sets of data.

(3) Imaging luminance meter for sky image data: The imaging luminance meter was used to take real-time measurements of the sky using the instant image mode to confirm the weather conditions on the night of the experiment. As the sky brightness is influenced by the sky light, a



fully cloudy or sunny day has the least effect on the change of sky brightness, with a total of 22 sets of data.

(4) Baseline pavement luminance measurement data: A section of the pathway underneath the Pingshang Surfing Homestay was selected, with only street lighting on the pathway and no other artificial light sources interfering, and its pavement luminance value was measured at 5.2 cd/m<sup>2</sup>.

## 2.2 Data processing

### 2.2.1 2D reconstruction of top view

Import the top view photos taken by the drone every hour into DJI SmartMap software. The software will automatically generate the location of the aerial photography points, check the 2D map reconstruction, and enter the height of 150 m in the advanced settings, and the software will automatically reconstruct the aerial top view of the drone.

The top view photographs taken at each hour were reconstructed. The reconstruction results are shown in Figure 3.

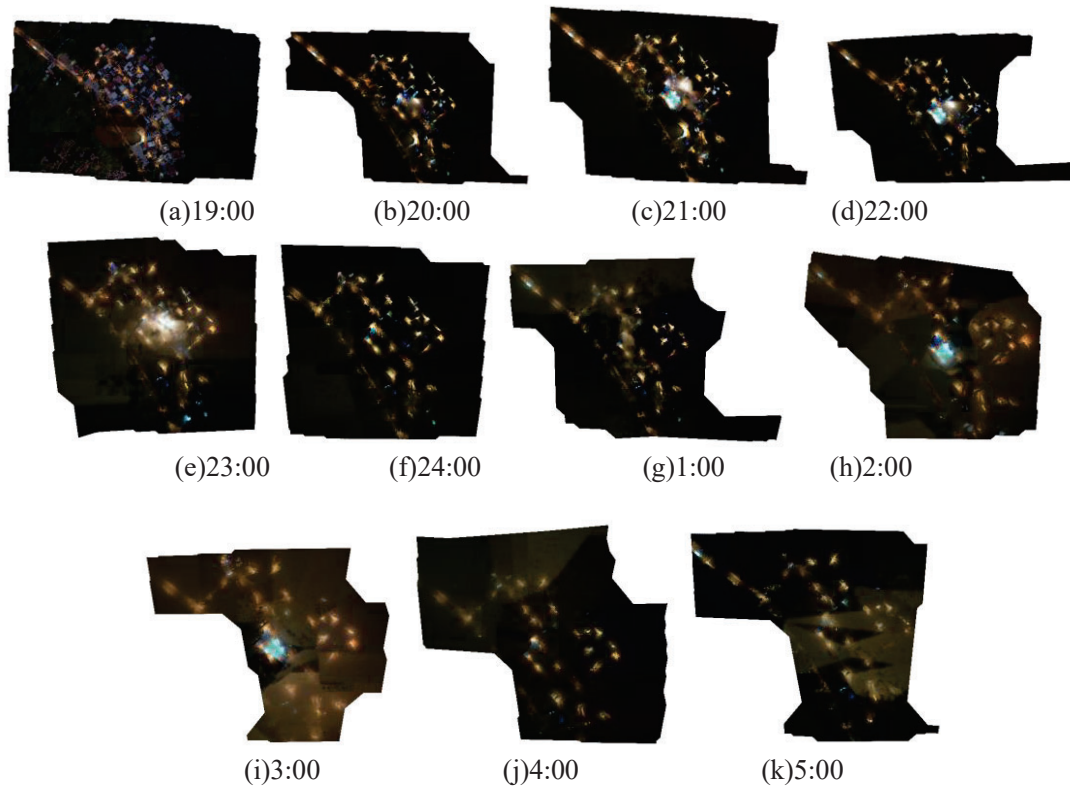


Figure 3 Overhead image after reconstruction

After the 2D reconstruction, the images obtained were further filtered. Due to the rain on the day after the experiment, which resulted in a foggy night on the day of the experiment, the reconstructed aerial data from 1:00-5:00 was not clear enough, which would affect the later analysis. And 19:00 near sunset sky brightness values are affected by sky light, so finally choose 20:00-24:00 total five groups of images for the subsequent study.

### 2.2.2 Artificial light source area circling

After two-dimensional reconstruction of the top view, the five sets of top views and the eight directions of aerial photography were used for artificial light source circling. According to the actual research situation in Xinwu Village, the artificial light sources on site were divided into five categories: street lights, decorative lights, commercial sign lights, residential lights and basketball court lights, as shown in Figure 4. The nighttime commercial lights were mainly defined as text-based signs used by shops, while the decorative lights were mainly defined as decorative coloured lights or light globes used by shops.

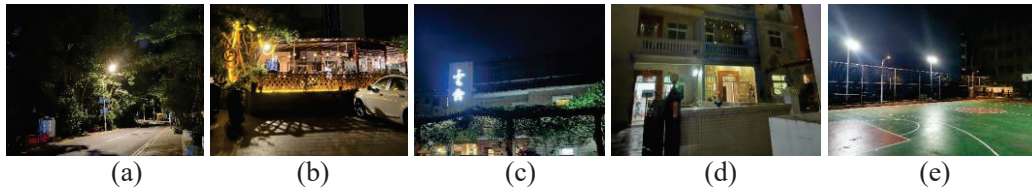


Figure 4 Five types of artificial light sources in Xinwu Village  
(a)Street light,(b)Decorative light,(c)Commercial sign light,(d)Residential light,(e)Basketball court light.

Import the top view and eight directions of the aerial photograph into the Photoshop software and manually circle the range of light emitted by each artificial light source in the picture, as shown in Figure 5.

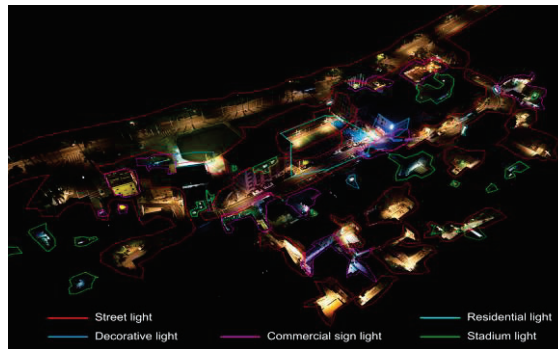


Figure 5 Example of artificial light source delineation

### 2.2.3 Image greyscale calculation and correction

Firstly, the photos obtained by the UAV were subjected to a light information crop acquisition operation. After conducting field research statistics and summarising, the author divided the types of lights into five categories, namely street lights, decorative lights, commercial sign lights, residential lights and Basketball court lights. In Photoshop, the different lights were intercepted to obtain png format pictures of the different lights. For the convenience of subsequent grey scale calculation, the output picture in this step has a horizontal to vertical ratio of 5:4, as shown in Figure 6.

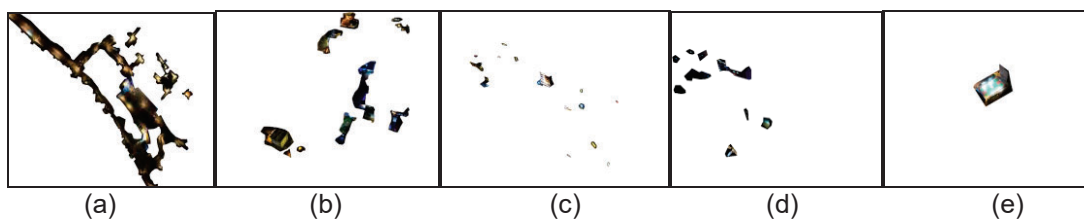


Figure 6 20:00 overhead view cutout images of various types of lights  
(a)Street light cutout image,(b)Decorative light cutout image (c)Commercial sign light cutout image,(d)Residential light cutout image,(e)Basketball court light cutout image

The grey scale is then calculated for a variety of lights taken in different orientations. On the one hand, there are two aspects to be considered when calculating the greyscale value of an image, on the other hand, there are two aspects to be considered, on the one hand, there is the problem of point selection, as there are too many pixel points in the image, this process requires a pixel selection design for the image, the image selection points can both cover the whole image evenly and reflect the effect of lighting on the greyscale of the area more accurately; on the other hand, there is the problem of data conversion, this step requires the operation to convert the colour information of the image into digital information, and according to the greyscale After a comprehensive comparison, Grasshopper programming can complete the job.

For this study, the number of sampling points was set to 500 horizontal and 400 vertical, for a total of 200,000 sampling points, based on the size of the intercepted image. The grey points were output as a decimal value between 0 and 1 according to the grey scale. The final output of the three data items for subsequent research is the number of points taken, the sum of the grey values and the average grey value.

After calculating the total and average greyscale values of the artificial light sources in different areas of all the aerial images, it was found that the average greyscale values obtained varied considerably between the different orientations of the photographs at different times. This was analysed and found to be due to the camera having different exposures and therefore the resulting grey values needed to be corrected. As the Basketball court lights were off at 20:00, 23:00 and 24:00, and as the Basketball court lights were on at 20:00, 23:00 and 24:00, the image of the stadium section contained enough pixel points and the light environment in the stadium was not affected by other artificial light sources, the overhead image at 20:00 was selected as the baseline image. After cropping out the stadium portion of the images from these three time periods, the average grey value of the stadium portion was again calculated, and the average grey value of the stadium from the 20:00 top view was used as a benchmark to grey-scale correct the other images from these three time periods. As the Basketball court lights were on at both 21:00 and 22:00, the images from these two time periods were first corrected using the average grey value of the stadium from the 21:00 top view as the base. Once the correction of the image data from 21:00 and 22:00 was complete, the 21:00 top view was then corrected using the 20:00 top view as the standard. Since the reference pavement appears in both images, the 21:00 top view was corrected using the reference pavement in the 20:00 top view as a benchmark, and the other 21:00 and 22:00 views were corrected together.

Conversion of image grey scale values into luminance values: On the day of the experiment the luminance value of the reference pavement was measured to be 5.2 cd/m<sup>2</sup>. In the top view image at 20:00, the average greyscale of the reference pavement is 0.81. It is therefore known that a greyscale value of 0.81 in the image is equivalent to 5.2 cd/m<sup>2</sup> in practice. The grey scale and luminance values of the artificial light sources in the different functional areas of all the images are therefore converted to obtain their luminance values in real life.

### 2.3 Data analysis

The background brightness of the sky in the darkest places on earth is about 22 mag/arcsec<sup>2</sup>, while in cities with brighter nighttime light conditions it is typically 16-17 mag/arcsec<sup>2</sup>. In order to convert SQM mpsas readings to cd/m<sup>2</sup>, the formula can be used:

$$\text{cd/m}^2 = 10.8 \times 10^4 \times 10^{(-0.4 \times [\text{mag/arcsec}^2])}$$

Converts all SQM measured sky brightness values into luminance values.

The SQM is known to have a field of view of 20 degrees, which indicates that it can measure a 20 degree cone of the sky directly above the instrument. Sky brightness values are affected by various artificial light sources on the ground, such as street lights, commercial lights, decorative lights, residential lights, etc. Because the effect of artificial light sources on sky brightness is affected by angle, in order to fully consider the effect of different angles on sky brightness, this paper selects nine angles for the same village for photographic recording: directly above, east, west, south, north, north-east, south-east, north-west and south-west, for each light, let its luminosity released to the sky be "b" and the luminosity released to the sky directly above be luminosity to the sky directly above is "b'" and the angle of view of the UAV to the horizontal is "θ", then the formula should be :

$$b' = b \times \sin \theta \quad (1)$$

The luminosity values emitted by the artificial light sources in the different functional areas of the nine photographs against the sky directly above were summed and averaged to obtain  $b_i$  :

$$b_i = \frac{b_1 + \sum_{j=2}^9 b_j'}{9} \quad (2)$$

Under either fully cloudy or fully sunny conditions, the sky brightness in a city will change as the light released into the sky from artificial light sources changes. Assuming that there are N different artificial light sources (e.g. street lights, decorative lights, commercial lights, residential

household lights, Basketball court lights, etc.) contributing to the overall sky brightness, the time course of the change in sky brightness,  $B(t)$ , expressed in units of luminance ( $\text{cd}/\text{m}^2$ ), can be written as

$$B(t) = \sum_{i=1}^N a_i b_i(t) \quad (3)$$

Here is the translation: "Where  $b_i(t)$ ,  $i=1, \dots, N$  are a set of functions describing the time process of emission from different types of light sources, and  $a_i$  are constants representing the relative contribution of artificial light sources in different functional areas recorded at the measurement location to the brightness of the sky. The normalization and units of " $a_i$ " and " $b_i(t)$ " can be freely chosen as long as their product in formula (1) has the correct brightness or luminance unit value. According to formula (1), the relative contribution of the  $k$ -th type of light source to the sky brightness at time  $t$ , " $P_k(t)$ ", is:"

$$P_k(t) = \frac{a_k b_k(t)}{\sum_{i=1}^N a_i b_i(t)} \quad (4)$$

Given the known constants  $a_i$  and the time-indicating function  $b_i(t)$ ,  $i=1, \dots, N$ , the relative contribution " $P_k(t)$ " at any time during the night can be directly obtained through formula (2).

### 3. RESULTS

#### 3.1 The contribution of light sources with different emission angles to sky glow:

First, the average gray values calculated from the artificial light sources in different functional areas in the 45 images are analyzed. Taking 20:00 as an example, the average brightness values calculated from the artificial light sources in different functional areas within the images at different angles are different, as shown in Figure 7.

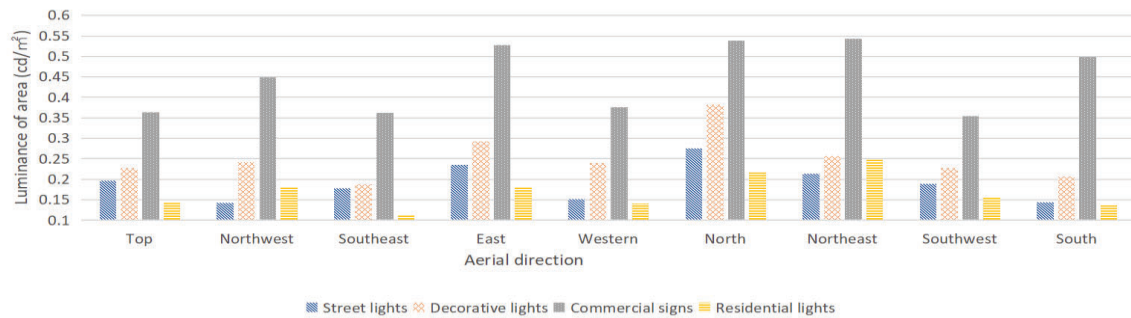


Figure 7 The average brightness value of artificial light sources in different functional areas within pictures from different angles

It can be seen that by taking photos of the artificial light sources on the ground of Xinwu Village from different angles, the average brightness of the artificial light sources in different functional areas at different angles can be calculated, and the final results show obvious differences. This is because when observing the ground from different angles, the situation of the artificial light sources on the ground that can be observed is different, as shown in Figure 8.

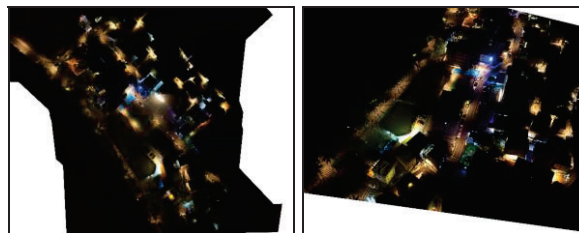


Figure 8 Comparison of the top view and top oblique photograph in the northeast direction at 20:00

This indicates that the results obtained from observing light sources with different emission angles from different angles are different. Therefore, in order to calculate the contribution of artificial light sources of different functions in a certain area to sky glow, it is not possible to observe and calculate from a single angle. The observation angle should be comprehensive enough.

### 3.2 Contribution of light from different functional areas to sky glow:

An experiment was conducted in Xinwu Village, Xichong International Dark Sky Community, from the night of May 6 to May 7, 2023. The sky brightness measurement location was selected on the roof of the Pingshang Surfing Homestay in the middle of Xinwu Village. SQM readings were recorded every five minutes, and the light information released by artificial light sources was obtained through drone aerial photography, with two sets of photos recorded every hour. After processing, nine photos were obtained every hour, including one overhead shot of Xinwu Village and eight side shots from eight directions around Xinwu Village. After calculating, the average brightness of the upwardly released light from artificial light sources in different functional areas in the nine images per hour was obtained. After converting the SQM values measured at each hourly aerial photography time point into brightness values, Figure 9 was obtained.

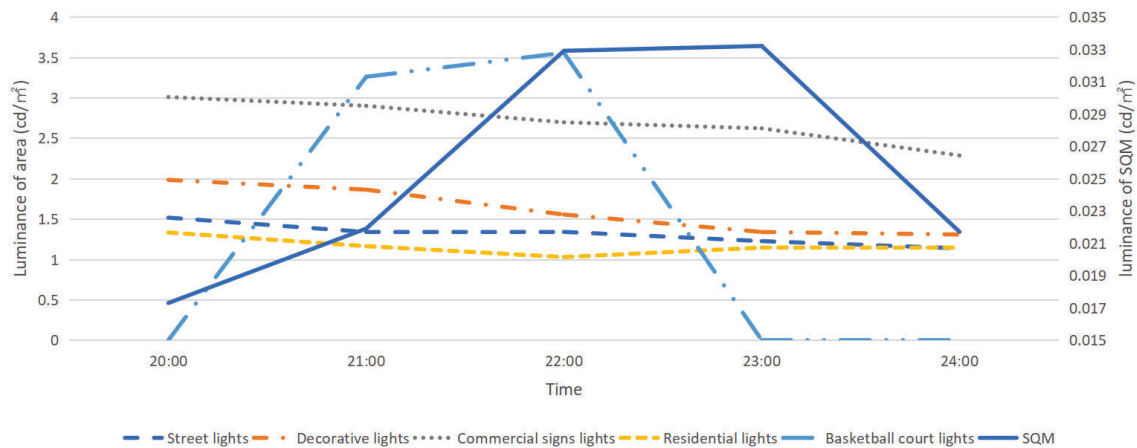


Figure 9 Average brightness line chart

Analyzing Figure 9, the Basketball court lights fluctuate greatly in a short period of time, which is due to the interference of human control. From 21:00 to 22:00, the stadium was in use and the Basketball court lights were turned on, causing a sudden change in the data. The average brightness of the decorative lights began to decline at 23:00, which was due to the gradual closing of stores after 23:00 and the turning off of decorative lights. It can also be seen from the figure that the average brightness of street lights showed a downward trend at 22:00, but the status of street lights did not change throughout the night. The author speculates that this is due to the large amount of light from decorative lights and commercial lights being projected onto the road surface before 22:00, causing the average brightness value of the road surface to increase. However, after 22:00, decorative lights gradually turned off and the road surface was no longer disturbed by light released by other artificial light sources, and the average brightness on the road surface returned to normal levels.

The linear fitting coefficients (representing the degree of influence of this type of light source on sky glow) of artificial light sources in different functional areas were calculated to be 0.0599, 0.0458, 0.0107, 0.0152, and 0.003 respectively. It can be seen that street lights have the greatest impact on sky brightness, followed by decorative lights, residential lights, commercial sign lights, and basketball court lights have the least impact.

The proportion of stray light from artificial light sources in different functional areas at different time periods is shown in Figure 10.



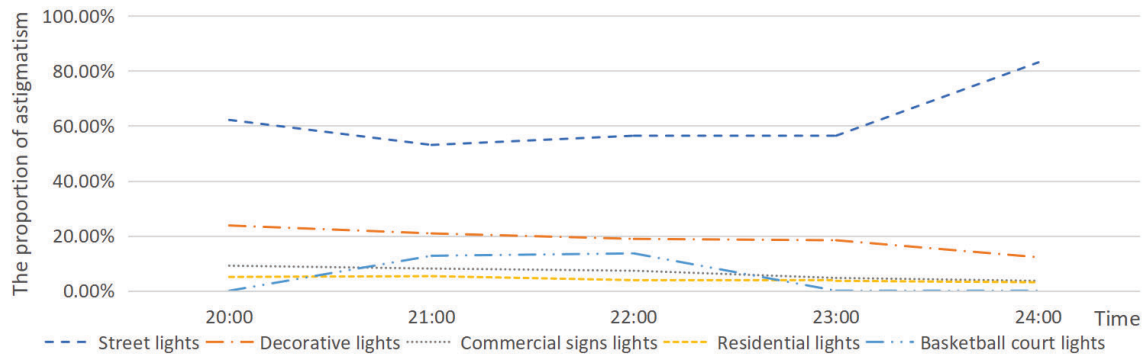


Figure 10 Proportion chart of stray light from artificial light sources in different functional areas at different time periods

As shown in Figure 12, the proportion of decorative lights and commercial lights began to steadily decline from 23:00, and the proportion of residential lights began to decline from 22:00. The proportion of artificial light sources in other functional areas showed a gradual downward trend. Since the light released by street lights is constant, the relative weight of the light released by street lights shows a gradually increasing trend. The Basketball court lights were turned on at 21:00, and at this time the light they released upwards accounted for 12.72% of the total amount of light released upwards by all artificial light sources on the ground.

At 24:00, the relative weight of the light released upwards by street lights was the largest, accounting for 83.09% of the total amount of light released upwards by artificial light sources on the ground. At this time, the contribution weight of commercial lights was the smallest, accounting for only 1.66%.

#### 4. CONCLUSIONS

This article uses drone aerial photography to decompose the current situation of light pollution in the Xichong International Dark Sky Community, and explores the degree to which various artificial light sources in the Xichong International Dark Sky Community affect sky brightness and the relationship between different emission angles of light sources and sky glow. The main conclusions are as follows. The contributions of light sources with different emission angles to sky glow are different, and the contributions of different types of light to sky glow are also different. The order of contribution to sky glow is street lights, decorative lights, residential lights, commercial sign lights, and basketball court lights. During the experiment, it was also found that some wall-washing lights used by some stores in the Xichong International Dark Sky Community caused serious light pollution to the sky. The conclusions of this study can be used to guide the transformation of subsequent dark sky communities.

#### REFERENCES

- [1] Davies T W, Bennie J, Inger R, et al. Artificial light alters natural regimes of night-time sky brightness[J]. Scientific Reports, 2013,3(1).
- [2] Falchi F, Cinzano P, Dan D, et al. The new world atlas of artificial night sky brightness[J]. Science Advances, 2016,2(6):e1600377.
- [3] Barentine J. Going for the Gold : Quantifying and Ranking Visual Night Sky Quality in International Dark Sky Places[J]. International journal of sustainable lighting (Online), 2016,18:9-15.
- [4] Yang Yanmei, Feng Kai, Liang Zheng. Dark Night Protection from Urban Lighting Planning: China Lighting Forum 2017 - Forum on Innovative Applications of Semiconductor Lighting and Smart Lighting Development, Chengdu, Sichuan, China, 2017[C].
- [5] International Dark Sky Association-DarkSky International[EB/OL]. <https://www.darksky.org/>.
- [6] Unihedron. Grimsby, Ontario, Canada. Available online[EB/OL]. <http://unihedron.com/projects/darksky/faqsqml.php>.

## **ACKNOWLEDGEMENTS**

Corresponding Author Name: Biao Yang

Affiliation: School of Architecture, Harbin Institute of Technology, Shenzhen

e-mail: yangbiao@hit.edu.cn

# EFFECTS OF LIGHTING DIFFUSENESS AND OBJECT SHAPE ON SURFACE APPEARANCE

Akira Kudo<sup>1</sup>, Yoshinori Dobashi<sup>2</sup>, Hiromi.Y Sato<sup>3</sup>, Yoko Mizokami<sup>3</sup>

(<sup>1</sup> Graduate School of Science and Engineering, Chiba University, Chiba Japan, <sup>2</sup> Graduate School of Information Science and Technology, Hokkaido University, Hokkaido, Japan,

<sup>3</sup> Graduate School of Engineering, Chiba University, Chiba, Japan)

## ABSTRACT

This study investigates the influence of surface bumpiness shape and lighting diffuseness on surface appearance reproduction by evaluating the impression of object appearance and the ideal appearance of the object. Lighting with medium lighting diffuseness close to natural lighting conditions yielded higher reproducibility than those with low and high diffuseness. This effect is more evident for the objects with higher surface bumpiness frequency in the case of gold but not plastic objects. This suggests that the influence of surface bumpiness for appearance under different lighting diffuseness may be critical for objects with very high specular components.

Keywords: Material appearance, Object shape, Lighting diffuseness

## 1. INTRODUCTION

The perception of material appearance is mainly influenced by three elements: material characteristics, an object's shape, and lighting conditions. Mizushima et al. [1] demonstrated that the perceived surface appearance of memorized objects is faithfully reproduced under lighting with medium diffuseness. Furthermore, our previous study [2] showed that the surface appearance could be enhanced by manipulating the surface shape of objects. However, the relationship between surface properties and surface appearance remains unclear.

This study investigates how object surface shape and photometric properties influence surface appearance when evaluating suitable lighting diffuseness for surface appearance reproduction.

## 2. EXPERIMENT

The experimental stimuli were created using Computer Graphics (CG). They consisted of three different materials, various shape variations with different surface bumpiness, and three types of environmental maps. We used MAYA for the CG modeling and Mitsuba for rendering. The stimuli were three types of materials: gold, plastic, and rough plastic, as shown in the left part of Figure 1. These materials were preset models in Mitsuba. The image resolution was 640 x 360 pixels. The surface's roughness was created by randomly moving each triangular mesh vertex in the normal vector's direction, as shown in the middle part of Figure 1. This moving method was determined using parameters from Perlin noise, which outputs corresponding three-dimensional coordinates ( $x'$ ,  $y'$ ,  $z'$ ) to input three-dimensional coordinates ( $x$ ,  $y$ ,  $z$ ). Perlin noise gives the shape with  $n$  peaks and valleys per centimeter when the frequency is  $n$ . The noise amplitude was set to 1, causing variation in the normal direction from -1 to 1. We refer to the frequency of created bumpiness as "bumpiness frequency." Additionally, three types of environment maps with naturalistic lighting diffuseness (0.55, 0.65, and 0.71) were prepared, as shown in the right part of Figure 1.

The environment shown in Figure 2 was created in CG to produce the images under various lighting diffuseness levels for evaluation, as shown in Figure 3. Inside a sphere with a radius of 20 cm, a point light source was placed 10 cm above the bottom surface. An experimental stimulus with a radius of 1 cm was positioned on the bottom surface. Seven levels of diffuseness (0.19, 0.26, 0.39, 0.54, 0.66, 0.79, and 0.91) were achieved by varying the reflectance of the sphere's inner wall.

It should be noted that there is no internationally established standard for lighting diffuseness. Therefore, we used the concept of diffuseness defined by Xia et al. [3], based on the illuminance measurement values of a cube according to Cuttle's definition [4]. The range of diffuseness values

is from the minimum value of 0 to the maximum value of 1. The detailed calculation method is as follows. First, the luminance from the six directions is measured (tilt angle  $+35^\circ$ , rotation angle  $0^\circ$  [ $E_{(u+)}$ ],  $120^\circ$  [ $E_{(v+)}$ ],  $240^\circ$  [ $E_{(w+)}$ ], tilt angle  $-35^\circ$ , rotation angle  $60^\circ$  [ $E_{(u-)}$ ],  $180^\circ$  [ $E_{(v-)}$ ],  $300^\circ$  [ $E_{(w-)}$ ]). The lighting vector components of the  $u$ ,  $v$ , and  $w$  axes are determined using equations (1), (2), and (3).

$$E_{(u)} = E_{(u+)} - E_{(u-)} \quad (1)$$

$$E_{(v)} = E_{(v+)} - E_{(v-)} \quad (2)$$

$$E_{(w)} = E_{(w+)} - E_{(w-)} \quad (3)$$

The magnitudes of the lighting vectors along the  $u$ ,  $v$ , and  $w$  axes are calculated using equation (4).

$$|E| = \sqrt{(E_{(u)}^2 + E_{(v)}^2 + E_{(w)}^2)} \quad (4)$$

The target components are derived from equations (5), (6), and (7), and the target illuminance is derived from equation (8).

$$\sim E_{(u)} = \frac{E_{(u+)} + E_{(u-)} - |E_{(u)}|}{2} \quad (5)$$

$$\sim E_{(v)} = \frac{E_{(v+)} + E_{(v-)} - |E_{(v)}|}{2} \quad (6)$$

$$\sim E_{(w)} = \frac{E_{(w+)} + E_{(w-)} - |E_{(w)}|}{2} \quad (7)$$

$$\sim E = \frac{\sim E_{(u)} + \sim E_{(v)} + \sim E_{(w)}}{3} \quad (8)$$

The scalar illuminance is then determined using equation (9), and the diffuseness is derived using equation (10).

$$E_{sr} = \sim E + \frac{|E|}{4} \quad (9)$$

$$D_{cuttle} = 1 - \frac{|E|}{4E_{sr}} \quad (10)$$








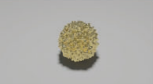

Material		Shape (bumpiness frequency)		Environment map (diffuseness)	
	<b>Plastic</b>		<b>0.5</b>		<b>0.55</b>
	<b>Rough Plastic</b>		<b>1.0</b>		<b>0.65</b>
	<b>Gold</b>		<b>2.0</b>		<b>0.71</b>

Figure 1. Experimental stimuli and environment maps

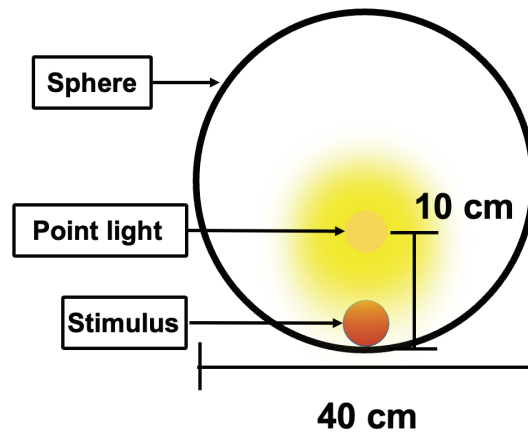


Figure 2. Method of creating lighting evaluation images

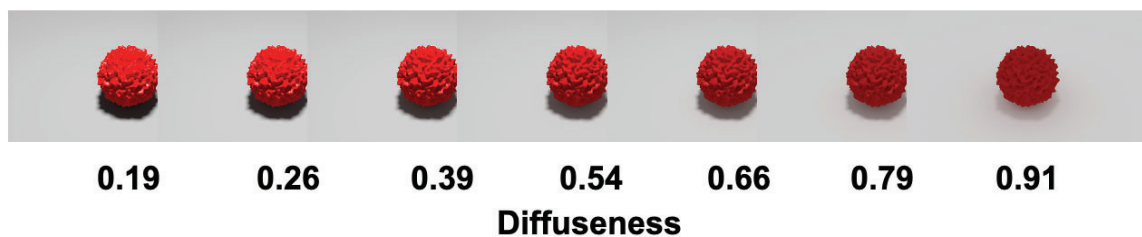


Figure 3. Examples of lighting evaluation images under different lighting diffuseness (Plastic, Bumpiness frequency 2.0)

The experiment was conducted using a 24.1-inch liquid crystal display in a darkroom. Participants observed stimuli images on the display with a viewing distance of 45 cm. The experimental procedure consisted of a preliminary observation part for object observation and pre-evaluation in three natural environment conditions conducted over two days and a lighting evaluation part under varied lighting diffuseness conducted over three days. During the object observation for memorizing the surface appearance, participants could observe images from six directions under three different environmental map conditions. In the lighting evaluation experiment, participants evaluated the appearance of one of the stimuli placed inside a sphere under seven levels of diffuseness.

The procedure for each part was as follows:

#### 1. Preliminary Object Observation Part

Participants freely observed each object for one minute from 6 directions (front, right, left, upper front, upper right, and upper left) to memorize the intrinsic surface appearance of each object.

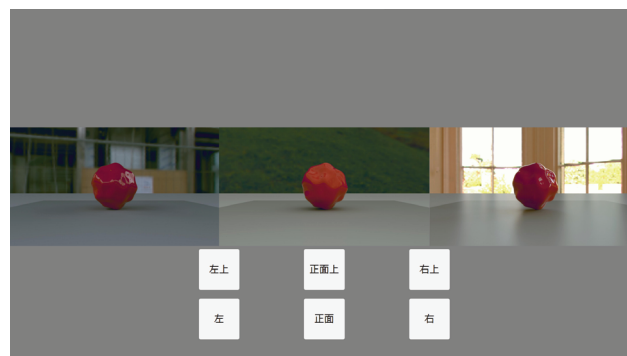


Figure 4. Display of presentation at object observation



## 2. Pre-Evaluation Part

Following dark, light, and gray background adaptation for 30 seconds each, participants evaluated the horizontally oriented images used in the object observation using a 7-point scale (-3 to +3 with a step size of 0.5) for ten evaluation factors: transparency, roughness, glossiness, brightness, hardness, heaviness, visibility, preference, value, and naturalness.

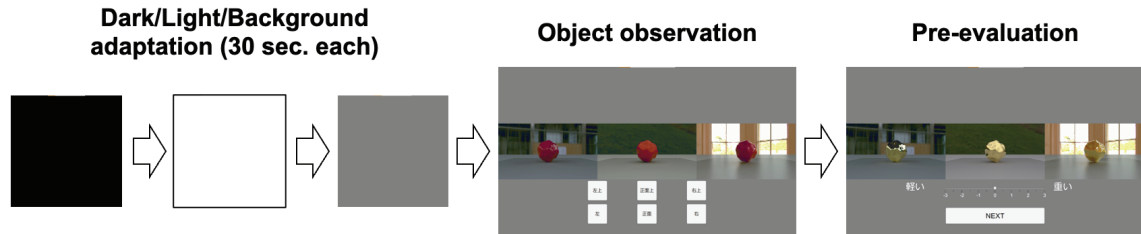


Figure 5. Pre-evaluation part procedure

## 3. Lighting Evaluation Part

Participants evaluated the images of objects under seven lighting diffuseness levels. In addition to the ten evaluation factors from the pre-evaluation, they also evaluated the fidelity and ideality of surface appearance reproduction. Participants were instructed to assess the degree of fidelity to the memorized surface appearance in the fidelity evaluation and the degree of the surface appearance's ideality as representing the object's intrinsic property in the ideality evaluation.

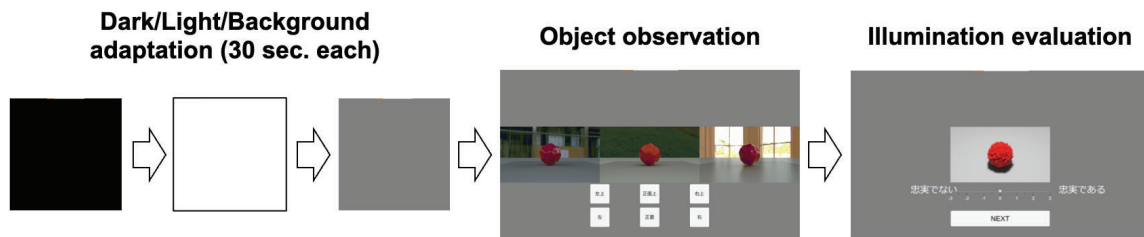


Figure 6. Lighting Part procedures

Five participants took part in the study. Each participant performed the preliminary object observation and pre-evaluation parts for two days, then the lighting evaluation for three days, one session each.

## 3. RESULTS AND DISCUSSION

Figures 7 and 8 show the average fidelity and ideality scores for each surface shape across all participants. The horizontal axis represents the lighting diffuseness, while the vertical axis represents the evaluation score. Error bars indicate the standard deviation. Like Mizushima et al. [1], fidelity and ideality evaluations were higher at medium than low or high diffuseness levels. Two-way ANOVA for lighting diffuseness showed significant effects for all three materials. (gold,  $F(6, 24) = 2.929$ ,  $p = .027$ ; plastic,  $F(6, 24) = 2.780$ ,  $p = .034$ ; rough plastic,  $F(6, 24) = 3.042$ ,  $p = .023$ )

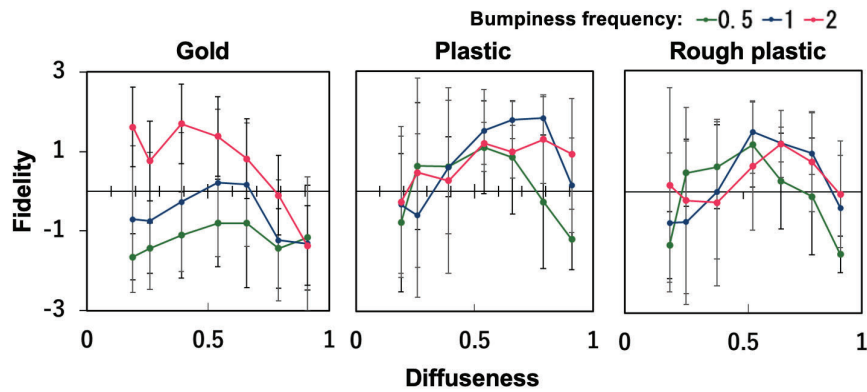


Figure 7. Relationship between lighting diffuseness and fidelity evaluation

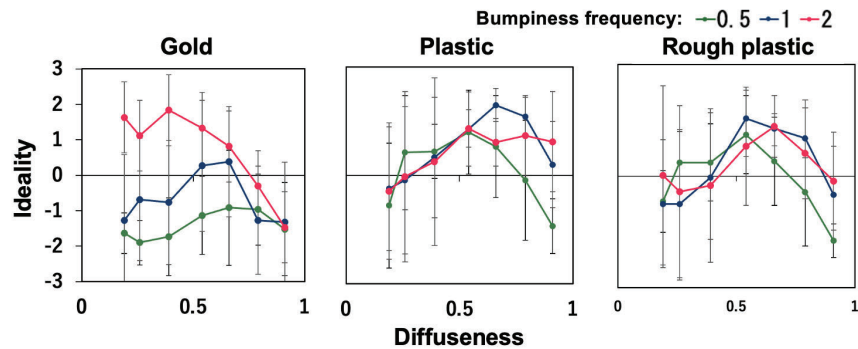
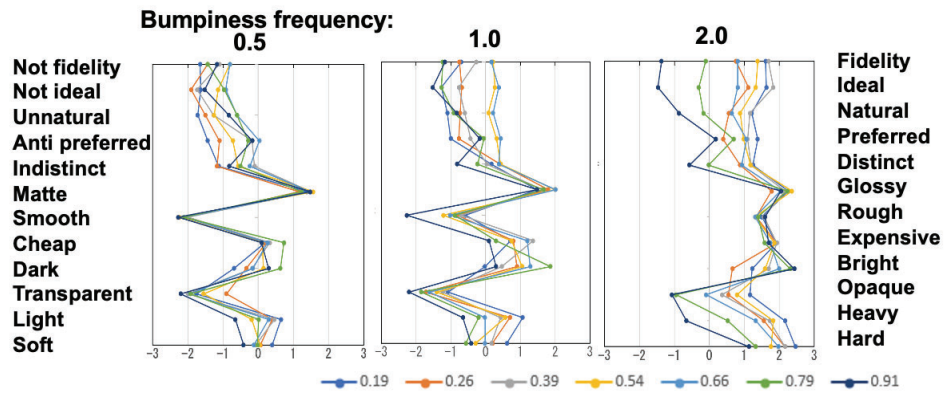


Figure 8. Relationship between lighting diffuseness and ideality evaluation

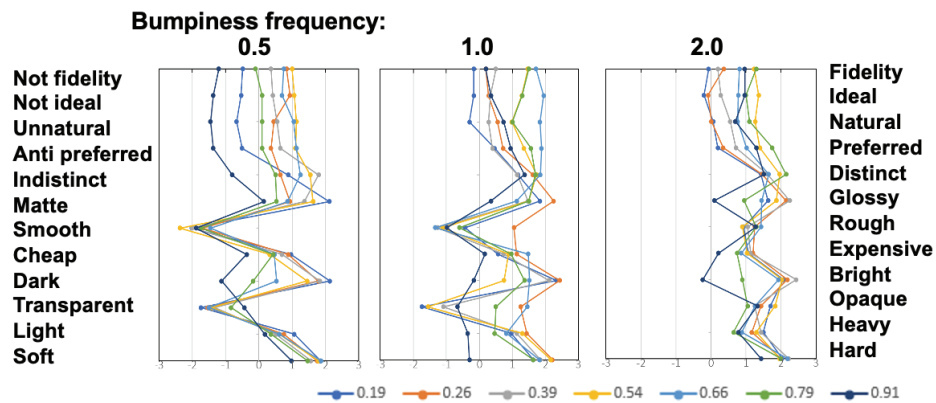
There were no clear differences in fidelity evaluation among different bumpiness frequencies for plastic and rough plastic. In the case of gold, fidelity evaluation increased with an increase in bumpiness frequency ( $F(2, 8) = 11.48, p < .05$ ). The interaction between bumpiness frequency and lighting diffuseness was significant ( $F(12, 48) = 1.958, p = 0.05$ ), suggesting that the influence of lighting diffuseness differs depending on the shape.

Furthermore, as shown in the impression evaluation results in Figure 9, gold exhibited significant variations in evaluations for factors such as roughness, transparency, and brightness based on surface shape. This suggests a shift in impressions depending on the shape.

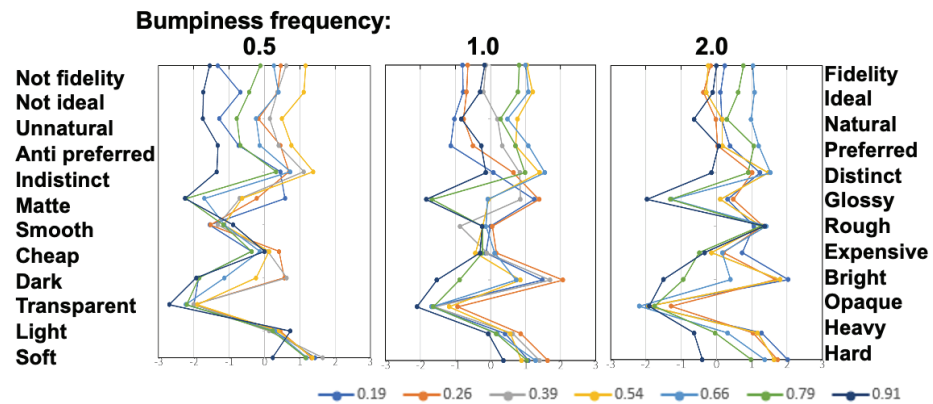
Our results suggest that the influence of surface bumpiness for appearance under different lighting diffuseness may be critical for objects with very high specular components. The multiple regression analysis of impression evaluations was performed to investigate the distinctive appearance of gold compared to other materials. The results indicated that as transparency decreased, both fidelity and ideality increased. Figure 10 shows the pixel heatmap and histogram of the gold and plastic for bumpiness frequency of 0.5 and 1.0 under medium diffuseness levels. The upper part of the object had lower luminance for gold, and the histogram showed a distribution towards lower luminance for the bumpiness frequency of 0.5 than that for 1.0. In contrast, plastic showed higher luminance in the upper part, and the histogram distribution is similar for bumpiness frequency of 0.5 and 1.0. These luminance distribution characteristics may affect the easiness of evaluating the differences in appearance due to lighting diffuseness.



a. Gold

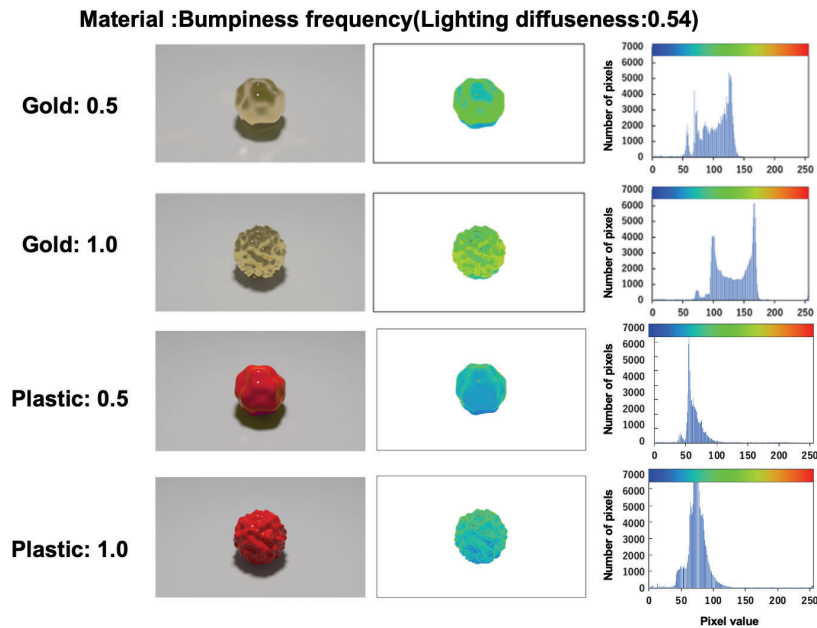


b. Plastic



c. Rough plastic

Figure 9. Results of impression evaluation



**Figure 10. Relationship between shape, material, and pixel histogram**

In summary, the surface appearance is faithfully reproduced under medium lighting diffuseness, and the influence of surface shape varies depending on the material. Specifically, the bumpiness frequency of the surface has a greater impact on fidelity for gold with high specular components. Therefore, it is necessary to consider the effects of material properties and surface shape on surface appearance reproduction.

## REFERENCE

- [1] Mizushima, S., & Mizokami, Y. Diffuseness of illumination suitable for reproducing a faithful and ideal appearance of an object. *Journal of the Optical Society of America A*, 2022, 39, 401-410.
- [2] Kudo, K., Dobashi, Y., Sato, H., & Mizokami, Y. Effect of object shape and lighting diffuseness on the reproducibility of object appearance. *Proc. of the Color Science Society of Japan Study Groups Meeting*, 2022, Nov., 37-39.
- [3] Xia, L., Pont, S. C., & Heynderickx, I. Diffuseness metric Part 1: Theory. *Lighting Research & Technology*, 2016, 49(4), 411-427.
- [4] Cuttle, C. Research note: A practical approach to cubic illuminance measurement. *Lighting Research and Technology*, 2013, 46(1), 31-34.

## ACKNOWLEDGEMENTS

Supported by JSPS KAKENHI JP19H04196.

Corresponding Author Name: Akira Kudo

Affiliation: Graduate School of Science and Engineering, Chiba University, Chiba Japan

e-mail: kudou.akiaki@chiba-u.jp

# BIRD RISK ASSESSMENT UNDER LIGHT POLLUTION IN URBAN ECOLOGICAL PATCH

Qingli Hao, Lixiong Wang, Gang Liu, Juan Yu

School of Architecture, Tianjin University, Tianjin, 300072, China

## ABSTRACT

The intensity and extent of artificial lighting at night are rapidly increasing, typified by urban ecological patches, altering the natural light environment where animals survive and thrive, thus creating a range of ecological risks. Nighttime remote sensing can provide the possibility to assess the ecological risk of light pollution on a large scale. However, in the light pollution evaluation studies, the light radiation data from remote sensing are inconsistent with the light environment evaluation indexes at the urban ecological level. In the case of birds, research on the evaluation of light pollution based on remote sensing did not establish a direct relationship with the behavior response of birds.

This paper explored the ecological risk assessment method, combining microscopic bird risk thresholds with macroscopic light pollution distribution data. First, at the micro level, we clarified the light risk thresholds to birds under light pollution stress. We proposed a technique for forecasting the risk thresholds of light intensity drawn from laboratory studies to those in outdoor light environments with compound spectral compositions, and estimated risk thresholds for light pollution to sleep behaviors of birds. Meanwhile, we obtained macroscopic light environment distribution data, Luojia 1-01 and Jinlin 1-07B. Using Yundang Lake in Xiamen, China, as a typical urban ecological patch, we combined microscopic bird risk thresholds and macroscopic artificial light data at night to evaluate and visualize the ecological risk of birds and analyze the ecological risk distribution characteristics under light pollution stress.

In the case of Eurasian Siskin and Chestnut Bunting, the results showed that: the irradiance risk thresholds were  $5 \text{ mW/m}^2$  ( $1.78 \text{ lx}$ ) and  $10 \text{ mW/m}^2$  ( $3.38 \text{ lx}$ ). Corresponding to the typical spectral energy distribution in Yundang Lake, the risk thresholds for the two species were  $118.28 \text{ nWcm}^{-2} \text{ sr}^{-1}$  and  $218.88 \text{ nWcm}^{-2} \text{ sr}^{-1}$  (radiation brightness of night light remote sensing), respectively. Thus, the preliminary correlation between nighttime remote sensing and ecological light pollution assessment was established. The method of ecological risk assessment proposed in this paper can provide a scientific and normative demonstration for research and techniques that support the rapid assessment of ecological risks by light pollution in large-scale urban areas.

Keywords: light pollution, ecological risk, birds, quantified threshold, risk assessment

## 1. INTRODUCTION

Light pollution generated by human activities is rapidly growing and expanding, invading ecological patches where birds survive and altering the nighttime light environment on which they depend[1]. Studies have shown that light pollution stress can alter the physiological rhythms of birds by affecting their perception of the light environment[2, 3]. Artificial light at night will continue to spread with urban expansion, and the impact on birds will continue to expand. Therefore, evaluating the ecological risk of birds caused by light pollution is necessary and urgent.

Both research directions have been studied, the micro-level "birds' behavior response to light stimulation" quantitative experiments and the macro-level light pollution ecological risk assessment. In experimental studies of artificial light stimulation, domestic and foreign scholars have obtained quantitative patterns between bird behavior and light environment properties (such as spectrum and illumination) [3, 4]. However, the evaluation index of the light environment in the experiment of "birds' behavior response to light stimulation" is inconsistent with the night light remote sensing image unit. At the same time, there are differences in the spectral energy distribution between the experimental light environment and the natural nighttime light environment, so the experimental conclusions can hardly fully reflect the influence of artificial light on birds in the urban environment. In macroscopic light pollution ecological risk assessment, nighttime light remote sensing provides the possibility to assess the ecological risk of light



pollution on a large scale. For example, combining nighttime light remote sensing data and bird data (such as the number of migratory birds, activity areas, or activity paths of birds) to explore the location, timing[5], and light pollution levels[6] of birds exposed to light pollution. However, the above ecological light pollution evaluation studies did not establish a direct relationship with the sensitive response characteristics of birds, and the light pollution class classification of urban areas using the natural breakpoint method may not reflect the degree of light pollution ecological risk faced by birds.

To address the shortcomings in the field of light pollution ecological risk evaluation, this paper explores the ecological risk thresholds of birds' sleeping rhythms under light pollution stress at the micro level, obtains macroscopic light pollution distribution data, and carries out ecological risk evaluation of urban ecological patches by combining the microscopic risk thresholds and macroscopic light pollution distribution data. This paper can provide methodological support for rapid diagnosis, evaluation, prevention, and control of ecological risks of urban light pollution.

## 2. METHODS

### 2.1 Quantification of ecological risk evaluation thresholds for light pollution

In this paper, we explored the irradiance thresholds of mixed light affecting the sleep behaviors of Eurasian Siskins and Chestnut Buntings. Previously, our research team conducted an experimental study on the sleep behaviors of birds under artificial light disturbance based on a standardized experimental method[7]. This experimental study used full-spectrum white and five spectral wavelengths (including violet, blue, green, yellow, and red-orange light) as experimental light sources, used three irradiances as experimental light intensity, and used four sleep parameters, including Sleep onset, Awakening time, Sleep duration and Frequency of awakenings, to measure the sleep behaviors. By summarizing the results of this experiment, we found the following pattern. For Eurasian Siskins, artificial light at 5 mW/m<sup>2</sup> delayed the Sleep onset, advanced the Awakening time, shortened Sleep duration by more than 1 h, and significantly increased the Frequency of awakening. When the light intensity increased from lower irradiance to 5 mW/m<sup>2</sup>, the four sleep parameters changed significantly; as the irradiance continued to increase, the trend of the parameters changed slowly. For Chestnut Buntings, artificial light at 10 mW/m<sup>2</sup> delayed the Sleep onset, shortened the Sleep duration by more than 1 h, and delayed the Awakening time, in contrast to the four parameters of artificial light at lower irradiance. By comparing the degree of combined effects of six light colors on sleep behavior parameters at different irradiances, we tentatively determined irradiance thresholds of 5 mW/m<sup>2</sup> and 10 mW/m<sup>2</sup> for Eurasian Siskins and Chestnut Buntings, respectively.

### 2.2 Conversion of ecological risk evaluation thresholds for light pollution to outdoor

The experimental scenes are difficult to reproduce the complex spectral distribution of the outdoor nighttime light environment. And the light environment evaluation parameters often used in experimental studies, such as illuminance (lx) and irradiance (mW/m<sup>2</sup>), are not consistent with the evaluation index of nighttime remote sensing data, radiance (nWcm<sup>-2</sup>sr<sup>-1</sup>). If we want to use the nighttime light remote sensing images for large-scale light pollution ecological risk evaluation, we need to convert the experimentally obtained irradiance thresholds into radiance thresholds by light intensity calibrations. Therefore, this paper proposed a method to estimate the radiance thresholds according to the irradiance thresholds of specific bird species consistent with the spectral energy distribution of the mixed light environment in the study area. The details are as follows:

1. Conduct laboratory monochromatic light radiance measurements.
  - In this paper, we use six customized monochromatic lights with precise peak band positions and more uniform distribution in the visible range, including Blue (448 nm), Cyan (501 nm), Lime (542-554 nm), Amber (594 nm), Red Orange (618 nm), and Red (660 nm). In the birds' sleep behavior experimental chamber, using the Topcon SR-3AR spectroradiometer, we measured the radiance of the diffusely reflective surface at the bottom of the chamber corresponding to six monochromatic lights with irradiances of 5 mW/m<sup>2</sup> and 10 mW/m<sup>2</sup>, respectively.
2. Determine the spectral energy distribution of the light environment in the study area.
  - The investigation found that road, architectural, and landscape lighting are the types of lighting that significantly impact the light environment at night. Using the Illuminance

Spectrophotometer CL-500A (Konica Minolta), we collected the spectral energy distribution of the nighttime light environment and obtained the typical spectral energy distribution characteristics.

3. Classify the representative bands of monochromatic lights.
  - We extracted the wavelengths at the five intersection points of the spectral energy distribution curves of the six monochromatic lights. Using the five intersection wavelengths as the boundary, we divided the visible light range (360–780 nm) into six representative bands. The monochromatic light with high spectral irradiance in each band is set as the main light so that the monochromatic lights correspond to the representative bands one by one.
4. Determine the energy weights occupied by each monochromatic light band in the spectral energy distribution of the light environment in the study area.
  - In the spectral energy distribution of the light environment in the experimental area, the ratio of the irradiance of the representative band to the total irradiance is used as the weight of the corresponding monochromatic light of the representative band.
5. Estimate the radiance thresholds consistent with the spectral energy distribution of the study area.
  - The monochromatic light weights obtained in step 4 are multiplied by the radiance values obtained in step 1 and summed to estimate the radiance thresholds that match the visible wavelengths of the real light environment.

### 2.3 Processing of nighttime light environment maps and light pollution risk maps

The light environment maps were obtained from the nighttime light remote sensing images acquired by the Luojia 1-01 satellite (LJ1-01) and the Jilin 1-7B satellite (JL1-07B), both with a spatial resolution of 130m[8] and 0.92m[6], respectively. Among them, the LJ1-01 images are from the Hubei High-Resolution Earth Observation System Data and Applications Network ([http://59.175.109.173:8888/app/login\\_zh.html](http://59.175.109.173:8888/app/login_zh.html), accessed on March 31, 2020), taken on August 21, 2018. The JL1-07B night-light remote sensing images were taken on April 9, 2020. The night-light remote sensing images were preprocessed, including median filtering, geometric correction, radiometric correction, and censored projection.

On the basis of the light environment maps, the risk thresholds of specific bird species were used as classification values for reclassification, and the study area was divided into safety and risk zones to obtain light pollution risk maps.

## 3. RESULTS

### 3.1 Demonstration study area

Xiamen, Fujian Province, is rich in bird resources, with 19.5% of the total number of bird species in China. The Eurasian Siskins and Chestnut Buntings are common songbirds in Xiamen. The Yundang Lake area (Figure 1), located in the west-central part of Xiamen Island, is a typical urban ecological patch and a haven for birds. It was found that all the areas shown in Figure 1a-e had frequent bird activity. Yundang Lake and its surroundings are the political, cultural, and financial center of Xiamen, with a high level of urbanization. Nighttime light pollution in the area is gradually becoming a potential risk factor affecting the survival of birds in the ecological patches. Therefore, this paper took the Yundang Lake area, a typical urban ecological patch, as a demonstration study area to explore how to combine macroscopic light pollution data with microscopic bird threshold data for ecological risk evaluation.

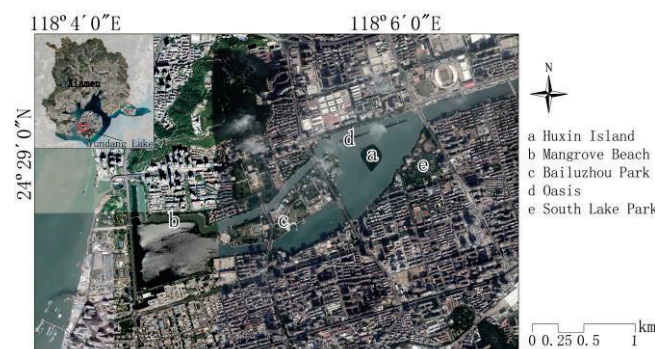


Figure 1. Map of Yundang Lake

### 3.2 Ecological risk evaluation thresholds for nighttime light pollution

The research found that the architectural lighting around Yundang Lake is the main source of light pollution. The intensity and vertical height of the building facade lighting in this area are high, significantly impacting the overall light environment. Therefore, the spectral distribution of the building lighting around Yundang Lake can represent the integrated spectral distribution of the region. Experimenters used CL-500A to collect the spectral energy distribution of the building lighting around the lake at the lake-center island (Figure 1a) to obtain the nighttime spectral energy distribution representing the Yundang Lake area (Figure 2).

According to the method proposed in section 2.2 for estimating the risk evaluation thresholds of the mixed spectrum, the final radiance thresholds conforming to the typical spectral energy distribution in the Yundang Lake were obtained: the radiance threshold corresponding to the artificial light risk threshold of 5 mW/m<sup>2</sup> for Eurasian Siskins was 118.28 nWcm<sup>-2</sup>sr<sup>-1</sup>, and the radiance threshold corresponding to the artificial light risk threshold of 10 mW/m<sup>2</sup> for Chestnut Buntings was 218.88 nWcm<sup>-2</sup>sr<sup>-1</sup>.

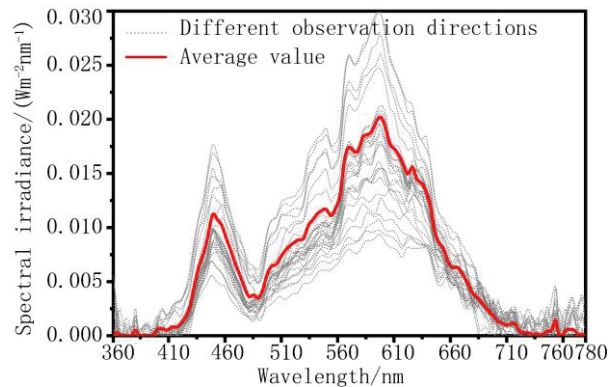


Figure 2. SPD of the nighttime light environment in Yundang Lake

### 3.3 Ecological risk evaluation

#### 3.3.1 Nighttime light environment maps and light pollution risk evaluation

The nighttime light environment map and the light pollution risk map are shown in Figure 3. Four typical areas of light pollution at night are selected in Figure 3e-g for municipal building lighting (Xiamen Municipal Government and People's Hall), h for residential building complex lighting, i for commercial building complex lighting (Wanxiang City), and j for road and landscape lighting around the lake.

As shown by the nighttime light environment maps (Figure 3), the distribution characteristics of the nighttime light environment in the Yundang Lake area are similar between the two types of nighttime light images. Concentrated lighting areas are formed around the roads and buildings, and local light pollution hotspots are formed in the building areas around the roads. The overall radiance level of the LJ1-01 map is higher than that of the JL1-07B due to the difference in resolution and the effect of spillover light. Taking the risk map of Chestnut Buntings as an example, the risk area of light pollution in the study area is 6.31 km<sup>2</sup>, as shown in LJ1-01, while the risk area is 0.96 km<sup>2</sup> as shown in JL1-07B. The area ratio of light environment risk overlap areas to JL1-07B risk areas is 84.0%, which shows that the two types of night light images are similar for identifying light pollution core risk areas.

JL1-07B night light image with high resolution can finely represent the nighttime lighting distribution, which is a good source of night light environment data at the urban area scale. Therefore, for the Yundang Lake in Xiamen, this paper described the bird risk areas with JL1-07B light pollution risk maps. The light pollution risk areas exceeding the risk threshold for Eurasian Siskins accounted for 24.6% of the study area, mainly from road lighting and decorative lighting of municipal, commercial, residential, and other building complexes. In contrast, the areas exceeding the risk threshold of Chestnut Bunting are relatively small, accounting for 6.9%, mainly from architectural decorative lighting and landscape lighting. This paper hypothesized that the high radiance areas that pose risks to the yellow finches and chestnut buntings are due to the lack of light interception measures for the lighting facilities.



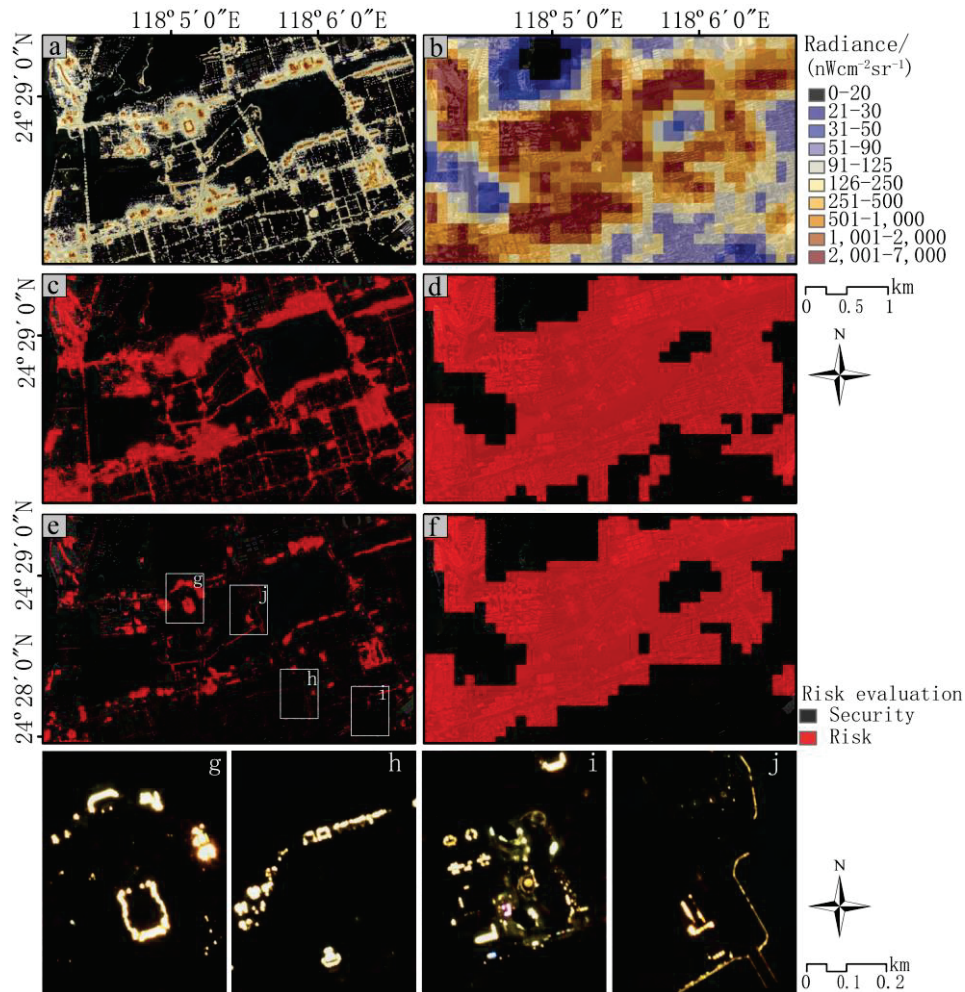


Figure 3. Light environment maps and light pollution risk maps of specific bird species

a: nighttime light environment map; b: LJ1-01 nighttime light environment map; c: JL1-07B light pollution risk map of Eurasian Siskin; d: LJ1-01 light pollution risk map of Eurasian Siskin; e: JL1-07B light pollution risk map of Chestnut Bunting; f: LJ1-01 light pollution risk map of Chestnut Bunting; g-j: JL1-07B images of selected typical light pollution area

### 3.3.2 Nighttime light pollution risk distribution pattern

Street lighting, architectural lighting, and landscape lighting are the types of lighting that need to be focused on, and the nighttime light levels of all three are closely related to the type of land use[9]. Exploring the relationship between urban land types and nighttime light pollution can help support the prevention and control of ecological light pollution and reduce ecological risks.

Based on satellite maps and field research, this paper obtained the distribution of land use types in the Yundang Lake area (Figure 4), including commercial, residential, administrative, greening, and other land use. Of these, residential accounts for the largest proportion, followed by commercial. To evaluate the contribution of different types of land use to nighttime light pollution, this paper superimposed the land use type map and JL1-07B nighttime image to calculate the total radiance of each patch, which is the sum of the radiance of all pixels within each patch (Figure 5 and Figure 7). According to the distribution maps and box plots of total radiance for each patch, it can be seen that among the five land use types, the total radiance of residential land is higher, followed by commercial. These two categories occupy a relatively large area and therefore contribute the most nighttime light to the overall light environment. Administrative, green, and other categories occupy a relatively small proportion of the area and contribute relatively little to light pollution. In order to distinguish the light intensity of different land uses, we further calculated the average irradiance of each land use patch (Figure 6 and Figure 8). The average radiance is the ratio of the total radiance of each patch to the total number of pixels. The results showed that the average radiance level of commercial land was the highest; administrative land

was the second highest, with localized over-bright lighting; and the light intensity of residential was relatively balanced.

In this paper, we calculated the percentage of light pollution risk areas in the five types of functional areas for the Eurasian Siskins and Chestnut Buntings (that is, the ratios of the areas exceeding the thresholds to the total area in each type of land use, Figure 9). The percentages of risk areas in the five land uses differed significantly between the Eurasian Siskins and Chestnut Buntings, but the general trend was consistent. Among them, commercial and administrative areas had the highest percentage over the threshold. For commercial areas, the percentages of risk areas for Eurasian Siskins and Chestnut Buntings were 55.0% and 24.9%, respectively; for administrative areas, the percentages were 44.8% and 19.4%, respectively. Secondly, the percentages of risk areas in residential areas are also relatively high, with 34.5% and 10.4% of risk areas in Eurasian Siskins and Chestnut Buntings, respectively. We speculated that this is due to unreasonable lighting outside buildings and landscapes in commercial and administrative areas, resulting in artificial light shining directly into the sky at night or shining onto building surfaces and pavement and reflecting into the sky, which is captured by satellite sensors. It was also found that most of the residences in the study area are high-rise buildings with widespread top decorative lighting and a lack of light-cutting measures.

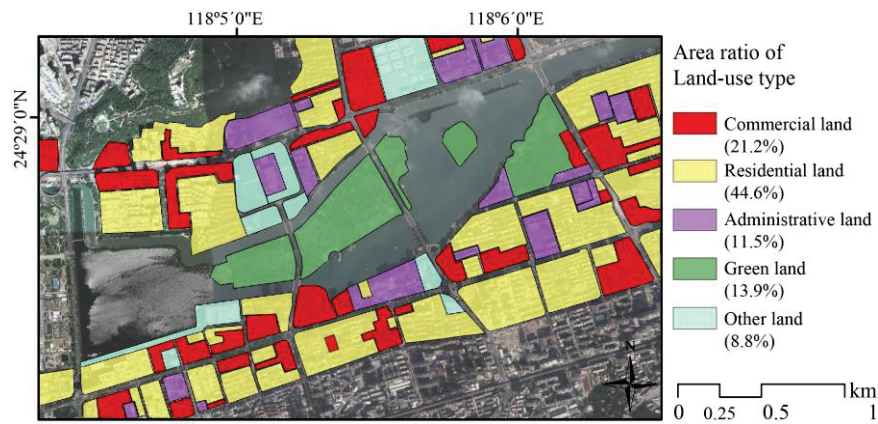


Figure 4. Urban land use distribution map in the study area

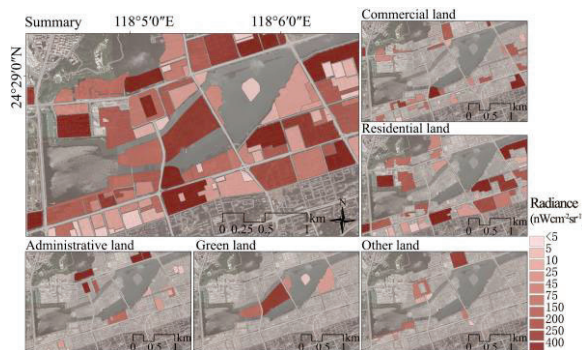


Figure 5. Total radiance distribution in each block

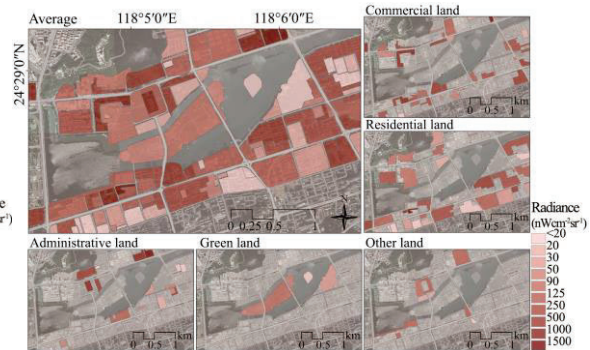


Figure 6. Average radiance distribution in each block

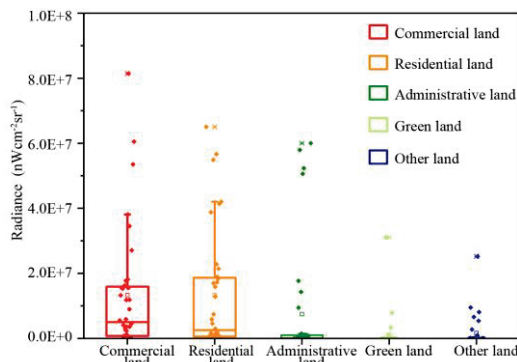


Figure 7. Total radiance of each land use

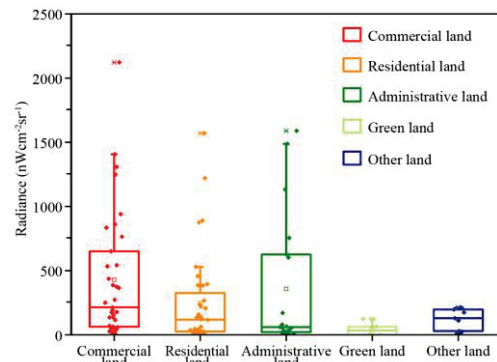


Figure 8. Average radiance of each land use



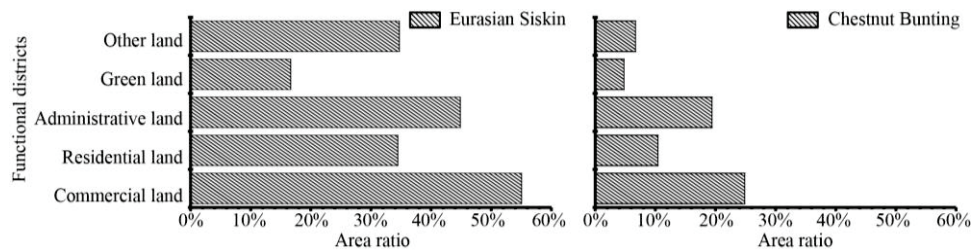


Figure 9. The proportions of risk areas of Eurasian Siskin and Chestnut Bunting in each land use

#### 4. CONCLUSION AND DISCUSSION

In this paper, with the support of GIS technology, microscopic risk thresholds are combined with macroscopic pollution maps to evaluate the ecological risk of birds under light pollution stress, taking the typical urban ecological patch of Yundang Lake area as an example, and the following conclusions are drawn and discussed.

##### 4.1 Microscopic light pollution risk thresholds

In this paper, based on the team's previous research, we initially concluded that the artificial light irradiance risk thresholds for Eurasian Siskins and Chestnut Buntings were  $5 \text{ mW/m}^2$  and  $10 \text{ mW/m}^2$ , corresponding to illumination risk thresholds of  $1.78 \text{ lx}$  and  $3.38 \text{ lx}$ , respectively. These risk thresholds are similar to the mixed light intensities that have been studied for their effects on birds. For example, artificial light at  $1.5 \text{ lx}$  advanced the onset of daytime activity by 55 min in the great tit (*Parus major*)[10]; artificial light at  $1.6 \text{ lx}$  may disrupt sleep behaviors in the great tit (*Parus major*)[3, 11]; artificial light at  $3.2 \text{ lx}$  may affect melatonin secretion and further affect the sleep-wake rhythm in scrub-jays (*Aphelocoma californica*)[12];  $10 \text{ mW/m}^2$  of artificial light delays the sleep behaviors in the embroidered silvereyes (*Zosterops lateralis*)[13]. In the heavy light pollution areas with an average illumination of  $3.91 \text{ lx}$ , the onset of dawn song chorus of the American robin was substantially earlier compared to the low light pollution areas[14].

In addition, this paper proposed a method to estimate the radiance thresholds according to the laboratory irradiance thresholds of specific bird species in accordance with the mixed spectral energy distribution of the real light environment, and obtained the radiance risk thresholds of  $118.28 \text{ nWcm}^{-2}\text{sr}^{-1}$  and  $218.88 \text{ nWcm}^{-2}\text{sr}^{-1}$  for the Eurasian Siskins and Chestnut Buntings, respectively, in accordance with the typical spectral energy distribution in the Yuandang Lake area. The sensitivity and tolerance of different bird species to artificial light intensity are different, and more research on the risk mechanism of different bird species is needed in future studies.

##### 4.2 Macroscopic light pollution maps and risk evaluation

This paper conducted a light pollution risk evaluation in the Yundang Lake area using bird risk thresholds combined with JL1-07B night light remote sensing images, and found that the percentages of light pollution risk areas in the area for Eurasian Siskins and Chestnut Buntings were 24.6% and 6.9%, respectively. In the Yundang Lake area, the overlap of the risk areas of Chestnut Bunting characterized by LJ1-01 and JL1-07B reached 84.0%, indicating that the risk distribution of light pollution characterized by LJ1-01 was similar to that of JL1-07B. Based on the respective characteristics of the two types of nighttime light images, this paper concluded that JL1-07B nighttime light images are suitable for light pollution risk evaluation at the urban regional scale, and LJ1-01 is more suitable for the large-scale evaluation of urban clusters.

Comparing the classification of bird habitat light pollution levels in the study of Xue et al.[6], the risk threshold of light pollution for Eurasian Siskins ( $118.28 \text{ nWcm}^{-2}\text{sr}^{-1}$ ) corresponded to primary light pollution ( $89.40\sim151.84 \text{ nWcm}^{-2}\text{sr}^{-1}$ ) in Xue's study, and the risk threshold for Chestnut Buntings ( $218.88 \text{ nWcm}^{-2}\text{sr}^{-1}$ ) corresponded to intermediate light pollution ( $151.85\sim334.60 \text{ nWcm}^{-2}\text{sr}^{-1}$ ). Although the study by Xue et al.[6] did not refer to bird risk thresholds, the light pollution classification can correspond to the risk thresholds of bird species in

this paper, indicating that the light pollution classification obtained using the natural breakpoint method can reflect the impact of typical artificial light on birds. However, due to the differences in the sensitivity of different bird species to artificial light, it is unclear whether the light pollution classes obtained by the natural breakpoint method can represent the light pollution risk faced by each typical bird species. Therefore, there is still a need to carry out research on the mechanism of birds' behavior response to artificial light to provide support for the reasonable classification of light pollution risk levels.

### 4.3 Light pollution risk distribution pattern and control suggestions

Among the five types of land use, commercial areas have the highest risk of light pollution, with 55.0% and 24.9% of the risk areas for yellow finches and chestnut buntings, respectively, followed by administrative and residential areas. The research found that during non-holiday nights, most of the building facade decorative lighting in the Yundang Lake area shuts down at 22:30, but the lighting of the stores along the streets on the lower floors of the commercial area, as well as the infrastructure lighting, basically runs overnight. Therefore, light pollution prevention measures need to be considered from the perspectives of both function and time. This paper suggests that urban management should focus on the light level in commercial and administrative areas according to the Frequency of bird activities and greening rates and take measures to reduce light intensity, reduce the number of light sources, and shorten lighting time for bird light pollution risk areas to reduce the ecological risk of light pollution.

### REFERENCES

- [1] Lyytimäki, J. Avoiding overly bright future: The systems intelligence perspective on the management of light pollution. *Environmental Development*, 2015, 16:4-14.
- [2] Raap, T., Sun, J. C., Pinxten, R., Eens, M. Disruptive effects of light pollution on sleep in free-living birds: Season and/or light intensity-dependent? *Behavioural Processes*, 2017, 144:13-19.
- [3] Raap, T., Pinxten, R., Eens, M. Artificial light at night disrupts sleep in female great tits (*Parus major*) during the nestling period, and is followed by a sleep rebound. *Environmental Pollution*, 2016, 215:125-134.
- [4] Zhao, X. B., Zhang, M., Che, X. L., Zou, F. S. Blue light attracts nocturnally migrating birds. *Condor*, 2020, 122(2):12.
- [5] Horton, K. G., Nilsson, C., Van Doren, B. M., La Sorte, F. A., Dokter, A. M., Farnsworth, A. Bright lights in the big cities: migratory birds' exposure to artificial light. *Frontiers in Ecology and the Environment*, 2019, 17(4):209-214.
- [6] Xue, X., Lin, Y., Zheng, Q., Wang, K., Zhang, J., Deng, J., Abubakar, G. A., Gan, M. Mapping the fine-scale spatial pattern of artificial light pollution at night in urban environments from the perspective of bird habitats. *Sci Total Environ*, 2020, 702:134725.
- [7] Fangbo, L. Study on the Sleeping Rhythm of Eurasian Siskin and Yellow-browed Bunting under Artificial Light Interference [D], 2018.
- [8] Jiang, W., He, G. J., Long, T. F., Guo, H. X., Yin, R. Y., Leng, W. C., Liu, H. C., Wang, G. Z. Potentiality of Using Luojia 1-01 Nighttime Light Imagery to Investigate Artificial Light Pollution. *Sensors*, 2018, 18(9):15.
- [9] Guk, E., Levin, N. Analyzing spatial variability in nighttime lights using a high spatial resolution color Jilin-1 image - Jerusalem as a case study. *ISPRS Journal of Photogrammetry and Remote Sensing*, 2020, 163:121-136.
- [10] Dominoni, D., Smit, J. A. H., Visser, M. E., Halfwerk, W. Multisensory pollution: Artificial light at night and anthropogenic noise have interactive effects on activity patterns of great tits (*Parus major*). *Environmental Pollution*, 2020, 256:9.
- [11] Raap, T., Pinxten, R., Eens, M. Light pollution disrupts sleep in free-living animals. *Scientific Reports*, 2015, 5:8.
- [12] Schoech, S. J., Bowman, R., Hahn, T. P., Goymann, W., Schwabl, I., Bridge, E. S. The effects of low levels of light at night upon the endocrine physiology of western scrub-jays (*Aphelocoma californica*). *Journal of Experimental Zoology Part A: Ecological Genetics and Physiology*, 2013:n/a-n/a.
- [13] Liu, G., Peng, X. T., Ren, Z. F., Liu, M., Dang, R., Chen, Y. Q., Liu, F. B. The effect of artificial light with different SPDs and intensities on the sleep onset of silvereyes. *Biological Rhythm Research*, 2019, 50(5):787-804.
- [14] Miller, M. W. Apparent effects of light pollution on singing behavior of American robins. *Condor*, 2006, 108(1):130-139.

### ACKNOWLEDGEMENTS

Corresponding Author: Juan Yu  
 Affiliation: School of Architecture, Tianjin University  
 e-mail : juan.yu@tju.edu.cn

# COLOR MATCHING AND HUE ESTIMATION EXPERIMENTS USING RGB LEDS

Minjeong Ko, Youngshin Kwak

Biomedical Engineering Department, Ulsan National Institute of Science and Technology,  
Ulsan, Republic of Korea

## ABSTRACT

Two RGB LED lightings having different spectral characteristics were used for color matching and hue estimation experiment. Seven observers conducted the color matching experiment between two RGB lightings and estimated hue of the colors for each RGB set. The results showed that though there were large color matching variations between two RGB LED conditions, hue perception under each condition were similar to each other.

Keywords: standard observer, color matching, color appearance

## 1. INTRODUCTION

Several studies reported that when two colors having the same CIE XYZ tristimulus values with different spectral characteristics were observed, people evaluate that the two colors look different [1] indicating the need for new standard observers. In this study, two RGB LED lightings were selected showing the large CIE colorimetry mismatch between them. Then hue estimation experiments were conducted using those two different RGB LED primary sets separately. The results of two experiments were compared to investigate the effect of color mismatch on color appearance of RGB LED lighting or display system.

## 2. COLOR MATCHING AND COLOR APPEARANCE EXPERIMENT

Two LED lighting booths having 15 channels were placed side by side, and the opened area was covered using a diffuser and a black paper to make a field of view of 6.3 degrees. Two test primary sets (P1: 635-505-445nm and P2: 670-525-445nm) were selected. Figure 1 displays the spectral power distribution (SPD) of the test primary sets.

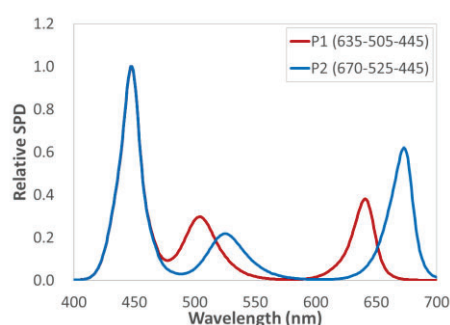


Figure 1. Spectral power distribution of Test primary sets

Both experiments were conducted in a dark room and the observers were located at the center of the two lighting booths. For color matching experiment, the observers were asked to manipulate the color mixed with P2 primary set to have the same color appearance as the reference stimulus generated with P1 primary set. Seven observers participated the experiments and matched 12 colors twice. All the test colors were low chromatic colors.

For hue estimation experiment, the reference white was shown on the left and various test colors were shown on the right. Both reference and test colors were generated using P1 or P2 primary sets. For each primary set, the number of test stimuli was 34 and both sets were adjusted to have the same CIE  $u'v'$  chromaticities. The observer took 2 minutes to adapt to the reference stimuli on

the left lighting booth. After adaptation, the test stimulus on the right lighting booth was shown for 2 seconds, and the observer were asked to evaluate the hue of test stimuli using magnitude estimation with four unique hues: red, yellow, green, and blue. A total of 544 evaluations (= 34 test color × 2 experimental session × 8 repeat) were performed for each observer. Seven observers (two females and five males) with normal color vision participated.

Figure 2(a) shows the color matching results, analyzed in the CIE  $u'_{10}v'_{10}$  chromaticity diagram and Figure 2(b) compares the hue estimation results between P1 and P2 primary sets. The arrow direction in Figure 2(a) represents the reference color coordinates to average color matching result showing large CIE colorimetry mismatch while there was little difference on hue perception when two RGB LEDs having the same CIE colorimetric values are shown independently.

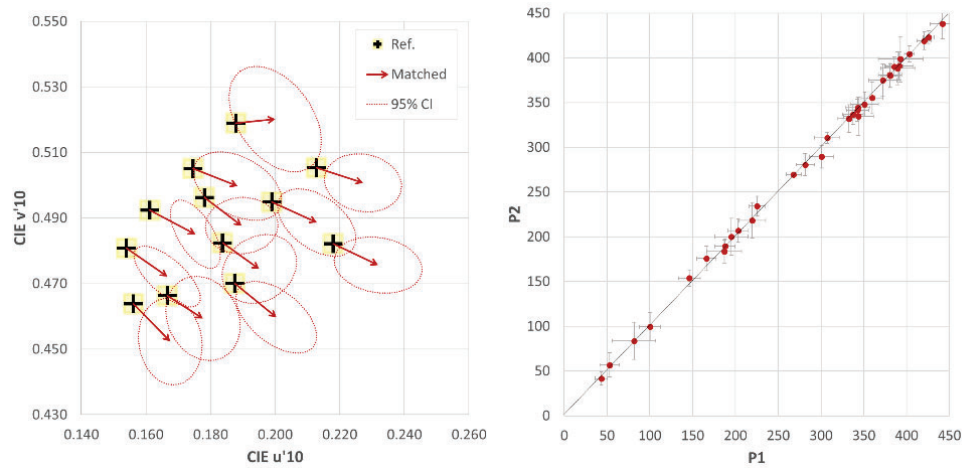


Figure 2. (a) Color matching results (left) and (b) Hue estimation results (right)

### 3. CONCLUSION

A color matching and color appearance experiments were conducted using two RGB LEDs. The results showed that there were differences in color matching results between two RGB LEDs, but when two lightings were shown separately, the same CIE colorimetric values showed the same hue perception. This result indicate that further research is needed to investigate new colorimetric observer and its impact on color appearance.

### REFERENCES

- [1] Ko, M., Kwak, Y., Seo, G., Kim, J., & Moon, Y. Reducing the CIE Colorimetric Matching Failure on wide Color Gamut Displays. *Opt. Express*, 2023, 31(4), 5670-5686.

### ACKNOWLEDGEMENTS

This work was supported by National Research Foundation of Korea (NRF-2021R1A2C1013610).

Corresponding Author Name: Youngshin Kwak  
Affiliation: Ulsan National Institute of Science and Technology  
e-mail: yskwak@unist.ac.kr

## **A study of daylight utilization in office spaces considering occupants' adaptation to changes in glare perception depending on their behavior and light color**

Akari Kawaguchi, Yuji Zhu, Hikaru Kobayashi

(Graduate School of Engineering, Tohoku University)

### **ABSTRACT**

Although use of natural daylight provides various benefits such as improved well-being and productivity, negative effects such as discomfort glare and increased heat load may also occur. While these risks may be mitigated by restricting the excessive use of natural light, it is desirable to promote daylight use through appropriate measures to improve indoor environmental quality (IEQ). However, discomfort glare evaluation indices used to assess the light environment in indoor spaces, such as daylight glare probability (DGP), are based on office work in a daylit environment. As an occupant's behaviors in a space may not be limited to office work, this evaluation system may unnecessarily restrict the diversity of indoor daylight environments. We suggest that depending on non-office activities (e.g. rest periods) and visible-light color, daylight may cause discomfort during office work but can also be perceived as pleasant, and that glare evaluation alone is thus an insufficient criterion for the design of interior spaces. We therefore conducted an experiment in a workplace under daylight conditions to obtain information on the mitigation of glare caused by occupant behavior and depending on the color of light perceived by occupants. We recorded the amount of light affecting the circadian rhythm as equivalent melanopic lux (EML), as well as vertical illuminance, wavelength spectral intensity, DGP, and correlated these to subjects' personal evaluation of glare. The results showed that glare perception was subjective, it was affected by light coloring, and different activities led to the glare mitigation being perceived differently. The reference values of WELL Certification EML were readily exceeded in the experimental environment.

Keywords: Daylighting, Glare, Subject experiment, Circadian rhythm, Workplace, Color

### **1. INTRODUCTION**

The use of daylighting in architecture is expected to have positive effects in terms of reducing lighting energy (energy benefits) and contributing to occupant comfort and health (non-energy benefits). However, a risk of negative effects, such as glare and increased heat load, may also be associated with daylight. Introducing daylight into an office space using daylighting louvers may cause glare, which must be appropriately suppressed. Conventional glare indices have been developed to evaluate light environments suitable for office work. However, this does not take into consideration that occupants may feel comfortable with glare during rest periods. This suggests that glare indices that assume only office work may not provide appropriate guidance for light environment planning, as they disregard some of the various activities occupants may carry out in an architectural space. Arata et al. [1] proposed a risk analysis method that divides the influence of the light environment on glare perception by office workers into three components: the distribution of light rays in the room (hazard), sensitivity to glare (vulnerability), and amount of exposure to the visual environment as determined by working conditions (exposure). They proposed an evaluation method that links these three elements. However, we suggest that the conventional glare index (daylight glare probability; DGP) [2], which evaluates only office work, is insufficiently descriptive with respect to the vulnerability component. Furthermore, glare



perception may differ based on perceived light color. In addition, some light may be dazzling but not unpleasant, or have a positive effect on aspects of human health such as circadian rhythms. These factors cannot be evaluated by general visible-light evaluation alone and require a broader perspective. In this study, we therefore conducted experiments on subjects in a workplace that actively uses daylight to correlate glare sensation to the activities of occupants, investigate the mechanism by which glare mitigation occurs, and determine the relationship between color and glare.

## 2. MATERIAL AND METHODS

### 2.1 Experimental Background and Objectives

The DGP is composed of three terms (Equ. 1): total amount of glare caused by the amount of light entering the pupil (vertical illuminance); contrast glare caused by luminance contrast in the visual field; and a constant term. Physiological responses that affect the amount of light entering the eye include the phototropic response, in which the pupil contracts (to a minimum diameter of 2 mm) in response to light intensity, and the near-vision response, in which the pupil contracts to bring a close object into focus, independent of light intensity [3]. Based on this, Arata et al. suggested that the mitigation of glare affects the total amount of glare, which is related to human physiological responses. Therefore, we focused on the vertical plane irradiance, which is related to total amount of glare. In this study, we investigated (1) the subjective perception of glare by experimental subjects, (2) illuminance in front of the eye (hereafter referred to as "vertical illuminance"), and (3) luminance image. We then tested whether glare perception was mitigated when the subject relaxed.

$$DGP = C_1 E_v + C_2 \log \left( 1 + \sum \frac{L_{si}^2 \cdot \omega_{si}}{E_v^{1.87} \cdot P_i^2} \right) + C_3 \quad (1)$$

$$C_1 = 5.87 \times 10^{-5}, C_2 = 9.18 \times 10^{-2}, C_3 = 0.16$$

$E_v$ : Vertical illuminance at eye position [lx],  $L_s$ : Brightness of glare source [cd/m<sup>2</sup>]

$\omega$ : Solid angle of glare source [sr],  $P$ : Position Index [-]

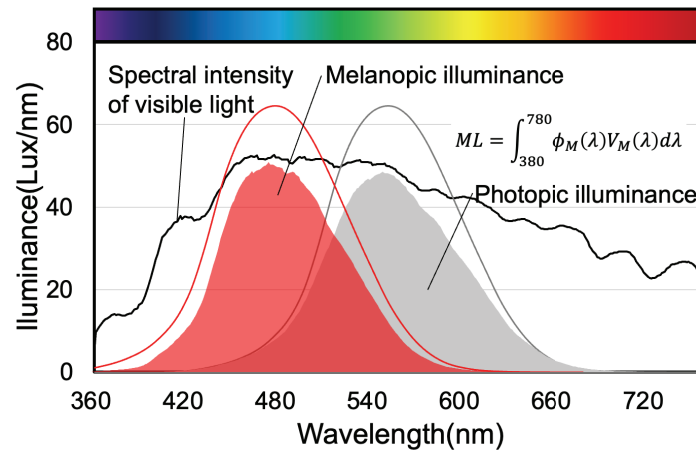


Figure 1. Equivalent melanopic lux (EML)

In addition, we investigated the relationship between light environment and comfort, including its effects on circadian rhythms. Equivalent melanopic lux (EML) [4][5] (Figure 1) was used to evaluate the amount of light acting on the circadian rhythm. This metric is based on the spectral sensitivity of the intrinsically photosensitive retinal ganglion cells (ipRGCs), the third and non-visual photoreceptor of the retina. The peak sensitivity of these cells is at 480 nm, a wavelength shorter than the photopic illuminance. The WELL Certification (WELL Building Standard) [6]

suggests a reference value of 150–200 EML for proper regulation of the circadian rhythm. We analyzed how much EML was obtained and whether the reference values were achieved.

## 2.2 Experimental Procedure

The subject experiment followed the experimental method of Jan et al., who proposed DGP [2]. A call for participation was put out at the authors' university, and a total of 12 university students (seven males and five females in their 20s, with no pre-existing eye disease) participated. The experiment was conducted 24 times, twice for each participant: once between December 5 and December 15 (with unfiltered instruments), and once more between December 17 and December 28 (with blue filters on all measurement instruments (Figure 2)). The subject experiments and light environment measurements were conducted in the same room with an east-facing window (Figure 3). No buildings or structures outside the window obstructed the sky or the view. Instruments installed at the side of the seated subject consisted of a digital SLR camera (Nikon D-300S) with a circumferential fisheye lens (SIGMA 4.5 mm F2.8 EX DC CIRCULAR FISHEYE HSM) for luminance image generation, an illuminance meter (T&D TR-74) for vertical illuminance measurement, a luminance meter (TOPCOM BM-9) for luminance measurement at representative positions for luminance image calibration, a gaze meter (NAC EMR-9) for measuring the relative pupil diameter and gaze point of the subject, and a spectroradiometer (UPRtek MK-350N) for measuring EML [lx] and CCT [K] (color temperature) to evaluate the light environment with respect to the circadian rhythm of the vertical plane.

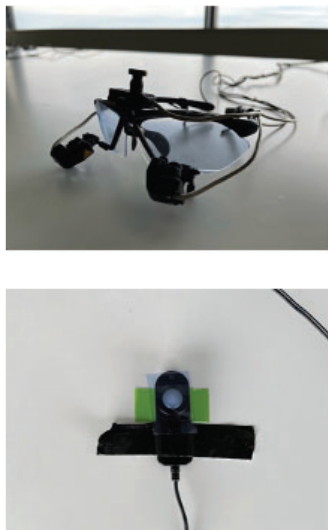


Figure 2. Equipment with blue filter installed (Upper panel: Line-of-sight meter, Lower panel: Illuminance meter sensor)

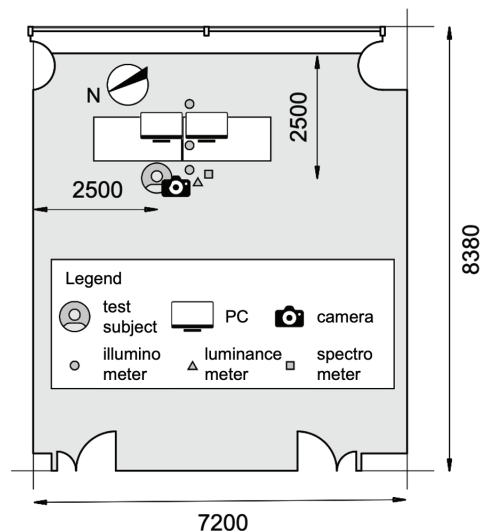


Figure 3. Laboratory layout. Distance units are in mm

## 2.3 Experimental Conditions

Figure 4 shows the experimental schedule for each participant. Activities consisted of three activities: text entry using a PC during the concentration period (CON), non-work-related internet browsing on the same PC during relaxation period A (R(A)), and looking at a view or at the room freely in relaxation period B (R(B)). Each activity was carried out for 10 min, and all three were done in sequence. Six combinations of activities of CON, R(A), and R(B) are possible; one combination was chosen for each subject, and the subject performed the chosen combination three times in a row with 10 min breaks between sequences. Each day, one subject was tested between 7:50 and 9:40, and a second between 10:10 and 12:00. Participants stated subjective evaluations of glare and discomfort every 2 min, using five evaluation levels ("not dazzling/slightly dazzling/dazzling/very dazzling/unbearable") for glare perception and four levels ("not

perceptible/perceivable/feeling uncomfortable/unbearable") for discomfort perception (Figure 5). In the analysis, 2-3 were rated as "discomfort".

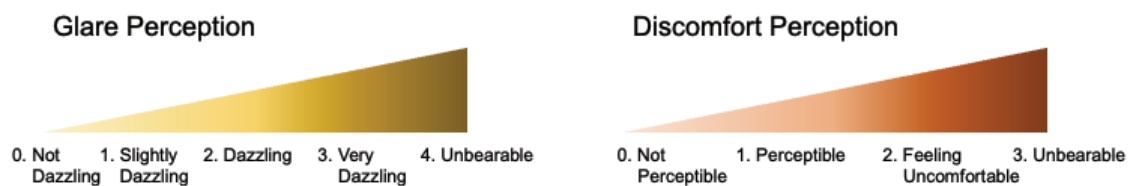
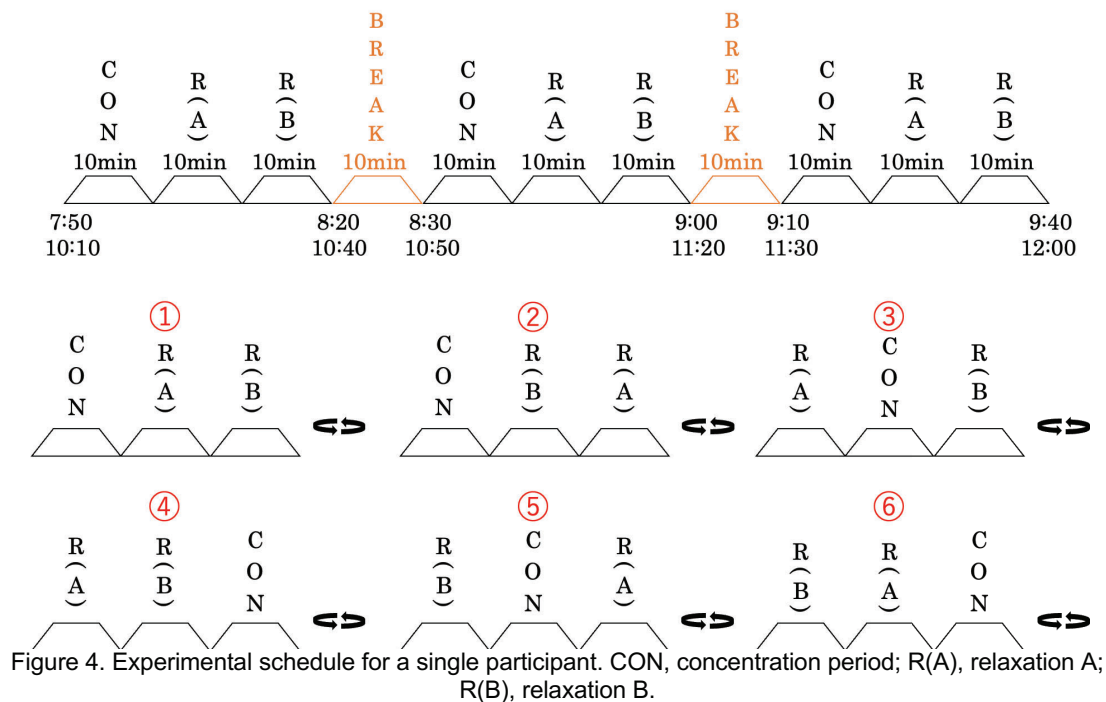


Figure 5. Subjective assessment levels stated by participants.

### 3. RESULTS

For each activity, the vertical illuminance was divided into 8 classes, and the percentage of subjects who stated discomfort in each class was regressed against average DGP calculated from the luminance images (Figure 6). In CON, DGP and discomfort had a close linear relationship (slope  $\sim 1.2$ ). For R(A), the slope of the regression was approximately 1.2, and mean discomfort percentages were approximately 12% lower, while for R(B) the slope was 0.79, and mean discomfort percentages were approximately 0.04 lower than in CON. This confirms that mitigation occurred for both R(A) and R(B) compared to CON, but that the trends for these activities were different.

The discomfort perception rates for vertical plane illumination are shown in Figure 7. The relationship is not as clear-cut as in Figure 6, and the effect of vertical surface illumination was not as apparent in this experiment. While a mitigation effect can be discerned for R(A), R(B) was little different from CON.

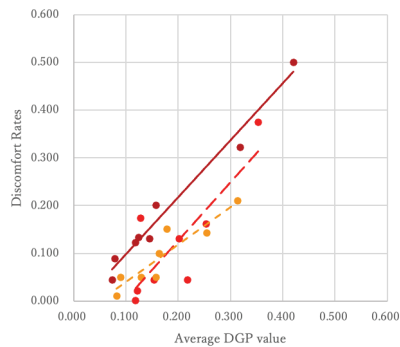


Figure 6.

Regression of discomfort perception rates against average DGP. CON, concentration period; R(A), relaxation A; R(B), relaxation B.

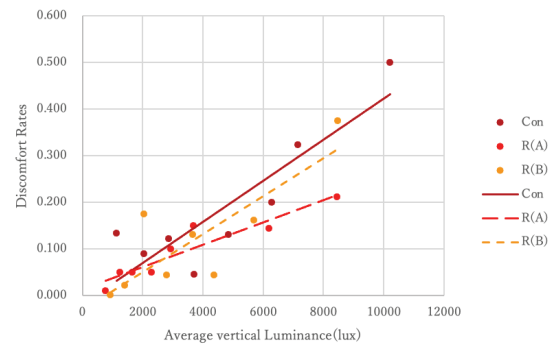


Figure 7.

Regression of discomfort perception rate against average vertical luminance. CON, concentration period; R(A), relaxation A; R(B), relaxation B.

### 3.1 Effect of Light Color

We compared discomfort and glare perception between experiments with and without an added blue light filter. Figure 8 shows discomfort rate regressed against DGP under blue filter conditions. There was still a clear linear relationship (slope  $\sim 1.0$ ) in CON. For R(A), the slope was approximately 1.4, with mean values  $\sim 7\%$  lower than in CON, while for R(B) the slope was 0.83, with mean values  $\sim 0.02$  lower. The slopes were similar to those without filters for both actions, but the intercepts of R(A) and R(B) were larger. Hence, the change between unfiltered and filtered light was small in CON, but glare perception increased in R(A) and R(B), indicating that glare perception was not mitigated during the relaxation activities.

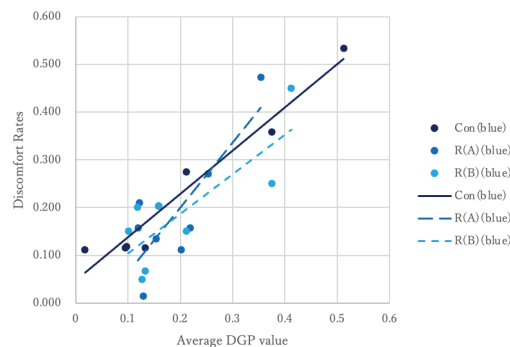


Figure 8. Regression of discomfort perception rate against average DGP, under blue light filtering. CON, concentration period; R(A), relaxation A; R(B), relaxation B.

Figure 9 shows the regression of glare perception against vertical illuminance for the three activities, with and without blue light filtering. Glare perception increased exponentially with vertical illuminance for all activities and was greater with than without the blue filter until a certain illuminance range was exceeded. This threshold occurred at approximately 8,000 lx for CON and at 6,500 lx for R(A) and R(B).

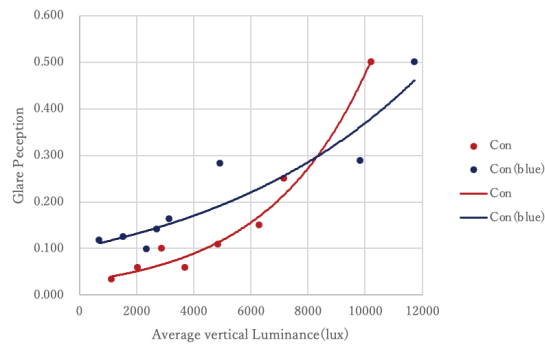


Figure 9.1. Regression of glare perception rate against average vertical luminance in CON, with and without blue light filtering.

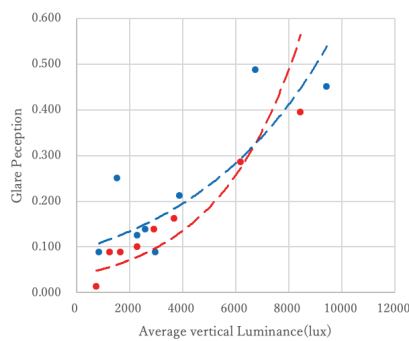


Figure 9.2. Regression of glare perception rate against average vertical luminance in R(A), with and without blue light filtering.

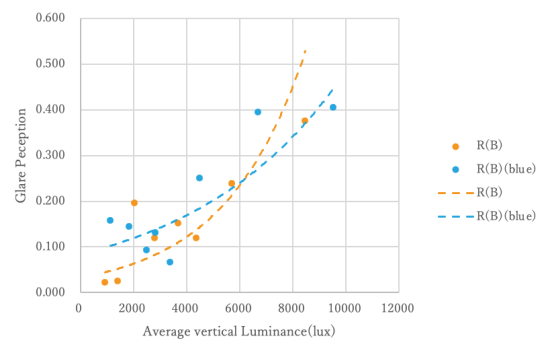


Figure 9.3. Regression of glare perception rate against average vertical luminance in R(B), with and without blue light filtering.

Figure 10 shows the regression of discomfort perception rate against vertical illuminance for the three activities, with and without blue light filtering. Similar to glare perception, discomfort perception increased exponentially with vertical surface illuminance for all actions, with greater percentages in the low-light range under blue light filtering. Discomfort rate in absence of blue light filtering reached and exceeded that under filtering at approximately 10000 lx in CON and approximately 6500 lx in R(B), whereas values approximately coincided at the end of the tested range in R(A). There was no significant difference in glare and discomfort sensation in R(B) between unfiltered and filtered light conditions, and in CON and R(A), perception rates under filtered conditions approached and exceeded those under unfiltered conditions at higher illuminance values. This shows that discomfort was merely moderate even if high illuminance caused glare under unfiltered conditions.

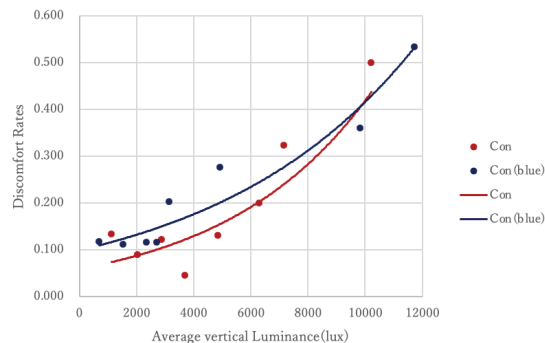


Figure 10.1. Regression of discomfort perception rate against average vertical luminance in CON, with and without blue light filtering.



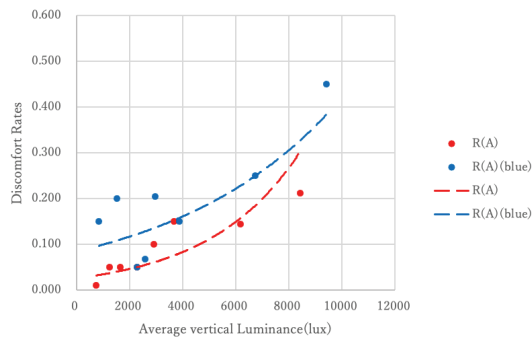


Figure 10.2. Regression of discomfort perception rate against average vertical luminance in R(A), with and without blue light filtering.

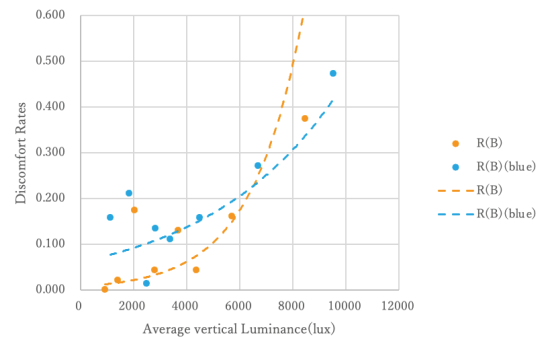


Figure 10.3. Regression of discomfort perception rate against average vertical luminance in R(B), with and without blue light filtering.

### 3.2 EML Evaluation

We compared the relationship of EML and spectral intensity without (10:10–12:00 AM on December 12) and with blue light filtering (10:10–12:00 AM on 23 December), assuming a similar irradiance distribution at these two times. Figure 11 shows timelines of both metrics over time. EML values were smaller than those of vertical illumination in absence of a filter. Values of 150–200 EML, which are defined as the standard for WELL Certification, were substantially exceeded throughout.

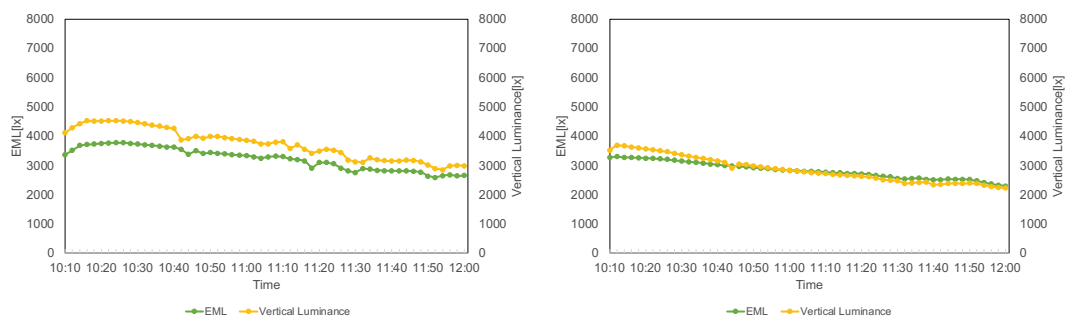


Figure 11. Vertical luminance and EML over two hours. Left, 12 December; right, 23 December.

Figure 12 shows spectral intensity over time at different wavelengths (40 nm increments across the tested spectrum) on both dates, and Figure 13 shows spectral intensity distribution at 10:12 AM on both dates. It is obvious that the yellow-green to yellow components at 560 nm and 600 nm were lost under filter use (23 December).

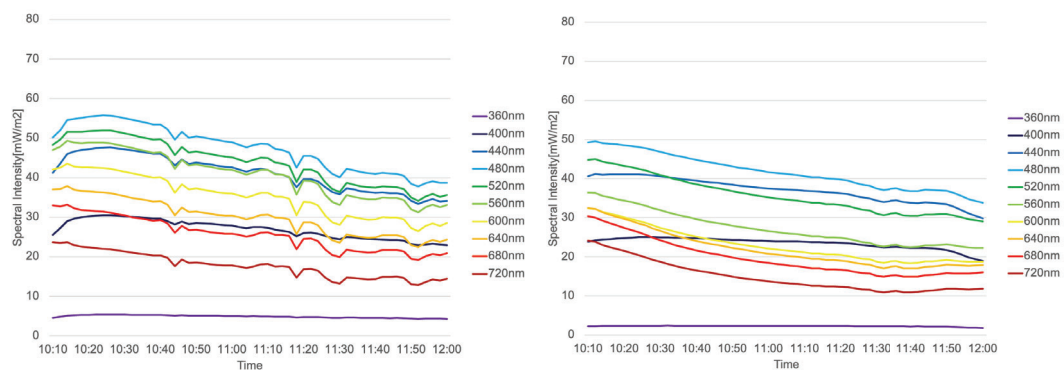


Figure 12. Spectral intensity at different wavelengths. Left, 12 December; right, 23 December.

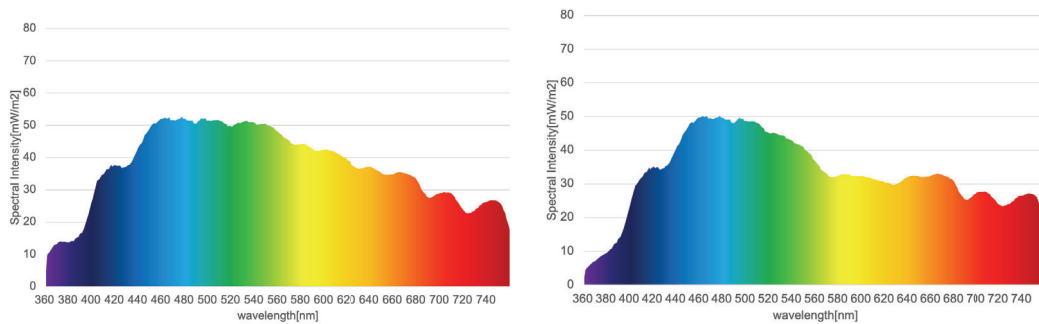


Figure 13. Spectral intensity across the spectrum at 10:12. Left, 12 December; right, 23 December.

#### 4. CONCLUSION

Our experiments based on the subjective perception of participants confirmed that different activities led to different experiences of glare mitigation and that glare perception was affected by light coloring. Suggested reference values of EML, a parameter related to circadian rhythms, were readily exceeded throughout in the experimental environment. Based on the relationship between EML values and glare perception, the development of a daylight utilization method that focuses on circadian rhythms should be considered.

#### REFERENCES

- [1] Keisuke Arata. Study on glare risk evaluation considering mitigation and adaptation of discomfort glare corresponding to worker's activities. Master's thesis, Graduate School of Engineering, Tohoku University, 2020, 2021.02.
- [2] Jan Wienold and Jens Christofferson. Evaluation methods and development of a new glare prediction model for daylight environments with the use of CCD cameras. *Energy and Buildings* 38, 2006, pp743–757.
- [3] Toyohiko Hatada. VDT and visual field characteristics. *Human Engineering*, vol22, 1986, pp45-52.
- [4] Ignacio Acosta, Miguel Ángel Campano, Russell Leslie, and Leora Radetsky. Daylighting design for healthy environments. Analysis of educational spaces for optimal circadian stimulus. *Solar Energy* 193, 2019, pp584-596.
- [5] Akari Kawaguchi. Research on lighting devices for regulating circadian rhythms. Conference proceedings, Architectural Institute of Japan, Hokkaido, Japan, 2022.09, pp515-516.
- [6] Brent Protzman. Current Standard WELL Certification: SSL lighting control for health. *LEDs Magazine Japan*, 2019.3, pp16-19.

#### ACKNOWLEDGEMENTS

We acknowledge support for this study by a grant from the Taisei Science Foundation.

Corresponding Author Name: Hikaru Kobayashi  
 Affiliation: Graduate School of Engineering, Tohoku University  
 e-mail: hikaru.kobayashi.c6@tohoku.ac.jp

# ARCHIVING THE PERSONAL MEMORIES OF ATTRACTIVE LIGHT: DATABASE BUILDING AND APPLICATIONS

Byeongjin Kim, Giyun Lee, Hyeon-Jeong Suk

(Department of Industrial Design, KAIST, Daejeon, South Korea)

## ABSTRACT

This study proposes a way to archive individuals' experiences with attractive light. As an initial stage of the database, a total of 255 cases were gathered from 43 professionals, including experts, researchers, and designers with expertise in light technology or application. Representative images accompanied each case in the database, and then judged in terms of the type of light, the optical property of the light, and the reason for the memorable quality. Based on the frequency, the cases were dominated by memories of sunlight, interior light, or art exhibition. The color hue of the light made a deep impression. Also, mood enhancement or interior styling was often mentioned as the reason for the memorable light. In this way, the database provides a trend about positive experiences with light in a specific manner. The archiving expects to build a body of knowledge about attractive light towards creating an emotionally enhanced user experience utilizing light source, device, or installation.

Keywords: Lighting, Experience, Database, Attractive Light

## 1. INTRODUCTION

Light is the most fundamental element in shaping our visual experience[1]. It has a wide range of potential, from functional purposes of perceiving the world to aesthetic ones such as inducing emotions or creating atmospheres[2,3]. Consequently, professionals in various fields such as architecture, design, and art have begun to take interest in understanding the aesthetic and emotional aspects of light.

However, understanding light as a design element poses a challenge compared to other elements such as materials or colors[4]. Unlike typical design elements, light is an intangible component. Furthermore, in everyday situations, we indirectly perceive light as it reflects off or is scattered by materials. This makes the documentation and reproduction of experiences related to light difficult. In addition, the experience of light is intricately connected to the intensity, direction, color of light, and the surrounding environmental factors. Consequently, to deeply understand such experiences, a multidisciplinary approach encompassing physics, psychology, and design is required. Therefore, to actively utilize light as a design element, it can be immensely helpful to apply the interpretations of professionals based on their expertise.

Nevertheless, systematic documentation and analysis of light experiences have yet to be conducted. This research proposes a methodology for preserving and classifying notable experiences related to light and lighting using online survey. Through this, we can provide systematic insights into the emotional and aesthetic aspects of light that have not been well-organized in previous research. This database could serve as empirical evidence to assist lighting, product, and user experience designers in effectively conveying emotions through lighting in the future.

## 2. ONLINE SURVEY

An online survey was conducted to collect the experience where people feel light to be attractive. The survey consisted of five questions. The participants (Q1) briefly described the experience, and (Q2) uploaded a photo or video that could represent the experience. Additionally, they responded to multiple-choice questions about (Q3) the type of the light, (Q4) the role of the light, and (Q5) the reason they found the light attractive in that experience. They were allowed to choose multiple options and were also permitted to add options. The survey was created using Google Forms. Figure 1 shows the survey questions and response options given to the participants.

**Q1. Please explain the experience.**

Any description, such as the name of the light or product, the manufacturer, or the situation, is acceptable.  
You can explain it freely.

**Q2. Please upload a photo or video file with light explaining your experience.****Q3. What kind of **field or type** of the light experience? (multiple choices)**

- |   |   |   |
|---|---|---|
| <input type="checkbox"/> Lighting Props                   | <input type="checkbox"/> Mobility Lighting                  | <input type="checkbox"/> Indoor Lighting  |
| <input type="checkbox"/> Artwork                          | <input type="checkbox"/> Home Appliances                    | <input type="checkbox"/> Outdoor Lighting |
| <input type="checkbox"/> Natural Light                    | <input type="checkbox"/> Exhibition and Stage Lighting      |   |
| <input type="checkbox"/> Fashion Clothing and Accessories | <input type="checkbox"/> Devices other than Home Appliances |   |
| <input type="checkbox"/> Others..                         |   |   |

**Q4. Which of the various **roles** of light would be the case you introduced? (multiple choices)**

- |  |  |  |
|--|--|--|
| <input type="checkbox"/> Decorative Effect           | <input type="checkbox"/> Creating Atmosphere             | <input type="checkbox"/> Help for Safety |
| <input type="checkbox"/> Brighten Space or Object    | <input type="checkbox"/> Provide Information Effectively |  |
| <input type="checkbox"/> Display Object Attractively | <input type="checkbox"/> Not Defined                     |  |
| <input type="checkbox"/> Others..                    |  |  |

**Q5. **Why** did you find this light attractive? (multiple choices)**

- |   |  |                                   |
|---|--|-----------------------------------|
| <input type="checkbox"/> Form                               | <input type="checkbox"/> User Interaction                | <input type="checkbox"/> Movement |
| <input type="checkbox"/> Color or Color Combination         | <input type="checkbox"/> Brightness                      |                                   |
| <input type="checkbox"/> Distribution or Direction of Light | <input type="checkbox"/> Technological Progress          |                                   |
| <input type="checkbox"/> Immersion                          | <input type="checkbox"/> Association with other Concepts |                                   |
| <input type="checkbox"/> Others..                           |  |                                   |

Figure 1. Online survey questions and choice options

To ensure a high quality and broad range of responses, this survey was conducted among 43 lighting professionals, designers, and researchers whose expertise has been proven. As a result of the survey, a total of 255 cases of lighting experiences were collected.

**3. RESULT**

The database of memorable experiences related to attractive light and lighting collected through the survey were subsequently analysed for design applications.

**3.1 Frequency Analysis**

Based on the frequency of experience cases, a summary was made about what kind of light people find attractive. The frequency analysis was based on the questions asked to the participants during the survey, and was conducted for the type of light, optical property, and the reason for the attraction.

**3.1.1 Type of Light**

Among the types of light collected in the database, the option that occupied the highest proportion was indoor lighting, followed by artwork, exhibition and stage lighting, and lighting props. These results indicate that artificial light used in artworks and performances can provide attraction to people. Figure 2 is a pie chart representing the frequency of the response about the types of light.

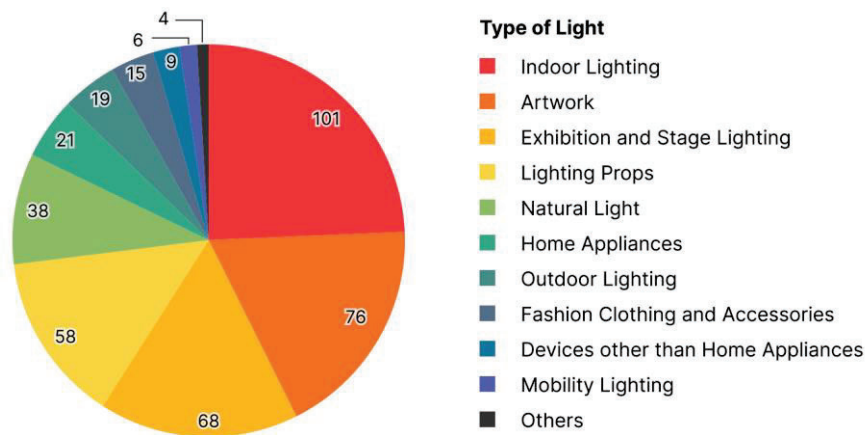


Figure 2. Frequency analysis of response about the types of light

### 3.1.2 Role of Light

Within the database, the roles of light that had high proportions were creating ambiance and decorative effects. It also frequently played a role in illuminating spaces or making displayed objects stand out attractively.

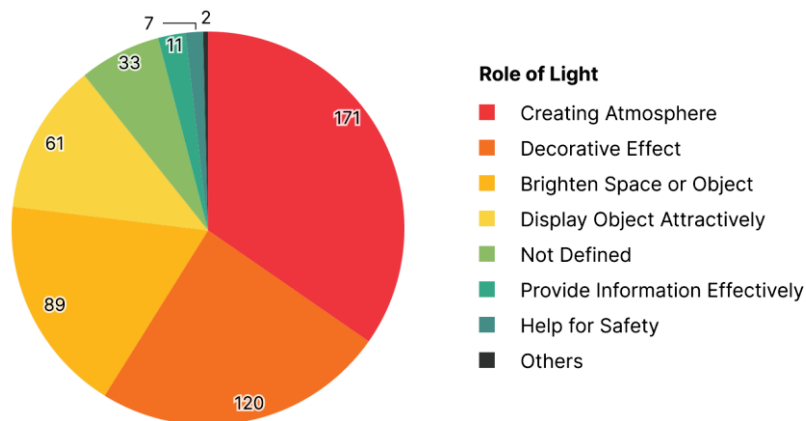


Figure 3. Frequency analysis of response about the role of light

### 3.1.3 Reason for the Attractiveness

The reasons participants found the light in their experiences attractive were diverse. They were impressed by the form and color of the light, and highly appreciated the immersion provided by the lighting. In addition, various optical elements such as distribution, movement, and brightness made the experience of light memorable.



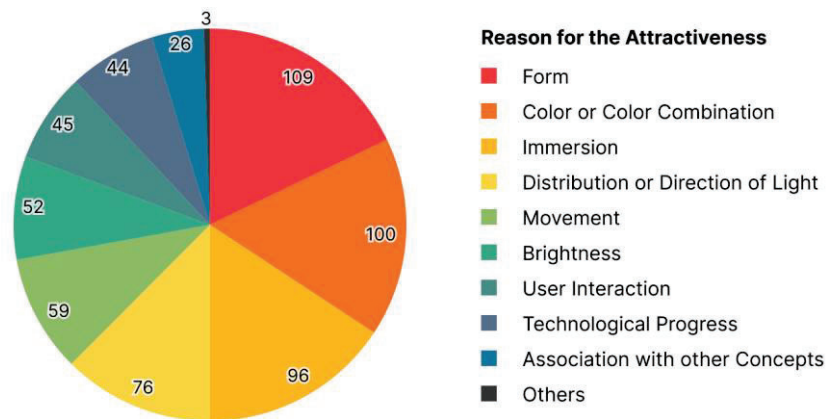


Figure 4. Frequency analysis of response about the reason of attraction

### 3.2 Association Between Factors

Based on the response database, we explored in what contexts and roles of light can be appealing to people. For this, we explored the relationships between the responses to the three questions provided for the participants. Since the attractiveness of light is caused by the composition of other factors, we intended to highlight the relationship between the reason for the attractiveness with other questions. Figure 5 is a Sankey diagram created from the responses of the participants to the three questions. To highlight the relationship between the reason for the attractiveness and other questions, responses to Q5 were placed in the middle of the figure.

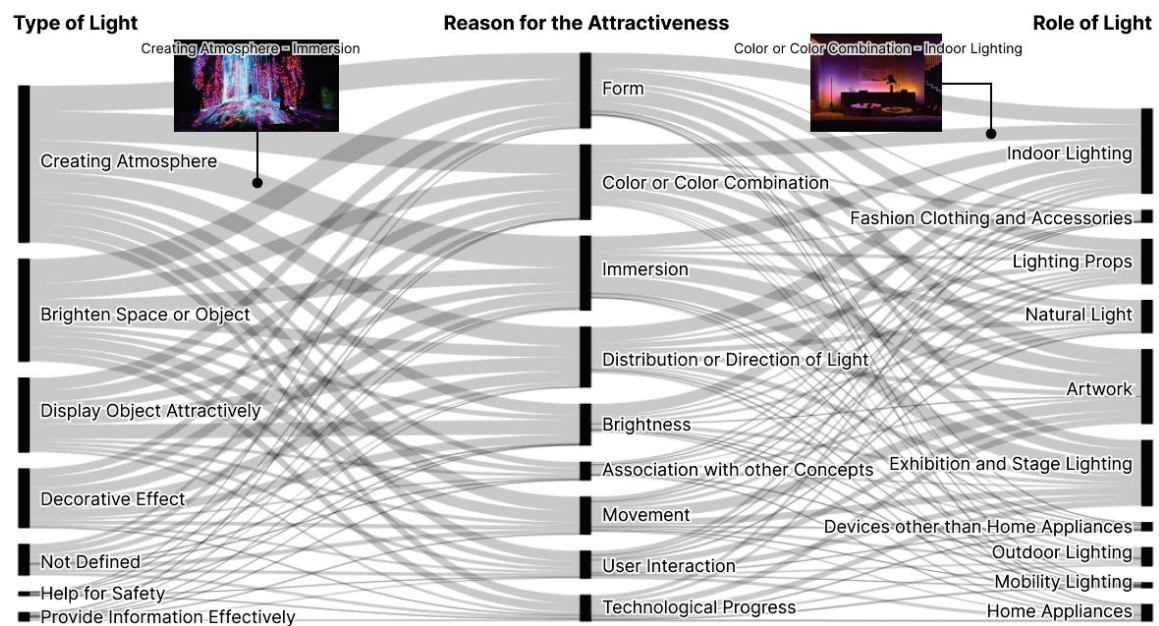


Figure 5. Sankey diagram of responses for three questions

Through the result, we can explore which factors can provide the memorable experience for people. For instance, when examining cases where lighting provided immersion to people, we found that the proportion was high when lighting was creating ambience. Additionally, lighting used in exhibitions and on stages often provided immersion.

#### 4. CONCLUSION AND DISCUSSION

This research aimed to build a database by collecting memorable experiences of lighting experts related to light and lighting. Based on this data, the frequency of responses and the relationship between the responses were analyzed to figure out the sentiments and emotions people can have provided through light. As a result of the analysis, we found out that people can be attracted to indoor lighting and lighting used in artworks and exhibitions. Light often used to create an ambiance and decorate the object and space. Moreover, the form and color of the light made the participants find the experience memorable.

The potential utility of this database extends beyond the frequency investigation and relational analysis. For example, terms can be extracted from the participants' description of their experience. This analysis can provide more detailed descriptions about the context in which people feel the light as attractive. Furthermore, emotional term analysis can work as a roadmap for what kind of emotions lighting can provide to people. Such research can provide the guideline to lighting designers or artists when they design their lighting works.

Also, the optical elements of lighting can be explored by analyzing the images submitted by participants to represent the experience. Notably, information such as brightness, shape, and color of light can be obtained through images. The extracted image metadata can be used to categorize the experiences. Such attempts can potentially develop the automated module that can extract the attraction elements from images. In addition, the extracted metadata can be supportive when generating lighting and art with attractive concepts that did not exist before.

#### REFERENCES

- [1] Cuttle, C. (1988). Lighting works of art for exhibition and conservation. *Lighting Research & Technology*, 20(2), 43-53.
- [2] Leccese, F., Salvadori, G., Maccheroni, D., & Feltrin, F. (2020). Lighting and visual experience of artworks: Results of a study campaign at the National Museum of San Matteo in Pisa, Italy. *Journal of Cultural Heritage*, 45, 254-264.
- [3] Schielke, T. (2020). Interpreting art with light: Museum lighting between objectivity and hyperrealism. *Leukos*, 16(1), 7-24.
- [4] Ramos, E. V. (2019). *Light in architecture: the intangible material*. Routledge.

#### ACKNOWLEDGEMENTS

Corresponding Author Name: Hyeon-Jeong Suk  
 Affiliation: Department of Industrial Design, KAIST, Daejeon, South Korea  
 e-mail: color@kaist.ac.kr

# VISIBLE LIGHT ID TRANSMITTER USING HIGH CIRCADIAN AND VISIBLE PERFORMANCES LED LIGHTING

Shogo Sakane, Saeko Oshiba

Graduate School of Science and Technology, Kyoto Institute of Technology

## ABSTRACT

In recent years, visible light positioning (VLP) using light-emitting diodes (LED) has been widely studied owing to its high precision. In this method, visible-light identifications (IDs) transmitter/receiving system is required to obtain location information as a visible-light ID by identifying the LEDs.

In addition, the light-emitting diode (LED), which is the transmitter in this system, must have high color-rendering properties to function as a general lighting fixture. Furthermore, human-centric lighting is becoming popular, and there is a growing demand for circadian lighting that can work with human circadian rhythms. Therefore, it is important to consider not only visual performance but also non-visual performance in lighting design.

In this study, we investigated the transmitter in a visible light ID transmitter/receiver system that used 8 color multi-chip LED lighting as the transmitter. It was found that the transmitter could produce light with correlated color temperatures ranging from 2700 K to 6500 K, a high color rendering index (CRI), CIE  $R_a > 80$ , constant illuminance, and different spectral distributions. Therefore, we demonstrated that the transmitter enables ID transmission while maintaining visual performance. Additionally, the possibility of using the transmitter for circadian lighting was studied by calculating its melanopic illuminance.

Keywords: Visible Light Communication, Visible Light ID, Human Centric Lighting, LED Lighting

## 1. INTRODUCTION

In recent years, indoor location estimation methods have been widely studied owing to the increasing demand for indoor location services and mobile devices, where it is difficult to acquire global positioning system (GPS) signals. Herein, visible light positioning (VLP) using visible light from light-emitting diodes (LEDs), which exhibit rapid spread, has been proposed [1] – [4]. VLP has the advantages of high accuracy, no radio interference, and compatibility with existing infrastructure compared with conventional indoor positioning technologies such as wireless LAN, infrared, and ultrasonic. In these methods, an identification (ID) representing the location information is obtained by identifying the LED lighting.

Human-centric lighting is becoming popular, and there is a growing demand for circadian lighting that can work with human circadian rhythms. Therefore, it is important to consider not only visual performance but also non-visual performance in lighting design. Circadian rhythm is an internal body rhythm with an approximately 24-hour cycle. It is responsible for regulating the body's environment, including body temperature and hormone secretion. Light significantly affects circadian rhythms. Continuous exposure to night lighting can disturb circadian rhythms. Recently, lighting designs using multi-chip LEDs have been proposed to create circadian lighting [5] – [9].

In this study, we focused on the use of a visible-light ID transmitter for circadian lighting. It is important to add a transmission function to avoid degrading the lighting quality, when lighting was used as the ID transmitter. By simulation, we studied whether the transmitter could transmit visible light IDs while being used for circadian lighting.

## 2. VISIBLE LIGHT ID TRANSMITTER

### 2.1 System Overview

Figure 1 shows the visible light ID system. The transmitter in this system was 8 color multi-chip LED lighting. The transmitted data ID are generated by changing the peak levels of each LED that constitutes the transmitter. The peak level of each LED is an optical code. A voltage corresponding to the peak levels is applied to the LED. The ID transmits and receives by visible light communication (VLC) using light mixed by the diffuser. A spectrometer was used as the receiver.

The output value from the spectrometer was analyzed to obtain the peak levels of LED1~8. The ID information was decoded by recognizing the peak levels of LED1~8. Therefore, the transmitter can transmit the ID information based on its spectral distribution.

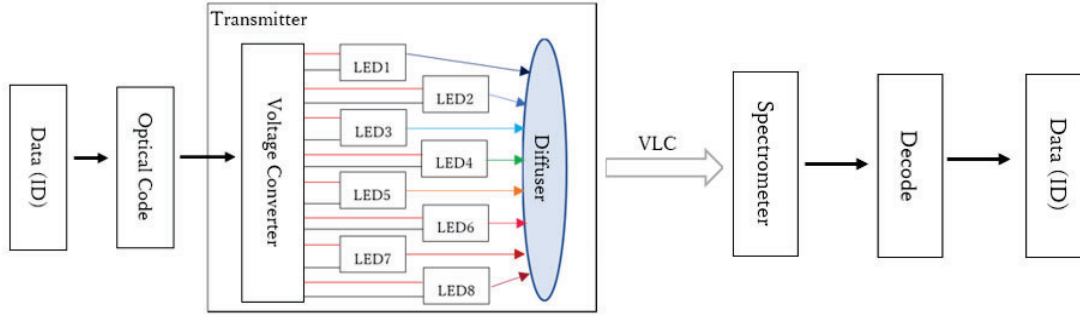


Figure 1. visible light ID system

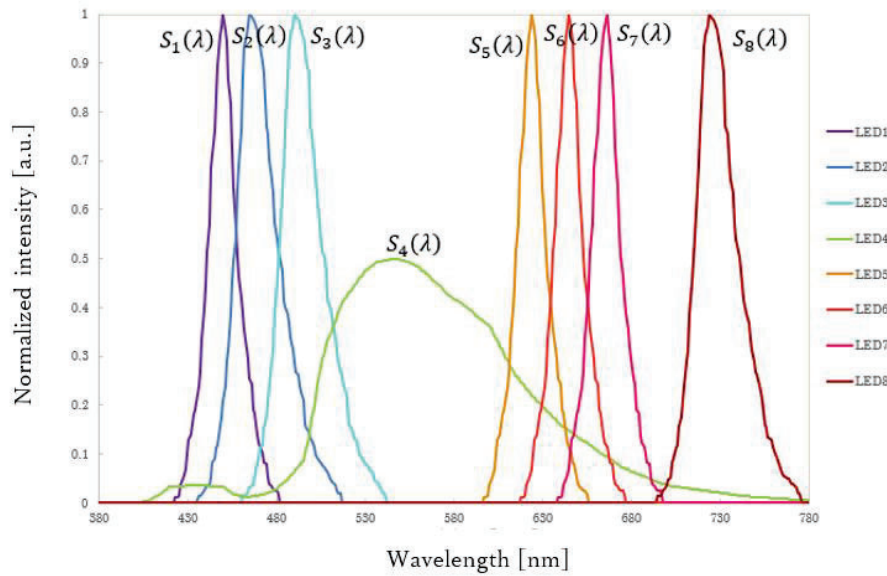


Figure 2. The spectral distribution of LED1~8

Figure 2 shows the spectral distribution of each LED consisting of a transmitter.  $S_1(\lambda) \sim S_8(\lambda)$  are the spectral distribution of LED1~8 when the illuminance of LED1~8,  $E_1 \sim E_8$ . The peak levels of LEDs 1-3 and 5-8 are equal, and LED 4 has a peak level of 0.5, relative to the other LEDs. Table1 shows the illuminance  $E_1 \sim E_8$  and the peak wavelength  $\lambda_n$  of LED1~8.

Table 1. illuminance and peak wavelength of LED1~8

LED <sub>n</sub>	1	2	3	4	5	6	7	8
$\lambda_n$ [nm]	450	465	490	546	624	645	666	724
$E_n$ [lux]	0.82	3.21	28.2	128.2	16.1	8.49	4.33	0.57

The spectral distribution  $S(\lambda)$  of transmitter light source given by Eq. (2.1):

$$S(\lambda) = k_1 S_1(\lambda) + k_2 S_2(\lambda) + k_3 S_3(\lambda) + S_4(\lambda) + k_5 S_5(\lambda) + k_6 S_6(\lambda) + k_7 S_7(\lambda) + k_8 S_8(\lambda) \quad (2.1)$$

The illuminance  $E$  at that time given by Eq. (2.2):

$$E = k_1 E_1 + k_2 E_2 + k_3 E_3 + E_4 + k_5 E_5 + k_6 E_6 + k_7 E_7 + k_8 E_8 \quad (2.2)$$

where  $k_n$ , ( $n = 1 \sim 3, 5 \sim 8$ ) are the peak levels of LED1~3, 5~8.  $k_n$  was varied in six steps of 0, 0.2, 0.4, 0.6, 0.8, and 1.0, and the peak level of LED 4 was fixed. Therefore, the transmitter can generate  $279936 = 6^7$  optical codes.

## 2.2 Design

The transmitter in this system is intended to meet the requirements of a visible light ID transmitter and circadian lighting. Therefore, the following three requirements were set for the visual performance in this study:

- ① CIE  $R_a > 80$
- ② Constant illuminance
- ③ Light source color exists within the correlated color temperature (CCT) range specified in ANSI C78.377

CIE  $R_a$  is a parameter that quantitatively indicates the color-rendering properties of lighting. This is commonly called the color rendering index (CRI). The CRI has been introduced as an indicator of color-rendering properties for general lighting.

For requirement ②, the range in which humans do not perceive any change in brightness is a constant illuminance in this study. In other words, if  $E$ , where the illuminance of the transmitter satisfies Eq. (2.3), the illuminance was considered constant [10].  $E_x$  is the illuminance constant.

$$0.92E_x \leq E \leq 1.06E_x \quad (2.3)$$

In requirement ③, in general, the CCT of the lighting color was divided into eight steps from 2700 K to 6500 K based on ANSI C78.377[11]. Figure 3 shows the nominal CCT for the eight categories in the CIE 1931  $(x, y)$  chromaticity diagram and their tolerances. Therefore, the color of the transmitter light source must be within the tolerances to be used for lighting.

Next, the light of the transmitter was investigated to determine the brightness of the light that affects circadian rhythms. In 2014, Lucas et al. proposed melanopic illuminance as a unit to quantitatively capture the brightness of light that affects circadian rhythms [12]. The melanopic efficiency of luminous radiation (MELR) was evaluated for the melanopic illuminance of the transmitter. The MELR is defined at CIE S 026/E:2018 and is represented as

$$\text{MELR} = \frac{\int_{380}^{780} S(\lambda) N_z(\lambda) d\lambda}{K_m \int_{380}^{780} S(\lambda) V(\lambda) d\lambda} \quad (2.4)$$

where  $V(\lambda)$  is the photopic luminosity function,  $N_z(\lambda)$  is the circadian action function,  $K_m = 683$  lm/W is the maximum spectral luminous efficacy of the visual system. MELR is set to 8 levels 0.5 ~ 1.2 and tolerances to  $\pm 0.05$ .

## 3. SIMULATION

The 279936 optical codes that can be generated by the transmitter include those that do not exhibit the visual performance described in section 2.2. Therefore, we conducted simulations to evaluate all the optical codes based on the requirements outlined in section 2.2 and examined the feasibility of using the visible light ID transmitter for circadian lighting.

### 3.1 Details

The simulation algorithm is described as follows: Figure 3 shows the process flow of the simulation. First, the peak levels  $kn$  of each LED consisting of a transmitter were determined to obtain the spectral distribution of the light source. The CIE 1931 chromaticity coordinate  $(x, y)$  and CCT were calculated [13][14] using the obtained spectral distribution of the transmitter. The obtained chromaticity coordinates  $(x, y)$  were determined to be within the tolerances of the CCT defined in ANSI C78.377. For optical codes determined to be between 2700 K and 6500 K, CIE  $R_a$  was calculated [15], and if  $R_a > 80$  illuminance was calculated using Eq. (2.2). The illuminance was determined to be constant by using Eq. (2.3). In this simulation, constant illuminance was set to  $E_x = 150$  lx. Therefore, 138–159 lx was the range in which the illuminance was constant. Finally, the MELR was calculated for optical codes that satisfied the aforementioned conditions using Eq. (2.4).



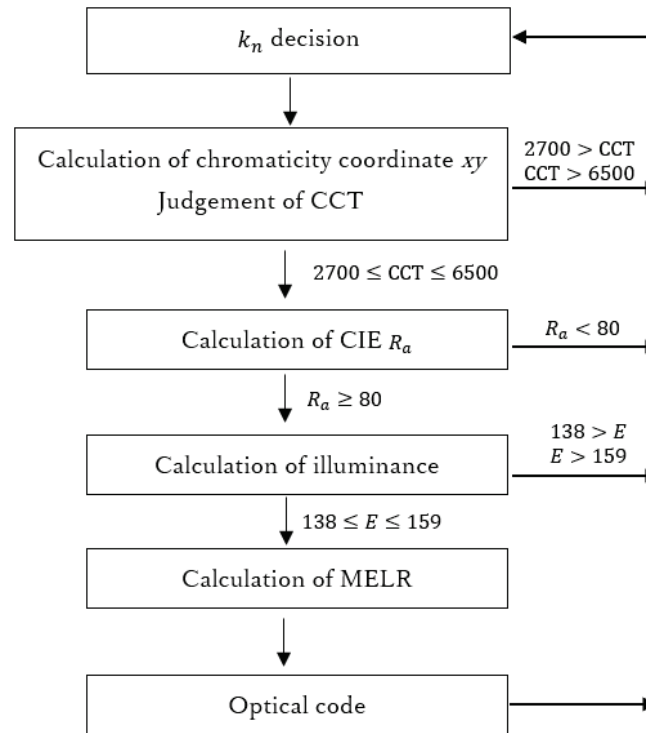


Figure 3. Process flow of the simulation conducted in this study

### 3.2 Result

The simulations presented in section 3.1 aimed to evaluate a total of 279936 different optical codes. Figure 4 shows the plot of the optical codes that satisfy the defined requirements ①–③ for visible performance on the MELR-CCT characteristics. The plots are divided into eight CCT, categories, as defined by ANSI C78.377, and are further divided into eight levels of MELR, as shown in Fig. 4.

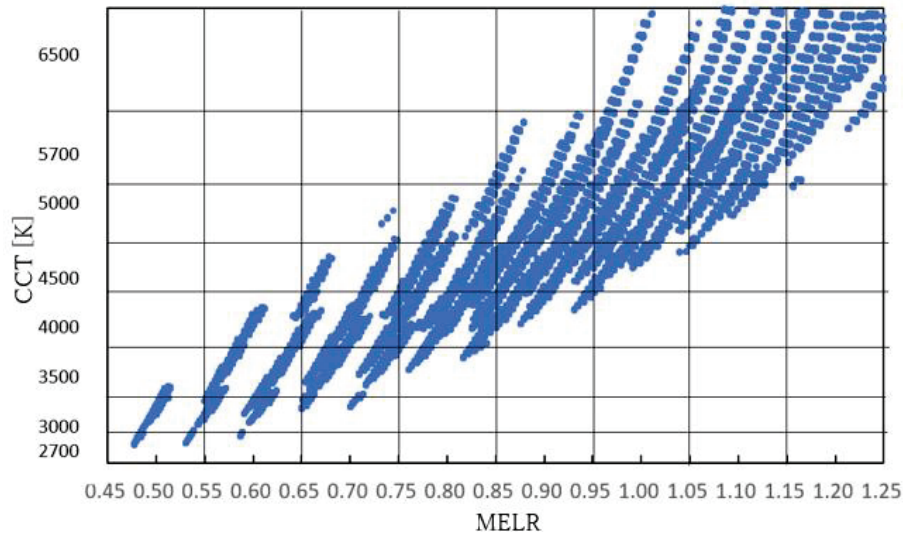


Figure 4. Plot of MELR-CCT characteristics

Table 3 lists the number of optical codes available in each area. In this section, we consider the application example of using transmission/reception self-location information for indoor drone flights as a waypoint system. Since the maximum number of waypoints that can be set for a drone is less than 99, using more than 99 optical codes ensures sufficient transmission of IDs. Table 4 lists the MELR ranges in eight categories of CCT, along with the corresponding colors. In [1] – [4], several transmitters were used simultaneously in the same space. If the colors of the transmitters are different, they cannot be used for lighting because they perceive color differences. Therefore, the

colors of the transmitters must be identical. From Table 4, it can be observed that the adjustable MELR varies only by two to four steps based on ANSI C78.377. However, by considering color classification, the range of adjustable MELR expands to five steps in white. Therefore, if the transmitter is white, it can be used for circadian lighting with a constant color and an adjustable MELR.

Further studies are needed to calculate the number of optical codes satisfying requirements ① – ③ in white color. Additionally, determining the range of adjustable MELR is also necessary at that time.

Table 3. Number of optical codes available in each area

		MELR							
		0.5	0.6	0.7	0.8	0.9	1	1.1	1.2
CCT [K]	6500	0	0	0	0	0	419	1636	1888
	5700	0	0	0	17	568	1896	1783	346
	5000	0	0	15	641	1572	1823	572	12
	4500	0	0	382	1249	1753	886	9	0
	4000	0	333	1295	1999	594	12	0	0
	3500	80	1037	1228	316	0	0	0	0
	3000	306	493	113	0	0	0	0	0
	2700	95	10	0	0	0	0	0	0

Table 4. Ranges of MELR in each CCT

Color	CCT [K]	MELR
Light	2700	0.5~0.7
	3000	
Warm White	3500	0.6~0.7
White	4000	0.6~0.9
	4500	0.7~1.0
Neutral	5000	0.8~1.1
Daylight	5700	0.9~1.2
	6500	1.0~1.2

#### 4. CONCLUSION

In this study, we investigated a visible-light ID transmitter that utilizes 8-color multi-chip LED lighting. The optical codes generated by the transmitter were evaluated through simulation, considering factors such as color-rendering properties, illuminance, and correlated color temperature. The aim was to identify practical optical codes suitable for lighting applications. Additionally, we calculated the MELR of the optical codes and explored the potential for circadian illumination, wherein the melanopic illuminance can be adjusted while maintaining a constant illuminance and CCT. The results indicate that a white transmitter can be utilized for circadian lighting, offering five-step adjustments in MELR ranging from 0.6 to 1.0 while adequately transmitting IDs.

#### REFERENCES

- [1] Canyu Xie, Weipeng Guan, Yuxiang Wu, Liangtao Fang, Ye Cai: The LED-ID Detection and Recognition Method Based on Visible Light Positioning Using Proximity Method. IEEE Photonics Journal, 2018, 10(2), 1-16.

- [2] Weipeng Guan, Shihuan Chen, Shangsheng Wen, Zequn Tan, Hongzhan Song, Wenyan Hou: High-Accuracy Robot Indoor Localization Scheme Based on Robot Operating System Using Visible Light Positioning. *IEEE Photonics Journal*, 2020, 12(2), 1-16.
- [3] Heqing Huang, Aiyang Yang, Lihui Feng, Guoqiang Ni, Peng Guo: Indoor Positioning Method Based on Metameric White Light Sources and Subpixels on a Color Image Sensor. *IEEE Photonics Journal*, 2016, 8(6), 1-10.
- [4] Rynosuke Inoshita, Saeko Oshiba: 3D-Self-Position Estimation Using Illumination and Image Sensors. *Proceeding of the 13<sup>th</sup> Asia Lighting Conference, China, 2022*, 37-44.
- [5] Jingxin Nie, Zhizhong Chen, Fei Jiao, Chengcheng Li, Jinglin Zhan, Yifan Chen, Yiyong Chen, Xiangning Kang, Yongzhi Wang, Qi Wang, Weimin Dang, Wentian Dong, Shuzhe Zhou, Xin Yu, GuoYi Zhang, Bo Shen: Tunable LED Lighting with Five Channels of RGCWW for High Circadian and Visual Performances. *IEEE Photonics Journal*, 2019, 11(6), 1-12.
- [6] Jeroen Cerpentier, Youri Meuret: Fundamental Spectral Boundaries of Circadian Tunability. *IEEE Photonics Journal*, 2021, 13(4), 1-5.
- [7] Yi Jiau Saw, Vineetha Kalavally, Chee Pin Tan: The Spectral Optimization of a Commercializable Multi-channel LED Panel with Circadian Impact. *IEEE Access*, 2020, 8, 136498-136511.
- [8] Tingzhu Wu, Yue Lin, Honghui Zhu, Ziquan Guo, Lili Zheng, Yijun Lu, Tien-Mo Shih, Zhong Chen: Multi-function Indoor Light Sources Based on Light-Emitting Diodes—A Solution for Healthy Lighting. *Optics Express*, 2016, 24(21), 24401-24412.
- [9] Akane Aoki, Saeko Oshiba: LED Lighting Considering Circadian Rhythm by Melanopic Illuminance Control, *Proceeding of 2022 International Conference on Emerging Technologies for Communications, ICETC, Tokyo, Japan, 2022*, 13-2.
- [10] Tomoaki Shikakura, Hiroyuki Morikawa, Yoshiki Nakamura: Perception of Lighting Fluctuation in a Luminous Offices Environment. *Journal of Light & Visual Environment*, 2003, 27(2), 75-82.
- [11] American National Standard Institute, Inc., ANSI C78.377 Electric Lamps Specifications for the Chromaticity of Solid State Lighting Products, National Electrical Manufacturers Association, 2015.
- [12] Robert J. Lucas, Stuart N. Peirson, David M. Berson, Timothy M. Brown, Howard M. Cooper, Charles A. Czeisler, et al.: Measuring and Using Light in the Melanopsin Age. *Trends in Neurosciences*, 2014, 37(1), 1-9.
- [13] Japanese Industrial Standards Committee, JIS Z 8781 Colorimetry, 2016.
- [14] Calvin S. McCamy: Correlated Color Temperature as an Explicit Function of Chromaticity Coordinates. *Color Research & Application*, 1992, 17(2), 142-144.
- [15] Japanese Industrial Standards Committee, JIS Z 8726 Method of Specifying Colour Rendering Properties of Light Sources, 1990.

## ACKNOWLEDGEMENTS

This research was also supported by the JSPS Grant-in-Aid for Scientific Research JP 23K03853.

Corresponding Author Name: Shogo Sakane

Affiliation: Graduate School of Science and Technology, Kyoto Institute of Technology

e-mail: m3621024.kit@gmail.com

# RESEARCH ON NOTICEABILITY OF DIGITAL BILLBOARDS FOCUSING ON VISUAL INFORMATION CHANGES

Yihan WANG and Miki KOZAKI

The University of Tokyo

## ABSTRACT

Digital billboards broadcasting dynamic advertisements have become a new type of lighting in urban landscapes. Pedestrians often noticed the digital billboards while moving. This raises the following research question: what properties of digital billboards draws people's attention. The reasons remain unclear, highlighting the need for further investigation on noticeability.

Usually, people will notice visual information change. Even if the visual information has changed the same degree, if the length of changing time is different, or if the visual information hasn't changed in the same direction, the noticeability level may also vary. For instance, the light source bright up in a second, or gradually bright up after a period of time, same degree has changed but with different time resulting in different mental feeling. Also, a light source condition changing from on to off, or from off to on, it changed the same degree but not in the same direction leads to different psychological tendencies. In order to clarify this, Visual Information Variation Rate (VIVR; visual information change amount divided by time period) was defined. Digital billboards broadcasting contents are considered to be the primary source of visual information in this paper, and a timeline is used as an extra dimension to present the entire visual information contents frame by frame. Visual information and time are also used for calculating the content change and measuring the speed of visual information change. The VIVR indicates the noticeability level of visual information, with a higher VIVR value indicating stronger noticeability. The VIVR is regarded as a vector which factors in the direction and time. By analyzing various elements contained in visual information, with a focus on the impact of changing rate in Visual Information and investigated the effects on visual attention attraction.

Experiment was conducted to prove the relationship between psychological quantities about noticeability and the Visual Information change. Subjects were shown 6 different commercial message short videos as visual information, and their attractive time spots were recorded by stopwatch. The noticeability level of the attractive time visual information was also gathered by using semantic differential methods.

VIVR was derived using the inter frame difference method to calculate the changing rate between each frame difference by timeline. Also, main properties like luminance, chroma and hue of the visual information itself, and other possible properties are also considered in the calculation process.

As a result, the correlation between noticeability and visual information variation rate was seen, an increase in VIVR leads to higher levels of visual information noticeability.

Keywords: Noticeability, Visual information, Variation rate, Digital billboard, Time period, Visual attention attraction, Inter frame difference method, Psychological tendency

## 1. INTRODUCTION

Out-of-home advertising is an essential part of the urban landscape and people's visual experience, continuously conveying visual information to pedestrians. Due to the increasing demand, many digital out-of-home advertising appeared in the urban space [1], and digital billboards are the most attractive one of them. Compared with traditional advertising media, digital billboards contain more visual information in the same unit time. Besides, advertisers prefer to use dynamic media to attract pedestrians' attention. These new dynamic advertisements not only carry the original information dissemination function, but also increase the density of visual information in the time dimension. People's attention can be easily attracted by dynamic advertisements, which makes an impact and influence on people's original visual experience. This research is trying to figure out the attractiveness level of visual information broadcasted by digital billboards.

Noticeability is normally used as an important factor to measure visual information [2]. The correlation between visual information's noticeability and people's visual experience is an important research direction in the future. There are many previous studies about noticeability in the architecture visual environment field, like using 3D simulations and luminance for prediction calculation [3], also using VR simulations research on "attractant area" by active searching [4]. However, due to the restriction of period, many researchers focus more on the static visual information, hardly regard digital billboards as the main research target. Besides, given the complexity of pedestrian activity and the dynamic content displayed on digital billboards, traditional optimization algorithms are inadequate for meeting the requirements of analyzing these scenarios. Conventional methods struggle to effectively handle the intricate measurement of time-varying visual information. A multi-angle approach is necessary to analyze the spatial relationship and visual information.

To effectively evaluate people's visual experience, with a particular focus on noticeability, this research is trying to get the correlation between visual information's physical elements and people's impression and reaction, aim to provide an effective solution to the challenges posed by time-varying visual information and its impact on assessing the noticeability of visual experiences.

## **2. HYPOTHESIS: NOTICEABILITY AND VISUAL INFORMATION VARIATION RATE**

Usually, people will notice visual information change. Even if the visual information has changed the same degree, if the length of changing time is different, or if the visual information hasn't changed in the same direction, the noticeability level may also vary. For instance, the light source bright up in a second, or gradually bright up after a period of time, same degree has changed but with different time resulting in different mental feeling. Also, a light source condition changing from on to off, or from off to on, it changed the same degree but not in the same direction leads to different psychological tendencies. In order to clarify this, Visual Information Variation Rate (VIVR; visual information change amount divided by time period) was defined.

Digital billboards broadcasting contents are considered to be the primary source of visual information in this paper, and a timeline is used as an extra dimension to present the entire visual information contents frame by frame. Visual information and time are also used for calculating the content change and measuring the speed of visual information change. The VIVR indicates the noticeability level of visual information, with a higher VIVR value indicating stronger noticeability. The VIVR is regarded as a vector which factors in the direction and time. By analyzing various elements contained in visual information, with a focus on the impact of changing rate in Visual Information and investigated the effects on visual attention attraction.

## **3. EXPERIMENT: IMPRESSION AND REACTION BY VISUAL INFORMATION**

### **3.1. EXPERIMENT SUMMARY**

The experiment investigates changes in subjects' perceived visual attractiveness when different types of visual information content are varied and conducts research to evaluate and analyze the visual information elements involved in the experiment.

Experimental environment: A "Meta quest 2" VR head-mounted display is used for the experiment, uses "Skybox video player" software to simulate the visual environment as a movie theater, and dynamic advertising media is played on the movie screen. The subjects' reaction time points are also recorded using a "Citizen 8RDA55-002" stopwatch. The 6 dynamic advertising visual information are selected by "YouTube's impressive commercial popularity ranking top 10" from January 2022 to February 2023, three 15s length and three 30s length, played in random order.

Experimental procedure: 1. Enter the laboratory and explain the content of the experiment to the subject; 2. Conduct reaction time test, repeat 5 times to take the average reaction time value; 3. Adjust the VR headset, to match the visual conditions of the subject; 4. The host will start to play the video and stopwatch at the same time. When the subject feels the visual information that attracts their attention, press the button on the stopwatch to record the time node. Keep record of attractive time nodes until the end of the video; 5. Visual information reaction evaluation; go back to the video images at the time nodes recorded by subjects, and ask the attracted level, the attracted object, its element and how they feel about it; 6. Visual information impression



evaluation; evaluate the video frame divided by equal time gap with 3 sets of adjectives; 7. Face sheet survey; answer to their background information.

Experiment period: May 16, 2023 to June 14, 2023.

Subject Information: There are 20 subjects (8 are female). For nationalities, 10 Chinese and 10 Japanese. Age from 22 to 36, the average age is 25.45; Subjects' height from 150cm to 185cm, average is 169.6cm. For subjects' dominant eyes, 17 are right and only 3 are left. 5 subjects wear contact lens, 8 wear glasses, and 7 are naked eye. Reaction time maximum is 0.427s, minimum is 0.248s, mean value is 0.294s. For subject's viewing history to the selected Visual Information, no subjects ever seen CM1, CM2 before the experiment; CM3 has 2 subjects seen once, and 2 subjects seen more than twice; CM4 has 1 subject seen more than twice; CM5 has 1 subject seen only once, and 1 subject seen more than twice; CM6 has 7 subjects seen it more than twice.

Evaluation items: the experiment records subjects' impression and reaction to the visual information. Visual information impression is evaluated using 3 sets of bipolar adjectives (7 Enjoyable - 1 Boring; 7 Lively - 1 Lonely; 7 Charming - 1 Mediocre) by 7-Point rating scale method. Visual information reaction is evaluated with an adjective (7 very attractive - 1 not attractive) by using the 7-Point rating scale method, also interviewing subjects' cognition and thoughts about the recorded time frames.

### 3.2. VISUAL INFORMATION PHYSICAL QUANTITIES ACQUISITION

The visual information needs to be measured to ensure its visual information variation rate (VIVR). In this research, the visual information is split into 6 elements (Luminance, Chroma, Hue, Delta E, Contrast, Content Change) to exactly measure its changes in different dimensions. Inter frame difference method is used to compute visual information changed, by differential the time period and compute the visual information changes frame by frame. In this part, the dynamic advertisement visual information is calculated as 30 frames per second, and the timeline is presented in "time frame number" way for calculation.

The elements are calculated by OpenCV, transfer the visual information media to CIE  $L^*a^*b^*$  color space and compute the Luminance, Chroma, Hue, Delta E and Contrast. The Content Change amount is directly equals to the number of content difference pixels divided by the whole frame pixel amount.

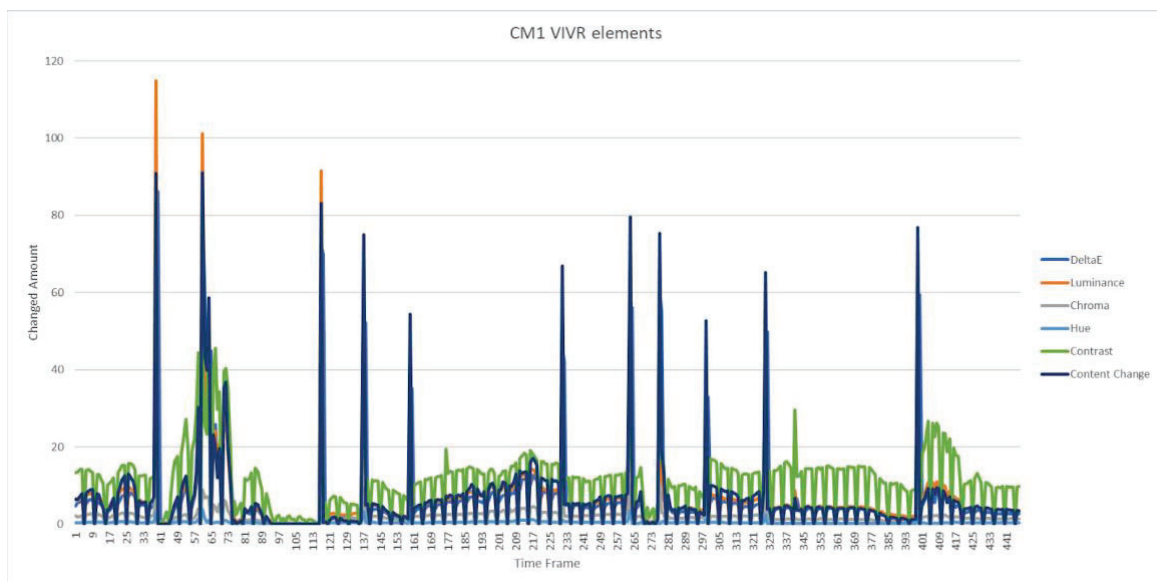


Figure 1. CM1 Visual Information Variation Rate Elements

As in Figure 1. shown above, VIVR elements are shown by timeline. Each value in the figure is subtract the element value corresponding to the previous frame from the element value of the next frame. In this way, the value divided by time (which equals to 1 after differential one second into 30 frames) is the variation rate of its element at its timeframe. The Shot number and its time length in time frame dimension is also recorded for further calculation and analysis.

#### 4. EXPERIMENTAL RESULTS AND DISCUSSION

A hypothesis of noticeability cognition model used in this research is shown in Figure 2. Visual information variation work as visual stimulation that attracts people's attention and changes the condition state from "see" to "noticed" perception period. After people's attention has changed to "noticed", the visual information will keep working together with long-term memory and finally form the "impression" of the visual information processing period. The amount of visual stimulation that attract people's attention, can make people's condition state change from "see" to "noticed" (evaluated in reaction evaluation), and how people evaluate the visual information's "impression" (evaluated in impression evaluation), are the points this research would like to figure out.

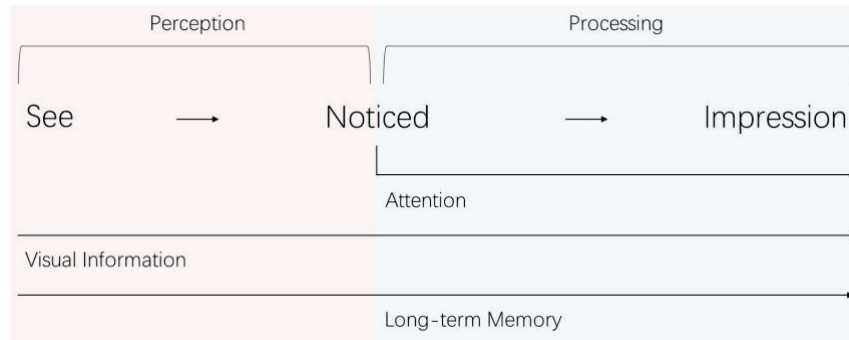


Figure 2. Noticeability Cognition Model

##### 4.1. RESULT OF VISUAL INFORMATION REACTION EVALUATION

This section will analysis and discuss in detail the correlation between the visual information reaction evaluation and subjects' personal attributes (results of face-sheet survey). It includes 8 sets of data, including Subject No., Gender, Nationality, Age, Dominant Eye, Eye condition, reaction time and viewing history. For the reaction evaluation, the attractiveness level in 7 rating scale is evaluated. Shot is a series of frame that runs for an uninterrupted period of time [5], and a dynamic advertisement is usually built up by a serious number of shots. Shot length is how long the shot lasts in time dimension. Shot number represents the order of shots, from 1 to the last shot based on timeline. It's hard to locate the accurate time frame that the subject's reaction happened with existing experiment equipment, and also based on the record of the interview part with subjects, the reaction time frame can be relocated by checking which time period it belongs to, to confirm its shot Number and figure out what kind of content that attracts subjects' attention.

Table 1. Reaction ANOVA test results of Overall

Factors	Subject No.	CM No.	Gender	Nationality	p-Value					
					Age	Dominant Eye	Eye Condition	Reaction Time	Viewing History	Shot Length
Reaction	<.0001	0.066	0.002	0.584	0.25	0.59	0.261	0.297	0.036	0.467

ANOVA test is done between the subjects' face sheet survey result and evaluated attractiveness level shown in Table 1. There's no strong evidence to show correlation between attractiveness level and shot length, gender, nationality, age, dominant eye, eye condition, reaction time and viewing history. The reaction results directly connect with visual information's physical quantities.

By combining the data and results both from "Reaction" and "Impression", the new subject grouping is reorganized between Gender and Nationality, the dataset is divided into 4 groups: "Male Japanese" (MJ), "Male Chinese" (MC), "Female Japanese" (FJ) and "Female Chinese" (FC) for the further analysis.

Table 2. New Group & reaction by CM No. ANOVA test result

CM No.		1	2	3	4	5	6
Group	FC	0.391	0.075	0.44	0.009	0.114	0.01
	FJ	0.134	0.147	0.216	0.003	0.065	0.486
	MC	0.244	0.447	0.167	0.001	0.173	0.042
	MJ	0.011	0.008	0.086	0.22	0.005	<.0001

An ANOVA test between the new group and reaction by CM Number is done, and the result is shown in Table 2. From the table “Male Japanese” show strong correlation in reaction evaluation except CM No.4&5, but other three groups met expectations in CM No.4, mainly because of the CM content difference.

Table 3. ANOVA test result of VIVR & attractiveness level by CM No. and Shot No.

CM No.	Shot No.	Delta E	Luminance	Chroma	Hue	Contrast	Content Change
1	6	0.038				0.019	
2	8		0.009	0.013		0.014	0.007
5	2	0.02					
5	6			0.028	0.009		
5	17	0.04					0.047
6	10					0.011	

An ANOVA test is held between these VIVR elements and attractiveness level evaluation of each shot in each CM, and the result is shown above in Table 3.

The test result shows the shot number in each CM, with correlation to the visual information changes. After checking the subject's interview record about impression and description, these shots are the target shots with high VIVR that attracted the subject's attention, they all have more than one VIVR elements that significantly huge move in its shot.

Table 4. record reaction counts & VIVR elements ANOVA test result

VIVR	p-Value	formula
Delta E	0.015	= 31.54 + 0.01 Delta E
Luminance	0.011	= 32.50 + 0.01 Luminance
Chroma	0.001	= 29.05 + 0.05 Chroma
Hue	0.01	= 45.79 + 0.17 Hue
Contrast	0.017	= 33.13 + 0.01 Contrast
Content Change	0.022	= 36.46 + 0.01 Content Change

Attractiveness level is not strong enough to proof the correlation between VIVR and subject's reaction. Another way to measure the VIVR is by counting subject's recorded reaction counts. As Table 4. shows, all the VIVR elements have a strong correlation with count numbers, and the formula shows the larger VIVR value, the higher count times.

Table 5. record reaction counts & VIVR elements ANOVA test result by CM No.

CM No.	reaction times	VIVR p-Value					
		Delta E	Luminance	Chroma	Hue	Contrast	Content Change
1	68	0.305	0.457	0.996	0.863	0.103	0.728
2	59	0.092	0.087	0.12	0.11	0.257	0.066
3	41	0.052	0.028	0.026	0.054	0.038	0.028
4	95	0.11	0.124	0.304	0.225	0.08	0.176
5	82	0.043	0.04	0.026	0.01	0.024	0.064
6	57	0.114	0.194	0.054	0.088	0.097	0.095

The Table 5 Shows the result of ANOVA test between reaction counts and VIVR elements by CM No., but only CM No.3 and CM No.5 has strong correlation which proof the hypothesis.

## 4.2. RESULT OF VISUAL INFORMATION IMPRESSION EVALUATION

Same as the reaction evaluation, this section will analysis and discuss in detail the correlation between the visual information impression evaluation and other attributes. For subjects' personal attributes, there 8 sets of data, including Subject No., Gender, Nationality, Age, Dominant Eye, Eye condition, reaction time and viewing history. For the impression evaluation, there are 3 sets of bipolar adjectives, enjoyable/boring, lively/lonely, and charming/mediocre. Before checking the experimental factors, other possible influential factors were tested, and ANOVA test result is shown below as Table 6.

By analyzing the subjects' information elements and impression evaluation, some significant findings were uncovered. Moreover, after obtaining positive results, favorable conditions that contributed to noticeability were identified by delved deeper into the data.

Table 6. Impression ANOVA test results of Overall

		p-Value								
Factors		Subject No.	CM No.	Gender	Nationality	Age	Dominant Eye	Eye Condition	Reaction Time	Viewing History
Impression	E/B	<.0001	<.0001	<.0001	0.878	0.323	0.039	<.0001	0.447	<.0001
	L/L	<.0001	<.0001	<.0001	0.081	0.906	0.03	<.0001	0.319	<.0001
	C/M	<.0001	<.0001	<.0001	<.0001	0.001	0.08	<.0001	0.003	<.0001

Gender: in CM No.1 to 5, female subjects evaluate visual information impression higher than male subjects in all 3 adjectives, and only in CM No.6, female subjects evaluate higher than male subjects in Enjoyable/Boring. The reason why CM No.6 have a higher impression score by male subjects might be because the main actress is a famous actress helped this CM got higher impression evaluation. In conclusion, except for the influence of the famous actress, usually female subjects are tending to rate higher than male subjects.

Nationality and Age: in CM No.4 Chinese / older subjects have higher evaluation on Enjoyable/Boring, Lively/Lonely; in CM No.5 Japanese / younger subjects have higher evaluation on Enjoyable/Boring, Lively/Lonely and Charming/Mediocre; in CM No.6, Japanese / younger subjects have higher evaluation on Charming/Mediocre. The ANOVA test result shows strong correlation between nationality and age. Most of the Japanese subjects are master course students, and most of the Chinese subjects are Doctor course students.

Dominant eye: Right eye subjects evaluate CM5 & 6 higher than Left eye subjects, but only have 3 left dominant eye subjects.

Eye condition: the overall result is subjects with contact lens rate a higher impression score than naked eye subjects than subjects wearing glasses. But in CM No. 2, 4, 6, there's no correlation between eye condition and Lively/Lonely, Charming/Mediocre.

Reaction time: CM No.5 shows correlation between reaction time and all 3 adjectives, and CM No.6 shows correlation with Charming/Mediocre. The higher reaction time, the lower the rate score.

Viewing history: there's no correlation between viewing history and impression evaluation score after the ANOVA test.

Table 7. New Group &amp; impression by CM No. ANOVA test result

CM No.	1			2			3			4			5			6		
Impression	E/B	L/L	C/M	E/B	L/L	C/M	E/B	L/L	C/M	E/B	L/L	C/M	E/B	L/L	C/M	E/B	L/L	C/M
Group	FC	0.178	0.016	0.449	0.643	0.81	0.909	0.606	0.965	0.239	0.257	0.07	0.221	0.854	0.765	0.976	0.986	0.963
	FJ	<.0001	<.0001	0.006	<.0001	<.0001	<.0001	0.001	0.691	0.004	<.0001	<.0001	0.001	<.0001	<.0001	<.0001	<.0001	0.0003
	MC	0.001	<.0001	0.006	<.0001	<.0001	<.0001	0.012	0.096	0.107	0.188	0.048	0.103	0.379	0.221	0.471	0.012	0.0003
	MJ	0.007	0.047	0.053	0.092	0.0003	0.356	0.571	0.686	0.821	<.0001	<.0001	<.0001	0.02	0.634	0.043	0.377	0.023

Same as reaction part, an ANOVA test between the new group and impression by CM Number is done, and the result is shown in Table 7. From the table "Male Japanese", "Male Chinese" and "Female Japanese" show strong correlation in all three impression dimensions, but the "Female Chinese" group only met expectations in the Lively/Lonely dimension, mainly because of the lack of diversity in female Chinese subjects.

Table 8. VIVR &amp; impression ANOVA test result &amp; formula

Impression	E/B		L/L		C/M	
VIVR	Formula	p-Value	Formula	p-Value	Formula	p-Value
Luminance	= 3.765 + 0.002 Luminance	<.0001	= 3.577 + 0.002 Luminance	<.0001	= 3.715 + 0.002 Luminance	<.0001
Chroma	= 3.765 + 0.002 Luminance	<.0001	= 3.546 + 0.011 Chroma	<.0001	= 3.639 + 0.011 Chroma	<.0001
Hue	= 3.890 + 0.384 Hue	<.0001	= 3.857 + 0.022 Hue	<.0001	= 3.831 + 0.040 Hue	<.0001
Delta E	= 3.749 + 0.002 Delta E	<.0001	= 3.555 + 0.002 Delta E	<.0001	= 3.702 + 0.002 Delta E	<.0001
Contrast	= 3.657 + 0.001 Contrast	<.0001	= 3.479 + 0.001 Contrast	<.0001	= 3.628 + 0.001 Contrast	<.0001
Content Change	= 3.820 + 0.002 Content Change	<.0001	= 3.627 + 0.002 Content Change	<.0001	= 3.770 + 0.002 Content Change	<.0001

From the linear fit test result show in Table 8., the higher the VIVR value, the better the impression rating score.

For the prediction formula, there are three methods to calculate. "Delta E / Contrast / Content Change" (DCC), "Luminance / Chroma / Hue" (LCh) and All6 by using all the visual information elements. An ANOVA test is held between these three methods, the result and its correlation level are shown in Table 8. From Table 9., it's clear that the DCC method works better than the other two in all group conditions.

Table 9. Formula method &amp; impression by Group ANOVA test result

Impression	L/L				E/B				C/M			
Group	FC	FJ	MC	MJ	FC	FJ	MC	MJ	FC	FJ	MC	MJ
method	DCC	DCC	DCC	DCC	DCC	DCC	DCC	DCC	DCC	DCC	DCC	DCC
Prob>F	0.046	<.0001	0.001	0.002	x	<.0001	0.001	0.006	x	<.0001	<.0001	0.006
method	LCh	LCh	LCh	LCh	LCh	LCh	LCh	LCh	LCh	LCh	LCh	LCh
Prob>F	0.304	<.0001	<.0001	0.0004	x	<.0001	0.003	0.008	x	<.0001	<.0001	0.065
method	All6	All6	All6	All6	All7	All6	All6	All6	All7	All6	All6	All6
Prob>F	0.273	<.0001	0.001	0.001	x	<.0001	0.006	0.015	x	0.0002	0.0003	0.026

The correlation formula between VIVR elements and subject's impression evaluation score can be defined as Table 10.

Table 10. VIVR and Impression formula (DCC method)

Impression	Group	Formula
Lively/Lonely	FC	= 3.989 - 0.002 DeltaE + 0.01 Contrast - 0.01 Content Change
	FJ	= 3.491 - 0.003 DeltaE + 0.001 Contrast + 0.005 Content Change
	MC	= 2.99 + 0.002 DeltaE + 0.001 Contrast - 0.001 Content Change
	MJ	= 3.681 - 0.001 DeltaE + 0.003 Content Change
Enjoyable/Boring	FJ	= 3.891 - 0.004 DeltaE + 0.001 Contrast + 0.004 Content Change
	MC	= 3.117 + 0.002 DeltaE + 0.002 Contrast - 0.002 Content Change
	MJ	= 3.673 + 0.002 Content Change
Charming/Mediocre	FJ	= 3.96 - 0.001 DeltaE + 0.003 Content Change
	MC	= 2.511 + 0.004 DeltaE + 0.003 Contrast - 0.002 Content Change
	MJ	= 4.094 - 0.005 DeltaE - 0.001 Contrast + 0.007 Content Change

## 5. CONCLUSIONS

This research aims to investigate the factors that attract people's attention to digital billboards and evaluate the noticeability of visual information changes. Visual Information Variation Rate (VIVR), by considering the degree and time of visual information changes, is proposed as a measure of noticeability. The experiment by showing subjects different dynamic advertisements on a VR headset and recording their attractive time spots using a stopwatch. The noticeability level and impression of the visual information are evaluated using semantic differential methods. The visual information is analyzed by calculating various physical quantities such as luminance, chroma, hue, delta E, contrast, and content change.

The results of the experiment suggest a correlation between noticeability and VIVR. The paper discusses the findings related to subjects' impressions and reactions to the visual information, considering factors such as gender, nationality, age, dominant eye, eye condition, reaction time, and viewing history. The research analysis from "reaction" and "impression" two parts, revealed a clear correlation between noticeability and the variation rate of visual information. An increase in VIVR led to higher levels of visual information noticeability. This indicates that factors such as the length of changing time and the direction of visual information changes play a significant role in attracting attention. Even if the visual information changes to the same degree, differences in time duration and direction can influence the noticeability level and individuals' psychological tendencies. The analysis also includes the prediction formula for noticeability based on VIVR elements and the subjects' impression evaluation scores.

Overall, the research paper focuses on understanding the noticeability of visual information changes in digital billboards and provides insights into the factors that influence people's attention and impressions. However, it's still necessary to dig out the correlation between other factors to approach an accurate interpretation. Also, there's still other elements need to be further dig out in the future, and it's also necessary improve the accuracy of time record to improve the experiment result.



## REFERENCES

- [1] McCarthy, Anna. (2001). Ambient Television. Durham, NC: Duke University Press Books.
- [2] Yoshihiko Tabuchi, Hajimu Nakamura, Visual requirements for legibility and readability of visual signs, JOURNAL OF THE ILLUMINATING ENGINEERING INSTITUTE OF JAPAN, 1992, Volume 76, Issue 1, Pages 8-12
- [3] Miki KOZAKI, Marina NISHIKAWA, Kotaroh HIRATE, RESEARCH ON VISUAL INFORMATION ACQUISITION OF SIGNBOARD IN SHOPPING MALL USING ANALOGY WITH ILLUMINANCE CALCULATION (PART 2): FOCUSING ON NOTICEABILITY, Journal of Environmental Engineering (Transactions of AIJ), 2019, Volume 84, Issue 766, Pages 1051-1058
- [4] Marina NISHIKAWA, Ye MA, Jaeyoung HEO, Kotaroh HIRATE, Yoshiki IKEDA, Kazuo ISHIMA, A STUDY USING VR ON THE EASE OF FINDING SIGNS IN STATION SPACE, Journal of Environmental Engineering, 2020, Volume 85, Issue 774, Pages 569-577.
- [5] Sklar, Robert. Film: An International History of the Medium. [London]: Thames and Hudson, [c. 1990]. p. 526.

## ACKNOWLEDGEMENTS

Corresponding Author Name: Miki Kozaki  
Affiliation: The University of Tokyo  
e-mail: kozaki@edu.k.u-tokyo.ac.jp

# TUNNEL LIGHTING SYSTEM FOR ENHANCED MAINTENANCE

Shigeru Muramatsu

SEIWA ELECTRIC MFG CO., Ltd.

## ABSTRACT

In recent years, the automation of the inspection of tunnel facilities has been progressing owing to the aging workers and labor shortages. A tunnel lighting system performs two-way communication between the tunnel lighting equipment and a control device. In addition to controlling the light, it can monitor abnormal situations using a status-monitoring function. Therefore, the introduction of tunnel lighting systems enables the maintenance of tunnel facilities, and this study presents the functions and features of these tunnel lighting systems.

## 1. Introduction

In recent years, there has been a decrease in work efficiency and an increase in workload in electrical equipment inspection tasks owing to aging workers and labor shortages. The inspection of tunnel lighting facilities is no exception. Therefore, studies are being conducted on tunnel lighting systems to reduce the man-hours required for inspection. This study proposes a tunnel lighting system that features a communication function for constant monitoring of the state of each tunnel light, in addition to the conventional lighting and dimming controls. This paper provides an overview of the proposed tunnel lighting system, its functionality, and its benefits.

## 2. Challenges in conventional tunnel lighting facilities

- Control and inspection of conventional tunnel lighting facilities

In conventional tunnel lighting facilities, the light-receiving unit of the automatic dimmer detects the brightness outside the tunnel and adjusts the tunnel lighting to an appropriate brightness in accordance with the natural light. However, because conventional tunnel lighting has no communication capability, inspectors go inside the tunnel to inspect the tunnel lighting and ensure it functions appropriately. Ideally, the inspection work should be carried out regularly. However, every time an inspection is carried out, the inspector has to go inside the tunnel, which requires significant time and effort.

- Maintenance of tunnel lighting

When a tunnel light reaches the end of its service life, its luminous flux drops or it fails to illuminate, making it impossible to guarantee the brightness that was originally required. Therefore, it is necessary to keep track of the cumulative lighting hours of tunnel lighting to determine when it would reach the end of its service life. Because the cumulative lighting hours vary depending on the type of tunnel lighting, the lighting hours may differ even among tunnel lights that entered service around the same time. In conventional tunnel lighting facilities, it is necessary to investigate the cumulative lighting hours for each type of tunnel lighting. Sunset and sunrise times also vary with the seasons, making it difficult to accurately manage the cumulative lighting hours in conventional tunnel lighting facilities.

## 3. Tunnel lighting system

- Tunnel lighting status monitoring function

The tunnel lighting system comprises the following equipment: tunnel lighting, tunnel lighting control unit, power reception and distribution, traffic safety facilities in the tunnel, and monitor and control devices. The capabilities of the tunnel lighting control unit include monitoring the status of each tunnel light, monitoring the status of the power reception and distribution system, collecting information on the presence of disaster prevention signals for traffic safety facilities in the tunnel,

and controlling the tunnel illumination for every situation. The tunnel lighting control unit also transmits its collected monitoring data to a remote monitor and control device in real-time, which allows the tunnel management office to quickly detect the status of tunnel facilities.

- Complementary brightness function

If the tunnel lighting malfunctions or fails to illuminate, it needs to be replaced as soon as possible to ensure safe lighting in the tunnel. However, it may not be possible to replace and restore the lighting immediately since arrangements need to be made to enforce the associated traffic regulations. Therefore, the proposed tunnel lighting system has a complementary brightness function that boosts the brightness of the adjacent lighting when a tunnel light fails to illuminate. This feature ensures safety in the tunnel by maintaining brightness until the tunnel lighting is replaced.

- Monitoring of cumulative lighting hours

The monitoring information that the tunnel lighting control unit receives from the tunnel lighting includes the lighting status of the tunnel lighting and fault monitoring, as well as the cumulative lighting hours. This makes it possible to monitor the cumulative lighting hours for each tunnel light and determine whether it has exceeded its service life. When a light exceeds its service life, the warning display on the tunnel lighting control unit alerts the maintenance manager. Knowing the cumulative lighting hours also facilitates light replacement planning.

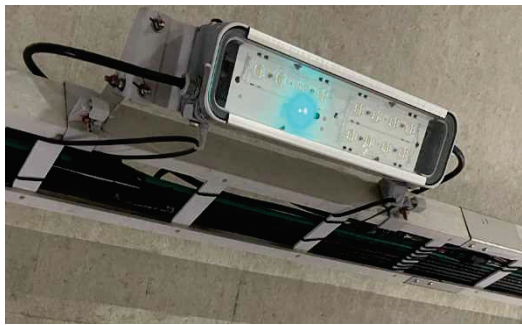


Fig. 1. Communication-controlled tunnel lighting



Fig. 2. Interior of the communication-controlled tunnel

#### 4. Conclusion

This study proposed a tunnel lighting system that reduces the man-hours required for inspection and enables efficient operation of tunnel lighting facilities. The system features added functionality to ensure safety in tunnels when the tunnel lighting malfunctions or fails to illuminate.

In the future, we hope to develop a system that ensures the safety of drivers driving in tunnels while reducing the man hours required for inspection.

Corresponding Author Name: Shigeru Muramatsu  
Affiliation: SEIWA ELECTRIC MFG CO., Ltd.  
e-mail: MURAMATU\_sigeru@seiwa.co.jp

# PROMOTING AFTERNOON NAP IN THE CAR: THE EFFECT OF ILLUMINANCE AND COLOR TEMPERATURE OF AUTOMOTIVE INTERIOR LIGHTING ON AFTERNOON SLEEPINESS, FATIGUE, AND SLEEP

Li N<sup>1, 2</sup>, Miao W<sup>1</sup>, Christopher W<sup>1</sup>, Lin Y<sup>1, 2, 3, \*</sup>

<sup>1</sup>Department of Illuminance & Light Source, School of Information Science and Engineering, Fudan University, Shanghai, 200438, China

<sup>2</sup>Human Phenome Institute, Fudan University, Shanghai, 201203, China

<sup>3</sup>Intelligent Vision and Human Factor Engineering Center, Shanghai 201306, China

## ABSTRACT

An afternoon nap during driving can reduce sleepiness and fatigue, thus ensuring driving safety and enhancing the passenger experience. Using automotive interior lighting before an afternoon nap can help people fall asleep more easily. This study aims to investigate the effects of illuminance and color temperature (CCT) on human performance, exploring the most suitable combination of lighting parameters to promote in-car napping. In this study, the environment inside the vehicle was transformed, and six lighting conditions were selected, consisting of 3 illuminances (10lx & 150lx & 300lx) and 2 CCTs (4500K & 2000K). Eleven participants participated in the experiment and received light interventions after lunch. The participants' sleepiness, fatigue, mood and subjective sleep quality were measured. The experimental results show that for illuminance and CCT, 300lx and 2000K light can effectively increase sleepiness and fatigue, reduce positive emotions, and thus help to fall asleep. However, light did not have a significant effect on sleep quality. This study proves that the lower CCT and higher illuminance automotive interior lighting promotes the napping experience and puts forward suggestions on the light parameter setting suitable for the lighting environment in the car, which provides an essential basis for future automotive interior lighting development.

Keywords: automotive interior lighting, nap, sleepiness, fatigue

## 1. INTRODUCTION

It is reported that traffic accidents are most likely to occur between 4 am-6 am and 2 pm-4 pm, which is related to drivers' drowsiness in the afternoon [1-4]. Afternoon drowsiness is not only caused by food but is also related to the inherent circadian rhythm of humans. Afternoon naps have been shown to prevent afternoon fatigue significantly and driver subjective sleepiness [5-11], cognitive performance [6,9,10] and driving performance [12,13]. In addition, with the development of self-driving cars in recent years, passenger cars have changed from ordinary means of transportation to one of the essential scenes of people's life and work. To sum up, having an afternoon nap in the car is necessary for the safety of driving and the comfort of passengers. Therefore, this study aims to set appropriate light to help fall asleep and improve napping.

External light is the most critical timing factor for humans. It directly interferes with the human body's circadian rhythm, directly or indirectly affecting sleep [14-18]. The light before going to bed at night is usually reported to be bad for subsequent sleep. Receiving light more than 10lx before bed will directly affect sleep homeostasis. Electronic use for a long time before going to bed has been shown to directly lead to an increase in sleep latency, a decrease in nocturnal sleepiness and a backward shift in circadian rhythm [19,20,22]. At the same time, bedside lights during sleep can also lead to light sleep and frequent awakening [21]. Therefore, the evidence suggests that a dark environment seems to be the most favourable for falling asleep compared to light. However, this conclusion may only apply to night sleep because it aligns with the diurnal cycle of natural light and the body's biological clock. Therefore, although the above studies focus on the effects of pre-bedtime light on night sleep, how daytime naps are affected by light still needs to be discovered, and individual studies have found that daytime conditions seem inconsistent with night sleep. Harrison's research shows that, compared with dark environments, 1 lx moonlight and 80 lx indoor light, 500 nm green light intervention during siesta does not affect falling asleep time and sleep quality [23]. This study shows that the effect of light on sleep does not exist in daytime sleep. Proper light can be used to help people fall asleep or improve the quality of sleep. Studies

had shown that subjects exposed to 2000K low CCT light before bed at night had better sleep quality and lower lethargy after waking up than 6000K light [24]. Exposure to a special 2700K pink light before bed at night has also been shown to improve sleep quality by more than 5000K light [25]. In addition, compared with high CCT light, low CCT is more conducive to eliminating pre-bedtime vigilance, thus helping to fall asleep.

A study of pilots showed a significant correlation between self-reported fatigue and daytime sleepiness [26,27]. For drivers, sleepiness is an essential indicator of fatigue, because the increased fatigue will significantly cause sleepiness [28]. An increase in the level of light has been shown to increase fatigue. In the narrow space inside the car, the human eye is closer to the light source, and the perception of brightness will be stronger. A study in limited space shows that the effect of environmental illuminance level on visual fatigue decreases at first and then increases [29]. When the illuminance of the working face is in the range of 0-300lx, the visual fatigue of readers decreases with the increase of illuminance but increases when it exceeds 300lx. Based on the non-visual effect of light and the response of ipRGCs to the rhythmic system, CIE proposes to use five equivalent illuminance models to describe the response of human visual cells to external light [30]. Therefore, the illuminance and spectrum of eye position are essential parameters to evaluate the non-visual effect of light on the human body. Because the scene in the car is different from the office scene, the illuminance of the working face has no reference value, so according to the correlation between the illuminance of the working face of the office and the vertical illuminance of the eye position [31], it is considered that the illuminance of the eye position of about 150lx is the lowest condition of visual fatigue, and exceeding 150lx will increase the degree of fatigue, which may cause a higher level of sleepiness. Therefore, in this experiment, the higher eye position illumination level of 300lx and the ordinary indoor eye position illumination level of 150lx is set, and 10lx is set as the lowest eye level illuminance according to the lighting scene in which the vehicle is parked in the basement. In addition, the CCT levels of 2000K and 4500K were set to compare the promoting effect of light on the degree of falling asleep. In addition, traditional car interior lighting usually uses a darker point light source to provide local lighting to meet the most basic lighting needs of the car. However, this study designed a space-filled environment similar to indoor lighting to achieve appropriate eye position illumination and avoid uncomfortable glare.

Therefore, this study aims to explore the influence of the lighting environment used in the passenger car before the afternoon nap on the subsequent degree of sleepiness and fatigue, to help fall asleep and improve the nap. In this study, we set up a new interior light environment of indirect lighting. We compared the effects of two kinds of light colour and three kinds of illumination on afternoon alertness, fatigue and sleep quality of passengers in small passenger vehicles. Even if light conditions do not necessarily affect sleep during the day, increasing light levels and fatigue in unique narrow spaces can increase sleepiness and help people fall asleep more easily.

## 2. METHODS

### 2.1 Experimental setting

This experiment was carried out in an actual sport utility vehicle. The experiment was carried out with four seats in the first and second rows, and an acrylic partition separated each seat to avoid interference. The seat is adjusted to an angle of 10 °between the seat and the ground and 55 °between the backrest and the ground, ensuring that the space between the front and rear rows of seats is ample enough for passengers. The temperature and humidity in the car are kept stable by air conditioning, and blankets are provided for subjects to use during their naps.

In this experiment, an intra-group design was adopted, in which each participant experienced all six light conditions randomly in sequence on different experimental days: using a combination of two specific spectra (4500K natural white light and a 2000K warm white light) and three illuminations (10lx, 150lx, 300lx). The adjustable 5-channel LED lamp belt is installed around the roof, the edge of the door, the floor and other positions through the combination of direct and indirect lighting to provide the lighting needed for the experiment, forming a uniform, space-filled lighting environment. All lamps and lanterns are set in the proper position and at a good angle to avoid uncomfortable glare when lying on the back. The brightness and CCT of LED lamp belts can be controlled by an external controller and computer program, and continuous dynamic change can be realized.



Table 1 Five equivalent daylight illuminance (EDI) calculated according to CIE S026 and CS values of eye positions provided by six light environments

Conditions	CCT (K)	Illuminance (lx)	$\alpha$ -opic equivalent daylight (D65) illuminance, EDI (lx)					Circadian stimulus, CS
			sc	mc	lc	rh	mel	
NL1	4545	10.05	7.30	9.10	10.02	7.72	7.26	0.012
NL2	4590	149.45	112.08	135.46	149.20	115.67	109.29	0.182
NL3	4599	306.78	241.73	277.79	307.17	239.28	227.76	0.329
WL1	1990	9.95	1.59	6.85	10.45	3.71	2.92	0.006
WL2	1977	146.17	24.42	104.09	159.24	55.97	43.82	0.102
WL3	1975	276.64	44.23	188.17	288.45	101.01	78.78	0.187

The spectral power distribution of eye position under six kinds of light conditions (NL1: 4500K, 10lx; NL2: 4500K, 150lx; NL3: 4500K, 300lx; WL1: 2000K, 10lx; WL2: 2000K, 150lx; WL3: 2000K, 300lx) is shown in Figure 1. The five equivalent daylight illuminations (EDI) of the eye positions provided by the six light environments calculated according to CIE S026 are shown in Table 1. At the same time, the circadian stimulus (CS) values are also calculated and listed (Mark Rea). The four seats' eye position spectrum and illuminance are measured using a spectrometer (CL-500A, Konika Minolta) to ensure that the difference between the four seats and the target illuminance and CCT does not exceed 10%. Shading curtains were used outside the car to prevent external light from entering.

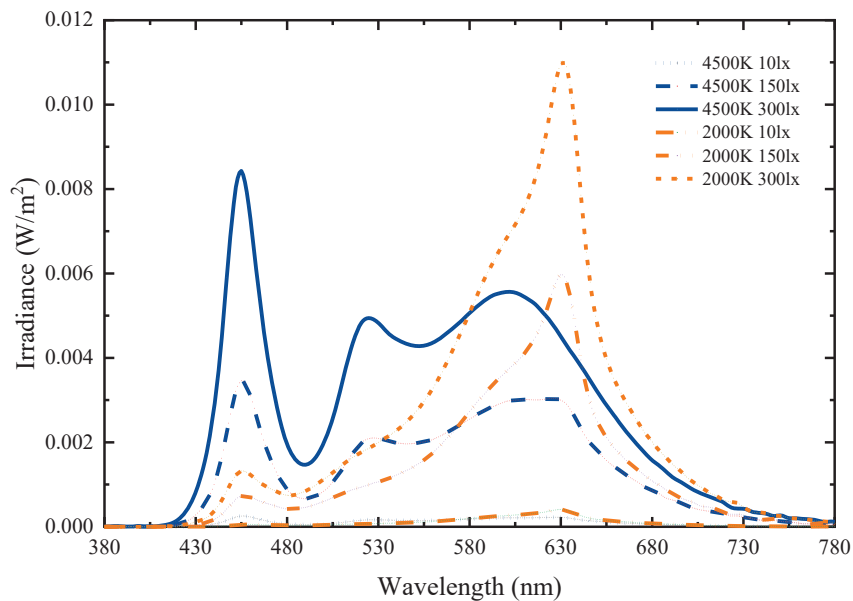


Figure 1. The spectral power distribution of eye position under six lighting conditions (two CCT \* three illuminances) was used in the experiment.

## 2.2 Participants

11 healthy adults (7 females) aged 25 to 49 years old (average,  $35.73 \pm 7.86$  years) participated in the current study. None of the participants was extreme chronotypes as per the Morningness-Eveningness Questionnaire (Horne & Ostberg, 1976), nor did they have physical or mental health problems or complaints about night sleep. All participants gave their written informed consent before participating. This study was conducted in agreement with the regulations of the Ethics Committee on Research Involving Humans at Fudan University (No. FE22028R).

**Measurements.** The scales measured subjects' subjective sleepiness, subjective alertness, and emotion.

**Karolinska Sleepiness Scale (KSS).** Subjective sleepiness was measured by Karolinska Sleepiness Scale (KSS) [32]. KSS is a 9-point Likert scale (1 representing 'extremely alert', 2

'very alert', 3 'alert', 5 'neither alert nor sleepy'..., and 9 'extremely sleepy'). It is sensitive to the alerting effects of light.

**Visual Analog Scales-Fatigue (VAS-F).** Subjective fatigue was also evaluated with 50 mm visual analogue scales (VAS) that were shown to have good reliability and validity [33,34]. The Fatigue Questionnaire consists of two parts. In the first part, eighteen items were to be evaluated, including tired, sleepy, drowsy, active, efficient and so on. In the second part, seven items describing visual fatigue were to be evaluated. The total score of these two parts is the total score of fatigue degree; the higher the score, the more fatigue. Participants were instructed to place a mark on a 50 mm long line to indicate their subjective feelings at that moment.

**Positive and Negative Affect Schedule (PANAS).** Mood states were assessed by the Positive and Negative Affect Schedule (PANAS) [35], which includes descriptions of both positive affect (PA) and negative affect (NA). The Chinese version of the PANAS has well-established validity and reliability. Subjects were required to rate their mood on a Likert scale ranging from 1 (little or not at all) to 5 (very much). PA and NA scores were calculated by the average of ten positive and ten negative items, respectively. The higher the PA or NA shows, the higher the positive or negative mood; the lower the score, the closer to no mood.

**Consensus Sleep Dairy (CSD).** Sleep quality was measured by modified Consensus Sleep Dairy [36]. The items included time to sleep, number of awakenings, length of awakenings, total length of sleep, and a five-point Likert scale of subjective sleep quality.

## 2.2 Procedure

The experiment was conducted from September to October 2022. Participants were scheduled to visit the laboratory for six days to experience six lighting conditions.

During the period from three days before entering the laboratory for the first time to the end of the experiment, the subjects were asked to follow the regular routine and report their sleep through an electronic questionnaire when they woke up every morning. On the day of the experiment, the subjects were asked to have lunch by themselves and came to the laboratory after the meal. The subjects were asked to use an appropriate amount of light meals to avoid over-satiety in order to avoid the differences caused by food intake. After coming to the laboratory, the subjects followed the process shown in Figure 2. At 11:50, the subjects went into the car under the baseline light to make preparations, and the operation sent instructions to the participants through a walkie-talkie that could talk in both directions. From 12:00, the subjects performed 10min dark adaptations in the dark environment. 12:10, the first measurement program was carried out in the set dark measurement environment as the baseline data, including KSS, PANAS and VAS-F. 12:20~12:50, the experimental lights were lit for light intervention. The subjects were told to open their eyes, during which the second measurement procedure, including KSS, PANAS and VAS-F, began at 12:40. From 13:00, the lights went out gradually in the 7min, and the subjects were told that they could close their eyes and try to fall asleep. 13:00 ~ 14:00 was the allowed nap time. At 14:00, the subjects woke up and took a third measurement in the set light, including CSD. At 14:10, the subjects left the laboratory. During the experiment, the subjects were told they could not talk and were prohibited from using electronic devices.

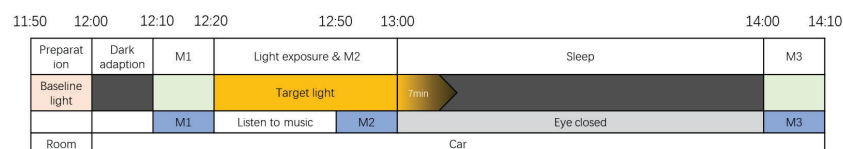


Figure 2. The experimental procedure and times of measurements for each experimental day. Each measurement process includes: M1:KSS, PANAS, VAS-F; M2:KSS, PANAS, VAS-F; M3: CSD.

## 2.3 Data Analysis

In this experiment, the visual analogue scale and Likert scale scores were calculated as continuous variables. After the light intervention, the scores of KSS, fatigue and mood were subtracted from the scores before the light intervention, and the difference was defined as the amount of change, which was recorded as  $d_{KSS}$ ,  $d_{Fatigue}$ ,  $d_{PA}$  and  $d_{NA}$ , respectively, to indicate the influence of lighting conditions. Unless otherwise noted, the data was expressed as an average  $\pm$  SD. Before data processing, the box diagram was used to determine the abnormal value and use the average value instead.

Two-factor ANOVA of 2\*3 was used to compare changes in subjective alertness, fatigue, and sleep quality measured by CSD. Post hoc comparisons were performed using Tukey's honestly significant difference (HSD) test. Non-parametric tests of independent samples compare the amount of change in PA and NA. All the statistics were conducted using SPSS Statistics version 20 (IBM, Armonk, NY, USA).

### 3. RESULT

#### 3.1 Subjective sleepiness

The paired t-test was performed on the KSS scores after and before the light intervention under each light condition, and all light conditions except HL2 led to a significant increase in KSS score, which meant a significant decrease in subjective alertness. The difference between KSS scores before and after the light intervention was taken as the change in subjective alertness, which was recorded as  $d_{KSS}$ . The results of one-way ANOVA showed that light conditions had a significant effect on  $d_{KSS}$  ( $F=2.886$ ,  $p=0.021$ ). The results of two-factor ANOVA using illuminance and CCT showed that illuminance ( $F=4.759$ ,  $p=0.012$ ) and CCT ( $F=4.461$ ,  $p=0.039$ ) had significant effects on  $d_{KSS}$ , but there was no interaction (Shown in Figure 3). The results of the post-hoc comparison showed that 300lx significantly improved the level of sleepiness compared with 10lx ( $p=0.029$ ) and 150lx ( $p=0.004$ ), and 2000K significantly improved the level of sleepiness ( $p=0.039$ ) compared with 4500K.

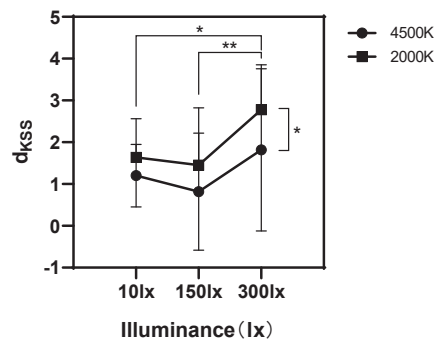


Figure 3 The effect of illuminance and CCT on the change of KSS.

#### 3.2 Subjective Fatigue on VAS

The paired t-test of fatigue scores after light intervention and before light intervention under each light condition showed that NL1 ( $t=5.502$ ,  $p=0.000$ ), NL3 ( $t=4.871$ ,  $p=0.001$ ), WL1 ( $t=6.418$ ,  $p=0.000$ ), WL2 ( $t=2.726$ ,  $p=0.021$ ), and WL3 ( $t=3.665$ ,  $p=0.004$ ) significantly increased the fatigue of subjects compared with before light intervention. NL2 ( $t=1.941$ ,  $p=0.081$ ) did not significantly affect fatigue. The difference between the fatigue score before and after the light intervention was used as the change in fatigue, which was recorded as  $d_{Fatigue}$ . The results of one-way ANOVA showed that light conditions had a significant effect on  $d_{Fatigue}$  ( $F=2.986$ ,  $p=0.018$ ). The results of two-factor ANOVA using illuminance and CCT showed that illuminance ( $F=5.949$ ,  $p=0.004$ ) had a significant effect on  $d_{Fatigue}$ , CCT had no significant effect on  $d_{Fatigue}$  ( $F=2.293$ ,  $p=0.135$ ), and there was no interaction between illuminance and CCT (Shown in Figure 4). The post-hoc comparison results show that 10lx ( $p=0.013$ ) and 300lx ( $p=0.002$ ) significantly increase fatigue levels compared with 150lx.

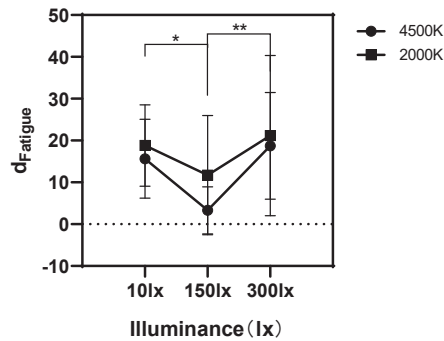


Figure 4 The effect of illuminance and CCT on the change of fatigue.

### 3.3 Mood

PA and NA scores were calculated with PANAS. Non-parametric tests were performed on relevant samples for PA and NA scores after and before each light intervention using the Wilcoxon method. The results showed that NL3( $Z = 2.567$ ,  $p = 0.010$ ) and WL3( $Z = 2.849$ ,  $p = 0.004$ ) led to a significant decrease in PA, indicating a significant decrease in positive emotions. All lighting conditions had no significant effect on NA. The difference between PA and NA scores before and after the light intervention was recorded as the change of positive and negative emotions and as  $d_{PA}$  and  $d_{NA}$ . The non-parametric test of independent samples showed that lighting conditions significantly affected  $d_{PA}$  ( $p = 0.000$ ). Similarly, CCT significantly affected  $d_{PA}$  ( $p = 0.005$ ). The results of the post-hoc comparison showed that compared with 4500K, 2000K significantly increased positive emotion. Illuminance had a significant effect on  $d_{PA}$  ( $p = 0.001$ ). Compared with 150 lx, 300 lx significantly decreased positive emotion ( $p = 0.000$ ). Light conditions had no significant effect on  $d_{NA}$ .

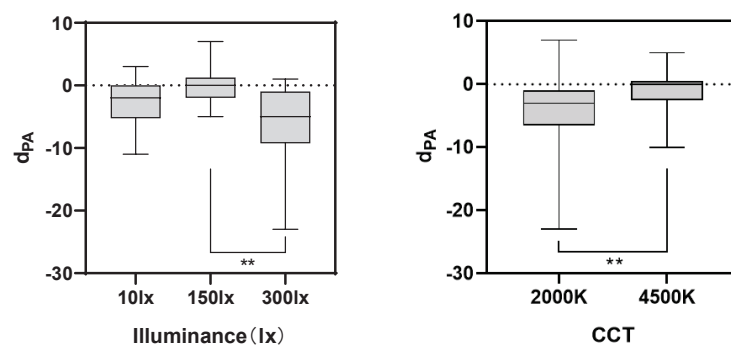


Figure 5 The effect of illuminance and CCT on the change of positive emotion.

### 3.4 Sleep Quality

The subjective scores of time to fall asleep, duration of sleep, and sleep quality in CSD were analysed separately. The results of the two-factor ANOVA of illuminance and CCT showed that illuminance and CCT both had no significant effect on sleep time, sleep duration and subjective score of sleep quality, and there was no interaction.

## 4. DISCUSSION

The primary purpose of this study is to explore which CCT and illuminance can promote nap when using car lighting before nap. When the CCT is set to 2000K, it significantly improves the level of sleepiness compared to 4500K, helping to fall asleep. This result is consistent with the research results of Wen et al. on nocturnal sleep and also indicates that low CCT light can promote sleep compared to high CCT [25]. Compared to low CCT photography, natural white light has also been proven to improve alertness and work performance in office settings. In this scenario, when the illuminance is set to 300lx, there is a significant increase in sleepiness after the light intervention, indicating that 300lx illumination can help fall asleep. This result is inconsistent with the research results before going to bed at night. More than 10lx of light before

bed at night can lead to increased alertness, melatonin inhibition, and sleep interference. However, research shows that light during daytime sleep does not seem to affect sleep, which may be related to the influence of natural light on circadian rhythm. Daytime lighting is different from the nighttime, lacking a pathway that significantly inhibits the secretion of melatonin and affects alertness, thus having a minor direct impact on sleepiness. The results of fatigue in this experiment indicate that 300lx light significantly causes fatigue compared to 150lx, and the increase in fatigue directly leads to an increase in subjective sleepiness [26,27], making people feel more likely to fall asleep. A study conducted in a narrow space showed that a working surface illuminance of 300lx was the lowest level of visual fatigue [29]. However, in this study, when the subjects were supine in the car, there was no working surface, such as a desktop, as a reference. The illuminance values reported in this study were all eye position illuminance. However, previous studies have rarely directly reported on eye position illuminance and often used horizontal illuminance of the working surface to characterize spatial illuminance, making it difficult to compare the illuminance level of this study with other studies. Based on the correlation between desktop horizontal illumination and eye position illuminance in previous studies [31], it is speculated that eye position illumination exceeding approximately 150lx leads to significant visual fatigue, which is consistent with the results of this study [29]. However, it is worth noting that in this experiment, the illumination of the 10lx eye position also caused higher fatigue but did not result in significantly more pre-sleep sleepiness.

The results of positive emotions in this experiment were consistent with those of alertness. 2000K and 300lx significantly increased sleepiness, decreased alertness, and reduced positive emotions [37-41], consistent with the conclusions of many studies that positive emotions and alertness constantly change consistently. Previous studies have shown that an increase in light levels increases positive emotions in the morning but causes a decrease in positive emotions in the afternoon [39]. The results of this study indicate that 300lx light significantly reduces positive emotions during the afternoon period, consistent with the conclusion of the afternoon. Therefore, the decrease in positive emotions at 300lx may also be the reason for the increase in sleepiness, corresponding to the result of no significant decrease in sleepiness at 10lx.

Finally, within the allowed hours of sleep in this experiment, although light intervention significantly affected the change in subjects' sleepiness and helped them fall asleep, the subjective sleep quality scale investigated after awakening showed that sleep quality was not affected by different light conditions. However, this study only used subjective questionnaires for investigation, and further research relying on objective sleep parameters of PSG should be conducted to explore the impact of different daytime lighting conditions on daytime sleep quality.

## 5. CONCLUSION

The results of this study suggest that using automotive interior lighting in passenger cars before an afternoon nap can help people fall asleep more easily. Low CCT and high illuminance lighting can effectively increase fatigue, reduce positive emotions, increase sleepiness, and thus help fall asleep. However, light did not have a significant effect on sleep quality. In summary, this study proposes light parameter settings suitable for this particular lighting environment in vehicles to promote afternoon naps and rest, help reduce accidents and improve driving safety.

## REFERENCE

- [1] Cook, C.C.H., Albery, I.P. SLEEP-RELATED VEHICLE ACCIDENTS. *British Medical Journal*. 1995, 310, 1411-.
- [2] Garbarino, S., Nobili, L., Beelke, M., De Carli, F., Balestra, V., Ferrillo, F. Sleep-related vehicle accidents on Italian highways. *Giornale italiano di medicina del lavoro ed ergonomia*. 2001, 23, 430-4.
- [3] Garbarino, S., Nobili, L., Beelke, M., De Carli, F., Ferrillo, F. The contributing role of sleepiness in highway vehicle accidents. *Sleep*. 2001, 24, 203-6.
- [4] Lucidi, F., Mallia, L., Violani, C., Giustiniani, G., Persia, L. The contributions of sleep-related risk factors to diurnal car accidents. *Accident Analysis and Prevention*. 2013, 51, 135-40.
- [5] Hayashi, M., Abe, A. Short daytime naps in a car seat to counteract daytime sleepiness: The effect of backrest angle. *Sleep and Biological Rhythms*. 2008, 6, 34-41.
- [6] Hayashi, M., Ito, S., Hori, T. The effects of a 20-min nap at noon on sleepiness, performance



- and EEG activity. *International Journal of Psychophysiology*. 1999, 32, 173-80.
- [7] Hilditch, C.J., Dorrian, J., Banks, S. A review of short naps and sleep inertia: do naps of 30 min or less really avoid sleep inertia and slow-wave sleep? *Sleep Medicine*. 2017, 32, 176-90.
- [8] Schnieder, S., Stappert, S., Takahashi, M., Fricchione, G.L., Esch, T., Krajewski, J. Sustainable Reduction of Sleepiness through Salutogenic Self-Care Procedure in Lunch Breaks: A Pilot Study. *Evidence-Based Complementary and Alternative Medicine*. 2013, 2013.
- [9] Takahashi, M., Arito, H. Maintenance of alertness and performance by a brief nap after lunch under prior sleep deficit. *Sleep*. 2000, 23, 813-9.
- [10] Tietzel, A.J., Lack, L.C. The short-term benefits of brief and long naps following nocturnal sleep restriction. *Sleep*. 2001, 24, 293-300.
- [11] Dutheil, F., Danini, B., Bagheri, R., Fantini, M.L., Pereira, B., Moustafa, F., et al. Effects of a Short Daytime Nap on the Cognitive Performance: A Systematic Review and Meta-Analysis. *International Journal of Environmental Research and Public Health*. 2021, 18.
- [12] Horne, J.A., Reyner, L.A. Counteracting driver sleepiness: Effects of napping, caffeine, and placebo. *Psychophysiology*. 1996, 33, 306-9.
- [13] Soleimanloo, S.S., Garcia-Hansen, V., White, M.J., Huda, M.M., Smith, S.S. Bright light alone or combined with caffeine improves sleepiness in chronically sleep-restricted young drivers. *Sleep Medicine*. 2022, 93, 15-25.
- [14] Aulsebrook, A.E., Jones, T.M., Mulder, R.A., Lesku, J.A. Impacts of artificial light at night on sleep: A review and prospectus. *Journal of Experimental Zoology Part a-Ecological and Integrative Physiology*. 2018, 329, 409-18.
- [15] Blume, C., Garbazza, C., Spitschan, M. Effects of light on human circadian rhythms, sleep and mood. *Somnologie*. 2019, 23, 147-56.
- [16] Hadi, K., Du Bose, J.R., Choi, Y.-S. The Effect of Light on Sleep and Sleep-Related Physiological Factors Among Patients in Healthcare Facilities: A Systematic Review. *Herd-Health Environments Research & Design Journal*. 2019, 12, 116-41.
- [17] Lee, J., Boubekri, M. IMPACT OF DAYLIGHT EXPOSURE ON HEALTH, WELL-BEING AND SLEEP OF OFFICE WORKERS BASED ON ACTIGRAPHY, SURVEYS, AND COMPUTER SIMULATION. *Journal of Green Building*. 2020, 15, 19-42.
- [18] Zhang, R., Campanella, C., Aristizabal, S., Jamrozik, A., Zhao, J., Porter, P., et al. Impacts of Dynamic LED Lighting on the Well-Being and Experience of Office Occupants. *International Journal of Environmental Research and Public Health*. 2020, 17, 7217.
- [19] Chang, A.M., Aeschbach, D., Duffy, J.F., Czeisler, C.A. Evening use of light-emitting eReaders negatively affects sleep, circadian timing, and next-morning alertness. *Proceedings of the National Academy of Sciences of the United States of America*. 2015, 112, 1232-7.
- [20] Santhi, N., Thorne, H.C., van der Veen, D.R., Johnsen, S., Mills, S.L., Hommes, V., et al. The spectral composition of evening light and individual differences in the suppression of melatonin and delay of sleep in humans. *Journal of Pineal Research*. 2012, 53, 47-59.
- [21] Gasperetti, C.E., Dolsen, E.A., Harvey, A.G. The influence of intensity and timing of daily light exposure on subjective and objective sleep in adolescents with an evening circadian preference. *Sleep Medicine*. 2021, 79, 166-74.
- [22] Chinoy, E.D., Duffy, J.F., Czeisler, C.A. Unrestricted evening use of light-emitting tablet computers delays self-selected bedtime and disrupt circadian timing and alertness. *Physiological Reports*. 2018, 6.
- [23] Harrison, E.M., Gorman, M.R., Mednick, S.C. The effect of narrowband 500 nm light on daytime sleep in humans. *Physiol Behav*. 2011, 103, 197-202.
- [24] Zheng, S.Q., Luo M. R., Wang M. L., Ren Z., Bao A. M., Qiang J. et al., Experiments show that a light that can improve sleep quality in terms of hormone concentration," 2017 14th China International Forum on Solid State Lighting: International Forum on Wide Bandgap Semiconductors China (SSLChina: IFWS), Beijing, China, 2017, pp. 101-104.
- [25] Wen, P., Tan, F., Wu, M., Cai, Q., Xu, R., Zhang, X., et al. The effects of different bedroom light environments in the evening on adolescents. *Building and Environment*. 2021, 206.
- [26] Alaminos-Torres, A., Martinez-Alvarez, J.R., Martinez-Lorca, M., Lopez-Ejeda, N., Serrano, M.D.M. Fatigue, Work Overload, and Sleepiness in a Sample of Spanish Commercial Airline Pilots. *Behavioral Sciences*. 2023, 13.
- [27] Reis, C., Mestre, C., Canhao, H., Gradwell, D., Paiva, T. Sleep complaints and fatigue of airline pilots. *Sleep science (Sao Paulo, Brazil)*. 2016, 9, 73-7.
- [28] Sun, J.Y., Sun, R.S. Development of a biomathematical model for human alertness and fatigue risk assessment based on the concept of energy. *Ergonomics*. 2022.
- [29] Xu, M., Jin, L., Tian, X., Wei, Y., Wang, L. Visual fatigue of VDT operation under different

illumination conditions in confined space. *Chinese Journal of Engineering*. 2020, 42, 1605-12.

[30] CIE. CIE TN006:2016-Visual Aspects of Time-Modulated Lighting Systems – Definitions and Measurement Models. 2016.

[31] Adamsson, M., Laike, T., Morita, T. Comparison of Static and Ambulatory Measurements of Illuminance and Spectral Composition That Can Be Used for Assessing Light Exposure in Real Working Environments. *Leukos*. 2019, 15, 181-94.

[32] Akerstedt, T., Gillberg, M. Subjective and objective sleepiness in the active individual. *International Journal of Neuroscience*. 1990, 52, 29–37.

[33] Aitken, R.C. Measurement of feelings using visual analogue scales. *Proceedings of the Royal Society of Medicine*. 1969, 62, 989–993.

[34] Folstein, M.F., Luria, R. Reliability, validity, and clinical application of the Visual Analogue Mood Scale. *Psychological Medicine* 1973, 3, 479–486.

[35] Watson, D., Clark, L.A., Tellegen, A. Development and validation of brief measures of positive and negative affect: The PANAS scales. *Journal of Personality and Social Psychology*. 1988, 54, 1063–1070.

[36] Carney, C.E., Buysse, D.J., Ancoli-Israel, S., Edinger, J.D., Krystal, A.D., Lichstein, K.L., et al. The Consensus Sleep Diary: Standardizing Prospective Sleep Self-Monitoring. *Sleep*. 2012, 35, 287-302.

[37] Rautkyla, E., Puolakka, M., Halonen, L. Alerting effects of daytime light exposure - a proposed link between light exposure and brain mechanisms. *Lighting Research & Technology*. 2012, 44, 238-52.

[38] Finucane, A.M., Whiteman, M.C., Power, M.J. The Effect of Happiness and Sadness on Alerting, Orienting, and Executive Attention. *Journal of Attention Disorders*. 2010, 13, 629-39.

[39] Zhu, Y., Yang, M., Yao, Y., Xiong, X., Zhou, G. Effects of Indoor Illuminance on Cognitive Performance: The Mediating Role of Subjective Mood and Alertness. *Journal of Psychological Science*. 2017, 40, 1328-34.

[40] Plitnick, B., Figueiro, M.G., Wood, B., Rea, M.S. The effects of red and blue light on alertness and mood at night. *Lighting Research & Technology*. 2010, 42, 449-58.

[41] Sawai, H., Inou, G., Koyama, E. Evaluating Optimal Arousal Level during the Task Based on Performance and Positive Mood Extracting Indices Reflecting the Relationship among Arousal, Performance and Mood. 2015.

## ACKNOWLEDGEMENT

Corresponding Author: yandan Lin

Affiliation: Fudan University

e-mail: ydlin@fudan.edu.cn

14th Asia Lighting Conference (Tokyo, Japan)

# Human-Centric Lighting LED Lighting Fixture with Visible Light Conversion Structure to Improve Melanopic Lux : Visible Light Conversion Structure to Improve Melanopixion HCL LED lighting fixture

Ga-Hee Yoon\*  
BY THE M Co., Ltd. KOREA

## Abstract

As the lighting industry continues to develop technology for smart LED lighting, considerable attention is being drawn to human-centric lighting (HCL), which is a technology at the forefront of the next-generation smart lighting that can improve human health and happiness. However, recent HCL development has focused solely on using ICT technology to change color temperature, increase user convenience, and conserve energy, without considering lighting's non-visual elements, that is, the biological effects of light. True HCL requires light that is optimized for the human body's circadian rhythms to help promote user health and welfare.

Each portion of the spectrum of light that is emitted by LED lighting plays a unique role that results from its effects on the human body and the properties of the lighting. Therefore, in this study, we used a material that is capable of light wavelength conversion to maintain a color rendering index (CRI) of 90 or more while reducing the light intensity of wavelengths in the waveband of 420 – 460 nm, which is harmful to the human body. In addition, the light intensity of wavelengths in the 470– 490 nm waveband, which are beneficial to the human body, was increased to create a lighting configuration that corresponds with circadian rhythms, thereby protecting the lighting users' eyesight, preventing eye aging, and improving sleep quality. These light wavebands were set by referencing previous studies. Official testing was performed in accordance with IEC/TR 62778(2014) and CIE S 026, and the results were compared and verified. This study can be used to maximize the value that lighting can provide to humanity and society in keeping with social trends, such as an aging society, health, quality of life, and well-being. In addition, to develop the lighting industry further, there is a need for institutional support and sustained research by universities and research organizations, as well as willingness and effort to develop technology by lighting companies.

Key Words : Smart LED lighting, human-centric lighting, circadian rhythm, light conversion material, spectrum wavelength

## 1. Introduction

### 1.1 Study Background

Light affects the perception of objects as well as human bio-rhythms. In humans, disruptions to bio-rhythms have negative psychological and physical effects. [1] Human bio-rhythms affect sleep quality, diseases, such as dementia, and work efficiency at the office. The intense signals that are required to reset human bio-rhythms to the earth's 24-h clock correspond to the amount of light that is exposed to the ipRGCs, which are the third class of photoreceptors in the human retina. [2] ipRGC cells, which exist at ratios of approximately 0.2– 0.8% in the human retina, are points at which non-visual reactions occur between the surrounding light environment and nervous system, and they convey information to the brain's suprachiasmatic nucleus (SCN) via the retinohypothalamic tract (RHT). When people are exposed to light early in the morning, the SCN increases body temperature and causes the release of the cortisol hormone in the body, which acts as a stimulant. At night, the SCN induces sleep through the release of the melatonin hormone, thereby regulating the circadian rhythm. [3] A considerable portion of insomnia and poor health that afflict most modern humans is caused by the modern lifestyle in which it is difficult to receive a sufficient amount of natural light. Therefore, there is a movement in architecture to promote designs that allow more natural light into buildings. In artificial lighting as well, the creation of lighting environments that humans can inhabit comfortably is considered an important task, and human-centric lighting (HCL) is attracting attention. Therefore, there is a demand for new

indoor lighting that is focused on the quality of the light as well as the function of the light. Researchers have published study results, which indicate that the secretion of hormones in the human body varies according to the wavelength changes caused by the spectrum of the light that is emitted by LED lighting and that HCL can maximize the efficiency of learning, the ability to concentrate at the office, and insomnia relief. Therefore, there is an increasing demand for HCL in the offices of educational facilities and public institutions. However, existing human-centric lighting mainly comprises dimming and color control functions, which focus on changing color temperature. In this study, we present a completely new LED lighting that increases melanopic lux while maintaining high color rendering and high efficiency. Focusing on the human circadian rhythm from waking to sleep, our approach uses an LED lighting fixture to regulate the provided spectrum of light, ranging from the spectrum, which provides energy during waking to the spectrum that provides relaxation before sleep. Thus, in this study, we implemented the circadian rhythm optimization spectrum lighting to support comfortable human lifestyles and optimize the internal clocks of modern humans who spend long hours indoors.

## 1.2 Study Purposes and Methods

Optical films and anti-static PET films that use quantum dot (QD) particles have been incorporated in LED modules with layered structures and applied to LED packages that have low color rendering and harmful blue light. Thereby, light spectrum conversion and color rendering changes that were once difficult to implement in LED lighting fixture manufacturing are now possible. The goal is to provide a higher color rendering of Ra 91 or greater, increased melanopic lux, and reduced harmful blue light wavelengths in comparison to conventional LED lighting. The 480 nm light wavelength, abundant in natural light yet often lacking in conventional indoor lighting, promotes mental and physical invigoration by promoting the secretion of serotonin, which is called the happiness hormone. If an abundance of serotonin is secreted in the body in the morning, it creates conditions in which melatonin, known as the sleep hormone, is likely to be secreted 14-16 h later. In this study, we focused on 480 nm wavelength light and developed a quantum dot optical member that effectively supplements light of that wavelength, and this was applied to an LED lighting fixture that can be effectively used in schools, hospitals, public institutions, and office spaces as a new style of LED lighting that regulates circadian rhythms.

### 1.2.1 LED Lighting's Spectrum Changes

Using QD nanomaterial technology, as well as the technology for making QD material into films and injectable material, we applied a light control technology that can control the wavelengths and intensity of light such that it is suitable for the location where the lighting is used to create the most ideal spectrum for HCL by reducing the intensity of wavelengths that harm humans and increasing the intensity of beneficial wavelengths in the spectrum provided by existing LED lighting.

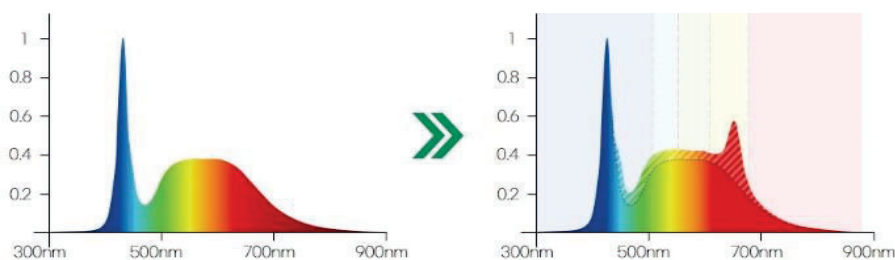


Figure 1. Light wavelength improvement using quantum dot light conversion material

Currently, most LED lighting comprises a spectrum of blue, yellow, green, and red color regions. Of these, the blue light waveband at 420–460 nm has high dispersibility and forms images at the front of the retina, and chromatic aberrations from the eyeball are felt more intensely than in the case of red light, which has a long wavelength. Blue light stimulates the optic nerve with strong energy and is the main wavelength that causes people to feel eye fatigue. In addition, problems have continually been reported regarding the negative effects of blue light, such as strong glare, increased heart rate through melatonin blocking, and accelerated aging of the human body through bio-rhythm disruptions. However, in the current lighting market, in which there is a well-

developed low-cost lighting market, most LED lighting companies have focused solely on light brightness because manufacturing costs increase when they change their LED package lineups or use additional materials to remove blue light separately. To resolve this, the intensity of the blue light wavelength, which has negative effects on the human body, is reduced using special QD optical members.

In addition, QD light conversion material is used in the light emission path of the LED lights in lighting fixtures to improve the properties of LED lighting by providing the optimal conditions for changing the spectrum, increasing efficiency, improving color deviation, and increasing the color rendering index. Through the QD light conversion material, the wavelength intensity of the 420–460 nm waveband is reduced, and the wavelength intensity of the 470–490 nm waveband is increased to provide human-centric lighting that protects the lighting user's sight, prevents eye aging, and affects circadian rhythms by optimizing bio-rhythms.

### **1.2.2 Color Rendering Index and Color Deviation Improvement**

The color rendering index represents the fidelity with which objects' colors are reproduced, and it quantifies the degree to which the color of an object under natural light (sunlight) is similar to the color of the object under certain lighting. The closer the index is to 100, the more similar the lighting's wavelength is to the wavelength of sunlight. In addition, the more uniformly the light is distributed, the better the color rendering. Recently, there has been a gradual increase in the demand for high-color rendering lighting in places where accurate colors are required. Because the human eye is accustomed to natural light, eye fatigue and a sense of artificiality can occur when people continuously view objects that are lit with lighting that has a low color rendering index. Conventional LED lighting's color rendering index of Ra 80-83 is improved by 7-9% to Ra 91-93 by using QD red waveband light conversion material to supplement the basic colors that constitute the general color rendering index.

To increase the accuracy of the method for evaluating the color rendering index, evaluations are performed using the ANSI TM30-18 standard, which performs evaluations based on 99 types of colors.

## **2. Technology Applied**

### **2.1 Quantum Dot Material Application**

QDs are nano-sized materials that emit light of different wavelengths according to the size of the material when it receives external light or electrical energy. Through QDs, LED lighting fixtures that approximate natural light for general lighting in homes, schools, and offices can be manufactured. Therefore, existing fixtures incorporate lighting technology that provides lighting close to natural light by reducing the wavelengths that are harmful to the human body and increasing the beneficial wavelengths by changing the spectrum of existing LED lighting through QDs, as well as wavelength conversion technology that creates optimal light quality through CCT and CRI conversion.



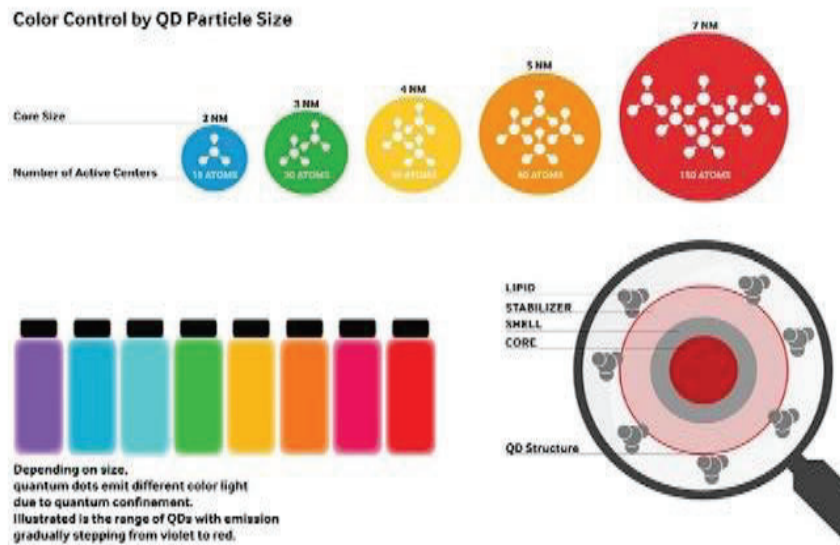


Figure 2. Quantum dot properties

LED lighting is equipped with QD films that ensure high reliability by blocking moisture and oxygen, powderizing the particles, and adopting RTR, which is a system for mass-producing single-layer films from powder-form QDs, using QD nanomaterial stabilization technology and technology for making this material into films and injectable material.

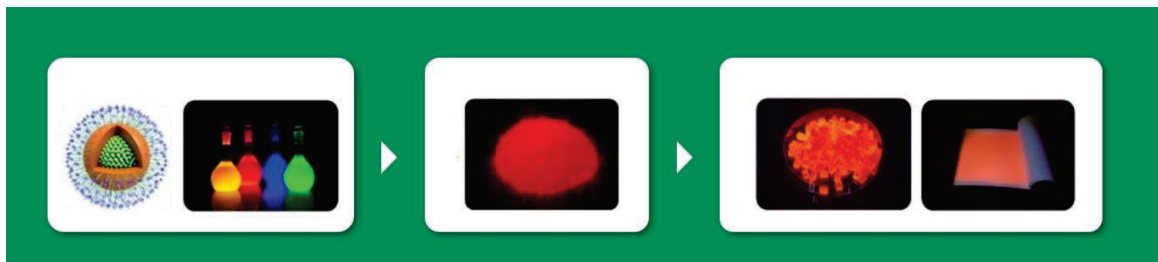
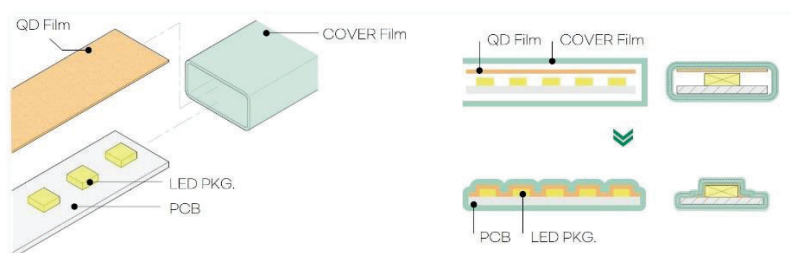


Figure 3. Quantum dot optical member lighting fixture use

## 2.2 Quantum Dot Optical Member Layered Structure LED Module

To manufacture LED modules that are equipped with wavelength control functions, a cover film that covers the outer surface of the QD film and protects it from external foreign material is applied, and the QD film is placed in between and installed/adhered to the PCB substrate using a vacuum suction method that uses suction air currents.



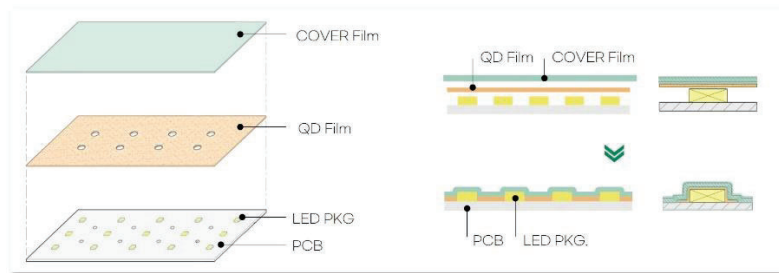


Figure 4. Quantum dot film layered structure LED module

### 2.3 LED Lighting Module Lifespan Extension

Dust adsorption and static electricity are prevented by installing and adhering to a high-transparency antistatic film to the surface of the LEDs that are attached to the PCB.

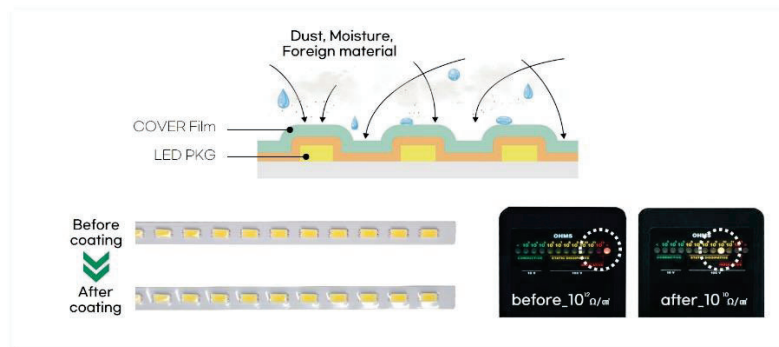


Figure 5. PET protection film composition

Durability is increased by preventing the LEDs from changing color due to infiltration by the moisture, sulfur, and other gases that are present in the external air and preventing/protecting against changes in the LED color temperature, reductions in luminous flux, and insulation failure.

### 3. Property Measurements

In this study, we performed a comparison of the light properties of existing products and light fixtures that use visible light conversion technology, including two types of light fixtures (direct and indirect type). A control group and the new R&D products were fabricated with a rated voltage of 220 V, a rated input power of 40 W, and an external size of 300 x 1200 x 40 mm, and their harmful blue light wavelength intensity, melanopic wavelength intensity, color rendering indices, and light efficiency were measured and compared by an official testing organization (Korea Institute of Lighting and ICT).



Figure 6. Lighting fixture shapes

Table 1. Direct lighting type performance comparison

		Existing product		R&D product	Notes
		BM53-4050-31NS	BM53-4057-31NS	BM53-4050-31QS	
Retina harmful blue light		-	-	Appropriate (RG0)	
Harmful blue light wavelength output		2580 mW	3196 mW	2453 mW	4.9%▼ 23.2%▼
Melanopic wavelength output		645 mW	629 mW	870 mW	34.9%▲ 38.3%▲
Color temperature		4929 K	5602 K	5116 K	
CRI	Ra	85.1	82.8	91.8	6.7(7.8%▲) 9(10.9%▲)
	R9	22	17	60	38(67%▲) 43(72%▲)
Optical flicker		-	-	0.0072	
MTBF		-	-	1,023,216 h	

Table 2. Indirect lighting type performance comparison

		Existing product		R&D product	Notes
		BM53-4050-31NSH	BM53-4057-31NSH	BM53-4050-31QSH	
Retina harmful blue light		-	-	적합 (RG0)	
Harmful blue light wavelength output		2172 mW	3013 mW	2125 mW	2.2%▼ 29.5%▼
Melanopic wavelength output		688 mW	597 mW	942 mW	36.9%▲ 57.8%▲
Color temperature		4979 K	5772 K	5026 K	
CRI	Ra	81.5	81.6	91.4	9.9(12.1%▲) 9.8(12%▲)
	R9	6	10	55	49(90%▲) 45(82%▲)
Optical flicker		-	-	0.017	
MTBF		-	-	972,531 h	

#### 4. Conclusions

In a comparison of existing direct-type panel lighting and the lighting fixture that used the visible light conversion mechanism technology, the 420–460 nm harmful blue light wavelength output was reduced by 4.9%, and the 470–490 nm melanopic wavelength output was increased by 34.9%. The color rendering index was improved to 91.8, which is a significant improvement in color reproducibility. Considering the performance of the indirect type lighting fixture that used the visible light conversion mechanism technology, the harmful blue light wavelength output was reduced by 2.2%, and the melanopic wavelength output was increased by 36.9%, while the color rendering index (Ra) was improved to 91.4.

Table 1. Comparison of wavelength intensity and color rendering of each waveband

	Existing product		R&D product		Notes
	BM53-4050-31NS	BM53-4057-31NSH	BM53-4050-31QS	BM53-4050-31QSH	
420–460nm	2580 mW	2172 mW	2453 mW	2125 mW	4.9% reduction 2.2% reduction
470–490nm	645 mW	688 mW	870 mW	942 mW	34.9% increase 36.9% increase
CRI	85.1	81.5	91.8	91.4	7.8% improvement 12.1% improvement

The difference between the existing normal lighting and the product that used the visual light conversion mechanism technology was that the light's melanopic intensity, which is a non-visual factor, was increased to maximize the light's melatonin hormone secretion regulating effect while the LED lighting's important technical aspects, such as light efficiency, light quality, and lighting fixture lifespan were maintained. As the best lighting fixture for protecting users' vision, the new lighting fixture will be combined with smart lighting technology to fully implement genuine human-centric lighting instead of simple light brightness and color temperature controls.

## REFERENCE

- [1] J. O. Kim and U. C. Ryu "A Spectral Combination Simulation Study on Improve Melanopic to Photopic Ratio and Color Rendering Index" Proceedings KIIEE Annual Conference, pp36, 2021.
- [2] S. I. Yun and A. S. Choi "Development of black-box model for evaluating melanopic lux with installed photo sensor" Proceedings KIIEE Annual Conference, pp4, 2020.
- [3] S. Y. Choi "Non-Visual Effects of Lights" Journal of KIIEE, pp26, 2019.3

## ACKNOWLEDGEMENT

GAHEE\_JEREMY YOON  
BY THE M Co., Ltd. | CEO  
bythemled@naver.com

# MINI LED APPLICATION FOR SMART HEAD LAMP

Jae Young Joo

Korea Photonics Technology Institute

## ABSTRACT

In this paper, we propose a high-resolution adaptive driving beam (ADB) with Mini LEDs, which enables better visibility by controlling the minimum angular resolution of a headlamp. Each LED has about 110  $\mu\text{m}$ , and arrayed with 32 by 32. The emitting source area was about 25mm<sup>2</sup>. This high-resolution pixel light source consumes less than 50W in 1,000 lm. Since many automotive headlamps manufacturing companies apply unique technology for better performance, we have developed a high-efficiency optical system with a diffractive kinoform lens. Optical efficiency was more than 50%, and the thickness of kinoform lens was in 2  $\mu\text{m}$ . Cross talk effect among LEDs was studied by the phosphor and LED fabrication type, and we finally prototyped a 1,024-resolution pixel source with projection optics in 3 lenses. And its illumination beam angle was 6 degrees with maximum illuminance intensity of 25,000 cd. Super positioning of two modules makes it possible to satisfy ECE R123 regulation successfully. The developed high-resolution headlamp can project various types of signals such as fogs, rainfall, snow, direction arrows on the driving roads. Also, This headlamp can make glare-free high beam within 0.2 degrees.

Keywords: Min LED, Smart Headlamp, Adaptive Driving Beam

## 1. INTRODUCTION

Major innovation of automotive head lamp technologies can be classified into three categories; Halogen, High Intensity Discharge (HID) Lamp, semiconductor i.e. Light Emitting Diodes(LEDs), Laser Diode(LD), Organic LEDs(OLEDs). Technological innovation in semiconductor photonics industry has contributed to the development of a wide range of technologies, starting from Center High Mount Stop Lamp (CHMSL) to HD resolution Digital Head Lamps. As a result of diffusion of such technologies, the innovation of automobile exterior design led us to the shift of the mainstream of the global automobile market from performance to design flexibility. Design driven innovation has redefined the global automotive market and opened new era of an automotive head lamp.

The BMW announced of adopting Laser Head Lamp in 2013, which used a reflective PC (Phosphor Ceramic) type[1]. The Audi developed a new concept of laser headlamp for slimmer technology, four to six Micro Laser Diodes were applied and a prism and a phosphor plate[2]. More recently, Micro LEDs have started to be adopted in this industry with high resolution pixel lighting. In this paper, we have used LEDs about 100  $\mu\text{m}$  size and those LEDs were arrayed in 32 row and column. Those LEDs were driven by CMOS black plane and controlled separately. Illuminated lights from each pixel were projected with plastic optics. The module shows significant variation in optical performance due to phosphor converting method.

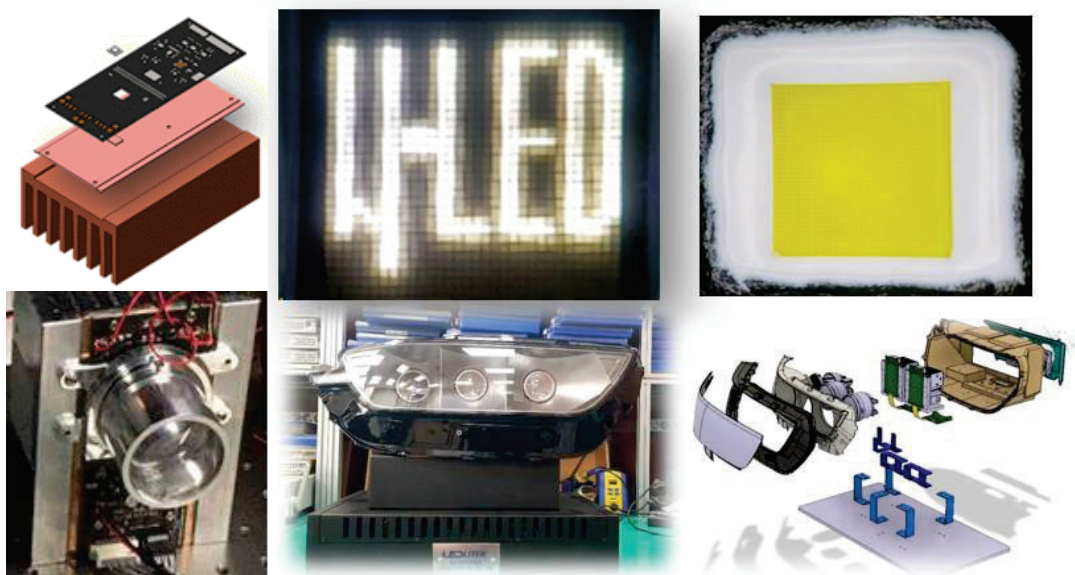
In this paper, we propose an high resolution adaptive driving beam (ADB) with Mini LEDs, and each rectangular pixel led has 110  $\mu\text{m}$  size , and arrayed with 32 by 32. Those LEDs consumes less than 50W in 1,000 lm in 1024 high-resolution pixel., We has developed high efficiency optical system in 50%, and cross talk effect among LEDs was studied by phosphor and LED fabrication type. Projection optics in 3 lenses illuminated in 6 degrees with maximum illuminance intensity of 25,000 cd. Super positioning of two module makes it possible to satisfy ECE R123 regulation success fully.

## 2. OPTICAL DESIGN AND PROTOTYPING OF HEAD LAMP

The Mini LEDs Module has basically three components. Each mini led are bonded with backplane PCB with directly metal bonded with cooper for heat dissipation. Also each mini leds are optically bonded with white light conversion phosphor plate individually. This kind of structure may decrease the optical efficiency of the mini led light source module, but dramatically reduced the colour stability of the module as well as cross talk effects. In Figure 1,



we can recognized clear view of projected letter '  $\mu$ LED' through 3 lens array. This projection lens optical system showed about 50% of optical efficiency in 6 degree view angle. Developed head lamp showed similar performance with that of Benz 's 1024 mini led head lamp.



**FIG. 1 fabricated min LEDs and Prototyped Head Lamp**

## REFERENCES

- [1] Dr. Tim Gock et al., "Lighting innovation of future BMW vehicles", ISAL 2015, p. 19-24
- [2] Burkard Wordewer, Jorger Wllascheck, Perter Boyce, Donald D. Hoffman, "Automotive Human Vision", Springer40, 6328 (2007).

## ACKNOWLEDGEMENTS

This research was supported by the Technology development Program(S1415186012) funded by the Korea Evaluation Institute of Industrial Technology(KEIT) grant funded by the Korea government (Title: Development of smart sensing based lighting optical parts and module technology)

Corresponding Author Name: Jae Young, Joo  
 Affiliation: Senior Researcher  
 e-mail: jyjoo@kopti.re.kr

# OBJECTIVE AND SUBJECTIVE EVALUATION FOR AUTOMOTIVE INTERIOR AMBIENT LIGHTS

Seo Young Choi, Jae Kyu Ko and Mi So Noh

(KIEL Institute, Bucheon-si, Gyeonggi-do, Republic of Korea)

## ABSTRACT

The application of interior lighting using LED is increasing in order to provide various ambient surrounds for driving experience improvement and differentiated brand image. The key objective quality components of the interior lighting are luminance, chromaticity, and spatial uniformity that are influenced by (1) the reflectance property of the finishing material, (2) the LED PKG colorimetric binning (dispersion of chromaticity), (3) the color-quality control deviations between manufacturers producing interior lighting parts, etc. Diverse affective factors (comfort, pleasant etc.) are formed by controlling the objective quality factors. The ambient light is designed by considering the interior of the car, visual impression, eye comfort, and distraction etc. The development of the objective evaluation method for the ambient light is not a simple matter due to such complex design factors. It is also important to understand changes in the affective factors according to the colour variation of interior lighting. This study therefore attempts to discover significant evaluation components through objective and subjective measurements and to determine the chromaticity map between affective factors and interior lighting colours.

**Keywords:** Automotive Ambient Lights, Perception of Space Atmosphere, Subjective Evaluation of Interior Lights

## 1. INTRODUCTION

The overall impression that users perceive about the interior space of the car is a major factor affecting the car brand image[1-2]. LED can freely implement various colours and has high degree of design freedom, so its application as an indoor lighting source for automobiles is increasing. Related research is active to provide a customized indoor atmosphere to users according to various indoor space utilization with the advent of autonomous cars. The interior atmosphere of an automobile is formed by a combination of hardware elements such as internal finishing materials, direct/indirect lighting, and displays, and lights and colours produced therefrom.

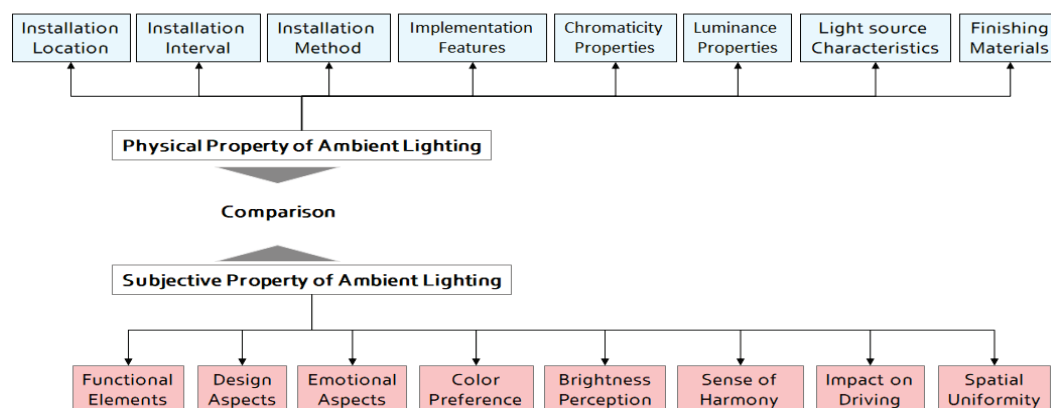


Figure 1. Effects of changes in physical characteristics of ambient lighting on user cognition

The design of these hardware components involves two objectives: (1) visual implementation of the identity pursued by the overall design of each vehicle, and (2) implementation of an interior lighting environment optimized for user safety and behaviour. In particular, ambient lighting, which can intuitively evoke the atmosphere through visual recognition, is a very important factor in automobile interior design. Indirect ambient lighting has quality factors such as luminance ( $\text{cd/m}^2$ ), chromaticity (specified by the spectrum of the light), and uniformity (in terms of luminance and chromaticity), and these characteristics are influenced by the visible reflection characteristics of

the finishing material. Figure 1 introduces the effect of changes in physical characteristics of ambient lighting on user cognition.

The colour appearance of ambient lights perceived by the end user may differ from that predicted by initial colorimetric characteristics of the LED PKG, since the lights of the LED PKG pass through the string and are reflected from the finishing materials shown in Figure 2. Therefore, not only the colour characteristics of the LED PKG but also the characteristics of the related parts (LED string, diffuser, finishing material) must be considered to manage the colour characteristics recognized by the end person. It can be said that the colour recognized in the last step affects the user's sensibility.

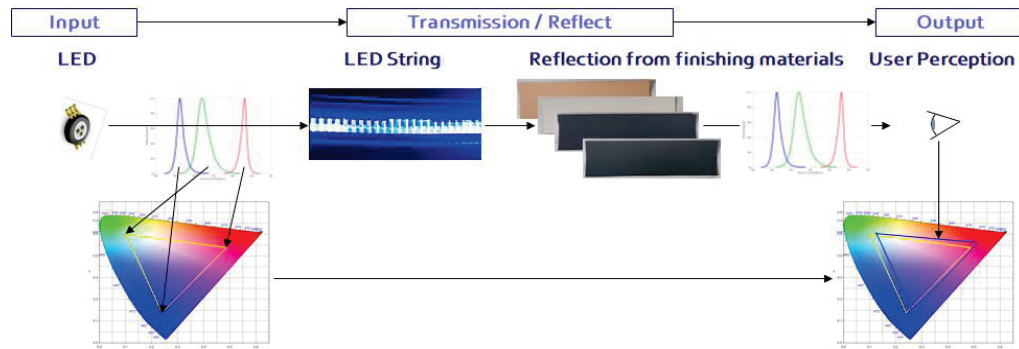


Figure 2. The process from the LED PKG to the user visual perception for automotive ambient lightings

## 2. Evaluation Results

### 2.1 Objective vs. Subjective Spatial Uniformity

The physical characteristics of ambient lighting are measured using a CMOS sensor-based luminance meter (LMK 6 of TechnoTeam, Germany) in this study. Figure 3 shows the physical measurement results for the luminance ( $Y$ ,  $\text{cd}/\text{m}^2$ ) and chromaticity ( $u'$  and  $v'$  in CIE 1976 Uniform Colour Space) uniformity of the ambient lighting installed in the vehicle. It can be seen that spatial uniformity is affected by the internal design of each automobile company and vehicle type. Benz E300 shows  $\Delta Y = -63\%$  to  $> +1000\%$  difference compared to the central luminance value ( $Y$  @ #3 location =  $0.52 \text{ cd}/\text{m}^2$ ) in Figure 3, while BMW 740e shows  $\Delta Y = -41\%$  to  $> +400\%$  difference compared to the central luminance value ( $Y$  @ #3 location =  $0.986 \text{ cd}/\text{m}^2$ ) in Figure 4. In the Benz E300, the luminance of both ends (#1, #6) where LED PKGs exist is observed to be more than 1000 % brighter than the luminance of the centre (#3). In the BMW 740e, the luminance of the left end (#6) where the LED PKG exist is observed to be more than 400% brighter than the luminance of the central part (#3). Benz E300 shows that both  $\Delta u'$  and  $\Delta v'$  are less than 0.005 compared to the central colour value ( $u'$  and  $v'$  @ #3 location) in Figure 3, while BMW 740e shows that the colour deviation increases toward the left end compared to the central colour value ( $u'$  and  $v'$  @ #3 location) in Figure 4.

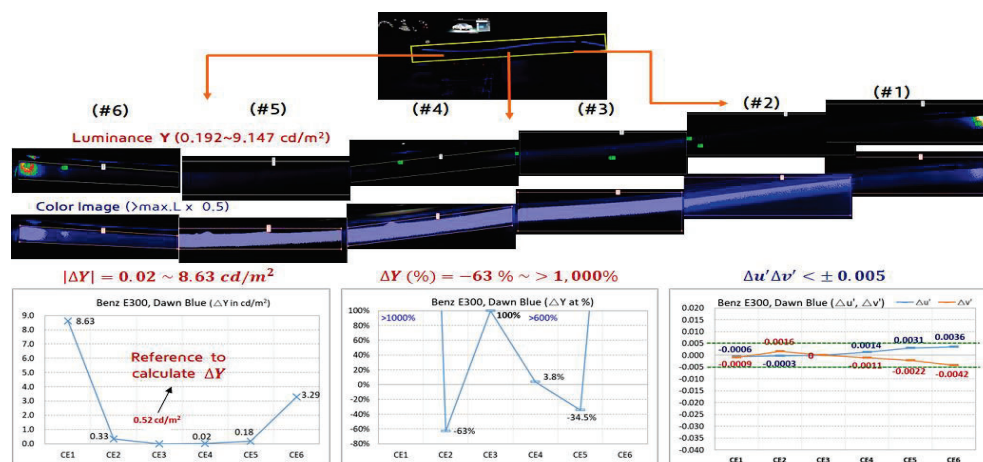


Figure 3. The luminance and chromaticity uniformity for the ambient lighting of Benz E300

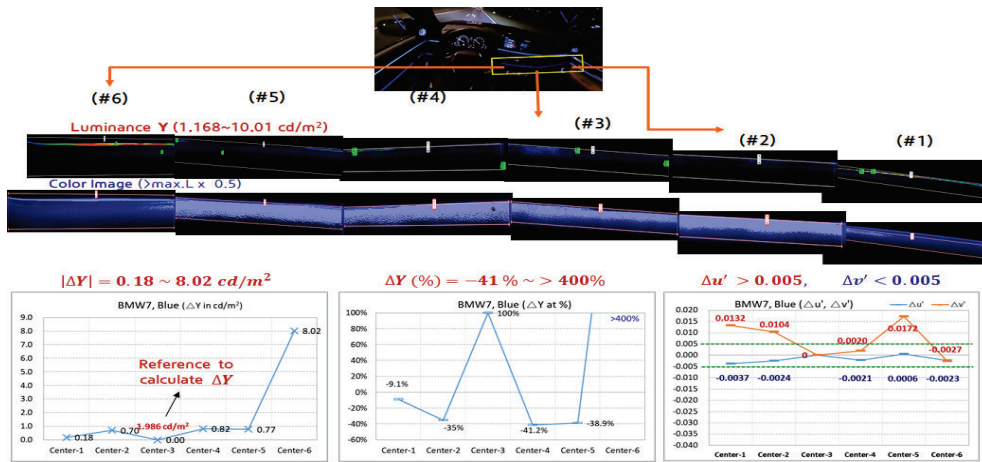


Figure 4. The luminance and chromaticity uniformity for the ambient lighting of BMW 740e

When the subjects are asked whether they would accept the luminance and chromaticity non-uniformity of the Benz E300 and BMW 740e using 5-point Likert scale (1 point is very difficult to accept, 3 points is normal, 5 points is very acceptable), they are all evaluated as acceptable (average between 3.5 and 4.5). Therefore, it seems that the subject evaluates the luminance non-uniformity phenomenon (the brightness becomes darker toward the centre or the opposite end from the brightest spot due to LED PKG) in the design aspect. In the case of interior ambient lighting in automobiles, it can be seen that the tolerance range in the physical-property (luminance and chromaticity) deviation for the spatial uniformity evaluation is greater than that in general lighting.

## 2.2 Emotional Colour Map for Automotive Interior Ambient Lighting

Ten preferred colour groups are firstly selected for interior ambient lightings through a huge set of observations and are illustrated in Figure 5: Green, Cyan, Blue 1 and 2, Purple, Magenta, Red, Orange, Warm White, and Cool White. Five adjectives are also chosen as the main emotions expected from interior ambient lightings of automobiles: Pleasant, Comfortable, Luxury, Secure/Stable, and Active.

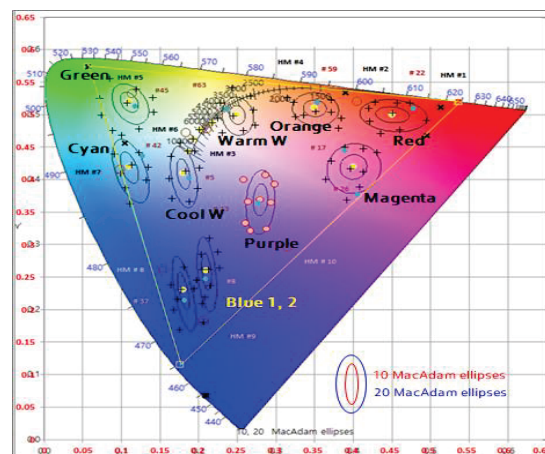


Figure 5. Ten preferred colour groups for interior ambient lightings

Additional experiments are conducted to determine corresponding colour groups representing these five main emotions. The matching results between five emotions and colour groups are shown in Figure 6. It mainly shows comfort in the blue, cyan, and cool white areas, and very comfortable sense is observed in the warm white, orange, and purple areas. It seems that the sense of secure/stable is also high in the warm white, orange, and purple areas. Hence, these colour groups can be classified into emotional areas such as comfortable and stable/secure. Active emotion is high in areas with high purity of orange and blue colour, and near cool white. In other words, orange and blue lights with high purity can inspire drivers to feel more active. It can



be seen that relatively luxury interior quality can be recognized in the blue and cool white areas. As the most preferred area (shown in the rightmost bottom graph of Figure 6) for ambient lighting in automobiles, comfortable, secure/stable, and luxury emotional areas are all included, so these three emotions are thought to have a great influence on preference.

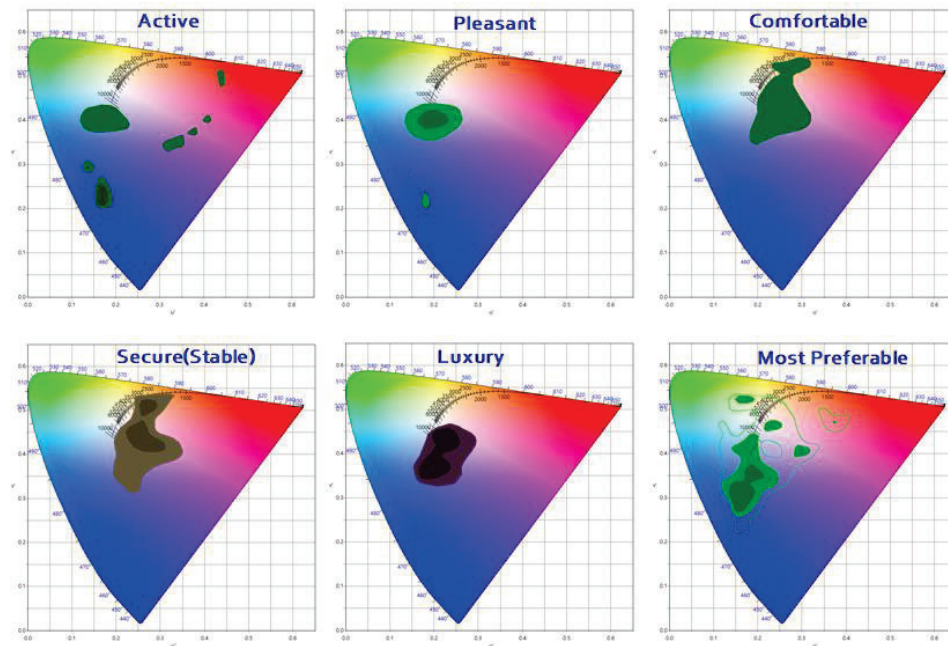


Figure 6. The corresponding chromaticity range to create each of five main emotions that are expected from interior ambient lightings

### 3. CONCLUSION

In this study, after measuring the physical characteristics of ambient lighting installed in ten vehicle models, user perception evaluation is conducted to derive evaluation factors that have a major impact on the interior atmosphere implemented by ambient lighting. The important evaluation factors of the ambient lighting that have a major influence on the interior atmosphere of automobiles are found as follows: (1) Hue (chromaticity, spectrum), (2) Luminance (gray level), (3) Finishing material (reflectance), (4) Installation type (direct or indirect lighting), (5) Spatial uniformity. Among these, only the results of spatial uniformity are introduced in this paper. The optimal chromaticity ranges are also proposed to maximize five key emotional stimuli (pleasant, comfortable, luxury, secure/stable, and active) in the application of interior ambient lighting.

### REFERENCE

- [1] Caberletti, L., Elfmann, K., Kumme, M. & Schierz, C. Influence of ambient lighting in a vehicle Interior on the driver's perceptions. *Lighting Res. Technol.*, 2010, 42, 297-311.
- [2] Hiamtoe, P., Steinhardt, F., Köhler, U. & Bengler, K. Subjective and objective evaluation of sense of space for vehicle occupants based on anthropometric data. 18th World congress on Ergonomics, 2012, 252-257.

### ACKNOWLEDGEMENTS

Corresponding Author Name: Seo Young Choi

Affiliation: KIEL Institute

e-mail: sychoi@kiel.re.kr



# EXPLORATION OF INTERIOR LIGHTING PREFERENCE CONDITIONS IN DIFFERENT SCENARIOS FOR AUTONOMOUS VEHICLES

Hyeran Kang, Hyensou Pak, Jemok Lee, Donguk Shin, Chan-Su Lee

Yeungnam University

## ABSTRACT

The development and expansion of autonomous vehicle technology is expected to enable various user activities inside the vehicle. In this study, automotive interior lighting scenarios were selected based on user activities that can be performed inside an autonomous vehicle. Five scenarios were selected: driving, office works, media watching, eating, and conversation. Lighting parameters(color temperature, illuminance) are adjusted to fit each participant preference to the given scenario. To this end, a test bed consisting of a PBV (Purpose Built Vehicle) test buck, four main lightings consisting of RGB, warm white, and cool white LEDs, and several ambient lightings consisting of warm white, cool white, and RGB LEDs were built. Eight subjects participated in the experiment and showed differences in light preference and color temperature between scenarios. The illuminance values with proper devices and objects required for activities in each scenarios show higher values than that of without proper devices and objects. The range of lighting parameters obtained in the experiment will be useful to determine the lighting conditions according to activities in the autonomous vehicle.

Keywords: Autonomous Vehicle, Interior Lighting, Lighting Scenario, Lighting Parameter

## 1. INTRODUCTION

The advancement of autonomous vehicle technology has opened up new possibilities for enhancing the in-vehicle user experience. With the potential for reduced driving responsibilities, passengers in autonomous vehicles can engage in various activities while traveling. More specifically, the temporal and spatial constraints within autonomous vehicles cars will be greatly reduced, and the freedom of the occupants' activities will be significantly increased. Therefore, it will be necessary to create various in-vehicle lighting scenarios that can meet the satisfaction and demands of passengers in areas such as emotion, safety, convenience, and performance. Several previous studies provide a basis for examining these scenarios [1-4]. Candidates for the in-vehicle activity scenarios can be considered, including working, relaxing, conversing, reading, sleeping, entertainment (watching & listening), smartphone usage (texting, searching & SNS), playing, eating, celebrating, alerting and refreshing, etc. As a result, if we know the most frequent and useful in-vehicle activities, we will be able to provide lighting environments or scenarios suitable for the activities.

In this study, we selected 5 scenarios among various passenger activities that can occur in autonomous vehicles, and tried to find out the preferred range of lighting parameters for each scenario and their subjective impressions on the lighting environment by asking the participants to adjust the illumination intensity and color temperature of the lighting in the test PBV buck. In addition, we tried to examine the difference between when there are proper devices and objects related to the scenario and when there are no devices and objects.

## 2. METHODS

In this study, a PBV test buck and four main lights consisting of warm white and cool white LED were used as the basis for developing automotive interior lighting that is automatically controlled according to occupant activity. We selected five scenarios for consideration: driving, office work, media watching, eating, and conversation. For each scenario, the seat's rotation angle was set to 0, 0, 30, 90, and 135 degrees, respectively.

Participants were seated in the driver's seat of the test buck and designed the lighting by adjusting the color temperature and illuminance for scenarios presented sequentially or in reverse order. At the end of each scenario, they were asked to complete a questionnaire.

The questionnaire included two short answer questions and three questions based on a 5-point Likert scale. The short answer questions consisted of 'Please describe the lighting design you created this time, using at least three words.' and 'Please describe, using at least three words, why you are either disappointed or satisfied with the designed lighting.' The Likert scale questions consisted of 'coziness', 'liveliness', and 'satisfaction'.

Participants took part in the experiment twice. In the first session, they conducted the experiment in a model free condition. In the second session, they conducted the scenarios with additional devices and objects such as a steering wheel, laptop, and fruit to be more realistic to given activities as shown in Figure 1.

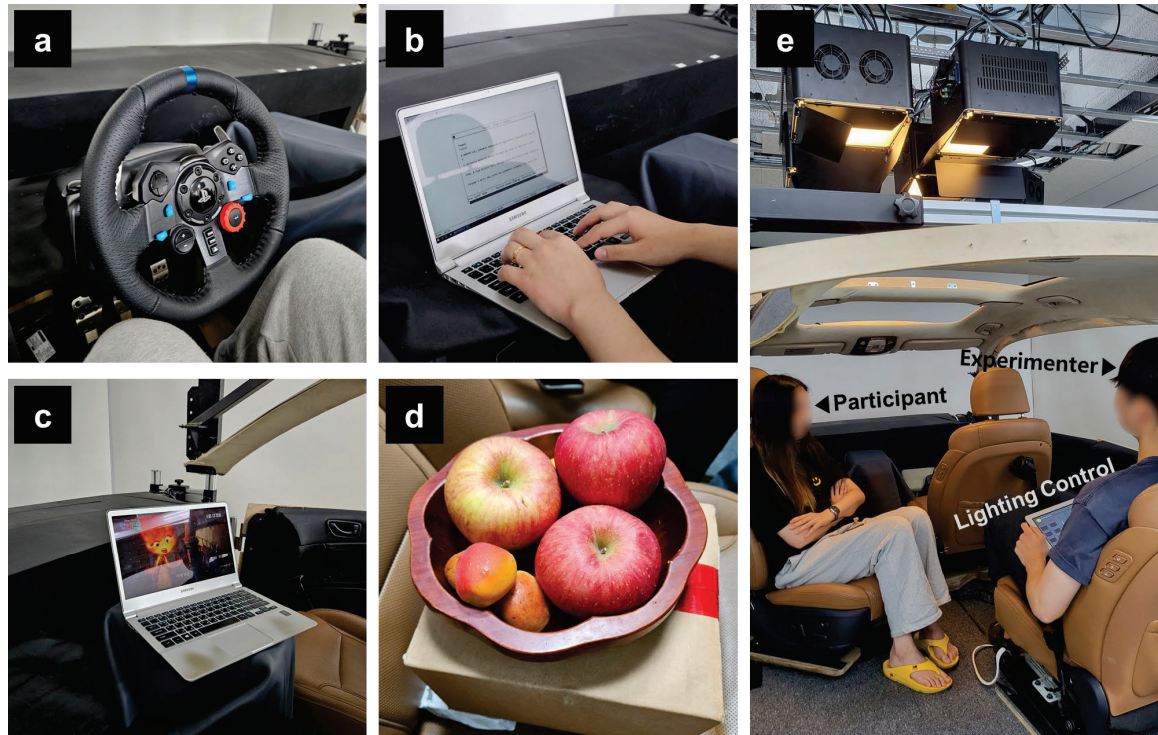


Figure 1. Scenarios for the evaluation of the lighting design in autonomous vehicle. a) driving, b) office works, c) media watching, d) eating, e) conversation

### 3. RESULTS

Eight participants participated in this experiment, their ages ranged from 22 to 25 years old (median = 23.5), with six males and two females and they self-reported with no color blindness or color weakness and strong interest in interior lighting.

**Lighting concepts for each scenario.** Participants designed lighting with at least three concepts for each scenario. For the driving scenario, they made for bright lighting to wake them up. In the office work scenario, they designed a cool and bright lighting, helpful for concentration. When watching media, they set the lighting to be dim and subtle, designing a cozy and comfortable atmosphere. For the eating scenario, participants preferred bright lighting that illuminated the food and contributed to a cozy mood. Lastly, during conversations, they aimed for a moderately bright lighting setup, creating a warm and comfortable environment. The presence or absence of items did not influence the lighting concepts, and consistent trends were observed across all scenarios.

**5-point Likert scale about coziness, liveliness, and satisfaction.** In terms of coziness, differences were observed among the scenarios, with the driving and office work scenarios receiving lower ratings compared to the media watching, eating, and conversation scenarios. In liveliness, in the driving scenario, the presence of a steering wheel resulted in higher scores. According to subjective responses, participants reported better concentration during driving when a steering wheel was present. Interestingly, in the eating scenario, the presence of fruit item led to lower scores. This could be attributed to the limited space resulting from the rotation of the seat to 90 degrees and the absence of a table, resulting in relatively lower ratings. In satisfaction, participants consistently expressed high levels of satisfaction, with ratings consistently above 4,

regardless of the presence or absence of item across all scenarios. These results are represented in Figure 2a and 2b.

**Illuminance and color temperature.** We used a Konica Minolta CL-200 chroma meter to measure illuminance and color temperature at the centre of the item. The results showed that for driving, office works, and media watching, illuminance below 100lux was preferred, while for eating and conversation scenarios, relatively high illuminance was preferred. Although bright and clear lighting was the main design concept for driving and office work, the main lights used in this experiment were limited by the roof of the vehicle. As a result, there may have been lower illuminance in these two scenarios when the chair rotation angle was 0 degrees due to shadows. According to the scenarios, we observed different preferences in color temperature. Driving, office work, and media watching scenarios had higher color temperatures compared to eating and conversation scenarios. In the illuminance, the presence of proper devices and objects resulted in higher illuminance than the absence of these devices and objects in each scenario (see Figure 2c).

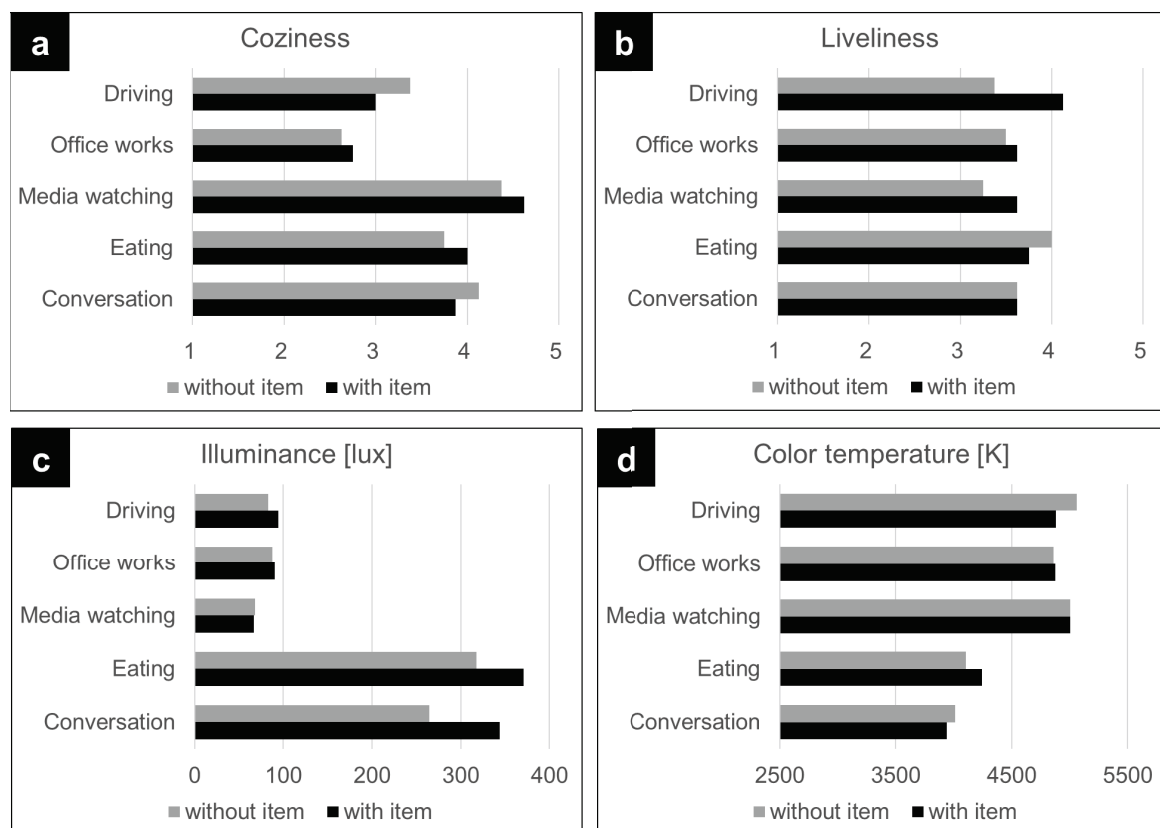


Figure 2. Scenario-based assessment of a) coziness, b) liveliness, preferences of c) illuminance and d) color temperature

#### 4. CONCLUSIONS

In this study, we constructed various scenarios that could occur in an autonomous vehicle and investigated the lighting preferences for each scenario, with and without specific items. The results show that occupants' lighting preferences vary depending on the scenario.

Thus, when designing interior lighting for autonomous vehicles, parameters such as illuminance and color temperature should be adjustable based on the activity. For example, scenarios that require high concentration, such as driving and office work, necessitate lighting with a high color temperature. Conversely, situations that require a relaxed concentration level, such as eating and conversation, demand warmer color temperature lighting.

The presence of physical items, such as a steering wheel, laptop, and fruit, had an impact on the perceived liveliness of the scenarios. These devices and objects also influenced the preferred illuminance of the lighting setup, with the introduction of these 3D devices and objects altering the overall illuminance compared to a scenario without such items. Participant feedback from short

answer questions indicated that the inclusion of a steering wheel and laptop aided in their focus. These findings suggest that while the nature of the activities dominated lighting preferences, the way the lighting environment is presented in each scenario also plays a significant role.

In summary, this research highlights the importance of personalization and adaptability in the design of autonomous vehicle lighting. Future research should expand on these findings by exploring a broader range of scenarios and activities, considering additional lighting parameters, and investigating the impact of other variables such as time of day, external weather conditions, and the passenger's mood.

## REFERENCES

- [1] Caberletti, L., Elfmann, K., Kummel, M., & Schierz, C. (2010). Influence of ambient lighting in a vehicle interior on the driver's perceptions. *Lighting Research & Technology*, 42(3), 297–311.
- [2] Betz, D., Westphal, K.M., & Schoneich, M. (2021). Adaptive interior light – An innovative technological approach for multifunctional interior lighting. In *Proceedings of the 14th International Symposium on Automotive Lighting (ISAL)*, 625-634.
- [3] Weirich, C., Lin, Y., & Khanh, T.Q. (2022). Evidence for Human-Centric In-Vehicle Lighting: Part 1. *Applied Sciences*, 12(2), 552.
- [4] Weirich, C., Lin, Y., & Khanh, T.Q. (2022). Evidence for human-centric in-vehicle lighting: Part 2-Modeling illumination based on color-opponents. *Frontiers in Neuroscience*, 16, 969125.

## ACKNOWLEDGEMENTS

This research was partly supported by Korea Evaluation Institute of Industrial Technology (KEIT) grant funded by the Korea government (MOTIE) (No. 20019078)

Corresponding Author Name: Chan-Su Lee  
Affiliation: Yeungnam University  
e-mail: chansu@ynu.ac.kr



The 14<sup>th</sup> Asia Lighting Conference

# Innovation of Lighting

August 17-18, 2023  
The University of Tokyo  
Tokyo, Japan

## Design Oral Session



Asia Lighting Conference



中国照明学会

CHINA ILLUMINATING ENGINEERING SOCIETY



一般社団法人 照明学会

THE ILLUMINATING ENGINEERING INSTITUTE OF JAPAN



대한민국조명·전기설비학회

THE KOREAN INSTITUTE OF ILLUMINATING AND ELECTRICAL INSTALLATION ENGINEERS



ALC Web Page



# A PRELIMINARY STUDY ON THE LIGHTING DESIGN OF COMMUNITY NURSING HOMES

Kehang Chen

(Faculty of Architecture and Urban Planning, Chongqing University, Chongqing, China)

## ABSTRACT

Community nursing homes have emerged as crucial settings for providing care services to elderly individuals, warranting careful consideration of lighting design for enhancing their well-being. This paper presents a preliminary study on the lighting design of community nursing homes. The research involved field investigations conducted at several community nursing homes, focusing on measuring key lighting parameters, including illuminance, uniformity ratio of illuminance, correlated color temperature, and color rendering index in critical areas such as activity rooms, reading rooms, and lounges. Additionally, questionnaires were administered to assess the visual satisfaction of elderly users. Correlation analysis was performed to explore the relationship between lighting design parameters and visual satisfaction. Based on the study's findings, distinctive lighting design characteristics and strategies were identified, accompanied by proposed suggestions to improve the well-being of elderly users in community nursing homes. The outcomes of this research provide valuable insights for the design of community nursing homes, underscoring the significance of lighting design in enhancing the overall quality of life for elderly individuals.

Keywords: lighting design, community nursing homes, elderly-oriented design, illuminance, visual satisfaction

## 1. INTRODUCTION

Since the beginning of the 21st century, China has experienced a rapid acceleration in the aging process, leading to an increasingly serious aging trend. By the end of 2021, the elderly population in China, aged 65 and above, is projected to exceed 200 million, accounting for 14.2% of the total population, reaching the national standard for moderate aging[1]. To effectively address the challenges posed by the aging population, China has placed significant emphasis on the development of an age-friendly society, with a particular focus on the robust expansion of community-based elderly care and the expedited construction of community nursing homes.

Within the realm of community nursing home design, lighting plays a pivotal role as a critical factor that directly impacts the visual comfort and spatial experience of the elderly residents[2-3]. Therefore, this paper aims to investigate and analyze the lighting design aspects in six community nursing homes located in Yubei Road, Shapingba District, Chongqing. By conducting field measurements of relevant lighting design parameters and administering visual satisfaction questionnaires to facility users, this study seeks to explore the correlation between lighting design and the overall satisfaction of elderly residents. The findings of this research endeavor are intended to serve as valuable references for future lighting design practices in community nursing homes.

## 2. RESEARCH ON LIGHT ENVIRONMENT AND VISUAL SATISFACTION

### 2.1 Research object

This study focuses on six specific community nursing homes located in Yubei Road Street, Shapingba District, Chongqing. The selected facilities are as follows: Hanyu Road Community Nursing Home, Shayang Road Community Nursing Home, Baiheling Community Nursing Home, Yanggongqiao Nursing Home, Shuangxiangzi Community Nursing Home, and Yangli Road Community Nursing Home. The research also involves the elderly users residing within these facilities.

The investigation primarily focuses on three distinct types of spaces within each of the six community nursing homes, namely the activity room, reading room, and lounges. The research involves an in-depth analysis of the lighting environment within these spaces. Additionally, a visual satisfaction study is conducted with the elderly users residing in each community nursing home, specifically pertaining to the aforementioned three types of spaces within their respective facilities.

## 2.2 Research content and methods

### 2.2.1 Light environment parameters

The light environment research in this study employed several parameters, including illuminance, uniformity ratio of illuminance, correlated color temperature, and color rendering index. To measure these parameters, the HPCS-320 portable spectral illuminance meter was utilized. The measurements were taken on a horizontal surface positioned at a height of 0.75m from the ground, which served as the designated measurement plane.

### 2.2.2 Visual satisfaction

In this study, the semantic difference method was employed to conduct a questionnaire-based investigation into the visual satisfaction of the elderly residents. The semantic difference method, originally proposed by Osgood (1957), is a psychometric approach that utilizes verbal scales to measure psychological perceptions[4]. By employing this method, the research aimed to capture the subjective feelings of the respondents and transform them into quantitative data, thereby facilitating a quantitative understanding of the psychological perceptions related to the research site.

The questionnaire utilized in the study employed a 5-point evaluation scale based on the semantic difference method. The scale assigned scores of 2, 1, 0, -1, and -2, with 0 representing the central axis (as shown in Table 1). These numerical scores were subsequently subjected to quantitative analysis to derive meaningful insights.

Table 1. Semantic Difference Scale

Very satisfied	Satisfied	Undecided	Dissatisfied	Very dissatisfied
2	1	0	-1	-2

## 2.3 Research Results and analysis

### 2.3.1 Light environment parameters research

The investigation of light environment parameters in the six community nursing homes revealed that the illuminance values in each space ranged from 200 lx to 700 lx. The activity room and reading room exhibited relatively high illuminance levels, while the lounge areas had lower levels of illuminance. As per the Building Lighting Design Standard (GB50034-2013), the recommended illuminance level for general activity areas in elderly living rooms should be at least 200 lx, and the writing and reading areas should have a minimum illuminance level of 500 lx. Based on this standard, the illuminance level in the reading rooms of most community nursing homes was found to be insufficient. However, the uniformity ratio of illuminance in all the reading rooms exceeded the international standard value of 0.8, indicating a favorable lighting condition in terms of uniformity. Furthermore, the correlated color temperature of each space in the six community nursing homes ranged from 3500K to 5500K, while the color rendering index was consistently above 80, meeting the international requirements in both cases.

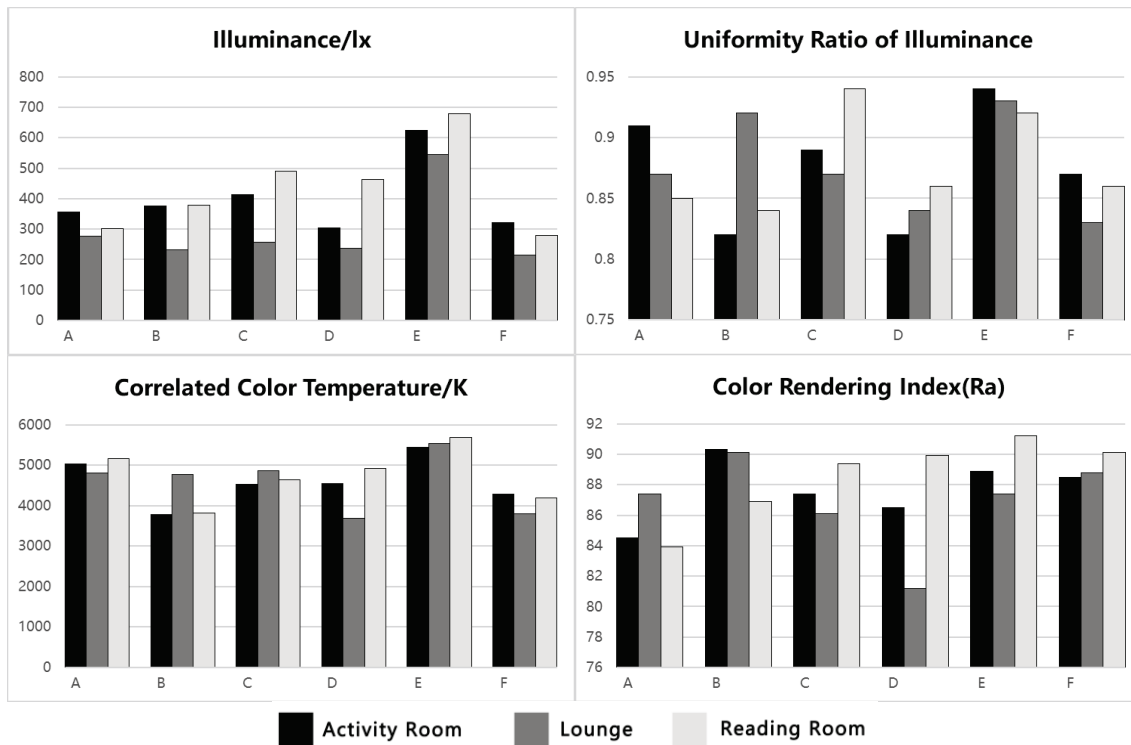


Figure 1. Light environment parameters of 6 community nursing homes

### 2.3.2 Visual satisfaction survey

The visual satisfaction evaluation questionnaire included participants selected randomly based on principles of gender, age stage, and visual condition. A total of 20 samples were collected from each community nursing home, resulting in a total of 120 samples. These samples were averaged to determine the visual satisfaction of the elderly users for each space within the six community nursing homes. The visual satisfaction scores obtained ranged from 0.25 to 1.25. These scores indicate that, overall, the elderly users expressed satisfaction with the light environment in each space of the six community nursing homes.

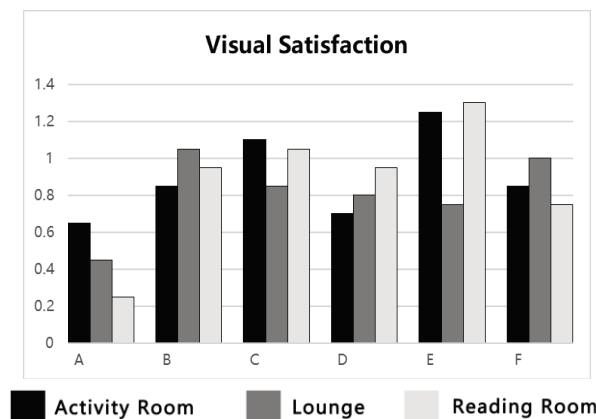


Figure 2. Visual Satisfaction of 6 community nursing homes

## 3. CORRELATION ANALYSIS OF LIGHTING PARAMETERS AND VISUAL SATISFACTION

In this study, Pearson's correlation coefficient was utilized to assess the correlation between visual satisfaction and each light environment parameter. The correlation coefficient, ranging from -1 to 1, indicates positive correlation for positive values and negative correlation for negative

values. A higher absolute value indicates a stronger correlation, while values closer to 0 indicate a weaker correlation.

Overall, visual satisfaction showed a moderate positive correlation with illuminance, uniformity ratio of illuminance, and color rendering index (0.4-0.6). However, there was a very weak positive correlation or no correlation with color temperature (0.0-0.2). The correlation between visual satisfaction and light environment parameters varied across different spaces.

For the activity room, there was a strong positive correlation between visual satisfaction and illuminance (0.6-0.8), indicating that higher illuminance levels led to increased visual satisfaction among the elderly participants. There was also a weak positive correlation with color temperature (0.2-0.4), suggesting that the elderly participants slightly preferred light sources with a color temperature above 5500K in the activity room.

In the reading room, visual satisfaction showed a strong positive correlation with illuminance, uniformity ratio of illuminance, and color rendering index (0.6-0.8), while demonstrating a very weak positive correlation or no correlation with color temperature (0.0-0.2). These results align with common sense, as reading requires appropriate illumination, high uniformity of illuminance, and favorable color rendering index. Additionally, individual preferences for color temperature may vary.

In contrast, the results for the lounge space differed significantly from the aforementioned spaces. In the measured interval, there was a weak negative correlation between visual satisfaction and illuminance and color temperature (-0.4 to -0.2), a weak positive correlation with color rendering index (0.2-0.4), and a very weak positive correlation or no correlation with the uniformity ratio of illuminance (0.0-0.2). These findings suggest that most elderly individuals preferred a lower illumination level and a warm light environment in the lounge. Additionally, the color rendering index was an important consideration for their visual satisfaction in this space.

Overall, the correlation analysis highlights the varying preferences and requirements of the elderly residents in different spaces, emphasizing the importance of considering individual needs and preferences when designing the lighting environment for community nursing homes.

Table 2. Correlation between visual satisfaction and light environment parameters

Pearson's correlation coefficient	visual satisfaction & illuminance	visual satisfaction & uniformity ratio of illuminance	visual satisfaction & correlated color temperature	visual satisfaction & color rendering index
all space	0.53	0.42	0.06	0.56
activity room	0.86	0.55	0.36	0.52
lounge	-0.29	0.02	-0.30	0.29
reading room	0.82	0.61	0.11	0.83

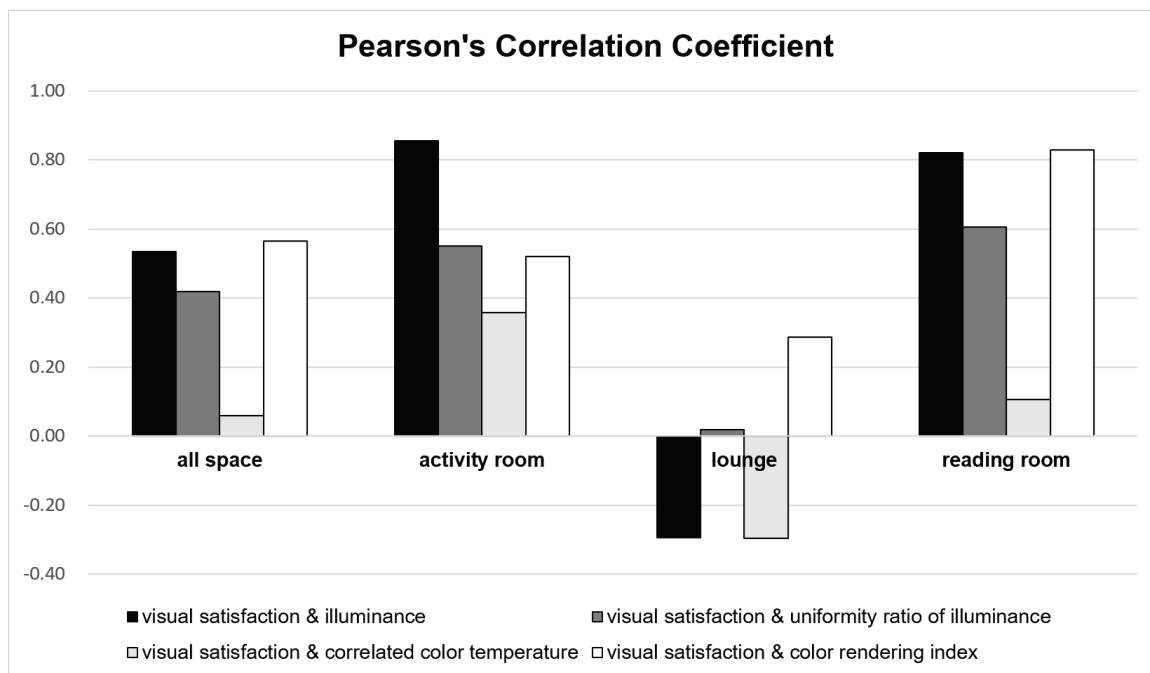


Figure 3. Correlation between visual satisfaction and light environment parameters

#### 4. LIGHTING DESIGN SUGGESTIONS OF COMMUNITY NURSING HOME

Based on the analysis of the research results, the following recommendations can be made for the design of aging-friendly lighting in community nursing homes:

1. Increase the illumination levels in activity rooms and reading rooms to ensure they reach a minimum of 500 lx. Since elderly individuals often experience vision degradation, higher illumination levels are necessary to create optimal lighting conditions for them[5]. On the other hand, it is advisable to slightly reduce the illumination in lounge areas to maintain privacy and create a comfortable resting environment.

2. Emphasize the importance of high uniformity of illumination, particularly in activity rooms and reading rooms. A higher level of uniformity ensures even distribution of light, facilitating object recognition and reading, while minimizing visual fatigue. To achieve this, a combination of general lighting in designated zones and localized surface light sources in reading areas can be employed to ensure both overall and localized uniformity of illumination.

3. Select appropriate color temperature for different spaces. In the activity room, neutral light sources with a color temperature of 5000K-5500K are recommended. This type of lighting promotes a vibrant and energetic atmosphere. In contrast, warm light sources with a color temperature of 3000K-3500K are preferable for the lounge area, as they create a cozy and relaxing environment.

4. Incorporate natural light as much as possible to enhance indoor illumination. Natural light provides the best color rendering index, which is beneficial for visual perception. If natural light is limited, high color rendering index LED lamps and fixtures should be utilized to ensure accurate color representation.

By implementing these suggestions, community nursing homes can enhance the lighting design to better meet the needs and preferences of the elderly residents, creating a more comfortable and visually satisfying environment for them.

#### REFERENCES

[1] 2021 年度国家老龄事业发展公报[EB/OL]. (2022-10-26)[2023-04-11]. [http://www.gov.cn/xinwen/2022-10/26/content\\_5721786.htm](http://www.gov.cn/xinwen/2022-10/26/content_5721786.htm).



- [2] Boyce P R. Human Factors in Lighting[M]. CRC Press, 2017.
- [3] Shariful, Shikder, Monjur, et al. Therapeutic lighting design for the elderly: a review[J]. Perspectives in Public Health, 2012, 132(6): 282.
- [4] 赵博阳, 乔丹惠, 张小弼. 基于 SD 法的儿童友好型老旧社区室外公共空间更新研究——以天津市体院北住区为例[J]. 河北工业大学学报(社会科学版), 2023, 15(01): 87-94.
- [5] ANSI. Lighting and the Visual Environment for Seniors and the Low Vision Population: IES RP-28-96[S]. IESNA, 2016.

## **ACKNOWLEDGEMENTS**

Corresponding Author Name: Kehang Chen  
Affiliation: Faculty of Architecture and Urban Planning, Chongqing University  
e-mail: 892241932@qq.com

# HEALTH-ORIENTED WARD LIGHTING DESIGN: TAKING THE DESIGN OF THE SMART HOSPITAL IN CHONGQING WESTERN SCIENCE CITY AS AN EXAMPLE

Guangzhi Hu<sup>1</sup>, Tongyue Wang<sup>2,3</sup>

(1. East China Architectural Design & Research Institute Co.,Ltd, Shanghai, China;

2. Shanghai Yangzhi Rehabilitation Hospital(Shanghai Sunshine Rehabilitation Center), School of Medicine, Tongji University, Shanghai, China;

3. School of Architecture and Urban Planning, Tongji University, Shanghai, China; )

## ABSTRACT

One of the most important functions of medical building is to provide healing space for patients. The ward is not only the largest proportion of medical buildings but also the long-term living space of hospitalized patients. Therefore, the natural light environment of the ward affects the patient's health deeply. In order to optimize the lighting effect of wards in hospital design, parametric design is used to establish a parameter model, which associates lighting effects with factors such as inpatient building layout, nursing unit layout, and lighting opening size, so as to conduct simulated lighting analysis. Furthermore, make an evaluation based on Dynamic Daylighting Performance Metrics - Useful Daylight Illuminance(UDI) and Daylight Glare Probability(DGP), and then optimize relevant design elements. Taking the actual project - the design of the Chongqing Western Science City Smart Hospital as an example, explain how to optimize the indoor lighting environment of the ward by adjusting relevant design elements including the shape of the inpatient building, the size of the daylight opening, and the parameters of the external sunshade, in order to create a healing ward space for patients.

Keywords: ward space; parametric design; daylighting simulation; dynamic daylighting performance metrics

## 1. Introduction

Hospitals need to go beyond fulfilling the function of treating diseases and pay more attention to creating healing environments. As the largest component among the seven major functional categories of hospitals, the area occupied by the inpatient department reaches 37-41%[1]. The patient ward space is the largest functional space within the inpatient department and serves as the long-term residence for hospitalized patients. Throughout history, the physical environment has always had a significant impact on human health[2]. Firstly, light can affect visual function in humans. Prolonged exposure to poor lighting conditions can lead to decreased visual acuity, visual fatigue, reduced task performance, hinder smooth activities, and contribute to eye conditions such as myopia and macular degeneration. Secondly, light also has a significant impact on circadian rhythms through the activation of the Intrinsically photosensitive retinal ganglion cells(ipRGCs) in the human eye. This affects biological rhythms, including sleep patterns, eating habits, metabolism, hormone secretion, and immune responses. Additionally, the lighting environment can influence a person's emotions and contribute to psychological well-being[3]. Therefore, in spaces such as hospital wards that emphasize the healing effect on patients, the comfort of the lighting environment is a crucial design element. The creation of a conducive lighting environment primarily depends on natural daylighting and artificial lighting. In the daily activity cycle, natural daylighting plays a more significant role for patients. Therefore, the focus here is on exploring the design principles and methods for natural daylighting in hospital wards.

## 2. Evaluation indicators for natural daylighting

To enhance daylighting design, it is important to select appropriate evaluation indicators for daylighting performance. There are various evaluation indicators for natural daylighting, which can be broadly categorized into two types: static daylighting performance metrics that evaluate the

daylighting performance at a specific moment in time, and dynamic daylighting performance metrics that reflect the annual daylighting performance. Dynamic daylighting performance metrics involve importing annual weather data of the building's location into software, establishing a sky model, and analyzing data such as illuminance and degree of glare on an hourly basis throughout the year. These indicators provide a comprehensive evaluation of daylighting performance and reflect the real indoor lighting conditions. They play a crucial and intuitive role in improving the healthy design of hospital ward spaces. Within the dynamic daylighting performance metrics, there are generally two directions: indicators that reflect the daylighting performance at specific observation points and indicators that reflect the daylighting performance within a specific spatial range. Among the numerous dynamic daylighting performance metrics, representative ones include the Daylight Autonomy (DA), Useful Daylight Illuminance (UDI), and Daylight Glare Probability (DGP). These indicators are commonly used for daylighting analysis. By utilizing appropriate evaluation indicators, designers can effectively analyze and optimize the daylighting design in hospital ward spaces, ultimately enhancing the health and well-being of patients.

## 2.1 Daylight Autonomy (DA)

DA is a dynamic daylighting performance metric that represents the percentage of time in which the minimum illuminance requirements are met solely by natural daylight throughout the year. It takes into account the daylighting conditions for all 8,760 hours of the year and provides a comprehensive description of the impact of weather, climate variations, and building factors on the indoor lighting environment. However, it has some limitations. DA only specifies the minimum illuminance requirements and does not consider issues such as glare that may arise from excessive illuminance. Nonetheless, the DA indicator still holds value as a reference, particularly in regions with limited natural lighting conditions.

## 2.2 Useful Daylight Illuminance (UDI)

UDI describes the proportion of time, out of the total 8,760 hours in a year, during which the indoor working plane is within the range of useful illuminance[4]. In 2006, Nabil et al. conducted a study where they divided the illuminance levels of the lighting environment into three ranges: less than 100 lx, 100-2000 lx, and greater than 2000 lx. When the illuminance is below 100 lx, the lighting environment is considered insufficient and not suitable for visual tasks. When the illuminance falls within the range of 100-2000 lx, the lighting environment is deemed suitable for various visual activities. However, when the illuminance exceeds 2000 lx, it may cause glare and other discomfort, making it unsuitable for visual tasks.

Compared to DA, UDI sets a specific range, which includes high illuminance conditions such as glare, allowing for a more comprehensive and accurate daylighting evaluation. Therefore, UDI is chosen as the indicator for subsequent daylighting simulation and evaluation, as it provides a more comprehensive assessment of the lighting conditions, including the potential issues of high illuminance and glare (As shown in Table 1).

Table 1: UDI Ranges

UDI ranges	Result
less than 100lx	Insufficient illuminance
100-2000lx	Suitable for human visual activities
greater than 2000 lx	Prone to glare and other phenomena

## 2.3 Daylight Glare Probability (DGP)

DGP is an indicator used to further assess the comfort level of the indoor lighting environment in relation to glare. It takes into account various factors such as overall luminance, glare range and luminance, visual contrast differences, and utilizes rigorous methods for calculation, effectively considering the user's perception[5]. The values of DGP are divided into several levels, as shown in Table 2. From the table, it can be observed that DGP levels below 0.4 are considered more ideal.

Table 2: DGP Classification (Table Source: Adapted by the author)

DGP	Level
$DGP < 0.35$	Imperceptible glare
$0.35 < DGP \leq 0.4$	Perceptible comfortable glare
$0.4 \leq DGP < 0.45$	uncomfortable glare
$0.45 \leq DGP$	Intolerable glare

For hospital wards, in order to create a natural lighting environment that is conducive to patient health, it is important to ensure adequate illumination. This allows patients to experience a sense of natural atmosphere despite being in a hospital room. Additionally, excessively high illuminance can lead to glare, affecting patients' visual comfort, especially those with eye-related conditions. Therefore, ideally, the indoor natural daylight illuminance should be within a sufficient but not excessively high range. It is suitable to use UDI100-2000lx as an evaluation criterion for the overall indoor lighting environment. Furthermore, glare analysis should be conducted for the areas where patients reside for extended periods. By quantifying glare using DGP values, the glare situation can be assessed to reduce the negative impact of light pollution on patients.

### 3. Basic Project Information

The project of the Chongqing Smart Hospital is located in the Shapingba District of Chongqing, specifically in Xianglushan Street, approximately 230 meters south of Chongqing University of Science and Technology (Huxi Campus), and on the north side of University City South Road. The surrounding area of the site is mostly residential, so when designing for natural lighting, the mutual influence between the hospital building and the high-rise residential buildings should be taken into consideration. The total land area of the project is approximately 22,000 square meters, with a total construction area of 78,910 square meters. It includes a secondary hospital, a disease control and experimental building, as well as a shared administrative building. The secondary hospital has a capacity of 400 beds. After conducting an analysis of the surrounding site, functional zoning, and the area requirements for various functional rooms, the following architectural layout and spatial relationships have been roughly formed: the Centers for Disease Control and experimental building are located at the downwind corner in the southeast, which is the dominant wind direction throughout the year. The inpatient area is situated on the north side to minimize the impact on the high-rise residential buildings on the south side of the site. The shared administrative building is located between them, serving as a transition and connection (As shown in Figure 1).

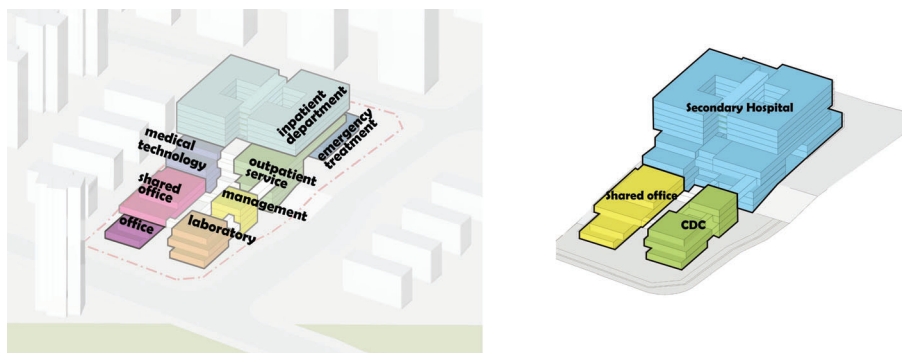


Figure 1: Preliminary Functional Layout and Spatial Relationships

Chongqing is located in Zone V, which is classified as a region with limited solar radiation in the Chinese daylight climate zone. It is one of the areas in China with the least solar energy resources. The city experiences overcast skies and a lack of sunshine throughout the year, with an annual average total illuminance of natural light in the range of less than 30 klx. Therefore, the lighting design of the hospital wards in this project is particularly important. The primary objective is to ensure sufficient illumination inside the wards. Due to the scarcity of sunlight, glare phenomena are also relatively rare. Therefore, the glare analysis for the west-facing direction is conducted at the most unfavorable time, which is the evening.

#### 4 Daylighting Simulation Analysis and Optimization

After the preliminary architectural massing design, the next step is to conduct corresponding daylighting design and lighting simulation for the hospital wards. This involves establishing functional relationships between the variables studied, allowing the parameters to mutually influence and determine each other while maintaining their respective correspondences. By utilizing existing "parameters" to determine and influence the required parameters, a dynamic parametric model is formed[6]. Based on the simulation results, the architectural design can be optimized to achieve the desired lighting environment in the wards.

##### 4.1 Factors Affecting Daylighting Effect

First, it is necessary to determine the architectural design variables that impact the daylighting conditions in the hospital wards. Since the overall layout has already been determined and there are no obstructions on the south side of the inpatient building, only the internal conditions need to be considered.

The first factor is the layout and form of the inpatient building itself, specifically whether there are any self-shading conditions. Under the current massing form, a comparison calculation can be conducted between a "O" shape and two "C" shapes (As shown in Figure 2).

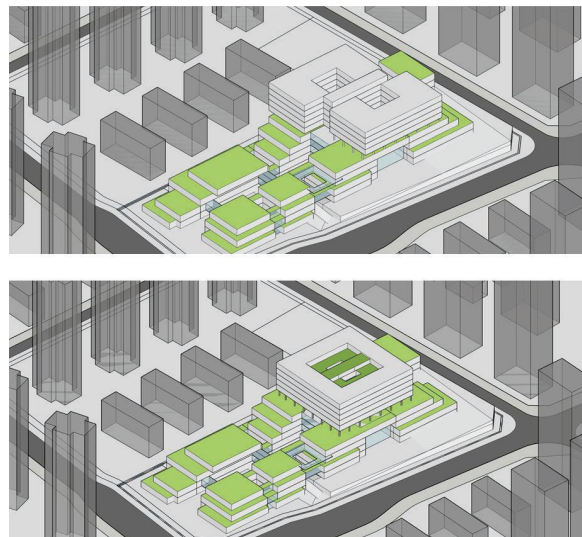


Figure 2: Forms of the Inpatient Building: "C" Shape(above) and "O" Shape(below)

Next is the arrangement of the nursing units on each floor of the inpatient building, whether the wards are arranged along the perimeter or along the south and east sides. However, in this project, due to the compact area, the wards can only be arranged along the east, west, and south sides while meeting the required number of beds. Therefore, no further consideration is needed in this regard.

Furthermore, the focus is on the daylighting openings in the wards themselves. The "Architectural Daylighting Design Standards" of China specify the window-to-floor ratio that buildings in different daylight climate zones should meet. Within the requirement of a certain window-to-wall ratio, the size of the daylighting openings also has a corresponding impact on the internal lighting environment. Additionally, to avoid glare and maintain a relatively comfortable DGP range, the influence of shading devices also needs to be considered.

##### 4.2 Model Creation and Daylighting Simulation

The established massing scale, column span, and ward dimensions are parameterized to create a model. The standard floor of the ward is selected for further study. The daylighting simulation is conducted using the Ladybug tools in the Grasshopper platform.

First, the room dimensions are determined based on an 8.4-meter column span: half of the span for the room width (4.2 meters) and one span for the room depth (8.4 meters). Additionally, considering the size of the inpatient building, to meet the required number of beds (40-50 beds on each floor) while maximizing the daylighting for the wards, they can only be arranged along the west, south, and east sides. The doctor's area, nursing area, and common activity area are located in the middle of the inpatient building. This configuration allows for the setting of dual nursing units on the same floor, with



the flexibility of being separated or combined. The ward area, nursing work area, doctor's work area, and common activity area complement each other. The patient meal service and waste collection service are arranged to achieve a "clean in, dirty out" layout pattern(As shown in Figure 3).



Figure 3: Rough Floor Layout of "C" Shape (Left) and "O" Shape (Right)

Next, the floor layout is transformed into a three-dimensional model. Since the focus is on studying the daylighting in the wards, each individual ward and its combination are expressed in the model. The requirements for materials such as walls and glass, as specified in the "Architectural Daylighting Design Standards" of China[7], are taken into account. Relative parameters are assigned to the enclosing surfaces of each ward in the Ladybug tools, creating a three-dimensional parametric model with optical attributes.

When determining the window size, according to the "Architectural Daylighting Design Standards," Chongqing belongs to the 5th category of daylight climate zones. In order to meet the requirement of a window-to-floor area ratio not less than 1/10, the minimum window area can be calculated as  $8.4 \times 4.2 \times 0.1 \approx 3.53$  square meters. On the southeast side of the ward building, there is an urban green area. The window sill height should ideally meet the needs of ventilation and daylighting while allowing patients to enjoy distant views. Therefore, the window sill height is set between 0.3-0.7 meters. Taking into account the thickness of beams and ceilings (approximately 0.9 meters) and a floor height of 4.2 meters, the height range of the window is 2.6-3.0 meters (in increments of 0.2 meters, with a total of 3 values). Considering the dimensions of the columns (0.6 meters wide) and the room depth (4.2 meters), the maximum width of the window is 3.6 meters. To meet the minimum window area of 3.53 square meters with the smallest window height and considering the overall facade aesthetics, the minimum width of the window is set at 2.1 meters. Therefore, the width range of the window is 2.1-3.6 meters (in increments of 0.3 meters, with a total of 6 values: 0.3, 0.45). Under the same ward building form, a total of 18 daylighting scenarios will be simulated and calculated.

The next step is to set the materials for each interface of the ward unit, as shown in table 3.

Table 3: Material and Related Parameters of Each Surface in the Ward

Face	Material	Reflectance	Transmittance
Floor	Light-colored wooden floor	0.58	
Wall	White paint	0.75	
Ceiling	Gypsum board	0.91	
Window	Low-E Insulated glass		0.76
Shade	Aluminum plate	0.8	

Then, import meteorological data specific to the Chongqing region and establish the CIE sky model. Based on the usage time regulations for hospital-type buildings in the "Architectural Lighting Design Standards," which is from 8:00 to 17:00, for 310 days a year, define the corresponding simulation time range. Conduct light simulation for the aforementioned ward parameter model for a total of 3,100 hours.

#### 4.3 Data Processing and Design Optimization

Analysis and processing of multiple sets of simulated data are conducted. Firstly, a comparison is made between the daylighting conditions of the "C" and "O" shaped ward layouts. To simplify the

calculations, a controlled variable approach is adopted, using a model with a window height of 3m and width of 2.1m for simulations. Due to the possibility of self-shading in the middle ward of the "C" shaped layout, the UDI values for this room are analyzed separately in addition to the average UDI100-2000lx value. The results are summarized in the table 4:

Table 4: UDI100-2000lx Values for Different Layout Forms

	"C" shape	"O" shape
Average UDI100-2000lx ( % )	65.92	65.93
Separate UDI100-2000lx ( % )	65.45	65.44

As we can see, both in terms of the average UDI100-2000lx value and the UDI100-2000lx value of the middle room on the south side, the results of the two layouts are similar. This is mainly because in the C-shaped layout, the self-shadowing portion is designated as a public resting area, minimizing the self-shadowing factor caused by the shape transition. Therefore, in terms of daylighting, there is no significant difference between the two layouts, and in design, the C-shaped nursing unit form with more varied form changes can be considered to enrich the architectural volume and shape.

Next, simulations were conducted for different window schemes in the C-shaped layout. Due to limited daylight resources in Chongqing, with a majority of the year being cloudy, glare is less of a concern. Therefore, the focus was primarily on UDI. The data were summarized in table5:

Table 5: Data for Different Daylighting Schemes in C-shaped Layout

Number	Width * Height of Daylight Opening (m * m)	Average UDI100-2000lx ( % )	Number	Width * Height of Daylight Opening (m * m)	Average UDI100-2000lx ( % )
1	3.6*3.0	62.24	10	2.7*3.0	64.82
2	3.6*2.8	63.30	11	2.7*2.8	64.79
3	3.6*2.6	63.37	12	2.7*2.6	64.75
4	3.3*3.0	63.97	13	2.4*3.0	65.44
5	3.3*2.8	64.01	14	2.4*2.8	65.37
6	3.3*2.6	64.01	15	2.4*2.6	65.29
7	3.0*3.0	64.15	16	2.1*3.0	65.88
8	3.0*2.8	64.15	17	2.1*2.8	65.77
9	3.0*2.6	64.15	18	2.1*2.6	65.61
			19	1.8*3.0	65.89

From the table 5, it can be observed that as the area of the daylight opening decreases, the overall trend of average UDI100-2000lx values is as follows: grouping the data with the same width, the value of each group increases. This is because with overly large daylight openings, there are more areas indoors with illuminance above 2000 lx. The growth trend tends to stagnate after number 16. Additionally, when the width of the daylight opening is constant, a smaller height leads to a lower UDI100-2000lx value. Therefore, it is not necessarily better to have larger daylight openings. Among the data above, numbers 16 and 19 represent the optimal sizes for daylight openings, but considering the human perception of panoramic views, it is preferable to choose the wider opening represented by number 16.

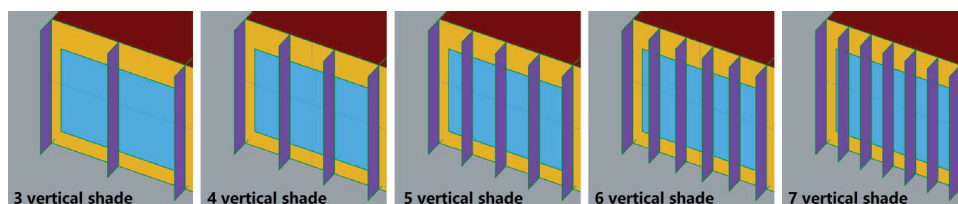
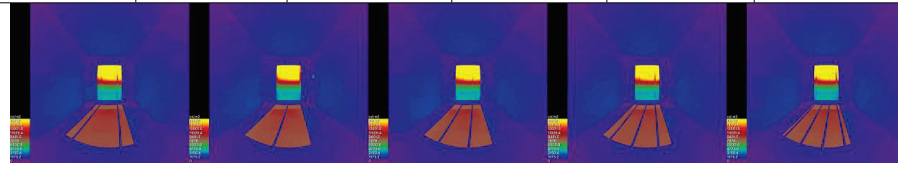


Figure 4: Establishment and Simulation of the Parameter Model

During the simulation process, it was observed that some situations experienced excessive glare. To address this issue, sunshades were introduced. Considering aesthetic factors, 3-7 vertically oriented sunshades were uniformly installed at the daylight opening of each patient room unit (As shown in Figure 4). The simulation analysis of DGP was conducted at 4:00 PM on the summer solstice, which is a time prone to glare. The glare analysis is based on a specific moment, viewpoint, line of sight, and resulting view, to analyse the brightness of objects in the image to assess glare. The resulting data is shown in 6.

Table 6: Improvement of Glare with Vertically Oriented Sunshades

	no sunshade	3 sunshades	4 sunshades	5 sunshades	6 sunshades	7 sunshades
South ward DGP	0.368	0.369	0.366	0.365	0.363	0.364
East ward DGP	0.360	0.356	0.370	0.357	0.356	0.354
West ward DGP	0.778	0.764	0.758	0.762	0.748	0.740
Average UDI100-2000lx	65.88%	65.99%	65.99%	66.11%	66.13%	66.11%
East ward view						

From Table 6, it can be observed that as the number of vertical sunshades increases, the glare values in west-facing rooms generally decrease, while the average UDI100-2000lx values increase. When the number of sunshades reaches 6 or 7, the glare values and UDI100-2000lx values tend to stabilize. However, having too many sunshades can also affect patients' viewing experience and the facade aesthetics. Therefore, the option of using 6 vertical sunshades per patient room is chosen.

In conclusion, there is no significant difference in terms of daylighting between the "C"-shaped and the "O"-shaped floor plans for the hospital building. In the design process, it is advisable to consider the more varied and dynamic "C"-shaped nursing unit layout to enhance the architectural massing. For the window openings, selecting Option 16 (2.1m \* 3.0m) would provide higher average UDI100-2000lx values and better scenic views. Additionally, it is recommended to uniformly install 6 vertical sunshades for each ward on the facade to reduce glare and increase UDI100-2000lx values to a certain extent.

## 5 Conclusion

The ward, as a space for long-term patient residence, has a close relationship with the health of the patients. The indoor lighting environment of the ward is influenced by various factors. Ward design should not only focus on the ward itself but also take into account the geographical characteristics of the building, the demands of the owners, contextual factors, and other relevant aspects for targeted ward lighting environment design, which is necessary.

Firstly, an analysis is conducted on the Chongqing Smart Hospital project to extract key elements that affect the ward lighting environment, including the ward's floor plan, the size of windows for daylighting, and external sun shading devices. Then, parameterized models are established to simulate the lighting effects of each influencing factor. Finally, using the UDI and DGP parameters as evaluation criteria, the experimental data is organized and evaluated to explore a relatively optimized design solution. From project analysis to establishing parameter models and then to data organization, the design is optimized in the end. This represents a health-oriented lighting environment design approach in practical projects.

## REFERENCE

- [1] Ministry of Housing and Urban-Rural Development of the People's Republic of China, National Development and Reform Commission. Code for design of polyclinic buildings (in Chinese): GB110-2021[S]. Beijing: China Planning Press, 2021: 1-5.
- [2] Rana Sagha Zadeh, Mardelle Mc Cuskey Shepley, Gary Williams, Susan Sung Eun Chung. The Impact of Windows and Daylight on Acute-Care Nurses' Physiological, Psychological, and Behavioral Health[J]. SAGE Publications, 2014, 7(4).
- [3] Luoxi Hao, Yixiao Cao. Evidence-based Research and Design Practice of Light Environment for Healthy Human Settlements (in Chinese)[J]. Time+Architecture, 2020(05): 22-27.
- [4] Azza Nabil, John Mardaljevic. Useful daylight illuminances: A replacement for daylight factors[M]. Energy and Buildings, 2006(38): 905-913.
- [5] Wienold J, Christoffersen J. Evaluation methods and development of a new glare prediction model for daylight environments with the use of CCD cameras[J]. Energy and Buildings, 2006, 38(7): 743-757.
- [6] Wolfram S. A New Kind of Science[M]. Champaign: Wolfram Media, 2002: 175-186.
- [7] Ministry of Housing and Urban-Rural Development of the People's Republic of China. Standard for daylighting design of buildings: GB 50033--2013 (in Chinese)[S]. Beijing: China Architecture Publishing & Media Co., Ltd, 2013: 5-10.

## ACKNOWLEDGEMENT

I am profoundly grateful to all those who have been instrumental in the successful completion of this academic thesis. First and foremost, I extend my sincere appreciation to my advisors, for their unwavering guidance and invaluable insights throughout the research process. Their expertise and constructive feedback have been vital in shaping the direction of this work. I also wish to acknowledge the support and encouragement provided by my family and friends, whose belief in my abilities has been a constant source of motivation. Lastly, I extend my thanks to the participants who generously contributed their time and insights, making this research possible.

Corresponding Author: Tongyue Wang

Affiliation: 1. Shanghai Yangzhi Rehabilitation Hospital (Shanghai Sunshine Rehabilitation Center), School of Medicine, Tongji University, Shanghai 201619, China; 2. School of Architecture and Urban Planning, Tongji University, Shanghai 200092, China  
e-mail: 1256559410@qq.com

# A STUDY ON THE APPLICATION OF LED EDGE LINEAR LIGHT TO LNG SHIP PASSAGEWAY

MINJEONG YOO, JIN KIM, ANSEOP CHOI  
SEJONG UNIVERSITY

## ABSTRACT

In general, most LNG ship Passageway ceilings are equipped with Ceiling Light, which is similar to flat-panel lighting installed inside buildings. However, unlike architectural lighting, as a precaution against fire, an insulation box is installed where the luminaire is recessed. In addition, lighting for marine use is basically divided into normal and emergency circuits, and in some cases, battery back up is also installed.

In this way, the application of Linear Light to Passageway was reviewed as an alternative to solving problems caused by difficulties in installation work and Gap differences with Ceiling after installation of Lighting. If it is installed in the form of linear light on both corners of the Passageway, it can reduce the ceiling work process, so that the difficulty of the work is resolved and the atmosphere of interior quality can be created. Compared to the existing Ceiling Light, this study aims to study the LED Passageway suitable for each type of ceiling by comprehensively comparing and analyzing installation, cost, and design.

Keywords: LIGHTING FOR MARINE USE, LNG CARRIER, PASSAGEWAY LIGHTING

## 1. INTRODUCTION (HEADING1)

Recently, large shipyards in Korea are considering changing the ceiling light of corridor to LED edge light. Usually, the no-Gap type ceiling on the ship except for cruiseship is repeatedly installed recessed ceiling light for each deck. However, in order to install the Ceiling Light, the ceiling must be configured in a flame retardant structure to satisfy the flame retardant grade depending on the conditions, and labor is consumed to cable the power. To improve this, a study was conducted to change to Linear Edge Light.

Compared to the existing Ceiling Light, a study was conducted to compare constructionability, economic feasibility, and design effect.



Figure 1. Recessed LED Ceiling Light installed in Passageway



## 2. REQUIREMENTS

### (1) Cable Partition between Normal and Emergency

Unlike architectural lighting, the lighting fixtures in the ship space must be equipped with Normal, Emergency, and Battery Back Up Light. When changing from Ceiling Light to Edge Light, it is necessary to consider a form in which the cable partition of normal and emergency can be separated.

### (2) The Height of LED Edge Light

The height of the passageway ceiling is very low, averaging 2.2 to 2.3m. In addition, considering the height of the door frame, the depth at which the luminaire can be recessed from the ceiling is narrow to 40 to 50 mm, so it is also necessary to consider the height of the luminaire.

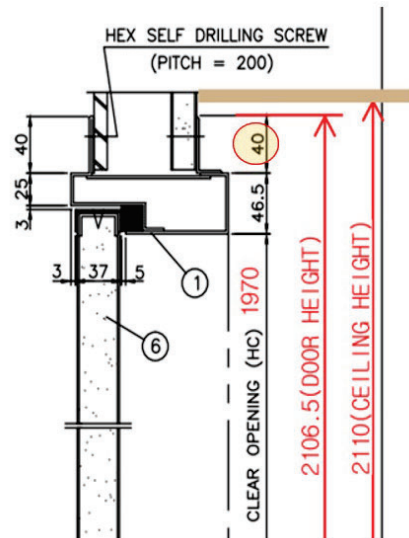


Figure 2. Inside the Passageway's Ceiling

### (3) Installation method of LED Edge Light

Fixing methods for lighting fixtures can be divided into ceiling fixing methods and wall fixing methods, and the effects of each fixing method must be compared and reviewed.

### (4) Maintenance

## 3. MOCK-UP

First of all, Mock-Up was carried out in a condition similar to that of the passageway of the LNG Ship. First of all, Mock-Up was carried out in a condition similar to that of the residential area of the ship lighting. A recessed ceiling light was installed in the conventional way, and an edge light was installed on the top of the wall so that it could be compared under the same conditions at the same time.

### (1) Floor Plan

The mock-up space was produced and on the same scale as the actual LNGC's Accommodate space. The total area is 594 m<sup>2</sup>, the length of the corridor is 33m, the width is 1.4m, and the height of the ceiling is 2.2m. One recessed ceiling light was installed every 3.3m, and the linear light was installed on both edges of the corridor. The circuit was divided into normal light and emergency light.

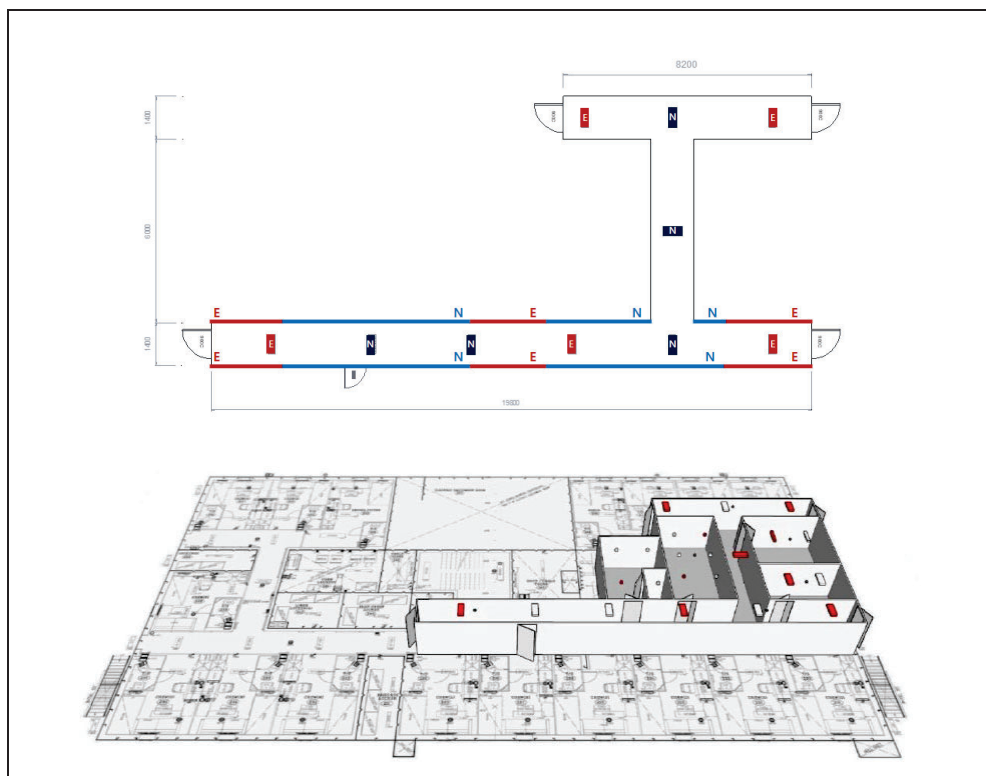





Figure 3. Inside the Passageway's Ceiling

## (2) Mock-up lighting specification

Recessed LED ceiling light is a lighting fixture generally installed in the passageway of LNG carriers built in major shipyards. In addition, the LED Edge Light, which is currently being reviewed as an alternative, was installed in the wall. Each lighting is divided into normal light and emergency light cables in the same way as the actual ship space.

Table 1. List of lighting fixtures[1]

Symbol	Image	Specification	Q'ty
		Lamp : LED 20W Dimension : (L)684 * (W)0282 * (H)100(mm) Protection Degree : IP20 Materials : Body – Electro zinc coated steel sheet / Globe - Polycarbonate Input : AC 220~240V	Normal : 5EA Emergency : 5EA
		Lamp : LED 18W/m Dimension : (L)12100/900/600/300/150 * (W)18 * (H)32 (mm) Protection Degree : IP20 Materials : Aluminum, PC Input : AC100-120V	L1000 : 3EA L500 : 7 EA L250 : 2EA

## (3) Installation

LED Edge Light is divided into ceiling fixing and wall fixing, and in this mock-up, it was fixed with a wall bracket.

Recessed Ceiling Light is divided into Normal and Emergency through cable connection, and main power is divided for each circuit, whereas in the case of LED Edge Light, in the case of the same circuit, it is possible to connect directly between luminaires without requiring cable connection. Because of these advantages, when applying LED Edge Light, cable costs can be reduced.






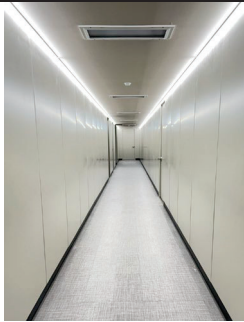
Figure 4. Classification of power cable wiring of Normal Light and Emergency Light

## 4. RESULTS

### (1) Visual Effects

As a result of comparing the average illuminance of LED Ceiling Light and LED Edge Light, the average illuminance of LED Edge Light was significantly higher. The average illuminance of Passageway specified by IEC is much higher than 100lx. And as the vertical surface became brighter than the recessed ceiling light, the uniformity was also improved. In addition, you can expect a high-end effect on the interior.

Table 2.

Recessed LED Ceiling Light	LED Edge Light		
	Normal	Emergency	All
			
Eavg : 570 lx	Eavg : 57.5 [lx]		Eavg : 1,167 lx

## (2) Complement to LED Edge Light

In the case of LED Edge Light, it is necessary to change the structure so that the cable division between Normal and Emergency can be clearly distinguished. In Mock-Up, the advantage of direct connection between lighting fixtures was demonstrated, but the disadvantage of having to install power cables in the first stage of the normal and the first stage of the emergency line occurred. In order to solve this problem, there is an advantage in that each cable can be separated by creating a cable path inside the lighting fixture, and at the same time, the cables can be smoothly connected inside the lighting fixture.

And, when installing the wall bracket, a phenomenon occurred that the bracket was exposed to the field of view from the side. A floating space is created between the wall and the bracket, and it may be difficult to level the bracket during construction, so these points must be supplemented.

## 5. CONCLUSION

By conducting a mock-up under the same conditions as the actual environment, the applicability of LED Edge Light and the points to be supplemented were confirmed. The points to be improved in order to meet the conditions necessary for installation in the ship space were reviewed, and they were reflected in the shape of the actual lighting fixture.

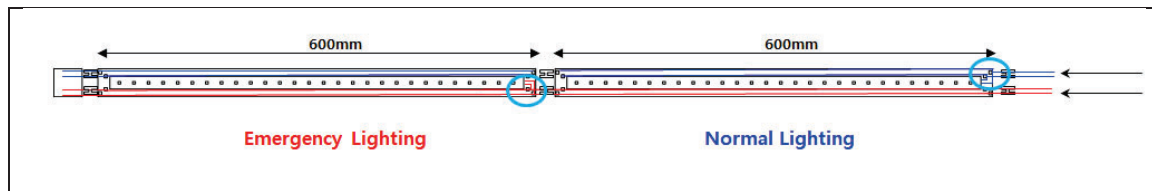


Figure 5. Conceptual diagram of Normal Light and Emergency Light

For smooth cable separation of normal light and emergency light, which is the most important part, the LED array itself in the lighting fixture is divided. Although normal and emergency LEDs are placed together inside one lighting fixture, it is divided into cable connections, and when connecting emergency cables, the normal line has been reviewed as a structure that can bypass.

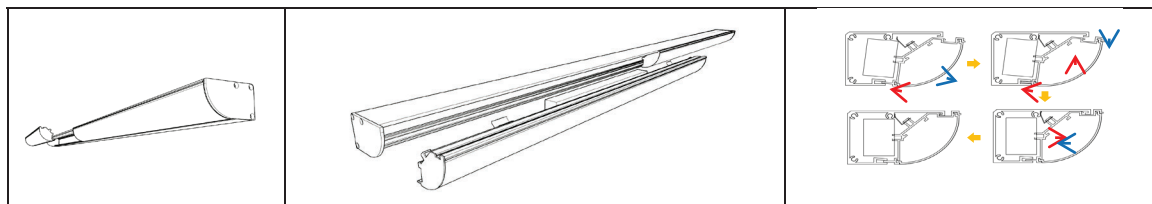


Figure 6. Molded structure led edge light

In order to supplement the exposure of the wall bracket, the entire luminaire was molded so that it could be fixed to the wall instead of the bracket. After pre-attaching the mold, we considered a method to push the LED lamp in and fix it inside the mold. In this case, it is possible to organize the wiring, and it is advantageous for future maintenance. The functions that can be connected between lighting fixtures applied in Mock-Up are maintained, but optical acid finishing materials and finishing caps are considered to reduce the dark point between lighting fixtures when connected.

Currently, this research is still in progress, and the concept and shape of a lighting fixture that can meet the requirements is manufactured and examined in detail.

## REFERENCES

- [1] DAEYANG Electric Company, Lighting Formal, Vol.22-2

## **ACKNOWLEDGEMENTS**

Corresponding Author Name: Yoo Min Jeong  
Affiliation: Sejong University  
e-mail: mjyou@daeyang.co.kr



## LIGHTING DESIGN AT MAIN LOBBY AS A BASE OF THE SCULPTURAL TOWER FACADE

Eunjeong Wang

BPI Studios Korea, Seoul, Republic of Korea

### ABSTRACT

An ethereal entry enhances this office tower in the center of a flourishing commercial district and transforms it into one of the city's crown jewels. As it rises to the heavens, the glimmering sculptural façade is delicately enhanced by the glowing interior. The lighting effect focuses on revealing solid surfaces through silhouettes of stainless-steel tubes. To maintain the flawless expression, ceiling and wall surfaces are illuminated through projected light and integrative lighting locations. The soft ambience provides a warm and welcoming experience, while highlights add a striking dramatic flair.

The design experience for this project will be presented a relationship between tower design and public interior lighting to achieve both aesthetical and functional program in the project.



Figure 1. Overall tower view from the site

### 1. INTRODUCTION

The glowing lobby immediately catches the eye of guests. The lobby serves as a significant foundation to the tower, while providing definition to the structure.

Beauty and strength are entwined within the lobby, creating a harmony of radiance and brilliance. The structure, enhanced by the illuminated interior features, reveals the strength and solidity of the tower base. Lighting systems, integrated within the architectural details, express a glow from interior to exterior.

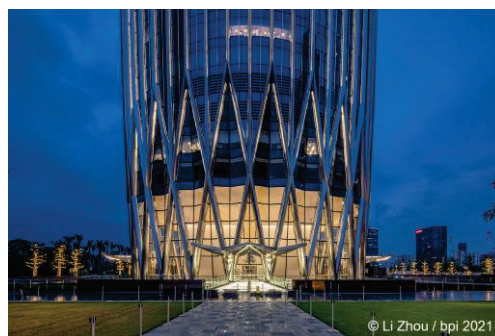


Figure 2. Exterior view from main entry approach

## 2. LIGHTING SYSTEMS AT MAIN LOBBY

The illumination reveals a massive cube core and multifaceted circular ceiling. Lighting defines delicate shapes and modern materials while contrasting against the sculptural façade. This combination of materials provides a warm and welcoming entrance into an impressive structure.

To keep lighting subtle, several studies were performed to analyze aiming and direction. Providing ambience from 17 meters high, while illuminating the floor 5 meters below, proved to be a complex challenge.

To preserve a quiet ceiling, studies evaluated providing illumination from the curved façade and structural steel, while avoiding shadows on the multifaceted ceiling system.



Figure 3. Exterior view sunken garden (core wall going down to B1 level)

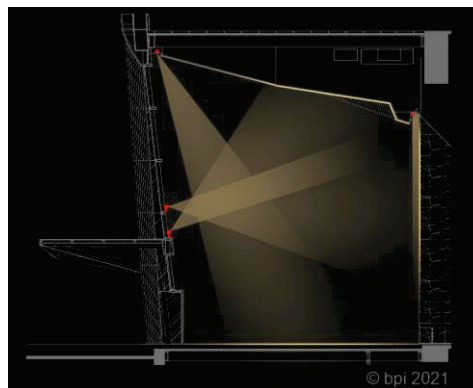


Figure 4. Lighting system sketch

As a result, ceiling and adjoining core walls are softly washed by accent lights from the opposing curtain wall. Grazers were applied between the wall and ceiling to create visual separation. To maintain the pristine ceiling, recessed lighting aligns the angular ceiling edges to provide ambient lighting.

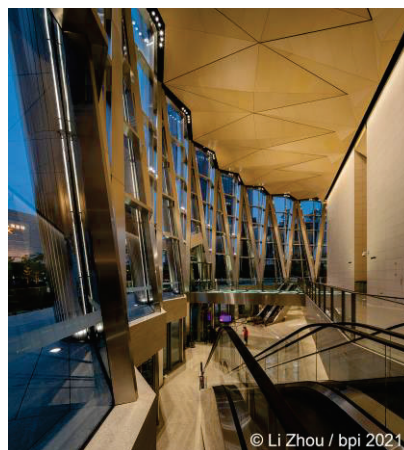


Figure 5. Interior view at open floor

The studies confirmed the lighting systems could be placed in a patterned radial array to correspond with the symmetrical architectural intent, maintaining an elegant and minimal system.



Figure 6. Interior view at ground floor

### 3. ELEVATOR LOBBY

Upon entering, visitors are drawn to an illuminated platform and elevator lobby. The frosted glass, grazed by fixtures within the bridge structure provide spatial sense.

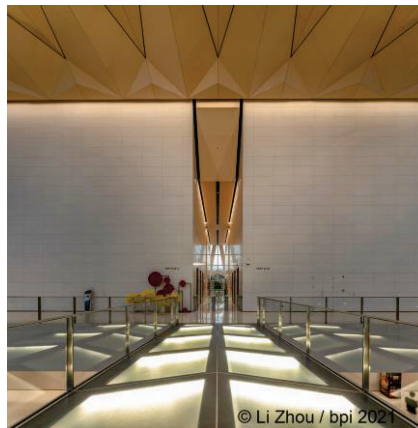


Figure 7. Elevator lobby approach

The elevator lobby divides the core in the for equal zones. Grazers at each side emphasize the ceiling cove while downlight within slots provide floor ambience

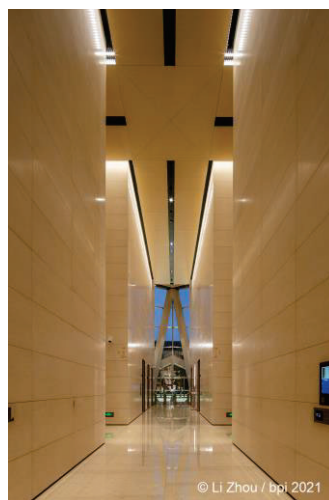


Figure 8. Elevator lobby core

The light density ratio, designed at 7:4:1 for the floor, walls, and ceiling, provides a balanced visual perception on all surfaces. Automatic lighting controls allows various levels: 95% full output for all systems from dusk to 9pm; 50% reduced density at the floor from 9pm to dawn; and 50% reduced density at core wall from midnight until dawn. This approach allows maximum energy savings, while maintaining safety and security.

## **ACKNOWLEDGEMENTS**

Design Architect: KPF, New York, USA

This work is accomplished by collaboration of BPI New York and BPI Shenzhen.

Design Team: Chou Lien, Robert Prouse, Eunjeong Wang (BPI New York)

Chiming Lin, Dandan Lin, Weina Lv, Zixuan Weng, Zefeng Lin (BPI Shenzhen)

This author worked at BPI New York as a director until July 2022 and currently is attending at BPI Studios Korea as a director in project bases.

Corresponding Author Name: Eunjeong Wang

Affiliation: BPI (Brandston Partnership Inc.) Studios Korea

e-mail: [Julie.wang@bpi.co](mailto:Julie.wang@bpi.co) / [julie.ej.wang@gmail.com](mailto:julie.ej.wang@gmail.com)



The 14<sup>th</sup> Asia Lighting Conference

# Innovation of Lighting

August 17-18, 2023  
The University of Tokyo  
Tokyo, Japan

## Poster Session



Asia Lighting Conference



中国照明学会

CHINA ILLUMINATING ENGINEERING SOCIETY



一般社団法人 照明学会

THE ILLUMINATING ENGINEERING INSTITUTE OF JAPAN



대한민국 조명·전기설비학회

THE KOREAN INSTITUTE OF ILLUMINATING AND ELECTRICAL INSTALLATION ENGINEERS



ALC Web Page



# THE APPROPRIATE LIGHTING TECHNIQUES CONSIDERING DAILY ACTIVITIES IN WORKING ENVIRONMENT

Ayano Nakamura<sup>1</sup>, Jaeyoung Heo<sup>1</sup>, Youko Inoue<sup>2</sup>

Nara Women's University<sup>1</sup>, The Open University of Japan<sup>2</sup>

## ABSTRACT

This study introduces a lighting method suitable for daily activities involving visual work and reports the evaluation results of subjects performing visual tasks. In addition, the results are compared with previous studies that are only imagined without doing the tasks.

Three visual tasks are experimented with typing on a PC, watching videos on a smartphone, and reading magazines. The lighting condition is six combinations of illuminance (50lx, 220lx, 700lx) and correlated color temperature (3000K, 5300K). The subjects evaluated 22 items related to illumination, ambiance, and workability using the 7-step semantic differential method.

Evaluation results are considered by evaluation items that are classified based on factor analysis. The propriety of each lighting condition in this experiment is ascertained using the average evaluation value of all subjects. Appropriate lighting under the conditions of this experiment is shown below. For typing on PC, in the case of 5300K, 220lx, and 700lx, and 700lx at 3000K are desirable. For watching videos on the smartphone, there is no problem with visibility under any lighting conditions in this experiment. However, 220lx and 700lx are desirable to enhance concentration regardless of the correlated color temperature. For reading magazines, 220lx and 700lx are desirable. Furthermore, 3000K is effective for impressing unobtrusive lighting while working and avoiding glare.

The imagined evaluation of reading newspapers in previous studies is compared to the actual evaluation of reading magazines in this study. The difference in results between newspapers and magazines is not the effect of the evaluation method. Unlike newspapers, magazines have many color pages, so it is conceivable that bright and colored lighting will make the colors look more vivid.

Keywords: lighting plan, daily activities, working environment, workability, lighting evaluation

## 1. INTRODUCTION

In recent years, as indoor time has increased due to the COVID-19 epidemic, there is a greater need to enhance the indoor environment. In addition, work styles are becoming more diverse, such as telecommuting and teleworking. This requires that the house not only function as a place to relax and enjoy life, but also have an environment that can accommodate a variety of tasks.

The lighting environment has a significant visual impact on visibility, atmosphere, and other aspects of work. Therefore, the purpose of this study is to clarify the lighting method suitable for the visual tasks among the daily activities.

Some studies have been conducted on daily activities and lighting using real spaces and models, but there are only a few in which subjects performed daily activities. This study reports the evaluation results of subjects performing visual tasks. Furthermore, the results are compared with previous study that only imagined without doing the tasks.

In addition, Internet usage time is increasing every year, so it is necessary to plan the proper lighting for using electronic equipment. However, there is insufficient documentation on these issues, electronic work is also considered.

## 2. EXPERIMENTAL ENVIRONMENT

### 2.1 SELECTION OF DAILY ACTIVITIES

In this study, reading newspapers was selected as a common item from previous studies. The magazine was changed to a magazine consisting of text and photographs, similar to a newspaper. This is to consider familiarity with young people and to verify the impact on color vision (color vibrancy).

Table 1 shows the results of the brainstorming session “How to spend your free time at home?” by five students at our university. Other daily activities were determined based on the highest number of responses. The total number of responses was 96. Excluding those difficult to perform in the laboratory, such as eating and drinking activities and household tasks, the number of responses was 43. Smartphone operation and PC operation, which had the highest number of responses out of 43 responses, were selected.

Table 1. The results of the brainstorming

Table 1: The results of the brainstorming					
Grand total				96	
Housework / Relaxation	Equipment (makeup・change of clothes etc.)	8	Work	Smartphone operation (SNS・game・telephone)	15
	Bathing (dry hair・skin care and facewash)	8		PC operation (typing work・game・watch movies)	7
	Meal・Tea break	7		Listen to music	5
	Cleaning・Housekeeping	6		Reading (include magazines, comics)	4
	Sleep・Rest	5		Study (writing study・reading study)	3
	Cooking	4		Watch television	3
	Do the laundry (wash・dry・fold)	4		Others (puzzle・drawing etc.)	6
	Exercise・Stretch・Massage	4		Total	43
	Dishwashing	2			
	Go to the lavatory	2			
	Others (enjoy with family and the pet etc.)	3			
	Total		53		

### 2.2 WORK CONTENTS

Table 2 shows the lighting conditions and daily activities in this experiment.

The PC device was a MacBook Pro (13-inch, 2018) and typing was performed for 1 minute using educational materials. The viewing distance to the screen was kept at about 40 cm, and the display angle was unified at 117 degrees. This angle was determined based on the average angle of 40 students at the university when using the PC. The luminance ratio between a near field of view and screen luminance was set to be within 1:3. The luminance ratio between a wide field of view and screen luminance was set to be within 1:10. These settings were determined from “the VDT (Visual Display Terminals) guidelines” to prevent glare in all lighting conditions.

The smartphone device was an iPhone SE (4.7-inch, 2020). The videos were the official PV of Nara Women’s University, edited into three videos of 1 or 1.5 minutes and played randomly. The brightness auto-adjustment was turned off and iPhone’s brightness setting was set to the median. The luminance ratio between a near field of view and screen luminance was set to be within 1:3 at 50lx and 220lx, and within 1:6 at 700lx, which was acceptable. The luminance ratio between a wide field of view and screen luminance was set to be within 1:7. Therefore, there is no problem with glare on the screen itself for video viewing.

The magazine was Casa Brutus Monthly (2018, vol.222, SEPTEMBER). About 30 pages that did not have a significant difference in the ratio of photos to text were selected. The reason for this is to minimize the difference in impression from different pages viewed. The bookstand was used for angle uniformity and fixed at 120 degrees to avoid reflection glare.

Table 2. Experimental condition

Illuminance	50lx, 220lx, 700lx
Color temperature	3000K (electric bulb color), 5300K (daytime white color)
Daily activity	Typing on PC, watching videos on a smartphone, Reading magazines

## 2.3 EXPERIMENTAL METHOD

The experimental location is Nara Women's University, building E, 4<sup>th</sup> floor laboratory (E413). The experiment was scheduled for October 20<sup>th</sup> – November 4<sup>th</sup>, 2022. Figure 1 shows a plan of the laboratory, W3.5m×D3.6m ×H2.4m. The interior is entirely white to eliminate non-lighting influences, and the lighting fixture is general diffusion LED ceiling lights. Subjects were 18 young people (21-23 years old) with normal color vision and were all females to eliminate gender factors.

Picture 1 shows the experiment in each daily activity. To eliminate the influence of clothing color and material, subjects were asked to wear white coats. The lighting fixtures are suspended from the ceiling to ensure sufficient illumination of the desk surface.

Figure 2 shows the experimental procedure. During acclimatization, subjects were instructed to look at the center of the desk surface where the illuminance was closest to the set value. The experiment lasted approximately 2 hours per person, with three time periods: 10:00-12:00, 13:00-15:00, and 15:30-17:30. The lighting conditions were changed for each activity, and a break of 3-5 minutes was taken before changing the activity to avoid the fatigue of the subjects.

Figure 3 shows an example of an evaluation item. The subjects evaluated 22 evaluation items related to illumination, ambiance, and workability using the 7-step semantic differential method. However, the evaluation of the lighting was done twice, once before and once after the work to confirm if there were any changes.

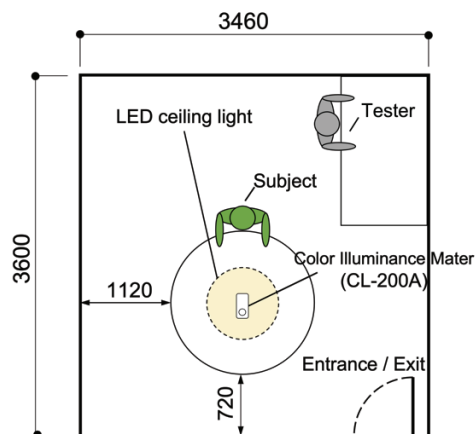


Figure 1. Floor Plan

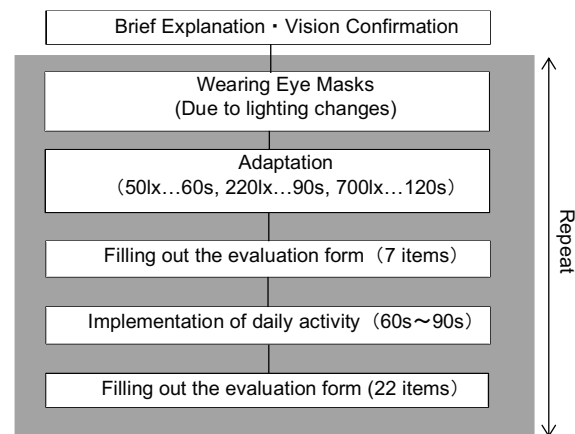


Figure 2. Experimental procedure



Picture 1. State of experiment in each daily activity

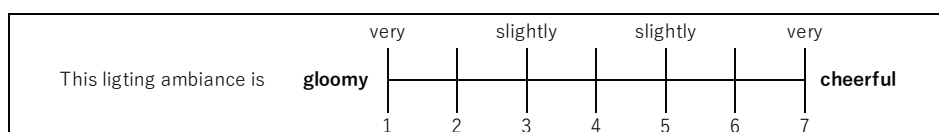


Figure 3. An example of evaluation items

### 3. RESULT AND DISCUSSION

Evaluation results are considered by evaluation items that are classified based on factor analysis (Principal Axis Factoring, Promax rotation). The propriety of each lighting condition in this experiment is ascertained using the average evaluation value of all subjects.

#### 3.1 ILLUMINATION AND ATOMOSPHERE

Table 3 shows the evaluation items and the results of the factor analysis for illumination light. The first factor is "comfortableness" and the second factor is "brightness".

Figure 4 shows the results of impression evaluation for illumination light. The "brightness" is rated high at 220lx, 700lx in 3000K. The difference in evaluation between 220lx, 700lx and 50lx does not depend on correlated color temperature. The second factor, "not dazzling - dazzling," indicates that 5300 K are more likely to glare at the same illuminance. The "bright – dark" is determined by illuminance, and there is no interaction between illuminance and color temperature.

Table 4 shows the evaluation items and factor analysis results for lighting ambiance. The first factor is "relaxation", the second factor is "liveliness", and the third factor is "visual temperature".

Figure 5 shows the results of impression evaluation for lighting ambiance. The "relaxation" is highly rated at 220 lx and 700 lx in 3000 K. There is no difference in the ratings for these two conditions. The "familiar - unfamiliar" 700lx/5300K is comparable to the 3000K 220lx, 700lx. The "(relaxing - distracted" and "natural - artificial" were largely influenced by color temperature and less by illuminance. The two items of the second factor were rated higher with higher illumination, suggesting that illumination is important for activeness. The third factor, "visual temperature", is rated differently based on color temperature. The difference between the highest and lowest ratings for each item is about 3-4. Thus, it can be confirmed that lighting has a significant impact on the ambiance.

Table 3. The evaluation items and factor analysis results for illumination light

Evaluation items	First factor (comfortableness)	Second factor (brightness)
This lighting environment is (comfortable—uncomfortable).	0.96	-0.07
This lighting environment is (pleasant—unpleasant).	0.92	-0.12
This lighting environment is (not tired—tired).	0.89	-0.29
This lighting color is (permissible—impermissible).	0.82	0.09
This lighting brightness is (permissible—impermissible).	0.73	0.22
This lighting environment is (not dazzling—dazzling).	0.27	-0.71
This lighting environment is (bright—dark).	0.44	0.68

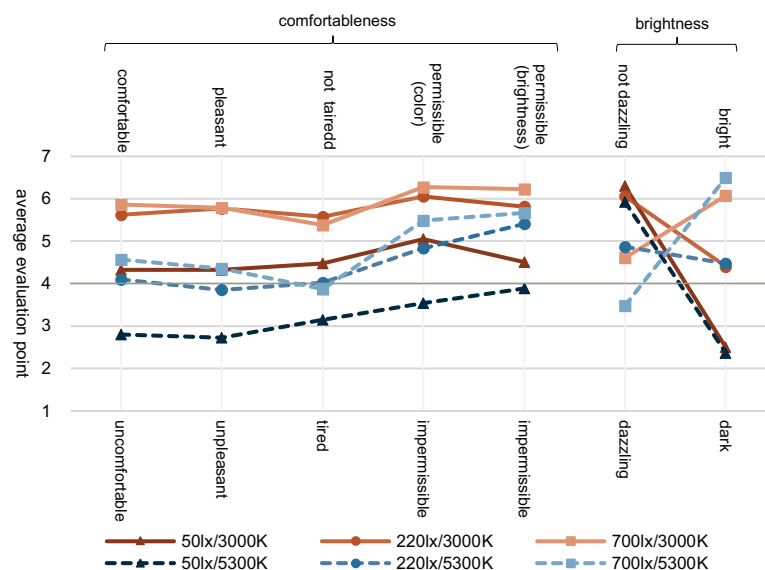


Figure 4. The results of impression evaluation for illumination light

Table 4. The evaluation items and factor analysis results for lighting ambience

Evaluation items	First factor (relaxation)	Second factor (liveliness)	Third factor (visual temperature)
This lighting ambience is (familiar—unfamiliar).	0.92	0.07	-0.13
This lighting ambience is (relaxing—distracted).	0.83	-0.21	0.18
This lighting ambience is (relieved—uneasy).	0.82	0.17	0.01
This lighting ambience is (natural—artificial).	0.56	-0.11	0.36
This lighting ambience is (active—restful).	-0.10	0.82	-0.20
This lighting ambience is (cheerful—gloomy).	0.20	0.74	0.27
This lighting ambience is (warm—cool).	0.08	-0.06	0.92

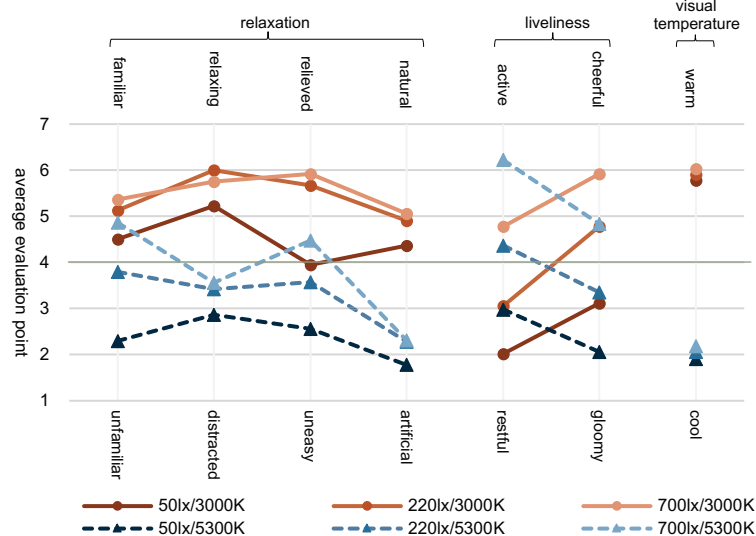


Figure 5. The results of impression evaluation for lighting ambience

### 3.2 WORKABILITY

Table 5 shows the evaluation items and factor analysis results for workability. The first factor is "concentration", the second factor is "visibility", and the third factor is "glare".

Typing: Figure 6 shows the results of impression evaluation for typing on PC. Overall, 700lx/5300K lighting is the highest rated. This is thought to be because 5300K is closer to the luminous color of the screen. A possible reason for this is that 5300 K is closer to the luminous color of the display. The "concentration" is highly rated at 220lx, 700lx and 700lx/3000K in 5300K, but the rating drops significantly at 50lx/5300K. The "visibility" is rated differently for each illuminance at 5300 K. It can be said that the effect of illuminance is more significant at 5300 K. The "glare" does not differ at any illuminance at 5300 K, but is affected by illuminance at 3000 K.

Watching videos: Figure 7 shows impression evaluation for watching videos on smartphones. The three items on the left, except for the first factor, "do not care - care," are highly rated regardless of color temperature, with no significant difference in evaluation at 220lx and 700lx. The "visibility" has an average rating score of 4.0 or higher for all lighting conditions. Therefore, in the case of video viewing, the effect of lighting on visibility is smaller than in other activities. In particular, there was almost no difference in "vivid - colorless". One possible reason for this is that, unlike typing, screens of various colors change one after another, making it difficult to recognize differences in color tones for each illumination. The "glare" shows little effect of color temperature, and the evaluation is divided by illuminance.

Reading magazines: Figure 8 shows the results of impression evaluation for reading magazines. Compared to typing and video viewing, lighting conditions affected magazine reading more. 700lx/3000K was the highest rated in each category. The left three items of the first factor have a marked difference in evaluation between 220lx, 700lx and 50lx lighting, regardless of color temperature. The "do not care - care" is especially highly rated at 220lx and 700lx in 3000K.



Therefore, in terms of concentration, it is desirable to maintain an illumination level of 220 lx or higher. 3000K is rated higher for "vivid - colorless" at the same illumination level. The "glare" at 5300 K is evaluated in accordance with physical quantities, while at 3000 K there is no difference in illuminance.

Table 5. The evaluation items and factor analysis results for workability

Evaluation items	First factor (concentration)	Second factor (visibility)	Third factor (glare)
Working under this lighting is (efficient—inefficient).	0.94	-0.12	-0.31
Working under this lighting is (suitable—unsuitable).	0.92	0.04	0.10
This lighting is (easy—difficult) to work.	0.88	0.08	0.02
You (do not care—care) about this lighting during work.	0.71	0.03	-0.10
The object can be seen (clear—vague).	0.02	0.89	-0.03
The object can be seen (vivid—colorless).	-0.51	0.73	0.05
The object can be seen (easily—difficultly).	0.48	0.50	-0.10
The object is (not dazzling—dazzling).	-0.02	0.01	0.92

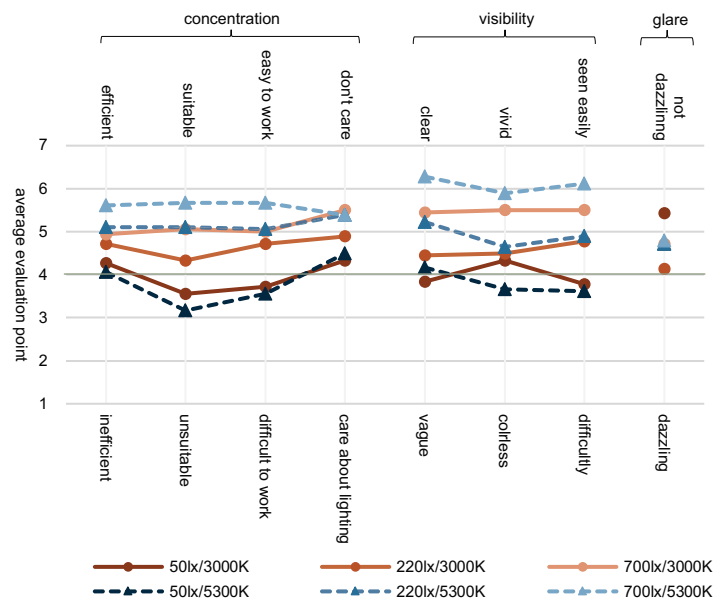


Figure 6. Typing on PC

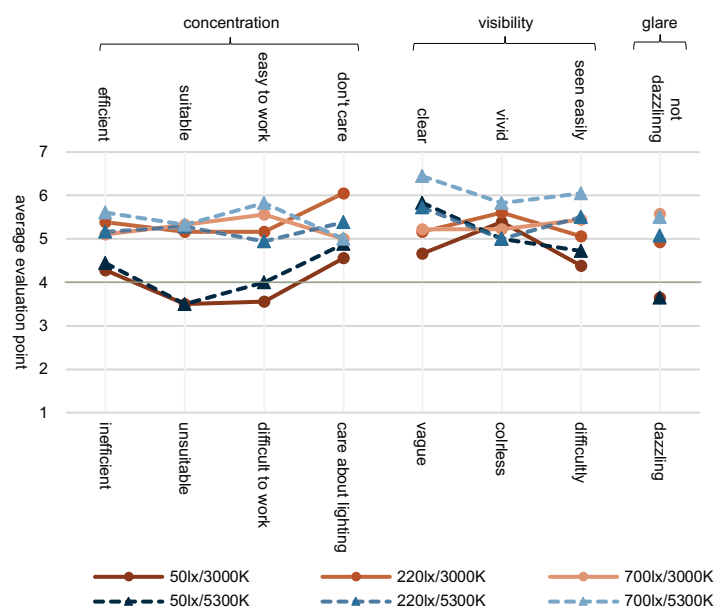


Figure 7. Watching videos on a smartphone

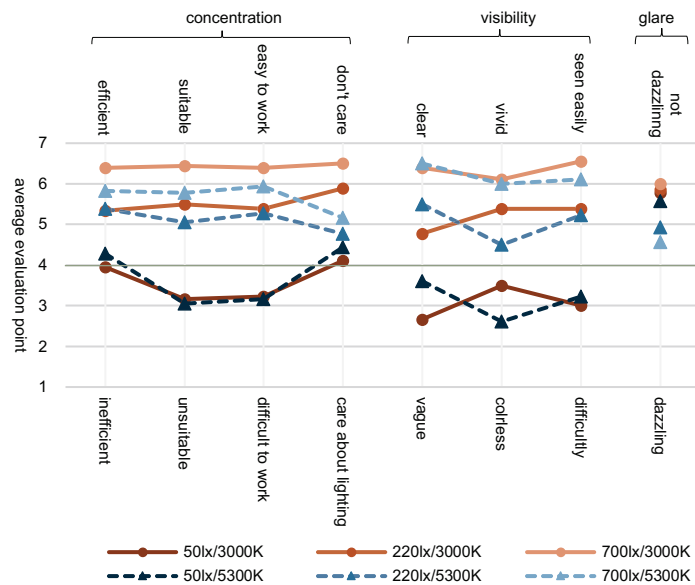


Figure 8. Reading magazines

#### 4. COMPARISON WITH PREVIOUS RESEARCH

The imagined evaluation of reading newspapers in previous studies is compared to the actual evaluation of reading magazines in this study.

Figure 9 shows an appropriate ratio of newspaper and magazine for young people. An appropriate ratio is the percentage of respondents who said the lighting conditions presented were suitable for the task.

Common to both tasks, the appropriate ratio increases as the illuminance increase. For newspapers, the correlated color temperature becomes higher; the appropriate ratio becomes higher too. Magazines have a highly appropriate ratio for both correlated color temperatures, with 3000K tending to be slightly higher. The difference in results between newspapers and magazines is not the effect of the evaluation method. Unlike newspapers, magazines have many color pages, so it is conceivable that bright and colored lighting will make the colors look more vivid. The results for the elderly in previous studies are similar to the present results.

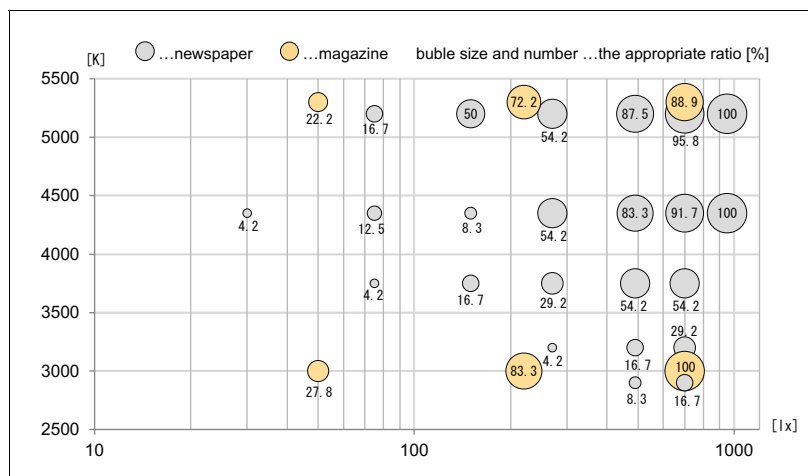


Figure 9. Appropriate ratio of newspaper and magazine (young people)

## 5. CONCLUSION

Through this experiment, it was confirmed that lighting changes the impression and ambiance, and that the appropriate lighting is different for each daily activity. Appropriate lighting under the conditions of this experiment is shown below.

From the evaluation results related to illumination and ambiance, Comfort and relaxation can be felt in the case of 3000K, 200lx, and 700lx. 5300K is more dazzling than 3000K, even with the same levels of illuminance. In addition, it is effective to increase illuminance to enhance activity.

The workability results indicate lighting conditions that don't interfere with work. For typing on PC, in the case of 5300K, 220lx, and 700lx, and 700lx at 3000K are desirable. For watching videos on the smartphone, there is no problem with visibility under any lighting conditions in this experiment. However, 220lx and 700lx regardless of the correlated color temperature are desirable to enhance concentration. For reading magazines, 220lx and 700lx are desirable. Furthermore, 3000K is effective for impressing unobtrusive lighting while working and avoiding glare.

## 6. FUTURE DEVELOPMENTS

In this experiment, three types of daily activities were evaluated. It is hoped that further studies will be conducted on various daily activities. In addition, it is necessary to conduct demonstration tests in an environment closer to real life, considering differences in age, lighting methods, and interior design. Further comparison of these results with those of previous studies will continue.

The ultimate goal is to create lighting systems appropriate for different situations, such as age, gender, and tasks. Further data collection is needed to achieve this goal.

## REFERENCES

- [1] Study on Lighting in Consideration of Age and Life Activities in Living Space -Suitable illuminance and CCT on steady adaptation state-, Yuki Oe, Youko Inoue and Mizuki Tango, Proceedings of the Architectural Institute of Japan, Vol.85, No. 776, pp. 725-732, 2020.10
- [2] Study on Required Brightness and Apparent Color for a Life Activity -Comparison between the young and the elderly-, Yuki Oe, Youko Inoue and Mizuki Tango, Proceedings of the Architectural Institute of Japan, Vol.86, No. 779, pp. 35-42, 2021.1
- [3] The Preference of The Indoor Illuminance and Color Temperature: Scale Model Experiment Assuming Daily Activity, Naoyuki Oi, Madoka Kasao, Hironobu Takahashi, Proceedings of the Architectural Institute of Japan, Vol.72, No. 614, pp. 87-92, 2007.4
- [4] Ministry of Internal Affairs and Communications, "Survey on Information and Communications Media Usage Time and Information Behaviour in2021. [https://www.soumu.go.jp/main\\_content/000831290.pdf](https://www.soumu.go.jp/main_content/000831290.pdf)
- [5] Manavision Free Typing Practice (Japanese version) <https://manabi-gakushu.benesse.ne.jp/gakushu/typing/nihongonyuryoku.html>
- [6] Ministry of Health, Labor and Welfare, "Guidelines for Occupational Health Management in Information Equipment Work" <https://www.mhlw.go.jp/content/000539604.pdf>
- [7] Nara Women's University Promotional Video <https://www.youtube.com/watch?v=x1SYzygfkOA>

## ACKNOWLEDGEMENTS

This work was supported by JSPS KAKENHI Grant Number JP21K02108. I would also like to thank everyone who willingly accepted our subjects.

Corresponding Author Name: Jaeyoung Heo  
Affiliation: Nara Women's University  
e-mail: heo@cc.nara-wu.ac.jp

# **STUDY ON OUTDOOR URBAN FARMING PLANTERS THROUGH DAYLIGHT SIMULATIONS: A FULL-SCALE EXPERIMENT IN SINGAPORE**

Chew Beng SOH, R HARIDARSHAN, Szu-Cheng CHIEN, Hui AN, Arijit SAHA, Mei Ting TEOH  
(Engineering Cluster, Singapore Institute of Technology, Singapore)

## **ABSTRACT**

The objective of this study was to examine the practicality and efficacy of utilizing a planter for outdoor urban farming at the Singapore Institute of Technology. The research encompassed various stages, commencing with an exploration of the optimal Photosynthetic Photon Flux Density (PPFD) and Daily Light Integral (DLI) values suitable for cultivating Asian greens. Subsequently, a comprehensive model of the urban farming structure and planter was generated using Revit and Rhino software.

To evaluate the planter's performance in an outdoor setting, daylight simulations were carried out utilizing ClimateStudio. These simulations were conducted during a period of clear sky conditions spanning from 28th March to 13th April, considering the material characteristics of the actual structure and planter. The chosen materials for both the outdoor structure and planter closely mirrored those employed in real-world scenarios. Through the analysis of the outcomes derived from the daylight simulations, this study assessed the feasibility and effectiveness of employing the planter for outdoor urban farming.

Keywords: Outdoor urban farming, Daylight simulation, PPFD and DLI, Singapore

## **1 INTRODUCTION**

One of the main drawbacks of Singapore's reputation as one of the world's smallest nations is the lack of available land. Unlike nations like the United States of America, Singapore was forced by a shortage of space to support housing with high-rise residential complexes. Furthermore, a lack of land might limit the availability of resources, such as the ability to cultivate food on the mainland. Singapore imports 90% of its freshly produced food from other countries. This illustrates the loss of independence that Singapore has experienced in the year 2020, when Covid-19 emerged and afflicted everyone in the entire world. In Singapore's situation, the inability to grow food locally has an economic impact because foreign manufacturers cannot deliver their fresh produce here.

According to Singapore Agro-Food Enterprises Federation Limited (SAFEF), Singapore's government has made the decision to establish a "30 by 30" vision that intends to generate 30% of the country's nutritional needs locally by 2030 in order to reduce the likelihood of food shortages [1]. By attaining this objective, Singapore can become more self-sufficient and ready in the event of future food shortages. To do this, however, it will be necessary to implement new innovative farming techniques in Singapore in order to address the country's land scarcity problem where one such solution would be the use of urban farming.

Due to its lack of available land, Singapore is intensively exploring urban farming as a means of increasing domestic food production and lowering its reliance on imports. Adequate sunlight is crucial for agricultural practices, as it directly impacts the growth and development of crops, including Asian greens. The presence of a sufficient amount of daylight is essential to ensure optimal conditions for successful crop growth. The design of the planters plays a key role in how much sunlight is being received by the crops therefore evaluation of the planter design needs to be conducted through simulations to evaluate the effectiveness of the planter design.

## 2 PAR, PPFD AND DLI

### 2.1 PAR

Unlike feet, inches, and kilos, PAR (Photosynthetically Active Radiation) is not a measurement. Instead, it identifies the kind of light on the light spectrum that encourages photosynthesis in plants. Plants employ photosynthesis to transform light energy into chemical energy, which serves as their food source and fuel for growth. Chlorophyll a and b are the major pigments that react with light in plants. Typically, the 400–700 nm wavelength range is used for PAR analysis [2, 3]. The light levels in greenhouses were formerly always indicated in lux. Human eyes normally respond to white light, hence lux or lumens is a measure of how much light is perceived by them. The S, M, and L receptors in our eyes are three light-receptors that mostly respond to blue, green, and yellow light. The representation of light levels of LED grow lights in lux is not applicable anymore since blue and red-light photons are the most effective for producing chlorophyll in plants. As a result, the new unit of measurement, which covers all light photons with wavelengths between 400 and 700 nm, is represented in micromoles per meter per second ( $\mu\text{Mol/m/s}$ ) [2].

### 2.2 PPFD

Photosynthetic photon flux (PPF) measures the amount of photosynthetically active radiation (PAR) produced by a lighting system per second. PPF determines the precise light available for plant photosynthesis, crucial for optimal growth conditions. Photosynthetic photon flux density (PPFD) combines PPF and surface area, measuring the number of PAR photons landing on a specific area in micromoles per square meter per second ( $\mu\text{Mol/m}^2/\text{s}$ ). PPFD reflects the quantity and effectiveness of photosynthetic photons reaching the growth area and the lighting system's performance [4]. In a study by Alahakoon in Singapore, Asian greens exhibited up to five times more growth when exposed to a PPFD of  $500\mu\text{Mol/m}^2/\text{s}$  compared to  $300\mu\text{Mol/m}^2/\text{s}$ . These higher PPFD levels also resulted in thicker leaves and larger leaf area [5]. Simulating light conditions involves obtaining illuminance, measured in lux, which can be converted to PPFD using a calibration factor of 0.0185 for sunlight [6].

### 2.3 DLI

The entire amount of light provided to a plant each day is gauged by the Daily Light Integral (DLI). The total number of photons that are absorbed by plants and algae daily is measured cumulatively by DLI. The DLI, which is measured in "moles" of photons per square meter per day in the Par region, is given as  $\text{mol/m}^2\cdot\text{per day}$ . The average DLI for Asian greens like Chinese kale and cabbage varies from 14 to  $16\text{mol/m}^2\cdot\text{per day}$  [7].

## 3 CLIMATIC CONDITIONS

Located at 1 degree north of the equator, Singapore falls under the classification of a tropical rainforest climate (Af) according to the Koppen climate classification system. Singapore experiences two distinct monsoon seasons with periods of inter-monsoonal weather in between. The Southwest Monsoon spans from June to September, whereas the Northeast Monsoon occurs from late December to early March [8].

### 3.1 DURATION OF SUNLIGHT

The duration of direct sun irradiance of at least  $120\text{ Watts/m}^2$  in an area is referred to as sunshine duration. Due to its close proximity to the equator, Singapore experiences relatively constant day length and sunshine duration throughout the year. The amount of sunshine received each day is largely influenced by cloud cover. During the wettest months, the duration of sunshine lasts around four to five hours, whereas during the driest months, it lasts around eight to nine hours. The months of February and March observe the highest number of sunshine hours, while the months of November and December observe the lowest number of sunshine hours [8].

During the June solstice, the sun rises at around 6:57 am at an azimuth of  $67^\circ$  and sets at approximately 7:12 pm at an azimuth of  $292^\circ$ . At solar noon, the altitude of the sun is  $63^\circ$  while the azimuth is at  $34^\circ$ . Similarly, during the December solstice, the sun rises at 7:01 am at an azimuth of  $113^\circ$  and sets at 7:04 pm at an azimuth of  $246^\circ$ . The daylight period lasts for approximately 12



hours throughout the whole year [8]. The positioning and alignment of buildings would be influenced by the path of the sun, which would impact the illumination and heating within the interior spaces.

### 3.2 CLOUD CAST

The most commonly observed low-cloud forms in Singapore include cumulus, stratocumulus, and cumulonimbus clouds. On a typical day, cumulus clouds start forming in the mid-morning and tend to increase to about 3-4 oktas (where one okta denotes one-eighth of the sky) by midday. Their bases are typically found at a height of 2,000 feet (0.6 km), while their tops can range from 8,000 to 12,000 ft (2.5-3.5 km). These cumulus clouds have the potential to transform into cumulonimbus clouds in the afternoon and early evening, with their tops reaching between 30,000 and 40,000 ft (9-12 km) in altitude [8].

### 3.3 MICROCLIMATIC CONDITIONS OF SITE

Figure 1 depicts an aerial view of SIT Dover campus, where the reference site is located. The campus is enveloped by dense clusters of vegetation that can be utilized to mitigate the Urban Heat Island (UHI) effect on and around the campus. The strategic arrangement and abundance of trees can cool the urban environment by providing shade and facilitating evapotranspiration. The temperature of unshaded surfaces can be 11-25°C higher than that of shaded surfaces [9]. Evapotranspiration can lower peak summer temperatures by 1-5°C either alone or in combination with shading [9]. Moreover, as observed in Figure 1, the majority of the SIT Dover campus does not have many high-rise buildings or infrastructure except for around three. Most of the high-rise buildings are located in the north, thus the sunlight exposure would not be significantly affected as the sun moves from east to west.

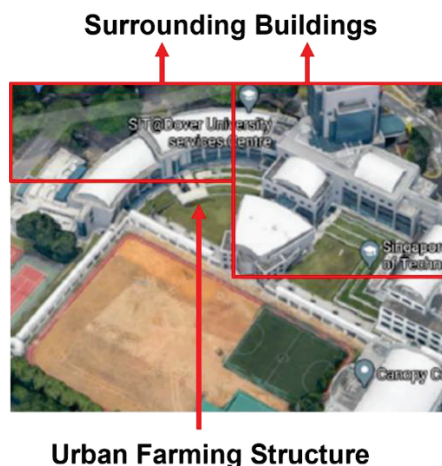


Figure 1. Masses of the Buildings around SIT Dover Campus

## 4 METHODOLOGY

Revit 2020 and Rhino 7 software were used to build the surrounding façade and outdoor urban farming structure. The façade orientation would follow the outdoor urban farming structure in SIT University Student Centre (USC) which takes into account the surrounding buildings structure (see Figure 2). Thus, when the simulations were conducted in ClimateStudio, the shadows overcasted by these buildings would be taken into consideration by the software. The urban farming structure contained three planters where daylight simulations will be run to determine the lux levels received by the planters throughout the day (see Figure 3).

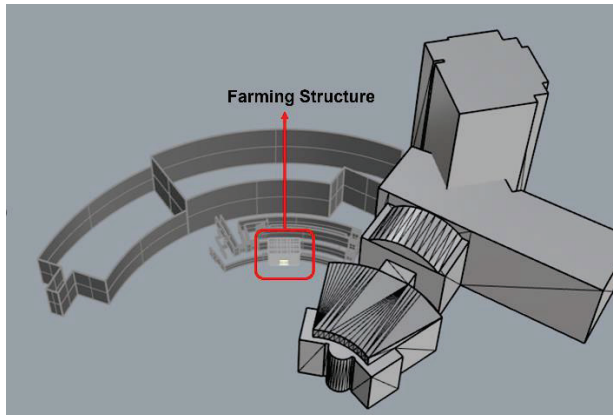


Figure 2. Site Layout of SIT USC



Figure 3. Urban Farming Structure

The urban farming structure had dimensions of 6050 mm in height, 4400 mm in width and 7800 mm in length while the planter had dimensions of 500 mm in height, 500mm in width and 2000 mm in length (see Figure 4-5).

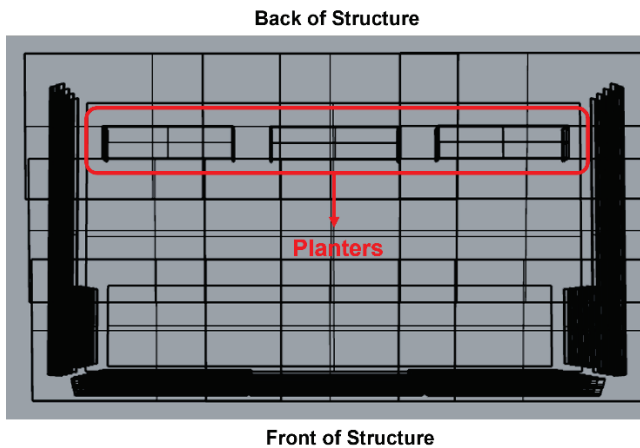


Figure 4. Top View of Structure

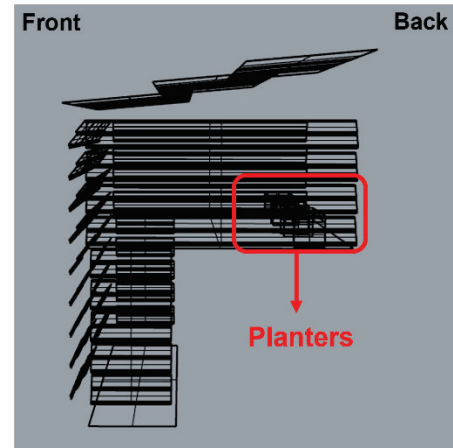


Figure 5. Side View of Structure

The material of the envelope of the structure was made of clear polycarbonate with a visible light transmission (Tvis) value of 90% while the planter was made from white plastic with a Tvis value of 0%. Due to the limitations of ClimateStudio in creating customized material specifications, a material that closely resembles the actual Tvis was chosen. The simulations were carried out based on the following parameters in Table 1 below.

Table 1. Simulation Parameters

Material of Urban Farming Structure	Starphire (Tvis 91%)
Material of Planter	White Plastic Chair (Tvis 0%)
Sky Conditions	Clear Sky
Simulations Dates	Alternate Days from 28 <sup>th</sup> March to 13 <sup>th</sup> April
Simulation Time	8am to 6pm

Sensors were placed on the left and right of each of the planters to derive the lux levels throughout the day (see Figure 6). With the derived lux values, the PPFD and DLI could be calculated based on the following formulas:

$$1\text{PPFD} = \text{Lux} \times 0.0185 \quad (1)$$

$$\text{DLI} = \text{PPFD} \times \text{Light Hours per day} \times \frac{3600}{1,000,000} \quad (2)$$

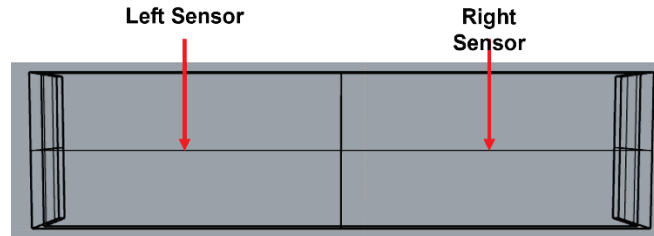


Figure 6. Sensor Placement on a Planter

## 5 RESULTS AND DISCUSSION

The PPFD and DLI values remain consistent across the left, middle, and right planters throughout the simulation period as shown in Figure 7, 8, and 9. Amongst these three planters, the highest recorded PPFD value was  $1540 \mu\text{Mol}/\text{m}^2/\text{s}$  at 1300 hrs, while the lowest value was  $30 \mu\text{Mol}/\text{m}^2/\text{s}$  at 0800 hrs. This observation can be explained by the sun's position at 1300 hrs, when the sun is directly overhead, the planters receive the maximum amount of sunlight, whereas at 0800hrs, when the sun is just beginning to rise, the amount of sunlight available is minimal. On the 3rd of April, the right and left planters experienced the highest DLI values, reaching  $30 \text{ mol}/\text{m}^2$  per day. Conversely, the lowest recorded DLI value of  $24 \text{ mol}/\text{m}^2$  per day was observed on the 9th of April for the middle planter (see Figure 8).

In general, results in the figures above show the PPFD values for the planters fell within the acceptable range of PPFD for Asian greens, approximately  $200$  to  $300 \mu\text{Mol}/\text{m}^2/\text{s}$ . Similarly, the calculated DLI values also fell within the acceptable DLI range for Asian greens, approximately  $14$  to  $16 \text{ mol}/\text{m}^2$  per day (see Figure10).

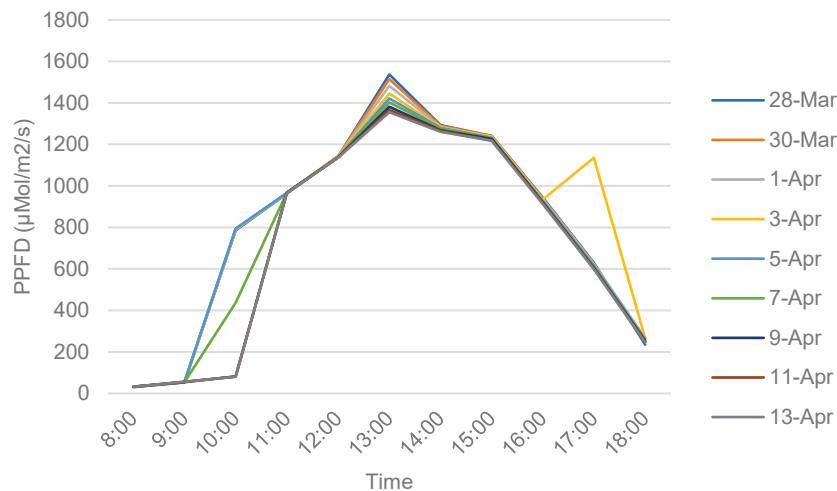


Figure 7. PPFD Results of Left Planter

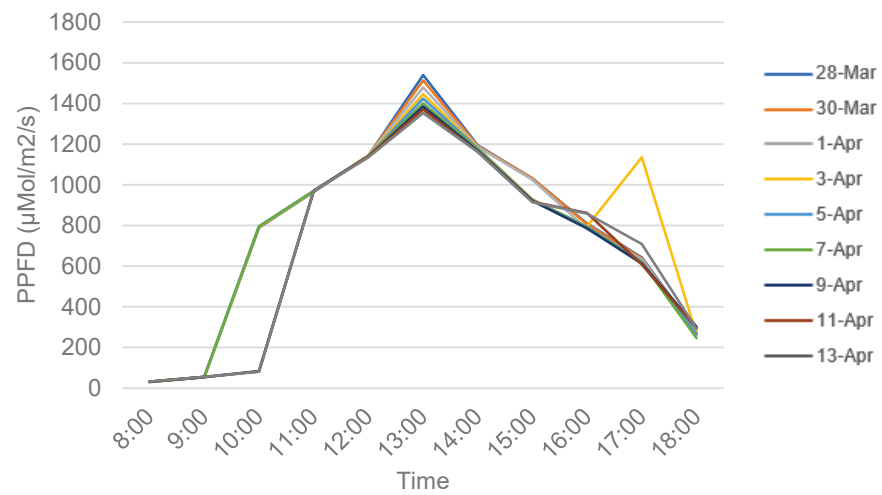


Figure 8. PPFD Results of Middle Planter

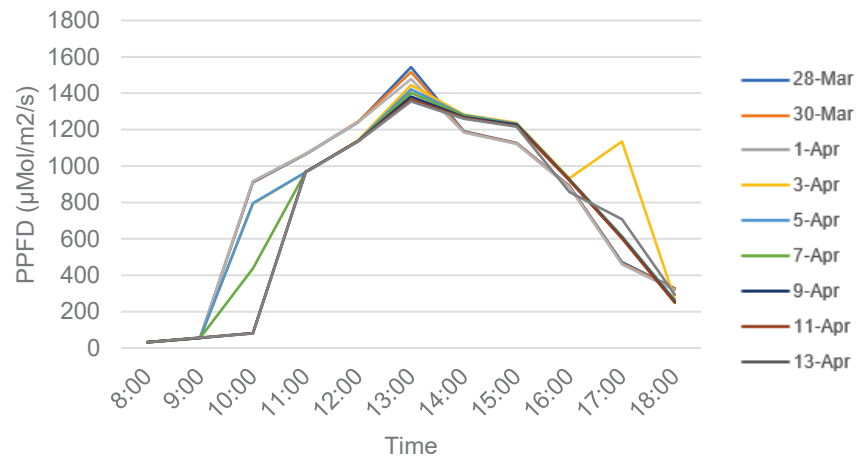


Figure 9. PPFD Results of Right Planter

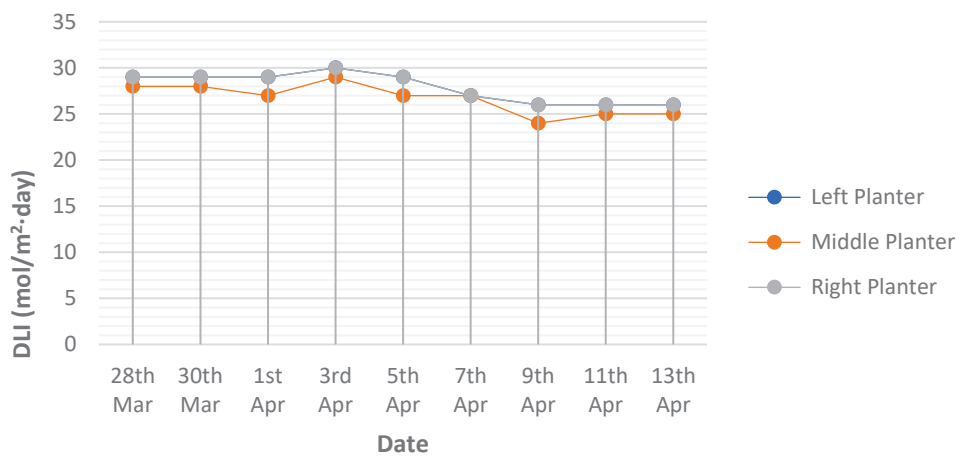


Figure 10. DLI Results of Planters

## 6 CONCLUSION AND FUTURE WORK

To sum up, the introduction of this type of planters in outdoor urban farming structure on an underutilized land has demonstrated its practicality and effectiveness, offering a potential means to support Singapore's objective of becoming a self-sufficient nation. With limited natural resources, integrating such planters in farms within the country has the capacity to diminish dependence on external exports and enhance self-sustainability. Nonetheless, it is important to note that simulation data may deviate from the actual data. Therefore, in order to validate the accuracy of the simulation data, it is necessary to measure the actual lux levels and derive the PPFD and DLI values and compare them with the simulated results to determine the viability of such planters in outdoor urban farming.

## REFERENCES

- [1] SAFEF, "How will COVID-19 impact Singapore's food security?" *Singapore Agro-Food Enterprises Federation Limited*. [Online]. Available: <https://safef.org.sg/blog/how-will-covid-19-impact-singapores-food-security/>.
- [2] "MechaTronix - PAR, PPF, YPF, PPFD and DLI," *Horti-growlight.com*. [Online]. Available: <https://www.horti-growlight.com/en-gb/par-ppf-ypf-ppfd-dli>.
- [3] "What are PAR, PPF and PPFD, and why should you care?" *Light Science Technologies*, 03-Mar-2021. [Online]. Available: <https://lightsciencetech.com/what-are-par-ppf-and-ppfd-and-why-should-you-care/>.
- [4] "PAR, PPF, PPFD and DLI – telos," *Teloslighting.co.uk*. [Online]. Available: <https://teloslighting.co.uk/par-ppf-ppfd-and-dli/>.
- [5] P. K. D. Alahakoon, "Productivity, photosynthesis and nitrogen metabolism of various leafy vegetables grown aeroponically under different combinations of light-emitting diodes (LEDs)," *NIE Digital Repository*, 2016. [Online]. Available: <https://repository.nie.edu.sg/handle/10497/22434>.
- [6] Apogee Instruments, "Conversion - PPFD to Lux," *Apogee*. [Online]. Available: <https://www.apogeeinstruments.com/conversion-ppfd-to-lux/>.
- [7] K. Liu et al., "Light intensity and photoperiod affect growth and nutritional quality of Brassica microgreens," 2022. [Online]. Available: <https://www.ncbi.nlm.nih.gov/pubmed/35164148>.
- [8] "Climate of Singapore," *Meteorological Service Singapore*. [Online]. Available: <http://www.weather.gov.sg/climate-climate-of-singapore/>.
- [9] O. Us Epa, "Using trees and vegetation to reduce heat islands," *United States Environmental Protection Agency*, 2014. [Online]. Available: <https://www.epa.gov/heat-islands/using-trees-and-vegetation-reduce-heat-islands>.
- [10] LANOUE, J., ST. LOUIS, S., LITTLE, C., & HAO, X. (2022). "Continuous Lighting Can Improve Yield and Reduce Energy Costs While Increasing or Maintaining Nutritional Contents of Microgreens". *FRONTIERS IN PLANT Science*, 13. <https://www.frontiersin.org/articles/10.3389/fpls.2022.983222>

## ACKNOWLEDGEMENTS

This research/project is supported by the Singapore Food Agency, Singapore, under its Singapore Food Story Theme 1 Programme (Award No. SFS\_RND\_SUFP\_001\_09)

Corresponding Author Name: Chew Beng SOH  
Affiliation: Singapore Institute of Technology  
e-mail: [ChewBeng.Soh@SingaporeTech.edu.sg](mailto:ChewBeng.Soh@SingaporeTech.edu.sg)

Corresponding Author Name: Szu-Cheng CHIEN  
Affiliation: Singapore Institute of Technology  
e-mail: [SzuCheng.Chien@Singaporetech.edu.sg](mailto:SzuCheng.Chien@Singaporetech.edu.sg)



# EVIDENCE-BASED RESEARCH AND APPLICATIONS FOR HEALTH LIGHTING DESIGN IN UNIVERSITY CLASSROOMS

Tongyue WANG<sup>1,2</sup>, Rongdi SHAO<sup>2,3</sup>, Yuyan WANG<sup>5</sup>, Guangzhi HU<sup>4</sup>, Luoxi HAO<sup>2,3</sup>

- (1. Shanghai Yangzhi Rehabilitation Hospital (Shanghai Sunshine Rehabilitation Center), School of Medicine, Tongji University, Shanghai 201619, China;
2. School of Architecture and Urban Planning, Tongji University, Shanghai 200092, China;
3. Key Laboratory of Ecology and Energy-saving Study of Dense Habitat (Tongji University), Ministry of Education, Shanghai 200092, China
4. Arcplus Group PLC East China Architectural Design & Research Institute Co.,Ltd
5. School of Architecture, the University of Sheffield, Sheffield S10 2TN, UK)

## ABSTRACT

In order to improve the current situation of classroom lighting, it is necessary to conduct evidence-based research and lighting design according to the existing problems of classroom lighting environment and the needs of students. Before the renovation, light environmental parameters were measured in typical classrooms at night. Interviews and questionnaires were conducted for students who have been using these classrooms for a long time to understand their evaluation and subjective preferences on lighting. Through the design of lighting lamps to improve visual efficiency and adapt to the health needs of teenagers, a new type of classroom lamps with upper and lower light emitting mode is developed, which makes the light distribution in the classroom more reasonable and the illuminance on the desktop significantly improved and more uniform. One year after the renovation of classroom lighting, field measurements and interviews were conducted again. A total of 41 valid questionnaires were collected to reevaluate the subjective satisfaction, sleep and emotional self-evaluation of the light environment in the classroom. The results showed that the students' evaluation of the brightness of the classroom changed from 48.57% slightly dark to 90.24% moderate after the reconstruction, and the illuminance of the working face was significantly improved (the horizontal illuminance of the desktop was 607.4lx). The evaluation of light color changed from 17.14% too cold white and 42.86% slightly cold white to 73.17% moderate. The evaluation of desktop evenness changed from 51.43% relatively unevenness to 7.32% relatively evenness (evenness is 0.9). The overall satisfaction degree of lighting was significantly improved. On the basis of visual function evaluation, the students' sleep and emotional state were evaluated subjectively. The self-evaluation of sleep quality improved overall, while the change of sleep time was not obvious. However, the score of the students' Self-rating depression scale (SDS) was significantly reduced, and the average score was reduced from 34.66 to 29.28, indicating that their depression mood was somewhat relieved. The design of indirect light emitting lamps is conducive to improving the overall visual comfort and uniformity of the desktop. It is not recommended to use lamps with too high color temperature in the classroom and warm white light is more appropriate. Light environment with high illuminance level in the daytime has a positive effect on students' sleep and can relieve their depression.

Keywords: Evidence-based research, Classroom, Integrative lighting, Post-Occupancy Evaluation

## 1. INTRODUCTION

In response to the rising rate of myopia among children and adolescents in China and the trend of younger age, the Ministry of Education and other eight departments jointly issued the "Implementation Plan for Comprehensive Prevention and Control of Myopia among Children and Adolescents", which clearly lists "improving the visual environment in schools" as an important measure for myopia prevention and control [1]. The classroom is the "main site" for the implementation of myopia prevention and control among children and adolescents, and a poor light environment can affect the working condition and development of the visual system of students [2], causing not only instantaneous hazards such as fatigue and cognitive decline, but also long-term cumulative effects such as poor visual acuity, sleep disorders and reduced academic performance [3].

Existing classroom lighting mainly has insufficient illumination, low uniformity and color rendering index, lamp glare, strobe, photobiological hazards, lamp damage and lack of maintenance and other problems [4][5], should be based on meeting the visual efficacy, pay more attention to the effective use of natural

light, reduce glare, choose a reasonable lighting methods and light patterns, balance the visual function [6], psychophysiology [7] and visual health of students and other aspects of demand, improve the quality of the classroom light environment [8][9].

In order to protect the learning needs and physical and mental health of students and improve the classroom lighting environment, the group carried out research-based design of lighting products to improve visual efficacy and adapt to the health needs of adolescents [10], developed classroom lamps with up and down light output methods to make the light distribution in the classroom more reasonable [11], and proposed intelligent control modes that consider teaching activities, rhythmic health, daylight supplementation and climate adaptation [12] [13]. In the process of practical application, the control modes can be selected according to the actual situation and partially combined to meet the needs of students in different aspects such as learning, activities, physical health and mental health. Eventually, the classrooms in the School of Architecture and Urban Planning of Tongji University were renovated in the field to improve students' learning efficiency and visual comfort, improve sleep quality, alleviate negative emotions, and promote students' physical and mental health development.

## 2. UNIVERSITY CLASSROOM LIGHT ENVIRONMENT STATUS STUDY

Through the data measurement of the lighting status of classrooms and lecture halls in Building D of the School of Architecture and Urban Planning of Tongji University (Figure 1), the desktop illuminance values are lower than the lighting standard value requirements, the average classroom uniformity is only 0.5, the average color rendering index is only 74, the color temperature of the lamps is high (close to 7000K), and there are some problems such as lamp glare and individual lamp damage (Table 1), where the color rendering index R9 of the saturated red is far below the requirement of WELL building standard of not less than 50. Among them, the art classroom color rendering index and illuminance value requirements higher than ordinary classrooms [14], we should make full use of natural light with good color rendering, and in order to avoid direct light, it is appropriate to use the north-facing skylight lighting [15]. Artificial lighting should choose a light source with good color rendering, use indirect lighting to realistically represent the shadows of objects, and also locally increase the floodlights as accent lighting [16].



Figure 1 Classroom lighting status at the School of Architecture and Urban Planning, Tongji University

Table 1 Classroom light environment measurement data in Building D (before renovation)

Current Status	Illumination average (Ev)	Color temperature (K)	Average CRI (color rendering index) /Ra	R9	Uniformity
Classroom D306	273.7	6868.9	73.9	-17.8	0.5
Lecture hall of Building D	197.5	6022.9	74.9	-45.5	0.6

On-site interviews and questionnaires were conducted with students before the classroom lighting renovation, 35 valid questionnaires were collected, and it was found that 54.3% of students thought the classroom light environment was too dark, 60.1% thought the classroom light color was cold white, 54.29% wanted yellow-white light but not warm yellow light (only 8.57%), and 51.43% thought the classroom light environment is more uneven. Therefore, there is a need to use lower color temperature lamps and to change the number and arrangement of lamps to improve the illumination and uniformity level of the work surface.

### 3. DESIGN STUDY OF CLASSROOM LIGHTING FIXTURES

Based on the results of the previous research, the group analyzed the behavior patterns and lighting needs of people using the classroom space, and completed a research-based design of lighting products to improve visual efficacy and adapt to the health needs of youth (Figure 2). The new classroom luminaire adopts a streamlined line design, breaking the traditional impression of straight and angular classroom luminaires, with a softer image; it adopts an up-and-down light distribution method, making the classroom light distribution more reasonable and improving students' learning efficiency and visual comfort; through its own shape design and microcrystalline anti-glare surface, it plays an anti-glare role to protect students' eyesight. The luminaire can be loaded with daylight sensing device to adapt to changes in time, weather and seasons, and can dynamically adjust the luminance and color temperature through the control system. In addition, the modular design of the luminaire on the line can be combined and spliced according to the actual situation inside the classroom.

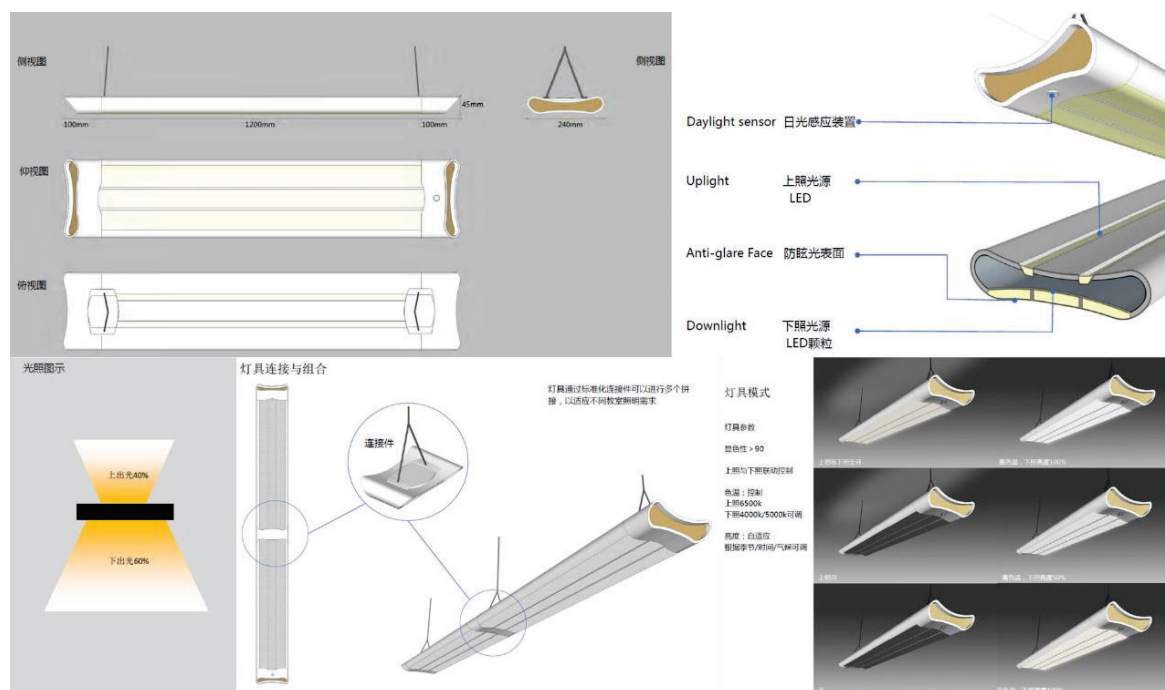


Figure 2 Health lighting lamps design scheme of classroom

Classroom intelligent control system can intelligently control the lighting from the following four aspects to achieve different effects. (1) teaching activities: according to different teaching activities such as class, morning and evening study, projection playback and other different teaching purposes, to set different modes of classroom lighting. (2) Rhythmic health: according to the human body rhythm of the day on the light of different illumination. Color temperature needs to intelligently control lighting. (3) Daylight fill light: according to the different illumination sensed by the induction device, intelligent fill daylight, so that the classroom illumination to maintain uniformity, but also to achieve the effect of energy saving. (4) climate adaptation: according to different seasons, climate and other factors intelligent adjustment of color temperature, illumination, light patterns, etc., not only to meet the requirements of students' visual work, but also to meet the psychological needs of students. In the actual use process, teaching activities + rhythmic demand, climate adaptation + teaching activities, teaching activities + daylight fill light can be integrated with each other.



#### 4. POST-OCCUPANCY EVALUATION (POE) OF NEW CLASSROOM LIGHTING FIXTURES

Based on the current situation of the light environment of the classroom in Building D of the School of Architecture and Urban Planning of Tongji University, the newly developed classroom lighting fixtures were selected for field renovation, with a color temperature of 5000K and an up-and-down light output to improve the uniformity of the illumination of the desktop, taking into account that the classroom in Building D is an art classroom, mainly used by students for drawing and model making, with high requirements for color rendering, the experiment uses a color rendering index of 90 or more lamps. Six months after the completion of the renovation, the classroom light environment was measured and interviewed on site again, and 41 valid questionnaires were collected (Figure 3). The average desktop illuminance of the renovated classroom was significantly improved to 607.4lx, the color temperature was reduced to 5376K, the average color rendering index and the special color rendering index R9 were significantly improved, and the illuminance uniformity of the desktop was significantly improved after adopting the lamps with up and down light output.

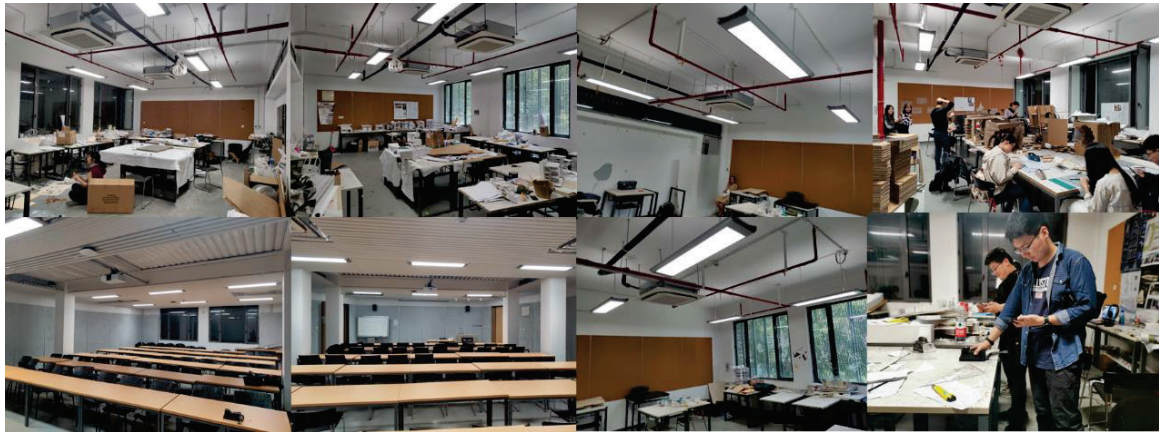


Figure 3 Classroom health lighting fixtures after the renovation of the actual effect and Post-Occupancy Evaluation

Table 2 Classroom light environment measurement data in Building D (after renovation)

Current Status	Illumination average (Ev)	Color temperature (K)	Average CRI (color rendering index) Ra	R9	Uniformity
Classroom D306	607.4	5376.6	93.4	73.5	0.9
Lecture hall of Building D	397.2	4817.1	94.5	80.7	0.7

Table 3 Evaluation of the brightness of the classroom lighting before and after the renovation

Options	Proportion (before renovation)	Proportion (after renovation)
Too dark	5.71%	0%
Slightly dark	48.57%	7.32%
Moderate	40%	90.24%
Slightly bright	5.71%	0%
Too bright	0%	2.44%

Table 4 Evaluation of the classroom lighting colors before and after the renovation

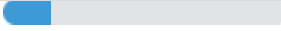
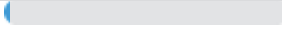
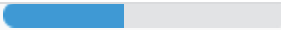
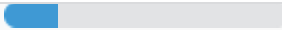
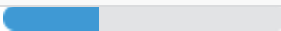

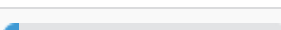
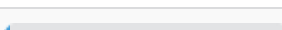
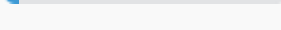
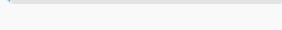
Options	Proportion (before renovation)	Proportion (after renovation)
Too cold white	 17.14%	 2.44%
Slightly cold white	 42.86%	 19.51%
Moderate	 34.29%	 73.17%
Slightly warm yellow	 5.71%	 2.44%
Too warm yellow	 0%	 2.44%

Table 5 Evaluation of the uniformity of classroom lighting before and after the renovation

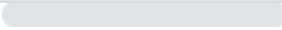
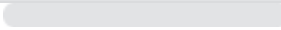

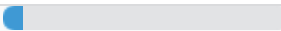
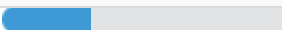
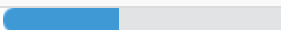
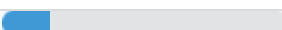
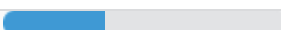
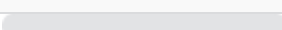
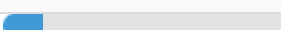
Options	Proportion (before renovation)	Proportion (after renovation)
Very uneven	 0%	 0%
More uneven	 51.43%	 7.32%
Moderate	 31.43%	 41.46%
More uniform	 17.14%	 36.59%
Very uniform	 0%	 14.63%

Table 6 Overall satisfaction level of classroom lighting before and after the renovation



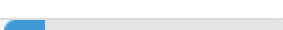
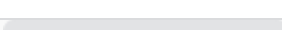
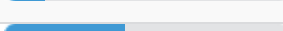
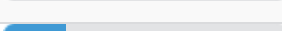
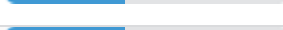

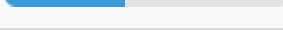

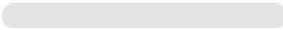
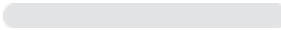
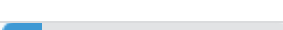
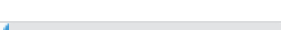
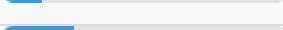
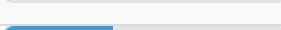
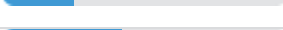
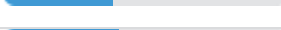
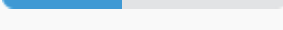
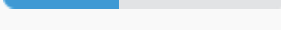
Options	Proportion (before renovation)	Proportion (after renovation)
Very dissatisfied	 0%	 0%
Dissatisfaction	 14.29%	 0%
General	 42.86%	 21.95%
Satisfaction	 42.86%	 60.98%
Very satisfied	 0%	 17.07%

Table 7 Self-evaluation of students' sleep quality before and after classroom renovation

Options	Proportion (before renovation)	Proportion (after renovation)
Very poor	 0%	 0%
Poor	 14.29%	 2.44%
Fair	 25.71%	 39.02%
Better	 42.86%	 41.46%
Very good	 17.14%	 17.07%



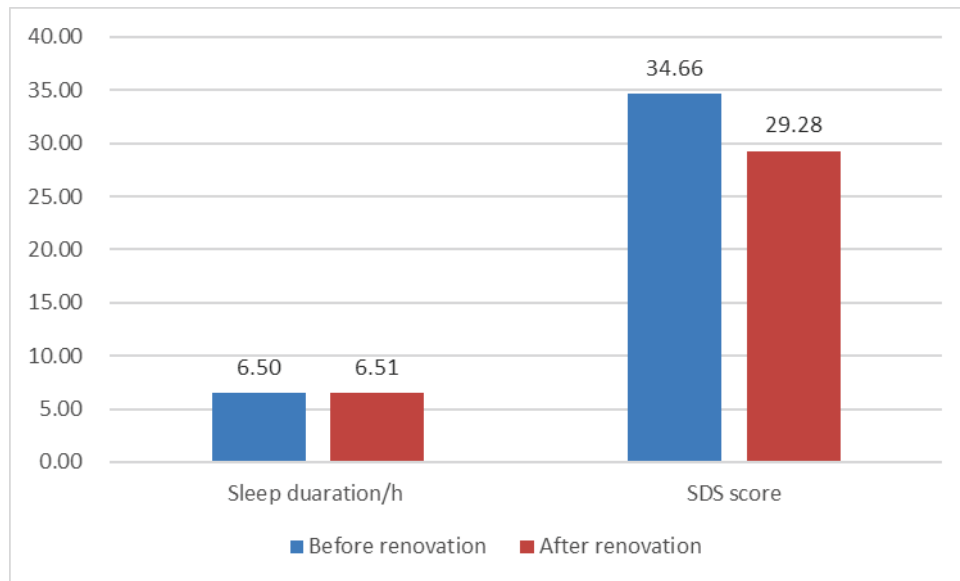


Figure 5 Comparison of students' sleep duration and depression self-assessment scale scores before and after classroom renovation

The group conducted a preliminary use evaluation of the classroom lighting before and after the renovation, and found that the students' evaluation of the brightness of the classroom shifted from 48.57% slightly dark before the renovation to 90.24% moderate after the renovation, and the illumination level of the working surface improved significantly; the evaluation of the lighting color shifted from 17.14% too cold white and 42.86% slightly cold white before the renovation to 73.17% moderate. Evaluation of desktop uniformity from 51.43% more uneven before the transformation to 7.32% more uneven, the overall lighting satisfaction improved significantly. On the basis of visual function evaluation, students' sleep and mood were evaluated subjectively respectively. The overall self-evaluation of sleep quality became better, and the change of sleep duration was not significant, but students' depression self-rating scale (SDS) score was significantly lower and depression was alleviated.

## 5. CONCLUSION

This study developed classroom lighting fixtures with upper and lower light output through the design of new classroom lighting fixtures, resulting in a more rational distribution of light space in the classroom. The changes in students' visual comfort, subjective satisfaction, sleep quality, and emotional state were evaluated through field modifications in university classrooms. Changing the color temperature, number and lighting method of the luminaires to improve the illumination and uniformity level of the working surface is significant to improve the visual efficacy of students with meeting the visual and physical and mental health needs of adolescents. In addition, it is necessary to further optimize the light parameters such as spectrum and illuminance, and to study appropriate dynamic light patterns and light patterns in different behavioral scenarios according to the characteristics of seasons, regions and students' ages and professions.

## REFERENCES

- [1] Qu J, Hou F, Zhou J, Hao L, Mou T, Lin Y, Zhao J, Yang Y, Yang C, Zhu X. Expert consensus on LED lighting for myopia prevention and control classrooms. *Journal of Lighting Engineering*, 2019, 30(06):36-40+46.
- [2] Lin Y. New advances in research and application of classroom lighting in the context of light health. *Journal of Lighting Engineering*, 2021, 32(04):3.
- [3] Hu ZG, Wei B, Ding WC, Huang YY, Dai Q. Research on classroom lighting in primary and secondary schools for visual and rhythmic health needs. *Journal of Lighting Engineering*, 2022, 33(06):17-26.
- [4] Ruan C, Huang Y, Zhang X, Wang Y. Research and application of classroom health lighting design. *Journal of Lighting Engineering*, 2020, 31(06):81-84.
- [5] Zong LJ. Analysis of the current situation and standardization and optimization of school classroom lighting. *Popular Standardization*, 2023(07):93-94+97.
- [6] Li W. Research on the effect of LED daylight simulation system on students' emotion and visual fatigue. Chongqing University, 2021.

- [7] Guo R. Research on the design of university smart classroom light environment based on behavioral psychological evaluation. Northern Polytechnic University, 2022.
- [8] Yang YJ, Ouyang F, Zhang JJ. School health lighting Shanghai in action - exploration and practice of improving classroom lighting in primary and secondary schools and kindergartens. China Modern Education Equipment, 2023(08):1-3.
- [9] Xu Jianxing. Analysis of the current situation of standards related to classroom lighting in primary and secondary schools. China Lighting Appliance, 2021(10):35-42.
- [10] Xuan H, Geng S, Hou J, Li C. Design and verification of classroom lighting retrofit based on LED light source. Anhui Architecture, 2022, 29(10):88-90.
- [11] Wei B, Ding WC, Liu YJ, Zhu YG, Dai Q, Hu ZG. Study on spatial light distribution of classroom lighting in primary and secondary schools. Journal of Lighting Engineering, 2023, 34(01):97-101.
- [12] Li J. Application of intelligent control in classroom health lighting. Light Sources and Lighting, 2022(02):86-88.
- [13] He W. Application of intelligent control in classroom health lighting. Light and Lighting, 2021, 45(03):24-26.
- [14] Wang W, Fu S, Bai Y. Research on the improvement of design classroom light environment: an example of professional classroom in Chongqing University College of Architecture and Urban Planning. Light and Lighting, 2022, 46(02):6-16.
- [15] Zheng S. Research on classroom lighting strategy combining natural lighting and artificial lighting. Light Sources and Lighting, 2022(01):1-3.
- [16] Huang Y. Study on the optimization design of classroom lighting in architecture. Chongqing University, 2020.

## ACKNOWLEDGEMENTS

This research was funded by the Scientific Research Project of Shanghai Municipal Science and Technology Commission (No. 20dz1207200).

Corresponding Author Name: Luoxi Hao

Affiliation: Tongji University

e-mail: haoluoxi@tongji.edu.cn

# THE EFFECT OF CEILING LAMPS' CONTRIBUTION TO HOME NIGHT READING ON VISUAL HEALTH

Yuanyi Luo<sup>1</sup>, Bing Cheng<sup>1</sup>, Yixiang Zhao<sup>1</sup>, Xin Zhang<sup>1</sup>, Hongxing Xia<sup>2</sup>, Wei Wang<sup>2</sup>

(<sup>1</sup> School of Architecture, Tsinghua University, Beijing, China;

<sup>2</sup> MCC Real Estate Group Co., Ltd, Beijing, 10084, China.)

## ABSTRACT

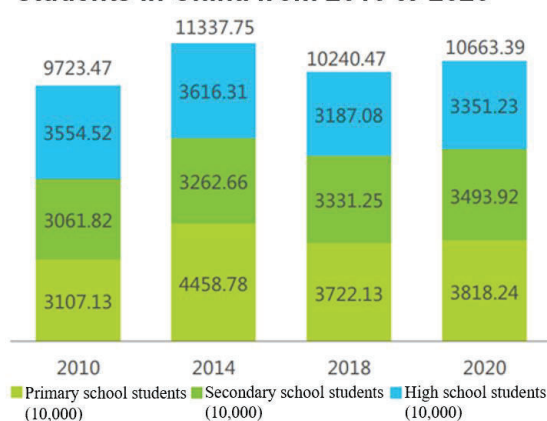
Increased youth myopia rate due to more home study time and lighting's effect on visual acuity emphasize the importance of a healthy home luminous environment. This study explored how ceiling lamps affected visual health based on the position of ceiling lamps (overhead vs. peripheral) and their contribution to task illuminance (1/3 vs. 2/3). The results showed that the position had a significant effect on visual performance. But visual fatigue and visual function showed no significant difference. These findings provide empirical backing and a theoretical basis for lighting practice in home offices.

Keywords: Ceiling lamps; Visual fatigue; Visual performance; Visual function; Ophthalmic equipment; Task-ambient lighting system.

## 1. INTRODUCTION

Myopia is a severe issue among youth. According to *World report on vision*, the overall prevalence of myopia is highest in high-income countries of the Asia-Pacific region (53.4%)[1]. In China, the number of youth myopia is still rising in 2020, and the prevention and control requirements in 2030 are strict (Figure 1)[2]. It is widely acceptable that luminous environment can affect visual health[3-5]. According to the scene, lighting research can be divided into office lighting, classroom lighting and home lighting. Most lighting studies on visual health focused on office and classroom. However, the number of hours adolescents spend studying at home is increasing, especially after COVID-19[6, 7]. Therefore, the study on visual environment of home learning is crucial to improving adolescents' visual health.

**The total number of myopia among primary, middle and high school students in China from 2010 to 2020**



**The change of myopia rate in children and adolescents from 2010 to 2020 and its prevention and control requirements**

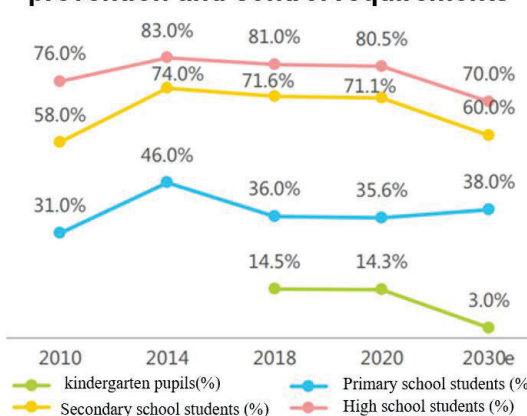


Figure 1. Changes in the number of students with myopia (Left), requirements for prevention and control of myopia in children and adolescents in 2030 (Right) (Source: iResearch)

Most lighting research have supported the relative visual performance model, which indicates that visual performance presents a marginal decreasing effect with the change of contrast[8, 9]. These studies are all focused on task area. However, except task area, non-task area occupies a significant part of visual field. With the development of visual neuroscience, the curve of contrast change of M pathway, which are responsible for "where", shows a trend similar to that of visual

performance[10, 11]. This suggests that non-task area in the visual field may also play a part in affecting visual performance.

In home office, most students use task-ambient lighting, which combines the ceiling lamp and desk lamp[6]. For task illuminance and interior surface's reflectance, there are corresponding standards, such as GB50034-2013, JIS Z9110-2011, ANSI IESNA RP-11-2017 and EN 12464. Based on these known conditions, there are still some important issues for non-task area: (1) where is the light coming from, i.e., where is ceiling lamps positioned? (2) when the task illuminance is determined, how much light is received by the non-task area, which can also be quantified by ceiling lamps' contribution to task illuminance.

For the position of ceiling lamps, it was noted that the overhead-peripheral lighting mode greatly influenced the impression of the luminous environment[12] and Indirect/ambient lighting can reduce people's negative emotions[13]. Although there is few research for the position of ceiling lamps, many studies about direct/indirect lighting can provide some basis for deduction. The pathway of ceiling lamps, namely the ratio of direct light to indirect light, will affect the brightness perception contributed by walls and ceilings, thus affecting the subjective response[13, 14]. Most studies on direct light and indirect light showed that more indirect lighting could make the room appear more spacious, make people more pleasant[13, 14] and reduce ocular symptoms[15]. Therefore, it can be inferred that changing the position of ceiling lamps can use wall reflection to obtain better brightness perception and improve visual health.

Numerous research studied task-ambient lighting, in which ambient lighting frequently refers to ceiling lamp[16-18]. In these cases, the provision of task lighting elevates pleasure and arousal, improves paper related task work and satisfaction[16]. While ambient lighting can maintain illumination on non-task surfaces and avoid extreme luminance ratio[18]. Therefore, it is possible to maintain the task illuminance but change ceiling lamps' contribution to task illuminance, which may improve visual health. The feasibility of task and ambient illuminance ratio around 1 was demonstrated early on[19]. When both task lighting and ambient lighting are at 50% output, luminance ratio in visual field are closer to IESNA recommendation, which can improve satisfaction[18]. But in those studies, either the definition of task and ambient illuminance ratio is not clear, or the findings are limited to output of the lamps used in that experiment, which cannot be generalized to provide recommendations in design practice. So, ceiling lamps' contribution to task illuminance needs to be further investigated to explore the possibility of improving visual health.

Based on existing research and lighting standards consensus, this study aims to investigate the effects of ceiling lamps' position (overhead vs. peripheral) and contribution to task illuminance (1/3 vs. 2/3) on visual health to select a relatively comfortable, efficient and healthy luminous environment. Self-report of visual fatigue, visual performance test, and ophthalmic examination are used to reflect the participants' visual health. This study will put forward more operational suggestions for lighting design in home offices and provide available measures to improve adolescents' visual health.

## 2. METHOD

### 2.1 Participants

Twenty-eight Chinese college students with normal naked or corrected visual acuity, normal color vision, no eye disease, and a regular lifestyle (17 females,  $M = 21.9$  years,  $SD = 2.1$ ) between the age of 18 and 27 participated in the experiment. Finally, after removing the extreme values, 24 valid experimental data were obtained.

### 2.2 Setting

The experimental space was a replica of the bedroom learning environment and measured 3.275 m(W) x 3.35 m(D) x 2.79 m(H). The desk was positioned facing the window. White full-blackout curtain was used to provide an entirely artificially lit environment. Figure 2 showed the participants' visual field.

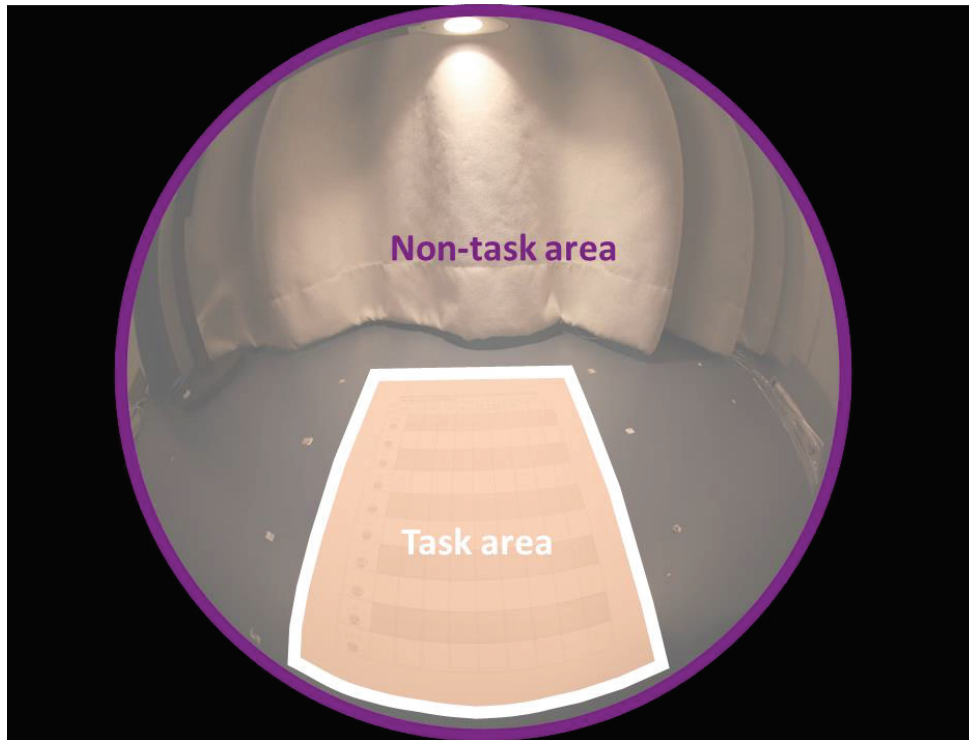


Figure 2. The visual field of the participants

In this study, both desk lamp and ceiling lamps used stepless dimming control. A 15-watt desk lamp was placed in front of the participant and its light source was positioned 45 cm above the desk (orange in Figure 3). The ceiling lamps were comprised of four groups of modular luminaires and each group consisted of six independently controllable units with a 12-watt output. Two groups were positioned on the periphery above the desk (yellow in Figure 3), while the other two groups were located overhead (red in Figure 3).

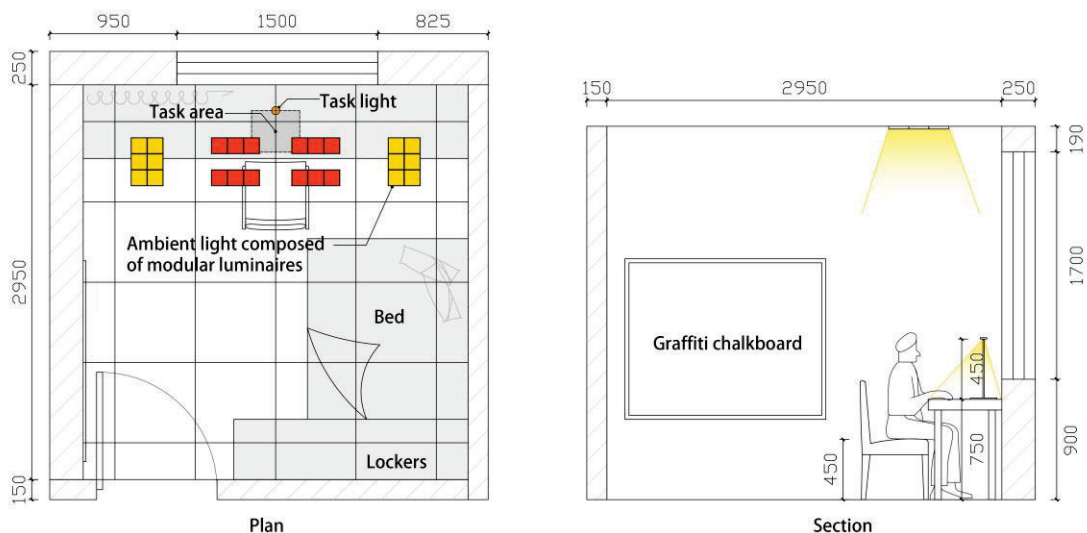


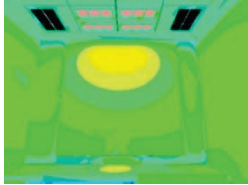



Figure 3. Room setting

In order to create four experimental scenes with varied ceiling lamps' contributions, this experiment adopted a two-factor experimental design with two positions of ceiling lamps (overhead, peripheral) and two ceiling lamps' contributions to task illuminance (1/3 vs. 2/3) (Table 1). According to the lighting standards, the recommended horizontal illuminance for home reading is 150 lx (GB 50034-2013), 200 lx (ANSI IESNA RP-11-2017), 500 lx (JIS Z9110-2011). Furthermore, Fotios proved that 500lx was sufficient to provide a pleasant environment and correlated color temperature had no effect on visual comfort and pleasure[20]. Therefore, the task illuminance of four scenes was set to 500 lx and CCT was set to 3300K.



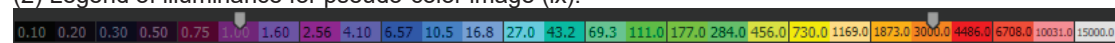
Table 1. Parameters of experimental scenes

Scene <sup>*(1)</sup>	Ceiling lamps		Measured task illuminance (lx)			Equivalent Melanopic Lux	Pseudo-color image <sup>*(2)</sup>
	Contribution to task illuminance	Position	Total (lx)	Ceiling lamps (lx)	Desk lamp(lx)		
1	1/3	Overhead	510.75	170	340.75	18.7	
2	1/3	Peripheral	513.56	172.81	340.75	18.2	
3	2/3	Overhead	508.66	344.37	164.29	22.6	
4	2/3	Peripheral	505.66	341.37	164.29	18.4	

\*Annotation:

(1) To facilitate description, four scenes are described as follows: scene 1 (Overhead-1/3), scene 2 (Peripheral-1/3), scene 3 (Overhead-2/3) and scene 4 (Peripheral-2/3).

(2) Legend of illuminance for pseudo-color image (lx).



## 2.3 Procedure

Each participant underwent four experiments over the same period of 4 days in the laboratory with constant temperature (20-23 °C) and humidity (35%-50%). The sequence of scenes and reading materials were in a counter-balanced order among the four experiments and participants to eliminate the potential for any result deviation.

Before the experiment, all participants should take adequate sleep, avoid consuming food or beverages containing alcohol or caffeine within 24 hours, and avoid long-term continuous eye use within 1.5 hours. Additionally, each participant should sign an informed consent and practice the visual performance test at least twice to counteract unfamiliarity.

The experimental procedure is shown in Table 2. Participants were instructed to take a seat in front of the desk. And then they need fill in the visual fatigue self-report, take ophthalmic examination (cooperate with a professional ophthalmologist) and visual performance test (Landolt-ring test). Next, the participants read English material for thirty minutes. After reading,

the participants filled in the visual fatigue self-report scale, took the visual performance test and ophthalmic examination again. At the end, an online questionnaire consisting of luminous environment appraisal, subjective alertness (KSS) and the emotional state (PAD) parts was administered.

Table 2. Experimental procedure

	Visual fatigue self-report	Ophthalmic examination	Visual performance test	Reading	Visual fatigue self-report	Visual performance test	Ophthalmic examination	Questionnaire
Duration	3 min	10 min	2 min	30 min	3 min	2 min	10 min	5 min

### 3. RESULTS

#### 3.1 Visual fatigue

The degree of visual fatigue was expressed as the sum of increments of visual fatigue symptoms, which was tested by Friedman test. The results showed that there was no significant difference between four scenes ( $p > 0.05$ ).

#### 3.2 Visual performance

The result of IMC reduction rate of visual performance was shown in Figure 4. The data all conformed to normal distribution. The interaction between ceiling lamps' position and contribution to task illuminance had no statistical significance ( $p > 0.05$ ). But the main effect of ceiling lamps' position on visual performance was statistically significant ( $F(1, 23) = 5.501, p = 0.021$ ). And it was found that scene 4 (Peripheral-2/3) is significantly better than scene 3 (Overhead-2/3) ( $p = 0.033$ ).

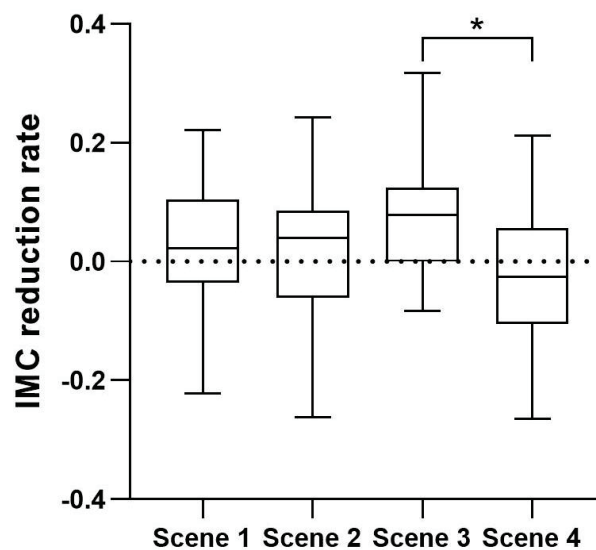


Figure 4. IMC reduction rate

#### 3.3 Visual function

The visual function included a variety of indicators, such as diopter, near eye position, adjustment sensitivity and melt phase change. In summary, the visual function of scene 3 (Overhead-2/3) had the greatest decline, while that of scene 1 (Overhead-1/3) had the smallest decline. But all the indicators showed no significant difference ( $p > 0.05$ ).

#### 3.4 Subjective questionnaire

The following three factors were extracted from the questionnaire through factor analysis: lighting satisfaction, brightness contrast and relaxation. For lighting satisfaction and brightness

contrast, there was no significant difference among the four scenes ( $p > 0.05$ ). This means that the change of ceiling lamps can basically maintain the consistency of subjective satisfaction. The interaction of ceiling lamps' position and contribution to task illuminance had a statistically significant effect on relaxation ( $F(1, 23) = 10.15, p = 0.004$ ) (Figure 5).

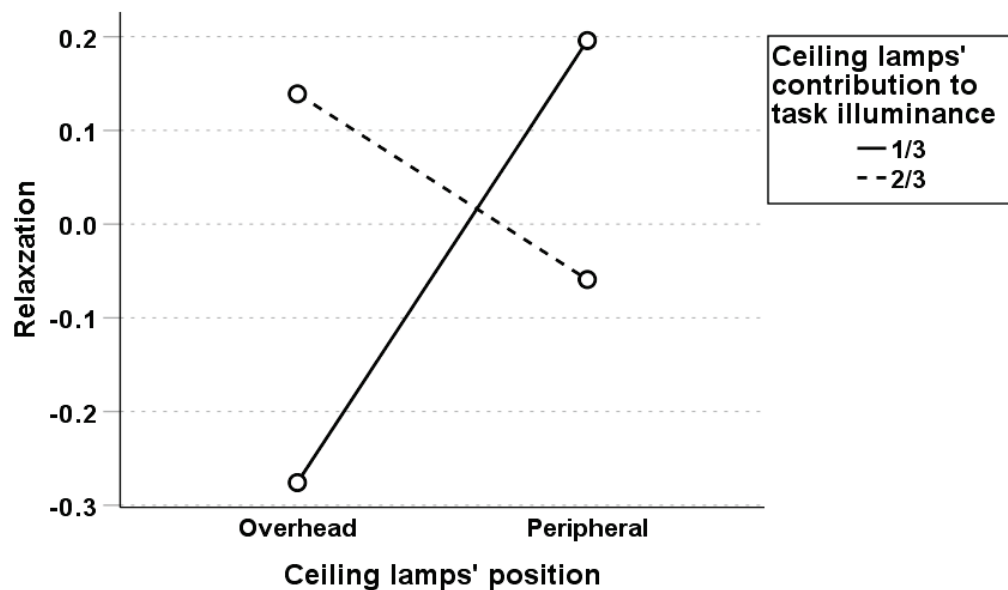


Figure 5. The effect of ceiling lamps on relaxation

#### 4. DISCUSSION

The results showed that ceiling lamps' position had significant effect on visual performance. For ceiling lamps' contribution to task illuminance, this study found that there showed no significant effect on visual fatigue, visual performance, visual function, lighting satisfaction and brightness contrast, which was consistent with the finding that the decreasing ambient lighting had no effect on satisfaction [21]. And the interaction of these two factors had a significant effect on relaxation in subjective evaluation. Although in this study, the interaction is not significant for visual performance. The apparent cross lines remind us that future research needs to consider the possibility of interaction between these two factors (Figure 6).

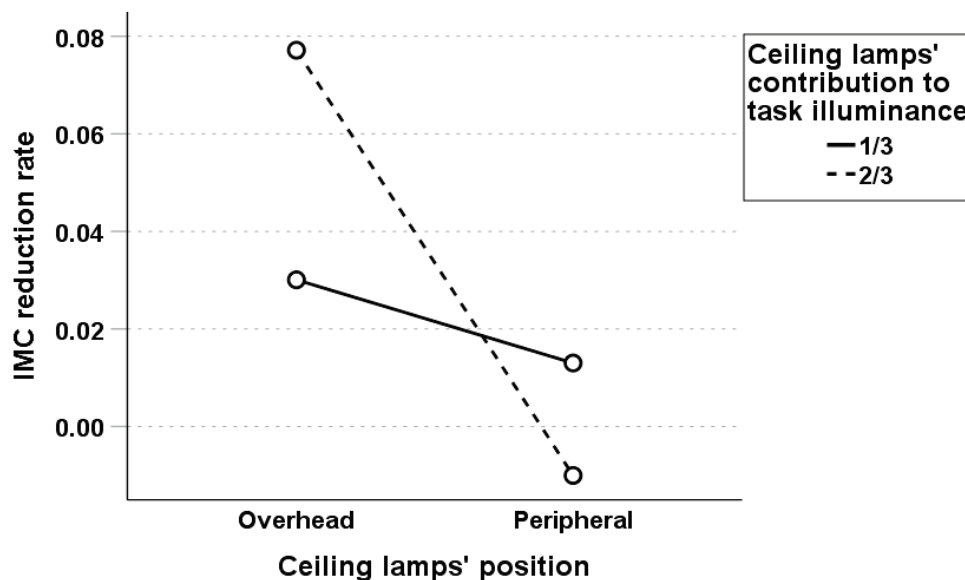


Figure 6. The effect of ceiling lamps on visual performance

Distributed ceiling lamps with local lighting make it easier to alter the luminous flux and achieve a reasonable light distribution. For example, ceiling lamps' position may be a thought-

provoking factor to achieve better visual performance, while ceiling lamps' position and contribution to task illuminance may be considerable factors to get better subjective evaluation. Therefore, for home office, distributed ceiling lamps with desk lamps can achieve self-regulation of task-ambient lighting to improve visual health.

However, visual function was not significantly different between four scenes. And there may be two reasons. Firstly, low sensitivity of visual function equipment may lead to low accuracy data. Secondly, changes in visual function are slow and subtle. So long-term monitoring, such as several months, may be required in the future vision study.

## 5. CONCLUSION

This study investigated the effect of ceiling lamps' position and contribution to task illuminance on visual health. And results showed that the visual performance was significantly influenced by the position of ceiling lamps. Additionally, position and contribution to task illuminance showed potential interaction. The findings provide practical and accessible lighting design recommendations for future applications in home learning environment. However, this study also indicates that using professional ophthalmic equipment to explore physiological changes in the eye may require long-term monitoring in future studies.

## REFERENCE

- [1] World Health Organization. World report on vision. 2019.
- [2] iResearch. White paper on visual health of children and adolescents in China. 2022(in Chinese).
- [3] Berman, S. M., Navvab, M., Martin, M. J., Sheedy, J., & Tithof, W. A comparison of traditional and high colour temperature lighting on the near acuity of elementary school children. *Lighting Research & Technology*, 2006, 38(1), 41-49.
- [4] Navvab, M. Visual acuity depends on the color temperature of the surround lighting. *Journal of the Illuminating Engineering Society*, 2002, 31(1), 70-84.
- [5] Wang, M. L., & Luo, M. R. Effects of LED lighting on office work performance. In 2016 13th China International Forum on Solid State Lighting (SSLChina). 2016. IEEE.
- [6] Amorim, C. N. D., Vasquez, N. G., Matusiak, B., Kanno, J., Sokol, N., Martyniuk-Peczek, J., Sibilio, S., Koga, Y., Giampi, G. & Waczynska, M. Lighting conditions in home office and occupant's perception: An international study. *Energy and Buildings*, 2022, 261.
- [7] Wang, J. Q., Fang, Y. H., Huang, Y. X., Chen, J. N., & Luo, X. Y. Study on the effect of home night lighting environment on students' eyestrain and visual efficacy. In *E3S Web of Conferences*. 2021. EDP Sciences.
- [8] Rea, M. S. Some basic concepts and field applications for lighting, color, and vision. *Glare and Contrast Sensitivity for Clinicians*, 1990, 120-138.
- [9] Rea, M. S., & Ouellette, M. J. Relative visual performance: A basis for application. *Lighting Research & Technology*, 1991, 23(3), 135-144.
- [10] Kaplan, E., & Shapley, R. M. The primate retina contains two types of ganglion cells, with high and low contrast sensitivity. *Proceedings of the National Academy of Sciences*, 1986, 83(8), 2755-2757.
- [11] Rea, M. The what and the where of vision lighting research. *Lighting Research & Technology*, 2018, 50(1), 14-37.
- [12] Flynn, J. E., Spencer, T. J., Martyniuk, O., & Hendrick, C. Interim Study of Procedures for Investigating the Effect of Light on Impression and Behavior. *Journal of the Illuminating Engineering Society*, 1973, 3(1), 87-94.
- [13] Shin, Y. B., Woo, S. H., Kim, D. H., Kim, J., Kim, J. J., & Park, J. Y. The effect on emotions and brain activity by the direct/indirect lighting in the residential environment. *Neuroscience letters*, 2015. 584, 28-32.
- [14] Houser, K. W., Tiller, D. K., Bernecker, C. A., & Mistrick, R. G. The subjective response to linear fluorescent direct/indirect lighting systems. *Lighting Research & Technology*, 2002, 34(3), 243-260.
- [15] Fostervold, K. I., & Nersveen, J. Proportions of direct and indirect indoor lighting—The effect on health, well-being and cognitive performance of office workers. *Lighting Research & Technology*, 2008, 40(3), 175-200.

- [16] Gene-Harn, L., Keumala, N. I. M., & Ghafar, N. A. Office Occupants' Mood and Preference of Task Ambient Lighting in the Tropics. In MATEC Web of Conferences. 2016. EDP Sciences.
- [17] Ishii, H., Kanagawa, H., Shimamura, Y., Uchiyama, K., Miyagi, K., Obayashi, F., & Shimoda, H. Intellectual productivity under task ambient lighting. *Lighting Research & Technology*, 2016, 50(2), 237-252.
- [18] Newsham, G., Arsenault, C., Veitch, J., Tosco, A. M., & Duval, C. Task Lighting Effects on Office Worker Satisfaction and Performance, and Energy Efficiency. *Leukos*, 2005, 1(4), 7-26.
- [19] Yamakawa, K., Watabe, K., Inanuma, M., Sakata, K., & Takeda, H. A study on the practical use of a task and ambient lighting system in an office. *Journal of Light & Visual Environment*, 2000, 24(2), 2\_15-2\_18.
- [20] Fotios, S. A revised Kruithof graph based on empirical data. *Leukos*, 2017. 13(1), 3-17.
- [21] Akashi, Y., & Boyce, P. R. A field study of illuminance reduction. *Energy and Buildings*, 2006, 38(6), 588-599.

## ACKNOWLEDGEMENTS

The project is a collaborative research and development effort with MCC Real Estate Group Co., Ltd, Beijing, China. And the authors appreciate Huizhou CDN Industrial Development Co., Ltd. for lighting devices used for this study.

## FUNDING

This work was supported by the National Natural Science Foundation of China (Grant No. 52078266), MCC Real Estate Group Co., Ltd, Beijing, China, and Tsinghua University Initiative Scientific Research Program (No. 20211080095).

Corresponding Author 1: Xin Zhang  
Affiliation: School of Architecture, Tsinghua University  
e-mail: zhx@tsinghua.edu.cn

Corresponding Author 2: Yuanyi Luo  
Affiliation: School of Architecture, Tsinghua University  
e-mail: yy-luo21@mails.tsinghua.edu.cn



# Research on Appropriate Lighting Methods that Take into account the Psychological Changes due to the Seasons

Minami Hagio, Heo Jaeyong, youko Inoue

(Nara Women's University, The Open University of Japan, Japan)

## ABSTRACT

Circadian rhythm is the biological rhythm of the annual cycle, and seasonal changes in daylight hours are known to affect the circadian rhythm. This study will clarify the relationship between season, psychology, and impression evaluation of the lighting environment.

Experiments were conducted in August, October, and December 2022. Subjects were the same in all experiments. The time of each subject was also the same for all experiments. The subjects were 13 young women in their 20s, all with normal color vision. Lighting was randomly presented after 120 seconds of dark adaptation in the laboratory. Lighting conditions are 50lx, 220lx, and 700lx, and color temperatures are 3000K, 4200K, and 5200K. The lighting evaluation was made using the 7-point semantic differential scale method for 10 evaluation items.

The evaluation of 3000 K was rated relatively high for all illuminance levels. In all lighting conditions, significant differences were found. Significant differences in seasons were found only in the Not-tired-Tired. Since the seasonal differences in each evaluation are largely influenced by individual differences, it is necessary to take individual differences into consideration. In addition, the Not-tired-Tired was rated lower in winter. This may be due to a decrease in melatonin secretion caused by a decrease in daylight hours during the winter and autonomic nervous system disturbances caused by differences in temperature.

Keywords: Seasonal Changes, Lighting Evaluation, Circadian Rhythm

## 1. INTRODUCTION

Circadian rhythm<sup>(1)</sup> is the biological rhythm of the annual cycle, and seasonal changes in daylight hours are known to affect the circadian rhythm<sup>(2)</sup>. For example, the difference in the monthly average of sunshine hours in Nara Prefecture over the 20-year period from 2001 to 2022 is about 1.7 times the difference between August and January. Thus, seasonal changes in sunlight hours are thought to affect circadian rhythms.<sup>(3)</sup> The autonomic nervous system, which regulates body temperature, heart, respiration, and digestion, is closely related to changes in the external environment, such as temperature changes. Since autonomic nervous system disorders are a factor in the occurrence of physical illnesses that are not generally judged to be diseases<sup>(5)</sup>, seasonal and weather changes affect the body and mind. In particular, short daylight hours in high latitudes are one of the factors causing seasonal affective disorder<sup>(6)</sup>.

Studies on the relationship between seasons and psychology in healthy subjects are fewer, and studies combined with seasons and lighting are also fewer. This study will clarify the relationship between season, psychology, and impression evaluation of the lighting environment.

## 2. EXPERIMENTAL METHOD

Lighting conditions are shown in Table 1. Experiments were conducted in August, October, and December 2022. Subjects were the same in all experiments to observe seasonal changes in individual psychology. Furthermore, to prevent circadian rhythms from influencing the evaluation, the time of each subject was also the same for all experiments. The subjects were 13 young women in their 20s, all with normal color vision. The monthly average total solar radiation and monthly average air temperature at the time of the experiment are shown in Table 2. The laboratory floor plan is shown in Figure 1.

First, 25 items were evaluated based on the GHQ30, which is effective for understanding, evaluating, and detecting symptoms of neuroticism. Also, questionnaires were administered to evaluate their impressions of each season and their residential area.

The seasonal questionnaire had the 14 evaluation items listed in Table 3 evaluated using 7-point semantic differential scale method. As for the three questionnaires, we report on the details separately, since the analysis is insufficient at this point.

Next, lighting was randomly presented after 120 seconds of dark adaptation in the laboratory. Lighting conditions are 50lx, 220lx, and 700lx, and color temperatures are 3000K, 4200K, and 5200K. After 60 seconds of acclimatization at 50 lx, 90 seconds at 220 lx, and 120 seconds at 700 lx, the subjects were asked to evaluate the lighting.

Table 1. Experimental conditions

Illuminance E	50, 220, 700lx
Color temperature Tc	3000, 4200, 5200K

Table 2. Monthly average total solar radiation and monthly average air temperature at the time of the experiment

	Monthly average total solar radiation	Monthly average air temperature
Summer(August)	18MJ/m <sup>2</sup>	28.3°C
Autumn(October)	12.5MJ/m <sup>2</sup>	17.2°C
Winter(December)	8.4 MJ/m <sup>2</sup>	6.1°C

Figure 1. Laboratory floor plan

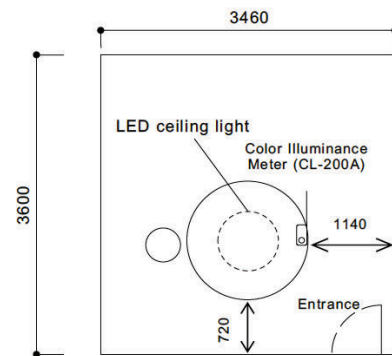


Table 3. Evaluation items

Evaluation items of Seasonal questionnaire	Evaluation items of Illuminance	Light-Dark Comfortable-Discomfortable Like-Dislike Warm-Cool Sharp-Unsharp Cheerful-Gloomy Relieved-Anxious Calming-Uncomfortable Concentrated-Not-concentrated Not-tired-Tired
		Delightful-Sad Refreshing-Not-refreshing Hot-Cold Dynamic-Static

### 3. LIGHTING EVALUATION

The 10 evaluation items shown in Table 3 were evaluated using 7-point semantic differential scale method. A score of 1 to 7 is given to the evaluation, with higher scores indicating a more positive impression on the item.

#### 3.1 Individual Results

Analysis of the results for each subject revealed that there were significant individual differences in the effects of the season. This report presents the results for subject A shown in Figure 2 and subject J shown in Figure 3. A showed little variation in the GHQ results with less than one standard deviation in the ratings across the three seasons. Seasonal differences were observed in the lighting evaluation results. The seasonal evaluation showed no particular change in Comfortable-Discomfortable, Relieved-Anxious, Calming-Uncomfortable, or Not-tired-Tired. The evaluation of 5200K in winter, which was low on average for all subjects discussed below, was relatively high for all illuminance levels. In particular, the 220 lx condition showed differences from summer in the like-dislike, Calming-Uncomfortable, and Concentrated-Not-concentrated. In addition, the winter evaluation was lower than the other seasons in the 700lx3000K condition in the Comfortable-Discomfortable, Like-Dislike, Concentrated-Not-concentrated. A is the subject who showed considerably lower results than the average of all subjects.

J scored the same in all three seasons in the GHQ results, but seasonal differences were observed in the lighting evaluation results. Seasonal differences were not seen in the seasonal evaluations either. However, the summer season was rated lower than the fall and winter seasons in Concentrated-Not-concentrated, Not-tired-Tired. Although not reflected in the GHQ results, the impression of the summer season was that people found it difficult to concentrate and tiring. Also, with the exception of 50lx in the summer season, subjects tended to rate higher at 4200K, a difference from the average of all subjects, which will be discussed later.

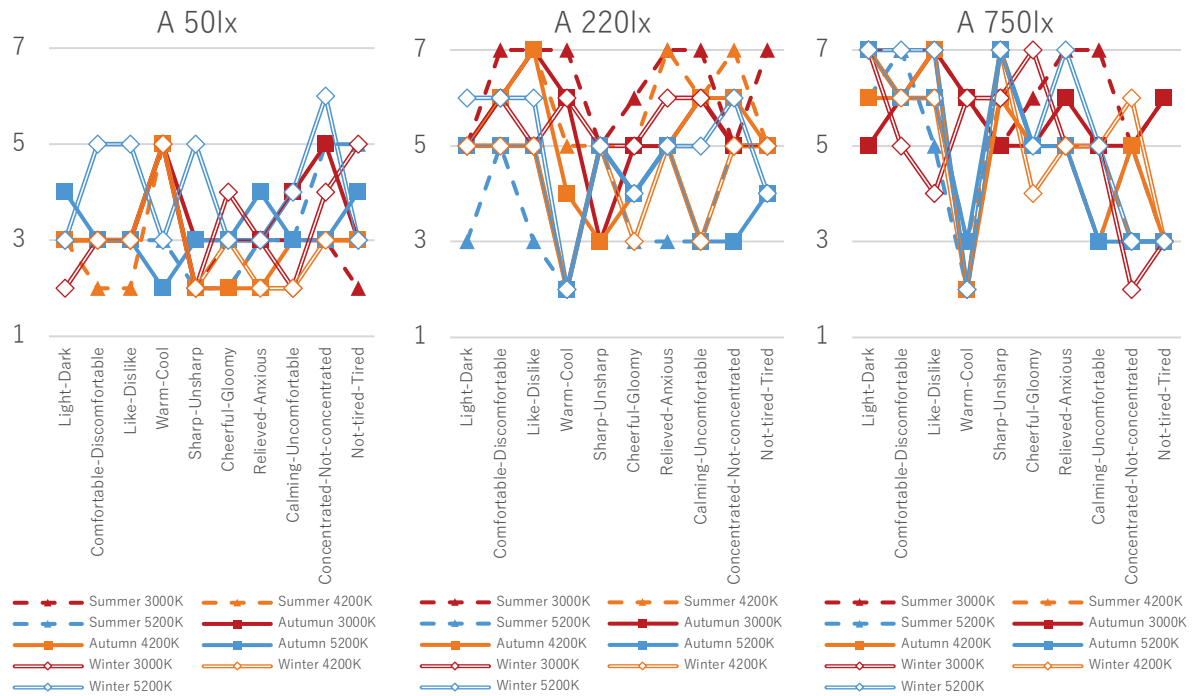


Figure 2. Results of A

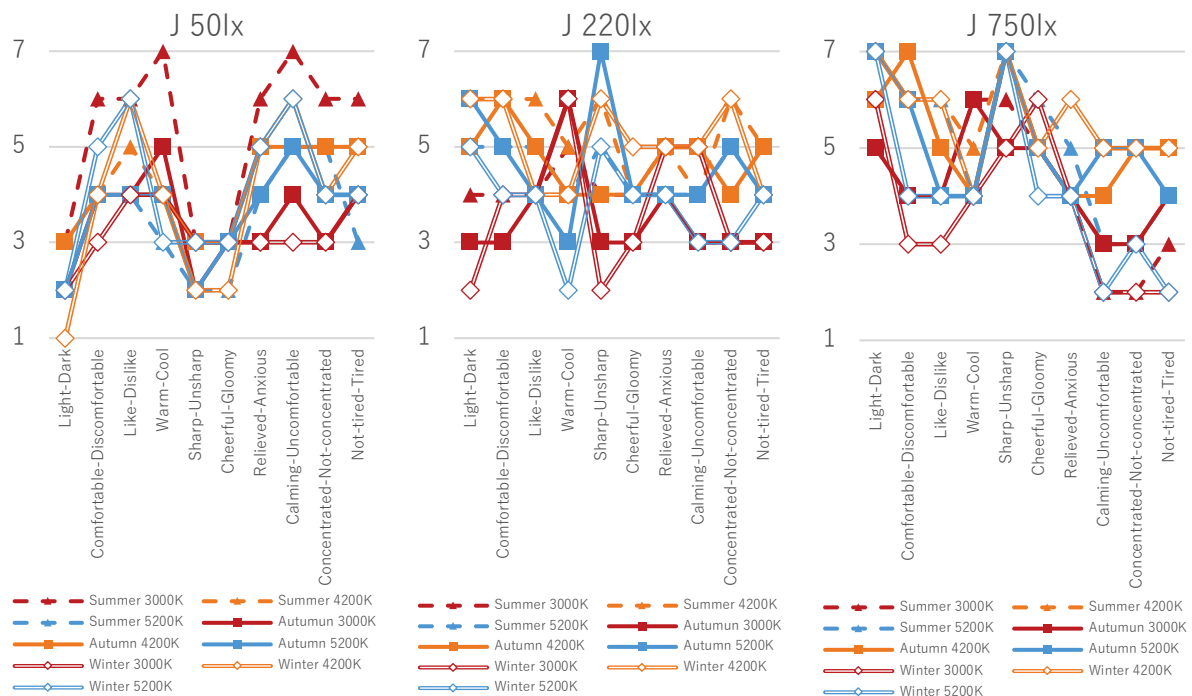


Figure 3. Results of J

### 3.2 Effects of illuminance and color temperature

Average for all subjects is shown in Figure 4. In all lighting conditions, significant differences were found. Significant differences in seasons were found only in the Not-tired-Tired. The three seasons showed the same trends in lighting ratings, with no significant differences. The evaluation of 3000 K was rated relatively high for all illuminance levels. The 3000 K showed higher values than the other conditions, especially for the Comfortable-Discomfortable, Like-Dislike, Relieved-Anxious, Calming-Uncomfortable, and Not-tired-Tired. And the 50 lx was rated low for all color temperatures. The evaluation of 700lx3000K condition was relatively high, but the evaluation of 220lx3000K was high in summer and fall, and 50lx3000K was high in winter in Not-tired-Tired.

It is understood from the examination of each subject that there are large individual differences in the seasonal differences in each evaluation.

This may be the reason why there are almost no significant seasonal differences from the mean of all subjects, and it is necessary to take individual differences into consideration.



Figure 4. Average for all subjects

### 3.3 Effects of Seasons

Seasonal Changes in Light-Dark conditions are shown in Figure 5. Seasonal Changes in Light-Dark conditions are shown in Figure 5.

The results showed that for Light-Dark, the ratings increased with each illuminance, and for Not-tired-tired, the ratings decreased with each increase in color temperature. There was little seasonal difference in the Light-Dark, representing physical quantities, while there was a seasonal difference in Not-tired-tired. Evaluations tended to be higher in summer and lower in winter.

The Not-tired-Tired was rated lower in winter. This may be due to a decrease in melatonin secretion caused by a decrease in daylight hours during the winter and autonomic nervous system disturbances caused by differences in temperature. However, there was no relationship between this condition and GHQ or seasonal evaluations in the August-December experiment, suggesting

that other factors, such as the subjects' usual lighting environment and lighting preferences, may have been involved.

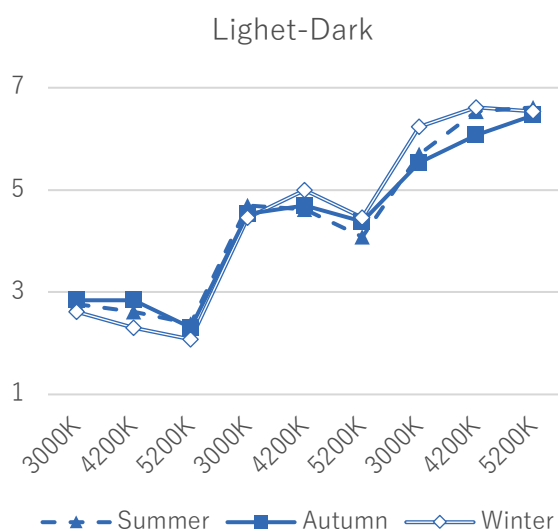


Figure 5. Seasonal Changes in Light-Dark condition

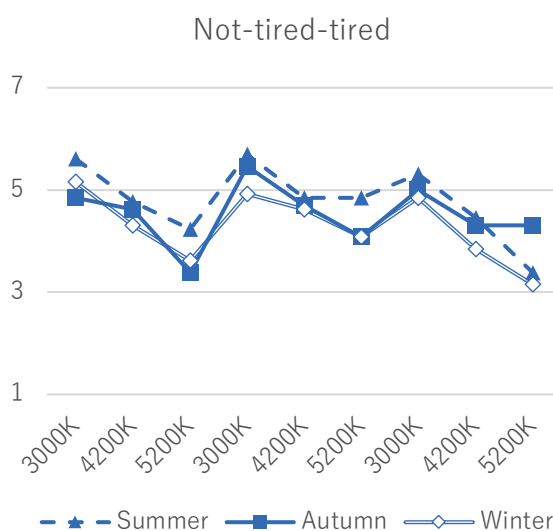


Figure 6. Seasonal Changes in Not-tired-tired condition

#### 4. CONCLUSION AND DISCUSSION

The three seasons showed the same trend in lighting evaluations, with no significant differences. It is understood from the subject-by-subject examination that there are large individual differences in the seasonal differences in each rating. This may be the reason why there were no significant seasonal differences in the mean of all subjects, and therefore, it is necessary to consider individual differences. Only in the Not-tired-Tired, there was a seasonal difference, with a tendency for lower ratings in the winter. This may be due to a decrease in melatonin secretion caused by a decrease in daylight hours during the winter and autonomic nervous system disturbances caused by differences in temperature.

The evaluation of the 700lx3000K condition was relatively high overall results. In the Not-tired-Tired, which showed significant differences by season, 220lx3000K was highly evaluated in summer and fall, and 50lx3000K was highly evaluated in winter. As a seasonal lighting technique to reduce fatigue caused by lighting, we propose changing the lighting to medium-light, low color temperature lighting in summer and fall, and low-light, low color temperature lighting in winter.

Future tasks include a discussion of lighting evaluation throughout the year with the addition of April results, the degree of intra-individual error in the same season, the relationship between physiological volume and understanding the effects of aging.

#### REFERENCES

- [1] Japanese Society for Chronobiology. "Glossary of Chronobiology terms". Japanese Society for Chronobiology. 2023. <https://chronobiology.jp/TechnicalTerms.html#circa-rhythm> (2023-01-25)
- [2] Jihwan Myung et al. : GABA-mediated repulsive coupling between circadian clock neurons in the SCN encodes seasonal time, Proceedings of the National Academy of Science of the United States of America.
- [3] Japan Meteorological Agency. "Historical data search Monthly value since the start of observation, Nara, Monthly average of daily temperature (°C)". Ministry of Land, Infrastructure, Transport and Tourism. 2023. [https://www.data.jma.go.jp/obd/stats/etrn/view/monthly\\_s3.php?prec\\_no=64&block\\_no=47780&year=&month=&day=&elm=monthly&view=a1](https://www.data.jma.go.jp/obd/stats/etrn/view/monthly_s3.php?prec_no=64&block_no=47780&year=&month=&day=&elm=monthly&view=a1) (2023-01-25)



- [4] Japan Meteorological Agency. "Nara, Monthly average of total solar radiation (MJ/m<sup>2</sup>), Monthly total value of sunshine hours (h)". Ministry of Land, Infrastructure, Transport and Tourism. 2023.  
[https://www.data.jma.go.jp/obd/stats/etrn/view/nml\\_sfc\\_ym.php?prec\\_no=64&block\\_no=47780](https://www.data.jma.go.jp/obd/stats/etrn/view/nml_sfc_ym.php?prec_no=64&block_no=47780) (2023-01-25)
- [5] Hiro Clinic Psychosomatic Medicine "What is the cause of winter fatigue that causes mental and physical discomfort [supervised by a physician]" . Medical Corporation Fukubikai Hiro Clinic Psychosomatic Medicine.2022-12-06. <https://www.hiro-clinic.or.jp/mental/winter-heat-fatigue/> (2023-01-30)
- [6] Rosenthal, N. E. and Sack, D. A. et al. : Seasonal affective disorder. A description of the syndrome and preliminary findings with light therapy, Arch. Gen. Psychiatry, 41-1. pp.72-80 (1984) .
- [7] Kyoko Ishida, Yoko Inoue, Hironobu Uchiyama, Junichi Kurata : The Effect of Season on Impression of Lighting : Part 1 Within- and between-subject variation. Journal of Science and Technology in Lighting. Vol. 95, No. 8A. p439-445, 2011
- [8] Shogo Imai : Factor Analysis of Sensations and Feelings about Seasonal Weather and Their Relationship to Personality. Jpn. J. Biometeor. Vol.17, No.3. 1980  
\*1 : GHQ Mental Health Questionnaire: Screening test for symptomatology, assessment, and detection of neuroticism

## ACKNOWLEDGEMENTS

This work was supported by JSPS KAKENHI Grant Number JP21K02108.

Corresponding Author Name: Heo Jaeyong  
Affiliation: Nara Women's University  
e-mail: heo@cc.nara-wu.au.jp

## VERIFICATION OF THE EVALUATION METHOD FOR THE SENSITIVITY TO LIGHT EXPOSURE

Taiki Saito<sup>1</sup>, Yuki Kawashima<sup>1</sup>, Kazuaki Ohkubo<sup>2</sup> and Yasuki Yamauchi<sup>1</sup>

<sup>1</sup> Graduate School of Science and Engineering, Yamagata University, Yamagata, Japan

<sup>2</sup> Systems Engineering Inc., Tokyo, Japan

### ABSTRACT

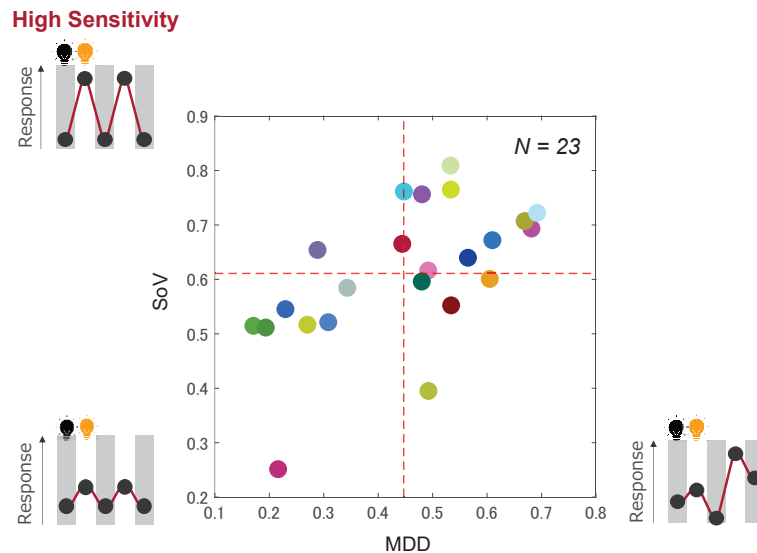
The purpose of this study is to validate our evaluation method for the sensitivity to light exposure. To validate the method, we used the vital data obtained from a previous experiment. We examined the correlation between the difference of means of the physiological responses obtained under the light exposure and those without light exposure and the index which expressed the subject's sensitivity derived from our method. The results showed that there was a strong negative correlation among these values, especially in one light exposure condition, suggesting that our evaluation method for the sensitivity is valid.

Keywords: physiological evaluation, individual difference, heart rate variability, sensitivity

### 1. INTRODUCTION

The role of lighting is not limited to illuminate space around us to assist our visibility. Many previous studies have shown that lighting may have different effects on human emotions and physiological functions depending on its condition [1-3]. For instance, higher CCT lighting promotes human alertness and activates autonomic nervous system [1,2]. A physiological evaluation is one of the methods to evaluate such influence of lighting on humans. It is generally conducted by measuring vital data such as electroencephalography of subjects. As the physiological evaluation uses vital data, which is very difficult to control intentionally, it is not likely that the results are affected by the preconception of subjects. Therefore, physiological evaluation has an advantage in obtaining objective and quantitative results. However, it is known that it is hard to get unified results, because there are inter-individual differences in physiological responses. Our previous study showed that there observed inter-individual differences in physiological responses, even when subjects were exposed to the same light in the same space [3].

Subject's sensitivity to light exposure may be one of the reasons that mediate the inter-individual differences. We have explored a novel method to evaluate the sensitivity to light exposure, and also an effective physiological index which can be accounted for it [4]. We assumed that the higher the sensitivity to light, the higher the physiological responses to the change in light exposure condition. Thus, we conducted an experiment that measured the heart rate variability of the subjects while they were exposed to a periodical turn-on/turn-off of the illumination. The results showed that a physiological index obtained from the heart rate variability can be effective for the evaluation of the sensitivity. If the subject were sensitive to light, 1) he/she would response equally to the transition of lighting: turn-on and turn-off, 2) the intensity of the response would be large. Based on these assumptions, we can calculate how symmetric the responses were, and how intense each response was. In order to classify the subject's sensitivity into several groups, we plotted these values for each subject on a scatter diagram (Fig. 1). The results showed that there were some inter-individual differences in these values, suggesting that these values are effective to evaluate the subject's sensitivity to light exposure. However, our evaluation method for the sensitivity have not fully verified yet. The purpose of this study is to examine whether our evaluation method for the sensitivity can also account for the inter-individual differences in physiological responses under the same lighting condition.



**Figure 1. The classification diagram for the sensitivity to light exposure obtained from 23 subjects [4]. MDD and SoV are indices which describe how symmetric the responses were and how intense each response was, respectively. Two red dot lines show means of each value. If the subject is sensitive to light exposure, he/she is classified in the second quadrant (low MDD and high SoV).**

## 2. METHODS

### 2.1 Overview of our previous experiment

In the previous experiment, we explored the relationship between the activity of autonomic nervous system and subjective/physiological alertness for the short-wavelength and the long-wavelength lights at night [5]. In order to validate our evaluation method for the sensitivity, we used the vital data obtained from this experiment.

#### *Subjects*

Eight subjects in their twenties participated in the experiment. All subjects had normal color vision, and normal or corrected-to-normal visual acuity. Subjects filled out questionnaires about their sleep-wake behavior (Munich ChronoType Questionnaire, MCTQ) [6]. None of the subjects were classified as either extreme morning or extreme evening types. All subjects were instructed to refrain from taking alcoholic and caffeine-containing beverages in the experimental day. In addition, they were instructed to sleep more than six hours before the experiment.

#### *Lighting Conditions*

We used LEDCube (Thouslite Ltd., Changzhou, China) as a light source. It can alter the spectral power distribution of light with fifteen types of internal LEDs. There were three light conditions: short-wavelength ( $\lambda_{\max}=475[\text{nm}]$ ), long-wavelength ( $\lambda_{\max}=635[\text{nm}]$ ) and white light (CCT = 5000[K]). Figure 2 shows the spectral power distribution of each light condition measured with a spectroradiometer (CL-500A, KONICA MINOLTA INC., Japan). The illuminance was 80[lx] in all lighting conditions at desk level. Other characteristics of lighting are shown in Table. 1.

#### *Procedure*

All experiments were carried out in an experimental booth(120cm × 200cm × 200cm) at night (21:00-24:00). A desk and a chair was installed in the booth. The light source was placed on the ceiling above the desk. Prior to the experiment, subjects sat on the chair in front of the desk. Subjects were exposed to either short-wavelength, long-wavelength, or white light for 10 minutes after dark adaptation of 3 minutes. We measured the physiological responses of the subjects including heart rate variability during the experiment. For measuring heart rate variability, we used myBeat (WHS-1, UNIONTOOL CO., Tokyo, Japan). The subject put the sensor on his/her chest area using a strap with electrodes. The experiment under the white light condition was conducted once, while those under short-wavelength and long-wavelength light conditions were conducted

three sessions each. The experiments were conducted over four days. White light conditions were conducted on the first day, and short-wavelength and long-wavelength light conditions were conducted in random order from thereafter.

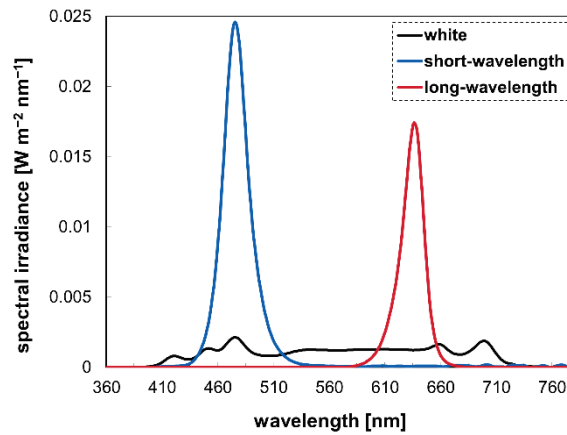


Figure 2. Spectral power distribution of each lighting condition

Table 1. The characteristics of each lighting condition

	short-wavelength	long-wavelength	white
(x,y)	(0.117,0.123)	(0.699,0.301)	(0.345,0.336)
Illuminance[lx]	80	80	80
Irradiance[W m <sup>-2</sup> ]	0.768	0.453	0.373
CCT[K]	-	-	5000
$\lambda_{\max}$ [nm]	475	635	475

#### Analysis for the heart rate variability

In order to clarify the transition of physiological responses during the experiment, we adopted a CSI as a physiological index. CSI is supposed to express the activity of the sympathetic nerve system [7]. It is calculated from the deviations from a diagonal line on a Lorenz plot, which was obtained based on the distribution of the successive RRIs (R-R intervals) during the experiment. When successive RRIs are expressed as  $RRI_k$  and  $RRI_{k+1}$ , the Lorenz Plot is obtained by plotting  $RRI_{k+1}$  against  $RRI_k$  (Fig. 3). CSI is calculated by following equation:

$$CSI = \frac{L}{T} \quad (1)$$

where  $L$  and  $T$  are four times of standard deviations for each diagonal line on the Lorenz plot. We calculated CSI of every one minute.

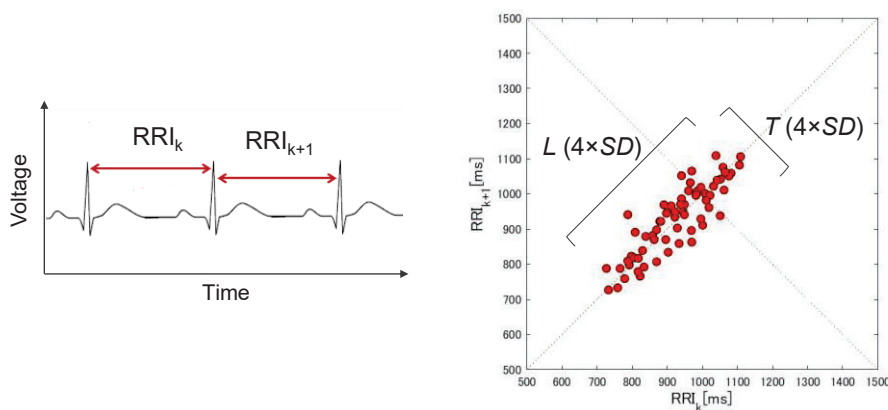


Figure 3. Example of Lorenz plot

## 2.2 Approach for the verification of our evaluation method

If the subject were sensitive to light, the trend of physiological responses without light exposure would differ from those with light exposure. Therefore, we made histograms of the CSI for each subject both during dark adaptation and during each light exposure condition. The histogram for the dark adaptation was obtained from CSI during dark adaptation in all lighting conditions. The histogram in each light condition was obtained from CSI for the first seven minutes during exposure to short- or long-wavelength light. Twenty-one data were used to make each histogram (dark adaptation: [3 minutes]  $\times$  [7 sessions], short-wavelength and long-wavelength: [7 minutes]  $\times$  [3 sessions]). Subject's CSIs were normalized for each subject before making the histograms. In addition, we quantified the difference of the trend in CSI with and without light exposure using the equation (2):

$$d = |\overline{CSI_{light}} - \overline{CSI_{dark}}| \quad (2)$$

where  $\overline{CSI_{light}}$  is the means of CSI during exposure to short- or long-wavelength light, and  $\overline{CSI_{dark}}$  is the means of CSI during dark adaptation in each subject.

We also thought that if our evaluation method were valid, there could be some correlation between the value of  $d$  and the index derived from our method. It was calculated for each subject by the equation (3):

$$E = \sqrt{w_x(x_i - x_0)^2 + w_y(y_i - y_0)^2} \quad (3)$$

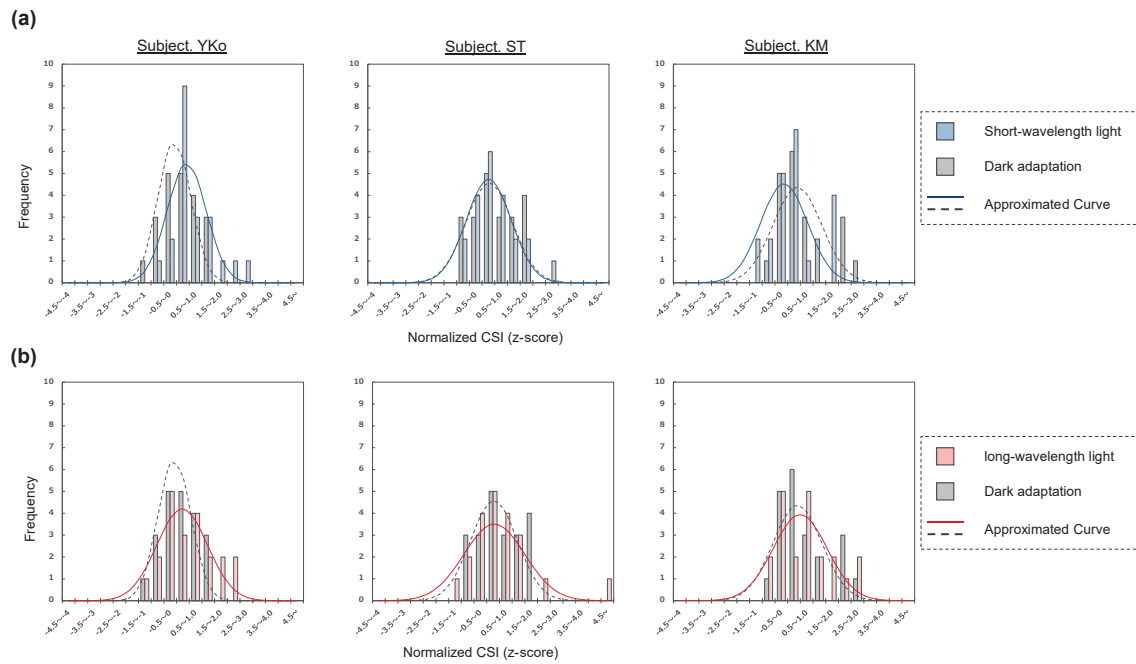
where  $x_i$  and  $y_i$  are the value of MDD and SoV of each subject, respectively. In this equation,  $x_0$  and  $y_0$  are the coordinates of the upper left point on the classification diagram shown in Fig. 1, and they were set to be 0 and 0.9, respectively. In addition,  $w_x$  and  $w_y$  were 1.  $E$  represents the euclidean distance of the data from the upper left point on the classification diagram. Therefore, the higher the sensitivity to light exposure, the lower the value of  $E$ . To validate our evaluation method, we examined the correlation between  $d$  and  $E$  for seven subjects.

## 3. RESULTS AND DISCUSSION

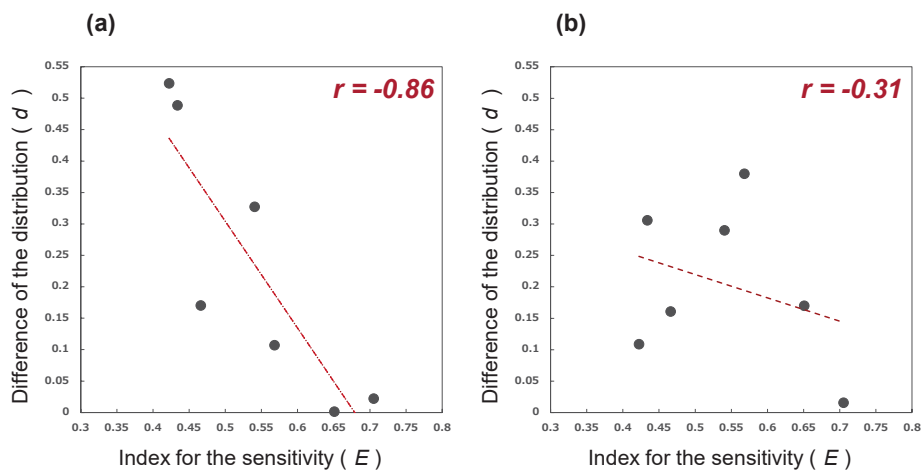
Figure 4 illustrates the histograms of the CSI for three subjects both during the dark adaptation and during the short-wavelength or the long-wavelength light exposure conditions. In this figure, gray bars show the histogram of CSI during the dark adaptation. Colored bars show the histogram of CSI during the short-wavelength or the long-wavelength light exposure conditions. In order to highlight the changes of the histogram, we plotted the approximated curves for each histogram. Black dot curves show the approximated curves for the histogram during the dark adaptation. Blue and red solid curves indicate the approximated curves for the histogram during the short-wavelength and the long-wavelength light conditions, respectively. The results showed that some subjects had different distribution of the CSI when they were exposed to the lights.

We plotted  $d$  against  $E$  for each subject on a scatter diagram (Fig. 5). The red dot lines represent the linear regression lines. In the short-wavelength condition (Fig. 5(a)), there was a strong negative correlation between  $d$  and  $E$  ( $r = -0.86$ ). This result indicates that the higher the sensitivity, the higher the difference of means in the CSI before and after light exposure, suggesting that our evaluation method can account for the inter-individual differences in physiological responses under the same lighting condition. On the other hand, we could not obtain similar results for the long-wavelength light condition ( $r = -0.31$ , Fig. 5(b)). These differences may be derived from the difference in irradiance between the short-wavelength and the long-wavelength light conditions. The irradiance of the short-wavelength light was about 1.7 times larger than that of the long-wavelength light. We thought that the irradiance of long-wavelength light was not intense enough to elicit the change of CSI, and this resulted in the trend in the small  $d$  overall subjects. That might be one of the reasons why strong negative correlation between  $d$  and  $E$  might not be obtained in the long-wavelength condition.





**Figure 4. Histograms of CSI during the dark adaptation and during the light exposure in three subjects. Panels (a) and (b) denote the conditions under the short-wavelength light and long-wavelength light, respectively.**



**Figure 5. Relationship between  $d$  and  $E$ . Panels (a) and (b) denote the conditions under the short-wavelength light and long-wavelength light, respectively.**

#### 4. CONCLUSION

In this study, we validate our evaluation method for the sensitivity to light exposure. We examined the correlation between the difference of means of the CSI obtained with and without light exposure and the index derived from our method. In conclusion, there was a strong negative correlation among these values, especially in short-wavelength light condition. It suggests that our evaluation method can account for the inter-individual differences in physiological responses under the same lighting condition. However, we validated our method using only the CSI. It would be necessary to examine the validity of our evaluation method for other physiological indices in future.

## REFERENCES

- [1] Michimori, A., Araki, K., Inbe, H., Hagiwara, H., Sakaguchi, T. Effects of Color Temperature of Light on the Alertness Level. (in Japanese). *Journal of the Illuminating Engineering Institute of Japan*, 1998, **82**(Appendix), 220.
- [2] Mukae, H., Sato, M. The effect of color temperature of lighting sources on the autonomic nervous functions. *The Annals of physiological anthropology*, 1992, **11**(5), 533–538.
- [3] Otsuka, T., Tashiro, T., Kawashima, Y., Nagai, T., Yamauchi, Y. Comparison of physiological response between LED and OLED during task execution. *Proceedings of CIE 2018*, 2018, 598-603.
- [4] Saito, T., Ohkubo, K., Yamauchi, Y. A study of individual differences in physiological response to light exposure. *The 11th Rajamangala University of Technology International Conference Book of Abstract*, 2022, 113.
- [5] Nanba, T., Ohkubo, K., Yamauchi, Y. Study of the effect of light on the alertness mechanism. (in Japanese). *Proceedings of Annual Conference of the Illuminating Engineering Institute of Japan*, 2021, 51.
- [6] Kitamura, S., Hida, A., Aritake, S., Higuchi S, Enomoto, M., Kato, M., Vetter, C., Roenneberg, T., Mishima, K. Validity of the Japanese version of the Munich ChronoType Questionnaire. *Chronobiology international*, 2014, **31**(7), 845–850.
- [7] Toichi, M., Sugiura, T., Murai, T., Sengoku, A. A new method of assessing cardiac autonomic function and its comparison with spectral analysis and coefficient of variation of R-R interval. *Journal of the Autonomic Nervous System*, 1997, **62**, 79-84.

## ACKNOWLEDGEMENTS

Corresponding Author Name: Taiki Saito  
Affiliation: Graduate School of Science and Engineering, Yamagata University  
e-mail: t222384m@st.yamagata-u.ac.jp

# COLOR APPEARANCE OF COLORED LIGHTING

Soonhyeng An, Youngshin Kwak\*

Dept. of Biomedical Engineering, Ulsan National Institute of Science and Technology,  
Ulsan, South Korea

## ABSTRACT

The color appearance of the colors that brighter than the reference white was investigated. Psychophysical experiment result conducted with 12 participants showed that the colored light tends to look more brighter and less colorful compared to CIELAB  $L^*$ ,  $C^*$  predictions.

Keywords: color appearance, colored light, lighting appearance

## 1. INTRODUCTION

Most of color appearance models such as CIECAM16 [1] are developed to predict the appearance of surface colors that are not brighter than the reference white. However, not only white light but also various colored lights are widely used nowadays though there is limited understanding of the appearance of the colors brighter than the reference white [2].

In this study, psychophysical experiments were conducted to compare the appearance of the colors that are brighter and more colorful than the surface colors with those of the surface colors.

## 2. PSYCHOPHYSICAL EXPERIMENT

12 participants with normal color vision took part in the experiment. To ensure accurate execution of the magnitude estimation for color appearance, participants were taken pre-training on the definitions and concepts of hue, brightness, and colorfulness using the Munsell student color set. An LCD with peak white of  $296 \text{ cd/m}^2$  was used in this experiment. A white color patch with a luminance of  $80 \text{ cd/m}^2$  with D65 chromaticity was used as the reference white for evaluating lightness, colorfulness, and hue. 53 color patches with luminance ranging from 0 to  $277.84 \text{ cd/m}^2$ , were presented as test colors. 26 colors within the DCI-P3 gamut at a reference white of  $80 \text{ cd/m}^2$  were classified as surface color, while 27 colors outside the gamut were classified as the lighting colors. After the adaptation time, each stimulus was shown for 2 seconds to participants, who were instructed to assign a numerical value representing their perceived brightness and colorfulness.

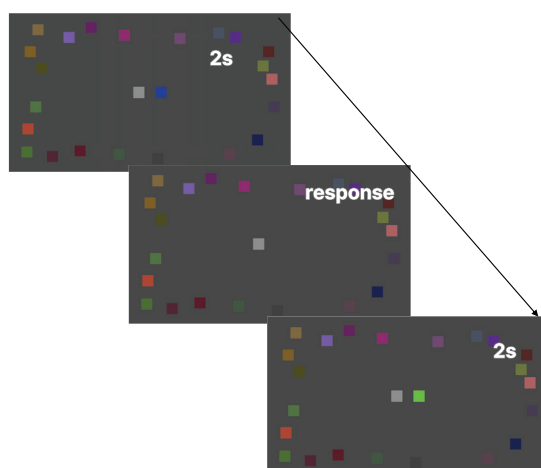


Figure 1. Configuration of color appearance scaling experiments.

For data analysis, geometric mean of the observers' responses was calculated and compared with CIELAB value of the color patches.

### 3. EXPERIMENTAL RESULT

Figure 2 compares the brightness scaling data with CIELAB  $L^*$  values and colorfulness scaling with CIELAB  $L^*$ . It is notable that CIELAB  $L^*$  aligns with the visual data for surface color but underestimates the lightness of colored lighting. On the contrary, in the case of colorfulness comparison, CIELAB  $C^*$  tends to overestimate colorfulness for colored lighting with higher chroma.

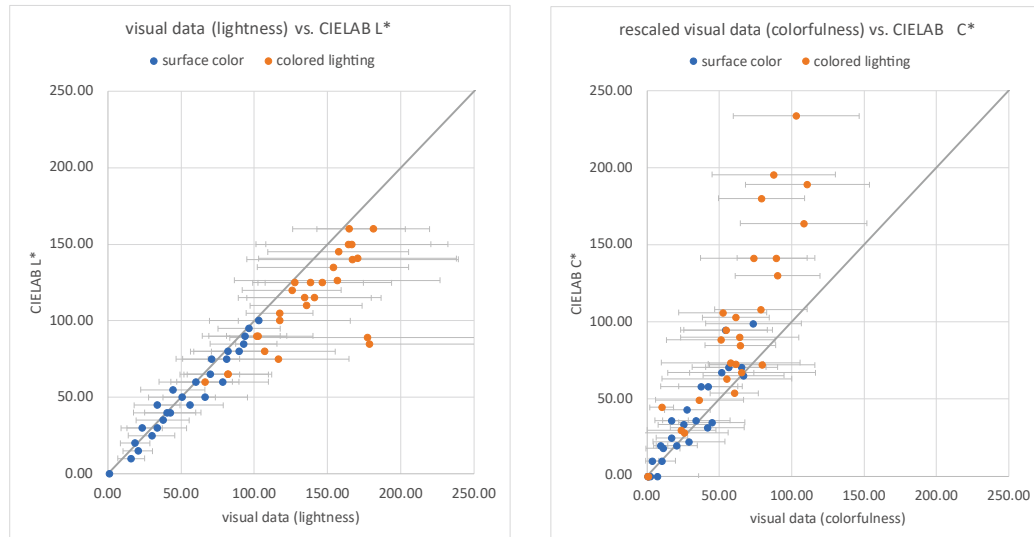


Figure 2. Comparison between visual data with CIELAB  $L^*$  (Left) and  $C^*$  (Right)

### 4. CONCLUSION

Color appearance of the surface and light colors are investigated using the magnitude estimation experiment. The experimental results based on 12 observers reveal distinct trends in the perception of lightness and colorfulness between surface color and colored lighting, while there is agreement in hue perception. While CIELAB reasonably predicts the perception of lightness and colorfulness for surface colors, CIELAB underestimate the brightness of colored lighting and overestimate its colorfulness. Therefore, it is suggested that further studies be made to develop color appearance models to predict the appearance of colored lighting more accurately.

### REFERENCES

- [1] CIE 248:2022 The CIE 2016 Colour Appearance Model for Colour Management Systems: CIECAM16
- [2] CHEN, Ping-Hsu; FAIRCHILD, Mark D.; BERNIS, Roy S. Scaling lightness perception and differences above and below diffuse white. In: Color and Imaging Conference. Society for Imaging Science and Technology, 2010. p. 42-48.

### ACKNOWLEDGEMENTS

This work were supported by Institute of Information & communications Technology Planning & Evaluation (IITP) grant funded by the Korea government(MSIT) (No.2021-0-00343, Development of metrology for the properties of reconstructed digital hologram's space and color)

Corresponding Author Name: Youngshin Kwak  
 Affiliation: Ulsan National Institute of Science and Technology  
 e-mail: yskwak@unist.ac.kr

# **HARNESSING SUNLIGHT FOR SUSTAINABLE URBAN FARMING: OPTIMIZING PHOTOVOLTAICS IN TROPICAL CONTAINER-BASED AQUAPONICS SYSTEMS**

Rui Xuan TENG, Szu-Cheng CHIEN, Andrew Keong NG

Engineering Cluster, Singapore Institute of Technology

## **ABSTRACT**

Currently, Singapore imports more than 90% of the food consumed. In order to be less reliant on external sources, Singapore aims to produce 30% of its nutritional needs by 2030 through alternative spaces for farming such as a Container-based Aquaponics System (CAS). This paper outlines the study into determining the optimal photovoltaics (PV) panel configuration on a CAS, which would ensure optimal daylight passing through and, as a result, allows for the favourable growth of crops. As these container-based aquaponics systems have yet to be implemented locally, the PV panel design of this CAS was studied and developed with reference to overseas case studies. A comprehensive review of the relevant case studies and lighting parameters such as Photosynthetic Photon Flux Density (PPFD) and Daily Lighting Integral (DLI) was performed, followed by a site investigation to examine if the conversion factor is influenced by the climate classification, sky conditions, and sunlight spectrum changes. The modelling process was carried out in Revit and Rhino, whereas the simulation processes were conducted with ClimateStudio. Based on the analysis and comparison of the research findings, the ideal container arrangement and PV installation (involving the transparency rate and tilt angle) that promoted the favourable growth of the crops was then recommended. Through this paper, the benefits of the CAS were studied; it was found that the CAS could increase crop yield towards the goal of food security. The findings from this study can provide a valuable basis for designing container-based aquaponics systems in metropolitan contexts with tropical climates, such as Singapore and other densely populated cities in Southeast Asia. By offering insights into optimizing daylight use and PV panel configurations, this research has the potential to increase the feasibility and efficiency of such systems in these regions. As a result, it contributes to the pursuit of sustainable urban farming and underscores the importance of alternative farming spaces in fostering a more self-reliant and environmentally conscious future.

**Keywords:** Aquaponics, Container-based aquaponics system, Tropical urban farming, Photovoltaics optimization, Sustainable agriculture, Daylight simulations

## **1. INTRODUCTION**

In Singapore, where agricultural land is limited, it imports more than 90% of its food supply from over 170 countries and regions [1]. The local agri-food sector in 2021 mainly consisted of farms that produced hen shell eggs, vegetables and seafood which accounted for up to 30%, 4% and 8% respectively of the total local food consumption [2]. Despite this, the country is still susceptible to emerging trends. Projection estimates that by 2050, global food demand will increase by 50% due to population growth [2]. The effects of climate change, including unpredictable weather patterns and loss of arable land, will also add stress to the global food supply [2]. Besides, the COVID-19 pandemic, which led to lockdowns in many countries, has highlighted the vulnerability of Singapore's reliance on imported food. As a result, the amount of locally produced food is insufficient to meet the needs of the country. Despite Singapore's efforts to boost local food production through urban farming and reduce its dependence on imports, the country continues to face challenges in optimizing crop yield due to the limited availability of agricultural land and the dynamic weather conditions in the country. Lighting plays a crucial role in agriculture, yet its effectiveness is hindered by the ever-changing weather conditions in Singapore. Thereby, this paper aims to simulate and analyze the container-based aquaponics system (CAS) design variations to determine the ideal configuration and specifications of the photovoltaic (PV) systems that will allow optimal light to pass through, ultimately maximizing crop yield.



## 2. METHODOLOGY

### 2.1 SITE

The proposed CAS at the Dover Campus of Singapore Institute of Technology in Singapore benefits from its surroundings, as seen in Figure 1, which depicts a dense vegetation cover that helps mitigate the Urban Heat Island effect not only on campus but also in the nearby areas.

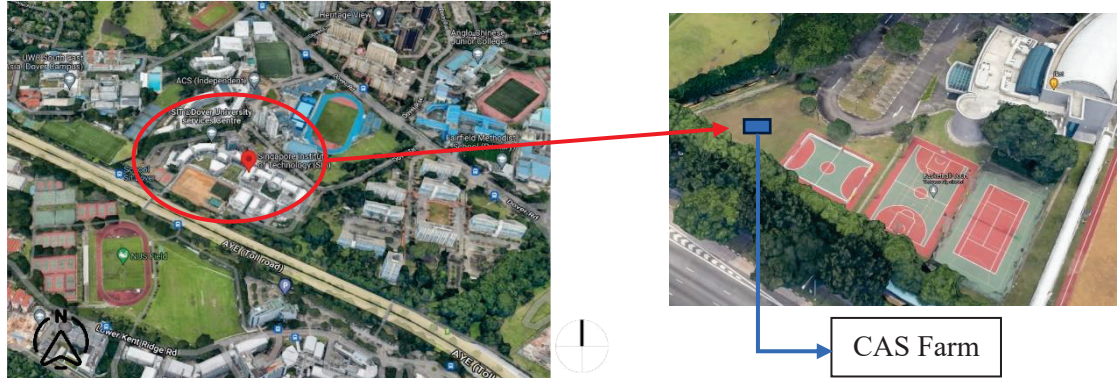


Figure 1. Google Maps images depicting the site context at SIT@Dover Campus in Singapore.

The campus features limited high-rise buildings and structures, primarily concentrated in the northern direction. Consequently, the impact on daylight exposure is minimal, with the sun's movement from east to west. To optimize sunlight access, careful consideration should be given to the placement of the CAS. Since it is positioned at ground level, it is advisable to select an open space where the crops can receive direct sunlight throughout the day, taking advantage of the farm's lower elevation compared to the campus buildings.

### 2.2 DESIGN SPECIFICATIONS OF THE CAS MODEL

The CAS design involves the vertical arrangement of two 20-foot shipping containers. The lower container houses the aquaculture, while the upper container accommodates the hydroponics. Modifications to the top container include replacing the aluminium cladding on the sides with mesh netting and substituting the top cover with polycarbonate material. Additionally, PV panels are added to the CAS structure. The CAS model adheres to the dimensions of a standard 20-foot storage container, measuring 2.6 m in height, 2.4 m in width, and 6.1 m in length. Initial simulations were conducted, excluding the PV panels and staircase, to obtain the PPFD and DLI values. These measurements are compared to the readings obtained during simulations, providing a benchmark for subsequent simulations and analysis. Specifically, this paper focuses on two primary configurations of PV modules. The first configuration, as shown in Figure 2, comprises a singular structure of six smaller PV modules arranged in a modular design. The second configuration, as depicted in Figure 3, comprises two structures consisting of three PV modules each. The conventional PV and Building-Integrated Photovoltaics (BIPV) with a visual transmittance rate of 50%, are compared and contrasted in this paper.

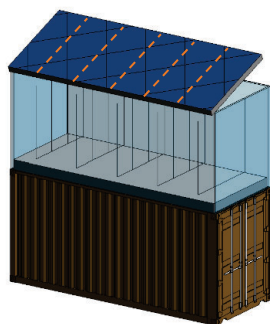


Figure 2. Configuration 1 - 1 PV

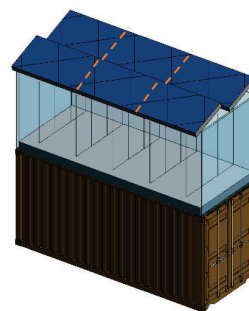


Figure 3. Configuration 2 - 2 PV

The orientation of the CAS is designed to maximize sunlight exposure for the crops throughout the day, with the longer sides facing North and South and the shorter ends facing East and West [3]. Furthermore, in accordance with the Building and Construction Authority Singapore, the PV modules are tested at a 10° inclination angle [3].

## 2.2 COMPUTATIONAL SIMULATION TOOLS

The models were constructed in Revit 2020 and Rhino 7, while the simulations were carried out using ClimateStudio. ClimateStudio is an advanced daylighting, electric lighting and conceptual thermal simulation software created by Solemma LLC. It facilitates a number of environmental analysis workflows for buildings and neighbourhoods, such as annual illuminance simulations and point-in-time illuminance simulations [4]. Rhinoceros, also known as Rhino, is a computer-aided design software programme. The daylighting simulations for this project would be run in Rhino 7 using the Climate Studio plugin for Rhino 3D.

The simulations were configured for the date of September 21<sup>st</sup> (Autumn Equinox) on Climate Studio, corresponding to the period of the September equinox. During this period, the sun is positioned directly above the equator, resulting in equal durations of day and night [5]. Given Singapore's proximity to the equator, sunlight in the region experiences higher degree of scattering and diffraction, leading to a less intense and more diffused quality of light compared to other days [6]. Table 1 provides an overview of the designated simulation parameters, while Table 2 outlines the settings for path-tracing.

Table 1. Simulation Parameters

Time	0700 – 1900 (Measurements were recorded at regular one-hour intervals over a 12-hour duration)
Sky Conditions	CIE Clear, CIE Intermediate, CIE Overcast
PV Module Dimensions	2580mm x 1080mm (Module), 158.75mm x 158.75mm (PV Cells)
Visual Transmittance Rates	0% (Opaque), 50% (BIPV), 100% (Empty)
Tilt Angle	10°

Table 2. Path-Tracing Settings

Sample per pass	64
Maximum number of passes	10
Ambient bounces	6
Weight limit	0.01
Acceleration Device	Intel(R) Core(TM) i7-10510U

## 2.3 PERFORMANCE METRICS FOR DAYLIGHTING

### 2.3.1 PHOTOSYNTHETIC PHOTON FLUX DENSITY

Photosynthetically Active Radiation (PAR) is a term used to describe the range of wavelengths between 400-700nm, which is vital for photosynthesis and plant growth [7]. Instead of measuring the total light, PAR can aid farmers in determining the specific type and quantity of light needed to optimize crop yield and health. Conversely, Photosynthetic Photon Flux (PPF) is a metric that measures the number of moles of PAR generated by a light source in a second [8]. Meanwhile, the term Photosynthetic Photon Flux Density (PPFD) incorporates both PPF and surface area, measuring the number of PAR photons that fall on a specific area, expressed in micromoles per square meter per second ( $\mu\text{Mol}/\text{m}^2/\text{s}$ ) [8].

After examining various literature reviews [9], it can be concluded that the conversion factor from Lux to PPFD typically falls between 0.017 to 0.02, with any differences being insignificant. Additionally, a site investigation utilising the Asensetek Lighting Passport Pro confirmed that the conversion factor remains within the range of 0.017 to 0.02, regardless of the sky conditions and sunlight spectrum changes. As such, a conversion factor of 0.0185 are employed in this paper.

Equation 1. Converting Lux to PPFD

$$PPFD = \text{Lux} \times 0.0185$$

Asian greens, such as Kai Lan and Nai Bai, typically require a PPFD between 200 and 300 ( $\mu\text{Mol}/\text{m}^2/\text{s}$ ) [10]. Moreover, when cultivated under a higher PPFD of more than 300 ( $\mu\text{Mol}/\text{m}^2/\text{s}$ ), these plants manifested greater leaf thickness and larger leaf area than those grown under a lower PPFD [10].

### 2.3.2 DAILY LIGHTING INTEGRAL

The total amount of photosynthetically active photons accumulated in a square meter throughout the day is represented by the daily lighting integral (DLI). The duration and intensity of light determine it, and it is expressed as a mole of light per square meter per day ( $\text{mol}/\text{m}^2\cdot\text{day}$ ) [11].

To calculate DLI, the PPFD is typically measured in ( $\mu\text{Mol}/\text{m}^2/\text{s}$ ) as it changes throughout the day. This information is then used to approximate the number of photons falling within the PAR range that a specific area receives over a 24-hour timeframe [12]. The conversion formula from PPFD to DLI used in this paper is [13]:

Equation 2. DLI Formula

$$DLI = \frac{PPFD \times (3.6 \times 10^3) \times \text{Light Hours per day}}{10^6}$$

For Asian Greens, the typical DLI ranges between 6 to 18 ( $\text{mol}/\text{m}^2\cdot\text{day}$ ) [14]. However, the farm industry partners have also indicated that for optimal growth, an ideal DLI range would be between 10 to 20 ( $\text{mol}/\text{m}^2\cdot\text{day}$ ).

## 3. RESULTS AND DISCUSSIONS

### 3.1 EMPTY MODEL

Figure 4 illustrates the recorded PPFD readings under three different sky conditions: CIE Clear, CIE Intermediate, and CIE Overcast. In all three conditions, the PPFD value begins at a low level in the morning, gradually increases and reaches its peak at 13:00. From there on, the PPFD values gradually decline.

Table 3 presents the tabulated PPFD and DLI values for all three sky conditions. Similar to the PPFD values, it is evident that the DLI results under CIE Intermediate and CIE Overcast sky conditions are significantly lower compared to those obtained under CIE Clear sky conditions. These findings will serve as a reference for subsequent simulations and analysis.

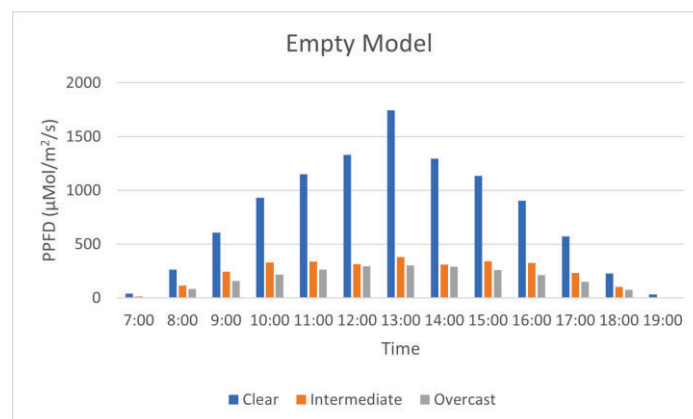


Figure 4. Recorded PPFD Values for Empty Model

Table 3. Recorded PPFD and DLI Values for Empty Model

PPFD ( $\mu\text{Mol}/\text{m}^2/\text{s}$ )	EMPTY		
	Clear	Intermediate	Overcast
Time			
7:00	42	14	8
8:00	265	117	86
9:00	607	244	157
10:00	933	331	219
11:00	1,150	340	266
12:00	1,333	313	294
13:00	1,745	380	304
14:00	1,298	311	293
15:00	1,136	342	261
16:00	906	326	213
17:00	573	234	151
18:00	230	104	78
19:00	35	8	0
<b>Average PPFD</b>	789	236	179
<b>DLI (<math>\text{mol}/\text{m}^2\cdot\text{day}</math>)</b>	34	10	8

### 3.2 CONVENTIONAL PV & BIPV

To assess the impact of conventional opaque PVs on light penetration, a series of simulations were conducted using these PVs in the project scenario. These PVs, unlike the transparent ones, prevent light from passing through.

Figure 5 presents the recorded PPFD readings under the three different sky conditions for the 1 PV configuration, while Figure 6 showcases the readings for the 2 PV configuration. Although there are no significant differences between the PPFD and DLI values between the two configurations, both exhibited a notable decrease compared to the empty model. The utilization of opaque conventional PVs resulted in the absence of direct sunlight, with all light sources being diffused solar radiation. This suggests that these conventional PVs significantly obstruct direct sunlight, leading to an observed drop in PPFD and DLI values.

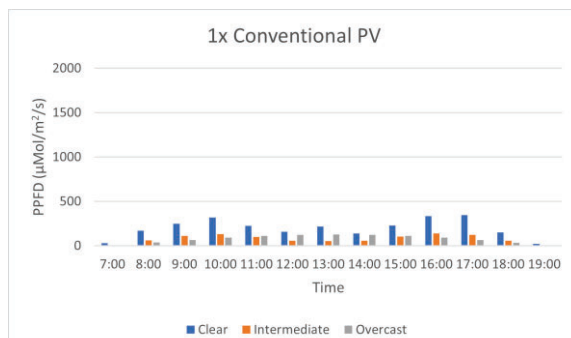


Figure 5. Recorded PPFD Values at 1x Conventional PV Configuration

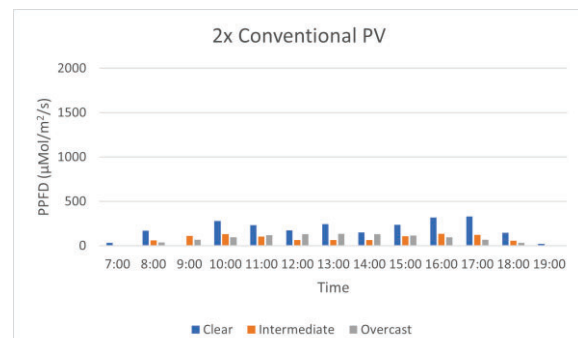


Figure 6. PPFD Readings at 2x Conventional PV Configuration

Furthermore, the average PPFD and DLI values, as seen in Table 4, cannot meet the requirements suggested for optimal crop growth.

This paper also examines another variation, namely the BIPVs with a visual transmittance rate of 50%, as depicted in Figure 7 and Figure 8. By analysing the results in Table 4, it is evident that the BIPVs closely resemble those of the empty structure, in contrast to the conventional PVs.

The BIPVs, with their higher visual transmittance rate, allow for greater light penetration, resulting in PPFD and DLI values that align more closely with the empty structure. This suggests that BIPVs with a 50% visual transmittance rate offer a promising alternative to conventional PVs, minimizing the light-blocking effect and maintaining favourable light levels for crop growth.

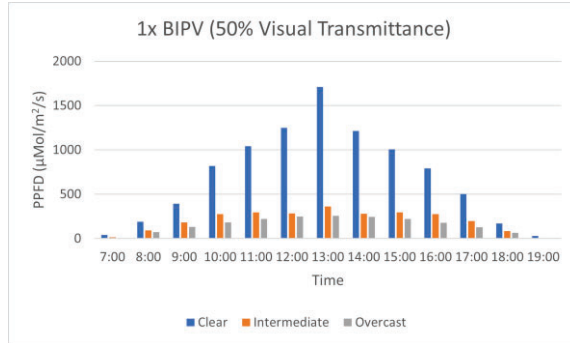


Figure 7. PPFD Readings at 1x BIPV (50% Visual Transmittance Rate) Configuration

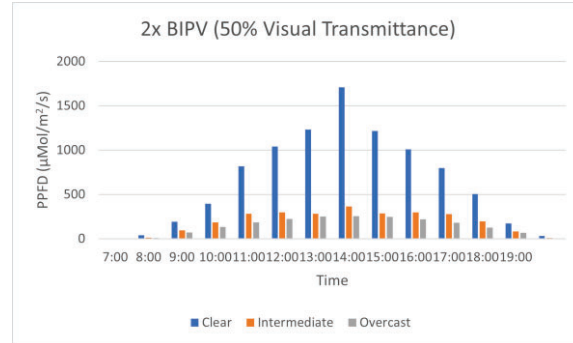


Figure 8. PPFD Readings for 2x BIPV (50% Visual Transmittance Rate) Configuration

Table 4. Recorded PPFD and DLI Values

PPFD ( $\mu\text{Mol}/\text{m}^2/\text{s}$ )	1 PV Configuration						2 PV Configuration					
	Conventional PV / $10^\circ$			BIPV / $10^\circ$			Conventional PV / $10^\circ$			BIPV / $10^\circ$		
	C	I	O	C	I	O	C	I	O	C	I	O
	Time											
7:00	31	8	3	41	13	7	32	8	4	41	13	7
8:00	169	62	36	192	92	72	169	63	38	193	93	72
9:00	248	111	66	394	181	132	0	110	70	394	184	132
10:00	318	133	92	818	276	184	281	132	97	818	280	183
11:00	225	99	112	1,042	296	222	235	105	119	1,041	296	222
12:00	158	57	125	1,248	285	247	173	64	130	1,232	282	249
13:00	216	52	129	1,711	363	255	246	65	135	1,709	363	255
14:00	139	57	124	1,213	280	246	152	64	130	1,215	284	246
15:00	228	103	110	1,007	296	220	237	109	116	1,009	297	219
16:00	334	137	90	794	278	179	318	136	95	796	277	179
17:00	346	125	64	503	199	127	332	123	67	504	197	127
18:00	149	56	33	170	84	65	149	57	34	171	84	65
19:00	21	4	0	30	7	0	22	4	0	30	7	0
Average PPFD	199	77	76	705	204	150	180	80	79	704	204	150
DLI	9	3	3	30	9	6	8	3	3	30	9	7

Upon analysing the results, it can be observed that there were minimal differences between the 1 PV and 2 PV configurations, regardless of whether conventional PVs or BIPVs were used. However, the PPFD and DLI readings showed a closer alignment with the data obtained from the empty structure.



Specifically, under the CIE Clear sky conditions, the DLI values have met the recommended threshold for optimal crop growth. Although under the CIE Intermediate and CIE Overcast sky conditions, the DLI readings fell slightly short of the suggested values, it is important to note that in a dynamic environment where sky conditions constantly change, crops are still likely to thrive within the optimal DLI range.

### 3.3 RECOMMENDATIONS

Based on the analysis of the simulation results, it is highly recommended to select BIPVs with a visual transmittance rate of 50% and a tilt angle of 10° in the first configuration (1 PV) due to two key factors.

#### Construction Complexity

While the recorded PPFD and DLI readings exhibit a comparable performance between the two configurations (1 PV and 2 PVs), the construction complexity varies significantly. Opting for the 1 PV variation involves modularly combining six BIPVs to form a single large PV module, which can be conveniently mounted at the top of the structure. In contrast, the 2 PVs variation requires the repetition of combining three BIPVs into one module, resulting in two PV modules that need to be mounted above the structure. This significantly increases the intricacy of the construction process, adding unnecessary complications.

#### General Maintenance

To maintain optimal performance, regular cleaning and maintenance are vital to remove accumulated dirt and debris from the PV panels, especially after storms or prolonged dry spells. The practicality of maintenance tasks is an important consideration, and it is worth noting that it is generally more convenient to clean and maintain a single large PV module compared to dealing with two separate PV modules.

By selecting BIPVs with a visual transmittance rate of 50% and a tilt angle of 10° in the 1 PV configuration, not only does it offer comparable performance to the 2 PV configuration, but it also simplifies the construction process and streamlines maintenance procedures. These factors contribute to the overall effectiveness, efficiency, and long-term viability of the CAS design, ensuring an optimized solution for sustainable crop production.

### 4 CONCLUSIONS

In conclusion, this study has developed a methodological framework for evaluating daylight availability in a CAS and conducted systematic simulations to optimize the CAS design. Future works include investigating the impact of the ventilation profile on crop yield to further enhance the CAS performance and productivity.

### REFERENCES

- [1] Singapore Food Agency, "30 by 30 - Strengthening our food security," 26 May 2022. [Online]. Available: <https://www.ourfoodfuture.gov.sg/30by30>.
- [2] Singapore Food Agency, "Our Singapore Food Story," 17 February 2022. [Online]. Available: <https://www.sfa.gov.sg/food-farming/sgfoodstory/our-singapore-food-story-the-3-food-baskets>.
- [3] Building and Construction Authority, "Green Handbook - Photovoltaic (PV) Systems in Buildings," [Online]. Available: [https://www.bca.gov.sg/greenmark/others/pv\\_guide.pdf](https://www.bca.gov.sg/greenmark/others/pv_guide.pdf).
- [4] Solemma, "Welcome to the ClimateStudio User Guide," 2020. [Online]. Available: <https://climatestudiodocs.com/>.

- [5] The Editors of Encyclopaedia Britannica, 2014. [Online]. Available: <https://www.britannica.com/science/autumnal-equinox>. [Accessed 2023].
- [6] Cleveland, Ohio Weather Forecast Office, "The Seasons, the Equinox, and the Solstices," [Online]. Available: <https://www.weather.gov/cle/Seasons#:~:text=At%20the%20equator%2C%20the%20sun,sun%20is%20below%20the%20horizon..> [Accessed 2023].
- [7] S. Mosharafian, S. Afzali, G. M. Weaver, M. v. Iersel and J. M. V. , "Optimal lighting control in greenhouse by incorporating sunlight prediction," 28 May 2020. [Online]. Available: <https://doi.org/10.1016/j.compag.2021.106300>.
- [8] D. O. Hall and K. Rao, Photosynthesis, 1999.
- [9] I. Ashdown, "Photometry and Photosynthesis," 10 December 2014. [Online]. Available: <https://www.allthingslighting.org/tag/lighting-fundamentals/>.
- [10] P. K. D. T. Alahakoon, "Productivity, photosynthesis and nitrogen metabolism of various leafy vegetables grown aeroponically under different combinations of light-emitting diodes (LEDs)," 2016. [Online]. Available: <https://repository.nie.edu.sg/handle/10497/22434>.
- [11] A. P. Torres and R. G. Lopez, "Measuring Daily Light Integral in a Greenhouse," 2010. [Online]. Available: <https://www.extension.purdue.edu/extmedia/ho/ho-238-w.pdf>.
- [12] P. C. Korczynski, J. Logan and J. E. Faust, "Mapping Monthly Distribution of Daily Light Integrals across the Contiguous United States," 2022.
- [13] V. Kollin and T. Nowell, "Battery Powered Adaptive Grow Light System Aiming at Minimizing Cost and Environmental Impact from Electricity Use," [Online]. Available: <https://www.diva-portal.org/smash/get/diva2:1670120/FULLTEXT02>.
- [14] N. Mattson, "Growing Hydroponic Leafy Greens," October 2016. [Online]. Available: <https://gpnmag.com/article/growing-hydroponic-leafy-greens/>.

## ACKNOWLEDGEMENTS

This research is supported by the Ministry of Education, Singapore, under its MOE Translational R&D and Innovation Fund (TIF) (MOE-MOE\_TIF-0009).

Corresponding Author Name: Rui Xuan TENG  
Affiliation: Singapore Institute of Technology  
e-mail: 1901955@sit.singaporetech.edu.sg

Corresponding Author Name: Szu-Cheng CHIEN  
Affiliation: Singapore Institute of Technology  
e-mail: SzuCheng.Chien@Singaporetech.edu.sg

Corresponding Author Name: Andrew Keong NG  
Affiliation: Singapore Institute of Technology  
e-mail: Andrew.Ng@SingaporeTech.edu.sg

# ANALYSIS OF TRANSMITTANCE BY LED WAVELENGTH TO IMPROVE ROAD LIGHTING VISIBILITY IN FOG CONDITIONS

Ji-myung Kim\*, Sung-gi Chae\*, Young-ju Cho\*, Meeryoung Cho\*, An-seop Choi\*\*

Korea Photonics Technology Institute (KOPTI)\*, Sejong University\*\*

## ABSTRACT

The purpose of this study is to find the best road lighting spectral distribution for foggy conditions. As a result of analysis, the visibility of each wavelength band in the fog situation targeting the currently used street light, the fog transmittance increased as the long wavelength regardless of the street light color. For future studies, in order to increase the accuracy of the test results, it is planned to secure data on the radiant flux reduction rate by wavelength through experiments on various fog generation conditions and lighting fixtures of various colors in the future.

Keywords: fog, road lighting, radial flux decreasing rate

## 1. INTRODUCTION

Road lighting plays a role in helping driving by recognizing the lanes of the road and the shape of the road through the light emitted from lighting fixtures not only at night when there is no light, but also in environments where it is difficult to secure visibility due to tunnels and specific weather conditions. However, it is difficult to secure forward visibility in foggy conditions, increasing the risk of traffic accidents. Therefore, it is necessary to develop a light source to secure the driver's visibility in a foggy environment.

This study aims to secure basic data for the development of light sources suitable for fog conditions by analyzing the spectral power reduction rate by wavelength in fog conditions by color temperature of lighting fixtures.

## 2. METHODS

### 2.1 Measurement overview



In this study, measurements were performed using a smog generator and a steam generator made of actual moisture particles to reproduce the fog situation. The LED lighting used is a module that can be changed to Cool White (correlated color temperature 4,800K) and Warm White (correlated color temperature 3,000K) in one module, and the correlated color temperature variable is driven by turning on/off each different LED PKG. The measurement conditions were set as in Table 1.

**Table 1. Measurement conditions**

	Fog generation method	Visibility distance measurement result		measurement space
		No fog	Fog	
CASE 1	Smog	2400m	50m	large dark room (W120m*D20m*H13m)
CASE 2	Steam	2400m	50m	small chamber (W3m*D3m*H2m)
Used Equipment		Visibility system: Biral SWS-100 Measuring equipment: Spectroradiometer (CL-500A)		

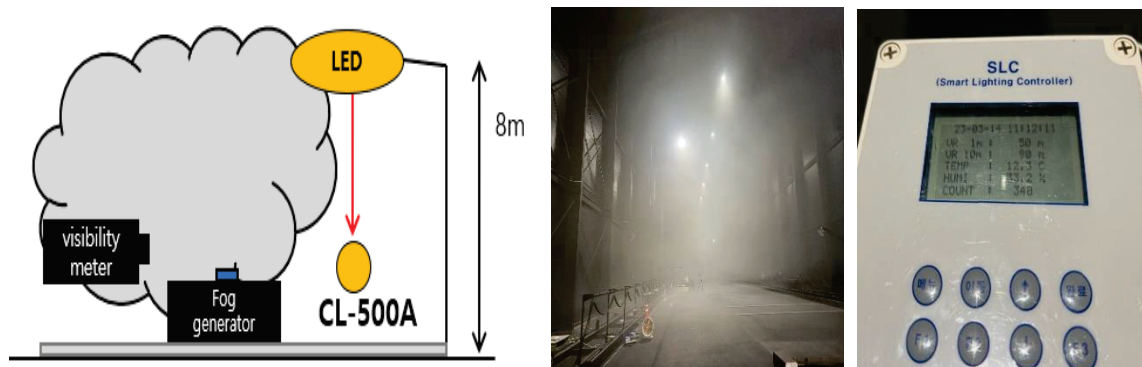
The characteristics of the light source used in the study are as follows in Table 2.

**Table 2. Optical characteristics analysis**

	Color temperature conversion LED PKG	
	3,000K	5,000K
Measurement image		
Luminous flux (lm)	1,515	1,494
Efficiency (lm/W)	65.29	63.69
Power Factor	0.96	0.96
Correlated color temperature (K)	3,015	5,018

## 2.2 Case 1: Smog generation method

The measurement using the smog generator reproduced the fog generation situation in the large dark room, and the visibility distance was confirmed by installing the visibility meter. In order to measure the radiant flux reduction rate by wavelength in the fog situation, a spectral irradiance meter (CL-500A) was installed at an interval of 8m directly below the lighting, and the spectrum for each color temperature was repeatedly measured 10 times before and after the fog situation, and the average value of the radiant flux for each wavelength compared.



**Figure 1. The measurement method using a smog generator**

## 2.3 Case 2: Steam generation method

The measurement using the steam generator reproduced the fog generation situation in a small chamber, and the visibility distance was confirmed by installing a visibility meter. In order to measure the radiant flux reduction rate by wavelength in the fog situation, a spectral irradiance meter (CL-500A) was installed at a distance of 1 m from the lighting, and the spectrum for each color temperature was repeatedly measured 10 times before and after the fog situation, and the average value of the radiant flux per wavelength was measured compared.

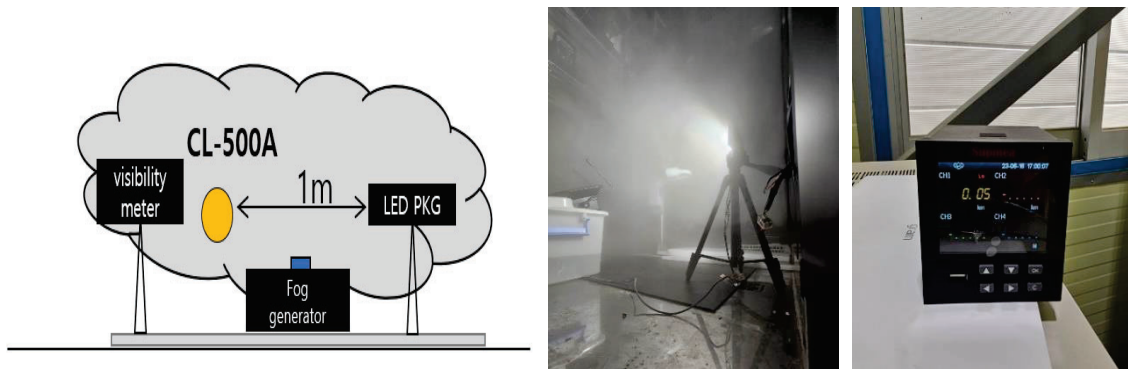


Figure 2. The measurement method using a steam generator

## 2.4 Measurement results

As a result of analyzing the reduction rate by the wavelength of radiant flux by reproducing the fog situation using the smog generator in case 1, It was confirmed that the longer the wavelength from 410 to 720(nm), the smaller the radiant flux decreases. However, 360~409 [nm] and 720~780 [nm] were excluded due to the significant deviation from the small measured radiant flux. And it was confirmed that Warm White had a higher reduction rate than Cool White.

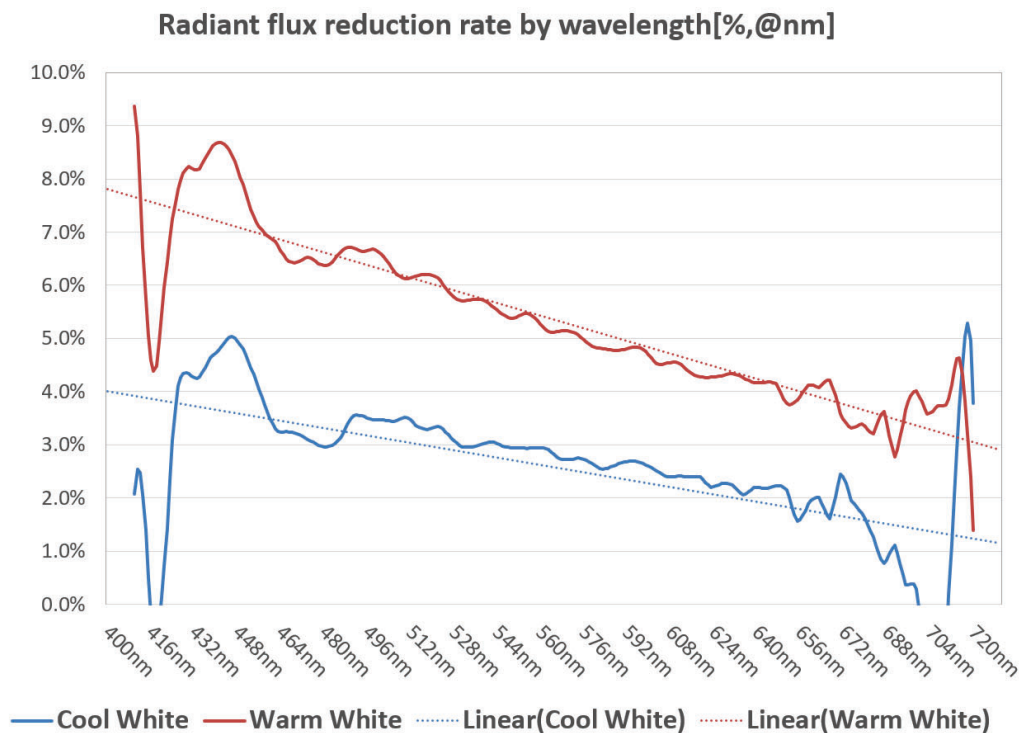
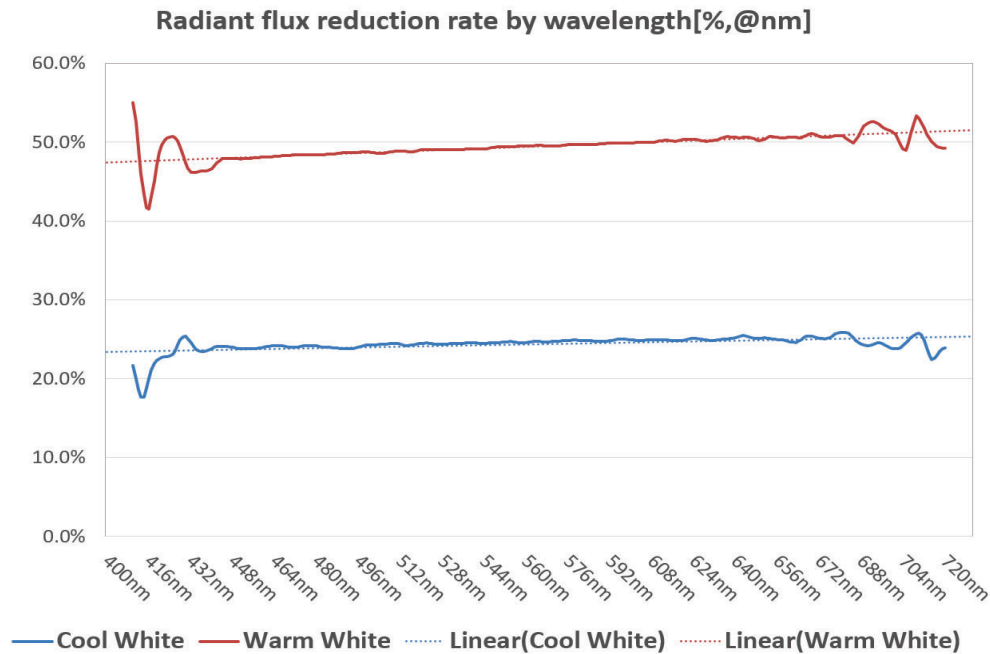


Figure 3. Radiant flux reduction rate graph using smog generator method

As a result of reproducing and analyzing the fog situation using the steam generator of case 2, it was shown that the radiant flux decreased at a constant rate in the wavelength range from 400 to 688 [nm]. The steam generator was also excluded from 360~409 [nm] and 720~780 [nm] due to the significant deviation due to the small amount of radiant flux measured. Contrary to case 1, it was confirmed that the reduction rate of Cool White was higher than that of Warm White.





**Figure 4. Radiant flux reduction rate graph using the steam generator method**

### 3. CONCLUSION

As a result of this study, in the smog generation method, regardless of color temperature, the longer the wavelength, the lower the radiant flux reduction rate, and it showed the characteristic of increasing the fog transmittance. However, a constant decreasing rate was maintained in the steam generation method. This difference in the rate of decrease occurred as a result of the difference in scattering characteristics of the smog-type particles used to reproduce the fog and the moisture particles of the steam-type method.

However, this paper is the result of a preliminary experiment measured using only two fog setting conditions and two correlated color temperature settings, respectively. Therefore, future studies are planned to supplement the experimental results by comparing the difference in Mie scattering characteristics with various conditions of fog density, particles, and correlated color temperature.

### REFERENCES

- [1] Ki Ho Nam, Chung Hyeok Kim, A Research on the Improvement of Visivility Using Low Deck Lighting in Bad Weather, J, Korean Inst. Electr. Electron. Mater. Eng. Vol.33, No.3, pp. 186-193, 2020

### ACKNOWLEDGEMENTS

Funding: This research was supported by an Institute of Information & Communications Technology Planning & Evaluation (IITP) grant funded by the Korea government (MSIT, MOIS, MOLIT, MOTIE) (No. 2020-0-00061, Development of integrated platform technology for fire and disaster management in underground utility tunnel based on digital twin).

This work was supported by the Korean Agency for Technology and Standards(KATS)(Contract No.00238178500, The de facto international standardization support and trend survey, 2023)

Corresponding Author Name: Ji-Myung Kim  
Affiliation: Korea Photonics Technology Institute (KOPTI)  
e-mail: sinji1230@kopti.re.kr

# Experiment of Healing Light For Sleep and Moods Relievement During Polar Night In South Pole Expediton Station

## ABSTRACTS:

**OBJECTIVES:** This experiment is a healing light experiment for the physical and mental stressful environment in the Antarctic station area. The main purpose of this experiment is to provide evidence for the regulation of the emotions and rhythms of the research team members at the Zhongshan Station during the polar night through the adjustment of indoor morning light and bedtime light. We propose light that is conducive to the physical and mental health of the explorers.

**METHOD:** A total of 8 young male subjects (aged 28-46 years) of the Zhongshan Station wintering crew were recruited and exposed to light for 2 consecutive weeks during the polar night. A within-group comparison experimental design was used, with the status quo baseline collection in week 1, using the status quo light pattern. In week 2, morning bright light stimulation and night time dark light protection were used, and salivary melatonin, interview questionnaire, state of mind scale, seasonal behaviour pattern questionnaire, the Self-rated Depression Scale (SDS), and sleep scale were collected from the scientists. Based on the subjective and objective data, the sleep and mood trends of the subjects were evaluated comprehensively.

**RESULTS:** The results showed that the length of sleep increased, the number of awakenings decreased, the latency to fall asleep, the time to wake up and the time to leave bed were all reduced, and the quality of sleep improved on the 14th day of the experiment. This indicates that light exposure was helpful in improving sleep quality and increasing sleep duration. By analysis of melatonin concentrations, at 7:00 am, day 14 was significantly lower relative to days 5 and 7 ( $p < 0.05$ ); at noon, day 14 was significantly lower relative to days 6 and 7, day 13 was significantly lower relative to day 6, and day 12 was significantly lower relative to days 5 and 7 ( $p < 0.05$ ); at 18:00 pm, day 7 was significantly elevated ( $p < 0.05$ ); at 20:00, day 14 was significantly higher relative to day 12 ( $p < 0.05$ ); and at 22:00, day 13 was significantly higher relative to day 7 ( $p < 0.05$ ). There was a significant trend of decrease in the scores of the Self-rated Mood Scale (POMS) on days 1 and 7, days 1 and 14 during the experiment, and a trend of decrease in the scores of the Self-rated Depression Scale (SDS) during the experiment, demonstrating that light changes contribute to mood regulation.

**CONCLUSION:** Indoor morning light and bedtime light combination helped to improve the sleep quality and sleep duration of the polar scientist, and reduced the number of wakings, sleep latency, awakening time, and time out of bed. This indicates that light is helpful in improving sleep quality and increasing sleep duration. The combination of light exposure was able to enhance the alertness of the scientist during the day, while the melatonin secretion was promoted at night. The subjects' emotional dimensions of depression, anger, tension, panic, and fatigue tended to decrease, which helped to improve negative emotions.

Key words: Healing Light, evidence-based experiments, circadian and sleep, mood reliefment

## 1. INTRODUCTION

The long-term isolation of Antarctica has a negative impact on human circadian rhythms, sleep, mood, mind and body, which has been well documented in medical and psychological studies. The application of health lighting technology to improve the physical and mental stress of the crew still needs more evidence-based research in multi-dimensional and multi-scale optical and biological studies to prove. Kennaway et al. found that the sleep rhythms of Antarctic over-winterers' underwent a natural shift (free running) in a constant darkness-like environment during the polar night (maximum 4.1 hours). Studies suggest that exposure to blue-rich (short wavelength) light as a countermeasure may prevent circadian rhythm disturbances in Antarctic wintering crews (Najjar et al., 2014).

This experiment is a healing light experiment for polar physical and mental stress environment, mainly through indoor morning light and bedtime adjusted healing light on the mood and rhythm regulation of the scientific researcher at Zhongshan Station during the polar night, to propose the light that is beneficial to the physical and mental health of the scientific researcher and promote the physical and mental habits of the scientific researcher at Zhongshan Station.

## 2. METHODS

### 2.1 Site

In this experiment, the ceiling lights in the explorers' dormitory were replaced to perform dimming control for a before-and-after comparison. The experimental period was the end of the Antarctic polar night. A two-week experimental light study was conducted from July 12 to July 26, 2018. The site is a typical explorers' dormitory with indoor dimensions of about 4.2m\*3m\*2.8m, one room for 2 people, two 1m-wide single beds, two tables and two sets of cabinets, a 600\*600 grille light panel on the roof, containing three 7W T8 double-ended lamps with a colour temperature of 6500K, and a wall button for on/off control.



Figure 1. Interior layout effect and lighting replacement program

The expedition trip lasted 15 months from December 2017 to February 2019. Most of the team members are participating in Antarctic scientific expeditions for the first time and experiencing continuous summer and wintering in Antarctica for the first time. The team consisted of six technical researchers, one administrative logistician and one teacher, who mainly performed expedition work such as housekeeping and fieldwork. The main activities of the subjects during their stay in Antarctica include the complex building, the dormitory building, the scientific observation building, the fieldwork and power generation building, the general store and the garage.

### 2.2 Subjects

The subjects were eight overwintering members of the Zhongshan Station, all male, aged between 28-46 years, with an average age of 33.6 years, BMI between 18.5 and 23.9, and in good health. They had a regular daily routine, no long-term habits of smoking, drinking alcohol or coffee, no history of drug dependence, no history of taking antipsychotics, normal vision or corrected vision, and no ophthalmic disease. All participants signed an informed consent form and received some remuneration for the experiment. Since the distant main subject on site was unable to participate, a team member on site, who was also the experiment operator, was asked to collect saliva as well as to summarize the questionnaires. The subjects signed an informed consent form before the experiment, and the experimental operator and the subjects were informed by the principal investigator of the relevant procedures and precautions.

### 2.3 Procedure

#### I. Interview Research

Research interviews were conducted with eight team members through questionnaires to understand the visual and psychological needs of the Zhongshan Station team members in order to propose a targeted design for the follow-up. These eight team members continued their scientific expedition in Antarctica from January 2018 to February 2019, for a total of 15 months, experiencing polar day and night processes during the year.

II. Experimental procedure (the first week and second week of the experiment need to be conducted consecutively). Week 1: 8 team members living in the general dormitory were invited to record the sleep scale every day, and saliva was collected five times a day on the first, fourth and seventh days (7:00, 12:00, 18:00, 20:00 and 22:00). Week 2: Eight team members were invited to conduct light experiments at regular intervals in the room where the experimental lights were

installed, the lights were adjusted to the appropriate scenes at the time required by the experiment every day, the sleep scale was recorded every day, saliva was collected five times a day on Thursday, Friday, Saturday, and Sunday (7:00, 12:00, 18:00, 20:00, and 22:00). Light hours and corresponding scene requirements (per day) for the second week of the experiment: The light time was 7:00-8:00 am to receive one hour of light, and the light was set by the experiment operator to scene A: full brightness mode)B. Light time for 20:00-21:00 to receive an hour of light, lights set by the experimental operator for the scene B: the lowest brightness, color temperature minimum)The experimental period was July 12-July 26, 2018 for a two-week experimental light study. At this time, there was no sunrise in Antarctica, almost no daylight outdoors, and the total daylight exposure is merely 0.

Table 1. Experimental procedure

	Day 1	Day 2	Day 3	Day 4	Day 5	Day 6	Day 7	Day 8	Day 9	Day 10	Day 11	Day 12	Day 13	Day 14	Day 21
Place	Room							Experimental Room							
Informed letter	Y														
Interview	Y														
POMS	Y						Y							Y	Y
SPAQ	Y														
SDS	Y													Y	Y
SLEEP	Y	Y	Y	Y	Y	Y	Y	Y	Y	Y	Y	Y	Y	Y	
Melatonin					Y	Y	Y					Y	Y	Y	
T1					7:00	7:00	7:00					7:00	7:00	7:00	
T2					7:30	7:30	7:30					7:30	7:30	7:30	
T3					19:00	19:00	19:00					19:00	19:00	19:00	
T4					19:30	19:30	19:30					19:30	19:30	19:30	
T5					22:00	22:00	22:00					22:00	22:00	22:00	

## 2.4 Methods

This experiment was conducted mainly by collecting salivary melatonin, interview questionnaire, state of mind scale, SPAQ, SDS, and sleep scale from the scientific research team members. The interview questionnaire was used to understand their basic information and preferences, and the questionnaire was designed to be as concise as possible, taking into account factors such as not interfering with the team members' work and experimental time control. The method has been developed over time and is assessed and measured in the form of scales or questionnaires. The first part of the questionnaire is the basic information, containing gender, age, sleep, etc. This part helps to classify and analyze the data later.

The scale data were scored and statistically summarized to find their mean and variance, and correlation analysis was performed for the collected data pairs to determine the correlation of two or more variables. Statistical analysis was performed using SPSS 25.0 software, and appropriate statistical methods were selected according to the type of data. For continuous variables, normality analysis was first performed, and if it conformed to a normal distribution, the statistical method of t-test or paired t-test was used. If it does not conform to the normal distribution, the Wilcoxon signed-rank test, which is a nonparametric test, is used. For discrete variables, the Wilcoxon signed-rank test was used directly.

## 3. Results

Rhythm indicators mainly included sleep logs and salivary melatonin concentrations, etc. Eight team members living in the general dormitory during the baseline week (week 1) and eight team

members performing light experiments at regular intervals during the light week (week 2) in the room where the experimental lights were installed were required to record sleep scales daily, respectively. Saliva was collected in five daily sessions (7:00, 12:00, 18:00, 20:00, and 22:00) on the first, fourth, and seventh days of the baseline week (week 1), and in five daily sessions (7:00, 12:00, 18:00, 20:00, and 22:00) on the fourth, fifth, sixth, and seventh days of the light week (week 2), respectively.

### 3.1. The effect of light on sleep quality

Using the sleep log to record sleep latency time, the subject's sleep time per night can be analyzed, with longer time indicating more difficulty in falling asleep. Based on the time of going to bed, falling asleep and waking up each night, we can calculate the time spent in bed and the actual length of sleep each night, and then calculate the sleep efficiency each night (sleep efficiency = time spent in bed/time spent in bed, if the result is more than 85%, it is considered normal and 90% means very good). The higher the sleep efficiency of the subject, the better the sleep quality. The number of awakenings, an important measure of sleep quality, was recorded by the subject each morning after waking up in a sleep diary for the number of awakenings from the previous night. An increase in the number of awakenings implied a deterioration in sleep quality.

#### 1. The analysis of the sleep diary

The analysis of the sleep diary revealed that there was an increase in sleep duration, a decrease in the number of awakenings, a decrease in sleep latency, wake-up time and bed departure time, and an improvement in sleep quality on the 8th day of the experiment (the first day of the start of the experimental light), and this trend continued on the 14th day of the experiment (the 7th day of the start of the experimental light). This indicates that light was helpful in improving sleep quality and increasing sleep duration.

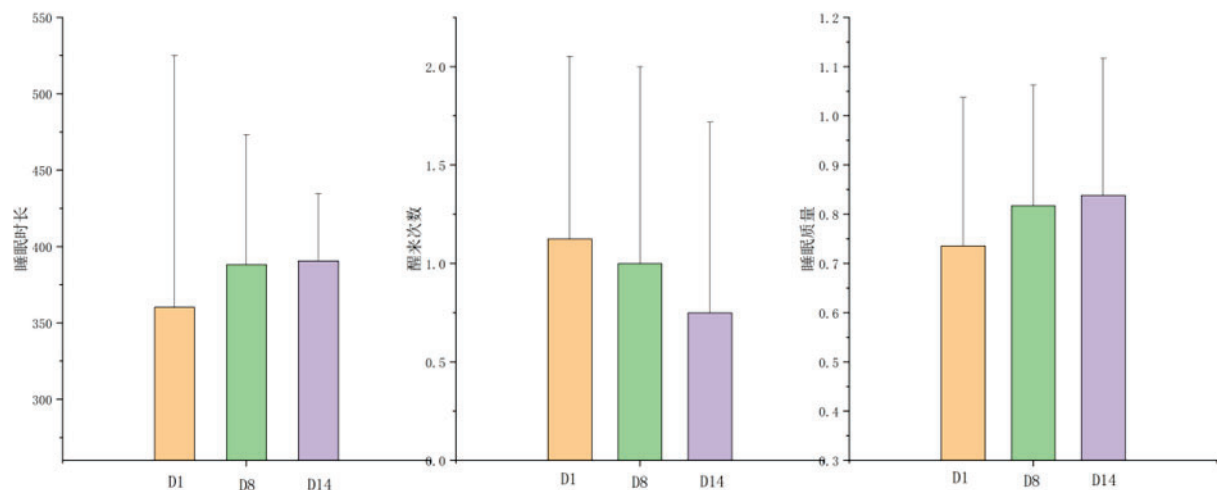


Figure 2. Effects of combined morning bright light and night dark light on sleep of polar crew members

#### 2. Effects of melatonin secretion

Saliva was collected five times a day (7:00, 12:00, 18:00, 20:00 and 22:00) on the first day, fourth day and seventh day of the first week, and five times a day (7:00, 12:00, 18:00, 20:00 and 22:00) on Thursday, Friday, Saturday and Sunday of the second week, and 1 ml of subject saliva was retained by the subjects on time and samples were obtained. The samples were sealed and stored in a refrigerator at  $-40^{\circ}$  by the experimenter, and then sent to the biological company for testing and analysis after returning to Shanghai with the Xuelong ship frozen the following year.

Salivary melatonin was detected by enzyme immunoassay, using an imported enzyme-linked immunoassay kit (IBL ELISA kit) for detection and analysis. The kit has 12 wells x 8 strips = 96T, with 8 wells reserved for standard comparison, and for each kit, 88 samples can be tested.



After statistical analysis, a total of 280 saliva sample data from 8 subjects were obtained, of which 269 were valid. The tested melatonin concentration data were first tested for normal distribution, and the results did not conform to a normal distribution, and the paired t-test could not be used, and the Wilcoxon signed-rank test, a non-parametric test, was required for statistical analysis (see Table 6.23). The results showed that at 7:00 am, day 14 was significantly lower relative to days 5 and 7 ( $p=0.046$ ,  $p=0.028$ ,  $p<0.05$ ); at 12:00 noon, day 14 was significantly lower relative to days 6 and 7 ( $p=0.046$ ,  $p=0.046$ ,  $p<0.05$ ), day 13 was significantly lower relative to day 6 ( $p=0.043$ ,  $p<0.05$ ), and significantly lower on day 12 relative to days 5 and 7 ( $p=0.036$ ,  $p=0.043$ ,  $p<0.05$ ); at 18:00 in the evening, significantly higher on day 7 relative to day 5 ( $p=0.046$ ,  $p<0.05$ ); at 20:00, significantly higher on day 14 relative to day 12 ( $p=0.043$ ,  $p<0.05$ ); and at 22:00, significantly higher on day 13 was significantly higher relative to day 7 ( $p=0.046$ ,  $p<0.05$ ). This indicates that the combination of light can suppress daytime melatonin secretion and enhance daytime alertness of the scientist, while nighttime can promote melatonin secretion and promote sleep.

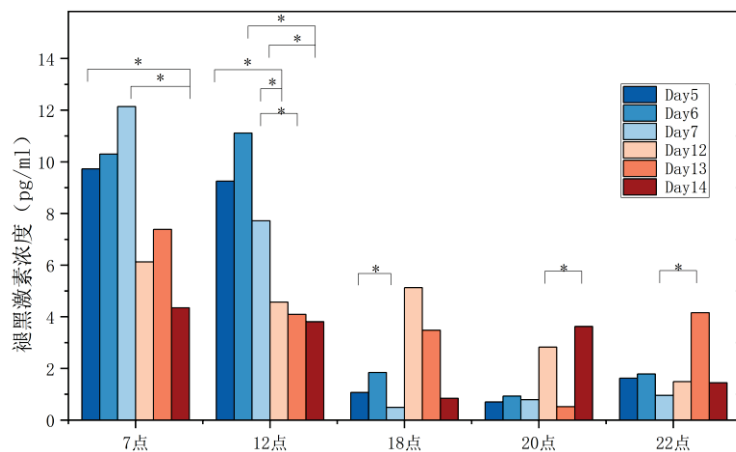


Figure 3. Comparison of salivary melatonin concentrations at different time points and light conditions

### 3.2. POMS and SDS mood impact analysis

Mood affects indicators mainly included the POMS mood scale and the SDS depressive mood scale, etc. The POMS mood scale was administered on the first, seventh, fourteenth, and twenty-first days of the experiment, and the SDS depressive mood scale was administered on the first, fourteenth, and twenty-first days of the experiment, respectively.

Because the POMS scores were not continuous variables, the statistical method of nonparametric tests was used. The analysis first revealed significant differences ( $p < 0.05$ ) between multiple data groups through the Fredman test, and then the statistical analysis was performed using the Wilcoxon signed-rank test for nonparametric tests. The scores on days 1, 7, 15, and 21 were also analyzed, and significant differences were found between days 1 and 7 ( $p=0.034$ ,  $p<0.05$ ) and between days 1 and 14 ( $p=0.046$ ,  $p<0.05$ ). Trends in the seven dimensions of mindfulness (depression, anger, nervousness, panic, fatigue, ego, and energy) could also be found, with all states of mind except ego showing a downward trend after two weeks of light, with more than 10% decreases in nervousness, panic, and anger, indicating that some improvement in the mindfulness factor could be achieved through light.

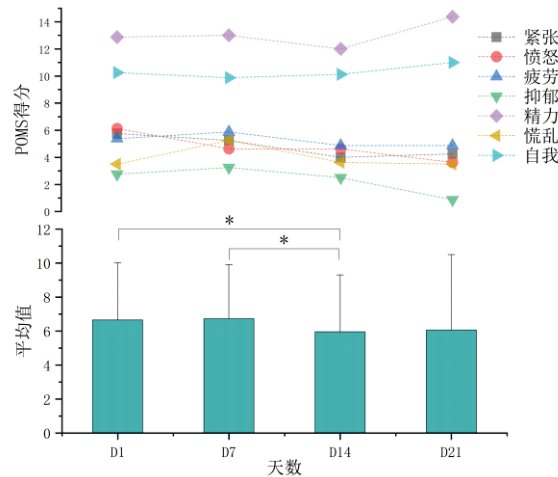


Figure 4 Analysis of the POMS Mindfulness Scale

The SDS self-rating scale scores were non-continuous variables, so the SDS self-rating scale data were tested non-parametrically. Statistical analysis was performed by Wilcoxon signed-rank test method. The results showed no significant difference ( $p>0.05$ ) between pre and post comparison. However, the results of the SDS self-rating scale showed a decrease in SDS scores in five of the eight subjects. This proves that light changes contribute to mood regulation.

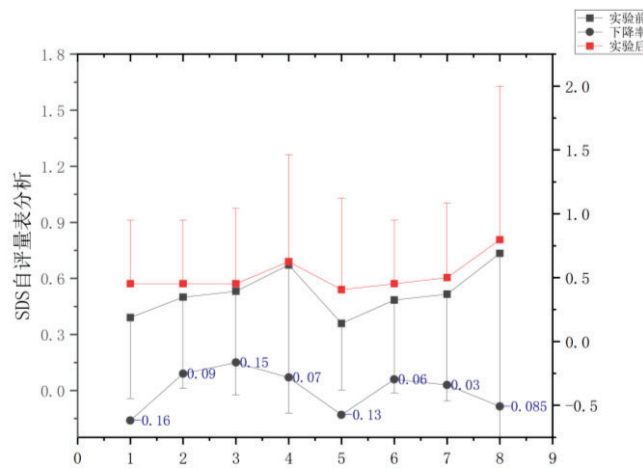


Figure 5. SDS self-assessment scale analysis

### 3. CONCLUSION

The experiment conducted at Zhongshan Station in Antarctica firstly verified the effects of a week of combined constant light patterns on personnel sleep and circadian rhythms, and then compared the active intervention effects of combined lighting patterns and baseline patterns on personnel rhythmic sleep, which were comprehensively evaluated in terms of rhythmic indicators, sleep quality, emotional state and other dimensions, respectively, in order to seek the appropriate combination of light parameters. Overall, a dynamic light combination of high M-EDI values in the morning and low M-EDI rhythmic light at bedtime enhanced daytime alertness and nighttime melatonin secretion in the polar wintering crew under normal operating conditions. Light exposure contributed to improved sleep quality and increased sleep duration, but was not significant. It shows that the dynamic lighting combination applied to the interior of the Zhongshan Station area in Antarctica can provide both visual and non-visual health performance enhancement. The above-mentioned healing lighting design strategies for Antarctic research stations can be applied to the construction of new stations in the future, and can also be used to improve the mood and sleep of personnel in existing stations during the winter and summer periods, and can also be applied in similar extreme habitat spaces such as spaceflight and deep-sea expeditions, which are isolated from the extreme day and night conditions in Antarctica.

## REFERENCE

- [1] Smolders, K. C. H. J., De Kort, Y. A. W., & van den Berg, S. M. Daytime light exposure and feelings of vitality: Results of a field study during regular weekdays. *Journal of Environmental Psychology*, 2013, 36, 270-279.
- [2] Boubekri, M., Cheung, I. N., Reid, K. J., Wang, C. H., & Zee, P. C. Impact of windows and daylight exposure on overall health and sleep quality of office workers: a case-control pilot study. *Journal of clinical sleep medicine*, 2014, 10(06), 603-611.
- [3] Steinach M, Kohlberg E, Maggioni MA, Mendt S, Opatz O, Stahn A, Gunga HC. Sleep Quality Changes during Overwintering at the German Antarctic Stations Neumayer II and III: The Gender Factor. *PLoS One*. 2016 Feb 26;11(2):e0150099. doi: 10.1371/journal.pone.0150099. PMID: 26918440; PMCID: PMC4769303.
- [4] Palinkas LA, Cravalho M, Browner D. Seasonal variation of depressive symptoms in Antarctica. *Acta Psychiatr Scand*. 1995 Jun;91(6):423-9. doi: 10.1111/j.1600-0447.1995.tb09803.x. PMID: 7676841.
- [5] Palmia G. (1963). Psychological observations on an isolated group in Antarctica. *Br. J. Psychiatry* 131 651–654.
- [6] Beute F, de Kort Y. A. (2014). Salutogenic effects of the environment: review of health protective effects of nature and daylight. *Appl. Psychol. Health Well Being* 6 67–95.
- [7] LeGates T. A., Fernandez D. C., Hattar S. (2014). Light as a central modulator of circadian rhythms, sleep and affect. *Nat. Rev. Neurosci.* 15 443–454.
- [8] Collet G., Mairesse O., Cortoos A., Tellez H. F., Neyt X., Peigneux P., et al. (2015). Altitude and seasonality impact on sleep in Antarctica. *Aerosp. Med. Hum. Perform.* 86 392–396.
- [9] Steinach M., Kohlberg E., Maggioni M. A., Mendt S., Opatz O., Stahn A., et al. (2016). Sleep quality changes during overwintering at the German Antarctic stations neumayer II and III: the gender factor. *PLoS One* 11:e0150099.
- [10] Pattyn N., Van Puyvelde M., Fernandez-Tellez H., Roelands B., Mairesse O. (2018). From the midnight sun to the longest night: sleep in Antarctica. *Sleep Med. Rev.* 37 159–172.
- [11] Do N., Mino V. L., Merriam G. R., LeMar H., Case H. S., Palinkas L. A., et al. (2004). Elevation in serum thyroglobulin during prolonged Antarctic residence: effect of thyroxine supplement in the polar 3,5,3'-triiodothyronine syndrome. *J. Clin. Endocrinol. Metab.* 89 1529–1533.
- [12] Chen N., Wu Q., Li H., Xu C. (2016). Different adaptations of Chinese winter-over expeditioners during prolonged Antarctic and sub-Antarctic residence. *Int. J. Biometeorol.* 60 737–747.
- [13] Bechtel R. B., Berning A. (1991). "The third-quarter phenomenon: do people experience discomfort after stress has passed" in *From Antarctica to Outer Space: Life in Isolation and Confinement* Vol. 26 eds Clearwater Y. A., Harrison A. A., McKay C. P. (New York, NY: Springer-Verlag; )
- [14] Kennaway D J, Van Drop C F. Free-running rhythm of melatonin , cortisol , electrolytes and sleep in human in Antarctica. *Am J Physiol* 1991 . 260: 1137 – 1144
- [15] Najjar R. P., Wolf L., Taillard J., Schlangen L. J. M., Salam A., Cajochen C., et al. (2014). Chronic artificial blue-enriched white light is an effective countermeasure to delayed circadian phase and neurobehavioral decrements. *PLoS One* 9:e102827.

## ACKNOWLEDGEMENT

This research was funded by the Scientific Research Project of Shanghai Municipal Science and Technology Commission (No. 20dz1207200).

Corresponding Author: Luoxi Hao  
 Affiliation: College of Architecture, Tongji University  
 e-mail : haoluoxi@tongji.edu.cn

# THE IMPACT OF WEARING YELLOW OR BLURRED LENSES ON DISCOMFORT GLARE FROM NIGHTTIME HEADLIGHTS

Tatsuya Iizuka, Shuya Suzuki, Takushi Kawamorita, Hitoshi Ishikawa

(Graduate School of Medical Sciences, Kitasato University, Kanagawa, Japan)

## ABSTRACT

**Purpose:** Headlights have become increasingly luminous, ensuring visibility and safety during nighttime driving. However, this has also caused ocular aversion due to the increasing headlight glare of oncoming vehicles. Designing light sources and driving glasses that reduce headlight glare while maintaining visibility is essential. The ISO 8980-3 standard recommends a 75% luminous transmittance for nighttime driving glasses. Nighttime driving glasses to reduce headlight glare and improving visibility are on the market. However, there is no supporting evidence which shows these glasses are effective. In addition, refraction is not always fully corrected with these glasses and some of drivers may still experience blurred vision due to post-work fatigue. The purpose was to evaluate the discomfort glare caused by headlights in a real driving environment, comparing the impact of three types of headlights under two lens conditions.

**Methods:** We enrolled 20 participants with a mean ( $\pm$  standard deviation) age of 21.3 ( $\pm$  1.6) years, with no history of ophthalmic surgery, retinal or optic nerve disease, or systemic diseases. The study assessed the effectiveness of color lenses (99% transmission: clear lens, 85% transmission: yellow lens Y1, 78% transmission: yellow lens Y2), and blurred lenses (+0.00, +0.50, +1.00 diopter sphere) in reducing various types of lower-beam headlight glare (halogen lamps, high-intensity discharge lamps, light-emitting diodes lamps) at a distance of 20 and 40 m using the De Boer scale.

**Results:** LED-headlight glare significant main effect for discomfort glare under yellow-lens conditions (20m:  $F_{2, 57} = 5.54$ ;  $p = 0.006$ , 40m:  $F_{2, 57} = 5.54$ ;  $p = 0.005$ ), indicating that the lower the transmittance of the lens, the slightly higher the average De Boer score, but the scores remained approximately the same. There was also a significant main effect observed under the blurred-lens condition (20m:  $F_{2, 57} = 15.9$ ;  $p < 0.001$ , 40m:  $F_{2, 57} = 30.3$ ;  $p < 0.001$ ), with glare enhancing as the blur increased (blur 0 versus blur 1.0 for all headlight,  $p < 0.001$ ). There was no significant main effect for the headlight condition (20 and 40m:  $F_{2, 57} = 0.01$ ;  $p = 0.99$ ).

**Conclusions:** The discomfort glare caused by each headlight glare is almost the same even with the use of yellow lenses (transmittance of 75% or higher). Therefore, eye-care professionals should not recommend these lenses for glare reduction purposes. Instead, refractive-corrected glasses should be prescribed, as they can help reduce the appearance of glare, halos, and starbursts.

**Keywords:** Headlight, Discomfort glare, Yellow lens, Refractive-corrected glasses

## 1. INTRODUCTION

Headlights have become increasingly luminous, ensuring visibility and safety during nighttime driving. However, this has also caused ocular aversion due to the increasing headlight glare (HLG) of oncoming vehicles [1-3]. Modern vehicle headlights have many variations, including halogen lamps, high-intensity discharge lamps (HID), and light-emitting diodes (LED), each with different spectral radiation intensities. This suggests that the light incident on the eye may affect photophobia and visual function differently [4-6]. In addition, discomfort glare from headlights can startle or distract the driver, leading to blinking, squinting, ocular aversion, and fatigue. Momentary lapses in judgment owing to headlight glare pose a significant accident risk.

Polarized glasses and sunglasses are commonly used during the day to prevent sun glare. They also effectively reduce headlight glare during nighttime use; however, most commercially available products have low luminous transmittance of approximately 20–30%, significantly reducing visibility and being dangerous at night. Designing light sources and driving glasses that reduce headlight glare while maintaining visibility is essential. Yellow-lens driving glasses could reduce glare by cutting short wavelengths of light that cause photophobia and improving contrast by transmitting wavelengths with high luminous sensitivity [7,8].

The International Organization for Standardization standardized the transmittance of lenses for nighttime use in 1999 with ISO 8980-3, updated in 2022 to advise against the outdoor use of lenses with a luminous transmittance of  $< 75\%$  [9].<sup>16</sup> Commercially available nighttime driving glasses claim to increase visibility and reduce headlight glare from oncoming vehicles. However, it is unclear whether they have been tested on vehicles or in actual nighttime driving conditions, and there is no scientific evidence to support these claims. Consequently, the optimal lens transmittance for reducing headlight glare and improving visibility during nighttime driving remains unclear. In addition, actual drivers do not always entirely correct for refraction with glasses, and some individuals may still experience blurriness due to post-work fatigue. Therefore, this study aimed to develop a vehicle headlight model to investigate the effects of discomfort glare from Halogen, HID, and LED headlights, as well as the potential benefits of yellow or blurred lenses.

## 2. METHODS

### 2.1 Participants

Twenty healthy, young individuals with a mean ( $\pm$  standard deviation [SD]) age of  $21.3 \pm 1.6$  years were included in this single-center study. We included all individuals with normal colour vision and corrected visual acuity of 20/20 or better. The mean spherical equivalent refractive error was  $-2.24 \pm 2.03$  ( $-0.25$  to  $-6.00$ ) diopter (D). Exclusion criteria included astigmatism  $> -1.00$  D, history of ophthalmic surgery, retinal or optic nerve disease, or systemic diseases (e.g., diabetes or cerebrovascular disease). The study was conducted following the principles of the Declaration of Helsinki and approved by the Ethics Committee of the School of Allied Health Sciences at Kitasato University (2022-004). Written informed consent was obtained from all participants in accordance with our Institutional Review Board protocol.

### 2.2 Lower-beam headlight model

This study used a lower-beam headlight model that could be switched between Halogen, HID, or LED to investigate the effects of different HLG. The model was based on a third-generation Prius (Toyota Motor Corporation, Aichi, Japan) and included the front body of the car (Figure 1A). The headlights were powered by the electrical circuit in Figure 1B. Their optical axis and cutoffs were adjusted following “Article 32 of the safety standards for road trucking vehicles: Headlight, etc.” of the Ministry of Land, Infrastructure, Transport and Tourism of Japan (Figure 1C, 1D) [10]. Luminous intensity and colour temperature from each headlight were measured at the point shown in Figure 1C, and the average values for the left and right headlights were recorded. For the halogen headlights, the luminous intensity and colour temperature were 10,370 cd and 3000 K, respectively; for the HID headlights, the values were 13,360 cd and 3700 K, respectively; and for the LED headlights, the values were 18,030 cd and 5200 K, respectively. The relative spectral intensity of each headlight type is shown in Figure 2A.



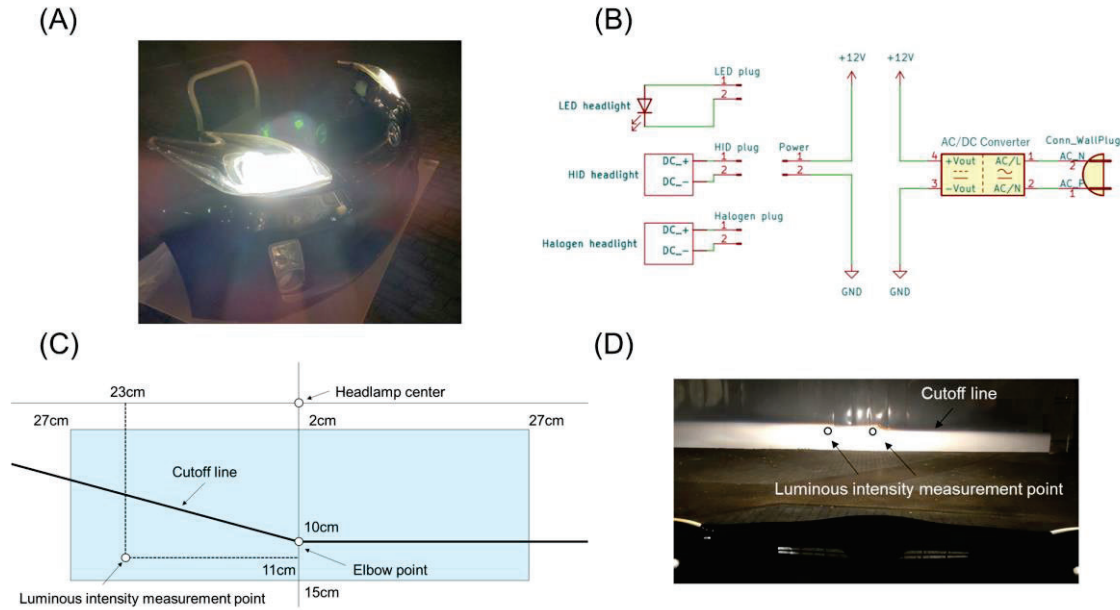


Figure 1. Lower-beam headlight model

### 2.3 Lens types and transmittance

This study utilized two commercially available yellow lenses, a clear lens and a blurred lens (convex spherical). The luminous transmittance of the lenses was measured: 99% for the clear and blurred lenses, 85% for the yellow Y1 lens (Actiview night drive: TOKAI OPTICAL Co., Ltd, Aichi, Japan), 78% for the yellow Y2 lens (Viewnal SP: TOKAI OPTICAL Co., Ltd, Aichi, Japan). The spectral transmittance of each lens is shown in Figure 2B. The Y2 lens was made of acrylic, whereas the other lenses were made of plastic.

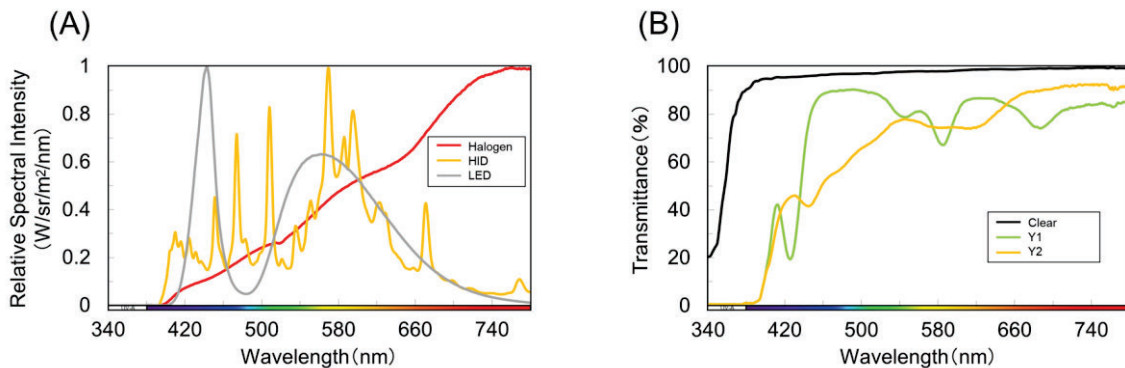


Figure 2. The relative spectral intensity of each headlight and spectral transmission of each lens

### 2.4 Research environment

The experiment was conducted on a flat field in Kitasato, Minami-ku, Sagami-hara-shi, Kanagawa, Japan (35-32-27N, 139-23-34E), with no nearby artificial light sources, between July and December 2022 when the outdoor horizontal and vertical illuminances were  $< 1.0$  lx. The road layout consisted of two 3.5-m-wide and 50-m-long lanes, in accordance with “Article 5 of road structure ordinance: Lane” of the Ministry of Land, Infrastructure, Transport and Tourism of Japan [11]. The observer was seated with an eye point adjusted to 1.3 m from the ground. The headlight model was placed on the side of the oncoming vehicle with the observer in the driver position. The headlights were positioned 40 and 20m from the observer to create a peripheral glare (Figure 3). A windshield with 75% transmittance was placed 10 cm away from the eyes of the observer, and the mounting angle of the windscreen was  $40^\circ$  from the horizontal to allow them

to see through it. The illuminance reaching the observer's eyes, caused by each headlight in the research environment, was measured using a spectral illuminance meter (IM-1000R; Topcon Technohouse Corporation, Tokyo, Japan). The measured illuminance values were as follows: 0.10 lx for halogen, 0.18 lx for HID, and 0.30 lx for LED headlights at a distance of 40 meters from the participants; and 0.60 lx for halogen, 1.08 lx for HID, and 1.30 lx for LED headlights at a distance of 20 meters from the participants.

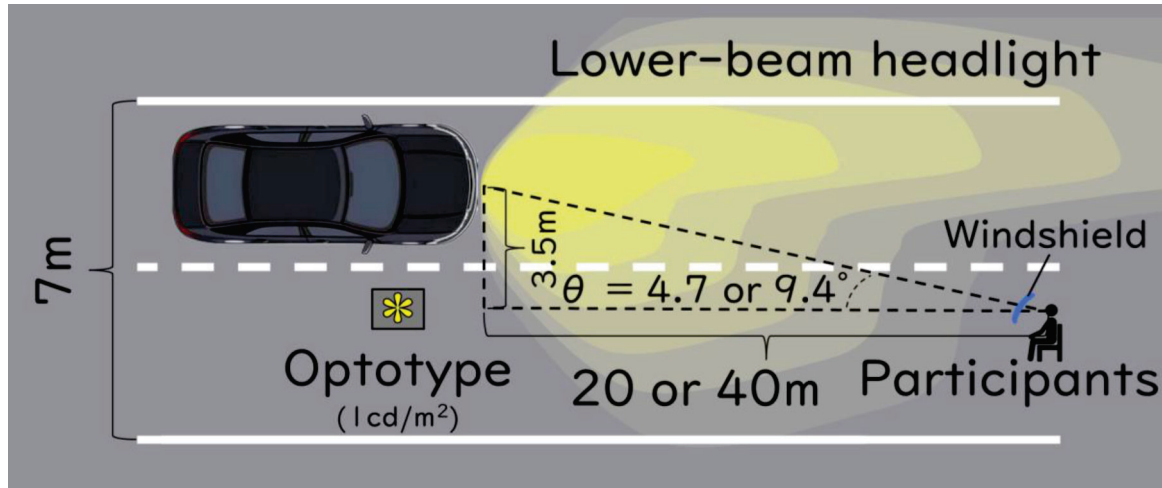


Figure 3. Research environment

## 2.5 Evaluation of discomfort glare

Discomfort glare was evaluated using the De Boer rating scale to assess subjective glare [12]. The 9-point scale consists of the following ratings: 9, Just noticeable; 7, Satisfactory; 5, Just admissible; 3, Disturbing; and 1, Unbearable. The observers evaluated the peripheral glare from the headlights, fixated on a yellow asterisk optotype displayed on a 15.6 inch Organic-LED (Guangxi Century Innovation Display Electronics Co.,Ltd) screen positioned at a distance of 50 m (Figure 2). This distance was based on a single scene of looking into the distance while driving. Measurements were taken under a combination of the three headlight conditions, three color-lens conditions (1: Clear, 2: Y1, 3: Y2), and three blurred-lens conditions (baseline refractive correction plus either +0.50 diopter sphere (DS) or +1.00 DS binocular spherical blur). The yellow lens conditions were measured at baseline refraction. Observers were instructed not to look directly at the headlights and rate the glare they experienced during the 3 s facing the front optotype. The observers were masked (specifically, the headlight portion) when not being evaluated and unmasked during the evaluation, with the assessment conducted continuously to minimize masked time. The headlight and lens combinations were randomized for each observer.

## 2.6 Diagnosis of visual acuity, ocular refraction and color vision

Participants will be evaluated by an ophthalmologist (HI) and orthoptist (TI) for refraction, visual acuity, and color vision. Visual acuity and ocular refraction when using blurred lenses were diagnosed using the VC-60(Takagi Seiko Co., Ltd, Nagano, Japan), and color vision when using yellow lenses was diagnosed using the Neitz anomaloscope OT-II (Neitz Instruments, Tokyo, Japan).

## 2.7 Statistical analysis

Statistical analyses were conducted using Microsoft Excel 365 (Microsoft Co., Albuquerque, NM, USA) and Bell Curve for Excel (Social Survey Research Information Co., Ltd., Tokyo, Japan). The Shapiro–Wilk test was performed to assess whether the data distribution was parametric or non-parametric. The De Boer rating scale was non-parametric. Aligned rank transform was used for non-parametric data analysis, as it is more robust and powerful than the traditional analysis of variance (ANOVA) [13,14]. To evaluate the effects of discomfort glare and color lenses in each headlight, a two-factor repeated-measures ANOVA was conducted with the De Boer rating scale index as the dependent variable, the headlight condition as the independent variable, and the

color-lens condition as the within-subject factor. A two-factor repeated-measures ANOVA was conducted to evaluate the effects of discomfort glare and blurred lenses. The De Boer rating scale index was the dependent variable, the headlight condition was the independent variable, and the within-subject factor was the blurred-lens condition.

These were assessed based on the interaction between the headlight and lens conditions and the main effect of each condition. Differences between the headlight and lens conditions were analyzed using Tukey's post-hoc test. Statistical significance was set at a two-sided p-value < .05.

### 3. RESULTS

#### 3.1 Visual acuity and color vision with yellow and blurred lenses

The mean ( $\pm$  SD) logarithm of the minimum angle of resolution of binocular visual acuity was  $-0.26 (\pm 0.06)$  at baseline,  $-0.06 (\pm 0.07)$  at blur 0.50, and  $0.10 (\pm 0.07)$  at blur 1.00 for the 20 individuals with baseline refractive correction and blurred lenses. Color vision remained normal for all participants throughout the yellow-lens wear period.

#### 3.2 Discomfort glare with yellow lenses

A two-factor repeated-measures ANOVA of discomfort glare at 40m (three headlight conditions  $\times$  three color-lens conditions) showed no significant interaction between the headlight and lens conditions ( $F_{4, 114} = 0.52$ ;  $p = 0.72$ ) for yellow lenses. There was a significant main effect of the lens condition ( $F_{2, 57} = 5.54$ ;  $p = 0.005$ ), and post-hoc multiple comparisons within lens conditions showed a significant difference between Y2 and Clear for Halogen-HLG (0.25 Boer score,  $p < 0.001$ ) and LED-HLG (0.30 Boer score,  $p = 0.003$ ), with lower transmission resulting in slightly higher average De Boer scores (Figure 4A). There was no significant main effect for the headlight condition ( $F_{2, 57} = 0.01$ ;  $p = 0.99$ ).

Similarly, a two-factor repeated-measures ANOVA of discomfort glare at 20m (three headlight conditions  $\times$  three color-lens conditions) showed no significant interaction between the headlight and lens conditions ( $F_{4, 114} = 0.13$ ;  $p = 0.97$ ) for yellow lenses. There was a significant main effect of the lens condition ( $F_{2, 57} = 5.54$ ;  $p = 0.006$ ), and post-hoc multiple comparisons within lens conditions showed a significant difference between Y2 and Clear for Halogen-HLG (0.40 Boer score,  $p < 0.001$ ), and LED-HLG (0.35 Boer score,  $p = 0.002$ ), with lower transmission resulting in slightly higher average De Boer scores (Figure 4B). There was no significant main effect for the headlight condition ( $F_{2, 57} = 0.01$ ;  $p = 0.99$ ).

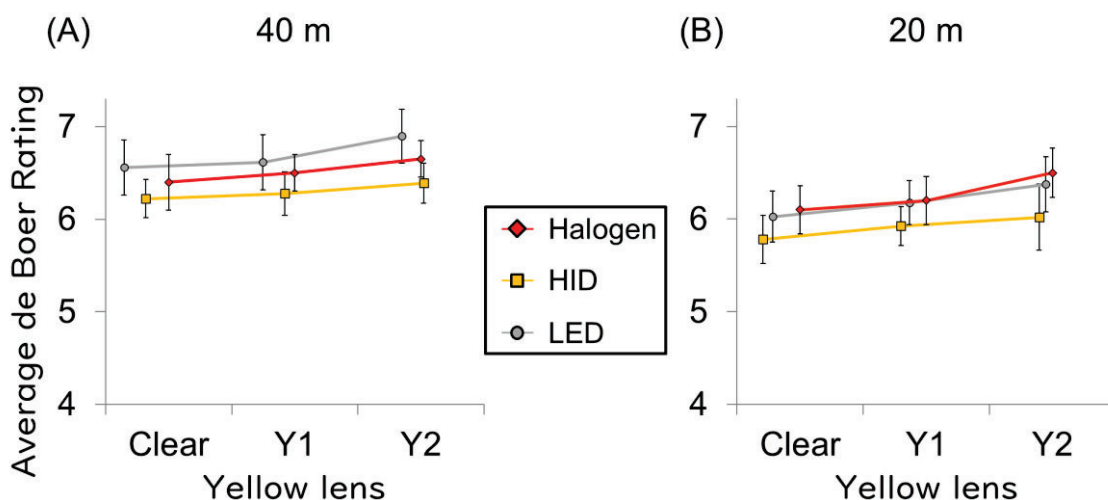


Figure 4. Impact of discomfort glare with yellow lenses and each headlight

### 3.3 Discomfort glare with blurred lenses

A two-factor repeated-measures ANOVA of discomfort glare at 40m (three headlight conditions  $\times$  three blurred-lens conditions) showed no significant interaction between the headlight and blur conditions ( $F_{4, 114} = 0.98$ ;  $p = 0.42$ ), but a significant main effect in the blur condition ( $F_{2, 57} = 30.3$ ;  $p < 0.001$ ). Post-hoc multiple comparisons within blur conditions showed a significant difference between blur 0 versus blur 0.5 and blur 0.5 versus blur 1.0 for all HLG ( $p < 0.01$ ) and blur 0 vs. blur 1.0 for Halogen- and LED-HLG ( $p < 0.01$ ). The average Boer score difference between blur 0 and blur 1.0 was 0.6 for halogen, 0.9 for HID, and 1.1 for LED (Figure 5A). The lower the blur, the higher the mean score and the lower the glare. There was no significant main effect for the headlight condition ( $F_{2, 57} = 0.01$ ;  $p = 0.99$ ).

Similarly, a two-factor repeated-measures ANOVA of discomfort glare at 20m (three headlight conditions  $\times$  three blurred-lens conditions) showed no significant interaction between the headlight and blur conditions ( $F_{4, 114} = 1.09$ ;  $p = 0.36$ ), but a significant main effect in the blur condition ( $F_{2, 57} = 15.9$ ;  $p < 0.001$ ). Post-hoc multiple comparisons within blur conditions showed a significant difference between blur 0 versus blur 1.0 for all HLG ( $p < 0.01$ ) and blur 0.5 vs. blur 1.0 for Halogen- and LED-HLG ( $p < 0.05$ ). The average Boer score difference between blur 0 and blur 1.0 was 0.75 for halogen, 0.4 for HID, and 0.7 for LED (Figure 5B). The lower the blur, the higher the mean score and the lower the glare. There was no significant main effect for the headlight condition ( $F_{2, 57} = 0.01$ ;  $p = 0.99$ ).

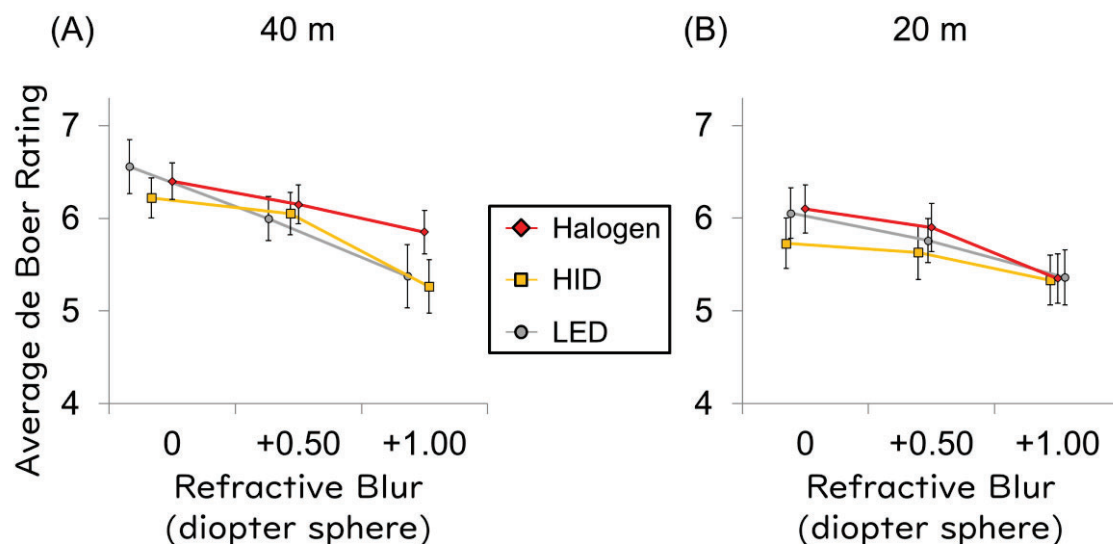


Figure 5. Impact of discomfort glare with blurred lenses and each headlight

## 4. DISCUSSION

This study aimed to investigate the impact of yellow and blurred lenses on headlight peripheral glare in a nighttime road environment. The results showed that when using yellow lenses adhering to ISO standard transmittance, no disturbances were observed on the De Boer rating scale. Additionally, no significant differences were found between the different of HLGs tested. Although yellow lenses had a minimal effect on reducing glare, it was noted that as the level of blur increased, there was an associated increase in perceived glare.

The physiological mechanisms of unpleasant glare are not fully understood, but the blue-sensitive short-wavelength-sensitive cone stimulation hypothesis is the most promising [15,16]. In our study, using the De Boer rating scale, we showed that no participant reported a “disturbing” level below a scale of 3 for HLG. LEDs are generally considered more dazzling than halogen or HID; however, no “disturbing” effect was observed with any of the HLGs, and there was no effect of the type of light source. To compare light sources, high disturbance light levels are necessary [17]. The LED-HLG did not cause any disturbance, suggesting no difference between it and other HLGs. We initially expected that discomfort glare would increase as the light source approached the visual axis; however, we observed slightly greater discomfort glare at a distance of 20 m,



which is farther from the visual axis. This may be attributed to the increased amount of irradiation into the eye, as well as a perception of greater glare due to the proximity of the HLGs. Nevertheless, the potential effectiveness of the yellow lens did not vary with distance. Yellow lenses slightly reduced glare, but no significant interaction effect was observed. It might be due to a reduction in the total amount of light entering the eye rather than a result of the short-wavelength cutoff. However, the De Boer rating scale showed a minimal average difference, making it unclear whether yellow lenses is meaningful for reducing photophobia while driving at night. Yellow lenses with a luminous transmittance of 75% or higher should not be recommended as glare measures.

We found that increasing blurriness resulted in more discomfort glare, which was unexpected. Light stimulus applied to the retina from a light source is generally uniform across the entire visual field and not influenced by optical correction [18,19]; however, our results do not support this finding, possibly because the blurred lens affects the size of the glare. The peripheral glare from low-beam headlights suggests that drivers experienced discomfort glare and evaluated changes in glare, halo, and starburst size through the blurred lens. Separating direct discomfort glare from the apparent evaluations of glare, halo, and starburst could lead to a more accurate discomfort glare evaluation. Notably, a stronger response was observed with the blurred lens than with the yellow lens, and additional research is needed to explore this finding. In addition, it is important to note that the experience of a person accustomed to driving with myopia blur may differ from the investigation conducted using optically reproduced blur. Visual acuity with the blurred lenses used in this study met the Japanese standard for acceptable driving binocular acuity, thus reproducing the poor quality of vision of actual drivers.

This study has limitations as it only considers the HLG in a stationary two-lane setting and does not simulate actual driving conditions. Therefore, the results of this study cannot be generalized to all driving situations. In addition, the windshield used was miniaturized for the experiment and fixed near the eye. The study used yellow lenses with a luminous transmittance of at least 75%, per the ISO standards, and pale-yellow lenses, preferred by the general public. However, neither lens type should be recommended for reducing glare, even though they do not worsen visual sensitivity. Lenses with < 75% luminous transmittance may also minimize glare if visual sensitivity is unaffected. Therefore, it is premature to dismiss glasses for nighttime driving completely. Finally, the results of this study were based on healthy young adults, and different results may be obtained in older adults owing to the impact of eye aging and cataracts on glare.

Our study revealed that there was no significant difference in discomfort glare caused by each HLG, even when yellow lenses were used. Based on these findings, it is not advisable for eye-care professionals to recommend yellow lenses for the purpose of reducing glare. Instead, the prescription of refractive-corrected glasses should be considered, as they have the potential to mitigate the perception of glare, halos, and starbursts.

## REFERENCE

- [1] Flannagan MJ, Sivak M, Gellatly A. Joint Effects of Wavelength and Ambient Luminance on Discomfort Glare from Monochromatic and Bichromatic Sources. Report No. UMTRI- 91-42. Ann Arbor: The University of Michigan Transportation Research Institute; 1991.
- [2] Bullough JD, Fu Z, Van Derlofske J. Discomfort and disability glare from halogen and HID headlamp systems (SAE paper: 2002-01-0010). In: Jiao J, Flannagan MJ, Karbowski RH, eds. *Advanced Lighting Technology for Vehicles*, SP-1668. Warrendale: Society of Automotive Engineers; 2002. p. 1-5.
- [3] Sivak M, Schoettle B, Mionda T, et al. Blue Content of LED Headlamps and Discomfort Glare. In: *Transportation Research Institute Report UMTRI-2005-2*. Ann Arbor: The University of Michigan; 2005.
- [4] Flannagan MJ, Sivak M, Gellatly A, et al. A Field Study of Discomfort Glare from High-Intensity Discharge Headlamps. Report No. UMTRI- 92-16. Ann Arbor: The University of Michigan Transportation Research Institute; 1992.
- [5] Fekete J, Sik-Lányi C, Schanda J. Spectral discomfort glare sensitivity under low photopic conditions. *Ophthalmic Physiol Opt* 2006;26:313-7.
- [6] Fekete J, Sik-Lányi C, Schanda J. Spectral discomfort glare sensitivity investigations. *Ophthalmic Physiol Opt* 2010;30:182-7.
- [7] Flannagan MJ, Sivak M, Traube EC. Discomfort Glare and Brightness as Functions of



- Wavelength. UMTRI-94-29. Ann Arbor, MI: University of Michigan Transportation Research Institute; 1994.
- [8] Flannagan MJ. Subjective and Objective Aspects of Headlamp Glare: Effects of Size and Spectral Power Distribution. Technical Report No. UMTRI-99-36. Ann Arbor, MI: University of Michigan Transportation Research Institute; 1999.
  - [9] Ophthalmic optics—Uncut finished spectacle lenses — Part 3: Transmittance specifications and test methods [internet]. International Organization for Standardization. Available from: <https://www.iso.org/obp/ui/#iso:std:iso:8980:-3:ed-4:v1:en>.
  - [10] Article 32 of the safety standards for road trucking vehicles: Headlight, etc. [internet]. Ministry of Land, Infrastructure, Transport and Tourism of Japan. Available from: [https://www.mlit.go.jp/jidosha/jidosha\\_fr7\\_000007.html](https://www.mlit.go.jp/jidosha/jidosha_fr7_000007.html)
  - [11] Article 5 of road structure ordinance: Lane. Ministry of Land, Infrastructure, Transport and Tourism of Japan. Available from: [http://www.mlit.go.jp/road/road\\_e/r1\\_standard.html](http://www.mlit.go.jp/road/road_e/r1_standard.html).
  - [12] De Boer JB. Visual perception in road traffic and the field of vision of the motorist. In: De Boer JB, ed. Public Lighting. Eindhoven: Philips Technical Library; 1967. p. 11-96.
  - [13] Wobbrock JO, Findlater L, Gergle D, et al. The aligned rank transform for nonparametric factorial analyses using only ANOVA procedures. In: Proceedings of the ACM Conference on Human Factors in Computing Systems (CHI '11). Vancouver, British Columbia. New York: ACM Press; 2011. p. 143-146.
  - [14] Elkin LA, Kay M, Higgins JJ, et al. An aligned rank transform procedure for multifactor contrast tests. In: Proceedings of the ACM Symposium on User Interface Software and Technology (UIST '21). New York: ACM Press; 2021. p. 754-768.
  - [15] Kooi FL, Alferdinck JWAM. Yellow Lessens Discomfort Glare: Physiological Mechanism(s); F-WR-2003-0023-H Report; TNO Human Factors. Soesterberg, The Netherlands; 2004.
  - [16] Sivak M, Schoettle B, Minoda T, et al. Short-wavelength content of LED headlamps and discomfort glare. LEUKOS 2005;2:145-54.
  - [17] Kooi FL, de Vries G. Een subjectieve beoordeling van optische hulpmiddelen bij het autorijden in het donker [The influence of optical aids on driving comfort at night]. Hum Factors. Soesterberg: TNO; 2002. (TNO-report TM-02-028, in Dutch).
  - [18] Pierson C, Wienold J, Bodart M. Review of factors influencing discomfort glare perception from daylight. LEUKOS 2018;14:111-48.
  - [19] Marié S, Montés-Micó R, Martínez-Albert N, et al. Evaluation of physiological parameters on discomfort glare thresholds using LUMIZ 100 tool. Transl Vis Sci Technol 2021;10:28.

## ACKNOWLEDGEMENT

The authors express their gratitude to Hidehiro Saeki of the Graduate School of Integrated Frontier Sciences, Kyushu University, and Atsushi Iizuka of Class 1 Car Mechanics for their valuable assistance in developing the headlight model. This study did not receive specific grants from public, commercial, or non-profit funding agencies. There are no conflicts of interest to declare.

Corresponding Author: Tatsuya Iizuka

Affiliation: Graduate School of Medical Sciences, Kitasato University

e-mail: [iizuka.tatsuya@st.kitasato-u.ac.jp](mailto:iizuka.tatsuya@st.kitasato-u.ac.jp)

# APPLICATION OF VISIBLE LIGHT COMMUNICATION TECHNOLOGY IN DIGITAL OPERATING ROOM

Xiaofei Wang<sup>1</sup>, Huafeng Yan<sup>2</sup>, Jian Song<sup>1</sup>

<sup>1</sup>Tsinghua University, Beijing, P.R.China

<sup>2</sup>Medpower Technology Co.,Ltd, Suzhou , P.R.China

## ABSTRACT

Visible Light Communication (VLC) is a wireless communication technology that uses visible light for illumination and communication at same time. Compared with the conventional wireless communication technology with radio channels, VLC transceiver units can be integrated with the existing lighting system. VLC system has advantages such as energy saving, easy deployment, no radio interference, electromagnetic compatibility and so on. It also has the disadvantages of being easily blocked by moving object, interrupted and interfered by sunlight. Finding the right application scenario for visible light communication has always been a challenge.

With the technology progress of medical digitization, traditional hospitals and are transforming into digital hospitals. More and more medical devices with wireless communication capabilities are being deployed, and more wearable devices are used in patients' body, such as pacemaker. Serious electromagnetic interference problem should be considered to affect medical safety. In this project, VLC technology is used in the digital operating room to reduce electromagnetic interference as an application experiment.

Keywords: Visible Light Communication, interference, transceiver, application experiment , ElectroMagnetic Compatibility

## 1. INTRODUCTION

Visible Light Communication (VLC) refers to communication method that directly transmits optical signals in the air by using Light in the visible band as information carrier. VLC technology is green and low-carbon, and can realize nearly zero energy consumption. It can also effectively avoid electromagnetic signal leakage and other weaknesses of radio communication, and quickly build an anti-interference and anti-interception safe information space. The idea is not new. On June 3, 1880, Alexander Graham Bell transmitted the first wireless telephone message on his newly invented "photophone," a device that allowed for the transmission of sound on a beam of light [1].

In the 21st century, with popularity of Light Emitting Diode (LED), VLC rises again and the technology is reinvented with new breakthroughs. LED can support faster switching on and off than traditional fluorescent and incandescent bulbs. By adding microchips to ordinary LED lights, they can be made to flash at extremely fast speeds and send data. As long as the overhead light is shining, it is theoretically easy to transfer data information, access the Internet, make voice and video calls, or adjust the switch of Internet of Things devices, and with the ultra-high transmission rate, the application experience is far better than WiFi and 4G networks. In the future, VLC will interact with WiFi, cellular networks (3G/4G/5G) and other communication technologies (such as zigbee and wsn), bringing innovative applications and value experience to the Internet of Things, smart city (home), aviation, navigation, subway, high-speed rail, indoor navigation, underground operations and other fields[2][3]. Visible light communications can be interfered with by sunlight and be blocked by objects, which physically limits the application range of VLC. The operating room is a good scene for VLC applications naturally. Furthermore, VLC can solve the Electro Magnetic Compatibility problem in the digital operating room.

Electro Magnetic Compatibility (EMC) defined as "the ability of equipment and systems to function properly in their electromagnetic environment without causing intolerable electromagnetic disturbance to anything in the environment." This definition has two meanings. First, the equipment should be able to work normally in a certain electromagnetic environment, a certain electromagnetic immunity (EMS). Secondly, the electromagnetic disturbance generated by the device itself should not have too much influence on other electronic products, namely electromagnetic disturbance (EMI).

EMC is not only related to the safety and reliability of the product itself, but also related to the protection of electromagnetic environment. Therefore, meeting EMC requirements is also a very important condition for products to enter digital operating room. With the progress of technology, more and more electronic equipment and medical equipment is miniaturization and wireless. Wearable devices and implantable medical devices, such as pacemakers, are used for the patients in digital operating room, rehabilitation centre and elderly care community. The density of electronic equipment is becoming higher and higher, with the requirement for EMC becomes more and more serious. The earth's EM environmental background noise is shown below, in Fig1.

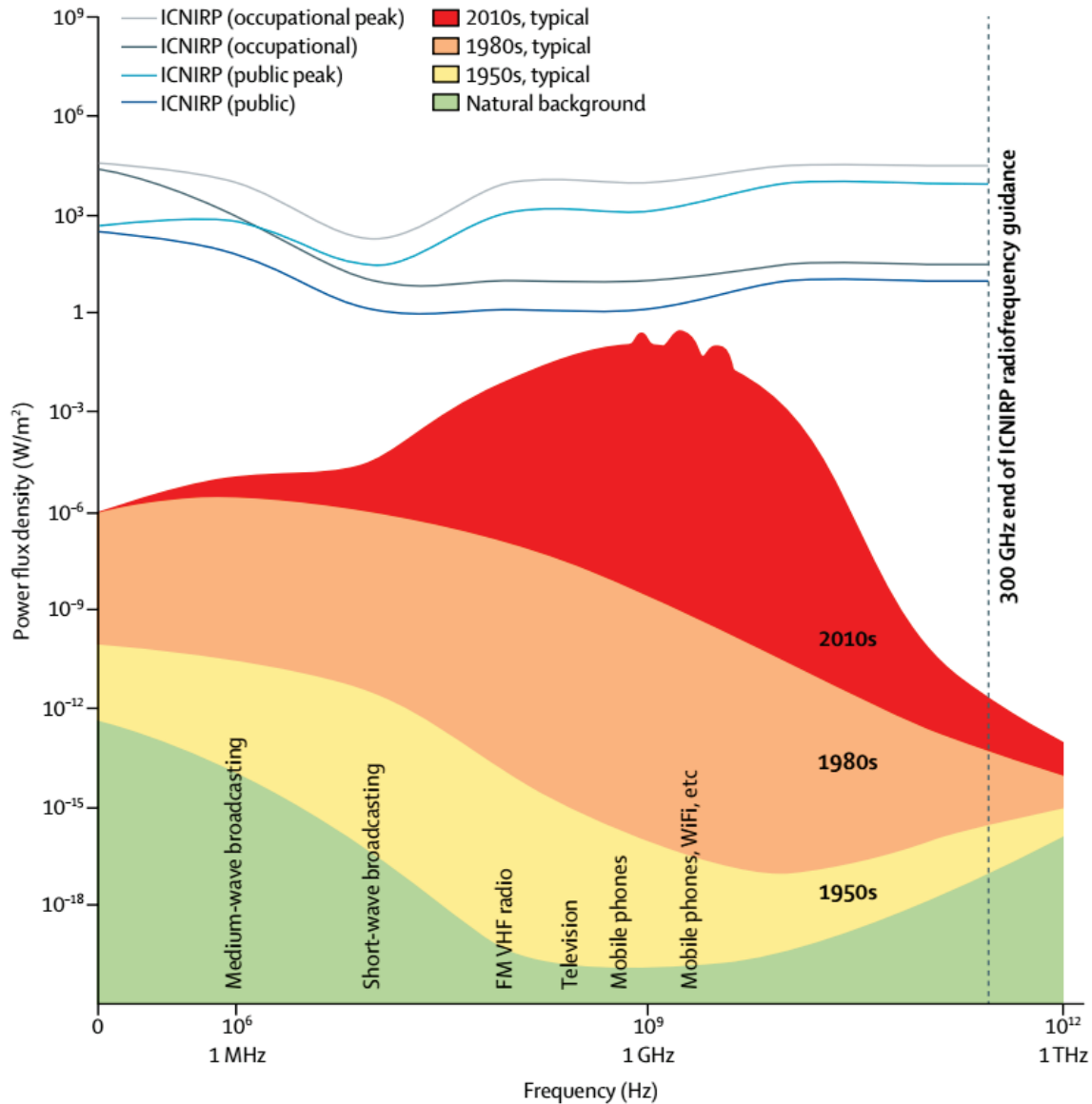


Fig1. Level of background EM noise [4]

As shown in the figure above, we can see that the increase of electronic equipment causes the change of spectrum utilization and spectrum noise. The appearance of VLC makes it possible to develop an innovative method to solve the problem of EMC in digital operating room.

With the architectural design of hospital and digital operating room, it is found that hospital operating room meet VLC requirement, no daylight and only artificial light. Therefore, in the research work of this paper, the possibility of using VLC in digital operating room to solve EMC problem is preliminary experimented and evaluated in a real world.

## 2. METHOD

The operating room always uses artificial lighting system and is a good place for VLC usage without interference of sunlight. With the increase of digital equipment, digital operating rooms are plagued by more and more radios interference. This situation will affect the safety of surgery and the patient's healthy with pacemaker and other important equipment inside the body. In the experiment, the project team with both electronic engineering ability and medical license, deploys VLC system in a real digital operating room and verified the effectiveness of VLC in operation.

The application experiment consists of two tasks:

- Verify the digital operating room environment can support video-level VLC applications. The light source in the operating room will not interfere with the video transmission of the VLC system.
- Verify the multi-emission source technology can be used to ensure that the VLC senders (8 in the experiment) would not be completely blocked by the body of the doctor and nurse during the operation. At least one transmitter of VLC system can work to maintain the communication functions.

For task one, shadow less operating lamp is modified as VLC receiving unit (Signal receiving module), the core receiving and control module of VLC system. Shadow less operating lamp, as the lighting source in the operating room, can theoretically produce a full range of transceiver without dead angle and solve the problem of visible light interruption caused by shading. The system is shown in Fig2. The sender of VLC video system is integrated with shadow less operating lamp.



Fig2. VLC video transmission system used in the digital operation room

For task two, in the operating room, eight potential device deployment points install the VLC sender (Signal transmitting module) module. In one hour simulated operation, the interference of doctors and nurses with VLC system at different locations was simulated. Experiment data are collected comprehensively as in Fig 3.





Fig3. Eight potential device deployment points to verify the VLC video transmission continues in the digital operation room

### 3. RESULT

The application of the VLC technology in the digital operating room achieved preliminary results. The experiment proved that it was feasible to carry out two-way data transmission through the multi-transmitting point method in the actual operation when shadow less operating lamp are used as the arbiter control. The communication would not be interrupted or interfered by the movements of doctors and nurses.

### 4. CONCLUSIONS

The experiment of VLC technology in the digital operating room proved that VLC can be well applied in the digital operating room, especially relying on shadow less operating lamp as the base station. VLC is a potential way to reduce electromagnetic interference, maintain the safety of patients' implantable electronic devices, and improve the security of communications in digital operating rooms and medical environments. Particularly, shadow less operating lamp is the natural VLC centre in the operating room.

### 5. FUTURE WORKS

The current combination method of the VLC system and shadow less lamp is unacceptable in the real operating room. Cooperation with the manufacturers of medical devices is needed to develop a customized shadow less lamps that support VLC which will meet the requirements of aseptic treatment in the operating room.

### ACKNOWLEDGEMENTS

The work was sponsored by Tsinghua-Toyota Joint Research Fund (From 2022/11 to 2024/11). The work was supported by Photomedicine Laboratory, Institute of Precision Medicine, Tsinghua University (No. 100010706).



## REFERENCES

- [1] Alexander Graham Bell's Photophone Was An Invention Ahead of Its Time, <https://www.thoughtco.com/alexander-graham-bells-photophone-1992318>
- [2] J. Cosmas, Y. Zhang and X. Zhang, "Internet of Radio-Light: 5G Broadband in Buildings," European Wireless 2017; 23th European Wireless Conference, Dresden, Germany, 2017, pp. 1-6.
- [3] Strategic Roadmap 2025 of the European Lighting Industry: [https://www.lightingeurope.org/images/160404-LightingEurope\\_Roadmap---final-version.pdf](https://www.lightingeurope.org/images/160404-LightingEurope_Roadmap---final-version.pdf)
- [4] P Bandara & D O Carpenter, The Lancet Planetary Health 2018

# BRIGHTNESS PERCEPTION THRESHOLDS OF LIGHT-EMITTING UNITS IN DIFFERENT FORMS: COMPARISON OF VIRTUAL REALITY AND REAL ENVIRONMENTS

Guangyan Kong<sup>1,2</sup>, Lixiong Wang<sup>1,2</sup>, Juan Yu<sup>1,2</sup>, Shuo Chen<sup>1,2</sup>

(<sup>1</sup>School of Architecture, Tianjin University, Tianjin, China;

<sup>2</sup> Tianjin Key Laboratory of Architectural Physics and Environmental Technology, Tianjin , China)

## ABSTRACT

Virtual reality (VR) technology is widely used in the study of light environments, and accurately setting the brightness of the light source in the VR environment is an important link to improve the accuracy of VR reproduction. Based on the theory of visual perception, this research adopts the minimal change method to carry out brightness perception experiments of light-emitting units in real environment and VR environment with similar settings. In both experiments, the shape, size and position of the light-emitting unit were used as variables, and a total of 20 groups of surface morphology were set. The experimental results show that: 1) In the real environment and the VR environment, the luminance, shape, and size are all significant factors affecting the brightness perception threshold (BPT) of the light-emitting unit, and the degree of influence in the VR environment is: initial brightness (0.893) > shape (0.465) > Size(0.046). 2) The BPT is negatively correlated with size. 3) There is a significant difference in the BPT between the center position and the non-center position, but there is no significant difference the non-center positions (the same viewing angle). To sum up, the influencing factors and changing rules of the BPT of different forms of light-emitting surface are consistent in the real environment and the virtual environment. This is important for the study of the calibration of luminance parameters in VR environments and realistic environments.

Keywords: Virtual reality, Brightness perception threshold, Luminance, Light-emitting units

## 1. INTRODUCTION

In recent years, the theory and technology behind virtual reality (VR) have been gradually improved and widely used in the research of indoor visual environment research [1-4]. Through a large number of comparative studies it was found that VR is the most promising alternative medium to replace the existent environment for light environment research, as it has more advantages over traditional alternative mediums for lighting research in terms of immersive experience [5], accurate reproduction of physical space, presentation of spatial ambience [6], and save on physical building costs. Although people's performance, perception and behavior in immersive virtual environments are not significantly different from those in physical environments, there is still room for improvement in the accuracy of VR applications in the study of optical environments [7]. The closer the results of optical parameter setting in VR are to the realistic environment, the more reliable are the experimental results obtained. The current VR technology changes the visual presentation brightness of the pre-rendered or photographed IVLE spatial surface by regulation, which essentially ensures the consistency of the visual perception of luminance contrast [8], and the set "luminance value" is a relative luminance value, which is not related to the actual physical value of luminance, especially when the regulation parameters of light in the VR light environment go through Especially when the light regulation parameters in the VR light environment are composed of algorithm simulation, exposure, Head Mounted Display (HMD) expression and other series of reproduction, the regulation input value will only retain the numerical properties, but does not have the actual physical meaning, i.e., it is impossible to directly obtain the actual physical luminance value of each surface in the VR scene. However, luminance is an important design element of the visual environment and a perceptually influential element of the light environment that is the focus of current research [9]. Therefore, obtaining the

physical luminance measures of each surface in VR scenes is an important problem to solve the accurate simulation of VR light environments [10].

Due to the visual characteristics of the human eye, it is necessary to consider the impact of various factors on the perception of visual brightness, such as human eye luminance adaptation, visual environment, and the morphology of the viewed object [11-12]. Among them, the form of the visual object itself includes its surface texture, shape, size, and position. The surface texture, i.e., the surface reflection characteristics and reflection coefficient [13], determines the direction and degree of luminance to be reflected. The shape, size, and position affect the field of view and viewing angle [14], and the variable field of view and viewing angle are the keys to the formation of the VR immersion experience. The two parameters of stereo angle and position index in the glare evaluation study also illustrate that the shape, size, and position of the luminous surface are essential factors affecting brightness perception. This study initially takes the morphology (shape, size and position) of the light-emitting surface as the research variables and conducts subjective brightness perception experiments using the brightness perception threshold (BPT), with the aim of trying to find a bridge between the VR environment and the real environment using the consistency of the human eye's subjective perception of brightness, and to provide a data base for future brightness calibration studies between the VR environment and the real environment.

## 2. METHODS

### 2.1 Experimental settings

The brightness perception threshold experiments of luminous surfaces were carried out in the real environment and VR environment, respectively. As shown in Table 1, different spatial interface materials, light-emitting modules and luminance adjustment methods were used in the two environments, but the aim was to ensure that both presented similar visualizations.

Table 1. Comparison of experimental settings

	Real environment	VR environment
Equipment	Physical space (includes a wall covered display)	HTC Vive Pro smart VR devices
Space Scale	$L \times W \times H = 4.5 \times 3.0 \times 3.0$ (m)	
Interface Materials	Black velvet (wall) + pvc floor leather (floor)	Gypsum board (UE4)
Light-emitting modules	LED full-color screen + translucent film	UE4 surface light source
Luminance adjustment method	0-255 grayscale images + screen luminance adjustment	Software input luminous flux
Light distribution forms	Lambertian body light distribution	
CCT	4000K	
Observation position	$(x, y, z) = 2.25\text{m}, 1.5\text{m}, 1.2\text{m}$	
Space model		

The experiments in the real environment were carried out in the comprehensive experimental platform of variable building space in Tianjin University, and the luminous surface was reproduced

by the LED display installed on the side of the space. The shape, position, size and other parameters of the luminous surface were set by a computer control system. To control the effect of background luminance and color temperature on luminance perception, the surface reflection coefficient, and background luminance were set to 0, and the color temperature was kept to the fixed value of 4000 K. The experiments were carried out with the luminance, shape, size and position of the luminous surface as independent variables.

We selected three traditional light source shapes (point, line, and surface), took 150 mm as the basic module of the light-emitting unit, and performed integer splicing to ensure a suitable size. Taking the center of the line of sight as the origin and combining the visual features of the human eye, we selected the upper, lower, and right regions as position variables. Therefore, a total of 20 light-emitting surfaces were set up in this experiment, as shown in Table 2. The coordinates of the center point of the light-emitting surface were used to represent the position parameters, and it was stipulated that the horizontal deviation of the line of sight to the right is positive, and the vertical upward deviation is positive, and vice versa.

Table 2. Light-emitting surface

Sizes				Positions	Sizes				Positions
Shape	Area / m <sup>2</sup>	L / m	W / m	Coordinates of	Shape	Area / m <sup>2</sup>	L / m	W / m	Coordinates of
				center point					center point
				(x, y)					(x, y)
Point (P)	—	0.15	0.15	(0, 0)	Vertical Line (VL)	0.09	0.60	0.15	(0, 0)
		0.15	0.15	(-2.175, 1.365)		0.27	1.80	0.15	(0, 0)
		0.15	0.15	(2.175, 1.365)		0.45	3.00	0.15	(0, 0)
		0.15	0.15	(-2.175, -1.365)		0.45	3.00	0.15	(-2.175, 0)
			0.45	3.00		0.15	(-2.125, 0)		
Surface (S)	0.09	0.30	0.30	(0, 0)		0.14	0.90	0.15	(0, 0)
	1.44	1.20	1.20	(0, 0)		0.41	2.70	0.15	(0, 0)
	1.44	1.20	1.20	(1.65, 0.84)	Horizontal	0.68	4.50	0.15	(0, 0)
	1.44	1.20	1.20	(-1.65, -0.84)	Line (HL)	0.68	4.50	0.15	(0, 1.365)
	5.76	2.40	2.40	(0, 0)		0.68	4.50	0.15	(0, -1.365)
	13.50	3.00	4.50	(0, 0)					



a).

P: 0.15×0.15m; (0, 0)



b).

VL: 1.80×0.15m; (0, 0)



c).

HL: 2.70×0.15m; (0, 0)



d).

S: 1.20×1.20m; (0, 0)

Figure 1. Example of light-emitting surface.

The VR light environment experiment platform contained an operation and an experiment area. The operation area includes a computer host with a VR control program installed to set the basic parameters of the experiment and adjust the experimental scenario. The participants wore HTC-Vive-PRO smart VR devices in the experimental area and conducted evaluation experiments according to specific procedures. In this study, the combination of 3d max and Unreal Engine 4 (UE4) was used to build the VR light environment experimental scene. To ensure that participants could clearly identify the form of the light-emitting surfaces, the material of the light-emitting surfaces was set to "Emissive" in UE4. The emissive intensity was set to 1.00, indicating that the surface luminance was equal to the input luminance. Also, the automatic exposure of the scene was turned off to ensure the correspondence between the VR scene rendering brightness and the actual input value.

## 2.2 Methodology

In this study, the minimal change method in psychophysics was used to measure the brightness perception threshold. The minimal change method is a common method for measuring the difference limen ( $DL$ ). The experiment consisted of two stimuli, standard luminance and comparative luminance, and participants provided feedback based on the alternating presented stimulus differences, with feedback divided into "+" "=" "-" three categories. Among them, "+" indicates that the comparison stimulus is stronger than the standard stimulus. In the experiment, the midpoint between "+" and non-"+" (i.e., "=" or "-") is the average upper limit ( $Lu$ ), and the midpoint between the first non-"-" and "-" is the average lower limit ( $Li$ ). The  $DL$  is equal to  $1/2$  the uncertainty interval ( $IU$ ) between the upper and lower limits. It is the relative change of the stimulus that determines the perceptual threshold, which is used in this study to calculate the luminance perception threshold (BPT) of the luminous surface, which in turn reflects the difference in luminance visual perception. In order to balance the practice and fatigue effects, the incremental and decremental series were arranged alternately according to the ABBA method.

## 2.3 Participants

In each experimental setting, four (2 male and 2 female) participants were recruited for a pre-experiment to obtain their feedback on the brightness differences and to determine the luminance range and adjustment steps for the formal experiment. In real environment, the participants in the formal experiment were 14 students aged 21-25 years (mean age = 23.85, standard deviation  $\sigma = 1.79$ ), with a male-to-female ratio of 1:1. Similarly, 14 participants were screened for the VR experiment with a mean age of 24.3 years (variance  $\mu_{age} = 1.48$ , standard deviation  $\sigma = 1.22$ ). The participants had a bare eye visual acuity of 5.0 or above or corrected visual acuity of equivalent visual acuity. Subjects were required to be well rested before the experiment, without feeling sleepy or tired, to exclude the effect of fatigue on the experimental results.

## 2.4 Procedures

(1) Pre-experiment: the BPT is related to the range of stimulus brightness. Therefore, a centrally positioned surface light-emitting unit ( $1.20\text{m} \times 1.20\text{m}$ ) was selected, and a pre-experiment was conducted. The purpose of the pre-experiment was to delineate the luminance range and to determine the applicable standard stimuli and the change step of the comparison stimuli at each luminance range. The detailed steps are shown in Figure 2. After participants performed dark adaptation, the luminance of the vertical light-emitting unit was gradually increased from the lowest until participants fed back to see the light-emitting surface, and the luminance value at this point was recorded as the initial perceptual step. With the initial perceptual step as the starting point, the luminance continued to increase until the participant indicated that he or she could not recognize the luminance change three consecutive times. The corresponding first luminance range was obtained at this point. Then, based on the upper limit of the first luminance range, the adjustment step was continued to increase until the participant was again unable to recognize the luminance change and obtained the second luminance range. The corresponding luminance ranges and change steps in real and VR environments were obtained by pre-experiments.

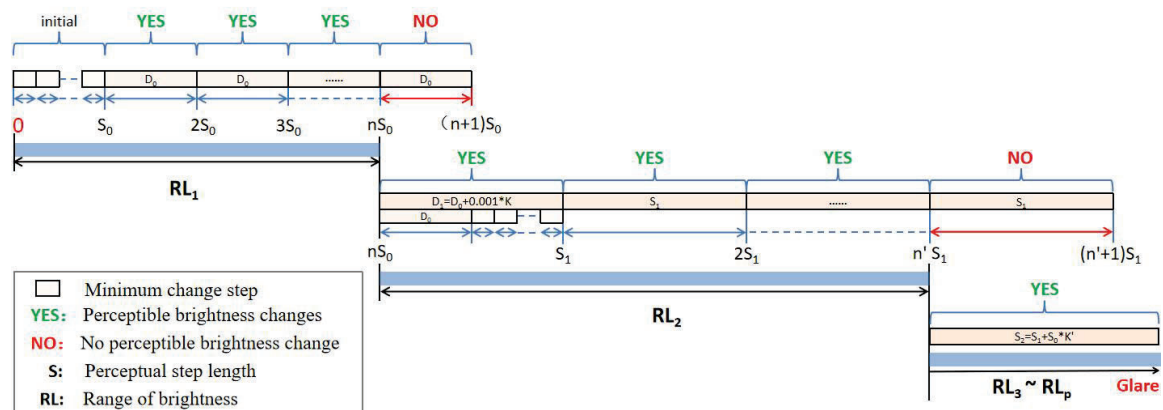


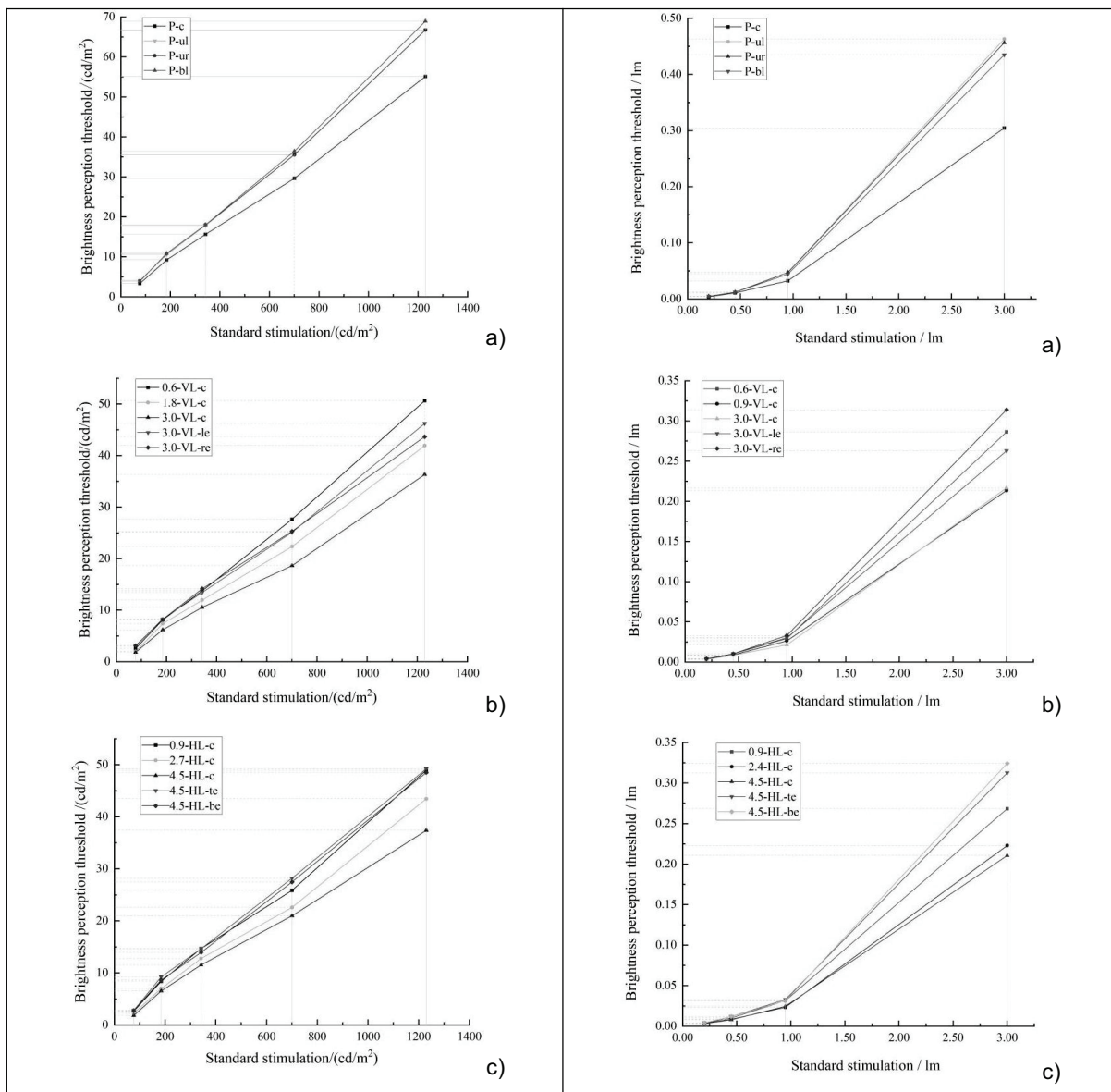
Figure 2. Pre-experiment process.



(2) Formal experiment: After introducing the relevant precautions to the participants, the experimenter adjusted the seat height so that the participants' visual height was uniformly 1.5 m, so that the point of view was consistent with the coordinates of the luminous surface position. The first luminous surface was randomly selected, and the experimenter changed the surface luminance according to the stimulus change step settings obtained from the pre-experiment, and the subject was verbally asked about the luminance perception for each change, and the subject rested with eyes closed for 2 min after each (two) ABBA lift cycle was completed; after each standard luminance stimulation experiment was completed, one luminous surface experiment was finished. One VR surface experiment lasted about 25 min, and then the subjects rested for 5 min; the next surface perception experiment was conducted.

### 3. RESULTS

The experimental data in the real environment and VR environment were input into SPSS 25 separately, and the outliers were detected, locked and replaced to calculate the BPT under different working conditions, and then the influence of the visual elements of the shape on the brightness perception was examined. As shown in Figure 3 and 4, BPT of the light-emitting surface under different operating conditions increases with the increase of standard stimuli.



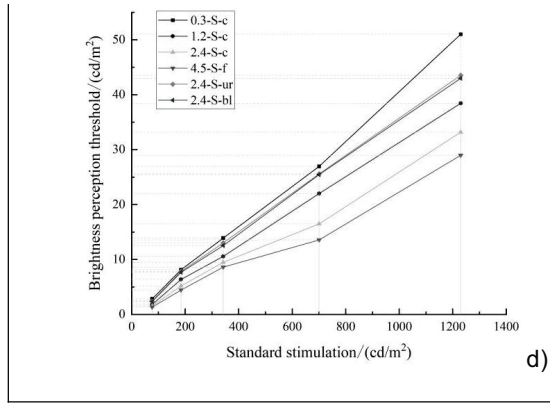


Figure 3. Results of BPT in Real environment.

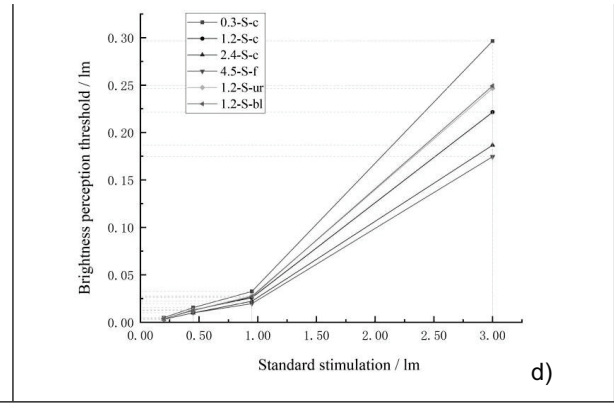


Figure 4. Results of BPT in VR environment

a) Points; b) Vertical line; c) Horizontal line; d) Surface    a) Points; b) Vertical line; c) Horizontal line; d) Surface

### 3.1 Regression analysis of influencing factors

To determine the influence degree of luminance of light-emitting surface, shape, size, and position on BPT, the author conducted linear regression analysis on all variables and established a multiple regression equation of VR surface BPT (Formula 1) according to the multiple linear regression theory. Take the results of the VR experiment as an example.

$$BPT_{VR} = \beta + k_1x_1 + k_2x_2 + k_3x_3 + k_4x_4 + k_5ay_1 + k_6by_2 + k_7cy_3 \quad (1)$$

Dt represents brightness perception threshold of VR surface.

$x_1, x_2, x_3, x_4, y_1, y_2,$  and  $y_3$  represent the independent variables of luminance, vertical view, horizontal view, area, vertical line, horizontal line, and surface, respectively.

$\beta$  represents constants.

$k_1 - k_7$  represent the regression coefficients.

$a, b, c$  represent the dummy variable encoding value (0 or 1).

Through SPSS's multiple linear regression analysis, the final model complex correlation coefficients were calculated and were  $R=0.906$  and  $R^2=0.820$ , indicating a good model fit. The analysis of variance (ANOVA) results showed that the significance of the F-test  $P=0.000<0.01$ , so the linear relationship established by the regression model is considered statistically significant at the 0.01 significance level. The regression coefficients and VIF values of each variable are shown in Table 3.

Table 3. Coefficient estimation of multiple linear regression model (VR)

Model	Unstandardized coefficient		Standardized coefficient		Collinearity statistics		
	B	Std. Error	Beta	t	Sig.	Tolerance	VIF
(Constant)	0.002	0.004		0.441	0.659		
luminance	0.101	0.001	0.893	75.296	0.000	1.000	1.000
vertical viewing angle	0.002	0.003	0.009	0.698	0.485	0.844	1.185
horizontal viewing angle	0.000	0.003	0.001	0.083	0.934	0.832	1.201
vertical line	-0.044	0.005	-0.157	-9.367	0.000	0.504	1.985
horizontal line	-0.042	0.005	-0.148	-8.857	0.000	0.503	1.990
surface	-0.043	0.005	-0.160	-8.508	0.000	0.397	2.521
area	-0.002	0.001	-0.046	-3.264	0.001	0.721	1.387

The results of the multiple linear regression analysis showed the following pattern. 1), VIF < 5 for all variables indicates that there is no covariance in all variables. 2), Vertical and horizontal perspectives ( $p > 0.05$ ), which were not statistically significant in this model, were removed from the regression model. 3), The p-values of the regression coefficient tests for the vertical lines, horizontal lines, and surfaces are less than 0.05, indicating that there are statistical differences between the luminous shapes of the vertical lines, horizontal lines, surfaces, and points. The variable coefficients B for the vertical line, horizontal line, and surface forms are  $-0.044$ ,  $-0.042$ , and  $-0.043$ , respectively, indicating that the brightness perception thresholds for the vertical line, horizontal line, and surface shapes are smaller than those for the point forms. 4), The standard regression coefficient data allows comparison of the contribution or magnitude of contribution between the coefficients, so the elements and order of influence of VR surface brightness perception threshold are luminance ( $0.893$ ) > shape ( $0.465$ ) > size ( $0.046$ ).

Substituting the significant effect variables into the regression equation (1), equation (2) is obtained.

$$10^2 BPT_{VR} = 0.2 + 10.1x_1 - 0.2x_4 - 4.4ay_1 - 4.2by_2 - 4.3cy_3 \quad (2)$$

Similarly, we obtained the regression model for the real environment as Equation 3. In a real environment, the luminance perception threshold is significantly correlated with the luminance and size of the emitting surface.

$$BPT_{REAL} = 6.944 + 0.038x_1 - 0.657x_4 - 7.727y_1 - 6.805y_2 - 7.129y_3 \quad (3)$$

### 3.2 The BPT law under each element

(1) Position. A one-way ANOVA concluded that the effect of position on the BPT of the light-emitting surface was highly consistent between the VR environment and the real environment. For point-like light-emitting surfaces, the significance of the F-test was  $P > 0.05$  for standard stimuli at low luminance levels, indicating that BPTs were not significantly different from position. For the standard stimuli with high luminance levels, the significance of the F-test was  $P < 0.05$ , indicating that the difference between BPTs and position was significant. For the line luminescent surface, the BPT was significantly different ( $P < 0.05$ ) with different luminance stimuli, and a post hoc comparison yielded a significant difference between center and non-center (same viewing angle). For the face-lit surface, there was no significant difference in BPT at different positions in the VR environment ( $P > 0.05$ ), while in the real environment, there was a difference only at a standard luminance stimulus of  $342.2 \text{ cd/m}^2$ .

(2) Size. The correlation analysis between the size of different shapes of light-emitting surfaces and BPT was performed for each luminance stimulus. Among the VR environments, the size of vertical lines did not correlate with BPT under the lowest luminance stimulus. The BPT was negatively correlated with the luminescent size of lines and surfaces under the rest of the standard stimuli, i.e., the BPT decreased with the increase of size. Similarly, in the real environment, the overall luminance perception thresholds of line and surface luminous units both decreased with increasing size, while the correlation degree was different under different standard luminance stimuli.

## 4. CONCLUSIONS

Establishing the correspondence between the perceived luminance of VR presentation and the actual scene is important for the reproduction accuracy of VR in light environment research. In this study, three visual morphological elements of luminous surface shape, size and position were selected as the main research variables, and the effects of the three on BPT were analyzed under different standard luminance stimuli in VR environment and real environment. The main findings of this study are as follows.

In both VR and real light environment experimental space, luminance, shape, and size are significant influencing factors of the light-emitting surface BPTs. The luminance of the VR space surface has the maximum impact on the brightness perception threshold ( $0.893$ ) and is positively correlated. The influence of form also had a great weight, with the shape ( $0.465$ ) having a much higher impact on the luminance perception threshold than size ( $0.046$ ).

The BPT of the light-emitting surface is negatively correlated with the size, and the larger the luminous surface morphology, the easier it is to perceive the brightness change. In addition, the brightness perception thresholds for the central position are smaller than those for the non-central position, while there is no significant difference between the non-central positions (same viewing angle).

In summary, the brightness perception thresholds of different forms of light-emitting surfaces, their influencing factors and change laws are consistent in real and virtual environments. This is of great significance for future research on the calibration of luminance parameters in VR environments and real environments.

## REFERENCE

- [1] Y. Lin, X. Zeng, Research on the influence of urban nightscape lighting on emotion perception: progress and prospect (in Chinese), *Urbanism and Architecture*. 17 (2020) 175-179.
- [2] K. Chamilothoni, J. Wienold, M. Andersen, Adequacy of immersive virtual reality for the perception of daylight spaces: comparison of real and virtual environments, *Leukos*. 15 (2018) 1-24.
- [3] M. Scorpio, R. Laffi, A. Teimoorzadeh, G. Ciampi, M. Masullo, S. Sibilio, 2022. A calibration methodology for light sources aimed at using immersive virtual reality game engine as a tool for lighting design in buildings, *J. Build. Eng.* 48, 103998.4 K. Chamilothoni, J. Wienold, C. Moscoso, B. Matusiak, M. Andersen, 2022. Subjective and physiological responses towards daylight spaces with contemporary facade patterns in virtual reality: Influence of sky type, space function, and latitude. *J. Environ. Psychol.* 82, 101839.
- [4] A. Bellazzi, L. Bellia, G. Chinazzo, F. Corbisiero, P. D'Agostino, A. Devitofrancesco, F. Fragliasso, M. Ghellere, V. Megale, F. Salamone, 2022. Virtual reality for assessing visual quality and lighting perception: A systematic review, *Build. Environ.* 209, 108674.
- [5] Y. Chen, Z. Cui, L. Hao, Virtual reality in lighting research: Comparing physical and virtual lighting environments, *Lighting Res. Technol.* 51 (2019) 820-837.
- [6] Iglesias MI, Jenkins M, Morison G. An Enhanced Photorealistic Immersive System using Augmented Situated Visualization within Virtual Reality[C]. *IEEE Conference on Virtual Reality and 3D User Interfaces (IEEE VR)*. 2021, 514-515.
- [7] Zhou Z, Zhou Y, Xiao J J. Survey on augmented virtual environment and augmented reality[J]. *SCIENTIA SINICA Informationis*, 2015, 45(02): 157-180. ( in Chinese )
- [8] Yvonne A. W. de Kort. Tutorial: Theoretical Considerations When Planning Research on Human Factors in Lighting[J]. *LEUKOS*, 2019, 15: 85-96.
- [9] Tian F, Xu H J, Wang P, et al. Evaluation criteria for visual comfort in 3D-VR[J]. *Journal of Shanghai University(Natural Science)*, 2017, 23(03): 324-332.
- [10] J. F. Barraza, A. Martin, The Effect of Texture on Brightness Perception in Simulated Scenes, *LEUKOS*, 16 (2020) 279-287.
- [11] S. Fotios, D. Atli, C. Cheal, K. Houser, Á. Logadóttir, Lamp spectrum and spatial brightness at photopic levels: A basis for developing a metric, *Light. Res. Technol.* 47 (2015) 80-102.
- [12] J. F. Barraza, A. Martin, The Effect of Texture on Brightness Perception in Simulated Scenes, *LEUKOS*, 16 (2020) 279-287.
- [13] R.F. Murray, 2013. Human Vision and Electronic Imaging- Human lightness perception is guided by simple assumptions about reflectance and lighting. *Proc. SPIE* 8651, 865106.
- [14] J. Yu, L. Wang, M. Zhang, J. Song, D. Yang, Threshold of the disruption to residents indoor activities by colored light from urban lighting, *J. Civil. Arch. Environ. Eng.* 41 (2019) 136-143.

## ACKNOWLEDGEMENT

The authors give special thanks to the National Natural Science Foundation of China (52278120) for funding this study. In particular, the authors are grateful to Jiaqiang Cui for his contributions to the pre-experiment.

Corresponding Author: Juan Yu  
Affiliation: School of Architecture, Tianjin University  
e-mail : 601463949@qq.com

## Study on the impact of alert sections inside long tunnels on reducing driver fatigue

**Abstract:** In long tunnel driving, tunnel lighting not only affects visual performance, but also non-visual effects, such as driver's physiological fatigue or psychological load. In the middle section of long tunnels, as a result of being in a confined space and exposed to a monotonous overall light environment for extended periods of time, drivers are more prone to experiencing physiological fatigue which can exacerbate their psychological load. In this study, the physiological signal testing system MP150 was used to study the curve changes of the subject's EEG indexes during the whole process of experiencing fatigue driving by taking the subject's EEG (EEG) energy ratio of specific bands ( $(\alpha+\theta)/\beta$ ) as the dependent variable, which was used as the basis for setting and establishing the long tunnel lighting alert section. The results and discussion have showed that: ① The best location for setting the alert section is within the section after driving for 286.8s under low luminance road illumination ( $3.5 \text{ cd/m}^2$ ), and under the condition that the length of the alert section is set at 200m, the most reasonable location for setting the illumination alert section is from 4780m to 7967m in the middle section of the tunnel; ② The higher average ambient luminance of the alert section can reduce the fatigue and psychological load of the subject in a short period of time, and the difference between the average ambient luminance and the decrease of  $(\alpha+\theta)/\beta$  in EEG in a short period of time present a quadratic function  $\Delta E = 30.091\Delta L s^2 - 3.74\Delta L s - 18.344$ ; ③ Comparing the 200m and 400m alert sections set in long tunnels, it was found that setting too long alert sections did not have a significant gain effect on the driver's alertness. This paper gives the recommended values of the length of the alert section, the recommended values of the road surface brightness and the average ambient brightness, and complements the study on the construction of the light environment in long tunnels to provide technical support for future research on driving comfort in long tunnels.

**Keywords:** middle section of long tunnel; alert section; perceived ambient brightness; EEG index; fatigue amelioration effect

China's long highway tunnels are developing rapidly, according to the statistics at the end of 2020, the number of long highway tunnels in China has increased to



1175, and the length of long highway tunnels has reached 52,700 km. However, it is far from enough to solve these problems for the lighting research of long tunnels, it takes the longest time to pass the middle section, and the existing domestic and foreign technical reports and specifications have not listed long tunnels separately to set corresponding lighting technical indicators although driving comfort in the middle section of long tunnels plays a crucial role in driving safety. Statistics (Pervez et al., 2020) of Chinese road tunnel traffic accident from 2012 to 2016 show that the number of casualties caused by tunnel rear-end collision increased from 244 in 2012 to 305 in 2016, and most of the accidents were caused by tunnel rear-end collision, which indicates that drivers' perception of speed and distance diminished in tunnels. In the middle section of long tunnels, due to low luminance of the road surface to some degree, the prolonged dim light environment will cause changes in non-visual effects such as drivers' physiological rhythms and psychological status, which will easily produce fatigue and drowsiness, thus reducing visual efficacy and posing serious safety risks, meanwhile drivers operating less and visual information being reduced 2/3 than in normal road sections are more prone to cause distracted fatigue (He et al., 2017b; Yan et al., 2020b; Pervez et al., 2020).

For a long time, research works related to illumination ray have been carried out based on human visual pathways and higher cognitive behaviors, and have been established to meet the requirements of illuminance levels and visual recognition, cognitive work efficiency, color-rendering properties of light source and glare evaluation methods. But research in the past 20 years have showed that lighting not only directly affects the human visual system, but also has significant effects on human both physiologically and psychologically. In 2002, David Berson of Brown University discovered a third photoreceptor cell, the retinal ganglion cell (RGC), in the retina of human eye, and verified its non-visual effects. PieR-Re Philip (2005) investigated the effect of fatigue on driving behavior by comparing the driving performance of the normal and sleep deprived groups, which demonstrated that the decrease in driving performance was closely related to driver fatigue and that drowsiness and fatigue had a significant effect on driver reaction time. Pia M. Forsman (2013) studied moderate driver fatigue, then concluded that steering wheel variability data and lane offset variability data can be used as parameters to characterize fatigue. Masaki Yamaguchi et al., (2006) used a handheld fatigue detection system to assess the driver's sympathetic excitability through salivary

enzyme activity, and when sympathetic excitability decreases, the driver is then in a state of fatigue. (deNauroisetal, 2019) found that some subjects reached a drowsy state after 10 minutes of driving in a simulated test, and the time for drivers to reach fatigue would be shorter in a real driving environment. Wang LZ et al. (2015) constructed a driving fatigue index calculation model based on fuzzy mathematical evaluation according to the changing pattern of dependent variables such as EEG, ECG, eye movements, and driving performance in a simulated driving. Although neuroimaging studies have shown the existence of light-induced activity in both prefrontal cortex and parietal lobe (Vandewalle et al, 2009), which are known to be related to visuospatial abilities and executive functions, but blue-light-rich illumination has been only partially explored for these processes. Exposure to high luminance light preferentially reduces reaction time, decreases subjective drowsiness, reduces auditory lapses, and increases alertness (West, Kathleen E, et al, 2011). There is growing evidence indicates that the spectral and luminance environment of light sources can have a significant impact on visual task performance as well as perceptions of safety and comfort (Knight C. PhD, 2007 ; Ahin, Levent et al, 2013). It is important to note that lighting choices increasingly tend to profit from the non-visual effects of light (Rea and Figueiro, 2016; Renzler M., 2018).

In summary, this section of the experiment will use the simulated driving time as the independent variable and the energy ratio of specific bands  $(\alpha+\theta)/\beta$  in the subject's electroencephalogram (EEG) as the dependent variable to study the curve changes of the subject's EEG indexes during the whole process of experiencing driving fatigue, which will be used as the basis for setting and establishing the long tunnel lighting alert segment. The experiment is conducted by observing and analyzing the patterns of changes in these two types of dependent variables in intermediate segment with different lighting environments of drivers, and then make a discussion of the following:

- ① How the physiological fatigue and psychological load of the driver change during driving in a situation where the overall average ambient luminance of the long tunnel is low;
- ② The location of the alert segment settings;
- ③ The length of the alert segment settings.

## 2. Method

### 2.1 Variables selected for the experiment

The driving behavior of the driver in a long tunnel, the impact of driving safety has been more than the road brightness, but the overall level of environmental lighting, including road and driver's field of vision, in the same condition of road brightness, the driver's visual perception and non-visual effects will be very different because of the difference in the visual area of the environmental brightness and color temperature. In longer tunnels, while driving too fast, the driver's visual area will be significantly reduced, which is inversely proportional to the speed obviously. In this paper, the average luminance within the visual area is defined as the perceived environmental luminance. To calculate the specific perception environment brightness of a vehicle speed, we can refer to the relationship between Thomas' perception range and the vehicle speed. for example, when driving speed is 80km/h, the background luminance perceived by the driver in the dynamic field of view is the polar range with the long tunnel as the center and the polar coordinates of  $31^\circ$ . The perceived ambient luminance is different from the overall background luminance and emphasizes the driver's visual perception range. However, the perceived ambient luminance is not easy to obtain accurately, and the maximum field of view of the traditional aiming point luminance meter is only  $1^\circ$ , so it is difficult to measure and calculate the perceived ambient luminance in such a large range, but thanks to the development of equivalent light curtain luminance meters, it is able to measure the ambient luminance value within the set polar coordinating in the light curtain luminance. In this paper, it is determined that both pavement luminance and perceived ambient luminance are considered as independent variables for the study.

Since the target of this paper is the middle section of a long highway tunnel, the selection of a real long tunnel for experimental preparation is extensive and time-consuming, and it is difficult to select a large number of samples for experiments to obtain relevant patterns, but indoor simulation experiments can solve these problems. In the process of studying the physiological and psychological effects of drivers in the middle section, the driving time in the long tunnel is one of the important independent variables, in the static laboratory simulation experiment, the electroencephalography (EEG) index is a sensitive dependent variable that changes with driving time, and the EEG data in the static simulation environment better reflects the fatigue level of the subject, while in the actual driving environment with

stress, electrocardiography (ECG) is more effective in reflecting the fatigue and psychological burden of the subject. Therefore, the selection of a better dependent variable and the determination of the duration of passage are particularly important for the success or failure of the experiment.

## 2.2 EEG signal experimental equipment and software

### ① MP150 polysomnographic recorder

MP150 polysomnographic recorder is an important instrument for collecting physiological indicators of the tested driver in this section of the experiment, the version used in this experiment is MP150-16 conductor version, this version of physiological signal recorder can complete 16 kinds of physiological electrical signal measurement such as ECG, EEG, EMG, EYE, etc. The working principle of this device is to digitally filter and anti-interference process the raw signal online or offline, and perform Fourier transform, then select the gain on the amplifier. The MP150 multi-conductor physiological recorder can be freely set to a maximum of 4000Hz, or 50Hz for indoor testing; the instrument can be triggered or recorded by selecting internal or external triggering, and the output has waveform size, shape, interval, etc.

The BIOPAC MP150-16 conductive physiological signal meter module selected for this experiment consists of the following components: a .BIOPAC electrode cable set (SS2L); b .BIOPAC disposable electrode sheet (EL503); c .BIOPAC experimental system: AcqKnowledge 5.0 software, MP150-16 conductor mainframe, EEG100C EEG module, MEC110C electrode cord set; d.The matching computer. In this experiment, the EEG module is mainly used for data collection and analysis, and the subject is connected to the instrument in a positive and negative way as shown in Figure 4.21.

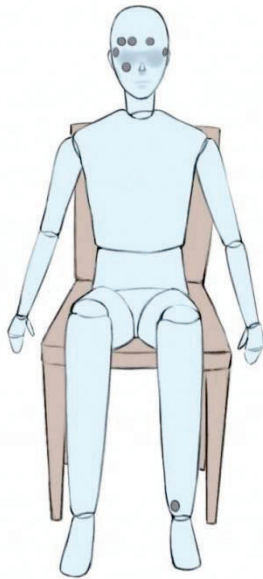


Figure 1 MP150 positive and negative connection position (source: author's own drawing)

## ② AcqKnowledge 5.0 software with MP150 polysomnography recorder

AcqKnowledge 5.0 software has two most important functions: recording and analyzing physiological information, which enables the acquisition settings to determine the basic nature of the data to be collected, such as the amount of time the data will be collected and the rate at which the data will be collected. In addition to collecting physiological data from the subjects, AcqKnowledge 5.0 also offers four additional features: brain wave preview, removal of eye movement signals from the EEG, digital filtering, and EEG wave segmentation. The energy curve of each segmented brain wave as shown in Figure 2.

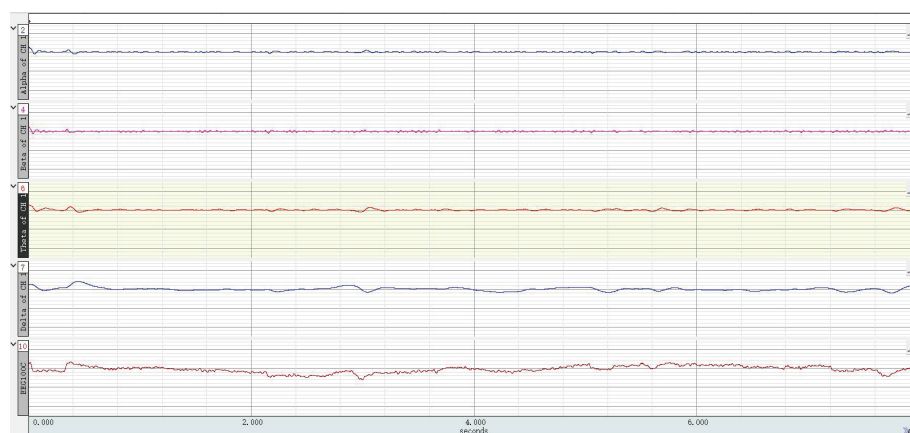




Figure 2 Energy profile of each waveform after EEG waveform splitting by using AcqKnowledge 5.0

### 2.3 Experimental subjects

20 drivers with long-distance driving experience were selected as the experimental subjects. The age group consisted of 10 drivers between 20 and 35 years of age (youth group) and 10 drivers between 35 and 50 years of age (middle-aged group), with average age  $M=37.1$ , and standard deviation  $SD: 3.9$ . The gender group consisted of 10 drivers of each sex. Each subject signed an informed consent form to participate in the experiment and was able to cooperate actively with the conduct of the experiment. The experiment was conducted at noon on the same day, and the subjects did not take a lunch break so that they simulated the exhaustion of having been driving for a longer period of time. Each subject had a valid driver's license corresponding to the vehicle tested, with an average driving experience of 6.6 years. The subjects had normal hearing and normal or corrected visual acuity. All subjects were proficient in driving multiple vehicle types, had no serious accident experience, and had a recent physiological examination and were free of physiological or psychological impairment, disease, or sleep disorders. Subjects were asked to avoid alcohol, caffeine, and drugs for 48 hours prior to testing, and all participants gave informed consent for the collection of their physiological information before entering the experiment.

### 2.4 Experimental test environment

#### ① Total time setting

The EEG index is the dependent variable that changes with the simulated driving time, therefore, the design of the simulation experiment length is particularly important for the success or failure of the experiment. At present, according to the data of the longest tunnel under construction in China, the length of a single tunnel has reached 20.8km, due to the speed limit is 80km/h in the tunnel, and it is impossible for the driver to maintain uniform speed at all times during the normal driving process, the overall driving process will be greater than 15minutes, this section integrates the mileage and design speed limit of most newly constructed long tunnels in China, and the driving process in the middle section of the tunnel is

considered as the ideal uniform speed status, set driver physiological and psychological effects of the experiment length control for 10minutes (600s), and simulated driving process are in the middle section of the long tunnel.

## ② Simulation of lighting scenes

The Highway Tunnel Lighting Design Rules (JTG/T D70/2-01-2014) stipulate that the luminance of the middle section of a long tunnel takes only the part about the road surface luminance, while the luminance takes the value related to whether it is two-way traffic, design speed, and car flow, the minimum value of road surface luminance within the middle section is  $3.5 \text{ cd/m}^2$ , and the corresponding average ambient luminance is  $1.54 \text{ cd/m}^2$ . The device used in this experiment is a homemade 1:20 scale model simulating the lighting of the middle section of a long tunnel, which can reproduce the lighting environment during the driving process of the middle section of a long tunnel, and test the changing pattern of driver physiological parameters after changing different light environment parameters (light source, road surface brightness, ambient brightness, ambient ratio).

This set of experimental equipment includes a simulated light box, tunnel wall reflective coating and other components. The simulated speed is set as 80km/h, so the average luminance of the environment is the cross section of the perspective projection under the dynamic field of view of the human eye at  $31^\circ$ . To ensure the uniformity of transmitted light distribution, a uniform diffuse transmission film is used inside the light box to cover the simulated tunnel sidewall coating, meanwhile retroreflective material is used inside the light box to simulate the contour marker, and a recurring car dynamic driving away animation is used after the light box. The structure diagram of the scaled-down model is shown in Figure 3.

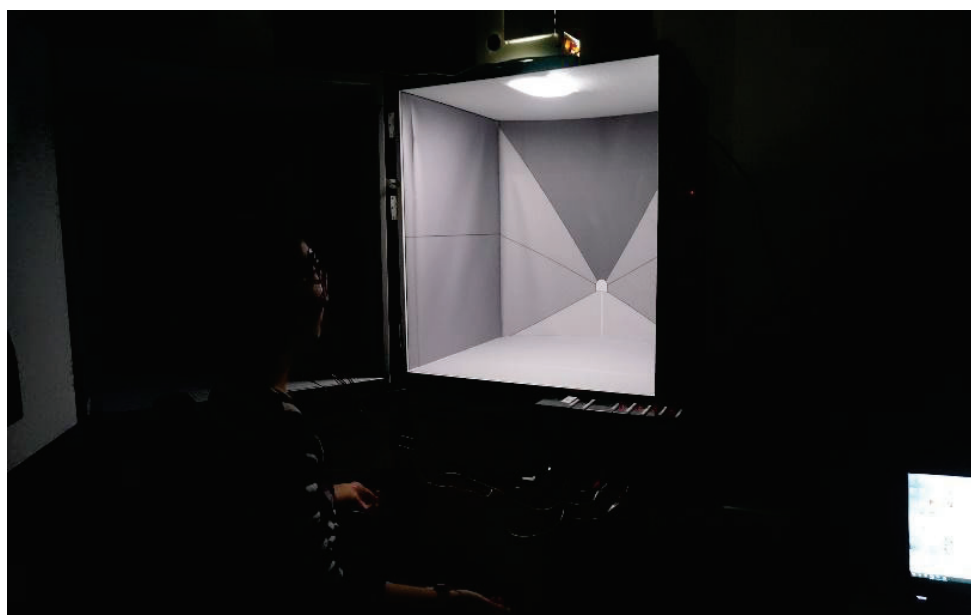


Figure 3 The structure of the scene in the middle section of the homemade simulated long tunnel

## 2.5 Experimental test content

The content of the experimental test in this chapter is divided into the subjective content part (subjective fatigue questionnaire and subjective alertness evaluation questionnaire) and the objective content (EEG index) part, for the physiological and psychological effects of the human factor effect of the driver in Chapter 3, along with the driving characteristics in long tunnels, the evaluation index is reasonably selected.

### ① Subjective test content

The main subjective test content adopted in this experiment is subjective alertness evaluation. Currently, the most widely used subjective alertness assessment method is the Karolinska Sleepiness Scale (KSS), which ranges from "extremely awake" to "extremely sleepy and uncontrollable", a total of 9 levels were used to describe the subjective alertness of the subjects, as shown in Table C1.

### ② Objective test content

The lighting in the tunnel is closely related to the physiological and psychological effects of the driver. From the contents of the literature review, it is clear that the energy of  $\theta$ -wave rhythm is elevated when the subject is fatigued, while the energy of  $\alpha$ -wave and  $\beta$ -wave rhythm is reduced. When the subject is tense, the brain mainly produces  $\beta$  waves; when the subject is relaxed and the brain is more active, the brain mainly produces  $\alpha$  waves; however, when the  $\alpha$  waves exceed a certain range, it indicates that the subject's attention cannot be focused. When the subject feels sleepy and less alert, the brain waves become theta waves. After comparing the results of the preliminary experiments, it was found that the most significant changes in the levels of physiological fatigue and psychological burden occurred in the  $(\theta+\alpha)/\beta$  ratio, as well as the  $\alpha/\beta$ 、 $(\theta+\alpha)/(\alpha+\beta)$ , and  $\theta/\beta$  combinations in the EEG. The  $(\theta+\alpha)/\beta$  ratio showed the highest increase in value as fatigue and psychological burden intensified. In the simulated experimental condition, these three status are simultaneous and each band produces energy values between 10-12V and 10-11 orders of magnitude, and it is more operational and significant to characterize the physical fatigue and psychological load of the subject using the ratio  $(\alpha+\theta)/\beta$ . Therefore, to address this issue, this paper calculates the wave energy ratio  $(\alpha+\theta)/\beta$  as

a characteristic index for judging the degree of psychological load of drivers based on the occurrence rates of three typical EEG waves:  $\alpha$ ,  $\beta$ , and  $\theta$  waves.

### 3. Results

After the completion of the MP150 test, the raw EEG data of 20 participants were filtered and the data with large fluctuations were removed. First, a Pearson correlation analysis was conducted between the sensitive frequency bands of the brain and the ratio between the bands. The statistical results are summarized in Table 1. After the Pearson test on the EEG indicators, the average of the group was also calculated. Based on the assumption that the experimental data follows a normal distribution, a Pearson correlation coefficient analysis was performed on the data. Figure 4 and Figure 5 respectively depict the temporal variations of  $(\alpha+\theta)/\beta$  in the simulated middle segment under low brightness lighting conditions and demonstrate the trend using a trend chart in Figure 5.

Table 1 Pearson correlation between EEG-related bands and ratio indicators of bands and simulated driving fatigue (source: based on experimental data)

Indicators	A lpha wave	Be ta wave	$\theta$ wave	$\alpha/\beta$	$\theta/\beta$	$(\alpha+\theta)/\beta$
Alpha wave	1					
Beta wave	*	1				
$\theta$ wave	*	/	1			
$\alpha/\beta$	*	/	/	1		
$\theta/\beta$	/	/	*	/	1	
$(\alpha+\theta)/\beta$	*	*	**	/	/	1
	*					

Note: \* represents correlation ( $P < 0.05$ ), \*\* represents significantly relevant ( $P < 0.01$ ), / represents not relevant

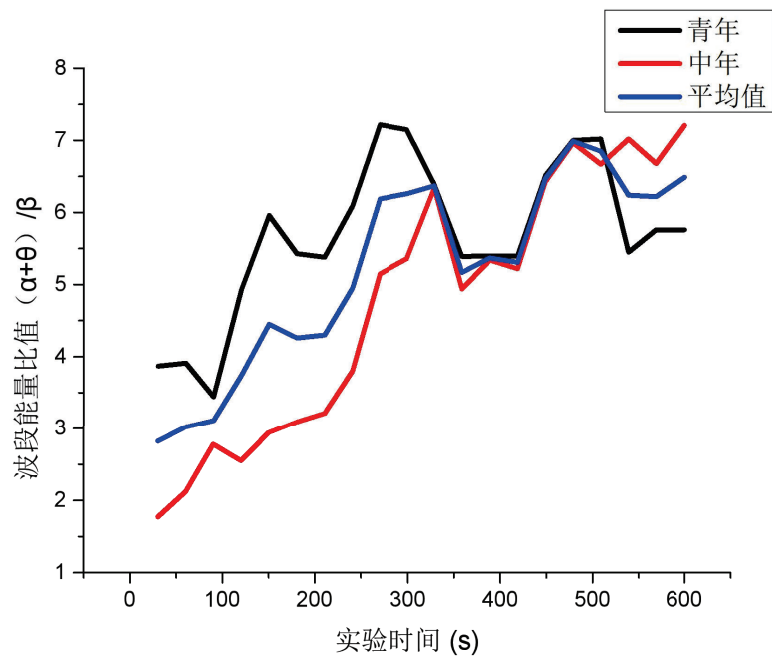


Figure 4 Trend of  $(\alpha+\theta)/\beta$  over time in the low luminance intermediate light environment for subjects of different ages

(Source: Self-drawn by the author)

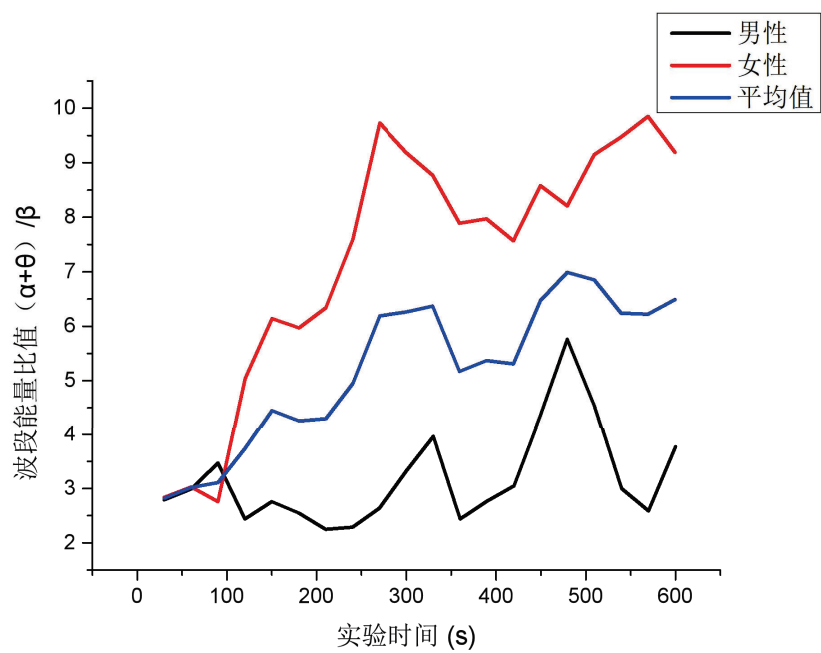




Figure 5 Trend chart of  $(\alpha+\theta)/\beta$  variation over time in the low luminance intermediate light environment for different gender subjects

(Source: Self-drawn by the author)

## 4. Discussion

### 4.1 Differences in age and gender of the subjects

When divided by age, the EEG band energy ratio  $(\alpha+\theta)/\beta$  (hereafter referred to as  $(\alpha+\theta)/\beta$ ) of the young subjects was similar to that of the middle-aged group, but the growth rate of  $(\alpha+\theta)/\beta$  was 48.8% for the young group and 307.3% for the middle-aged group, which was 6.29 times that of the young group, suggesting that the middle-aged group, which was older, was more affected in the middle section of the light environment with low luminance. From the trend of  $(\alpha+\theta)/\beta$  changes over time during the whole experiment, it can be observed that the increasing process of psychological load and fatigue of the subjects has been in a fluctuating status, especially between 360s and 420s there even appeared a U-shaped change interval, but the overall change trend of  $(\alpha+\theta)/\beta$  of the subjects was increasing over time.

When divided by the gender of the driver, it can be found that the difference between genders is more obvious than the difference between ages. The  $(\alpha+\theta)/\beta$  of females rose rapidly to high values right after the start of the experiment, while the  $(\alpha+\theta)/\beta$  of males experienced a period of plateauing and then gradually increased. This indicates that female drivers are more prone to psychological load and physiological fatigue rises faster than male drivers in the middle section of the light environment with low luminance.

### 4.2 Subject mean regression optimization

In the experiment near to 300s the subject's  $(\alpha + \theta) / \beta$  experiences a rapid increase process, which shows that the psychological load and fatigue of the subject are difficult to control when the subject exceeded a certain critical status, at this time if driving in the real tunnel, drivers are very easy to judge inaccurately, follow the car too close, or even be drowsy, which significantly increase the probability of major traffic accidents occurrence; after this stage, the person's own willpower will antagonize the psychological load, and after decreasing  $(\alpha+\theta)/\beta$ , it will rise again and

keep to a higher level. The average  $(\alpha+\theta)/\beta$  of all subjects was fitted to the data to obtain Figure 6.

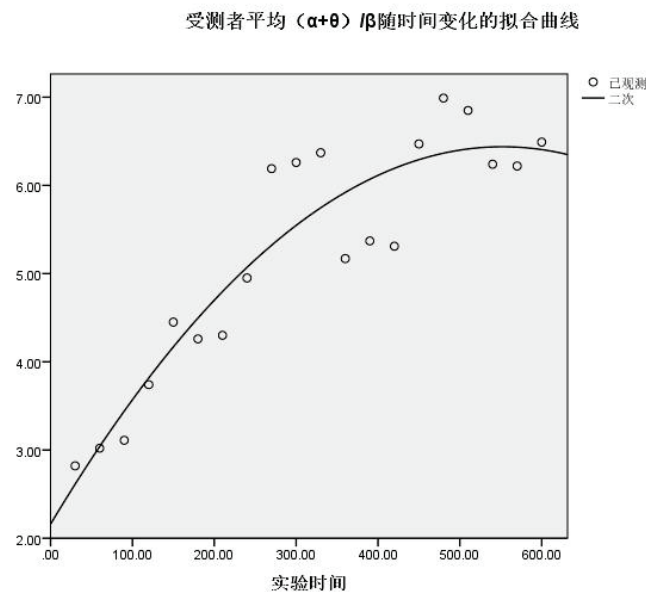


Figure 6 Fitted curve of average  $(\alpha+\theta)/\beta$  over time for subjects (source: software derived)

The fitted curve of the subject's mean  $(\alpha+\theta)/\beta$  over time the fitted equation is shown in equation (1):

$$y = 2.16 + 0.16x - 1.404E^{-5}x^2 \quad (1)$$

The goodness of fit of this fitted equation,  $R^2 = 0.861$ , is a good fit and can illustrate more obviously the pattern of the wave energy ratio  $(\alpha + \theta)/\beta$  of the tested driver changes with time at the lowest pavement brightness allowed by the specification. It can be seen from the fitted equation that  $y/x$  is the slope of this fitted curve, which indicates the growth rate of  $(\alpha+\theta)/\beta$  over time, and when  $x$  takes the value of 286.8, the slope  $y/x$  value can achieve the maximum value, at this time in the dim light environment, the subject is more easy to be fatigue and judge inaccurately, which will lead to serious traffic accidents. If setting lighting alert section in this time point, it will put the best effect on the driver's alertness. According to the speed limit of vehicles in the tunnel (60~100km/h), this paper calculates that it is most reasonable to set the lighting alert section at the position of 4780m~7967m into the middle section of the tunnel.

#### 4.3.9 Location and length of alert segment setting

The experimental study in this paper is to investigate the whole process of changes in simulated driving fatigue of drivers of different genders and ages in a long intermediate light environment with low ambient mean luminance, by using the physiological quantities (EEG parameters) of the subjects as the main dependent variables, and to give that there was a significant correlation between each band and band ratio separated from the EEG of the tested driver and the length of driving time in the lowest road brightness lighting environment allowed by the setting specification. The trend curves formed with driving duration are similar to those in the literature<sup>[123][120][37]</sup>. From the changing trend of the average values and the fitting results, the EEG band energy ratio  $(\alpha+\theta)/\beta$  varied significantly with time. When the polar point of  $y/x$  appeared at 286.8s, the ratio of  $(\alpha+\theta)/\beta$  for the tested driver is showing the highest upward trend. If taking the overall light environment changes before and after this moment to enhance the driver's alertness, it can change the situation of continuing increasing their fatigue and psychological load. According to the speed limit of vehicles in the tunnel (60~100km/h), this paper calculates that it is most reasonable to set the lighting alertness section at the position of 4780m~7967m into the middle section of the tunnel.

A study conducted for the age of the subjects found that age had a significant effect on the subjects. The initial values of the specific EEG energy ratio  $(\alpha+\theta)/\beta$  were higher in the youth group than in the middle-aged group in the environment with low mean luminance, in detail, 151% higher in the female group and 65.6% higher in the male group, suggesting that the initial values of the specific EEG energy ratio  $(\alpha+\theta)/\beta$  were higher in young people aged 20 to 35 years than in middle-aged people aged 36 to 50 years due to their physiological characteristics, which may be related to the intensity of their neural activity and does not indicate that they were already in a more fatigued status before starting the experiment in the low luminance situation. However, it is worth noting that when comparing the energy ratio  $(\alpha+\theta)/\beta$  of specific EEG bands in the last 30s before the end of the experiment, the rise was significantly smaller in the youth group, suggesting that the youth subjects were more capable of self-regulating their fatigue status even under the conditions of unfavorable average ambient luminance.

For the study of the effect of subject gender on the EEG band energy ratio  $(\alpha+\theta)/\beta$  in the environment with low mean luminance, the results show that the gender

factor also affects the trend of driver fatigue changes when the lighting is unfavorable. Comparing Fig. 4.39, the specific EEG band energy ratio  $(\alpha+\theta)/\beta$  curve for male drivers was above the mean curve, and the change trend was approximately the same as the mean, and the  $(\alpha+\theta)/\beta$  ratio increased faster and had a higher slope as time passed by; while the specific EEG band energy ratio  $(\alpha+\theta)/\beta$  curve for female drivers was below the mean curve, and the change trend was different between middle-aged female and young female, and the reasons may be due to: ① The male drivers' driving age is generally long, and they are in a more relaxed status in the simulated driving, and are more likely to reach fatigue under dim lighting conditions, while the female drivers' driving age is short, and they are in a cautious status in the simulated driving until the end of the experiment, and it is worth noting that the average driving age of the selected middle-aged female drivers is lower than that of the young female drivers, therefore, although the fatigue status was also entered in the second half of the experiment, the specific EEG band energy ratio  $(\alpha+\theta)/\beta$  in the last 30 s of the experiment was only 64.2% higher than the initial value, and the curve was flatter. ② The hormone secretion of male drivers was relatively more vigorous, and the original EEG band energy  $\alpha$ ,  $\theta$ , and  $\beta$  were all higher than those of females, so the initial EEG band energy ratio  $(\alpha+\theta)/\beta$  of male drivers and the final value at the end of the experiment were significantly higher than those of female drivers.

In summary: ① The pattern of the wavelength energy ratio  $(\alpha+\theta)/\beta$  of the subjects as time passes by is more influenced by age and gender, young drivers have a tendency to slow down or decrease slightly after the psychological load rising to a certain stage, but middle-aged drivers show a continuous increase in the psychological load when driving in the middle section of the tunnel under the same experimental conditions, which can be seen from the goodness of fit that improving the single light environment in the middle section of a long tunnel is more beneficial for older drivers, and for male drivers than female drivers. ② Based on the combined results of all subjects, the set position of the alert section should be at 286.8 seconds after driving into the middle section of the long tunnel, and for further convenient calculation of subsequent experiments, the position of the alert section was set at 300 seconds after driving at 80 km/h in the middle section.

## 5. Conclusion

Long tunnel lighting needs to meet the three requirements of "safety, comfort and energy saving". And when vehicles pass through long tunnels, driving safety and comfort are equally important. Traditional tunnel lighting research focuses on the visual efficacy of drivers, while pays little attention to the impact of long tunnels' overall light environment on the physiological and psychological effects of drivers. In this paper, we propose the concept of ambient lighting level to set the middle section of the long tunnel by increasing the brightness of the road surface and the average brightness of the environment as well as changing the light source, thus to solve the scientific problems of the influence mechanism and the changing pattern of the physiological and psychological effects of the driver's driving, based on which a method for designing environmental assisted lighting in the middle section of a long tunnel using materials for traffic safety is constructed, then to achieve the purpose of safety of tunnel operation, driving comfort and energy saving and consumption reduction. The main conclusions of the thesis are as follows:

(1) . In scenes with low ambient luminance in the middle section of long tunnels, setting alert segments can effectively improve driver fatigue and increase driving alertness.

(2) . Through laboratory simulated experiments, the study investigated the changes in driver's psychological workload over time under low lighting conditions. It was found that the optimal setting for alertness period is to drive within a section of low illuminated road ( $3.5\text{cd/m}^2$ ) after driving for 286.8 seconds.

(3) . Under the condition that the alert section length is set to 200m in a long tunnel, it is most reasonable to set the lighting alert section at the position of 4780m~7967m in the middle section of the tunnel.

This study proposes that the average brightness of the driver's environment has a clear impact on the non-visual effects of driving in long tunnels. It provides a new design concept for the lighting in the middle section of long tunnels, which aims to enhance the driver's alertness and reduce fatigue without increasing the existing lighting energy consumption. This is achieved by utilizing traffic safety settings such as contour markings within the tunnel. However, it should be noted that the study subjects were similar in age and did not consider gender differences. This aspect can be further improved in future indoor simulation experiments.



## References

- Commission Internationale de l'Éclairage, CIE, 2004. CIE 88-2004 Guide for the lighting of road tunnels and underpasses. CIE Publ. 88, Vienna.
- Commission internationale de l'éclairage, 2014. CIE 206-2014 The Effect of Spectral Power Distribution on Lighting for Urban and Pedestrian Areas. Vienna.
- Commission Internationale de l'Eclairage, Research roadmap for healthful interior lighting application, CIE Technical Report 218 (2016).
- Berson , D. M. , Dunn , F. A , Motoharu Takao, 2002. Phototransduction by retinal ganglion cells that set the circadian clock . Science , 295 , 1070-1073.
- Wout J . M. van Bommel, 2006. Non-visual biological effect of lighting and the practical meaning for lighting for work .Applied ergonomics 37 ,461~466.
- Katsuura, Tetsuo, Xinqin Jin, Yasushi Baba, Yoshihiro Shimomura, and Koichi Iwanaga, 2005. Effects of Color Temperature of Illumination on Physiological Anthropology and Applied Human Science 24, no. 4: 321-325.
- JIAO Fangtong, DU Zhigang, WANG Shoushuo, et al. Research on drivers' visual characteristics in different curvatures and turning conditions of the extra-long urban underwater tunnels[J]. Tunnelling and Underground Space Technology, 2020(99): 1-9.
- FENG Zhongxiang, YANG Miaomiao, ZHANG Weihua, et al. Effect of longitudinal slope of urban underpass tunnels on drivers' heart rate and speed: A study based on a real vehicle experiment[J]. Tunnelling and Underground Space Technology, 2018(81): 525-533.
- Zhang, H., 2006. New Progress Among the Lighting Science. China Illuminating Engineering Journal - Chinese Version, vol. 17, no. 3, 1-3.
- Yang, G., 2006. The third photoreceptor in the human eyes 1. Chinese Journal of Lamps and Lighting, no. 2, pp. 30-31.
- Yang, G., 2006. The third photoreceptor in the human eyes 2. Chinese Journal of Lamps and Lighting, no. 3, pp. 28-30.
- Steven W. Lockley, PhD, Erin E. Evans, et al. 2006. Short-wavelength sensitivity for the direct effects of light on alertness, vigilance, and the waking Short-wavelength sensitivity for the direct effects of light on alertness, vigilance, and the waking electroencephalogram in humans. sleep physiology vol. 29, no. 2:161-168

S.Y. He, L. Tähkämöb, M. Maksimainenb, B. Liangc, G.B. Pana, L. Halonenb, 2017. Effects of transient adaptation on drivers' visual performance in road tunnel lighting, *Tunn. Undergr. Space Technol.* 70 (2017 ) 42 -54.

Renzler M., Reithmaier, N., Reinhardt, R., Pohl, W., Ußmüller, T., 2018. a road tunnel model for the systematic study of lighting situations. *tunn. Undergr. Space Technol.* 72, 114-119. <https://doi.org/10.1016/j.tust.2017.11.017> .

Chiara Burattinia, Laura Piccardib, Giuseppe Curcioc, Fabio Ferlazzoe, Anna Maria Gianninie, Fabio Bisegnaa 2019, Cold LED lighting affects visual but not acoustic vigilance, *Building and Environment* 151 (2019) 148-155.

Zhu Tong, Wu Ling, Hu Yueqi, et al. Research on the physiological load characteristics of drivers in extra-long highway tunnel based on factor model[J]. *Chinese Journal of Highways*, 2018, 31(11): 165-175.

Du Zhigang, Huang Faming, Yan Xinping, et al. The adaptation time to the brightness and darkness of a highway tunnel based on the changes in the size of the pupil[J]. *Highway Traffic Technology*, 2013, 30(05): 98-102.

Hu Jiangbi, Li Ran, Ma Yong. Evaluation method of lighting safety threshold for highway tunnel entrance section[J]. *Chinese Journal of Highways*, 2014, 27(03): 92-99.

Xie Jijian, Liu Chengping. Fuzzy mathematical methods and their applications, 4th edition [M]. Wuhan: Huazhong University of Science and Technology Press, 2013.

Bor-Shong Liua, Yung-Hui Leeb. In-vehicle Workload Assessment: Effects of Traffic Situations and Cellular Telephone Use [J]. *Journal of Safety Research*, 2006, (37):99-105

Byung Chan Min, Soon Cheol Chung. Autonomic Responses of Young Passengers Contingent to the Speed and Driving Mode of a Vehicle [J]. *International Journal of Industrial Ergonomics*, 2002,(29):187-198

Ashley Craig , Yvonne Tran. A Controlled Investigation into the Psychological Determinants of Fatigue [J]. *Biological Psychology*, 2006,(72):78-87

# RESEARCH ON LED ADVERTISING SCREEN TRESPASS BASED ON URBAN LIGHT ENVIRONMENT ZONING AND SCENE SETTINGS

FAN Qing, ZHANG Mingyu, LV Chenge

(Tianjin Key Laboratory of Architectural Physics and Environmental Technology, Tianjin University, Tianjin 300072, China)

## ABSTRACT

The rapid development of nighttime lighting in Chinese cities has led to a significant increase in the number of LED advertising screens in different lighting environments, causing excessive light intrusion into surrounding residential buildings, directly or indirectly affecting the physical and mental health of surrounding residents. Therefore, 22 LED advertising screens from five cities in China were selected for subjective and objective research. Based on the mixed urban layout of commercial and residential areas in China, the basic background brightness ranges for different lighting environment zones were given, and the basic data of LED advertising screen light intrusion was mastered. Six influencing factors of LED advertising screen light intrusion were determined. In order to control the main influencing factors and propose reasonable setting suggestions, a computer simulation analysis experiment was designed using orthogonal experimental method. The ranking of the influence weights of each factor was obtained as follows: screen brightness>screen area>horizontal linear distance between screen and window>relative vertical height>horizontal angle between screen and window surface normals>background brightness, with screen brightness and area having the greatest impact. Provide guidance for the setting of LED advertising screens in different lighting environment areas.

Keywords: LED advertising screens, The windows of residential buildings, Light trespass, Light environment partitions, Relative position relationships

## 1. INTRODUCTION

Against the backdrop of rapid urbanization, the urban night lighting industry in China has developed rapidly, and the urban night light environment is becoming increasingly bright. Traditional lighting methods are gradually being replaced by light emitting diodes (LEDs), which has led to a diversification of types and forms of urban night scene lighting. Due to the needs of commercial promotion, a large number of LED advertising screens are installed<sup>[1]</sup>, which do not control the number and location of settings, do not control the screen size, brightness, and color, and even add dynamic images for promotional purposes<sup>[2]</sup>. The problem of high-frequency flashing screen images is becoming increasingly apparent, leading to a large amount of light pollution on LED advertising screens, leading to abnormal environmental light and dark cycles, and affecting the ecosystem Human health<sup>[3]</sup> and even astronomical observation activities bring enormous pressure.

Nowadays, LED advertising screens are spread throughout various areas of human activity, including urban parks, community center road intersections, building facades, and even rural squares. As a result, the problem of visual intrusion<sup>[4][5][6]</sup> on residents, road drivers, nighttime travelers, and activity groups near the advertising screens is becoming increasingly common and serious. According to statistics, in some cities' environmental complaint cases, the number of complaints about light pollution is increasing year by year, and the causes of light pollution are mostly directed towards LED advertising screens. The research on LED advertising screen setting and light pollution control at home and abroad mainly focuses on setting suggestions<sup>[7]</sup> on controlling its brightness, opening and closing time, Switching frequency, etc., as well as providing limit reference for LED advertising screen brightness according to environmental zoning and screen area division. In theoretical research, more efforts are made to avoid its impact on human visual comfort<sup>[8]</sup>, road drivers<sup>[9]</sup>and pedestrians<sup>[10]</sup> The residents of surrounding residential buildings<sup>[11][12]</sup> have an impact. In the relevant research on residents in residential areas, it

focuses on exploring the subjective impact of various factors on residents<sup>[13][14]</sup>, and achieves the goal of reducing light pollution by controlling the influencing factors. The research method is mainly based on on-site inspection and research, as well as subjective evaluation experiments, supplemented by software simulation and other methods. However, in previous studies, there has not been much research on LED advertising screens with different lighting environment zones, and there has been no consensus on the zoning standards and recommended brightness limits for different areas formulated by relevant regulations<sup>[15][16][17][18]</sup>. At the same time, there has been less consideration of discussing the location relationship with the intrusion source in residential building light intrusion research.

At present, the restrictions on outdoor lighting light pollution in China<sup>[19][20][21]</sup> and the restrictions on LED display screens<sup>[22]</sup> both refer to the CIE Technology No. 150<sup>[15]</sup> regulations, and their division of environmental areas is more based on foreign urban layout models. However, there is a mixed commercial and residential urban layout characteristic in China, which leads to a greater impact of LED advertising screens on the windows of surrounding residential buildings. Therefore, further research is needed on the setting standards of domestic LED advertising screens based on different lighting environment zones.

## 2. METHODS

### 2.1 TESTING AND RESEARCH ON TYPICAL SCENARIOS OF LED ADVERTISING SCREENS FOR LIGHT INTRUSION IN RESIDENTIAL AREAS

On site data monitoring on light intrusion of 22 LED advertising screens in five cities of Hangzhou, Guangzhou, Chongqing, Beijing and Nu Cygni, the LED advertising screen location shall be selected based on covering as many light environment areas as possible, and in areas with large population flow or easy to disturb people in surrounding residential areas, while ensuring the diversity of types of intrusion.

#### 2.1.1 QUESTIONNAIRE INVESTIGATION

In order to fully grasp the current views of residents in residential buildings on the installation of LED advertising screens, understand the specific impact of LED advertising screens on surrounding residents, the types of activities that affect residents, and the tolerance of residents to various factors that cause light intrusion by LED advertising screens, identify the factors that have a significant impact and conduct key research, providing theoretical support for subsequent on-site measurement and simulation research.

The survey questionnaire mainly aims to understand the personal situation, home activity habits, and subjective feelings related to LED advertising screen light intrusion of the survey subjects. The light intrusion evaluation in the questionnaire design mainly starts with the overall intrusion degree and various possible intrusion factors. According to the residents' possible daily feelings, the LED advertising screen brightness, screen Switching frequency, area, relative position with the window, broadcast content, lighting time and other influencing factors are screened out to understand the impact of various factors on residents. The Likert scale is used to set up questions related to satisfaction and impact. A total of 233 questionnaires were distributed and 214 valid questionnaires were collected. Gender balance of the surveyed subjects; Balanced coverage of age groups; Eye health conditions vary and are covered.

#### 2.1.2 ON SITE TESTING

Referring to relevant domestic regulations<sup>[24]</sup>, it is divided into two forms: single frame image type (with a single image staying for too long) and rolling video type (with a continuous playback image), based on the area of LED advertising screens.

##### (1) LED advertising screen brightness:

For advertising screens with an area less than or equal to 2m<sup>2</sup>, select at least 6 measurement points; If the advertising screen area is greater than 2m<sup>2</sup>, at least 9 measurement points should be selected. The tester is located in the area affected by the interference of the LED advertising screen. The single frame image measurement uses a point brightness meter (CL10W) to conduct a 9-point brightness test on the single frame image played by the LED advertising screen, and record the data results. Rolling video measurement uses a brightness meter to continuously measure the same measurement point at equal time intervals (20s~60s), with 6 readings taken at each measurement point and 54 readings taken at 9 measurement points. After the test is

completed, a single frame image measurement can be used to supplement the testing of single frame images that appear multiple times and stay for a long time on the advertising screen.

(2) Illuminance of the measuring point window disturbed by LED advertising screen

The tester stands at the window interfered by the LED advertising screen and adopts the "center layout method" to divide the outdoor surface of the bedroom window into rectangular grids, with the center point of each grid being a vertical illuminance measurement point. If the window area is less than  $1\text{m}^2$ , at least 6 measuring points should be selected; If the window area is greater than or equal to  $1\text{m}^2$ , at least 9 measuring points should be selected; And evenly arrange the measuring points. The single frame image measurement tester is tested synchronously with brightness, and the rolling video measurement is conducted continuously at equal time intervals (20s~60s). Each measurement point is read 6 times, and 6 or 9 measurement points are read 36 or 54 times.

(3) LED advertising screen playback content and playback method

Using camera photography and video recording functions to record the playback content and format of LED advertising screens (single frame image type, rolling video type).

(4) LED advertising screen size

The tester chooses Leica Disto D5), tape measure, step measurement, visual inspection and other methods to measure the length and width of LED advertising screen according to the actual situation, and calculate its area.

(5) Relative position relationship between LED advertising screen and measuring point

The relative position relationship between the LED advertising screen and the measuring point includes the horizontal straight distance, the horizontal angle between the measuring point and the surface normal of the LED advertising screen, and the vertical height from the bottom of the LED advertising screen to the measuring point.

(6) LED advertising screen surrounding background brightness

Due to the specific study of LED advertising screen light intrusion based on different light environment zones, the background brightness around the LED advertising screen should be synchronously measured during the research.

Referring to the previous research<sup>[2]</sup>, the background range is defined as the nine grid area centered on the LED advertising screen (Figure 1). The Sky brightness, building facade brightness, outdoor advertising and signs brightness, road brightness, etc. included in the background range are measured uniformly, and the average value is calculated according to the proportion of each part in the background range, which is used as the background brightness ( $L_b$ ) of the LED advertising screen. Refer to the following equation (1):



Figure 1 Definition of the Background Range of LED Advertising Screen

$$L_b = \gamma \times L_s + \rho \times L_{\text{build}} + \varepsilon \times L_{\text{sign}} + \tau \times L_r \quad (\gamma + \rho + \varepsilon + \tau = 1) \quad (1)$$

In the formula:  $L_b$ —background brightness,  $\text{cd/m}^2$ ;  $L_s$ —Sky brightness,  $\text{cd/m}^2$ ;  $\gamma$ —Percentage of sky area within the background range, %;  $L_{\text{build}}$ — Building facade brightness,  $\text{cd/m}^2$ ;  $\rho$ — Percentage of building facade area within the background range, %;  $L_{\text{sign}}$ — Outdoor advertising and signage brightness,  $\text{cd/m}^2$ ;  $\varepsilon$ —Percentage of outdoor advertising and signage area within the background range, %;  $L_r$ — Road brightness,  $\text{cd/m}^2$ ;  $\tau$ — Percentage of road area within the background range, %

### 2.1.3 DIVISION OF LIGHT ENVIRONMENT AREAS

This article focuses on the previous research and standardization of CIE150<sup>[16]</sup>, which divides the light environment into E1 (dark area), E2 (low brightness area), E3 (medium brightness area), and E4 (high brightness area) based on the mixed commercial and residential



urban layout in China. The division criteria are shown in Table 1. Dividing and defining the functional areas of the 22 research points mentioned above is more in line with China's urban planning model, and can provide a more comprehensive foundation for further research on the standardization of LED advertising screen settings.

Table 1 Division of Light Environment Areas

Light environment zoning	E1 (dark area)	E2 (low brightness area)	E3 (medium brightness area)	E4 (high brightness area)
Division basis(The level of prosperity in the surrounding area)	Not bustling, shops and pedestrian flow scarce	Moderate, with some shops and low pedestrian flow	Busy, with many shops and high pedestrian flow	Extremely bustling, with numerous shops and high pedestrian flow
Research points	/	1;12;20	2;3;4;5;10;11;21;22	6;7;8;9;13;14;15;16;17;18;19
Functional Zone	Industrial and residential areas	Residential, office, and commercial areas	Residential, office, and commercial areas	Residential, office, and commercial areas

## 2.2 RESEARCH ON INTRUSION SIMULATION OF SCENE SETTING CONDITIONS FOR URBAN LIGHT ENVIRONMENT ZONING

### 2.2.1 Simulation process

This article mainly studies the light intrusion of residential windows by factors such as LED advertising screen brightness, area, relative position with the window, and background brightness. Due to the fact that the "vertical illuminance of the exterior surface of residential building windows" (hereinafter referred to as "illuminance at the window") is an important indicator for determining the degree of visual interference among residents, and has been clearly defined as a limit in China's industry standard<sup>[20]</sup>, this article calculates the illuminance value at the window using simulation software and judges the degree of window interference based on specifications.

The simulation adopts the software GWLE2015 developed on AutoCAD, which utilizes the principle of LED display Lambert body luminescence to divide the LED screen into several small pieces, and uses the segmented center point as the Lambert body point light source for simulation calculations. By setting the light source surface, the average illumination of building windows disturbed by LED advertising screens can be accurately calculated.

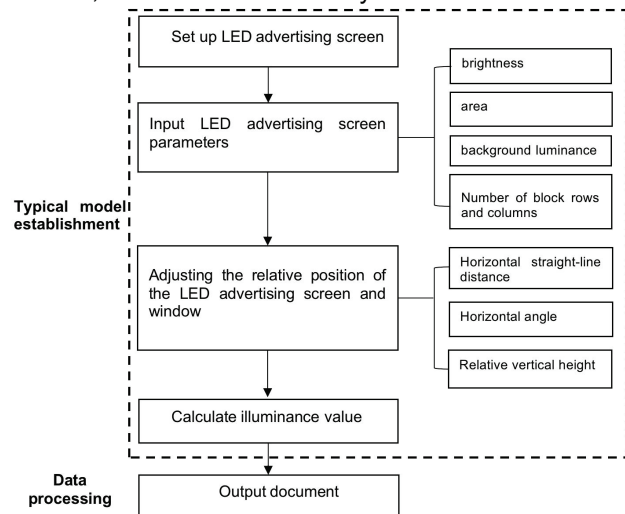


Figure 2 The specific model construction and process

### 2.2.2 Setting of influencing factors

The main source of intrusion in typical intrusion light models is LED advertising screens, and the intrusion factors of this intrusion source include advertising screen brightness, background brightness, advertising screen size, and relative position with the object being invaded. This simulation is set to static light intrusion mode.

In order to reduce the visual intrusion on the window under the LED advertising screen, this paper establishes a Relational model between the typical position of the LED advertising screen and the affected window as shown in Figure 3 for simulation and discussion. Based on field research, questionnaire survey, and literature review, determine the LED advertising screen area  $S$  ( $m^2$ ), the horizontal straight distance  $L$  ( $m$ ) between the LED advertising screen and the window, the brightness  $W_s$  of the LED advertising screen ( $cd/m^2$ ), and the horizontal angle between the LED screen and the window surface normal  $\alpha$ , The vertical height  $H$  ( $m$ ) of the LED advertising

screen relative to the window and the background brightness  $W_b$  ( $\text{cd}/\text{m}^2$ ) are the main factors that affect the window illumination value. Simulation research mainly focuses on these six influencing factors.

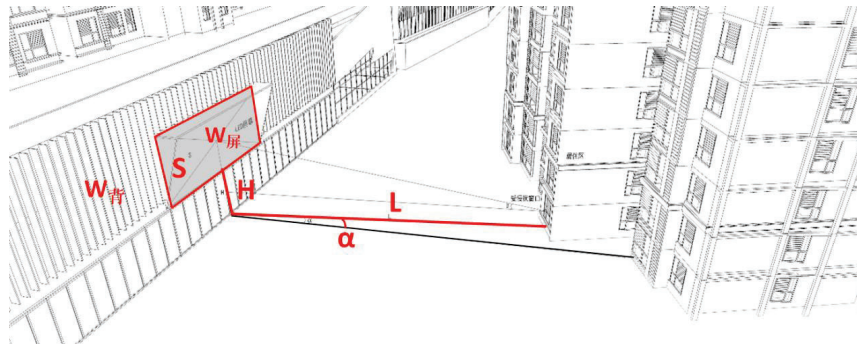


Figure 3 Relational model between LED advertising screen and the typical position of the disturbed window

(1) LED advertising screen area  $S$

According to the actual survey results, the area of LED advertising screens ranges from  $1.6\text{m}^2$  to  $367.5\text{m}^2$  (with lengths ranging from 1.6m to 35m and heights ranging from 1m to 14m), and most of them are above  $25\text{m}^2$ . The simulated LED advertising screen is set to have an area range of  $25\text{m}^2 \sim 400\text{m}^2$ . It is divided into five steps by Geometric progression. The boundary area is set to be  $25\text{m}^2$ ,  $50\text{m}^2$ ,  $100\text{m}^2$ ,  $200\text{m}^2$ ,  $400\text{m}^2$ , and the length height ratio is set to 2:1.

(2) Horizontal straight-line distance between LED screen and window  $L$

According to on-site research data, the horizontal straight distance between LED advertising screens and the affected window is between 28 and 120.5m, and most of them are above 30m. In most cases, LED advertising screens beyond 100m have a small impact<sup>[6]</sup>, so a distance of 30~100m is selected for simulation, and the Arithmetic progression is graded into 5 steps. The distance  $L$  is set as 30m, 45m, 60m, 75m and 90m respectively.

(3) Brightness of LED screen  $W_s$

According to the actual measurement and research results, the brightness range of LED advertising screens is between  $0.25 \sim 5927\text{cd}/\text{m}^2$ , with a large range. The brightness range values come from certain extreme brightness values rather than average values, which is not representative. Therefore, referring to the average brightness range of LED advertising screens ( $164.34 \sim 3752.33\text{cd}/\text{m}^2$ ), the brightness division is carried out using  $200 \sim 3200\text{cd}/\text{m}^2$  as simulated values. The brightness of LED screen is set as  $200\text{cd}/\text{m}^2$ ,  $400\text{cd}/\text{m}^2$ ,  $800\text{cd}/\text{m}^2$ ,  $1600\text{cd}/\text{m}^2$ ,  $3200\text{cd}/\text{m}^2$  respectively by grading Geometric progression into five steps.

(4) Horizontal angle between LED screen and window surface normal  $\alpha$

The measurement points selected in the research range from  $0^\circ$  to  $60^\circ$  from the horizontal angle of the surface normal of the LED advertising screen. With the line of sight perpendicular to the LED advertising screen as the axis, the visual perception of the window in the left and right directions of the LED advertising screen is similar, so only a simulation point needs to be set on one side of the LED advertising screen. According to the field survey results, the Arithmetic progression is divided into five steps, and the angles are set as  $0^\circ$ ,  $15^\circ$ ,  $30^\circ$ ,  $45^\circ$  and  $60^\circ$  respectively.

(5) Vertical height of LED advertising screen relative to window  $H$

According to the actual survey results, the Elevation between the LED advertising screen and the measuring point is between 1.4 and 21m, and most of the settings are based on the height of multi-storey buildings above the ground. Therefore, the height from the bottom of the LED advertising screen to the ground is controlled between the first floor and the fifth floor ( $0 \sim 20\text{m}$ ). With the single floor height (about 4m) as the tolerance, the Arithmetic progression is graded into 5 steps, and the height from the ground can be set as 4m, 8m, 12m, 16m, 20m, respectively, The relative vertical height between the actual window and the LED advertising screen is also determined based on this value.

(6) Background brightness  $W_b$

The actual survey results show that the background brightness of LED advertising screen varies from 0.75 to 68.36cd/m<sup>2</sup>, and is between 0 and 25cd/m<sup>2</sup> except for very few cases. Combining the simulation with the actual survey, the background brightness is set to be 0cd/m<sup>2</sup>, 6cd/m<sup>2</sup>, 12cd/m<sup>2</sup>, 18cd/m<sup>2</sup>, 24cd/m<sup>2</sup> respectively by grading the Arithmetic progression into five steps.

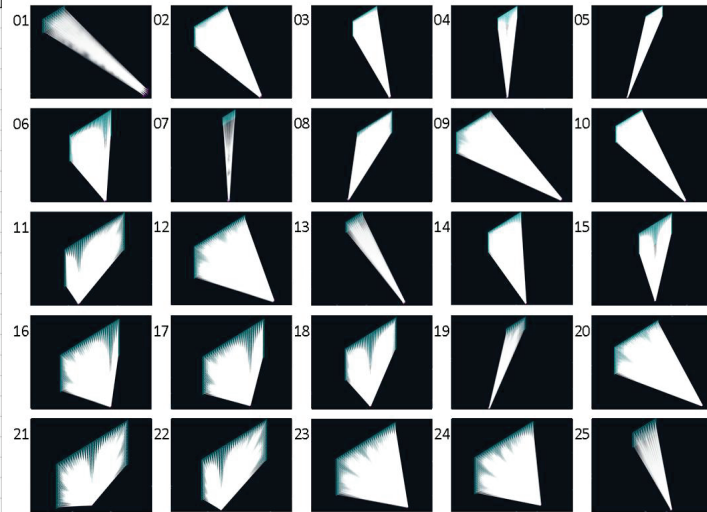
### 2.2.3 Simulation Experiment Settings

According to the scientific method of orthogonal experiments<sup>[24]</sup>, this article conducts value selection for various factors, aiming to select representative and typical appropriate points from a large number of experimental points. By reducing the number of experiments and selecting representative experiments, complete the experimental tasks. After design, a total of 25 equivalent simulation experiments are required for the 6 factors and 5 steps listed. The specific simulation combination of the experimental design scheme is shown in Figure 4. Model 25 sets of LED advertising screen light intrusion scenarios selected through orthogonal experimental schemes, as shown in Figure 5.

Figure 4 Simulation combination of orthogonal experimental design scheme

实验计划表	1	2	3	4	5	6
因素	面积	距离	亮度	水平角度	相对垂直高度	背景亮度
实验1	25	30	200	0	4	0
实验2	25	45	400	15	8	6
实验3	25	60	800	30	12	12
实验4	25	75	1600	45	16	18
实验5	25	90	3200	60	20	24
实验6	50	30	400	30	16	24
实验7	50	45	800	45	20	0
实验8	50	60	1600	60	4	6
实验9	50	75	3200	0	8	12
实验10	50	90	200	15	12	18
实验11	100	30	800	60	8	18
实验12	100	45	1600	0	12	24
实验13	100	60	3200	15	16	0
实验14	100	75	200	30	20	6
实验15	100	90	400	45	4	12
实验16	200	30	1600	15	20	12
实验17	200	45	3200	30	4	18
实验18	200	60	200	45	8	24
实验19	200	75	400	60	12	0
实验20	200	90	800	0	16	6
实验21	400	30	3200	45	12	6
实验22	400	45	200	60	16	12
实验23	400	60	400	0	20	18
实验24	400	75	800	15	4	24
实验25	400	90	1600	30	8	0

Figure 5 Schematic diagram of simulation model creation



## 3. ANALYSIS OF RESULTS

### 3.1 Questionnaire data analysis

(1) 42.6% of respondents reported being strongly disturbed by LED advertising screen light, while only 10.3% of respondents reported being insensitive to the light intrusion generated by LED advertising screens outside the window;

(2) The surveyed subjects engage in a variety of activities in rooms facing LED advertising screens, and all activities are subject to varying degrees of intrusion from LED advertising screens. Among them, they are more susceptible to light intrusion during rest, sleep, and work and learning that require focused attention.

(3) The brightness of LED advertising screens is the most intrusive to the respondents; In addition to brightness, the factors that have a greater impact are area, distance from the screen, horizontal angle with the normal of the screen surface, contrast with background brightness, and screen switching speed. Therefore, in field measurements, the above factors should be emphasized. Whether the content is dull or not has a relatively small impact on the respondents.

Therefore, it is recommended to control the brightness of the screen first in the setting of LED advertising screens; Secondly, appropriately reduce the screen area, set the screen as far away from residential building windows as possible, twist the angle to avoid facing the window in a large area, and avoid setting high brightness advertising screens in situations where the background is too dark; In addition, the screen switching speed of LED advertising screens should be controlled; If there is spare time, you can choose more interesting and attractive

playback content, reduce the aversion of surrounding residents to dull content, and control the opening and closing time of LED advertising screens to avoid continuous light pollution in the late night.

### 3.2 Research data analysis

(1) Based on the level of bustling surrounding environment and background brightness, the light environment can be divided into different zones to make it more suitable for the urban layout model of mixed commercial and residential areas in China;

(2) According to the measured brightness data, there are 9 screens that exceed the standard; According to the measured illuminance data at the measuring points, there are 19 screens that exceed the standard. This indicates that although some screens have their brightness controlled within the specified limits, other reasons such as large area, close proximity to the measurement point, background brightness, and surrounding stray light may cause the illumination value of LED advertising screens at the measurement point to exceed the standard, leading to light pollution. It has been found that the current regulations and previous studies that only specify brightness limits are insufficient to control the light pollution of surrounding residential buildings. In the future, more factors should be explored to influence the degree of light intrusion.

### 3.3 Weight analysis of influencing factors

Simulate 25 sets of LED advertising screen light intrusion scenarios selected through orthogonal experimental schemes, and the results are shown in Table 6.

Table 6 Simulation Results of Orthogonal Experimental Schemes

Serial number	Illumination at the window (lx)	Serial number	Illumination at the window (lx)	Serial number	Illumination at the window (lx)
01	5.35	02	5.05	03	5.00
04	5.00	05	4.73	06	17.38
07	10.46	08	11.27	09	28.64
10	1.94	11	47.26	12	74.91
13	75.21	14	3.27	15	4.11
16	171.16	17	272.98	18	13.79
19	6.81	20	19.34	21	699.50
22	24.63	23	42.59	24	63.15
25	66.24	/	/	/	/

The processing and analysis of the experimental results obtained in the orthogonal experimental design method are shown in Table 7. The first columns I, II, III, IV, and V in the table respectively represent the sum of simulation results when the LED advertising screen area is taken as 25m<sup>2</sup>, 50m<sup>2</sup>, 100m<sup>2</sup>, 200m<sup>2</sup>, and 400m<sup>2</sup>; The I, II, III, IV, and V in the second column are the sum of the simulation results when the horizontal linear distance between the screen and the window is taken as 30m, 45m, 60m, 75m, and 90m, respectively. The rest of the results are similar. Then subtract the extreme values of all I~V values of the same factor to obtain the corresponding T values of each factor. By comparing the T values, the influence weights of different influencing factors can be analyzed.

Table 7 Weight analysis of various influencing factors

Test number	Screen area	Straight line distance from window	Screen brightness	Horizontal angle	Relative vertical height	Background brightness
I	25.13	940.65	48.98	170.83	356.86	164.07
II	69.69	388.03	75.94	316.51	160.98	738.43
III	204.76	147.86	145.21	364.87	788.16	233.54
IV	484.08	106.87	328.58	732.86	141.56	369.77

Test number	Screen area	Straight line distance from window	Screen brightness	Horizontal angle	Relative vertical height	Background brightness
V	896.11	96.36	1081.06	94.7	232.21	173.96
T	870.98	844.29	1032.08	638.16	646.60	574.36

The following conclusions are obtained through calculation:

(1) Among the six factors that affect window illumination, the order of degree of influence is screen brightness>screen area>horizontal linear distance between screen and window>relative vertical height>horizontal angle between screen and window surface normals>background brightness. The brightness of the LED advertising screen has the greatest impact on the illumination at the window, while the background brightness of the LED advertising screen has the smallest impact on the illumination at the window;

(2) As the brightness and area of the LED advertising screen increase and the background brightness increases, the illumination at the window increases, and residents are more affected by the interference of the LED advertising screen.

(3) As the distance between the LED advertising screen and the window, the horizontal angle with the window surface normal, and the relative vertical height with the screen increase, the illumination at the window decreases, and residents are less affected by the interference of the LED advertising screen.

(4) The relative vertical height between the LED advertising screen and the window, the horizontal angle between the surface normal, and the background brightness have little impact on the illumination value at the window, with the background brightness having the smallest impact.

#### 4.CONCLUSION

This study conducted a subjective questionnaire survey on the light intrusion of residents around LED advertising screens, in order to understand the activity behavior characteristics of surrounding residents, their subjective feelings and degree of intrusion towards LED advertising screen light intrusion, the types of activities affected by intrusion, and the specific manifestations of intrusion, And through the Likert scale, we learned that the subjective evaluation of the weight of each possible factor that may cause light intrusion to LED advertising screen by residents is: screen brightness>screen area>>window to screen distance>horizontal angle between window and screen surface normal>brightness contrast with background>screen switching speed>playing content.

Complete on-site research and measurement of 22 LED advertising screens in five cities in China, and divide the lighting environment areas (E1~E4) that are more suitable for the mixed layout of commercial and residential areas in China based on the bustling surrounding environment and background brightness; At the same time, understand the current situation of LED advertising screens invading residential buildings in China, and obtain basic data such as LED advertising screen brightness, area, relationship with surrounding residential building window positions, background brightness, illuminance, etc., to provide data support for subsequent simulation research. It is found that only the brightness meeting the specification can not completely control the light intrusion to the window, so other factors such as area and relative position should be considered simultaneously. The orthogonal experiment method was used to design the weight simulation experiment of LED advertising screen light intrusion effect. Six factors were selected: LED advertising screen brightness  $W_s$ , area  $S$ , horizontal linear distance from residential building window  $L$ , horizontal Angle from window surface normal  $\alpha$ , relative vertical height  $H$ , background brightness  $W_b$ , and the illumination of the window was simulated. The weight of the influencing factors is sorted as follows: screen brightness > screen area > horizontal straight distance from the window > relative vertical height > horizontal Angle > background brightness, so it is recommended to first control the brightness and area of the LED advertising screen; In summary, it is suggested that when controlling the LED advertising screen, the relevant specifications should give priority to controlling the brightness and area of the LED advertising screen, and mainly control the brightness level of the LED advertising screen to reduce the interference to the window.



## REFERENCE

- [1] LI Nong, LI Yao. Research about the Design Standard and Calculation of Advertising Lighting[J]. China Illuminating Engineering Journal, 2016, 27(02): 87-91 .
- [2] Youwu Yuan, Evaluation of Urban Outdoor LED Display Brightness and Setting [D]: Chongqing University. 2014 .
- [3] Park Choul Yong. Night Light Pollution and Ocular Fatigue[J]. Journal of Korean Medical Science, 2018, 33(38).
- [4] LIU Ming, LI Weishan, etc. Study on the Influence of Outdoor Advertising LED Screen on Urban Planning[J]. China Illuminating Engineering Journal, 2016, 27(05): 13-20 .
- [5] LIU Ming, MA Jian, etc. Effects of Dynamic Obtrusive Light on Vision-Psychology and Emotion [J]. Chinese Journal of Ergonomics. 2009, 15(04): 21-24 .
- [6] Gao Chengkang, Qin Wei, etc. The Monitoring and Evaluation of Light Pollution from LED Screen's at Night[J]. China Illuminating Engineering Journal, 2015, 26(01): 88-93 .
- [7] HAO Ying , ZHANG Peng. Investigation of Light Pollution Management Policy and Analysis of Interference Light Limit Standard of LED Advertisement Screen[J]. Environmental Monitoring in China, 2022, 38(03): 199-206 .
- [8] Zissis Georges. Sustainable Lighting and Light Pollution: A Critical Issue for the Present Generation, a Challenge to the Future[J]. Sustainability, 2020, 12(11): 4552.
- [9] YU Tingting, Lighting in the City intersection area visual disturbance of outdoor LED display An Investigation on the drivers [D]: Tianjin University, 2012.
- [10] MENG Yingying, LI Jian, YANG Biao. Potential Influencing Factors of the Commercial Signage at Night on Visual Comfort of Pedestrians[J]. China Illuminating Engineering Journal, 2021, 32(3): 134-141 .
- [11] Zalesinska Malgorzata. The impact of the luminance, size and location of LED billboards on drivers' visual performance — Laboratory tests[J]. Accident Analysis & Prevention, 2018, 117: 439-448.
- [12] Zhuang Xiaobo, Lin Jigang, Residential buildings[J]. Lamps & Lighting. 2022, No. 174(S1): 58-60 .
- [13] Ho Chen Ying, Lin Hsien Te, Huang Kuang Yu. A Study on Light Trespass of Dynamic LED Advertising Sign Flickering on Adjacent Residents at Night[J]. Applied Mechanics and Materials, 2013, 368-370: 593-598.
- [14] Ho C Y, Lin H T. Analysis of and control policies for light pollution from advertising signs in Taiwan[J]. Lighting Research & Technology, 2015, 47(8): 931-944.
- [15] International Commission on illumination, CIE150:2017, Guide on the Limitation of the Effects of Obtrusive Light from Outdoor Lighting Installations[R]. CIE Central Bureau, Vienna Austria, 2004.
- [16] Illuminating Engineering Society of North America. TM-11-2000. Light Trespass: Research, Results and Recommendations[R]. New York: IESNA, 2000.
- [17] AS4282-1997 Control of the obtrusive effects of outdoor lighting, Australian national standard
- [18] Institution of Lighting Engineers: Guidance Notes for the Reduction of Light Pollution 1992, UK Prevention and Control Guidelines.
- [19] JGJ/T 163-2008, Code for lighting design of urban nightscape[S]. China.
- [20] GB/T 35626-2017, Specification for limitation to obtrusive light of outdoor lighting[S]. China.
- [21] GB 55016-2021, General Code of Building Environment[S]. China.
- [22] CJJ/T 149-2021, Technical standards for urban outdoor advertising and signage facilities [S].
- [23] GB/T 34973-2017 , On-site measurements of obtrusive light of LED panels[S]. China.
- [24] Wang Naikun, Application of Orthogonal Design of experiments Method in Design of experiments[J]. Communications Science and Technology Heilongjiang, 2003, 056(8).

## ACKNOWLEDGEMENT

Corresponding Author Name: ZHANG Mingyu  
 Affiliation: School of Architecture, Tianjin University, Tianjin 300072, China  
 e-mail: 294634856@qq.com

# THE INTERVENTION EXPERIMENT OF LIGHTING IN WORKING SPACES ON HUMAN EMOTIONS

Yi Su, Weiwei Chen, Yaowu Yang  
(SPT Lighting Co., Ltd., Jiangsu, China)

## ABSTRACT

This study is aimed at people who work continuously in a fully artificial lighting environment. In the interval of work, different LED lighting environments are given to observe their mental state, emotional changes, work quality and efficiency. Here, we set up three different experimental schemes by adjusting the LED parameter configurations, e.g. color temperature, blue light proportion and luminous intensity. The experimental results make it clear that the blue-rich and strong lighting environment before starting work should increase the excitement level of employees, and then possibly improve work efficiency and reduce operation mistake.

Keywords: Fully artificial lighting environments, LED parameter configurations, Excitement level.

## 1. INTRODUCTION

Nowadays, the confined spaces, all of which are illuminated by artificial light, are required for many working environments, such as isolated laboratories, clean workshops, etc. In the design of these artificial lighting environments, people only consider functional lighting and often overlook non-visual light, which not only easily leads to work fatigue of operators, but also affects people's emotions. A good lighting environment can improve people's visual and non-visual effects, and many studies on this aspect have been carried out and further prove this point. Recently, the efforts that the exposure level of the artificial light is regulated in preparation of the work, have been already taken to discuss the possibility of blocking the work fatigue of the assembly-line operators. As previously reported, the light exposure experiment in the assembly-line workshop lounge illuminated by the artificial light was carried out to observe the changes in the alertness, attention and mood of the assembly-line workers, where three luminous intensities and two color temperatures were set up.<sup>1</sup> Herein, our study is only for the specific workers in a fully artificial lighting environment. A certain amount of lighting intervention at the working interval is provided for observing their psychological and physiological changes, which is a main part of our researching project named "The research of light on employee health". In this study, we concentrate on studying the changes in the participants' working quality and efficiency after such lighting intervention at the working interval.

## 2. EXPERIMENTAL DETAILS

The participants are a group of operators who are engaged in the quality inspection of chemical pharmaceutical bottles. In a completely closed clean room, they are responsible for sorting out unqualified ampoules from a batch of products to be inspected, which is a routine work of the drug inspection line in the pharmaceutical factory. The LED parameter configuration in the regular working environment is shown as No.1 of Table 1, which meets the national standards and production requirements. Meanwhile, the LED lighting conditions at working intervals are shown as No.2 and No.3 of Table 1, respectively. And on this basis, we set up three different experimental schemes as follows.

Table 1. The LED parameter configurations in different lighting environments.

Serial NO.	Color temperature	Blue light proportion	GCRI	Luminous intensity	Uniformity of illuminance	UGR
NO.1	4500 K	15%	80	300 cd	0.7	19
NO.2	4000 K	5%	80	150 cd	0.6	19
NO.3	6000 K	25%	80	1000 cd	0.6	19

Notes: GCRI represents general color rendering index. UGR is the abbreviation for 'Unified glare rating'.

### 3. RESULTS AND DISCUSSION

*Experimental scheme 1:* The experimental participants are ten skilled workers and engaged in the same work as the above mentioned. After two hours of continuous work in the production line, 10 minutes available for rest were provided for them under completely unchanged lighting environment (No.1 of Table 1). Subsequently ten participants were arranged to detect unqualified ones from 1000 bottles, where 1% unqualified ones were intentionally mixed. The experimental results are illustrated in Table 2.

Table 2. The results based on experimental scheme 1.

Serial NO.	Total amount	Unqualified amount	Pass rate	Fallout rate	Sampling time /minute
1	1000	9	90%	0%	13.50
2	1000	10	100%	0%	14.20
3	1000	11	100%	10%	13.70
4	1000	10	100%	0%	14.50
5	1000	10	100%	0%	14.20
6	1000	9	90%	0%	15.20
7	1000	10	100%	0%	13.90
8	1000	10	100%	0%	13.70
9	1000	10	100%	0%	14.60
10	1000	10	100%	0%	14.50
Average	1000	/	98%	1%	14.20

*Experimental scheme 2:* Ten participants conducted two hour periods of work under the lighting environment (No.1 of Table 1), and then took a 10-minute break under the another lighting environment (No.2 of Table 1). After this short rest, they went on with the same task, that is, to detect unqualified ones from 1000 bottles involving 1% unqualified rate. The experimental results are shown in Table 3.

Table 3. The acquired results on basis of experimental scheme 2.

Serial NO.	Total amount	Unqualified amount	Pass rate	Fallout rate	Sampling time /minute
1	1000	10	100%	0%	13.80
2	1000	11	100%	10%	13.50
3	1000	10	100%	0%	13.70
4	1000	10	100%	0%	14.20
5	1000	10	100%	0%	14.20
6	1000	11	100%	10%	15.20
7	1000	9	90%	0%	14.20
8	1000	10	100%	0%	13.50
9	1000	10	100%	0%	14.20
10	1000	10	100%	0%	14.50
Average	1000	/	99%	2%	14.10

*Experimental scheme 3:* After two hours of continuous work under the lighting environment (No.1 of Table 1), ten participants were firstly scheduled a five-minute break under the lighting environment involving a low proportion of blue light and low illumination intensity (No.2 of Table 1), and then went on with a five-minute break under the another lighting environment with a particularly high proportion of blue light and high illumination intensity (No.3 of Table 1). After that, they conducted the same work to detect unqualified ones from 1000 bottles containing 1% unqualified rate. The experimental results are shown in Table 4.

Table 4. The experimental results according to scheme 3.

Serial NO.	Total amount	Unqualified amount	Pass rate	Fallout rate	Sampling time /minute
1	1000	10	100%	0%	12.50
2	1000	10	100%	0%	13.20
3	1000	10	100%	0%	13.20
4	1000	10	100%	0%	13.60
5	1000	10	100%	0%	14.10
6	1000	10	100%	0%	13.80
7	1000	10	100%	0%	14.00
8	1000	9	90%	0%	13.20
9	1000	10	100%	0%	14.20
10	1000	10	100%	0%	14.20
Average	1000	/	99%	0%	13.60

By contrast between Table 2 and Table 3, the specific lighting environment at the working intervals, that possesses a low proportion of blue light and low illumination intensity, provides the employees with a possibility to relieve fatigue. Furthermore, the experimental results of Table 4 are detailedly compared with ones of Table 3. Before starting work, introducing the blue-rich and strong lighting environment (the experimental scheme 3 ) should increase the excitement level of employees, and then possibly improve work efficiency (sampling time) and reduce operation mistake (fallout rate). With these findings, this study may open an attractive direction for a wide range of design possibilities in terms of LED lighting environments at the working intervals.

#### 4. CONCLUSION

Long-term working in an artificial lighting environment enables the workers to feel tired, and even causes decreased visual function or discomfort, which directly leads to a decline in work quality and efficiency. According to the above three different experimental schemes, the acquired results show that the lighting intervention at working intervals, especially the blue-rich and strong lighting, is capable of increasing the excitement level of workers, and then potentially improving work quality and efficiency. The experiment is still in progress, the report is only our periodic work, and the results need to be verified in future studies.

#### REFERENCE

- [1] Yan Y. H., He S. Q., Hu Y. Q. and Zhang W. L. Impact of LED lighting exposure prior to work on alertness, attention and mood of assembly-line workers[J]. South Architecture, 2019, 0(3): 70-75.

#### ACKNOWLEDGEMENT

Corresponding Author: Yaowu Yang

Affiliation: SPT Lighting Co., Ltd.

e-mail : yang@sptlighting.com

# EFFICIENT AND PERSONALIZED HUMAN-CENTRIC LIGHTING DESIGN WITH MEDI AND AI: A CLOUD-BASED SOLUTION FOR CIRCADIAN RHYTHMS OPTIMIZATION

Shaokun Chen<sup>1</sup>, Shu Yi<sup>2</sup>, Heng Li<sup>1</sup>, Huaming Chen<sup>1</sup>

(1. LEDVANCE Operation & Management (Shenzhen) Co., Ltd., Shenzhen, China. 2. The Hong Kong Polytechnic University, Hong Kong, China)

## ABSTRACT

The visual and non-visual impacts of lighting on humans are increasingly understood. However, a lack of systematic organization of this knowledge makes it challenging for lighting designers to apply it to real-world projects. As demand for Human-centric Lighting (HCL) grows, there is a pressing need for new design software to assist in its implementation. This paper proposes an innovative automated system for HCL design that considers the impact of lighting on human circadian rhythms, specifically reflected in the Melanopic Equivalent Daylight Illuminance (mEDI). Based on cloud computing technology, the system incorporates artificial intelligence and big data algorithms to provide efficient and personalized HCL design solutions. Dialux simulation result shows our solution can successfully fulfil subjects' circadian system need and significantly reduced design time. The proposed system represents an important step forward in HCL design and has significant implications for the health and well-being of building occupants.

Keywords: Human Centric Lighting, Circadian Rhythm, Automated Lighting Design, AI, Cloud Computing, Well Being

## 1. INTRODUCTION

Human Centric Lighting (HCL) is a lighting concept which is intended to achieve beneficial effects in humans by supporting their visual, non-visual and emotional requirements on the light in an optimal way [1]. The research on visual performance, experience, and comfort has been thoroughly conducted, serving as the basis for lighting industry standards, regulations, and design guidelines. The non-visual impact (also known as biological impact) is currently a hot research topic, with extensive research results in alertness [2] [3], melatonin suppression [4] [5], circadian rhythm [5] [6], fatigue levels [7], attention [8], and subjects' performance [9]. As for emotional impact, research mainly focuses on users' subjective assessment [10], comfort [11], interest [12], and awareness propagation [12]. In terms of usage scenarios, in addition to laboratory scenarios, offices [13], education [14], nursing homes and hospitals [15] are currently the focus of research.

Among these effects, the circadian system, as the most in-depth and thorough part of research in human centric lighting, has yielded significant results. Melanopic Equivalent Daylight Illuminance, melanopic EDI, or 'mEDI' for short, is the illuminance of standard daylight (D65), at a point, that provides equal melanopic irradiance as the test source. mEDI has been defined for the description of light related to its for non-visual effects in CIE S 026 [16]. Such parameter is related to influencing factors such as age, spectral power distribution of the light source (SPD), illuminance at the eye position, and dynamic changes.

However, in practical applications, many existing design processes are too complex to consider and are disconnected from real-life scenarios. Currently, CIE [16], UL [17], WELL [18], CEN [19] and DIN [20] [21] have all begun to quantify and evaluate the design standards for HCL, but there are differences in the factors considered. Designers also find it difficult to integrate standards and design. Currently, professional lighting researchers and some designers can integrate non-visual effects into the lighting design process through existing research results and standards [22]. But this process involves cumbersome procedures and multiple new parameters that need to be considered and calculated, which is not friendly for most lighting designers. As a new design emphasis, designers do not have enough energy and time to complete this process.

To solve this problem, we rely on the Light & Space cloud platform which is based on artificial intelligence and big data algorithms, and design a new digital simulation tool that incorporates the factors and algorithms of human centric lighting into it. This forms an automated solution for HCL design,



generating practical lighting solutions based on quantified HCL research results quickly and professionally. We conducted experiments to demonstrate that this solution can meet the actual needs of the mEDI.

## 2. METHODS

### 2.1 Main influence factors of light environment on human circadian system

There is currently a vast amount of research on the factors that influence the human circadian rhythm system based on light environment. In consideration of our platform's intended purposes as a provider of professional and accurate HCL design schemes, rather than being focused on scientific research, we will prioritize the inclusion of industry-accredited academic association standards, regional regulations, and widely recognized certifications as the key factors to consider in our design process. These considerations will ensure that our HCL designs have high industry credibility.

CIE S 026 (2018) for measurement and assessment of light for non-visual effects has strong credibility and authority, and is highly recognized among designers. It defined  $\alpha$ -optic quantities based on five photoreceptors, and leave uncertainty about impact of single photoreceptors [16]. Different light sources can be calculated and corrected, which close to daylight is preferable. Age-related corrections also need to be considered, for example,  $+1/3$  illuminance at eye sight is required for 50 years old users and  $+2/3$  for 80 years. And based on the distribution of different photoreceptor cells in the retina, it's field of view need to be considered in design stage, forwards and upper viewing angles is preferred. Meanwhile, regional standard European CEN TR 16791 (2017) and German Standard DIN/TS 5031-100 (2021) for measurement and assessment, focused on melanopic weighting but other receptors ignored [19] [20]. This simplification is reasonable for lighting design applications and has been justified. These standards provide detailed biological basis for the impact of light on the human circadian rhythm, summarize widely recognized research literature, and provide quantitative explanations for the measurement and assessment factors. However, they do not provide enough standard reference values and design recommendations for applications.

As the first national standard which provide definite design guide value for biologically effective illumination, DIN/TS 67600 clearly point out that 250lux mEDI for daytime applications and marked 250lux should be measured vertically on eye level. At the same time, age correction, correction for spectrum deviating from daylight, room factor (ratio horizontal/vertical illuminance), light dynamic factor, maintenance factor will all be used as correction factors to ensure that the mEDI of the eye position truly meets the needs of people [21]. As for certifications such as WELL and UL, although the requirements for the impact of various light environment parameters on human rhythm are also gradually clarified, UL is based on the Circadian stimulus Evaluation (CS) [17] and WELL is based on the Equivalent melanopic Lux Evaluation (EML) (but point out 218 mEDI if electric light only) [18]. At present, this article only points out these influence factors for reference.

To sum up, we will select mEDI=250lux as the core requirement of the HCL algorithm on our cloud platform, select the eye position 1.2m from the ground as the test height (using room factor as the conversion coefficient), horizontal illuminance as the test method, and age, MDER of light fittings, lighting dynamic changes and maintenance factor for correction.

These influence factors are also recognized by the lighting industry in new publications and have reached consensus among best known and recognized experts in this field [23]. These articles not only recognize that mEDI can reliably approximate the light sensitivity of human physiological responses under most practically relevant situations, but also give specific recommendations for mEDI during daytime, evening and sleep. These recommendations are supported by detailed analysis of sensitivity of human circadian, neuroendocrine, and alerting responses to ocular light and provide a straightforward framework for our personalized Human-centric Lighting Design cloud platform with AI

### 2.2 Implementation mechanism of Light & Space AI Cloud Platform

Light & Space is an AI-based automatic lighting design cloud platform. Based on the input floor plan, spatial properties, and space functions, lighting fixtures best for the spaces are selected from the lighting fixture library, then placed according to spatial calculation lighting standards and predefined designers' project experience by our rule engine. The result is a full set lighting solution package with outputs of lighting layout plans, illuminance distribution maps, product catalogues, 3D views, quotations, etc.



Figure 1. Main interface of Light and Space

Automatic design typically uses machine learning and deep learning methods [24]. However, there are often issues with accuracy, large sample sizes, and high training costs when facing a lack of samples [25]. Specialized lighting systems must adhere to lighting standards, architectural design, and installation standards, requiring higher accuracy. Therefore, we use dynamic programming to break down this problem into multiple sub-problems and store previously solved problems to reduce complexity. To further enhance accuracy and efficiency beyond neural networks, we have developed an expert system that relies on a combination of supervised learning and rule-based dynamic programming.

Dynamic programming is an algorithm for solving optimization problems that have the property of optimal substructure, meaning that the optimal solution to the problem can be decomposed into optimal solutions to subproblems. The basic idea of dynamic programming is to gradually construct the optimal solution to the problem by using the optimal solutions to its subproblems. The cost-to-go represents the minimum cost required to reach the final state of the problem, usually using a recursive relationship called the bellman equation [26].

$$J(s) = \min_a \sum_{s'} P(s'|s, a) [R(s, a, s') + \gamma J(s')]$$

$J(s)$ : The cost to go function. The optimal value function for states, representing the maximum expected return from states to the terminal state.

min: Enumerate all the actions that can be taken in states, and choose the one that minimizes the equation.

$\sum_{s'}$  : Sums over all possible next states  $s'$ .

$P(s'|s, a)$ : The transition probability function, representing the probability of transitioning from states to the next states' after taking action  $a$ .

$R(s, a, s')$ : The reward function, representing the immediate reward obtained when action  $a$  is taken in state  $s$  and transition to state  $s'$  occurs.

$\gamma$ : the discount factor, representing the importance of future rewards decreases with time.

$J(s')$ : The maximum expected return from state  $s'$  to the terminal state.

Our system includes several key components:

- **Spatial Calculation:** The spatial calculation module places lighting fixtures based on the current space's geometric shape, usage attributes, functional partition, and placement of crucial lighting furniture. Lighting fixture placement is mainly based on geometric placement methods and machine learning models. Geometric placement methods include uniform distribution, binary placement, and centerline placement. The uniform arrangement suits most spaces and provides the best lighting uniformity. Binary placement is suitable for areas such as meeting rooms, while centerline placement is used for narrow areas such as corridors. For irregular spaces, lighting fixtures are placed based on the quadtree algorithm, which partitions the space into rectangles and uses the Voronoi uniformization process for lighting fixture placement. The centerline is located using the skeleton search algorithm. Pretrained models are a set of model data trained by random forests regarding the placement of lighting fixtures in previous engineering floor plans.

- **Illuminance Calculation:** The illuminance calculation part calculates the illuminance, eye illuminance, and lighting uniformity of each characteristic point on the walls, ceilings, work plane, and floors of the entire space based on the current space and lighting fixture placement using the reflection method and Monte Carlo method simplification [27]. The basic reflection formula is based on the Lambert diffuse reflection model [28].

$$L = k_d \cdot I \cdot \cos \theta$$

where  $L$  is the reflected illuminance,  $k_d$  is the diffusion reflection coefficient of the surface,  $I$  is the illuminance of the incident light, and  $\theta$  is the angle between the incident light and the normal of the surface. all surfaces in the spaces are divided into lambert pieces, and the total illuminance is calculated from reflections to and from the lambert surfaces.

- **Lighting Standards:** The lighting standards include the required illuminance for work surfaces, eye illuminance standard (for HCL), uniformity standard, power standard, and others, as per region & country standards.
- **Lighting Fixture Library:** The available lighting fixtures for each country and region are stored in the library.
- **Rule Engine:** The rule engine selects lighting fixtures and judges whether the lighting fixture placement is reasonable, whether the lighting standards are met and whether the lighting fixture placement can be output as the final design. The lighting designer's predefined rules, such as lighting fixture placement spacing and placement principles, are also considered.
- **Input and Visualization:** The final lighting plan and its effects are displayed using the three.js rendering engine. All the design details are compiled into a complete lighting report in PDF, Word, and Excel format for output.
- **Learning and Training System:** Completed projects are stored in the training library as input for future AI training, enabling continuous system improvement.

The system structure are as follows.

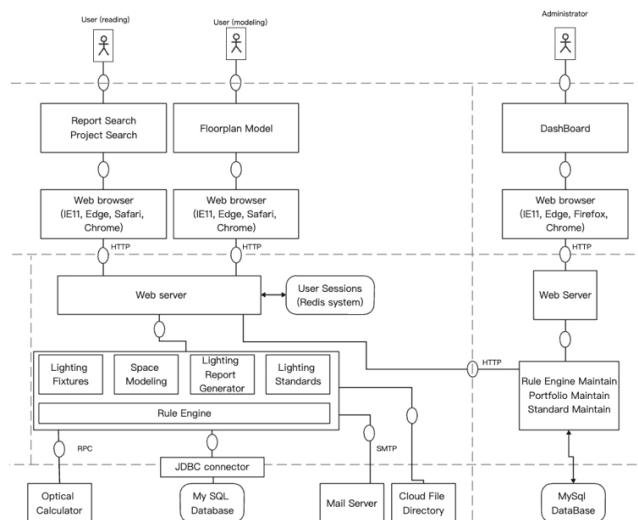


Figure 2. System Structure of Light and Space



Figure 3. Lighting Layout Sample for three hotel rooms

## 2.3 Human-Centric Lighting Design Process Involvement in Light and Space

Based on the implementation mechanism and algorithm flow of the Light & Space AI Cloud Platform, an efficient and personalized human centric lighting design solution is architected for optimizing circadian rhythms. The entire design process follows five steps of HCL design proposed by Kevin and Tony [22]. We have limited our design solution to be prepared for people who work and study during the daytime and have regular and controllable light application, sleep cycles, and sleep requirements. We have also completed the review of lighting guidelines. Next steps involve implementing algorithms that will put all design elements together.

In the first part of method, mEDI has been selected as the design target, the eye position as the testing location, the spectral power Distribution (SPD) of the light source, user age, dynamic lighting changes, and maintenance coefficient as correction factors. The correction calculation formula is as follows:

$mEDI = \text{Horizontal illuminance} \times \text{Room factor} \times mDER \times \text{Age correction} \times \text{Dynamic change percentage} \times \text{Maintenance coefficient} = 250 \text{ lux}$

Correcting factors need to be thoroughly considered to accurately adjust the true value of mEDI. This will help our algorithm become more accurate and reliable. Here are explanations for each correction factor:

### 2.3.1 Room factor

We aimed to select the eye position 1.2m from the floor as the test height. However, considering that designers often do not specifically mark the positions of room users, this makes it difficult to measure the vertical illuminance at the position of the human eye. To simplify the operation and design process, room factor was used as the conversion coefficient. Generally speaking, for workers sitting in an office scene, the ratio of the vertical illuminance at the eye position of 1.2m to the horizontal illuminance of the desktop at 0.8m is 1:2 [21].

### 2.3.2 SPD

Because the photoreceptor cells of the visual system are sensitive to different wavelengths, different SPDs will have different effects on the suppression or promotion of melatonin levels in the human body [16]. Melanopsin containing photoreceptors are sensitive in the blue spectral region. Melanopic daylight (D65) efficacy ratio (mDER) is the ratio of the illuminance of the standard illuminant D65 (mEDI) to the illuminance of the test illuminant  $E_v$  (in lx) when the absolute melanopic efficacy of both illuminants is set equal [16]. So mDER is used as an important parameter to measure the impact of luminaires on the human circadian system. We perform SPD analysis on the products in the cloud luminaire library through optical testing to calculate their mDER values. The SPD analysis formula and mDER value of common light sources are as follows [16].

$$X_{e,mel} = \int_{\lambda_u}^{\lambda_0} X_{\lambda}(\lambda) \cdot s_{mel}(\lambda) \cdot d\lambda$$

$X_{e,mel}$  is the melanopic quantity of target luminaire provided,  $X_{\lambda}(\lambda)$  is the SPD and  $s_{mel}(\lambda)$  is the action spectra of retinal photoreceptors (ipRGC) for melanopsin sensitivity.

Table 1. mDER value of common light sources

Common illuminant or light source	Illuminance $E_v$ (lx)	Melanopic irradiance $E_{mel}$ (mW·m <sup>-2</sup> )	Melanopic equivalent daylight (D65) illuminance $E_{v,mel}^{D65}$ (lx)	Melanopic efficacy of luminous radiation (of the light source) $K_{mel,v}$ (mW·lm <sup>-1</sup> )	Melanopic daylight (D65) efficacy ratio $r_{D65/mel,v}$
Equi-energy spectrum	100	120,1	90,6	1,201	0,906
CIE standard illuminant A	100	65,7	49,6	0,657	0,496
Fluorescent 3 000 K (CIE illuminant FL 12, interpolated to 1 nm)	100	53,4	40,4	0,534	0,404
Fluorescent 4 000 K (CIE illuminant FL 11, interpolated to 1 nm)	100	74,5	56,2	0,745	0,562
CIE illuminant D55 (daylight 5 500 K)	100	119,9	90,4	1,199	0,904
CIE standard illuminant D65 (daylight 6 500 K)	100	132,6	100,0	1,326	1,000

### 2.3.3 User age

The circadian rhythm of human beings changes with age. Due to these selective wavelength absorptions of the aged lens, a significant variation in the level of mEDI is present in the retina. Older people tend to have less sensitivity to light, which requires the design to consider appropriate lighting levels. Some studies have attempted to correct for this effect [29]. The age correction formula of mEDI and correction factor reference for different ages are as follows [16] [29].

$$E_{v,mel}^{D65}(\alpha) = E_{v,mel}^{D65} \cdot k_{mel,\tau}(\alpha) = E_{v,mel}^{D65} \cdot \frac{\int_{380\text{ nm}}^{780\text{ nm}} \phi_{e,\lambda}(\lambda) c(\alpha, \lambda) s_{mel}(\lambda) \cdot d\lambda}{\int_{380\text{ nm}}^{780\text{ nm}} \phi_{e,\lambda}(\lambda) s_{mel}(\lambda) \cdot d\lambda}$$

$k_{mel,\tau}(\alpha)$  is the age-related transmittance ratio of melanopic efficacy,  $\phi_{e,\lambda}(\lambda)$  is the spectral radiant flux,  $c(\alpha, \lambda)$  is the age-related spectral correction function defined for an observer of age  $\alpha$  and spectrum modified by the absorption of the anterior media of the eye, shifted for different-aged observers (from 10 to 90 years old).

Table 2. Age correction factors of common light sources

Common illuminant or light source	$k_{mel,\tau}$ (25 years)	$k_{mel,\tau}$ (32 years)	$k_{mel,\tau}$ (50 years)	$k_{mel,\tau}$ (75 years)	$k_{mel,\tau}$ (90 years)
Equi-energy spectrum	1,052	1,000	0,835	0,589	0,459
CIE standard illuminant A	1,042	1,000	0,863	0,646	0,523
Fluorescent 3 000 K (CIE illuminant FL12, interpolated to 1 nm)	1,045	1,000	0,857	0,641	0,524
Fluorescent 4 000 K (CIE illuminant FL11, interpolated to 1 nm)	1,050	1,000	0,842	0,608	0,484
CIE illuminant D55 (daylight 5 500 K)	1,050	1,000	0,840	0,598	0,468
CIE standard illuminant D65 (daylight, 6 500 K)	1,052	1,000	0,835	0,589	0,457

### 2.3.4 Dynamic lighting changes

Many lighting systems, especially those claimed to be "human-centric" lighting systems, provide a changeable lighting environment during operation through the lighting control system. These systems can dynamically change the brightness, color temperature, and wavelength of the lighting fixtures to simulate natural light and promote melatonin secretion or inhibit it depending on the time of day in order to achieve better lighting effects and physiological benefits for humans. The correction should consider these changes in the lighting environment and adjust accordingly.

### 2.3.5 Maintenance coefficient

Over time, the SPD of lighting fixtures can change due to ageing, dust accumulation, and other factors. The maintenance coefficient reflects the impact of such changes and adjusts the actual mEDI/mDER value accordingly.

### 2.3.6 Other luminaire screening conditions and luminaire arrangement algorithm optimization

There are many other factors that may affect mEDI that need to be considered. For luminaires selection, high CRI, low glare, no flickering and color consistency is recommended to ensure high lighting quality. Also, some design experience and preferences from designers shall be included, for example, the location of table, seat and sub-zone for significant functions inside rooms should be considered to ensure environmental illumination to be designed in users' eyelids in 50 above 0 to 70 below 0 of vertical extend, 180 of horizontal extent [16]. The correction flow chart based on the Light and Space algorithm is:

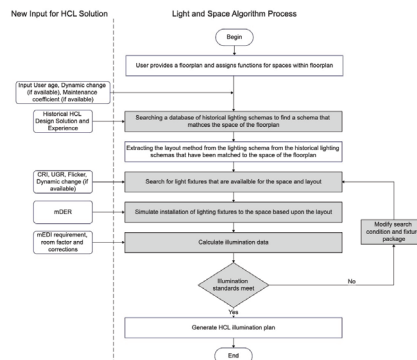




Figure 4. The correction flow chart based on the Light and Space algorithm

Based on the cloud platform, the optimal lighting options that meet the requirements are selected through a screening process. Then, the illuminance calculation is performed on the automatically proposed lighting layout, which is compared with the standard values. If the results do not comply, the lighting quantity and distribution are adjusted, and the verification process is repeated until an HCL scheme that meets the standards is found. The space properties and scheme are recorded and retained as part of a pre-trained model for subsequent use.

### 3. RESULT AND EVALUATION

As an example, we applied the human-centric lighting algorithm to an open office space with dimensions of 20.00 x 15.00 x 3 meters. The average age of the occupants in this office was set to be 50 years old, with a maintenance factor of 0.8 by default. After a few seconds of response time by clicking intelligent design button, the platform provided us with a complete lighting solution. The lighting layout plan and the optical simulation results are shown below.

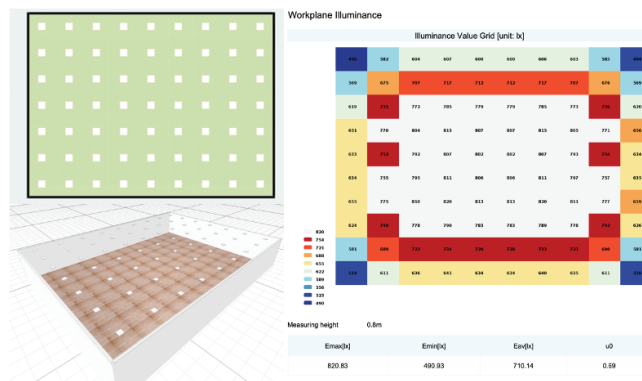


Figure 5. The lighting layout plan and the optical simulation results

From the distribution of the lighting fixtures, the AI selected a uniformly distributed lighting fixture layout, which provided an illuminance value of 710.14lx on the workplane for the office. In terms of lighting fixture selection, the AI selected the BIOLUX 600 \* 600 40W panel light fitting from a company's lighting fixture library as the recommended lighting fixture. This lighting fixture uses a light source which SPD is highly similar to natural daylight with an MDER of 0.95 and UGR less than 16. Additionally, this lighting system has several lighting scene modes, among which the most commonly used natural mode simulates the color temperature and intensity variation of natural light outside throughout the day based on GIS information of the lighting system's location. The change in luminous flux during the daytime is about 90% of the full-output. The entire process from clicking on the intelligent design to obtaining the design scheme took 3-5 seconds. If the time to construct the spatial information is included, the process took about 1 minute.

Based on the design generated by this digital tool, after verification with the adjustment formula, the effective value of mEDI is 253.49lux, which meets the HCL design standards requirements (250lux). The distribution of the lighting fixtures produces a uniform desktop lighting environment ( $u0 = 0.69$ ), ensuring the visual and circadian rhythms optimization needs of each workstation user. At the same time, the automatically selected lighting fixtures have the characteristics of low UGR and high MDER, which are in line with the selection principles of the HCL design scheme. This design scheme meets the requirements of Human-centric Lighting Design and can be customized based on the characteristics of the users such as age and preferences.

To evaluate the effectiveness of the Light & Space platform's HCL design function, we recreated the same spatial environment and lighting layout in Dialux Evo 11.1 and placed eight calculation points at a height of 1.2 meters, corresponding to users' actual eye positions. The resulting simulation (as shown in the figure below) demonstrates that the lighting scheme can satisfy average calculation surfaces' mEDI requirements while effectively, affirming the reliability of the Light & Space HCL Design Function. We have found that calculation objects 1, 2, 5, and 6 meet the requirements of mEDI. However, objects 3, 4, 7, and 8 did not meet the standards. This discrepancy is related to the direction of vertical illuminance measurements. Although the average values meet our requirements, we recommend that officers face the direction with a larger view of the ceiling area while sitting, to ensure that more light sources stimulate the retina and meet the requirements of mEDI.

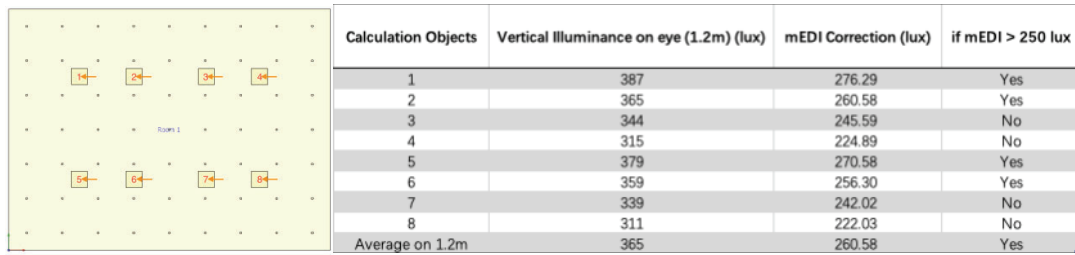


Figure 6 & Table 3. Calculation points locations, directions and the optical simulation results by Dialux

Moreover, reproducing the lighting scene using this existing scheme took about 4 minutes, with the computer simulation process lasting roughly 30-40 seconds, which are both far more than using Light & Space. This indicates that, even with an experienced designer, trying to recreate the design in traditional simulation software would take far longer than using the Light & Space platform's AI-based tool. These results underscore the efficiency of our solution.

#### 4. CONCLUSION

By leveraging AI algorithms and cloud platforms, our solution for human-centric lighting design exhibits superior efficiency. This new tool allows us to quickly and accurately tackle the complex and difficult-to-quantify design challenges involved in human-centric lighting. Through the incorporation of an age factor, we can truly achieve individualized lighting schemes customized to each person's needs.

#### 5. DISCUSSION

Human-centric lighting design encompasses a wide range of considerations. However, as we continue to accumulate adequate quantitative data and develop more design schemes, we can rely on our platform and machine learning algorithms to create a greater variety of lighting scenarios. By incorporating more influential factors, we can really achieve intelligent generation and simulation of human-centric lighting design schemes.

#### REFERENCE

- [1] C. Blume, C. Garbazza, and M. Spitschan, "Effects of light on human circadian rhythms, sleep and mood," *Somnologie*, vol. 23, no. 3, pp. 147–156, 2019. doi:10.1007/s11818-019-00215-x
- [2] C. Cajochen, J. M. Zeitzer, C. A. Czeisler, and D.-J. Dijk, "Dose-response relationship for light intensity and ocular and electroencephalographic correlates of human alertness," *Behavioural Brain Research*, vol. 115, no. 1, pp. 75–83, 2000. doi:10.1016/s0166-4328(00)00236-9
- [3] Lockley SW, Evans EE, Scheer FAJL, Brainard GC, Czeisler CA, Aeschbach D. "Short-wavelength sensitivity for the direct effects of light on alertness, vigilance, and the waking electroencephalogram in humans," *Sleep*, 2006. doi:10.1093/sleep/29.2.161
- [4] A. J. Lewy, T. A. Wehr, F. K. Goodwin, D. A. Newsome, and S. P. Markey, "Light suppresses melatonin secretion in humans," *Science*, vol. 210, no. 4475, pp. 1267–1269, 1980. doi:10.1126/science.7434030
- [5] J. M. Zeitzer, D. Dijk, R. E. Kronauer, E. N. Brown, and C. A. Czeisler, "Sensitivity of the human circadian pacemaker to nocturnal light: Melatonin phase resetting and suppression," *The Journal of Physiology*, vol. 526, no. 3, pp. 695–702, 2000. doi:10.1111/j.1469-7793.2000.00695.x
- [6] C. A. Czeisler et al., "Bright light induction of strong (type 0) resetting of the human circadian pacemaker," *Science*, vol. 244, no. 4910, pp. 1328–1333, 1989. doi:10.1126/science.2734611
- [7] J. S. Martin, M. Hébert, É. Ledoux, M. Gaudreault, and L. Laberge, "Relationship of chronotype to sleep, light exposure, and work-related fatigue in student workers," *Chronobiology International*, vol. 29, no. 3, pp. 295–304, 2012. doi:10.3109/07420528.2011.653656
- [8] A. Green, M. Cohen-Zion, A. Haim, and Y. Dagan, "Evening light exposure from computer screens disrupts sleep, biological rhythms and attention abilities," *Sleep Medicine*, vol. 40, 2017. doi:10.1016/j.sleep.2017.11.343
- [9] A. U. Viola, L. M. James, L. J. Schlangen, and D.-J. Dijk, "Blue-enriched white light in the workplace improves self-reported alertness, performance and sleep quality," *Scandinavian Journal of Work, Environment & Health*, vol. 34, no. 4, pp. 297–306, 2008. doi:10.5271/sjweh.1268

- [10] A. C. Allan, V. Garcia-Hansen, G. Isoardi, and S. S. Smith, "Subjective assessments of lighting quality: A Measurement Review," *LEUKOS*, vol. 15, no. 2–3, pp. 115–126, 2019. doi:10.1080/15502724.2018.1531017
- [11] S. Carlucci, F. Causone, F. De Rosa, and L. Pagliano, "A review of indices for assessing visual comfort with a view to their use in optimization processes to support building integrated design," *Renewable and Sustainable Energy Reviews*, vol. 47, pp. 1016–1033, 2015. doi:10.1016/j.rser.2015.03.062
- [12] S. Chen, K. Fu, B. Yang, and X. Lian, "Using light art installation in urban nightscapes to raise public awareness of carbon neutrality," *Science Communication*, p. 107554702211472, 2023. doi:10.1177/10755470221147286
- [13] P. R. Mills, S. C. Tomkins, and L. J. Schlangen, "The effect of high correlated colour temperature office lighting on employee wellbeing and work performance," *Journal of Circadian Rhythms*, vol. 5, no. 0, p. 2, 2007. doi:10.1186/1740-3391-5-2
- [14] O. Keis, H. Helbig, J. Streb, and K. Hille, "Influence of blue-enriched classroom lighting on students' cognitive performance," *Trends in Neuroscience and Education*, vol. 3, no. 3–4, pp. 86–92, 2014. doi:10.1016/j.tine.2014.09.001
- [15] M. Royer et al., "Light therapy for seniors in long term care," *Journal of the American Medical Directors Association*, vol. 13, no. 2, pp. 100–102, 2012. doi:10.1016/j.jamda.2011.05.006
- [16] Commission Internationale de l'Eclairage, *CIE System for Metrology of Optical Radiation for ipRGC-Influenced Responses to Light*. Vienna: CIE S 026/E:2018, 2018.
- [17] Underwriters Laboratory, *Design Guidelines for Promoting Circadian Entrainment with Light for Day-Active People*. UL Design Guideline 24480, Edition 1, 2019.
- [18] International Well Building Institute., *WELL Building Standard v2, Q3 2020 Version*. Section L03: Circadian Lighting Design. 2020.
- [19] "Quantifying irradiance for eye-mediated non-image-forming effects of light in humans," *CEN/TR 16791*: 2017, 2017. doi:10.3403/30310356u
- [20] German Institute for Standardisation, "Optical Radiation Physics and Illuminating Engineering—Melanopic Effects of Ocular Light on Human Beings—Quantities, Symbols and Action Spectra," *DIN/TS 5031-100:2021*, 2021.
- [21] German Institute for Standardisation., "Complementary criteria for lighting design and lighting application with regard to non-visual effects of light.," *DIN SPEC 67600:2022-08*, 2022.
- [22] K. W. Houser and T. Esposito, "Human-centric lighting: Foundational considerations and a five-step design process," *Frontiers in Neurology*, vol. 12, 2021. doi:10.3389/fneur.2021.630553
- [23] T. M. Brown et al., "Recommendations for daytime, evening, and nighttime indoor light exposure to best support physiology, sleep, and wakefulness in healthy adults," *PLOS Biology*, vol. 20, no. 3, 2022. doi:10.1371/journal.pbio.3001571
- [24] V. Bolón-Canedo, N. Sánchez-Maróño, and A. Alonso-Betanzos, "Distributed feature selection: An application to microarray data classification," *Applied Soft Computing*, vol. 30, pp. 136–150, 2015. doi:10.1016/j.asoc.2015.01.035
- [25] P. Linardatos, V. Papastefanopoulos, and S. Kotsiantis, "Explainable AI: A Review of Machine Learning Interpretability Methods," *Entropy*, vol. 23, no. 1, p. 18, 2020. doi:10.3390/e23010018
- [26] D. E. Kirk, *Optimal Control Theory: An Introduction*. Englewood Cliffs (New Jersey): Prentice-Hall, 1998.
- [27] C. M. Goral, K. E. Torrance, D. P. Greenberg, and B. Battaile, "Modeling the interaction of light between diffuse surfaces," *Seminal graphics*, pp. 137–146, 1998. doi:10.1145/280811.280985
- [28] T. Tsesmelis, "Measuring and understanding light in real life scenarios," thesis, Doctoral Thesis, University of Verona, 2019
- [29] A. Sanchez-Cano, E. Orduna-Hospital, G. Fernández-Espinosa, and J. Aporta, "Method to calculate melanopic light reaching the retina depending on the optical density of an aging crystalline lens," *Applied Sciences*, vol. 13, no. 4, p. 2569, 2023. doi:10.3390/app13042569

## ACKNOWLEDGEMENT

Corresponding Author: Shaokun Chen

Affiliation: LEDVANCE Operation & Management (Shenzhen) Co., Ltd.

e-mail : shawnchen\_ucl@163.com

## Light&Space: Rule-Based Software for Efficient and Code-Compliant Office Lighting Design

Shu Yi<sup>1</sup>, Shawn Chen<sup>2</sup>, Heng Li<sup>2</sup>, Huaming Chen<sup>2</sup>, Kevin Wang<sup>2</sup>

(1. The Hong Kong Polytechnic University, Hong Kong, China 2. LEDVANCE Operation & Management (Shenzhen) Co., Ltd., Shenzhen, China.)

### ABSTRACT

Traditional lighting design software is limited to providing simulation capabilities for verifying lighting effects in drawing layouts, and computer-aided lighting design has not fully realized its potential in improving the project process. This study proposes a novel lighting design software called Light&Space (L&S), which aims to replicate the workflow of experienced lighting designers by incorporating their design rules to generate lighting solutions that satisfy both functional and aesthetic requirements, specifically for office spaces. L&S integrates lighting simulation algorithms and design rules to produce complete lighting layouts and luminaire selection schemes with varying prices. The software was tested on representative office space types, and the generated lighting solutions met the workplace design standards outlined in BS EN 12464-1:2021. To validate its feasibility, the study constructed an actual lighting scene based on the solutions generated by L&S and demonstrated their compliance with the standards. In conclusion, L&S is a valuable tool for expediting the design process and producing reliable office lighting design schemes that meet both functional and aesthetic criteria. Future research should focus on enhancing the user experience in the office environment to promote lighting designs that improve employee well-being.

Keywords: Lighting design, simulation, automated design, office lighting, space syntax

### 1. INTRODUCTION

Most lighting design software currently available is primarily focused on simulating the photometric performance of an already-designed lighting concept<sup>1</sup>. While designers use the simulation results to make decisions regarding the design's validation and fixture selection criteria<sup>1, 2</sup>, Simulation is an early step in the architecture design procedure. To complete the project entirely, however, several tasks still must be performed manually. These actions, which include designing proposals, predicting performance, and evaluating performance, form a continuous cycle that concludes when the desired performance is attained. This complete process of completing the loop is known as "design iteration"<sup>3</sup>. And since lighting design is typically performed by professionals, the duration and quality of the lighting design process is highly dependent on the responsible lighting professionals<sup>4</sup>.

The efficacy of lighting design is vital to the success of the overall architecture design process, as it has an impact on the visual appeal of the space, energy consumption, and cost estimation<sup>5-7</sup>. It is crucial to make well-informed decisions regarding lighting design. In order to tackle this challenge, a new lighting design software is being introduced in this study. This software not only verifies the illumination performance but also takes into consideration the fundamental aspects of lighting design as a crucial component of the architecture design process. At the building level, the allocation of light is no longer the sole issue that needs to be resolved. Hence, it is essential to clearly specify the type of space while entering information, and comprehensive information can be readily accessed to aid in decision-making when reviewing the results<sup>8</sup>.

The proposed design tool aims to automate the complete lighting design process and provide multiple comprehensive lighting design solutions following the pre-defined lighting layout rules from in a short timeframe. This study outlines the working mechanism of this new tool and validates its effectiveness through a case study.

## 2. METHODS

The proposed software emulates the lighting scheme design process, generating solutions automatically and adapting them based on the evaluation criteria. This leads to a comprehensive design report rather than just a simulation outcome. The software incorporates two sets of rules: first, it adheres to the lighting requirements of office lighting specifications to produce light layouts; second, it selects luminaire types, installation accessories, and installation guidelines based on the type and characteristics of the space.

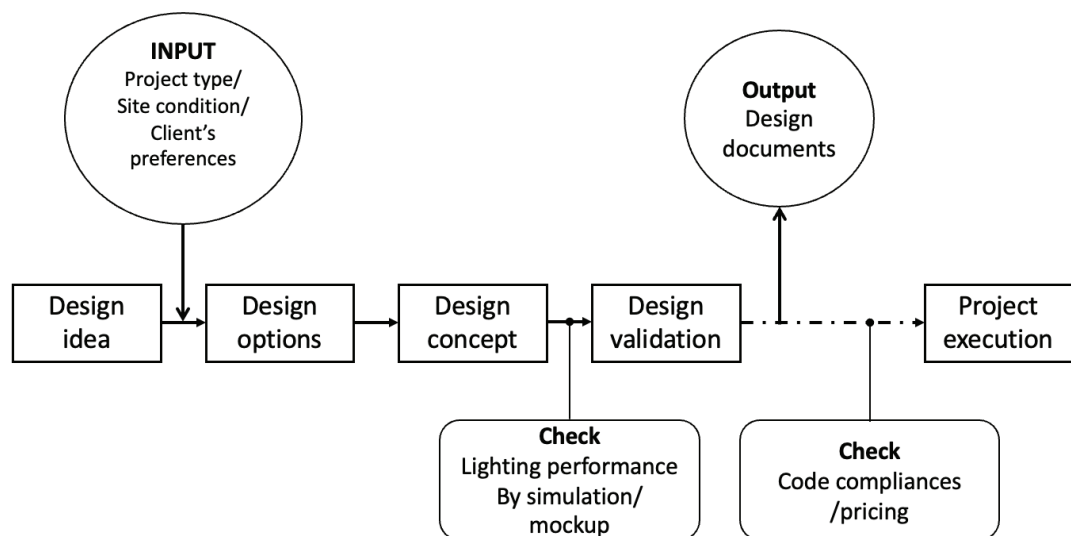


Figure 1 workflow of the software

### 2.1 Modeling

The software includes an easy-to-use tracing function that enables users to efficiently generate a 3D model, which is employed as the fundamental input for the space. To simplify the modelling process, users can draw one or more rectangular or polygon shapes, where each shape represents a room or conceptual area. These spaces may include function rooms, such as small meeting rooms or areas with partial walls. Basic spatial condition such as ceiling type is needed to input for the software to suggest proper mounting methods.

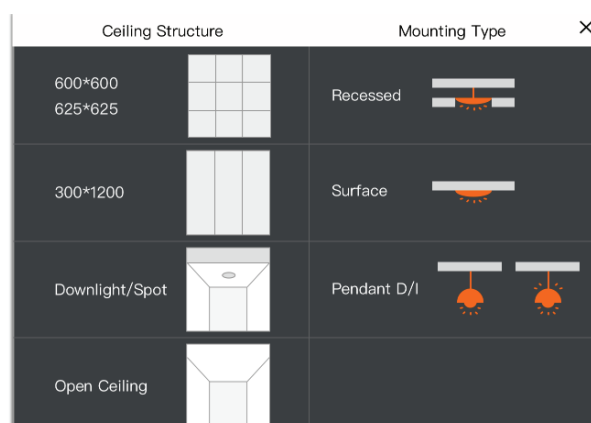


Figure 2 user interface, selection of room structure condition



Subzones can be created within a room, representing special function that require additional lighting or accent lighting, such as sofa area in an individual office.

Each space and subzone must be assigned a function, such as an office, pantry, meeting room etc. These functions impact fixture selection, location logic, and code compliance verification. For example, function options may include small or open offices, corridors, large warehouses, and classrooms.

## 2.2 Generate Lighting Layout

To enhance decision-making efficiency and reduce complexity, we apply a dynamic programming algorithm that decomposes the problem into smaller subproblems and preserves the solutions of previously solved subproblems. This step involves an iterative process. The following procedures are followed for each space in the floorplan: generating an initial lighting fixture layout, performing lighting calculations, and conducting compliance verification. If the layout does not meet the standards, the process returns to the first step to optimize the layout until a compliant lighting solution is generated.

### 2.2.1. Generating fixture placement:

Firstly, the social attributes of the space and lighting preferences are considered to select the most suitable fixture type from the fixture library's defined rules.

For rectangular spaces, the initial required number of fixtures  $N$  is calculated based on the initial optical parameters:

$$(E_{av}) = (N * \phi) * (CU) * \text{factor}(MF) / \text{area}(m^2)$$

Here,  $E_{av}$  represents the average illuminance,  $N * \phi$  represents the total luminous flux of the light source,  $CU$  represents the utilization factor,  $\text{factor}(MF)$  represents the maintenance factor, and  $\text{area}(m^2)$  represents the area of the space.

For non-rectangular cases, three processing options are provided. The first option involves enclosing the space in a maximum bounding rectangle and then performing rectangle approximation using the quadtree algorithm<sup>9</sup>. The second option involves dividing the space into triangular grid cells and calculating each cell's required number of fixtures  $N$ . Additionally, a skeleton searches algorithm can be employed to calculate the centerline skeleton of the space if needed.

For rectangular areas or spaces divided into rectangles, fixtures are placed based on the calculated number  $N$ . Three main principles for placement are as follows:

(a) Uniform distribution:  $N \approx n \times m$ , where the ratio of  $n$  and  $m$  should closely match the aspect ratio of the space.

(b) Binary symmetric distribution: Arranging two rows of fixtures symmetrically on both sides of the centerline.

(c) Centerline distribution: Placing  $N$  fixtures at evenly spaced intervals along the centerline.

### 2.2.2 lighting calculation

After completing the initial fixture placement, the illuminance values on the work surface, floor, and walls are calculated using the reflection method<sup>10</sup>.

- Dividing the surfaces of the space into smaller elements: The interior space is divided into smaller elements or regions, and the size and shape of each element can be adjusted as needed.

- Calculating direct lighting between the elements: The direct lighting between the element and all point light sources is calculated for each element. Then, the contribution to the surrounding elements is computed based on the element's reflection coefficient.

- Iteratively calculating indirect lighting between the elements: Using an iterative approach, the indirect lighting between the elements is computed. This process continues until convergence or a predefined number of iterations is reached. During the computation, the indirect lighting values

of each element are continuously updated and propagated. Currently, 4 or 5 iterations are typically used based on empirical values.

### 2.2.3. The results and reports

Consequently, the lighting uniformity, average illuminance, Lighting Power Density (LPD), and other calculations conform to the lighting standards of the space. If the results fail to meet the standards, automatic adjustments are made to modify the number of fixtures or arrangement logic. The process then restarts with the rearrangement of fixture placement and recalculating the lighting until a lighting solution that aligns with the lighting standards of the space is achieved.

Unlike conventional lighting software that prioritizes light distribution calculations, a comprehensive report that includes three different lighting schemes at varying price points is automatically generated at the end of the calculation process.

## 4. FEASIBILITY STUDY

To validate the effectiveness of the software, this research employed the L&S software to generate an office lighting solution for a typical laboratory at the Ledvance R&D center. Based on the automatically generated lighting scheme, the lighting design was implemented in the actual space. Subsequently, the space was measured, and the results demonstrated that the measured average illuminance achieved was in compliance with the lighting standards, with a difference of less than 5% compared to the lighting solution generated by the software. This confirms the efficacy of the solution generated by the software, which is simple and rapid in its generation.

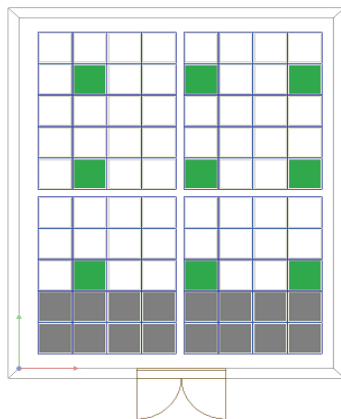


Figure 3 fixture plan suggested by L&S software.



Figure 4 lab setting.

#1 Light & Space suggested illuminance distribuion

434.22	589.54	664.04	699.01	729.52	734.09	710.5
598.76	781.08	900.37	935.21	971.22	1000.6	961.35
650.74	870.27	980.71	1034.3	1080.1	1098.1	1085.7
678.88	896	1018.3	1068.1	1115	1141.6	1117
667.33	877.11	998.04	1049.9	1091.9	1121.4	1092.8
622.05	831.24	933.68	985.15	1029.9	1046.5	1037.6
586.28	764.44	877.69	913.27	948.75	980.04	944.68
432.29	572.05	644.48	678.85	708.1	721.65	710.1
250.74	328.09	366.53	388.7	406.08	407.47	399.27

avg.(lx)	809	105%
min.(lx)	251	88%
max.(lx)	1142	109%
u0	0.31	84%

Table 1. Illuminance level on the task plane. suggested by L&S software.

#2 One site measurement

430.2	583.2	624.8	667.9	698.6	690.6	605.1
582.2	780.2	853.5	908.7	939.2	918.6	816.6
645.9	852	947.5	993	1023	997	899.2
680.6	896.3	968.9	1030	1049	1024	928.5
649.1	869.5	966.2	999	1025	1002	915.2
608.5	829.7	908.3	954.3	979.5	959.6	866.4
549.4	750.9	842.1	894.5	922.7	914.8	819.5
429.7	603.2	642.6	679.7	696.5	692.1	627.5
284	372.7	414	431.4	430.2	422.2	384.2

avg.(lx)	768	100%
min.(lx)	284	100%
max.(lx)	1049	100%
u0	0.37	100%

Table 2. Illuminance level on the task plane. Measured on site.

## 5. DISCUSSION AND CONCLUSION

Incorporating industry knowledge into the lighting design software can substantially decrease the design cycle while guaranteeing that the resultant office lighting design solution conforms to design principles. The current research stage prioritizes the correlation between the luminaire and the space, as well as the adherence to code requirements in the lighting scheme generated. In upcoming research, it is imperative to pay more attention to the users' perception of the office environment to facilitate office lighting design that improves the well-being of employees.

## REFERENCE

1. Ochoa CE, Aries MB and Hensen JL. State of the art in lighting simulation for building science: a literature review. *Journal of Building Performance Simulation* 2012; 5: 209-233.
2. De Wilde P and Prickett D. Preconditions for the use of simulation in M&E engineering. 2009.
3. Petersen S and Svendsen S. Method and simulation program informed decisions in the early stages of building design. *Energy and Buildings* 2010; 42: 1113-1119. DOI: <https://doi.org/10.1016/j.enbuild.2010.02.002>.
4. Sorger J, Ortner T, Luksch C, et al. LiteVis: Integrated Visualization for Simulation-Based Decision Support in Lighting Design. *IEEE Transactions on Visualization and Computer Graphics* 2016; 22: 290-299. DOI: 10.1109/TVCG.2015.2468011.
5. Duff J, Kelly K and Cuttle C. Perceived adequacy of illumination, spatial brightness, horizontal illuminance and mean room surface exitance in a small office. *Lighting Research & Technology* 2015; 49: 133-146. DOI: 10.1177/1477153515599189.
6. Odabaşioğlu S and Olguntürk N. Effects of Coloured Lighting on the Perception of Interior Spaces. *Perceptual and Motor Skills* 2015; 120: 183-201. DOI: 10.2466/24.PMS.120v10x4.
7. Cuttle C. Making the switch from task illumination to ambient illumination standards: Principles and practicalities, including energy implications. *Lighting Research & Technology* 2019; 52: 455-471. DOI: 10.1177/1477153519857465.
8. Attia S, Beltrán L, De Herde A, et al. "Architect Friendly": a comparison of ten different building performance simulation tools. In: *11th International IBPSA Building Simulation Conference (BS 2009), July 27-30, 2009, Glasgow, UK* 2009, pp.204-211. International Building Performance Simulation Association (IBPSA).
9. Har-Peled S. *Geometric approximation algorithms*. American Mathematical Soc., 2011.
10. Tsemlis T. Measuring and understanding light in real life scenarios. 2019: 43-44 DOCTORAL THESIS.

## ACKNOWLEDGEMENTS

The software discussed in the article is an outcome of a research and development project conducted by Landevance Shenzhen R&D center.

Corresponding Author Name: YI Shu  
 Affiliation: The Hong Kong Polytechnic University  
 e-mail: shu-nancy.yi@connect.polyu.hk

# ANALYSIS OF TRANSMITTANCE BY LED WAVELENGTH TO IMPROVE ROAD LIGHTING VISIBILITY IN FOG CONDITIONS

Ji-myung Kim\*, Sung-gi Chae\*, Young-ju Cho\*, Meeryoung Cho\*, An-seop Choi\*\*

Korea Photonics Technology Institute (KOPTI)\*, Sejong University\*\*

## ABSTRACT

The purpose of this study is to find the best road lighting spectral distribution for foggy conditions. As a result of analysis, the visibility of each wavelength band in the fog situation targeting the currently used street light, the fog transmittance increased as the long wavelength regardless of the street light color. For future studies, in order to increase the accuracy of the test results, it is planned to secure data on the radiant flux reduction rate by wavelength through experiments on various fog generation conditions and lighting fixtures of various colors in the future.

Keywords: fog, road lighting, radial flux decreasing rate

## 1. INTRODUCTION

Road lighting plays a role in helping driving by recognizing the lanes of the road and the shape of the road through the light emitted from lighting fixtures not only at night when there is no light, but also in environments where it is difficult to secure visibility due to tunnels and specific weather conditions. However, it is difficult to secure forward visibility in foggy conditions, increasing the risk of traffic accidents. Therefore, it is necessary to develop a light source to secure the driver's visibility in a foggy environment.

This study aims to secure basic data for the development of light sources suitable for fog conditions by analyzing the spectral power reduction rate by wavelength in fog conditions by color temperature of lighting fixtures.

## 2. METHODS

### 2.1 Measurement overview



In this study, measurements were performed using a smog generator and a steam generator made of actual moisture particles to reproduce the fog situation. The LED lighting used is a module that can be changed to Cool White (correlated color temperature 4,800K) and Warm White (correlated color temperature 3,000K) in one module, and the correlated color temperature variable is driven by turning on/off each different LED PKG. The measurement conditions were set as in Table 1.

**Table 1. Measurement conditions**

	Fog generation method	Visibility distance measurement result		measurement space
		No fog	Fog	
CASE 1	Smog	2400m	50m	large dark room (W120m*D20m*H13m)
CASE 2	Steam	2400m	50m	small chamber (W3m*D3m*H2m)
Used Equipment		Visibility system: Biral SWS-100 Measuring equipment: Spectroradiometer (CL-500A)		

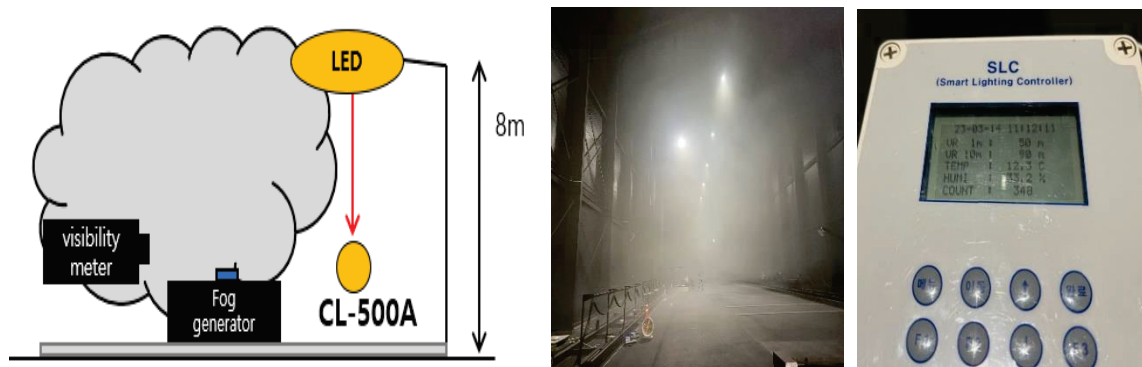
The characteristics of the light source used in the study are as follows in Table 2.

**Table 2. Optical characteristics analysis**

	Color temperature conversion LED PKG	
	3,000K	5,000K
Measurement image		
Luminous flux (lm)	1,515	1,494
Efficiency (lm/W)	65.29	63.69
Power Factor	0.96	0.96
Correlated color temperature (K)	3,015	5,018

## 2.2 Case 1: Smog generation method

The measurement using the smog generator reproduced the fog generation situation in the large dark room, and the visibility distance was confirmed by installing the visibility meter. In order to measure the radiant flux reduction rate by wavelength in the fog situation, a spectral irradiance meter (CL-500A) was installed at an interval of 8m directly below the lighting, and the spectrum for each color temperature was repeatedly measured 10 times before and after the fog situation, and the average value of the radiant flux for each wavelength compared.



**Figure 1. The measurement method using a smog generator**

## 2.3 Case 2: Steam generation method

The measurement using the steam generator reproduced the fog generation situation in a small chamber, and the visibility distance was confirmed by installing a visibility meter. In order to measure the radiant flux reduction rate by wavelength in the fog situation, a spectral irradiance meter (CL-500A) was installed at a distance of 1 m from the lighting, and the spectrum for each color temperature was repeatedly measured 10 times before and after the fog situation, and the average value of the radiant flux per wavelength was measured compared.



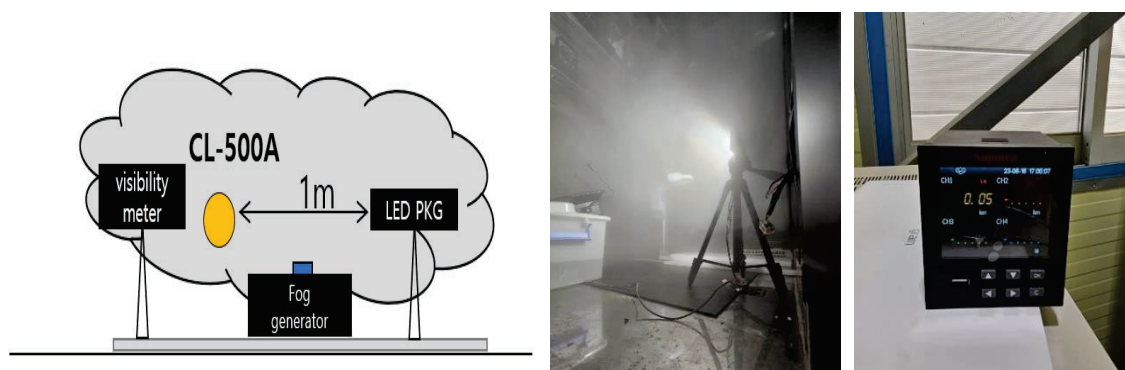


Figure 2. The measurement method using a steam generator

## 2.4 Measurement results

As a result of analyzing the reduction rate by the wavelength of radiant flux by reproducing the fog situation using the smog generator in case 1, It was confirmed that the longer the wavelength from 410 to 720(nm), the smaller the radiant flux decreases. However, 360~409 [nm] and 720~780 [nm] were excluded due to the significant deviation from the small measured radiant flux. And it was confirmed that Warm White had a higher reduction rate than Cool White.

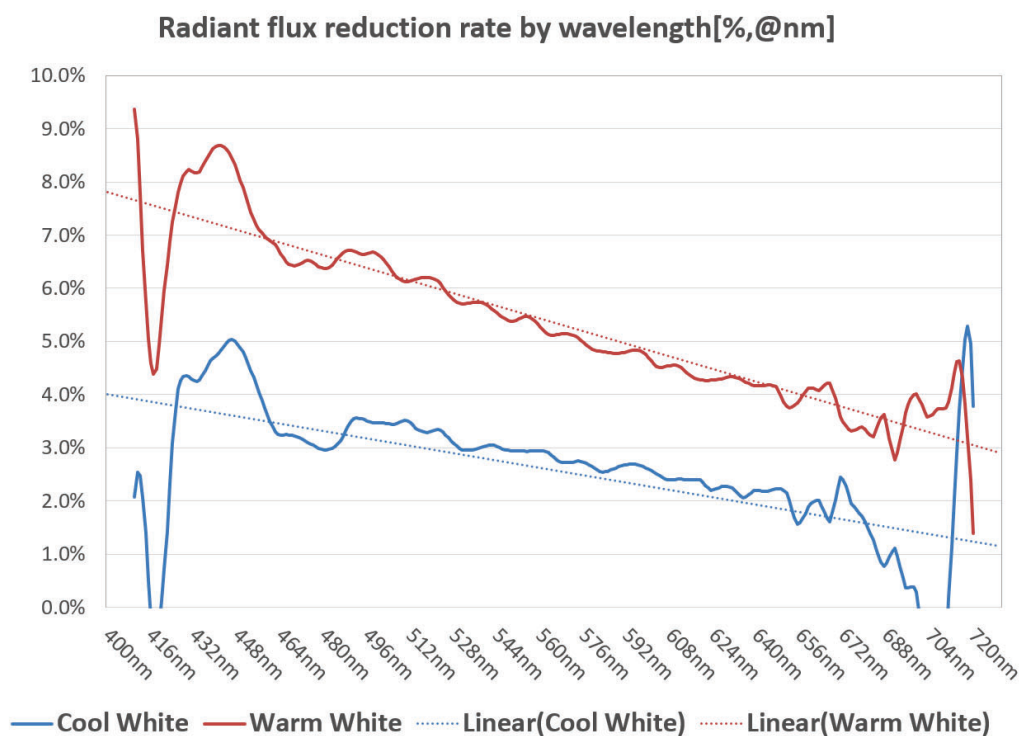
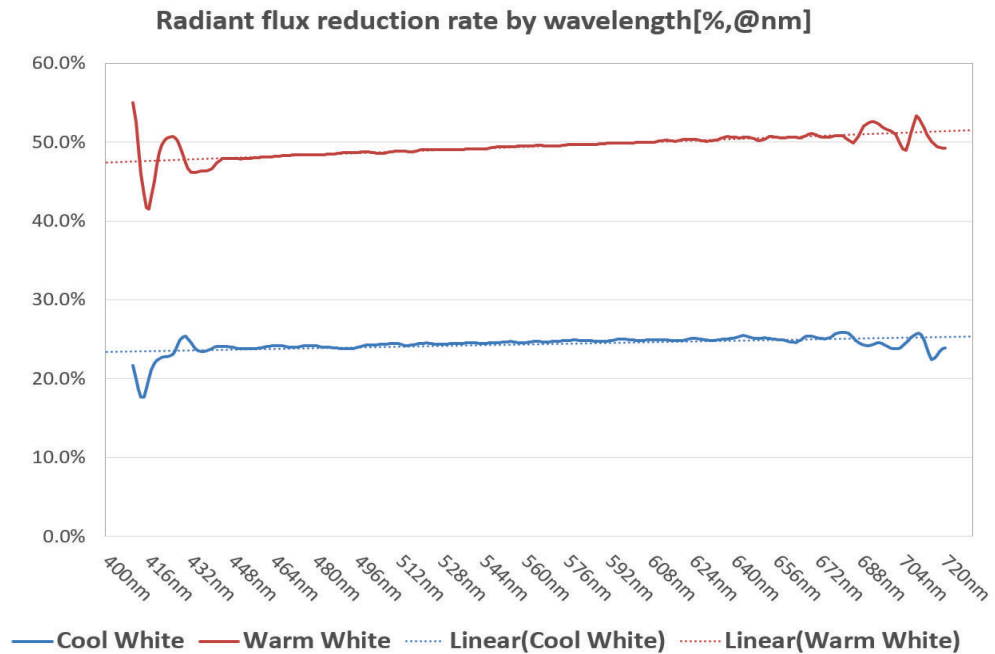


Figure 3. Radiant flux reduction rate graph using smog generator method

As a result of reproducing and analyzing the fog situation using the steam generator of case 2, it was shown that the radiant flux decreased at a constant rate in the wavelength range from 400 to 688 [nm]. The steam generator was also excluded from 360~409 [nm] and 720~780 [nm] due to the significant deviation due to the small amount of radiant flux measured. Contrary to case 1, it was confirmed that the reduction rate of Cool White was higher than that of Warm White.



**Figure 4. Radiant flux reduction rate graph using the steam generator method**

### 3. CONCLUSION

As a result of this study, in the smog generation method, regardless of color temperature, the longer the wavelength, the lower the radiant flux reduction rate, and it showed the characteristic of increasing the fog transmittance. However, a constant decreasing rate was maintained in the steam generation method. This difference in the rate of decrease occurred as a result of the difference in scattering characteristics of the smog-type particles used to reproduce the fog and the moisture particles of the steam-type method.

However, this paper is the result of a preliminary experiment measured using only two fog setting conditions and two correlated color temperature settings, respectively. Therefore, future studies are planned to supplement the experimental results by comparing the difference in Mie scattering characteristics with various conditions of fog density, particles, and correlated color temperature.

### REFERENCES

- [1] Ki Ho Nam, Chung Hyeok Kim, A Research on the Improvement of Visivility Using Low Deck Lighting in Bad Weather, J, Korean Inst. Electr. Electron. Mater. Eng. Vol.33, No.3, pp. 186-193, 2020

### ACKNOWLEDGEMENTS

Funding: This research was supported by an Institute of Information & Communications Technology Planning & Evaluation (IITP) grant funded by the Korea government (MSIT, MOIS, MOLIT, MOTIE) (No. 2020-0-00061, Development of integrated platform technology for fire and disaster management in underground utility tunnel based on digital twin).

This work was supported by the Korean Agency for Technology and Standards(KATS)(Contract No.00238178500, The de facto international standardization support and trend survey, 2023)

Corresponding Author Name: Ji-Myung Kim  
Affiliation: Korea Photonics Technology Institute (KOPTI)  
e-mail: sinji1230@kopti.re.kr

# ANALYSIS OF CLASSROOM LIGHTING RENOVATION PROJECT FOR SCHOOLS AND KINDERGARTENS IN THE YANGTZE RIVER DELTA REGION

Yuting Tong<sup>1, 2</sup>, Weijia Jiang<sup>1, 2</sup>, Jun Zhao<sup>3</sup>, Lihua Chen<sup>4</sup>, Nianyu Zou<sup>5</sup>, Pengpeng  
Guo<sup>6</sup>

(1.CQC Standard (Shanghai) Testing Technology Co.,Ltd., Shanghai, China,

2. China National Machinery Industry Test Center of Intelligent and Healthy Lighting,  
Shanghai, China,

3.Oppl Lighting Co.,Ltd.Suzhou,China,

4.Fujian Inspection and Research Institute for Product Quality,Fujian,China,

5.Research Institute of Photonics, Dalian Polytechnic University, Dalian, China,

6. Zhejiang Lierdalux Intelligent Technology Co., Ltd.,Zhejiang,China )

## ABSTRACT:

Adolescent myopia has become the focus of the whole society, classroom lighting is one of the causes of students' myopia, the Yangtze River Delta region is a demonstration area for classroom lighting transformation in China. However, requirements of the standard is difficult to achieve due to the complexity of classroom environmental facilities and the non-standard transformation construction. This paper tests the maintained average illuminance and uniformity ratio of illuminance of the desk and the blackboard, the correlated color temperature, color rendering index and unified glare rating of typical classrooms in the Yangtze River Delta region, then analyzes the reasons leading to low lighting quality in classrooms. The result shows that the maintained average illuminance and uniformity ratio of illuminance of the blackboard and unified glare rating are the main parameters that affect the substandard quality of the classroom lighting. By selecting suitable luminaires, formulating reasonable design schemes and optimizing luminaire installation methods, etc., the quality of classroom lighting can be improved and students' visual health can be protected. By analyzing the problems existing in classroom lighting transformation, this paper proposes solutions to optimize classroom lighting quality, and provides guidance for classroom lighting transformation not only for the Yangtze River Delta region but also the whole of China.

Keywords: classroom lighting renovation; luminous environment of the classroom; illuminance of the blackboard ;unified glare rating;

## 0 INTRODUCTION

In recent years, with the continuous increase in myopia rate and the emergence of younger

age, the visual environment of adolescents has received widespread attention from society and government departments. More than 60% students in China spend their time in the classroom every day during their school years, so classroom lighting is an important factor affecting the visual development and health of adolescents<sup>[1]</sup>. Whether the quality of classroom lighting Compliances standards has a significant impact on students' visual health and learning efficiency. The quality of the lighting environment affects students' physical health directly and a reasonable and high-quality luminous environment of the classroom can enhance students' learning enthusiasm. Therefore, ensuring a high-quality luminous environment of the classroom is crucial for students.

Due to the former campus environment and long construction time of some classrooms, the complexity of related facilities in the classrooms has increased the difficulty of renovation. Additionally, non-standard renovation construction in some typical classrooms may indirectly or directly result in some parameters still not meeting the standard requirements. In response to the above issues, analyze and explore the corresponding problems arising from the renovation of different luminous environment of the classrooms, and provide corresponding adjustment plans and guidance suggestions to fundamentally improve the current problems in luminous environment of the classroom<sup>[2]</sup>.

## 1 MEASUREMENT METHOD

In accordance with the requirements of the national myopia prevention and control policy, according to DB31/T 539-2020, GB 7793-2010, GB/T 5700-2008 and GB 50034-2013, the maintained average illuminance of the desk, uniformity ratio of illuminance of the desk, maintained average illuminance of the blackboard, uniformity ratio of illuminance of the blackboard, light power density per 100 lx, uniform glare rating, correlated colour temperature, general colour rendering index  $R_a$  and the special colour rendering index  $R_9$  are tested. The test items and relevant limit requirements are shown in Table 1<sup>[3-6]</sup>.

Table 1. Testing Items and Related Limit Requirements

Number	Testing items	Limit
1	maintained average illuminance of the desk	$\geq 300 \text{ lx} / \geq 500 \text{ lx}$
2	uniformity ratio of illuminance of the desk	$\geq 0.7$
3	maintained average illuminance of the blackboard	$\geq 500 \text{ lx}$
4	uniformity ratio of illuminance of the blackboard	$\geq 0.8$
5	Light power density per 100 lx	$\leq 1.8 \text{ W/m}^2/100 \text{ lx}$
6	Unified glare rating	$\leq 16$
7	Correlated colour temperature	3300 K-5300 K
8	General colour rendering index $R_a$	$\geq 90$
9	Special colour rendering index $R_9$	$> 50$

## 2 SUMMARY OF CLASSROOM SPOT CHECK DATA AND EXISTING PROBLEMS ON

## SITE

In the typical classrooms of primary and secondary schools and kindergartens sampled, the most problematic detection items are the uniformity ratio of illuminance of the blackboard and uniform glare rating. The main reason for disqualification of correlated color temperature, General colour rendering index  $R_a$  and Special colour rendering index  $R_9$  is the selection of luminaires, which can be avoided by selecting products with better quality. In the typical classrooms of primary and secondary schools being tested, preliminary size parameter research is particularly important, and corresponding simulations should be conducted based on the surveyed data and different acceptance standards in different regions. Insufficient research, lack of professional simulation, and unprofessional installation personnel can directly lead to issues such as low uniformity ratio of illuminance of the blackboard, high uniform glare rating, and certain safety hazards during installation.

In the typical kindergarten classrooms tested, due to the complexity of the environmental facilities in the kindergarten classroom, the installation of lighting fixtures in the kindergarten classroom is often due to the artistic design of the ceiling or irregular shape of the classroom. The lighting fixtures cannot be uniformly arranged and installed in a regular manner, which is also an important factor that can easily lead to inconsistent glare values and classroom illumination uniformity in the kindergarten classroom.

Based on the results of on-site testing and research, the typical classrooms tested mainly have the following issues:

1. The problem of luminaire selection is the main reason that the unified glare rating, correlated color temperature, general colour rendering index and special colour rendering index are not up to standard;
2. The installation position and angle of the blackboard are the main reasons for the unsatisfactory maintained average illuminance and uniformity ratio of illuminance of the blackboard;
3. The issue of the installation position of classroom lights is the main reason why the unified glare rating, maintained average illuminance of the desk, and uniformity ratio of illuminance of the desk do not meet the standard;
4. Safety hazards during on-site construction and installation.

Below, we will focus on analyzing and exploring corresponding solutions to the above issues.

### 3. OVERALL ANALYSIS AND IMPROVEMENT OF SPOT CHECK ISSUES

#### 3.1 Selection of Luminaires



In some schools, the optical parameters of the LED chips inside the lighting fixtures used in certain classrooms are poor. Improper selection of the LED chips inside the lighting fixtures can lead to the relevant optical and color parameters of the classroom lighting fixtures not meeting the standard requirements, as shown in Figure 1. At the same time, the optical components of such luminaires are mostly not subjected to anti glare treatment, and uneven light output can easily lead to excessive local brightness of the luminaires, resulting in low maintained average illuminance of the desk and poor uniformity ratio of illuminance of the desk. It is also easy to cause low background luminance of the ceiling, floor, and side walls in the classroom, resulting in high uniform glare ratings in the classroom.

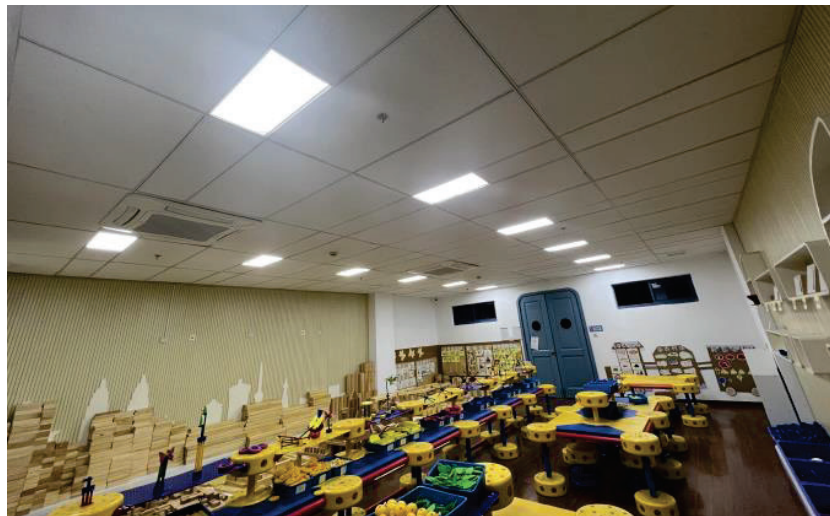


Figure 1. Classrooms with Poor Related Data

The type of classroom lighting fixture shown in Figure 2 is an LED bulb. After actual measurement, it was found that its relevant optical and color parameters do not meet the standard requirements. In addition, the light source has a small luminous area and a large output per unit area, which can easily cause uniform glare rating too high.



Figure 2. Classroom with LED light bulbs

In summary, the selection of lighting fixtures in the classroom should choose lighting fixtures with high-quality LED chips, good overall optical parameters, and optical components that require anti glare treatment. On the basis of ensuring that the color related measurement indicators in the classroom meet the standards, the output of the lighting fixtures can be evenly distributed in the classroom, thereby increasing the maintained average illuminance of the desk, uniformity ratio of illuminance of the desk, and background luminance in the classroom.

### 3.2 Blackboard illumination and uniformity issues

In the on-site spot check, the insufficient number of blackboard lights installed in some classrooms (as shown in Figure 3) resulted in the average illumination and uniformity of the blackboard not meeting the standards. It is recommended to simulate the size of the blackboard before installing it, in order to determine the number of blackboard lights installed.

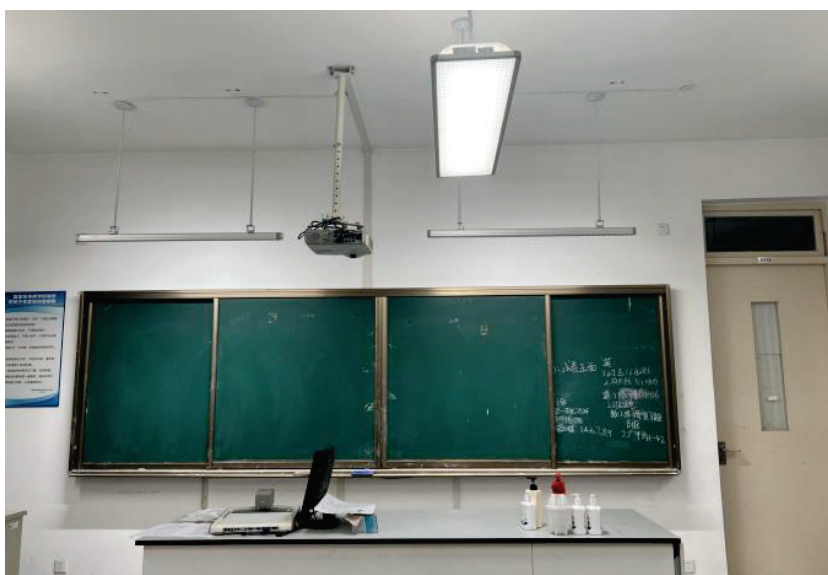


Figure 3. Classroom with insufficient number of blackboard lights

When simulating and installing the blackboard luminaire, many manufacturers' installation drawings only provide the distance between the blackboard luminaire and the upper edge of the blackboard. It was not considered that there are significant differences in the types and sizes of different blackboards and supporting electronic teaching equipment in actual installation.

The width of the blackboard has an impact on the placement of the testing points for the illumination of the blackboard luminaire (as shown in Figure 4). So in order to avoid measuring the average illumination and uniformity of the blackboard as much as possible, on the basis of meeting the standard that the blackboard luminaire is 0.2m higher than the upper edge of the blackboard, the vertical distance between the lower edge of the blackboard luminaire and the horizontal centerline of the blackboard should be considered during installation to prevent installation errors caused by different widths of the blackboard in the design of the lighting fixtures. At the same time, the distance between the two lights of the blackboard luminaire and the horizontal distance between the edge of the blackboard luminaire near the blackboard surface should also be determined.

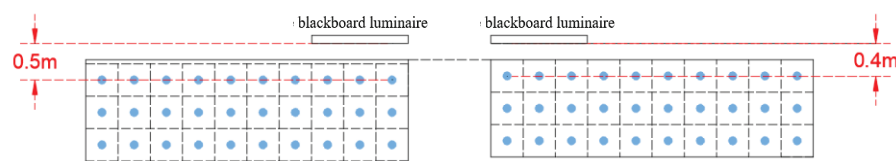


Figure 4. Effect of Different Blackboard Widths on the Distance from Blackboard Measurement Points to Blackboard Luminaire Installation

At the same time, it should also be considered that the height and size of different projectors equipped with different blackboards may affect the installation position of blackboard lights. Therefore, simulation of the installation of blackboard lights can be conducted based on the projector position to ensure that the test results meet the standard requirements. During on-site testing, we also found that in the case of projectors or all-in-one machines, most blackboard lights do not have shunt control. For blackboards with multimedia devices, single light control should be implemented to avoid discomfort caused by reflective glare and contrast glare when students and teachers use multimedia devices in class<sup>[7-8]</sup>.

### 3.3 Installation location and uniform glare rating of classroom lights

In the typical classrooms sampled, the common problems with classroom lighting in primary and secondary school classrooms and kindergarten classrooms are mainly the unreasonable and concentrated installation of lighting fixtures, which leads to excessive local illumination (as shown in Figure 5).



Figure 5. Classroom with overly concentrated lighting installation positions

Some kindergarten classrooms have low floor height and suspended ceilings (as shown in Figure 6). However, when the classroom floor height is low, it is not advisable to install too many and too concentrated classroom lights. If the installation location is not designed properly, it can easily cause local brightness to be too high and background luminance to be too dark, leading to high uniform glare rating in the classroom.



Figure 6. Classroom with lower height

In typical classrooms in primary and secondary schools, different types of blackboards can also have an impact on the uniform glare rating. At present, there are three main types of blackboards we encounter in the Yangtze River Delta region: dark green material, milky white material, and black blackboards with multimedia display screens. The three types of blackboards are shown in Figures 7, 8, and 9.





Figure 7. Dark green blackboard



Figure 8. Milk White Blackboard

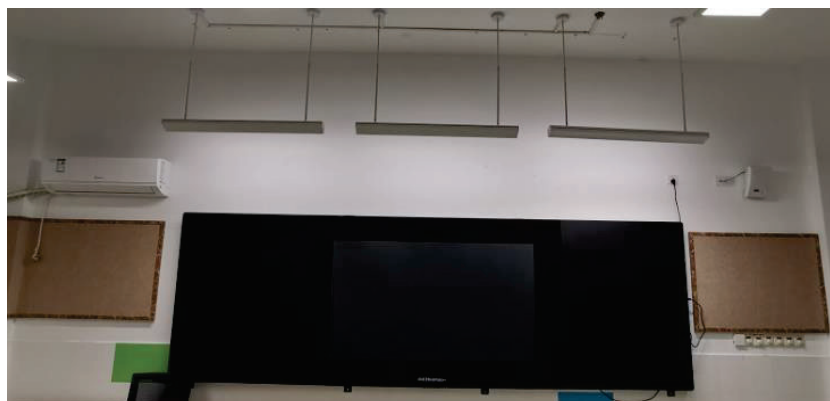


Figure 9. Black Multimedia Integrated Writing Pad

The materials of the three mainstream blackboards are different, resulting in differences in their corresponding reflectivity. The reflectivity of different blackboards can also have a certain impact on the background luminance in the classroom. For example, when the blackboard surface in the classroom is black, the reflectivity of the board surface is lower. Therefore, installing a black blackboard in the classroom will have a lower background luminance than installing a dark green blackboard. If the color and reflectivity of the blackboard are not taken into account during simulation, the unified glare value will be higher during actual testing. If the color and reflectivity of the blackboard are not taken into account during simulation, the uniform glare rating will be higher during actual testing. Therefore, blackboard materials with different



reflectivity should also be considered during simulation.

According to the calculation formula of the unified glare value, if we want to reduce the unified glare value, we can pull the luminaires as high as possible or close to the walls around the classroom. On the basis of increasing the background luminance, we can make the last row of luminaires as close to the back wall as possible, so that the unified glare value Test point can not observe the last row of luminaires.

In terms of increasing background luminance, the unified glare values measured in the classrooms of most newly built schools are lower than those of old schools. The main reason is that the background luminance of newly built schools is relatively high. Therefore, the method of increasing the reflectivity of walls, related facilities, and curtain materials to brighten the surrounding walls, related facilities, and ceilings in the classroom to improve the background luminance and reduce the uniform glare rating is also worth referring to.

So when simulating the light environment in the early stage, factors such as the reflectivity of materials such as walls, ceilings, and curtains in the classroom should also be taken into account, which will reduce the data differences between the simulated design in the early stage and the actual on-site testing results in the later stage.

In terms of reducing the brightness of the lighting fixtures, anti glare treatment can be applied to the optical components of the lighting fixtures. However, when performing anti glare treatment, it is also necessary to consider the direct impact of changing the optical components on the lighting angle and luminous flux of the classroom lighting fixtures, as well as the indirect impact on the average illumination and uniformity of the classroom lighting, in order to avoid attend to one thing and lose sight of another.

### **3.4 On site installation issues**

In the process of testing typical classrooms, many typical classroom lighting fixtures are installed too rough, with problems such as poor uniformity of lighting fixtures, installation of blackboard lights or classroom lights not on a horizontal line, inadequate handling and repair of wiring slots and installation holes, and so on. Due to the fact that the main personnel in the classroom are students, their safety awareness is relatively weak, and the consequences of safety accidents such as the detachment of luminaire suspension rod screws are unimaginable.



Figure 10. Classroom with Unneatly Installed Luminaires

The installation of lighting fixtures is too inclined, which can easily lead to uneven stress on the suspension rods of the lighting fixtures. As the service life increases, the risk of the suspension rods falling off can increase, leading to safety accidents. At the same time, tilted lighting fixtures will also have a certain impact on the unified glare rating of luminous environment of the classroom indicators, as well as the illuminance and uniformity of the desktop.



Figure 11. Classroom light with exposed power cord

The wiring in some typical classrooms after renovation is very rough and there is no wiring slot installed, and the power cord is exposed. The holes after installation construction are visible to the naked eye.

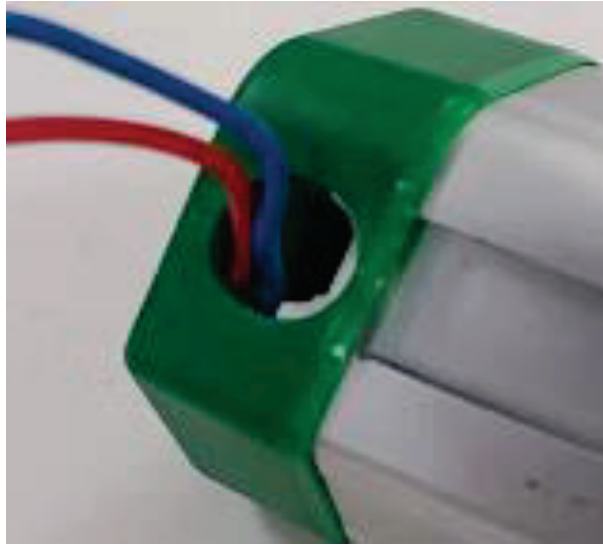


Figure 12. Blackboard light with nominal IP40

In a typical classroom, it was found that the nameplate of the lighting fixture claimed to have a dust and water resistance level of IP40, but in reality, it did not meet the declared dust and water resistance level. At the same time, the wiring was too simple, and the wires were exposed and hung outside, which could easily lead to poor contact of the lighting fixture wires and lead to electric shock accidents.

In the early stage of engineering design, the lighting design drawings should be designed and simulated using professional lighting design software according to the acceptance standards shown in the bidding documents. During the construction phase, the lighting fixtures in the classroom should be installed by professional lighting fixture installation personnel or professional testing personnel. Due to difficult to estimate on-site environmental factors, it is necessary to avoid significant errors between the on-site installation position and the simulated installation position, which may result in significant differences between the actual test results and the simulated results, thereby affecting subsequent acceptance work.

#### **4 CONCLUSION**

Choosing safe and energy-saving lighting products is essential for ensuring high-quality luminous environment of the classroom. It is necessary to conduct sufficient research on on-site environmental facilities and developed a diversified lighting distribution design for complex environmental facilities. In terms of installation, the simulation design must be carried out in advance according to the on-site investigation, and the construction and installation must be strictly carried out according to the specific installation position and angle parameters of the luminaires in the design. After construction, regular cleaning and maintenance of lighting fixtures should be carried out to ensure a sustainable high-quality lighting environment.

Therefore, for different classroom types, by selecting appropriate lighting fixtures, developing reasonable design plans, and optimizing the installation methods of lighting fixtures, a good luminous environment of the classroom should follow four requirements from beginning to end: good lighting fixtures, good design, good installation, and good maintenance. Surrounding the above four requirements, a specific analysis of the problems that can arise during the renovation process is conducted, providing excellent improvement plans and guidance suggestions for the problems that may arise during the classroom lighting renovation work in the Yangtze River Delta region and even the whole country.

## 5 REFERENCES

- [1] CAO Jun, JIA Hailong. Analysis Report on Classroom Lighting in Primary and Secondary Schools [J]. Scientific and Technological Innovation, 2019, 0(21): 26-27
- [2] Li Jiangtao, Sun Fang, He Yonghu, Zhang Zhixin, Miao Zhongcui. Investigation and analysis of classroom lighting and poor eyesight of students in primary and middle schools [J]. Gansu Medical Journal, 2022, 41(8): 748-749 757
- [3] Specification for lighting design of classrooms in primary and middle schools and kindergartens: DB31/T 539—2020 [S].
- [4] Measure methods for lighting: GB/T 5700-2008 [S].
- [5] Hygienic standard for day lighting and artificial lighting for middle and elementary school: GB 7793-2010 [S].
- [6] Standard for lighting design of buildings: GB 50034-2013 [S].
- [7] QIAN Cheng, CHENG Min, CHEN Jianqiu. Testing and Simulation Analysis of UGR at Different Places in Classroom [J]. China Illuminating Engineering Journal, 2020, 31(6): 75-80
- [8] LIN Yandan, QIU Jingjing, LIU Yihong. Research Status and Development on Discomfort Glare [J]. China Illuminating Engineering Journal, 2016, 27(2): 7-13

Corresponding Author Name: Pengpeng GUO

Affiliation: Zhejiang Lierdalux Intelligent Technology Co., Ltd

e-mail: gpp@lierda.com

# **A STUDY ON THE EFFECT OF SOUND AND LIGHT INTERFERENCE ON HUMAN COMFORT IN URBAN NIGHTSCAPES**

Yifei Li, Xiaoxi Liu

( School of Film and Cinematic Arts, Communication University of China, Beijing, China )

## **ABSTRACT**

As the urban nocturnal landscape continues to evolve, certain inadequately designed elements have become sources of pollution. Both sound and light pollution can have significant impacts on individuals' physical and mental well-being in contemporary society. In reality, individuals are exposed to environments where multiple factors interact with one another. However, it remains unclear which of these factors - sound or light - exerts a greater impact on people's comfort levels and whether they interact with each other in an enhancing or inhibiting manner. Therefore, it is crucial to investigate the intricate interplay among these factors.

This paper aims to investigate the impact of audiovisual sensory experiences on individuals' comfort levels, with dynamic light's colour and flicker frequency as well as sound decibel serving as research factors. A quantitative subjective evaluation experiment is conducted to explore the extent of influence that acousto-light complex factors have on people's comfort and to examine the interaction between sound and light. Finally, the study postulates on the impact of various forms of combined stimuli involving dynamic lighting and background noise as opposed to single stimuli, offering insights and recommendations for designing nighttime light environments and controlling pollution.

Keywords: sound-light interference, subjective evaluation experiment, nightscape, flicker frequency, decibel

## **1. INTRODUCTION**

At the same time as the development of urban nocturnal landscape, some unreasonable design has caused serious pollution (light pollution, noise pollution, etc.) to the surrounding environment. In promoting the development of urban nocturnal landscape, it is necessary not only to consider how to better integrate regional culture with digital media art, but also to develop an environmentally friendly night economy without damaging the natural ecological environment. Much of the light pollution that occurs at night is caused by the flickering of coloured light, while noise pollution is often caused by high decibels. Both types of pollution have serious effects on the physical and mental health of people in today's society.

Most of the existing studies on the main factors influencing the nighttime visit experience are from a qualitative perspective and are relatively macroscopic. They focus on the design methods of the nighttime landscape and are mainly based on case studies. However, the night environment is a complex object composed of multiple elements, not only the visual single element will affect the overall feeling of space, the remaining four senses for the comprehensive impact of space should not be ignored, and the sense of hearing has a variety of interaction with vision. It is well known from the literature that an additional visual representation of the sound source can significantly influence the attitude towards it (e.g. Shams L. Kamitani Y Shimojo S et al. 2000[1], Shams L. Kamitani Y Shimojo S et al. 2002[2], Wolfson and Case et al. 2000[3], Kosuke Itoh et al. 2019[4]). Therefore, in outdoor urban landscapes, and even in urban nightscapes, the impact of the interaction of multisensory elements is inevitable and urgent to explore.

The aim of this study is to investigate the interaction effects of sound and light on people, and ultimately to speculate on the perceptual differences induced by different forms of dynamic light and background noise, in order to provide new theoretical underpinnings for further research on the multisensory comfort experience at night. The results of the study will provide guidance and suggestions for the future design and control of nighttime light environments.



## 2. EXPERIMENT

### 2.1 Stimuli

#### 2.1.1 The colour and flicker frequency of dynamic light

In this experiment, an LED screen is used as a simulated dynamic light source, and visual stimuli are presented through pre-made videos. The light colour is red, blue and warm yellow, which are the main light colours of artificial lighting in daily life at night, representing warm light, cool light and warm yellow light, respectively. On the other hand, according to the existing research on dynamic lighting, the dynamic frequency range of flickering dynamic light is limited to 0.5-4Hz[5]. Therefore, four different flicker frequencies were set for each colour, which were 0.5Hz, 1Hz, 2.5Hz and 4Hz from low to high. A total of 12 groups were set after the light stimulus was mixed. To ensure the same surface brightness of the three colour dynamic lights, their brightness was adjusted in Photoshop and measured with a luminance meter in the experimental room. (During the experiment, the surface brightness of the three colours presented through the display is controlled at  $210\text{cd/m}^2$ . As shown in Figure 1.)

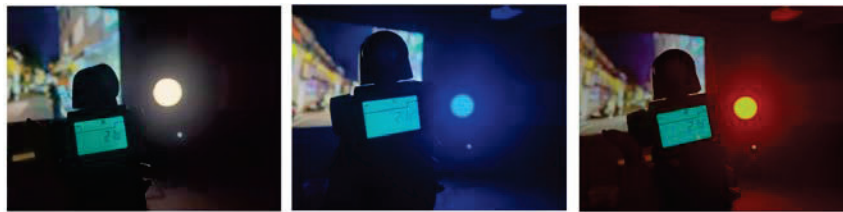


Figure 1. On-site measurement of the surface brightness of three light-coloured light sources (author's own photo)

#### 2.1.2 The loudness level of sound

Most of the sounds involved in urban nightscapes are mostly background sounds and do not exist as the core of the main body. People do not need to pay too much attention to these sounds. Therefore, in this experiment, in order to simulate the ambient sound of the outdoor environment at night, a stereo is chosen for external playback, which is the real noise sampling of the street environment at night.

According to the study of Nicolas Pellerin et al. [6], when people are in an environment of 85dB, they will become very restless and feel seriously uncomfortable at the same time; however, sounds below 55dB do not constitute irritability. Therefore, in this experiment, after considering the hearing safety and emotional state of the subjects, the sound pressure level was chosen above 55dB and below 85dB. Finally, taking into account the total duration of the test and the actual effect, three sound levels were chosen, 55dB, 65dB and 75dB, corresponding to relatively quiet, slightly noisy and very noisy.

#### 2.1.3 Design of test conditions

According to the experimental factors and levels selected above, the acousto-optic stimuli are combined ( $3 \times 4 \times 3$ ) and 36 sets of stimuli were eventually obtained.

## 2.2 Methods

### 2.2.1 Site

This experiment was conducted in the Light Environment Laboratory of Communication University of China in April 2023. The interior size is  $15\text{m} \times 8\text{m} \times 3.5\text{m}$ , movable baffles are installed around the walls, and shading curtains are installed on the windows, which can ensure the dark room environment. The background noise of the detected laboratory is about 45dB, and the noise decibel level set in this experiment is above 55dB, so it will not affect the simulated acoustic environment in the experiment.

For the size, shape and height of the light source displayed on the LED screen, as well as the distance between the subject and the screen, the solid angle was calculated, and the scale comparison between it and the night street presented by the projection was referred to. The

height of the sitting position is 1.2 m, the centre of the light source is ensured on the horizontal line of sight, the seat is placed in a circular arc, and the distance to the LED screen is 3 m. The angle between the screen and the vertical direction of the wall is  $45^\circ$ . Three seats were placed in the centre of the room within the range of the computer monitor. After actual observation, the declination angle between the three seats and the monitor did not exceed  $60^\circ$ , which could ensure a good viewing effect.

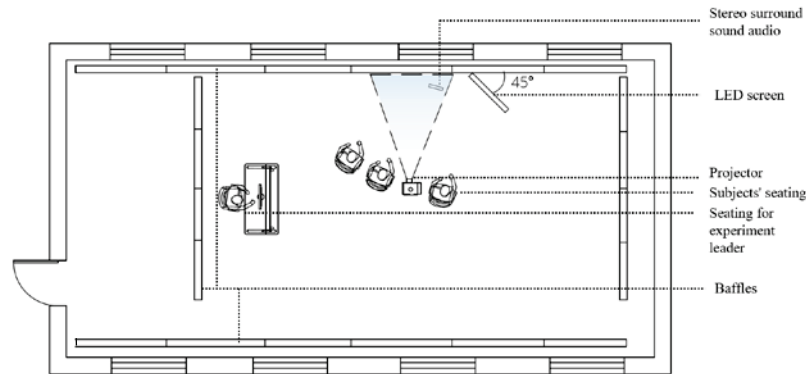


Figure 2. Laboratory layout plan (self-drawn by the author)

The projection scenario simulation was set up to better integrate the subjects into the set scene environment: by playing the photos of the outdoor street at night with depth, taken by the author from a human perspective, the subjects could feel more involved.

The tools used in this period include: (1) computer; (2) noise meter (model UNI-T UT353 BT); (3) luminance meter (model UNI-T UT383 BT); (4) luminance meter (model Shiguang L-758D); (5) projector; (6) LED screen; (7) stereo surround sound audio.

### 2.2.2 Questionnaire design

In order to achieve the expected purpose of this experiment, the method of experimental design and the establishment of evaluation indexes of a large number of related studies were referred to. Considering that this experiment had too many variables and the overall environment was complex, and at the same time, individual judgments were found to be somewhat different in the pre-experiment, a ten-point scoring system of 1-10 was established for this experiment, with smaller numbers representing more comfortable and vice versa uncomfortable. At the same time, in order to unify the scoring criteria, a standard stimulus of 1 point was established, on the basis of which the subjects scored the comfort of the subsequent stimulus groups.

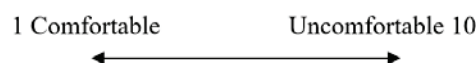


Figure 3. Questionnaire scoring evaluation scale (author's own drawing)

### 2.2.3 Subjects

The experiment was based on the subjective evaluation of the subjects, and 35 students and teachers from Communication University of China were gathered. All the subjects participated voluntarily and had no colour blindness or weakness. The basic information of the subjects is shown in Table 1 and Figure 4 below.

Table 1. Age and gender distribution of subjects (author's own drawing)

			Age range			Total
			11~20	21~30	31~40	
Gender	Female	Count	4	19	1	24
		Percentage of age range	57.1%	73.1%	100.0%	70.6%
	Male	Count	3	7	0	10
		Percentage of age range	42.9%	26.9%	0.0%	29.4%
Total	Count	7	26	1	34	
	Percentage of age range	100.0%	100.0%	100.0%	100.0%	

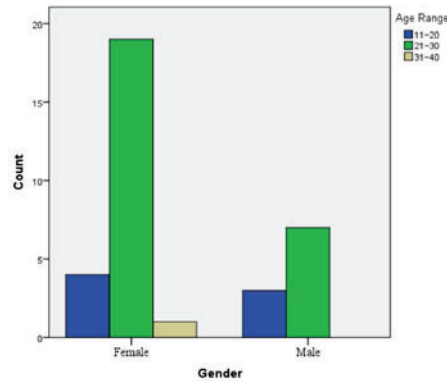


Figure 4. Age and gender distribution of subjects (author's own drawing)

#### 2.2.4 Procedure

The flow of this experiment is shown in the following Figure 5:

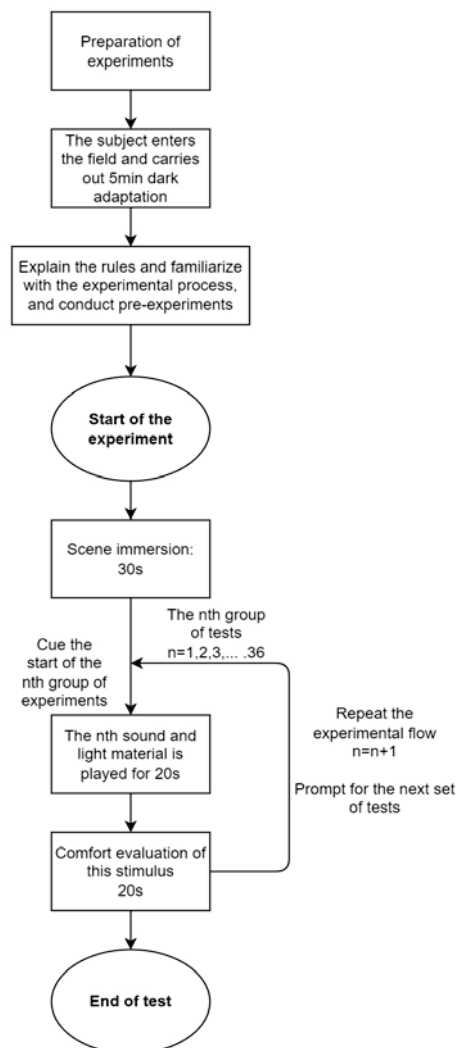


Figure 5 . Experimental flow chart (author's own drawing)

After arriving at the laboratory at the scheduled time, subjects will first undergo a 5-minute dark adaptation session. The pre-experiment will begin after the precautions have been explained, and the formal experiment will begin after the pre-experiment has been completed without objection. Subjects were asked to remain seated throughout the experiment and were not allowed to use electronic devices.

There were 6 sets of acousto-optic stimuli in the pre-experiment and 36 sets of acousto-optic stimuli in the formal experiment. The duration of each group of stimuli was 20 s. After each group of stimuli, the subjects had to score the questionnaire corresponding to the serial number, and the time to answer each serial number was 20s. In the pre-experiment, six sets of acousto-optic stimuli were scored first and will be used as the scoring criteria for the formal session of the experiment: the first stimulus is representative of a 1-point stimulus.

### 3.RESULTS AND DISCUSSION

#### 3.1 Analysis of pre-experimental results

The pre-experiment at the beginning of the formal experiment simulated the procedure of the formal experiment. Subjects were provided with the stimulus of the "1 point" scoring standard while receiving the stimulus of the single element, in order to understand the influence of the single light colour and the single sound loudness on the comfort level, and to provide basic data support for the later formal experiment of the composite factors. After averaging the scores of the 6 stimulus groups, the following Figure 6 is obtained.

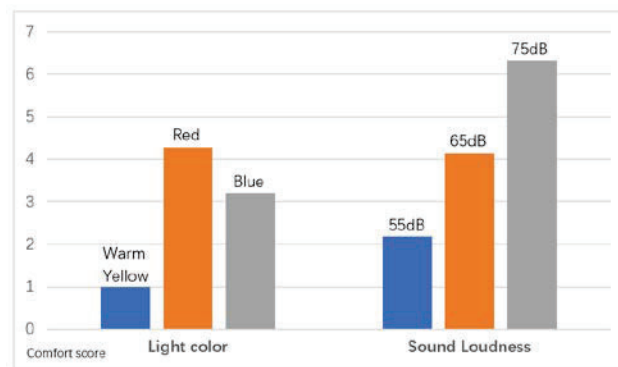


Figure 6. Histogram of the mean of subjects' comfort scores under single-element stimulation (author's own drawing)

According to the figure, it can be clearly seen that for the stimulation of single light colour variables, the subjects' comfort level of warm yellow light is significantly higher than that of coloured light (red light, blue light). Meanwhile, red light has the greatest influence on the comfort level of people, and makes people feel the most uncomfortable under the condition of the same luminous area and surface brightness. As for the influence of sound loudness on human comfort, it follows the general cognition and research, that is, the higher the decibel, the more uncomfortable.

#### 3.2 The significance analysis of the effects of dynamic light colour, flicker frequency and sound decibels on human comfort

In the formal experiment of this study, the score of human comfort under different conditions of sound and light environment was obtained by means of a subjective questionnaire. A total of 35 questionnaires were collected, 34 of which were valid. The reliability analysis is shown in the table below: Cronbach  $\alpha$  coefficient value = 0.976 > 0.8, indicating high reliability.

Table 2. Formal experimental data reliability analysis (author's own drawing)

Cronbach's Alpha	Cronbach's Alpha Based on Standardized Items	N of Items
.976	.979	34

Then, the data of the experiment were sorted out and the single-factor analysis of variance (ANOVA) in SPSS was used to study the correlation of the influence of the three influencing factors on the human comfort level. Then, the significance values of the three factors and the mean value of the comfort score are shown in Table 3:

Table 3. Results of significance analysis of the effects of dynamic light colour, flicker frequency and sound decibels on human comfort (author's own drawing)

	Light		Sound
	Light color	Blinking frequency (Hz)	Decibel (dB)
Significance	.350	.025	.000

According to the results of ANOVA analysis, the correlation significance between light colour and comfort level is  $0.35 > 0.05$ , and comfort level is not significantly affected by light colour. However, the correlation significance between light scintillation frequency and comfort level was 0.025, and the significance of sound decibel was 0.000, both  $< 0.05$ . Therefore, both light scintillation frequency and sound decibel had a significant effect on people's comfort level, and the effect of sound decibel was the most significant.

### 3.3 The variation rule of human comfort level under the interaction of dynamic light and sound

The stimuli in the experiment were grouped and analysed according to light colour and sound loudness, and the mean and standard deviation of each group could be obtained as shown in Table 4.

Table 4. Light colour as a classification method of comfort scoring (author's own drawing)

	Average value	Standard deviation	Number of cases
Warm yellow light	4.983333333	1.3118248180	12
Red light	5.221428571000001	1.338130671	12
Blue light	5.764285714000001	1.345045192	12

	Average value	Standard deviation	Number of cases
55dB	4.211904762000001	.849180186	12
65dB	5.040476190000001	.921196	12
75dB	6.716666667	.7401006133	12

By analysing the data using the light colour classification standard, it can be seen that the subjects' comfort level follows the rule that warm yellow light is more comfortable than coloured light; however, the level of discomfort under blue light is slightly higher than that under red light. Contrary to the experimental results obtained by changing the single light colour, it is speculated that the dynamic light scintillation frequency and pressure level may affect the results.

Using loudness as a classification standard to analyse the data obtained, it can be seen that the change still follows the rule that the higher the decibel, the more uncomfortable, which is consistent with the results obtained by changing the loudness of single sound. It is speculated that the change of decibels in acousto-optical interaction stimuli is the main factor affecting the comfort level of people. This conjecture is consistent with the results of ANOVA analysis above.

### 3.4 The effect of sound-light interaction on human comfort under the influence of different light colours

First, the 36 groups of stimuli were grouped according to the light colour analysis, and the score of each stimulus was averaged to get the following Figure 7.

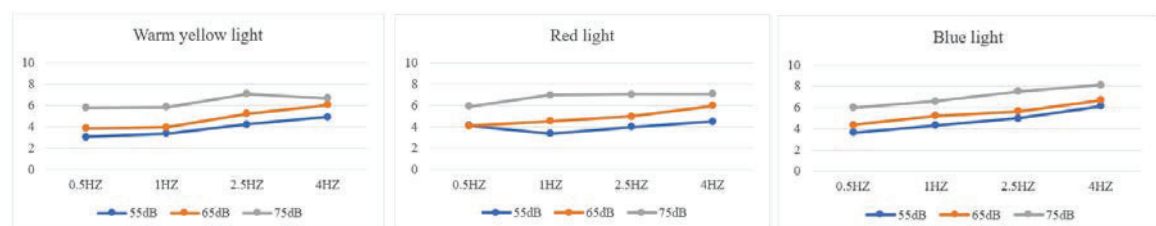


Figure 7. The influence curve of sound and light interaction on human comfort under the influence of different light colours (author's own drawing)



(1) In the blue light condition, the influence of dynamic light scintillation frequency and sound loudness all follows the trend that the higher the scintillation frequency, the higher the sound pressure level and the more uncomfortable.

(2) For red light, the higher the scintillation frequency, the higher the sound pressure level and the more uncomfortable the sound pressure level of 65dB and 75dB followed the trend; however, at 55dB, people are most comfortable when the scintillation frequency is 1Hz. Therefore, when the noise level of the outdoor environment is at a low pressure level of 55dB, red light with a flashing frequency of about 1Hz can be considered for landscape design to improve people's comfort.

(3) Under the condition of warm yellow light, the sound pressure level of 55dB and 65dB follows the trend that the higher the flicker frequency, the higher the sound pressure level, the more uncomfortable; however, under the sound pressure level of 75dB, people were most uncomfortable at the flicker frequency of 2.5Hz, and the discomfort was relieved when the flicker frequency increased to 4Hz. Therefore, if the noise level of the outdoor environment is at the lower pressure level of 75dB, dynamic light with a flicker frequency of 2.5Hz should be avoided in the design.

The obtained data were imported into SPSS to analyse the correlation between dynamic light scintillation frequency and ambient sound pressure level and human comfort, and the significance of mutual influence under the same light colour. The scintillation frequency was numbered as 0.5 Hz-1, 1 Hz-2, 2.5 Hz-3, 4 Hz-4, and the sound pressure level was numbered as 55dB-1, 65dB-2, 75dB-3. Scintillation frequency, sound pressure level and comfort level were all defined as numerical values. Correlation analysis resulted in the following Table 5:

Table 5. Correlation between sound pressure level, dynamic light flicker frequency and comfort under three light colours (author's own drawing)

Warm yellow light					Red light					Blue light				
分列	Pearson Correlation	1	.000	.794**	分列	Pearson Correlation	1	.000	.885**	分列	Pearson Correlation	1	.000	.727**
	Sig. (2-tailed)		1.000	.002		Sig. (2-tailed)		1.000	.000		Sig. (2-tailed)		1.000	.007
N	12	12	12	12	N	12	12	12	12	N	12	12	12	12
闪烁频率	Pearson Correlation	.000	1	.540	闪烁频率	Pearson Correlation	.000	1	.337	闪烁频率	Pearson Correlation	.000	1	.661*
	Sig. (2-tailed)	1.000		.070		Sig. (2-tailed)	1.000		.285		Sig. (2-tailed)	1.000		.019
N	12	12	12	12	N	12	12	12	12	N	12	12	12	12
平均分	Pearson Correlation	.794**	.540	1	平均分	Pearson Correlation	.885**	.337	1	平均分	Pearson Correlation	.727**	.661*	1
	Sig. (2-tailed)	.002	.070			Sig. (2-tailed)	.000	.285			Sig. (2-tailed)	.007	.019	
N	12	12	12	12	N	12	12	12	12	N	12	12	12	12

\*.Correlation is significant at the 0.05 level (2-tailed).

\*\*.Correlation is significant at the 0.01 level (2-tailed).

From the above table, it can be analysed that:

(1) Under the conditions of warm yellow light and red light, the correlation coefficients of the background sound pressure level and the average value of the comfort score are 0.794 and 0.885, and the Sig values (significance test results) are 0.002 and 0.000, indicating that there is a strong and significant positive correlation between the background sound pressure level and the comfort level under these conditions. However, under the warm yellow light and red light conditions, the Sig value (significance test result) of the moving light scintillation frequency and the mean value of the comfort score Therefore, under this article, the correlation between the dynamic light scintillation frequency and the comfort level is not significant, that is, there is no significant correlation between the two. Therefore, when warm yellow light and red light are used in the design, the speed of the flicker frequency will not have a significant effect on the comfort level of the experiencers. More attention should be paid to the setting of the background sound pressure level in the design: to make the experiencers feel more comfortable, the sound pressure level should be reduced.

(2) Under the blue light condition, the correlation coefficient between the background sound pressure level and the average comfort level is 0.727, the correlation coefficient between the dynamic light scintillator frequency and the average comfort level is 0.661, and the sig value (significance test result) is 0.019, indicating that under this condition, there is a highly significant positive correlation between the background sound pressure level and the comfort level and between the dynamic light scintillator frequency and the comfort level. Therefore, when blue light is used in the design, the speed of the flicker frequency and the setting of the background sound

pressure level will have a significant effect on the comfort level of the subjects. Blue light should be chosen with great care in the design.

#### 4.CONCLUSION

This article combines dynamic light colour, flicker frequency and sound pressure level in an experiment to investigate the effect of the interaction of two elements of the three factors on human comfort. The article explores the interaction of the sound and light composite factors through quantitative subjective evaluation experiments, and the following conclusions are drawn from the full study:

(1) Human comfort follows the rule that warm yellow light is more comfortable than coloured light when stimulated by sound and light alone; the higher the sound pressure level, the more uncomfortable it is. Dynamic coloured light brings a different feeling of comfort than static coloured light of the same colour.

(2) Human comfort is not significantly affected by light colour, but light flicker frequency and sound decibels both have a significant effect on human comfort, and the effect of sound decibels is the most significant.

(3) The effect of light colour on human comfort was not as significant as the effect of dynamic light flicker frequency and background sound pressure level in the combined sound and light stimulus conditions. However, separate analysis of the difference between dynamic light flicker frequency and background sound pressure level for each light colour showed that there was a strong positive correlation between background sound pressure level and comfort level in the warm yellow and red light environments, i.e. the higher the sound pressure level, the more uncomfortable it was; however, the correlation between dynamic light flicker frequency and comfort level was not significant, i.e. there was no significant correlation between the two. In contrast, there is a strong positive correlation between dynamic light flicker frequency and background sound pressure level and comfort level in blue light environments.

#### REFERENCES

- [1] Shams L, Kamitani Y, Shimojo S. What you see is what you hear[J]. *Nature*, 2000, 408(6814): 788-788.
- [2] Shams L, Kamitani Y, Shimojo S. Visual illusion induced by sound[J]. *Cognitive brain research*, 2002, 14(1): 147-152.
- [3] Wolfson S, Case G. The effects of sound and colour on responses to a computer game[J]. *Interacting with computers*, 2000, 13(2): 183-192.
- [4] Itoh K, Sakata H, Igarashi H, et al. Automaticity of pitch class-colour synesthesia as revealed by a Stroop-like effect[J]. *Consciousness and Cognition*, 2019, 71: 86-91.
- [5] Wang Yajiang. Experimental study on the intrusion of instantaneous change of coloured luminance to residents from LED advertising screen [D]. *Tianjin University*, 2018, 29. [in Chinese]
- [6] Pellerin N, Candas V. Combined effects of temperature and noise on human discomfort[J]. *Physiology & Behavior*, 2003, 78(1):99-106.

#### ACKNOWLEDGEMENTS

This paper was funded by the project (22YTC025) of Beijing Social Science Foundation Youth Program : Research on the construction of Beijing city night image from the cross-media perspective.

Corresponding Author Name: Yifei Li  
 Affiliation: School of Film and Cinematic Arts, Communication University of China  
 e-mail: 1073418231@qq.com

# DISCUSSION OF THE INFLUENCE OF LIGHT ENVIRONMENT BEFORE BEDTIME ON SLEEP QUALITY BASED ON MULTI-LEVEL POPULATION SURVEY

Kehui Zhao<sup>1</sup>, Ming Liu<sup>1,\*</sup>, Baogang Zhang<sup>2</sup>, Lie Feng<sup>1</sup>, Jiamin Li<sup>1</sup>

(<sup>1</sup> School of Architecture and Fine Art, Dalian University of Technology, Liaoning, China; <sup>2</sup> Faculty of Infrastructure Engineer, Dalian University of Technology)

## ABSTRACT

In contemporary society, the increasing amount of time individuals spend indoors highlights the significance of lighting as a crucial component of the indoor environment. Light affects the physiological rhythm system through the non-visual system of the human body, influencing the secretion of substances such as melatonin, thyroid hormones, cortisol, which in turn impact vital functions. Sleep, being an essential physiological phenomenon for the body, plays a vital role in maintaining individual health, necessitating good sleep quality.

This study aims to investigate and analyze the demographic characteristics, pre-sleep lighting environment, and sleep quality of various dimensions of the population, and to explore the impact of demographic characteristics and pre-sleep lighting environment on sleep quality of the population. A convenient sampling method was employed to select 412 participants from all dimensions of the country in December 2022 through an online platform. The Pittsburgh Sleep Quality Index (PSQI) and the MEQ-5 Chinese version were used to evaluate sleep quality and sleep behaviors. The mean PSQI score of the participants was  $(7.54 \pm 3.597)$  points, and the average sleep duration was 7 hours. The differences in PSQI scores among gender, age, education level, occupation category, work pressure, living status, and time spent using electronic devices in a dark environment were statistically significant ( $P < 0.05$ ). The MEQ-5 score was  $(14.42 \pm 2.545)$  points, and the majority of the population belonged to the intermediate type, while the morning and evening types coexisted. The differences in MEQ-5 scores among age, occupation category, time spent using electronic devices in a dark environment, and whether the lighting environment affects sleep were statistically significant ( $P < 0.05$ ). In conclusion, the pre-sleep lighting environment (time spent using electronic devices in a dark environment) has a significant impact on sleep quality and sleep behavior evaluation. Differentiated and targeted health measures for pre-sleep lighting should be taken into account to improve sleep quality.

**Keywords:** Sleep quality, Sleep health, Pre-sleep Lighting environment, Demographic characteristic

## 1. INTRODUCTION

Sleep, as a highly conserved life phenomenon, is intricately related to biological evolution, species reproduction, and individual survival and development. The brain's function during sleep plays a crucial role in normal life activities and major diseases. Consistently sleeping less than 6-7 hours per night can compromise the immune system and more than double the risk of developing cancer. Sleep disorders can exacerbate mental illnesses such as depression, anxiety and suicidal tendencies, and insufficient sleep can even lead to weight gain. In recent years, the average daily sleep duration of Chinese residents has been progressively decreasing, accompanied by a decline in sleep quality and an increase in the prevalence of sleep disorders. Sleep problems such as forced staying up late, sleeplessness, and poor sleep have become common. According to the "China Sleep Research Report (2022)"<sup>[1]</sup>, in the past 10 years, China's per capita sleep duration has been reduced from 8.5 hours in 2012 to 7.06 hours in 2021, sleep duration has been significantly reduced, and the delay in falling asleep is serious.

## 2. OBJECTS AND METHODS

### 2.1 Object

In December 2022, the respondents were selected as the research subjects using a convenience sampling method through an online platform, ensuring representation from diverse dimensions across the country. Prior to distributing the questionnaire, the purpose of the survey and the instructions for completing it were explained to the participants. and 412 valid questionnaires were collected. The survey population was characterized by a high degree of randomness, thereby ensuring the survey's relevance and universal significance.

## 2.2 Methods

### 2.2.1 Pittsburgh Sleep Quality Survey

Pittsburgh Sleep Quality Index ( PSQI ) was used to evaluate the sleep quality of the subjects. The internal consistency coefficient of PSQI was 0.842, and the reliability and validity were good, which met the purpose of the survey. PSQI consists of 19 self-evaluation items and 5 other-evaluation items, of which the 19th self-evaluation item and the 5 other-evaluation items are not involved in the scoring. The 18 self-assessment items involved in the scoring were composed of 7 components, which were subjective sleep quality, Fall-sleep time, Sleep duration, sleep disorder, sleep efficiency, the application of hypnotic drugs and the impact on daytime function. Each component was scored according to the 0-3 score level, and the cumulative score of each component was calculated as the PSQI total score, ranging from 0 to 21. The higher the score, the worse the sleep quality. <sup>[2]</sup>. In this study, PSQI score of 0-5 indicates good sleep quality, 6-10 indicates good sleep quality, 11-15 indicates general sleep quality, and 16-21 indicates poor sleep quality. Sleep disorders: The total score of the Pittsburgh Sleep Quality Index is more than 8 points, suggesting that there is sleep disorder. The higher the score, the more serious the sleep disorder <sup>[3]</sup>.

### 2.2.2 Morning and Night Scale- MEQ-5 Chinese version

The Chinese version of MEQ-5 consists of five items ( item 1, 7, 10, 18, 19 ) of the Chinese version of MEQ-19, and the total score of MEQ-5 ranges from 5 to 25 points. The demarcation proposed by Adan and Almirall : 5-7 is absolute night type ; 8-11 is divided into moderate night type ; 12-17 is divided into intermediate type ; 18-21 is divided into moderate morning type ; 22-25 is divided into absolute morning type <sup>[4]</sup>.

### 2.2.3 Statistical Methods

SPSS26.0 software was adopted to establish a database and input data, and mean process,  $\chi^2$  test, t test and variance analysis were performed.  $P < 0.05$  was considered statistically significant.

### 2.2.4 Quality control

At the beginning of the questionnaire, the intention and purpose of the questionnaire are described in text to help the people who fill in the questionnaire better understand the intention of the questionnaire. In the questionnaire questions, the filling methods and filling requirements are stipulated, and the explanation is added to the objection questions. After the questionnaire was recovered, the investigators conducted self-examination and mutual examination; data entry ensures double repeated entry.

## 3 RESULTS

### 3.1 Demographic characteristics of respondents

Table 3-1 shows that the sex ratio of the respondents was 1.57: 1, and women were more than men. Mainly for young and middle-aged groups, 20-40 years old accounted for 48.8 %, 40-60 years old accounted for 48.3 %; The proportion of warm light and cold light in bedtime lighting environment was 35.7 % and 64.3 % respectively. The proportion of people sleeping with lights on was 7.3 %; 64.4 % of people will use electronic products in a dark environment within one hour, and one third of people will use electronic products in a dark environment for more than one hour; The number of people with sleep disorders accounted for 36.2 % of the total. It can be seen from Figure 3-1 that education and the use of electronic products in the dark environment have a significant correlation with the frequency of sleep disorders.

Table 3- 1 The demographic characteristics and composition ratio of the respondents

Feature	classification	Frequency	Constituent ratio (%)	Frequency of sleep disorders	Characteristic proportion (%)
Gender	Males	252	61.2	109	43.3
	Female	160	38.8	40	25.0
Age	Under 20 years old	4	1.0	2	50.0
	21-30 years old	116	28.2	25	21.6
	31-40 years old	85	20.6	43	50.6
	41-50 years old	77	18.7	36	46.8
	51-60 years old	122	29.6	41	33.6
	Over 61 years old	8	1.9	2	25.0
Educational	Junior high school and below	10	2.4	6	60.0

<b>background</b>	Senior high	60	14.6	25	41.7
	University	252	61.2	100	39.7
	Postgraduate	85	20.6	18	21.2
	Doctoral students	5	1.2	0	0
	Mental work	151	36.7	51	33.8
<b>Occupation type</b>	Physical labour	46	11.2	28	60.9
	Mental and physical work	129	31.3	54	41.9
	Student	64	15.5	10	15.6
	Retire	22	5.3	6	27.3
	No pressure	44	10.7	9	20.5
<b>Working pressure</b>	Pressure is relatively small	123	29.9	38	30.9
	More stressful	186	45.1	63	33.9
	The pressure is very high	59	14.3	39	66.1
<b>Pre-sleep Lighting environment</b>	Cold colour tone (white light)	147	35.7	44	29.9
	Warm colour tone (yellow light)	265	64.3	105	39.6
<b>Turn on the lights to sleep</b>	Yes	30	7.3	12	40.0
	No	382	92.7	137	35.9
<b>Time of using electronic devices in dark environments</b>	0-0.5h	163	39.6	46	28.2
	0.5-1h	102	24.8	29	28.4
	1-1.5h	56	13.6	25	44.6
	1.5-2h	51	12.4	31	60.8
	≥2h	40	9.7	18	45.0
<b>Believed that light has an effect on sleep.</b>	Yes	370	89.8	133	35.9
	No	420	10.2	16	38.1
<b>Living conditions</b>	No pressure	49	11.9	12	24.5
	Pressure is relatively small	144	35.0	35	24.3
	More stressful	167	40.5	66	39.5
	The pressure is very high	52	12.6	36	69.2
<b>Total</b>				149	36.2

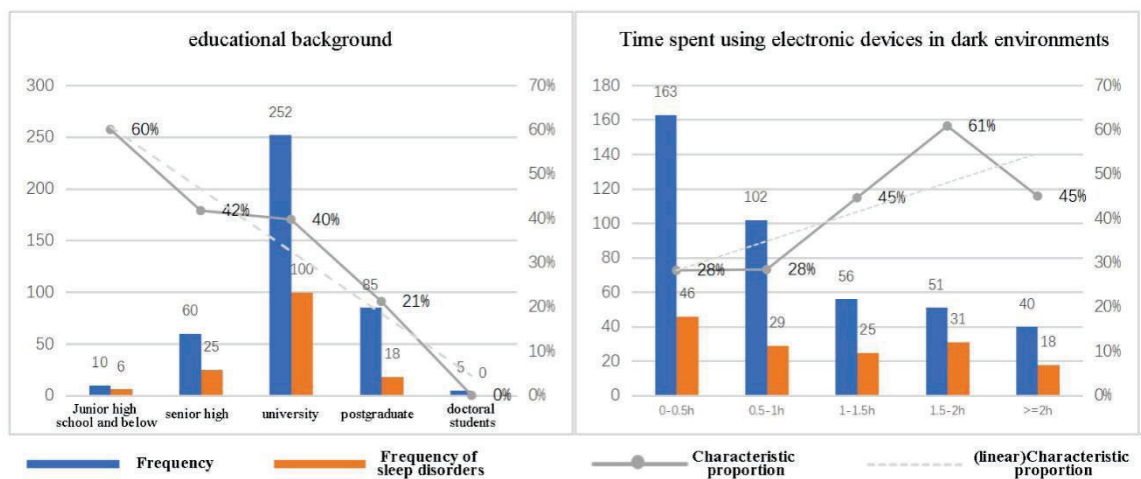


Figure 3-1 Trends in academic qualifications and time characteristics of using electronic devices in dark environments

### 3.2 Analysis of the status quo of sleep quality in the population

Table 3-2 shows that the mean score of sleep quality is 0.99 ( good sleep quality ), the mean score of Sleep duration is 1.45 ( sleep time is about 7 hours ), the mean score of sleep efficiency is 0.80 ( sleep efficiency is about 80 % ), the mean score of PSQI is 7.54 ( good sleep quality ), and the mean score of MEQ-5 is 14.42 ( intermediate type ).

Table 3-2 Analysis of sleep quality in population



Sleep dimension	Frequency	Minimum value	Maximum value	Mean value(E)	Standard deviation
Sleep quality	412	0	3	0.99	0.743
Fall-sleep time	412	0	3	1.45	0.933
Sleep duration	412	0	3	1.62	1.253
Sleep efficiency	411	0	3	0.80	1.059
Sleep disorders	412	0	3	1.21	0.603
Hypnotic drugs	412	0	3	0.11	0.447
Daytime dysfunction	412	0	3	1.37	0.971
PSQI score results	411	0	20	7.54	3.597
MEQ-5 score results	412	5	21	14.42	2.545

Table 3-3 presents a comparison of different demographic characteristics with PSQI score and MEQ-5 score. Regarding the PSQI score, female sleep is better than male sleep. The PSQI score index of the 31-40 age group was the highest, and the sleep quality was worse than other age groups. The higher the education, the lower the score, the better the sleep quality. In the occupational category, the physical labor score was the highest, followed by mental and physical labor, mental labor, retirement and students, and the student group had the best sleep quality compared with other groups. In terms of work pressure and living conditions, the greater the pressure, the higher the score, the worse the quality of sleep. Among them, gender, age, education, occupational category, work pressure and living status had statistically significant differences in PSQI scores (  $P < 0.05$  ). In the MEQ-5 score, the older the age group, the higher the MEQ-5 score index, and the closer to the morning type ; in the occupational category, the middle school students tend to be moderate night type, and the retirement group tends to be moderate morning type. Among them, there were statistically significant differences in MEQ-5 scores between age and occupational category (  $P < 0.05$  ). However, there was no significant difference in gender, education, work pressure and living status.

Table 3-3 Differences between different demographic characteristics and PSQI score and MEQ-5 score

demographic characteristic	classification	PSQI			MEQ-5		
		Mean $\pm$ Standard Deviation	T or F value	P value	Mean $\pm$ Standard Deviation	T or F value	P value
Gender	Males	8.11 $\pm$ 3.586	4.095	<0.01**	14.55 $\pm$ 2.500	1.230	0.219
	Female	6.65 $\pm$ 3.439			14.23 $\pm$ 2.612		
	Under 20 years old	7.50 $\pm$ 4.796			12.75 $\pm$ 3.775		
Age	21-30 years old	6.45 $\pm$ 3.215	4.023	<0.01**	13.38 $\pm$ 2.248	8.903	<0.01**
	31-40 years old	8.52 $\pm$ 3.548			14.41 $\pm$ 2.362		
	41-50 years old	8.13 $\pm$ 3.679			14.65 $\pm$ 2.437		
	51-60 years old	7.59 $\pm$ 3.653			15.17 $\pm$ 2.634		
	Over 61 years old	6.38 $\pm$ 3.204			17.00 $\pm$ 1.512		
Educational background	Junior high school and below	8.70 $\pm$ 4.644	3.912	<0.01**	13.90 $\pm$ 4.012	2.069	0.084
	Senior high	7.93 $\pm$ 3.560			14.98 $\pm$ 2.678		
	University	7.83 $\pm$ 3.710			14.52 $\pm$ 2.514		
	Postgraduate	6.51 $\pm$ 2.864			13.87 $\pm$ 2.277		
	Doctoral students	4.00 $\pm$ 2.915			13.60 $\pm$ 2.191		
Occupation type	Mental work	7.17 $\pm$ 3.471	7.628	<0.01**	14.89 $\pm$ 2.171	8.613	<0.01**
	Physical labour	9.33 $\pm$ 4.397			14.11 $\pm$ 3.261		
	Mental and physical work	8.17 $\pm$ 3.496			14.26 $\pm$ 2.602		
	Student	6.02 $\pm$ 2.780			13.25 $\pm$ 2.233		
	Retire	7.18 $\pm$ 3.217			16.32 $\pm$ 2.056		
Working pressure	No pressure	5.93 $\pm$ 3.500	12.018	<0.01**	14.89 $\pm$ 3.127	2.157	0.093
	Pressure is relatively small	7.01 $\pm$ 3.522			14.55 $\pm$ 2.218		
	More stressful	7.59 $\pm$ 3.289			14.46 $\pm$ 2.430		
	The pressure is very high	9.73 $\pm$ 3.814			13.71 $\pm$ 2.960		
Living conditions	No pressure	6.18 $\pm$ 3.946	12.512	<0.01**	14.49 $\pm$ 3.373	0.413	0.744
	Pressure is relatively small	6.81 $\pm$ 2.978			14.49 $\pm$ 2.415		
	More stressful	7.87 $\pm$ 3.511			14.47 $\pm$ 2.315		

The pressure is very high	9.79±3.977	14.06±2.747
---------------------------	------------	-------------

Note : \* indicates the difference at the significance level of 0.05, \*\* indicates the difference at the significance level of 0.01.

Table 3-4 compares different bedtime lighting environments with PSQI scores and MEQ-5 scores. In the PSQI score, the time of using electronic devices in the dark environment increases with the time of use within two hours. The longer the sleep quality is worse, the time of using electronic devices in the dark environment has a statistically significant difference in PSQI scores (  $P < 0.05$  ). In the MEQ-5 score, the light-on sleep was closer to the morning type than the non-light-on sleep ; the time of using electronic devices in the dark environment increased with the time of use within two hours, and the longer the use, the closer to the morning type ; the group that believes that the light environment has an impact on sleep is closer to the early morning type. There were significant differences in MEQ-5 scores between the time of using electronic equipment in dark environment and whether the effect of light environment on sleep was considered (  $P < 0.05$  ).

Table 3-4 Differences between different bedtime lighting environments and PSQI scores and MEQ-5 scores

Bedtime lighting environment	classification	PSQI			MEQ-5		
		Mean ± Standard Deviation	T or F value	P value	Mean ± Standard Deviation	T or F value	P value
Pre-sleep Lighting environment	Cold colour tone (white light)	7.18±3.533	-1.516	0.130	14.17±2.503	-1.525	0.128
	Warm colour tone (yellow light)	7.74±3.623			14.57±2.562		
Turn on the lights to sleep	Yes	7.63±3.810	0.142	0.887	13.53±3.071	-1.999	0.046*
	No	7.54±3.584			14.49±2.491		
Time of using electronic devices in dark environments	0-0.5h	6.90±3.593	7.187	<0.01**	15.04±2.280	4.579	<0.01**
	0.5-1h	7.00±3.221			14.27±2.442		
	1-1.5h	8.39±3.268			13.75±2.322		
	1.5-2h	9.57±3.910			13.78±3.061		
	≥2h	7.80±3.488			14.08±2.947		
Believed that light has an effect on sleep.	Yes	7.53±3.570	-0.188	0.851	14.55±2.454	3.026	<0.01**
	No	7.64±3.869			13.31±3.056		

Note : \* indicates the difference at the significance level of 0.05, \*\* indicates the difference at the significance level of 0.01.

### 3.3 Correlation analysis of different demographic characteristics and bedtime lighting environment and sleep quality

From Table 3-5, it can be seen that the PSQI score is significantly correlated with gender, education, work pressure and living conditions, and the MEQ-5 score is significantly correlated with age, education and work pressure.

Table 3-5 Correlation between different demographic characteristics and PSQI and MEQ-5 scores.

	PSQI score	MEQ-5 score	Gender	Age	Educational background	Occupation type	Working pressure	Living conditions
PSQI score	1							
MEQ-5 score	-0.076	1						
Gender	-0.198**	-0.061	1					
Age	0.082	0.301**	-0.289**	1				
Educational background	-0.163**	-0.106*	0.185**	-0.510**	1			
Occupation type	-0.043	-0.088	0.181**	-0.134**	0.084	1		
Working pressure	0.266**	-0.110*	-0.174**	-0.193**	0.046	-0.138**	1	
Living conditions	0.279**	-0.038	-0.077	-0.218**	0.044	-0.124*	0.745**	1

Note : \* indicates the difference at the significance level of 0.05, \*\* indicates the difference at the significance level of 0.01.

It can be seen from Table 3-6 that the PSQI score is significantly positively correlated with the time of using electronic equipment in the dark environment, and the MEQ-5 score is significantly correlated with whether the light is on, the time of using electronic equipment in the dark environment and whether the light environment has an effect on sleep.

Table 3-6 Correlation between different bedtime lighting environments and PSQI and MEQ-5 scores

	PSQI score	MEQ-5 score	Pre-sleep Lighting environment	Turn on the lights to sleep	Time of using electronic devices in dark environments	Believed that light has an effect on sleep.
<b>PSQI score</b>	1					
<b>MEQ-5 score</b>	-0.076	1				
<b>Pre-sleep Lighting environment</b>	0.075	0.075	1			
<b>Turn on the lights to sleep</b>	-0.007	0.098*	-0.072	1		
<b>Time of using electronic devices in dark environments</b>	0.195**	-0.173**	-0.007	0.051	1	
<b>Believed that light has an effect on sleep.</b>	0.009	-0.148**	0	-0.183**	0.138**	1

Note : \* indicates the difference at the significance level of 0.05, \*\* indicates the difference at the significance level of 0.01.

### 3.4 Differences and correlation analysis between the time of using electronic devices in dark environment and the scores of sleep dimensions

Table 3-7 compares the time of using electronic devices in different dark environments with the scores of various sleep dimensions. Among them, except for the MEQ-5 score, the lower the score of each sleep dimension is, the better. In terms of sleep quality, Fall-sleep time, and daytime dysfunction, the score of time less than 2 hours is positively correlated with the time of use ; in terms of Sleep duration and sleep efficiency, the score of time greater than 0.5 h was positively correlated with the time of use ; no obvious rules were found in sleep disorders and hypnotic drugs.

Table 3-7 Differences between the time of using electronic devices in dark environment and the scores of sleep dimensions

Time of using electronic devices in dark environments	Sleep quality	Fall-sleep time	Sleep duration	Sleep efficiency	Sleep disorders	Hypnotic drugs	Daytime dysfunction
0-0.5h	0.82±0.728	1.26±0.900	1.55±1.248	0.87±1.072	1.20±0.565	0.05±0.310	1.15±0.913
0.5-1h	1.01±0.738	1.41±0.848	1.37±1.202	0.60±0.967	1.13±0.520	0.13±0.520	1.35±0.886
1-1.5h	1.13±0.470	1.66±0.880	1.79±1.232	0.75±0.995	1.43±0.657	0.09±0.345	1.55±1.043
1.5-2h	1.29±0.901	1.96±0.894	1.90±1.269	0.88±1.177	1.37±0.747	0.31±0.735	1.84±1.084
2h	1.02±0.768	1.43±1.130	1.93±1.309	0.95±1.131	1.00±0.555	0.08±0.267	1.40±0.928
<b>Total</b>	0.99±0.743	1.45±0.933	1.62±1.253	0.80±1.059	1.21±0.603	0.11±0.447	1.37±0.971

Table 3-8 shows that the time of using electronic equipment in dark environment is significantly positively correlated with sleep quality, sleep time, sleep time, hypnotic drugs and daytime dysfunction.

Table 3-8 The correlation between the time of using electronic devices in dark environment and the scores of sleep dimensions

	Time of using electronic devices in dark environments	Sleep quality	Fall-sleep time	Sleep duration	Sleep efficiency	Sleep disorders	Hypnotic drugs	Daytime dysfunction
Time of using electronic devices in dark environments	1							
Sleep quality	0.171**	1						
Fall-sleep time	0.177**	0.485**	1					
Sleep duration	0.125*	0.217**	0.101*	1				

Sleep efficiency	0.021	0.161**	0.192**	0.542**	1			
Sleep disorders	0.016	0.386**	0.290**	0.135**	0.122*	1		
Hypnotic drugs	0.102*	0.231**	0.126*	0.114*	0.171**	0.275**	1	
Daytime dysfunction	0.181**	0.525**	0.339**	0.114*	0.011	0.361**	0.121*	1

Note : \* indicates the difference at the significance level of 0.05, \*\* indicates the difference at the significance level of 0.01.

#### 4 DISCUSSIONS

Through the utilization of PSQI scale survey, this study provides insights into the overall sleep status of various individuals across the country. According to the content of the scale, the scoring criteria and the results of this study, the average sleep duration of the population in this study was 7 hours, which was in line with the trend of the " China Sleep Research Report ( 2022 )" report. <sup>[1]</sup> The results of this study found that the average score of the sleep PSQI scale of the population surveyed was ( 7.54 ± 3.597 ) points, of which 149 people ( 63.8 % ) scored more than 8 points, suggesting that there were sleep quality problems. The total score of the MEQ-5 scale showed a normal distribution among 412 subjects, which reflected the objective distribution of circadian rhythm types, that is, most of the population belonged to the intermediate type, but the morning type and the night type coexisted.

Among the demographic characteristics, the number of sleep disorders in the 31-40 age group reached 50 %, and the PSQI score was also the highest compared to other age groups, which was the main group that needed to pay attention to adjusting sleep quality ; in terms of academic qualifications, the higher the academic qualifications, the lower the proportion of people with sleep disorders, and the lower the PSQI score, the better the sleep quality, which indirectly proves that improving academic qualifications helps to improve sleep quality ;In the occupational category, the number of people with sleep disorders in the manual labor group reached 60.9 %, and the PSQI score was also higher than other work categories. The number of students with sleep disorders was the least, and the sleep quality was the best. The less pressure on work pressure and life pressure, the fewer the number of sleep disorders, the better the quality of sleep. Young and middle-aged people generally live and work under great pressure. They face a small situation in the family. There is also competition for promotion at work. How to balance health under pressure is also a problem that needs to be paid attention to. Therefore, based on the above, we can preliminarily infer that the portrait of people with better sleep quality is a female group with a high degree of mental work and a short time of using electronic equipment in a dark environment. The poor sleep quality group portrait is a group of men with low education engaged in manual labor and long time using electronic equipment in dark environment.

Before going to bed, the time of using electronic equipment in the dark environment had different degrees of influence on the seven dimensions of sleep, among which the number of sleep disorders in 1.5-2h reached 60.8 %, and the PSQI score was the highest and the sleep quality was the worst. Bedtime entertainment is also an important factor affecting people 's sleep quality. With the popularity of the Internet and the widespread use of smart phones, people generally sleep late, and the phenomenon of staying up late for entertainment is very common, which directly affects physical health and work efficiency. Multivariate logistic analysis of sleep quality showed that the factors affecting people 's sleep quality included gender, educational background, work pressure, Living conditions and the time of using electronic equipment in the dark environment, which were the direct factors affecting sleep quality and must be targeted intervention.

This study also has some limitations to further investigate. First, the study uses cross-sectional data, so causality cannot be established; secondly, this study adopts the network platform convenience sampling method. Although it can widely collect national data, teenagers and the elderly receive less data due to the low popularity of the network. Therefore, the conclusions of this article are more suitable for young and middle-aged groups. Finally, in order to ensure complete anonymity in this study, there is no sample territory in the questionnaire, which limits the comparison between different regions.

#### 5 PROSPECT

In recent years, the rapid advancement of intelligent control technology and the deepening research on the influence of light on the human body and mind have propelled the

development of the light environment beyond its original visual function. It now encompasses various aspects related to sleep, emotion, cognition, and rhythm, leading to the emergence of dynamic lighting. This entails adjusting the spectrum and intensity of lighting based on user behavior and time to create a safe, comfortable, and healthy lighting environment.

When designing lighting sources, it is crucial not only to control the energy of harmful bands such as infrared and ultraviolet but also to consider their impact on the human body's rhythm. This consideration enables lighting to actively contribute to sleep quality, emotional regulation, and other physiological functions.

The influence of light environment on sleep is intricate and multifaceted. Exploring a healthy light environment not only involves the field of construction engineering, but also encompasses disciplines such as medicine, psychology, behavior science and mathematics. Besides the retina, there are photoreceptors in the human body, including those present in the skin. Therefore, further research is needed to determine how to adjust the light environment parameters to ensure the mental health and improve sleep quality. It is also a further move towards the green and healthy development of the country.

The objective of this research is to investigate the relationship between light environment and sleep quality, as well as the relationship between light, human health and mood under different circumstances. To address the diverse requirements of different user groups and different scenarios, an intelligent light control system is established. By enhancing the light environment, the user's physiological rhythm can be indirectly adjusted, thereby improving sleep quality, overall health, mood and memory. The intelligent light control system will be designed and developed accordingly. Different light sources will be tailored to accommodate various usage habits, dynamically adjusting the spectral brightness and composition of each band. This approach aims to provide users with a positive impact on sleep, mood, and overall well-being, ultimately realizing an intelligent optimization design scheme for a healthy light environment.

## REFERENCES

- [1] Yangyang Liu, Junxiu Wang & Heng Zhang, Chinese Sleep Research Report 2022, 2022: Beijing.
- [2] Ling Guo, Improving people's sleep quality should become a 'livelihood project'. Insight China, 2022(15): 30-31.
- [3] Jie Yang, Correlation Between Traditional Chinese Medicine Constitution and Sleep Quality Among Medical Students. Journal of Anhui University of Chinese Medicine, 2019. 38(06): 16-20.
- [4] Adan and H. Almirall, Horne & "stberg morningness-eveningness questionnaire: A reduced scale. Personality and Individual Differences, 1991.

## ACKNOWLEDGEMENTS

Declaration of Competing Interest. The authors declare no conflict of interest. This research was funded by The National Natural Science Foundation of China, grant number 52178067.

Corresponding Author: Ming Liu

Affiliation: School of Architecture and Art, Dalian University of Technology

e-mail : liumingyitj@163.com



# DEVELOPMENT OF A LIGHTING CONTROL AND CONDITION MONITORING SYSTEM

Yumi Hayashi, Tatsuya Nagai, Hiroki Okamoto, Kazuki Fujimoto

(SEIWA ELECTRIC MFG.CO.,LTD, Kyoto, Japan)

## ABSTRACT

Industrial lighting equipment installed in expansive and dangerous areas regularly requires time-consuming service and maintenance. The lighting control and condition monitoring system developed in this study enables the remote monitoring of equipment status (leakage current value, life of lighting equipment, etc.) measured by the lighting equipment itself. Furthermore, it enables the dimming control of the lighting equipment. Accordingly, an operator can remotely identify malfunctioning equipment and determine the status of the lighting equipment. This prevents accidents in dangerous areas and simplifies system inspection. Additionally, this system reduces energy consumption by facilitating minute lighting control.

Keywords: lighting control, condition monitoring, accident prevention, simplification of inspection, energy saving

## 1. INTRODUCTION

Many pieces of industrial lighting equipment ("lighting equipment" hereafter) are installed in factories. This lighting equipment is installed in various locations, including high and dangerous areas, and workers must visit the site in person to check whether the lighting equipment is on or off. This form of servicing and maintaining lighting equipment consumes a significant amount of time. Furthermore, leakage current is typically checked in individual circuits to which multiple pieces of lighting equipment are connected. If an abnormal value is detected, the worker must then check the wiring for each piece of lighting equipment. Therefore, time is consumed in identifying which lighting equipment is causing the problem.

Work sites and other locations continue to be automated to minimize the number of workers required, and companies are under constant pressure to streamline their work. Additionally, awareness is increasing in the field of factory management to transition to so-called smart factories. Innovative technologies such as Internet of Things (IoT) and Artificial Intelligence (AI) are expected to streamline workflow and reduce energy consumption.

To address these requirements, we are developing a system capable of remotely monitoring the conditions of lighting equipment, with the aim of streamlining maintenance work. By developing this lighting control and condition monitoring system, we aim to significantly reduce the time and effort required to service and maintain lighting equipment and make factory management more efficient.

## 2. SYSTEM OVERVIEW

### 2.1. SYSTEM CONFIGURATION

The lighting control and condition monitoring system consists of lighting equipment, a base unit, a server, a Web application, and an operation terminal. The lighting equipment is connected to a network and operated using a Web application. The configuration of this system is shown in Figure 1. The system is administered and managed from a server on the network. The system application is installed on the server. This application is used to control the lighting equipment and record condition monitoring data. The application is operated using a Web browser from the operation terminal (personal computer [PC] or tablet computer) connected to the system network.

The lighting equipment in this system consists of control, power supply, and light source sections. The control section contains a control board, which includes an antenna for wireless communication and a control circuit. Lighting equipment is dimmed through Pulse Width Modulation (PWM) control, based on control commands received from the server. The lighting equipment and the base unit are capable of wireless communication in the 920-MHz band and connect wirelessly to form a network. The base unit can communicate over Wi-Fi and serves as the gateway connecting the network formed by the lighting equipment with the network of the server. The system communicates wirelessly, eliminating the necessity to install control lines or other wiring, and enabling layout changes to be made during or after installation.

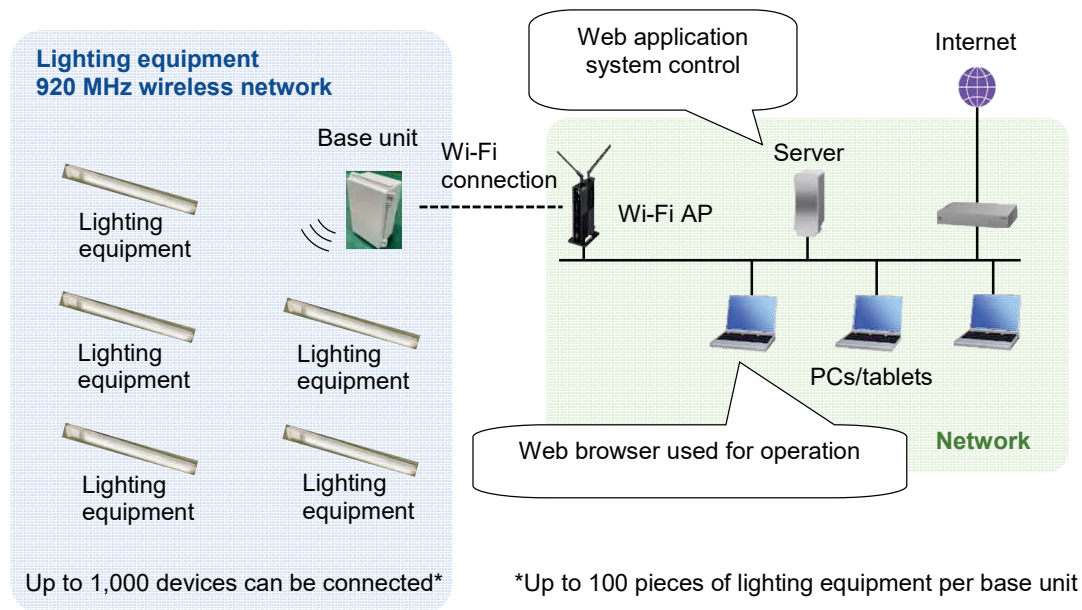


Figure 1. System configuration

## 2.2. FUNCTIONS

This section describes lighting control and condition monitoring, which are the major functions provided by the lighting control and condition monitoring system.

The lighting control function enables lighting equipment to be remotely turned on/off or dimmed through the use of an application. Figure 2 shows the control mechanism. When lighting control is performed, control commands are sent through the base unit to applicable lighting equipment. Lighting equipment dimming is performed by receiving these control commands. Lighting equipment can be controlled individually, together (such as controlling all lighting equipment on a particular floor), or separated into groups of multiple pieces of lighting equipment. This facilitates different types of lighting control. Some examples include turning off lighting equipment for idle production lines or dimming lighting equipment near windows during the day. The lighting control application can also be used to check the lighting status of lighting equipment in real time, as shown in Figure 3. This enables workers to check the lighting status of lighting equipment without requiring them to visit the site in person.

In addition to manual control, lighting control can be performed automatically on a schedule (scheduled control). Scheduled control enables users to set time slots and actions, with control performed automatically according to these settings. Actions can be repeated on certain days of the week or performed on specific days, enabling users to set different usage patterns during the week and on holidays (Figure 4). Scheduled control can be used to ensure that lighting equipment is turned off when not in use and can make it easier to turn lighting equipment on when needed.

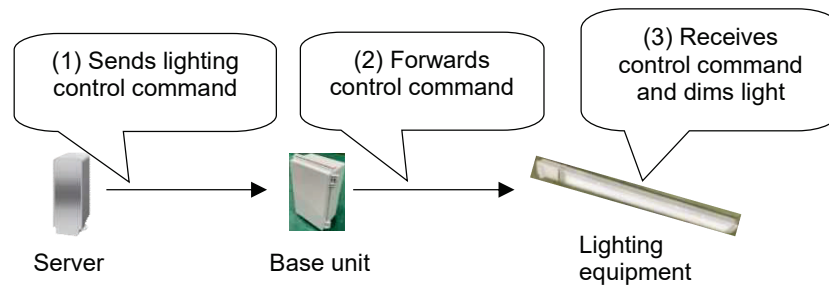


Figure 2. Lighting control



Figure 3. Lighting control operation screen

Figure 4. Schedule configuration screen

The condition monitoring function enables the condition measured for lighting equipment to be remotely viewed using an application. Specifically, it can be used to detect lighting equipment that cannot be turned on and to check leakage current values, cumulative lighting time, lighting equipment temperature, lighting equipment lighting status, and signal strength. Figure 5 shows the method of obtaining condition monitoring data. The base unit periodically sends commands to obtain data from the lighting equipment. When the lighting equipment receives this command, it returns the condition monitoring data to the base unit. The base unit then forwards the data received from the lighting equipment to the server. Data obtained by the server is shown as a list in the application, as shown in Figure 6. An alert is displayed if lighting equipment cannot turn on, or if data exceeds a preset threshold. This enables lighting equipment defects to be discovered without having to visit the site in person. Alerts are shown for each piece of lighting equipment, making it easy to identify defects.

Condition monitoring data is also stored on the server at regular intervals. This data can be used to display a graph, such as that shown in Figure 7. These graphs can be used to identify lighting equipment trends and estimate when lighting equipment should be replaced.

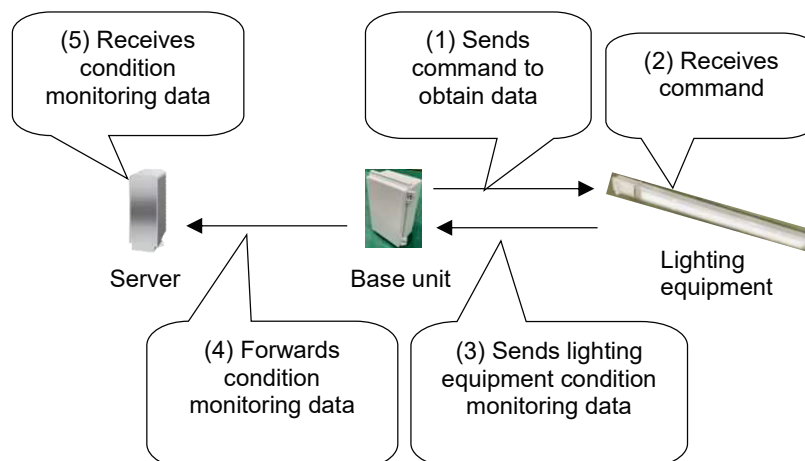


Figure 5. Obtaining monitoring data

照明器具	設置位置	消費電流	実測点灯時間	機体内温度
2021-12-12 15:00:00	グート南1-1	1.25 mA	27.00	33 °C
2021-12-12 15:00:00	グート南1-2	1.25 mA	27.00	33 °C
2021-12-12 15:00:00	グート南1-3	1.25 mA	5700h	33 °C
2021-12-12 15:00:00	グート南1-4	1.25 mA	6000h	33 °C
2021-12-12 15:00:00	グート南1-5	1.25 mA	27.00	33 °C
2021-12-12 15:00:00	グート南1-6	5mA	27.00	33 °C
2021-12-12 15:00:00	グート南1-7	10mA	27.00	33 °C
2021-12-12 15:00:00	グート南1-8	1.25 mA	27.00	33 °C
2021-12-12 15:00:00	グート南1-9	1.75 mA	27.00	33 °C

Figure 6. Data list screen



Figure 7. Graph display screen

### 3. CONCLUSION

The new lighting control and condition monitoring system we have developed can remotely perform lighting control and condition monitoring functions for lighting equipment. This system provides three benefits: The first is streamlining maintenance work. The conditions of individual pieces of lighting equipment can be remotely monitored, which can reduce the amount of work required for workers to visit a site in person. This can also prevent accidents in high or dangerous places. The second benefit is reducing energy consumption. Different types of lighting control can be performed, and the lighting status can be checked to ensure that lighting equipment is turned off when not in use. This can reduce the amount of power consumed by equipment, which can contribute toward the Sustainable Development Goals (SDGs). The system can also be used to respond immediately when authorities request that power usage be limited. The third benefit is that it makes the planning of equipment replacements easier. Data obtained from lighting equipment can be used to predict trends, which can be of use in planning when to replace lighting equipment. In the near future, we will continue to enhance this system through methods such as linking external sensors and using AI to analyze data.

Corresponding Author Name: Yumi Hayashi  
 Affiliation: SEIWA ELECTRIC MFG. CO., LTD  
 e-mail: HAYASI\_yumi@seiwa.co.jp

# RESEARCH ON THE EFFECTS OF LIGHTING ENVIRONMENT ON HUMAN VISUAL PERFORMANCE AND BIOLOGICAL REACTIONS

Toru Kitano, Kunio Kanemaru  
(Iwasaki Electric Co., Ltd., Tokyo, Japan)

## ABSTRACT

We studied the effects of lighting environment on human visual performance and biological reactions. We measured the heart rate variability (HRV) of 12 subjects under three lighting conditions, and asked them to perform visual tasks and answer subjective evaluation questions. The LF/HF values obtained from frequency analysis of HRV were significantly lower in the lighting environment with a correlated color temperature of 2,700 K than in that of 5,000 K. This study showed the importance of lighting control based on people's emotions and behavior objectives.

Keywords: Circadian rhythm, Lighting control, CCT, Visual performance, HRV, LF/HF

## 1. INTRODUCTION

In recent years, office rooms, hotels, and hospital rooms have increasingly adopted lighting control systems that automatically change the room brightness and light color according to time of day. Generally, the illuminance and correlated color temperature (CCT) are set higher in the morning to daytime period, and set lower in the evening to night-time period. Some studies [1] have shown that such lighting control systems regulate a person's circadian rhythm, resulting in quality sleep. On the other hand, the effects of the lighting environment on visual performance and psychological state are not fully understood. We therefore constructed a laboratory mounted on the ceiling with a multi-wavelength variable light source device capable of arbitrarily adjusting the spectral distribution of the light source to conduct a basic investigation about the effects of lighting conditions on human visual performance, subjective comfort, fatigue, and biological reactions.

## 2. METHODS

The experimental room was 2.0 m wide, 2.0 m deep, and 2.0 m high, with the interior walls and ceiling covered with gray Kent paper (with approximately 20% reflectivity) and a black carpet laid on the floor. A wall was erected in the center of the room to separate the spaces on either side, and a multi-wavelength variable light source device (Light Replicator; Telumen, California, USA) was installed to the ceiling of each space. A chair and a desk were placed in the left and right spaces, respectively, so that two subjects can conduct experiments simultaneously in a seated position. Figure 1 shows the room's interior during experiment and Figure 2 a multi-wavelength variable light source device used in the experiment. The lighting environment in the laboratory can be adjusted by controlling the multi-wavelength variable light source device through dedicated software installed on a PC, and the CCT were pre-set to be 2,700 K at 500 lx, 5,000 K at 500 lx, and 5,000 K at 50 lx at the measurement points on the desk. Figure 3 shows the spectral power distributions at CCTs of 2,700 K and 5,000 K. The color rendering index (CRI) of all light sources was 98.



Figure. 1: View of the laboratory interior



Figure. 2: Multi-wavelength variable light source device



Before starting the experiment, the heart rate sensor (WHS-1; UNION TOOL, Tokyo, Japan) shown in Figure 4 was attached to an electrode pad and affixed to the subject's left chest to measure the heart rate and heart rate variability (HRV) of the subject continuously until the end of the experiment. The experiment was conducted according to procedural steps I through VI shown in Figure 5, in which the subjects were asked to perform simple visual tasks under one of the three lighting conditions and answer subjective evaluation questions of comfort and fatigue.

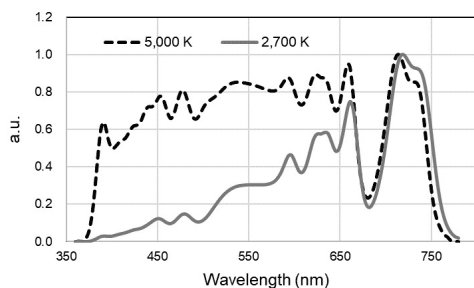


Figure 3 Spectral power distributions



Figure 4: Heart rate sensor

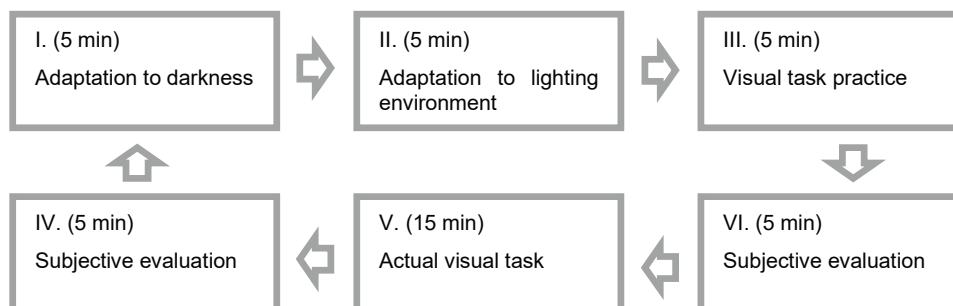


Figure 5: Experimental procedure

In the visual tasks, the subjects were given a sheet of paper with a string of characters (17 characters per line) that randomly combined the kanji representing the color names (red, yellow, green, blue, and black) shown in Figure 6 with the colors of the characters (red, yellow, green, blue, and black), and asked to count and enter the number of matches between the meaning of the kanji and the color of the character for each line. The subjects were instructed to answer as many questions as possible within the time limit.

Name : \_\_\_\_\_ Age : \_\_\_\_\_ years old Starting time : \_\_\_\_\_

Circle all characters that match the "kanji meaning" and "font color" and fill in the number of ○ in the blank on the right. Answers should be given line by line, and after filling in the number of circles, proceed to the next line. It is not necessary to answer all the questions within the time limit, but please answer them accurately and quickly.

Sample answer

黄	緑	黄	青	黒	青	青	黒	青	緑	黄	青	緑	緑	黄	赤	青	6
黄	赤	赤	赤	青	青	青	黒	青	黄	黒	黄	黄	青	黒	緑	緑	3

1	赤	黒	黒	緑	黒	青	黒	赤	黒	青	赤	緑	緑	黄	赤	黒	青	
2	青	赤	青	赤	黄	青	黒	青	青	赤	緑	赤	赤	黒	緑	黒	黄	
3	青	黄	緑	青	赤	黒	赤	赤	緑	黒	赤	黒	黒	黒	緑	青	黒	
4	黄	赤	黒	黒	赤	青	青	黄	緑	黄	青	青	黄	黄	黄	黄	緑	
5	赤	青	赤	青	青	緑	赤	黄	赤	赤	青	黒	赤	赤	黄	緑	緑	

Figure 6: Answer sheet for visual tasks

In the subjective evaluation of comfort, the subjects were given the following items: "The room was bright enough," "It was easy to work," "I was able to concentrate on my work," and "It was easy to read the characters." They were asked to rate each question item on a scale of 1 to 5: 1. disagree, 2. somewhat disagree, 3. can't say either way, 4. somewhat agree, and 5. agree.

In the subjective evaluation of fatigue, the subjects were asked to rate a total of 25 question items, with five questions each on “sleepiness,” “instability,” “discomfort,” “sluggishness,” and “blurriness.” They were asked to rate each item on a scale of 1 to 5: 1. not true at all, 2. slightly true, 3. somewhat true, 4. substantially true, and 5. very true. Experimental steps I through VI were repeated three times under all three lighting conditions. The subjects were 12 males aged between 26 and 62 years (average age 44.8 years).

### 3. CONCLUSION

Figure 7 shows the number of answers, the number of correct answers, and the percentage of correct answers for visual tasks under the three lighting conditions. Statistical analysis of each average value of the 12 subjects by t-test showed that the number of correct answers and the percentage of correct answers were both significantly better ( $p = 0.05$ ) in the lighting environment with a horizontal illuminance of 500 lx than in that with 50 lx. On the other hand, when compared under the condition of 500 lx with equal horizontal illuminance, there was a trend toward better visual performance in the lighting environment with a CCT of 5,000 K compared with that with 2,700 K, but no significant difference was observed. These results show that the horizontal illuminance contributes to visual performance.

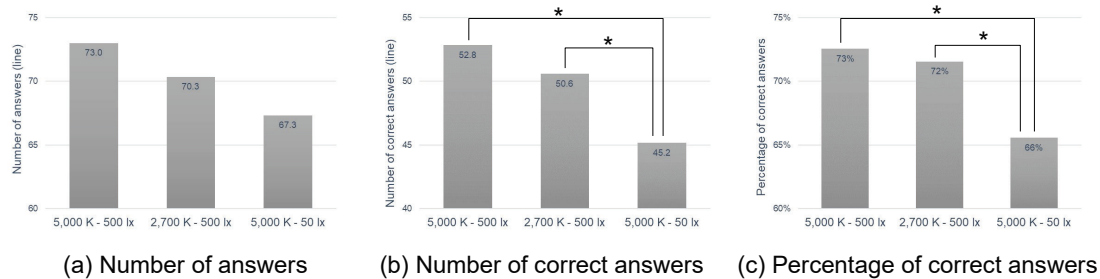


Figure 7: Results of visual task (\*: 5% level of significance)

Figure 8 shows the results of the subjective evaluation of comfort in lighting environments. Our statistical analysis of the average of the subjective evaluation of the 12 subjects by t-test shows that the lighting environment with a horizontal illuminance of 500 lx was significantly better ( $p = 0.05$ ) than that with 50 lx for the question items “the room was bright enough” and “it was easy to work.” For the question item “I was able to concentrate on my work,” the results showed that the lighting environment with a higher horizontal illuminance (5,000 K at 500 lx) was rated significantly better ( $p = 0.01$ ) than that with a lower horizontal illuminance (5,000 K at 50 lx). For the question item “The characters were easy to read,” the results were statistically significantly better ( $p = 0.01$ ) for 5,000 K at 500 lx, 2,700 K at 500 lx, and 5,000 K at 50 lx, in that order. These results showed that lighting conditions with higher horizontal illuminance and higher CCTs are preferred for the lighting environment under which visual tasks are performed. The results also showed that the lighting environment with a higher visual performance and that with a higher comfort were generally similar.

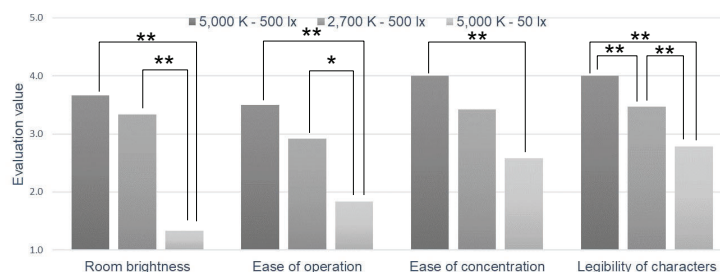


Figure 8: Results of subjective evaluation of comfort (\*: 5% level of significance, \*\*: 1% level of significance)

Figure 9 shows the results of subjective evaluation of fatigue before and after visual tasks. Statistical analysis was performed on the average value of subjective evaluation of the 11 subjects by t-test, excluding as an outlier the result of one subject who was extremely high in

“sleepiness,” “instability,” “discomfort,” and “sluggishness” in subjective evaluation before performing visual tasks. In the lighting environment with a high horizontal illuminance of 500 lx, “sluggishness,” which indicates physical fatigue, increased significantly ( $p = 0.01$ ) before and after visual tasks, and in the lighting environment with a high CCT of 5,000 K, “instability,” which indicates mental fatigue, increased significantly ( $p = 0.05$ ) before and after visual tasks. The results showed that both physical and mental fatigue increased before and after visual tasks in the lighting environment of 5,000 K at 500 lx with a higher horizontal illuminance and a higher CCT. The results also showed that “blurriness,” which is an indicator of eyestrain, increased significantly ( $p = 0.05$ ) in the lighting environments with 2,700 K at 500 lx and 5,000 K at 50 lx before and after visual tasks. These results may indicate that the horizontal illuminance and CCT affect the type of fatigue perceived.

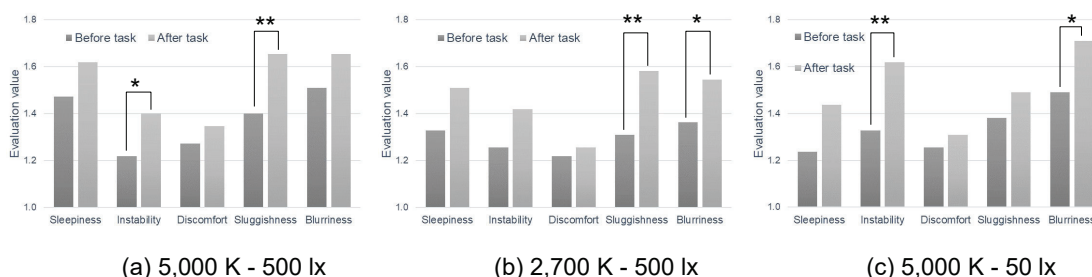


Figure 9: Results of subjective evaluation of fatigue  
(\*: 5% level of significance, \*\*: 1% level of significance)

Finally, Figure 10 shows the ratio of low frequency to high frequency (LF/HF) results obtained from frequency analysis of HRV. A high LF/HF value is said to indicate sympathetic nervous system dominance, which increases blood pressure and causes the body to enter an active state. A low LF/HF value is said to indicate parasympathetic nervous system dominance, which results in lower blood pressure and a relaxed, calm state. Our statistical analysis for the average LF/HF value of the 12 subjects by t-test shows that LF/HF values were significantly lower ( $p = 0.05$ ) in the lighting environment with a CCT of 2,700 K than in that with 5,000 K. The results may indicate that the CCT affects the balance between sympathetic and parasympathetic nervous system activities.

A lighting control system that automatically changes the brightness and light color of a room according to time of day may regulate a person's circadian rhythm and bring about quality sleep. On the other hand, this investigation also showed the importance of controlling the room brightness and light color according to people's emotions and behavioral objectives. In the future, more personalized and highly controlled lighting control systems will need to be realized.

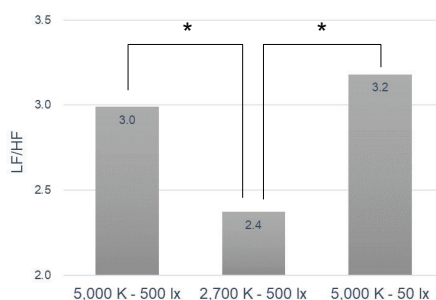


Figure 10: Results of LF/HF (\*: 5% level of significance)

## REFERENCE

- [1] Brown TM et al. (2022) Recommendations for daytime, evening, and nighttime indoor light exposure to best support physiology, sleep, and wakefulness in healthy adults. PLoS Biol 20(3): e3001571.

Corresponding Author: Toru Kitano  
Affiliation: Iwasaki Electric Co., Ltd.,  
e-mail : kitano-tooru@eye.co.jp

# RESEARCH ON THE PREDICTION OF LIGHTING LOAD IN PUBLIC BUILDINGS BASED ON GA-SEQ2SEQ MODEL

Haozhe Zhu, Qingcheng Lin, Xuefeng Li, Hui Xiao

(College of Electronic and Information Engineering, Tongji University, Shanghai, China)

## ABSTRACT

Lighting load is an important component of building energy consumption, and accurate prediction can not only promote the reduction of energy consumption but also optimize the allocation of power resources. However, due to the variability of climates, the variability of working days and holidays, and the uncertain behavior of personnel, the daily operating state of lighting equipment is random in regularity, which affects the accuracy of the prediction algorithm in analyzing the distribution of lighting load behavior.

To address the above problems, a Sequence-to-Sequence (Seq2Seq) model based on Genetic Algorithm (GA) optimization under classification is proposed in this study to solve the uncertainty of lighting load prediction. Using the lighting load of a public building in Shanghai and the corresponding meteorological data as the analysis sample, the energy consumption behavior patterns are classified based on the load value of a certain off-peak hour of the daily lighting load to obtain three categories of labels: high lighting load, medium lighting load, and low lighting load, and then the Seq2Seq model with the hybrid genetic algorithm is used to predict the lighting load during the peak hours of the forecast day. The three types of labels obtained by the classification are used as input for the features together with the building lighting loads and the related meteorological data, which can further improve the fit of the model. Also, the optimization of model hyperparameters based on genetic algorithm can reduce the uncertainty interference and further improve the prediction accuracy. The proposed method in this study is validated by analyzing actual data cases. The results show that the method proposed in this study shows the optimal MAE, RMSE, and  $R^2$  indexes, which can solve the problem more effectively in the direction of lighting load prediction and provide technical support to improve buildings' intelligent operation and maintenance management.

Keywords: lighting load prediction, classification, energy consumption behavior patterns, genetic algorithm, Seq2Seq model

## 1. INTRODUCTION

Building energy consumption accounts for about 30% of the total global energy consumption, and building energy efficiency is a key link to reduce carbon emissions in the construction sector [1]. At the same time, lighting energy consumption occupies a very large proportion of the overall building energy consumption during the use phase of building projects, and reducing lighting energy consumption and improving energy utilization is the first task to alleviate the energy shortage problem[2].

However, reducing lighting energy consumption without losing lighting quality requires accurate lighting load prediction. In addition, some building research institutes and related building enterprises have collected a large amount of lighting load data by building energy consumption monitoring platforms [3] to provide data sets for lighting load prediction, but there is still the problem of poor utilization.

Currently, in the field of load prediction, Yongchao Cui et al [4] applied the Seq2Seq-LSTM model to short-time series load prediction, which has a better performance compared with traditional ANN and LSTM. However, it is not reasonable to directly predict without analyzing the building load behavior patterns if the dataset is complex and large, which leads to a decrease in prediction accuracy [5]. On this basis, Zaki Masood et al [6] reaped good results in load prediction by the Seq2Seq model based on the results obtained from single-family electricity load clustering. However, only single variable load values are considered in this method, while climate factors also play a crucial role in actual load forecasting [7], and its lack of ability to mine Seq2Seq superior superparameters leads to uncertainty in load forecasting results. At the same time, in practical applications, the load pattern of the forecast day cannot be obtained in advance, and

because most of the short-term load forecasting tasks are focused on the peak load time [8]. In this paper, based on the above problems, a Seq2Seq model based on genetic algorithm optimization under classification is proposed for single-user lighting load forecasting, which divides three load intervals into high lighting load days, medium lighting load days, and low lighting load days, classifies and labels the load values of a certain off-peak period of the knotted daily load curve, and uses them as features along with lighting loads and relevant climate data as Finally, the Seq2Seq model optimized by the genetic algorithm is used to predict the lighting load during the peak hours, and the genetic algorithm can help us find the optimal hyperparameters of the model so that the lighting load prediction can achieve better prediction accuracy.

## 2. BACKGROUND AND RELATED WORK

### 2.1 Algorithm Introduction

#### 2.1.1 Genetic Algorithm

Hyperparameters are parameters that need to be set before the model training process starts, and excellent hyperparameters can greatly improve the performance of the model [9]. In this study, to optimize the hyperparameters, the model is optimized using a genetic algorithm. Genetic algorithm is an optimization search algorithm that simulates the law of superiority and inferiority in natural selection [10,11,12], and is capable of adaptively adjusting the search space with a high global search capability. Genetic algorithms have a wide range of application areas, and in deep learning, they can effectively search for hyperparameters of neural networks to achieve structural as well as parametric optimization of the network.

#### 2.1.2 LSTM-based Seq2Seq

Seq2Seq is a network model with an encoder and decoder structure, which has good performance in the field of time series multi-step prediction [13,14,15,16,17]. Compared with the traditional RNN, LSTM as the encoder and decoder of the Seq2Seq model can better solve the gradient disappearance problem and the long-term dependence problem that occurs during the backpropagation [18].

Seq2Seq has a better performance compared to LSTM in scenarios with different input and output lengths. In this study, Seq2Seq is more applicable for predicting the future 4-moment load by inputting 24-moment load, and its better fit is demonstrated in the later experimental section. The structure of the Seq2Seq model is shown in the figure below.

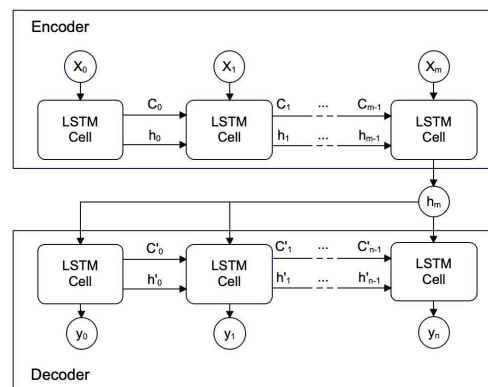


Figure 1. Structure of single-layer Seq2Seq model

Figure 1 shows the structure of the single-layer Seq2Seq model, which consists of two parts: encoder and decoder, each part is implemented based on LSTM. The encoder takes the input sequence as input and passes the parameters of the hidden node  $h_m$  at moment  $m$  and the memory cell  $C_m$  as the state vector to the decoder, which generates the target sequence based on this.



## 2.2 Data preparation

### 2.2.1 Data collection

In this study, an office building located in Shanghai was selected for analysis, and the load data collected from its internal equipment was highly segmented to better filter the lighting load data. The lighting load data of this office building is shown in Figure 2. This study selected the building lighting load data for the building from February 2019 to May 2020, which contains normal lighting, emergency lighting, etc., and obtained relevant climate data, which contains data related to atmospheric temperature, humidity, and total cloudiness.

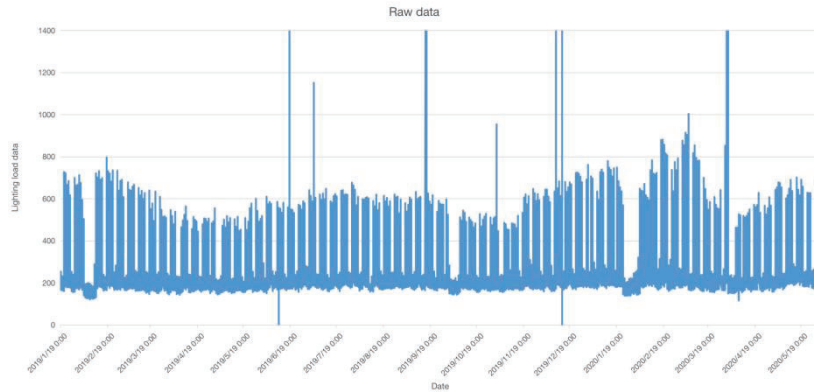


Figure 2. Original lighting load data graph

### 2.2.2 Data processing and feature selection

To improve the prediction accuracy of the lighting load model, the missing and outlier values of the data need to be processed. For missing values, the fill function in the Python library is used to fill the vacant data with the average value. For the outliers, a box line plot (quartile method) is used to detect the outliers and replace them with the mean value[19]. After data processing, the lighting load data of this office building is shown in Figure 3.

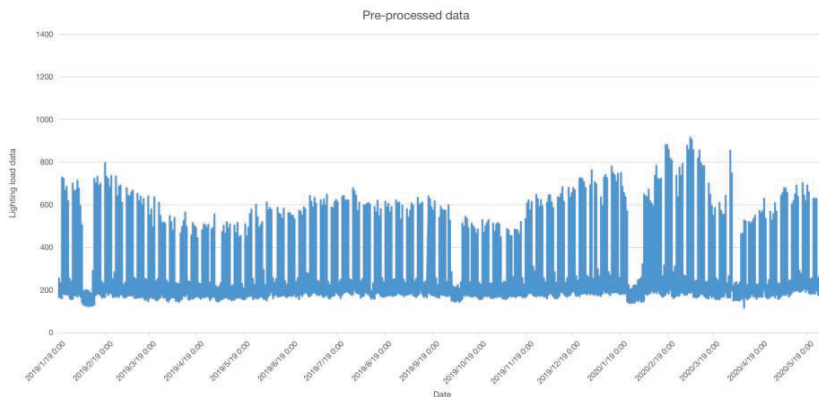


Figure 3. Lighting load data graph after data processing

Table 1. Table of partial input features of the model

ID	variable	explain	Unit
1	Value	Building lighting load data	kW·h
2	Temp	Atmospheric temperature	°C
3	Hum	Relative Humidity	%
4	wd_power	Wind Speed	m/s
5	Cloud	Total Cloud Volume	%

A reasonable feature analysis not only can reduce the dimensionality of the data and remove redundant or irrelevant features, but also can improve the prediction accuracy of the model as

well as the generalization ability. This study takes into account the close relationship between lighting loads and weather. Building lighting load data, atmospheric temperature, relative humidity, wind speed, and total cloudiness are selected as some of the inputs to the model, as shown in Table 1.

### 3. RESEARCH METHODOLOGY

#### 3.1 Training set and test set division

To verify the feasibility of the method in this study, the data need to be divided into training and test sets first. The data from February 2019 to February 2020 are used as the training set, and the data from February 2020 to May 2020 are used as the test set. The training set is mainly used for the training of the GA-Seq2Seq prediction model, and the test set is used to verify the accuracy of the model.

#### 3.2 Classification method

In order to improve the prediction accuracy, this study divided three load intervals into [0,250], (250,430], and (430,800] corresponding to low lighting load days, medium lighting load days, and high lighting load days, and judged whether the load values during the non-peak hours of 8:00-9:00 in the daily lighting load. The category labels are used as input to the model along with the lighting load and related climate data, and the classification results are shown in Figure 4.

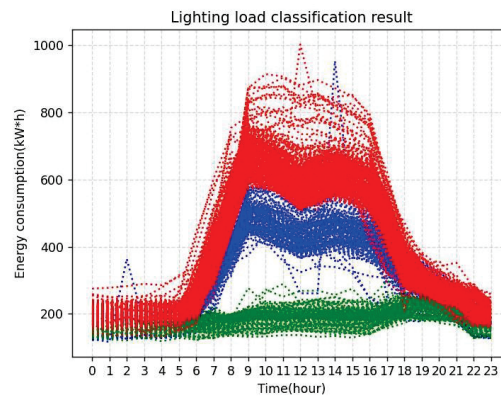


Figure 4. Schematic diagram of the results of lighting load classification

#### 3.3 Model Predictions

To eliminate the scale differences between different features and to unify the feature values to the same scale, the data were normalized using the min-max scaling approach [20], where the values of all features were deflated to between 0 and 1 according to Equation 1.

$$X'_1 = \frac{X_i - X_{\min}}{X_{\max} - X_{\min}} \quad (1)$$

To verify the superiority of the model proposed in this study, RNN, GA-LSTM, BiLSTM, CNN-LSTM, and our proposed GA-Seq2Seq model are compared. The model input features include lighting load, relevant climate data, and daily classification labels, and the predicted values are chosen after 9:00 a.m. daily. The experiments are based on the Pytorch framework, Adam is chosen as the optimizer, and the MSE mean square loss function is used for the loss function with 140 iterations. The evaluation metrics are chosen as MAE, RMSE, and R2 for prediction result evaluation. A comparison of the test set prediction results is shown in Figure 5.

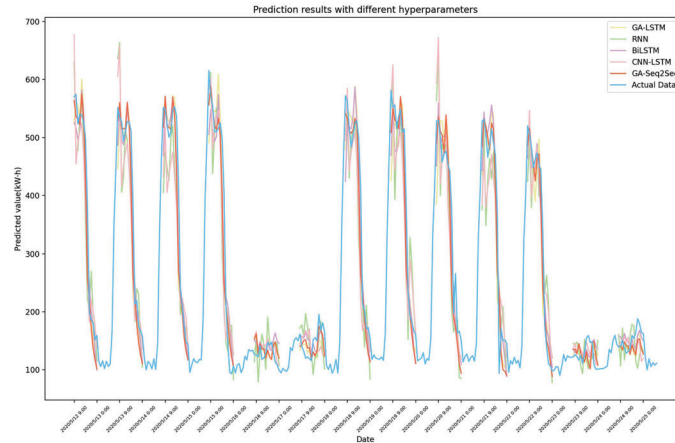


Figure 5. Comparison of the actual load curve and the predicted load curve of the method in this paper and the other four evaluation models

Table 2. Comparison of the performance indexes predicted by the method in this paper and the other four evaluation models

Predictive Models	MAE	RMSE	R <sup>2</sup>
GA-Seq2Seq	0.0333	0.0503	0.889
GA-LSTM	0.0353	0.0539	0.873
BiLSTM	0.0396	0.0557	0.869
CNN-LSTM	0.0374	0.0544	0.871
RNN	0.0468	0.0699	0.786

The above experiments show that using our proposed GA-Seq2Seq model in this study has better MAE, RMSE, and R<sup>2</sup> metrics compared to GA-LSTM, BiLSTM, CNN-LSTM, and RNN.

The GA-Seq2Seq model is optimized by genetic algorithm to find the hyperparameters. In this study, the selected hyperparameters are the number of layers and the hidden size of the model, and the number of layers and the hidden size of the encoder and decoder are set to be the same. The number of iterations of the genetic algorithm is set to 20, and the number of populations in each generation is 20. Since the number of hyperparameters is 2, the size of each DNA is set to 2. The optimization results are shown in Figure 6.

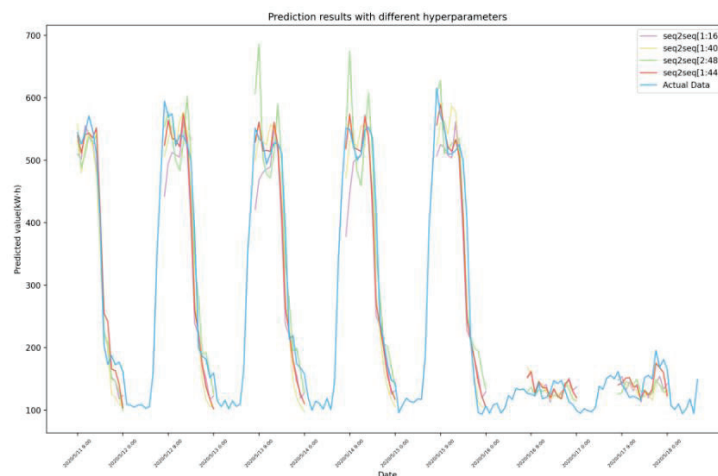


Figure 6. Comparison of the actual lighting load curve and the predicted load curve with the four optimal hyperparameters of GA-Seq2Seq

Table 3. Comparison of performance indexes under hyperparameters of genetic algorithm optimization

Hyperparameters [num_layers:hidden_size]	MAE	RMSE	R <sup>2</sup>
[1,44]	0.0333	0.0503	0.889
[1,16]	0.0358	0.0527	0.879
[1,40]	0.0356	0.0530	0.877
[2,48]	0.0358	0.0536	0.875

According to Table 3, the Seq2Seq model has better performance when num\_layers=1,hidden\_size=44. In summary, it can be seen that the hyperparameter optimization of Seq2Seq by the genetic algorithm can improve the performance of the model and thus further improve the prediction accuracy.

In order to further verify the superiority of the method, this study compared the methods of classification without using classification labels and the traditional sense of classification with both weekday and holiday labels, and the experimental results are shown in Figure 7.

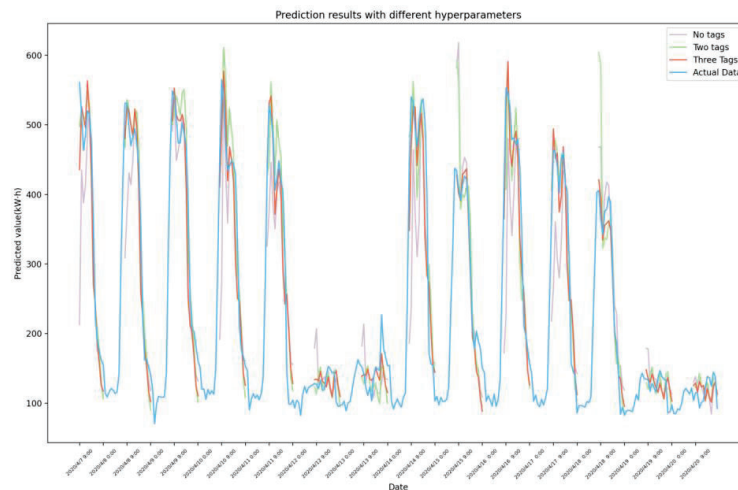


Figure 7. Comparison of the actual lighting load curve and the predicted load curve with different label numbers

Table 4. Comparison table of evaluation indexes under different label numbers

Number of tags	MAE	RMSE	R <sup>2</sup>
3	0.0333	0.0503	0.889
2	0.0389	0.0607	0.841
1	0.0442	0.0709	0.786

As can be seen from Figure 7, the method in this study has a better fit; the method without the use of categorical labels is the least effective, and its prediction error for holidays is larger; the method based on two types of labels for weekdays and holidays does not perform well in the case of fluctuating load changes during weekdays. In addition, according to Table 4, the method that analyzes the trend of a certain off-peak period to obtain three types of classification labels as part of the characteristics and inputs them into the GA-Seq2Seq model for load forecasting has lower MAE, RMSE, and higher R<sup>2</sup> index than the method that does not use classification labels and forecasts based on two types of labels for weekdays and holidays. In summary, the method not only has good performance in forecasting on holidays but also fits the load usage trend well in the face of load fluctuations on weekdays, effectively reducing the forecast error.

#### 4. CONCLUSION

In order to predict building lighting loads more accurately, this paper proposes a Seq2Seq model based on genetic algorithm optimization under classification, which classifies energy consumption behavior patterns based on the trend of daily lighting loads during a certain off-peak period to obtain three types of labels: high lighting loads, medium lighting loads and low lighting loads, and uses the obtained classification labels with lighting loads and related meteorological data as the input features of the GA- Seq2Seq model and optimize the hyperparameters of the model by genetic algorithm to further improve the prediction accuracy of the model and compare it with other models (GA-LSTM, BiLSTM, CNN-LSTM, and RNN). In addition, this paper also compares the methods that do not use daily classification labels and those that are traditionally classified with both weekday and holiday labels in order to closely verify the superiority of the proposed method. The results show that the multi-step time series prediction method proposed in this study has better MAE, RMSE, and  $R^2$  metrics in both comparison experiments, which confirms that the method proposed in this paper can have better performance and is a reliable method for lighting load prediction in the field of lighting load prediction.

#### REFERENCE

- [1] Nalcaci G, Özmen A, Weber G W. Long-term load forecasting: models based on MARS, ANN and LR methods[J]. *Central European Journal of Operations Research*, 2019, 27: 1033-1049.
- [2] Hammad M A, Jereb B, Rosi B, et al. Methods and models for electric load forecasting: a comprehensive review[J]. *Logist. Sustain. Transp*, 2020, 11(1): 51-76.
- [3] Hong Wang, Khalid A. Alattas, Ardashir Mohammadzadeh, Mohammad Hosein Sabzalian, Ayman A. Aly, Amir Mosavi, Comprehensive review of load forecasting with emphasis on intelligent computing approaches, *Energy Reports*, Volume 8, 2022, Pages 13189-13198, ISSN 2352-4847, <https://doi.org/10.1016/j.egyr.2022.10.016>.
- [4] Y. Cui, B. Yin, R. Li, Z. Du and M. Ding, "Short-time Series Load Forecasting By Seq2seq-LSTM Model," 2020 IEEE 9th Joint International Information Technology and Artificial Intelligence Conference (ITAIC), Chongqing, China, 2020, pp. 517-521, doi: 10.1109/ITAIC49862.2020.9339110.
- [5] Zhenxiang Dong, Jiangyan Liu, Bin Liu, Kuining Li, Xin Li, Hourly energy consumption prediction of an office building based on ensemble learning and energy consumption pattern classification, *Energy and Buildings*, Volume 241, 2021, 110929, ISSN 0378-7788, <https://doi.org/10.1016/j.enbuild.2021.110929>.
- [6] Masood, Z.; Gantassi, R.; Ardiansyah; Choi, Y. A Multi-Step Time-Series Clustering-Based Seq2Seq LSTM Learning for a Single Household Electricity Load Forecasting. *Energies* 2022, 15, 2623. <https://doi.org/10.3390/en15072623>.
- [7] Maryam Imani, Electrical load-temperature CNN for residential load forecasting, *Energy*, Volume 227, 2021, 120480, ISSN 0360-5442, <https://doi.org/10.1016/j.energy.2021.120480>.
- [8] Zhe Chen, Yongbao Chen, Tong Xiao, Huilong Wang, Pengwei Hou, A novel short-term load forecasting framework based on time-series clustering and early classification algorithm, *Energy and Buildings*, Volume 251, 2021, 111375, ISSN 0378-7788, <https://doi.org/10.1016/j.enbuild.2021.111375>.
- [9] Li Yang, Abdallah Shami, On hyperparameter optimization of machine learning algorithms: Theory and practice, *Neurocomputing*, Volume 415, 2020, Pages 295-316, ISSN 0925-2312, <https://doi.org/10.1016/j.neucom.2020.07.061>.
- [10] Goldberg, D. E., & Holland, J. H. (1988). Genetic algorithms and machine learning. *Machine Learning*, 3(2), 95-99.
- [11] A. Lambora, K. Gupta and K. Chopra, "Genetic Algorithm- A Literature Review," 2019 International Conference on Machine Learning, Big Data, Cloud and Parallel Computing (COMITCon), Faridabad, India, 2019, pp. 380-384, doi: 10.1109/COMITCon.2019.8862255.
- [12] Katoch, S., Chauhan, S.S. & Kumar, V. A review on genetic algorithm: past, present, and future. *Multimed Tools Appl* 80, 8091 - 8126 (2021). <https://doi.org/10.1007/s11042-020-10139-6>.
- [13] Xu, J.; Wang, K.; Lin, C.; Xiao, L.; Huang, X.; Zhang, Y. FM-GRU: A Time Series Prediction Method for Water Quality Based on seq2seq Framework. *Water* 2021, 13, 1031. <https://doi.org/10.3390/w13081031>.
- [14] Gong, G.; An, X.; Mahato, N.K.; Sun, S.; Chen, S.; Wen, Y. Research on Short-Term Load Prediction Based on Seq2seq Model. *Energies* 2019, 12, 3199.



- <https://doi.org/10.3390/en12163199>.
- [15] Ge Zhang, Xiaoqing Bai, Yuxuan Wang, Short-time multi-energy load forecasting method based on CNN-Seq2Seq model with attention mechanism, Machine Learning with Applications, Volume 5, 2021, 100064, ISSN 2666-8270. <https://doi.org/10.1016/j.mlwa.2021.100064>.
  - [16] M. Razghandi, H. Zhou, M. Erol-Kantarci and D. Turgut, "Short-Term Load Forecasting for Smart Home Appliances with Sequence to Sequence Learning," ICC 2021 - IEEE International Conference on Communications, Montreal, QC, Canada, 2021, pp. 1-6, doi: 10.1109/ICC42927.2021.9500767.
  - [17] Lopez-Martin, M.; Sanchez-Esguevillas, A.; Hernandez-Callejo, L.; Arribas, J.I.; Carro, B. Novel Data-Driven Models Applied to Short-Term Electric Load Forecasting. Appl. Sci. 2021, 11, 5708. <https://doi.org/10.3390/app11125708>
  - [18] Xiang, Z., Yan, J., & Demir, I. (2020). A Rainfall-Runoff Model With LSTM-Based Sequence-to-Sequence Learning. Water Resources Research, 56(1). <https://doi.org/10.1029/2019WR025326>
  - [19] Zhu, Q. & Ye, L. & Zhao, Yongning & Lang, Y. & Song, Xueguan. (2015). Methods for elimination and reconstruction of abnormal power data in wind farms. Dianli Xitong Baohu yu Kongzhi/Power System Protection and Control. 43. 38-45.
  - [20] Lemuel Clark P. Velasco, Karl Anthony S. Arnejo, Justine Shane S. Macarat, Performance analysis of artificial neural network models for hour-ahead electric load forecasting, Procedia Computer Science, Volume 197, 2022, Pages 16-24, ISSN 1877-0509, <https://doi.org/10.1016/j.procs.2021.12.113>.

## ACKNOWLEDGEMENT

The success of this work was made possible by the careful guidance of Ms. Xiao and Mr. Li, for which I would like to express my sincere gratitude. In addition, I am also very grateful to Qingcheng Lin for her help.

Corresponding Author: Xuefeng Li

Affiliation: College of Electronic and Information Engineering, Tongji University, Shanghai, China

e-mail : [lixuefeng@tongji.edu.cn](mailto:lixuefeng@tongji.edu.cn)

# RESEARCH AND ANALYSIS OF LIGHTING ENVIRONMENT DESIGN OF MOTHER AND BABY ROOM IN COMMERCIAL SPACE IN SHANGHAI

Shujian Dai<sup>1</sup>, Lei Shi<sup>2</sup>, Luoxi Hao<sup>1</sup>.

(1.College of Architecture and Urban Planning, Tongji University, Shanghai, China

2. Architectural Design & Research Institute of Tsinghua University)

## ABSTRACT

The mother and baby room is a special public space for maternal and infant breastfeeding, nursing or resting, and its light environment design should fully consider the needs of mothers and infants, from color temperature, luminaire arrangement, lighting methods and other aspects. We conducted field research on the natural and artificial light environments in 33 commercial spaces in Shanghai, and summarized the common luminaire arrangements and lighting methods in mother and baby rooms. Subsequently, the color temperature, illuminance, and uniformity of the main area (nursing area, breastfeeding area, resting area and so on) of four mother and baby rooms with different lighting methods were measured and calculated. Through the statistical and analytical results of the research data, lighting design recommendations for the mother and baby rooms were presented.

Keywords: maternity, infant, light environment design, field research; artificial lighting

## 1. INTRODUCTION

Breastfeeding can help reduce postpartum weight retention and also the risk of breast and ovarian cancer, and is recommended by the WHO (World Health Organization), UNICEF (United Nations International Children's Emergency Fund) and American Academy of Paediatrics to support optimal growth and development in infants [1]. Existing design standards for mother and baby rooms provide recommendations from perspective of artificial lighting, natural lighting, illumination, and so on. Some commercial spaces in Shanghai are well-equipped for mother and baby rooms, which provide travel convenience for lactating women, but their light environment may not be finely designed. Based on the design standards of mother and baby rooms, this study investigated and statistically analyzed 33 mother and baby rooms in commercial spaces in terms of luminaire types, natural lighting, interior light color, lighting design of the guidance system, and so on. The parameters of horizontal illuminance, color temperature and uniformity of each functional area in 4 mother and baby rooms which representing different types of lighting methods were measured to explore the advantages and disadvantages of different lighting arrangements and to provide reference for the design of indoor light environment in mother and baby rooms.

## 2. RECOMMENDATIONS OF EXISTING DESIGN STANDARDS FOR MOTHER AND BABY ROOMS

UNICEF posed the points that breastfeeding is key to the comprehensive development of children, their mothers and society. It provided recommendations that natural light and soft lighting are preferred environment in creating a comfortable environment for breastfeeding rooms [2]. WELL Building Standard™ version 2 feature also requires ambient lighting of dedicated lactation rooms to help nursing mothers breastfeeding. Lactation rooms design guidelines given by AIA (American Institute of Architects) suggested that uniform ambient lighting and task lighting over the sink and the pump area should be provided for pumping milk and breastfeeding [3]. Murrye recommended windows of lactation room should be fitted with shades or opaque glass [4]. In China, the Shenzhen Housing and Construction Bureau issued the "Design Regulations for Mother and Baby Rooms in Public Places in Shenzhen City", which makes recommendations on lighting parameters such as ground illumination, glare value, color rendering index, and power density in 2019 (Table 1). The latest "Civil Airport Mother and Baby Room Planning and Construction and Facilities and Equipment Configuration Guide" issued by the Airport Department of the Civil Aviation Administration of China contains more detailed recommendations on lighting: warm light is recommended for the lighting of the breastfeeding and nursing areas, avoiding direct light sources (Figure 1). It also posed the point that mirrors are preferably equipped with internal light strips as a supplementary light source for makeup.

Table 1. Recommended Lighting Indicators of 'Design Regulations for Mother and Baby Rooms in Public Places in Shenzhen City'

Surface	Illuminance (lx)	Unified Glare rating	Color rendering index ( Ra )	Lighting Power Density ( W/m <sup>2</sup> )	
				Current value	Target value
Ground	200	19	80	6.5	5.5

Figure 1. Schematic diagram of positive and negative examples of luminaires  
(left: embedded strip, right: spotlight)

### 3. ANALYSIS OF LIGHT ENVIRONMENT DESIGN PROFILE OF MOTHER AND BABY ROOMS IN SHANGHAI COMMERCIAL SPACE

Field research was conducted on 33 mother and baby rooms in Shanghai, and statistical analysis was conducted on natural lighting and artificial lighting (type of luminaires, light color, lighting design of the guidance system, and whether the color temperature illumination is adjustable). The statistical results in Table 2 showed that there was no natural light in any of the 33 mother and baby rooms. For artificial lighting, the most common types of light fixtures in the room were strips and spotlights. 24 mother and baby rooms were equipped with strips and 20 mother and baby rooms were equipped with spotlights. There were 5 mother and baby rooms with ceiling lights and downlights which are the next most numerous lamp types. In terms of artificial light color temperature, 29 mother and baby rooms were equipped with warm light (<4000K) and 4 mother and baby rooms were equipped with cool light ( $\geq 4000K$ ). In addition, 4 mother and baby rooms were equipped with colored light to create a warm and special indoor lighting atmosphere (Figure 3). Five of the 33 of the mother and baby room's guidance system are designed with lighting which are not only more identifiable, but also more aesthetic and interesting. It is worth noting that only 2 of the 33 rooms equipped with adjustable color temperature or illumination, while most lighting environment of the mother and baby rooms are fixed.

Table 2. Field research and records of natural lighting and artificial lighting in 33 mother and baby rooms in commercial spaces in Shanghai

Number		1	2	3	4	...	33
Location		Suhe Bay Vientiane world 2F	Qiantan Taikooli 2F	AI Plaza 2F	L+MALL 2F		JingAn Kerry Center2F
With natural lighting?		No	No	No	No		No
Artificial lighting	Luminaire types	trips, spotlights	Strip, wall light, spot light, mirror front light	strips	Strips, downlights		strips, spotlights
	warm/cool/colored lighting	Cool lighting	Warm lighting	Warm lighting	colored lighting		Warm lighting
	Guide system lighting design	Yes	No	No	No		No
	Color temperature or illumination adjustable	No	No	No	No		Yes

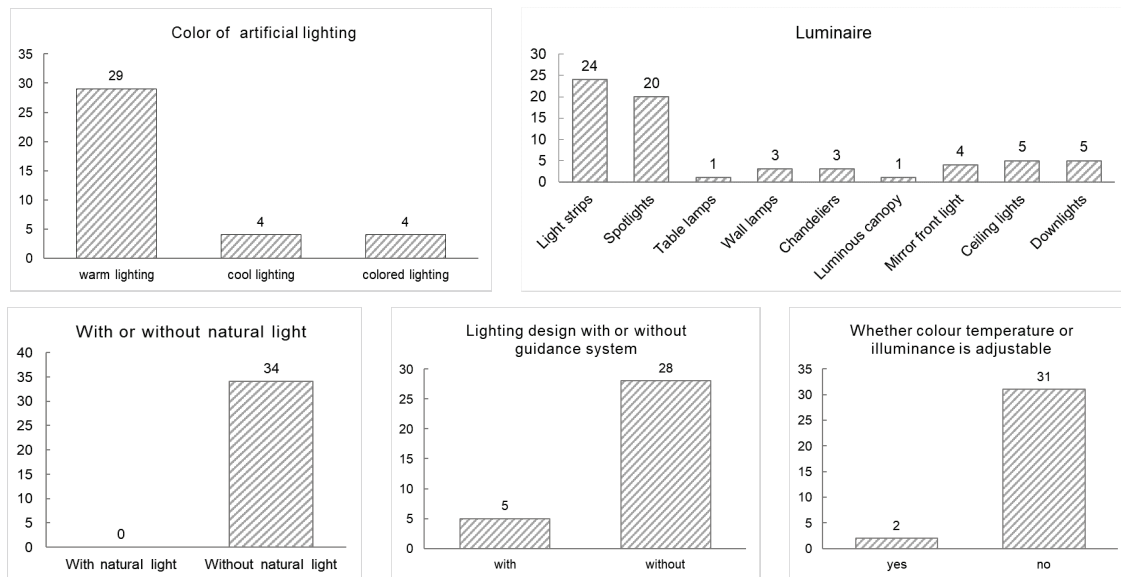


Figure 2. Statistical results of the survey on the design of the light environment of mother and baby rooms in commercial spaces in Shanghai

During the field research process, we found that the following lighting methods are common in mother and baby rooms. The first is indirect lighting with only light strips, such as lighting environment of the mother and baby room on 2nd floor of Wanxiang City on Wu Zhong Road and the 3rd floor of LCM Hkland and Cifi Plaza where light strips are placed in the ceiling recesses, at the bottom of the sink, and on the back of the mirror to light for the breastfeeding and nursing areas. The second type of light environment is direct lighting. Only down-illuminated spotlights or downlights are set on ceilings illuminating washbasins and diaper tables. The mother and baby rooms on the 2nd floor of Ruihong Hall of the Sun, 2nd floor of IFC and the 3rd floor of Reo Department Store are representative mother and baby rooms. Another lighting environment is a combination of direct and indirect lighting with light strips and downlights or ceiling lights, which is the most common. Mainly indoor lamps are light strips combined with downlights, spotlights or ceiling lights. For instance, the mother and baby room on the 2nd floor of the First Babaiban Mall, 2nd floor of Suhe Bay Vientiane world, and JingAn Kerry Centre set light strips to provide ambient lighting for the overall space and breastfeeding area, and downlights to directly shine down on the diaper table and hand washing pool in the nursing area to provide task lighting. A ceiling light is installed in the mother and baby room on the 3rd floor of Sun Moon Light Center to provide task lighting. In addition, the mother and baby rooms on the 3rd floor of Sun and Moon Light Center and the 4th floor of Plaza 66 are equipped with mirror front lights to improve facial illumination.

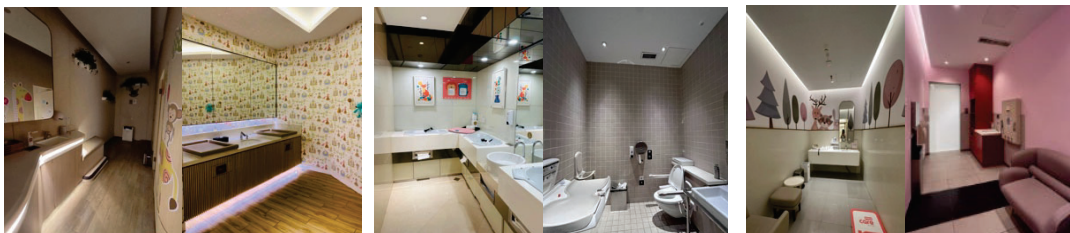


Figure 3. three kinds of different lighting methods and luminaire arrangements of mother and baby rooms (Left: indirect lighting. Middle: direct lighting. Right: indirect and direct lighting)

#### 4. LIGHT ENVIRONMENT MEASUREMENT AND PROBLEM IDENTIFYING OF 4 MOTHER AND CHILD ROOMS

After analyzing the indoor light environment of 33 mother and baby rooms, we selected four mother and baby rooms on the 2nd floor of Al Plaza (indirect lighting), the 2nd floor of Ruihong Hall of the Sun (direct lighting), the 3rd floor of Sun Moon Center and 2F floor of Qiantan Taikooli (direct lighting and indirect lighting) to conduct light environment measurements and interviews to investigate whether the light distribution of different lighting methods can meet the actual usage needs of mothers and babies. The mother and baby room on the 2nd floor of Qiantan Taikooli is a large mother and baby room (area >30m<sup>2</sup>), with 3 nursing rooms, 2 diaper tables and children

play area. The other three are small mother and baby rooms (area  $\leq 10\text{m}^2$ ), consisting of a breastfeeding area, a nursing area and a waiting area. A spectral illuminance meter (Yuanfang spic-300aw) was used to measure the illuminance and color temperature in different spatial areas. And the type of indoor luminaires was recorded. The illuminance data was measured by the center point method in GB/T5700-2008 Lighting Measurement Method (as shown in Figure 2.2), which divides the space into a rectangular grid and measures the illuminance at the center point of each rectangular grid on the horizontal surface of 0.75m from the ground, and takes the average value to obtain the average illuminance of the indoor working surface. The uniformity ratio illuminance is calculated by the ratio of the minimum illuminance to the average illuminance in the measurement point.

Table 3. Research records of natural lighting and artificial lighting in mother and baby rooms in commercial spaces in Shanghai

Area	Size	Area			
		Breastfeeding area	Nursing area	Waiting area	Play area
AI Plaza2F	Small	√	√	√	
Qiantan Taikooli 2F	Large	√	√	√	√
Ruihong Hall of the Sun 2F	Small	√	√	√	
Sun Moon Light Center 3F	Small	√	√	√	

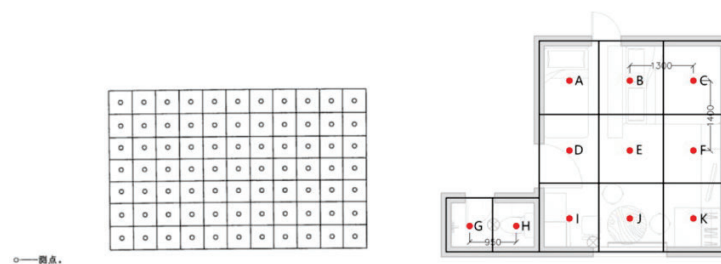


Figure 4. Central pointing method for illuminance measurement

#### 4.1 Light environment measurement result and problem summary in the mother and baby room on the 2nd floor of AI Plaza

Table 4. Light environment parameters in the mother and baby room on the 2nd floor of AI Plaza

Area	Nursing Area (Hand washing sink)	Nursing area (Diaper table)	Breastfeedi ng area	Waiting area	Illumination uniformity
Illuminance (lx)	289.9	204.2	59.2	259.5	0.98
Color temperature (K)	2578	2986	2403	2940	
Luminaires type	strip	strip	strip	Strips, Spotlights	
Lighting method	Indirect lighting	Indirect lighting	Indirect lighting	Direct&indirect lighting	
Photo					



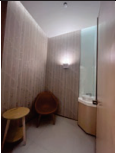
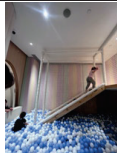


The lighting environment in the mother and baby room on the 2nd floor of AI Plaza is indirect lighting, with strips behind the mirror, at the bottom of the sink, and at the top of the ceiling decoration. The horizontal illumination of the sink and diaper table can reach over 200lx, which can meet the needs of hand washing and baby care. The lactation room is also equipped with



indirect light-emitting strips, and the horizontal illuminance of the breastfeeding sofa is 59.2lx without visible glare. The overall light in the room is soft and uniform. Interviews with users showed that most of them were satisfied with the space.

#### 4.2 Light environment measurement result and problem summary in the mother and baby room on the 2nd floor of Qiantan Taikooli

Table 5. Light environment parameters in the mother and baby room on the 2nd floor of Qiantan Taikooli




Area	Nursing Area (Hand washing sink)	Nursing area (Diaper table)	Breastfeeding area	Play area	Waiting area	Illumination uniformity
Illuminance (lx)	890.1	311.87	53.32	331.8	57.6	0.76
Color temperatur e (K)	3421	3170	2872	3362	3318	
Luminaires type	Strip, Wall light, Spotlights , Mirror front light	Strip, Wall light, Spotligh ts, Mirror front light	Strip, Wall light,	Spotlights	Spotlights, Strip	
Lighting method	Direct lighting	indirect lighting	indirect lighting	Direct lighting	Direct&indi rect lighting	
Photo						

The mother and baby room on the 2nd floor of Qiantan Taikooli on the is a large mother and baby room, clearly divided internally into a play area, a nursing area and a breastfeeding area. The nursing area provides ambient lighting with light strips, functional lighting with spotlights shining down on the sink and diaper table, and ambient lighting with low color temperature wall luminaires. The horizontal illumination level of the sink and diaper table is well above the standard requirement of 200 lx. However, Babies lying on the diaper table can see significant direct glare by spotlights. The ceiling of the play area is also spotlighted with strong glare. The light environment of breastfeeding area is indirect lighting, with light strips and wall luminaires. The horizontal illuminance of the sofa in the nursing area is 53.32lx, which can basically meet the illuminance demand of the baby nursing in a lying position.

#### 4.3 Light environment measurement result and problem summary in the mother and baby room on the 2nd floor of Ruihong Hall of Sun

Table 6. Light environment parameters in the mother and baby room on the 2nd floor of Ruihong Hall of Sun

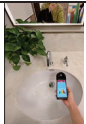




Area	Nursing Area (Hand washing sink)	Nursing area (Diaper table)	Breastfeeding area	Waiting area	Illumination uniformity
Illuminance (lx)	508.36	151.97	416.07	194.8	0.36
Color temperature (K)	3182	2978	3052	2869	
Luminaires type	Strip	Spotlights	Spotlights	Strip	
Lighting	Direct lighting	Direct lighting	Direct lighting	indirect	

method				lighting	
Photo					

The mother and baby room on the 2nd floor of Ruihong Hall of the Sun is equipped with only three spotlights on the ceiling, which are located near the entrance, the washbasin and the nursing chair. The horizontal illumination level at the sink is more than 500 lx. While the illumination level at the diaper table is only about 150 lx. The illumination level at the breastfeeding area is above 400 lx. The illuminance at the diaper table is dark, which cannot fully meet the baby's care needs. And the illuminance at the nursing area is too high, which will cause the baby's visual discomfort. Besides, the internal illuminance distribution is unreasonable. And the uniformity of illuminance in the space is only 0.38. Most of the nursing mothers interviewed were not satisfied with the indoor lighting. They thought the harsh light was unfriendly to their little babies.

#### 4.4 Light environment measurement result and problem summary in the mother and baby room on the 2nd floor of Sun Moon Light Center

Table 7. Light environment parameters in the mother and baby room on the 2nd floor of Sun Moon Light Center

Area	Nursing Area (Hand washing sink)	Nursing area (Diaper table)	Breastfeeding area	Waiting area	Illumination uniformity
Illuminance (lx)	496.7	456.4	91.7	276.4	0.83
Color temperature (K)	3257	3154	2986	3580	
Luminaires type	Mirror front light	Strip	Strip	Strip, Spotlights	
Lighting method	Direct lighting	Direct lighting	Indirect lighting	Direct&indirect lighting	
Photo					

The mother and baby room on the 3rd floor of Sun Moon Light Center provides ambient lighting with a combination of uniformly illuminated ceiling lights and light strips. And the mirror of the sink is set with a mirror front light. The overall brightness of the space is high with good uniformity. The illumination levels of the nursing areas are above 400lx. Although indirectly illuminated, the luminance at the nursing chair still reaches 90 lx. The luminance at the 1.2m level of the mother and baby room is more than 200 lx, which can meet the visual demand. However, some mothers interviewed thought the space make them feel too bright and uncomfortable.

## 5、CONCLUSION

By statistics and analysis of the natural and artificial light environment of 33 commercial space mother and baby rooms in Shanghai, as well as light environment measurements and interviews in four mother and baby rooms with different lighting methods and luminaire layout, it is found that the light environment of mother and baby spaces has problems such as lack of natural lighting, irrational luminaire settings, non-adjustable color temperature illumination, insufficient illumination in the nursing area, excessive illumination in the breastfeeding area, and glare. The light environment design of mother and baby room could be optimized from the following aspects:

1. Light strips or uniformly illuminated ceiling luminaires are recommended, while spotlights are not recommended, whether in the breastfeeding area, nursing area, or play area. The color temperature and illumination of the luminaires should be adjustable to meet the needs of mothers and babies for nursing, sleeping and breastfeeding.

2. Indirect lighting environment is softer and more uniform, bringing a stronger sense of privacy. So it is recommended to use indirect light-emitting strip in mother and baby rooms. The light strip can be set in the ceiling, behind the mirror, under the sink countertop recess or ground recess, to meet the increased horizontal illumination and ensure the overall space illumination uniformity.

3. In order to increase the comfort, pleasure and relaxation of the space, the color temperature of the light is recommended to be controlled below 3000K. Local colored light can be used to create a relax atmosphere, but the overall space is not recommended to use colored light because the overall illumination may be too low for caring for babies.

4. The guide system of mother and baby room could be designed with low color temperature light box or backlight, which can not only keep consistent with the sense of light atmosphere inside the mother and baby room, but also increase the identifiability of mother and baby room in public places.

## REFERENCES

- [1] U.S. Department of Health and Human Services. Executive Summary: The Surgeon General's Call to Action to Support Breastfeeding. Off SurgGen. 2011.
- [2] United Nations International Children's Emergency Fund. Breastfeeding room guide. 2020.
- [3] York L, Lee J. Best Practices: Lactation/Wellness Room Design. New York, NY: American Institute of Architects, 2016.
- [4] Anthony K H, Bernard M. Priming the Pump-Lactation Room Design Guidelines. 2018.

## ACKNOWLEDGEMENTS

Corresponding Author Name: Luoxi Hao  
Affiliation: Tongji University  
e-mail: [haoluoxi@tongji.edu.cn](mailto:haoluoxi@tongji.edu.cn)

Corresponding Author Name: Shujian Dai  
Affiliation: Tongji University  
e-mail: [529457841@qq.com](mailto:529457841@qq.com)

# EFFECTS OF CHROMATIC LIGHT WITH DIFFERENT SPECTRAL DISTRIBUTION ON EEG DURING EYES CLOSED CONDITION

Jun Mukondo, Hiroshi Takahashi

(Department of Electrical and Electronic Engineering, Kanagawa Institute of Technology,  
Japan)

## ABSTRACT

Sleep is an essential part of peoples' daily lives. Most people adjust the room lighting before falling asleep. Numerous studies have shown that light affects alertness and work efficiency; however, the effects of exposure to light when the eyes are closed, such as during sleep, is unclear. In this study, we examined the effect of light colours with different spectral distributions on the electroencephalogram (EEG) of subjects in the setting of closing their eyes and falling asleep. This was analyzed based on the content of theta waves, and the results showed that blue light, which contains more short-wavelength components, is the most suitable for falling asleep.

Keywords: spectral distribution, EEG, LED, falling asleep

## 1. INTRODUCTION

Medical care has developed dramatically with advances in medicine and equipment. In the field of nursing, treatment is being improved not only in terms of instrumental treatment, but also in terms of patient physical management. In particular, the quality of patient's sleep is considered important, and various studies are being conducted daily. Sato et al. observed the difference in sleep quality between subjects under warm and cold lighting for 7 days and found that the warm lighting was superior to the cold lighting[1]. In addition, Yoshinaga et al.'s experiments on the effects of different light preferences on sleep quality showed that sleep quality was superior when subjects were under their preferred light environment compared to when they were not[2]. While these studies are among the few studies on sleep and lighting environments, both experiments were characterized as comparisons of two conditions. The purpose of this study is to clarify the effects on sleep quality of the three primary colours of light, red, green, and blue, under two conditions with different spectral distributions, assuming any light environment, based on physiological indices using electroencephalogram(EEG).

## 2. EXPERIMENT

### 2.1 Method

The experiment was conducted in a darkroom, which was equipped with a reclining chair open to the prone position and a lighting environment adapted to the conditions. The darkroom environment was shielded from the outside world to eliminate physical factors other than illuminance as much as possible, and the room temperature was kept at a comfortable level for the subjects. Subjects were asked not to wear jackets and clothes that would cause physical discomfort while in the supine position. After entering the darkroom, subjects were asked to close their eyes on cue, which signalled the start of the experiment. The duration of the experiment was 20 minutes after the subjects entered the darkroom and closed their eyes. Electrodes of the electroencephalograph were placed at three points on the occiput (P3, P4) and earlobe (A1) according to the international 10/20 method. Electrodes of the electroencephalograph were placed from the beginning of the experiment (eyes closed) to the end of the experiment (20 minutes later).

### 2.2 Conditions

The subjects were eight males in their 20s with normal colour vision. For each of the three primary colours of light (red, green, and blue), two types of light with different spectral distributions were used: RGB, which contains more short-wavelength components, and RGB, which contains more long-wavelength components. The illuminance of all light sources was set so that the subject's face was illuminated at 6 lx. These conditions are shown in Table 1.

Table 1. Experimental conditions

Subjects	8 males in their 20s with normal colour vision
Light colour	R,G,B short wavelength, long wavelength ( $R_S, R_L$ $G_S, G_L$ $B_S, B_L$ )
Illuminance [lx]	6
Duration of experiment [min]	20
Subject's condition	Closed eyes, Elevated position

### 2.3 Analysis

To make measurements based on physiological indices, this experiment was conducted using EEG as an index. The analysis was performed from the time the subject's eyes closed on cue until the end of the experiment 20 minutes later. EEG analysis was based on content rate, and the content rate of theta waves generated during that time was analysed in 2-minute increments over the duration of the experiment. The next section, "Experimental Results," will deal with the content rate of the theta group as a measure of sleep depth.

## 3. RESULTS

### 3.1 Variation in the content rate of theta in each condition

Figures 1 to 3 show the variation in the content rate of theta in each condition; from Figure 1, the red light colour was almost the same from the initial to the final value with almost no difference between  $R_S$  and  $R_L$  over time. Figure 2 shows that the initial content rate of green light colour was approximately 19% for  $G_L$  and  $G_S$ , respectively, while the final values were 21.6% for  $G_S$  and 26.9% for  $G_L$ , indicating that  $G_L$  had a higher content rate than  $G_S$ . Figure 3 shows that the initial value of blue light for both  $B_S$  and  $B_L$  is about 19%, while the final value for  $B_S$  is 31.0% and 23.7% for  $B_L$ , indicating that  $B_L$  has a higher content rate than  $B_S$ . No trend was observed between the long wavelength component-rich ( $R_L$ ,  $G_L$ ,  $B_L$ ) and short wavelength component-rich ( $R_S$ ,  $G_S$ ,  $B_S$ ) groups.

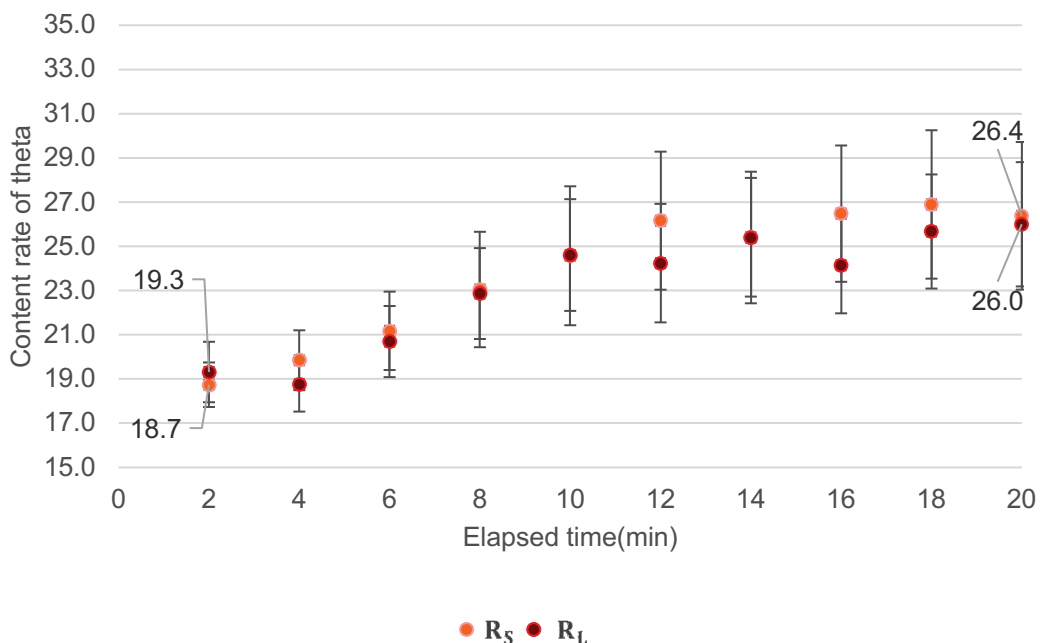


Figure 1 Relationship between elapsed time and content rate of theta wave in red light



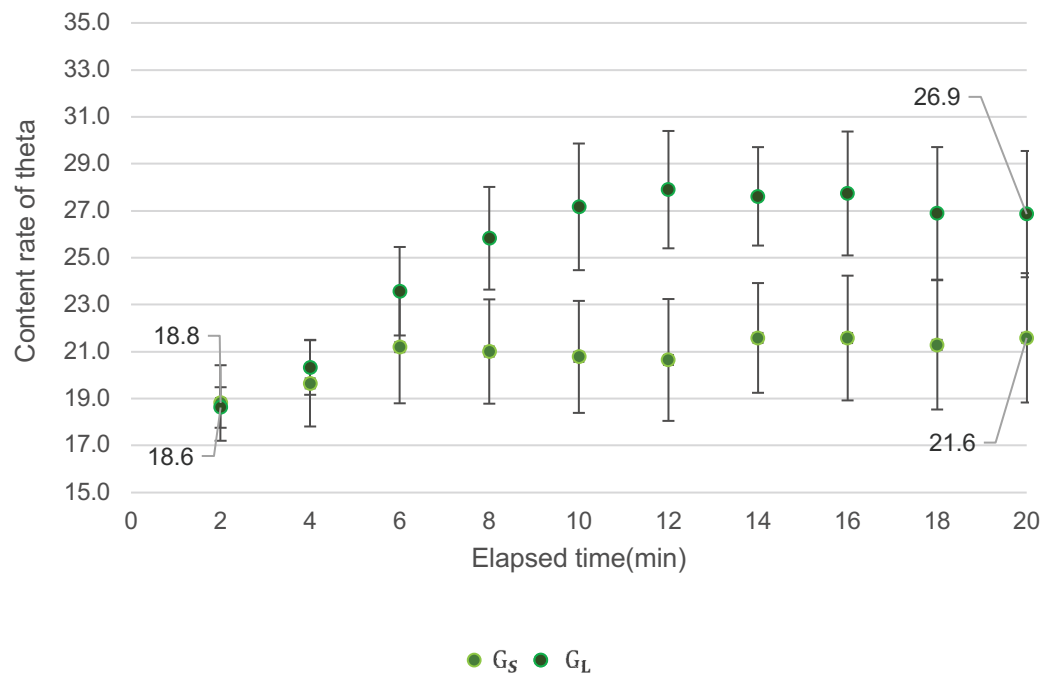


Figure 2 Relationship between elapsed time and content rate of theta wave in green light

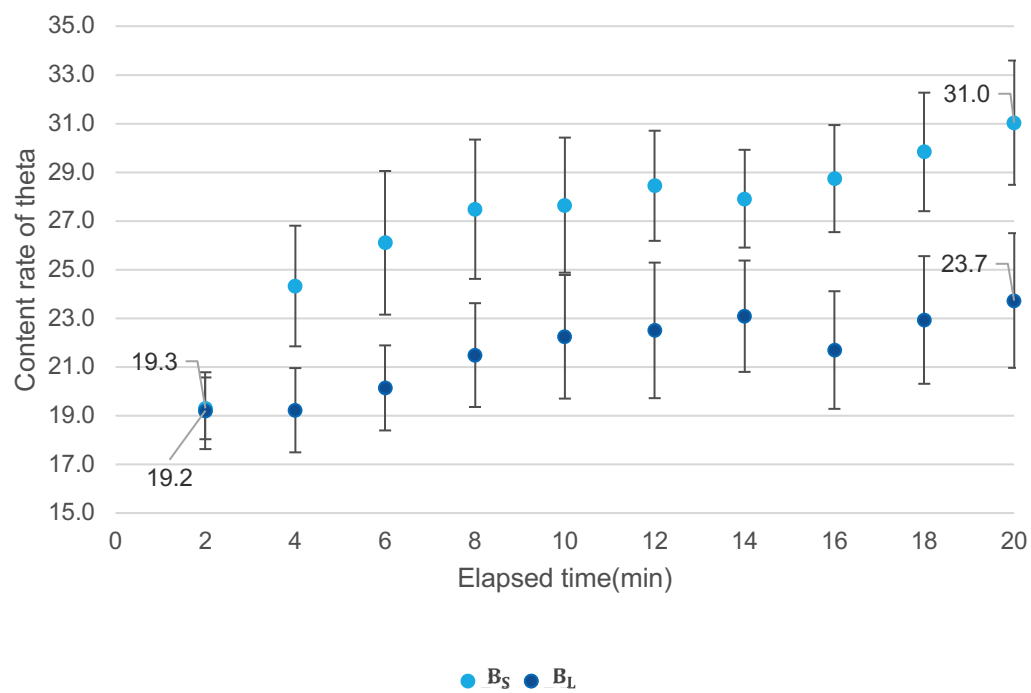


Figure 3 Relationship between elapsed time and content rate of theta wave in blue light

### 3.2 Comparison of initial and final values of content ratio for each light condition

Table 2 compares the initial and final values of the content rate under each light condition and summarizes them as a percentage increase. Table 2 shows that the highest rate of increase was observed for the B<sub>s</sub> light condition, followed by the G<sub>L</sub> and R<sub>s</sub> conditions, in that order. Conversely, the lowest rate of increase was observed for the G<sub>s</sub> condition.

Table 2 Comparison of initial and final values of content rate under each lighting condition

	Initial values (%)	Final values (%)	percentage increase
<b>R<sub>s</sub></b>	18.7	26.4	<b>1.41</b>
<b>R<sub>L</sub></b>	19.3	26.0	<b>1.35</b>
<b>G<sub>s</sub></b>	18.8	21.6	<b>1.15</b>
<b>G<sub>L</sub></b>	18.6	26.9	<b>1.44</b>
<b>B<sub>s</sub></b>	19.3	31.0	<b>1.61</b>
<b>B<sub>L</sub></b>	19.2	23.7	<b>1.24</b>

According to a study by Sato et al., "the warm colour tendency was predominant for sleep in warm and cold lighting"[1], which is different from the experimental results of the present study. In addition, a comparison of this experiment with the experiment by Sato et al. shows a difference in the time of day and night, and it is possible that the difference in the generation rate of melatonin in the body between the experiment conducted at night and the experiment conducted during the daytime caused a difference in physiological indices in response to illuminance, which requires further investigation. However, according to a study by Ogasawara et al., "blue light has the effect of inducing sleep"[3], and we would like to take this into account in the results of this experiment, which assumes falling asleep.

### 4. CONCLUSION

The highest rate of increase in theta waves was observed in the B<sub>s</sub> light condition and the lowest rate of increase in theta waves was observed in the G<sub>s</sub> light condition.

This study was approved by the Ethical Review Board for the use of human subjects of Kanagawa Institute of Technology (No.20220325-01).

### REFERENCE

- [1] Akemi Sato, Tomoe Kikuchi, Rie Sugawara, Megumi Imano, Kimiko Hurukawa, Noriko Watanabe: "Verification of light colours that do not disturb the sleep of patients requiring observation," National Hospital Organization Sendai Medical Centre, Nursing Department, East Wing, Ward 6 (March 7, 2010)
- [2] Naoki Yoshinaga, Mizuho Fujita, Yuji L. Tanaka: "Basic Research on Individual Differences in Preferences and Biological Responses to Illuminance at Sleep Onset: Effects on Physiological Function and Subjective Evaluation," Journal of the Japanese Society of Nursing Technology Vol. 10, No. 2 (2010).
- [3] Ogasawara Masahiro, Hirao Takahashi, Shizuo Fujita: "Medical Applications of Light Emitting Diodes: Effects on Sleep," Materials Vol. 66 (2017), No. 9.

Corresponding Author: Mukondo Jun

Affiliation: Department of Electrical and Electronic Major subject, Kanagawa Institute of Technology

e-mail : nekomander0127@outlook.com

# POSSIBLE IMPACT ON SLEEP QUALITY CAUSED BY EXTERIOR LIGHTING IN COMMERCIAL BUSINESS DISTRICTS AT NIGHT

Shenfei Chen<sup>1</sup>, Yi Lin<sup>1\*</sup>, Qi Yao<sup>2</sup>, Xianxian Zeng<sup>1</sup>, Bing Zhang<sup>1</sup>

<sup>1</sup>College of Architecture and Urban Planning, Tongji University, Shanghai, China

<sup>2</sup>Academy for Engineering and Technology, Fudan University, Shanghai, China)

## ABSTRACT

Industrialization and urbanization have dramatically altered the daytime and nighttime light exposure in cities, and the wide-spread artificial light at night (ALAN) is altering human health. Policymakers, researchers and lighting management bodies are exploring strategies for controlling light pollution from external lighting. We report a series of field measurements to quantify the responses of different human photoreceptors and the possible suppression of melatonin production caused by the exterior lighting in metropolises. A total of 17,612,800 spectral and 50 hyperspectral imaging images were collected at 5.6 ft. above the ground in seven commercial business districts in Shanghai. The investigation of seven commercial districts reveals that the luminance distribution of urban nighttime illumination primarily falls within the range of 5-25 cd/m<sup>2</sup>, with certain scenes exhibiting luminance levels of 25-50 cd/m<sup>2</sup>. A significantly large proportion of scenes display higher luminance exceeding 200 cd/m<sup>2</sup>, which can be attributed to the presence of self-luminous fixtures within the scenes. It was found that all lighting scenes could potentially affect the sleep quality of nighttime pedestrians, as characterized using melanopic equivalent daylight (D65) illuminance (melanopic EDI), because they had at least 40% area (in some areas exceeding 90%) with melanopic EDI values beyond 10 lx, a working threshold for the maximum melanopsin cell EDI before bedtime by 3 hours.

Keywords: Artificial light at night; Light pollution; Circadian rhythm

## 1. INTRODUCTION

The industrialization and urbanization have had significant impacts on the illumination of urban areas during both day and night. The widespread dissemination of artificial light at night (ALAN) is currently affecting human health. Research has revealed that human health is regulated by the photoperiodic rhythm<sup>[1-4]</sup>, while extensive ALAN during the night prolongs the duration and intensity of urban nocturnal illumination, disrupting physiological processes such as the internal circadian clock and melatonin secretion in the human body. This may lead to health issues including insomnia, depression, and metabolic disorders. For a long time, the lack of effective regulation and assessment indicators has resulted in the misuse of artificial light worldwide, and both urban and rural areas are living under increasingly brighter night skies<sup>[5, 6]</sup>. Moreover, excessive nighttime lighting also has negative effects on wildlife, plant ecosystems, and stargazing<sup>[7-10]</sup>. Policymakers, researchers, and lighting management organizations are exploring strategies to control external light pollution.

Previous studies have revealed that even in individuals with complete blindness, there are persistent physiological responses to light stimulation on the eyes<sup>[11-13]</sup>. Consistent evidence from human and animal research indicates that these non-visual responses, including impacts on the circadian system, melatonin secretion, sleep/wakefulness, and pupil constriction, are mediated by a specialized type of retinal neurons called intrinsically photosensitive retinal ganglion cells (ipRGCs)<sup>[2, 14]</sup>. The photopigment within ipRGCs is melanopsin, which in humans, is most sensitive to photons in a distinct portion of the visible light spectrum separate from cone photopigments ( $\lambda_{max} \approx 480\text{nm}$ )<sup>[15-17]</sup>.

In 2013, the Lucas team proposed a system that weighted irradiance based on the spectral sensitivity of five known human retinal photopigments (melanopsin, rhodopsin, S-, M-, and L-cone opsins)<sup>[18]</sup>. In 2018, this framework was formally established as an international standard and incorporated into a measurement system that complies with the SI standards to quantify the impact of ipRGCs on light (Commission Internationale de l'Eclairage (CIE) S 026)<sup>[19]</sup>. In this system, the effective photon capture rate of each human retinal photopigment under given lighting conditions is equated to the illuminance characteristics (such as intensity) of a standard 6500K (D65) daylight

spectrum that produces the same photon capture rate. This approach defines an  $\alpha$ -opic equivalent daylight illuminance (EDI) for each class of photoreceptor, where  $\alpha$ -opic represents one of the five classes of human photoreceptors that can contribute to the effects on ipRGCs, such as melanopsin.

In 2022, recommendations regarding lighting were provided based on expert scientific consensus, using a readily measurable quantity defined in the standard as melanopsin equivalent daylight illuminance (melanopic EDI). 1) The minimum vertical plane Melanopic EDI on surfaces should be 250 lx during daytime; 2) The maximum vertical plane Melanopic EDI at a position 1.2 meters prior to bedtime should be 10 lx within the last three hours<sup>[20]</sup>. These recommendations were supported by a detailed analysis of the sensitivity of human circadian rhythms, neuroendocrine systems, and alert responses to ocular light exposure. They provide a straightforward framework for lighting design and practice.

This study collected high-spectral data of architectural facade night lighting in the core commercial area of Shanghai, China, at a near-ground scale from a pedestrian's perspective. Unlike the traditional method of satellite photography from high altitudes, this high-spectral data is closer to human visual perception and offers finer-grained information. Through the analysis of the collected data, the brightness distribution of architectural facades and melanopic EDI were obtained, enabling an assessment of the impact of urban commercial area architectural facade landscape lighting on human health.

## 2. METHODS

### 2.1 Data Collection

We conducted research and data collection on the urban nighttime light environment in seven core commercial districts in Shanghai. These areas include: North Bund, Lujiazui, Bund, Nanjing East Road, Nanjing West Road, Xujiahui and Wujiaochang, as shown in Figure 1, which provides geographical location information for each region. The data was collected at a height of 5.6 ft above the sidewalk using a TOPCON SR5000-HS 2D spectroradiometer to capture hyperspectral imaging (HSI) data for each scene. The spatial resolution of the spectroradiometer is  $688 \times 512$  pixels, and it scans wavelengths from 380 to 780 nm with an interval of 5 nm. Therefore, each captured scene obtained HIS data consisting of 81 spectral layers, with 352,256 pixels per layer. This means that each pixel has spectral radiation distribution data, as shown in Figure 2. The data collection period spanned from December 2021 to October 2023. In the end, we obtained lighting data for a total of 46 scenes from 6 locations, as shown in Table 1.

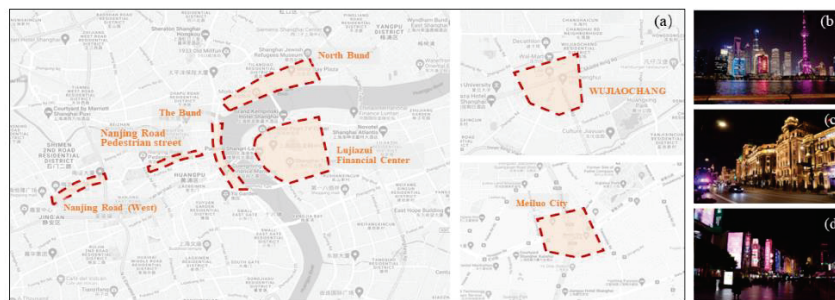


Figure 1 (a) Geographical location of seven commercial districts and (b~d) some night.

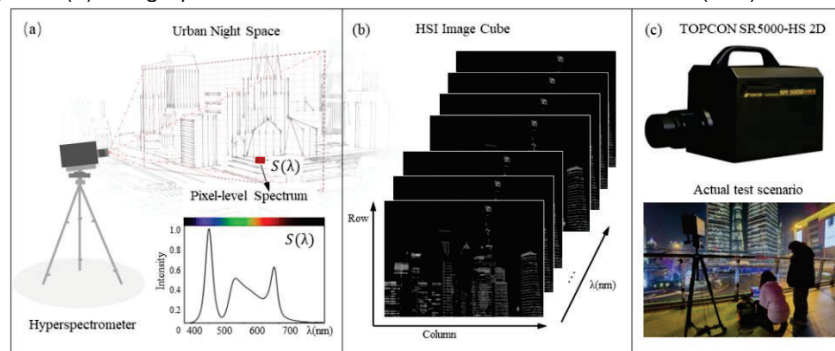


Figure 2. Hyperspectral imaging acquisition diagram.

Table1 The geographical location corresponding to the 46 scenes

location	Scene number
North Bund	1, 2, 3, 4, 5, 6, 33
Lujiazui	7, 8, 9, 25, 26, 27, 8, 29, 30, 31, 32
Bund	10, 36, 37, 38, 39, 40, 41, 42, 43, 44, 45, 46
Nanjing East Road	11, 12, 13, 14
Nanjing West Road	15, 16, 17, 18, 19
Xujiahui	20, 21, 22, 23, 24
Wujiaochang	47,48, 29, 50

## 2.1 Data Analysis

Regarding the collected nighttime landscape data, we extracted the brightness value and spectral intensity for each pixel. The brightness data was used to analyze the proportion of scene brightness intensity, while the spectral data was utilized to calculate the equivalent melanopic lux (EML) and Melanopic equivalent daylight (D65) illuminance (melanopic EDI) of the scene<sup>[18]</sup>. Detailed explanations for the calculation method can be found in the work by Robert J. Lucas et al.<sup>[21]</sup>.

$$EML = \frac{K_M \int E_{e,\lambda}(\lambda) N_Z(\lambda) d\lambda \cdot \int V(\lambda) d\lambda}{\int N_Z(\lambda) d\lambda} \quad (1)$$

$\lambda$  is the wavelength of the radiation;

$K_M = 683.002 \text{ lm/W}$ , the maximum spectral luminous efficacy;

$V(\lambda)$  is the spectral luminous efficacy function for photopic vision;

$E_{e,\lambda}(\lambda)$  is the spectral power distribution;

$N_Z(\lambda)$  is the Melanin spectral optical efficacy function;

As  $\int V(\lambda) d\lambda = 106.857$  and choosing to define  $\int N_Z(\lambda) d\lambda = 1$ , equation (1) can be simplified to an equivalent form to that calculations for photopic lux:

$$EML = 72983.25 \int E_{e,\lambda}(\lambda) N_Z(\lambda) d\lambda \quad (2)$$

Melanopic equivalent daylight (D65) illuminance (melanopic EDI) refers to the illuminance value of the standard light source D65 when it produces the same melanopic equivalent illuminance as defined by the CIE standard. The calculation formula for melanopic EDI is as follows:

$$\text{melanopic EDI} = EML \times \gamma \quad (3)$$

Whereas EML represents the melanopic equivalent lux, and  $\gamma$  is a constant with a value of 0.9063, which serves as the conversion coefficient between the numerical values of EML and melanopic EDI.

The brightness data is divided into ten levels in academic research, namely 1-5, 5-25, 25-50, 50-75, 75-100, 100-125, 125-150, 150-175, 175-200, and above 200  $\text{cd/m}^2$ . The Melanopic Effective Daylight Index (EDI) is categorized into the following ranges: 0-1, 1-10, 10-50, 50-100, 100-150, 150-200, 200-250, and beyond 250 lx.

## 3. Results

### 3.1 Luminance Distribution of Building Facades

In areas where multiple lighting types are used, there is a significant variation in façade brightness distribution. Heatmap shows the brightness proportion of 50 scenes from seven commercial districts. As show in Figure 3. The majority of areas have brightness levels below 25  $\text{cd/m}^2$  (International Commission on Illumination, 2017), but in some areas, the proportion of higher brightness levels has significantly increased. Scenes such as 5, 11, 12, 13, 14, 20, 21, 22,



23, 32, and 49 show a noticeable increase in the proportion of brightness greater than 50 cd/m<sup>2</sup>, mainly because these scenes include lights near billboards, LED screens, and projected light sources. Some areas reach brightness levels exceeding 200 cd/m<sup>2</sup>, like scenes 13, 22, 23, 24, and 32. These improperly illuminated areas on building facades pose a significant threat of light pollution to the nighttime environment on the ground.

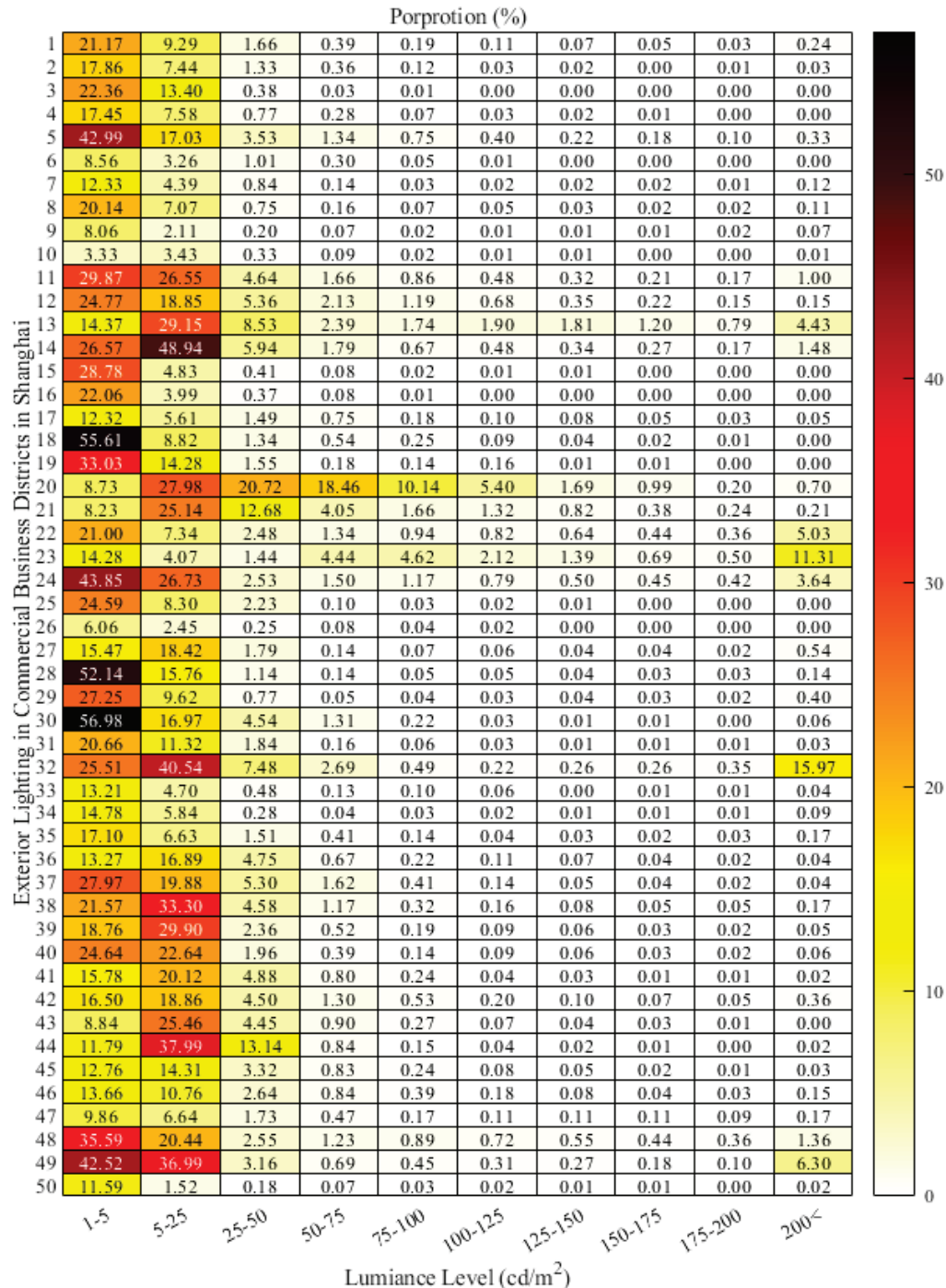


Figure 3. Proportion of luminance in different ranges of night lighting scenes in 50 commercial areas.

According to CIE:150-2017 (International Commission on Illumination, 2017), the lighting environment in this survey corresponds to well-residential urban areas and commercial zones, representing medium and high bright zones (E3 and E4), with maximum recommended luminance limits of 800 cd/m<sup>2</sup> and 1000 cd/m<sup>2</sup>, respectively. Although the proportion of high-brightness facades is relatively low across the entire surveyed area, some screens and billboards exceed 1000 cd/m<sup>2</sup> of brightness, creating a strong contrast with the surrounding darker environment, as shown in Figure 4.

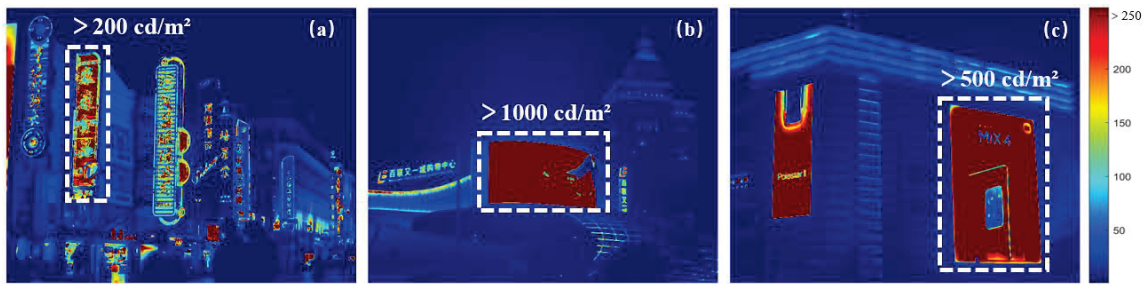


Figure 4. Brightness distribution of some scenes: the brightness of the signboard in (a) is greater than 200  $\text{cd/m}^2$ , the display brightness in (b) is greater than 1000  $\text{cd/m}^2$ , and the brightness of the advertisement in (c) is greater than 500  $\text{cd/m}^2$ .

### 3.2 Melanopic EDI for the spectral dose of the building façade

The spectral data of each pixel in the scene was calculated to obtain the Melanopic Effective Daylight Index (EDI) at the pixel location using formulas (1)-(3), as shown in Figure 5. Similarly, we generated a Heatmap image representing the Melanopic EDI values in each scene based on the analysis methodology outlined in Section 2.1, as depicted in Figure 6.



Figure 5 Live-action images in some scenes and distributed images of Melanopic EDI.

Based on Figure 6, it is evident that the majority of scenes exhibit a significant proportion of Melanopic Effective Daylight Index (EDI) values below 1 lx, which is closely related to the proportion of sky present in the scenes. This implies that excluding the portion below 1 lx, the remaining proportion can be attributed to artificial lighting. Among them, the mean proportions of 1-10, 10-50, 50-100, 100-150, 150-200, 200-250 and greater than 250 lx were 17.85%, 9.68%, 6.13%, 4.27%, 3.15%, and 19.68, respectively. Among them, 1-10, 10-50, and larger than 250 lx proportions are the largest. In certain scenes, the proportion of EDI exceeding 250 lx exceeds 60%, indicating a greater influence of artificial lighting on the suppression of melatonin production in such scenarios. In 2022, experts reached a consensus regarding illumination recommendations for daytime and nighttime conditions: 1) The minimum vertical plane Melanopic EDI on surfaces should be 250 lx during daytime; 2) The maximum vertical plane Melanopic EDI at a position 1.2 meters prior to bedtime should be 10 lx within the last three hours<sup>[20]</sup>. Figure 7 illustrates the percentage of scenes with Melanopic EDI values exceeding 10 lx in 50 urban commercial districts' nighttime lighting. It is evident from the graph that the majority of scenes exhibit a proportion exceeding 40% for EDI values above 10 lx, with some even exceeding 90%.

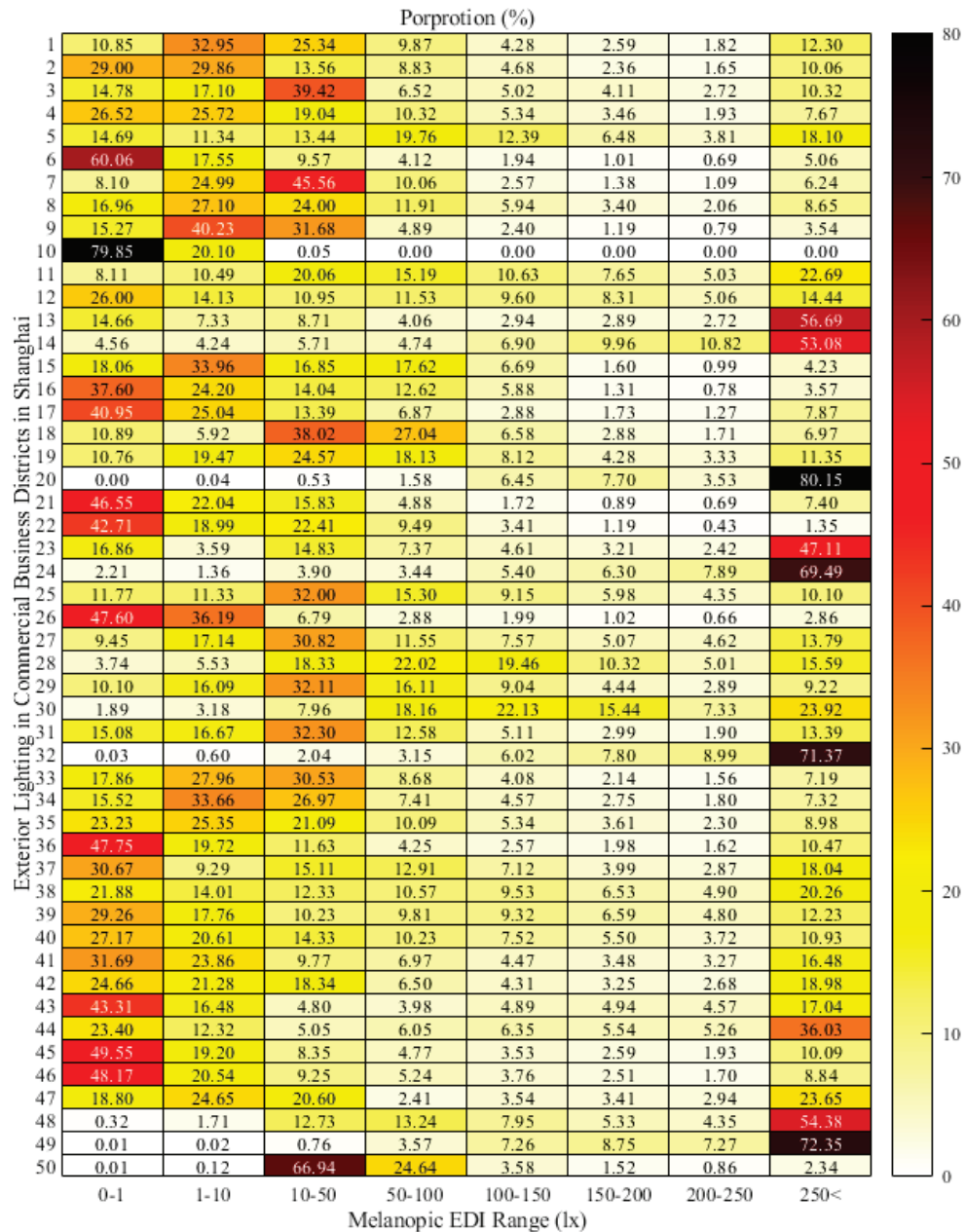


Figure 6 Proportion of Melanopic EDI in different ranges of night lighting scenes in 50 commercial areas.

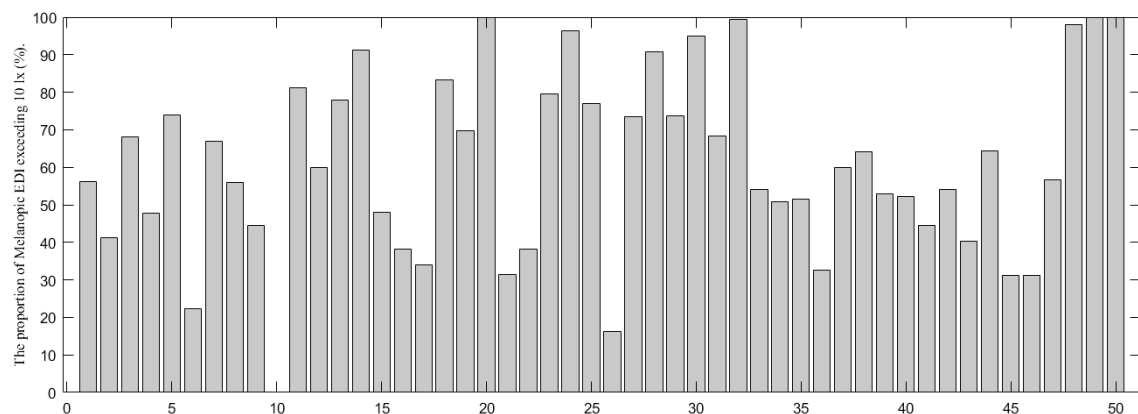


Figure 7. Proportion of Melanopic EDI with a scale greater than 10 lx in 50 commercial areas.

#### 4. CONCLUSION

In the investigation of seven commercial districts in Shanghai, the luminance distribution of urban nighttime lighting mainly falls within the range of 5-25 cd/m<sup>2</sup>, with some scenes reaching a luminance of 25-50 cd/m<sup>2</sup>. A significant proportion of scenes exhibit higher luminance exceeding 200 cd/m<sup>2</sup>, which is primarily attributed to the influence of large-scale self-luminous facilities such as billboards, architectural signage, and media facades within the scenes. Consequently, effectively controlling the luminance of commercial district signage, advertisements, and media screens becomes a necessary measure for mitigating light pollution. Among the 50 nighttime lighting scenes in commercial districts, the mean proportions of luminance ranging from 1-10, 10-50, 50-100, 100-150, 150-200, 200-250, and greater than 250 lx are 17.85%, 9.68%, 6.13%, 4.27%, 3.15%, 19.68%, respectively. The highest proportions are observed in the ranges of 1-10, 10-50, and greater than 250 lx. According to expert consensus, it is recommended that the Melanopic Effective Daylight Index (EDI) be below 10 lx in the three hours prior to sleep onset. However, in the majority of these 50 lighting scenes, the proportion of scenes with an EDI exceeding 10 lx surpasses 40%, with some scenes even exceeding 90%, indicating a certain impact of urban nighttime lighting on the sleep quality of nocturnal pedestrians.

#### REFERENCE

- [1] LUCAS R., HATTAR S., TAKAO M., BERSON D., FOSTER R. & YAU K.-W. Diminished pupillary light reflex at high irradiances in melanopsin-knockout mice *Science* (New York, NY), 2003, 299: 245-7.
- [2] BERSON D. M. Strange vision: ganglion cells as circadian photoreceptors *Trends in Neurosciences*, 2003, 26(6): 314-20.
- [3] REA M. S., BULLOUGH J. D. & FIGUEIRO M. G. Phototransduction for human melatonin suppression *Journal of Pineal Research*, 2002, 32(4): 209-13.
- [4] THAPAN K., ARENDT J. & SKENE D. J. An action spectrum for melatonin suppression: evidence for a novel non-rod, non-cone photoreceptor system in humans *The Journal of Physiology*, 2001, 535(1): 261-7.
- [5] FALCHI F., FURGONI R., GALLAWAY T. A., RYBNIKOVA N. A., PORTNOV B. A., BAUGH K., CINZANO P. & ELVIDGE C. D. Light pollution in USA and Europe: The good, the bad and the ugly *Journal of Environmental Management*, 2019, 248: 109227.
- [6] FALCHI F., CINZANO P., DURISCOE D., KYBA C. C. M., ELVIDGE C. D., BAUGH K., PORTNOV B. A., RYBNIKOVA N. A. & FURGONI R. The new world atlas of artificial night sky brightness *Science Advances*, 2016, 2(6): e1600377.
- [7] WALKER W. H., BUMGARNER J. R., BECKER-KRAIL D. D., MAY L. E., LIU J. A. & NELSON R. J. Light at night disrupts biological clocks, calendars, and immune function *Semin Immunopathol*, 2022, 44(2): 165-73.
- [8] MURPHY S. M., VYAS D. K., SHER A. A. & GRENIS K. Light pollution affects invasive and native plant traits important to plant competition and herbivorous insects *Biol Invasions*, 2022, 24(3): 599-602.
- [9] LI D., HUANG J., ZHOU Q. M., GU L., SUN Y. F., ZHANG L. & YANG Z. Artificial Light Pollution with Different Wavelengths at Night Interferes with Development, Reproduction, and Antipredator Defenses of *Daphnia magna* *Environ Sci Technol*, 2022: 11.
- [10] ŚCIEŻOR T. Light pollution as an environmental hazard *Technical Transactions*, 2019, 116: 129 - 42.
- [11] HULL J. T., CZEISLER C. A. & LOCKLEY S. W. Suppression of Melatonin Secretion in Totally Visually Blind People by Ocular Exposure to White Light: Clinical Characteristics *Ophthalmology*, 2018, 125(8): 1160-71.
- [12] KLIERMAN E. B., SHANAHAN T. L., BROTMAN D. J., RIMMER D. W., EMENS J. S., RIZZO J. F., 3RD & CZEISLER C. A. Photic resetting of the human circadian pacemaker in the absence of conscious vision *J Biol Rhythms*, 2002, 17(6): 548-55.
- [13] CZEISLER C. A., SHANAHAN T. L., KLIERMAN E. B., MARTENS H., BROTMAN D. J., EMENS J. S., KLEIN T. & RIZZO J. F., 3RD. Suppression of melatonin secretion in some blind patients by exposure to bright light *The New England journal of medicine*, 1995, 332(1): 6-11.
- [14] M. B. D. Phototransduction by Retinal Ganglion Cells That Set the Circadian Clock *Science*, 2002, 295(5557): 1070-3.



- [15] BAILES H. J. & LUCAS R. J. Human melanopsin forms a pigment maximally sensitive to blue light ( $\lambda_{\text{max}} \approx 479 \text{ nm}$ ) supporting activation of G(q/11) and G(i/o) signalling cascades *Proceedings Biological sciences*, 2013, 280(1759): 20122987.
- [16] GOOLEY J. J., HO MIEN I., ST HILAIRE M. A., YEO S. C., CHUA E. C., VAN REEN E., HANLEY C. J., HULL J. T., CZEISLER C. A. & LOCKLEY S. W. Melanopsin and rod-cone photoreceptors play different roles in mediating pupillary light responses during exposure to continuous light in humans *The Journal of neuroscience : the official journal of the Society for Neuroscience*, 2012, 32(41): 14242-53.
- [17] ZAIDI F. H., HULL J. T., PEIRSON S. N., WULFF K., AESCHBACH D., GOOLEY J. J., BRAINARD G. C., GREGORY-EVANS K., RIZZO J. F., 3RD, CZEISLER C. A., FOSTER R. G., MOSELEY M. J. & LOCKLEY S. W. Short-wavelength light sensitivity of circadian, pupillary, and visual awareness in humans lacking an outer retina *Current biology : CB*, 2007, 17(24): 2122-8.
- [18] LUCAS R. J., PEIRSON S. N., BERSON D. M., BROWN T. M., COOPER H. M., CZEISLER C. A., FIGUEIRO M. G., GAMLIN P. D., LOCKLEY S. W., O'HAGAN J. B., PRICE L. L. A., PROVENCIO I., SKENE D. J. & BRAINARD G. C. Measuring and using light in the melanopsin age *Trends in Neurosciences*, 2014, 37(1): 1-9.
- [19] 026/E:2018 C. S. CIE System for Metrology of Optical Radiation for ipRGC-Influenced Responses to Light: [S]. Vienna: CIE Central Bureau, 2018:
- [20] BROWN T. M., BRAINARD G. C., CAJOCHEN C., CZEISLER C. A., HANIFIN J. P., LOCKLEY S. W., LUCAS R. J., MÜNCH M., O'HAGAN J. B., PEIRSON S. N., PRICE L. L. A., ROENNEBERG T., SCHLANGEN L. J. M., SKENE D. J., SPITSCHAN M., VETTER C., ZEE P. C. & WRIGHT K. P., JR. Recommendations for daytime, evening, and nighttime indoor light exposure to best support physiology, sleep, and wakefulness in healthy adults *PLoS biology*, 2022, 20(3): e3001571.
- [21] LUCAS R. J., PEIRSON S. N., BERSON D. M., BROWN T. M., COOPER H. M., CZEISLER C. A., FIGUEIRO M. G., GAMLIN P. D., LOCKLEY S. W., O'HAGAN J. B., PRICE L. L. A., PROVENCIO I., SKENE D. J. & BRAINARD G. C. Irradiance toolbox user guide *Trends in Neurosciences*, 2014.

## ACKNOWLEDGEMENT

This work was supported by the National Natural Science Foundation of China (grant no. 52078357).

Corresponding Author: Yi Lin

Affiliation: College of Architecture and Urban Planning, Tongji University

e-mail: [linyi\\_tjcaup@tongji.edu.cn](mailto:linyi_tjcaup@tongji.edu.cn)



# MULTI-OBJECTIVE ANALYSIS OF VISUAL AND ENERGY PERFORMANCE OF SOLAR FAÇADES FOR OFFICE BUILDINGS IN FIVE DIFFERENT DAYLIGHT CLIMATE ZONES IN CHINA

Yuyan WANG<sup>1</sup>, Tongyue WANG<sup>2,3</sup>, Lixing YANG<sup>4</sup>, Luoxi HAO<sup>3,5</sup>

1. School of Architecture, The University of Sheffield, Sheffield S10 2TN, UK
2. Shanghai Yangzhi Rehabilitation Hospital (Shanghai Sunshine Rehabilitation Center), School of Medicine, Tongji University, Shanghai 201619, CHINA,
3. College of Architecture and Urban Planning, Tongji University, Shanghai, CHINA,
4. China Construction Seventh Bureau Urban Investment Operation Management Co., Ltd, Zhengzhou, CHINA,
5. Key Laboratory of Ecology and Energy-saving Study of Dense Habitat (Tongji University), Ministry of Education, Shanghai 200092, CHINA

## ABSTRACT

Population growth and urban expansion have led to increasing demand for buildings. Optimizing building façade design with integrated photovoltaic shading (PVSD) can reduce building energy consumption while ensuring a comfortable indoor light and thermal environment. However, few studies have focused on optimizing façades based on indoor light comfort with integrated PV. Therefore, this study investigates the association of high-density urban office building façades with indoor light environments and their potential as a productive integration. The indoor light environment of typical office buildings in five different Daylight Climate Zone in China and their façades were investigated. Visual comfort, power generation and a set of workflows for regulating the indoor lighting environment with self-produced power are considered, and the optimal façade configuration is selected from the established model library. The integrated module effectively improves the indoor lighting and visual comfort of the space, resulting in an average light comfort of 66.5%. And it also met 7-13.5% of the annual per capita electricity demand of the office. This study can guide other densely populated cities to promote the research and construction of solar façades to improve the visual comfort of office spaces and reduce energy consumption.

Keywords: Solar façade; photovoltaic shading; Daylighting; Useful daylight illuminances; visual comfort; Energy production

## 1. INTRODUCTION

In most developed countries, the building sector accounts for over one-third of the total energy consumption[1] and contributes to global greenhouse gas emissions[2]. Given the prevailing energy crisis, there has been a growing emphasis on energy efficiency in architectural design. Particularly in China, which boasts the world's largest building market[3], rapid urbanization and expansion have increased energy demand and carbon emissions[4]. Public buildings comprise 21.3% of the overall building stock in China, with their energy consumption amounting to 33.2% of the total building energy consumption, with office buildings representing the largest portion[5].

Given that the building envelope plays a crucial role in the energy consumption of buildings, numerous studies have been dedicated to reducing net energy consumption while maintaining indoor comfort[6]. Grondzik and Kwok[7] have identified that the energy consumption of office buildings is influenced by orientation and factors such as layout patterns and geometric forms. Additionally, Lim et al. [10] emphasize that well-designed glazing on the façade and appropriate shading devices can significantly improve daylight conditions and reduce the demand for lighting energy. However, excessive direct solar radiation can result in user discomfort due to overheating and glare issues[11]. Consequently, shading devices are typically strategically oriented and inclined to mitigate unnecessary direct sunlight and radiation effectively, thereby preventing overheating and glare.

Solar energy is one of the most popular renewable sources due to its abundance, cleanliness, and inexhaustibility. Moreover, photovoltaic technology enables the capture and conversion of light

energy into usable energy at a reasonable cost. Building-integrated photovoltaics (BIPV) entails the incorporation of photovoltaic modules into the building envelope[12], thereby granting the building the capability to generate electricity. On the other hand, photovoltaic shading devices (PVSD), as one of these integration methods, not only produce electricity but also regulate and block the influx of sunlight and solar radiation through windows[13]. This functionality contributes to reduced cooling requirements during summers and improved natural indoor lighting conditions, ultimately enhancing the overall energy performance of buildings[14]. Research has demonstrated that the implementation of photovoltaic devices can yield savings of 50-80% in artificial lighting[15], as well as reductions of 11% in cooling energy consumption and 13% in electricity consumption[16]. These advanced building components form a complex boundary between the internal and external spaces of a building, and their performance significantly influences the visual and thermal quality of the indoor environment, as well as the energy conversion efficiency of the system[17].

Optimal lighting conditions in the workspace significantly enhance productivity by improving visual comfort[18]. Additionally, the solar gain facilitated by PVSD aids in reducing energy consumption for both space heating and electric lighting. However, using large shading devices that excessively block solar radiation may result in increased reliance on artificial lighting, counteracting some of the original benefits, despite greater energy conversion by the PV material. Consequently, the modulation of sunlight through PVSD becomes a complex yet crucial measure to maintain comfortable thermal and visual conditions. The most effective control methods for PVSD should be adaptable to factors such as climate characteristics, building type, and building orientation[13]. Consequently, research on PVSD focuses on four primary aspects: the angle and arrangement of PV panels, the axis of rotation, the PV cell material, and the panel size, as these factors are closely intertwined with the energy efficiency and indoor comfort achieved through PVSD implementation.

This study focuses on office buildings in five distinct Daylight-climate zones in China: Lhasa, Kunming, Beijing, Shanghai, and Chongqing. The optimization of building-integrated photovoltaic (BIPV) systems and office building facades varies across regions due to the differences in average solar radiation levels among the light-climate zones. This study aims to investigate the methods and potential of integrating PV shading into office buildings in these five cities situated in diverse daylight-climate zones in China. A multi-objective analysis of the integrated façade configuration was conducted to determine the optimal PV tilt angle and application form for the specific building environment. The study aimed to enhance daytime indoor light comfort for office occupants and reduce unnecessary energy consumption.

## 2. METHODS

### 2.1 framework for optimization methods

Figure 1 illustrates the workflow employed in this study. The initial step involved determining the dimensions of the module model suitable for the specific office space. A model representing an open office measuring 7.8 m (width), 8.5 m (depth), and 3.6 m (height) was established, as depicted in Figure 2. Subsequently, evaluation criteria were defined for the façade module, with the Useful daylight illuminances (UDI) selected as an indicator for assessing indoor light comfort; while electricity production served as an indicator for evaluating the performance of the PV panel application. The next step entailed defining the variable parameters of the façade module. These parameters encompassed the size and number of rows of PV panels, the direction of the rotation axis, the tilt angle, and the type of PV cell. Combining the various permutations of these variable elements generated a library of façade prototypes, forming the basis for subsequent simulations.

In the simulation process, the initial step involved selecting representative cities from five distinct Daylight-climate zones in China and extracting their corresponding weather data[19] for subsequent simulations. The chosen cities were Lhasa (Zone I), Kunming (Zone II), Beijing (Zone III), Shanghai (Zone IV), and Chongqing (Zone V). The multi-objective optimization process relied on Rhinoceros and Grasshopper parametric modelling tools alongside performance analysis tools such as Ladybug[20], OpenStudio, Daysim[21], EnergyPlus[22], and Radiance[23]. Through these parametric simulation tools, 2,880 programs were executed for each façade module across 16 representative time points throughout the year, encompassing all five cities. Subsequently, a meritocratic procedure was employed to identify each city's most efficient façade components and determine the optimal combination of axis directions (horizontal, vertical, diagonal). A visual heat map depicting the Useful daylight illuminances of each optical module was generated.

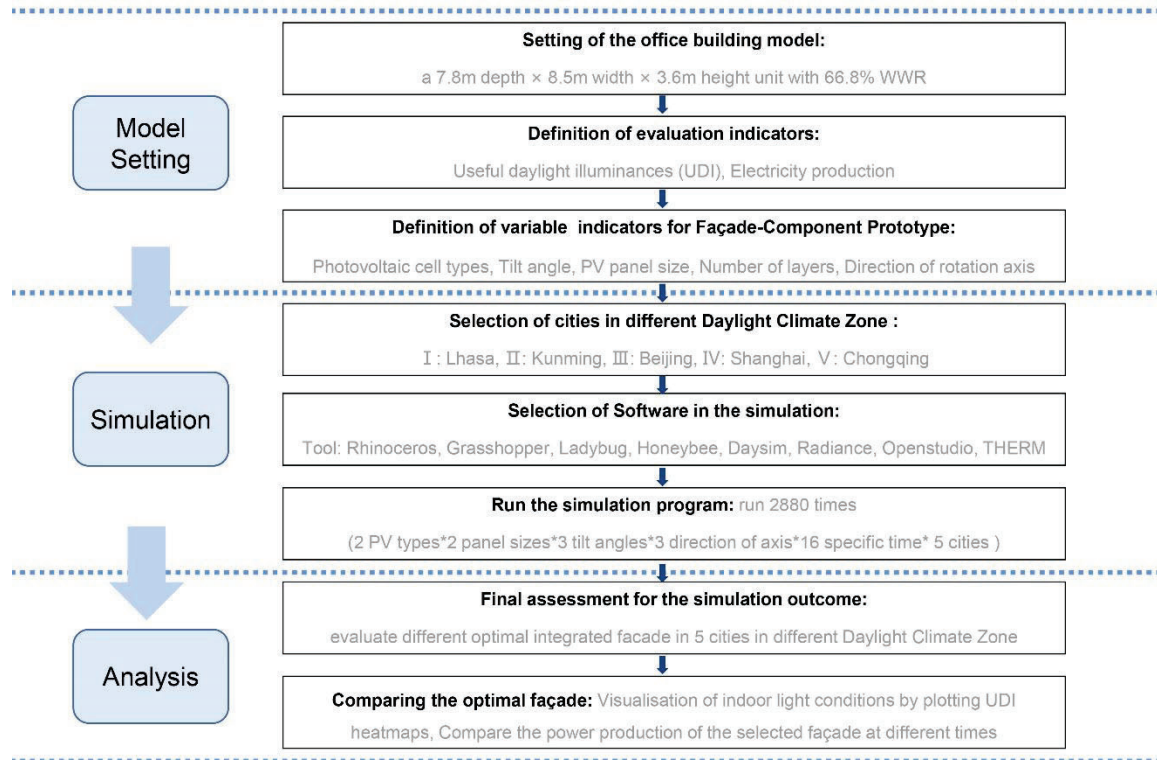


Figure 1. Overview of methodology

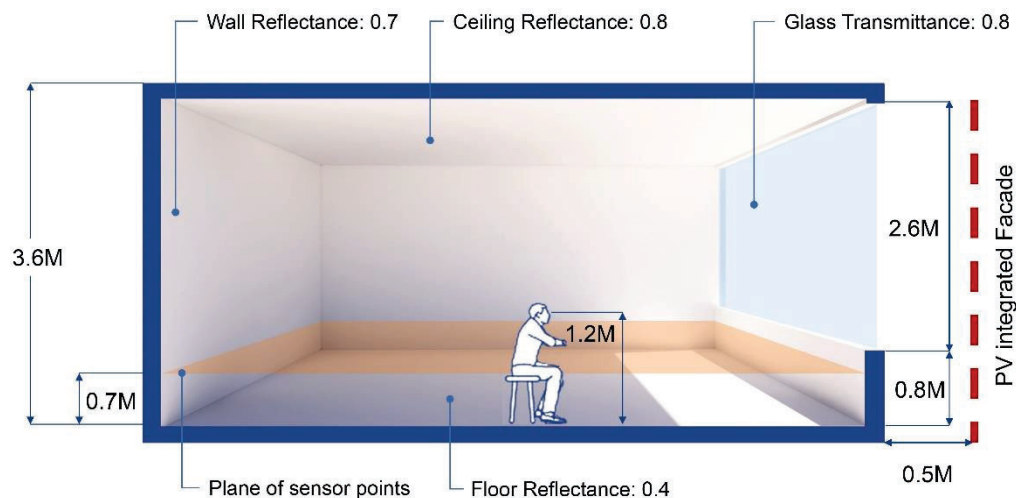


Figure 2. Settings of typical office building space

## 2.2 Model setup

Figure 2 presents the dimensional settings of the selected typical office space, the reflection parameters, and the plane where the simulated sensor points are positioned. Initially, a model of an open-plan office was established, taking reference from the studies conducted by Shi[24] and Wang[25]. The internal space dimensions were set at 7.8 m (width), 8.5 m (depth), and 3.6 m (height). The elevation of the office space included a bay window with a height of 0.8 m and a standard window with a height of 2.6 m. Subsequently, the plane for the simulated sensor points, which assess indoor lighting conditions, was determined to be 0.7 m above the floor surface. Additionally, the vertical surface where the PV panels are situated was positioned 0.5 m away from the original building façade, providing ample space for the rotation of the equipment and PV panels.

## 2.3 Evaluation indicators and optimization formula

In terms of the evaluation indicators, the assessment considers both the electricity generation and the impact of PVSD modules on indoor lighting. The output power of the PV panels is denoted as  $P$ , representing the resource output for electricity generation. Visual comfort refers to the subjective perception of comfort in the visual environment. Given the significant temporal and spatial variations in actual daylight levels within buildings, the traditional concept of illuminance uniformity is inadequate in reflecting realistic lighting conditions[26]. A more appropriate metric for evaluating the indoor light environment is the useful daylight illuminance (UDI), typically ranging from 100 to 2000 lx. UDI is commonly used to calculate light distribution within a building[26].

The screening process was devised using a multi-objective optimization method described by equation (1). Subsequently, the Rhinoceros + Grasshopper tool was employed to process the data and extract the optimal component forms for the five cities.

The design prototype merit formula was calculated as follows:

$$O_{best} = \text{Min} \left( \sqrt{\left( \frac{(P_i - P_{max})}{P_{max}} \right)^2 + \left( \frac{(UDI_i - UDI_{max})}{UDI_{max}} \right)^2} \right) \quad (1)$$

UDI = average effective natural daylight illuminance (UDI 200–3000 lx).

$P$  = output power of the adaptive façade dynamic PV shading system.

#### 2.4 Definition of variable indicators for the façade

The PVSD system should be configured to prioritize indoor light comfort while maximizing power production. The system involves several key design variables, including the PV cell type, PV panel size, number of PV panel layers, rotation axis direction, and tilt angle. Thin film PV and crystalline PV are the most commonly used PV cell types in the market. For the PV panel size, a choice of 0.2m x 0.2m is selected, which corresponds to the largest commercially available monocrystalline size commonly used, with a dimension of 210mm[27].

Table 1. Characteristics of the different PVSD devices.

Photovoltaic Type	Panel Size	Tilt Angle	Number of rows	Axis Orientation
Crystalline silicon	0.4 m × 0.4 m	30°	6	Horizontal
Thin film	0.8 m × 0.8 m	20°	3	Vertical
		15°		Oblique

As depicted in Table 1, the available sizes for photovoltaic panels are 0.4m × 0.4m and 0.8m × 0.8m. The number of photovoltaic layers is limited to six or three, depending on the chosen façade size. Each layer can accommodate up to 10 panels, considering the original building façade opening width of 7.8m. Drawing inspiration from various design forms commonly observed in adaptive façades, three types of rotation axis—horizontal, vertical, and inclined—are implemented. A tilted PV configuration yields 20–40% higher power generation than a flat vertical layout [28]. Therefore, three tilt angles of 15°, 20°, and 30° are selected for the PV panels. A prototype encompassing all elevations is constructed by arranging and combining all the variables above, as depicted in Figure 3.



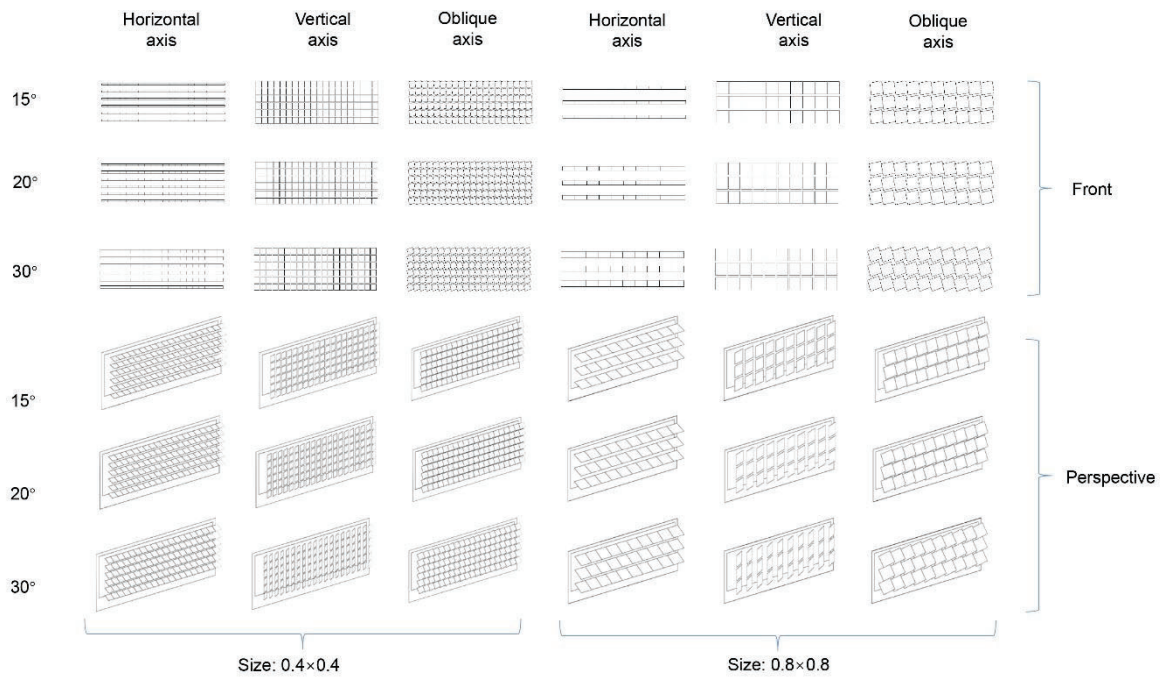


Figure 3. Façade library.

## 2.5 Settings of Simulation

Ladybug[20] and Honeybee can retrieve weather data to simulate the lighting, thermal, and wind environment of the building. All simulations rely on performance simulation software such as Daysim[21], Radiance[23], THERM, and OpenStudio. With the aid of this software and plugins, energy and lighting simulations can be conducted, and the output data can be visualized. The weather and lighting data used in the simulations were obtained from the epwmap website[19].

The simulations were conducted in five representative cities in China: Lhasa (Zone I), Kunming (Zone II), Beijing (Zone III), Shanghai (Zone IV), and Chongqing (Zone V). The objective was to investigate the lighting conditions in different regions of China and, based on these findings, design and optimize the energy efficiency of PVSD façades. The simulations were performed on four selected dates throughout the year: March 22nd, June 22nd, September 22nd, and December 22nd. For each date, simulations were conducted at four different time points: 9:00 a.m., 12:00 p.m., 3:00 p.m., and 6:00 p.m. This approach enables a comparison of results across different seasons and visually represents the variations in indoor lighting and PV power production throughout the day. With all the variable combinations, a total of 2,880 simulations were conducted.

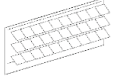
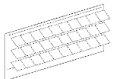
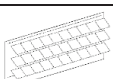
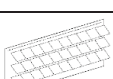
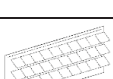
## 3. RESULTS

The filtering results presented in Table 2 indicate that the optimal configuration for the southward orientation of PVSD is a crystalline silicon PV panel with a horizontal axis rotation of 30° and a size of 0.8m x 0.8m. All lead to this result, even in different light-climate zones. This finding suggests that the most suitable tilt angle between the module and the horizontal plane is 30°, with equal weightage given to the indoor light environment and power generation, and it remains unaffected by geographical location. Figure 4 illustrates the substantial variations in PVSD power production across different light-climate zones, influenced by the varying availability of light in different cities. For instance, as observed from Table 2, power production in light-climate zone I such as Lhasa is significantly higher compared to several other cities. At the same time, areas like Chongqing are less suitable for PV installation.

In contrast, the cities of Kunming, Beijing, and Shanghai exhibit similar levels of electricity production. Although the daily illumination levels may appear comparable across the cities, the Useful daylight illuminances (UDI), being a range ratio, limits the visualization of detailed light differences. For a more comprehensive understanding, please refer to Figure 5.

Table 2. Best performance results in different cities.



Type	City	Size	Tilt Angle	PV Type	Axis Orientation	UDI	Electricity Production (Annual)
	Lhasa (I)	0.8 m × 0.8 m	30°	Monocrystalline	Horizontal	0.61	7990.6 kWh
	Kunming (II)	0.8 m × 0.8 m	30°	Monocrystalline	Horizontal	0.66	4152.87 kWh
	Beijing (III)	0.8 m × 0.8 m	30°	Monocrystalline	Horizontal	0.62	4691.27 kWh
	Shanghai (IV)	0.8 m × 0.8 m	30°	Monocrystalline	Horizontal	0.69	5463.36 kWh
	Chongqing (V)	0.8 m × 0.8 m	30°	Monocrystalline	Horizontal	0.70	1105.63 kWh

As depicted in Figure 4, Lhasa exhibits the highest and most consistent overall electricity production performance, maintaining a consistently high level throughout the year. Shanghai demonstrates notably high electricity production performance during the summer and autumn seasons. Conversely, Chongqing is deemed the least suitable city for PV integration on building façades within the selected parameters. The electricity production in each city positively correlates with the total light availability within its respective daylight-climate zone.

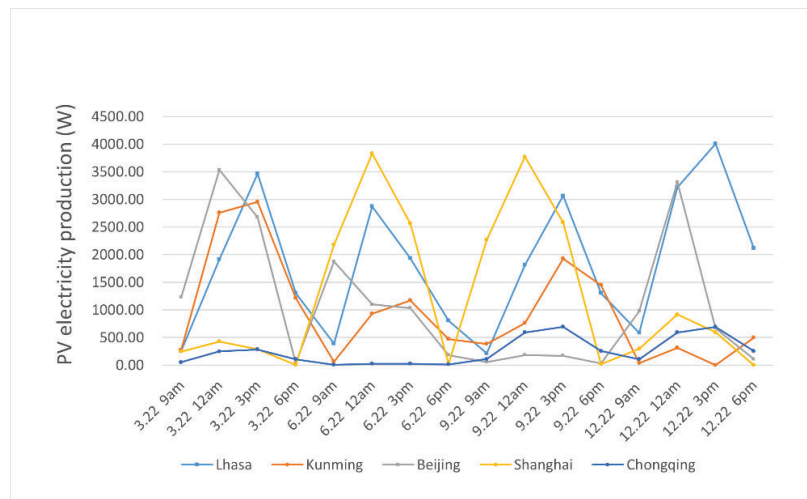


Figure 4. PV electricity production in different time.

As shown in Figure 5, Lhasa exhibits the highest light levels, which remain consistently high throughout the year. This may result in potential glare issues and visual discomfort due to excessive illumination. Similar to Lhasa, Kunming and Beijing display comparable light environments. However, Lhasa benefits from longer daylight hours in winter and maintains a high level of daylight even at 6:00 p.m. Shanghai showcases a pleasant light environment during the spring, summer, and autumn seasons while experiencing relatively higher glare levels during winter. However, it is essential to note that this discrepancy in winter may be attributed to the specific sample dates chosen for analysis. In contrast, Chongqing experiences high illumination levels during the summer and autumn seasons, a relatively comfortable light environment in spring, and significantly reduced illumination levels in winter, necessitating artificial lighting to compensate.

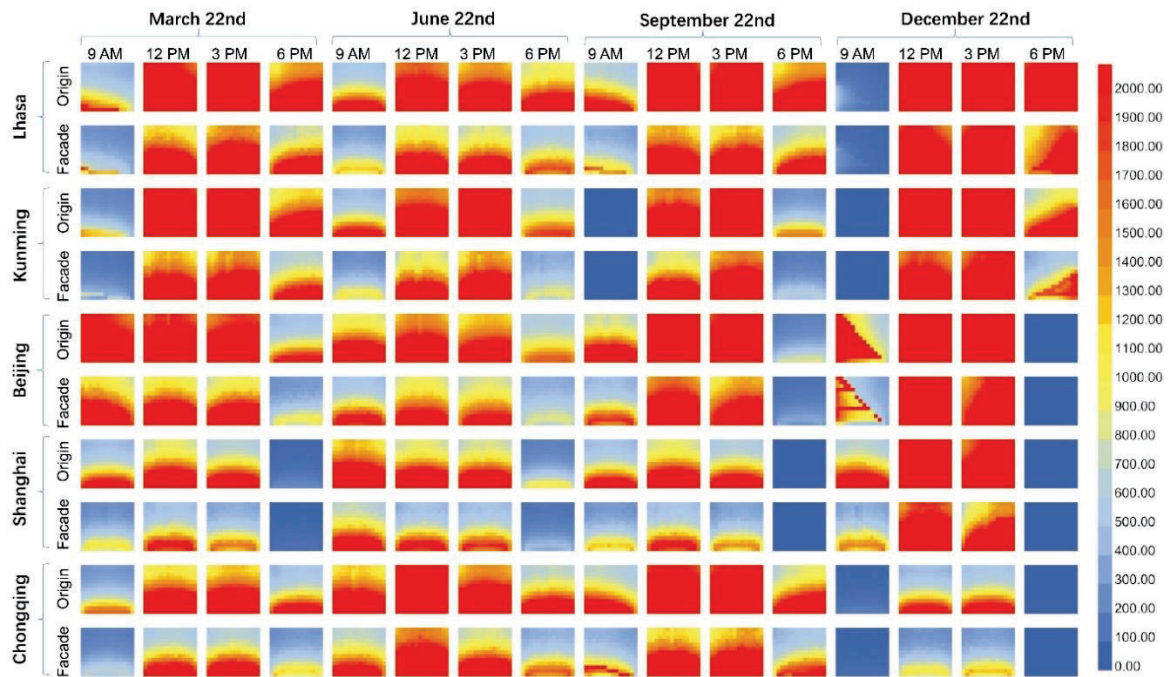


Figure 5. UDI Heatmap.

#### 4. CONCLUSION

The study examined the indoor light environment and integrated solar facades of typical office buildings across five distinct daylight climate zones in China. It develops a collaborative design mechanism that considers multiple factors and evaluates its application potential across different daylight climate zones. A multi-objective optimization approach was employed to conduct a quantitative analysis, performance simulation, resource output calculation, and design selection process for the facade design. After parametric simulation has been carried out, an optimal configuration for the building façade was selected from a library of established models. The integration of the selected module effectively enhanced the indoor lighting and visual comfort of the office space, resulting in an average light comfort level of 66.5%. Furthermore, the integrated module met 7-13.5% of the annual per capita electricity demand of the office building. The findings of this study can serve as a guide for other densely populated cities in promoting research and construction of solar façades, aiming to improve visual comfort in office spaces and reduce energy consumption.

#### REFERENCES

- [1] IEA. World Energy Outlook 2013. International Energy Agency: Paris, France, 2013, <https://doi.org/10.1787/20725302>.
- [2] Zhang, X., & Wang, Y. How to reduce household carbon emissions: A review of experience and policy design considerations. *Energy Policy*, 2017, 102, 116-124.
- [3] Global Buildings Performance Network. China: The World's Largest Single Market in New Construction, 2023.
- [4] THUBERC Annual Report on China Building Energy Efficiency; China Architecture & Building Press: Beijing, China, 2018.
- [5] Research Center for Building Energy Efficiency, Tsinghua University. Annual Development Report on Building Energy Efficiency in China 2020. Beijing: China Construction Industry Press, 2020.
- [6] Coma, J., Pérez, G., Solé, C., Castell, A., Cabeza, L.F. New green facades as passive systems for energy savings on buildings. *Energy Procedia*, 2014, 57, 1851-1859. <https://doi.org/10.1016/j.egypro.2014.10.049>.
- [7] Grondzik, W.T., Kwok, A.G. Mechanical and Electrical Equipment for Buildings. John Wiley & Sons, 2014.
- [8] Hamdan, M. A. The Influence of Roof Form and Interior Cross Section on Daylighting in the Atrium Spaces in Malaysia. University of Manchester, Doctor of Philosophy, 1996.

- [9] Fadzil, S. F. S., & Sia, S. J. Sunlight control and daylight distribution analysis: the KOMTAR case study. *Building and Environment*, 2004, 39(6), 713-717.
- [10] Lima, K. M. D., Bittencourt, L. S., Caram, R. M. Ranking configurations of shading devices by its thermal and luminous performance. *Sustainable Architecture for a Renewable Future*, 2013, 29th.
- [11] Jakubiec, J. A., Reinhart, C. F. The 'adaptive zone'-A concept for assessing discomfort glare throughout daylight spaces. *Lighting Research and Technology* 2012, 44, 149-70. <https://doi.org/10.1177/1477153511420097>.
- [12] Cardona, A. J. A., Chica, C. A. P., & Barragán, D. H. O. *Building-Integrated Photovoltaic Systems (BIPVS)*. Springer, 2018.
- [13] Hensen, J. L. M., Loonen, R. C. G. M., & Kin, S. Building performance evaluation of integrated transparent photovoltaic blind system by a virtual testbed, 2014.
- [14] Assoa, Y. B., Mongibello, L., Carr, A., Kubicek, B., Machado, M., Merten, J., Misara, S., Roca, F., Sprenger, W., Wagner, M., Zamini, S., Baenas, T., & Malbranche, P. Thermal analysis of a BIPV system by various modelling approaches. *Solar Energy*, 2017, 155, 1289-1299. <https://doi.org/10.1016/j.solener.2017.07.066>
- [15] Bodart, M., & De Herde, A. Global energy savings in offices buildings by the use of daylighting. *Energy and buildings*, 2002, 34(5), 421-429.
- [16] Lam, J. C., & Li, D. H. An analysis of daylighting and solar heat for cooling-dominated office buildings. *Solar energy*, 1999, 65(4), 251-262.
- [17] Taveres-Cachat, E., Lobaccaro, G., Goia, F., & Chaudhary, G. A methodology to improve the performance of PV integrated shading devices using multi-objective optimization. *Applied Energy*, 2019, 247, 731-744. <https://doi.org/10.1016/j.apenergy.2019.04.033>
- [18] Leslie, R. P. Capturing the daylight dividend in buildings: why and how?. *Building and environment*, 2003, 38(2), 381-385.
- [19] Ladybug Tools. epwmap. Retrieved from <https://www.ladybug.tools/epwmap/>
- [20] Roudsari, M. S., & Pak, M. Ladybug: a parametric environmental plugin for grasshopper to help designers create an environmentally-conscious design, 2013.
- [21] Reinhart, C. F., & Walkenhorst, O. Validation of dynamic RADIANCE-based daylight simulations for a test office with external blinds. *Energy and buildings*, 2001, 33(7), 683-697.
- [22] Romero, R., Simon, J., Ryan, T., Peterson, Z., Torcellini, P., Kandt, A., ... & Colgan, C. US Department of Energy Solar Decathlon Competition Guide: 2021 Design Challenge and 2023 Build Challenge (No. NREL/BK-7A40-78944). National Renewable Energy Lab.(NREL), Golden, CO (United States), 2021.
- [23] Ward, G. J. The RADIANCE lighting simulation and rendering system. In *Proceedings of the 21st annual conference on Computer graphics and interactive techniques*, 1994, 459-472.
- [24] Shi, X., Abel, T., & Wang, L. Influence of two motion types on solar transmittance and daylight performance of dynamic façades. *Solar Energy*, 2020, 201, 561-580.
- [25] Wang, Jiawei. Simulation of dynamic daylighting in office spaces under typical shading strategies. *Urban Architecture*, 2020.
- [26] Nabil, A., & Mardaljevic, J. Useful daylight illuminances: A replacement for daylight factors. *Energy and buildings*, 2006, 38(7), 905-913.
- [27] Beinert, A. J., Romer, P., Heinrich, M., Mittag, M., Aktaa, J., & Neuhaus, D. H. The effect of cell and module dimensions on thermomechanical stress in PV modules. *IEEE Journal of Photovoltaics*, 2019, 10(1), 70-77.
- [28] Freitas, S., & Brito, M. C. Maximizing the solar photovoltaic yield in different building facade layouts. In *Proceedings of the European Photovoltaic Solar Energy Conference and Exhibition*, Hamburg, Germany, 2015, 14-18.

## ACKNOWLEDGEMENTS

Corresponding Author Name: Luoxi Hao  
 Affiliation: Tongji University  
 e-mail: haoluoxi@tongji.edu.cn

# AN FIELD STUDY ON ENERGY USAGE AND HUMAN COMFORT IN A SMART LIGHTING OFFICE

Songbo Zhang, Hang Su, Biao Yang\*

(School of Architecture, Harbin Institute of Technology, Shenzhen, China)

Intelligent control systems can effectively reduce energy consumption during building operation, but there is a lack of rigorous empirical research of its energy-saving effects and impact on comfort. This study carried out a 129-day four-stage study by intelligently retrofitting the OCC intelligent system in real office spaces, while introducing an initial baseline and a parallel control group into the experimental design. A total of 69 volunteers participated in the empirical experiment. During the demonstration period, the data of environment sensors, human perception sensors and wireless intelligent controllers were collected, and structured questionnaire surveys were carried out for the treated group and the control group in four stages respectively. The comparative analysis results show that the intelligent retrofitting effectively reduces lighting energy consumption by 11.8% without compromising comfort.

Keywords: smart lighting; human factor; energy usage control

## 1. INTRODUCTION

The area of public buildings in China exceeds 15.2 billion square meters. The growth of large-scale public buildings and the increase in energy demand have caused an increase in the unit energy consumption of public buildings from 17 kgce/m<sup>2</sup> (in 2001) to over 26 kgce/m<sup>2</sup>, indicating a rapid growth in energy consumption intensity. Heating, ventilation, and air conditioning (HVAC) systems and lighting systems are the key contributors to building energy consumption. The comfort and work efficiency of users are also significantly influenced by the thermal and visual environments from the ergonomics perspective [1]. To achieve a green and sustainable built environment and reduce carbon emissions, it is important to reduce energy consumption during building operation. Nowadays LED replacement have significantly reduced the lighting power density, hence the detection, control, and optimization of equipment operating becomes critical. In public spaces, especially in typical open-office scenarios, integrating intelligent lighting control and human-centric lighting is necessary to achieve energy efficiency while satisfying the comfort needs of occupants [2].

Current OCC systems often focus on either lighting or HVAC systems without integrating them, which presents a challenge in the entire system. Existing experiments are often performed in experimental scenarios such as university campuses, which differ from actual open office working scenarios. Thus, conducting empirical research in actual scenarios can improve research effectiveness.

In this paper, building upon relevant prior research, we conducted an Intelligent Integrated Occupant Centered Control (IOCC) retrofitting within a real open office space around 200 m<sup>2</sup>. The office layout comprised an open office area and three individual offices, which accommodated workforce of 100 individuals. The primary goal for this retrofitting was to conduct empirical research aimed at evaluating the impact of the system on both building energy consumption and human comfort.

Throughout this study, we assessed user satisfaction levels concerning the built environment before and after implementing the IOCC. Furthermore, we evaluated changes in both energy consumption and equipment usage time as results. Ultimately, we developed the IOCC framework that combined occupants' satisfaction with the air conditioning and lighting while simultaneously reducing energy consumption.

The remainder of this paper is structured as follows: Section 2 presents the background of the IOCC, including details regarding the office's situation, hardware installation, evaluation metrics

and occupant-centric experimental design. Section 3 outlines the main results of our experiment. Lastly, we provide an analysis and discussion of the research in Section 4.

## 2. METHODS

### 2.1 Experimental Design

We employ an empirical research approach within an interior design company located in Shenzhen, Guangdong Province, China. The study was conducted between July 26, 2022 and December 8, 2022. Two open office spaces located on the same floor, similar in size and symmetrically arranged along the central axis, were selected for our research, as depicted in Figure 1. Specifically, the experimental group faced west, while the control group faced east.

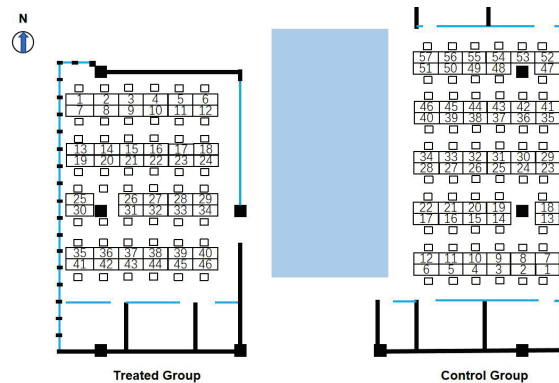


Figure 1 Floor plan of the experimental site

The project is located in Shenzhen, having subtropical monsoon climate. Summer in Shenzhen is hot with rainfall, while winter is mild with little rainfall. The average monthly highest temperature ranges between 26°C and 32°C with high humidity levels, while the coldest month averages between 12°C to 20°C. The environmental needs indicates high need for HVAC system to meet cooling and dehumidification requirements. The yearly average sunshine hours in Shenzhen are 1980 hours. October is the most sun-filled month with an average of 223 hours of sunshine per month while the least sunny month is usually March with an average of 136 sunshine hours per month. Having adequate sunshine hours, however, the site choose close shading curtains regularly, with lighting fixtures left on.

Both sites' occupants participated in this study. The primary experimental site was the Department A of the company, comprising a four-row open office space accommodating approximately 40 occupants, along with three additional offices, particularly a personal office (office 1), a meeting room (office 2), and a storage room (office 3). The control group has an east-facing orientation, accommodating approximately 50 occupants with similar layout and spatial proportions.

Due to the company's characteristics, the occupants have flexible working hours. It is common that only several occupants work late to complete their task, keeping the the entire office equipment on constantly. Therefore, air conditioning and lighting usage have a potential in achieving energy conservation targets by applying Occupant-Center Control.

In this experiment, Millimeter-Wave radar was used as the main tool for perceiving the presence of occupants. The Millimeter-Wave radar obtains environmental information by emitting and receiving specific wavelengths of millimeter waves. After filtering out any unnecessary interference, it records and analyzes the presence and movement of individuals. Prior to the experiment, the site was divided into sections, and a Millimeter-Wave radar was placed in each corresponding section and calibrated. The corresponding sections were further divided into grids and specific grids were selected to ensure that only the behaviors of individuals in the designated areas were recorded. As shown in Figure 2, this is an example of a Millimeter-Wave radar grid



after delineation. When individuals work or move in the corresponding areas, their behavior trajectories are generated, which provide a basis for subsequent control of intelligent devices.

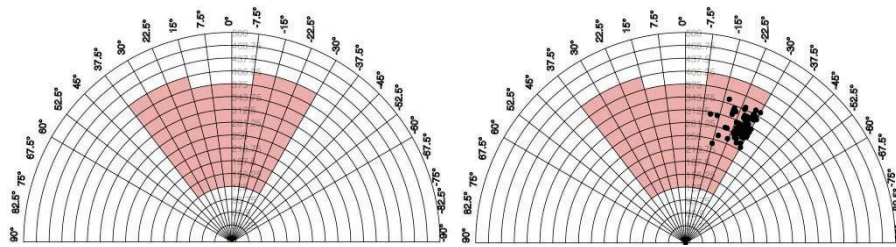


Figure 2 The division of detection grids and recording of personnel presence using Millimeter-Wave radar.

The intelligent OCC system contains four parts, including Occupant Detection Sensors, Environmental Information Sensors, Wireless Smart Switches, Smart Meters. To achieve space management, firstly, the Occupant Detection part relies primarily on millimeter-wave radar to analyze personnel occupants and deliver signals [3]. Then, combining the information received by Environmental Information part, the system uses these signals to determine the corresponding disturbance pattern in the area, generate its trajectory, filter out invalid disturbances, interpret the behavior trajectory of personnel, and utilize it as the basis for activating the corresponding Wireless Smart Switches in the given space [4]. Also, system utilizes intelligent switches to gather hourly air conditioning and lighting fixture operation hours data and site-wide energy usage by Smart Meter. The equipment will deactivated after TD once the system detects that the personnel have departed. Figure 3 illustrates the building's terminal intelligent control system architecture.

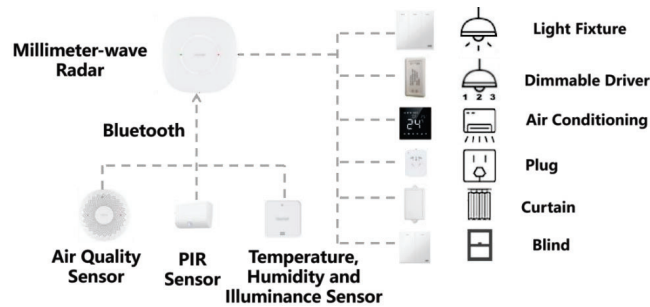


Figure 3 the Architecture of OOC smart system

By implementing a grid-based system and leveraging the capabilities of Millimeter-Wave radar, it is possible to accurately monitor and record the presence of individuals in different areas of interest. This information can further be utilized for various applications, such as smart building management, security surveillance, or optimizing space utilization.

The experiment process was partitioned into four stages labeled A-B-C-D, as demonstrated in Table 1. During Stage A, the OCC system was installed but not operated, and users were not informed. During Stage B, the OCC system was installed, and users were informed of its operating, yet it was not activated. During Stage C, the smart control system was actively running. During Stage D, the OCC system was disabled, and users were not informed.

Table 1 Intelligent System Strategy Schedule

Stage	Stage Content	Duration Date	Event	Event Time
Stage A	The intelligent system is installed but the policy is not started; The consumer is not informed that the system is installed	7/24-7/26	Install the system	2022/7/24 17:38
			First questionnaire	2022/7/26 15:00

Stage B	The intelligent system is installed but the policy is not started; The consumer is informed that the intelligent system is enabled	7/27-11/2	Second questionnaire	2022/9/15 15:00
Stage C	The intelligent system has the policy installed and started	11/3-11/25	Turn on Strategy	2022/11/3 14:40
			Third questionnaire	2022/11/24 15:00
Stage D	The intelligent system turned off the policy; The user is not informed that the system is shut down	11/26-12/7	Close Strategy	2022/11/26 0:21
			Fourth questionnaire	2022/12/7 15:00

To minimize the influence of extraneous variables, we utilized a difference-in-differences (DID) method in our experimental design [5]. Data collection during each stage involved observing the duration of lighting fixture and air conditioning hourly usage [6], user occupancy, and environmental parameters (i.e., temperature, humidity, illuminance, and air quality) for the experimental group. Moreover, questionnaire was collected during each stage for both groups, the control group received no other interventions except the questionnaire. By applying the difference-in-difference approach, the impact of applying interventions on users' comfort perception was ascertained by contrasting the outcome differences between the experimental group and the control group before and after the intervention.

## 2.2 Site Retrofitting

To enhance the intelligence of the experimental site, the retrofitting project involves installing various equipment and sensors. In summary, the smart retrofitting project involves installing smart meters, environmental information sensors [7], millimeter-wave radar and PIR sensors, and wireless smart switches. These are designed to obtain energy consumption data, environmental parameters, and personnel behavior status, as well as to remotely control lighting, air conditioning, and window pushers the real scenario and its digital twin model [8] are shown in Figure 4.

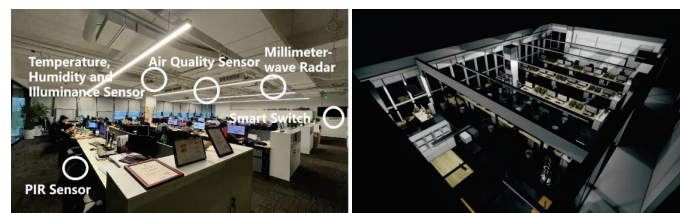


Figure 4 Real retrofitting scenario(left) and its digital twin model (right)

After installation of the equipment, control strategies was configured according to realistic scenarios and specific requirements. The purpose of these strategies is to reduce inconsistencies between occupant behavior and operation of the equipment. The IOOC system controls the operation of the equipment based on the presence of occupants, turn on lights and air conditioning when recognize the occupants and turn them off when they leave [9]. In order to avoid causing inconvenience to users, several strategies are also set to prevent misjudgments. For example, the time delay (TD) strategy of 10 minutes will be implemented before turning off the equipment. Additionally, environmental parameters are used to determine whether immediate activation of air conditioning is necessary when personnel are detected [10], for example, if the temperature is below 26 degrees, the air conditioning will not activate immediately [11].

## 2.3 Analysis of Users' Comfort

To investigate the comfort situation of the occupants, we conducted the questionnaire survey throughout the entire experiment and mainly consists of five parts: basic information; sleep quality; Perceived Stress; Subjective vitality; environmental perception and psychological feelings.

The basic information section of the questionnaire mainly collects the seat number, gender, age, and work intensity of the subjects this week, with a total of three questions. The personal factors section mainly investigates the subjects' personal situation this week, including subjective performance with a total of three items.

Sleep quality and sleepiness with a total of ten items. The PSQI questionnaire [12] was used as the international standard questionnaire for sleep (a score greater than or equal to 8 indicates poor sleep quality). Perceived stress with a total of 14 items. The Perceived Stress Scale questionnaire [13] was used for perceived stress ( $\leq 28$  means "low,"  $\leq 42$  means "moderate,"  $\leq 56$  means "high," and  $\leq 70$  means "very high"). Subjective vitality with a total of seven items. The Subjective Vitality Scale questionnaire [14] was used for vitality (the higher the score, the more positive emotions). The questionnaire design is based on Hedge's Sick Building Syndrome model [15], and it primarily consists of four parts: personal basic information, environmental factors, environmental perception, and psychological feelings.

The environmental factors section is mainly recorded by the experimenters, including indoor temperature and humidity, special point illuminance, etc. The investigation of environmental perception and utility includes thermal environmental quality with a total of three items, light environmental quality with a total of six items, and other factors with a total of two items. Two open-ended questions about optimization suggestions were included.

### 3 Results

#### 3.1 Electricity consumption analysis

The power consumption analysis of the venue: After collecting the total daily power consumption for Phase B and Phase C (i.e., before and after the strategy was implemented) and excluding holidays (shown in Table 2), the average daily power consumption before the strategy was implemented was approximately 77.34 kWh. After the implementation of the strategy, the average daily power consumption was 68.16 kWh, which represents an 11.87% reduction. When further excluding weekends, the power consumption before the strategy was implemented was 83.65 kWh, and after implementation was 75.69 kWh, which leads to a reduction of 9.52%. The power consumption comprises the indoor socket power. Energy-consuming equipment, such as computer hosts, monitors, and water heaters, remain in a long-term power-on state, and thus the actual energy-saving rate may be underestimated to some extent.

Table 2 Power Consumption before and after the Implementation of Intelligent Control Strategies

Stage	Average Power Consumption (Excluding Holidays)	Average Power Consumption (Excluding Holidays and Weekends)
Stage B	77.34	83.65
Stage C	68.16	75.69
Energy Savings (%)	11.87%	9.52%

Based on the analysis of power consumption before and after the strategy was implemented, it can be concluded that the intelligent control system is effective in reducing the energy consumption of office building operations, and the energy-saving effect is more significant on weekends, possibly due to the more dispersed presence of personnel on weekends.

#### 3.2 Energy Usage of lighting fixtures

As per Table 3, the usage time of lighting fixtures in the open space has reduced for fixtures 1, 3, and 4, with a maximum reduction rate of 30.25%. Fixture 2's usage time has increased by 8.23%. Before implementation, the average usage time was 14.50 hours with a sample variance

of 3.0. After implementation, the average usage time was 12.55 hours with a sample variance of 0.73, representing a decrease of 13.36%. Fixture usage time after the strategy was uniformly lower, which may be because people have certain preferences when manually operating the equipment, while the intelligent control system can control the equipment opening more objectively.

For individual offices, the intelligent system is more effective in reducing energy consumption when people leave, achieving a reduction rate of 56.09%. In meeting rooms, the reduction rate was 25.89%, while the usage time reduction in the storeroom was negligible for comparison purposes.

Table 3 Usage Time of Lighting Fixtures (hours)

	Row1	Row2	Row3	Row4	Personal Office	Conference Room	Store Room
Before Strategy	14.85	12.44	16.62	14.08	3.40	3.49	0.91
After Strategy	13.05	13.46	11.59	12.13	1.49	2.59	0.90
Time Reduction	1.79	-1.02	5.03	1.95	1.91	0.90	0.00
Reduction Rate (%)	12.07%	-8.23%	30.25%	13.87%	56.09%	25.89%	0.38%

### 3.3 Energy Usage of air conditioning

Table 4 shows the usage time of air conditioning equipment in the experimental area. For the open space, the usage time of air conditioning units 1, 2, and 4 has decreased, and the highest reduction rate has reached 51.08%. The usage time of unit 3 has increased by 19.73%. The average usage time before implementation was 12.39 hours with a sample variance of 18.6. The average usage time after implementation decreased to 9.2 hours with a sample variance of 1.0, indicating a decrease of 25.96%. The usage time of air conditioning equipment after the strategy's implementation was more uniform, probably because people have certain preferences when manually operating the equipment, while an intelligent control system can control the equipment more objectively. In individual offices, the reduction rate of usage time was 86.45%. In the meeting room, the reduction rate of usage time was 34.02%, while the overall usage time in the storeroom was too low to be meaningful for comparison.

Table 4 Usage of Air Conditioning Equipment

	Row1	Row2	Row3	Row4	Personal Office	Conference Room	Store Room
Before Strategy	12.88	12.37	6.89	17.42	12.87	1.28	0.01
After Strategy	9.63	10.41	8.25	8.52	1.74	0.84	0.02
Time Reduction	3.25	1.96	-1.36	8.90	11.13	0.43	0.00
Reduction Rate (%)	25.26%	15.85%	-19.73%	51.08%	86.45%	34.02%	-19.67%

### 3.4 User Questionnaire Analysis

A total of 233 questionnaires were distributed to both experimental and control groups at four different stages. 24 valid questionnaires (96 pages) were fully completed in all four rounds of the survey. Detailed information on the questionnaire collection process are shown in Figure 4.

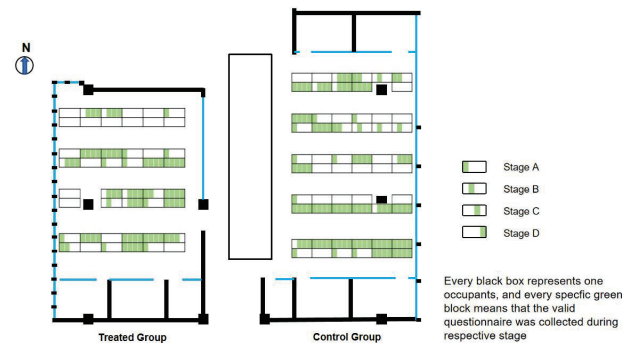


Figure 5 Questionnaire distribution and collection statistics

The distribution and collection of survey questionnaires are statistically summarized in Figure 4. The Double Difference Estimation (DID) analysis method was used to analyze the questionnaires collected to evaluate the subjective effects of the intelligent system on user comfort. The specific results are shown in Table 7. According to the survey results, the overall temperature( $p=0.000$ ), excessive sunlight( $p=0.043$ ), and thermal environmental comfort( $p=0.003$ ) were significantly improved( $P<0.05$ ) in Stage C compared to Stage A. However, no significant differences were found in the content of research between Stage B and Stage C or between Stage C and Stage D, which may be due to the Hawthorne effect, wherein users had an improved perception of the thermal environment [16]. Based on the questionnaire results, it was found that the glare near the window was significantly stronger. This is one of the reasons why curtains are commonly closed in such scenarios and artificial lighting is used. It also provides a reference for integrating daylighting and artificial lighting in the next step.

#### 4. CONCLUSION

This study is based on intelligent retrofitting in real scenes, and through the analysis of human behavior and environmental information, explores the energy-saving potential and environmental comfort impact of intelligent retrofitting. According to the analysis of energy consumption and user behavior data in the experimental site for 129 days, it was found that after the experimental group used the intelligent strategy to automatically control lighting based on personnel detection, the electricity consumption was reduced to a certain extent. Before opening the strategy, the average daily electricity consumption was about 77.34 kWh, after opening the strategy, it was 68.16 kWh, a decrease of 11.87%. The average lighting time of the open office space decreased by 13.36%, the average air conditioning time decreased by 25.96%, and the uniformity of the equipment's opening time significantly improved. The lighting equipment usage time in personal offices decreased by 56.09%, and the air conditioning equipment usage time decreased by 86.45%, greatly reducing the usage time of terminal devices. The lighting equipment usage time in the conference room decreased by 25.89%, and the air conditioning equipment usage time decreased by 34.02%, which significantly reduced the usage time of terminal devices.

Using the DID method to analyze the impact of the intelligent control system on user perception, a questionnaire survey was conducted on both groups in four stages to collect individual factors and environmental perception conditions, including work performance, sleep quality, alertness, perceived pressure, subjective vitality, physical fitness, and indoor environmental impression. The survey results showed that compared with the situation before the strategy was informed and opened, the actual opening of the strategy significantly improved the thermal environment perception conditions and utility ( $p<0.05$ ), and there was no significant



difference between the actual opening before and after the strategy, indicating that thermal comfort was not affected by the physical environment terminal intelligence retrofitting.

This study still has shortcomings, and the following issues need to be further studied: 1) Due to the different orientations of the experimental group and control group, it is not convenient to directly compare energy consumption data. Future cases should choose the same orientation; 2) The existing site shading curtains are kept closed, and natural light is not fully utilized. Through the use of a refined daylighting and lighting integration system, intelligent terminals may have greater potential for energy saving and human comfort.

## REFERENCE

- [1] Han Zhu, Xiangchao Lian, Yuxin Liu, et al. Consideration of occupant preferences and habits during the establishment of occupant-centric buildings: A critical review. *Energy and Buildings*, 2023, 280, 112720.
- [2] Christoph F. Reinhart. Lightswitch-2002: a model for manual and automated control of electric lighting and blinds. *Solar Energy*, 2004, 77(1), 15-28.
- [3] Miguel García-Monge, Belén Zalba, Roberto Casas, et al. Is IoT monitoring key to improve building energy efficiency? Case study of a smart campus in Spain. *Energy and Buildings*, 2023, 285, 112882.
- [4] Zhao P, Lu C X, Wang J, et al. mID: Tracking and Identifying People with Millimeter Wave Radar. 2019 15th International Conference on Distributed Computing in Sensor Systems (DCOSS). 2019, 33-40.
- [5] Stephan Lindner, K. John McConnell. Difference-in-differences and matching on outcomes: a tale of two unobservables. *Health Services and Outcomes Research Methodology*, 2019, 19(2-3), 127-144.
- [6] Mahdavi A, Mohammadi A, Kabir E, et al. Occupants' operation of lighting and shading systems in office buildings. *Journal of Building Performance Simulation*, 2008, 1(1), 57-65.
- [7] Pei Zhou, Gongsheng Huang, Zhengwei Li. Demand-based temperature control of large-scale rooms aided by wireless sensor network: Energy saving potential analysis. *Energy and Buildings*, 2014, 68, 532-540.
- [8] D.R.G. Hunt. The use of artificial lighting in relation to daylight levels and occupancy. *Building and Environment*, 1979, 14(1), 21-33.
- [9] Rijal Wagiman K, Noor Abdullah M, Yusri Hassan M, et al. A review on sensing-based strategies of interior lighting control system and their performance in commercial buildings. *Indonesian Journal of Electrical Engineering and Computer Science*, 2009, 16(1), 208.
- [10] Pei Zhou, Gongsheng Huang, Linfeng Zhang, et al. Wireless sensor network based monitoring system for a large-scale indoor space: data process and supply air allocation optimization. *Energy and Buildings*, 2015, 103, 365-374.
- [11] Zhe Wang. How frequent should we measure the indoor thermal environment. *Building and Environment*, 2022, 222, 109464.
- [12] Buysse D J, Reynolds C F, Monk T H, et al. The Pittsburgh sleep quality index: A new instrument for psychiatric practice and research. *Psychiatry Research*, 1989, 28(2), 193-213.
- [13] Eleni Andreou, Evangelos C. Alexopoulos, Christos Lionis, et al. Perceived Stress Scale: Reliability and Validity Study in Greece. *International Journal of Environmental Research and Public Health*, 2011, 8(8), 3287-3298.
- [14] Ryan R M, Frederick C. On Energy, Personality, and Health: Subjective Vitality as a Dynamic Reflection of Well-Being. *Journal of Personality*, 1997, 65(3), 529-565.
- [15] A. Hedge, P.S. Burge, A.S. Robertson, et al. Work-related illness in offices: A proposed model of the "sick building syndrome". *Environment International*, 1989, 15(1-6), 143-158.
- [16] Rob McCarney, James Warner, Steve Iliffe, et al. The Hawthorne Effect: a randomised, controlled trial. *BMC Medical Research Methodology*, 2007, 7(1), 30.

## ACKNOWLEDGEMENT

Corresponding Author: Biao Yang

Affiliation: School of Architecture, Harbin Institute of Technology, Shenzhen

e-mail: yangbiao@hit.edu.com

# HOW CAMPUS LANDSCAPE LIGHTING INFLUENCES VISUAL ATTENTION AND RESTORATIVE PERCEPTION: A SPATIAL MEASUREMENT STUDY EMPLOYING EYE TRACKING

Xianxian Zeng<sup>1</sup>, Yi Lin<sup>1,2,3</sup>, Bing Zhang<sup>1</sup>, Shenfei Chen<sup>1</sup>

(1. College of Architecture and Urban Planning, Tongji University, Shanghai, China; 2. Key Laboratory of Ecology and Energy-saving Study of Dense Habitat, Ministry of Education, Shanghai, China; 3. Tongji Architectural Design (Group) Co., Ltd, Shanghai, China)

## ABSTRACT

Due to academic pressure, social competition, and interpersonal communication, psychological problems like anxiety and depression are common among college students. The campus outdoor space, as a vital venue for students, not only serves practical functions but also plays a crucial role in enhancing psychological recovery. Lighting, as a significant factor in shaping the landscape, has a profound impact on human perception. This research aimed to investigate the influence of different lighting environments on visual perception and restorative experiences among college students. Three lighting conditions (daytime, nighttime with landscape lighting + street lighting, and nighttime with street lighting only) were set up along a university campus pathway. Eye-tracking data, interviews, and subjective questionnaires were used to gather participants' experiences. The findings indicate that lighting conditions influence visual perception and cognitive preferences. Moreover, pedestrians displayed diverse fixation patterns depending on the lighting environment. Nighttime scenes with well-designed lighting exhibited a higher restorative effect compared to other scenes. This study provides insights into the role of lighting design in guiding visual attention and supports the potential benefits of night landscapes for restoration.

Keywords: College students, Psychological problems, Lighting environments, Visual perception, Eye-tracking

## 1. INTRODUCTION

College students face serious physical and mental health issues, including heavy academic workload, intense job competition, and interpersonal relationships, among other complex factors, which have drawn widespread attention from society [1][2]. As the space where college students spend the majority of their time, the outdoor campus environment not only serves basic functions of public activities, aesthetics, and ecology but also significantly influences their psychological restoration and physiological stress levels [3][4][5]. Light, including natural sunlight and artificial lighting, plays a vital role in shaping the spatial image. Under different lighting conditions, the same campus space may present different visual images, thus eliciting varying visual preferences and restorative perceptions. However, further research is needed to determine how to measure these perceptual differences effectively.

The campus landscape, as the most encountered "second nature environment" in the daily lives of college students, holds significant importance for positive psychological intervention. Current research mainly focuses on exploring the effects of daytime environment and campus landscape on emotions [6]. However, the night time is one of the main periods for students' socializing, leisure, and studying activities, and a high-quality campus nightlife can provide a comfortable, safe, and pleasant environment for students. A good campus nighttime scenery not only satisfies students' basic mobility needs but also serves as a valuable restorative landscape resource, effectively reducing students' physical and mental stress and helping them restore their original state of well-being. Therefore, investigating the perceptual effects of different lighting conditions on campus nightlife is of great significance.

Studying human experience and perception has always been an important issue in the field of environmental psychology. Traditional evaluation methods for landscape preference, emotional experience, and restorative quality can be categorized into two approaches. One method is phenomenological interviews that require participants to recall event details as fully as possible. Another method is psychological measurement scales, such as mood scales, Perceived Recovery

Scale (PRS), and State-Trait Anxiety Inventory (STAI) [7]. However, traditional measurement methods like phenomenological interviews and psychological measurement scales demand high experiential requirements from the participants, and the data collection process can be labor-intensive and resource-consuming, limited by the experiences of the participants themselves. With the development of wearable sensor technologies, eye-tracking devices, which directly measure visual attention, have been applied in studies on environmental perception. Analysing indicators such as fixation points, fixation durations, and pupil size while participants view landscapes, in conjunction with subjective evaluations, can facilitate a better understanding of differences in perception between day and night landscapes. [8][9][10]

Consequently, the primary objective of this research endeavor pertains to dual facets: (1) investigating the viability of employing eye-tracking as a tool for evaluating the perceptual aspects of landscapes in diurnal and nocturnal settings; (2) examining the effects of diverse lighting conditions on the restorative perception of college students traversing a predefined campus route.

## 2. METHODS

### 2.1 Participants

In the first stage, 13 subjects were recruited, all of whom were undergraduate students who usually stayed in campus, so all of them were familiar with the experimental road. They were required to be in good health, have a regular living schedule and normal vision (the naked eye vision of both eyes is greater than 0.8), no colour blindness, colour weakness, glaucoma and other eye diseases, also no alcohol abuse or smoking habits. After preliminary screening and confirmation, 8 students participated in the experiment finally (see Table 1). The results of Self-rating anxiety scale (SAS) and Self-rating depression scale (SDS) showed that their anxiety and depression levels were all normal. The subjects were estimated through Morningness-Eveningness Questionnaire (MEQ), showing that 6 of them were "intermediate" and 2 were "intermediate evening". There was no "definite morning" or "definite evening", and the sleep habits were basically similar.

Table 1. Description of participants.

Characteristics	Mean	SD	Maximum	Minimum
Age (years old)	18.63	1.11	21	18
Self-rating anxiety scale (SAS)	33.75	6.06	42	23
Self-rating depression scale (SDS)	37.75	8.35	50	22
Morningness-Eveningness Questionnaire (MEQ)	45.13	6.27	55	33
Body Mass Index (BMI)	20.66	2.25	24.30	18.22

### 2.2 Study Area

This study selected a road route on Siping Road at Tongji University, with a total round-trip distance of 700 meters. The walking route was divided into three segments, and three fixed stopping points were established along the way to capture participants' perception of the static environment. The experiment included three different lighting conditions: a daytime scene (overcast), nighttime scene A (streetlights and landscape lights), and nighttime scene B

(streetlights).

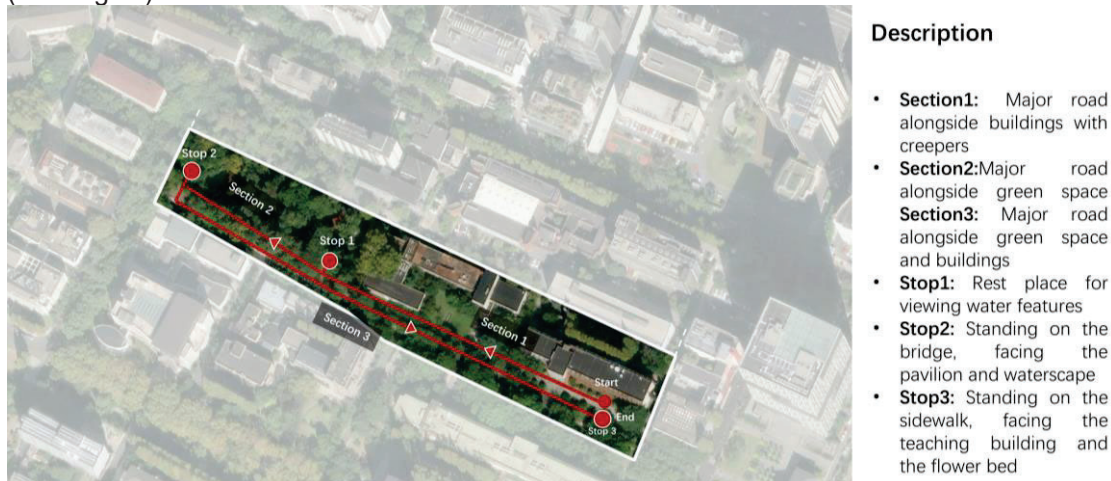


Figure 1 Experimental Site

### 2.3 Research Process

The experiment was conducted from November 12th, 2022, to November 26th, 2022, during a period characterized by mild weather and cloudy skies with dry ground conditions. To minimize interference, the experiment was conducted during periods of low student traffic. Daytime experiments took place from 8:00 AM to 11:00 AM, while nighttime experiments occurred from 7:00 PM to 10:00 PM. The experiment utilized a repeated measures design, where each participant started by completing a series of tasks indoors to induce stress perception. Participants then experienced three scenes in random order, with the experimental procedures for each scene being the same. Participants gathered at Room 115 of Wenyuan Building according to a predetermined schedule. Before the experiment, participants were provided with the designated route and stopping points and were asked to imagine the following scene: "After a busy day of studying, taking a stroll alone or with companions on campus. Except for the three fixed stopping points, participants could stop and continue at their discretion and use an iPad to capture photos of campus environments that interested them and share them with family and friends. The duration of stays at the stopping points was self-controlled."

Each participant was equipped with Tobii Glasses eye-tracking glasses and a GPS device (Garmin eTrex 221X GPS), allowing the linkage of GPS locations with visual experiences. After the experiment, participants completed Perceived Restorativeness Scale (PRS). between sessions. During the experiment, participants were not allowed to speak, eat, or consume energy drinks. In the case of unexpected events such as coughing, noise, or interference from other individuals, the experimenter recorded audio and video throughout the experiment.

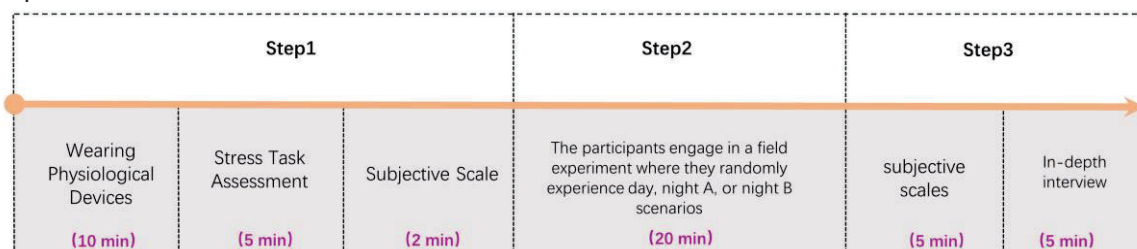


Figure 2 Research Process





Figure 3 Overview of research

### 3. RESULTS

During the process of appreciating landscape spaces, individuals form aesthetic perceptions of space through exploration. The presentation of landscape elements in space is orderly, and perceptual preferences may vary based on the observer's viewing methods and locations. Therefore, in this study, eye-tracking data was analysed using both quantitative and qualitative methods in the context of two behavioural modes: walking and pausing.

#### 3.1 Analysis of eye movement data during walking

##### 3.1.1 Analysis of the eye movement data

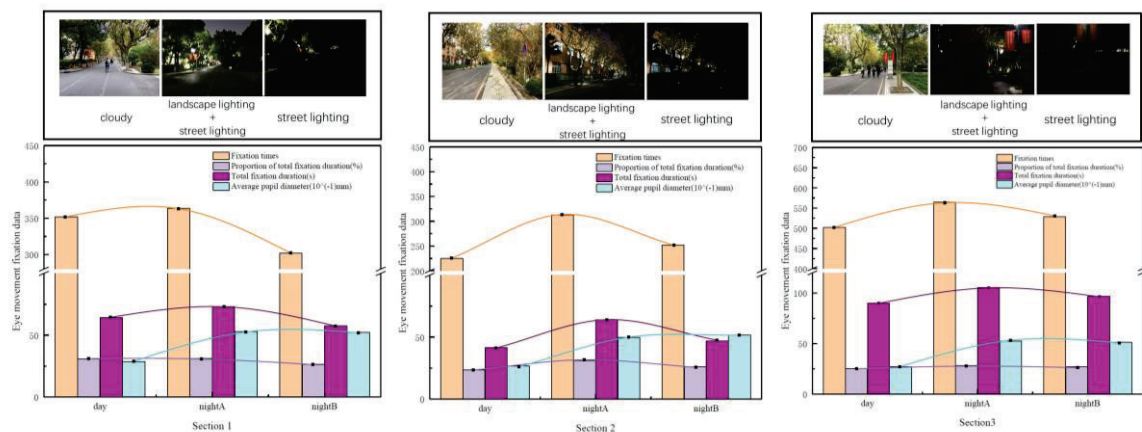


Figure 4 Eye movement fixation data statistics during walking

When observers were exposed to nighttime scene A, they exhibited the highest number of fixations and longest total fixation duration, indicating a visual preference for nighttime scene A. The illuminated buildings, seating, and sculptures in nighttime scene A captured the observers' attention. In comparison between daytime and nighttime scenes, observers showed slightly higher fixations counts and total fixation duration in daytime scene than in nighttime scene B, while in Section 2 and 3, observers exhibited slightly higher fixations counts and total fixation duration in nighttime scene B than in daytime scene.


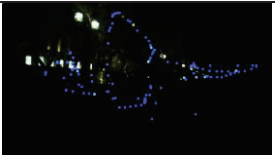




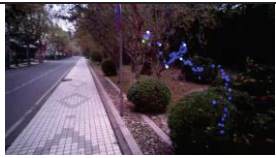













Attention allocation remained relatively consistent across all scenes. In terms of pupil size, nighttime scene A had the largest pupils, slightly larger than nighttime scene B, while daytime scene had the smallest pupils. These findings suggest that changes in lighting conditions influence visual perception and behavioural responses, leading to differences in attention allocation and cognitive load across different environments.

### 3.1.2 Analysis of the cognitive and area of interest

In order to investigate the impact of the same landscape elements under different lighting conditions on the visual attraction of participants, we analysed eye-tracking data of key landscape elements during walking and generated interest area heatmaps. By combining eye-tracking heatmaps with task performance and subjective evaluation results, we were able to uncover the relationship between participants' eye movements and their cognition and behaviour (as shown in Table 2).

Table2 Eye movement, filming tasks and subjective interviews during walking

Location	Content	Daytime Scene	Nighttime Scene A	Nighttime Scene B
Section1	Eye-track			
	Photo			
	AOI elements	Plants, Roads, Buildings	Streetlights, Roads, Illuminated plants.	The sky, Streetlights, Tree shadows
	Evaluation	" On this road, there are people, birds, and trees. I feel that they are dynamic and full of vitality, which makes me feel very comfortable."	"On the way back, I noticed that the area beneath the column with the school emblem was illuminated by lights. It looked quite beautiful and created a memorable spot that brought a sense of joy."	"It feels like some of the lights in the North Building have been adjusted and dimmed a bit. However, seeing classmates still in class gives an overall sense of softness."
Section2	Eye-track			
	Photo			
	AOI elements	Plants, Roads.	Streetlights, Roads.	Streetlights
	Evaluation	"Today's weather is quite good, with sunshine. The sunlight shines through the leaves and onto the ground, giving a vibrant and uplifting feeling. Compared to the nighttime, the daytime is	"There is a small pathway paved with little stones that slowly leads to the depths of that garden. Alongside the path, there are small, scattered lights that accompany it. The overall feeling is quite attractive and	"The streetlights form a continuous line, creating a distinct contrast with the darkness on the right side. They stand out and appear vivid against the black backdrop."

		much more enriched."	has a sense of mystery."	
Section3	Eye-track			
	Photo			
	AOI elements	Plants, Road	Buildings, Road	Buildings, Road
	Evaluation	"I find this area facing the academic building to be quite boring. The construction noises around here also make me uncomfortable."	"The main entrance of the North Building gives me a visual appeal."	"It makes me feel anxious because the lighting there is not bright. Although there are some lights in the direction of the North Building, the area beneath the benches is quite dark. The presence of someone lurking in that area could create a sense of unease and insecurity"

Analysis of gaze points revealed that participants exhibited different patterns of visual fixation under various lighting conditions. During daytime scenes, participants showed a primary interest in plants, roads, and unique signage along the roadside. In nighttime Scene A, their main areas of interest were streetlights, buildings, and roads. In nighttime Scene B, streetlight elements were the main focus. Furthermore, due to some segments being poorly illuminated at night, participants required additional time to identify the road conditions while walking. However, it does not necessarily indicate a positive correlation between duration and areas of interest.

### 3.2 Analysis of eye movement data during standing

#### 3.2.1 Analysis of the eye movement data

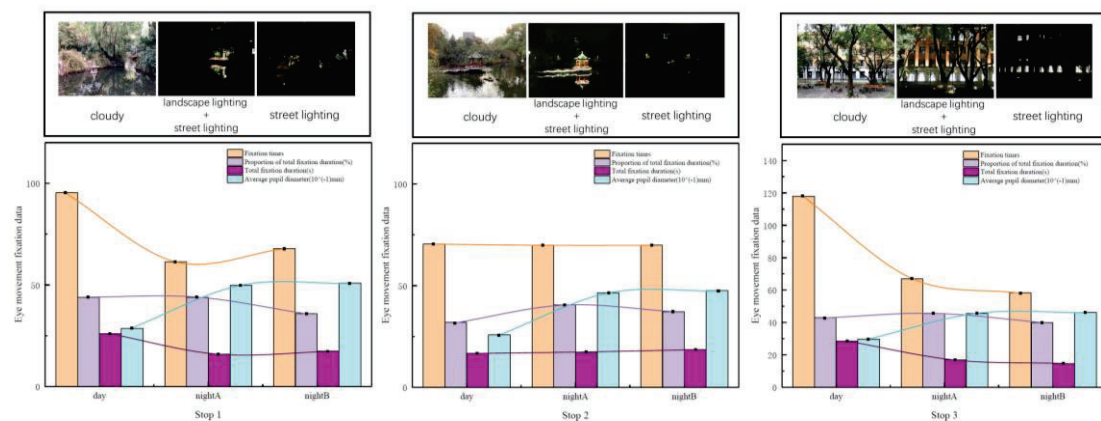


Figure 5 Eye movement fixation data statistics during standing

Results of the study on gaze points revealed that at Stop 1 and Stop 3, participants exhibited the highest number of fixations, the longest total fixation duration, and the highest proportion of gaze time in daytime environments. The data for nighttime Scene A and Scene B were relatively similar in these aspects. However, at Stop 2, participants showed comparable numbers of

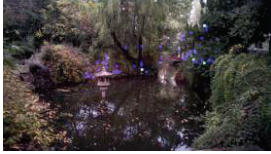
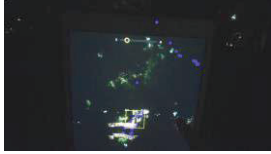
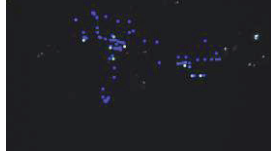





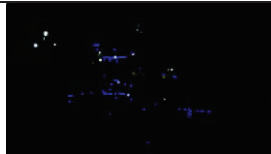
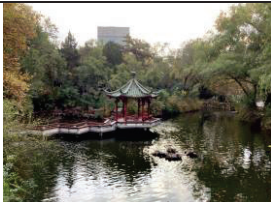


fixations and total fixation duration across all three scenes. This finding contrasts with the trends observed during walking.



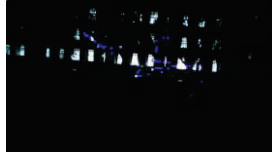


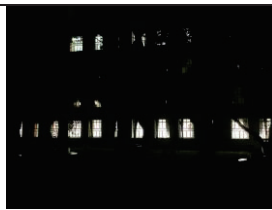
At Stop 1, participants observed dense vegetation and a water feature in the daytime scene, while nighttime Scene A and Scene B showed similar observations of bridges illuminated by landscape lights and illuminated bridges internally, respectively. Stop 2, a pavilion, had distinct landscape lighting in nighttime Scene A compared to only streetlight illumination in nighttime Scene B. Stop 3, located in front of a teaching building, exhibited architectural facade illumination and seating in nighttime Scene A, while only interior light transmission was present in nighttime Scene B. In the 'all section,' participants' pupil size was slightly larger in nighttime Scene B compared to nighttime Scene A, while the smallest pupil size was observed during the daytime.

### 3.2.2 Analysis of the cognitive and area of interest

The study selected eye-tracking data within the first 5 seconds after participants' arrival at each stop to analyze their preferences for the landscape elements at the stops. By combining photography tasks and in-depth interviews, it was possible to reveal the relationship between eye-tracking patterns and cognitive-behavioural aspects (as shown in Table 3).

Table3 Eye movement, filming tasks and subjective interviews during standing

Location	Content	Daytime Scene	Nighttime Scene A	Nighttime Scene B
Stop 1	Eye-track Heat map			
	Photo			
	AOI elements	Plants, Water features, bridge	A bridge illuminated with lights; stars scattered in Sky; Water surface	A translucent storefront; the sky above
	Evaluation	"The bridge stands out with its striking color, it looks beautiful. The reflection in the water is mesmerizing, with the stone pillars creating a sense of depth. The plants are arranged in a scattered manner, creating a visually pleasing effect."	"The reflection is unique, with vibrant colours and a feeling of flowing water. The soft and gentle glow of the small light strips adds the perfect touch to it."	"Now it's not illuminated, so it feels quite dark. However, this intersection still has some traffic, especially at night when some electric scooters don't have lights. When they approach from behind, it makes me feel a bit anxious and uncomfortable."
Stop 2	Eye-track Heat map			
	Photo			
	AOI elements	Water scenery, plants, pavilion.	Pavilion, reflection on the water, plants.	Street lamp, fountain, and building.

	Evaluation	<p>"It looks more comfortable during the day. The pavilion is not glaring at night, and you can see more details of the plants: the gradient colors of the leaves, the layering effect, and even the stones of the fountain. The water area doesn't appear as empty."</p>	<p>"The pavilion stands out under the lighting effects and, when combined with a calm water surface, creates a sense of serenity. The predominant colors of the lights are red, green, and yellow, complemented by the deep green and deep blue of the background. The overall picture appears harmonious."</p>	<p>"I think the colors in this photo are a bit monotonous. I only feel that the illuminated building contrasts with the darkness around it, but I don't find this photo particularly appealing."</p>
Stop 3	Eye-track Heat map			
	Photo			
	AOI elements	The building, Plants	The building and the illuminated seats	interior translucency
	Evaluation	<p>"I find the North Building to be quite attractive from this spot. Standing here, I can see the entire facade of the North Building, including some small benches at the entrance, plants, and the sky. Overall, it looks quite beautiful."</p>	<p>"While observing at the resting point, I noticed that there were seating areas beneath the big trees, resembling fenced enclosures. The seats were adorned with light strips that emitted a glow. I found the scene to be quite cozy and inviting, making me want to sit there. It felt very pleasant and comfortable."</p>	<p>"I find the sequential presentation of internal translucency in the photo quite boring."</p>

The analysis at the stopping points revealed that participants exhibited different patterns of visual attention under various lighting conditions. At stop1, participants paid attention to a wide range of landscape elements, including water features, vegetation, pavilions, bridges, and buildings, during the daytime scene. The overall subjective evaluation was high, and the eye movement distribution was relatively dispersed. Under nighttime scene A, participants' gaze primarily focused on illuminated elements, such as illuminated pavilions, bridges, and buildings, or self-luminous lighting fixtures. Under nighttime scene A, participants' gaze primarily focused on illuminated elements, such as illuminated pavilions, bridges, and buildings, or self-luminous lighting fixtures.

### 3.3The result of Perceived Recovery Scale

The results of the restoration scale showed that "readability" and "confusion" were not applicable in this study and were subsequently removed. After removing them, the overall reliability of the scale was good (Cronbach's Alpha: 21 items overall: 0.88, distance: 0.81, fascination: 0.90, coherence: 0.73, compatibility: 0.87). The scores of the scale (Table 4) showed that participants rated restoration perception highest in nighttime scene A, followed by the daytime scene and nighttime scene B.

Table 4 The result of Perceived Recovery Scale

	Being-Away	Fascination	Extent	Compatibility	All
--	------------	-------------	--------	---------------	-----



	Mean	Std.	Mean	Std.	Mean	Std.	Mean	Std.	Mean	Std.
Day	3.80	1.82	4.52	1.46	4.63	1.58	3.45	1.53	4.40	1.74
Night A	4.13	1.63	4.67	1.64	4.17	1.70	4.25	1.53	4.59	1.70
Night B	4.48	1.80	4.09	1.42	4.08	2.04	3.63	1.65	4.32	1.75

#### 4. DISCUSSION

Previous research has shown a positive correlation and strong consistency between eye-tracking indicators (such as fixation count and fixation duration) and landscape preferences[11][12]. Similar findings were observed in this study. In the scenes of interest mentioned by participants during interviews and subjective interviews, such as fixation point 1 and fixation point 3 in the daytime scene, a diverse range of landscape elements was observed, and participants rated them highly in in-depth interviews, resulting in a significant increase in their fixation count and fixation duration.

In some studies on landscape preferences, pupil size has been used to indicate emotional preferences[13]. However, pupil size is not as suitable for studies on diurnal and nocturnal landscape perception preferences. Pupil size is influenced by various factors including lighting, emotions, cognitive load, and attention. During intense lighting conditions, people's pupils tend to be larger. Pupils usually dilate when people feel excited, interested, or focused on a particular landscape, and they tend to contract when experiencing dislike, fear, or disinterest. Our experiment found that the influence of lighting conditions on pupil size was much greater than that of emotional representation, making it challenging to evaluate emotional characteristics of participants in diurnal and nocturnal landscapes based on pupil size.

Furthermore, this study revealed the potential of nighttime scenery for addressing psychological issues among college students. SangHyu et al.'s research found that daytime views are more beneficial for restorative purposes[14]. However, the results of this experiment suggest that the therapeutic effects of the campus nighttime environment, which has undergone lighting design improvements, may be even more significant than those of the daytime environment. This indicates the possibility that well-designed nighttime landscapes can surpass the restorative effects of daytime landscapes, demonstrating the potential for nighttime designs to have superior restorative effects.

#### 5. CONCLUSION

The research findings indicate that:(1) Eye-tracking data, in-depth interviews, and subjective rating scales demonstrate that the same scene elicits different visual perceptions and cognitive preferences under different lighting conditions.(2)Eye-tracking results reveal that the fixation of pedestrians is more diverse in daytime scenes, with the most common environmental elements being vegetation, buildings/structures, and water features. In contrast, in nighttime scenes, pedestrians tend to focus their visual attention more on illuminated environmental elements, particularly buildings/structures and streetlights.(3)The perceived restoration scale indicates that compared to other scenes, Nighttime Scene A has a higher restorative effect, suggesting the potential of well-designed night scenes to surpass the restorative effects of daytime scenes. For future studies, building upon human factors engineering, eye-tracking experiments will be conducted in virtual environments to better control experimental scenes and comprehensively analyse the perception between participants and lighting conditions.

#### REFERENCES

[1] Casey, S. M. , Varela, A. , Marriott, J. P. , Coleman, C. M. , & Harlow, B. L. . (2022). The influence of diagnosed mental health conditions and symptoms of depression and/or anxiety on



- suicide ideation, plan, and attempt among college students: findings from the healthy minds study, 2018-2019. *Journal of affective disorders*(298PA-), 298PA.
- [2] Wang J , Mao Z , Wei D ,et al. Prevalence and associated factors of anxiety among 538,500 Chinese students during the outbreak of COVID-19: A web-based cross-sectional study. *Psychiatry Research*, 2021, 305:114251-..
- [3] Li D , Sullivan W C .Impact of views to school landscapes on recovery from stress and mental fatigue. *Landscape and Urban Planning*, 2016, 148:149-158.
- [4] Kelz C , Evans G W , Roederer K .The Restorative Effects of Redesigning the Schoolyard: A Multi-Methodological, Quasi-Experimental Study in Rural Austrian Middle Schools. *Environment & Behaviour*, 2013, 47(2):119-139.
- [5] Alvarsson J J , Wiens S , Nilsson M E .Stress Recovery during Exposure to Nature Sound and Environmental Noise. *International Journal of Environmental Research & Public Health*, 2010, 7(3):1036-1046.
- [6] Zhang H .The Relationship between the Restorative Perception of the Environment and the Physiological and Psychological Effects of Different Types of Forests on University Students. *International Journal of Environmental Research and Public Health*, 2021, 18.
- [7] Bolouki A .Exploring the association between self-reported and objective measures in search of the restorative quality of natural environments: a systematic review. *International journal of environmental health research*, 2022:1-15.
- [8] Chen Z , Schulz S , Qiu M ,et al. Assessing affective experience of in-situ environmental walk via wearable biosensors for evidence-based design. *Cognitive Systems Research*, 2018, 52(DEC.):970-977.
- [9] Bolouki A .Exploring the association between self-reported and objective measures in search of the restorative quality of natural environments: a systematic review. *International journal of environmental health research*, 2022:1-15.
- [10] Birenboim A , Dijst M , Scheepers F E ,et al. Wearables and location tracking technologies for mental-state sensing in outdoor environments. *Routledge*, 2019(3).
- [11] Cottet M , Vaudor L , Tronchere H ,et al. Using gaze behaviour to gain insights into the impacts of naturalness on city dwellers' perceptions and valuation of a landscape. *Journal of Environmental Psychology*, 2018, 60(DEC.):9-20.
- [12] Kim, M., Kang, Y., Abu Baker, S.. A nightscape preference study using eye movement analysis. *Alam Cipta J.* 2013, 6 (2), 85-99.
- [13] Li Z , Sun X , Zhao S ,et al.Integrating eye-movement analysis and the semantic differential method to analyze the visual effect of a traditional commercial block in Hefei, China.*Frontiers of Chinese Architecture and Civil Engineering: English Version*, 2021(002):010.
- [14] Cheon S H , Han S , Kim M ,et al. Comparison between Daytime and Nighttime Scenery Focusing on Restorative and Recovery Effect. *Sustainability*, 2019, 11.

## ACKNOWLEDGEMENTS

Funding: This work was supported by the National Natural Science Foundation of China (No. 52078357), Tongji Architectural Design (Group) Co., Ltd. independently initiated research project (2019KY24).

Corresponding Author Name: Yi Lin

Affiliation: School of Architecture, Tongji University

e-mail: linyi\_tjcaup@tongji.edu.cn

# INVESTIGATION AND SIMULATION ABOUT LIGHT EXPOSURE AND ACTIVITIES ON THE ELDERLY: A CASE STUDY OF THE THIRD TYPE OF DAYLIGHT CLIMATIC ZONE OF URUMQI

Juanjie Li<sup>1,2</sup>, Rongdi Shao<sup>1,2</sup>, Chuang Yu<sup>1,2</sup>, Tongyue Wang<sup>3</sup>, Yanni Wang<sup>1,2</sup>, Luoxi Hao<sup>1,2</sup>,

1 School of Architecture and Urban Planning, Tongji University, Shanghai 200092, China;

2 Key Laboratory of Ecology and Energy-saving Study of Dense Habitat (Tongji University) Ministry of Education, Shanghai 200092, China

3 Shanghai Yangzhi Rehabilitation Hospital (Shanghai Sunshine Rehabilitation Center)

## ABSTRACT

Light has both visual and non-image effects on people. The design of an indoor lighting environment for elderly people should consider both the aging visual system and higher circadian, emotional, and cognitive needs to light. In the fourth type of daylight climate zone of Shanghai, which has rich daylight sources, a comprehensive solution of daylighting and artificial lighting throughout the day should be developed, which is conducive to achieving healthy and energy-saving indoor lighting goals. Abstract the typical behavior (standing, sitting, lying, going out) and activity characteristics (frequency, duration) of the elderly indoors as human factors parameters (reference planes, directions, heights, and residence time), and simulate the characteristics change in spectrum, timing, duration, and spatial distribution of light indoor during the 24 hours of four solar terms in a normal year, and calculate the compliance rate of integrative lighting needs based on relevant standards.

The conclusion proposes dynamic lighting modes and indoor design suggestions that meet the integrative lighting needs: (1) Long stay positions such as beds and sofas should be arranged parallel to the lighting surface, with a best distance of 0.5m-1.5m from the window; (2) Adding circadian strengthen lightings such as desk lamps in winter and spring; (3) Wall reflectance higher than 0.6, ceiling reflectance higher than 0.7, and the use of non-direct luminaires all contribute to the circadian lighting quality of the elderly room; (4) The active elderly and the quiet elderly should adopt different indoor lighting strategies: the former should focus on protection from exceed light before sleep, while the latter should focus on circadian light at daytime; (5) The linkage of import and shade of daylight, as well as artificial light, can achieve the optimum indoor lighting environment goals about human health and energy conservation.

Keywords: light exposure; the elderly; activities; visual and NIF lighting; circadian lighting; melanopic EDI (equivalent daylight illuminance); indoor lighting

## 1 INTRODUCTION

Light has both visual and non-image-forming effects on people [1], the design of an elder-friendly indoor lighting environment should consider the aging visual system, as well as the wakened circadian, emotional, and cognitive functions especially [2,3]. Although studies indicated that the circadian timing system has functional plasticity, it's difficult to ignore an advanced or disordered circadian phase in most old adults [4]. Given that the appropriate ocular light exposure on healthy adults had been published by CIE professionals and experts [5], the recommendation for the elderly should refer to it and take aging circadian, neuroendocrine, and neurobehavioural into consideration. CIE's recommendation, 250lx melanopic EDI (equivalent daylight illuminance) is the minimum level of daytime light exposure, while 10lx melanopic EDI and 1lx melanopic EDI are the maximum light exposure level 3 hours before sleep and at night respectively, can be interpreted in two ways, daytime light stimulus, and protection from light at night. Higher bright light levels, which means higher illuminance and blue light percentage in the spectrum, as well as longer exposure time, synchronize the human circadian rhythm well, on the condition of balancing energy efficiency, avoiding glare, and satisfying visual performance. Aging mechanisms including macular degeneration, decrease in the densities of ganglion cells, and more sedentary behavior cause less bright environmental light exposure, studies show that it was the direct output of rhythm with reduced amplitudes, advance, and disorder. The elderly need brighter lighting and twice as the recommended melanopic EDI level may be an appropriate value. Taking D65 standard illumination

as an example, the equal vertical illuminance level around the elderly eyes reached 500lx, which brings superior requirements to the light environment.

Xinjiang Urumqi belongs to the fifth type of daylight climate region in China, which was abundant in daylight resources. Regarding daylight as a primary circadian light source will achieve multi-purpose goals such as saving energy, fulfilling high-quality circadian lighting (daylight has a high melanopic DER), and promoting the elderly outdoor activities, which benefits their health. As a consequence, a comprehensive solution of daylighting and artificial lighting throughout the day should be developed, which is conducive to achieving healthy and energy-saving indoor lighting goals.

There is a crossover between different classification methods and the age segment classification method was taken in this paper. NIH (National Institutes of Health) defined the “elderly” as persons age 65 and older [6]. For different age segments, the elderly can be divided into the young old (aged 60-69), the old old (aged 70-79), and the oldest old (aged 80+) [7]. For functional status, which was measured by ADLs (activities of daily living) and IADLs (instrumental activities of daily living), the elderly can be divided into 5 levels with a range of low to high functional impairment and frequency of exercise [8]. The Law on the Protection of the Rights and Interests of the Elderly in China stipulates that the starting age standard for the elderly is 60 years old [9].

## 2 METHOD

Three typical old people were observed, measured, and analysed on their daily activities, light exposure, and sleep condition for one week through August 2022. Then simulated the daylight vertical illuminance around their eye all year round in 2022, based on the hypothesis of stability of their daily routines. At last of the article, a full-day dynamic lighting solution was given, which take considerably differentiates the daylight regionality and the elderly's types, as well as a recommendation to the elderly about physical activities and home design.

### 2.1 Investigation

Three typical old people were brought into the investigation, detailed information and activity zone were shown in Table 1 and Figure 1. All of them lived in the same town, but have different activity trajectories. Participant A was a young old male in perfect functional status, his sleep quality was not bad and was a definite morning chronotype. Although retired, A had a busy life schedule, and his daily life cycle is about 5 km. Participant C is A's mother, who had been demented and paralyzed for two years, thus A had the worst functional status and had a disordered circadian phase taking several naps during the daytime and sleeping late and bad at night. C was taken upstairs in a wheelchair for sun bask every morning or afternoon if she wants to, and her life cycle is 1km around her house. Participant B was A and C's neighborhood, and was in good functional status, and her sleep quality and chronotype were both intermediate types. B lived by herself and with children visiting every weekend. She took a small walk every day in the nearest park and went to her friend's house sometime, whose life cycle is about 3km.

Table 1 Personal information about three participants

	Age	Gender	MEQ	PSQI	Social Personality	Functional Status (ADLs, IADLs)
Participants A	60	male	81 Definite morning	4	Active	0
Participants B	74	female	57 Intermediate	10	Active	1
Participants C	84	female	39 Moderate evening	17	Quiet	4

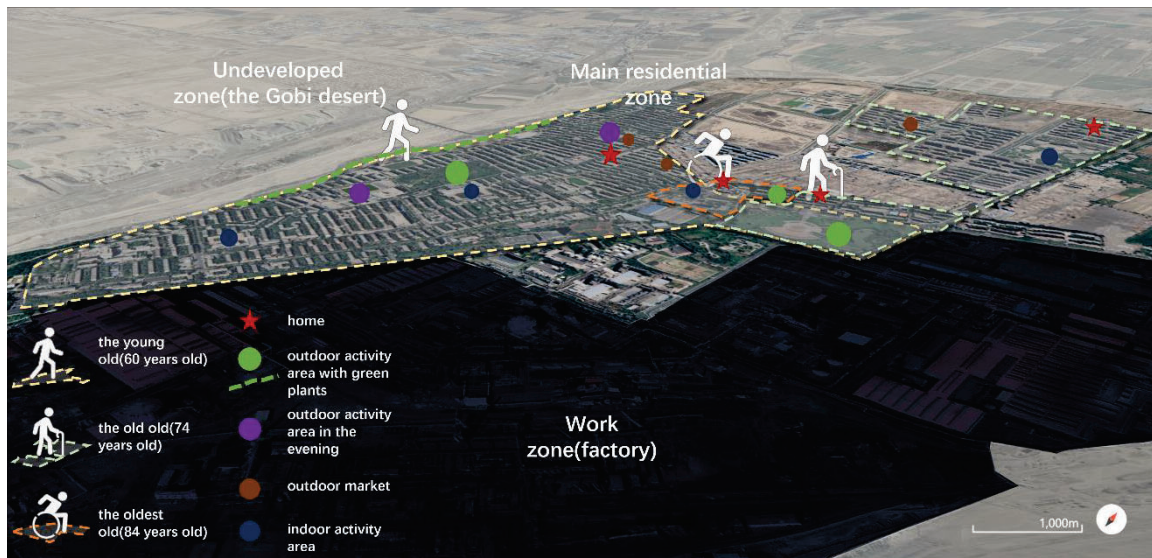


Figure 1 Activity zone of three participants

Through a week following and measuring these participants, a plot of vertical illuminance around the eyes of a typical day was shown below (see Figure 2). It can be easily observed that 1) daytime light exposure level:  $A > B > C$ . 2) A had high light exposure during morning and commuting time, while B had enough light exposure during daytime for taking outdoor activities, and C was lack of light exposure. 3) A seldom took a nap during the day, and his chronotype was definite morning, go to bed early then get up early, and sleep well; B had a siesta habit, and she was intermediate chronotype; C was always snoozing during the day, especially after the meal with high blood glucose, and C was moderate evening chronotype with bad sleep quality. It's also seen that B and C were likely to catch evening naps.

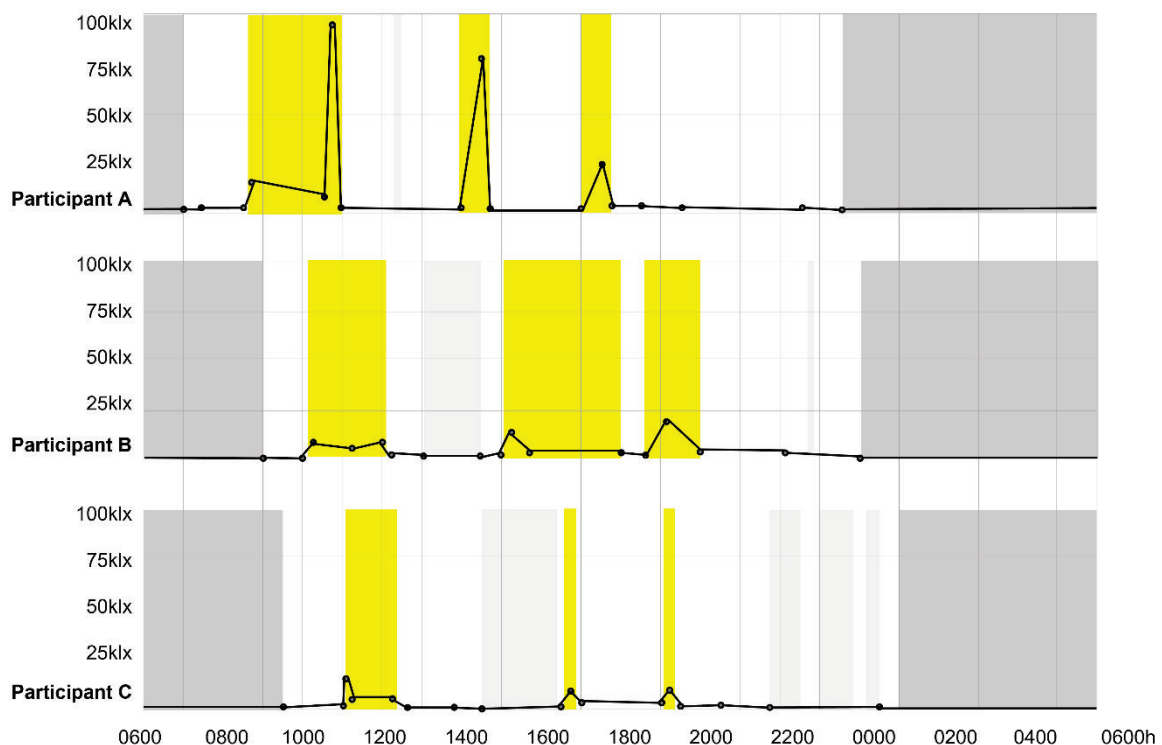


Figure 2 Vertical illuminance of the participants' eye

## 2.2 Calculation

### 2.2.1 Outdoor daylight calculation

Based on three types of standard general sky models, three typical days (the clear sky, the overcast sky, and the cloudy sky) were selected to measure the daylight illuminance of the vertical plane at 1.6m high (illuminance of eye position). All three typical days supplied abundant circadian stimulus



at the eye position, which means outdoor daylight can create more than 500lx melanopic EDI and maintain longer than four hours (see Figure 3). The sky condition in August was composed of three types of standard general sky models, which were twelve days of clear sky, two days of overcast sky, and seventeen days of cloudy sky, while the mean  $\pm$ SD of duration of sunshine and total irradiance in twelve months of a year were  $7.26E+08 \pm 3.44E+08$  and  $362.0 \pm 57.3$ , it is obvious that the outdoor daylight supplies enough circadian stimulus to the elders through the entire month and the whole year in Urumqi.

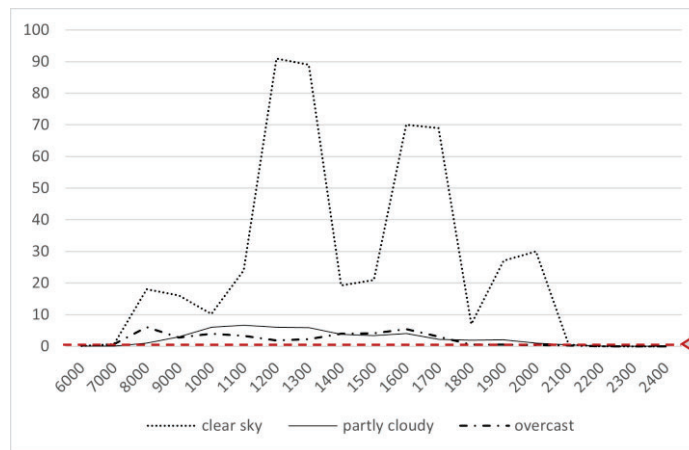


Figure 3 Illuminance of eye position in the clear sky, the overcast sky, and the cloudy sky conditions (the red dot line represents 500lx melanopic EDI)

The standard for daylighting design of buildings (GB50034) illustrates that even in the deficient fifth daylight climate zone, the outdoor daylight illuminance was 12klx of an average year, which is about 4klx eye position illuminance and far more than the recommended values. As a consequence, to keep enough daylight exposure, it should be encouraged to prolong the elders' outdoor activities duration and frequency during the daytime, and as for those demented and paralyzed elders, electronic luminaires were equipped to enhance indoor circadian lighting.

### 2.2.2 Indoor daylighting model

The indoor daylighting model needs to consider the daylighting indoors and the elder's behaviors, the former was related to the geographical latitude, altitude, absolute humidity, sunshine duration, total irradiance, daylight factor, and daylight climate coefficient, while the latter need to first abstract the typical behavior (standing, sitting, lying, going out) and activity characteristics (frequency, duration) of the elderly being indoor and outdoor, then figure out human factor parameters (reference planes, directions, heights), as well as light parameters (spectrum, timing, duration, and spatial distribution of light) around the year, finally calculate the gap between the elderly needs and recommended value. The model will be discussed in future research. Referring to the elementary measurement data indoors, facing towards the window and staying within a range of one-meter distance around the window or the balcony, the daylighting indoors will benefit the elder's circadian system, furniture arranged towards the window was also encouraged.

## 3 RECOMMENDATIONS

### 3.1 Lighting and physical activity solution

Recommendations for lighting and exercise for the elderly were as followed (see Table 2), based on CIE (International Commission on Illumination) and ACSM (American College of Sports Medicine) recommendations:

Table 2 Recommendation for the elderly light exposure and exercise

Types	daytime	night	Participant A, the young old	Participant B, the intermediate old	Participant C, the oldest old



Healthful visual lighting	Above 200lx at the 1.2m height vertical plane [10]		1)More morning exercise, in moderate and vigorous intensity, like, running, yoga, and ball game, both benefit physical health and circadian health;	1) More morning exercise, in moderate intensity, like Taiji, walking, jogging, etc;	1)More morning exercise and morning bright light. Exercise intensity depends on the individual level, for example, take a morning walk outdoors; walk outside and bask in the sun; for paralysis or demented people, just facing toward a window or light therapy devices and doing some stretching will helps inducing daytime alertness and entraining the circadian rhythm;
Healthful circadian lighting [5]	Above 500lx melanopic EDI during the day	Below 10lx, 3 hours before bedtime;  Below 1lx, at night	2)Too much light before sleep, it's better to wear a blue-light-filtered glass or avoid outdoor activities at night with bright light	2) Too much light before sleep, it's better to switch on night mode and turn down the brightness on electronic devices, like television and phone screens	2) Too much light before sleep, better to use low color temperature (below 3000K) dimming inductive nightlight for getting up at night.
Healthful physical activity	A combination of moderate- and vigorous-intensity exercise to achieve a total energy expenditure of $\geq 500-1000$ MET•min•wk <sup>-1</sup> . On 2-3 d•wk <sup>-1</sup> for adults. [11]	Intense exercise right before bedtime may lead to phase delay. [12]			

### 3.2 Indoor design

The dynamic lighting modes and indoor design suggestions to meet the integrative lighting needs: (1) Long stay positions such as beds and sofas should be arranged parallel to the lighting surface, with the best distance of 0.5m-1.5m from the window; (2) Adding circadian strengthen lightings such as desk lamps in winter and spring; (3) Wall reflectance higher than 0.6, ceiling reflectance higher than 0.7, and the use of non-direct luminaires all contribute to the circadian lighting quality of the elderly room; (4) The active elderly and the quiet elderly should adopt different indoor lighting strategies: the former should focus on protection from exceed light before sleep, while the latter should focus on circadian light at daytime; (5) The linkage of import and shade of daylight, as well as artificial light, can achieve the optimum indoor lighting environment goals about human health and energy conservation.

#### REFERENCE

- [1]. Brown TM, Brainard GC, Cajochen C, Czeisler CA, Hanifin JP, Lockley SW, Lucas RJ, Münch M, O'Hagan JB, Peirson SN, Price LLA, Roenneberg T, Schlangen LJM, Skene DJ, Spitschan M, Vetter C, Zee PC, Wright KP Jr. Recommendations for daytime, evening, and nighttime indoor light exposure to best support physiology, sleep, and wakefulness in healthy adults. *PLoS Biol.* 2022 Mar 17;20(3):e3001571.
- [2]. Owsley C. Aging and vision. *Vision Res.* 2011 Jul 1;51(13):1610-22.
- [3]. Dzierzewski JM, Perez E, Ravyts SG, Dautovich N. Sleep and Cognition: A Narrative Review Focused on Older Adults. *Sleep Med Clin.* 2022 Jun;17(2):205-222.
- [4]. Eus J.W. Van Someren, Rixt F. Riemersma, Dick F. Swaab, Functional plasticity of the

- circadian timing system in old age: light exposure, *Progress in Brain Research*[J], Elsevier, Volume 138, 2002, Pages 205-231.
- [5]. Brown TM, Brainard GC, Cajochen C, Czeisler CA, Hanifin JP, et al. (2022) Recommendations for daytime, evening, and nighttime indoor light exposure to best support physiology, sleep, and wakefulness in healthy adults. *PLOS Biology* 20(3): e3001571.
  - [6]. <https://www.ncbi.nlm.nih.gov/books/NBK235450/#:~:text=Traditionally%2C%20the%20%E2%80%9Celderly%E2%80%9D%20are,persons%20age%2065%20and%20older.>
  - [7]. Chou K-L, Chi I. Successful Aging among the Young-Old, Old-Old, and Oldest-Old Chinese. *The International Journal of Aging and Human Development*. 2002;54(1):1-14.
  - [8]. Edemekong PF, Bomgaars DL, Sukumaran S, Schoo C. Activities of Daily Living. 2022 Nov 19. In: StatPearls [Internet]. Treasure Island (FL): StatPearls Publishing; 2023 Jan.
  - [9]. [https://www.gov.cn/banshi/2005-05/25/content\\_952.htm](https://www.gov.cn/banshi/2005-05/25/content_952.htm)
  - [10]. BS EN 12464-1, Light and lighting. Lighting of work places. Part1 : Indoor work place
  - [11]. Garber C.E., Blissmer B., Deschenes M.R., Franklin B.A., Lamonte M.J., Lee I.-M., Nieman D.C., Swain D.P. Quantity and quality of exercise for developing and maintaining cardiorespiratory, musculoskeletal, and neuromotor fitness in apparently healthy adults: Guidance for prescribing exercise. (2011) *Medicine and Science in Sports and Exercise*, 43 (7), pp. 1334 - 1359.
  - [12]. O.M. Buxton, C.W. Lee, M. L'Hermite-Baleriaux, F.W. Turek, E. Van Cauter. Exercise elicits phase shifts and acute alterations of melatonin that vary with circadian phase. *Am. J. Physiol. Regul. Integr. Comp. Physiol.*, 284 (3) (2003), pp. R714-R724, 10.1152/ajpregu.00355.2002

## ACKNOWLEDGEMENT

Corresponding Author: Juanjie Li

Affiliation: College of Architecture and Urban Planning, Tongji University

e-mail : 490711356@qq.com

# A META-ANALYSIS OF THE INDOOR LIGHTING DESIGN PARAMETERS FOR PROMOTING HEALTHY SLEEP

Yixiao Cao, Rongdi Shao, Luoxi Hao

(Beijing institute of architectural design, Beijing, China)

(Tongji University, Shanghai, China)

## ABSTRACT

The achievement of adequate sleep is vitally necessary for the maintenance of physical and mental health. Indoor lighting conditions have a considerable impact on the consistency of daily sleep. In the field of evidence-based design, meta-analyses are often regarded as the most authoritative kind of evidence, offering a solid foundation for making wise judgements. In order to evaluate the establishment of ideal indoor lighting conditions supportive of fostering good sleep patterns, the current study uses a meta-analysis technique. This study examined the effects of various lighting interventions, including nighttime blue light restriction, dynamic daylighting, and bright light, on sleep duration, delayed sleep period, the proportion of rapid eye movement sleep. The meta-analysis findings highlight the importance of the light environment for sleep and the beneficial influence of a dynamic, cyclical light environment throughout the day on sleep quality.

Keywords: Lighting design, Lighting interventions, Sleep environment, Workplace

## 1. INTRODUCTION

There exist a multitude of light environment factors that exert an impact on the quality of sleep[1-3]. By combining different light parameters, diverse forms of light therapy for promoting healthy sleep can be devised, each yielding distinct effects. These interventions directly and indirectly influence sleep quality by modulating circadian rhythms and engaging multiple neural pathways. The assessment of sleep quality encompasses multiple dimensions, and the impact of light varies across diverse indicators. The optimal configuration of light and combination of parameters for the sleep environment is still uncertain in terms of its underlying mechanisms. Numerous researchers have endeavored to employ experimental designs and statistical analyses in order to identify patterns that encapsulate the relationship between light parameters and sleep. However, the presence of diverse experimental conditions, subject heterogeneity, and disparate experimental protocols have contributed to a multitude of conflicting findings across various studies. Consequently, a consensus regarding the resolution to this inquiry has yet to be reached. The utilization of meta-analysis offers a novel perspective by amalgamating the outcomes of numerous experiments via statistical analysis. This approach enhances the sample size and test effectiveness, thereby bridging the gap between the obtained results and the actual scenario[4]. Hence, this study employs a meta-analysis approach to examine and contrast the impacts of high retinoid lighting, nighttime blue light restriction, dynamic daylight, and other light modalities on various sleep parameters, including sleep duration, sleep latency, and rapid eye movement (REM) sleep. This study employs a meta-analysis to examine the impact of bright light, blue light restriction, and dynamic daylight on various sleep parameters, including sleep duration, delayed sleep period, the proportion of rapid eye movement sleep and the proportion of slow wave sleep. The findings contribute to the identification of optimal indoor lighting conditions for promoting healthy sleep, addressing the current dearth of parametric evidence for designing sleep environments. Further investigation into the underlying mechanisms and accumulation of experimental data will enhance the reliability of the conclusions.

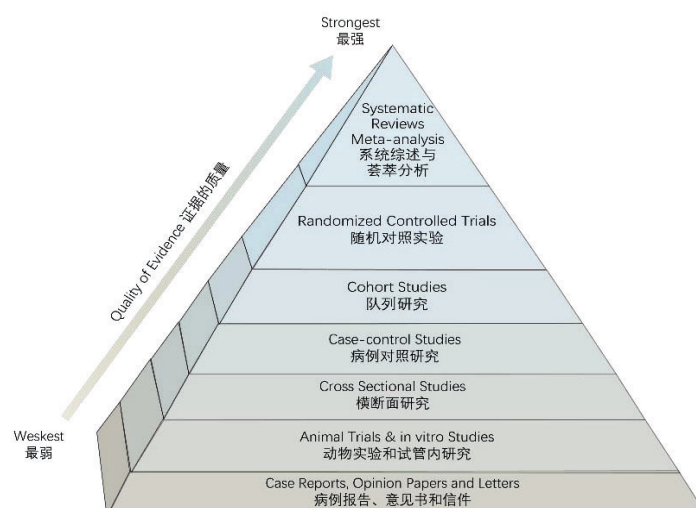


Figure 1. Meta-analysis is widely regarded as a highly dependable foundation for decision-making within the realm of evidence-based design.

## 2. METHODS

### 2.1 Light conditions

This thesis aims to conduct a meta-analysis on the impact of five different light patterns on various indicators of sleep. These light patterns include:

- (1) High intensity bright light, characterized by horizontal illuminance levels exceeding 2000lx or eye illuminance levels surpassing 1000lx.
- (2) Standard room lighting, with illumination levels between 50 and 1000 lx and color temperatures between 3000K and 6000K.
- (3) Blue-rich lighting, high colour temperature white light illumination mode or wavelength 410nm-480nm narrow band monochromatic light illumination mode.
- (4) Blue-light-restricted lighting, warm white light with a color temperature less than 3000K, or coloured lighting with orange and red tones.
- (5) Dynamic lighting, a combination of day and night light interventions, or artificial lighting that simulates natural light forms

### 2.2 Literature search strategy and screening

The literature utilized in the meta-analysis was retrieved from four databases, namely "Web of Science," "PubMed," "The Cochrane Library," and "Embase." The search duration spanned from 1980 to June 2022. The search strategy employed consisted of a blend of subject terms related to light and sleep, as well as additional free terms. Search terms for light include "light", "light exposure", "light therapy", "bright light", "color temperature", "light intensity", and "spectrum"; search terms for sleep include "sleep", "sleep quality", and "sleep structure".

The criteria for inclusion in the meta-analysis studies were as follows:

- (1) Randomized controlled experiments employing either a crossover or parallel group configuration;
- (2) Utilization of visible light as a means of improving sleep quality
- (3) Investigation conducted on individuals who are in good health, devoid of sleep disorders, and without any underlying medical ailments;
- (4) The participants fall within the age range of 18 to 65 years;
- (5) Experimental investigations encompassing a sample size exceeding 5 subjects;
- (6) Study participants consist of individuals adhering to a regular work schedule, devoid of shift work or transcontinental travel.
- (7) Light does not operate as an autonomous intervention.

The following were the study's exclusion criteria:

- (1) The study did not meet the criteria for inclusion;
- (2) Animal experiments or experiments on isolated cells;

- (3) Screen luminescence studies using natural light or video terminals;
- (4) Experimental procedures involving sleep restriction or sleep deprivation;
- (5) Different studies but using duplicate subject data;
- (6) Literature with incomplete reporting of outcome data.

Two people independently searched for and screened articles, and after thorough discussion between the screeners and the methodological caliber of the included research, the literature that seemed to differ was either included or deleted by consensus. Using the Cochrane Risk of Bias Assessment Tool, independent evaluation.

### 2.3 Data extraction

The following study characteristics were extracted from the included literature: the author, year of study, and region. Additionally, it includes details about the study subjects, such as their age and gender. Furthermore, the characteristics of the sleep intervention light are described, encompassing factors such as light intensity, spectral composition, duration, length, and form of the intervention. The sleep indicators that were extracted encompassed various aspects, such as sleep duration, sleep onset latency, proportion of rapid eye movement (REM) sleep, and proportion of slow wave sleep (SWS). The study's outcome data were derived by extracting the means, standard deviations, and sample sizes of subjects in both the intervention and control groups.

### 2.4 Statistical analysis

RevMan 5.3 was employed as the statistical software for conducting the meta-analysis. The effect size indicator chosen for this study was the Weighted Mean Difference (WMD) due to the fact that all intervention outcomes reported in the included studies were continuous variables. The researchers opted to use the Standardised Mean Difference (SMD) as the effect measure in cases where multiple measures were employed to assess the same intervention target, where different units of measurement were utilized, or where the reported mean values for the same measure varied by a factor of 10 or more in the literature. The statistical values were represented as mean differences accompanied by 95% confidence intervals. The measurement of heterogeneity between studies was conducted using the Cochran Q test and the  $I^2$  statistic.

## 3. Results

### 3.1 Studies description

During the initial stage of the investigation, scholarly articles were obtained from four distinct databases, yielding a cumulative total of 2190 outcomes. From a selection of 1990 articles, research content that was deemed irrelevant, such as titles related to non-English and Chinese literature, animal experimental studies, and studies involving non-visible light sources (including natural light, spontaneous light electronic screens, light filters, and ultraviolet light), was excluded. The abstracts of the literature were reviewed and subsequently excluded if they pertained to populations that were not considered healthy, if they involved age groups that were outside the scope of the analysis, if they focused on sleep deprivation and shift work in an experimental paradigm, or if they did not meet the criteria for inclusion or exclusion. Ultimately, a total of 22 articles were identified for the purpose of conducting a meta-analysis. According to the guidelines outlined in the Preferred Reporting Items for Systematic Reviews and Meta-Analyses (PRISMA), it is recommended that efforts be made to contact the original authors in cases where literature lacks complete outcome data or only presents statistical effects. However, it is acknowledged that there may be challenges in contacting these authors, which can hinder the acquisition of such data. These items were temporarily excluded due to factors such as the unavailability of the original authors for contact or the non-disclosure of data.



Table 1. Information on included literature

No	Basic study information			Intervention condition			Control condition			Time	Hour/ day	day	Facil ity	Age	male( %)	indicat ors
	Author, year of publication, country			lx	CCT	n	lx	CCT	n							
1	J Carrier	1995	CA	6000-13000	/	8	<100	/	8	8:30-13:30	5	3	lp	22.9	75	bc
		1996		6000-13000	/	7	<100	/	7	18:30-23:30	5	3	lp	22.6	85.7	bc
		1997		6000-13000	/	8	<100	/	8	13:30-18:30	5	3	lp	23	75	bc
2	Danilenko, K. V.	2000	RUS	0.001-1000	/	9	dark	/	9	3:30-6:00-7:30	0.5	6	sd	24.0±4.8	100	a
3	Wakamura, T.	2000	JP	6000	/	7	200	/	7	wake-18:00	≈8	4	fl	20±2	0	a
4	Munch, M.	2016	DE	750	3573	18	40	2600	18	8:00-11:00	3	3	fl	23.± 3.3	75	ab
5	Knaier, R.	2017	CH	4400	Peak 545 nm	24	230	Peak 545nm	24	17:00-18:00	1	1	tl	18-35	100	a
				230	Peak 469 nm	24	230	Peak 545nm	24	17:00-18:00	1	1	tl	18-35	100	a
6	Hea Ree Park	2020	KR	150 (LED)	4000	24	<10	/	24	18:00-24:00	6	1	rl	26.9±5.7	25	b
				150 (OLED)	4000	24	<10	/	24	18:00-24:00	6	1	rl	26.9±5.7	25	b
7	Cajochen, C.	1992	CH	2500	/	7	6	/	7	21:00-0:00	3	2	lp	23-32	100	ab
8	Munch, M.	2006	CH	82.61	460nm	8	dark	/	8	21:30-23:30	2	1	gl	24.6±3	100	ac
				68.64	550nm	8	dark	/	8	21:30-23:30	2	1	gl	24.6±3	100	ac
9	Viola, A. U.	2008	UK	310±98.9	4000	94	409. 11	/	94	8:30-16:45	8.25	28	rl	34.9±1.4	52.1	a
				421±128.5	17000	94	409. 11	/	94	8:30-16:45	8.25	28	rl	34.9±1.4	52.1	a
10	Mottram, V.	2011	UK	30±18	5000	15	53±28	/	15	8:00-18:00	10	21	lb	32.5 ± 8	66.7	ab
				30±18	17000	15	53±28	/	15	8:00-18:00	10	21	lb	32.5 ± 8	66.7	ab
11	Chellappa, S. L.	2013	CH	40	6000	9	40	2500	9	Before sleep -2:45-0:45	2	1	rl	25.9 ± 1.2	100	ac
				40	6000	9	40	2500	9	Before sleep -2:45-0:45	2	1	rl	25.9 ± 1.2	100	ac

12	Chellappa, S. L.	2014	CH	27	2500	30	29.8	3000	30	Before sleep -2:45-0:45	2	1	rl	25.2± 3.1	53.3	a
				27.8	6000	30	29.8	3000	30	Before sleep -2:45-0:45	2	1	rl	25.2± 3.1	53.3	ac
13	Cho, C.	2014	KR	5	6000	11	dark	/	11	23:00-7:00	8	1	lb	22.26±2.65	100	ab
				10	6000	12	dark	/	12	23:00-7:00	8	1	lb	22.26±2.65	100	ab
14	Moniek Geerdink	2016	NL	2306	Peak 470 nm	15	70	Peak 590nm	19	After wake 0.5h	0.5	9	lb	23.1±8.6	50	ab
15	Danilenko, K. V.	2016	RUS	140	organge	26	140	organge	26	19:30-20:15, 7:13-7:43	0.8 0.5	13	at	37	7.69	a
16	Momoko Kayaba	2016	JP	46.9	Peak 465nm	9	dark	/	9	21:30-23:30	2	1	rl	22.7±1.5	100	ab
17	Chul-Hyun Cho	2018	KR	5	5779.1	12	dark	/	12	23:00-7:00	8	1	lb	23.86±2.97	0	ab
				10	5779.1	13	dark	/	13	23:00-7:00	8	1	lb	23.86±2.97	0	ab
18	Yang, M. Q.	2018	CN	1000	6000	15	<5	3600	15	Before sleep3h	3	3	lb	20±3.4	46.7	ab
19	Chamorro,Rodrigo	2021	DE	<5	/	20	dark	/	20	23:00-7:00	8	2	lb	23.4±6.71	100	a
20	Ishizawa, Masao	2021	JP	Blue light		11	/	/	11	Before sleep1h	1	7	lb	20.9±1	100	ac
				Blue light restricted		11	/	/	11	Before sleep1h	1	7	lb	20.9±1	100	ac
21	Vethe, D.	2021	NO	55-124	Filtering 460nm	12	dark	/	12	18:30-06:50	12	5	rl	23.0±3.1	41.7	ab
22	Choi, Y. J.	2021	JP	10000	/	10	0.03	/	10	21:00-24:00	3	1	lb	26±3.16	100	ab

Note 1: Intervention modalities are represented by abbreviated letters, lp:illuminated panels, sd:simulated dawn, fl:fluorescent lamp, rL:room light, tl:table light, gl:Light-emitting glasses, lb:light box, at:artificial twilight

**Note 2:** Intervention modalities are represented by letters, a:sleep duration, b:sleep latency, c:Proportion of rapid eye movement (REM) sleep.

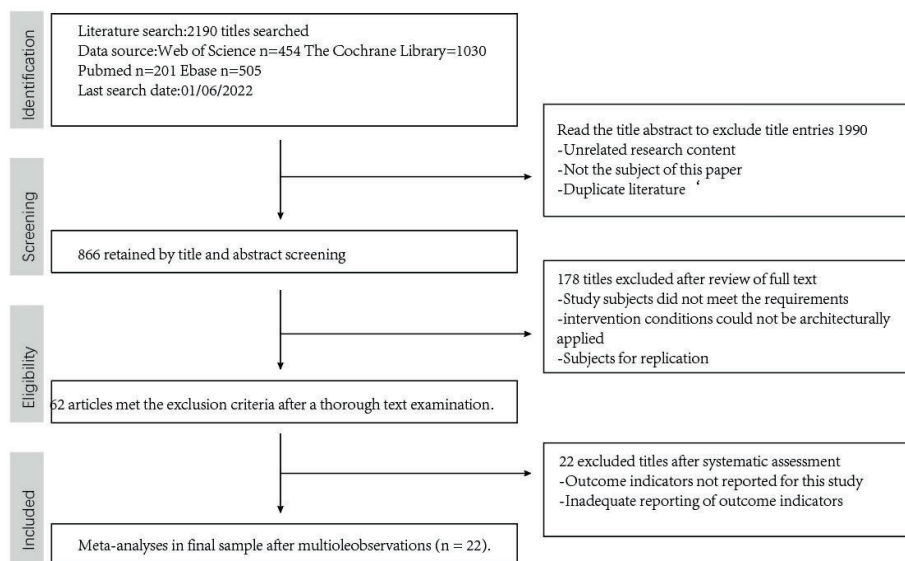


Figure2. The literature screening process

### 3.2 Sleep duration

#### (1) The Impact of Light Intensity and Spectral Composition Characteristics

The group that optimized the room light received a p-value of 0.16 and an  $I^2$  value of 37% from the statistical analysis used to determine the degree of study heterogeneity. The blue light restriction group displayed a p-value of 0.09 and an  $I^2$  value of 59% in a similar manner. The  $I^2$  value for the final three groups was 0. In contrast. Thus, it can be assumed that the aforementioned studies showed homogeneity, which is what led to the choice of a fixed effects model for the meta-analysis of the length of sleep. Both the indoor light stimulation (weighted mean difference [WMD] = -6.63, 95% confidence interval [CI]: -12.64, -0.2,  $p = 0.003$ ) and low intensity light (WMD = -10.15, 95% CI: -15.86, -0.44,  $p = 0.0005$ ) groups showed a statistically significant difference between the combined impact of the stimulation and control groups. Light exposure was given to both experimental groups while they were dozing off. The total amount of sleep time decreased as a result of exposure to low light and the application of room light stimulation at levels similar to those used for daily activity lighting. As a result, it is essential to create a dark, dark environment that effectively blocks any outside sources of illumination while you sleep.

#### (2) The impact of the timing of light stimulation

The data was divided into five distinct subgroups based on the time periods of early morning, daytime, evening, sleep phase, and a combination of early morning and evening. The  $I^2$  values for each subgroup were found to be below 50 during the heterogeneity test, leading to the adoption of a fixed-effects model for the meta-analysis. There was no statistically significant impact of light stimulation observed during any of the light periods, except for the combined findings of the three studies in the continuous low-intensity light group during the sleep phase (weighted mean difference [WMD] = -10.15, 95% confidence interval [CI]: -15.86 to -0.44,  $p = 0.0005$ ).

### 3.3 Sleep latency

#### (1) The Impact of Light Intensity and Spectral Composition Characteristics

The study conducted a meta-analysis to examine the relationship between the intensity and spectral characteristics of light stimuli and sleep latency. The analysis categorized the data into four groups: intense light stimulation, room light, blue-rich light, and low-light continuous light. The overall heterogeneity of the four groups that were included in the study was found to be  $I^2=56\%$ , with a p-value of 0.003. Additionally, it was observed that there was a high level of heterogeneity among the literature. Therefore, a random-effects model was selected for combining the effect sizes. There was no statistically significant difference in sleep latency observed between the groups exposed to different forms of light stimulation and the control group, when considering their combined effects. The observed alterations in sleep latency exhibited variability across studies employing similar forms of light stimulation. In addition to the potential influence of light

intensity and spectral composition on sleep latency, other light-related factors may also play a role in modulating this aspect of sleep.

## (2) The impact of the timing of light stimulation

The meta-analysis employed a fixed-effects model due to the  $I^2$  test indicating a heterogeneity of less than 50 across the four subgroups of studies, namely early morning, daytime, nighttime, and sleep stages. The collective findings of the three studies conducted within the early morning light group demonstrated a significant reduction in sleep latency due to early morning light stimulation (weighted mean difference [WMD] = -4.77, 95% confidence interval [CI]: -7.42, -2.12). The collective findings from the six studies encompassed in the nocturnal light group indicate that exposure to nocturnal light is associated with an increase in sleep latency (weighted mean difference = 1.67, 95% confidence interval: 0.4, -2.93). The concurrent exposure to daytime light and continuous light during sleep did not yield a statistically significant impact on sleep latency.

## 3.4 Proportion of rapid eye movement (REM) sleep.

### (1) The Impact of Light Intensity and Spectral Composition Characteristics

Room light and blue-rich light decreased REM sleep. Room light had a weighted mean difference (WMD) of -0.54 (95% CI=-1.67,0.79,  $p=0.43$ ), whereas blue-rich light had -1.48 (95% CI=-4.34,1.57,  $p=0.36$ ). These impacts were not statistically significant compared to the control group's results. Light stimulation increased REM sleep (WMD=1.15, 95% CI=-0.28, 2.59) compared to the dark control group. Note that this effect was not statistically significant (Figure 3).

### (2) The impact of the timing of light stimulation

The findings from the group exposed to nocturnal light indicated a minor decrease in the proportion of rapid eye movement (REM) sleep due to light stimulation (WMD=-0.56, 95% CI=-1.73, 0.6). However, it is important to note that this outcome did not reach statistical significance. Based on the findings of the meta-analysis, it was observed that light stimulation did not yield any significant alteration in the proportion of rapid eye movement (REM) sleep duration.

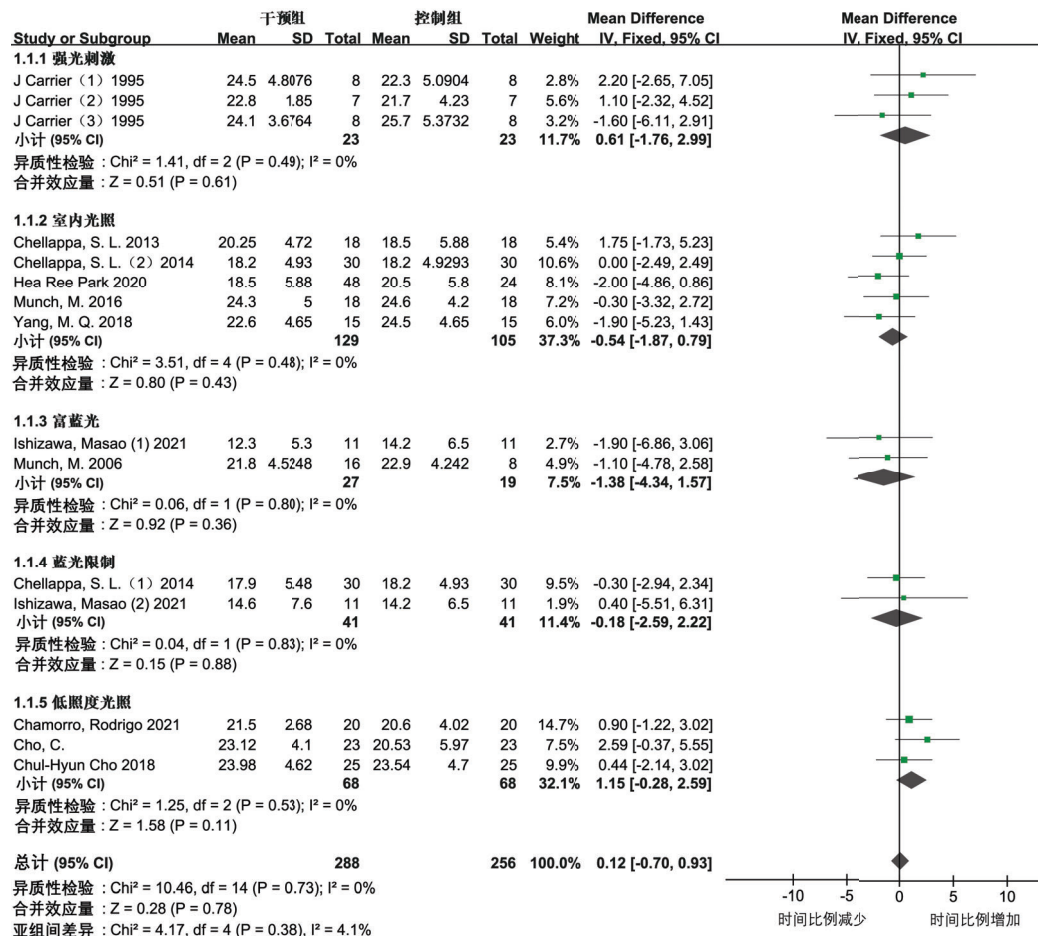


Figure3. Forest plots of rapid eye movement sleep and light stimulation intensity and spectrum.

#### 4. DISCUSSION

The meta-analysis of light's effects on three sleep markers highlighted the following concerns for this thesis.

(1)Light Intensity: Only a few investigations on bright light stimulation and sleep showed a statistically meaningful effect. The circadian system requires adequate light stimulation to start. However, inhibiting bright light stimulation may not activate the sleep homeostasis system. Light stimulation and other factors may regulate sleep quality. To investigate further, more literature is needed.

(2)Temporal parameters :Light stimuli affect sleep indices, especially in the evening. Light stimulation during the nocturnal period might potentially affect sleep quality. Nighttime light stimulation decreases sleep latency and efficiency.

(3)Light-free sleep: This meta-analysis shows how uninterrupted light exposure during sleep affects sleep quality. The most important, constant, and notable aspect is this effect. This analysis included only low-intensity, high-color-temperature trials with illuminance levels below 10lx. Despite the low light intensity, subjects reported significant sleep quality and architectural changes. The study reveals that the sleep maintenance system is very sensitive to external light cues before and after sleep. Thus, light avoidance and shading must be used to create a dark sleep environment and limit exposure to even low light levels.

#### 5.CONCLUSION

The thesis summarizes the following tactics for designing healthy lighting for sleeping environments based on the findings of the meta-analysis.

(1) Create a lighting schedule and an all-weather lighting program. To lessen the negative effects of nighttime light, the design can increase the amount of light stimulation received in the morning and during the day.

(2) Create a "healthy sleep outcome" oriented design with a variety of light parameter combinations and multi-level interventions, depending on the precise desired outcomes, such as normalizing sleep duration and reducing daytime sleepiness.

The small sample size of the literature and the conclusions drawn from the meta-analysis are still premature and should be treated with caution because the meta-analysis used strict inclusion criteria to prevent the influence of confounding variables like age and health status on the results.

#### REFERENCE

- [1] Papatsimpa C, Linnartz J P. Personalized office lighting for circadian health and improved sleep. *Sensors*, 2020, 20(16): 4569.
- [2] Figueiro M G, Rea M S. Office lighting and personal light exposures in two seasons: Impact on sleep and mood. *Lighting Research & Technology*, 2016, 48(3): 352-364..
- [3] Faulkner S M, Bee P E, Meyer N, et al. Light therapies to improve sleep in intrinsic circadian rhythm sleep disorders and neuro-psychiatric illness: A systematic review and meta-analysis. *Sleep medicine reviews*, 2019, 46: 108-123.
- [4] L'ABBÉ K A, Detsky A S, O'ROURKE K. Meta-analysis in clinical research. *Annals of internal medicine*, 1987, 107(2): 224-233.

#### ACKNOWLEDGEMENT

Corresponding Author: luoxi Hao  
Affiliation: School of Architecture, Tongji University  
e-mail : 2573898116 @ qq.com



## A basic study on the effects of interaction between pure tone frequencies and lighting luminance on the psychological state

Kato, Y.<sup>1</sup>, Yu, H.<sup>1</sup>, Akita, T.<sup>1</sup>, Hirate K.<sup>1</sup>, and Sano, N.<sup>1</sup>

(<sup>1</sup>Tokyo Denki University, Tokyo, Japan)

### ABSTRACT

It is known that the sense of comfort in the built environment is greatly influenced not only by the interaction of visual and auditory factors, but also by the sense of harmony. Therefore, it is necessary to study the relationship between the sense of harmony and the sense of comfort by taking a composite view of the physical characteristics of sound and light. Therefore, as a basic study, this research focused on the interaction between the frequency of pure tone and the luminance of lighting and examined the effects of this interaction on the psychological sense of harmony and comfort.

In the experiment, a ratio of 1:10 scale model of a school space was used. The two experimental factors were the frequency of pure tone (7 levels between 63 and 4000 Hz) and the luminance of the lighting (11 levels between 96 and 4080 cd/m<sup>2</sup>). Subjects were asked to rate their impressions on five factors: harmony, comfort, spatial brightness, tone level, and appropriateness for light work on a seven-point scale. Subjects were asked to look into the model space, listen to whether the tone and the brightness of the space were in harmony, and evaluate their impressions. After that, the light was dimmed until the harmony was changed, and another evaluation was made after it was changed. The point at which there was a change was the turning point. The same was done for the feeling of comfort. The subjects were 14 healthy students between the ages of 21 and 25.

A two-way ANOVA was conducted on tone and luminance for subjects who had a turning point, and significant differences were found in the interaction between luminance and tone and luminance for the sense of harmony, and between tone, luminance, and tone and luminance for the sense of comfort. Next, an iso-evaluative chart was created and analyzed for the sense of harmony and sense of comfort. As a result, it was found that the sense of harmony was found at low frequencies with low luminance, high frequencies with high luminance, and the sense of comfort was found at high frequencies with high luminance. The subjects were divided into two groups for "preferred lighting brightness," dark and light, based on the preliminary survey. The results showed that the subjects who preferred dark lighting in terms of harmony rated the combination of low brightness at low frequencies, medium brightness at medium frequencies, and high brightness at high frequencies, while the subjects who preferred bright lighting rated the combination of low brightness at low frequencies and high brightness at high frequencies. The group of subjects who preferred dark lighting for a sense of comfort preferred a combination of low luminance at low frequencies and medium luminance at medium frequencies, while the group of subjects who preferred bright lighting preferred a combination of low luminance at low frequencies and high luminance at high frequencies. The results of this study suggest that comfort is not necessarily perceived when a sense of harmony is perceived.

**Keyword:** Comfort, Harmony, Tone frequency, Luminance, Interaction, Adjustment method

### 1 Introduction

When designing architectural spaces, it is important to consider the sense of comfort. According to Gassho et al.[1], the overall sense of comfort is not only influenced by the interaction of visual and auditory factors, but also by the "sense of harmony. On the other hand, the

architectural space in which we usually live contains a variety of environmental information such as sound, light, heat, and smell. When people are in an architectural space, they do not perceive and judge these pieces of information in isolation, but rather they perceive them simultaneously and unconsciously judge their combined impressions. It is also known that there is a resonance phenomenon through the psychological properties common to sight and hearing, and that there is a concerted phenomenon in which sight and hearing interact with each other to give a better impression when sound and images are superimposed [2]. Based on the above, in order to create a comfortable architectural space, it is necessary to consider sound and light in a composite manner and study their relationship to the "sense of harmony" and "sense of comfort."

In a study by Someya et al.[3], they focused on the "sense of harmony" caused by the high frequency of pure tone and the brightness of achromatic colors in a model space that imitates a real space, and described under what conditions a sense of harmony is created in an audiovisual complex and the impressions that are created when subjects arbitrarily change the brightness of lighting by using the adjustment method. The study also describes the conditions under which a sense of harmony is created in an audiovisual complex and the impression that is created. As a result, it is stated that the values of illuminance and luminance that harmonize increase exponentially with the brightness of walls, etc., but that the values of illuminance and luminance that harmonize decrease when the low frequencies are matched. Furthermore, the results show that the sense of spaciousness increases with increasing luminance, indicating the need to conduct experiments under realistic space conditions. Furthermore, by expressing the results in contour plots, the trend of the evaluation changed depending on the subject's preference for the brightness of the illumination. However, the difference in frequency range was only two octaves, so it is necessary to examine the results in more detail.

The overall idea and purpose of this study was to investigate the effects of the interaction between the frequency of pure tone and the luminance of lighting on the psychological state, focusing on the "sense of harmony" and "sense of comfort. This will provide basic knowledge for planning architectural spaces. In previous studies [1-9] dealing with audiovisual complex sensory perception, visual perception was examined in terms of visual images and various scenic slides and hues, and auditory perception was examined in terms of everyday sound events such as music, traffic sounds, and natural sounds, as well as music and pink noise. Therefore, in this study, we decided to focus on the frequency of physical pure tones and the luminance of lighting and examine them quantitatively.

Based on the above, this experiment focused on "a sense of harmony" and "a sense of comfort," and aimed to examine the effect of the interaction between frequency and lighting luminance by the adjustment method on the psychological state, and to examine the psychological state for environments where lighting brightness can be controlled by the adjustment method. In addition, the results of the experiment are expressed as contour plots, which can be applied to real spaces, and the differences in evaluations due to differences in lighting brightness preferences are also discussed.

## 2 Method

### 2.1 Study design

The size of the booth used for the experiment was W2000 x D2200 x H2800 mm, with a desk (W750 x D1500 x H680 mm) and chairs. The size of the model is W4500 x D7500 x H2800 mm at a ratio of 1:10 [Figure 1-2]. For the wall, floor, and ceiling surfaces, in order to study the application to a real space, a color with a lightness similar to that of the walls of a laboratory, classroom, or office was used out of the grayscale used by Someya [3]. A dimmable LED bulb (AKARUE JJ-TGTSQ-9W) with a color temperature of 5000 K and total luminous flux of 1000 lm was used, with 11 brightness levels, box illuminance ranging from 38.7 lx to 1683 lx, and luminance from 96 cd/m<sup>2</sup> to 4080 cd/m<sup>2</sup>. The pure tone frequencies and pink noise were created by Audition. The equivalent noise level in the room was 32-33.5 dB(A) (Laeq, 10s ), the average illuminance of the room was 621 lx, the temperature of the room was 22.3-24.6°C, and the

humidity was 23-46%. The two factors were auditory (frequency of pure tone) and visual (luminance of illumination). Next, the auditory stimuli were set at seven pure tone frequencies (63, 125, 250, 500, 1000, 2000, and 4000 Hz) in order to obtain a more detailed understanding of the trends. The visual stimuli to be adjusted were dimming LED bulbs with luminances of 96, 453, 790, 1258, 1720, 2170, 2600, 3020, 3400, 3760, and 4080 cd/m<sup>2</sup> (lighting brightness 1 to 11). Subjects were 14 healthy Japanese students (9 males and 5 females) aged 21-25 years with normal color vision and hearing.

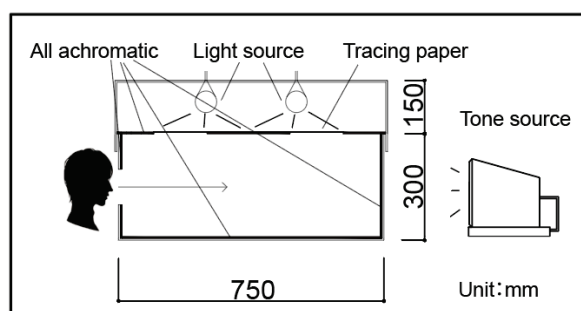


Figure 1 . Diagram of experimental model

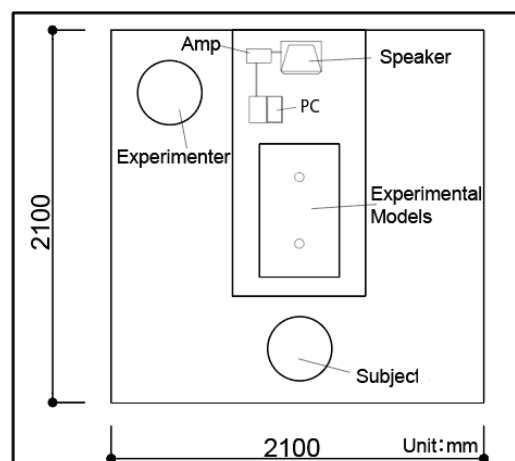


Figure 2 . Diagram of experimental system

## 2.2 Procedure

After the subjects entered the laboratory and filled out the face sheet, the experiment was taught. After practicing light dimming, the experiment was started on the basis of “harmony”. First, the subjects were asked to rest with their eyes closed for 1 minute. Next, the subjects were asked to meditate before each stimulus tone and, after 10 seconds of 35 dB(A) pink noise was played, they were asked to open their eyes and look into the experimental chamber, where each stimulus tone was presented through a speaker. The stimulus level was set at 50 dB(A). The subjects were then asked whether the brightness of the stimulus tone and the Spatial brightness they looked into were “in harmony” or “out of harmony,” and were asked to evaluate their impressions of the combination [Table 1-2].

Table 1 . Impression evaluation items

Indicator	Scale	
	Harmonious	Disharmonious
Sense of harmony	Harmonious	Disharmonious
Sense of comfort	Comfortable	Uncomfortable
Spatial brightness	Bright	Dark
Sound Height	High	Low
Appropriateness of light work	Appropriate	Inappropriate

Table 2. Evaluation scale

Rating scale						
7: Extremely	6: Moderately	5: Slightly	4: Neither	3: Slightly	2: Moderately	1:Extremely

The participants were then asked to continue dimming until their judgment changed, and if their judgment changed, they were asked to evaluate their impression of the combination. When the light dimming was completed, the subjects were asked whether their judgment had changed or not, and then they were asked to evaluate their impression of the last combination. When the stimulus tone was switched, the subject was asked to meditate for 1 minute to avoid retaining the impression of the previously presented stimulus tone. This procedure was repeated seven times. The same procedure was repeated seven times with "comfort" as the criterion. The brightness was controlled by the experimenter using a remote control in accordance with the subject's instructions. In this process, the subject was first asked to dim the lights in two patterns: the brightest and the darkest (descending and ascending series). The experiment was terminated by having the participants fill out a face sheet after all the steps were completed. The order of presentation was set using the Latin case method to eliminate order effects. In the experiment, "harmony" means harmony when each person has a "common impression" of the frequency of the pure tone and the brightness of the lighting. In addition, the experiment was conducted under the definition that "comfort" is comfortable when looking into the experiment box. Finally, "ease of light work" in Table 1 was defined as light work such as working on a computer or taking notes or memos.

### 3 Results

#### 3.1 Impressions

A two-way ANOVA was performed in the tone and luminance conditions on subjects who had a turning point [Table 3]. The results showed that the main effects for "sense of harmony" were observed in the luminance and tone and luminance conditions, and for "sense of comfort" in the tone, luminance, and tone and luminance conditions. This suggests that a "sense of harmony" is influenced by the luminance condition and the mutual influence of tone and luminance, while a "sense of comfort" is influenced by the tone and luminance conditions.

Table3. Two-Way ANOVA Results

Analysis of variance table	Sense of harmony	Sense of comfort	Brightness of space	Sound Height	Appropriateness of light work
Tone	0.143	0.001	<.0001	0.320	0.766
Luminance	0.002	0.007	0.013	<.0001	<.0001
Tone * Luminance	<.0001	<.0001	0.358	0.143	0.166

#### 3.2 Analysis of harmony and comfort

The "sense of harmony" was judged to be harmonized by the interaction between low frequency and low luminance, and high frequency and high luminance. The "sense of comfort" was judged to be harmonized by the interaction between high frequency and high luminance. [Figure 3- 4].

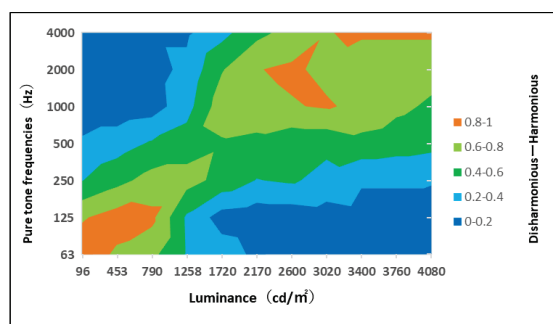


Figure 3 . Contour map of Harmony

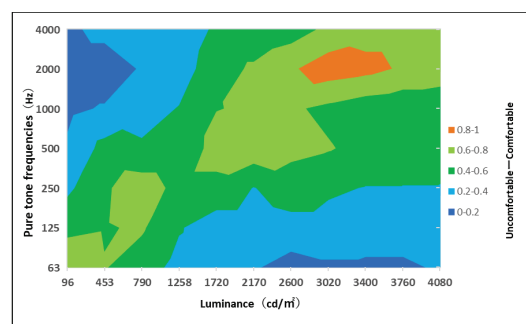


Figure 4 . Contour map Diagram of Comfort

### 3.3 Analysis by brightness preference

The ratio of the number of subjects who judged “not harmonious and uncomfortable” to be 0 and “harmonious and comfortable” to be 1 for those who had a turning point was tabulated, and a contour plot was created by connecting the sense of harmony and the sense of comfort with an almost equal line. The contour plots were then drawn for the dark preference group (dark group), which consisted of one person who selected “dark” and three people who selected “somewhat dark,” and the brightness preference group (light group), which consisted of five people who selected “normal” and five people who selected “somewhat bright. The “sense of harmony” and “sense of comfort” were compared and discussed, and the two groups were compared and discussed.

As a result of drawing contour plots for the dark and light groups, it was found that the dark group for “sense of harmony” was judged to be in harmony with a steadily rising trend, especially in the interaction between low frequency and low luminance, medium frequency and middle luminance, and high frequency and high luminance [Figure 5]. The light group was judged to be in harmony in the interaction between low frequency and low luminance and high frequency and high luminance [Figure 6]. This suggests that the combination of “sense of harmony” is judged to be comfortable in different combinations depending on lighting preference. Next, the dark group of “comfort” was judged to be comfortable by the interaction between low frequency and low brightness, medium frequency and medium brightness, and 2000 Hz and medium to high brightness [Figure 7], while the light group was judged to be comfortable by the interaction between high frequency and high brightness [Figure 8]. This suggests that the combination of “comfort” judged to be comfortable differs depending on lighting preference.

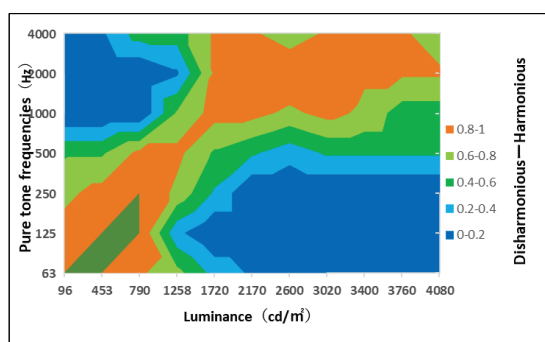


Figure 5. Contour map of Harmony  
(Dark group)

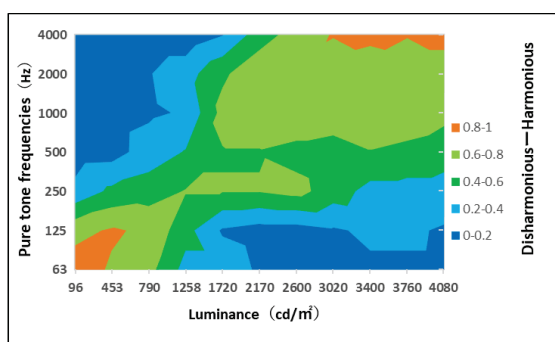


Figure 6. Contour map of Harmony  
(Light group)

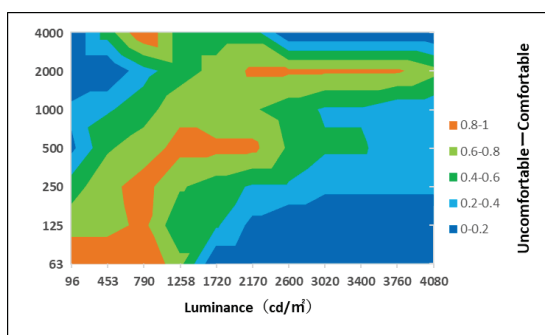


Figure 7 . Contour map of Comfort  
(Dark group)

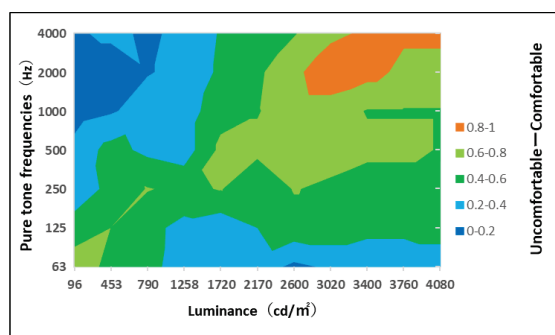


Figure 8 . Contour map of Comfort  
(Light group)



## 4 Discussion

When looking at the relationship between "sense of harmony" and "sense of comfort" on the contour map, not all combinations that are judged to be harmonious are judged to be comfortable, which suggests that being harmonious does not necessarily mean being comfortable. Therefore, when planning places where many people gather, such as school classrooms, laboratories, and offices, the environment should be planned to be favorable to many people in terms of audible tone and brightness of lighting. However, when designing a space used by a limited number of people, such as a house, it is better to plan an environment preferred by the people who use the space. The results of a study by Gassho et al. [1] also revealed that even in environments where visual and auditory factors are highly evaluated, the overall evaluation is lowered when the two factors are not in harmony. The same tendency was observed in the case of pure tone frequency and lighting luminance in this study. Therefore, we believe that the sense of harmony when visual and auditory senses are combined is a point that must be taken into consideration when creating architectural spaces.

In the results of the study by Iwamiya [2], a resonance phenomenon was observed in which the auditory impression emphasized the visual impression. In a two-way ANOVA, main effects were found in the luminance and tone and luminance conditions. Therefore, it is thought that the "sense of harmony" was emphasized by the accompanying tone condition. The results of the study by Iwamiya [4] indicated that the higher the degree of harmony between tone and image, the greater the effect of the evaluation. In this study, low frequency and low luminance and high frequency and high luminance were seen to harmonize with each other at the same magnitude. Therefore, it is considered that tone and luminance are preferred to be of equal magnitude.

From the above, it is thought that when planning a place where many people gather, such as a school classroom, laboratory, or office, an environment should be planned that is desirable to many people in terms of audible tone and brightness of illumination. Therefore, it is necessary to understand what is ideal for many people. However, when designing a space used by a limited number of people, such as a house, it is better to plan an environment preferred by the people who will use the space.

## 5 Conclusion

In this study, we investigated the effects of the interaction between the frequency of pure tone and the luminance of illumination on the psychological state of people by using a model space adjustment method, focusing on "a sense of harmony" and "a sense of comfort. As a result, the following were found.

- The "sense of harmony" was judged as being in harmony when there was the interaction between low frequency and low luminance and high frequency and high luminance. The "sense of comfort" was judged to be comfortable by the interaction between high frequency and high luminance.
- The "sense of harmony" and "sense of comfort" were different depending on the lighting preference. The light group was evaluated to be more comfortable with a combination of higher luminance.
- The contour plot of the relationship between "sense of harmony" and "sense of comfort" showed that not all combinations that were judged as harmonious were also evaluated as comfortable.

Therefore, it is possible that being in harmony does not necessarily mean being comfortable.

## Reference

- [1] GASSHO, A., TAMURA, A., MATSUBARA, N. and KURAZUMI, Y. The possibility of the improvement in the comprehensive comfortableness by the harmony with visual and auditory stimuli. Architectural Institute of Japan. Journal of architecture, planning and environmental engineering, 2001, 544, 55-62.  
[https://www.jstage.jst.go.jp/article/aija/66/544/66\\_KJ00004230347/\\_article/-char/ja/](https://www.jstage.jst.go.jp/article/aija/66/544/66_KJ00004230347/_article/-char/ja/)
- [2] IWAMIKY, S. The interaction between auditory and visual processing when listening to music via audio-visual media. Acoustical Society of Japan, 1992, 48(3), 146-153.  
[https://www.jstage.jst.go.jp/article/jasj/48/3/48\\_KJ00001456413/\\_article/-char/ja/](https://www.jstage.jst.go.jp/article/jasj/48/3/48_KJ00001456413/_article/-char/ja/)
- [3] SOMEYA, T. Study on audiovisual harmony by lighting dimming in model space: Examination Examination by contour maps. Architectural Institute of Japan. Summaries of technical papers of annual meeting, 2021, 11-12.  
<https://www.aij.or.jp/paper/detail.html?productId=658637>
- [4] IWAMIKY, S. The effect of the matching of sound and video on the interactions between auditory and visual process-ing in communication via audio-visual media. Acoustical Society of Japan, 1992,48(9), 649-657.  
[https://www.jstage.jst.go.jp/article/jasj/48/9/48\\_KJ00001456541/\\_article/-char/ja/](https://www.jstage.jst.go.jp/article/jasj/48/9/48_KJ00001456541/_article/-char/ja/)
- [5] MIYAKAWA, M., NAKATSUKASA, T. and AONO, S. The Effects of Visual and Auditory Information on the Impression of Sound Environment. Institute of Noise Control Engineering of Japan, 2002, 26(1), 53-59.  
[https://www.jstage.jst.go.jp/article/souonseigyo/1977/26/1/26\\_1\\_53/\\_article/-char/ja/](https://www.jstage.jst.go.jp/article/souonseigyo/1977/26/1/26_1_53/_article/-char/ja/)
- [6] SU, X., KIM, K. and IWAMIYA, S. Subjective congruence between complex transforma-tion patterns of an image and monotonous pitch shift patterns of a sound. Acoustical Society of Japan, 2010,66(10), 497-505.  
[https://www.jstage.jst.go.jp/article/jasj/66/10/66\\_KJ00006628143/\\_article/-char/ja/](https://www.jstage.jst.go.jp/article/jasj/66/10/66_KJ00006628143/_article/-char/ja/)
- [7] KOBAYASHI, S., INUI, M., NAKAMURA, Y. and KITAMURA, A. Illuminance level and uniformity of interior ambient lighting for behaviors of daily life. Architectural Institute of Japan. Journal of architecture, planning and environmental engineering, 1996, 481, 13-22.  
[https://www.jstage.jst.go.jp/article/aija/61/481/61\\_KJ00004221507/\\_article/-char/ja/](https://www.jstage.jst.go.jp/article/aija/61/481/61_KJ00004221507/_article/-char/ja/)
- [8] LEE, S., ISHIHARA, T., HIRATE, K. and YASUOKA, M. Effects of brightness distribution on psychological appraisal in a living room. Architectural Institute of Japan. Journal of architecture, planning and environmental engineering, 1997, 497, 1-6.  
[https://www.jstage.jst.go.jp/article/aija/62/497/62\\_KJ00004222140/\\_article/-char/ja/](https://www.jstage.jst.go.jp/article/aija/62/497/62_KJ00004222140/_article/-char/ja/)
- [9] MIYAKAWA, M., SUZUKI, S., AONO, S and TAKAGI, K. The effects of visual information on the impressions of environmental sounds. Acoustical Society of Japan, 2000, 58(6), 427-436.  
[https://www.jstage.jst.go.jp/article/jasj/56/6/56\\_KJ00001457386/\\_article/-char/ja/](https://www.jstage.jst.go.jp/article/jasj/56/6/56_KJ00001457386/_article/-char/ja/)

## Acknowledgments

We would like to thank Ikezawa Makoto, Someya Tsubasa, and all the subjects for their cooperation in conducting this experiment.

# INVESTIGATION OF ERRORS DUE TO SELF-ABSORPTION CORRECTION IN INTEGRATING SPHERE MEASUREMENTS

Matsumoto, K<sup>1</sup>. Ohkubo, K<sup>2</sup>. Yamauchi, Y<sup>1</sup>.

<sup>1</sup>Graduate School of Science and Engineering, Yamagata University, Yamagata, Japan

<sup>2</sup>Systems Engineering Inc., Tokyo, Japan

## ABSTRACT

An integrating sphere (IS) is widely used to measure the total luminous flux (TLF). The method determines the TLF of a DUT by comparing the values obtained with the standard lamp with those with the DUT. However, since light absorption of DUT causes errors in the measurement, self-absorption correction is generally performed. In this study, SRDF was obtained by the optical simulation, and the TLF measurement error of the DUT was examined from the self-absorption of the standard lamp and that of the DUT. It was found that the larger the self-absorption of the DUT, the larger the error in the TLF value of the detector.

Keywords: integrating sphere, total luminous flux, self-absorption, photometry

## 1. INTRODUCTION

An IS is widely used to measure the total luminous flux of lamps. With the spread of LED lamps, total luminous flux measurement has become more important for performance evaluation and energy saving evaluation. For the measurement of total luminous flux with the IS, the difference in the luminous intensity distributions between the standard lamp and the DUT causes an error in the total luminous flux measurement value due to the non-uniformity of the spatial response distribution function (SRDF) of the IS. The error can be corrected by determining the luminous intensity distributions of the standard lamp and those of DUT<sup>1)</sup>. Previous researches showed that the error can be corrected by determining the SRDF of each lamp and the IS<sup>1-2)</sup>. On the other hand, the SRDF varies depending on the size of the lamp<sup>3)</sup>. In this study, we report the effects of the size of the lamp on the total luminous flux measurement by the optical simulation<sup>4)</sup>.

## 2. SRDF SIMULATION

The optical model of the IS used in the simulation was based on an actual IS of 1 m diameter, as shown in Figure 1. The optical model consists of a lamp, a lighting stand that holds the upward lamp, a detector placed at a vertical angle  $\theta = 90^\circ$  (at the equator), and a baffle (a circular plate with a diameter of 125 mm at the distance of 160 mm from the detector). The lamp was supported in the center of the IS by a lighting stand of a  $\Phi 30$ mm diameter rod. Its surface reflectance is the same as that of the IS inner wall.

The inner wall of the IS was assumed to completely diffuse reflective, and the reflectance  $\rho$  was varied from 80% to 95%. The reflectance of the baffle was the same as that of the inner wall of the IS on both the detector and lamp sides. The change in SRDF was analysed by optical simulation when the DUT of either  $\Phi 100$ mm,  $\Phi 140$ mm,  $\Phi 200$ mm,  $\Phi 250$ mm,  $\Phi 300$ mm or  $\Phi 350$ mm (surface absorption 100%) was placed at the center of the IS. Lumicept by Integra Inc. was used for the analysis<sup>4)</sup>. Figure 2 shows the change of SRDF of the horizontal angle at  $\theta=90^\circ$  when a  $\Phi 100\sim\Phi 350$ mm lamp was placed at the center of the IS.

The results were obtained by multiplying the SRDF without the lamp by the SRDF with the given size of the lamp. The standard lamp used in this experiment was a JCV100V200WA/F with light distribution in  $4\pi$  geometry and was analysed under the assumption that it has no self-absorption.

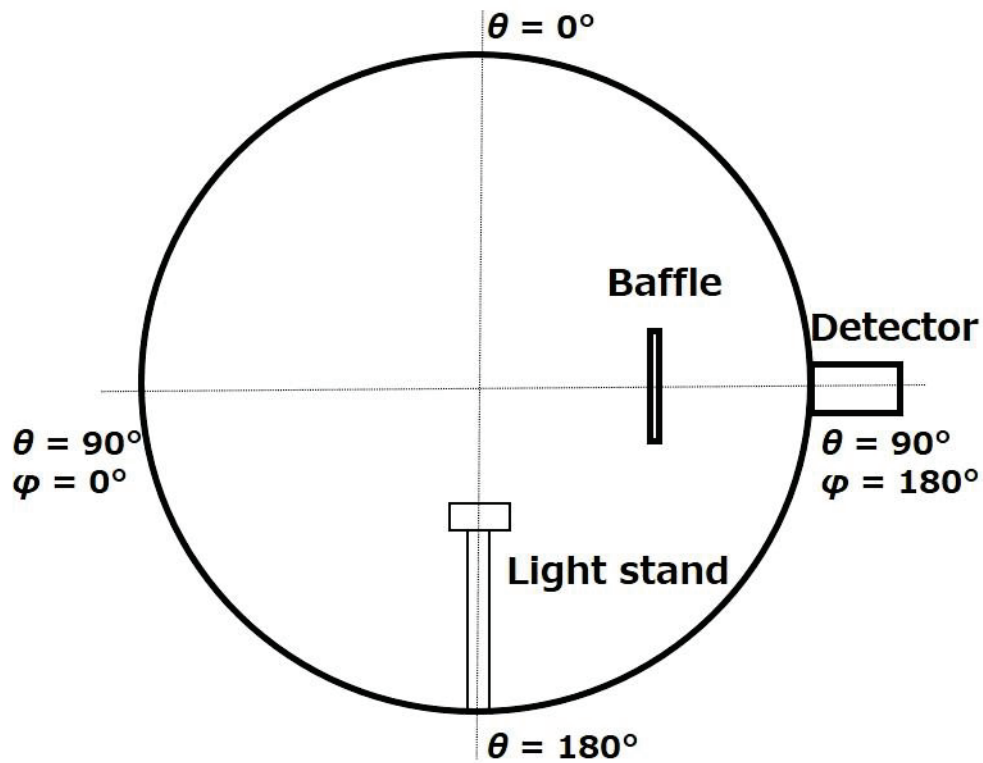


Figure 1 : 1m IS structure(Side view). While the standard lamp is assumed to be a point light source, the DUT has a diameter of 100 to 350 [mm]

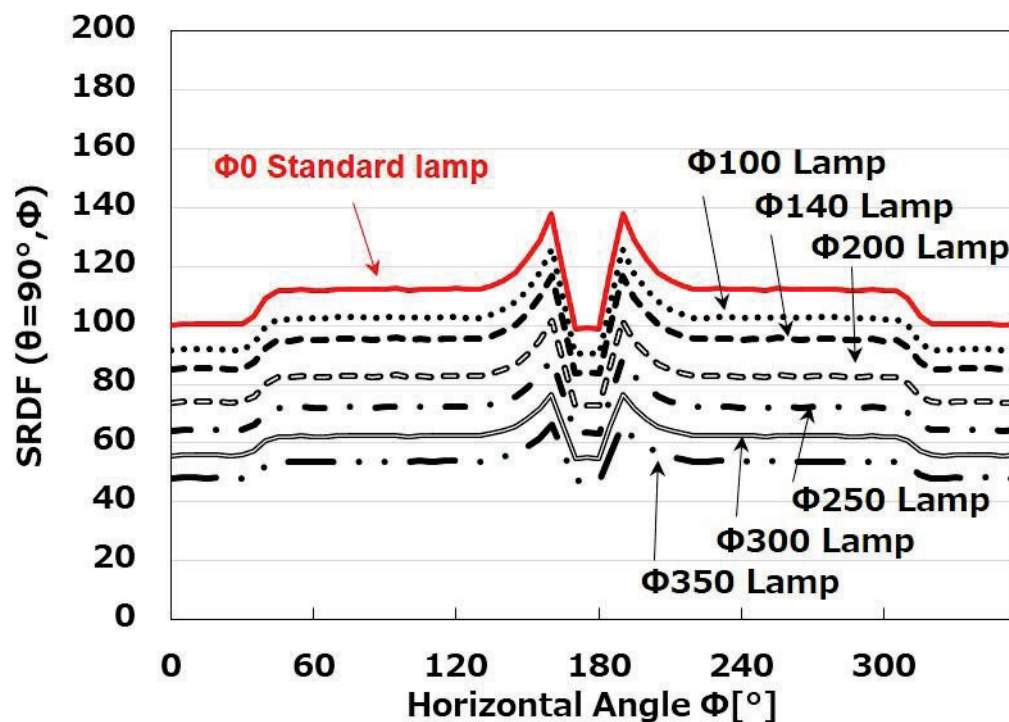


Figure 2 : SRDF with  $(\theta, \phi) = (90^\circ, 0 \sim 355^\circ)$  of IS. The degradation of the SRDF response due to self-absorption is shown by multiplying the ratio of the DUT's detector output by the standard lamp detector output.

### 3. CALCULATION OF TOTAL LUMINOUS FLUX BY SRDF

The changes in SRDF with respect to the diameter of the lamp (100% absorption) is mediated due to the self-absorption of the lamp. The actual IS has an auxiliary lamp for the self-absorption measurement which is not shown in Figure 1. The diffuse light of the inner wall of IS is used to correct for self-absorption. The self-absorption correction factor for each DUT were obtained according to the definition of LM-79<sup>5)</sup> using the SRDF simulation results when the lamp was mounted in the integrating sphere. In this experiment, the self-absorption correction factor is calculated using the ratio of standard lamp and DUTs of SRDF simulation value of  $\theta = 0^\circ$  and the correction formula of IES LM-79<sup>5)</sup>. Using these self-absorption correction factors,  $K^*(\theta_i)$  (without the lamp) was corrected to obtain  $K^*(\theta_i)$  (with the size of each lamp).

If the average luminous intensity of the lamp in the horizontal direction at the vertical angle  $\theta_i$  is  $\overline{I(\theta_i)}$  and the spherical band coefficient at the vertical angle  $\theta_i$  is  $Z(\theta_i)$ , the total luminous flux  $P_{ls}$  of the lamp is calculated by the following formula.

$$P_{ls} = \sum_{i=1}^n K^*(\theta_i) \cdot Z(\theta_i) \cdot \overline{I(\theta_i)} \quad \dots (1)$$

where  $n$  is the number of cross sections of the horizontal angle in the light distribution measurement.  $K^*(\theta_i)$  are the average value of the IS SRDF in the horizontal angular direction at vertical angle  $\theta_i$ . The  $K^*(\theta_i)$  of each lamp, which was corrected for self-absorption, is shown in Figure 3. The reflectance of IS inner wall was assumed to be 90%.

It is clear from Figure 3 that the larger the surface area of the lamp, the larger the change of  $K^*(\theta_i)$  with respect to the vertical angle  $\theta_i$ . These values were used to obtain the SRDF correction factor  $A_{SRDF}$  for 18 different lamps with different 50% beam angles of light distribution. The light distributions of these 18 lamps are shown in Figure 4. Figure 5 shows  $A_{SRDF}$  of 18 lamps, under the condition of the reflectance value of the inner wall of 90%.

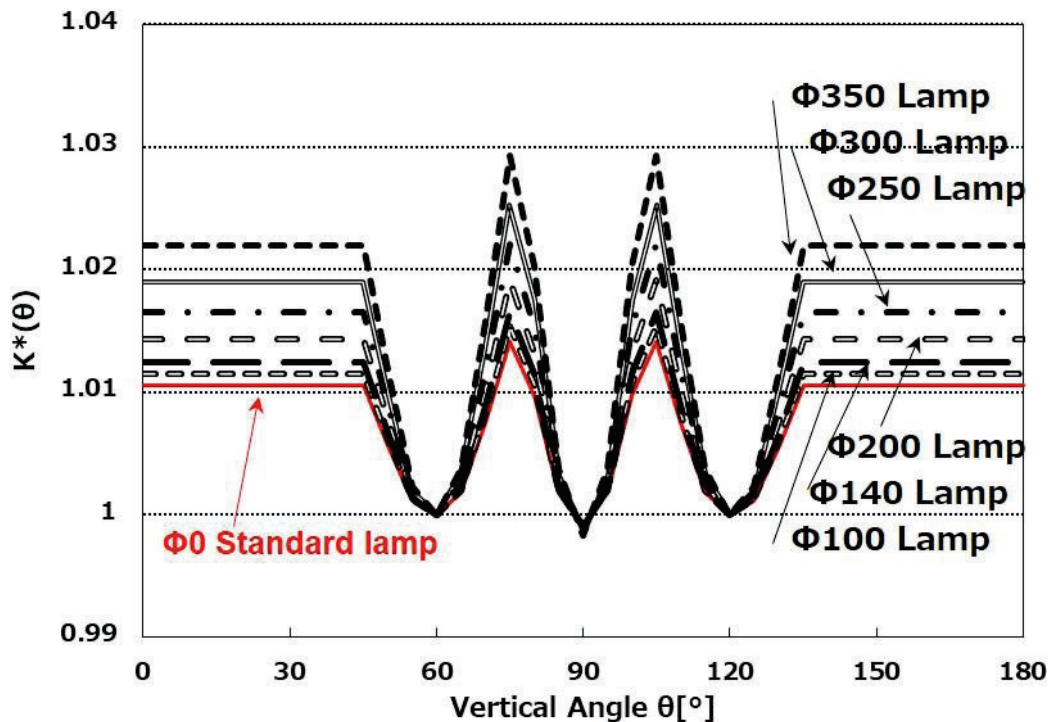


Figure 3 : Horizontally mean SRDF with the size of the DUT as a parameter.



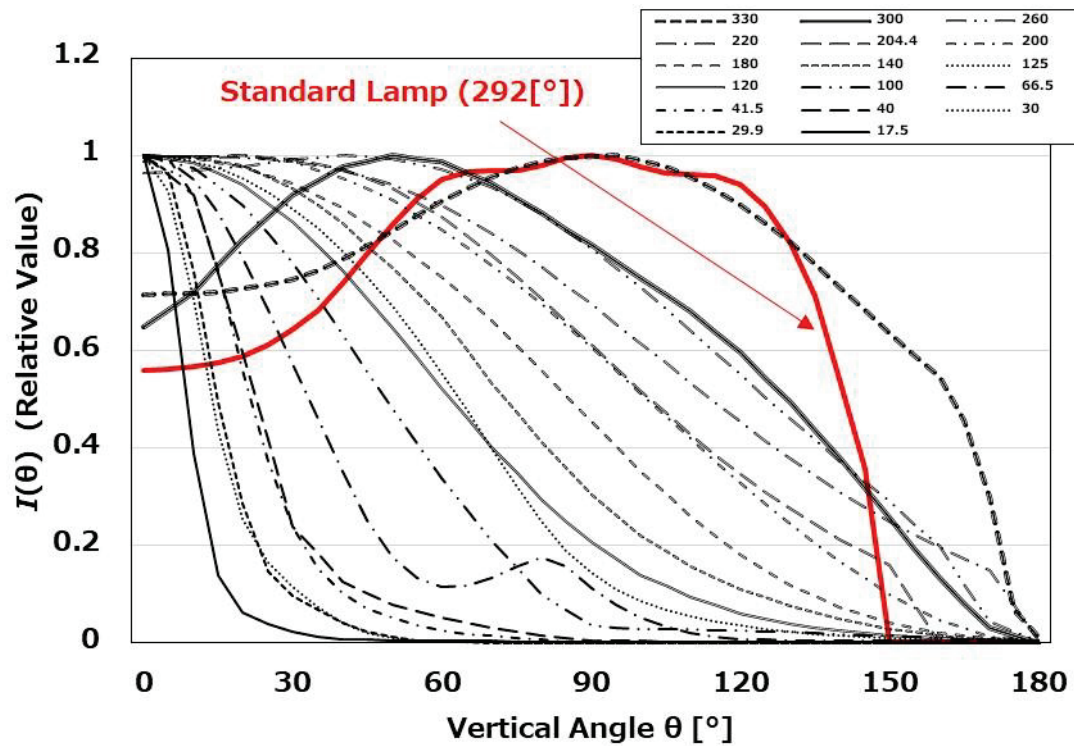


Figure 4 : Light distribution data  $I(\theta)$  used to calculate SRDF correction factor.

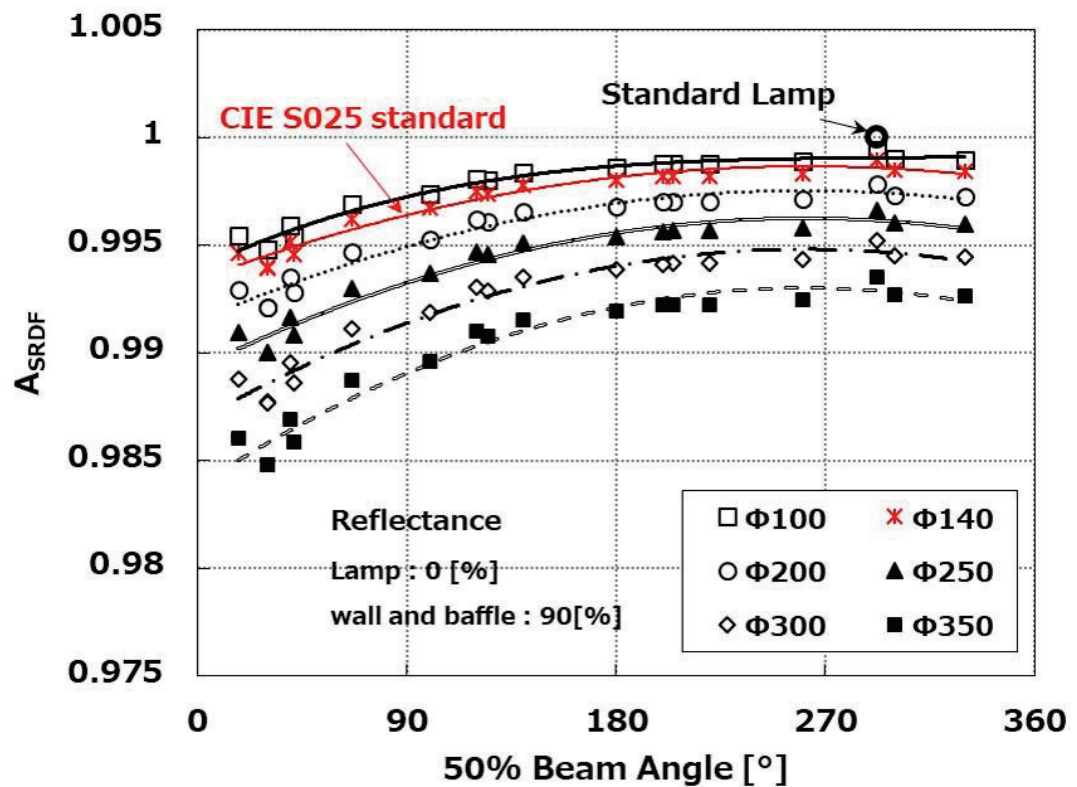


Figure 5 : SRDF correction factors of the DUT for the different size, calculated from simulated SRDF and light distribution data.

JIS C7801<sup>6)</sup>, which specifies the requirements for IS measurement, requires that the inner wall reflectance of the IS should be 90% or higher. Under these conditions, if the ratio of the surface area of the lamp to the inner wall area of the IS is smaller than 1% ( $\Phi 100\text{mm}$  lamp), the deviation of the measured value can be suppressed to be less than 0.5%. CIE S025/E:2015<sup>7)</sup> defines the size of the lamps that can be measured with a IS, where the reflectance of the inner wall of the IS is higher than 90% or more. The surface area of the lamp should be less than 2%<sup>7)</sup> of the total area of the inner wall of the IS. For the lamp shown in Figure 4, the error in the total luminous flux measurement is less than 0.7%.

#### 4. CONCLUSION

In an IS with a diameter of 1 m, the internal structure (detector, baffle, lighting stand, etc.) is used as an optical model, and SRDFs were obtained using the IS inner wall reflectance as a parameter by optical simulation. The deviation of the total luminous flux measurement value was evaluated from the size of various lamps. Errors in the measurement are partially caused by the SRDF, which contains the self-absorption error. If the IS is designed to have the reflectance of the inner wall 90% or more, and the surface area of the lamp (in the case of absorption of 100%) is less than 1% of the IS inner wall area, it is expected that the error due to SRD will be suppressed to less than 0.5%.

#### REFERENCES

- [1] Ohkubo, Yamauchi : Uncertainty of photometry caused by SRDF of integrating sphere (in Japanese), *J. Illum. Engng. Jpn*, 2019, 103-4, pp142-147.
- [2] Ohkubo et al. : Uncertainty of photometry caused by SRDF of integrating sphere. - Influence of lighting posture of light source - (in Japanese), *Proc. Annual Conf. IEI Jpn*, 2019, 8-O-01.
- [3] Ohkubo et al. : Investigation of the effect of the size of the light source on the SRDF of the integrating sphere (in Japanese), *Proc. Annual Conf. IEI Jpn*, 2019, 8-O-07.
- [4] Matsumoto et al. : A study of an integrating sphere without a baffle 2 (in Japanese), *Proceedings of the illuminating Engineering Institute of Japan Tokyo Branch Conference*, 2021, H-7.
- [5] IES LM-79-08 : Approved Method : Electrical and Photometric Measurements of Solid-State Lighting Products.
- [6] JIS C7801:2019 : Measuring methods of lamps for general lighting.
- [7] CIE S025/E:2015 : Test Method for LED Lamps, LED Luminaires and Modules

#### ACKNOWLEDGEMENTS

Corresponding Author Name: Kazuma Matsumoto  
 Affiliation: Yamagata University  
 e-mail: t222558m@st.yamagata-u.ac.jp

# AESTHETIC EVALUATION STANDARD OF ARCHITECTURE LIGHTING EXTERIOR

Xing Zhang

Southeast University, Nanjing, Jiangsu, China

Qian, Liu

Longt Lighting Group Inc. Jiangsu Branch, Nanjing, Jiangsu, China

## ABSTRACT

This article attempts to establish an aesthetic reference for light on building facades based on common sense understanding. The reference is one of the aesthetic standards for beginners. Compare the knowledge in the fields of architecture and lighting with other fields, especially in the field of graphic design, we want to find the principles of graphic aesthetics based on the human visual system from the knowledge of patterns design. Correspond this principle to architecture and lighting, we deduce a lighting aesthetic reference that conforms to the basic principles of design through analogy.

This aesthetic standard can help lighting beginners analyze successful cases, establish a basic aesthetic understanding, and assist them in doing simple lighting design. It can also serve as a reference for the design team to evaluate the quality of lighting schemes, in order to compare design schemes that are more suitable with the client's requirements.

Keywords: aesthetic standard, architecture, exterior lighting, graphic design, pattern aesthetics, human visual system,

## 1. INTRODUCTION

Background of this article: Outdoor lighting beginners' confusion about the aesthetic of architectural night scenes

Maybe different persons can tell different standards on their favorite interests, which are based on different civilizations. Two lighting designers may even provide vastly different design solutions for the same building, even if they come from countries with the same culture. The evaluation team may also have different evaluation results when facing the same lighting design scheme, even if the evaluation team is based on the same interests. For a developing industry, without a reasonable aesthetic evaluation standard, it will seriously restrict the growth of the industry and be not conducive to attracting new people to join the industry.

## 2. FURTHER CLAUSE

Many lighting beginners often feel an aesthetic confusion when facing night lighting projects on building facades where is the advantage of other successful solution, how to carry out new solutions, and so on. So, they can only blindly follow industry success proposal or carry out projects solely based on our own feelings. This article attempts to find a method to establish a common sense based aesthetic reference for architectural night scenes for beginners, to assist them in reading successful cases and applying the knowledge learned to their own lighting plans. Of course, this auxiliary approach is not unique, and this article discusses it from a new perspective.

## REFERENCES

Paul Jackson. How to Make Repeat Patterns: A Guide for Designer, Architects, and Artists, 2020. ISBN: 9789864592210.  
Qinghua Xing. Modern Pattern Design from the Perspective of Typology, 2017.

## ACKNOWLEDGEMENTS

Corresponding Author Name: Jing Zhang  
Affiliation: Zhongshe Zhubang Beijing Architectural Design and Research Institute  
e-mail: 22418378qq.com

# AESTHETIC EVALUATION STANDARD OF ARCHITECTURE LIGHTING EXTERIOR

Xing Zhang

Southeast University, Nanjing, Jiangsu, China

Qian, Liu

Longt Lighting Group Inc. Jiangsu Branch, Nanjing, Jiangsu, China

## SECTION 1: CHARACTERISTICS OF THE APPEARANCE OF BUILDINGS AT NIGHT

During the day, under sunlight and skylight, the shadows received on the surface of the building make it look layered. At night, due to the lack of sufficient light to form shadows, it is visually impossible to recognize surface feature, and the building appears flattened, transforming the visual sense of three-dimensional into a flat feeling.

Unlike during the day, without intentionally increasing external lighting, relying solely on the scattering effect of the night sky and urban light, the colour of building materials cannot be correctly recognized, the texture of the materials cannot be clear, and even the boundaries of the contour appearance are difficult to recognize. The brightest element of night architecture is the projection of indoor lights through glass. However, the human eye cannot judge the distance and proximity of a building solely through internal light transmission. Under the cover of night, the city's architectural complexes are like silhouette paintings that have been flattened and pasted on the night sky.

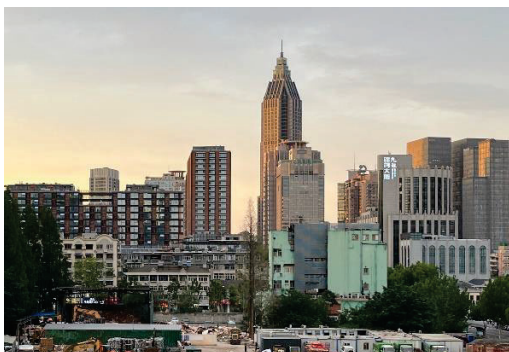


Figure 1-1 Daytime under the sunlight and skylight

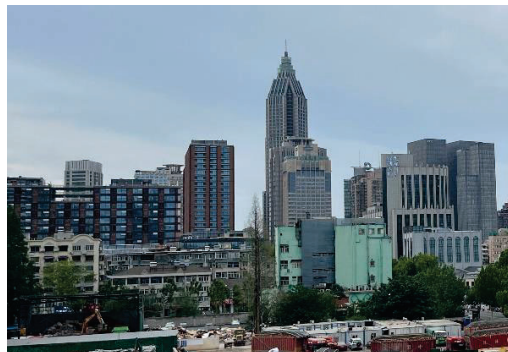


Figure 1-1 Daytime without direct sunlight

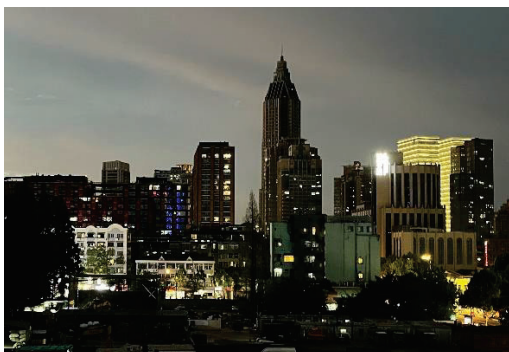


Figure 1-3 Evening with insufficient skylight

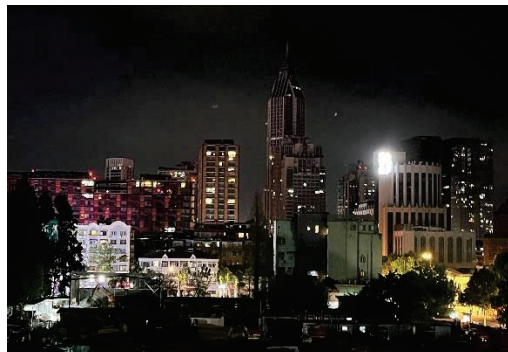


Figure 1-4 Night scene with weak light

## SECTION 2: ESTABLISHING THE FOUNDATION OF NIGHT SCENERY

Establishing aesthetic standards for nightscape requires a simplified model of nightscape architecture, and the simplification process requires a basic understanding of architecture. The essential task of lighting designers is to emphasize buildings from the night sky, forming a unique style of the building at night. This premise requires designers to understand architectural features.



From a visual perspective, the most important elements of architecture in the night scene are contour, material, and texture.

The process of simplifying the nighttime appearance of a building is to topology the building from a three-dimensional space to a flat surface. The outline of the building's appearance is refined into the main area of the plane, and the material, colour, and texture styles of the building's surface are identified within the outline, gradually forming a simplified model.



Figure 2-1 Daytime appearance of buildings (computer graphic)

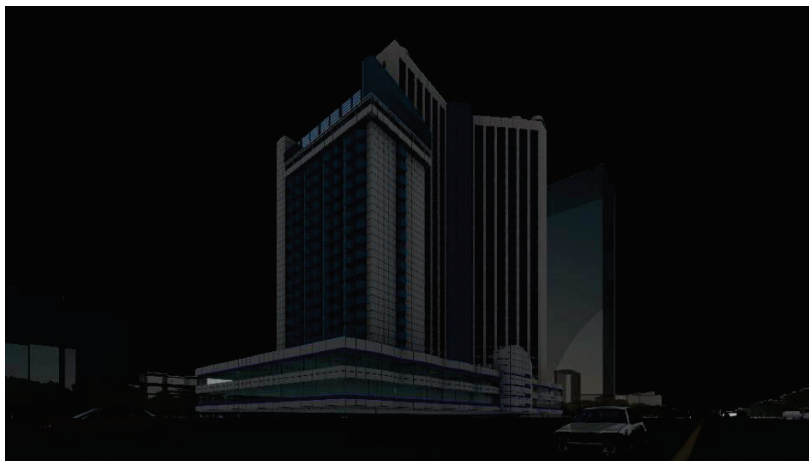


Figure 2-2 Night appearance of buildings (computer graphic)



Figure 2-3 Nighttime visual simplified model of buildings



After refining the simplified model, sketching night features in the building is like playing a coloring game on the simplified model. After analysing the characteristics of the building itself, the lighting designer fills in colours and lines to draw the characteristics of the building itself, thus achieving a beautiful night view of the building. This aesthetic perception has actually shifted from three-dimensional architecture to graphic design.

### SECTION 3: ESTABLISHING AESTHETIC COGNITION THROUGH SUCCESSFUL CASE ANALYSIS

How to create excellent images on paper with simplified model? This article attempts to find a feasible method from the fields of architecture and other design, especially in the field of graphic design, we want to establish a basic aesthetics standard suitable for beginners to evaluate the night scenes. In graphic design, the three main elements of pattern are form, colour, and texture. This corresponds to several major elements of architecture: contour, material, and texture.

Through the knowledge of pattern studies and successful case studies, we establish a cognitive understanding of night scenery aesthetics. The important criteria for evaluating the quality of patterns can also be referred to as the aesthetic standards of night view architecture. The following are examples:

1. Symmetry and Balance: The natural symmetry method relies on visual perception to obtain symmetrical patterns, while the psychological symmetry method relies on cultural knowledge to obtain balanced symmetry. For example:



Figure 3-1 Raffles city in Chongqing by BPI

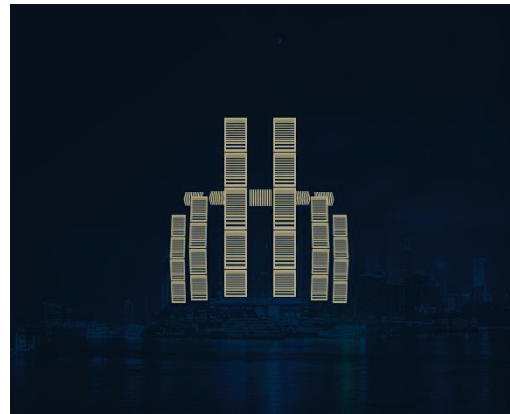


Figure 3-2 raffles city simplified model

2. Comparison and Harmony: Derived from change and unity, contrast is the difference and conflict of elements, and harmony is to make the contrasting elements appear harmonious. For example:



Figure 3-3 North star in Changsha by BPI

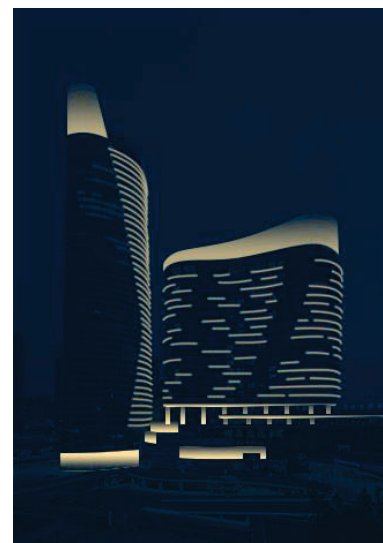


Figure 3-4 North star simplified model

3. Beats and Rhythm: It is a description of the trend of element changes, and the evolution of the same rhythm is dull. Changes bring fun, but they cannot change randomly and require rhythmic support. For example:

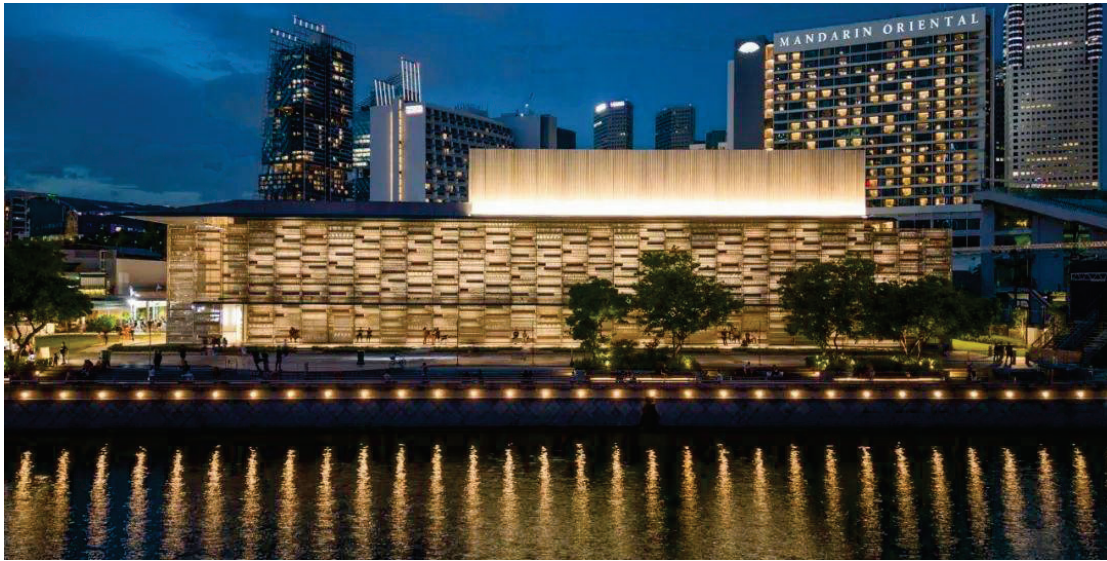


Figure 3-5 Singtel Waterfront Theatre in Singapore by LPA



Figure 3-6 Singtel Waterfront Theatre simplified model

There are many other design factors, such as the concept of drawing focus, variation and uniformity, proportion and contrast, etc. Due to limited space, we do not provide examples one by one.

#### SECTION 4: FROM PATTERN STUDIES TO A NIGHTSCAPE PLAN FOR BEGINNERS

With the assistance of simplified models and the knowledge of patterning, we will create architectural night scene plans.

Here, a very common modern architecture is chosen as a typical case for analysis. Firstly, the architecture is abstracted into a simplified model of the night scene, as follows:



Figure 4-1 Common modern architecture

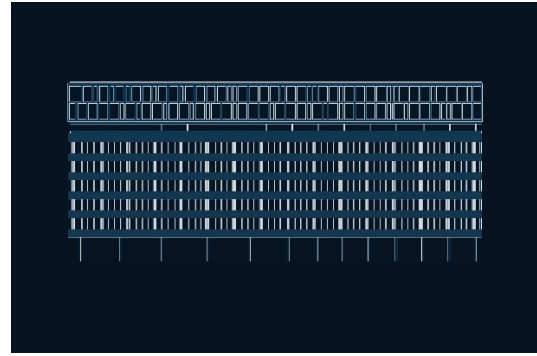


Figure 4- Nighttime simplified model

Firstly, using the principles of symmetry and balance, we analyse the structure direction of the upper, middle, and lower parts of the building clearly to find the biggest characteristics of the building. As shown in the figure:

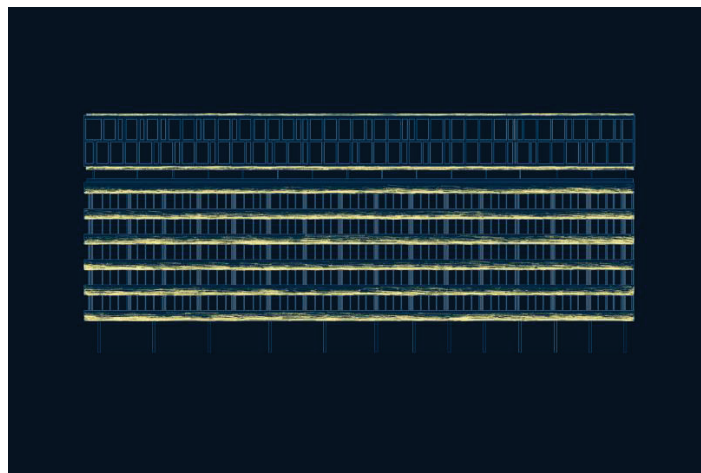


Figure 4-3 Principle of Symmetry and Balance

Next, the principle of comparison and harmony is added. Using only the principle of symmetry and balance often leads to monotonous solutions. By utilizing the different upper and lower structures of the building, a different form of lighting is used at the top. This creates a sense of building volume through the comparison of the upper and lower parts, as shown in the figure:

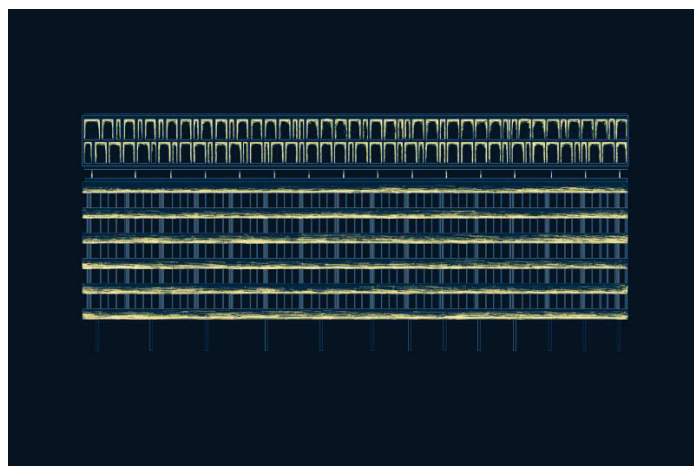


Figure 4-4 Adding the principle of comparison and harmony

Finally, incorporating the principles of beats and rhythm, incorporating unified elements into variations, giving a sense of rhythm to light and dark, creating visual rhythm and showcasing the unique charm of architectural night scenes. As shown in the figure:



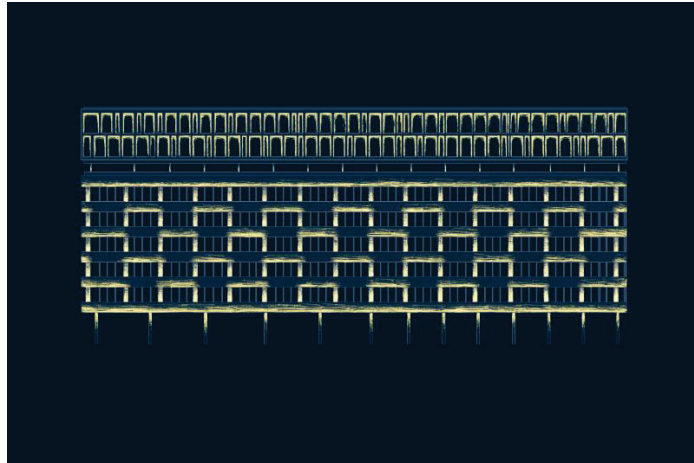


Figure 4-5 Adding the principle of Beats and Rhythm

Referring to the scale of nature, the scale of the composition of the picture, and the scale of the human body, the corresponding method used in night scenes is to compare the scale of the city, the scale of the building itself, and the scale of the human observation perspective. By relying on the extension of this principle, it can be concluded that the principles of patterning can be extended from individual architectural design to the design of urban palm.

## CONCLUSION

Outdoor lighting is a complex territory, and factors such as materials, light color temperature, light distribution, building texture, ambient light, and internal transparency can all affect the external performance. The combination of simplified models and pattern design cannot solve all problems, but it can assist beginners in establishing preliminary aesthetic evaluation reference. Integrating further knowledge, beginners will learn in the lighting industry from shallow to deep.

The purpose of proposing this aesthetic reference and standard is not to persuade everyone to accept it, but to present personal experience, and reflecting on the various confusions I experienced from beginner to proficient. Let's see if it can resonate with everyone's cognition, we hope it can be of some help to others.

According to this method, there are even some tricks to form the aesthetic concept of night scenery for beginners, whether these concepts can serve as standards for professionals still requires careful consideration and proof. But it can alleviate some beginners' confusion in the industry. With the deepening of later learning and the addition of knowledge on lighting material, beginners will gradually expand their understanding of the lighting industry. Establishing a pathway for learning, of course, there must also be other methods for establishing aesthetic standards. Welcome everyone to discuss together.

## REFERENCE

- [1] Paul Jackson. How to Make Repeat Patterns: A Guide for Designer, Architects, and Artists, 2020. ISBN: 9789864592210.
- [2] Lighting Design Professional Committee of Beijing Lighting Society. Lighting Design Manual (Third Edition), 2017. ISBN: 9787519801274.
- [3] Qinghua Xing. Modern Pattern Design from the Perspective of Typology, 2017.
- [4] Jiakang Hu. Fundamentals and Applications of Patterns (Second Edition), 2023, ISBN:9787566921864.
- [5] Li Sun, Yu Kang, Jin Zhang. Fundamentals of Patterns, 2013, ISBN:9787560058530.
- [6] Yan Qin, Ben Zhang. From Pattern to Design Art: An Analysis of Zhuge Kai's Academic Thought, 2023,5(02), 10.19798/j.cnki.2096-6946.2023.02.002.
- [7] Ning Mao. The Formation of the "Folk" Perspective in the Construction of Lei Guiyuan's Chinese Pattern Studies System, 2022(07),Journal Art Observation.

# CHARACTERISTICS OF BRIGHTNESS SENSITIVITY BY TWO LIGHT SOURCES PRESENTED TO PERIPHERAL VISION

Kouya Yamamoto and Hiroshi Takahashi  
(Kanagawa Institute of Technology, Atsugi, Japan)

## ABSTRACT

Various studies have been conducted on brightness perception. However, the influence of the positional relationship of light sources on brightness perception when multiple light sources are presented in the visual field has not been well studied. In the present study, we investigated the brightness perception characteristics depending on the positional relationship between two light sources using a brightness matching method. The experimental results showed a tendency for the perceived brightness to one light source to decrease when the number of lights presented is increased. In addition, when the phase difference of the light sources was  $180^\circ$ , the perceived brightness tended to be slightly higher than when the phase difference was other than  $180^\circ$ .

Keywords: positional relationship by two light sources, peripheral vision, brightness sensitivity

## 1. INTRODUCTION

The degree of brightness in a full space as perceived by humans, and the consideration of a sense of brightness within a space, can be expected to serve as an index for the design of an agreeably illuminated space. Although numerous research studies have evaluated brightness sensitivity, investigations have not yet extended to the characteristics of brightness sensitivity for multiple light sources directed to the peripheral visual field. The purpose of this study was to clarify the effect on brightness sensitivity of the positional relationship by two light sources presented to an area within the peripheral visual field.

## 2. METHODS

Figure 1 shows the experimental environment. The experiment was conducted in a dark room with a large display. The distance between the subject and the display was 400 mm, and the background luminance was  $0.2 \text{ cd/m}^2$ . The brightness matching method, in which the subject could adjust the brightness of the test light to be equal to that of the reference light, was used as the experimental method. Both the reference light and the test light were circles with a diameter of  $2^\circ$  and presented alternately. The direction of the light in the peripheral visual field was  $0^\circ$  to the horizontal right and every  $45^\circ$  from  $0^\circ$  to  $315^\circ$ , for a total of eight directions.

The experimental procedure is described below.

1. Acclimatize to the display luminance for 10 minutes.
2. Gaze at the central fixation point. Maintain this state throughout the experiment.
3. The test light is dimmed to the same brightness as the reference light. The luminance of the test light when dimmed is  $L_t$ .
4. The luminance of the test light is returned to its initial value. Repeat step 3 by randomly changing the direction and eccentricity of the light in the peripheral visual field. The procedure in step 4 is intended to counter the practice effect and the order effect, respectively.



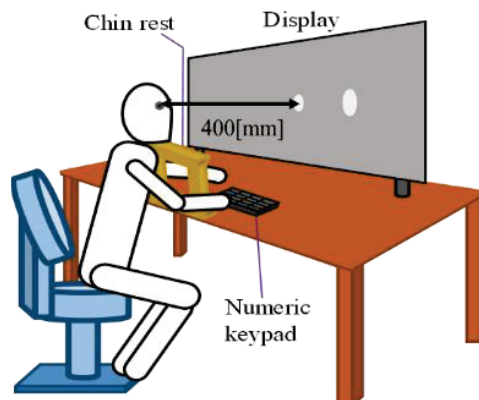


Figure 1. Experimental environment

### 2.1 Brightness sensitivity when one light source is presented in the peripheral visual field

A reference light was presented in the center and a test light was presented in the peripheral visual field.

The eccentricities of the test light were 5°, 10°, 15°, 20°, 25°, and 30°. The luminance of the reference light ( $L_m$ ) was set at 10  $\text{cd/m}^2$ , and the initial value of the test light was set at 1.52  $\text{cd/m}^2$ .

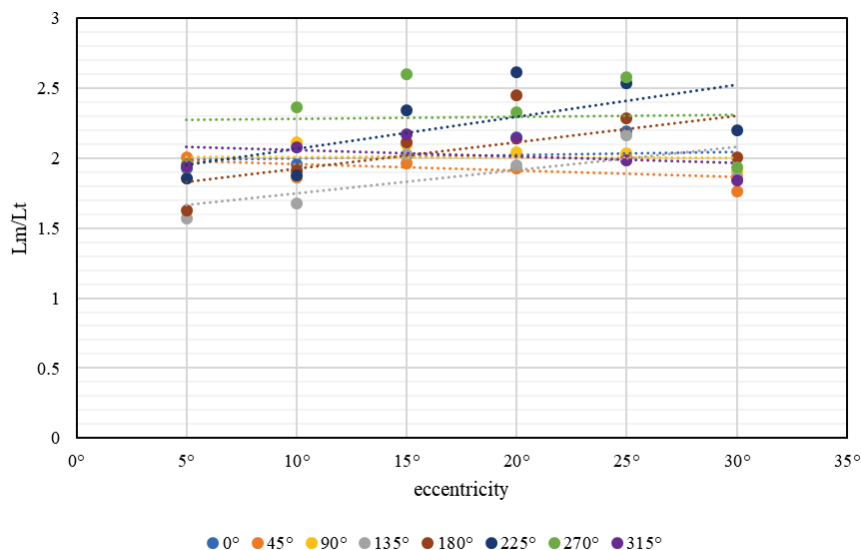
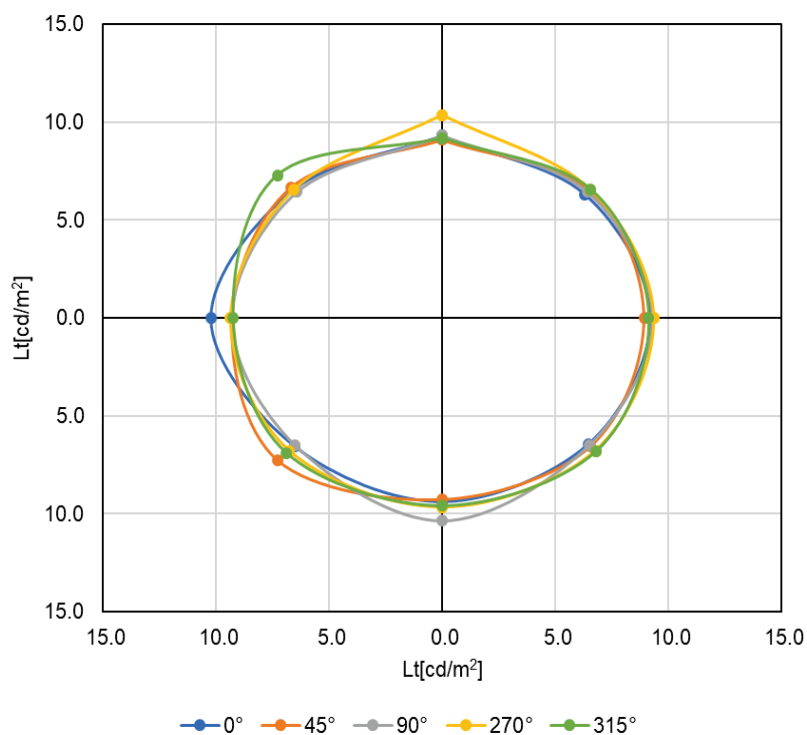
### 2.2 Brightness sensitivity when two light sources are presented

A test light was presented in the center and two reference lights were presented in various positions in the peripheral visual field.

The eccentricities of the reference light were 5°, 10°, 15°, 20°, 25°, and 30°. The reference light was presented at the same brightness and perceived luminance as the 10  $\text{cd/m}^2$  presented light at the center of each presentation position measured in section 2.1. Since two light sources were presented, the initial value of the test light was set to 10  $\text{cd/m}^2$ , because it was expected that the perceived brightness would increase compared to when one light source was presented.

## 3. RESULTS

Figure 2 shows  $L_m/L_t$  in eccentricity in Experiment 2.1. Figure 2 shows that  $L_m/L_t$  tends to increase with increasing eccentricity. This shows a similar trend to previous studies. Figure 3 shows the  $L_t$  curve for the amount of  $L_t$  from the center on the graph in Experiment 2.2. It is the average of  $L_t$  when two light sources, one shown in the direction of the data series and the other in the direction from the center, are presented, respectively. Figure 3 shows that the brightness sensitivity was lower when two light sources were presented in the peripheral visual field, which would result in the same brightness sensitivity as 10  $\text{cd/m}^2$ , than when one light source was presented in the peripheral visual field. This result suggests that when fewer light sources are visible, the brightness of those light sources may be perceived more attentively. The brightness sensitivity was high when the two light sources were in a phase difference relationship of 180°, suggesting that brightness sensitivity in the peripheral visual field may change depending on the phase difference between the light sources. Brightness sensitivity was higher when two light sources in the peripheral visual field were presented in two different presentation directions from among the directions of 225°, 270°, and 315°. This result suggests that brightness sensitivity in the peripheral visual field may change depending on the presentation position of the light sources.

Figure 2.  $L_m/L_t$  in eccentricityFigure 2.  $L_t$  curve

#### 4. CONCLUSIONS

In the present study, we investigated the influence of the positional relationship of light sources on brightness perception when two light sources are presented in the peripheral visual field. The results suggest that the presentation position and the phase difference of the two light sources are related to brightness sensitivity. Since this study was conducted under one condition of brightness sensitivity as the reference brightness sensitivity, the effect of the positional relationship of the light source on the brightness sensitivity under different conditions of reference brightness remains unclear. Future studies should be conducted using more reference brightness conditions.

## REFERENCES

- [1] Byoungwoo Ko, Takaaki Koga, Bin Lu, Kotaroh Hirate, Masaaki Mizuno, Naoyuki Suzuki, Brightness of a Space in Terms of Variation of Luminance. J. Illum. Engng. Jpn. Vol. 97 No.8A 2013
- [2] Qianying Dai, Yoshiki Nakamura, Effects of Central Luminance on Perceived Brightness of Surrounding Area. J. Illum. Engng. Jpn. Vol. 96 No.5 2012
- [3] Tasuku Watanuki, Hiroshi Takahashi, Takashi Irikura, Brightness Perception Throughout the Entire Visual Field. J. Illum. Engng. Jpn. Vol. 99 No.5 2015

Corresponding Author: Kouya Yamamoto  
Affiliation: Kanagawa Institute of Technology  
e-mail: s2282001@cco.kanagawa-it.ac.jp

# EXPLORING KEY METRICS FOR HUMAN-CENTRIC LIGHTING DESIGN IN MULTI-APPLICATION SCENARIOS: A COMPREHENSIVE STUDY

Luo Luya<sup>1</sup>, Chen Huaming<sup>1</sup>

<sup>1</sup>LEDVANCE Operation & Management (Shenzhen) Co., Ltd., Shenzhen 518000, China

## ABSTRACT

This research seeks to investigate the critical indicators of human-centric lighting design in the process from functional design to actual implementation. While the current emphasis in human-centric lighting is on parameters that related to the non-visual effects, particularly spectrum, merely discussing the light source is insufficient. Therefore, this paper conducted a status survey to identify potential issues in the lighting design process that solely focuses on light source parameters. Relevant indicators in domestic and foreign standards and certifications were compiled, and key indicators were selected for further statistical analysis. The study concludes with the establishment of a comprehensive and innovative lighting design system that spans from light source to scene and then to system, guiding the next stage of human-centric indoor lighting design. This system includes multiple aspects such as spectrum parameters, luminaire selection, and scene design, contributing to improving user health and well-being, as well as enhancing the utilization rate of lighting devices.

The implementation of the proposed design system will have significant implications in the field of indoor lighting, providing a more holistic approach to human-centric lighting design. This study provides valuable insights into the factors that must be considered when designing lighting systems for indoor environments, ensuring that all aspects of the lighting system are optimized for the benefit of users. The proposed design system is expected to serve as a valuable tool for designers, architects, and other professionals involved in the indoor lighting industry, facilitating the creation of lighting systems that prioritize the needs and well-being of users.

Keywords: Human-centric lighting, spectrum, lighting scenarios, lighting design parameters

## 1. INTRODUCTION

In addition to stimulating the visual system, light incident on the retina stimulates other biological functions, also referred to as non-visual responses. Human-centric lighting is a lighting concept that delivered the combination of excellent visual, biological, and emotional effects of light.<sup>1</sup> The CIE (International Commission on Illumination) is advocating similar concepts for “integrative lighting”<sup>2,3</sup>. In conclusion, human-centric lighting prioritizes non-visual effects far more than traditional lighting, highlighting its emphasis on the overall well-being of human.

According to CIE, to successfully design and commission an efficient human-centric lighting solution, four parameters must be carefully considered: intensity, spectrum, spatial pattern, timing and duration.<sup>4</sup> At any given time, the biological potency of a light stimulus can be altered first by adjusting light level and second by adjusting light spectrum. A study by *Figueiro et al.*, 2017, shows that compared to office workers receiving low levels of circadian-effective light, those who had receiving high levels is associated with reduced sleep onset latency (especially in winter), increased phasor magnitudes and sleep quality.<sup>5,6</sup> Research also found that the third kind of photoreceptor ipRGCs, which importantly associated with non-visual pathways of human brain, are most sensitive to shortwave blue light.<sup>7,8</sup> With respect to the spatial pattern of light, light exposure on the lower retina more effectively suppresses melatonin than light on the upper retina, and light exposure on the nasal side of the retina is more biologically potent than light exposure on the temporal side of the retina.<sup>9,10</sup> Sleep consolidation is optimal when sleep timing coincides with the period of melatonin secretion<sup>11</sup>, this indicates that proper alignment with lighting approaches between sleep–wakefulness and biological (internal circadian) time is crucial. The same light stimulus may be beneficial at one time of day but detrimental at another.<sup>12</sup> Although light source features mentioned above are of great importance, we must have a clear

understanding of how to apply them in all aspects of human-centric lighting design. After all, human-centric lighting begins with effective prioritization of design goals and is an outcome of good decision making at every step in the lighting design process. All of this includes the continuous demonstration of support of positive human outcomes in operation and use.

## 2. STATUS SURVEY OF LIGHTING IN WORKPLACE

Based on two studies of visual and non-visual effects carried out in offices,<sup>13,14</sup> we have analysed possible problems in human factors lighting design. The sample offices in the first study met the minimum horizontal illuminance ( $>300\text{lx}$ ) specified in the Chinese and CIE standards, and the light sources met the standard usage requirements, but users reported varying degrees of visual fatigue and eye discomfort because the lighting was not properly integrated with the VDT office style. In another study, the majority of workstations ( $>75\%$ ) in the sample met the WELL standard of no less than 200 equivalent melanopic lux (EML) under certain circumstances,<sup>15</sup> but according to the analysis, there were factors in the light environment that could be improved. Further analysis shows that the non-visual effects of office lighting are influenced by weather and lighting, with large differences in conversion factors for the same spectrum on sunny and cloudy days. Thus, the comprehensive human-centric lighting needs a more full-range and flexible implementation to ensure that it maximizes the health effects of light in all aspects.

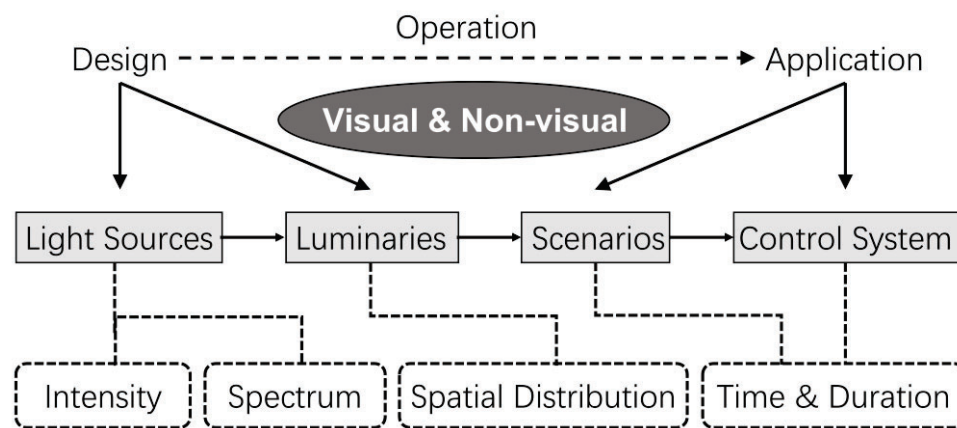


Figure 1. Comprehensive lighting design process for visual and non-visual considerations

## 3. CONSIDERATIONS IN DIFFERENT STAGES OF HUMAN-CENTRIC LIGHTING DESIGN

### 3.1 Light Exposure

Light exposure, especially the spectral composition and intensity, has a significant impact on our visual performance and circadian rhythm. Light with low blue light (long wavelength: 415-455nm) and high colour rendering index ( $\text{CRI}>90$ ) can be visually comfortable and soothing to our eyes while mimicking the spectrum of natural daylight can promote the synchronization of the body's internal clock<sup>16,17</sup>. For instance, bright and cool-toned lighting in the morning can help increase alertness and wakefulness<sup>18</sup>, and blue lighting can accelerate the relaxation process after stress.<sup>19</sup>

### 3.2 Luminaire Selection

The selection of luminaires in human-centric lighting is often overlooked, despite its paramount importance for the visual health of users. Even when utilizing high-quality light sources, pairing them with inappropriate luminaires and drivers can lead to issues such as glare and strobe, significantly disturbing and impairing visual function.<sup>20</sup> Therefore, it is crucial to allocate attention to uniformity, encompassing factors like luminance contrast on the same work surface and the contrast of luminance between the overall environment and the visual subject. By addressing these aspects, the risk of visual fatigue and eye discomfort can be mitigated, ultimately prolonging effective work and reading durations.<sup>21,22</sup>



### 3.3 Light Scenarios

Different tasks require varying levels and qualities of light for optimal performance. For example, reading or working on a computer requires focused and brighter lighting, while relaxing or watching TV calls for a softer and dimmer ambiance. By having different light scenes that adapted to changing needs, individuals can easily adjust the lighting to suit the specific task at hand, enhancing comfort, productivity, and visual performance.<sup>23,24</sup>

### 3.4 Control System and Sensor

The lighting control system allows for personalization by monitoring and responding to individual preferences, activities, and environmental conditions. Integrating luminance sensor to control system can enhance task performance, as well as contribute to energy efficiency by ensuring that lighting is only active when needed<sup>25</sup>. With daylight sensor, the lighting level can be automatically dimmed or adjusted based on natural daylight availability, promoting a healthy sleep-wake pattern and people's overall satisfaction.

## 4. INTEGRATION OF KEY METRICS INTO A HOLISTIC SYSTEM

The design of human-centric lighting encompasses a holistic approach that aims to optimize the visual, non-visual, energy, safety and usability aspects of lighting systems. To ensure the successful implementation of such designs, a comprehensive checklist of key metrics becomes indispensable. This checklist serves as a practical tool for designers, architects, and lighting professionals, enabling them to evaluate and incorporate essential considerations into their solutions.

Table 1. key metrics for human-centric lighting design

Visual	<ul style="list-style-type: none"> <li>• Lumen output</li> <li>• Dimming range</li> <li>• Lowest dim level</li> <li>• Glare assessment</li> <li>• Luminance distribution, uniformity, local deviations</li> <li>• Color rendering index</li> <li>• Color uniformity of different product samples</li> <li>• Color consistency (SDCM)</li> <li>• Maximum deviation from black body line</li> <li>• Seamless, smooth transitions without visible steps</li> <li>• Flickering (<math>p^{LM}_{ST}</math>), temporal light artefacts, stroboscopic effects (SVM) at all dim levels</li> </ul>
Non-visual	<ul style="list-style-type: none"> <li>• Melanopic daylight efficacy ratio</li> <li>• Melanopic dynamic range</li> <li>• Color temperature range</li> <li>• Characteristics of the dynamic daylight-curves</li> <li>• Spectral power distribution</li> </ul>
Safety and Usability	<ul style="list-style-type: none"> <li>• Electrical safety</li> <li>• Photobiological safety</li> <li>• Safety instructions</li> <li>• Resilience against technical failures</li> <li>• Ease of installation and commissioning</li> <li>• Individually user-selectable lighting scenarios</li> </ul>
Energy	<ul style="list-style-type: none"> <li>• Luminous efficacy</li> <li>• Sensor integration</li> </ul>

By addressing visual parameters such as glare control and luminance contrast, non-visual factors like circadian rhythm regulation, energy efficiency considerations, safety measures, and user-friendly interfaces, the checklist acts as a guide for creating lighting environments that prioritize human well-being and satisfaction. Through the systematic integration of these metrics, human-

centric lighting design can fulfil its potential in positively influencing human health and enhancing lighting experiences.

## 5. CONCLUSION

In conclusion, the scope of human-centric lighting extends beyond the mere specifications of the light source, necessitating meticulous control over various parameters encompassing light source selection, scene design, and management systems. While human-centric lighting design is still in its nascent phase of exploration, it is evident that heightened awareness regarding the capacity of light to positively impact human health calls for the adoption of comprehensive design approaches and applications. Further research in this field holds promise as a valuable contribution towards advancing the standardization of designs that prioritize human well-being.

## REFERENCES

- [1] LightingEurope. Joint position paper with IALD on Human Centric Lighting. [S/OL]. 2017. <https://www.lightingeurope.org/newspublications/position-papers/118-jointposition-paper-with-iald-on-human-centriclighting>
- [2] CIE. Commission Internationale de l'Eclairage. CIE Position Statement on Non-Visual Effects of Light: Recommending Proper Light and the Proper Time. 2nd ed. Vienna: CIE (2019).
- [3] ISO/CIE. International Standards Organization and Commission Internationale de l'Eclairage. Light and lighting—Integrative lighting—Non-visual effects. Under development (2020). Report No. ISO/CIE TR 21783.
- [4] Van bonmmel W, Van den Beld G. Lighting for work: a review of visual and biological effects [J]. *Lighting Research & Technology*, 2004, 36(4):255-269.
- [5] Figueiro M G, Steverson B, Heerwagen J, et al. The impact of daytime light exposures on sleep and mood in office workers[J]. *Sleep Health*, 2017 (3) : 204-215.
- [6] Huiberts L M, Smolders K C H J, De Kort Y A W. Non-image forming effects of illuminance level: exploring parallel effects on physiological arousal and task performance[J]. *Physiology & Behavior*, 2016, 164:129-139.
- [7] Brainard G C. Action spectrum for melatonin regulation in humans: evidence for a novel circadian photoreceptor[J]. *Journal of Neuroscience*, 2001, 21(16): 6405-6412.
- [8] Thapan K. An action spectrum for melatonin suppression: evidence for a novel non-rod, non-cone photoreceptor system in humans[J]. *The Journal of physiology*, 2001, 535 (1) : 261-267.
- [9] Glickman G, Hanifin JP, Rollag MD, Wang J, Cooper H, Brainard GC. Inferior retinal light exposure is more effective than superior retinal exposure in suppressing melatonin in humans[J]. *Biol Rhythms*. (2003) 18:71–9.
- [10] Visser EK, Beersma DGM, Daan S. Melatonin suppression by light in humans is maximum when the nasal part of the retina is illuminated[J] *Biol Rhythms*. (1999) 14:116–21.
- [11] Dijk D. J., Cajochen C. Melatonin and the circadian regulation of sleep initiation, consolidation, structure, and the sleep EEG[J]. *Journal of Biological Rhythms*, (1997)12, 627-635.
- [12] Chang A M, Santhi N, St Hilaire M, et al. Human responses to bright light of different durations[J]. *The Journal of physiology*, 2012, 590(13): 3103-3112.
- [13] Luo Luya, Shao Rongdi, Hao Luoxi. Research and Analysis of Status of Visual Display Terminal Task Lighting in Shanghai[J]. *China Illuminating Engineering Journal*, 2022, 33(4):99-106.
- [14] Zeng Yunyi, Yu Juan, Zhang Qinyi, et al. Field evaluation and influencing factor analysis of office light environment based on non-visual effect[J]. *China Illuminating Engineering Journal*, 2022, 33(5):183-191.
- [15] WELL Building Institute. Circadian Lighting Design[S/OL]. 2019. <https://standard.wellcertified.com/light/circadian-lighting-design>.

- [16] Brainard J, Gobel M, Scott B, et al. Health implications of disrupted circadian rhythms and the potential for daylight as therapy[J]. *Anesthesiology*, 2015, 122(5): 1170-1175.
- [17] Wright K P, McHill A W, Birks B R, et al. Entrainment of the human circadian clock to the natural light-dark cycle[J]. *Current Biology*, 2013, 23(16): 1554-1558.
- [18] Motamedzadeh M, Golmohammadi R, Kazemi R, et al. The effect of blue-enriched white light on cognitive performances and sleepiness of night-shift workers: a field study [J]. *Physiology & behavior*, 2017, 177: 208-214.
- [19] Minguillon J, Lopez-Gordo M A, Renedo-Criado D A, et al. Blue lighting accelerates post-stress relaxation: Results of a preliminary study[J]. *PloS one*, 2017, 12(10): e0186399.
- [20] Huang Y Y, Menozzi M. Effects of discomfort glare on performance in attending peripheral visual information in displays[J]. *Displays*, 2014, 35(5): 240-246.
- [21] Xie X, Song F, Liu Y, et al. Study on the effects of display color mode and luminance contrast on visual fatigue[J]. *IEEE Access*, 2021, 9: 35915-35923.
- [22] Bangor A W. Display technology and ambient illumination influences on visual fatigue at VDT workstations[D]. Virginia Polytechnic Institute and State University, 2000.
- [23] Kompier M E, Smolders K C H J, Kramer R P, et al. Contrasting dynamic light scenarios in an operational office: Effects on visual experience, alertness, cognitive performance, and sleep[J]. *Building and Environment*, 2022, 212: 108844.
- [24] Kompier M E, Smolders K C H J, de Kort Y A W. A systematic literature review on the rationale for and effects of dynamic light scenarios[J]. *Building and Environment*, 2020, 186: 107326.
- [25] Wagiman K R, Abdullah M N, Hassan M Y, et al. A new optimal light sensor placement method of an indoor lighting control system for improving energy performance and visual comfort[J]. *Journal of building engineering*, 2020, 30: 101295.
- [26] Houser K W, Boyce P R, Zeitzer J M, et al. Human-centric lighting: Myth, magic or metaphor?[J]. *Lighting research & technology*, 2021, 53(2): 97-118.
- [27] Houser K W, Esposito T. Human-centric lighting: Foundational considerations and a five-step design process[J]. *Frontiers in neurology*, 2021, 12: 25.
- [28] Boyce P, Hunter C, Howlett O. The benefits of daylight through windows[J]. Troy, New York: Rensselaer Polytechnic Institute, 2003.
- [29] Boyce P. Exploring human-centric lighting[J]. *Lighting Research & Technology*, 2016, 48(2): 101-101.
- [30] Yoshimura K, Sakakibara H, Ikeda M, et al. Effect of blue light from LCD on VDT work: Experiment using blue light reduction function LCD [J]. *Journal of the Socielgfor Information Display*, 2020, 28 (8) : 691-697.
- [31] Haves B K, Brunye T T, Mahoney C. I, et al. Effect d four workplace lighting technologies on perceptions cognition and affective state[J]. *International Journal d Industrial Ergonomics*, 2012, 42 (1) : 122-128.
- [32] Konis K. Field evaluation of the circadian stimulus potential of daylit and non-daylit spaces in dementia care facilities[J]. *Building and Environment*, 2018, 135:112-123.
- [33] Lucas R J. Measuring and using light in the melanopsin age[J]. *Trends in Neurosciences*, 2014, 37 (1) : 1-9.
- [34] CIE System for Metrology of Optical Radiation for ipRGC-Influenced Responses to Light: CIE S 026: 2018 [S].
- [35] Hao Luoxi, Cui Zhe, Zeng Kun, et al. Research Trends and Application Prospects on Light and Health effect[J]. *China Illuminating Engineering Journal*, 2017, 28(06):1-15+23.

## ACKNOWLEDGEMENTS

Corresponding Author Name: Luo Luya

Affiliation: LEDVANCE Operation & Management (Shenzhen) Co., Ltd., Shenzhen 518000, China

e-mail: luoluya@163.com

# EFFECTS OF IMMERSIVE VIRTUAL EXHIBITION ON VISUAL PERCEPTION: A COMPARATIVE EXPERIMENT

Haoyu Wu, Xin Zhang

(School of Architecture, Tsinghua University, Beijing, China)

## ABSTRACT

The study focuses on the effects of VR immersive exhibitions on visitors' visual perception compared with traditional physical showrooms, conducting on-site experiments in a real showroom and simulating the showroom in VR Lab at Tsinghua University. The experiment introduces ergonomic metrics into immersive virtual environment study, indicates the correlations between visual perception and lighting strategies by analyzing eye movement data of the participants. The study aims to optimize spatial experience design in virtual display space, and provide theoretical support for the application of digital technology in museums.

Keywords: Immersive exhibition, Lighting strategy, Naked-eye 3D virtual reality, Eye-tracking, Visual perception

## 1. INTRODUCTION

Immersive experiences are flourishing with the development of technological strategies, penetrating into various scenarios. Mobilizing the user's multiple senses and providing real-time interaction, the immersive environment creates a deep experience beyond the physical world. In recent years, immersive technologies have been widely used in digital exhibitions. Digital exhibition space is becoming a significant aspect of museum design and an effective way to enhance audience experience[1].

Immersive information and communication technologies such as virtual reality (VR), augmented reality (AR), mixed reality (MR) and naked-eye 3D have changed the concept of interacting with the reality[2]. Many scholars are concerned with advance in these immersive technologies. Some focus on technical application paths and research methods[3-5], while others study the spatial experience in virtual space and its effects[6-8]. Some experimental research has been done to investigate the factors of immersion and interactivity in virtual environments. The comparative studies between the real space and virtual space are relatively fewer.

Ergonomic metrics such as EDA, ECG and eye-tracking data have provided an effective approach to measure spatial experience. Ergonomic analysis in virtual environment is still being established. Eye-tracking is a useful method for eye-related signal collecting, analysing metrics such as pupil size, gaze direction, fixation and saccade. Many studies have indicated the correlation between eye movements and cognitive load[9-11], task difficulty[12], emotional arousal[13], visual perception[14], etc.

This research aims to reveal the effects of immersive virtual exhibition on visitors' visual perception, optimize spatial experience design in virtual display space, and provide theoretical support for the application of digital technology in museums. Eye-tracking experiments were conducted both in a physical exhibition hall and immersive virtual exhibition hall supported by Unreal Engine and naked-eye 3D technology. We analysed eye movement characteristics in these two environments from pupil diameter and fixation duration data obtained by eye-tracking device.

## 2. METHODS

To investigate the effects of immersive virtual exhibition on visual perception, a comparative experiment was conducted. We have selected a small-scale exhibition hall in Beijing, China, and then replicate the exhibition in a naked-eye 3D-based panoramic simulation laboratory. An eye-tracking experiment was preformed separately both in the physical and immersive virtual showrooms.



aSee Glasses from 7INVENSUN (Figure 1) and its eye movement analysis system were applied to collect eye-tracking data of the participants. The device records more than 20 items of eye movement data while capturing real scenes. In this study, aSee Glasses was connected to a cell phone recording device, which enabled the participants to move around without restriction and have more authentic exhibition visiting experiences. The essential parameters of aSee Glasses are shown in Table1.



Figure 1. aSee Glasses eye-tracking device

Table1. Parameters of aSee Glasses

Parameter	Sampling rate	Accuracy	Delay	Glasses weight
data	60Hz	<0.5°	≤10ms	40±3g

## 2.1 Physical exhibition experiment

### 2.1.1 Site

The physical exhibition experiment was carried out in a small-scale showroom (Figure 2-3) in Yizhuang, Beijing, China. The room has a width of 3.30 meters, a depth of 5.50 meters, and a height of 2.88 meters. The opaque curtains were kept closed to avoid the influence of daylighting during the experiment, ensuring that the showroom was illuminated by artificial lights only.

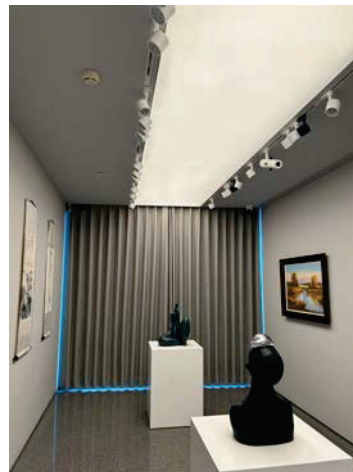


Figure 2. Physical exhibition hall

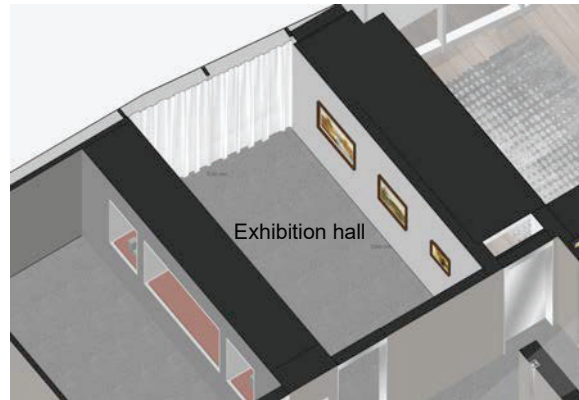


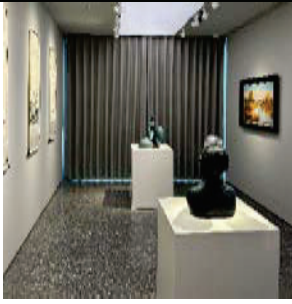


Figure 3. Axonometric diagram of the exhibition hall

### 2.1.2 Lighting mode selection

The exhibition hall was equipped with a lighting control system, including seven different lighting modes. To test participants' eye movement and visual perception under different lighting strategies, we have selected 3 lighting modes as 3 experiment scenarios (Table 2), which are ambient lighting mode, accentuated lighting mode with focal glow on exhibited works, and a mixed lighting mode that combines the previous two.

Table 2. Three lighting modes

Lighting mode	1	2	3
Feature	Ambient lighting	Accentuated lighting	Mixed lighting
Picture			

### 2.1.3 Participants selection and experimental procedure

A total of 13 people participated in this experiment. All participants had normal naked or corrected vision, did not wear contact lenses that changed pupil color or iris shape, and did not use eye makeup.

The experimental procedure is as follows.

- First, the participant would learn the basic process and experimental scenarios to gain a preliminary understanding of the experiment.
- Then the participant wore aSee Glasses eye-tracking device, and completed a three-point calibration under guidance. After successful calibration, the participant tried to adapt to the vision of aSee Glasses for one minute and entered the showroom.
- In each test, the participant visited the paintings on the wall in the counterclockwise direction, during which the eye-tracking device was connected to the aSee Glasses cell phone recording assistant to record the participant's eye movement data.
- After the test, the participant left the exhibition hall to relax for one to two minutes, and then repeated the former step in another lighting mode. Each participant had completed 3 tests. The order of the lighting modes was chosen randomly to minimize the impact of the order of different lighting scenes on participants' perception.

## 2.2 Immersive virtual exhibition experiment

### 2.2.1 Site

The immersive exhibition experiment was performed in the Panoramic Simulation VR Lab at the School of Architecture in Tsinghua University. The laboratory has been built to display virtual environments to conduct ergonomic research. Supported by n'Space naked-eye 3D virtual reality system, the devices capture and react to users' movements, providing photorealistic immersive experience and real-time interaction.

In this study, the immersive virtual exhibition hall that replicated the physical showroom was presented in the lab.



Figure 4. Panoramic Simulation VR Lab, Tsinghua University

### 2.2.1 Virtual environment building

An immersive virtual environment was built in VR Lab, replicating the spatial and visual information of the physical exhibition hall. The technical approach is shown in Figure 5. First, a SketchUp model was made after measuring relevant data of the showroom and paintings. Second, we added material details and lighting effects in Twinmotion. Then exhibition scenes and interactive elements were established in Unreal Engine 5.0. UE5 is a widely applied virtual engine that enables multi-purpose 3D rendering. The three lighting modes in physical exhibition experiment (ambient, accentuated and mixed lighting) were simulated separately. Finally, after connecting the n'Space naked-eye 3D virtual reality system, the immersive virtual exhibition was built and human-machine interaction was also generated.

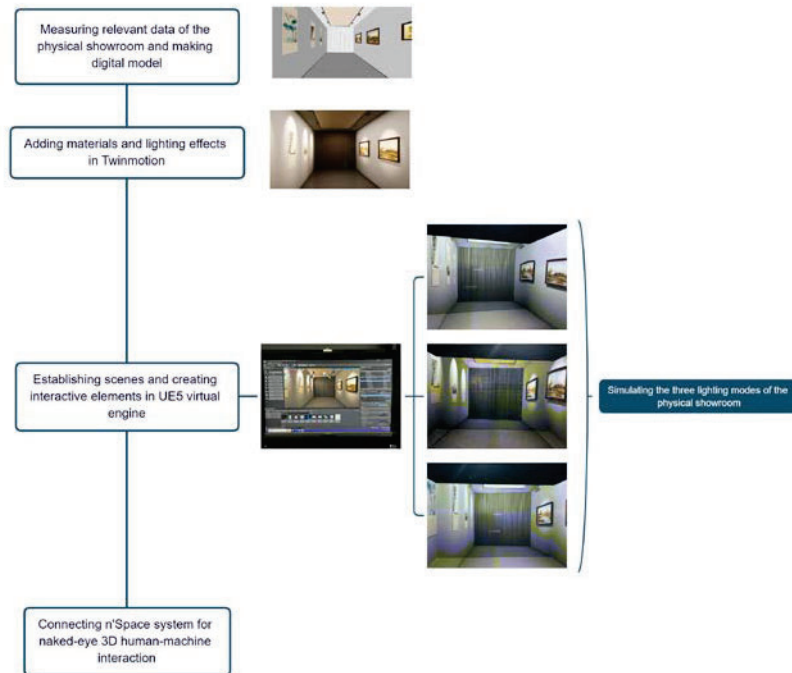


Figure 5. Technical approach to build the virtual environment

### 2.2.2 Participants selection and experimental procedure

A total of 16 participants were invited to the experiment. All participants had normal naked or corrected vision, did not wear contact lenses that changed pupil color or iris shape, and did not use eye makeup or have obvious 3D motion sickness.

See 2.1.3 for the experimental procedure.

## 3. RESULTS

In the physical exhibition hall experiment, a total of 13 people participated and 13 sets of valid data were obtained. There were 16 participants in the immersive virtual exhibition experiment, and 15 sets of valid data were obtained.

We selected pupil diameter and fixation duration as main metrics of eye movement. Pupil diameter has been considered as an effective index of cognition[9, 15, 16]. It is noted that pupil diameter is related to ambient light[17], task difficulty[18] and other factors. Fixation index is also a significant metric in eye-tracking research. Some studies have used total fixation duration to reveal the cognitive activities[19, 20], while other visual research used average fixation duration[21, 22]. However, some studies indicate that average fixation duration should vary depending on the processing demands of the task[23]. There is research using both average pupil diameter and average fixation duration to classify emotions and comparing the validity of these two metrics[24].

### 3.1 Average pupil diameter

Figure 6-9 illustrate the participants' average pupil diameter in three different lighting modes in the physical and virtual showrooms. In light mode 2, namely, accentuated lighting with focal glow on the paintings, participants had the highest average pupil diameter among all experimental scenarios. The pattern appeared in both physical and virtual showroom experiments, with the physical showroom being more obvious.

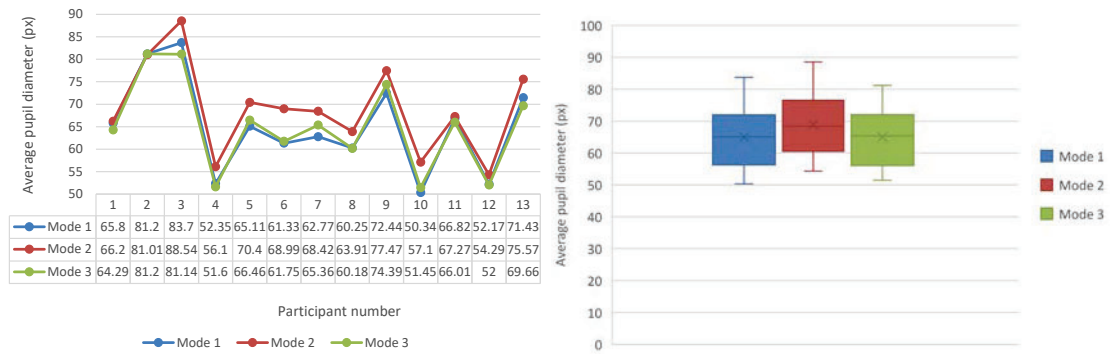


Figure 6 (Left). Average pupil diameter in three lighting modes in physical exhibition hall

Figure 7(Right). Box plot of average pupil diameter in three lighting modes of the physical exhibition hall

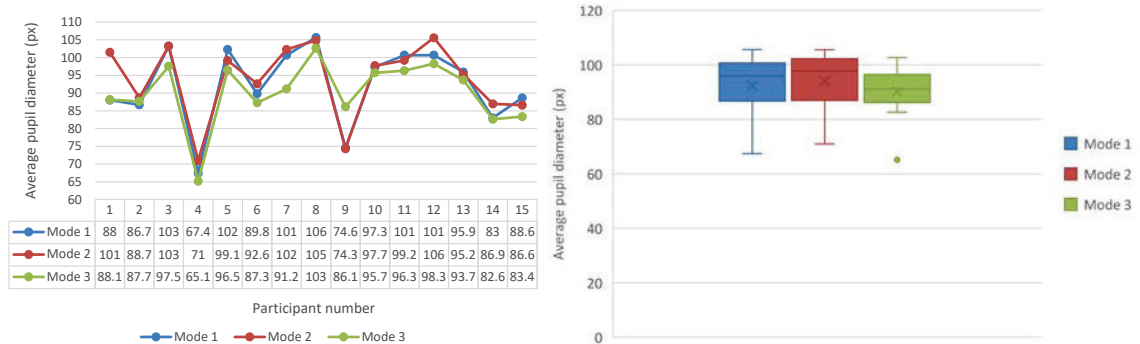


Figure 8 (Left). Average pupil diameter in three lighting modes virtual exhibition hall

Figure 9 (Right). Box plot of average pupil diameter in three lighting modes of the virtual exhibition hall

### 3.2 Average fixation duration

Figure 10-13 show the participants' average fixation duration in three different lighting modes in the physical and virtual showrooms. In physical exhibition, participants had higher average fixation duration in ambient lighting mode than that in the other two modes. This metric does not differ significantly across modes in the immersive virtual showroom experiment.

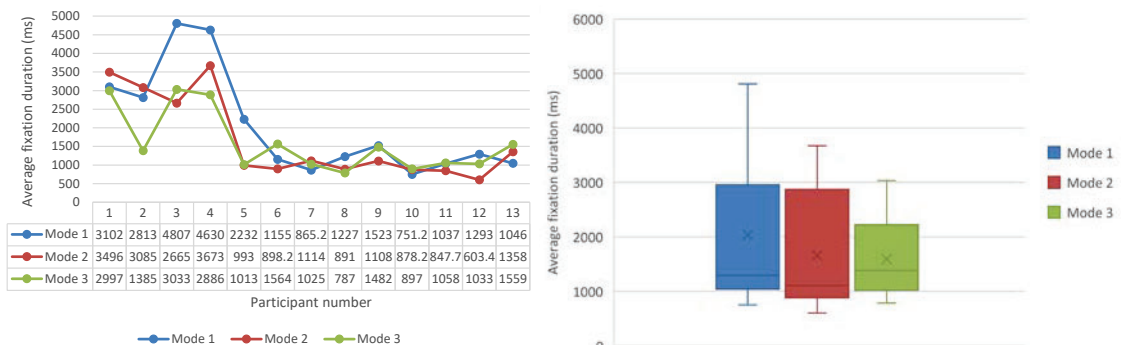


Figure 10 (Left). Average fixation duration in three lighting modes in physical exhibition hall

Figure 11(Right). Box plot of average fixation duration in three lighting modes of the physical exhibition hall



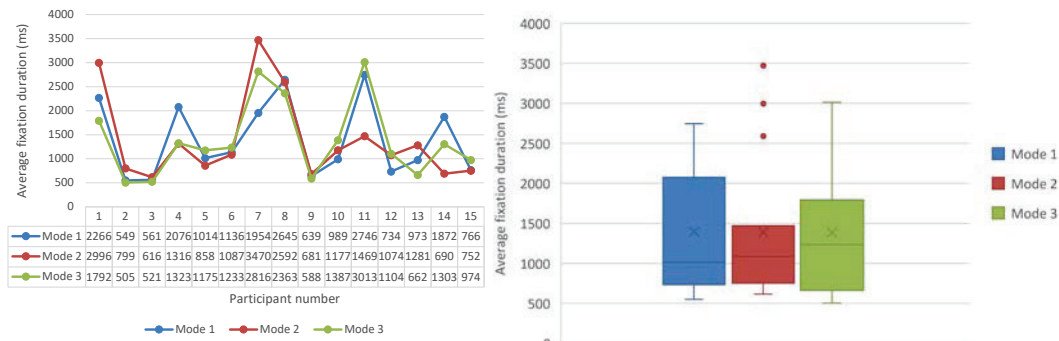


Figure 12 (Left). Average fixation duration in three lighting modes in virtual exhibition hall

Figure 13 (Right). Box plot of average fixation duration in three lighting modes of the virtual exhibition hall

### 3.3 Effects of immersive virtual exhibition on eye movement

In all three lighting modes, compared to physical exhibition, virtual exhibition had higher average pupil diameter (Figure 14), which might represent a higher level of excitement and arousal. Participants' average fixation duration was lower in immersive virtual exhibition than that in physical showroom (Figure 15). This indicated that either it was harder to extract information from the environment in physical exhibition, or visual targets in physical showroom appeared to be more attractive.

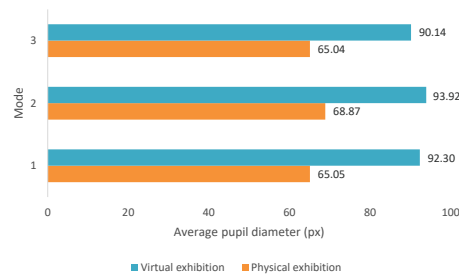


Figure 14. Average pupil diameter in three lighting modes in physical and virtual exhibitions

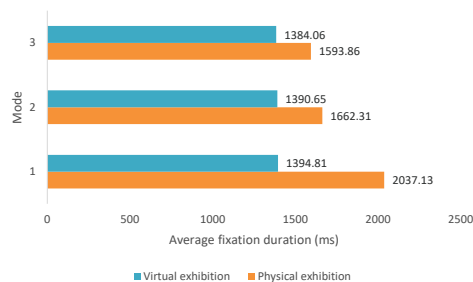


Figure 15. Average fixation duration in three lighting modes in physical and virtual exhibitions

## 4. CONCLUSION

Immersive virtual exhibitions are rapidly evolving with technological progress and higher demand for user experience. Meanwhile, the interactions between users and the environment remains complex. This research studies the effects of immersive exhibition on eye movement through a comparative experiment. Through a comparative experiment of a physical exhibition and an immersive virtual exhibition, we had noted some differences of pupil diameter and fixation duration between the two environments. The research shows that an immersive environment may provide greater excitement and arousal for visitors.

In follow-up study, the generalizability of research can be enhanced by expanding the number of participants, improving the 3D rendering fineness and interaction fluency, and introducing other

ergonomic indicators such as EDA and ECG to comprehensively evaluate the effect of immersive virtual environments on visual perception.

## REFERENCES

- [1] Kamariotou, V., M. Kamariotou, & F. Kitsios, Strategic planning for virtual exhibitions and visitors' experience: A multidisciplinary approach for museums in the digital age. *Digital Applications in Archaeology and Cultural Heritage*, 2021, 21, p. e00183.
- [2] Rubio-Tamayo, J.L., M. Gértrudix-Barrio, & F.G. García, Immersive Environments and Virtual Reality: Systematic Review and Advances in Communication, Interaction and Simulation. *Multimodal Technol. Interact.*, 2017, 1, 21.
- [3] Lazar, J., J. Feng, & H. Hochheiser. *Research Methods in Human-Computer Interaction*. 2010.
- [4] Lin, W., et al. Design of Hand Gestures for Manipulating Objects in Virtual Reality. in *Interacción*. 2017.
- [5] Loomis, J.M., J. Blascovich, & A.C. Beall, Immersive virtual environment technology as a basic research tool in psychology. *Behavior Research Methods, Instruments, & Computers*, 1999, 31, 557-564.
- [6] Kober, S.E., et al. Effects of a 3D Virtual Reality Neurofeedback Scenario on User Experience and Performance in Stroke Patients. in *International Conference Games and Learning Alliance*. 2016.
- [7] Moussaïd, M., et al., Crowd behaviour during high-stress evacuations in an immersive virtual environment. *Journal of the Royal Society Interface*, 2016, 13.
- [8] Xia, G., et al., The effects of colour attributes on cognitive performance and intellectual abilities in immersive virtual environments. *Computers in Human Behavior*, 2023: p. 107853.
- [9] Krejtz, K., et al., Eye tracking cognitive load using pupil diameter and microsaccades with fixed gaze. *PLoS ONE*, 2018, 13.
- [10] He, D., et al., Classification of Driver Cognitive Load: Exploring the Benefits of Fusing Eye-Tracking and Physiological Measures. *Transportation Research Record*, 2022, 2676, 670 - 681.
- [11] Souchet, A.D., et al., Measuring Visual Fatigue and Cognitive Load via Eye Tracking while Learning with Virtual Reality Head-Mounted Displays: A Review. *International Journal of Human-Computer Interaction*, 2021, 38, 801 - 824.
- [12] Cho, Y., Rethinking Eye-blink: Assessing Task Difficulty through Physiological Representation of Spontaneous Blinking. *Proceedings of the 2021 CHI Conference on Human Factors in Computing Systems*, 2021.
- [13] Pengnate, S. Measuring Emotional Arousal in Clickbait: Eye-Tracking Approach. in *Americas Conference on Information Systems*. 2016.
- [14] Lisińska-Kuśnierz, M. & M.P. Krupa, Suitability of Eye Tracking in Assessing the Visual Perception of Architecture—A Case Study Concerning Selected Projects Located in Cologne. *Buildings*, 2020, 10, 20.
- [15] Hess, E.H. & J.M. Polt, Pupil Size in Relation to Mental Activity during Simple Problem-Solving. *Science*, 1964, 143, 1190 - 1192.
- [16] Beatty, J. & D. Kahneman, Pupillary changes in two memory tasks. *Psychonomic Science*, 1966, 5, 371-372.
- [17] Beatty, J.K. & B. Lucero-Wagoner. *The pupillary system*. 2000.
- [18] Siegenthaler, E., et al., Task difficulty in mental arithmetic affects microsaccadic rates and magnitudes. *European Journal of Neuroscience*, 2014, 39.
- [19] Liu, P.-L., Using eye tracking to understand learners' reading process through the concept-mapping learning strategy. *Comput. Educ.*, 2014, 78, 237-249.
- [20] Mitra, R., K.S. McNeal, & H.D. Bondell, Pupillary response to complex interdependent tasks: A cognitive-load theory perspective. *Behavior Research Methods*, 2017. 49: p. 1905-1919.
- [21] Rayner, K., Eye movements in reading and information processing: 20 years of research. *Psychological bulletin*, 1998, 124(3), 372-422.
- [22] Rayner, K., et al., Eye Movements as Reflections of Comprehension Processes in Reading. *Scientific Studies of Reading*, 2006, 10, 241 - 255.
- [23] Negi, S. & R. Mitra, Fixation duration and the learning process: an eye tracking study with subtitled videos. *Journal of Eye Movement Research*, 2020, 13.
- [24] Zheng, L.J., J. Mountstephens, & J. Teo, Eye Fixation Versus Pupil Diameter as Eye-

Tracking Features for Virtual Reality Emotion Classification. 2021 IEEE International Conference on Computing (ICOCO), 2021, 315-319.

## **ACKNOWLEDGEMENTS**

This work was supported by the National Natural Science Foundation of China (No. 52078266) and Ergonomic Analyses in Built Space Design and its Product Research (No.20223930099).

Corresponding Author Name: Xin Zhang  
Affiliation: School of Architecture, Tsinghua University  
e-mail: zhx@mail.tsinghua.edu.cn

# Reflections on Optical Linguistics from the Perspective of Eastern Philosophy

Hao Shen

(Dalian Polytechnic University, Dalian City, Liaoning Province, China)

## ABSTRACT

As a catalyst of space, light can realize visual metaphor under the support of interface and structure, and the language of light can be strengthened. In the Oriental philosophical system that takes reality as virtual, light always occupies an important position. Through the empowerment of light, the spatial sequence of environment has a richer level. The flowing spatial sequence makes the character of space more charming and makes it have special significance. At present, the language of light becomes more important to the construction of environmental culture.

**Keywords:** Philosophy/catalyst/space/character/cultural/space structure/verve /cosmetics

## INTRODUCTION

With the steady improvement of people's attention to the living environment and the rapid updating of science and technology, we have found more factors closely related to the quality of the light environment in observation and evidence collection. In the past, we habitually included the subject of light source as a subject of engineering, and the part of light efficiency into the category of aesthetics category, which caused the light source and the light effect to belong to two systems, which were difficult to integrate. It should to learn the knowledge of light control, to engage in the design of light environment, in addition to learning photoelectric research light source, is more inseparable from the environment, requires a deep understanding of the environment, architecture and interior space, master the space composition style and material properties, in order to make Light melts into space and is higher than space, creating and enhancing space temperament.

It is said that philosophy began with the appearance of real people. Philosophy has inspired and guided the development of human society for a long time, and the development of many fields closely related to human life cannot be separated from the promotion of philosophical thought. Philosophy guides the development of various fields with its own logic and language.

## 1. THE FORMATION AND STATUS QUO OF SPACE FORMAT

Nourished by traditional culture, Chinese people are born to respect and learn from nature. The Tao Te Ching says: Man's law is the earth's law, the earth's law is heaven's law, the heaven's law is Tao's law, and the road is nature's law. The highest state of light is to learn from nature. Man imitates earth, earth imitates heaven, and heaven imitates Tao, and the way is natural. Cutting-edge technology represents fashion and a sense of technology, and Eastern culture blends Yin and Yang.

Zen, the essence of Oriental traditional culture, is a state of mind, a return, a pursuit, a belief, it helps us integrate into nature, regain a new life, away from the hustle and bustle, have great wisdom.

Ancient Chinese philosophy is an important part of Chinese civilization, among which traditional thoughts such as Taoism and Confucianism are deeply loved and respected by people. This paper will introduce the most distinctive and representative philosophical thoughts of ancient China and explore their influence on Chinese culture.

Confucianism is the most widely spread and far-reaching ideological system in ancient China. Its core concepts are "benevolence" and "rule by etiquette", emphasizing the relationship between individuals and society, and pursuing social harmony and stability. Confucius is the founder of Confucianism, he put forward the "benevolent lover", "do not do to others what you do not want to do to yourself" and other famous remarks. In the later development, Confucianism gradually formed a complete theoretical system and was regarded as the orthodox thought of the ruling class.

Taoism emphasizes "ruling without doing anything" and advocates the pursuit of ruling without doing anything under the natural state in order to achieve the realm of physical and mental unity and freedom. Laozi is the founder of Taoism, he put forward "the way can be very road", "heaven and earth are not benevolent, take all things as dogs". The core idea of Taoism is "Tao", that is, the origin and law of all things, and the pursuit of harmony between man and nature.

Mohist thought advocates "universal love" and "non-aggression", opposes war and violence, and emphasizes equality and cooperation between people. Mozi is the representative figure of Mohist thought. He put forward the slogan of "universal love for the public" and believed that only through mutual help and cooperation can social harmony and progress be realized. Mohist thought once had a glorious history in ancient China, but later it gradually declined.

Legalist thought advocates the rule of law and emphasizes the authority and effect of law. It believes that political power should be concentrated in the hands of a single person or a small group of people and that social order should be maintained through law. Han Feizi is the representative of legalist thought, he put forward the theory of "heavy punishment and light punishment", "educate the people by law" and so on. Although it had a certain political influence in ancient China, legalism was not widely accepted in the cultural field.

In a word, ancient Chinese philosophical thoughts have rich and colorful connotations and profound wisdom, which have had an important impact on the development and evolution of Chinese culture. Confucianism emphasizes the relationship between individual and society and pursues social harmony and stability. Taoist thought advocates the pursuit of non-action in the state of nature, in order to achieve physical and mental unity, freedom; Mohist thought emphasizes equality and cooperation among people; Legalist thought advocated the rule of law and emphasized the authority and effect of law. These philosophical thoughts are not only an important part of Chinese civilization, but also add a unique and precious piece to the history of world philosophical thoughts.

## **2. Space theory**

### **2.1 Spatial concept**

Space is a relative concept, which constitutes the abstract concept of things, and the abstract concept of things exists with reference to space. Length, width, height, if we call this "mathematical space", then how to express the emotional, cognitive space. Light can make space produce wonderful changes, in the highly developed lighting technology today, the skilled use of human lighting technology combined with a deep understanding of the meaning of space, coupled with the comprehensive expression of optics, aesthetics, materials science, psychology, we have a higher expectation of the artistic value and commercial value of space. The civilization of dialogue has replaced the civilization of instruction in more areas, and we need the massive interaction of public opinions to produce multi-directional interaction and communication, so as to form a communication medium and promote the spread and development of symbols of artistic value.

### **2.2 Virtual space**

When using lights to create atmosphere, not only can the lighting be used, but also the lighting shape and light color tone can be combined to create an artistic realm and atmosphere in the space. In order to create a rich spatial texture, comprehensive control of lighting can be carried out, such as the combination of virtual and real, the combination of static and dynamic, and the comprehensive control of the direction of light, and reasonable control of the light area to achieve rich light chroma changes. For the image art treatment of lighting fixtures, it can effectively increase the atmosphere effect in the living room, play a finishing touch and icing on the cake effect, and make the atmosphere in the space lively and interesting, fully reflect the characteristics and style of the living room design. It can be seen that in the interior, the decoration of lighting can be better integrated with the indoor links.

## **3. Artistic treatment of space lighting**

### **3.1 Spatial processing**

In the actual design, lighting can be used to achieve the division of space, select different lights in different areas, partition lighting of the overall space, or use different colors to achieve the division of the region. Different lighting can be used to divide large areas to increase people's curiosity and increase the interest of indoor space. For example, different lights can be used to divide the number of diners in a restaurant to help customers sit down quickly and save manpower.

### **3.2 Light and Shadow Effect**



In the space decoration, you can choose the combination of light and shadow to show different effects. For example, the light is reflected to the place where attention is drawn, advertising words, new products, etc., the contrast of light and shadow is used to highlight the key points, guide people or attract attention, and the light and shadow are combined with the indoor environment and objects to create an amazing feeling.

### **3.3 Highlight Key points**

For people, the space is usually an important content worth highlighting, so it is necessary to choose different lights to attract the attention of customers, and cooperate with music to create another artistic atmosphere.

### **3.4 Play Up the atmosphere**

When designing space lighting, it is necessary to combine light and shadow with light and color, and combine space decoration to form a unique charm style. Combined with the actual situation, the use of lighting color, shadow, intensity, make the space decoration more eye-catching, can use the color of the lamp to create a unique interior style.

Light can be the brilliance of divinity, or it can be the brilliance of life, and the spiritual core is set by the designer. Confucianism's "benevolence", Taoism's "ruling without doing anything", Mohism's equal cooperation, legalism's authority and other philosophical thoughts can be transformed into design ideas and design propositions, which determine the pattern of light in space. In this era where midjourney can use several keywords at any time, design ideas have become particularly important and precious. What is irreplaceable for human beings, the answer is obvious, it is thought, and only thought can reflect the artistry and uniqueness of design. What can solve this? Perhaps we should return to the "core" – philosophy. And start again.

## **REFERENCES**

- [1] Cui Zhe, Hao Luoxi, Lin Yi. Current International Research Trends on Circadian Rhythm. Zhaoming Gongcheng Xuebao, 2014, 25(3)
- [2] Xu Dongliang, Approach To Lighting Design, 江苏凤凰科学技术出版社; 第 1 版 (2016 年 12 月 1 日)

# COMPARISON OF LUMINANCE MEASUREMENT BETWEEN SPOT LUMINANCE METER AND ILMD

Xiaobo Zhuang<sup>1,2</sup>, Xilong Yu<sup>2</sup>, Xin He<sup>1,2</sup>

1. Shanghai Alpha Lighting Equipment Testing Ltd., Shanghai 201114, China,

2. Shanghai Institute of Quality Inspection and Technical Research, Shanghai 201114, China

## ABSTRACT

Luminance measurement has been widespread used, such as road lighting, landscape lighting, and glare evaluation, etc., especially light pollution. The spot luminance meter and ILMD (imaging luminance measurement device) are used to test the luminance. Since luminance is a physical quantity related to direction and the luminance meter measures the average luminance, which is related to the field angle and test distance, the test results vary widely.

Three kinds of spot luminance meter and two types of ILMD are used to test uniformly emitting panel luminaires and non-uniformly emitting floodlights along the normal direction. Analyses are conducted to compare the results across the 5 instruments but also to compare results among different view angle and test distance.

Keywords: luminance, luminance meter, ILMD, luminaire, brightness

## 1. INTRODUCTION

The definition of luminance is the density of luminous intensity with respect to projected area in a specified direction at a specified point on a real or imaginary surface [1]. So Luminance is a physical quantity related to direction, independent of distance. However, the luminance meter measures the average luminance, which is related to the measuring angle and test distance [2].

Due to different of the field of view angle, test distances, and test directions of the luminance meter, and the calibrated problems, the measured luminance results vary greatly, sometimes even by orders of magnitude. Furthermore, the repeatability of test results is awful.

The uniformly emitting panel luminaire and non-uniformly emitting road lighting luminaire have been measured the luminance along the normal direction by three kinds of spot luminance meter (Konica Minolta LS-160, LMT L1009 and Konica Minolta CS-2000) and two types of ILMD (Radiant Vision Systems ProMetric Y-16 and Konica Minolta CA-2500).

## 2. UNIFORM ILLUMINANT

### 2.1 Luminance of the LED panel luminaire

Fix a 36 W LED panel luminaire with an external dimension of 320\*1220 mm and a light-emitting area of 254\*1148 mm on the vibration isolation platform.

Radiant Vision Systems ProMetric Y-16 (CCD resolution is 5312\*3032, standard lens) and Konica Minolta CA-2500 (CCD resolution is 980\*980, standard lens) color luminance meters are used to measure at a distance of 3 meters from the normal direction of the LED panel luminaire. The measured luminance and false color charts are shown in Figure 1. The measured normal center luminance is 4057 cd/m<sup>2</sup> and 4336 cd/m<sup>2</sup>.

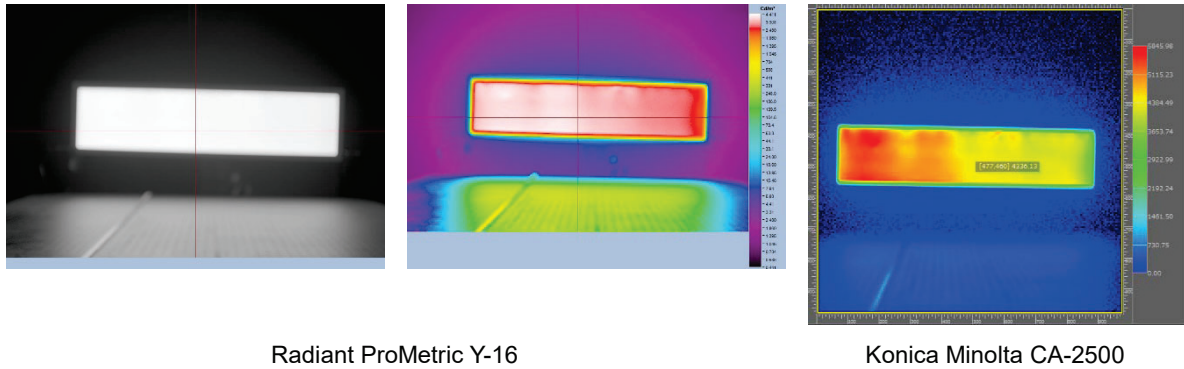


Figure 1. Luminance false color charts tested by 2 ILMD

The LED panel luminaire is fixed vertically in the optical darkroom, and the center of the emitting area is 310 mm above the table. We use the Konica Minolta LS-160 and LMT L1009 spot-luminance meter with a measuring angle of 20' to test the luminance of the normal center point of the LED panel luminaire at different distances. In the same field angle of 20', the luminance test results of different spot-luminance meters are shown in Figure 2.

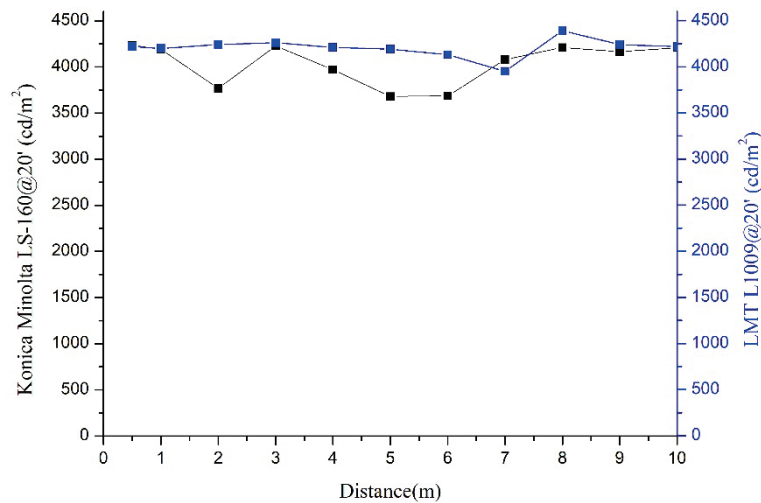


Figure 2. Luminance comparison test of LED panel luminaire under the same field angle of 20'

Moreover, the Konica Minolta CS-2000 and LMT L1009 spot-luminance meter with a measuring angle of 1° to measure the luminance of the normal center point of the LED panel luminaire at different distances. In the same field angle of 1°, the luminance test results of different spot-luminance meters are shown in Figure 3.

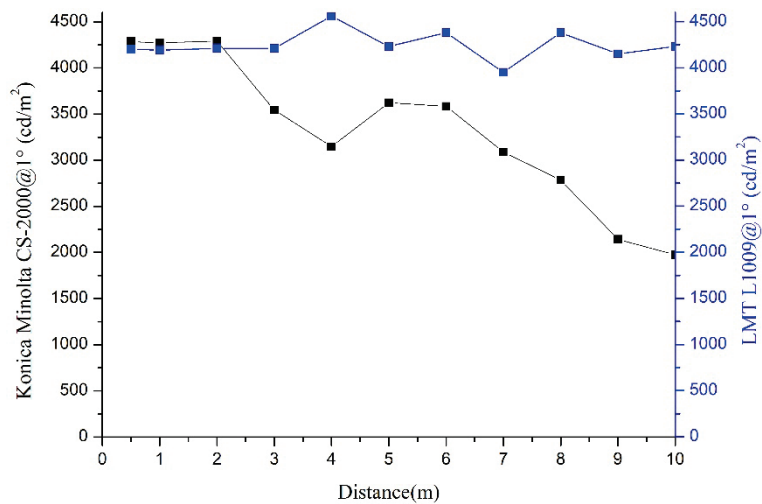


Figure 3. Luminance comparison test of LED panel luminaire under the same filed angle of 1°

With the same spot-luminance meter, the luminance test results of different field angle are shown in Figure 4. When the test distance is greater than 6 meters and the viewing angle is 3°, the measured luminance is significantly lower than before and other viewing angles. This is because the measured actual dimension has exceeded the width of the LED panel light, so the measured area includes the non-luminous background, and then the average luminance would be low.

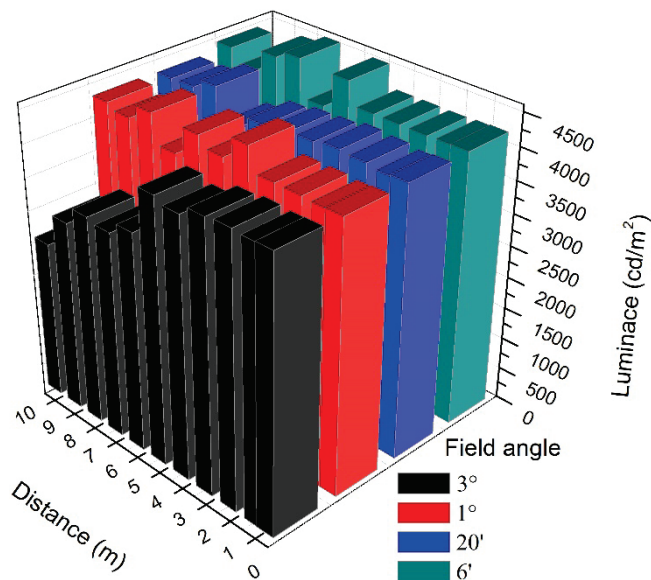


Figure 4. Luminance comparison test of LED panel luminaire under the same spot luminance meter of LMT L1009

## 2.2 Light distribution of the LED panel luminaire

The LED panel luminaire is installed on the LMT GO-V 1920 goniophotometer to measure the light distribution. The light distribution curve of LED panel luminaire is shown in Figure 5. The light distribution of the LED panel luminaire is similar to the cosine illuminator, especially near the normal line. Therefore, it is almost a uniform illuminant.

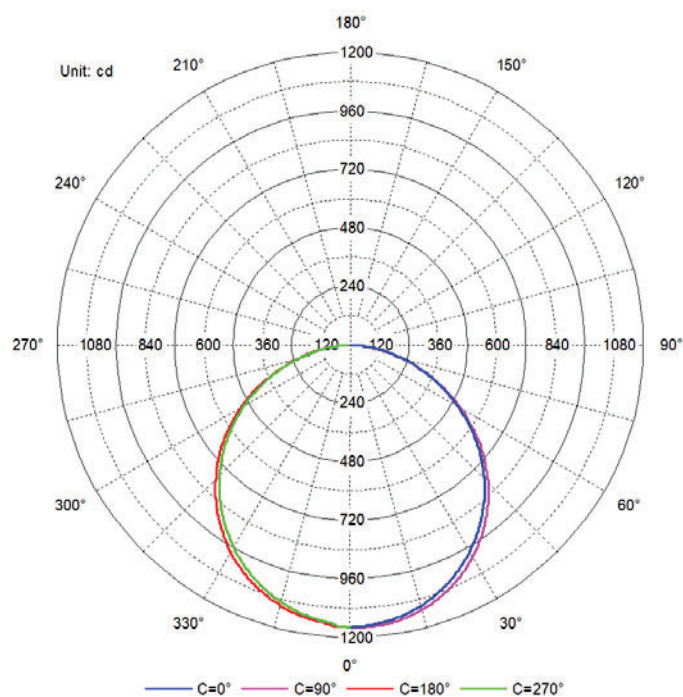


Figure 5. Light distribution curve of LED panel luminaire

### 3. NON-UNIFORM ILLUMINANT

#### 3.1 Luminance of the LED road lighting luminaire

A 150 W LED road lighting luminaire with an external dimension of 365\*750 mm and a light-emitting area of 210\*450 mm is installed vertically on the vibration isolation platform.

Since the surface brightness of the street lamp is too high, the Konica Minolta CA-2500 is overexposed and cannot be photographed. Only the Radiant Vision Systems ProMetric Y-16 is used to measure at a distance of 4 meters from the normal direction of the LED road lighting luminaire. The measured luminance and false color charts are shown in Figure 6. The measured normal center luminance is 22112  $\text{cd/m}^2$ .



Figure 6. Luminance false color charts tested by Radiant ProMetric Y-16

Under the same spot-luminance meter, the luminance of road lighting luminaire test results of different field angle are shown in Figure 7. When the viewing angle is large than  $1^\circ$ , the test luminance is over range of the meter. When the field of view is  $20'$  or  $6'$ , and the normal center of the test is just the light-emitting chip, although the farther the distance is, the larger the measured area will be, then the measured area will include the dark area between chips. On the other hand, the luminance of the chip is too high, so the average brightness is high, and the result is not much different.

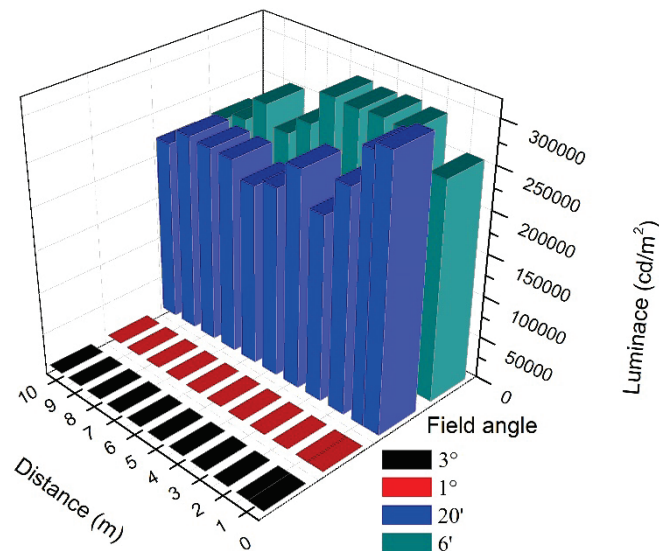


Figure 7. Luminance comparison test of LED road lighting luminaire under the same spot luminance meter of LMT L1009

#### 3.2 Light distribution of the LED road lighting luminaire



The LED road lighting luminaire is also fixed on the LMT GO-V 1920 goniophotometer to measure the light distribution. The light distribution curve of LED road lighting luminaire is shown in Figure 8. The light distribution across the luminaire is asymmetrical is clearly evident from the curve through the plane across the road (C270°- C90° plane): more light is radiated towards the road rather than towards the kerb [2]. From this point of view, the road lighting luminaire is a non-uniform illuminant.

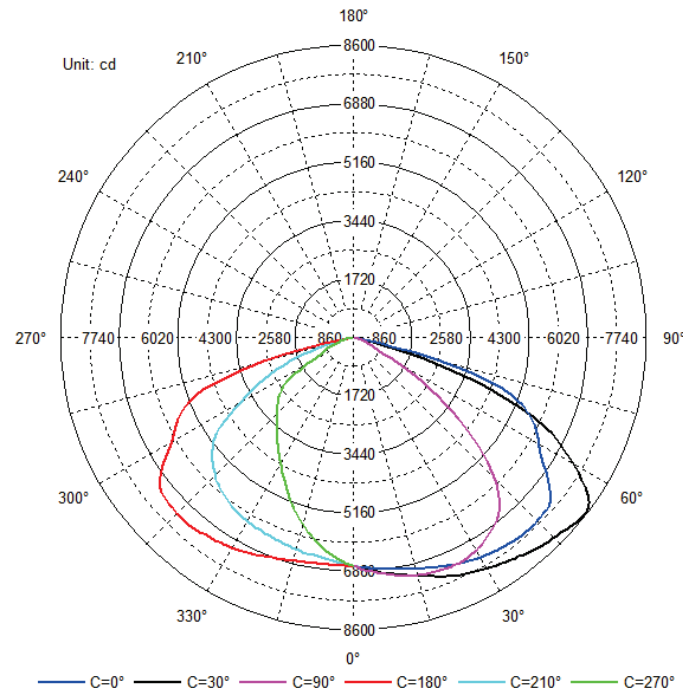


Figure 8. Light distribution curve of LED road lighting luminaire

#### 4. DISCUSSION

The luminance test results of Figure 2-4 are in good agreement with the conclusion of luminance is independent of distance. However, the luminance test requires a luminance meter. The luminance meter tests the average luminance of the measured area, and the measured area is related to the field angle and distance. The relationship between the field angle and the measured area is shown in Figure 9. The size of the measured area is proportional to the measured distance. When the measured area is larger than the size of the measured object, the luminance value is low, as shown in Figure 4 with a 3° of view angle. When the measured object is a non-uniform luminous body, and the measured area is larger than the luminous area, it often contains dark areas, resulting in low test values, and when the test direction is changed, the luminance value will change drastically, and the repeatability of the test is poor, as shown in Figure 7.

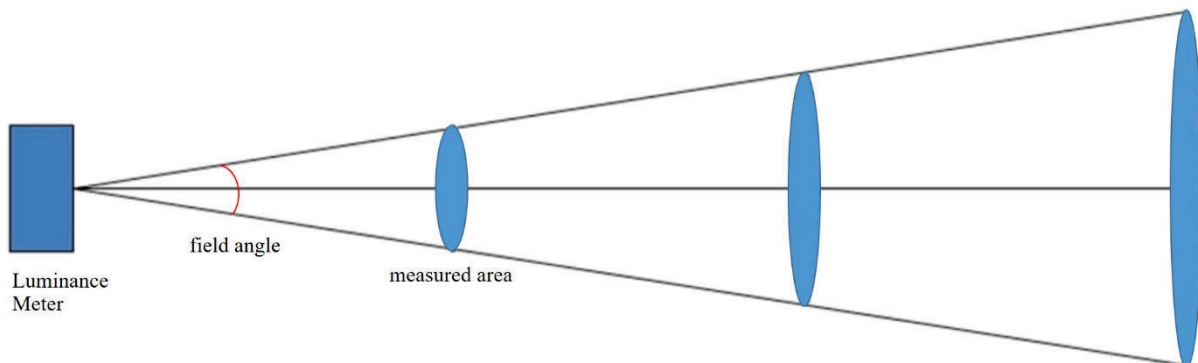


Figure 9. Schematic diagram of the relationship between the field angle and the measured area

Furthermore, compare the result between Figure 1 and Figure 4, the test results of luminance are close for uniform illuminant by spot-luminance meter and ILMD. But for non-uniform illuminant, the luminance values vary widely through Figure 6 and Figure 7 between spot-luminance meter and ILMD.

In fact, the luminance meter has  $V(\lambda)$  correction, it can only be used to measure white light, not for colour light [3]. However, brightness is the perceptual response to luminance. Though luminance is usually the most important stimulus to brightness perceptions, size, gradient, surround luminance, adaptation, and spectral composition can have important effects on brightness [4]. There is still a tremendous need for research related to the accurate measurement of luminance and accurate assessment of brightness, etc.

## REFERENCE

- [1] IEC, 2020. IEC 60050-845:2020. International Electrotechnical Vocabulary (IEV) - Part 845: Lighting [S].
- [2] Bommel W v. Road Lighting: Fundamentals, Technology and Application [M]. Switzerland: Springer International Publishing, 2015.
- [3] Bommel W v. Interior Lighting: Fundamentals, Technology and Application [M]. Switzerland: Springer International Publishing, 2019.
- [4] DiLaura D, House K, Mistrick R, et al. The Lighting Handbook: Reference and Application. 10th ed. [M]. New York: The Illuminating Engineering Society of North America, 2011.

## ACKNOWLEDGEMENT

Corresponding Author: Xiaobo Zhuang  
Affiliation: Shanghai Alpha Lighting Equipment Testing Ltd.  
e-mail :13501902696@163.com

# STUDY ON THE OPTIMIZATION OF THE CURVES THAT COMPOSE THE REFLECTOR OF A REGULAR-REFLECTION LIGHT SHELF

Ryota Higashino and Hirotaka Suzuki

(Graduate School of Engineering, Kobe University, Kobe, Japan)

## ABSTRACT

Recently, it is considered that it is important to reduce primary energy consumption in buildings. One way to do this is to use daylight. To use daylight as lighting, the author focused on a light shelf, one of the daylighting devices. This study aimed to clarify the cross-sectional shape of light shelf that can bring in a sufficient amount of light evenly into a room. In order to derive a cross-sectional shape with high daylighting performance, we focused on a reflector composed of multiple quadratic curves. A numerical program was constructed to constitute the optimal shape of the light shelf, and the performance of the derived light shelf was verified.

Keywords: light shelf, specular reflection, daylight, quadratic curves, energy conservation

## 1. INTRODUCTION

In recent years, there is a growing movement in the building sector to reduce energy consumption, and one way to do this is using daylight to save energy. Since lighting energy amount to more than 20% of an office building's total primary energy consumption[1], the use of daylight is expected to be effective. Against this background, many studies have been conducted on the development and performance verification of daylighting devices[2][3][4][5], and similar studies have been seen on light shelves, one of the lighting devices[6]. However, there are few examples of previous studies on light shelves, and there is room for performance improvement in terms of daylighting performance with the use of a method of daylighting by positive reflection.

In this study, as an effective device in terms of uniformly introducing light into a room, we proposed a regular-reflection light shelf based on a combination of quadratic curves obtained through optimization calculations, and clarified its usefulness through performance verification.

## 2. OPTIMIZATION METHODS FOR LIGHT SHELVES

### 2.1 Optimization policy

This study deals only with reflected light from direct sunlight on a light shelf installed on a window surface in a space that is assumed to be an office with a window on the south face. Assuming that the ceiling surface is a uniform diffusion surface, it is considered that the light entering the ceiling surface should be uniform in order to bring light into the room evenly. Therefore, in optimizing the device, the objective was to form a reflector shape that reflects light uniformly on the ceiling surface.

### 2.2 Optimization theory

In order to make the reflected light to the ceiling surface uniform, a reflector composed of reflective surfaces having multiple quadratic curves as cross sections was used. The number of quadratic curves constituting the cross-section of the reflector is  $n$ . In this case, the reflector is composed of a combination of reflective surfaces with  $n$  curved cross sections. When the apparent area of each reflective surface as viewed from the direction of direct sunlight irradiation is equal (Figure 1.), the number of incident rays on each reflective surface is equal. In addition, if the ceiling surface is divided into  $n$  equal parts and reflected light is incident from each reflected surface on each of the equally divided ceiling sections, as shown in Figure 1, the number of incident rays on each equally divided ceiling section is equal. In such a case, it is thought that by increasing the number of reflective surface divisions  $n$ , reflected light could be delivered to the ceiling surface uniformly. We clarified the combination of quadratic curves that would satisfy the above conditions

by finding the solution of the equation of a quadratic curve constituting a reflective surface using the Newton method, a method of convergence calculation.

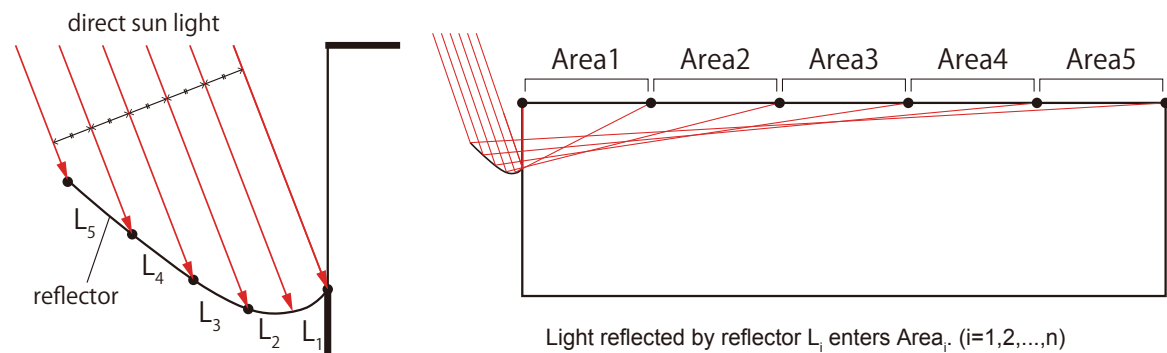


Figure 1. Optimization theory( $n=5$ )

### 3. PERFORMANCE VERIFICATION

In order to verify the light harvesting ability of the reflector of the regular reflective light shelf created using the optimization method described in Chapter 2, ray visualization images were created and the Uniformity ratio was calculated under the experimental conditions shown in Table 1 and Figure 2.

Table 1. Condition setting in verification

Location	Kobe, Japan (34.69°N, 135.20° E)
date	Sep.23(vernal equinox)
time	12:00
Solar altitude	55.33°
Solar orientation	183.61°
Profile angle	55.38°

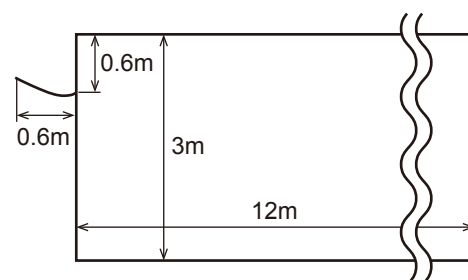
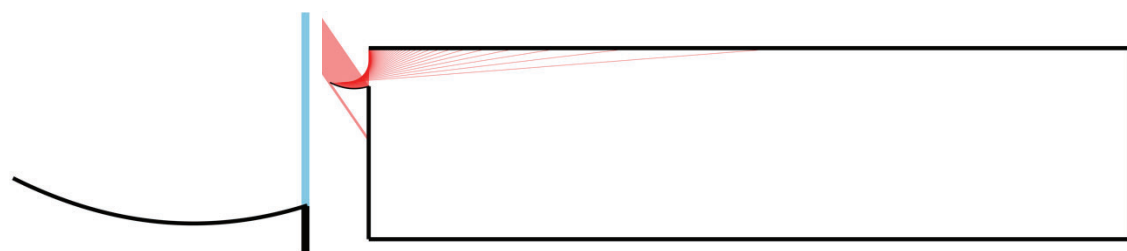


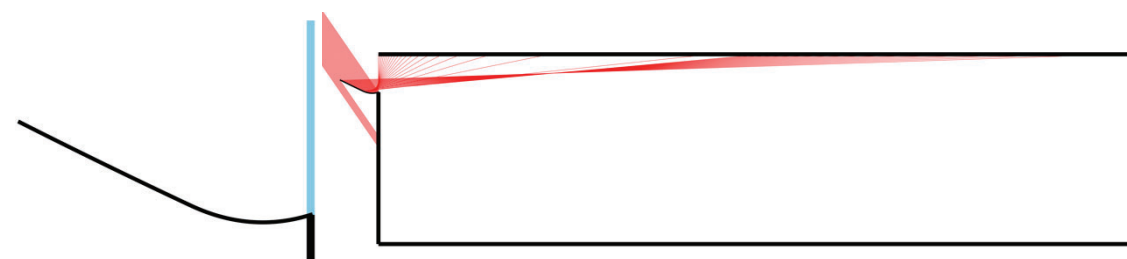
Figure 2. Target room (cross section)

#### 3.1 Ray visualization image

Figure 3 shows the reflection of direct sunlight on three patterns of light shelf reflector shapes with 1, 2, 10, 50, and 100 divisions. The number of rays was set to 50 for clarity of each ray.



(a) divisions  $n=1$



(b) divisions  $n=2$

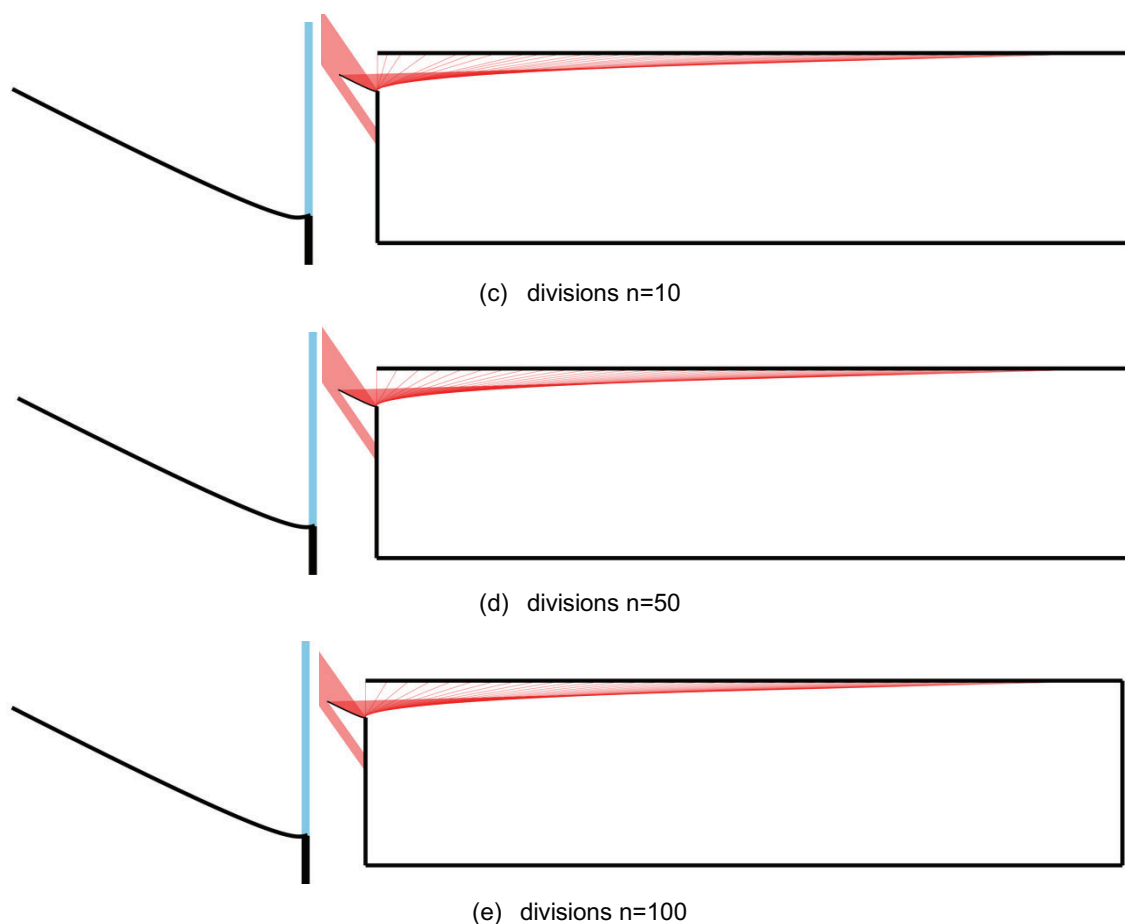


Figure 3. Ray visualization image (Upper left:  $n=2$ , Upper right:  $n=10$ , Lower left:  $n=50$ , Lower right: 100)

Comparing the reflections at each number of divisions in Figure 3, it was visually confirmed that the reflected light was not uniformly incident on the ceiling surface when the number of divisions was small, but became closer to uniform when the number of divisions was increased. If the ceiling surface is assumed to be an even diffusion surface, increasing the number of divisions is considered to uniformly brighten the room. The number of divisions 1 is the so-called parabolic column reflector shape, and with the simple shape, the reflected light illuminated only a limited area of the room. The fact that increasing the number of divisions allows the light to be reflected uniformly over a wide area indicates that the study of the reflector shape through optimization is significant.

### 3.2 Uniformity ratio of illumination

Uniformity ratio was used to quantitatively evaluate the degree of uniformity of direct sunlight reflected by a regular reflective light shelf and incident on the ceiling surface. Illuminance is the luminous flux incident on a unit area, and a ray of light can be considered a luminous flux of a certain size. Therefore, the ceiling surface was divided into 100 equal parts, and the number of incident rays on each part was considered to represent the ratio of illuminance at each ceiling surface. Using this idea, the illuminance ratio per unit area was calculated, and the uniformity ratio was calculated by (average value of illuminance) / (maximum value of illuminance). The calculation results for 8 patterns with 1, 2, 5, 10, 20, 30, 40, 50, 60, 70, 80, 90 and 100 divisions are shown in Figure 4. The number of rays was 10,000.



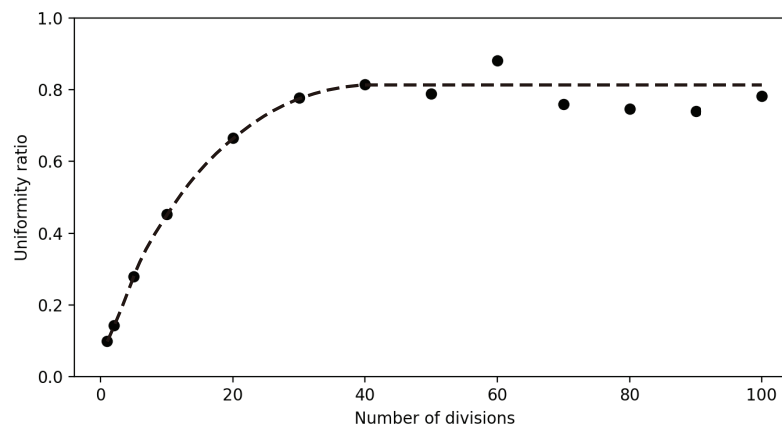


Figure 4. Uniformity ratio

Figure 4 shows that when the number of divisions is small, the uniformity ratio increases as the number of divisions increases. Besides, when the number of divisions was 40 or more, the uniformity ratio remained around 0.8. Since the method of convergence calculation was used in the optimization calculation, the obtained solution is an approximate solution, and it is thought that errors against the true value may have occurred. However, if this is taken into consideration, it is considered that the uniformity ratio increases as the number of divisions increases, and converge to about 0.8 eventually. Therefore, it can be said that the number of divisions for practical use is about 40, which is sufficient to ensure uniformity.

#### 4. CONCLUSION

It has been confirmed that a regular-reflection light shelf, which is based on a combination of quadratic curves obtained through numerical calculations, can bring light into a room evenly. Besides, by quantifying the change in uniformity ratio with the number of divisions, we were able to identify the number of divisions that would result in sufficient uniformity ratio. In the future, in addition to clarifying what the actual working surface illuminance will be, how to cope with changes in the position of the sun depending on the time of day and the season will be an issue to be addressed.

#### REFERENCES

- [1] Ministry of Economy, Trade and Industry (2021) 2018 Publicity and research project on electricity supply and demand measures.
- [2] Yusuke, T. & Hirotaka, S. Geometric feature of a structure composed of concave and convex parabolic mirrors. *Journal for geometry and graphics*, 2019, 23(2), 235-244
- [3] Yusuke, T. & Hirotaka, S. Combination of concave and convex paraboloids: Theoretical model of new-type daylighting system. *Journal of science and technology in lighting* 2021,45,22-27
- [4] Marina, I. & Hikaru, K. Development of transparent nonimaging daylighting device using refraction and total reflection. *journal of environmental engineering*, 2018,83(747),435-441
- [5] Maki, I., Kazuyoshi, H., Taisuke, O., Takafumi, K., Tomoo, K. & Etsuko, M., Studies on demonstrations and evaluations of urban ZEB: Part4 Outline and field measurement results of lighting system with daylighting device
- [6] Heangwoo, L., janghoo, S. & Chang-ho, C., Preliminary study on the performance evaluation of a light shelf based on reflector curvature. *MDPI Energies* 2019,12(22),4295

Corresponding Author Name: Ryota Higashino

Affiliation: Graduate School of Engineering, Kobe University

e-mail: 228t041t@stu.kobe-u.ac.jp

## **A study on crystal lighting for transparent display using PET film**

Sang-hoon Lee, Yeon-ho Yang\*

Glow One Co., Ltd.

Seoul, Korea

### **ABSTRACT**

The downside of crystal lighting is that crystal lighting is expensive. Also, crystal lights are heavy because they are made of glass. And it's fragile, and it's also dangerous. Moreover, difficulty in cleaning is also a major drawback of crystal lighting. The glare of crystal lamps affects children's eyesight.

In order to solve this problem, we researched and developed a product that can create a crystal lighting effect using a transparent display. The transparent display uses PET (Poly Ethylene Terephthalate) film, which has excellent heat resistance and transparency, and develops a module combined with LED parts using a material with printing and adhesiveness to emit light. you can feel the effect

It has been confirmed that the transparent display using PET film eliminates the disadvantages of crystal lighting, can feel the effect of crystal lighting several times, and is competitive in terms of product design diversification, safety and price.

Keywords: PET film, Transparent display, Crystal lighting, LED, Silicon

### **1. INTRODUCTION**

Crystal lighting is a lighting product made using precious crystal material known for its luxury and beauty. Crystal is a transparent material similar to glass that has been developed. When it passes through a light source, it reflects, refracts, and scatters light to give off a beautiful light. Because of these characteristics, crystal lighting shoots colorful light into the space, creating a luxurious and sophisticated atmosphere.

The price is relatively high because it requires expensive materials and manufacturing processes, and it is fragile and dangerous because it is partially implemented with glass to realize luxury.

In order to solve these problems, after identifying the problems of the existing technology, we grafted a new technology. In the prior art, since the surface of the coating layer has a smooth flat or curved surface, the direction of light transmitted through the coating layer is constant and the light reflected on the surface of the coating layer tends to be reflected at a certain angle. That is, in the prior art LED lighting device, the light generated from the plurality of LED elements was scattered or diffused in a very small degree in the process of being transmitted through or reflected through the coating layer. Therefore, the prior art LED lighting device can exhibit aesthetic effects and crystal effects in addition to illuminating the surroundings because light is emitted in a certain direction from the light emitting part and there is no intensity variation of each light, like a commonly seen LED light. couldn't

## **2. BODY**

Research and development was conducted to solve these problems. The LED lighting device is a transparent printed circuit board, a plurality of LED elements mounted on the transparent printed circuit board and transparent, formed on the outer surface of each of the plurality of LED elements and the transparent printed circuit board, and generated from the plurality of LED elements. and an amorphous coating layer configured to diffusely reflect at a plurality of angles while passing or reflecting light.

The amorphous coating layer may be configured to cause scattered reflection by hitting the uneven surface of the portion coated with the plurality of LED elements. The amorphous coating layer may be configured to cause scattered reflection by hitting the uneven surface of the portion covering the plurality of LED elements. The transparent printed circuit board may include a flexible material, and the transparent printed circuit board may include a curved structure. The transparent printed circuit board may include a cylindrical structure in which a body is bent such that one end and the other end meet each other. LED elements may be arranged in longitudinal and transverse directions along the inner surface of the cylindrical structure of the transparent printed circuit board. The irregular coating layer may be formed by applying a spray to the surface of each of the transparent printed circuit board and the plurality of LED elements.

As an effect of research and development, the LED lighting device is transparent, formed on the outer surface of each of the plurality of LED elements and the transparent printed circuit board, and diffused reflection at a plurality of angles as the light generated from the plurality of LED elements passes or is reflected. By including an amorphous coating layer configured to be formed, the light of the LED element scattered and diffusely reflected by the amorphous coating shines as if a crystal shines, providing a user with a beautiful aesthetic experience.

In the transparent printed circuit board, at least two or more LED elements are surface mounted. The transparent printed circuit board may include a transparent material. The transparent printed circuit board may include a flexible (flexible) film or sheet. For example, the transparent printed circuit board may include a transparent sheet. For example, the transparent printed circuit board may include a sheet using Poly Ethylene

Terephthalate (PET) or Polyimide (PI) resin. Power lines and signal lines are formed in a pattern on the surface of the transparent printed circuit board. The signal line may be configured to transmit an electric signal for adjusting light emission color and intensity of light to a plurality of LED elements. The power line may be configured to supply power to a plurality of LED elements. For example, the signal line and the power line may include any one or more of an alloy, a carbon structure, and a conductive polymer. For example, signal lines and power lines may include copper or silver (Ag).

The LED device includes at least one light emitting diode chip (114) and an IC chip that controls light emission of the light emitting diode chip. The IC chip is configured to individually control the amount of current supplied to the light emitting diode chips to control the color coordinates and beam angle, thereby controlling the light emitting diode chips having different colors so that the LED element emits not only white light but also various colors. can The IC chip is mounted on a transparent printed circuit board. For example, the LED device may be an RGB LED Package or a White LED Package (warm type or cool type). The light emitting diode chip may include at least one of a red light emitting diode chip, a green light emitting diode chip, and a blue light emitting diode chip. Light emission of the light emitting diode chip may be controlled by an IC chip.

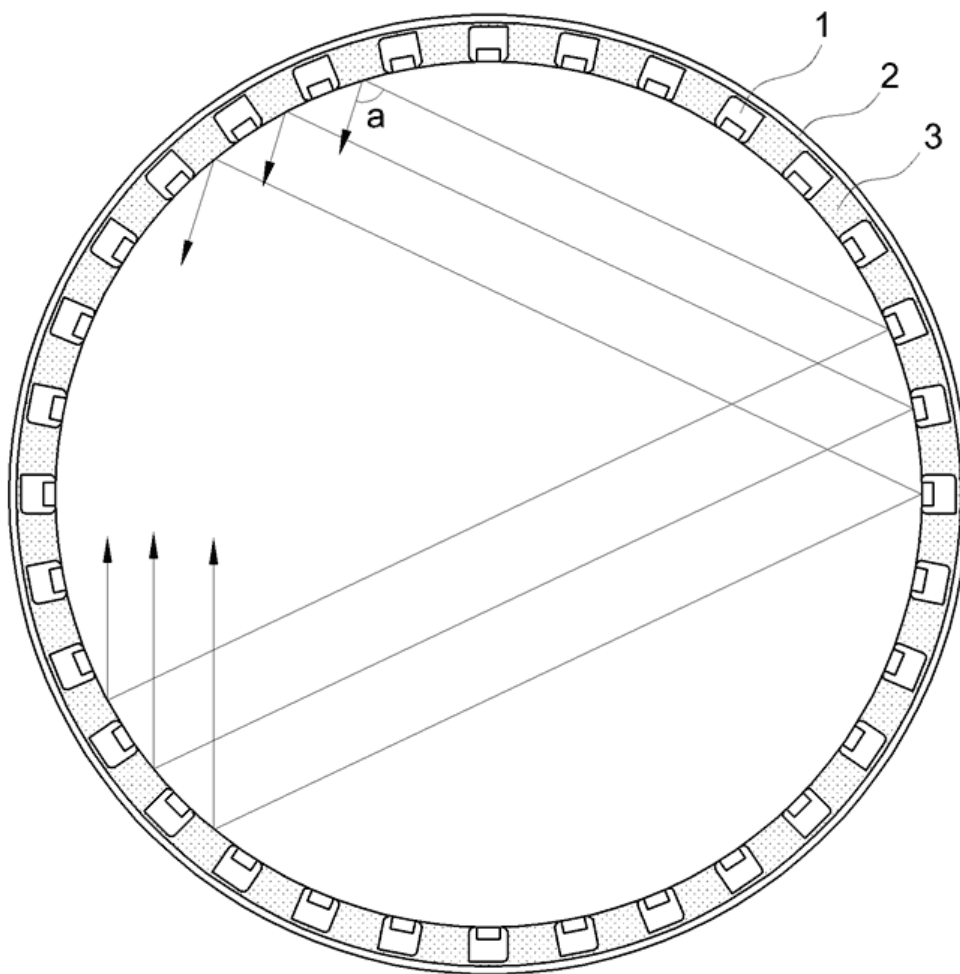


Figure 1. Existing horizontal section

1; LED element, 2; printed circuit board, 3; coating layer



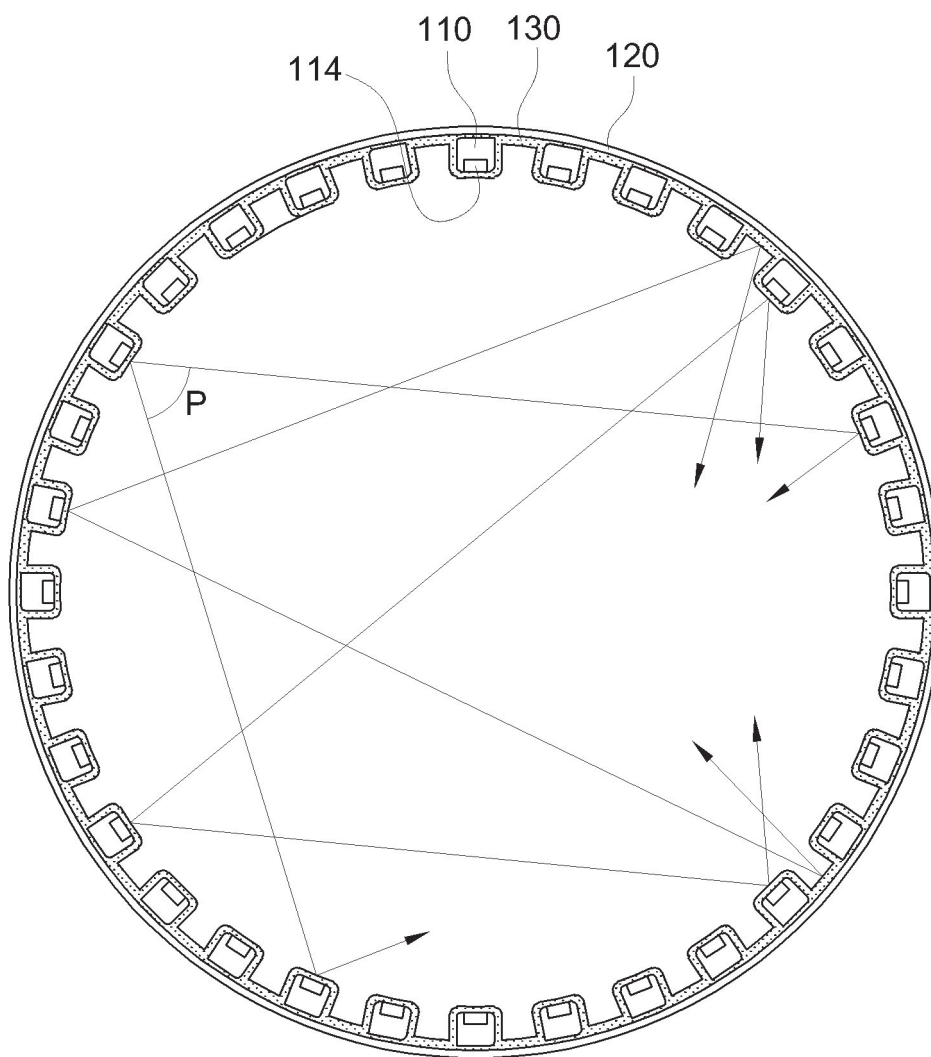


Figure 2. New horizontal section

110; LED element, 120; printed circuit board, 130; irregular coating layer 114; light emitting diode chip

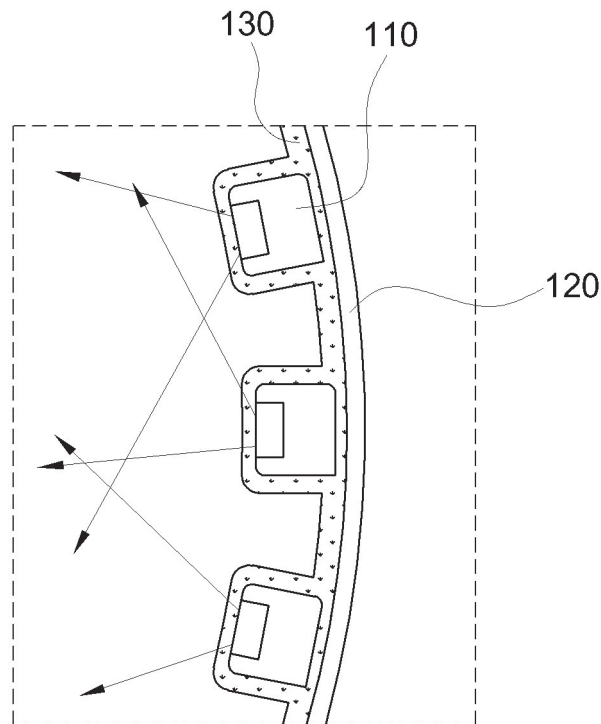


Figure 3. New partial enlarged cross section

It is a horizontal cross-sectional view schematically showing the appearance of some components of the LED lighting device. It is a partial cross-sectional view schematically showing the appearance of some components of the LED lighting device with a partial area enlarged.

The amorphous coating layer (130) is transparent. The irregular coating layer may be formed on outer surfaces of each of the plurality of LED elements (110) and the transparent printed circuit board (120). In addition, the amorphous coating layer may be configured such that light generated from a plurality of LED devices is scattered or diffusely reflected. That is, when light passes through the irregular coating layer, the light may be dispersed (scattered) at various angles  $P$ . In addition, the amorphous coating layer may be configured to cause scattered reflection by hitting the uneven surface of the portion coated with the plurality of LED elements.

For example, after passing through an irregular coating layer generated by one of a plurality of LED elements, when the passing light is reflected on the uneven surface of the irregular coating layer coated on another LED element located on the opposite side, that The reflected reflection angle may not be constant for each surface position (point) where the reflection is reflected.

Here, the irregular coating layer is a coating layer having an uneven thickness and a bumpy surface in which the height of the coating layer is different depending on the outer surface of a metal pattern mounted on the surface of a transparent printed circuit board or a plurality of LED elements. For example, the irregular coating layer may be formed by applying a spray to the surface of each of the transparent printed circuit board and the plurality of LED elements.

Therefore, the LED lighting device of the present disclosure includes a transparent amorphous coating layer formed on the outer surface of each of the plurality of LED elements and the transparent printed circuit board and configured to diffusely reflect at a plurality of angles while passing or reflecting light generated from the plurality of LED elements. By doing so, the light of the LED element scattered and diffusely reflected by the amorphous coating shines like a shining crystal, providing a beautiful aesthetic experience to the user.

### **3. Conclusion**

The transparent printed circuit board may include a flexible (flexible) material. The transparent printed circuit board may include a curved structure. For example, the transparent printed circuit board may include a cylindrical structure in which a body is bent so that one end and the other end meet each other.

Therefore, the LED lighting device includes a transparent printed circuit board having a curved structure or a cylindrical structure, so that light generated from each of a plurality of LED elements is coated on an adjacent LED element or an opposite LED element facing each other. Since it can be diffusely reflected or scattered, it is possible to maximize the diffused reflection or scattering of light, so that the lighting device can shine like a crystal by emitting light having different light intensities.



Figure 4. Crystal lighting

## REFERENCE

(1) Korean Intellectual Property Office Publication No. 2016-0092761

## ACKNOWLEDGEMENT

This work was supported by the Korea Evaluation Institute of Industrial Technology (KEIT) and the Ministry of Trade, Industry & Energy (MOTIE) of the Republic of Korea (No.20018805).

Author Name: Yeon-ho Yang

Affiliation: Glow One Co., Ltd. laboratory

Email: yhyang04@glowone.com

# **MANUFACTURING AND EVALUATION OF POLYTOPE TENSEDRITY LAMPSHADE -PRACTICAL APPLICATION AND FABRICATION OF LAMPSHADE METHOD BASED ON DODECAHEDRAL SUPER PRISM AND ANTIPRISM**

Anqi Duan and Hirotaka Suzuki  
Kobe University

## **ABSTRACT**

The purpose of this paper is to explore the use of dodecahedron as the base cell super prisms and anti-prisms to produce innovative lampshade models. According to previous studies, lampshade design can be performed by projecting high-dimensional shapes in three-dimensional space, and there is a more complete study on the fabrication of lamps with hypercube. Based on the study of hypercube, super prisms with dodecahedron have also been proposed. In contrast, an anti-prism formed by twisting the prism without projection has also been proposed to be used for lampshade. In this paper, we have tried to make lampshades in the form of both super-prisms and anti-prisms based on the existing research results. The results show that the dodecahedron super-prism and anti-prism structures can provide unique and exquisite lampshade designs and provide excellent results for interior lighting. This study provides new ideas and methods for innovation in the field of lampshade design and provides a practical reference for the design and fabrication of geometry-based decorative elements.

Keyword: lampshade design, super prism, anti-prism, lampshade making, polytope

## **1. INTRODUCTION**

This paper is a description of the method and process of lampshade fabrication, which explores not only the feasibility of the existing design but also how to fabricate it by properly selecting the appropriate materials and ensuring the stability of the structure. In this paper, the lampshade is based on a super prism based on a hyper-dimensional figure projected into three-dimensional space as proposed by Suzuki <sup>[1]</sup>, with a dodecahedron as the base cell as shown in Fig. 1. Also this paper tries the method of lampshade design based on the anti-prism.



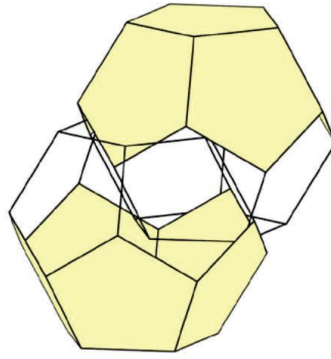


Fig1. Axonometric projection of super prism with a dodecahedron as a base cell

The purpose of this paper is to try to make a model of the lampshade based on the available research results, taking into account the plasticity and weight of the materials used to reduce the difficulty of making the structure of the lampshade, without focusing on the light transmission. Choose materials that can be easily processed and shaped to achieve the desired shape and structure of the design. Soft plastic or elastic materials may be more suitable for some complex shapes of lamps. After comprehensive consideration, it was decided to use thin strips of wood that are easy to cut as the main material. The nodes and other joints between the strips are fixed with tape, which can get a more stable structure and easier to make than using glue. Thin wires are used to connect the cells to each other.

## 2. MAKING THE SUPER PRISM LAMPSHADE

First, determine the size of the lampshade model. The size of a dodecahedron unit is about the size of a hand, so the side length of the dodecahedron is assumed to be 3 cm. For the sake of stability and ease of production, the dodecahedron can be disassembled into twelve pentagons and then the pentagons can be combined to form the dodecahedron.

Based on Suzuki's 3D drawing, the thin strips of wood were cut to a length of 3cm and wrapped with tape to connect the five strips at the end. As the tape is malleable, it can be bent to form a pentagon, and the tape is wrapped around the final node to secure it. After the pentagon has been made, the sides of the pentagon are secured with tape wrapped around the edges, and the two pentagons together form one edge of the dodecahedron, making the structure more stable. However, when carrying out the assembly, it is necessary to take into account the part of the two dodecahedron where the crossover takes place. The top corner of one dodecahedron and the bottom corner of the other dodecahedron cross into each other, at which point three sides of each of the two dodecahedron cross the edge of the other unit, so these six sides need to be eliminated. The two crossed dodecahedron frames are shown in Fig 2.

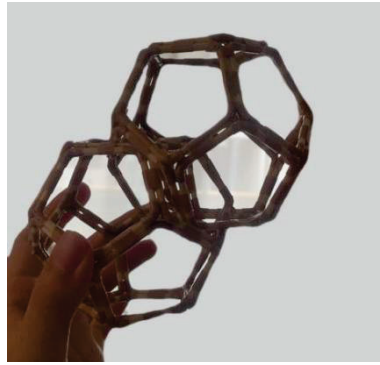


Fig 2. The photos of the two dodecahedron base cell

### 3. STABILITY OF THE SUPER PRISM LAMPSHADE

Once the dodecahedron has been assembled, the desired shape of the lampshade and the position of the light bulb are the factors to be considered for fixing the two cells to each other. According to the tension structure of the hypercube proposed by Suzuki<sup>[2]</sup> in 2021, a thin wire was chosen as the tension material to connect the two intersecting cells in order for the lampshade to produce a levitating effect. In addition, even if the two dodecahedron intersect, a tension material must suspend the lower end point of the upper member to the upper end point of the lower member. Structural stability and the distribution of the center of gravity of the lampshade should be considered when joining. In order to ensure the stability of two dodecahedron in horizontal and vertical directions, the lower end point of the upper member is first suspended on the upper end point of the lower member to connect the two apexes that produce intersection, and then four groups of points with equal distance and corresponding to each other are selected for connection according to the structural stability.

Center of gravity is the center of gravity or balance point of the object relative to the fulcrum. A balanced design of a lampshade can be achieved by properly distributing the location of elements, materials and components within the lampshade. This helps to reduce the risk of tilting, falling or instability. Depending on the shape and material of the lampshade, the location of the center of gravity needs to be determined. By adding weight blocks to the bottom-most position of the Super Prism, the position of the center of gravity can be adjusted to improve the lampshade's stability. By properly distributing the center of gravity and considering how the lampshade is supported, you can ensure that the lampshade is stable and reliable during use and reduce the risk of tilting or instability. The completed super prism is shown in Fig 3.

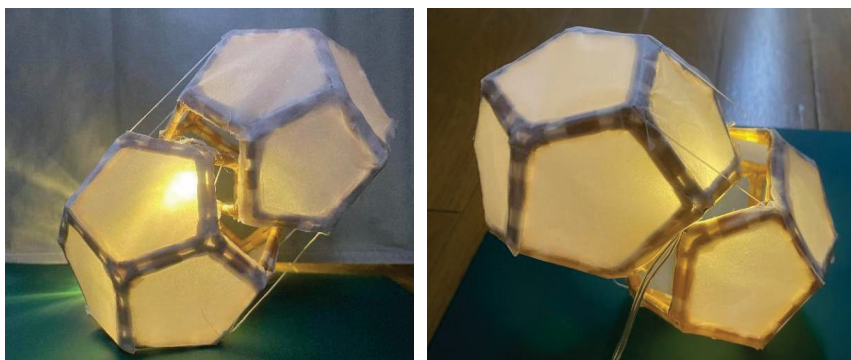


Fig 3. The photos of the lampshade Super prism with a dodecahedron as a base cell  
(Left: front view, Right: Oblique top view)

#### 4. MAKING THE ANTIPRISM LAMPSHADE

The antiprism column is formed based on a normal square transformed by rotating the top surface of the square by forty-five degrees and connecting each vertex on the top surface to the corresponding vertex on the bottom surface, an octahedral antiprism column. As shown in Fig 4, the bottom and top surfaces of the antagonistic column are squares with a side length of 5 cm, and the connecting surface has a side length of 10 cm, forming six isosceles triangles.

The focus of the production of the antiprism column is to consider the connection of the nodes, to find the appropriate node connection method instead of using the same graphic combination method as the production of dodecahedron can get a more lightweight structure.

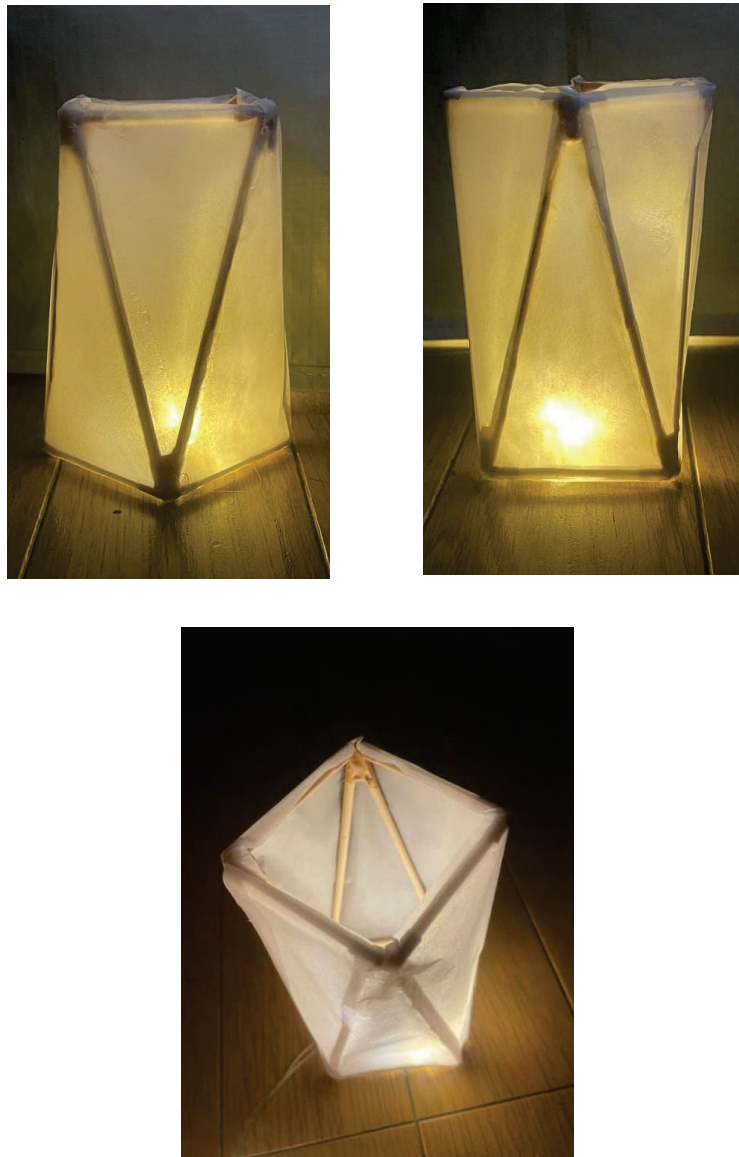


Fig.4 The photos of the lampshade antiprism (Above: Side view, Below: Oblique top view)

## **5. CONCLUSION**

In summary, the creation of lampshades based on three-dimensional shapes is an innovative and interesting approach to design, combining geometry and spatiality with lighting effects to create unique and artistic lampshades. This approach is based on the understanding and application of three-dimensional shapes and brings more creativity and expressiveness to lampshade design.

## **6. REFERENCE**

- [1] Hirotaka SUZUKI. Lampshade Design That Takes Advantage Of The Shape Derived From High-dimensional Polytopes. Making Good Use Of Super Prism And Rotation Of Polytopes, Proc. of the Asia Light-ing Conference 2020
- [2] Hirotaka SUZUKI. The Lampshade Design Making Use Of Geometric Forms: The Lampshade Form Based On four Dimnsional Polytope with Tensegrity Structure, Revista Brasileira de Expressão Gráfica, Vol. 9, No. 2, 2021, ISSN 2318-7492

## **ACKNOWLEDGEMENTS**

Corresponding Author Name: Anqi Duan

Affiliation: Kobe University

e-mail: duananqi1223@163.com

# EFFECTS OF TASTE-ASSOCIATED COLORS ON TASTE THRESHOLDS

**Takuma Hashimoto and Hiroshi Takahashi**  
**(Kanagawa Institute of Technology, Atsugi, Japan)**

## ABSTRACT

The purpose of the present study was to investigate the colors associated with sweet, salty, sour, and bitter tastes, and to determine the taste thresholds under light of the associated colors. We defined the threshold for perceiving taste as the detection threshold and the threshold for recognizing taste as the recognition threshold and investigated the thresholds for each subject. For physiological assessments, stress indices under colored light were measured using electrocardiograms. The results indicate that both detection and recognition thresholds were lower under colored light associated with sweetness than under colored light associated with other tastes.

Keywords: Taste, Cross-modal perception, Chromatic light

## 1. INTRODUCTION

Meals should not only provide the required nutrition, but also taste good. Taste is determined by various characteristics related to the food (e.g., appearance, smell, texture, mouthfeel, and flavor) and eating (e.g., psychological, physiological, innate, acquired, and environmental factors). The modulation of one sense by another is called cross-modal perception, and vision (appearance) has been shown to influence taste (flavor), even in eating. It has been reported that humans associate sweetness with high brightness of red and red-purple, saltiness with high brightness of blue and white, sourness with high brightness and high saturation of yellow, and bitterness with low brightness of green and yellowish green. However, the relationships between the light colors associated with such tastes and taste thresholds have not been clarified. The purpose of the present study was to investigate the influence of light color on taste thresholds.

## 2. EXPERIMENT

even male subjects in their 20s participated in the experiment. We investigated the subjects' associations of four colors with each of sweet, salty, sour, and bitter tastes, and conducted taste threshold measurements for each of these tastes. To reduce individual differences due to physiological conditions, certain restrictions were placed on how subjects spent the day before and the day of the experiment.



The restricted contents were as follows:

[The day before]

- Sleep for more than 6 hours
- Avoid strenuous exercise
- Do not consume alcohol

[The day]

- Lunch at least 1 hour before the experiment
- Avoid stimulant foods

Saliva is responsible for dissolving taste substances and transporting them to the taste buds, and its secretion can be affected by changes in psychological conditions due to stress. Therefore, stress indices were measured from electrocardiograms, which were recorded using electrodes attached to both wrists. From electrocardiogram (ECG) data, which were recorded throughout the experiments, low-frequency/high-frequency (LF/HF) values, which act as sympathetic nervous function indicators, were extracted. Figure 1 shows the experimental environment. Taste presentations were ordered from lowest concentration based on interaction level, and subjects were instructed to write "X" if they could not identify the taste, " $\triangle$ " if they could detect the taste even if they could not identify the type, and the actual name of the taste if they could identify it. The detection threshold was defined as the point at which the presence of any taste could be identified, and the recognition threshold was defined as the point at which a specific taste could be identified. The solutions with the different tastes were presented in a specific order to account for taste interactions, i.e., the contrast and inhibitory effects. Table 1 shows the taste solution concentrations.

The experimental procedure was as follows:

1. Subjects were given 10 minutes to acclimatize to chromatic lighting conditions.
2. Electrocardiogram measurements were taken after color adaptation.
3. Taste threshold measurements were then performed.

Steps 1 to 3 were repeated for each light color, which was selected randomly to avoid creating an order effect.



Figure 1. Experimental environment

Table 1. Taste solution concentration [%]

	sweetness	saltiness	sourness	bitterness
<b>1</b>	0.05	0.025	0.001	0.0001
<b>2</b>	0.1	0.05	0.002	0.0002
<b>3</b>	0.15	0.075	0.004	0.0003
<b>4</b>	0.2	0.1	0.006	0.0004
<b>5</b>	0.25	0.15	0.007	0.0005
<b>6</b>	0.3	0.2	0.008	0.0006
<b>7</b>	0.35	0.25	0.009	0.0007
<b>8</b>	0.4	0.3	0.01	0.0008
<b>9</b>	0.45	0.35	0.0125	0.0009
<b>10</b>	0.5	0.4	0.015	0.001
<b>11</b>	0.55	0.45	0.0175	0.0015
<b>12</b>	0.6	0.5	0.02	0.002
<b>13</b>	0.65	0.55	0.0225	0.0025
<b>14</b>	0.7	0.6	0.025	0.003
<b>15</b>	0.75	0.65	0.0275	0.0035
<b>16</b>	0.8	0.7	0.03	0.004

### 3. RESULTS

In the present experiment, sweetness was associated with high-brightness red, saltiness with white, sourness with yellow, bitterness with low-brightness green. Figure 2 shows the experimental results of taste threshold. Colors associated with sweetness are defined as Sweet Color, colors associated with saltiness as Salty Color, colors associated with sourness as Sourness Color, colors associated with bitterness as Bitter Color, and colors associated with other tastes as Other Colors. The taste threshold results indicated that for sweet tastes, the taste sensitivity was higher when the Sweet Color. On the contrary, for bitter tastes, the taste sensitivity was lower when the Bitter Color. No significant differences in taste threshold were observed for any of the tastes. Figure 3 shows the relationship between recognition threshold and stress indices. The results for the taste threshold and stress index indicated that for sourness, taste sensitivity decreased with increasing stress index. On the other hand for saltiness, where taste sensitivity increased as the stress index increased.

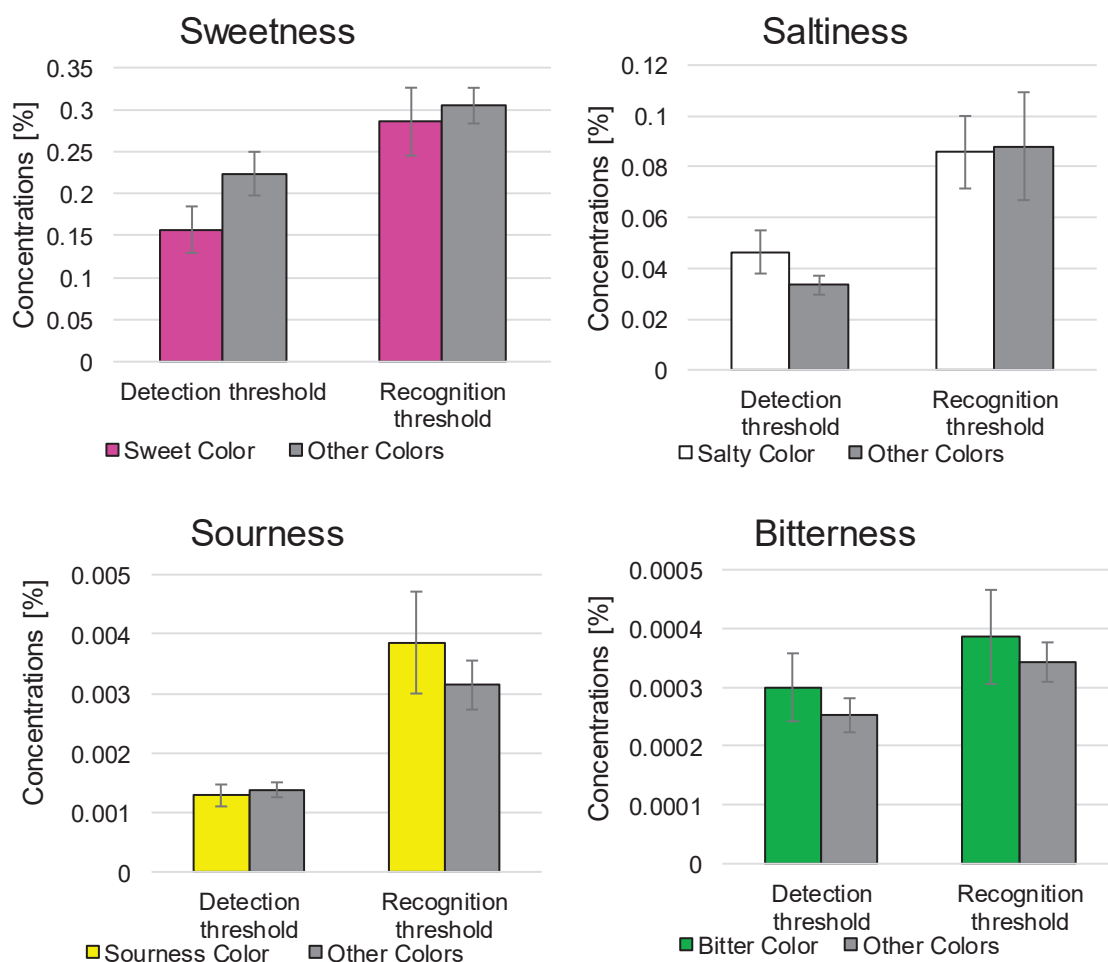


Figure 2. Taste threshold Average

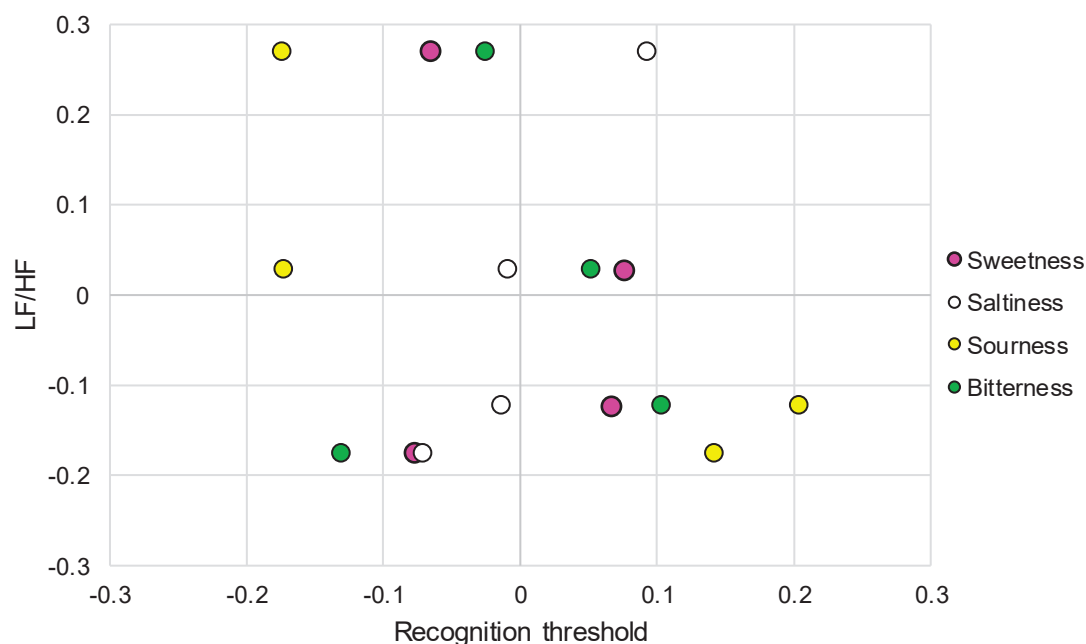


Figure 3. recognition threshold and stress indices

## REFERENCE

- [1] Yuko,K., Koko,S. and Sigeko,S., Association of tastes with colors and foods, Journal of Human and Living Environment, 2018, 25(2), 125-134
- [2] Noriko,H., Taste Interrelationships (Part1): Relationship between Saltiness and Sweetness, Journal of home economics of Japan, 1969, 20(1), 19-23
- [3] Noriko,H., Taste Interrelationships (Part2): Relationship between Saltiness and Sourness, Journal of home economics of Japan, 1976, 27(4), 255-261
- [4] Noriko,H., Taste Interrelationships (Part3): Relationship between Saltiness and Bitterness, Journal of home economics of Japan, 1977, 28(4), 278-281
- [5] Noriko,H., Taste Interrelationships (Part4): Relationship between Sweetness and Sourness, Journal of home economics of Japan, 1977, 28(4), 282-286
- [6] Noriko,H., Taste Interrelationships (Part5): Relationship between Saltiness and Bitterness, Journal of home economics of Japan, 1981, 32(2), 156-161
- [7] Noriko,H., Taste Interrelationships (Part6): Relationship between Sourness and Bitterness, Journal of home economics of Japan, 1981, 32(3), 241-245

Corresponding Author: Takuma Hashimoto

Affiliation: Kanagawa Institute of Technology

email: s2382012@kait.jp

# EFFECTS OF TASTE-ASSOCIATED COLORS ON TASTE THRESHOLDS

**Takuma Hashimoto and Hiroshi Takahashi**  
**(Kanagawa Institute of Technology, Atsugi, Japan)**

## ABSTRACT

The purpose of the present study was to investigate the colors associated with sweet, salty, sour, and bitter tastes, and to determine the taste thresholds under light of the associated colors. We defined the threshold for perceiving taste as the detection threshold and the threshold for recognizing taste as the recognition threshold and investigated the thresholds for each subject. For physiological assessments, stress indices under colored light were measured using electrocardiograms. The results indicate that both detection and recognition thresholds were lower under colored light associated with sweetness than under colored light associated with other tastes.

Keywords: Taste, Cross-modal perception, Chromatic light

## 1. INTRODUCTION

Meals should not only provide the required nutrition, but also taste good. Taste is determined by various characteristics related to the food (e.g., appearance, smell, texture, mouthfeel, and flavor) and eating (e.g., psychological, physiological, innate, acquired, and environmental factors). The modulation of one sense by another is called cross-modal perception, and vision (appearance) has been shown to influence taste (flavor), even in eating. It has been reported that humans associate sweetness with high brightness of red and red-purple, saltiness with high brightness of blue and white, sourness with high brightness and high saturation of yellow, and bitterness with low brightness of green and yellowish green. However, the relationships between the light colors associated with such tastes and taste thresholds have not been clarified. The purpose of the present study was to investigate the influence of light color on taste thresholds.

## 2. EXPERIMENT

even male subjects in their 20s participated in the experiment. We investigated the subjects' associations of four colors with each of sweet, salty, sour, and bitter tastes, and conducted taste threshold measurements for each of these tastes. To reduce individual differences due to physiological conditions, certain restrictions were placed on how subjects spent the day before and the day of the experiment.



The restricted contents were as follows:

[The day before]

- Sleep for more than 6 hours
- Avoid strenuous exercise
- Do not consume alcohol

[The day]

- Lunch at least 1 hour before the experiment
- Avoid stimulant foods

Saliva is responsible for dissolving taste substances and transporting them to the taste buds, and its secretion can be affected by changes in psychological conditions due to stress. Therefore, stress indices were measured from electrocardiograms, which were recorded using electrodes attached to both wrists. From electrocardiogram (ECG) data, which were recorded throughout the experiments, low-frequency/high-frequency (LF/HF) values, which act as sympathetic nervous function indicators, were extracted. Figure 1 shows the experimental environment. Taste presentations were ordered from lowest concentration based on interaction level, and subjects were instructed to write "X" if they could not identify the taste, " $\triangle$ " if they could detect the taste even if they could not identify the type, and the actual name of the taste if they could identify it. The detection threshold was defined as the point at which the presence of any taste could be identified, and the recognition threshold was defined as the point at which a specific taste could be identified. The solutions with the different tastes were presented in a specific order to account for taste interactions, i.e., the contrast and inhibitory effects. Table 1 shows the taste solution concentrations.

The experimental procedure was as follows:

1. Subjects were given 10 minutes to acclimatize to chromatic lighting conditions.
2. Electrocardiogram measurements were taken after color adaptation.
3. Taste threshold measurements were then performed.

Steps 1 to 3 were repeated for each light color, which was selected randomly to avoid creating an order effect.



Figure 1. Experimental environment

Table 1. Taste solution concentration [%]

	sweetness	saltiness	sourness	bitterness
<b>1</b>	0.05	0.025	0.001	0.0001
<b>2</b>	0.1	0.05	0.002	0.0002
<b>3</b>	0.15	0.075	0.004	0.0003
<b>4</b>	0.2	0.1	0.006	0.0004
<b>5</b>	0.25	0.15	0.007	0.0005
<b>6</b>	0.3	0.2	0.008	0.0006
<b>7</b>	0.35	0.25	0.009	0.0007
<b>8</b>	0.4	0.3	0.01	0.0008
<b>9</b>	0.45	0.35	0.0125	0.0009
<b>10</b>	0.5	0.4	0.015	0.001
<b>11</b>	0.55	0.45	0.0175	0.0015
<b>12</b>	0.6	0.5	0.02	0.002
<b>13</b>	0.65	0.55	0.0225	0.0025
<b>14</b>	0.7	0.6	0.025	0.003
<b>15</b>	0.75	0.65	0.0275	0.0035
<b>16</b>	0.8	0.7	0.03	0.004

### 3. RESULTS

In the present experiment, sweetness was associated with high-brightness red, saltiness with white, sourness with yellow, bitterness with low-brightness green. Figure 2 shows the experimental results of taste threshold. Colors associated with sweetness are defined as Sweet Color, colors associated with saltiness as Salty Color, colors associated with sourness as Sourness Color, colors associated with bitterness as Bitter Color, and colors associated with other tastes as Other Colors. The taste threshold results indicated that for sweet tastes, the taste sensitivity was higher when the Sweet Color. On the contrary, for bitter tastes, the taste sensitivity was lower when the Bitter Color. No significant differences in taste threshold were observed for any of the tastes. Figure 3 shows the relationship between recognition threshold and stress indices. The results for the taste threshold and stress index indicated that for sourness, taste sensitivity decreased with increasing stress index. On the other hand for saltiness, where taste sensitivity increased as the stress index increased.

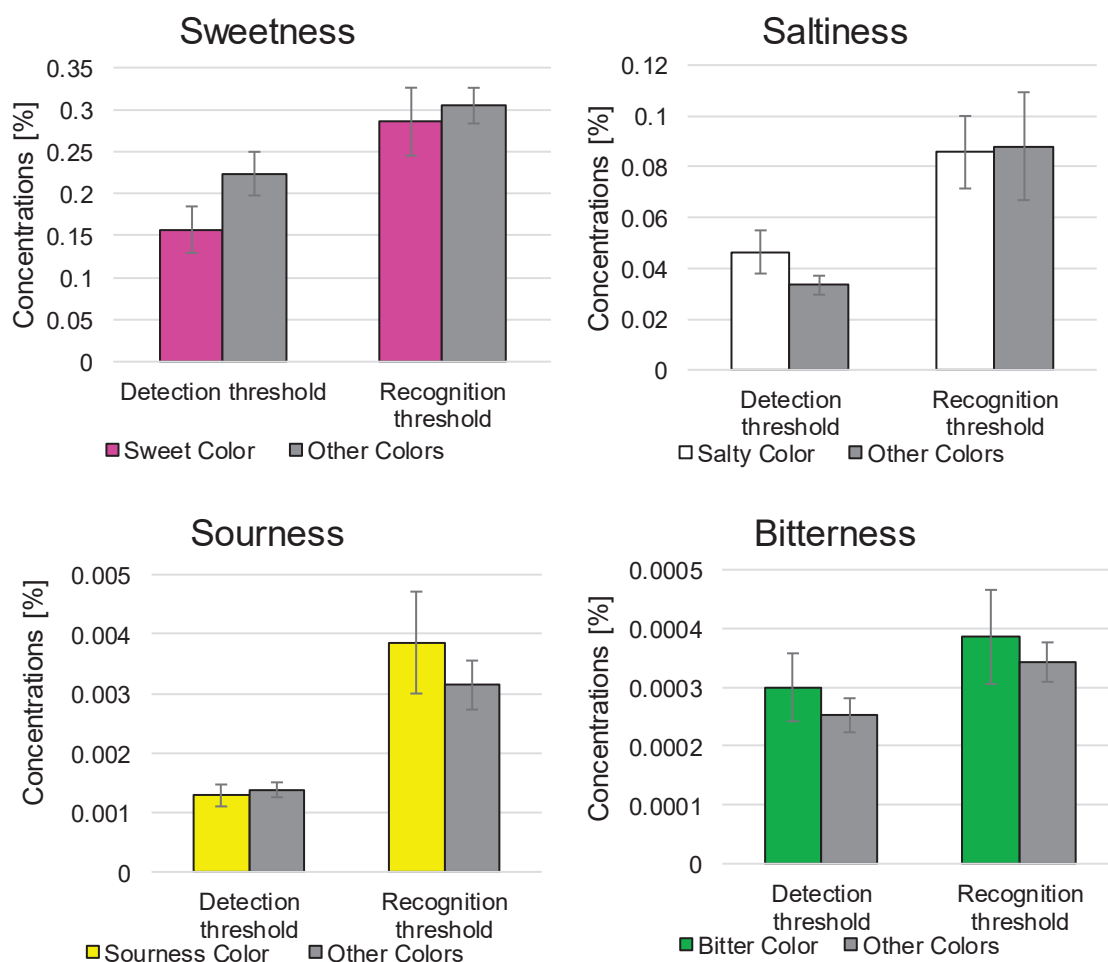


Figure 2. Taste threshold Average

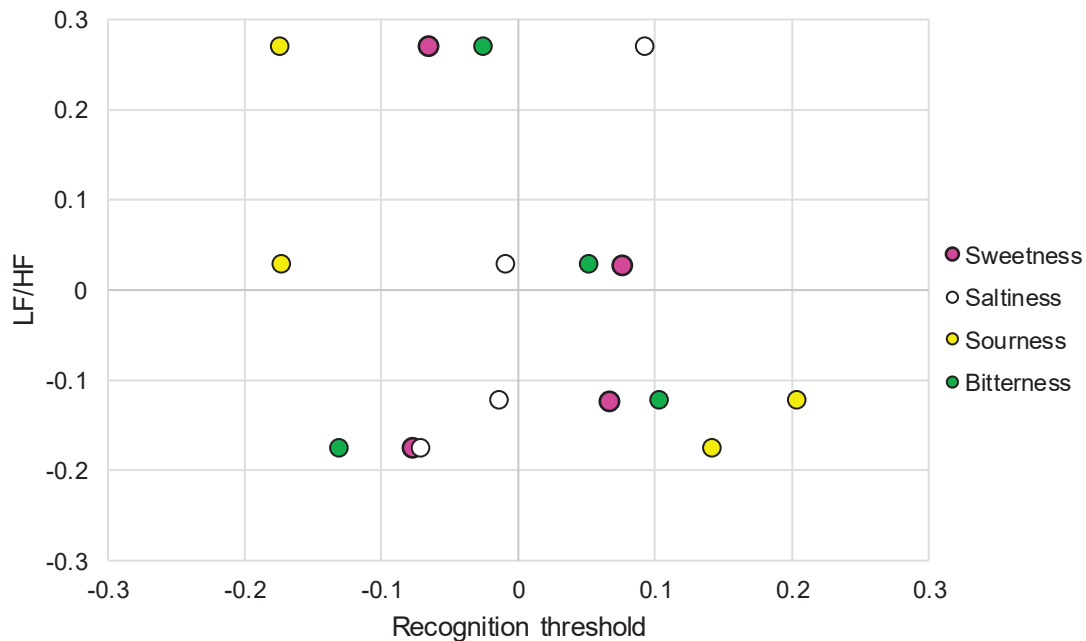


Figure 3. recognition threshold and stress indices

## REFERENCE

- [1] Yuko,K., Koko,S. and Sigeko,S., Association of tastes with colors and foods, Journal of Human and Living Environment, 2018, 25(2), 125-134
- [2] Noriko,H., Taste Interrelationships (Part1): Relationship between Saltiness and Sweetness, Journal of home economics of Japan, 1969, 20(1), 19-23
- [3] Noriko,H., Taste Interrelationships (Part2): Relationship between Saltiness and Sourness, Journal of home economics of Japan, 1976, 27(4), 255-261
- [4] Noriko,H., Taste Interrelationships (Part3): Relationship between Saltiness and Bitterness, Journal of home economics of Japan, 1977, 28(4), 278-281
- [5] Noriko,H., Taste Interrelationships (Part4): Relationship between Sweetness and Sourness, Journal of home economics of Japan, 1977, 28(4), 282-286
- [6] Noriko,H., Taste Interrelationships (Part5): Relationship between Saltiness and Bitterness, Journal of home economics of Japan, 1981, 32(2), 156-161
- [7] Noriko,H., Taste Interrelationships (Part6): Relationship between Sourness and Bitterness, Journal of home economics of Japan, 1981, 32(3), 241-245

Corresponding Author: Takuma Hashimoto

Affiliation: Kanagawa Institute of Technology

email: s2382012@kait.jp

# COMPARATIVE ANALYSIS AND STUDY ON THE EVALUATION OF COLLEGE STUDENTS' MENTAL HEALTH UNDER NATURAL LIGHT AND ARTIFICIAL LIGHT ENVIRONMENT IN UNIVERSITY LIBRARY

Shouyi Wang, Fanpu Meng, Hua Feng

(School of Architecture and Art, Hebei University of Engineering, Handan, China)

## ABSTRACT

As an area for college students to study for a long time, the light environment is the key to affect students' mental health. In this paper through the way of field measurement and subjective evaluation of Hebei university of engineering library reading room natural light, artificial light environment mental health comprehensive evaluation, through weight analysis, multiple index comprehensive evaluation way to determine two kinds of light environment students mental health comprehensive score, and regression analysis, get natural light, artificial light environment best desktop illumination threshold. The study found that the illumination value of natural light environment in the range of 0-3000lx and the mental health evaluation model was  $y = 1.42871 + 0.01612 * x^1 + (-1.73959E-5) * x^2 + (6.99447E-9) * x^3 + (-9.68541E-13) * x^4$ , where y was the comprehensive evaluation score and x was the illumination value of natural light environment, and the optimal illumination threshold was 513.68lx-1101.76lx. The illumination value in artificial light environment in the 0-600lx interval and the mental health evaluation model was  $y = 2.45175 + 0.0148 * x^1 + (-7.07218E-5) * x^2 + (1.90631E-7) * x^3 + (-1.6971E-10) * x^4$ , where y is the comprehensive mental health evaluation score, and x is the desktop illumination value in artificial light environment, and the optimal illumination threshold was 430.56lx-598.65lx. It provides a theoretical basis for the lighting and lighting design of the library reading room in the future.

Key words: reading room luminous environment mental health comprehensive evaluation of multiple indicators

## 1. INTRODUCTION

The 2023 Mental Health Blue Book: Chinese National Health Development Report pointed out that 21.48% of college students are prone to depression, 7.02% of college students have anxiety tendency [1], the mental health of college students should be paid attention to. Light can have an impact on human physical and mental health through visual effects and non-visual effects. On the one hand, through the visual system, inappropriate light environment will affect the visual effect, resulting to visual discomfort, visual fatigue and other [2]. On the other hand, light can influence the circadian rhythm, alertness, cognitive behavior, emotion and others through non-visual channels [3]. Previous studies have found that under the same illumination, the visual efficiency is 5%~20% [4] higher than that under artificial illumination. Wu Zhu [5] analyzed the changes of the pupil size and subjective feeling in the natural light environment in Chongqing. Grunberger et al [6] found that in the afternoon, students' attention was more concentrated in high illumination environment than in low illumination. Cajochen [7] Again confirmed that high illumination environment can improve alertness and reduce drowsiness, and alertness showed a significant positive correlation with the degree of light inhibition on melatonin. Through a literature review, Shilu et al. [8] concluded that high illumination lighting environmental stimuli can enhance alertness. Yan Yonghong [9] studied the effects of T5 fluorescent lamp on learning efficiency, visual fatigue and brain fatigue under different color temperature and illumination levels.

Yang Huanyu [10] evaluates the lighting comfort through the lighting simulation of the library reading room, and uses the multi-objective optimization system to optimize the reading space. Zhang Jingyi [11] concluded the importance of different influencing factors on reading comfort in the general lighting situation of the library. Guo Qi [12] established a prediction model for the subjective evaluation of visual satisfaction and lighting parameters. Feng Zilong [13] proposed a multi-objective optimization method for lighting environment of electronic reading room with illuminance, related color temperature, reflection coefficient and VDT screen brightness as variables.

In the past, the studies on the environment health evaluation of light in library reading rooms were mostly focused on natural light or artificial light alone, but both are important ways



of lighting in reading rooms. This paper comprehensively evaluates and analyzes the natural light environment of the reading room of Hebei University of Engineering from the subjective and objective dimensions, and compares the influence of natural light and artificial light environment in the reading room on students' mental health.

## 2. METHODS

### 2.1 Survey location

The research site is the open reading room of Hebei University of Engineering Library, with the opening time of 8:00-22:00. The space of the reading room is different in size and the depth is large. Only the unilateral window opening is considered. The outdoor environment is open and there are no tall trees. The new campus of Hebei University of Engineering is located in the longitude: 114.603217, latitude: 36.651677, and according to the division of China photolithing Design Standard GB50033-2013 [14], which belongs to the optical climate zone. Most reading rooms are arranged in the east, south and west, and less on the north. The windowsill height is 1 m and the window height is 2.1 m. The wall is large white painting, the reflection ratio is 0.75, the ground is white gray black terrazzo, the reflection ratio is 0.52, the desktop material is wood veneer desktop, and the reflection ratio is 0.7. The lighting fixture is grille type LED lamp, downlight, the height of 3.1 meters, parallel and perpendicular to the desktop layout, horizontal interval of 1-2m, vertical interval of 2-3 meters. Surrounding environment of the library The indoor space environment and light environment are shown in Figure 1.

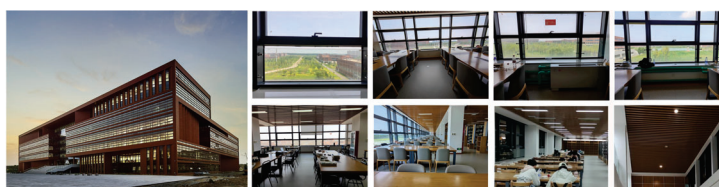


Figure 1. Overview of the library environment

### 2.2 Objective measurement method

The measurement method of the illumination in the reading room according to the characteristics of the operation, combined with the lighting measurement method GB / T5699-2017 [15], the lighting Measurement method GB / T5700-2008 [16], select the desktop illumination measurement method, select the height of the desktop, the measurement point to select the center point of the desktop. The measurement time is selected to measure the desktop illumination value in the natural light environment every one hour in mid-May, 2023, sunny days, 8-20 hours, and when there is no direct sunlight into the room and other artificial light sources. Measure the desktop illumination value in the artificial light environment during the period of 20-22, and extinguish other light sources when measuring. A tape measure and rangefinder are used for dimensional measurement, and a JTG 01 handheld illuminance meter is used for illumination measurement. The illumination value measurement points are shown in Figure 2.

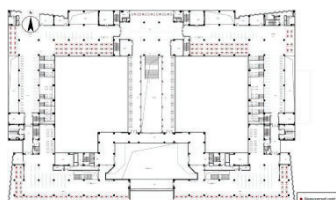


Figure2. Location diagram of the illumination measurement point

### 2.3 Subjective evaluation method

Research object for the students in the reading room, in order to ensure that the results are representative and universality, using personal basic information table to be research students preliminary screening, choose normal mood, no other physiological problems, psychological problems, and daily learning time in 3 hours, learning more than 4 days a week of students to fill in the next step of subjective questionnaire.

Subjective questionnaire content reference the light environment evaluation method (GB / T12454-2017) [17] and guan Yang for Chongqing classroom daytime health lighting study [18],

the introduction of light environment satisfaction evaluation, visual perception evaluation, emotional perception evaluation, cognitive ability evaluation four aspects of natural light, artificial light environment under the mental health level of comprehensive evaluation. The seven-level semantic difference scale was designed, and the corresponding scores of the 7 levels were 1,2,..., 7.

## 2.4 Analysis methods

(1)CRITIC Method, is an objective empowerment method, is through comprehensively considering the contrast intensity of the evaluation index and the conflict between the indicators Sex determines the objective weight of the indicators. It is not that the higher the weight, the more important the index, but the correlation between the variation of the index and the index, and completely uses the objective attributes of the data itself for scientific evaluation. Jiang Minyu [19] used the CRITIC method to analyze the weight of the light environment index of the cruise ship cabin.

(2)The comprehensive evaluation method, also known as the multi-index comprehensive evaluation method, is to establish a statistical index system according to the research purpose, right Several aspects of the development of the phenomenon are described quantitatively, combining the information provided by each index to get a comprehensive evaluation value, and making an overall evaluation of the research object for comparison.Hu Hao [20] studied the computer operation efficiency and fatigue degree of the office personnel under the artificial lighting environment through the method of multi-index comprehensive evaluation.This paper obtains the index data set through the establishment of the evaluation system  $Z = \{Z_1, Z_2, \dots, Z_6\}$ , and the corresponding weight of each index  $W = \{W_1, W_2, \dots, W_6\}$ , Using the weighted average method, the score results of multiple indicators are integrated into a comprehensive evaluation score. The numerical calculation formula of the comprehensive evaluation score is shown as follows:

$$I = \sum_{i=1}^n Z_i \times W_i \quad (1)$$

In the formula,  $0 \leq W_i \leq 1$  and meet  $\sum_{i=1}^n W_i = 1$

## 3. Results

### 3.1 Objective data analysis

#### 3.1.1 Natural light environment

The orientation and the number of floors of the building in the natural light environment will affect the desktop illumination. The average illumination value of the reading room in the reading room is shown in Table 1.

Table 1. Measurement results of desktop illumination in natural light environment all sunny days

time	Average desktop illumination / lux			
	East reading room	South reading room	West reading room	North reading room
8-9	6146	306	235	258
9-10	7482	435	400	383
10-11	811	479	425	380
11-12	699	1035	464	414
12-13	522	8082	395	415
13-14	504	7215	710	356
14-15	439	1089	1333	443
15-16	514	932	4699	439
16-17	357	621	3433	366
17-18	294	334	655	225
18-19	99	202	96	84
19-20	31	46	39	21

During the sunny day, the average of the east reading room from 8-10, the southward reading room from 12-14, and the average of the west reading room from 15-17. In the north reading room, the average illumination of the desktop changes little with time, and the light

environment is relatively stable, but the overall illumination level is low. South, west and north reading rooms in 8,8-10, east, south and north reading rooms in 16-18, east, west, south and north reading rooms in 18-20, the illumination value is lower than the standard value stipulated in GB50033-2013 [14] 450 lx.

### 3.1.2 Artificial light environment

The lowest illumination, highest illumination, average illumination and uniformity of illumination on the desktop from 20-22 in the artificial light environment are shown in Table 2.

Table 2. Measurement results of the desktop illuminance in the lighting environment

Position	Average desktop illumination / lux	The desktop illumination uniformity
East reading room,sixth floor	259	0.93
South reading room,sixth floor	262.5	0.91
West reading room,sixth floor	268.5	0.91
East reading room,fifth floor	266.5	0.95
South reading room,fifth floor	132	0.89
West reading room,fifth floor	239.5	0.88
East reading room, fourth floor	477.5	0.85
Southern reading room,fourth floor	118.5	0.88
Western reading room,fourth floor	550.5	0.90
North reading room,fourth floor	143	0.87
East reading room,third floor	209	0.92
Southern reading room,third floor	143.5	0.92
Western reading room,third floor	125.5	0.89
North reading room,third floor	70	0.94

It is found that the light color of the artificial light environment in the reading room is all white light. The illumination value was generally low, with only 14% of the average desktop illumination area above 300 lx, meeting the requirements of [21], 35.7% between 200 lx and 300 lx, 42.8% between 100 lx and 200 lx, and 7% between 0 and 100 lx. The overall light environment is relatively uniform, and the uniformity of the desktop illumination is basically above 0.8, which is higher than the 0.6 required by the building lighting design standard [21].

### 3.2 Subjective data analysis

Through the preliminary analysis, it is found that students have great differences in their attention to different evaluation indicators of natural light environment and artificial light environment. In order to excavate the students' attention to different indicators, CRITIC weight analysis method is applied to analyze the relative weight of each index.

#### 3.2.1 Natural light environment

The subjective evaluation results of the whole natural light environment in the reading room are shown in Table 3,4.

Table 3. Statistics of the survey results of the natural light environment questionnaire

Classification	Index	Describe	Average value	Standard deviation
Light environment evaluation	Overall satisfaction	Not satisfied / Satisfied	4.930	1.233
	Light color satisfaction	Cold / Warm	5.000	1.700
	No glare evaluation	Dazzling / Not dazzling	3.250	1.274
	Brightness satisfaction	Dark / Bright	4.990	1.679
Visual perception evaluation	Visual comfort	Not comfortable / Comfortable	4.760	1.288
	Visual fatigue	Fatigue / No fatigue	4.370	1.779
	Visual clarity	Fuzzy / Clear	4.630	1.674
	Colour truth	Not real / Real	4.910	1.596
Emotional perception evaluation	Vitality degree	Durbine / Active	4.030	1.636
	Pleasure degree	Frustration / Pleasure	4.220	1.829
	Calm degree	Disturbed / Calm	4.310	1.637
	Relax degree	Nervous / Relax	4.090	1.564
Cognitive appraisal	Cognitive speed	Slow / Fast	4.030	1.636
	Cognitive accuracy	Low accuracy / High accuracy	3.890	1.588

Table 4. Weight analysis of natural light environment evaluation indicators

Classification	Index	Indicator variability	Indicators are conflicting	Quantity of information	Weight
----------------	-------	-----------------------	----------------------------	-------------------------	--------

Classification	Index	Indicator variability	Indicators are conflicting	Quantity of information	Weight
Light environment evaluation	Overall satisfaction	1.233	12.312	15.181	7.77%
	Light color satisfaction	1.700	8.847	15.037	7.70%
	No glare evaluation	1.274	14.573	18.570	9.51%
	Brightness satisfaction	1.679	9.014	15.131	7.75%
Visual perception evaluation	Visual comfort	1.288	10.974	14.134	7.24%
	Visual fatigue	1.779	11.449	20.368	10.43%
	Visual clarity	1.674	8.254	13.815	7.07%
	Colour truth	1.596	10.908	17.409	8.92%
Emotional perception evaluation	Vitality degree	1.636	6.481	10.601	5.43%
	Pleasure degree	1.829	6.864	12.554	6.43%
	Calm degree	1.637	6.801	11.135	5.70%
	Relax degree	1.564	6.594	10.314	5.28%
Cognitive appraisal	Cognitive speed	1.636	6.481	10.601	5.43%
	Cognitive accuracy	1.588	6.560	10.420	5.34%

According to the results of the questionnaire, the students scored more than 4 points on the evaluation indicators of the overall natural light environment under all sunny days, and the overall evaluation is relatively high, indicating that the students are generally satisfied with the natural light environment in the reading room, but the evaluation score of no glare is low.

It can be found from Table 4 that the order of different evaluation indicators in natural light environment is Visual fatigue (10.43%)> No glare evaluation (9.51%)> Colour truth (8.92%)> Overall satisfaction (7.77%)> Brightness satisfaction (7.75%)> Light color satisfaction (7.70%)> Visual comfort (7.24%)> Visual clarity (7.07%)> Pleasure degree (6.43%)> Calm degree (5.70%)> Vitality degree (5.43%) = Cognitive speed (5.43%)> Cognitive accuracy (5.34%)> Relax degree (5.28%).

### 3.2.2 Artificial light environment

The subjective evaluation of the overall artificial light environment in the reading room are shown in Table 5,6.

Table 5. Statistics of the survey results of the artificial light environment questionnaire

Classification	Index	Describe	Average value	Standard deviation
Light environment evaluation	Overall satisfaction	Not satisfied / Satisfied	3.050	1.513
	Light color satisfaction	Cold / Warm	3.900	1.528
	No glare evaluation	Dazzling / Not dazzling	4.980	1.279
	Brightness satisfaction	Dark / Bright	3.060	1.530
Visual perception evaluation	Visual comfort	Not comfortable / Comfortable	2.990	1.367
	Visual fatigue	Fatigue / No fatigue	3.040	1.428
	Visual clarity	Fuzzy / Clear	3.050	1.513
	Colour truth	Not real / Real	3.720	1.102
Emotional perception evaluation	Vitality degree	Durbine / Active	3.140	1.504
	Pleasure degree	Frustration / Pleasure	2.960	1.325
	Calm degree	Disturbed / Calm	3.130	1.587
	Relax degree	Nervous / Relax	3.090	1.491
Cognitive appraisal	Cognitive speed	Slow / Fast	3.070	1.559
	Cognitive accuracy	Low accuracy / High accuracy	2.980	1.497

Table 6. Weight analysis of artificial light environment evaluation indicators

Classification	Index	Indicator variability	Indicators are conflicting	Quantity of information	Weight
Light environment evaluation	Overall satisfaction	1.513	4.373	6.618	4.84%
	Light color satisfaction	1.528	12.291	18.774	13.74%
	No glare evaluation	1.279	23.283	29.780	21.80%
	Brightness satisfaction	1.530	4.349	6.652	4.87%
Visual perception evaluation	Visual comfort	1.367	4.276	5.845	4.28%
	Visual fatigue	1.428	4.639	6.624	4.85%
	Visual clarity	1.513	4.373	6.618	4.84%
	Colour truth	1.102	14.866	16.378	11.99%
Emotional perception evaluation	Vitality degree	1.504	4.333	6.519	4.77%
	Pleasure degree	1.325	4.424	5.862	4.29%
	Calm degree	1.587	4.347	6.898	5.05%
	Relax degree	1.491	4.324	6.448	4.72%
Cognitive appraisal	Cognitive speed	1.559	4.409	6.873	5.03%

Classification	Index	Indicator variability	Indicators are conflicting	Quantity of information	Weight
	Cognitive accuracy	1.497	4.491	6.724	4.92%

According to the results of the questionnaire survey, the score of various evaluation indicators in the overall artificial light environment of the library reading room is basically about 3, indicating that the overall evaluation of the artificial light environment is general, but the evaluation score of non-glare is relatively high.

It can be found from Table 6 that the order of different evaluation indicators in artificial light environment is No glare evaluation (21.80%)> Light color satisfaction (13.74%)> Colour truth(11.99%)> Calm degree(5.05%)> Cognitive speed (5.03%)> Cognitive accuracy (4.92%)> Brightness satisfaction (4.87%)> Visual fatigue (4.85%)> Overall satisfaction (4.84%) = Visual clarity (4.84%)> Vitality degree(4.77%)> Relax degree (4.72%)>Pleasure degree (4.29%)> Visual comfort (4.28%).

### 3.3 Analysis of objective data and subjective data

In order to explore the relationship between subjective data and objective data, the desktop illumination and subjective perception evaluation in natural light and artificial light environment were compared and analyzed, and a regression model of comprehensive score and illumination was established. The preliminary investigation found that there was no student learning in the area where the desktop illumination value of natural light was higher than 3000 lx, so only the illumination measured illumination within 0-3000 lx was considered in the next study. According to the preliminary investigation of the artificial light environment, the measured illumination within 0-600 lx was selected in the next study. In this study, a total of 286 valid questionnaires were collected in the reading room, and SPSS was used to test the validity of the obtained data. The KMO measurements of subjective questionnaire data in natural and artificial light environments were 0.928,0.868, and the Cronbach Alpha coefficient was 0.927,0.931, respectively.

#### 3.3.1 Natural light environment

The change trend of natural light environment illumination value and subjective evaluation index is shown in Figure 3.

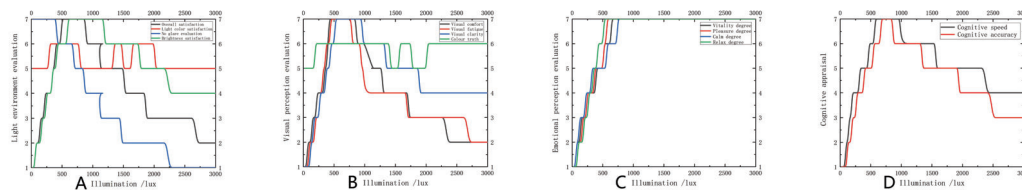


Figure 3. Comparative analysis of illumination and subjective perception evaluation

In the range of mood perception evaluation and illumination is the same change, not glare evaluation and illumination opposite change, light color satisfaction, color reality and illumination value relationship is not obvious, visual comfort, visual fatigue, visual clarity and cognitive evaluation, overall satisfaction, brightness satisfaction with illumination increased after the change.

The regression model fit of the illuminance values in natural light environment and mental health comprehensive evaluation scores is shown in Figure 4.

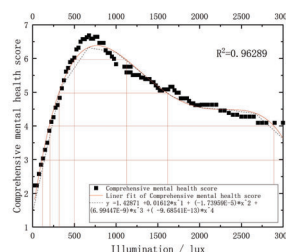


Figure 4. Lance values and mental health composite scores

A function model of 0-3000lx,  $R^2=0.96289$ , F value test,  $P < 0.05$ , whose expression was  $y = 1.42871 + 0.01612 * x^1 + (-1.73959E-5) * x^2 + (6.99447E-9) * x^3 + (-9.68541E-13) * x^4$

$x^4$ , where  $y$  is the comprehensive evaluation score of mental health, and  $x$  is the illumination value of natural light environment. The comprehensive score of mental health first increased and then decreased with increasing illumination, with the highest value of 6.21 and the illumination of 596.95lx, and when the combined score was above 6, the illumination threshold was 513.68lx-1101.76lx. When the combined score is above 5, the illuminance threshold is 316.48-1593.28. When the combined score is above 4, the illuminance threshold is 198.87-2886.12. When the composite score is above 3, the illumination threshold is 109.95-3126.49lx.

### 3.3.2 Artificial light environment

The change trend of the artificial light environment illumination value and the subjective evaluation index is drawn as shown in Figure 5.

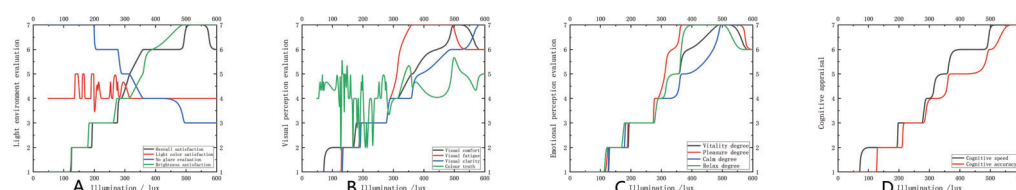


Figure 5. Comparative analysis of illumination and subjective perception evaluation

Under the measured illumination range of the artificial light environment, the overall satisfaction degree, visual comfort degree, visual fatigue degree, activity degree, pleasure degree and relaxation degree all increased first and then decreased with the increase of the illumination degree. Non-glare evaluation gradually decreased with increasing illuminance. Brightness satisfaction, visual clarity, calmness, cognitive speed, and cognitive accuracy all increased with the increasing illuminance. The relationship between light and color satisfaction, color authenticity and illumination value is not obvious.

The regression model fit of the illuminance values in the artificial light environment and the comprehensive evaluation of mental health is shown in Figure 6.

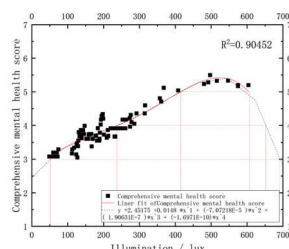


Figure 6. Lance values and mental health composite scores

A function model of 0-600 lx,  $R^2=0.90452$ , F value test passed,  $P < 0.05$ , whose expression is  $y = 2.45175 + 0.0148 * x + (-7.07218E-5) * x^2 + (1.90631E-7) * x^3 + (-1.6971E-10) * x^4$ , where  $y$  is the score of comprehensive mental health and  $x$  is the illumination of artificial light environment. When the composite score is above 5, the illumination threshold is 430.56lx-598.65lx. When the composite score is above 4, the illuminance threshold is 239.66-660.68lx. The illumination threshold was 45.93-694.34lx when the composite score was above 3.

## 4. CONCLUSION

The results of the mental health of the students in the natural light and artificial light environment are as follows.

1. The natural light environment changes diverse, which is not easy to control, and is easy to appear problems such as large changes in illumination in the same region in the daytime and large differences in illumination in different regions at the same time. Artificial light environment due to unreasonable lighting layout and partial damage, resulting in lighting quality deviation in some areas.



2. Students' evaluation of natural light environment is higher than that of artificial light environment. Most students are more satisfied with the evaluation of natural light environment, and the evaluation of artificial light environment is more general.

3. Comprehensive evaluation of students' mental health, the best desktop illumination threshold in natural light environment is 513.68lx-1101.76lx, and the best desktop illumination threshold in artificial light environment is 430.56lx-600lx.

## REFERENCE

- [1] Fu Xiaolan, Zhang Kan, Chen Xuefeng, et al. Chinese National Mental Health Development Report 2021-2022 [M]. Beijing: Social Sciences Academic Press, 2023:75-84.
- [2] Jiang Jincai, Wu Wei. Review of evaluation methods for non-visual effects of light and lighting [J]. Journal of Lighting Engineering, 2018,29 (03): 129-136 + 140.
- [3] Peter R. Boyce. The Impact of Light in Buildings on Human Health[J]. Indoor and built environment: Journal of the International Society of the Built Environment,2010,19(1).
- [4] William A. Gosling. To Go or Not to Go? Library as Place[J]. American Libraries,2000,31(11).
- [5] Wu Zhu. Research on natural lighting in office space based on photobiological effect [D]. Chongqing University, 2013.
- [6] Grünberger J.,Linzmayr L.,Dietzel M.,Saletu B.. The effect of biologically-active light on the mood and thymoppsyche and on psychophysiological variables in healthy volunteers[J]. International Journal of Psychophysiology,1993,15(1).
- [7] Christian Cajochen,Jamie M Zeitzer,Charles A Czeisler,Derk-Jan Dijk. Dose-response relationship for light intensity and ocular and electroencephalographic correlates of human alertness[J]. Behavioural Brain Research,2000,115(1).
- [8] Stone road. Effect of illumination source color temperature on the physiological function of human CNS [J]. Human ergonomics, 2006(02):59-61+71.
- [9] Yan Yonghong, Guan Yang, Liu Xiangde, etc. The effect of classroom fluorescent light color temperature on student learning efficiency and physiological rhythm [J]. Civil Construction and Environmental Engineering, 2010,32 (04): 85-89.
- [10] Yang Huanyu. Research on light environment of Kunming University Library based on Octopus optimization algorithm [D]. Kunming University of Science and Technology, 2020.
- [11] Zhang Jingyi. Evaluation of coupled reading comfort in library lighting environment [D]. Tianjin University, 2019.
- [12] Guo Qi, Wang Lixiong. Visual satisfaction prediction model of e-reading in a library lighting environment [J]. Journal of Civil and Environmental Engineering (Chinese and English), 2019,41 (01): 144-149.
- [13] Feng Zilong, Wang Lixiong. Multi-objective optimization method for reading comfort lighting in library electronic reading room [J]. Journal of Lighting Engineering, 2022,33 (04): 115-122.
- [14] GB 50033-2013,Design standards for building lighting[S].
- [15] GB / T 5699-2017, Daylighting measurement method [S].
- [16] GB / T 5700-2008, Lighting measurement method [S].
- [17] GB / T 12454-2017, Light environment assessment method [S].
- [18] Guan Yang. Study on daytime health lighting of classrooms in Chongqing area [D]. Chongqing University, 2017.
- [19] Jiang Minyu, Ge Wenjing, Yang Xiu. Comprehensive evaluation of light environment of cruise cabin combining subjective and objective [J]. Journal of Shanghai Maritime University, 2023,44(01):104-110.
- [20] Hu Hao. Research on the computer operation efficiency and fatigue degree in the artificial lighting environment of administrative office space [D]. Chongqing University, 2018.
- [21] GB 50034-2013, Building Lighting Design Standard (attached provision description) [S].

## ACKNOWLEDGEMENT

Corresponding Author: Fanpu Meng

Affiliation: School of Architecture and Art, Hebei University of Engineering

e-mail : 2423078106@qq.com

# THE COMPARISON AND ACCURACY EVALUATIONS OF CIRCADIAN SENSITIVITY MODELS FOR LIGHT INDUCED CIRCADIAN RESPONSE

Yingying Huang<sup>1</sup>, Qi Dai<sup>2\*</sup>

(1. Institute of Future Lighting, Academy for Engineering & Technology, Fudan University, Shanghai, 200433, China

2. Institute for Electric Light Sources, Department of Light Sources and Illuminating Engineering, School of Information Science and Technology, Fudan University, Shanghai, 200433, China)

\*Corresponding author: Qi Dai, Email: qidai@fudan.edu.cn

## ABSTRACT

Light exposure has been shown to affect human circadian rhythms, including suppressing the production of melatonin. These light-induced circadian effects are regulated by melanopsin-based intrinsically photosensitive retinal ganglion cells, with partial contributions from visual photoreceptors. Various approaches have been proposed by different groups to quantify light-induced melatonin suppression, including the widely used melanopic illuminance model, which the EML and m-EDI metrics derived from, and visual photoreceptor-combined CS model. However, these models adopt different hypothesis on visual photoreceptors' contribution in circadian pathway, leading to conflicting predictions of circadian effects and pose challenges for lighting applications.

To evaluate the accuracy of these popular circadian sensitivity models, we collected data from multiple laboratory studies that measured human melatonin suppression in response to different light stimulus types and durations. The goodness of fit for the 4-parameter sigmoid curves that described the overall datasets (adjusted R<sup>2</sup>) as adopted as to compare the accuracy of each model. Our results showed that melanopic illuminance and CS models provided overall comparable goodness-of-fit, and outperformed photopic illuminance across the studies. Though the CS model has been fixed to CS 2.0 model, we found that this new model did not provide better description of light-induced melatonin suppression compared with the original one. Given the lack of broad consensus on the exact visual photoreceptors' contribution, the melanopic illuminance approach appears to be a preferable strategy compared to the CS model. Moreover, our analysis revealed a limitation in previous research, as the spectra used rarely covered the controversial regions between different metrics, resulting in challenges in compare their accuracy. To address this, we proposed a methodology for designing comparative spectra that can emphasize the fundamental differences between the circadian metrics. This approach could be employed in future human-factor studies to establish a precise and practical "circadian illuminance" metric.

Keywords: circadian sensitivity, melanopic illuminance, CS model, melatonin suppression

## 1. INTRODUCTION

In modern society, a large proportion of individuals spend an increasing amount of time indoors. This often leads to restricted daylight access and excessive evening light exposure. These patterns of light stimulus are misaligned with the circadian clock, resulting in detrimental effects on the acute production of the sleep hormone melatonin and disrupting the natural sleep-wake cycle [1,2]. Consequently, a range of circadian-disruption-related problems would arise [3-5]. These light-induced non-visual effects are primarily mediated by intrinsically photosensitive retinal ganglion cells (ipRGCs), which contain the photopigment melanopsin [6,7]. The ipRGCs convert optical signals into electrical signals and transmit them to the suprachiasmatic nucleus, synchronizing the biological clock and regulating the melatonin secretion [8-10]. Additionally, ipRGCs receive extrinsic signals originating from visual photoreceptors, including rods and cones [11,12]. Converging evidences suggest that both ipRGCs and visual photoreceptors contribute to

the circadian phototransduction process under certain conditions [13,14]. But the precise contribution of visual photoreceptors in modulating human circadian rhythms and neuroendocrine light responses is not yet fully understood.

Researchers and organizations have pursued different strategies to evaluate the impact of light on the circadian system. Due to the lack of specific contributions from each known photoreceptors (rods, S-cone, M-cone, L-cone and ipRGCs), Lucas et al. suggested to record the corresponding counterpart of illuminance named  $\alpha$ -opic illuminance [11]. This approach provides comprehensive information for the stimulus experienced by each type of photoreceptors that would be investigated in future studies, but it currently does not allow for the determination of the specific circadian output, such as the “circadian illuminance”. Following that, based on the ipRGCs-related melanopic illuminance, one of the five  $\alpha$ -opic illuminances, the International WELL Building Institute and the International Commission on Illumination recommended the metrics of equivalent melanopic lux (EML) [15] and melanopic equivalent daylight D65 illuminance (m-EDI) [16], respectively. Differing from the melanopic illuminance approach, Rea et al. [19,20] proposed the Circadian Stimulus (CS) model initially in 2005 and introduced the metric of Circadian Light (CLA) as the “circadian illuminance”. The CS model not only rely on the contribution of ipRGCs, but also assumes that the human circadian system exhibits S-cone based b-y color opponency, and taking into account the interplay of rod and cone photoreceptors in circadian phototransduction [18-20].

The mechanisms underlying circadian sensitivity models are illustrated in Fig. 1. It reveals that the melanopic illuminance and CS models differ significantly, particularly concerning the incorporation and integration of visual photoreceptors. Consequently, their spectral sensitivities exhibit considerable inconsistency, leading to contradictory predictions of circadian effect for the same light stimulus [25]. Such uncertainty regarding the accuracy of the melanopic illuminance and CS models poses challenges for the practical application of circadian lighting. Experts in the field have been engaged in intense discussions over the merits of the two models, and showing a serious division of opinions [26,27]. A fundamental question remains unanswered: Can models that integrate the complex interplay of visual photoreceptors, as hypothesized by the CS model, offer superior predictions of circadian effects?

## 2. Methods

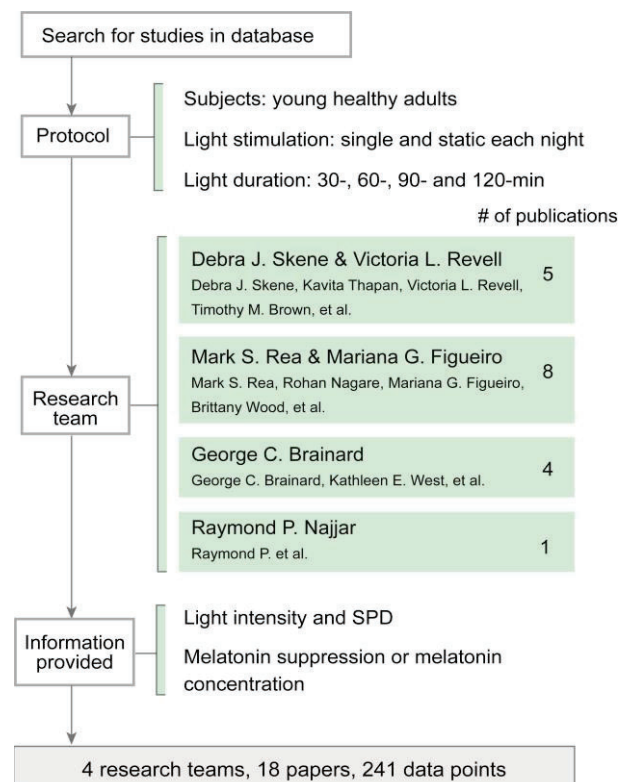


Figure 1. Procedure for publications screening.

In this study, we conducted a comprehensive analysis using data from multiple laboratory studies that measured human melatonin suppression in response to various light stimuli with differing spectra and durations. The selection procedure, depicted in Fig. 1, followed specific criteria:

(i) Protocol: We included publications that investigated evening light-induced melatonin suppression in healthy young adults. The experiments were needed to utilize a single static light stimulation throughout the study night. Prior to each light stimulation, a period of dim light exposure was required. We considered the common intervals for melatonin collection (15, 30, or 60 minutes) and selected publications that reported data within 30, 60, 90, or 120 minutes.

(ii) Research team: Publications sharing the same corresponding author or first co-authors, indicating similar experimental protocols, were grouped as works from the same research team. We identified a total of four research teams, which are: (i) Debra J. Skene & Victoria L. Revell team, (ii) Mark S. Rea & Mariana G. Figueiro team, (iii) George C. Brainard team, and (iv) Raymond P. Najjar team. Within each research team, we re-evaluated the experimental protocols adopted and excluded publications that exhibited significantly inconsistent key setups. Specifically, publications deviating significantly in the starting time of light exposure (deviation exceeding 60 minutes) or using different melatonin suppression calculation methods were excluded. The method of melatonin suppression calculation which was not align with that adopted by other studies within the same research team were also excluded.

(iii) Information provided: Selected publications needed to provide detailed information on light intensity and spectral power distributions (SPD) for calculating the circadian effects of the lighting conditions. Light intensity could be expressed in terms of illuminance, irradiance, or photon density. In cases where monochromatic light was used but spectral power distributions were not provided, peak wavelength and half-wave width were necessary. If only melatonin concentration was reported, we calculated the melatonin suppression values using the baseline melatonin concentration provided in the publication.

A total of 18 publications [21-23,28-42] contributed by four research teams were included in our analysis. These publications provided data for 241 lighting conditions along with corresponding melatonin suppression information.

The SPDs of the light sources, typically presented in figures, were extracted from the published works using WebPlotDigitizer software (Version 4.4). For the SPD of monochromatic light which were not presented in the figures, we generated SPDs using Gaussian functions based on the provided peak wavelength and half-wave width. For the analysis, we utilized directly reported melatonin suppression values whenever available. In cases where melatonin suppression and concentration data were only presented in figures, we employed WebPlotDigitizer (Version 4.4) to extract the relevant data. We used the four-parameter logistic function to fit the different circadian metrics with melatonin suppression. The equation for four-parameter sigmoid fit was as follows:

$$Y = \frac{Y_{max} - Y_{min}}{1 + 10^{(X_{50}-X)*P}} + Y_{min} ,$$

where  $X$  was the log value of effective circadian illuminance based on different models,  $X_{50}$  was log circadian illuminance producing a response halfway between  $Y_{max}$  and  $Y_{min}$ , and  $P$  determined the slope of the curve. Following the physiological assumptions suggested in previous studies [28], we constrained the fits to have minimum at 0 and a maximum  $\leq 100\%$  ( $Y_{min} = 0$ ,  $Y_{max} = 100\%$ ). The  $Y$  equals zero when  $X$  was zero, which conformed to the fact that the dark control group has no melatonin suppression. Fits were performed using Origin 2017 (OriginLab). Adjusted R-square values reported in the study reflected the correspondence between the fitted curves and the mean responses across the relevant data sets.

### 3. Results

#### 3.1 Fitting results of experimental data after 30 min light exposure

The adjusted R-squared for melanopic illuminance was 0.541, indicating that this model could not provide a satisfactory overall description of the data. The adjusted R-squared of CS model 2005 was 0.717, showing that the CS model 2005 was still able to adequately predict sensitivity across test spectrum. In contrast, the adjusted R-squared of CS model 2.0 was 0.600, which declined by 16.0% compared to that of the CS model 2005. Therefore, the accuracy of circadian efficiency prediction has not been improved based on the CS model 2.0. When quantify using photopic

illuminance, the adjusted R-squared was only 0.101. This result shows that the photopic illuminance alone is not a reliable predictor of melatonin suppression.

To further investigate the impact of spectrum on the fitting results, we arranged all spectra and numbered on the x-axis in ascending order of melanopic illuminance values in Fig. 2A. The left and right y-axes represent the corresponding melanopic illuminance values (indicated in blue) and CLA values (indicated in red) of each spectrum, respectively. Disputed spectra were identified as pairs with equivalent EML values (difference less than 5%) but large difference in CLA values (more than 50%). A total of 11 pairs of disputed spectra (34.4%) were found, as shown in Fig. 2B. The disputed spectra included monochromatic light in short wavelength stimuli (424, 456 and 496 nm), and polychromatic spectra with CCT of 4000 K and 17000 K. When including these disputed spectra, EML model showed lower level of goodness-of-fit, suggesting that the accuracy of circadian efficiency model may depend on the spectra adopting in the analysis.

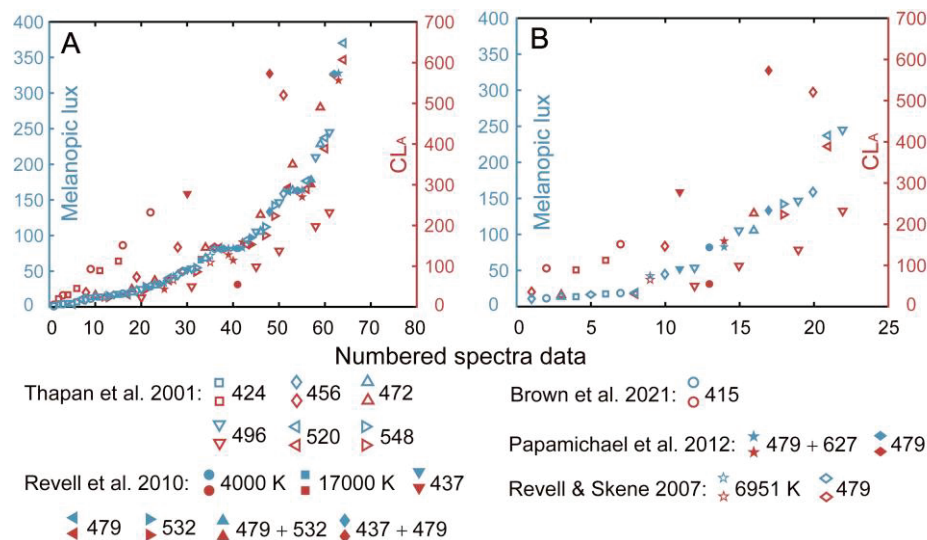


Figure 2. Comparison of the melanopic illuminance and CLA values for the spectra (A) adopted in current study and (B) that showed disputable results in current study. The spectra data were arranged in ascending order of melanopic illuminance values and numbered. The left and right y-axes represent the corresponding melanopic illuminance (indicated in blue) and CLA (indicated in red) of each spectrum, respectively.

### 3.2 Fitting results of experimental data after 60 min light exposure

The results based on the data from Najjar team were illustrated in Fig. 5. The adjusted R-squared value for the melanopic illuminance was 0.985, indicating that the melanopic illuminance adequately accounts for the variations in sensitivity across different monochromatic light types. However, the adjusted R-squared values for CLA, and CLA 2.0 were 0.693 and 0.684, respectively, which were lower than that of the melanopic illuminance. This discrepancy was primarily due to the CS models overestimating the circadian sensitivity to a monochromatic light with a wavelength of 420 nm. Additionally, the predictive accuracy of photopic illuminance for sensitivity to all test wavelengths was found to be extremely low, with an adjusted R-squared value of  $-0.126$ . Moving on to the spectra and melatonin suppression data collected from the Rea & Figueiro team, the goodness-of-fit were calculated. The adjusted R-squared of EML, CS model 2005 and CS model 2.0 were 0.755, 0.714 and 0.750. These findings indicate that accuracy among these models is comparable for predicting the evening light-induced melatonin suppression effect. The photopic illuminance still exhibited lower accuracy, with an adjusted R-squared value of 0.583.

Furthermore, we conducted a detailed analysis of the spectra used during the 60-minute light exposure (Fig. 3 Left), focusing on the data from the Rea & Figueiro team. Within their data, there were only a few spectra that displayed disputed characteristics. As a result, the differences in accuracy between the melanopic illuminance and CS models may be overshadowed by the majority of spectra that showed no disputes, thus explaining the comparable goodness-of-fit observed between these models. Three examples of disputed spectra are illustrated in the inset figure, representing different CCTs of 3000 K, 4900 K and 6400 K. The CLA value of 6400 K and 4900 K were identical, while their melanopic illuminance values exhibited a significant difference.



Contrasting results were also observed when comparing the melanopic illuminance and CLA values between spectra in 4900 K and 3000 K.

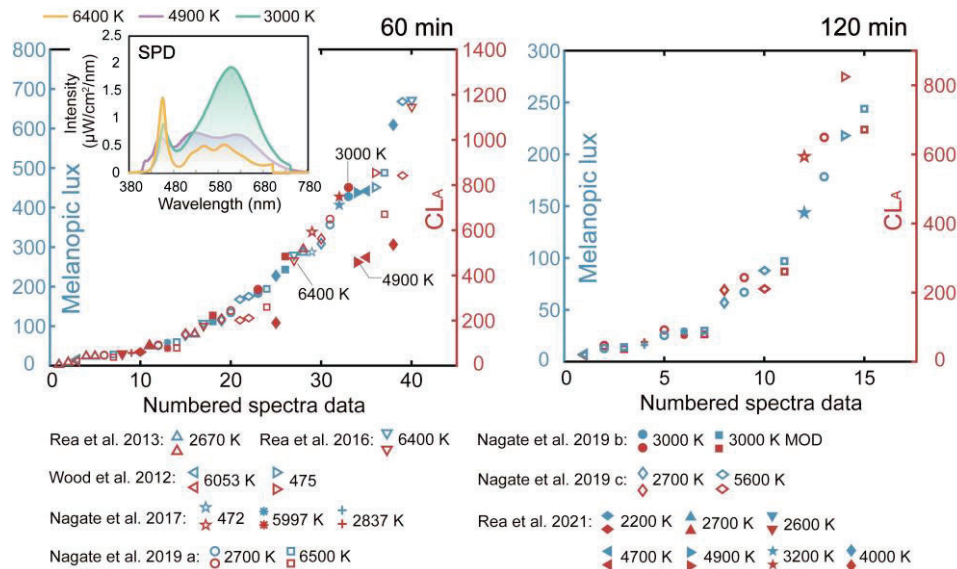


Figure 3. Comparison of the melanopic illuminance and CLA values for the spectra (Left) adopted in analysis of 60-min light exposure and (Right) that adopted in analysis of 120-min light exposure. The spectra data were arranged in ascending order of melanopic illuminance values and numbered. The left and right y-axes represent the corresponding melanopic illuminance (indicated in blue) and CLA (indicated in red) of each spectrum, respectively. Inset figure represented the three disputed SPDs.

### 3.3 Fitting results of experimental data after 90 min light exposure

The data corresponding to the 90-minute light duration was collected from the Brainard team. The adjusted R-squared of melanopic illuminance, CLA and CLA 2.0 were 0.667, 0.706 and 0.650, respectively. These metrics demonstrated similar accuracy in predicting light-induced melatonin suppression. Compared with the CLA metric, CLA 2.0 did not show improved accuracy. When quantify using photopic illuminance, the adjusted R-squared was only 0.220, which still could not provide reliable prediction.

Fig. 4 (Left) illustrated the prediction of melanopic illuminance and CLA to all spectra used in 90-min analysis. Within this data group, we identified 44 out of 113 spectra (38.9%) that displayed significant discrepancies between the EML and CS models, which were shown in Fig.4 (Right). Similar to the observations for the 30-minute duration, the disputed spectra mainly consisted of monochromatic light stimuli in the short-wavelength range (424-440 nm), as well as polychromatic spectra with CCT of approximately 4000 K and 17000 K.

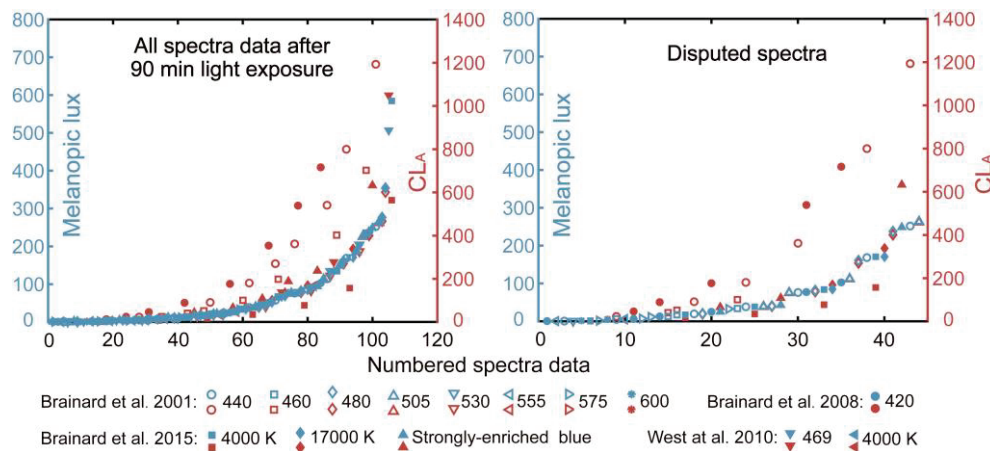


Figure 4. Comparison of the melanopic illuminance and CLA values, for the prediction to all spectra adopted in 90 min analysis (Left), and that showed disputable results (Right). The spectra data were arranged in ascending order of melanopic illuminance values and numbered. The left and right y-axes represent the corresponding melanopic illuminance (indicated in blue) and CLA (indicated in red) of each spectrum, respectively.



### 3.4 Fitting results of experimental data after 120 min light exposure

The data for 120-minute light stimuli were derived from studies conducted by the Rea & Figueiro team. For these experimental data, we found that the goodness-of-fit for the melanopic illuminance, CLA and CLA 2.0 was found to be 0.857, 0.845 and 0.837 respectively. In contrast, the goodness-of-fit based on photopic illuminance was only 0.139. Therefore, all of the models except for photopic illuminance demonstrated reliable predictability of light-induced melatonin suppression. The fitting quality among the melanopic illuminance, CLA and CLA 2.0 was comparable. Moreover, both the melanopic illuminance and CS models exhibited a strong level of goodness-of-fit, with adjusted R-squared values exceeding 0.8. As shown in Fig. 3 (Right), no disputed spectra were observed for the spectra adopted in the 120-minute light exposure, indicating a high level of consistency in the predictions of the melanopic illuminance and CS models for these SPDs.

Fig. 5 presented the adjusted R-squared values of the melanopic illuminance, photopic illuminance, CS model 2005, and CS model 2.0 across different durations of light exposure. The goodness-of-fit results of the melanopic illuminance and CS models were found to be relatively similar. In addition, both melanopic illuminance and CS models showed increased adjusted R-square under the light exposure of 120 minutes, which were higher than 0.80. This result indicated melanopic illuminance and CS models could effectively predict the melatonin suppression for the long-term light exposure. Conversely, the predictive capacity of photopic illuminance were proved to be unreliable across all durations of light exposure. These findings suggested that high levels of photopic illuminance may not necessarily correlate with greater circadian effects.

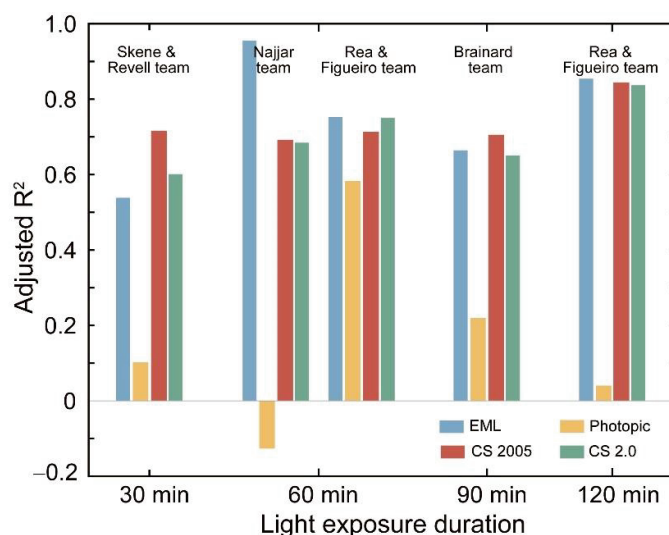


Figure 5. The adjusted R-squared of melanopic illuminance, photopic illuminance, CLA and CLA 2.0 on the experimental results after 30-, 60-, 90- and 120-minute light exposure.

### 4. SPDs solution for circadian efficiency model comparison

Though the melanopic illuminance and CS models should have achieved large difference in accuracy by adopting different visual photoreceptors contribution, their adjusted R-square values observed were consistent (only differed by around 5%) using existing spectra. This was mainly due to that there were rarely spectra that yielded disputed results between the melanopic illuminance and CS model. To further reveal the fundamental discrepancies between melanopic illuminance and CS models, a larger and more diverse set of disputed spectra are needed. Here, we explored a lighting design method by self-developed multi-component color mixing algorithm [45] to efficiently compare the accuracy of circadian efficiency models. A five-component color mixing with commercial light-emitting diode (LED) sources were used for the spectral design analysis. Following the principles of color science, when the target color locates inside the gamut area formed by connecting the coordinates of all components, there exist infinite numbers of spectral mixing solutions, as shown in Fig. 6A (Left). To ensure the selection of appropriate spectra for human studies, considerations were given to achieving white color and reasonable color rendering index.

As an example, we presented SPD-1, SPD-2 and SPD-3 in Fig. 6A (Right), which were calculated using the color mixing algorithm. These SPDs were white light ( $Duv = 0$ ), with color rendering index higher than 70 and equivalent photopic illuminance. Regarding the illuminance level for each photoreceptor, these SPDs exhibit equivalent values in terms of melanopic, rhodopic, chloropic and erythroptic illuminance, while their cyanopic illuminance values differ significantly. As a result, their relative circadian effects predicted by EML and CS models are completely different as shown in Fig. 6C. According to the EML model, these SPDs showed equivalent circadian effect (all EML = 200). However, based on the CS model, the spectral circadian efficacy experiences a significant drop from SPD-1 to SPD-2 (contrast:  $CL_{ASPD-1}/CL_{ASPD-2} = 2.3$ ), followed by an increase from SPD-2 to SPD-3 ( $CL_{ASPD-3}/CL_{ASPD-2} = 2.0$ ).

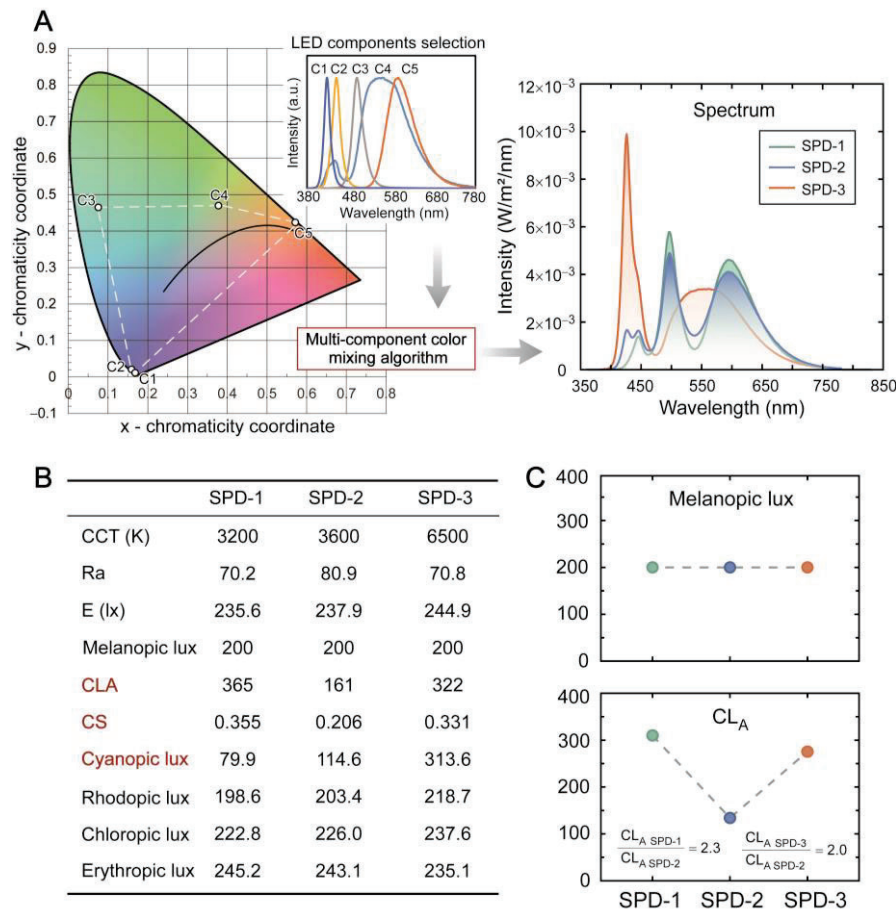


Figure 6. SPDs for accuracy comparison of circadian efficiency models based on multi-component color-mixing algorithm. (A) Left: the SPDs and color chromaticity coordinates of five LED components adopted in calculation. Right: three designed SPDs (SPD-1, SPD-2 and SPD-3) for explanation, (B) the corresponding visual and non-visual parameters of three SPDs, and (C) different relative circadian efficiency results to these three SPDs when based on melanopic illuminance and CS models.

## 5. Conclusion

In conclusion, our study demonstrated that the EML and CS models offer comparable descriptions of data from numerous previous studies, while photopic illuminance proved to be an unreliable predictor of melatonin suppression. Despite the complexity of CS models, they did not show better accuracy compared with the simpler EML model. Thus, the melanopic illuminance approach, which the EML model based on, would be a more reasonable approximation. Our findings also highlight the importance of using well-designed lighting spectra for comparison of circadian efficiency models. With our self-developed multi-component color mixing method, we are able to provide valuable experiment solutions in the form of SPDs, which could achieve large difference in circadian efficiency based on one model, while keep equivalent level by other models. This method could meet the requirements of general lighting, and be utilized to investigate the specific contributions of each photoreceptor in the human circadian pathway. Our

study provides important insights for in circadian efficiency model evaluation in indoor health lighting and light-related circadian researches.

## REFERENCE

- [1] Chang A. M, Aeschbach D. , Duffy J. F. , & Czeisler C. A. (2014). Evening use of light-emitting Ereaders negatively affects sleep, circadian timing, and next-morning alertness. *Proceedings of the National Academy of Sciences*, 112(4), 1232-1237.
- [2] Burns AC, Saxena R, Vetter C, Phillips AJK, Lane JM, Cain SW. Time spent in outdoor light is associated with mood, sleep, and circadian rhythm-related outcomes: a cross-sectional and longitudinal study in over 400,000 UK Biobank participants. *J Affect Disord*. 08 27, 2021.
- [3] Roenneberg T, Allebrandt KV, Merrow M, Vetter C. Social jetlag and obesity. *Curr Biol* 2012;22:939–43.
- [4] Scheer FAJL, Hilton MF, Mantzoros CS, Shea SA. Adverse metabolic and cardiovascular consequences of circadian misalignment. *Proc Natl Acad Sci U S A* 2009;106:4453–8.
- [5] Boubekri M, Cheung IN, Reid KJ, Wang CH, Zee PC. Impact of windows and daylight exposure on overall health and sleep quality of office workers: a case-control pilot study. *J Clin Sleep Med* 2014;10(6):603-611.
- [6] Provencio I, Rodriguez IR, Jiang G, et al. A novel human opsin in the inner retina. *J Neurosci*. 2000;20:600–605.
- [7] D.M. Berson, F.A. Dunn, M. Takao, Phototransduction by retinal ganglion cells that set the circadian clock, *Science* 295 (2002) 1070–1073.
- [8] Dacey DM, Liao H-W, Peterson BB, et al. Melanopsin-expressing ganglion cells in primate retina signal colour and irradiance and project to the LGN. *Nature*. 2005;433:749–754.
- [9] Czeisler CA and Klerman EB (1999) Circadian and sleep dependent regulation of hormone release in humans. *Recent Prog Horm Res* 54:97-132.
- [10] Zeitzer JM, Dijk DJ, Kronauer R, Brown E, Czeisler C (2000) Sensitivity of the human circadian pacemaker to nocturnal light: Melatonin phase resetting and suppression. *J Physiol* 526(Pt 3):695–702.
- [11] R. J. Lucas, S. N. Peirson, D. M. Berson, T. M. Brown, H. M. Copper, C. A. Czeisler, M. G. Figueiro, P. D. Gamlin, S. W. Lockley, J. B. O'Hagan, L. L.A. Price, I. Provencio, D. J. Skene, and G. C. Brainard, Measuring and using light in the melanopsin age, *Trends Neurosci*. 37 (2014) 1-9.
- [12] M. S. Rea, M. G. Figueiro, A. Bierman, and R. Hamner, Modelling the spectral sensitivity of the human circadian system, *Light. Res. Technol*. 44 (2012) 386-396.
- [13] R. J. Lucas et al., Diminished pupillary light reflex at high irradiances in melanopsin-knockout mice. *Science*. 299 (2003) 245–247.
- [14] J. J. Gooley et al., Spectral responses of the human circadian system depend on the irradiance and duration of exposure to light. *Sci. Transl. Med*. 2, 31ra33 (2010).
- [15] Circadian lighting design – WELL standard, <https://standard.wellcertified.com/light/circadian-lighting-design>, Accessed 8 February 2020.
- [16] CIE, "CIE System for Metrology of Optical Radiation for ipRGC-Influenced Responses to Light," 2018, doi: 10.25039/S026.2018
- [17] Rea MS, Figueiro MG, Bullough JD, Bierman A. A model of phototransduction by the human circadian system. *Brain Res Rev*. 2005;50(2):213-228.
- [18] M. G. Figueiro, A. Bierman, M. S. Rea, Retinal mechanisms determine the subadditive response to polychromatic light by the human circadian system, *Neurosci. Lett*. 438 (2008) 242-245.
- [19] Figueiro, M. G., Bullough, J. D., Parsons, R. H., and Rea, M. S. (2004). Preliminary evidence for spectral opponency in the suppression of melatonin by light in humans. *Neuroreport* 15, 313–316.
- [20] Rea MS, Nagare R, Figueiro MG. Modeling circadian phototransduction: retinal neurophysiology and neuroanatomy. *Frontiers in Neuroscience* 2021; 14: 615305.
- [21] G.C. Brainard, J.P. Hanifin, J.M. Greeson, B. Byrne, G. Glickman, E. Gerner, and M.D. Rollag, Action spectrum for melatonin regulation in humans: evidence for a novel circadian photoreceptor, *J. Neurosci*. 21 (2001) 6405-6412.
- [22] K. Thapan, J. Arendt, and D. J. Skene, An action spectrum for melatonin suppression: evidence for a novel non-rod, non-cone photoreceptor system in humans, *J. Physiol*. 535 (2001) 261-267.

- [23] Rea, M. S., Nagare, R., & Figueiro, M. G. (2021). Modeling Circadian Phototransduction: Quantitative Predictions of Psychophysical Data. *Frontiers in neuroscience*, 15, 615322.
- [24] Underwriters Laboratories Inc. Design Guideline for Promoting Circadian Entrainment With Light for Day-Active People, Design Guideline 24480, Edition 1. Report # DG 24480. Northbrook, IL: Underwriters Laboratories Inc., 2019.
- [25] Dai, Q, Huang, Y, Hao, L, Lin, Y, & Chen, K. (2018). Spatial and spectral illumination design for energy-efficient circadian lighting. *Building and Environment*, 146, 216-225.
- [26] Schlangen L, Belgers S, Cuijpers R, Zandi B, Heynderickx I. Correspondence: Designing and specifying light for melatonin suppression, non-visual responses and integrative lighting solutions – establishing a proper bright day, dim night metrology. *Lighting Research & Technology*. 2022;54(8):761-777.
- [27] Brown TM, Brainard GC, Cajochen C, Czeisler CA, Hanifin JP, Lockley SW, et al. (2022) Recommendations for daytime, evening, and nighttime indoor light exposure to best support physiology, sleep, and wakefulness in healthy adults. *PLoS Biol* 20(3): e3001571.
- [28] T.M. Brown, K. Thapan, J. Arendt, V.L. Revell, D.J. Skene, S-cone contribution to the acute melatonin suppression response in humans, *J. Pineal Res.* 71 (2021) 1–12.
- [29] V. L. Revell, D. J. Skene, Light-induced melatonin suppression in humans with polychromatic and monochromatic light, *Chronobiol. Int.* 24(2007) 1125-1137.
- [30] Revell VL, Barrett DC, Schlangen LJ, and Skene DJ (2010) Predicting human nocturnal nonvisual responses to monochromatic and polychromatic light with a melanopsin photosensitivity function. *Chronobiol Int* 27:1762-1777.
- [31] C. Papamichael, D. J. Skene, V. L. Revell, Human nonvisual responses to simultaneous presentation of blue and red monochromatic light, *J. Biol. Rhythms* 27(2012) 70-78.
- [32] R. P. Najjar, C. Chiquet, P. Teikari, P. L. Cornut, B. Claustrat, P. Denis, H. M. Cooper, C. Gronfier, Aging of non-visual spectral sensitivity to light in humans: Compensatory mechanisms? , *PLoS One* 9(2014) e85837.
- [33] R. Nagare, M. S. Rea, B. Plitnick, M. G. Figueiro, Effect of white light devoid of "cyan" spectrum radiation on nighttime melatonin suppression over a 1-h exposure duration, *J. Biol. Rhythms* 34(2019) 195-204.
- [34] R. Nagare, M. S. Rea, B. Plitnick, M. G. Figueiro, Nocturnal melatonin suppression by adolescents and adults for different levels, spectra, and durations of light exposure, *J. Biol. Rhythms* 34(2019) 178-194.
- [35] R. Nagare, B. Plitnick, M. G. Figueiro, Effect of exposure duration and light spectra on nighttime melatonin suppression in adolescents and adults, *Light. Res. Technol.* 51(2018) 530-543.
- [36] B. Wood, M. S. Rea, B. Plitnick, M. G. Figueiro, Light level and duration of exposure determine the impact of self-luminous tablets on melatonin suppression, *Appl. Ergon.* 44(2013) 237-240.
- [37] R. Nagare, B. Plitnick, M. G. Figueiro, Does the ipad night shift mode reduce melatonin suppression? , *Light. Res. Technol.* 51(2018) 373-383.
- [38] M. S. Rea, M. G. Figueiro, Light as a circadian stimulus for architectural lighting, *Light. Res. Technol.* 50(2016) 497-510.
- [39] M. G. Figueiro, M. S. Rea, A working threshold for acute nocturnal melatonin suppression from "white" light sources used in architectural applications, *J. Carcinogene. Mutagene.* 04(2013) 100150
- [40] G. C. Brainard, D. Sliney, J. P. Hanifin, G. Glickman, B. Byrne, J. M. Greeson, S. Jasser, E. Gerner, M. D. Rollag, Sensitivity of the human circadian system to short-wavelength (420-nm) light, *J. Biol. Rhythms* 23(2008) 379-386.
- [41] G. C. Brainard, J. P. Hanifin, B. Warfield, M. K. Stone, M. E. James, M. Ayers, A. Kubey, B. Byrne, M. Rollag, Short-wavelength enrichment of polychromatic light enhances human melatonin suppression potency, *J. Pineal Res.* 58(2015) 352-361.
- [42] K. E. West, M. R. Jablonski, B. Warfield, K. S. Cecil, M. James, M. A. Ayers, J. Maida, C. Bowen, D. H. Sliney, M. D. Rollag, J. P. Hanifin, G. C. Brainard, Blue light from light-emitting diodes elicits a dose-dependent suppression of melatonin in humans, *J. Appl. Physiol.* 110(2011) 619-626.

# EFFECT OF LUMINOUS ENVIRONMENT ON VISUAL PERCEPTION AND MOOD IN SUBMARINE ENCLOSED SPACE

Chenyao Zhao<sup>1</sup>, Yandan Lin<sup>1,2,3,4\*</sup>, Yixuan Zhao<sup>5</sup>

(<sup>1</sup>Institute for Electric Light Sources, School of Information Science and Technology, Fudan University, Shanghai 200438, China

<sup>2</sup>Institute for Six-sector Economy, Fudan University, Shanghai 200433, China

<sup>3</sup>Human Phenome Institute, Fudan University, Shanghai 201203, China

<sup>4</sup>Intelligent Vision and Human Factor Engineering Center, Shanghai 201306, China

<sup>5</sup>Guanghua Port Engineering Application Technology R & D (Shanghai) Co., Ltd.)

## ABSTRACT

The submarine is a typical military isolated and closed environment, its light environment is completely composed of artificial lighting, which can affect people's emotions and visual perception, and in turn affect their rest. Color and light are two important environmental factors of space. This study targets the submarine lounge and explore the impact of environmental color and light on mood and visual perception. A submarine lounge model cabin was builded for a realistic feeling, all participants expericed 8 light conditons (2 environment colors × 2 illuminances × 2 CCTs). The BRUMS mood scale and the visual-semantic difference scale were used to investigate if the environment color, illuminance and CCT would affect the emotional state and visual perception. The results showed that participants felt lower levels of tension, fatigue, and distress and higher level of vigour in the white walnut grain cabin with high illumination and CCT. High illuminance induces brighter perception and is attributed to create a lively and cozy atmosphere, high CCT induces cooler and brighter perception and also appears more lively. Moreover, participants seem to prefer bright environments. In the design of enclosed space, both light and environment color need to be considered. Among them, the illuminance seems to be more sensitive and more important.

Keywords: submarine cabin, color, illuminance, CCT, mood, visual perception

## 1. INTRODUCTION

The isolated and closed environment is an operating environment in remote areas with inconvenient transportation, limited communication, poor entertainment, and lack of social interaction[1], such as spacecraft, vessels, and remote islands. Submarine is a typical military isolated and closed environment, which has the characteristics of being far away from the base, self-supply, long-term closed, and extreme environment[2, 3]. During the voyage, the crew will be in the claustrophobic, confined and extreme environment for a long time, and due to the importance of mission objectives, they need to undertake a lot of high-intensity works, which causes them to accumulate so much fatigue that have to need a good rest. However, the submarine environment is very complex, the prominent factors such as narrow space, air pollution, continuous noise and lack of natural light continue to affect the rest of the crew, leading them to feel fatigue or tired[4]. Vgontzas AN et al. [5] conducted a survey of 143 U.S. Navy submariners who had served for more than one year and found that more than 45% of the sailors reported that they often, frequently, and always felt bodily or mental exhaustion, more than 60% of the crew said that they "rarely" or "never" felt energetic.

Compared with vessels, aircraft, and spacecraft, in few other places like a submarine are completely composed of artificial lighting and with a serious lack of natural light exposure, which may easily lead to a decrease in visual comfort and an increase in negative emotions, in turn cause psychological problems and affect work performance[6-8]. Liu et al.[9] found that submarine soldiers were the arm with the worst emotional state in the survey of various arms of the navy. Ma et al.[10] surveyed 103 submariners and found that more than 50% of the crew members responded to a significant increase in negative emotions in terms of psychologically affected choices. Therefore, when crew are constantly exposed to an inappropriate light environment during rest, the negative emotions such as anxiety and depression will be more



serious under a large amount of external/self pressure[11], which implies it is particularly important to provide a scientific and suitable light environment.

Light and color are two important attributes of an indoor light environment[12]. Past studies have shown that light can affect the nervous system such as the cerebral cortex and hypothalamus to produce changes in feelings, emotions, and psychology through visual and non-visual effects[13, 14]. Recent studies have shown that light-induced non-visual effects, intrinsically photosensitive retinal ganglion cells[15, 16], rod and cone photoreceptors[17, 18] all play a very important role. Illuminance and correlated color temperature (CCT) are two important factors to describe light. Under the same illuminance, low CCT (warm light) is more likely to produce positive emotions than high CCT (cold light), and the visual evaluation may be better; under the same correlated color temperature, low illuminance is more likely to reduce positive emotions than high illuminance[19-21]. Color is similar to light, and can also participate in the emotional and psychological adjustment process in the brain. Although everyone's favorite color is different, according to many research results, red has the strongest visual stimulation, blue and green are more comfortable colors, and white is considered insensitive and boring. In terms of regulating emotions, blue is considered refreshing, comfortable, calm, and harmonious, while some colors can cause anxiety, restlessness. In addition, researchers believe that individual differences (such as gender, age, culture, etc.) also affect emotional responses to colors[22-24]. Therefore, In order to provide the crew with a reasonable and comfortable rest environment, both light and color are important factors to be considered.

This paper studies the influence of cabin environment color and lighting on people's visual perception and emotion in a simulated submarine lounge, in order to obtain a light environment suitable for rest.

## 2. METHODS

### 2.1 Participants

In this experiment, 8 healthy males with work experience of ship (engineers, retired soldiers) were recruited as subjects, with an average age of 29 years ( $29 \pm 4.7$  years). All the subjects had a professional health examination in the hospital, showing good health, no gastrointestinal, nervous system, and cardiovascular diseases, normal corrected vision (uncorrected vision 4.6 or corrected vision 4.9 and above), no color blindness, Color weakness or other eye diseases.

### 2.2 Experiment environment

In order to simulate the real submarine rest environment, we built a 1:1 submarine lounge model cabin in the laboratory according to the real submarine cabin. The area of the simulation cabin is  $4.1\text{m} \times 2.5\text{m} \times 2.5\text{m}$ , and all the walls are painted white. The lounge is a comprehensive cabin that combines amusement and rest functions. The internal structure includes: three beds, a large conference table, a small folding table and several three-dimensional cabinets. The light source consists of two panel lights with adjustable illuminance and color temperature, which are embedded on the ceiling. The ichnography of the simulation cabin are shown in Figure 1. The subjects sat on the bed 1 and bed 2 and experienced different light environments.

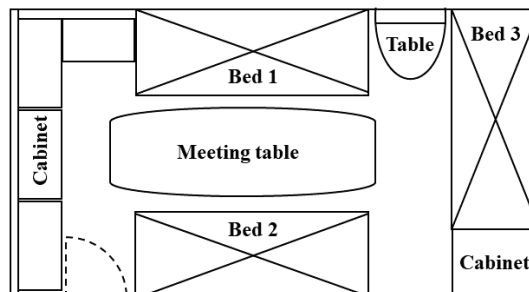


Figure 1. The ichnography of the simulation cabin

### 2.3 Color environment and light parameters

The light environment in the simulated cabin takes into account the two factors of environmental color and light. For the environmental color, two typical colors of interior decoration were designed: white walnut grain (56% reflectance) and black walnut grain (8% reflectance),



which were represented by WW and BW, respectively, as shown in Figure 2. Since the submarine is far away from the land, electricity is a very precious resource. In order to save electricity, the brightness of the lamps is generally lower. So for the light, it is divided into four light conditions according to two light parameters (illuminance and CCT), illuminance changes between 100 lx and 300 lx, which were represented by the character low (L) and high (H), respectively. CCT changes between 3000 K and 5500K, which were represented by the character warm (W) and cool (C), respectively. Therefore, the eight stimulated conditions are summarized in Table 1.



Figure 2. The schematic diagram white walnut grain (left) and black walnut grain (right)

Table 1. The details of eight stimulated conditions in this experiment.

Symbols	illuminance/lx	CCT/K
WW_L_L	99	2937
WW_L_H	109	5456
WW_H_L	297	2950
WW_H_H	301	5548
BW_L_L	100	2954
BW_L_H	110	5466
BW_H_L	299	2943
BW_H_H	318	5546

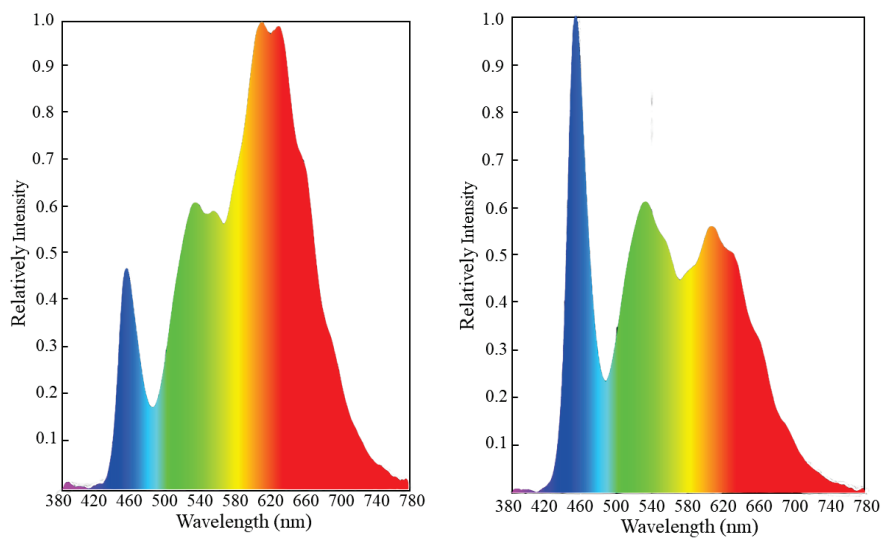


Figure 3. The spectral power distribution of 3000K (left) and 5500K (right).

## 2.4 Questionnaire

In this study, the BRUMS mood scale and the visual-semantic difference scale were used to investigate the emotional state and visual perception of the subjects. BRUMS The mood scale was proposed by Terry, Lane et al. It only contains 24 mood descriptors and can be completed in only 1-2 minutes. After being introduced into China, it was translated and revised. The revised BRUMS scale has 6 dimensions and 23 descriptors. The Cronbach's  $\alpha$  coefficient of each dimension is 0.71-0.84, the Cronbach's  $\alpha$  coefficient of the total table is 0.94, and the RMSEA is 0.064. Good reliability and validity. The Visual Semantic Difference Scale consists of 19 positive/negative word pairs in 3 dimensions selected from scales in 3 past studies (Vogels, Liu, Vienot). And Liu's scale is used as a reference for Chinese translation, and the Chinese and English sources of vocabulary pairs are shown in the table. The Brums Mood Scale uses a 5-point scale and the Visual-Semantic Difference Scale uses a 7-point scale.

## 2.5 Experiment procedure

The subjects were required to ensure at least 7-8 hours of sleep the night before the start of the experiment. First, the subjects entered the experimental room and underwent dark adaptation for 5 minutes, and then adjusted the illuminance and CCT to the experimental conditions. The subjects were asked to adapt to the light environment for 5 minutes, and then performed a 15-minute reading task. All books are science books, their content will not cause emotional changes. After reading, complete the Brums Emotion Scale and Visual Perception Semantic Difference Scale. Before experiencing the next light environment, the subjects are allowed to rest in dark for 5 minutes to avoid the influence of the previous light stimulus.

## 3. RESULTS

### 3.1 Mood state

Multivariate analysis of variance was used. Table 2 shows the impact of single variables and interaction of environmental color, illuminance and CCT on the mood state. The statistically significant differences are indicated by their p value. From the result, the tension was not only affected by environmental color, illuminance and CCT, but also by the interaction of environmental color \* CCT and illuminance \* CCT. The illuminance change has a significant effect on vigour, fatigue and depression. Moreover, the fatigue is also affected by CCT.

Table 2. the statistical difference of mood states at the variables changes

Mood	Tension	Vigour	Anger	Fatigue	Confusion	Depression
Environmental color	0.023					
Illuminance	< 0.001	0.003		0.001		0.004
CCT	< 0.001			0.003		
Environmental color * CCT	0.032					
Illuminance * CCT	0.016					

The statistically significant effect between variables and mood states are presented in Figure 4. For the environment color, the participants appear a higher tension level in the BW environment than to WW environment. For the illuminance, when illuminance increased from 100 lx to 300lx, the negative mood related to tension, fatigue and depression gradually decreased, whereas, the positive mood related to vigour increased. For the CCT, the tension and fatigue level were lower at cool light. From figure 4 (d), the tension mood was affected by the interaction of CCT and environment color, the participants had experienced a higher tension level in warm light, especially in the BW environment, and there was a significant difference of tension between cool and warm light in BW environment. However, the differences between cool and warm light in WW environment were not significant. As shown in figure 4 (e), the interaction of illuminance and CCT also has a statistically significant effect on tension mood, the low illuminance increased the tension level significantly in present of warm light, there was the lowest tension level in the high illuminance and high CCT. While in high illuminance, CCT changes did not have a significant effect.

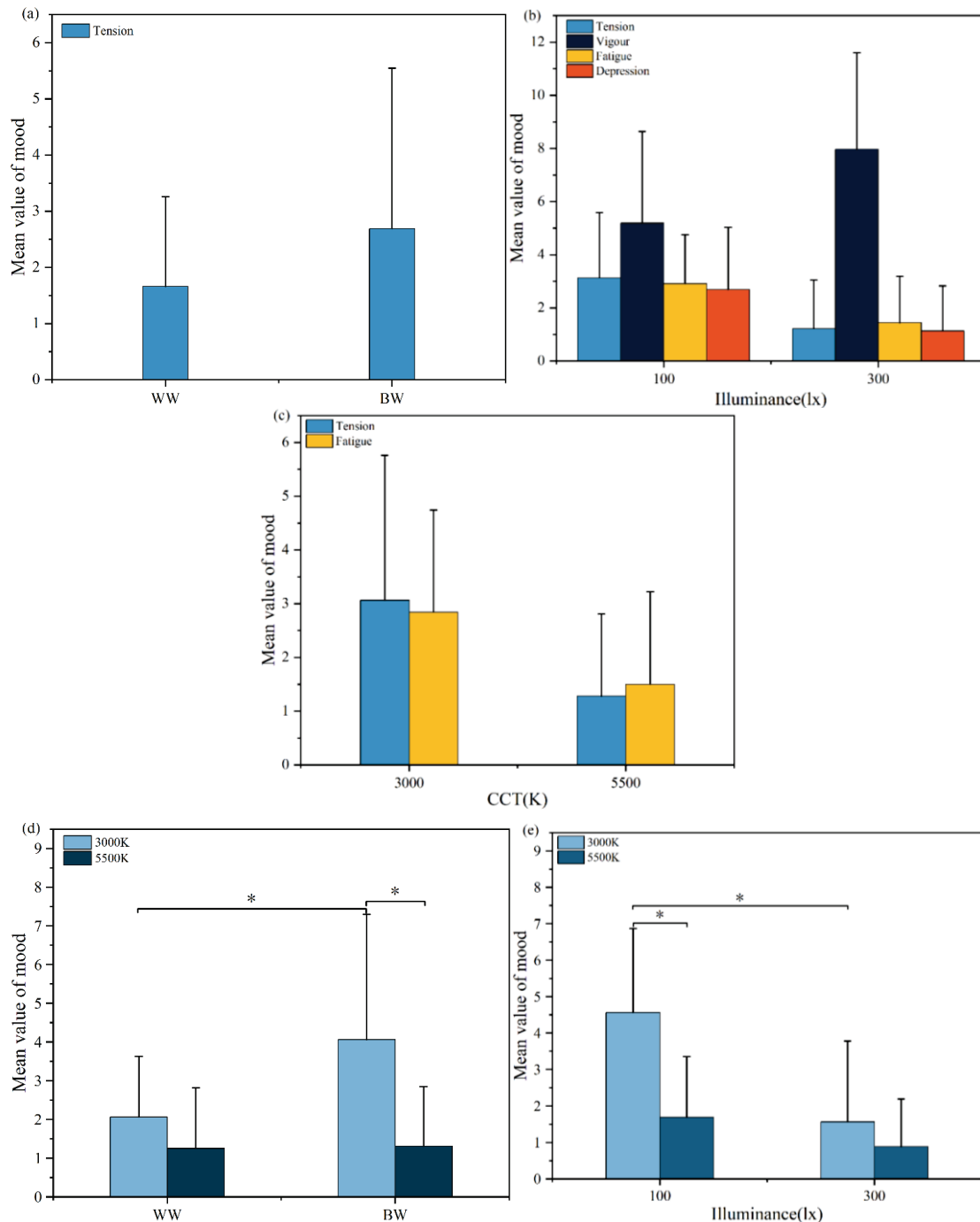


Figure 4. the main effect of (a) environment color, (b) illuminance, (c) CCT and the interaction effect of (d) environment color and CCT, (e) illuminance and CCT on mood.

The results demonstrated that environment color, illuminance and CCT all have a significant effect on mood states, especially tension mood. In addition to the main effect, there are both interaction effects of environment color and CCT or illuminance and CCT. The WW environment may be more appropriate due to lower tension level, there was a negative relationship of illuminance and negative mood, this trend was also found in CCT changes. Meanwhile, increasing illuminance leads to a higher vigour. The 300 lx and 5500 K condition has a lowest tension level.

### 3.2 Visual perception

In this experiment, a questionnaire with 3 dimensions (Lighting environment, Perception of atmosphere and Preference) was designed to study visual perception. Among them, perception of atmosphere consists of 14 scales. In order to explore the effect of variables on perception of atmosphere, factor analysis was used, the underlying factors of atmosphere terms was extracted

with principal component analysis and varimax orthogonal rotation. Table 3 lists the results of factor analysis. Two main factors are extracted and labelled as Factor 1 and 2, which account for 76.02% of total variance and has variance explained of 42.72% and 33.3%, respectively. We can see that the scales lifeless-lively, artificial-natural, informal-formal, tired-energetic, lethargic-arousing have the high loadings for Factor 1, while the high loadings on Factor 2 are related to the scale hostile-hospitable, dangerous-safe, tense-relaxed, terrifying-close. As shown in Figure 5, each scale was plotted on the Factor 1 versus Factor 2 diagram according to their factor loadings. It is clearly that the scales related to Factor 1 and Factor 2 are well separated from each other. By comparing the scales of factor with previous studies, we get similar dimensionality reduction results. Hence, Factor 1, associated with lively, energetic and arousing with high loading, was labelled as liveliness. Factor 2, related to cozy, hospitable and relaxed with high loading, was labelled as coziness. Therefore, these two underlying dimensions, liveliness and coziness, substituting for all the atmosphere scales can be used to describe the atmosphere perception. Finally, warmth (cool-warm), brightness (dim-bright), beauty (ugly-beautiful), favor (unlike-like), liveliness and coziness are employed for exploring the effect of light on visual perception in simulated color cabin.

Table 3. Factors coefficient matrix of atmosphere perception using 14 scales

Total variance: 76.02% Scales	Factor 1 42.72%	Factor 2 33.30%
Lifeless-Lively	<b>0.881</b>	0.232
Artificial-Natural	<b>0.866</b>	0.237
Informal-Formal	<b>0.838</b>	0.344
Tired-Energetic	<b>0.832</b>	0.347
Lethargic-Arousing	<b>0.816</b>	0.315
Blurred-Clear	<b>0.767</b>	0.418
Cabined-Spacious	<b>0.716</b>	0.487
Hostile-Hospitable	0.23	<b>0.884</b>
Dangerous-Safe	0.299	<b>0.825</b>
Tense-Relaxed	0.412	<b>0.775</b>
Terrifying-Close	0.209	<b>0.775</b>
Uncomfortable-Cozy	0.622	<b>0.634</b>
Depressed-Cheerful	0.466	<b>0.623</b>
Unpleasant-Pleasant	0.575	<b>0.59</b>

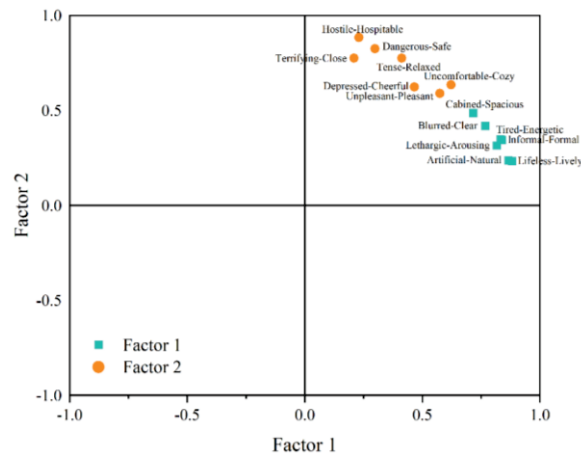


Figure 5. Factors plotted on the Factor 1 versus Factor 2 diagram.

Multivariate analysis of variance was used to study the effect of variables on the factors of visual perception including warmth, brightness, beauty, favor, liveliness and coziness. Table 4 shows the statistically significant differences of factors, which are demonstrated by p values. From the result, the illuminance level has a significant effect on spatial brightness perception, preference (Beauty and Favor) and atmosphere perception (Liveliness and Coziness). While only spatial warmth/brightness perception and liveliness are significantly affected when CCT changes occur, the CCT level doesn't affect preference. The reason that environment color isn't listed in Table 4 is that it doesn't have a significant effect on 6 factors.

The two main factors, liveliness and coziness, are characterized by the mean value of 7 scales, respectively. The effects of different illuminance and CCT level on the visual perception are demonstrated in Figure 6. When the illuminance changes, for spatial brightness perception, the participants felt brighter at a higher illuminance. For preference, a higher score implied that participants think the light looks better and like it more, significantly 300 lx light is more popular. For liveliness, the atmosphere was perceived as livelier when the illuminance increased. For coziness, it is similar that coziness is related to the trend of illuminance change, the participants felt cozier at 300 lx. When the CCT changes, for spatial warmth perception, the higher CCT induced relatively colder feeling, while for spatial brightness perception, perceived brightness alters in a opposite way, the score of brightness is higher at high CCT, which indicates a brighter lighting. For liveliness, the participants tend to perceive a livelier atmosphere under a higher CCT level. Variation in CCT do not have a significantly effect on preference and coziness factor.

Table 4. the statistical difference of factors of visual perception at the variables changes.

	Warmth	Brightness	Beauty	Favor	Liveliness	Coziness
Illuminance		0.001	0.001	0.001	0.001	0.001
CCT	0.001	0.013			0.016	

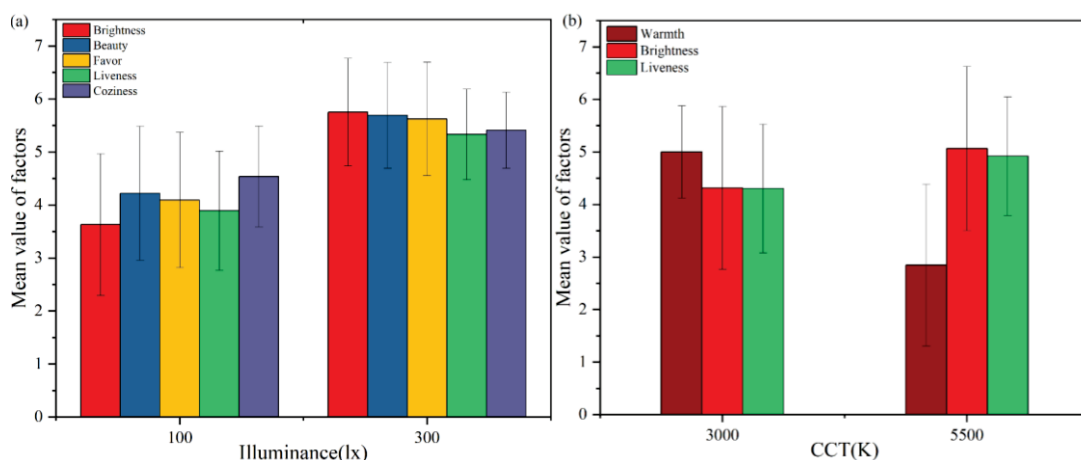


Figure 6. effect of Illuminance(a) and CCT(b) changes on the warmth, brightness, beauty, favor, liveliness and coziness factors.

#### 4. CONCLUSION

This study investigated the effect of environment color and lighting on mood states and visual perception. Illuminance and CCT as two critical factors significantly affect many parameters of mood and visual perception, the environment color also has a certain effect on tension and there are also two interaction effects. the participants experienced lower negative moods (tension, fatigue, depression) and a higher positive mood (vigour) in a higher illuminance and CCT environment. For visual perception, the two main factors characterizing atmosphere perception, liveliness and coziness, were obtained by principal component analysis. The high illuminance appears a more lively and cozy environment, the participants prefer a brighter feeling. The high CCT also appear a more lively environment. suggesting that brightness may be a more important factor to consider in the design of light environment in submarine non-operating cabin due to its reflection on the atmosphere perception and preference evaluation.

In the further work, more color, illuminance and CCT need to be studied. In submarine, crew's Circadian rhythm and sleep quality are both very important, and the effect of light on these two physiological parameters is also the focus of future research

#### REFERENCES

- [1] Tu Z, Li H, He J, et al. Application feasibility of sociometric badges in team studies of military isolated and confined environments[J]. Acad J Sec Military Med U, 2021,42:916-21.
- [2] Chabal S, Welles R, Haran FJ, et al. Effects of sleep and fatigue on teams in a submarine environment[J]. Undersea Hyperbar M, 2018,45:257-72.
- [3] Weng ZX, Wei LZ, Song J, et al. Effect of Enclosed Lighting Environment on Work

- Performance and Visual Perception. 2020 17th China International Forum on Solid State Lighting & 2020 International Forum on Wide Bandgap Semiconductors China (SSLChina: IFWS)[C], 2020.
- [4] Trousselard M, Leger D, van Beers P, et al. Sleeping under the Ocean: Despite Total Isolation, Nuclear Submariners Maintain Their Sleep and Wake Patterns throughout Their Under Sea Mission[J]. Plos One, 2015,10.
  - [5] Vgontzas AN, Zoumakis E, Bixler EO, et al. Adverse effects of modest sleep restriction on sleepiness, performance, and inflammatory cytokines[J]. J Clin Endocr Metab, 2004,89:2119-26.
  - [6] Canazei M, Pohl W, Bliem HR, et al. Artificial skylight effects in a windowless office environment[J]. Build Environ, 2017,124:69-77.
  - [7] Laurentin C, Bermtto V, Fontoynt M. Effect of thermal conditions and light source type on visual comfort appraisal[J]. Lighting Res Technol, 2000,4:223-33.
  - [8] Van Cutsem J, Abeln V, Schneider S, et al. The impact of the COVID-19 lockdown on human psychology and physical activity; a space analogue research perspective[J]. Int J Astrobiol, 2022,21:32-45.
  - [9] Liu C, Wang Z, Wu G. A study of the mental health status of military personnel under settings of special military operations[J]. Med J Chin PLA, 2003,28:597-8.
  - [10] Ma Q, Wang J, Chen X, et al. Influence of submarine environment on submariners' operational performance[J]. Mil Med Sci, 2020,6:406-9.
  - [11] Kuller R, Ballal S, Laike T, et al. The impact of light and colour on psychological mood: a cross-cultural study of indoor work environments[J]. Ergonomics, 2006,49:1496-507.
  - [12] Savavibool N. The Effects of Colour in Work Environment: A systematic review[J]. Enviro-Behav Proc J, 2016,1:262-70.
  - [13] Hou DD, Lin CX, Lin YD. Diurnal Circadian Lighting Accumulation Model: A Predictor of the Human Circadian Phase Shift Phenotype[J]. Phenomics, 2022,2:50-63.
  - [14] Yan L, Lonstein J S, Nunez A A. Light as a modulator of emotion and cognition: Lessons learned from studying a diurnal rodent[J]. Horm Behav, 2019,111:78-86.
  - [15] Berson DM, Dunn FA, Takao M. Phototransduction by retinal ganglion cells that set the circadian clock[J]. Science, 2002,295:1070-3.
  - [16] Richter CP. Psychopathology of periodic behavior in animals and man. Proceedings of the annual meeting of the American Psychopathological Association[C]. 1967,55:205-227.
  - [17] Moore RY, Speh JC, Card JP. The Retinohypothalamic Tract Originates From A Distinct Subset Of Retinal Ganglion-Cells[J]. J Comp Neurol, 1995,352:351-66.
  - [18] Takahashi Y, Katsuura T, Shimomura Y, et al. Prediction Model of Light-induced Melatonin Suppression[J]. Lighting Res Technol, 2011,35:123-35.
  - [19] Zhou L, Fu TY, Miao WQ, et al. Lighting Intervention with Different Colors on Emotion: A Bayesian Network Meta-Analysis. 19th China International Forum on Solid State Lighting / 8th International Forum on Wide Bandgap Semiconductors (SSLCHINA) (IFWS)[C], 2022.
  - [20] Te Kulve M, Schlangen L, Schellen L, et al. Correlated colour temperature of morning light influences alertness and body temperature[J]. Physiol Behav, 2018,185:1-13.
  - [21] Ru Tt, De Kort Y, Smolders K, et al. Non-image forming effects of illuminance and correlated color temperature of office light on alertness, mood, and performance across cognitive domains[J]. Build Environ, 2019,149:253-63.
  - [22] Shahidi R, Golmohammadi R, Babamiri M, et al. Effect Of Warm/Cool White Lights on Visual Perception and Mood in Warm/Cool Color Environments[J]. Excli J, 2021,20:1379-93.
  - [23] Kurt S, Osueke K K. The Effects of Color on the Moods of College Students[J]. SAGE Open, 2014.
  - [24] Savavibool N, Moorapun C. Effects of Colour, Area, and Height on Space Perception. 3rd Association-of-Behavioural-Researchers-on-Asians (ABRA) International Conference on Quality of Life (AQoL)[C]. 2017,2:351-9.

## ACKNOWLEDGEMENTS

Corresponding Author Name: Yandan Lin

Affiliation: Institute for Electric Light Sources, School of Information Science and Technology, Fudan University

e-mail: ydlin@fudan.edu.cn



# TEST GUIDANCE FOR 'U ZERO' CLASSIFICATION OF OUTDOOR LUMINAIRE ACCORDING TO IES LM-75-19

Jun-Seok, Oh, Hee-suk Jeong, Eun-cheol Jeong, Minkyu-Kang, Hyo-seok Oh  
(KIEL Institute, Bucheon-si, Gyeonggi-do, Republic of Korea)

## ABSTRACT

Recently, the design of light distribution pattern emitted by fixture becomes very important issue regarding light pollution. In particular, 'uplight light pollution', which is directed upward at night, makes people feel uncomfortable. For the prevention of light pollution, IES TM-15-11 requires that a luminaire with an uplight rating of U0 emits zero lumen into the upper hemisphere. Lighting manufacturers are developing and evaluating their products to achieve U0 rating. However, there is a limit to measure '0' value due to the measurement configuration of indoor environment. This study therefore introduces a measurement guide to solve this problem.

Keywords: UGR, Zero Uplight, Light Pollution

## 1. INTRODUCTION

The luminaire shown in Figure 1 is designed to emit light only inside the enclosure. This type of luminaire is not capable of emitting lights in the angle over 90 degrees in the vertical direction. However, a positive measured value (non-zero) can be obtained at 90 degrees or higher of the vertical angle due to the stray light when a measurement is conducted using a light distributor. For this reason, the luminaire cannot be classified as 'U0' according to IES TM-15-11[1]. Therefore, in this study, a method is proposed to prevent non-zero value appearing at an angle of 90 degrees or more in the vertical direction due to the stray light.

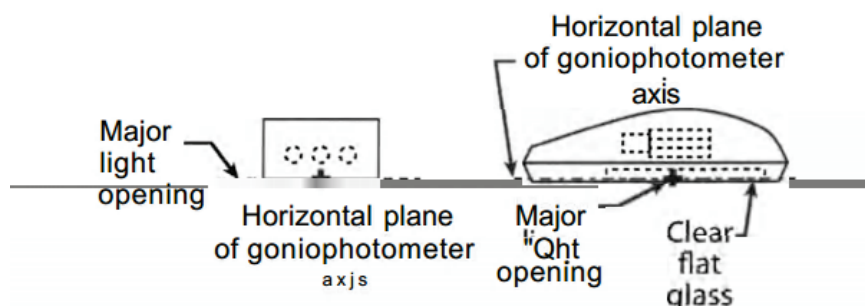


Figure 9-2. Luminaire with horizontal flat light-emitting opening.

Figure 1. The luminaire with horizontal flat light-emitting opening illustrated in IES LM-75-19[2]

## 2. METHODS

The following requirements are proposed for an actual implementation in order to make 'zero' of the stray light measured at 90 degrees or higher of the vertical angle.

A cylinder shall be prepared with a halogen lamp as defined in the specification of IES LM-79-19[3]. This cylinder should have a structure that does not emit light above 90 degrees of vertical angle. The lamp should be fixed inside the cylinder and the light distribution is then measured. The zonal lumen value of upper-light is checked whether this value is less than 1.0% of the total luminous flux value. This is **the first condition** which should be fulfilled. The usage of light trap, baffle, and matte black finishing material is recommended to minimize stray light.

The distribution of stray light is measured using the black material mask at the measurement setting condition described in the previous paragraph. It should be verified after the correction of the stray light that the zonal lumen value for the upper-light emitted at 90 – 180 degrees of vertical

angle is less than 0.1 % of the total luminous flux. This is **the second condition** which should be satisfied.

If **the first (< 1.0 %) and second (< 0.1 %) conditions** about the measured zonal lumen value for the upper-light are satisfied, a luminaire with the zonal lumen value less than 0.25 % of the total luminous flux can be achieved 'U0' rating. This is because the zonal lumen value measured from the upper-light emitted at 90 – 180 degrees of vertical angle can be assumed to be zero.

Here is what we should keep in mind. The negative value of the luminous intensity generated in the subtraction of the stray light shall be handled according to the following cases.

- To maintain negative value of the luminous intensity when used to calculate luminous flux
- To convert to zero value when representing an angular luminous intensity distribution

The following statement should be written on the test report:

**[The device under test emits no detectable upper-light, as defined by ANSI/IES LM-75-19]**

**[For the purpose of this report, certain non-zero upper-light readings have been assigned zero value, in accordance with the requirements of ANSI/IES LM-75-19]**

The following statement should be added to the IES form header code:

**[OTHER] The reported results were measured in a facility that meets the requirements of ANSI/IES LM-75-19. The device under test emits no detectable upper-light, as defined by ANSI/IES LM-75-19.**

### 3. CONCLUSION

**Table 1. Summary of Test Results**

Photometric Items	Unit	Detection threshold analysis		
		Uplight Measurement without stray light correction	Uplight Measurement with stray light correction	
			Stray Light	Corrected
Total Luminous Flux	lm	4456.74	78.7	4378.04
Zonal Luminous Flux (90 – 180 degree)	lm	4.72	0.86	3.86
	%	0.11	N/A	0.09
IES LM-75 Required	%	< 1.0	N/A	< 0.1
Input Voltage	V	120.9 VAC	120. 876 VAC	-
Input Current	A	4.2417 A	4.2322 A	-
Input Power	W	512.834 W	511. 580 W	-

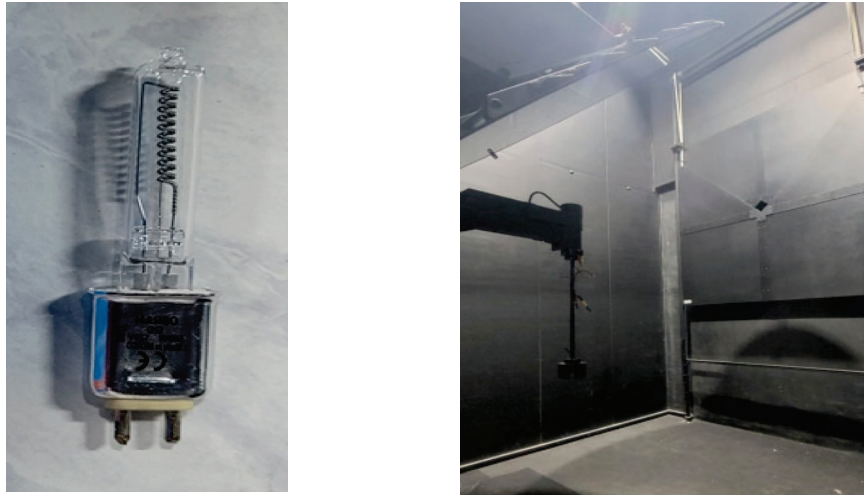


Figure 1. Tungsten Halogen Lamp(Left) and Goniometer(Right)

#### REFERENCE

- [1] IES TM-15-11, 2011, Luminaire Classification System for Outdoor Luminaires
- [2] IES LM-75-19, 2019, Approved Method: Guide to Goniometer Measurements and Types, and Photometric Coordinate Systems
- [3] IES LM-79-19, 2019, Optical and Electrical Measurements of Solid-State Lighting Products

#### ACKNOWLEDGEMENTS

Corresponding Author Name: Oh Jun-Seok

Affiliation: KIEL Institute

e-mail: ojunsuk@kiel.re.kr

# HOW TO LIGHT UP A PLANE UNIFORMLY USING TWO ROWS OF LUMINAIRES

Xingwu Chu

(Guangzhou Xiaoxing Design Ltd., Guangzhou, China)

## ABSTRACT

We hope to light up a plane uniformly using two rows of luminaires in some lighting design projects. Firstly, we will study the aim theoretically. Secondly, we solve it using mathematical tools. Lastly, a numerical example will be shown.

Keywords: Wall wash luminaire, Average illuminance, Uniformity ratio of illuminance  $U_0$

## 1. INTRODUCTION

It is difficult to light up a plane uniformly using a single row of luminaires, as the illumination decreases rapidly with increasing distance. But two rows of luminaires can complement each other, making the illumination on the plane more uniform. Our aim is to achieve the ratio of minimum average illuminance up to 0.95.

## 2. ANALYSIS

Axisymmetric light distribution with simple LED lens and processing high light output efficient luminaires is selected.

If we can make the illuminance generated by a single side luminaire decay linearly with distance, then the illuminance generated by two side luminaires with the same light distribution must be a constant value. To simplify the problem, we accurately align the centreline of the light axis of the luminaire with the farthest end of the illuminated surface. The cross-sectional view of the calculation model is shown in Figure 1.

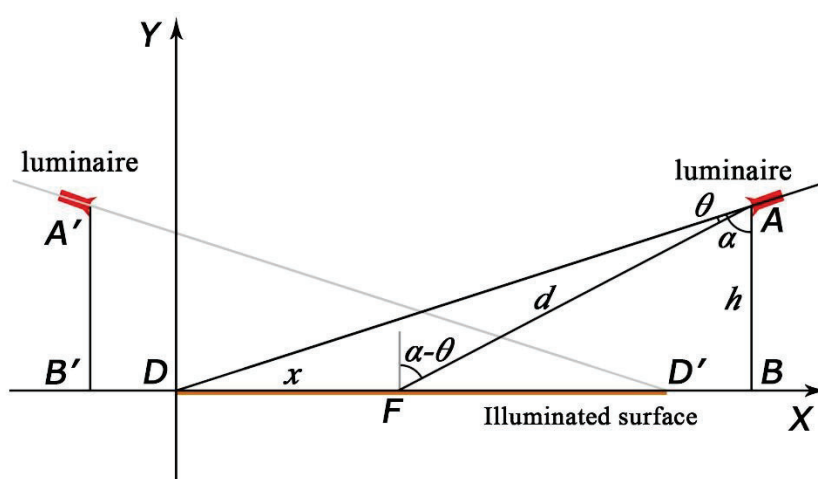


Figure 1. Section drawing of calculation model

We know that the formula for calculating the horizontal illumination generated by the luminaire at point A on any point F of the illuminated surface is:

$$E(\theta) = \frac{I(\theta)\cos(\alpha - \theta)}{d^2} = \frac{I(\theta)\cos^3(\alpha - \theta)}{h^2} \quad (1)$$

Where,

$I(\theta)$ : Light intensity the angle  $\theta$  of the centreline with the light axis of the luminaire.

$d$ : The distance between point A and point F.

$h$ : Vertical height difference between point A and the illuminated surface.

In order to achieve the goal of "making the illuminance generated by a single side luminaire linearly decay with distance" mentioned earlier, that is, the illuminance value increases linearly with the increase of  $x$  in Figure 1, we construct a light intensity function:

$$I(\theta) = \frac{k(bx + c)}{\cos^3(\alpha - \theta)} = \frac{k(bh(\tan\alpha - \tan(\alpha - \theta)) + c)}{\cos^3(\alpha - \theta)} \quad (2)$$

$$0 \leq \theta \leq \alpha$$

The above equation has three coefficients  $k$ ,  $b$ , and  $c$ . Among them,  $k$  is the light intensity scaling coefficient, which will be determined by the efficiency of the luminaire. To determine the relationship between two coefficients  $b$  and  $c$  of a linear function, let's find the first derivative of variable  $\theta$  for the equation above.

$$\frac{dI(\theta)}{d\theta} = \frac{kbh}{\cos^5(\alpha - \theta)} - \frac{3k\tan(\alpha - \theta)(bh(\tan\alpha - \tan(\alpha - \theta)) + c)}{\cos^3(\alpha - \theta)} \quad (3)$$

Make the derivative value equal to zero at  $\theta = 0$ , so that the light intensity function (2) is smooth at  $\theta = 0$ . That is, the tangent of the curve of the light intensity function (2) at its maximum value is a horizontal line. We obtained:

$$c = \frac{bh}{3\sin\alpha\cos\alpha}$$

### 3. NUMERICAL EXAMPLE

The transverse cross-section of a pedestrian bridge is shown in Figure 2. Two rows of luminaires are arranged at a height of 0.75 meters on both sides of the handrail to light up the bridge deck uniformly.

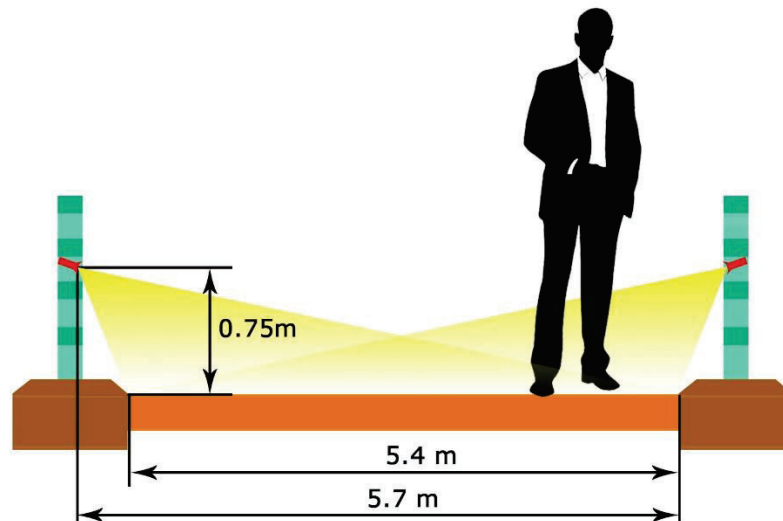


Figure 2. Section drawing of bridge

The main design parameters of calculation example are as Table 1.

Table 1. Main design parameters of calculation example

Item	Design parameter
Maintenance factor	0.8
Distance between luminaires	0.5 m
Lamp power	2.0w
Luminous Flux of one lamp	200.0 lm
Luminaire efficiency	72%
Width of calculation plane	7.5 m

$$\alpha = \tan^{-1}\left(\frac{5.7}{0.75}\right) \approx 82.5^\circ$$

In this example, the value of  $b$  is taken as 1.00.

$$c = \frac{0.75}{3 \sin \alpha \cos \alpha} \approx 1.932$$

Therefore, the light intensity function:

$$I(\theta) = \frac{k(0.75(5.7/0.75 - \tan(82.5^\circ - \theta)) + 1.932)}{\cos^3(82.5^\circ - \theta)} = \frac{k(7.632 - 0.75 \tan(82.5^\circ - \theta))}{\cos^3(82.5^\circ - \theta)}$$

When the efficiency of the luminaire is 72%, it is calculated that:

$$k = 1.3211$$

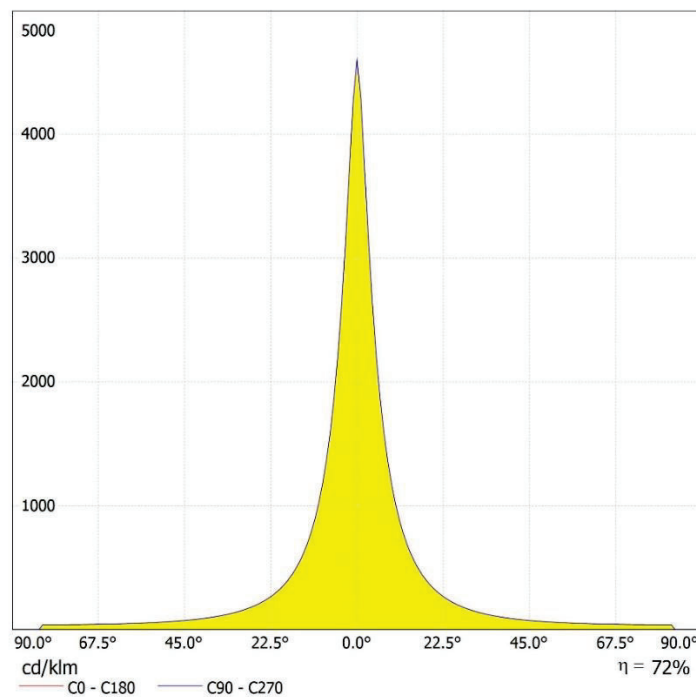


Figure 3. Light intensity distribution curve of luminaire



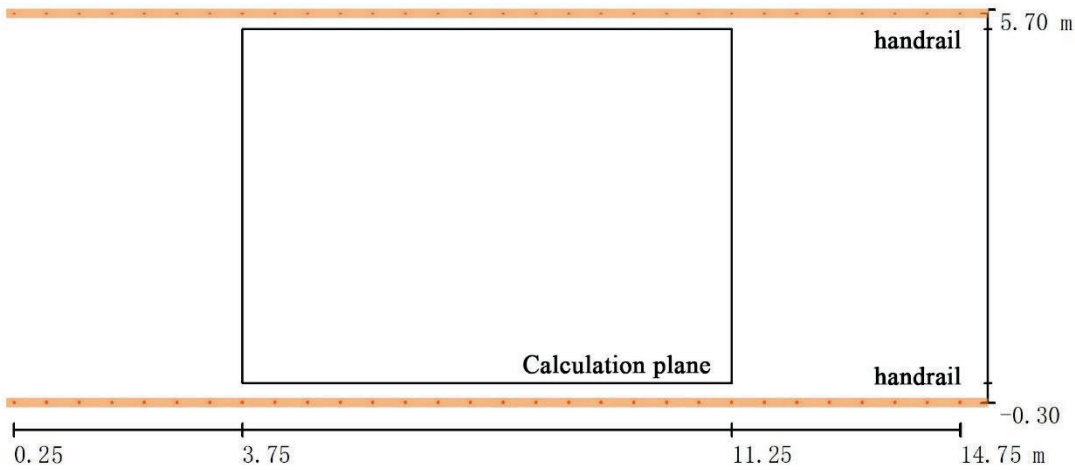


Figure 4. Location of calculation plane

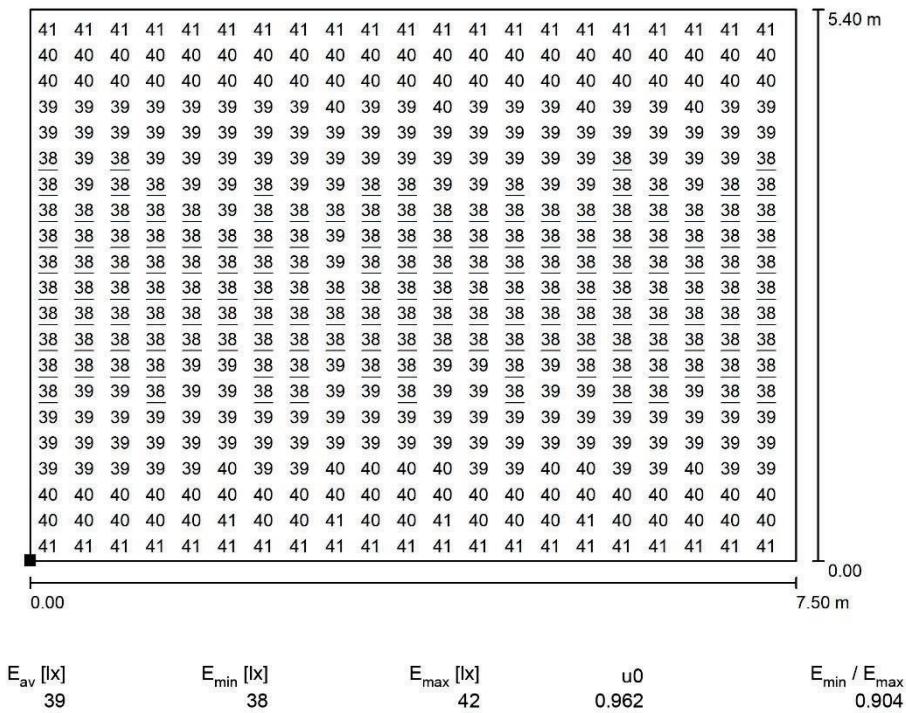


Figure 5. Illumination values of calculation plane

4. IES DOCUMENT

- IESNA:LM-63-2002
- [TEST]
- [TESTLAB]
- [MANUFAC]
- [LUMCAT]

[LUMINAIRE]20220605-3

[LAMP] LED

[BALLAST] N/A

[ISSUE DATE] 200304

[OTHER] B-Angle = 0.00 B-Tilt = 0.00

TILT=NONE

2 100.00 0.80 93 1 1 2 0.010 0.010 0.010

1.0 1.0 2.00

0.00 1.00 2.00 3.00 4.00 5.00 6.00 7.00 8.00 9.00 10.00

11.00 12.00 13.00 14.00 15.00 16.00 17.00 18.00 19.00 20.00

21.00 22.00 23.00 24.00 25.00 26.00 27.00 28.00 29.00 30.00

31.00 32.00 33.00 34.00 35.00 36.00 37.00 38.00 39.00 40.00

41.00 42.00 43.00 44.00 45.00 46.00 47.00 48.00 49.00 50.00

51.00 52.00 53.00 54.00 55.00 56.00 57.00 58.00 59.00 60.00

61.00 62.00 63.00 64.00 65.00 66.00 67.00 68.00 69.00 70.00

71.00 72.00 73.00 74.00 75.00 76.00 77.00 78.00 79.00 80.00

81.00 82.00 83.00 84.00 85.00 86.00 87.00 88.00 89.00 90.00

90.50

180.00

0.00

1149.6484 1069.2371 925.6417 782.6536 657.7886

553.6164 468.1298 398.2707 341.0936 294.0926

255.2365 222.9124 195.8492 173.0462 153.7140

137.2270 123.0870 110.8949 100.3289 91.1283

83.0803 76.0105 69.7749 64.2541 59.3486

54.9749 51.0629 47.5531 44.3951 41.5459

38.9686 36.6316 34.5075 32.5728 30.8067

29.1915 27.7116 26.3530 25.1040 23.9537

22.8928 21.9131 21.0071 20.1682 19.3907

18.6692 17.9991 17.3762 16.7967 16.2572

15.7547 15.2863 14.8497 14.4424 14.0626

13.7082 13.3777 13.0695 12.7822 12.5146

12.2654 12.0336 11.8183 11.6186 11.4336

11.2628 11.1054 10.9608 10.8285 10.7081

10.5990 10.5009 10.4134 10.3363 10.2692

10.2121 10.1645 10.1264 10.0978 10.0783

10.0681 10.0670 10.0751 0.0000 0.0000  
0.0000 0.0000 0.0000 0.0000 0.0000  
0.0000 0.0000 0.0000

## REFERENCE

- [1] Xingwu Chu, Lighting and Mathematics, The 5<sup>th</sup> Lighting Conference of China, Japan and Korea, 2012.8, Tokyo, Japan.
- [2] Architectural Lighting Design Standards: GB50034-2013[S], 2014. 4, China Construction Industry Press (In Chinese).

Corresponding Author: Xingwu Chu  
Affiliation: Guangzhou Xiaoxing Design Ltd.  
e-mail: 553043027@qq.com

# The effect of illumination color temperature on visual fatigue in VDT working environment

Given name Family name: Zheng dong, Li

Affiliation: Chongqing University

## abstract

In the environment where the visual display terminal ( VDT ) and the surrounding environment are used as the visual operation surface, 15 subjects were randomly assigned to three groups : low color temperature ( 3000K ), medium color temperature ( 5000K ) and high color temperature ( 7000K ). In the experimental environment, visual operations such as Landau ring recognition and visual classification tasks were performed, and subjective evaluation questionnaires were filled out and physiological indicators were measured to study the effect of illumination color temperature on visual fatigue under certain VDT characteristics. The results showed that the subjective fatigue and eye discomfort of the subjects in the high color temperature environment were significantly higher than those in the low color temperature and medium color temperature environment. Among them, the work efficiency and visual comfort of the subjects under low color temperature light source are the highest, but the lower limit threshold of color temperature remains to be further studied.

Keys: VDT operation, Visual fatigue, Color temperature of light, Simulation experiment

## 1 Introduction

With the development of science and technology, people's exposure time to digital reading media has gradually increased. In the results of the 17th national reading survey conducted by the China Press and Publication Research Institute, the national exposure rate to digital reading media was 79.3% in 2019, and the daily cell phone exposure time per adult was 100.41 minutes. Digital reading has replaced traditional paper-based reading media to dominate people's daily reading. Along with the massive popularity of VDT reading, a number of health problems have come to the fore, including a variety of symptoms related to excessive eye use and musculoskeletal disorders. <sup>[1-2]</sup> Among them, the most significant problems include visual fatigue, blurred vision, burning sensation in the eyes, and deficient color perception. The results of the study surface that work content, workload, and environmental requirements are the main factors that affect the perception of VDT reading and thus cause eye health problems. Among the environmental factors, the color temperature of the lighting environment directly affects the visual effect, mood, and fatigue of people who generate behavioral activities in the space. About lighting color temperature, the International Commission on Illumination (CIE) No. 158 document pointed out that different color temperatures lead to differences in the spectrum will have an impact on human efficiency and health. China's "Architectural Lighting Design Standards" also stipulates the relevant color temperature range of the color table characteristics that should be used in office premises. Today, when VDT reading is fully popular, how to make

environmental color temperature selection and consider the appropriate color temperature range to adapt to the new reading habits and eye behavior is a necessary choice to improve work efficiency and create a healthy indoor environment. In this paper, a laboratory experimental method was used to investigate the effect of color temperature selection on the visual fatigue of VDT reading behavior personnel.<sup>[3]</sup>

## **2 Experiment Overview**

Based on the relevant parameters determined through literature reading, optical experiments are designed and the experimental space is set up. The following is a description of the experimental space, experimental objects, measurement methods and experimental instruments.<sup>[4]</sup>

### **(1) Experimental subjects**

In this experiment, 15 school students were selected as subjects. The subjects were in good health, without symptoms of red-green color blindness, color weakness, corrected visual acuity of 4.8 or above and without hearing weakness, heart disease and other diseases. The subjects were required to get enough sleep, eat properly, avoid drinking alcohol, maintain emotional stability, and avoid stress and anxiety during the experiment.

### **(2) Experimental space**

In order to reduce the interference of external ambient light, the experiment chose to close the indoor space, indoor ceiling for white gypsum board, the walls are painted with white latex paint. <sup>[5]</sup>And in the indoor set up blackout curtains and sliding blackout panels surrounding the experimental area, the indoor space is divided into two areas, the experimental area outside the observation area. The experimental controller observed the state of the subject outside the experimental area throughout the experiment to reduce interference. The space was completely closed during the experiment to create a fully illuminated environment.

The experimental work surface was selected as an ordinary desk with a wood-like surface, the standard value of illumination was 500lx, and the ambient background illumination was set to 100lx.

### **(3) Visual fatigue measurement indexes**

The experimental measurement indexes include two categories: The first. Physiological indexes. Heart rate was obtained by the photoelectric volumetric pulse tracing method, measured by wearing an infinite pulse sensor.<sup>[6]</sup> Second, objective measurement indexes: the international standard logarithmic visual acuity scale was selected for visual acuity testing. The purpose of the visual acuity test is to evaluate the subject's object recognition ability, and compare the recognition ability of the subject before and after the experiment, the greater the difference, the more serious the degree of visual fatigue, and vice versa to a lesser extent.

## **3 Experimental procedure**

The experiment was conducted in April, and the time period chosen was 8:30-12:00. 20 subjects were divided equally into three groups of five each and tested under a color temperature lighting environment of 3000K, 5000K, and 7000K, respectively. And data were collected for each subject at the end of the test. After entering the experimental environment,

the subjects sat still for 5 min to adapt to the lighting environment, and wore a pulse sensor during this period, and performed visual acuity tests after the sitting. The test results were analyzed for stability and confirmed to be correct before entering the experimental phase. During the experiment, the subject adjusted to the state and started the test, including the visual test tasks such as Landauer's cycle and visual classification. The task duration lasted thirty minutes through and the visual acuity test was performed immediately after the end. The brightness of the display screen was constant during the experiment, and subjects were allowed thirty minutes without long-term eye closure and other fatigue-relieving activities.

#### 4 Experimental results and analysis

The experimental data were collected and organized, and the ECG data were processed as follows: moderate wavelet noise reduction was selected to remove white noise; passband filtering from 0.5 to 20 Hz was selected: mean correction was taken for singularities. After processing, 15 sets of data were collected from 15 subjects, and the signal acquisition was complete and the heart rate values were normal in all fifteen sets of data.

Figure 1 7000K color temperature environment experimental data statistics results

No.	Pre	Post	Heart rate /bpm									
1	5.1	5.0	70	75	74	83	71	71	69	73	74	80
2	5.1	5.0	74	76	77	73	75	74	76	80	72	75
3	5.0	4.9	64	65	70	66	64	66	66	63	61	61
4	5.0	4.9	72	68	70	71	75	68	73	71	73	76
5	5.0	4.8	62	66	63	62	61	63	65	70	63	67

Figure 2 5000K color temperature environment experimental data statistics results

No.	Pre	Post	Heart rate /bpm									
6	5.1	5.1	70	73	74	76	72	73	78	75	72	73
7	5.1	5.1	74	76	75	74	75	74	76	74	72	75
8	5.1	4.9	64	71	70	66	68	72	72	75	73	70
9	5.0	5.0	72	76	72	74	74	71	70	71	69	72
10	4.9	4.8	62	66	63	61	64	66	62	65	61	64

Figure 3 3000K color temperature environment experimental data statistics results

No.	Pre	Post	Heart rate /bpm									
6	5.1	5.1	70	73	73	76	75	74	75	76	77	73
7	5.1	5.1	74	70	68	69	74	73	70	72	70	69
8	5.0	5.0	64	71	70	70	71	72	72	71	73	75
9	4.9	4.9	72	76	75	74	74	77	73	72	73	74
10	4.9	4.9	62	64	65	63	62	63	64	65	65	63

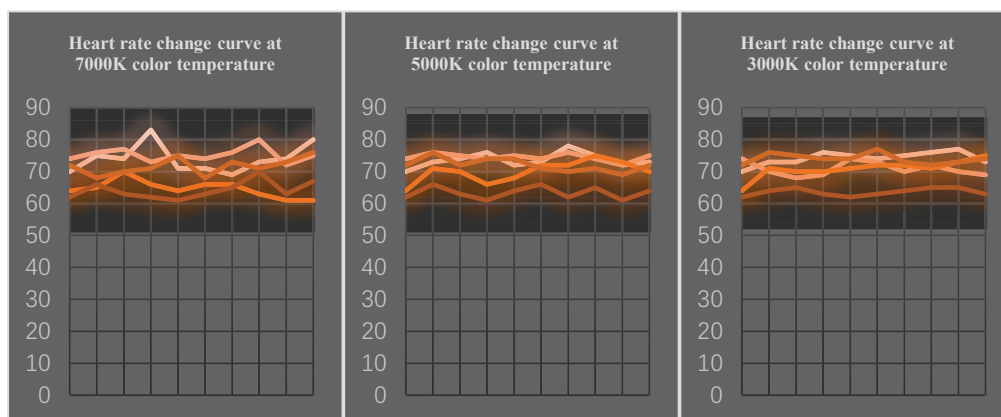


#### 4.1 Visual acuity changes and visual fatigue

After analyzing the data, it was found that the subjects' visual acuity test results decreased in 7000K color temperature environment, more than half of the subjects' visual acuity decreased in 5000K color temperature environment, while the subjects' visual acuity test results did not decrease in 3000K color temperature environment. After the subjective perception survey, the subjects in the 7000K high color temperature environment all had some sense of visual fatigue.

#### 4.2 Heart rate variability and visual fatigue

The main way to judge the degree of visual fatigue was by the fluctuation of heart rate during the experiment. In the VDT reading mode, the heart rate curves of the subjects in the three color temperatures were compared, and the curve fluctuations were more obvious in the 7000K color temperature environment, while the curve was more gentle in the 3000K color temperature environment, indicating that the visual fatigue level was higher in the high color temperature visual environment.



### 5 Conclusion

Comparing the experimental data results of different experimental groups, it can be concluded that under the VDT reading mode, the change of ambient lighting color temperature has a significant effect on the visual fatigue of the readers. Among them, compared with the low color temperature of 3000 K, the visual measurement results of the subjects in the high color temperature visual environment decreased more significantly and the heart rate curve fluctuated more drastically, so it can be concluded that the VDT readers were more prone to visual fatigue under the high color temperature condition.

## References

- [1] Courtin Romain, Pereira Bruno, Naughton Geraldine, et al. Prevalence of dry eye disease in visual display terminal workers: a systematic review and meta-analysis.[J]. *Bmj Open*, 2016, 6(1).
- [2] Mohammad Nooruz Zaman, Varsha Singh. Computer Vision Syndrome in Visual Display Terminal users (VDT)[J]. *Indian Journal of Public Health Research & Development*, 2018, 9(12).
- [3] Weng Ji, Zhang Xiao, Cao Xin. The effect of background reflection coefficient on visual fatigue of visual work surface in visual display terminal environment[J]. *Journal of Lighting Engineering*, 2022, 33(6): 27-34.
- [4] Liang, Shu ying, Yang, Chun yu, Li, Juan jie. Experimental protocol of visual fatigue suitable for multimedia classroom light environment research[J]. *Journal of Lighting Engineering*, 2019, 30(3): 43-47, 101.
- [5] Wu, J. W. A comprehensive study on the effect of indoor local lighting arrangement pattern and color temperature selection on VDT reading behavior[D]. *Suzhou University of Science and Technology*, 2022
- [6] Wang Yan. Research on fatigue analysis of VDT operation and its improvement measures[D]. *Xi'an University of Architecture and Technology*, 2009

# OPTIMIZING CLASSROOM LIGHTING AND VIEW CLARITY WITH A NOVEL SWITCHABLE BLIND WINDOW SYSTEM

Yanan Chen, Yu Bian

(School of Architecture, State Key Laboratory of Subtropical Building and Urban Science, South China University of Technology, Guangzhou, China)

## ABSTRACT

This study evaluates the performance of a new window system with switchable blinds designed to balance daylight availability, visual comfort, and view in classrooms. The method used Radiance-based simulation with bidirectional scattering distribution function (BSDF) data and was validated against experimental measurements. The results show that, regardless of the classroom orientation (south/east/west), the studied window system can: a) meet LEED requirements for spatial daylight autonomy; b) reduce discomfort areas on the blackboard, and c) maintain a satisfactory openness of the window with a clear image of the exterior. The developed simulation method can be useful for designing and evaluating daylighting systems in classrooms.

Keywords: window system, switchable blinds, visual comfort, contrast ratio

## 1. INTRODUCTION

Daylighting is essential for creating a healthy and energy-efficient environment. Studies have shown that increasing daylighting can improve occupants' mood, performance, and well-being [1-4]. In particular, studies have demonstrated a high correlation between students' perceptions and dynamic daylight indicators when defining the daylit area [5], as well as the availability of daylight and its effects on electrical energy demand [6]. Despite the benefits of daylighting, maximizing its use while ensuring visual comfort and window views remains a challenge [7-11]. Most studies have focused on discomfort glare, but visual discomfort issues in classrooms may have unique sources [12, 13]. For example, poor text legibility resulting from daylight reflections on the board area was found to be the most concerning discomfort issue [14]. Daylight availability and visual comfort are essential requirements in most daylight regulations, as well as window design, to create comfortable and beneficial learning environments [15, 16]. The degree of openness in window design is also crucial in school buildings, as it allows for a better view [17]. BSDF (Bidirectional Scattering Distribution Function) data has been found to accurately predict daylight performance and high-performance shading devices can improve visual comfort and reduce energy consumption [18-20].

This paper proposes a window system that includes switchable blinds, which are described by BSDF files, and a simulation method that incorporates these files. The aim of this study is to improve daylight availability, visual comfort, and view in a classroom with a novel window system with switchable blinds.

## 2. WINDOW SYSTEM WITH SWITCHABLE BLINDS

### 2.1 The limitations of conventional window blinds

Window blinds are commonly used in classrooms to control light, but they can limit view clarity and daylight availability [21]. Tzempelikos found that the ratio of slat width to spacing is important in reducing the impact of blinds on daylight availability and view openness [22]. Venetian blind control strategies have been developed to consider daylight utilization and glare protection [23].

### 2.2 The Proposed Window System

The proposed window system with switchable blinds aims to address the limitations of conventional window blinds. The system consists of frosted thin aluminium sheets, with each slat composed of three equal-width sections hinged together. The slat spacing is three times wider than the slat width, as illustrated in Figure 1.

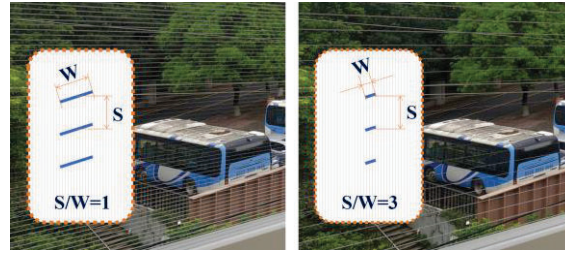


Fig 1. Comparison of the window openness between window blinds with a slat spacing ( $S$ ) to a slat width ( $W$ ) ratio of 1 and 3.

### 2.3 Functionality of the Proposed Window System

The proposed window system with switchable blinds can be unfolded at a specific angle (marked as  $\theta$ ) or folded tightly together. Figure 2 shows a schematic of the window prototype with switchable blinds. Figure 3 illustrates the conditions that trigger control and the resulting effects. When disturbing daylight reflections reduce the contrast in any one-quarter of the board to less than 1.3, the blinds switch to the open mode to either obstruct or redirect the daylight, otherwise, the blinds remain closed.

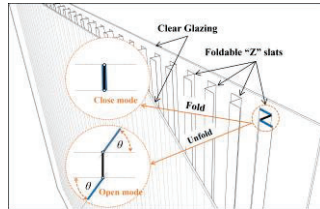


Fig 2. Schematic diagram of the window.

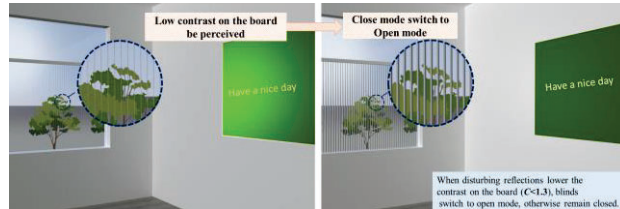


Fig 3. The control logic of the window system.

## 3. METHODOLOGY

### 3.1 Overview of the research methodology

This paper presents a workflow for investigating daylight availability, visual comfort, and openness of a secondary classroom using simulation-based methods. The simulation results were validated by comparing the simulated results with measured values in a real test room. The methodology involves generating BSDF files for the proposed window system using the *Radiance* program *genBSDF*, applying annual DA, assessing the contrast ratio on the board using HDRI renderings with specific model settings, and analysing the window openness.

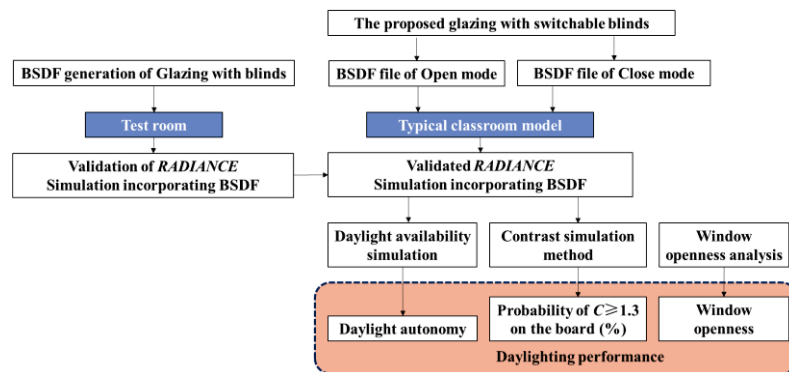


Fig 4. Workflow diagram of the simulation-based daylighting performance study.

### 3.2 The generation of the BSDF file

In this study, computational methods were employed using the *Radiance* program *genBSDF*, which could virtually generate BSDF with ray-tracing methods [24]. The process for generating the BSDF files for the CFS is illustrated in Figure 5, and typical material properties utilized for the simulation are outlined in Table 1. Selected BSDF plots of the proposed window system in both open and closed modes are presented in Figure 6. The transmission values range from 8.0% to 27.6% in open mode and from 7.4% to 40.8% in closed mode.

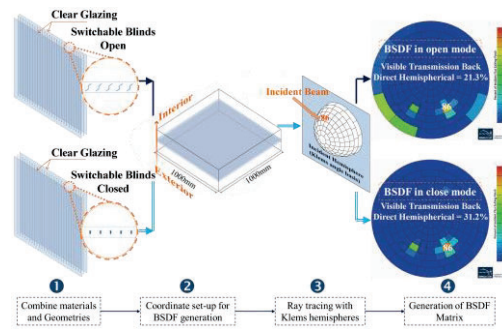
Fig 5. Workflow diagram for BSRF generation of glazing with blinds in *genBSDF*.

Table 1. Typical material properties used for the simulation.

	Reflectance			Roughness	Specularity
	R	G	B		
slats	0.663	0.702	0.767	0.05	0.95
overhang	0.7	0.7	0.7	0	0
	Transmittance			Refractive Index	
	R	G	B		
clear glazing	0.83	0.83	0.83	1.52	

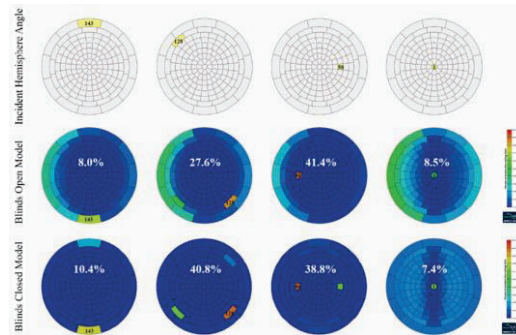


Fig 6. Selected BSRF plots of the proposed window system in both open and closed modes.

### 3.3 Simulation method for daylight availability and contrast ratio on the board

The typical classroom model was based on the average requirement in Code for Design of School (GB50099-2011) [25], measuring  $9.3 \times 7.5 \times 3.8$  m ( $L-W-H$ ). The schematic classroom model with marked dimensions is shown in Figure 7(a). The walls, ceiling, and floor elements were opaque plastic material, with a diffuse reflectance of 35%. The sensor grid arrangement was placed in the occupied area of the classroom and is positioned 0.75 m above the floor (Figure 7(b)). The radiance material files of the typical dark-green and white portions of the board are described in Table 2. The worst scenario for observing contrast on the board is from the seat at the far end of the window in the front row. Therefore, the contrast study scenario is shown in Figure 7(c).

The luminance contrast on a blackboard ( $C$ ) is defined as:

$$C = \frac{L_t - L_b}{L_b} \quad (1)$$

Where  $C$  is luminance contrast on a blackboard;

$L_t$  is the luminance of chalk writings ( $\text{cd/m}^2$ );

$L_b$  is the luminance of the dark-green area on the blackboard ( $\text{cd/m}^2$ ).

The statistical analysis indicated that the level of disturbing reflection was correlated with the contrast ratio ( $C$ ) between the white and dark-green portions of the board. Further numerical analysis revealed that a contrast ratio greater than 1.3 could ensure good legibility [26].

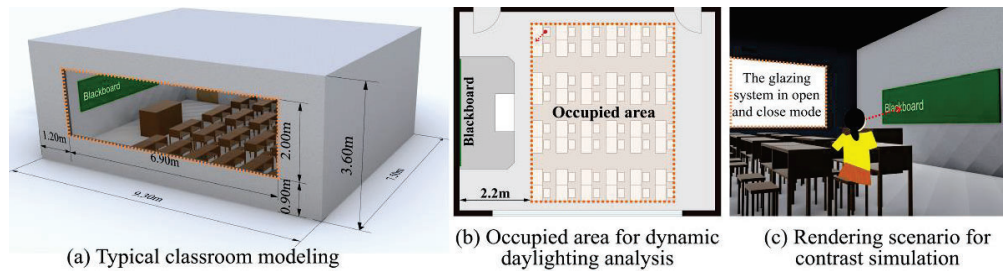


Fig 7. Test model information.

Table 2. Typical material properties of the blackboard (dark-green) and white chalk.

	Reflectance			Roughness	Specularity
	R	G	B		
Blackboard (dark-green)	0.14	0.20	0.14	0.02	0.0009
white chalk	0.8	0.8	0.8	0	0

### 3.4 Validation of Radiance simulation using BSDFs

This section provides a brief overview of the validation experiment procedure, focusing on the validation of contrast values on the board. The validation study is generally divided into two stages. The first stage is determined by the difference between the simulated and measured illumination at desk height ( $E_h$ ). The second stage is validated by comparing the contrast ratio from rendered and measured HDRI of the observer's FOV.

#### 3.4.1 Test room setup

The test room used for the validation study is a 50 m<sup>2</sup> room located in the building lighting laboratory of South China University of Technology in Canton, China. The actual luminance of the target material was measured. Figure 8 shows the test room during the experiment, with the primary instruments numbered and briefly described.

#### 3.4.2 Validation of illuminance

This is the first stage of a two-stage validation study, spanning the period from 11th to 15th July 2022, from 8:00 to 17:00 daily. The sensor points in the model were set in accordance with the correct positions of physical sensors in the test room, and a series of illuminance data was obtained for each sensor. The average error between simulated and measured illuminances is 14%, with a root mean square error (RMSE) of 16.9%.

#### 3.4.3 Validation of contrast ratio on the board

After the first validation stage was completed, the second study was conducted. The resulting HDR images have a luminance value integrated into each pixel, and the luminance values of the white and dark-green portions of these 16 blocks could be read from the calibrated HDR image. Figure 9 shows a sample picture of the HDR image taken in the second stage validation study.



Fig 8. Test room setup for the validation study.

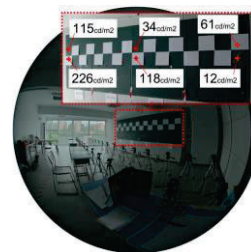


Fig 9. A sample of HDR image.

Based on the measured and simulated contrast values during the test period, the average error of the simulated absolute value is 17% for  $L_t$  and 19% for  $L_b$ . The statistical results for the 16 patterns indicate a simulation error of 17% for  $C$ .



### 3.5 Method for assessing view through the window system

To evaluate the performance of fenestration systems with integrated blinds, a key factor to consider is the ratio of the unobstructed area within the window. We used a metric called the "Openness Factor", which measures the ratio of the unobstructed area in the window as observed from the viewer's field of view [27, 28]. This ratio determines the openness of the window system, with smaller areas obstructed by the slats leading to higher openness.

## 4. RESULTS & ANALYSIS

### 4.1 Contrast ratio distribution on the blackboard

The contrast ratio distribution values on the board are statistics taken from 8:00 to 17:00 on the Summer Solstice, Autumn Equinox, and Winter Solstice days under CIE standard clear sky conditions with the sun. These values are presented in a  $4 \times 16$  grid with the probability of occurrence greater than or equal to 1.3 (probability of  $C \geq 1.3$ ). All the related contrast ratio distribution information is displayed in Figure 10.

Orientation	Blinds mode	Contrast on the board (probability of $C \geq 1.3$ )	The area ratio of (probability of $C \geq 1.3$ ) $\geq 75\%$
South	Non-blinds, Single-layer clear glazing	49 52 57 60 60 63 63 63 66 66 100 100 100 100 100 100	31%
		44 44 47 50 50 60 63 63 63 66 66 100 100 100 100 100	
	Blinds in closed mode	44 44 47 50 50 60 63 63 63 66 66 100 100 100 100 100	77%
		45 49 52 54 60 60 63 63 63 66 66 100 100 100 100 100	
	Blinds in open mode	48 55 77 75 100 100 100 100 100 100 100 100 100 100 100	100% (Improve 23% by the closed mode)
		44 58 70 70 100 100 100 100 100 100 100 100 100 100 100	
East	Non-blinds, Single-layer clear glazing	44 44 47 50 50 60 63 63 63 66 66 100 100 100 100 100	50%
		44 44 47 50 50 60 63 63 63 66 66 100 100 100 100 100	
	Blinds in closed mode	44 44 47 50 50 60 63 63 63 66 66 100 100 100 100 100	81%
		45 49 52 54 60 60 63 63 63 66 66 100 100 100 100 100	
	Blinds in open mode	48 55 77 75 100 100 100 100 100 100 100 100 100 100 100	100% (Improve 19% by the closed mode)
		44 58 70 70 100 100 100 100 100 100 100 100 100 100 100	
West	Non-blinds, Single-layer clear glazing	44 44 47 50 50 60 63 63 63 66 66 100 100 100 100 100	50%
		44 44 47 50 50 60 63 63 63 66 66 100 100 100 100 100	
	Blinds in closed mode	44 44 47 50 50 60 63 63 63 66 66 100 100 100 100 100	75%
		45 49 52 54 60 60 63 63 63 66 66 100 100 100 100 100	
	Blinds in open mode	48 55 77 75 100 100 100 100 100 100 100 100 100 100 100	100% (Improve 25% by the closed mode)
		44 58 70 70 100 100 100 100 100 100 100 100 100 100 100	

The data is the statistic from 8:00 to 17:00 each day on the summer solstice, autumn equinox, and winter solstice days under CIE standard clear sky conditions with the sun.  
Location: Guangzhou, CN  
Weather file: Meteonorm TMY weather file

Fig 10. Simulation results of the contrast ratio distribution on the board of the typical classroom model.

### 4.2 Daylight availability of the switchable window system

#### 4.2.1 Daylight autonomy

The DA distributions of a typical classroom with the switchable window system in open mode and closed mode are depicted in Figure 11. The simulation results suggest that all three orientation cases have a high probability of failing to meet LEED requirements, where the sDA threshold is 55%. To address this issue, incorporating other materials with higher light-transmitting properties into the building façade, along with the novel window system, may be a feasible solution.

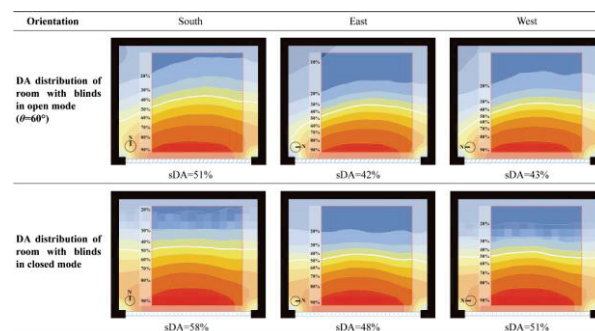


Fig 11. Daylighting performance of the optimized fenestration design for East/South/West orientation.

#### 4.2.2 Solution to improve daylight availability

Based on the simulation results, it is necessary to improve the window layout design to increase

daylight harvesting. Figure 12 is an example of a quick shading analysis on the façade section located in Guangzhou, China. During the winter solstice in Guangzhou, when the solar altitude angle is  $43^{\circ}64'$ , the room inside will be well-shaded if the relationship between the depth of the fixed internal overhang ( $D$ ) and the height of the upper portion ( $H_1$ ) is satisfied such that  $D \approx H_1$ .

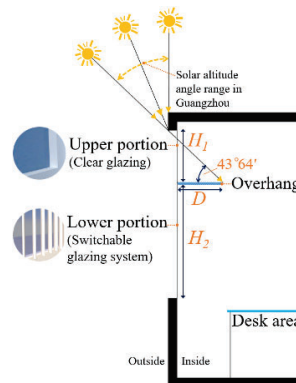


Fig 12. The window layout shown on the façade section and a rapid shading analysis at the site location.

When the height of single-layer clear glazing ( $\tau = 0.83$ ) in the upper portion of the window ( $H_1$ ) = 400 mm, the height of the switchable window system ( $H_2$ ) = 1600 mm, and the length of the internal overhang ( $D$ ) = 400 mm. The typical optical properties of the internal overhang were described in Table 1. The simulated DA for the typical classroom model with the improved window layout is plotted in Figure 13. The presence of switchable window systems and other transparent materials in a well-designed fenestration could meet the LEED requirement for daylight availability in a typical classroom.

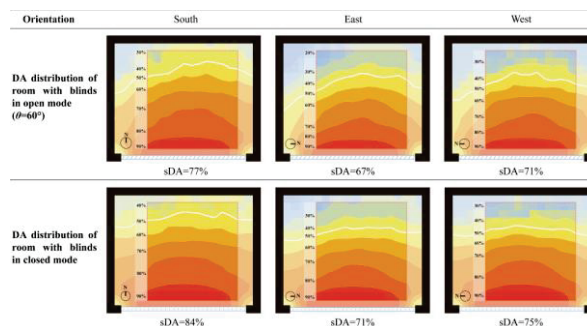


Fig 13. DA of the typical classroom model with improved window layout in South / East / West orientation.

### 4.3 The openness of window

As a result, the overall performance of the window in terms of daylighting and view is improved, and reflected light through daylight redirection is avoided. To fully evaluate the window's openness, we assessed it in three viewing directions (i.e.,  $-45/0/45$  degrees), as shown in Figure 14.

The images and values presented in Figure 15 depict the partial image and calculated openness factor of the window system in both open and closed modes in three view directions. This unique feature of the system allows the blinds to be closed when there are no disturbing daylight reflections on the board, which not only provides sufficient daylighting but also ensures a significant degree of window openness. This contributes to the subjective perception of the well-being of the occupants in the room.

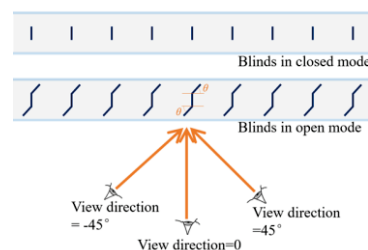


Fig 14. View directions to study the openness of the proposed window system in open and closed modes.

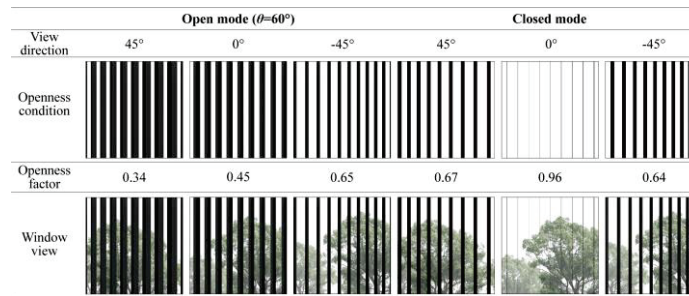


Fig 15. The openness of the glazing with switchable blinds from various view directions.

## 5. DISCUSSION

The design of daylight environments in civil buildings requires careful consideration of various factors, including daylight availability, visual comfort, and view, to achieve energy conservation, carbon emission reduction, physical health, and positive psychological effects. Building simulation is an effective tool for understanding and optimizing these aspects.

In summary, this study validates a comprehensive simulation method and evaluates the performance of a novel window system that improves openness and visual comfort in a typical secondary school classroom in China. Future work will focus on addressing the limitations of the proposed system and optimizing its performance in different climate conditions and building types.

## 6. CONCLUSION

The following conclusions are drawn:

1. *Radiance*-based simulation using BSDF is an effective method for evaluating the daylight performance of complex fenestration systems in illuminance-based metrics as well as luminance renderings.
2. The method of rating the visual comfort of a classroom from the contrast ratio on the blackboard proved to be feasible and applicable.
3. In classrooms, a window system with switchable blinds that can be opened and closed provides a suitable balance between daylight availability, visual comfort, and view.

This study found that the current modelling method has an error of approximately 20%, which is acceptable for assessing the lighting performance of a fenestration system in room spaces. However, there is still room for improvement, and future studies will explore the use of higher-resolution BSDF files and simulation methods with improved accuracy.

## REFERENCES

- [1] D.H.W. Li, K.L. Cheung, S.L. Wong, T.N.T. Lam, An analysis of energy-efficient light fittings and lighting controls, *Applied Energy*. 87 (2010) 558–567. doi: 10.1016/j.apenergy.2009.07.002.
- [2] A.D. Galasiu, J.A. Veitch, Occupant preferences and satisfaction with the luminous environment and control systems in daylit offices: a literature review, *Energy and Buildings*. 38 (2006) 728–742. doi: 10.1016/j.enbuild.2006.03.001.
- [3] L. Edwards, P. Torcellini, Literature Review of the Effects of Natural Light on Building Occupants, 2002. doi: 10.2172/15000841.
- [4] J. Heerwagen, Green buildings, organizational success and occupant productivity, *Building Research & Information*. 28 (2000) 353–367. doi: 10.1080/096132100418500.
- [5] L. Heschong, R.L. Wright, S. Okura, Daylighting Impacts on Human Performance in School, *Journal of the Illuminating Engineering Society*. 31 (2002) 101–114. doi: 10.1080/00994480.2002.10748396.
- [6] S. Markussen, K. Røed, Daylight and absenteeism – Evidence from Norway, *Economics & Human Biology*. 16 (2015) 73–80. doi: 10.1016/j.ehb.2014.01.002.
- [7] Z.S. Zomorodian, M. Tahsildoost, Assessing the effectiveness of dynamic metrics in predicting daylight availability and visual comfort in classrooms, *Renewable Energy*. 134 (2019) 669–680. doi: 10.1016/j.renene.2018.11.072.
- [8] S.J. and C. Kwon, Evaluation of visual comfort with daylighting levels using Daysim in different transparency and orientation in the UK, *International Journal of Sustainable Building Technology and Urban Development*. 9 (2018) 266–278. doi: 10.22712/susb.20180025.
- [9] P. Tregenza, D. Loe, *The design of lighting*, Routledge, London; New York, 2014.
- [10] S.J. Oh, S. Dutton, S. Selkowitz, H.J. Han, Application of a coelostat daylighting system for energy

- savings and enhancement of indoor illumination: A case study under clear-sky conditions, *Energy and Buildings*. 156 (2017) 173–186. doi: 10.1016/j.enbuild.2017.08.081.
- [11] L.T. Doulos, A. Kontadakis, E.N. Madias, M. Sinou, A. Tsangrassoulis, Minimizing energy consumption for artificial lighting in a typical classroom of a Hellenic public school aiming for near Zero Energy Building using LED DC luminaires and daylight harvesting systems, *Energy and Buildings*. 194 (2019) 201–217. doi: 10.1016/j.enbuild.2019.04.033.
  - [12] J. Xiong, A. Tzempelikos, I. Bilionis, N.M. Awalgaonkar, S. Lee, I. Konstantzos, S.A. Sadeghi, P. Karava, Inferring personalized visual satisfaction profiles in daylight offices from comparative preferences using a Bayesian approach, *Building and Environment*. 138 (2018) 74–88. doi: 10.1016/j.buildenv.2018.04.022.
  - [13] S.A. Sadeghi, S. Lee, P. Karava, I. Bilionis, A. Tzempelikos, Bayesian classification and inference of occupant visual preferences in daylight perimeter private offices, *Energy and Buildings*. 166 (2018) 505–524. doi: 10.1016/j.enbuild.2018.02.010.
  - [14] P. Ricciardi, C. Buratti, Environmental quality of university classrooms: Subjective and objective evaluation of the thermal, acoustic, and lighting comfort conditions, *Building and Environment*. 127 (2018) 23–36. doi: 10.1016/j.buildenv.2017.10.030.
  - [15] A. Tzempelikos, Advances on daylighting and visual comfort research, *Building and Environment*. 113 (2017) 1–4. doi: 10.1016/j.buildenv.2016.12.002.
  - [16] M.B. Hirning, G.L. Isoardi, I. Cowling, Discomfort glare in open plan green buildings, *Energy and Buildings*. 70 (2014) 427–440. doi: 10.1016/j.enbuild.2013.11.053.
  - [17] R.G. Hopkinson, Glare from daylighting in buildings, *Applied Ergonomics*. 3 (1972) 206–215. doi: 10.1016/0003-6870(72)90102-0.
  - [18] K. Van Den Wymelenberg, M. Inanici, A Critical Investigation of Common Lighting Design Metrics for Predicting Human Visual Comfort in Offices with Daylight, *LEUKOS*. 10 (2014) 145–164. doi: 10.1080/15502724.2014.881720.
  - [19] J. Jakubiec, C. Reinhart, The “adaptive zone” – A concept for assessing discomfort glare throughout daylight spaces, *Lighting Research & Technology*. 44 (2011) 149–170. doi: 10.1177/1477153511420097.
  - [20] J.Y. Suk, M. Schiler, K. Kensek, Investigation of existing discomfort glare indices using human subject study data, *Building and Environment*. 113 (2017) 121–130. doi: 10.1016/j.buildenv.2016.09.018.
  - [21] Y. Sun, R. Liang, Y. Wu, R. Wilson, P. Rutherford, Glazing systems with Parallel Slats Transparent Insulation Material (PS-TIM): Evaluation of building energy and daylight performance, *Energy and Buildings*. 159 (2018) 213–227. doi: 10.1016/j.enbuild.2017.10.026.
  - [22] A. Tzempelikos, The impact of venetian blind geometry and tilt angle on view, direct light transmission and interior illuminance, *Solar Energy*. 82 (2008) 1172–1191. doi: 10.1016/j.solener.2008.05.014.
  - [23] Y.-C. Chan, A. Tzempelikos, Efficient venetian blind control strategies considering daylight utilization and glare protection, *Solar Energy*. 98 (2013) 241–254. doi: 10.1016/j.solener.2013.10.005.
  - [24] A. McNeil, Tutorial-genBSDF\_v1.0.1.pdf — Radsite, (2015). [https://www.radiance-online.org/learning/tutorials/Tutorial-genBSDF\\_v1.0.1.pdf/view](https://www.radiance-online.org/learning/tutorials/Tutorial-genBSDF_v1.0.1.pdf/view).
  - [25] MOHURD, GB 50099-2011: Code for design of school. Ministry of Housing and Urban-Rural Development of China (MOHURD), Beijing: China Architecture and Building Press, 2010.
  - [26] Y. Bian, J. Luo, T. Leng, Contrast demand on the blackboard in typical secondary school classrooms of China: Effects of daylight reflections on text legibility, *Energy and Buildings*. 261 (2022) 111974. doi: 10.1016/j.enbuild.2022.111974.
  - [27] A. Ozdemir, The effect of window views' openness and naturalness on the perception of rooms' spaciousness and brightness: A visual preference study, *Scientific Research and Essays*. 5 (2010) 2275–2287.
  - [28] L. Koprivec, M. Zbašnik-Senegačnik, Ž. Kristl, Analysis of Survey Responses to the Window Views, *Igra Ustvarjalnosti - Creativity Game*. 2021 (2021) 14–23. doi: 10.15292/iu-cg.2021.09.014-023.

## ACKNOWLEDGEMENTS

The work was supported by the National Natural Science Foundation of China (No.51978277 and No.52278107), Guangdong Department of Housing and Urban-Rural Development 2022 Science and Technology Innovation Plan (2022-K2-450970).

Corresponding Author Name: Yu Bian

Affiliation: School of Architecture, State Key Laboratory of Subtropical Building Science, South China University of Technology, Guangzhou, China

e-mail: aryubian@163.com

# A LABORATORY STUDY ON DYNAMIC DURATION PREFERENCE IN SHADING LIGHTING: BASED ON VISUAL COMFORT EVALUATION AND AOI OF EYE MOVEMENT

Luoxi Hao<sup>1</sup>, Kai Feng<sup>2</sup>,

(1: College of Architecture and Urban Planning, Tongji University, Shanghai, China

2: Faculty of Architecture and City Planning, Kunming University of Science and Technology, Kunming, China)

## ABSTRACT

Shading lighting is a widely-used way of dynamic lighting in urban nightscapes, in which the change of dynamic duration (DD) would affect observers' visual comfort directly. Field evaluation in urban environments would be influenced by numerous (inner and the external) factors, so it's necessary to conduct pilot research in an laboratory environment. The preference towards 5 DD (2s/4s/6s/8s/10s) were evaluated in lab under variables of 3 observation distances (3m/6m/9m) and 3 monochromatic lights (3000K/4000K/5000K) and 30 subjects participated in the experiment. Subjective questionnaire (analyzed by Principal Component Analysis using R language) and Area of Interest (AOI) of eye movement data were used in the analyzing procedure. When "-3" (representing "unbearable") appeared in the subjective evaluation, the previous (longer) DD would be defined as DD<sub>P</sub> (Peak Value of Dynamic Duration) to express the minimum acceptable DD value and DD<sub>R</sub> (Recommended Value of Dynamic Duration) was defined to explain more (75%) participants' preference towards DD. It was found that DD<sub>R</sub> in most conditions were around 4s, indicating that 4s can be used as the DD<sub>R</sub> in shading scenarios both in relative studies or construction works.

Keywords: Dynamic duration preference, Subjective evaluation, AOI of eye movement, R language, DD<sub>R</sub> (Recommended value of dynamic duration)

## 1. INTRODUCTION

The World Health Organization (WHO) proposed the strategic principle of "everyone's health" in the mid-1970s and introduced the concept of "healthy cities" in 1984[1]. Health Impact Assessment (HIA) is an important way to promote the development of healthy cities, aiming to quantify the health impact of planning policies or projects on local residents[2]. With the rapid development of research related to healthy cities, nighttime health issues are also being discussed. Different scholars have conducted extensive research on the daily behavior of the public [3,4], eye health [5,6], physiological rhythms [7,8], specific diseases [9,10], and special populations [11,12] from urban lighting (or nightscape lighting). However, there is still relatively little research on the impact of lighting on people in outdoor neighborhoods, especially the impact on observer comfort (such as visual, emotional, etc.).

With the development of LED and its related technologies, dynamic lighting has become an important way of night scene expression. Through research on more than 100 cases in Shanghai, Shenzhen, Guangzhou and other cities, nearly 60% of the scenes are shading scenes (or its combination with other dynamics modes), indicating that shading scenes are widely used in urban environments. In contrast to its widespread presence in cities, there is a lack of control over dynamic lighting in standard documents. After analyzing multiple relevant standard and specification documents, it can be seen that there's very few quantitative requirements for dynamic lighting; although some documents are being developed to explore the introduction of relevant content, they mainly focus on defining or qualitative requirements, quantitative requirements are still significantly insufficient. How to propose targeted control indicators based on dynamic lighting characteristics is an urgent problem that needs to be considered and solved.

Through on-site research and questionnaires, it was found that the evaluation of the comfort of dynamic lighting is influenced by factors such as the amount of surrounding lighting construction,



the variables of lighting itself, observation distance (and angle), real-time emotions, and even (individual) past learning cognition, cultural background, etc. There is mutual influence among variables, which is a comprehensive and complex process. Direct on-site evaluation can be influenced by multiple variables, so conducting pilot studies in a laboratory environment can simplify the variables as much as possible and obtain the impact of a single variable on the subjects. Subsequently, exploring the impact between variables will have more reference value.

This study focuses on shading dynamics and analyzes the impact of dynamic duration on observer comfort. In the experiment, a combination of subjective questionnaires and eye movement AOI was used to achieve a comprehensive discussion of both subjective and objective dimensions. The article proposes two indicators,  $DD_P$  and  $DD_R$ , which will provide reference for the selection of quantitative indicators in future relevant standard documents. The research ultimately proposed specific numerical suggestions, which can provide reference for future related evaluation work.

## 2. METHODS

### 2.1 Variable selection

An analysis of the dynamic duration(DD) in cities (referring to the duration of completing a complete translation of dynamic mode) found that in most cases is less than 10s. It was further divided into 5 intervals: less than 2s, 2-4s, 4-6s, 6-8s, and 8-10 seconds. It was found that the proportion of the middle 3 intervals was slightly higher. Considering the operability and completeness of the study, comfort evaluation was conducted using 2s, 4s, 6s, 8s, 10s as objects. In the selection of light colors, online image retrieval (789 copies), on-site research (over 100 items), and public questionnaires (97 copies) were conducted to find 6 most widely used light colors in cities, namely 3000K, 4000K, 5000K, red, blue, and RGB. Considering the feasibility of the research, only 3000K, 4000K, and 5000K were selected as the research subjects. In the process of determining the observation distance, the feasibility of the laboratory was mainly considered, and three distances of 3m, 6m, and 9m were ultimately selected.

### 2.2 Experimental environment and equipment

Based on the laboratory site conditions, an experimental setup consisting of a light source component, an observation box, and an observer was formed (Figure 4). The light source component consists of 15 lamps (length 500mm, power 12W/m, control system DMX512, commonly used in dynamic lighting cases) installed at equal intervals (40mm) on a black matte wood base plate. The signal line forms a series connection at the back of the base plate, and is powered and scene controlled through an external power supply and controller. The observation box is composed of multiple unit boxes (600\*600\*600mm) assembled, each of which is composed of 4 black matte chevrolet plates (serrated edges) spliced together to form a rectangular hole shape. With the help of the black and matte surface characteristics of the material, it can effectively reduce reflected light and create a diffuse reflection experimental environment (to avoid reflection and potential glare problems), The assembly of multiple unit boxes at the same time can achieve convenient adjustment of observation distance (in 600mm units). Compared to similar studies in the past [23,24], the observation box has been optimized in terms of material selection, surface treatment, assembly method, reuse, storage and transfer.



Figure 1. Experimental setup and scenario diagram

### 2.3 Experimental methods and processes

The experimental process includes: ① the first subject sits in the observation position (wearing an eye tracker) and enters the experimental state; ② The first light variable lights up and the



subject observes for 1 minute; ③ The light is turned off, and the subjects close their eyes and rest for 1 minute. During this period, the subjects will ask questions about comfort conditions; ④ The second light variable lights up, and the evaluation and data collection of all variables (with the same light color) are completed according to the ① - ③ process; ⑤ Replace with the second subject and complete the corresponding data collection according to ① - ④; ⑥ Two participants conducted a cross experiment and completed the collection of all light color data. The experiment ended (Figure 5). In the end, 30 participants (14 males and 16 females) participated in the experiment.



Figure 2. Photos of the experimental process

## 2.4 Analytical methods

Subjective questionnaire data: sorting out the subjective data of each participant, When "-3" (representing "unbearable") appeared in the subjective evaluation, the previous (longer) DD would be defined as  $DD_P$  (Peak Value of Dynamic Duration) to express the minimum acceptable DD value for the subject. To explore the commonality of  $DD_P$  among all participants,  $DD_R$  (Recommended Value of Dynamic Duration) was defined: box plot was used and the upper quartile was selected as the  $DD_R$  which was used to explain "when the DD exceeds the  $DD_R$  (i.e. the dynamic speed is slower), more (75%) participants believe that the DD is within an acceptable range".

Eye movement AOI: Analyze the changes in the fixation points of each subject in different DD (represented as AOI) to learn the a more comfortable DD and analyze the scanning distance in different DD scenarios at the same time to assist in proving their eye comfort. During the analysis process, the total amount of physiological data under different DD scenarios were also counted, and comfort issues were further explored through the duration of eye closure.

## 3. CONCLUSION

Subjective evaluation showed that with the shorten of DD (from 10s to 2s), the comfort value of most subjects decreases. There is no significant difference between light colors (3000K/4000K/5000K), but the lower comfort value in 5000K scenes appeared (slightly) earlier than that in 3000K and 4000K, possibly due to its higher luminance. Under the variable of observation distance, the D-value between 10s and 2s in 6m/9m scenes are higher than that in 3m scene (3m changes from "no sensation" to "very uncomfortable", while 6m/9m changes from "comfortable" to "very uncomfortable"), indicating that in longer DD scenes (mainly referring to 8s/10s), a further observation distance will bring better comfort, while in shorter DD scenes (mainly referring to 2s) the impact of observation distance is relatively little.

Eye movement AOI shows that the concentration of gaze points in the middle scenes (4s/6s/8s) is higher than that in the other two side scenes (10s/2s), representing a better comfort feeling occurred. Meanwhile, in 2s scenes the scanning distance was closer, and fewer concentrated gaze areas occurred, indicating that subjects were in a continuous short-distance-scanning state (indicating a poor comfort condition). it was also found that when DD gets shorter, the amount of eye movement data received would decrease, which means with the shorten of DD, subjects has a more possibility of eye-closed state ( indicating an uncomfortable condition).

It was found that  $DD_R$ s in all conditions were 4s, indicating that 4s can be used as the  $DD_R$  in the shading scenarios in the future studies or construction works.

## REFERENCE

- [1] Be loyal. Introduction to the World Health Organization (WHO) - Origin and Development% J Beijing Medicine [J] 1981, (06): 377
- [2] Zhang Yalan, Cai Chunting, Wang Lan. Application of Health Impact Assessment in Urban Redevelopment: A Case Study of the Atlanta Ring Road Revitalization Project [J] 2017, 33 (11): 113-9
- [3] Shao Ligang, Liu Bei. Urban Light Pollution and Its Prevention and Control Measures [J] 2006, (01): 13-5
- [4] NGARAMBE J, KIM G J S. Sustainable Lighting Policies: The Contribution of Advertisement and Decorative Lighting to Local Light Pollution in Seoul, South Korea [J]. 2018, 10(4): 1007.
- [5] Zhou Ti. The Problem of Light Pollution in Urban Night Scene Lighting and Design Countermeasures [D]; Huazhong University of Science and Technology, 2004
- [6] FALCHI F, FURGONI R, GALLAWAY T A, et al. Light pollution in USA and Europe: The good, the bad and the ugly [J]. 2019, 248: 109227.
- [7] PAULEY S M J M H. Lighting for the human circadian clock: recent research indicates that lighting has become a public health issue [J]. 2004, 63(4): 588-96.
- [8] HURLEY S, NELSON D O, GARCIA E, et al. A cross-sectional analysis of light at night, neighborhood sociodemographics and urinary 6-sulfatoxymelatonin concentrations: implications for the conduct of health studies [J]. 2013, 12(1): 1-9.
- [9] HANSEN J J E. Increased breast cancer risk among women who work predominantly at night [J]. 2001, 12(1): 74-7.
- [10] KLOOG I, HAIM A, STEVENS R G, et al. Global co - distribution of light at night (LAN) and cancers of prostate, colon, and lung in men [J]. 2009, 26(1): 108-25.
- [11] LUNN R M, BLASK D E, COOGAN A N, et al. Health consequences of electric lighting practices in the modern world: A report on the National Toxicology Program's workshop on shift work at night, artificial light at night, and circadian disruption [J]. 2017, 607: 1073-84.
- [12] FONKEN L K, WORKMAN J L, WALTON J C, et al. Light at night increases body mass by shifting the time of food intake [J]. 2010, 107(43): 18664-9.

## ACKNOWLEDGEMENT

Corresponding Author: Kai Feng

Affiliation: Faculty of Architecture and City Planning, Kunming University of Science and Technology, Kunming, China

e-mail : ciochie@163.com

# A CROSS-CAMERAS COLOR CONSISTENCY APPROACH IN RAW DOMAIN FOR ARBITRARY LIGHTING SCENES

Minhang Yang, Haisong Xu, Yiming Huang

(State Key Laboratory of Modern Optical Instrumentation, College of Optical Science and Engineering, Zhejiang University, Hangzhou 310027, China)

## ABSTRACT

The color appearance of images captured by different cameras for the same scene may vary significantly due to the individual sensor spectral sensitivities and built-in image signal processing (ISP) pipelines, resulting in dissatisfactory color consistency or low visual quality of the images. Many correction approaches have already been developed, including color transfer, color correspondences alignment and histogram matching. However, these methods focus on post-processing images and are limited to some particular assumptions, so it is difficult and challenging to achieve accurate color consistency. In this study, we aim to tackle the color consistency in the raw domain to reduce color discrepancies between the different camera images. Based on the illumination information of an arbitrary scene, a viable color mapping strategy is proposed to convert a raw image from one camera to another. Utilizing paired images captured respectively by two cameras under various lighting conditions with different correlated color temperatures (CCT), the pre-trained matrixes are deduced in order for estimating the corresponding mapping matrix of actual scenes. The experimental results indicate that the proposed approach achieves better performance compared to the existing methods, and the cross-cameras color consistency is also acceptable to the human visual system (HVS).

Keywords: Color consistency, Color mapping, Cross-cameras, Raw domain, Arbitrary lighting scenes

## 1. INTRODUCTION

With the development of imaging technology, various imaging devices are constantly emerging. Meanwhile, there are also gradually increasing demands for image quality. However, owing to the differing optics, sensor spectral sensitivities, field of view, hardware processing and built-in image signal processing (ISP) pipelines employed by the cameras, the images acquired by different cameras for the same scene would generally output different color response values, leading to inconsistent color appearance as demonstrated in Fig. 1. This color inconsistency problem brings about an unpleasant visual experience when people view such images. Hereby, there are various color consistency approaches have been put forward to lower the color discrepancies among images through different techniques. Some of them introduce color transfer function following the statistical distribution of the images [1, 2]. Others adopt histogram matching [3] or local feature matching [4, 5] methods. However, most methods address the color mapping in the standard color spaces (e.g., standard RGB [6], or Adobe RGB). So far, the prior work has not been sufficiently focused on the mapping in the raw domain. Nguyen et al. [7] adopted two linear transformations, one global and another illumination-specific, to deal with the color inconsistency caused by cameras. In [8] a semi-supervised raw-to-raw mapping method was proposed through lightweight deep learning network. Such methods have the advantages of the global accuracy, but their applicability in real scenarios is limited.



Figure 1. The images captured by different cameras from dataset [9]: (a) and (d) CanonPowerShotG9, (b) and (e) CasioEX-Z55, (c) OlympusE500, (f) SonyDSC-F828.

The goal of this study is to reduce the color differences between the images acquired by different cameras for the same scene. We delve into the color mapping strategy that works in the raw domain

to obtain a transformation matrix. Upon converting the raw images between cameras, the white balance correction is performed on the images using white point, and finally the algorithms are evaluated in terms of color difference, color difference without lightness difference and chroma difference in CIELAB color difference.

## 2. METHODOLOGY

Camera images can be saved in the raw format, which is linearly related to the scene radiance and presents the raw sensor responses without any post-processing operations. Mathematically, the construction of a raw image can be expressed as [10]

$$I_c(x) = \int_{\omega} \rho(x, \lambda) R(x, \lambda) S_c(\lambda) d\lambda \quad (1)$$

where  $c = \{R, G, B\}$ ,  $x, \lambda, \omega$  respectively denote three color channels, pixel location, wavelength, and the visual spectral range, and  $S(\cdot)$  is the camera sensor spectral sensitivity. The terms  $\rho(\cdot)$  and  $R(\cdot)$  refer to the spectral power distribution (SPD) of the scene illumination and the object spectral reflectance, respectively.

The global method can be performed using a linear transformation without considering the practical scene lighting. Thereupon, inspired by the idea of color correction matrix (CCM) interpolation, we come up with an illumination-aware interpolation method based on the correlated color temperatures (CCTs). Taking no account of the color metamerism, it is assumed that the more similar the scene lighting is, the more consistent the raw color response of the same target is. According to the range and shape of the color gamut, the whole CCT range are divided into four sections, including below 2500K, 2500K-4500K, 4500K-6500K and above 6500K. For the CCTs of 2500K, 4500K and 6500K, the corresponding color mapping matrixes are pre-trained by color calibration chart images captured under several controlled lighting conditions by multiple cameras. For a practical scene image, the CCT of the scene illumination can be estimated via white point [11], and then the appropriate pair of pre-trained mapping matrixes are selected to derive the final illumination-aware matrix as follows:

$$M_{scene} = wM_1 + (1-w)M_2 \quad (2)$$

$$w = (CCT_{scene}^{-1} - CCT_2^{-1}) / (CCT_1^{-1} - CCT_2^{-1}) \quad (3)$$

where  $M_1, M_2$  are two pre-selected mapping matrixes with differing CCTs, and  $w, (1-w)$  present their corresponding interpolation weights.

## 3. EXPERIMENTS AND RESULTS

### 3.1 Experiments

In the experiment, three cameras were employed, including Nikon D3x DSLR camera, the main-camera and ultra-wide sub-camera of HUAWEI P50 Pro smartphone, being denoted as C1, C2 and C3, respectively, to build a raw image dataset consisting of various scenes. As shown in Fig.2, it is obvious that the raw color distributions of the color chart image for three cameras in the [R/G, B/G] color space are significantly different due to their diverse sensor spectral sensitivities, indicating the necessity of color consistency correction.

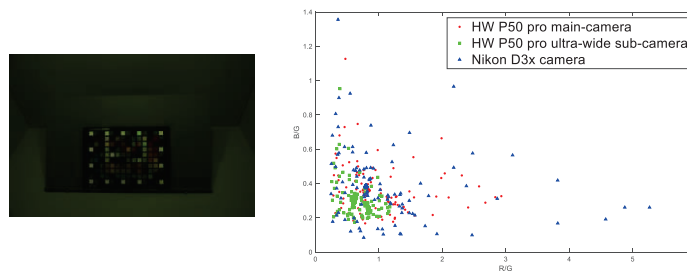


Figure 2. Example raw image and color distribution of the X-Rite Digital SG ColorChecker captured by three cameras under A illumination.

### 3.2 Results

Since the white balance algorithm is not the focus of this study, we use the 21<sup>st</sup> neutral grey block of X-Rite ColorChecker Classic as the reference of white point. Before estimating the related metrics, a scale factor  $k$  is set to adjust the two images for minimizing the exposure discrepancy. The color difference between the source image and target image (without applying color consistency approach) is regarded as a benchmark, and this method is compared with the traditional global method and Nguyen's method [7]. In the evaluation, the following CIELAB color metrics are adopted:

$$\Delta E_{ab}^* = \sqrt{(\Delta L^*)^2 + (\Delta a^*)^2 + (\Delta b^*)^2} \quad (4)$$

$$\Delta E_{ab, w/o \Delta L^*}^* = \sqrt{(\Delta a^*)^2 + (\Delta b^*)^2} \quad (5)$$

$$\Delta C_{ab}^* = C_{ab1}^* - C_{ab2}^* = \sqrt{(a_1^*)^2 + (b_1^*)^2} - \sqrt{(a_2^*)^2 + (b_2^*)^2} \quad (6)$$

The evaluation results with the built dataset are listed in Tables 1 and 2, from which it can be seen that, among the compared approaches, our method presents better performance on the whole. Nguyen's method is poor since it requires two transformation functions and so is more likely to accumulate conversion errors. Compared with the global method, our method shows comparable perceptual color performance while with the least color difference. As found in Table 2, the proposed approach could reduce the chroma difference by 49.09% in comparison with the benchmark.

Table 1. Color consistency comparisons among Nikon D3x camera (C1), the main-camera (C2) and ultra-wide sub-camera (C3) of HUAWEI P50 Pro smartphone.

Method		$\Delta E_{ab, w/o \Delta L^*}^*$		$\Delta E_{ab}^*$		$\Delta C_{ab}^*$	
		Mean	Median	Mean	Median	Mean	Median
C3→C2	Benchmark	3.00	2.40	3.71	3.15	2.27	1.72
	Nguyen [7]	2.21	1.91	2.76	2.48	1.59	1.29
	Global	2.11	1.90	2.78	2.55	1.46	1.22
	Ours	<b>1.81</b>	<b>1.64</b>	<b>2.36</b>	<b>2.20</b>	<b>1.19</b>	<b>1.02</b>
C2→C1	Benchmark	2.89	2.21	3.65	3.20	2.55	1.80
	Nguyen [7]	2.74	2.22	3.25	2.82	2.21	1.72
	Global	2.08	1.79	2.84	2.62	1.61	1.34
	Ours	<b>1.76</b>	<b>1.60</b>	<b>2.35</b>	<b>2.20</b>	<b>1.26</b>	<b>1.11</b>

Table 2. The color consistency improvement of the compared methods relative to the benchmark.

	Method	C3→C2	C2→C1	Average
$\Delta E_{ab, w/o \Delta L}^*$	Nguyen [7]	26.24%	5.30%	15.77%
	Global	29.50%	28.01%	28.76%
	Ours	<b>39.66%</b>	<b>39.00%</b>	<b>39.33%</b>
$\Delta E_{ab}^*$	Nguyen [7]	25.80%	11.05%	18.43%
	Global	25.12%	22.21%	23.67%
	Ours	<b>36.32%</b>	<b>35.51%</b>	<b>35.92%</b>
$\Delta C_{ab}^*$	Nguyen [7]	29.89%	13.19%	21.54%
	Global	35.97%	36.65%	36.31%
	Ours	<b>47.49%</b>	<b>50.69%</b>	<b>49.09%</b>



The visual comparison is also carried out as illustrated in Fig. 3. To aid visualization, a gamma operation with 1/2.2 encoding gamma and a rough image registration operation are applied. Fig. 3 shows that our method gives more reasonable visual color consistency for cross-camera images, especially for the colors with significant discrepancy in saturation, such as the red calendar in the first row and the green grass in the third row. It is considered that our method takes into account the scene illumination information so that it could be adaptive to color mapping of the complex lighting scenes and exhibits better robustness. Nevertheless, compared with the global method, the advantages of our approach on the visual perception is not yet significant, of which the reason may be that the accuracy of CCT estimation in our method would affect the choice of the pre-trained mapping matrixes and the corresponding interpolation weights, so finally impacts the color consistency.

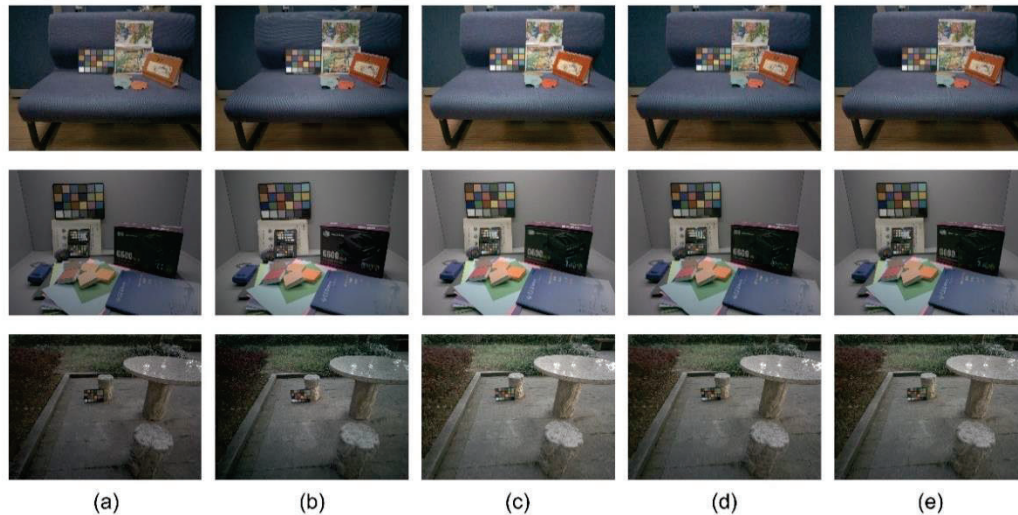


Figure 3. Visualization comparisons with our dataset. (a) Input C3 image, (b) Target C2 image, (c) Nguyen method, (d) Global method, (e) Our method.

#### 4. CONCLUSION

In this study, with the assistance of the CCT information of arbitrary lighting scenes, a cross-camera color consistency approach is proposed to compensate the color differences caused by individual camera sensor spectral sensitivities in the raw domain. The comprehensive evaluation and comparison indicate that the proposed method effectively improves the color consistency between the images acquired by different cameras for the same scene. In the future, more information, such as image contents and shooting parameters, will be involved to further enhance the performance and robustness of the color consistency algorithm.

#### REFERENCES

- [1] Reinhard, E., Adhikhmin, M., Gooch, B., & Shirley, P. Color transfer between images. *IEEE Computer graphics and applications*, 2001, 21(5), 34-41.
- [2] Xiao, X., & Ma, L. Color transfer in correlated color space. In *Proceedings of the 2006 ACM international conference on Virtual reality continuum and its applications*, 2006, 305-309.
- [3] Ding, C., & Ma, Z. Multi-camera color correction via hybrid histogram matching. *IEEE Transactions on Circuits and Systems for Video Technology*, 2020, 31(9), 3327-3337.
- [4] Yamamoto, K., Yendo, T., Fujii, T., Tanimoto, M., & Suter, D. Color correction for multi-camera system by using correspondences. *ACM SIGGRAPH 2006 Research posters*, 2006, 73.
- [5] Tehrani, M. P., Ishikawa, A., Sakazawa, S., & Koike, A. Iterative colour correction of multicamera systems using corresponding feature points. *Journal of Visual Communication and Image Representation*, 2010, 21(5-6), 377-391.
- [6] Ssstrunk, S., Buckley, R., & Swen, S. Standard RGB color spaces. *Proc. IS&T/SID 7th Color Imaging Conference*, 1999, 7, 127-134.



- [7] Nguyen, R., Prasad, D. K., & Brown, M. S. Raw-to-raw: Mapping between image sensor color responses. Proceedings of the IEEE Conference on Computer Vision and Pattern Recognition, 2014, 3398-3405.
- [8] Afifi, M., & Abuolaim, A. Semi-supervised raw-to-raw mapping. British Machine Vision Conference (BMVC), 2021.
- [9] Chakrabarti, A., Scharstein, D., & Zickler, T. E. An Empirical Camera Model for Internet Color Vision. BMVC, 2009, 1(2), 4.
- [10] Basri, R., & Jacobs, D. W. Lambertian reflectance and linear subspaces. IEEE transactions on pattern analysis and machine intelligence, 2003, 25(2), 218-233.
- [11] Robertson, A. R. Computation of correlated color temperature and distribution temperature. JOSA, 1968, 58(11), 1528-1535.

## **ACKNOWLEDGEMENT**

This study was supported by the Fundamental Research Funds for the Central Universities (No. S20220156).

Corresponding Author: Haisong Xu

Affiliation: College of Optical Science and Engineering, Zhejiang University

e-mail: chsxu@zju.edu.cn

# RESEARCH ON COLOUR QUALITY MANAGEMENT TECHNOLOGY IN LIGHTING FOR CULTURAL TOURISM

Xian Tang, Xiong Yang, Qian Li, Jianguan Pan

(EVERFINE Corporation, Hangzhou, Zhejiang, China)

## ABSTRACT

By skillfully integrating lighting and landscape through elaborate design and implementation, captivating visual effects and aesthetic atmosphere can be created. The colour displayed by the landscape is influenced by both the spectral power distribution (SPD) of the lighting source and the spectral transmittance/reflectance of the materials in the landscape. The colour quality management should be implemented throughout the entire process, from the initial design to construction and subsequent maintenance. This paper analyzes the interaction between objects and light sources in landscape lighting scenarios. Furthermore, it explores the measurement methods for assessing the transmittance, reflectance, and absorption characteristics of materials. By measuring the spectral properties of typical materials and light sources and simulating their combined visual effects, this study aims to provide a data foundation for design and construction. This paper also investigates the solutions for field measurement of lighting systems and objects within a lighting scene. These solutions enable accurate and convenient measurement of colour and luminance, beneficial for in time adjustment of light sources especially when dealing with multi colour mixing illumination. Moreover, the digitized expression of colour for lighting scene and objects can improve communication efficiency for engineering record and confirmation.

Keywords: lighting for cultural tourism; colour management; colour measurement

## 1. INTRODUCTION

Currently, there is an increasingly opportunity to utilize lighting in cultural tourism. Whether it's immersive night tourism that corporates local resources, cultural IP theme parks, or stages within scenic areas, creating an aesthetic atmosphere through landscape lighting scenarios is a major focus. The ambiance is manifested through the interplay of light and scenery, light and architecture, and light and objects.

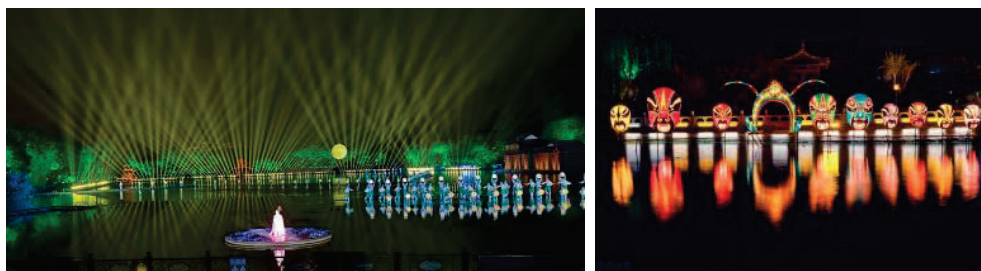


Figure 1: Examples of lighting for cultural tourism

In lighting design, it is essential to consider the impact of light absorption, reflection, and transmission by objects or materials. The overall lighting effect is the result of combining light from sources with light reflection/transmission by objects .

The on-site evaluation of cultural tourism landscape lighting is also a complex undertaking, which involves multiple scenes and lighting combinations, as well as diverse environments such as water, roads, bridges, mountains, walls of buildings, etc. The most convenient and efficient method for in field measurement of lighting systems and objects in a lighting scene is to obtain the imaging colour distribution of the scene.

## 2. COLOUR QUALITY MANAGEMENT IN LIGHTING DESIGN

### 2.1 The interaction between light and object

When light reaches the surface, several phenomena related to the optical properties of the object will occur, including reflection, transmission, and absorption, as shown in Figure 2, of which the value can be expressed as the ratios of reflected, transmitted, and absorbed radiant flux to the

incident radiant flux, defined as  $\rho$ ,  $\tau$ , and  $\alpha$ , respectively. The colour appearance of the object can be characterized by the spectral reflection  $\rho(\lambda)$ , the spectral absorption  $\alpha(\lambda)$ , and the spectral transmission  $t(\lambda)$ .

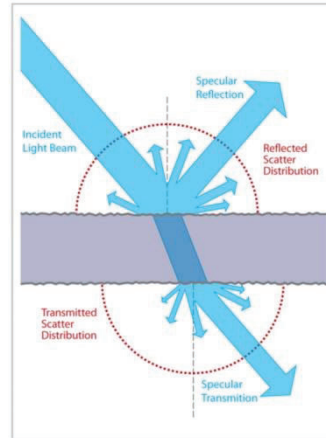


Figure 2. The interaction between light and object

The colour of an object as perceived visually is generally decided by the spectral reflectance/transmittance of the material and the spectral power distribution (SPD) of the light source. Take the example of the red wall of historic buildings in China: when illuminated by light sources with different spectra, the reflected spectrum will vary significantly leading to distinct visual effects. In Figure 3, when a red paint is illuminated by two different light sources, one being illuminant A with a correlated colour temperature (CCT) of 2856K and the other being illuminant D65 with a CCT of 6500K, the two reflected spectra show notable differences, resulting in completely different visual effects. The change in spectral power distribution of the lighting source is the primary reason behind the significant visual contrast between buildings during the day and at night.

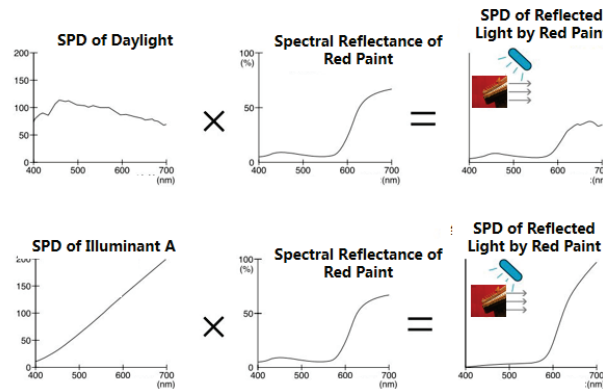


Figure 3. The effect of red paint illuminated by different light sources

As shown in Figure 3, when the red paint is illuminated by illuminant D65, the red portion of the lighting spectrum overlaps with the reflection spectrum of the red paint, and the blue-green portion of the lighting spectrum is absorbed. In comparison, the illuminant A has a higher proportion of red light. When weighted with the reflection spectrum of the red paint, the rising edge of SPD becomes steeper, which increases not only the colour saturation of red paint, but also its brightness.

The colour of an object is generally represented by CIE 1976  $L^*a^*b^*$  colour space, which is a three-dimensional spherical colour space. As shown in Figure 4,  $L$  represents the lightness scale, where a lightness value of 0 represents black, a value of 100 represents white, and a value of 50 corresponds to a wide range of colours on the equatorial plane. The  $a$ -axis indicates the degree of red-green colour, with positive values indicating a bias towards red, and negative values indicating a bias towards green. The  $b$ -axis represents the degree of yellow-blue colour, with positive values indicating a bias towards yellow, and negative values indicating a bias towards blue.

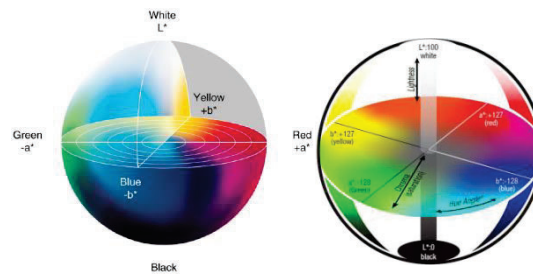


Figure 4. CIE 1976 L\*a\*b\* colour space

Due to the absorption of objects, if the SPD of light source overlaps with the absorption spectrum of objects, the lighting efficiency will be reduced significantly. Conversely, if the SPD of light source overlaps with the reflection spectrum of objects, the efficiency is much higher. Therefore, in the design phase, measurement and selection should be conducted based on the spectrum of light sources and spectral reflectance/transmittance of materials. At the same time, power selection of the light source should be taken into consideration to present the landscape effect, while balancing the lighting efficiency.

## 2.2 SPD measurement of light sources

LEDs have become mainstream in cultural tourism lighting, due to their ability to emit wide-spectrum white light and colourful narrow-band light. The wavelength shift of narrow-band light sources often has a great impact on light colour.

The SPD of LED light sources is usually measured by a spectroradiometer, and the key performance of a spectroradiometer lies in bandwidth and wavelength accuracy. As illustrated in Figure 5, if the measured light source has a narrow bandwidth, using two spectroradiometers with different bandwidths will yield notable differences in the obtained SPD. The SPD obtained by the spectroradiometer of narrow-bandwidth is more precise, while the wider-bandwidth instrument may introduce errors, particularly at steep changes (as indicated by the red circle area in Figure 5).

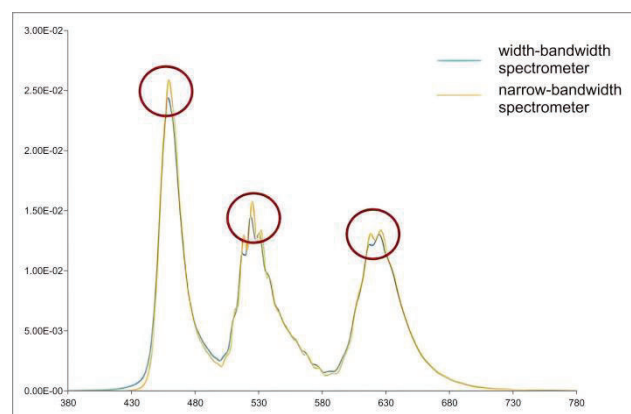


Figure 5. SPD by two spectrometers with different bandwidths

Therefore, during the design phase for cultural tourism lighting, it is highly recommended to use narrow-bandwidth spectroradiometers with high wavelength accuracy, such as the HAAS series spectroradiometer depicted in Figure 6, for the selection and testing of light sources. And it offers the following advantages:

- Bandwidth is smaller than 3 nm, which is ideal for testing typical blue-violet lights with bandwidth around 10-15 nm;
- Wavelength accuracy is better than  $\pm 0.3\text{nm}$  which is highly suitable for wavelength binning of coloured light sources in cultural tourism lighting, enabling better control over light colour consistency.



Figure 6. EVERFINE HAAS series high accuracy spectrometer

### 2.3 Reflection/transmission measurement

Reflection/transmission characteristics of material need to be measured under specific geometric conditions defined by the publication of CIE 15. Typically, material selection and quality management involve measuring spectral reflectance by  $d_i/8^\circ$  or  $d_e/8^\circ$  measurement geometry, as shown in Figure 7, and spectral transmittance by  $d/0^\circ$  measurement geometry. The  $d_i/8^\circ$  measurement geometry captures information that includes contributions from both surface reflection and diffuse reflection, while  $d_e/8^\circ$  measurement geometry excludes surface reflection, which is closer to the diffuse reflection perceived by human eyes. The appropriate geometry can be selected according to the specific requirements of application.

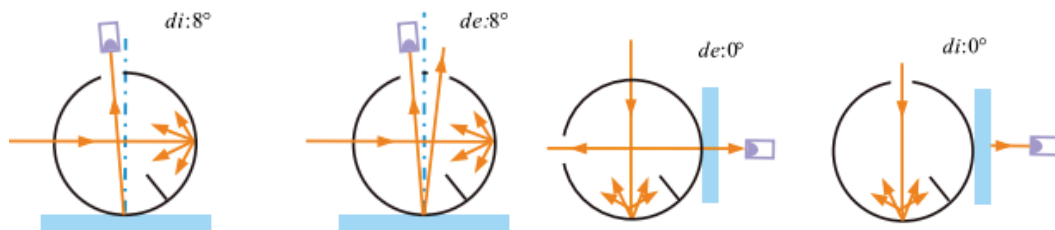


Figure 7. Spectral reflectance and transmittance measurement geometry

When selecting measurement equipment for reflection/transmission characteristics of material in cultural tourism, the following recommendations are suggested:

- 1) Measurement geometry:  $d/8^\circ$  measurement geometry specified in CIE 15 is used for spectral reflectance measurement of materials which is insensitivity to various textures such as clothing, wall coatings, metals, etc.;
- 2) Measurement bandwidth: according to the CIE 15:2018, it is recommended to use a spectrometer with a bandwidth below 5 nm, which also ensures accurate measurement of highly saturated colours;
- 3) Measurement range: the measurement instrument should have good sensitivity and stability across the entire range from black velvet with a reflectivity of about 0.3% to white textiles with a reflectivity close to 100%;
- 4) Software simulation and analysis functions: a measurement instrument is better to include features for analyzing colour differences of materials under different illuminants, as well as simulating colour and other parameters.
- 5) Material colour management: the stability and repeatability of the instrument are also very important, and it is generally recommended to choose a spectrometer with a dual optical path design as it can effectively monitor and compensate for the light source fluctuation.

Figure 8 shows a typical instrument with  $d/8^\circ$  geometry. By considering these factors and selecting appropriate measurement equipment, accurate and reliable colour management can be achieved for materials used in cultural tourism lighting applications.

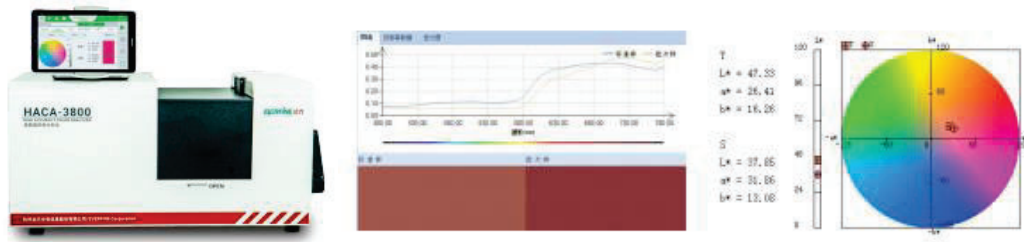


Figure 8. EVERFINE HACA-3800 High Accuracy Colour Analyzer

## 2.4 Practical analysis

The dance-poem drama “The Journey of a Legendary Landscape Painting” presents a unique challenge in stage light design, aiming to achieve a “blue-green” effect. To support this design, the SPD of the stage lights can be measured using the EVERFINE integrating sphere system with HAAS-2000 spectroradiometer. The spectral reflectance and transmittance of materials can be measured by HACA-3800 High Accuracy Colour Analyzer. The tristimulus values X/Y/Z of the materials under any given light source with reflectance can be calculated using formula (1):

$$X = \frac{\sum_{\lambda=380nm}^{780nm} S(\lambda) \cdot R(\lambda) \cdot \bar{x}(\lambda)}{\sum_{\lambda=380nm}^{780nm} S(\lambda) \cdot \bar{x}(\lambda)}; \quad Y = \frac{\sum_{\lambda=380nm}^{780nm} S(\lambda) \cdot R(\lambda) \cdot \bar{y}(\lambda)}{\sum_{\lambda=380nm}^{780nm} S(\lambda) \cdot \bar{y}(\lambda)}; \quad Z = \frac{\sum_{\lambda=380nm}^{780nm} S(\lambda) \cdot R(\lambda) \cdot \bar{z}(\lambda)}{\sum_{\lambda=380nm}^{780nm} S(\lambda) \cdot \bar{z}(\lambda)} \quad (1)$$

Where:

- $R(\lambda)$  is the spectral reflectance of the material
- $\bar{x}(\lambda)$ 、 $\bar{y}(\lambda)$ 、 $\bar{z}(\lambda)$  are the colour matching functions defined by CIE 1931 Chromaticity system
- $S(\lambda)$  is the spectral power distribution of the illuminating light source

According to formula (2) tristimulus values X/Y/Z can be converted to CIE  $L^*a^*b^*$  colour coordinates of the materials in the corresponding colour space.

$$\begin{aligned} L^* &= 116f(Y/Y_n) - 16 \\ a^* &= 500[f(X/X_n) - f(Y/Y_n)] \\ b^* &= 200[f(Y/Y_n) - f(Z/Z_n)] \end{aligned} \quad (2)$$

In formula (2),  $X_n$ ,  $Y_n$ ,  $Z_n$  are the tristimulus values of perfect diffuse reflectors.

The colour coordinates and simulated colours under different combinations of lights were calculated and simulated as shown in Figure 9. The colours of cyan, blue-green and green coatings under illuminant D65 are shown in first column. When illuminated by an illuminant A, all three colours shift towards yellow hue. When illuminated by a 5000K LED light source, the green colour changes minimally, while the blue colour shifts towards purple hue and the blue-green colour becomes closer to green. When illuminated by a single-colour LED light source with a typical wavelength of 560nm, due to the SPD overlap between illuminating light source and the material's spectral reflectance with the bandwidth of light source being narrower than the spectral reflectance of the material, the reflected colour becomes closer to the colour of the light source. These results highlight the significant impact of the light source on the perceived colour of objects.

As shown in Figure 10, the colour coordinates of the reflected colours may vary across quadrants in the  $L^*a^*b^*$  colour coordinate system when different light sources illuminate typical colour coatings. Reflected colour becomes closer to the colour of the light source when illuminated by highly saturated single-colour light.









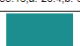
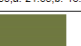
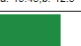
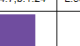
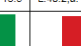

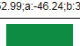
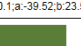
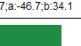
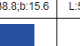
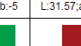

	illuminant D65	illuminant A	5000K white LED	typical wavelegth 450nm LED	typical wavelegth 560nm LED	typical wavelegth 640nm LED
cyan	L:50.1,a:-13.49,b:-30.13 	L:51.02,a:-21.03,b:-37.85 	L:51.55,a:-2.08,b:-39.3 	L:71.78,a:8.9,b:-4.36 	L:51.1,a:-13.4,b:-19.6 	L:41.73,a:-0.34,b:-51.3 
blue green	L:55.18,a:-26.4,b:-8.68 	L:51.55,a:-21.65,b:-16.22 	L:52.7,a:-19.45,b:-12.9 	L:60.55,a:-4.7,b:1.24 	L:53.6,a:-15.4,b:-13.5 	L:40.2,a:-0.97,b:-34.04 
green	L:52.99,a:-46.24,b:33.03 	L:50.1,a:-39.52,b:23.5 	L:52.77,a:-46.7,b:34.1 	L:39.26,a:-38.8,b:15.6 	L:56.56,a:-20.3,b:-5 	L:31.57,a:-2.55,b:-8.6 

Figure 9. Colour effects of different combinations of light sources and materials

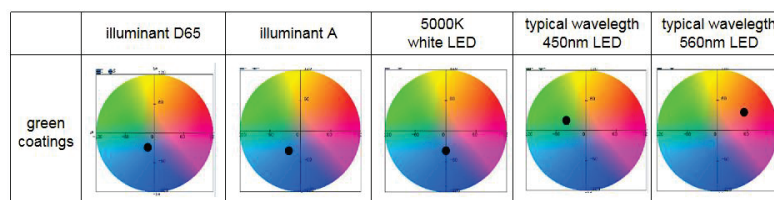


Figure 10. Changes in colour coordinates of green coatings under different light sources

In summary, the strategic use of light sources can greatly enhance the colour expression of clothing and effectively highlight the performance themes, ultimately achieving the desired "blue-green" effect.

### 3. FIELD MEASUREMENT FOR CULTURAL TOURISM LIGHTING

On-site evaluating conditions for cultural tourism lighting are usually complex. It is recommended to use an imaging luminance & colour meter for accurate and efficient in field measurement. An imaging luminance & colour meter allows for the capture of overall lighting effect images, enabling the analysis of colour variations, colour uniformity, chromatic aberration, and more. This capability proves especially valuable when dealing with multi-colour mixing light sources, as adjustments can be made promptly based on the measured results.

In dark backgrounds commonly found in cultural tourism lighting scenarios, accurate colour measurement of lighting system in such environments requires the meter with high dynamic range and great linearity. In addition, in order to improve colour measurement accuracy, a spectroradiometer can be used for colour calibration.

The EVERFINE ILC series imaging luminance Colourimeter features a high  $V(\lambda)$  matching accuracy and patented cooling technology to reach the test limit down to  $0.0005 \text{ cd/m}^2$ . Additionally, it has a high dynamic range up to  $10^8$  and an ultra-high measurement repeatability, which ensures accurate measurement of luminance, chromaticity, and uniformity of field lighting. Furthermore, it is recommended to be used along the spectral radiance meter (e.g. EVERFINE SRC series), which can achieve colourimetric mismatch measurements. The test results of a spectral radiance meter can be imported into the software of an ILC imaging luminance colourimeter with a simple, enabling precise calibration of chromaticity and the accuracy of field colour measurements. The colour uniformity and luminance uniformity in the lighting scene can be easily measured and analyzed using the method described.

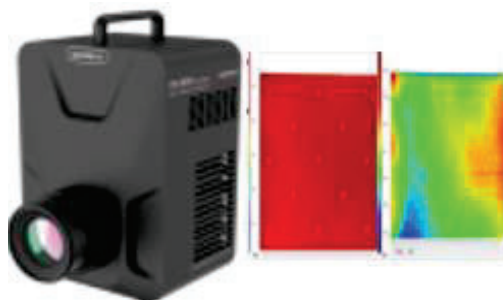


Figure 11 EVERFINE ILC series Imaging Luminance Colourimeter

#### **4. CONCLUSION**

In the design and selection phase of lighting for cultural tourism, by measuring and analyzing the various parameters of light sources and the light reflection and transmission performance of the materials, we can evaluate the lighting design effect more intuitively. This provides great convenience for various lighting applications. During the on-site evaluating phase, it becomes essential to accurately, quickly, and conveniently restore the colour and luminance of the lighting scene, to make timely adjustments for achieving the best lighting effect. An imaging luminance and colour meter is the suitable and convenient solution for on-site conformity measurement. Further by utilizing statistical analysis software, panoramic, regional, and key evaluation parameters can be quickly obtained. Digitized expression of colours for lighting scenes and objects can also improve the communication efficiency for engineering record and confirmation.

#### **REFERENCES**

- [1] CIE 015:2018 Colourimetry(4rd Edition)
- [2] Jiangen Pan, Hongxuan Yue, Haiping Shen,etc. Uncertainty Analysis of LED Colour Measurement by Spectroscopy[J]. Photoelectron . Laser, 2008, 19(2):3

#### **ACKNOWLEDGEMENTS**

This work is supported by the National Key R&D Program of China, under Grant No. 2022YFF0705500

Corresponding Author Name: Jiangen Pan

Affiliation: EVERFINE Corporation, Hangzhou, Zhejiang, China

e-mail: tech@everfine.cn

# RESEARCH ON COLOUR QUALITY MANAGEMENT TECHNOLOGY IN LIGHTING FOR CULTURAL TOURISM

Xian Tang, Xiong Yang, Qian Li, Jiangen Pan

(EVERFINE Corporation, Hangzhou, Zhejiang, China)

## ABSTRACT

By skillfully integrating lighting and landscape through elaborate design and implementation, captivating visual effects and aesthetic atmosphere can be created. The colour displayed by the landscape is influenced by both the spectral power distribution (SPD) of the lighting source and the spectral transmittance/reflectance of the materials in the landscape. The colour quality management should be implemented throughout the entire process, from the initial design to construction and subsequent maintenance. This paper analyzes the interaction between objects and light sources in landscape lighting scenarios. Furthermore, it explores the measurement methods for assessing the transmittance, reflectance, and absorption characteristics of materials. By measuring the spectral properties of typical materials and light sources and simulating their combined visual effects, this study aims to provide a data foundation for design and construction. This paper also investigates the solutions for field measurement of lighting systems and objects within a lighting scene. These solutions enable accurate and convenient measurement of colour and luminance, beneficial for in time adjustment of light sources especially when dealing with multi colour mixing illumination. Moreover, the digitized expression of colour for lighting scene and objects can improve communication efficiency for engineering record and confirmation.

Keywords: lighting for cultural tourism; colour management; colour measurement

## 1. INTRODUCTION

Currently, there is an increasingly opportunity to utilize lighting in cultural tourism. Whether it's immersive night tourism that corporates local resources, cultural IP theme parks, or stages within scenic areas, creating an aesthetic atmosphere through landscape lighting scenarios is a major focus. The ambiance is manifested through the interplay of light and scenery, light and architecture, and light and objects.

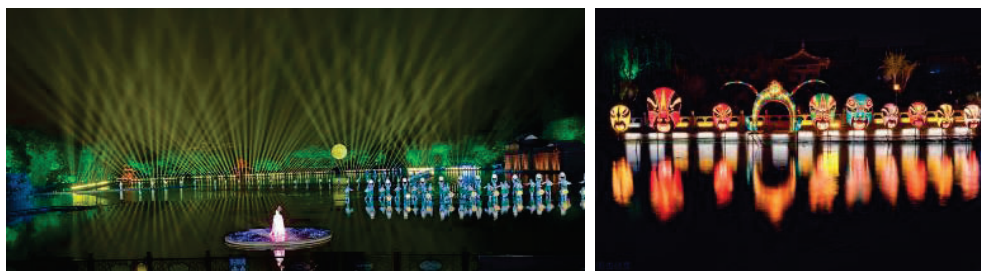


Figure 1: Examples of lighting for cultural tourism

In lighting design, it is essential to consider the impact of light absorption, reflection, and transmission by objects or materials. The overall lighting effect is the result of combining light from sources with light reflection/transmission by objects .

The on-site evaluation of cultural tourism landscape lighting is also a complex undertaking, which involves multiple scenes and lighting combinations, as well as diverse environments such as water, roads, bridges, mountains, walls of buildings, etc. The most convenient and efficient method for in field measurement of lighting systems and objects in a lighting scene is to obtain the imaging colour distribution of the scene.

## 2. COLOUR QUALITY MANAGEMENT IN LIGHTING DESIGN

### 2.1 The interaction between light and object

When light reaches the surface, several phenomena related to the optical properties of the object will occur, including reflection, transmission, and absorption, as shown in Figure 2, of which the value can be expressed as the ratios of reflected, transmitted, and absorbed radiant flux to the

incident radiant flux, defined as  $\rho$ ,  $\tau$ , and  $\alpha$ , respectively. The colour appearance of the object can be characterized by the spectral reflection  $\rho(\lambda)$ , the spectral absorption  $\alpha(\lambda)$ , and the spectral transmission  $t(\lambda)$ .

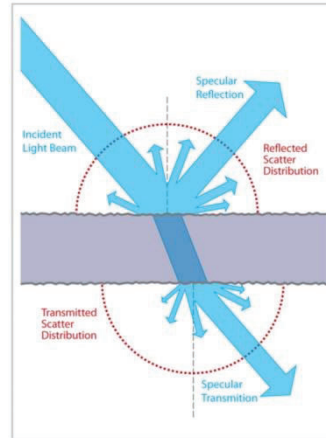


Figure 2. The interaction between light and object

The colour of an object as perceived visually is generally decided by the spectral reflectance/transmittance of the material and the spectral power distribution (SPD) of the light source. Take the example of the red wall of historic buildings in China: when illuminated by light sources with different spectra, the reflected spectrum will vary significantly leading to distinct visual effects. In Figure 3, when a red paint is illuminated by two different light sources, one being illuminant A with a correlated colour temperature (CCT) of 2856K and the other being illuminant D65 with a CCT of 6500K, the two reflected spectra show notable differences, resulting in completely different visual effects. The change in spectral power distribution of the lighting source is the primary reason behind the significant visual contrast between buildings during the day and at night.

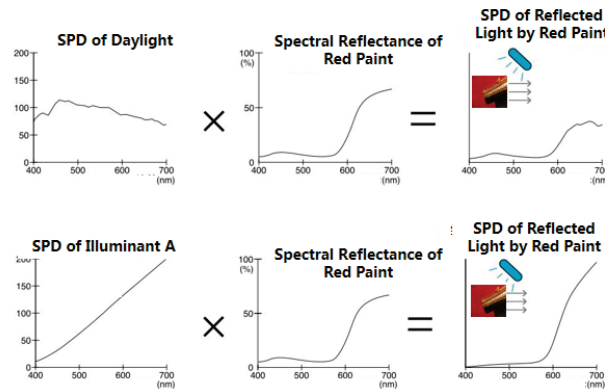


Figure 3. The effect of red paint illuminated by different light sources

As shown in Figure 3, when the red paint is illuminated by illuminant D65, the red portion of the lighting spectrum overlaps with the reflection spectrum of the red paint, and the blue-green portion of the lighting spectrum is absorbed. In comparison, the illuminant A has a higher proportion of red light. When weighted with the reflection spectrum of the red paint, the rising edge of SPD becomes steeper, which increases not only the colour saturation of red paint, but also its brightness.

The colour of an object is generally represented by CIE 1976  $L^*a^*b^*$  colour space, which is a three-dimensional spherical colour space. As shown in Figure 4,  $L$  represents the lightness scale, where a lightness value of 0 represents black, a value of 100 represents white, and a value of 50 corresponds to a wide range of colours on the equatorial plane. The  $a$ -axis indicates the degree of red-green colour, with positive values indicating a bias towards red, and negative values indicating a bias towards green. The  $b$ -axis represents the degree of yellow-blue colour, with positive values indicating a bias towards yellow, and negative values indicating a bias towards blue.

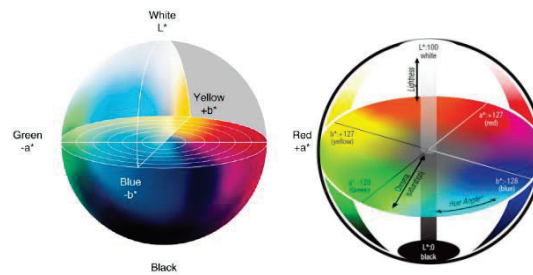


Figure 4. CIE 1976 L\*a\*b\* colour space

Due to the absorption of objects, if the SPD of light source overlaps with the absorption spectrum of objects, the lighting efficiency will be reduced significantly. Conversely, if the SPD of light source overlaps with the reflection spectrum of objects, the efficiency is much higher. Therefore, in the design phase, measurement and selection should be conducted based on the spectrum of light sources and spectral reflectance/transmittance of materials. At the same time, power selection of the light source should be taken into consideration to present the landscape effect, while balancing the lighting efficiency.

## 2.2 SPD measurement of light sources

LEDs have become mainstream in cultural tourism lighting, due to their ability to emit wide-spectrum white light and colourful narrow-band light. The wavelength shift of narrow-band light sources often has a great impact on light colour.

The SPD of LED light sources is usually measured by a spectroradiometer, and the key performance of a spectroradiometer lies in bandwidth and wavelength accuracy. As illustrated in Figure 5, if the measured light source has a narrow bandwidth, using two spectroradiometers with different bandwidths will yield notable differences in the obtained SPD. The SPD obtained by the spectroradiometer of narrow-bandwidth is more precise, while the wider-bandwidth instrument may introduce errors, particularly at steep changes (as indicated by the red circle area in Figure 5).

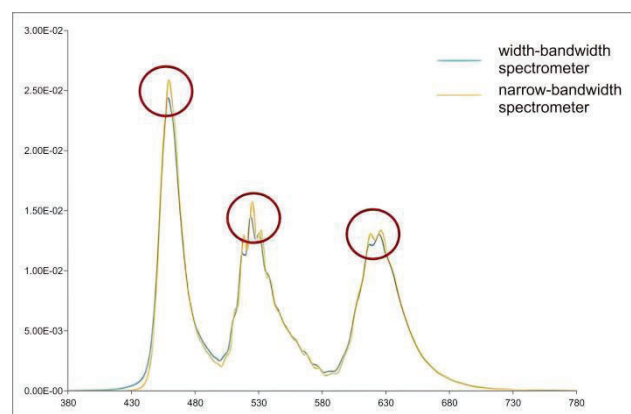


Figure 5. SPD by two spectrometers with different bandwidths

Therefore, during the design phase for cultural tourism lighting, it is highly recommended to use narrow-bandwidth spectroradiometers with high wavelength accuracy, such as the HAAS series spectroradiometer depicted in Figure 6, for the selection and testing of light sources. And it offers the following advantages:

- Bandwidth is smaller than 3 nm, which is ideal for testing typical blue-violet lights with bandwidth around 10-15 nm;
- Wavelength accuracy is better than  $\pm 0.3\text{nm}$  which is highly suitable for wavelength binning of coloured light sources in cultural tourism lighting, enabling better control over light colour consistency.



Figure 6. EVERFINE HAAS series high accuracy spectrometer

### 2.3 Reflection/transmission measurement

Reflection/transmission characteristics of material need to be measured under specific geometric conditions defined by the publication of CIE 15. Typically, material selection and quality management involve measuring spectral reflectance by  $d_i/8^\circ$  or  $d_e/8^\circ$  measurement geometry, as shown in Figure 7, and spectral transmittance by  $d/0^\circ$  measurement geometry. The  $d_i/8^\circ$  measurement geometry captures information that includes contributions from both surface reflection and diffuse reflection, while  $d_e/8^\circ$  measurement geometry excludes surface reflection, which is closer to the diffuse reflection perceived by human eyes. The appropriate geometry can be selected according to the specific requirements of application.

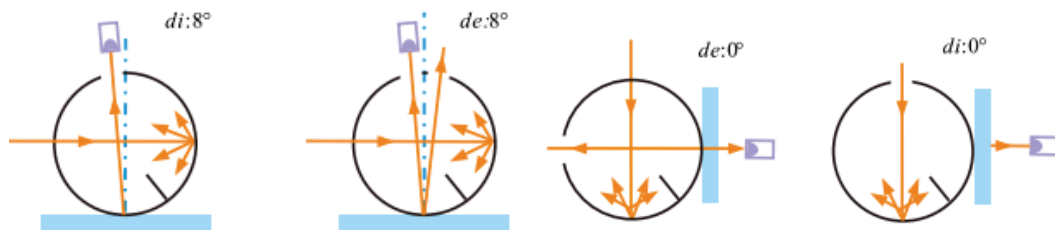


Figure 7. Spectral reflectance and transmittance measurement geometry

When selecting measurement equipment for reflection/transmission characteristics of material in cultural tourism, the following recommendations are suggested:

- 1) Measurement geometry:  $d/8^\circ$  measurement geometry specified in CIE 15 is used for spectral reflectance measurement of materials which is insensitivity to various textures such as clothing, wall coatings, metals, etc.;
- 2) Measurement bandwidth: according to the CIE 15:2018, it is recommended to use a spectrometer with a bandwidth below 5 nm, which also ensures accurate measurement of highly saturated colours;
- 3) Measurement range: the measurement instrument should have good sensitivity and stability across the entire range from black velvet with a reflectivity of about 0.3% to white textiles with a reflectivity close to 100%;
- 4) Software simulation and analysis functions: a measurement instrument is better to include features for analyzing colour differences of materials under different illuminants, as well as simulating colour and other parameters.
- 5) Material colour management: the stability and repeatability of the instrument are also very important, and it is generally recommended to choose a spectrometer with a dual optical path design as it can effectively monitor and compensate for the light source fluctuation.

Figure 8 shows a typical instrument with  $d/8^\circ$  geometry. By considering these factors and selecting appropriate measurement equipment, accurate and reliable colour management can be achieved for materials used in cultural tourism lighting applications.



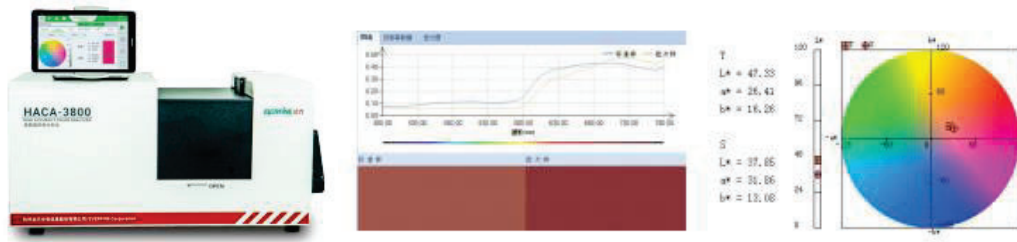


Figure 8. EVERFINE HACA-3800 High Accuracy Colour Analyzer

## 2.4 Practical analysis

The dance-poem drama “The Journey of a Legendary Landscape Painting” presents a unique challenge in stage light design, aiming to achieve a “blue-green” effect. To support this design, the SPD of the stage lights can be measured using the EVERFINE integrating sphere system with HAAS-2000 spectroradiometer. The spectral reflectance and transmittance of materials can be measured by HACA-3800 High Accuracy Colour Analyzer. The tristimulus values X/Y/Z of the materials under any given light source with reflectance can be calculated using formula (1):

$$X = \frac{\sum_{\lambda=380nm}^{780nm} S(\lambda) \cdot R(\lambda) \cdot \bar{x}(\lambda)}{\sum_{\lambda=380nm}^{780nm} S(\lambda) \cdot \bar{x}(\lambda)}; \quad Y = \frac{\sum_{\lambda=380nm}^{780nm} S(\lambda) \cdot R(\lambda) \cdot \bar{y}(\lambda)}{\sum_{\lambda=380nm}^{780nm} S(\lambda) \cdot \bar{y}(\lambda)}; \quad Z = \frac{\sum_{\lambda=380nm}^{780nm} S(\lambda) \cdot R(\lambda) \cdot \bar{z}(\lambda)}{\sum_{\lambda=380nm}^{780nm} S(\lambda) \cdot \bar{z}(\lambda)} \quad (1)$$

Where:

- $R(\lambda)$  is the spectral reflectance of the material
- $\bar{x}(\lambda)$ 、 $\bar{y}(\lambda)$ 、 $\bar{z}(\lambda)$  are the colour matching functions defined by CIE 1931 Chromaticity system
- $S(\lambda)$  is the spectral power distribution of the illuminating light source

According to formula (2) tristimulus values X/Y/Z can be converted to CIE  $L^*a^*b^*$  colour coordinates of the materials in the corresponding colour space.

$$\begin{aligned} L^* &= 116f(Y/Y_n) - 16 \\ a^* &= 500[f(X/X_n) - f(Y/Y_n)] \\ b^* &= 200[f(Y/Y_n) - f(Z/Z_n)] \end{aligned} \quad (2)$$

In formula (2),  $X_n$ ,  $Y_n$ ,  $Z_n$  are the tristimulus values of perfect diffuse reflectors.

The colour coordinates and simulated colours under different combinations of lights were calculated and simulated as shown in Figure 9. The colours of cyan, blue-green and green coatings under illuminant D65 are shown in first column. When illuminated by an illuminant A, all three colours shift towards yellow hue. When illuminated by a 5000K LED light source, the green colour changes minimally, while the blue colour shifts towards purple hue and the blue-green colour becomes closer to green. When illuminated by a single-colour LED light source with a typical wavelength of 560nm, due to the SPD overlap between illuminating light source and the material's spectral reflectance with the bandwidth of light source being narrower than the spectral reflectance of the material, the reflected colour becomes closer to the colour of the light source. These results highlight the significant impact of the light source on the perceived colour of objects.

As shown in Figure 10, the colour coordinates of the reflected colours may vary across quadrants in the  $L^*a^*b^*$  colour coordinate system when different light sources illuminate typical colour coatings. Reflected colour becomes closer to the colour of the light source when illuminated by highly saturated single-colour light.



















	illuminant D65	illuminant A	5000K white LED	typical wavelegth 450nm LED	typical wavelegth 560nm LED	typical wavelegth 640nm LED
cyan	L:50.1,a:-13.49,b:-30.13 	L:51.02,a:-21.03,b:-37.85 	L:51.55,a:-2.08,b:-38.3 	L:71.78,a:8.9,b:-4.36 	L:51.1,a:-13.4,b:-19.6 	L:41.73,a:-0.34,b:-51.3 
blue green	L:55.18,a:-26.4,b:-8.68 	L:51.55,a:-21.65,b:-16.22 	L:52.7,a:-19.45,b:-12.9 	L:60.55,a:-4.7,b:1.24 	L:53.6,a:-15.4,b:-13.5 	L:40.2,a:-0.97,b:-34.04 
green	L:52.99,a:-46.24,b:33.03 	L:50.1,a:-39.52,b:23.5 	L:52.77,a:-46.7,b:34.1 	L:39.26,a:-38.8,b:15.6 	L:56.56,a:-20.3,b:-5 	L:31.57,a:-2.55,b:-8.6 

Figure 9. Colour effects of different combinations of light sources and materials

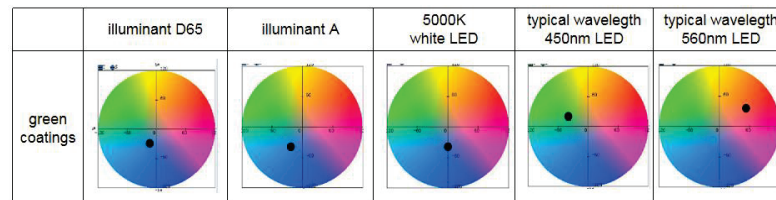


Figure 10. Changes in colour coordinates of green coatings under different light sources

In summary, the strategic use of light sources can greatly enhance the colour expression of clothing and effectively highlight the performance themes, ultimately achieving the desired "blue-green" effect.

### 3. FIELD MEASUREMENT FOR CULTURAL TOURISM LIGHTING

On-site evaluating conditions for cultural tourism lighting are usually complex. It is recommended to use an imaging luminance & colour meter for accurate and efficient in field measurement. An imaging luminance & colour meter allows for the capture of overall lighting effect images, enabling the analysis of colour variations, colour uniformity, chromatic aberration, and more. This capability proves especially valuable when dealing with multi-colour mixing light sources, as adjustments can be made promptly based on the measured results.

In dark backgrounds commonly found in cultural tourism lighting scenarios, accurate colour measurement of lighting system in such environments requires the meter with high dynamic range and great linearity. In addition, in order to improve colour measurement accuracy, a spectroradiometer can be used for colour calibration.

The EVERFINE ILC series imaging luminance Colourimeter features a high  $V(\lambda)$  matching accuracy and patented cooling technology to reach the test limit down to  $0.0005 \text{ cd/m}^2$ . Additionally, it has a high dynamic range up to  $10^8$  and an ultra-high measurement repeatability, which ensures accurate measurement of luminance, chromaticity, and uniformity of field lighting. Furthermore, it is recommended to be used along the spectral radiance meter (e.g. EVERFINE SRC series), which can achieve colourimetric mismatch measurements. The test results of a spectral radiance meter can be imported into the software of an ILC imaging luminance colourimeter with a simple, enabling precise calibration of chromaticity and the accuracy of field colour measurements. The colour uniformity and luminance uniformity in the lighting scene can be easily measured and analyzed using the method described.



Figure 11 EVERFINE ILC series Imaging Luminance Colourimeter

#### **4. CONCLUSION**

In the design and selection phase of lighting for cultural tourism, by measuring and analyzing the various parameters of light sources and the light reflection and transmission performance of the materials, we can evaluate the lighting design effect more intuitively. This provides great convenience for various lighting applications. During the on-site evaluating phase, it becomes essential to accurately, quickly, and conveniently restore the colour and luminance of the lighting scene, to make timely adjustments for achieving the best lighting effect. An imaging luminance and colour meter is the suitable and convenient solution for on-site conformity measurement. Further by utilizing statistical analysis software, panoramic, regional, and key evaluation parameters can be quickly obtained. Digitized expression of colours for lighting scenes and objects can also improve the communication efficiency for engineering record and confirmation.

#### **REFERENCES**

- [1] CIE 015:2018 Colourimetry(4rd Edition)
- [2] Jiangen Pan, Hongxuan Yue, Haiping Shen,etc. Uncertainty Analysis of LED Colour Measurement by Spectroscopy[J]. Photoelectron . Laser, 2008, 19(2):3

#### **ACKNOWLEDGEMENTS**

This work is supported by the National Key R&D Program of China, under Grant No. 2022YFF0705500

Corresponding Author Name: Jiangen Pan

Affiliation: EVERFINE Corporation, Hangzhou, Zhejiang, China

e-mail: tech@everfine.cn

# RESEARCH PROGRESS OF BUILDING DAYLIGHT ENVIRONMENT BASED ON CLIMATE-BASED DAYLIGHT MODELING

Shuying Liang<sup>1, 2</sup>, Yi Yang<sup>1, 2</sup>

(1. Key Laboratory of New Technology for Construction of Cities in Mountain Area, Ministry of Education, Chongqing University, Chongqing 400045, China.

(2. School of Architecture and Urban Planning of Chongqing University, Chongqing 400045, China)

## ABSTRACT

As a green energy source, natural light has great significance for sustainable development. The research, development and utilization of natural light have received more and more attention. Correct assessment of natural lighting in buildings is a key factor in the active use of natural light, while current natural lighting research is mainly based on static calculation assessment, without taking into account the highly dynamic of natural light and the influence of geographic differences on indoor lighting. Therefore, the proposal of Climate-based Daylight Modeling has put forward new requirements for the applicability application of natural lighting in buildings. This paper reviews the research results on Climate-based Daylight Modeling in the past ten years, sorts out the research results from the three dimensions of "quantitative research", "simulation technology" and "measurement standard", summarizes the research progress of natural light based on Climate-based Daylight Modeling. The future development trend of natural lighting and some research problems that need to be solved have been proposed.

Keywords: Daylighting, Climate-Based Daylight Modeling, Daylight climate data, Sky brightness model, Dynamic daylighting

## 1. INTRODUCTION

Since the energy crisis of the 1970s, the study, development, and utilization of daylight as a green energy source to support human activities and physical health has received increasing attention. With the growing understanding of the health effects of daylight, numerous studies have shown that compared to artificial lighting environments, indoor spaces in daylight conditions not only allow for optimal visual effects, but also provide psychological comfort and pleasure. In recent years, more and more scholars have begun to study the correlation between daylighting quality and visual comfort [1-2], circadian rhythm [3] and non-visual factors [4].

Since the 1950s, Daylight Factor (DF) has been widely used as an objective evaluation indicator for building daylighting design. The DF takes the overcast sky condition as the boundary condition of building daylighting design, so that buildings can meet people's daylighting needs under the most unfavorable daylighting conditions [5]. However, daylight is dynamic and climatic, and the DF is computed only statically at a given point, without taking into account the effects of orientation, area, climate, and other factors. The DF does not accurately reflect the illumination level. Therefore, it is clear that traditional static daylighting evaluation methods cannot meet the need for more accurate daylighting analysis and better daylighting environments.

The emergence of Climate-Based Daylight Modeling (CBDM) is a significant progress in the field of daylighting research. It is a method of predicting various radiation amounts or light measurements by using solar and sky conditions from standardized annual weather data sets. CBDM can accurately predict absolute values (such as irradiance, illuminance, radiation, and brightness)[6]. The dynamic daylighting analysis technique based on CBDM takes into account time variables, sky conditions and local climate, which not only reflects the regional climate characteristics, but also allows for a more accurate assessment of the daylighting performance of buildings. Climate-based metrics, such as Useful Daylight Illuminance (UDI) and Daylight Autonomy (DA), have been proposed and gradually incorporated into design criteria. In the last decade, there has been positive progress in the study of daylighting in buildings based on CBDM. The emphasis on CBDM-based daylighting design research is crucial for a comprehensive understanding of the interplay between daylight, architecture, and people to create healthy and effective living spaces.

## 2. QUANTITATIVE STUDY OF DAYLIGHT

The CBDM relies heavily on accurate climate data. Climate data commonly include hourly solar irradiance, diffuse horizontal irradiance, and direct normal irradiance. These values can reflect the brightness distribution of the sun and sky at different times [7]. These values are fed into an accurate building simulation software to reconstruct a realistic model of the sky brightness distribution in successive hourly or sub-hourly steps. The comparison between the CBDM and CIE standard overcast sky options is shown in Fig.1. Thus, the fundamental study of CBDM includes the fields of daylight climate data and sky brightness models.

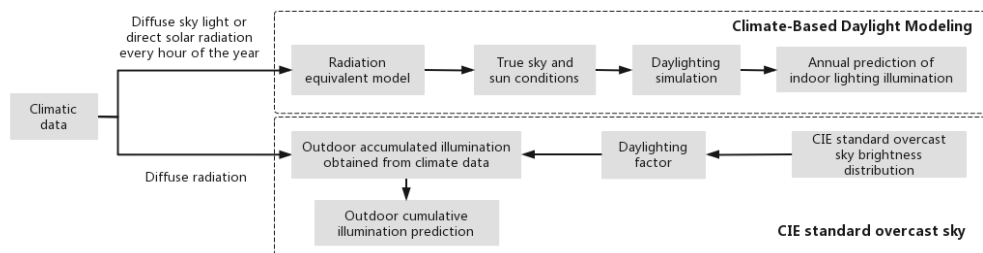


Figure 1. Comparison between CBDM and CIE standard overcast sky options

### 2.1 Research on daylight climate observation

In 1991, the WMO and the CIE established the IDMP. The project is to set up a series of ground stations around the world for the collection of daylight climate data. The establishment of IDMP can help researchers to understand and grasp the characteristics of daylight climate, and to conduct systematic studies of daylight availability around the world. Most of the IDMP observatories are located in the Northern Hemisphere, with the largest number, 19, located in Japan. In contrast, there are only three observatories in China: the Chongqing General Observation Station, the Beijing Research Observation Station, and the Hong Kong Research Observation Station [8].

Since its establishment in 1991, the observatory in Chongqing has been engaged in the study of daylight climate observation and has made positive progress. From 1991 to 1993, Zhang Qingwen [9] made continuous observation of Chongqing for two and a half years, and collected 11 quantities of data such as solar radiation, illuminance and zenith brightness, which provided a scientific basis for the study of daylight climate in Chongqing. He Ying et al. [10] studied and analyzed the weather parameters that affected the sky brightness distribution. Combined with 1min daylight climate data from the IDMP Chongqing Observatory, the reference sky was divided into six sky types, which laid the foundation for the study of the sky brightness distribution. Luo Tao et al. [11] used the IDMP Beijing observation station, combined with the self-developed spectral sky scan brightness meter, collected one-year data of sky illuminance distribution in Beijing, proposed the classification of sky brightness in the Beijing area. Then, based on the Matlab algorithm program, he obtained the law of the sky brightness distribution in the Beijing area, which provided data support for domestic daylight climate research. Hong Kong leads the research of the daylight climate in China. In 2003, Danny.H.W et al. [12] collected and processed the sky brightness data in Hong Kong for one year and obtained the distribution rule of the sky brightness in Hong Kong. Later, Edward et al. [13] conducted optimization research on the basis of Danny.H.W's research and proposed a "Hong Kong Representative Sky" (HKRS), which represented the real sky conditions in Hong Kong, and demonstrated that using this sky model gave better predictions of daylight availability and reduced errors by 20% to 40%.

### 2.2 Daylight climate data

The CBDM uses dynamic daylighting simulation techniques, and weather data has a direct impact on its results. The dynamic daylight simulation commonly uses the Perez All-Weather sky model, which mostly uses climate data of typical years in recent decades (IWE/CSWD files, etc.) to generate sky brightness distribution, and then develops daylight simulation based on regional daylight climate. However, with the development of cities in recent years, the regional daylight climate is also changing, and the use of typical annual climate data can also form large errors [14]. Meanwhile, the existing climate files take hourly step as the simulation, which to some extent also



has an impact on the simulation accuracy [15]. Therefore, in order to provide a more realistic external light environment for building daylight simulation and improve the simulation accuracy of daylighting in buildings, numerous researchers begin to explore which climate data is more accurate to be applied in local building lighting simulation, and try to apply measured data in building daylight simulation.

The research achievement of Tianjin University "Regional Daylight-climate Information System Based on GIS" can obtain outdoor illumination value and sky brightness data by inputting measured solar radiation data of a place. The research and development of this system is a great enrichment of Chinese daylight climate data [16-17]. On this basis, Wang Shuyi et al. [18] based on the measured solar radiation data in Tianjin, compared the modified data of typical years with the measured daylight data through experimental simulation, and concluded a set of building daylighting simulation process based on DEST typical years. It has been tentatively demonstrated that the simulation time steps based on the DAYSIM climate files have an effect on the simulation accuracy. Sun Wenchao [19] based on one-year solar radiation data in Tianjin area, compared and analyzed different climate files including ChinaTMY2, DEST typical year and CSWD, founded that the DEST typical year was in better agreement with the measured data. After that, he revised the climate data for typical years on a month-by-month basis to get climate data for typical years that better reflect Tianjin's true daylight climate conditions.

### 2.3 Sky brightness model

The accuracy of daylighting simulation is extremely dependent on the sky brightness condition [20]. Therefore, the construction of accurate sky brightness models has been the goal of various researchers for a long time. Foreign studies of sky brightness models started earlier, with relatively complete studies since the 1940s. Currently, the CIE standard sky model, the Igawa sky model and the Perez All-Weather sky model are widely used in the world. Ferraro [21] conducted a comparative study of different sky brightness models, and found that the CIE standard sky model can more accurately represent the true sky brightness. The study of Yuje Wu et al. [22] showed that the simulated value of indoor illuminance obtained by Perez All-Weather Sky Model was more than 300% different from the measured value. It has also been demonstrated that real sky conditions play an essential role in the accuracy of daylighting simulations.

Kittler [23] proposed the standard sky brightness distribution theory in 1991 and determined 15 sky brightness types. Bartzokas et al. [24] confirmed the applicability of the distribution frequencies of these 15 sky types in the application of daylight climate research. However, the sky brightness distribution is also influenced by additional factors, such as solar position, cloudiness, turbidity, the level of pollutants in the atmosphere and so on [25]. There are also significant differences in the distribution of sky brightness in regions with different climatic and geographical characteristics. Therefore, in order to calculate the brightness distribution accurately, it is necessary to determine the closest sky type at a given place and time based on regional daylight climate measurements. Zi Ying et al. [26] used a sky scanner to collect sky brightness data, determined the sky type which is closest to Harbin in winter by comparing the sky brightness data with 15 CIE standard skies. Bian Yu et al. [27] used a fisheye lens to continuously acquire sky images in South China for a lengthy period of time, obtained the distribution of sky brightness from the sky images, and analyzed the three types of standard sky with the most frequency in South China. Later, he obtained a model of the typical sky brightness distribution in South China by superimposing the linear components of the occurrence frequencies of these three standard skies. In addition, the simulation accuracy of building daylighting can be considerably improved by modifying the sky brightness model adopted in the simulation of the measured daylight climate data. Wang Hongzhen [28], by comparing the simulated data with the measured data, proved that the Perez All-Weather sky model modified by the real measured climate data had higher simulation accuracy. Wang Zhao [29] used the solar irradiance data measured by local meteorological stations to modify the Perez All-Weather sky model.

### 3. THE TECHNICAL APPLICATION OF CBDM

The proposal of CBDM has fundamentally changed the practice of daylighting in buildings. In 2006, Professor J.Mardaljevic from Loughborough University described CBDM in the annual conference of CIBSE: The assessment of the luminous conditions within the built environment that makes use of representative climate data to recreate realistic sky luminance distributions, at hourly or sub-hourly consecutive steps, by means of physically accurate lighting simulation tools.



### 3.1 Analysis and simulation of CBDM

There are two principal analysis methods for CBDM: cumulative and time series. Cumulative methods can be used to predict microclimate and solar access in urban environments, long-term exposure of artworks to daylight, and quick assessment of seasonal daylight availability and/or solar shading at the early design stage. Du Jiangtao et al. [30] used climate data of Harbin, obtained the annual value of vertical sunshine illumination from 6 a.m. to 6 p.m. (hourly step) through the DAYSIM simulation, evaluated three typical urban layout, and completed a comprehensive analysis of daylighting potential. Time series analysis is used to assess, for example, the overall daylighting potential of a building, the occurrence of excessive or insufficient illumination, as an input to behavioral models for light switching and/or blind usage, and the potential of daylight responsive lighting controls to reduce building energy usage. Konis [31] developed a simulation tool that integrated multi-spectral lighting simulations of biological lighting effects into CBDM workflows, enabling automated hourly (or half-hourly) time series assessments on selected days throughout the year, which can be used to directly assess the daylighting performance of future projects during the design process.

Over the past 16 years, CBDM simulation technology has undergone a rapid development process. Radiance has been adopted as the primary CBDM simulation tool due to its precise computing capabilities, and has produced five CBDM simulation techniques: DAYSIM, 4-Component method (4-CM), 2-phase method (2-PM), 3-phase method (3-PM) and 5-phase method (5-PM) [32]. Among them, DAYSIM, 3-PM and 5-PM are used more. In addition, simulation software tools such as ADELIN, Ecotect Analysis, DIVA, Rhinoceros-based Ladybug and Energy Plus, DALI are also widely used and still under development.

### 3.2 Application research of CBDM

As the foundation of daylight simulation matures, there is a growing demand for CBDM to address increasingly challenging applications. In order to improve the quality and efficiency of daylighting, Jun Wang et al. [33] used three different simulation techniques: Daylight Coefficient method(DC), 3-PM and 5-PM, and two kinds of weather data: TMY data and actual measured weather data, simulated the CBDM of 400 apartments in 8 residential buildings for a whole year, and derived various metrics associated with CBDM, and founded that a flat with an average sDA<sub>300/50%</sub> above 66% and a maximum average daylight illuminance above 5 624 lx, to provide acceptable daylight quality for typical residential buildings in Hong Kong. Mahsan Mohsenin et al. [34] took the climate zone three of the United States as the climate background and adopted CBDM as the evaluation strategy to evaluate and optimize the types and proportions of atrium. Jiafeng Fang et al. [35] used the 5-PM to compare the annual daylight performance and glare levels of the three CFSs with dynamic metal louvers, dynamic micro-prism film louvers and micro-prism film, and analyzed the control strategy of dynamic micro-prism film louvers in south-facing offices to reduce the glare incidence in spaces near windows.

Based on CBDM, related researchers have further explored improving the comfort of the light environment. Lars Oliver Grobe [36] proposed an image generation method for visual comfort assessment, which only required two computational steps to achieve accurate image synthesis for visual comfort assessment, achieving an accuracy equivalent to 5-PM. Ali Omid et al. [37] conducted quantitative analysis of CBDM metric on Orosi window elements, and concluded that glass color played the most effective role in visual comfort. With the rapid development of non-visual research, CBDM has received increasing attention in the field of non-visual research. Konis [38] developed procedures using annual, climate-based daylight modeling of eye-level light exposures to analyze and map indoor environments in regard to spatial and seasonal changes in the availability of a circadian-effective daylight stimulus.

In addition, CBDM makes it possible to assess long-term daylight conditions and facilitates integration with other building performance analysis, such as energy consumption assessment from the same weather data. Esquivias et al. [39] used the DC to analyze the effect of fixed shading devices on the lighting of an open-plan office, and showed that excessive obstruction may increase lighting energy consumption. Tsikra et al. [40] took a primary school in C climate zone of Greece as an example, simulated its energy consumption and daylighting by using simulation software, and founded that inappropriate orientation and shading facilities had a great impact on energy consumption and lighting quality.

## 4. CLIMATE-BASED DAYLIGHT METRICS

#### 4.1 Dynamic daylight evaluation system

The daylighting performance metric is a standard for measuring the daylighting performance of buildings. The daylighting performance metric based on CBDM can simulate the illumination value of each point in the space at different time periods, also known as dynamic daylight metric. In contrast to static daylighting metrics, dynamic daylighting metrics provide a better understanding of the changing process of daylight in the interior space of buildings. As a result, dynamic daylighting metrics are more complicated.

Since the late 1990s, researchers have proposed different daylight measurement methods for CBDM. Unlike DF, time is an essential parameter in the daylight metric of CBDM. Its essence is to calculate the proportion of time during the whole year when the room can only rely on daylight. Since 2010, in order to investigate the reliability of these daylight metrics in evaluating architectural daylighting, researchers have investigated these metrics to understand their potential ability to describe a building's lighting design as excellent, poor or moderate. At present, some green building evaluation standards, such as LEED v4, CABSEE, and Green Building Evaluation Standard (GB/T 50378-2019), not only put forward more strict requirements on DF, but also add daylight metrics of CBDM to evaluate the building daylighting, such as DA and UDI. Meanwhile, the IESNA issued the IES LM-83-12 standard in 2013. This standard mainly regulated building daylighting through Spatial Daylight Autonomy(sDA) and Annual Sunlight Exposure (ASE) [41]. These are the most common climate-based daylight metrics shown in Table 1, which have been inserted into most simulation tools since their introduction in the building guidelines. However, there are many additional metrics that have been proposed as daylight performance metrics and calculated from the data produced by CBDM evaluations. Some of these metrics include: Daylight Saturation (DS), Lighting Dependency (LD), Daylight Excess(DE) and so on.

Although the daylight metrics of CBDM has not yet formed a unified evaluation standard, it has played an increasingly significant role in daylighting design and applications. After a gradual change from research to practice, it was gradually used by researchers and designers to achieve the goal of favorable daylight environments.

Table 1. the most common climate-based daylight metrics

Indices	Definition	Range
Useful daylight illuminance(UDI)	Percentage of occupied hours where the illuminance level falls into certain ranges. It is calculated at each sensor point and then averaged over the working plane. The sum of all UDI results has to add up to 100% for the same space.	<ul style="list-style-type: none"> <li>• 0–100 lx : UDI-n for non-sufficient,</li> <li>• 100–300 lx : UDI-s for supplementary</li> <li>• 300–3000 lx : UDI-a for autonomous</li> <li>• over 3000 lx : UDI-x for exceeded</li> </ul>
Daylight Autonomy (DA)	Percentage of occupied hours where the illuminance level is higher than a certain threshold (300 lx here) for each of the sensor points. The final value is the average between all sensor points.	<ul style="list-style-type: none"> <li>• Fully daylight: DA150lx[50%]</li> <li>• Partially daylight: DA300lx[50%]</li> <li>• Overlit: DA3000lx[5%]</li> </ul>
Spatial Daylight Autonomy(sDA)	The percentage of a space that receives a minimum target illuminance of 300 lx for at least 50% of the annual occupied hours.	<ul style="list-style-type: none"> <li>• &gt;55% acceptance</li> <li>• &gt;75% preference</li> </ul>
Continuous Daylight Autonomy(cDA)	As a basic modification of DA. cDA awards partial credit in a linear fashion to values below the user defined threshold.	
Annual Sunlight Exposure (ASE)	Represents the portion of the working plane where the sensor points recorded illuminances higher than 1 000 lx for more than 250 occupied hours.	<ul style="list-style-type: none"> <li>• &lt;10% acceptance</li> <li>• &lt;7% neutrality</li> <li>• &lt;3% preference</li> </ul>
Total Annual Illumination (TAI)	The sum of the illuminance recorded at every sensor point, for every occupied hour. The results are then averaged over the working plane.	

#### 4.2 Application Research on climate-based daylight metrics

Numerous researchers have discussed climate-based daylight metrics to validate its plausibility and applicability. Bian Yu et al. [42] used DF, DA and UDI indicators in four different elevations, different window wall ratios and shade sizes in a study of a side window lighting classroom in Guangzhou, and founded that DA and UDI were more reasonable than DF. Wu Wei et al. [43] discussed the applicability of UDI in-depth, simulated and concluded the characteristics of UDI by taking the DF as the contrast.

As the climate-based daylight metric has been intensively studied, relevant researchers have applied it to the study of optimizing daylighting in buildings. Huang Y et al. [44] carried out daylight simulation for buildings with double atriums through the DAYSIM, evaluated the results using two metrics: DA and UDI, and founded that the larger the atrium area, the better the lighting effect. Man gkuto et al. [45] discussed and analyzed the influence of various daylight metrics and lighting energy consumption on the window-to-wall ratio, wall reflection coefficient and window orientation of buildings under tropical climate conditions, and founded that the window-to-wall ratio had the greatest influence, while the building orientation had the least. Shan Rudai et al. [46] studied the daylighting design scheme for office space in Shenyang area with UDI as an indicator, through parametric modeling using a lighting simulation plug-in based on Radiance simulation. Xiang Luyao et al. [47] studied the characteristics of the light environment of the reading space by using the year-round dynamic light environment simulation method in combination with the amount of lighting and UDI. Bian Yu et al. [48] extended the application objects of sDA and ASE to the building group or urban design, and proposed the optimization design method of spatial layout of the building group to improve the overall daylighting and visual comfort level of the teaching building.

Climate-based daylight metrics are still in development, and more daylighting performance metrics have been proposed. Xin Zhang et al. [49] proposed an index of the "poor utilization time ratio" of daylight for each column of desks. Its essence is also the dynamical daylighting evaluation of space-time level subdivisions. Sudan et al. [50] applied the CBDM approach to building assessment for evaluating indoor daylighting. It is a new daylighting performance metric for atrium spaces to account for both direct and diffuse components. T Dogan et al. [51] proposed a new climate-based analysis framework for cold and temperate climates, called residential daylight score (RDS), which aims to capture the basic characteristics of residential daylight.

## 5. SUMMARY

The theoretical basis and practical application of natural lighting in buildings is undergoing a fundamental re-evaluation [6]. The rapid development of CBDM has led to more accurate analytical methods and more realistic daylighting assessments as the basis for a new generation of daylighting guidelines. The research and application of daylighting in buildings is gradually shifting from traditional static daylighting to CBDM-based dynamic daylighting analysis models. Its application is gradually expanding from daylighting efficiency, visual comfort, shading system etc. to non-visual effects, complex fenestration systems, thermal comfort and new daylighting evaluation and analysis, which is more and more widely used. This paper reviews the research results on Climate-based Daylight Modeling at home and abroad in the past ten years, sorts out the research results from the three aspects of "quantitative research", "simulation technology" and "metric standard". Basic studies should discuss each aspect in-depth to provide a theoretical basis for the effective design of daylighting in buildings.

However, the research and application of CBDM in China is still in its infancy due to the lack of daylight climate data, the absence of consensus on climate-based daylighting metrics, and the complexity of computation and simulation. Currently, the research trend of daylighting is moving towards human-oriented, healthy, and energy-efficient. An in-depth study of CBDM is not only important for creating a healthy and pleasant light environment and better achieving energy conservation and emission reduction, but can also provide a foundation and guidance for the design and application of daylighting in buildings. At the same time, these theories and techniques can also provide the basis and guidelines for the design and application of daylighting in buildings, as well as the theoretical basis and application reference for the future large-scale construction of healthy, low-energy buildings.

## Reference

- [1] LU Zhen. Research on Natural Lighting in College Classrooms Based on Visual Comfort [D]. Guangxi University, 2020.
- [2] Bian Yu, Ma Yuan. Dynamic lighting simulation and lighting energy consumption analysis

- considering visual comfort [J]. Journal of Zhejiang University: Engineering Science, 2018, 52(9): 1638-1643.
- [3] Bella L, Pedace A, Barbato G. Daylighting offices: A first step toward an analysis of photobiological effects for design practice purposes[J]. Building and Environment, 2014, 74(2): 54-64.
  - [4] Zhang Xin, Du Jiangtao, "Non-visual" trends and health orientation in natural light research and design [J]. Architectural Journal, 2017(05):87-91.
  - [5] Zi Ying. Study on simulation method of natural lighting for buildings in Cold areas based on field measurement of local sky brightness [D]. Harbin Institute of Technology, 2019.
  - [6] Zhang Bing, et al. Daylighting for Buildings [M]. Intellectual Property Publishing House, 2019.
  - [7] Eleonora Brembilla. Applicability of Climate-Based Daylight Modelling[D]. Loughborough University, 2017.
  - [8] Zhang Qingwen, Yang Chunyu, et al. Review and Prospect: A natural light and daily radiation observation station in Chongqing [J]. Lamps and Lighting, 2010, 34(04): 12-16+21.
  - [9] ZHANG Q W. Natural light and daily radiation observation station in Chongqing [J]. Journal of Chongqing Institute of Civil Engineering and Architecture, 1994(01): 68-73.
  - [10] He Ying, Hu Yingkui, Weng Ji. Classification of reference sky in natural lighting design [J]. Civil, Architectural and Environmental Engineering, 2010, 32(06): 105-109.
  - [11] Luo Tao. Research on Energy Consumption Simulation Method of Office Building Lighting [D]. Tsinghua University, 2014.
  - [12] Li D W, Lau C S, Lam J. A Study of 15 Sky Luminance Patterns against Hong Kong Data[J]. Architectural Science Review, 2003, 46(1): 61-68.
  - [13] Edward Ng, Cheng V, Gadi A, et al. Defining standard skies for Hong Kong[J]. Building & Environment, 2007, 42(2): 866-876.
  - [14] Bian Y, Ma Y. Analysis of daylight metrics of side-lit room in Canton, south China: A comparison between daylight autonomy and daylight factor[J]. Energy and Buildings, 2017, 138: 347-354.
  - [15] Liu Lei. Research on Low Energy Consumption Design of office buildings in Cold Regions based on photothermal performance simulation [D]. Harbin Institute of Technology, 2017.
  - [16] Wang Aiyong, Jin Hai, Li Wenwen. Regional photoclimatic information system based on GIS [J]. Journal of Lighting Engineering, 2010, 21(04): 37-40.
  - [17] Wang Aiyong, Jin Hai, et al. Calculation of outdoor illuminance value by solar radiation conversion method [J]. Civil, Architectural and Environmental Engineering, 2011, 33(03): 88-93.
  - [18] Wang Shuyi, Wang Yajiang, et al. Experimental simulation of building daylighting based on DeST typical year Data [J]. Journal of Lighting Engineering, 2022, 33(02): 145-151.
  - [19] Sun Wenchao. Application of DeST Typical annual Data to building daylighting simulation in Tianjin [D]. Tianjin University, 2018.
  - [20] nanici M, Hashemloo A. An investigation of the daylighting simulation techniques and sky modeling practices for occupant centric evaluations[J]. Building and Environment, 2017, 113(6): 220-231.
  - [21] Ferraro V, Mele M, et al. Sky luminance measurements and comparisons with calculation models[J]. Journal of Atmospheric and Solar-Terrestrial Physics, 2011, 73(13): 1780-1789.
  - [22] Yujie Wu, Jérôme Henri Kämpf, Jean-Louis Scartezini. Daylighting simulation for external Venetian blinds based on HDR sky luminance monitoring with matrix algebraic approach[J]. Energy Procedia, 2019, 158: 2677-2682.
  - [23] Tregenza P I. Standard Skies for Maritime Climates[J]. Lighting Res & Technol, 1999, 31(31): 97-106.
  - [24] Bartzokas A, Darula S, Kambezidis H D, et al. Sky luminance distribution in Central Europe and the Mediterranean area during the winter period[J]. Journal of Atmospheric and Solar-Terrestrial Physics, 2003, 65(1): 113-119.
  - [25] Kittler, S. Darula. Scattered Sunlight Determining Sky Luminance Patterns[J]. Renewable and Sustainable Energy Reviews, 2016, 62: 575 - 584.
  - [26] Zi Ying, Sun Cheng, Han Yunsong. Sky type classification in Harbin during winter [J]. Journal of Asian Architecture and Building Engineering, 2020, 19(5): 515-526.
  - [27] Ma Yuan, Bian Yu, Chen Jianhua. Observation of sky brightness distribution in South China. Chinese Journal of Lighting Engineering, 2015, 26(1): 1-5.
  - [28] Wang Hongzhen. Research on Building Daylighting Simulation based on Regional photoclimatic [D]. Tianjin University, 2012.
  - [29] Wang Z. Study on the Form design strategy of office buildings in cold regions under the guidance of light comfort [D]. Harbin Institute of Technology, 2018.



- [30] Ming Lu, Jiangtao Du. Dynamic evaluation of daylight availability in a highly-dense Chinese residential area with a cold climate[J]. *Energy & Buildings* 193 (2019) 139 – 159.
- [31] Konis, Kyle. A circadian design assist tool to evaluate daylight access in buildings for human biological lighting needs[J]. *SOLAR ENERGY*, 2019, 191:449-458.
- [32] E. Brembilla, J. Mardaljevic. Climate-Based Daylight Modelling for compliance verification: Benchmarking multiple state-of-the-art methods[J]. *Building and Environment*, 2019, 158 (2019) 151 – 164.
- [33] Wang J , Wei M , Ruan X . Characterization of the acceptable daylight quality in typical residential buildings in Hong Kong[J]. *Building and Environment*, 2020, 182.
- [34] Mohsenin, Mahsan, et al. Assessing daylight performance in atrium buildings by using Climate Based Daylight Modeling[J]. *Solar Energy*, 2015, 119:553-560.
- [35] Fang J , Zhao Y , Tian Z , et al. Analysis of dynamic louver control with prism redirecting fenestrations for office daylighting optimization[J]. *Energy and buildings*, 2022(May):262.
- [36] Grobe L O . Photon-Mapping in Climate-Based Daylight Modelling with High-Resolution BSDFs[J]. *Energy and Buildings*, 2019, 205.
- [37] Omid, Ali, Golchin, Navid, Masoud, Seyed Ehsan. Evaluating the visual comfort of Orosi windows in hot and semi-arid climates through climate-based daylight metrics: a quantitative study[J]. *Journal of Asian Architecture and Building Engineering*, 2021, 21(5):2114-2130.
- [38] Konis, Kyle. A novel circadian daylight metric for building design and evaluation[J]. *Building & Environment*, 2017, 113:22-38.
- [39] Esquivias, P. M., Munoz, C. M., et al. Climate-based daylight analysis of fixed shading devices in an open-plan office[J]. *Lighting Research and Technology*, 2016, 48(2):205-220.
- [40] Tsikra P, Andreou E. Investigation of the Energy Saving Potential in Existing School Buildings in Greece[C]. *The role of Shading and Daylight Strategies in Visual Comfort and Energy Saving - ScienceDirect*, 2017:204-211.
- [41] Bian Yu. *Daylighting For Buildings*[M]. China Architecture and Building Press, 2019.
- [42] Bian Yu, Yuan Lei, Leng Tianxiang. Dynamic daylighting index analysis and side window daylighting range [J]. *Journal of Harbin Institute of Technology*, 2017, 49(10):172-176.
- [43] Wu Wei, Liu Kunpeng. A brief analysis of new natural daylighting evaluation parameters that can replace daylighting coefficient [J]. *Journal of Lighting Engineering*, 2012, 23(2):1-7.
- [44] Huang Y, Borong L. Functional Relationship Between Lighting Energy Consumption And The Main Parameters For Double Atrium Offices[J]. *Procedia Engineering*, 2015, 121:1869-1879.
- [45] Mangkuto R A, Rohmah M, Asri A D. Design optimisation for window size, orientation, and wall reflectance with regard to various daylight metrics and lighting energy demand: A case study of buildings in the tropics[J]. *Applied Energy*, 2016, 164:211-219.
- [46] Shan Rudai, XI Mingming, YAN Yunbo, XIA Xiaodong. A comparative study of natural lighting evaluation index based on parameterization - taking a typical office space in Shenyang area as an example [J]. *Building Science*, 2016, 32(12):102-106+134.
- [47] Xiang Luyao, Ni Weichao, Wu Enrong. Research on the design of typical reading space parameters based on year-round dynamic light environment simulation conditions[J]. *Journal of Lighting Engineering*, 2017, 28(3):24-29,35.
- [48] Bian Yu, Pang Yuzhi, et al. Space optimization design of teaching building based on lighting and visual comfort[J]. *Journal of Lighting Engineering*, 2023, 34(01):68-72.
- [49] Zhang X, Zhou XY, Chen XD. From "classroom lighting" to "desk lighting"-a reassessment of lighting standards for primary and secondary school classrooms based on the percentage of poor utilization time[J]. *World Architecture*, 2021(03):36-41+126.
- [50] Sudan M , Mistrick R G , Tiwari G N . Climate-Based Daylight Modeling (CBDM) for an atrium: An experimentally validated novel daylight performance[J]. *Solar Energy*, 2017, 158:559-571.
- [51] Dogan T , Park Y C . Testing the residential daylight score: Comparing climate-based daylighting metrics for 2444 individual dwelling units in temperate climates[J]. *Lighting Research and Technology*, 2020, 52(8):991-1008.

## ACKNOWLEDGEMENT

Corresponding Author Name: Shuying Liang

Affiliation: School of Architecture and Urban Planning, Chongqing University

e-mail: Lsyarch@163.com

# THE DIFFERENCE OF PERFORMANCE IN THE COMPLEX LIGHT ENVIRONMENT OF METAMERISM

Yan Li, Junxian Chen, Xiong Zhou, Daqing Zhu\*, Xiaohan Zhou, Wu Song

(College of Mechanical Engineering and Automation, Huaqiao University,  
Design and Ergonomics Research Center, Xiamen, China)

## ABSTRACT

This article introduces an illumination human factor experiment that examines the subjective experience, emotions, alertness, memory, and semantic cognitive abilities of participants in the isochromatic environment produced by metameric light. It was conducted during the spring period (March 13, 2023 -- April 2, 2023) in the human Factors Laboratory at the Huaqiao University using a light environment provided by a light box, in which subjective alertness (Karolinska Sleepiness Scale, KSS), feeling (Self-Assessment Manikin, SAM), mood (Visual Analog Mood Scales, VAMS), and task performance in sustained attention (Psychomotor Vigilance Test, PVT), working memory (Paced Visual Serial Addition Test, PVSAT), and semantic recognition (Lexical Decision Task, LDT) were measured. Findings are as follows: Blue dominated white light (BWL) and Red dominated white light (RWL) is more conducive to improving alertness and work performance than Normal office white light (NWL), which has an influence trend but is not statistically significant; Different metamerism compound lights have no effect on human emotional and semantic cognition.

Keywords: Metameric light, Alertness and emotion, Semantic cognition, Light environment, Compound light

## 1. INTRODUCTION

Recent discoveries in biology have shown that intrinsically photosensitive retinal ganglion cells (ipRGCs), a third type of photosensitive cells different from traditional rods and cones, can constitute a non-visual optical system [1]. In view of this finding, people realized that light signals could be sensed by ipRGCs and transmitted to the suprachiasmatic nucleus (SCN) of the brain, which then controlled the body's biological rhythm, hormone secretion and other vital signs. At the same time, the extensive neural projection association between SCN and many regions of cerebral cortex can regulate the body's alertness, emotion and cognitive processing, and even social psychology and behavior. This is often referred to as non-image forming function (NIF) [2-7]. A large number of existing literatures show that light can affect human alertness, cognitive performance and physiological response [8-11]. However, there are few studies on lighting with complex isochromatic light as ambient light. Following hypotheses were observed and proposed.

Firstly, the influence of the isochromatic light with different spectral power distribution (SPD) on the emotion is different. H Lee & E Lee [12] compared the emotional impact of lighting color on subjects in different monochromatic light environments, and found that blue was the most pleasant lighting color, but red is the most unpleasant. Christoph von Castell Hlee et al [13], compared the emotional impact of the same white light on the environmental background of different colors, and the results showed that the same white light on the environmental background of different colors did not show the influence of the color of the learning environment on students' emotions. Based on this, we assume that different wavelength spectra of isochromatic light will affect the emotions of the subjects, in which BWL and RWL can improve subjective alertness; in addition, BWL can improve pleasure, RWL will cause discomfort.

Secondly, the influence of the isochromatic light with different spectral power distribution (SPD) on the objective alertness and memory is different. Segal A Y [14], Łaszewska K [15] and Wolska A et al [16] respectively found that monochrome red light and monochrome blue light both increased physiological markers of alertness in electroencephalogram (EEG). Based on this, we hypothesized that isochromatic lights with different SPD would affect the alertness and performance of subjects differently. BWL and RWL could both improve alertness and performance. In addition, RWL showed a more obvious trend of increasing alertness.

Thirdly, the influence of the isochromatic light with different spectral power distribution (SPD) on semantic discrimination and semantic priming ability is different. Lorenzo Tonetti et al [17].



found that blue light exposure enhanced semantic priming significantly. Based on this, we hypothesized that tisochromatic lights with different SPD would affect the semantic ability of the subjects, and BWL could have stronger semantic priming ability than others.

## 2. METHODS

### 2.1 Participant

This study collected subjective experience and behavior data of 28 subjects (7 females, age:  $23.22 \pm 1.20$  years old) respectively in BWL, NWL and RWL. The recruited subjects did not have color discrimination disorders such as color blindness and color weakness, and kept more than 7 hours of sleep for a long time. The subjects read and signed the informed consent before the experiment. After the experiment was completed, each subject was paid 90 ¥ as participation fee. It was approved by the Medical Ethics Committee of Huaqiao University School of Medicine.

### 2.2 Experimental procedure

Subjects were required to expose to three light conditions, with a one-week washout interval. Different light environments: BWL (502.3lx, 5473K), NWL(506.1lx, 5416K), RWL(495.3lx, 5437K). The experiment began at 8:20 am and ended at 11:35 am. Four subjects were tested in one day, and each experiment lasted about 40 minutes. Each subject first completed the information collection of the pre-test questionnaire, and then was exposed to dim environment ( $<5\text{lx}$ ) for 5min light adaptation. In Addition, the Psychomotor Vigilance Test (PVT) for 7min to assess alertness and the Paced Visual Serial Addition Test (PVSAT) for 10min to investigate memory were carried out in turn under different light conditions test and 10min Lexical decision task (LDT). Shall be set for 2min rest between each task. After completing the normal form task, post-trial questionnaire information shall be collected. The above paradigm tasks were designed and completed on the basis of E-Prime 3.0. A one-minute video demonstration was conducted before the experiment to let the subjects know the experimental process in advance. Figure 1 provides to help understand.

### 2.3 Experimental task

#### 2.3.1 Subjective experience and emotion questionnaire

##### a) Karolinska Sleepiness Scale (KSS)

KSS scale is an indicator of subjective alertness and is used to measure participants' subjective sleepiness. This scale is scored on a scale of 1 to 9, where 1= "extremely awake," 3= "awake," 5= "not very awake but also not sleepy," 7= "sleepy but not requiring much effort to stay awake," and 9= "very sleepy and requiring great effort to stay awake."

##### b) Self-Assessment Manikin (SAM)

SAM is a image-oriented tool that directly assesses pleasure, arousal, and dominance associated with an object or event. The scale score is also between 1 and 9, where 1= "most unpleasant/unawake/undominated" and 9= "most pleasant/excited/dominated", and the dominance dimension represents the change in control and the change in SAM size.

##### c) Visual Analog Mood Scales (VAMS)

VAMS An intuitive visual state measure in which the evaluator marks a number of subjective emotional states between the two ends of a scale. The feelings of "Sleepy-Alert", "Calm - Stressed", "Sad - Happy", "Health - Sick", "Energetic - Exhausted", "Exhausted - Sharp", "Tired - Fresh", and "Motivated - Unmotivated" were evaluated with a scale of 1-9 points from left to right.

#### 2.3.2 Objective behavioral response paradigm

##### a) Psychomotor Vigilance Test (PVT)

Objective alertness and sustained attention were assessed using a 7-minute visual psychomotor alertness test, a measure of visual reaction time that requires sustained attention and is highly sensitive to attentional neglect. During the task, participants were asked to place their dominant hand on the space bar and react as soon as they saw a number appear on the screen, using random stimulus intervals of 2000-6000 ms. The average reaction rate of the whole experiment and the concentration rate of reaction based on 10% before and after the average reaction rate were calculated respectively.

##### b) Paced Visual Serial Addition Test (PVSAT)

The experiment used the 10-minute PVSAT, a visual reaction-based memory task that requires not only constant attention to the presence of numbers, but also immediate memory calls. The number of units (5-15) appears on the screen, and each number needs to be added to the previous one, except for the first one reporting its own number, and the resulting answer is entered via the numeric keypad (the "sum" of adjacent pairs, not the total of all the numbers). The number renders 2000 ms, then allows for an additional 5000 ms maximum range of responses, or disappears until a response is detected, and then the number appears again after an interval of 1000ms. The correctness and speed of reaction were measured respectively.

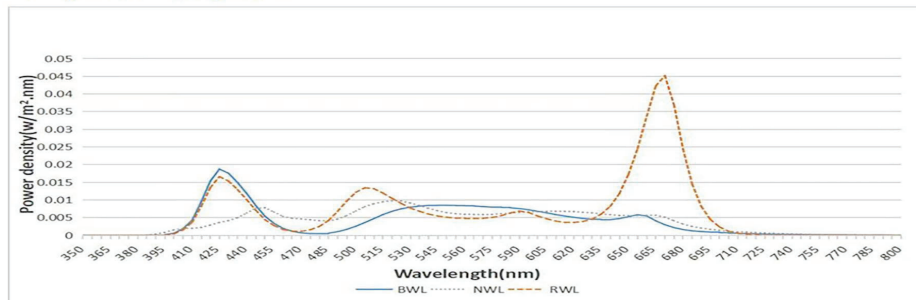
### c) Lexical decision task (LDT)

The experiment adopted a 10-minute LDT, taking word judgment as the experimental task. First, "+" was presented in the center of the screen for 500 ms, and then the stimuli (true or false words) were presented randomly for 1000 ms. The subjects were asked to accurately and quickly judge whether the presented words were true or false words, and responded by pressing keys. The subjects used their left hand to press "Q" for true words and their right hand to press "P" for false words. Subjects who do not respond within 1000 ms will automatically move on to the next trial. Each stimulus was randomly presented in a thesaurus consisting of 100 true words and 100 false words.

### A: luminous environment



### B: Spectral distribution



### C: Light condition data

Lighting condition	LUX (lx)	CCT (K)	x	y	u	v	Deep UV	CIE Ra
BWL	502.3	5473	0.333	0.3339	0.2101	0.4739	-0.0039	66.5
NWL	506.1	5416	0.335	0.3718	0.1973	0.4927	0.0139	94
RWL	495.3	5437	0.3338	0.3338	0.2106	0.474	0.0043	62.7

### D: experimental flow chart

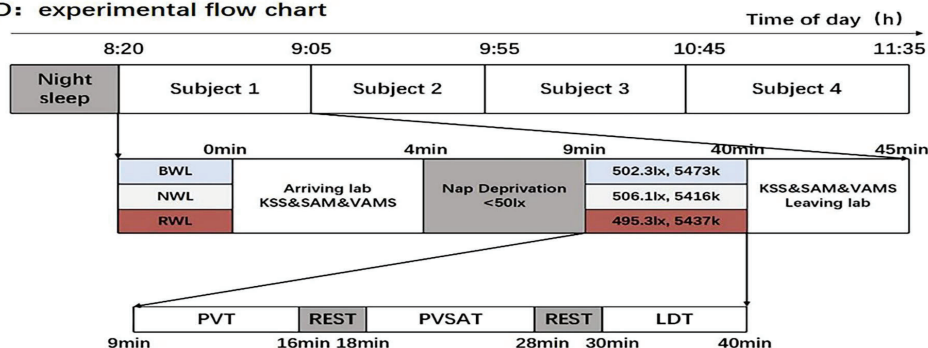


Figure 1. Experimental design of this study. (A) Luminous environment. (B) Spectral distribution. (C) Light condition data. (D) Experimental procedure: the task order was pseudo-random and remained unchanged for three days of the experiment. BWL(white light dominated by blue); NWL(normal office lighting white light); RWL(white light dominated by red); KSS(Karolinska Narcolepsy Scale); SAM(Self-Assessment Manikin); VAMS(Visual Analog Mood Scales); PVT(Psychomotor Vigilance Test); PVSAT(Paced Visual Serial Addition Test); LDT(Lexical Decision Task).

### 3. RESULTS

#### 3.1 Subjective sleepiness, mood, and health

Table 1. Mean  $\pm$  standard deviation of subjective test results and variance analysis result values

Test outcome	BWL		NWL		RWL		F (p-value)
	M (DIFF) (SD)	N	M (DIFF) (SD)	N	M (DIFF) (SD)	N	
KSS	-0.88 (2.00)	28	-1.27 (2.10)	28	-0.80 (1.67)	28	0.45 (0.64)
valence	0.64 (1.69)	28	0.71 (1.64)	28	0.54 (1.27)	28	0.09 (0.91)
arousal	0.75 (1.84)	28	0.61 (1.65)	28	0.64 (1.74)	28	0.05 (0.95)
dominance	0.89 (1.61)	28	0.82 (1.67)	28	1.07 (1.56)	28	0.17 (0.84)
Sleepy—Alert	0.96 (2.10)	28	0.96 (2.03)	28	0.93 (1.91)	28	0.00 (1.00)
Calm—Stressed	-0.57 (1.84)	28	-0.86 (2.07)	28	-0.29 (1.89)	28	0.59 (0.56)
Sad—Happy	0.25 (1.66)	28	0.64 (1.47)	28	0.36 (1.23)	28	0.52 (0.60)
Healthy—Sick	-0.75 (1.70)	28	-0.86 (1.92)	28	-0.46 (1.55)	28	0.37 (0.69)
Energetic—Exhausted	-1.14 (1.83)	28	-0.93 (1.71)	28	-0.89 (1.61)	28	0.17 (0.85)
Exhausted—Sharp	0.64 (1.95)	28	0.93 (1.91)	28	0.39 (1.72)	28	0.56 (0.57)
Tired—Fresh	0.71 (2.03)	28	1.29 (1.69)	28	0.89 (1.61)	28	0.72 (0.49)
Motivated—Unmotivated	0.71 (1.73)	28	1.04 (1.61)	28	0.82 (1.65)	28	0.26 (0.77)

A comparative analysis of the data before and after light exposure showed that there was no difference in subjective sleepiness, pleasure, excitement, alertness, health, adaptation and other aspects (Table 1). In the follow-up interview, nobody could distinguish the three light environments.

#### 3.2 PVT

Excluding the data caused by excessive standard deviation, the remaining 21 subjects of data (6 females) were subjected to variance analysis, F-test, T-test and multiple comparison.

##### 3.2.1 Individual performance

###### a) accuracy

Although there was a difference trend in the accuracy performance of PVT under three kinds of isochromatic environment produced by metameric lights, there was no significant difference in multiple comparisons ( $P_{\text{blue}\&\text{red}}=0.07$ ,  $P_{\text{blue}\&\text{white}}=0.28$ ,  $P_{\text{red}\&\text{white}}=0.44$ ). The accuracy of subjects under BWL ( $M=0.43, SD=0.12$ ) was lower than that under NWL ( $M=0.47, SD=0.13$ ), while the accuracy under RWL ( $M=0.50, SD=0.12$ ) was higher than that under NWL.

###### b) reaction time

Also find a trend of difference in the performance of PVT reaction time, but still no significant difference under multiple comparisons ( $P_{\text{blue}\&\text{red}}=0.06$ ,  $P_{\text{blue}\&\text{white}}=0.19$ ,  $P_{\text{red}\&\text{white}}=0.58$ ). The reaction time of subjects under BWL ( $M=365.14, SD=13.43$ ) was increased compared with that under NWL ( $M=346.71, SD=6.71$ ), that is, the reaction time required under BWL was longer, while the reaction time under white light dominated by RWL ( $M=339.06, SD=7.79$ ) was reduced compared with NWL. That is, shorter reaction times are required under RWL.

##### 3.2.2 Gender performance

###### a) accuracy

There were differences in the accuracy of PVT between male and female under three isochromatic environment produced by metameric lights, although there was no significant

difference in accuracy between male and female (male:  $P_{\text{blue}\&\text{red}}=0.14$ ,  $P_{\text{blue}\&\text{white}}=0.22$ ,  $P_{\text{red}\&\text{white}}=0.79$ )(female:  $P_{\text{blue}\&\text{red}}=0.31$ ,  $P_{\text{blue}\&\text{white}}=0.98$ ,  $P_{\text{red}\&\text{white}}=0.30$ ), but the trend was different between male and female under different light conditions. The accuracy of male students under BWL ( $M=0.43, SD=0.03$ ) was lower than that under NWL ( $M=0.49, SD=0.03$ ) and RWL ( $M=0.50, SD=0.02$ ). The accuracy of female students under BWL ( $M=0.44, SD=0.07$ ) was close to but slightly higher than that under NWL ( $M=0.44, SD=0.14$ ), both of which were lower than that under RWL ( $M=0.51, SD=0.11$ ).

#### b) reaction time

There were differences in the performance of PVT responses between male and female under three kinds of isochromatic environment produced by metameric lights, among which there were significant differences in the response time of male in BWL and RWL ( $P_{\text{blue}\&\text{red}}=0.04$ ,  $P_{\text{blue}\&\text{white}}=0.13$ ,  $P_{\text{red}\&\text{white}}=0.55$ ). The response time of subjects under BWL ( $M=375.01, SD=17.79$ ) was increased compared with that under NWL ( $M=336.19, SD=9.46$ ), that is, the response time required under BWL was longer, while that under RWL ( $M=347.07, SD=8.71$ ) was reduced compared with NWL. That means shorter reaction times are required under RWL. However, the mean response time of female in the three light environments increased successively from BWL ( $M=340.47, SD=11.81$ ), NWL ( $M=345.81, SD=9.94$ ), RWL ( $M=346.22, SD=14.42$ ), and there was no obvious trend to approach each other. There was no significant difference under multiple comparison ( $P_{\text{blue}\&\text{red}}=0.74$ ,  $P_{\text{blue}\&\text{white}}=0.76$ ,  $P_{\text{red}\&\text{white}}=0.98$ ).

### 3.3 PVSAT

Excluding the data caused by excessive standard deviation, the remaining 23 subjects of data (7 females) were subjected to variance analysis, F-test, T-test and multiple comparison.

#### 3.3.1 Individual performance

##### a) accuracy

Although there was a difference trend in the PVSAT accuracy performance under three isochromatic environment produced by metameric lights, there was no significant difference under multiple comparisons ( $P_{\text{blue}\&\text{red}}=0.28$ ,  $P_{\text{blue}\&\text{white}}=0.55$ ,  $P_{\text{red}\&\text{white}}=0.10$ ). The correct rate of subjects under BWL ( $M=0.87, SD=0.21$ ) and RWL ( $M=0.90, SD=0.12$ ) was higher than that under NWL ( $M=0.85, SD=0.23$ ), and the correct rate under RWL was higher than that of BWL.

##### b) reaction time

There was no significant difference in the performance of PVSAT reaction under three isochromatic environment produced by metameric lights under multiple comparisons ( $P_{\text{blue}\&\text{red}}=0.80$ ,  $P_{\text{blue}\&\text{white}}=0.74$ ,  $P_{\text{red}\&\text{white}}=0.56$ ). The response time of subjects under BWL ( $M=823.49, SD=57.34$ ) and RWL ( $M=804.58, SD=47.70$ ) was shorter and faster than that under NWL ( $M=848.69, SD=52.26$ ), and the response time under RWL was shorter than that under BWL, but there was little difference between the mean values of the three.

#### 3.3.2 Gender performance

##### a) accuracy

Male and female showed the same trend in the PVSAT accuracy performance under three isochromatic environment produced by metameric lights, and there was no significant difference in the accuracy (male: ( $P_{\text{blue}\&\text{red}}=0.42$ ,  $P_{\text{blue}\&\text{white}}=0.53$ ,  $P_{\text{red}\&\text{white}}=0.15$ )(female:  $P_{\text{blue}\&\text{red}}=0.50$ ,  $P_{\text{blue}\&\text{white}}=0.86$ ,  $P_{\text{red}\&\text{white}}=0.40$ ). The accuracy of both male and female under BWL was close to but slightly higher than that under NWL, and the accuracy of male under BWL ( $M=0.88, SD=0.02$ ) and NWL ( $M=0.86, SD=0.03$ ) was slightly higher than that of female under BWL ( $M=0.84, SD=0.05$ ) and NWL ( $M=0.83, SD=0.05$ ). The accuracy of male ( $M=0.90, SD=0.01$ ) female ( $M=0.88, SD=0.02$ ) was the highest in RWL.

##### b) reaction time

The mean values of PVSAT responses of both male and female were determined by RWL (male:  $M=781.87, SD=64.21$ )(female:  $M=856.50, SD=56.64$ ) BWL (male:  $M=799.73, SD=72.93$ ) (female:  $M=877.80, SD=92.30$ ) NWL (male:  $M=805.57, SD=68.08$ ) (female:  $M=947.27, SD=63.97$ ) was increased successively, and there was no significant difference under multiple comparisons (male:  $P_{\text{blue}\&\text{red}}=0.86$ ,  $P_{\text{blue}\&\text{white}}=0.95$ ,  $P_{\text{red}\&\text{white}}=0.81$ )(female:  $P_{\text{blue}\&\text{red}}=0.84$ ,  $P_{\text{blue}\&\text{white}}=0.51$ ,  $P_{\text{red}\&\text{white}}=0.39$ ).



### 3.4 LDT

After the analysis of experimental data, 28 groups of data (21 males and 7 females) were analyzed by variance analysis, F test, t test and multiple comparison.

#### 3.4.1 Individual performance

##### a) accuracy

The accuracy rate of LDT under three isochromatic environment produced by metameric lights was densely distributed, which was successively improved by BWL ( $M=0.9537, SD=0.0054$ ) RWL ( $M=0.9555, SD=0.0049$ ) NWL ( $M=0.9568, SD=0.0050$ ) and was close to each other. There was no significant difference in multiple comparisons ( $P_{blue\&red}=0.80$ ,  $P_{blue\&white}=0.67$ ,  $P_{red\&white}=0.86$ ).

##### b) reaction time

The LDT reaction of three kinds of isochromatic environments was also densely distributed, which was successively increased by NWL ( $M=654.05, SD=15.06$ ) RWL ( $M=659.46, SD=15.47$ ) BWL ( $M=674.81, SD=17.97$ ) and was close to each other and difficult to distinguish. There was no significant difference in multiple comparisons ( $P_{blue\&red}=0.51$ ,  $P_{blue\&white}=0.37$ ,  $P_{red\&white}=0.81$ ).

#### 3.4.2 Gender performance

##### a) accuracy

The LDT accuracy rates of male and female were distributed intensively and showed no trend difference (male:  $P_{blue\&red}=0.64$ ,  $P_{blue\&white}=0.80$ ,  $P_{red\&white}=0.83$ )(female:  $P_{blue\&red}=0.84$ ,  $P_{blue\&white}=0.72$ ,  $P_{red\&white}=0.58$ ) under three isochromatic environments. The accuracy rate of male subjects was increased according to BWL( $M=0.9551, SD=0.0063$ ), NWL( $M=0.9588, SD=0.0048$ ), RWL( $M=0.9571, SD=0.0053$ ). The accuracy rate of female subjects was increased according to RWL( $M=0.9459, SD=0.0110$ ), BWL( $M=0.9495, SD=0.0136$ ), NWL( $M=0.9559, SD=0.0125$ ).

##### b) reaction time

There were differences in LDT responses between male and female under three isochromatic environment produced by metameric lights, but there was no significant difference under multiple comparisons (male:  $P_{blue\&red}=0.70$ ,  $P_{blue\&white}=0.28$ ,  $P_{red\&white}=0.48$ )(female:  $P_{blue\&red}=0.48$ ,  $P_{blue\&white}=0.86$ ,  $P_{red\&white}=0.38$ ). The response time of males under BWL ( $M=681.40, SD=21.41$ ) and RWL ( $M=670.64, SD=19.34$ ) was longer than that under NWL ( $M=651.24, SD=17.48$ ). In female, the response time under BWL ( $M=655.03, SD=33.82$ ) and RWL ( $M=625.91, SD=17.86$ ) was shorter than that under NWL ( $M=662.48, SD=31.79$ ).

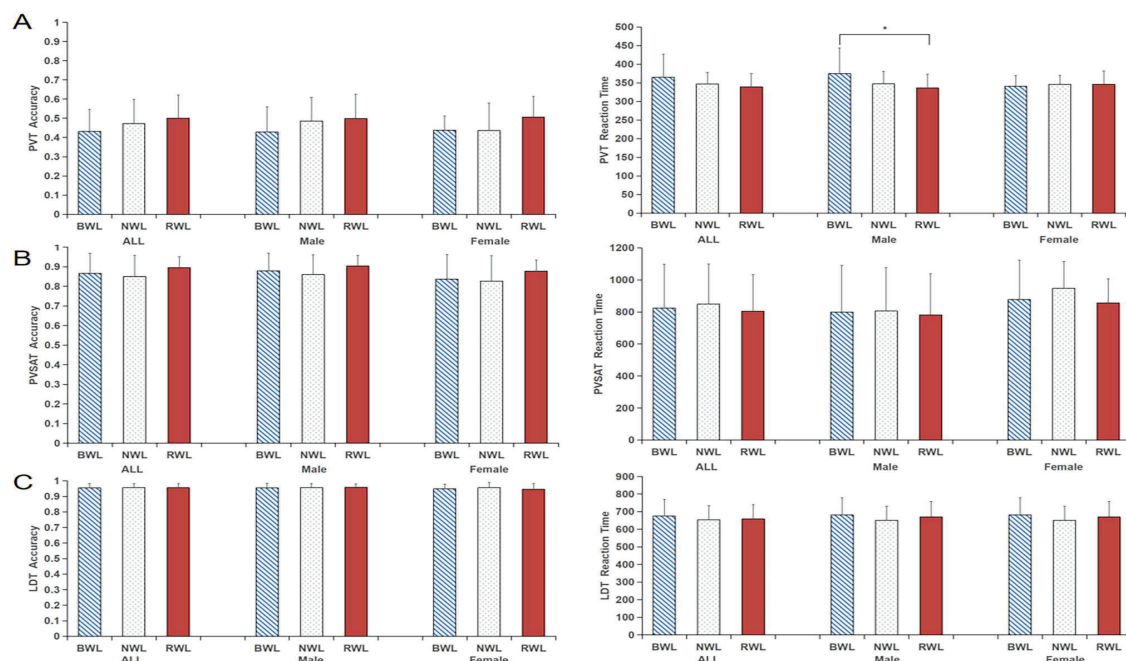


Figure 2. Data analysis chart(A)PVT paradigm. Accuracy & Reaction time.

(B)PVSAT paradigm. Accuracy & Reaction time (C)LDT paradigm. Accuracy & Reaction time

#### 4. CONCLUSION & DISCUSSION

In this study, a light box was used as a light environment, and NWL was used as a positive control to compare the differences in subjective feelings and physiological responses brought by BWL and RWL conditions, so as to verify the previous hypothesis accordingly.

First, it can be found in the subjective questionnaire that the subjects did not show the systematic response and subjective alertness of color to the emotional state in the unconscious light environment and color light state, negating the hypothesis before the experiment. Combined with the research of H Lee and Christoph von Castell, it can be inferred that the emotional changes brought by color light have nothing to do with spectrum, but are related to the color temperature of the light environment, that's mean metameric light expression cannot be perceived by consciousness to affect emotions.

Second, by examining the PVT and PVSAT paradigms, it was found that subjects' alertness and recall performance in BWL and RWL were different from those in NWL, which verified the pre-experiment hypothesis. Combined with study of Segal A Y and Wolska A et al. that both monochromatic red and blue light reported increased physiological markers of alertness, it can be inferred that red and blue light in complex light still has the ability to intervene. In addition, the pathways affecting alertness of RWL and BWL may not be the same. The trend of increasing alertness of RWL in this study and that of monochrome red light in the above study can be seen, while the alertness performance of BWL in PVT decreases compared with that of NWL. However, Cheung I N et al[18]. showed that exposure to low intensity blue light during the day would reduce the alertness performance of PVT, that is, exposure to blue light during the day may have a certain negative impact on alertness and attention.

Third, LDT normal form data analysis showed that there was no difference trend in semantic discrimination or semantic priming ability among NWL, BWL and RWL, which negated the pre-experiment hypothesis. Combined with study of Lorenzo Tonetti et al. that blue light exposure enhances semantic priming ability, it can be inferred that the influence of semantic priming ability may be related to the subjective emotional influence brought by monochromatic blue light, or related to the selection of special wavelength of blue light.

In summary, this study found a trend of differences between alertness and memory task performance among environments of isochromatic light with different SPD, among which there was a significant difference in PVT response time between BWL and NWL for males, indicating that both BWL and RWL had changes in alertness and memory compared with NWL, which was corresponding to previous studies. We can therefore conclude that Blue dominated white light and Red dominated white light have the ability to enhance some of the physiological correlation compared to the Normal office white light commonly used in the office. However, this experiment is short in duration and lacks continuous observation and long-term research. Whether these changes can be translated into improvements in task performance and subjective experience requires further research to determine the optimal characteristics of light intervention, such as color temperature, illuminance and color render, so as to improve alertness and psychological performance in daytime office environments.

At the same time, there are still some deficiencies in the experiment of this study, which need to be adjusted and optimized later. First of all, in terms of behavioral science, the number of subjects in this experiment is small, so it is difficult to exclude the influence of random factors well, and the difference analysis of small set of samples is not significant. Secondly, without the long period experiments, it cannot guarantee whether the existing trend results can be maintained under long-term lighting. Finally, it is difficult to ensure the absolute consistency of parameters in light environment due to the limitation of light box. It can be expected that future experiments will increase the number of subjects, carry out long-term lighting observation, improve the existing dimming and other problems. Future explorations in this area could adapt the cognitive effects of monochromatic light to compound light studies, providing evidence for improvements in indoor office lighting.

#### FOUNDATIONS

This study was supported by the following foundation projects:

2019 Natural Science Foundation Program, Fujian Province, China (2019J01061);



2020 General Project of Humanities and Social Sciences Research, Ministry of Education, China (20YJA760067);

Cooperative Research Project between CRRC Zhuzhou Locomotive CO., LTD and Huaqiao University (2021-0015).

## REFERENCE

- [1] Berson D M, Dunn F A, Takao M. Phototransduction by retinal ganglion cells that set the circadian clock[J]. *Science*, 2002, 295(5557): 1070-1073.
- [2] Cajochen C. Alerting effects of light[J]. *Sleep medicine reviews*, 2007, 11(6): 453-464.
- [3] Perrin F, Peigneux P, Fuchs S, et al. Nonvisual responses to light exposure in the human brain during the circadian night[J]. *Current Biology*, 2004, 14(20): 1842-1846.
- [4] Vandewalle G, Balteau E, Phillips C, et al. Daytime light exposure dynamically enhances brain responses[J]. *Current Biology*, 2006, 16(16): 1616-1621.
- [5] Vandewalle G, Maquet P, Dijk D J. Light as a modulator of cognitive brain function[J]. *Trends in cognitive sciences*, 2009, 13(10): 429-438.
- [6] 陈庆伟, 汝涛涛, 周菊燕, 等. 光照对社会心理和行为的影响[J]. *心理科学进展*, 2018, 26(6): 1083.
- [7] 朱莹莹, 汝涛涛, 周国富. 照明的非视觉作用及其脑神经机制[J]. *心理科学进展*, 2015, 23(8): 1348.
- [8] Askaripoor T, Motamedzade M, Golmohammadi R, et al. Effects of light intervention on alertness and mental performance during the post-lunch dip: a multi-measure study[J]. *Industrial health*, 2019, 57(4): 511-524.
- [9] Cajochen C, Zeitzer J M, Czeisler C A, et al. Dose-response relationship for light intensity and ocular and electroencephalographic correlates of human alertness[J]. *Behavioural brain research*, 2000, 115(1): 75-83.
- [10] Smolders K C H J, De Kort Y A W, Cluitmans P J M. A higher illuminance induces alertness even during office hours: findings on subjective measures, task performance and heart rate measures[J]. *Physiology & behavior*, 2012, 107(1): 7-16.
- [11] Huiberts L M, Smolders K, De Kort Y A W. Shining light on memory: Effects of bright light on working memory performance[J]. *Behavioural Brain Research*, 2015, 294: 234-245.
- [12] Lee H, Lee E. Effects of coloured lighting on pleasure and arousal in relation to cultural differences[J]. *Lighting Research & Technology*, 2022, 54(2): 145-162.
- [13] von Castell C, Stelzmann D, Oberfeld D, et al. Cognitive performance and emotion are indifferent to ambient color[J]. *Color Research & Application*, 2018, 43(1): 65-74.
- [14] Segal A Y, Sletten T L, Flynn-Evans E E, et al. Daytime exposure to short-and medium-wavelength light did not improve alertness and neurobehavioral performance[J]. *Journal of biological rhythms*, 2016, 31(5): 470-482.
- [15] Łaszewska K, Goroncy A, Weber P, et al. Influence of the spectral quality of light on daytime alertness levels in humans[J]. *Advances in cognitive psychology*, 2018, 14(4): 192-208.
- [16] Wolska A, Sawicki D, Nowak K, et al. Method of Acute Alertness Level Evaluation after Exposure to Blue and Red Light (based on EEG): Technical Aspects[C]//*Proceedings of the 6th International Congress on Neurotechnology, Electronics and Informatics (NEUROTECHNIX 2018)*, Seville, Spain. 2018: 20-21.
- [17] Tonetti L, Natale V. Effects of a single short exposure to blue light on cognitive performance[J]. *Chronobiology international*, 2019, 36(5): 725-732.
- [18] Cheung I N, Zee P C, Shalman D, et al. Morning and evening blue-enriched light exposure alters metabolic function in normal weight adults[J]. *PLoS one*, 2016, 11(5): e0155601.

## ACKNOWLEDGEMENT

Thanks to Professor Daqing Zhu and his team for providing the light box environment and technical basis. It's helpful to explore the cooperative research of heterochromatic compound light.

Corresponding Author: Daqing Zhu

Affiliation: College of Information Science & Engineering, Huaqiao University,  
Fujian Key Laboratory of Light Propagation and Transformation

e-mail : zhudaqing@hqu.edu.cn

# A REVIEW OF DAYLIGHT PREDICTION BASED ON MACHINE LEARNING ALGORITHMS

Qiuping LIU , Yaodong CHEN\*, Yang LIU, Yuanfang LEI

(School of Architecture, Southwest JiaoTong University, Chengdu, China)

## ABSTRACT

Daylight confers extensive benefits for building occupants and improves energy efficiency; thus, its prediction and performance are significant for design decision-making on building and lighting. However, real-time prediction with high precision is difficult since daylight is spatiotemporal correlated and highly dynamic (e.g., periodic, irregularity). In recent years, numerous studies have been focused on machine learning algorithms (MLAs) due to their high generalization ability, robustness, and accuracy in dealing with complex problems. In contrast, selecting the optimal MLAs for a specific research problem is time-consuming and challenging, especially for new learners. This review attempts to provide a systematic summary of MLAs-based daylight-prediction studies by: 1) discussing the main principles and characteristics of the most representative algorithms; 2) conducting a whole process statistical analysis on the MLAs-based daylight-prediction studies and their technologies. This study will benefit the research field and support theoretical references for an extensive field that uses MLAs.

Keywords: daylight prediction, machine learning algorithms, artificial neural network

## 1. INTRODUCTION

Humans spend an average of 86.9% of their time living or working in enclosed buildings [1]. An indoor environment comprising daylight and artificial light is essential to human health and well-being. Appropriate lighting levels maintain visual comfort and productivity while regulating physiological and psychological conditions such as circadian rhythms and moods. Daylight prediction is beneficial for decision-making on indoor lighting and building design (energy efficiency-oriented design, comfort-oriented design). Hence, investigating the predictability of daylight is of great significance.

Daylight exhibits spatiotemporal correlation and periodic regularity, but it is also highly dynamic with random irregularity, making it predictable but challenging to obtain accurately in real-time [2]. In recent years, robust data-driven tools with intelligence algorithms for conducting data analysis, mining, and forecasting [3], have become increasingly popular as an alternative to simulation-derived tools, such as EnergyPlus and Radiance. Machine learning algorithms (MLAs), as a type of intelligence algorithms, can search, learn, and optimize data to recognize data patterns, construct complex relationships between input and output data, and perform prediction. Moreover, MLAs exhibited promising potential in numerous fields, including weather prediction [4], environmental monitoring [5], traffic [6], and energy efficiency [7].

MLAs were first applied to daylight prediction in 2006 [8]. After a brief period of growth and stagnation around 2011, sustained exploration of machine learning-based (ML-based) daylight prediction commenced in 2014, focusing on deep learning algorithms since 2020. Building layouts, facades, and external environments have been discussed in the related studies to support building design decision-making. Initially, for discussing building layouts [2, 9-24], Han et al. [2] simulated 415 effective rooms and proposed an fully connected neural network-based annual model that uses 16 building parameters to predict useful daylight illuminance (UDI) and spatial daylight autonomy (sDA) on the work-plane, with the  $R^2$  is 0.988 and 0.996, respectively. Second, for discussing facades optimization [2, 10-16, 21-23, 26-38], Lin et al. [37] tested 225 different facade designs and proposed a back propagation neural network (BPNN) model that utilizes facade-equivalent parameters to predict sDA and annual sunlight exposure, with deviations of 1.7-6.1% and 0.3-2.1 h, respectively. Several studies have focused on shading systems. Hu and Olbina [25] developed a BPNN model that uses horizontal illuminance and sun angle to predict the work-plane illuminance and the optimal slat angles of split blinds, with an accuracy of 94.7% and 98.5%, respectively. Third, for discussing the external environment, someone most involve climate conditions and external obstructions [12, 35, 39]. Ahmed et al. [12] compiled a dataset, including weather conditions, obstruction data, and room data. They established support vector

machine (SVM) and linear regression models to predict indoor daylight levels, with the MAE being 4.06 for SVM.

This study presents a comprehensive review of MLAs for daylight predictions. Firstly, the main principles and characteristics of 3 categories of MLAs are discussed, resulting in a fundamental understanding of their superiority. Secondly, constructing an MLA model based on 39 relevant studies published within the past 17 years is comprehensively reviewed and statistically analyzed. Finally, the potential use of ML technology and optimization methods are discussed.

## 2. REVIEW PROCEDURE

This study was conducted in accordance with the Preferred Reporting Items for Systematic Reviews and Meta-Analyses (PRISMA) guidelines [41] to ensure the quality of the review. Several search engine databases were utilized, including Sci-E, Scopus, Elsevier Science-Direct, and Engineering Village, to search for keywords in journal articles, and allowing the combination of relevant keywords and search operators (e.g., 'and' and 'or') to query detailed results. The initial keywords included 'daylight prediction', 'daylight illumination', 'machine learning', 'artificial neural network', 'support vector machine', and 'random forest'. For a further search, these keywords were combined in various ways when searching the databases, such as 'daylight prediction' AND 'machine learning', 'daylight prediction' AND 'artificial neural network', etc. The screening process of literature was conducted using the following inclusion and exclusion criteria: (i) The literature reviewed was limited to articles published in English between 2000 and 2023 that focused on daylight prediction using MLAs; (ii) Articles that were published in journals not cited in SCI were excluded; articles in the last quarter of JCR partition gave priority to be excluded; (iii) Articles with highly influential citations or high impact factors were evaluated as reliable and credible. Through the above process, a total of 39 studies related to MLA-based daylight prediction were collected.

## 3. MACHINE LEARNING ALGORITHMS

### 3.1 Artificial Neural Network-Based Algorithms

Artificial neural network (ANN) imitates the function of biological neural networks and can learn and recognize patterns [42, 43], effectively solving various complex problems. ANN comprises many neurons and three types of neuron layers, such as the input layer, the hidden layers, and the output layer. Neurons are the primary units of an ANN, which are interconnected through weighted connections between layers [42]. ANN can optimize itself to modify the influence of connections between neurons by adjusting the weights ( $w_{ij}$ ) or bias ( $\theta_i$ ), thereby minimizing the prediction error between the predicted value ( $y'$ ) and the actual value ( $y_j$ ) [43]. Based on data-flow directions, ANNs are mainly divided into feedforward neural network (FNN) and recurrent neural network (RNN). The information in FNN flows in a forward direction from one layer to the next without any connections between neurons within each layer. Multiple FNN-based variants have been developed, such as back propagation neural network, fully connected neural network (FCNN), and convolutional neural network. The RNN is inspired by the recurrent feedback system and the reverberating circuit hypothesis [44]. Its information not only flows forwards within different layers but also flows between neurons within the same layers, forming recurrent propagation. Additionally, its neurons in the hidden layers have a memory function, which can capture sequential data relations. Therefore, RNN is effective at sequence recognition tasks and has been widely applied in time series prediction. Various RNN-based variants have been developed, such as long short-term memory (LSTM), and gated recurrent unit network.

### 3.2 Support Vector Machine-Based Algorithms

The basic concept of support vector machine [45] is to find a line or plane that can dichotomize a dataset and maximize the geometric interval between two data groups. For those inseparable datasets in low dimensions, SVM maps them to a high-dimensional space to find a hyperplane for dichotomy. SVM is characterized by slight complexity, high tolerance to local disturbances of training samples, high generalization ability, and prediction accuracy [3]. Data samples nearest the decision margin are defined as support vectors. Hence, SVM is primarily used for classification by maximizing the distance between two support vectors. Variants of SVM, such as support vector regression (SVR), were developed for regression by minimizing the distance between two different support vectors.

### 3.3 Decision Tree-Based Algorithms

The basic concept of decision tree (DT) is to find the optimal splitting features and splitting rules for accurately classifying the dataset utilizing a binary or multi-ary recursive structure. DT comprises branches and nodes [46, 47]. Branches contain given classification rules and divide data samples into nodes with corresponding class labels [47]. Nodes include a root node, leaf nodes, and decision nodes. The root node consists of all input samples. Leaf nodes are those that no longer split down, and contain the model's output. Decision nodes contain samples that have not reached a decision yet and require further classification based on the given splitting rules. Feature selection is the key to the classification process, selecting the current node's splitting feature from input features. The optimal splitting features and features' splitting point (the value of splitting numerical interval) can be evaluated and chosen by various splitting criteria, including information gain, information gain ratio, and Gini index. Thus, DT can classify samples into categories best suited to their features; it is interpretable and can handle redundant features. ID3, C4.5, and classification and regression tree (CART) are the three primary variants of DT. In addition, ensemble DTs can be combined using various ensemble schemes, such as random forest (RF), boosting tree (BT), gradient boosting decision tree (GBDT), and eXtreme gradient boosting (XGBoost).

## 4. STATISTICS OF THE MLA PROCESS IN THE RELATED STUDIES

The main information from the studies that have used MLAs for daylight prediction, as follows: (i) research problems, including statistical issues, and prediction tasks; (ii) model selection and building information, including MLA selection, hyperparameters, input and output parameters; (iii) model evaluation, including model accuracy, and calculation speed.

### 4.1 Research Problem

#### 4.1.1 Statistical Issues

Statistical issues determine the type of model output and are categorized into regression and classification. Generally, regression produces more accurate daylight metric values, e.g., illuminance. Classification produces labels, perceptions, or other, e.g., 'insufficient, sufficient, excessive' [11] and 'imperceptible, perceptible, disturbing, intolerable' [36]. Figure 1(a) shows that most studies have aimed to obtain specific illuminance values or other metrics using regression, accounting for 71.4%. Another 16.7% of the studies have aimed to obtain a label representing the range of values using classification, where it was easier to develop a qualified model when sacrificing the demand for specific values prediction with high precision. Additionally, Figures 1(b) and (c) show the distribution of MLA types used in statistical issues. For regression, the most used algorithm types are ANN-based (55.4%), followed by DT-based (17.9%), other (17.9%), and SVM-based (8.9%), of which BPNN, uninterpreted ANN, and RF are widely adopted. For classification, the most used algorithm types are other (38.9%), followed by SVM-based (27.8%), DT-based (22.2%), and ANN-based (11.1%), of which SVM is widely adopted.

#### 4.1.2 Prediction Tasks

Different research purposes require various input features or parameters, sequence arrangements of dataset, and complexity of input-output mapping relations. Accordingly, research problems are categorized into 3 types of prediction tasks: time series prediction, spatial prediction, and spatiotemporal prediction. As shown in Figure 1(d), 57.5% of the studies have focused on spatial prediction, while 12.5% of them have focused on time series prediction. Spatial prediction is based on stable physics principles with fewer random variables, making it easy to achieve high accuracy. In contrast, time series prediction has received less attention because it is more challenging, and its time variations are accompanied by random variations, such as climate, weather, and clouds. Spatiotemporal prediction involves the complex simultaneous prediction of variations in space and time, has not been studied, and is more suitable for integration with intelligent lighting control systems than daylight prediction. Figure 1(e) and (f) show the distribution of MLA types used in prediction tasks. For spatial prediction, the most used algorithms are ANN-based (48.8%), followed by DT-based (19.5%), other (22.0%), and SVM-based (9.7%), of which BPNN, uninterpreted ANN, and RF are the most used algorithms. For time series prediction, the most used algorithms are ANN-based (77.8%), followed by DT-based (11.1%), and others (11.1%), and some algorithms that are advantageous in extracting time features were applied sporadically, such as LSTM and RF [29, 33].



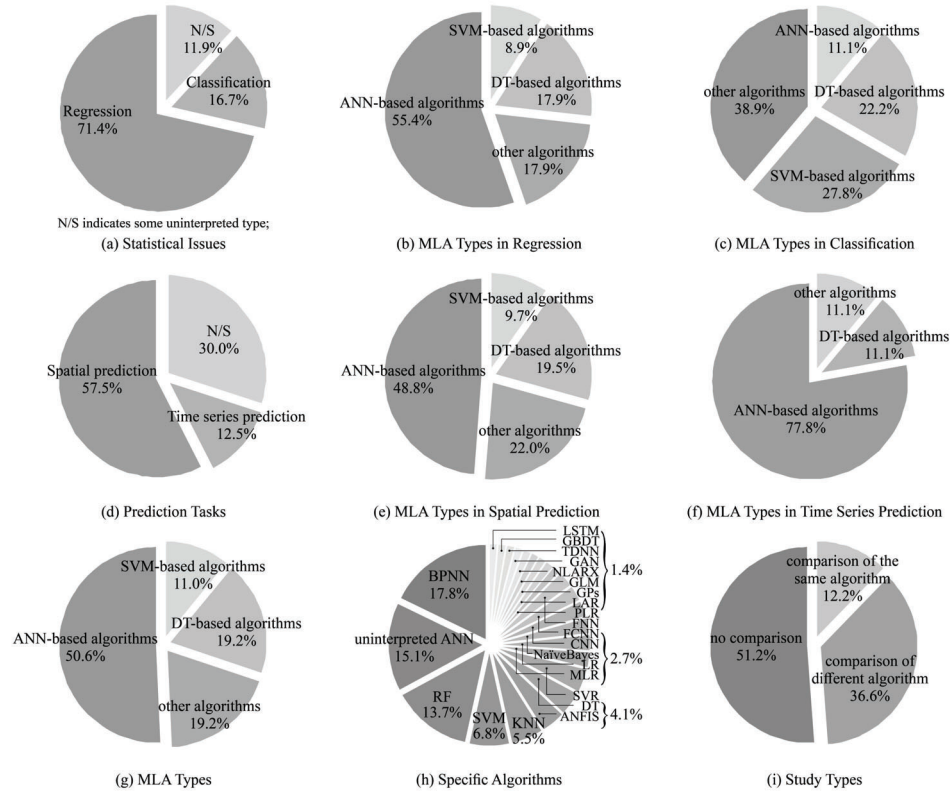


Figure 1. The distribution of statistical issues, prediction tasks, and MLA selection in the related studies

## 4.2 Model Selection and Building Information

### 4.2.1 MLA Selection

Figure 1(g) reveals the application frequency of various MLA types, with ANN-based being the most used algorithms (50.6%), followed by DT-based (19.2%), other (19.2%), and SVM-based (11.0%). This distribution can be attributed to the fact that most studies focus on solving regression and providing approximation algorithms. From the perspective of specific algorithms, Figure 1(h) summarizes nearly 20 kinds of MLAs involved, where BPNN and RF are the most used algorithms that have shown high accuracy in several studies [24, 33, 35]. Additionally, various studies employed one or multiple MLAs for daylight prediction. These studies are divided into: (i) no comparison, (ii) comparison of the same algorithm (with different structures), and (iii) comparison of different algorithms. Figure 1(i) reveals that 51.2% of the studies did not compare algorithms, 36.6% compared different algorithms, and 12.2% compared the same algorithm. These comparative studies aimed to identify the optimal algorithm by comparing models' accuracy. For example, Ngarambe et al. [33] found that BPNN outperformed GLM, RF, and gradient boosting model in predicting illuminance.

### 4.2.2 Hyperparameters

The hyperparameters refer to predefined configurations, which are essential for controlling the learning process of an MLA-based model and can be initialized or optimized. 84.6% of the studies have discussed their hyperparameter settings. These settings are summarized as follows: (i) For ANN models, the hyperparameters include hidden layers, neurons, epoch, max-epoch, batch size, learning rate, activation function, and loss function. Hidden layers often range from 1 to 15 and are mostly set as 1 layer. The number of neurons and epoch vary drastically among studies, ranging from 3 to 800 and 8 to 5000. They are mostly defined as 5, 10, and 200. Moreover, other hyperparameters are often set to default values; (ii) For SVM models, the hyperparameters include the kernel function, parameter C, and specific kernel parameters. The kernel function often uses RBF and Linear Kernel. The parameter C ranges from 1 to 500 and is typically defined as 15; (iii) For the RF model, the hyperparameters include the number of trees, the number of estimators, the maximum number of features, the maximum tree depth, the maximum number of leaf nodes, the minimum number of leaf nodes' samples, the minimum leaf nodes' total weight, the minimum number of samples for splitting, the criterion, and the loss

functions. The range of number of trees, number of estimators, and maximum tree depth are 1 to 1000, 38 to 264, and 1 to 6, respectively, of which the number of trees is typically set to 10 and the maximum tree depth is typically defined as 5.

#### 4.2.3 Input Parameters

The input is essential for accuracy, interpretability, and computational speed. A total of 109 input parameters involved in the related studies are counted, analyzed, and divided into: spatial feature inputs and temporal feature inputs. (i) Spatial feature inputs are static and include: (i-i) building information, e.g., room size/coordinates/orientation/elevation, latitude and longitude, wall reflectance/thickness/color, ceiling reflectance/color, floor reflectance/color, storey number; (i-ii) window information, e.g., window size/orientation/transmissivity/number/position, window to wall ratio (WWR), solar heat gain coefficient; (i-iii) sensor point, e.g., measured value, point distance from window/facade/wall/obstacle, position, direction; (i-iv) devices information, e.g., shading device type/position/size, blind angle/width/reflectance/number; (i-v) external obstructions, e.g., obstruction size/elevation/reflectance, external ground reflectance, site coverage. (ii) Temporal feature inputs are dynamic and include (ii-i) temporal parameters, e.g., solar altitude/azimuth/hour angle, year, month, day, hour, minutes, sunshine hours, and (ii-ii) temporal-feature climatic parameters, e.g., diffuse horizontal irradiance/illuminance, direct normal irradiance/illuminance, global horizontal irradiance/illuminance, exterior illuminance. Based on the analysis, the following findings are concluded: i) the mostly discussed spatial feature inputs are WWR (31%), followed by room size (28%) and window size (23%); while the mostly discussed temporal feature inputs are solar altitude/azimuth angle and diffuse horizontal irradiance (23%), followed by hour (18%); ii) climate change, e.g., cloud cover, has unpredictability caused by randomness, which significantly affects daylight prediction. Thus, few studies have explored the impact of instantaneous climate factors, and some ignored it using average sky data, e.g., typical meteorological year [36]; iii) window and device information are generally combined with other information.

#### 4.2.4 Output Parameters

Among the related studies, 22 output parameters are collected and analyzed, including the absolute illuminance and performance metrics. Absolute illuminance metrics include illuminance, mean/average illuminance, vertical eye illuminance (Ev), and daylight uniformity. Performance metrics include (i) standardized metrics, such as daylight autonomy (DA), spatial daylight autonomy (sDA), mean daylight autonomy (mDA), useful daylight illuminance (UDI), daylight glare probability (DGP), daylight glare index (DGI), annual sunlight exposure (ASE), and daylight factor (DF); (ii) self-defined metrics, such as illumination distribution, illumination level, luminance error, success rate, real perception, room status, view range/depth/factor, and spatial visual discomfort (sVD). As shown in Figure 2(a), the most used output parameters are illumination (19.4%), followed by sDA (14.9%), DA and UDI (10.4%), DGP (9.0%), and ASE (6.0%), etc. Among them, illumination relates to visual performance and comfort; DA, sDA, and UDI can evaluate annual daylight amount and distribution; DGP and DGI focus on evaluating the degree of perceived discomfort glare. In recent years, these output parameters have been used to meet the demands of work efficiency, visual comfort, energy conservation, and occupants' personalized design.

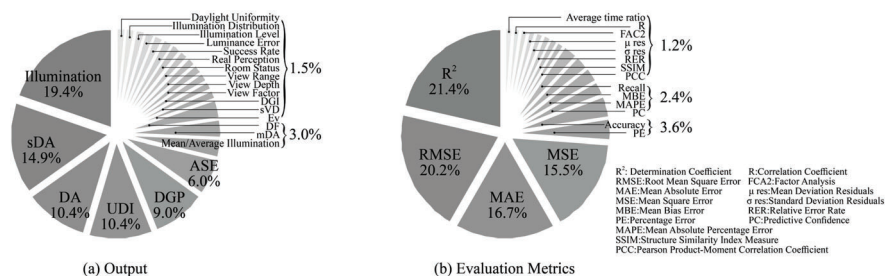


Figure 2. The distribution of output and evaluation metrics in the related studies

### 4.3 Model Evaluation

#### 4.3.1 Model Accuracy

Various evaluation metrics are typically used to evaluate the models' accuracy. Figure 2(b) shows that the most used evaluation metric is  $R^2$  (21.4%), followed by RMSE, MAE, and MSE. The  $R^2$ , accuracy-c (for classification), and recall are selected for model comparison because they



have relatively high utilization rates and normalized metrics ranging from -1 to 1 and are not affected by any input and output values, with the value closer to 1, indicating better accuracy. Accordingly, the model accuracy of 39 studies was analyzed as follows:

- For regression. ANN-based algorithms and RF achieve  $R^2 \geq 0.99$  when predicting mean illuminance, sDA, mDA, UDI, and ASE, but only the BPNN reaches 0.99 for predicting illuminance;
- For classification. NaïveBayes, DT, and SVM achieve accuracy-c  $\geq 0.99$  for predicting illuminance, and SVM reaches recall  $\geq 0.99$  for predicting DGP, while only ANN with principal component analysis achieves accuracy-c  $\geq 0.95$  for predicting UDI;
- For spatial prediction. ANN-based algorithms (i.e., FCNN) and RF achieve  $R^2 \geq 0.99$  for predicting mean illuminance, sDA, mDA, and ASE. Besides, BPNN, uninterpreted ANN, and CNN also reach 0.99 for predicting illuminance, UDI, and DGP, respectively. In contrast, the performance of SVM-based algorithms is weaker, and most studies are below 0.95;
- For time series prediction. Only ANN-based algorithms and RF were involved. Adaptive-Network-Based Fuzzy Inference System (ANFIS), RF, and BPNN are the best models in their respective studies, where ANFIS and RF achieve  $R^2 \geq 0.98$ .

Overall, ANN-based algorithms and RF were dominant in most studies on regression, spatial prediction, and time series prediction, and regression, performing excellently with  $R^2 \geq 0.99$  in most cases, while SVM outperformed others in classification.

#### 4.3.2 Calculation Speed

20.5% of the studies have compared the calculation speed of various simulation tools to prediction models and found that the prediction models significantly improve the computational speed. For instance, Han et al. [2] proposed that FCNN is 250 times faster than the conventional simulation. Additionally, some studies have explored reducing the training time by reducing input features or incorporating optimization algorithms [17, 18, 27]. For instance, Aydin et al. [27] improved the speed by 1224000 times by introducing the NSGA-II optimization algorithm.

## 5. DISCUSSION

Based on the review analyzed, two research areas require further exploration to fully leverage ML technology's potential. These areas are (i) real-time and high-precision oriented prediction, which is challenging because the trade-off between real-time and accuracy is easily influenced by specific research problems, hyperparameter structures, data size, measurement error, variables, and external environmental factors; (ii) the design of intelligent daylight-artificial light control systems for personalized demand and multi-objective optimization, which involves balancing various demands such as sufficient daylight, energy saving, thermal and visual comfort, physical and psychological health, occupants' preferences, and customized requirements.

## 6. CONCLUSION

This study aims to present a comprehensive review of machine learning methods for daylight predictions. Accurate daylight prediction is crucial for indoor building light quality and quantity optimization and occupants' satisfaction. Moreover, it allows considerable energy saving when coupled with automation. Machine learning algorithms provide powerful tools, surpassing traditional analytical models. Due to the importance of those technologies, the review for daylight prediction studies and their technologies will benefit the research field and the application of machine learning for personalized demands.

## REFERENCES

- [1] Klepeis, N.E., Nelson, W.C., Ott, W.R., et al. The National Human Activity Pattern Survey (NHAPS): a resource for assessing exposure to environmental pollutants. *Journal of Exposure Analysis and Environmental Epidemiology*, 2001, 11, 231-252.
- [2] Han, Y., Shen, L., & Sun, C. Developing a parametric morphable annual daylight prediction

- model with improved generalization capability for the early stages of office building design. *Building and Environment*, 2021, 200, 107932.
- [3] Xu, L., Chen, N., Chen, Z., Zhang, C., & Yu, H. Spatiotemporal forecasting in earth system science: Methods, uncertainties, predictability and future directions. *Earth-Science Reviews*, 2021, 222, 103828.
  - [4] Hamidi, O., Tapak, L., Abbasi, H., & Maryanaji, Z. Application of random forest time series, support vector regression and multivariate adaptive regression splines models in prediction of snowfall (a case study of Alvand in the middle Zagros, Iran). *Theoretical and Applied Climatology*, 2018, 134, 769-776.
  - [5] Das, M., & Ghosh, S.K. A probabilistic approach for weather forecast using spatio-temporal inter-relationships among climate variables. *ICIIS*, 2014, 1-6.
  - [6] Polson, N.G., & Sokolov, V.O. Deep learning for short-term traffic flow prediction. *Transportation Research Part C-emerging Technologies*, 2017, 79, 1-17.
  - [7] Seyedzadeh, S., Rahimian, F.P., Oliver, S., Rodriguez, D.S., & Glesk, I. Machine learning modelling for predicting non-domestic buildings energy performance: A model to support deep energy retrofit decision-making. *Applied Energy*, 2020, 279, 115908.
  - [8] Kurian, C.P., George, V.I., Bhat, J., & Aithal, R.S. ANFIS Model for the Time Series Prediction of Interior Daylight Illuminance. *International Journal on Artificial Intelligence & Machine Learning*, 2006, 6(3), 35-40.
  - [9] Le-Thanh, L., Nguyen-Thi-Viet, H., Lee, J., & Nguyen-Xuan, H. Machine learning-based real-time daylight analysis in buildings. *Journal of Building Engineering*, 2022, 104374.
  - [10] Kazanasmaz, T., Günaydın, M., & Binol, S. Artificial neural networks to predict daylight illuminance in office buildings. *Building and Environment*, 2009, 44, 1751-1757.
  - [11] Ahmed, A., Korres, N.E., Ploennigs, J., et al. Mining building performance data for energy-efficient operation. *Adv. Eng. Informatics*, 2011, 25, 341-354.
  - [12] Ahmed, A., Otreba, M., Korres, N.E., et al. Assessing the performance of naturally day-lit buildings using data mining. *Adv. Eng. Informatics*, 2011, 25, 364-379.
  - [13] Chatzikonstantinou, I., & Sariyıldız, S. Approximation of simulation-derived visual comfort indicators in office spaces: a comparative study in machine learning. *Architectural Science Review*, 2016, 59, 307 - 322.
  - [14] Lorenz, C., & Jabi, W. Predicting daylight autonomy metrics using machine learning. In: *International Conference for Sustainable Design of the Built Environment*, 2017, 991-1002.
  - [15] Radziszewski, K., & Waczyńska, M. Machine learning algorithm-based tool and digital framework for substituting daylight simulations in early-stage architectural design evaluation. In: *proceedings of the symposium on simulation for architecture and urban design*, 2018.
  - [16] Lorenz, C., Packianather, M.S., Spaeth, A.B., & Souza, C.B. Artificial Neural Network-Based Modelling for Daylight Evaluations. In: *proceedings of the symposium on simulation for architecture and urban design*, 2018.
  - [17] Lorenz, C., Packianather, M.S., Souza, C.B., Spaeth, A.B., & Lorenz, T.I. Input feature selection and optimization for ANN models predicting daylight in buildings. 2019.
  - [18] Lorenz, C., Spaeth, A.B., Bleil de Souza, C., et al. Artificial Neural Networks for parametric daylight design. *Architectural Science Review*, 2019, 63, 210 - 221.
  - [19] Liu, Y., Colburn, A., & Inanici, M. Deep neural network approach for annual luminance simulations. *Journal of Building Performance Simulation*, 2020, 13, 532 - 554.
  - [20] He, Q., Li, Z., Gao, W., Chen, H., Wu, X., Cheng, X., & Lin, B. Predictive models for daylight performance of general floorplans based on CNN and GAN: A proof-of-concept study. *Building and Environment*, 2021, 206, 108346.
  - [21] Nourkojouri, H., Shafavi, N.S., Tahsildoost, M., & Zomorodian, Z.S. Development of a Machine-Learning Framework for Overall Daylight and Visual Comfort Assessment in Early Design Stages. *Journal of Daylighting*, 2021, 8 (2), 270-283.
  - [22] Zou, Y., Zhan, Q., & Xiang, K. A comprehensive method for optimizing the design of a regular architectural space to improve building performance. *Energy Reports*, 2021, 7, 981-996.
  - [23] Deshpande, R., Nisztuk, M., Cheng, C., et al. Synthetic Machine Learning for Real-time Architectural Daylighting Prediction. *CAADRIA proceedings*, 2022.
  - [24] Daneshi, M., Fard, R.T., Zomorodian, Z.S., et al. Development of a hybrid machine -learning and optimization tool for performance-based solar shading design. 2022.
  - [25] Hu, J., & Olbina, S. Illuminance-based slat angle selection model for automated control of split blinds. *Building and Environment*. 2011, 46 (3), 786 -796.
  - [26] Logar, V., Kristl, Ž., & Škrjanc, I. Using a fuzzy black-box model to estimate the indoor

- illuminance in buildings. *Energy and Buildings*, 2014, 70, 343-351.
- [27] Aydin, E.E., Dursun, O.B., Chatzikonstantinou, I., & Ekici, B. Optimisation of energy consumption and daylighting using building performance surrogate model. 2015.
  - [28] Navada, S.G., Adiga, C.S., & Kini, S.G. Prediction of Daylight Availability For Visual Comfort. *International journal of applied engineering research*, 2016, 11, 4711 - 4717.
  - [29] Ahmad, M.W., Hippolyte, J., Mourshed, M.M., & Rezgui, Y. Random forests and artificial neural network for predicting daylight illuminance and energy consumption. 2017.
  - [30] Uribe, D., Vera, S., Bustamante, W. Optimization of complex fenestration systems using an artificial neural network (ANN) considering energy and daylighting performance of office buildings. 2017.
  - [31] Lu, Y., Liu, S.W., Hong, Y., & Xiao, Y.Q. Multivariable Optimization of Dynamic Translucent Solar Screen on West-Facing Offices. *IOP Conference Series: Earth and Environmental Science*, 2019, 238.
  - [32] Jung, S.K., Kim, Y., & Moon, J.W. Performance Evaluation of Control Methods for PV-Integrated Shading Devices. *Energies*, 2020, 13 (12), 3171.
  - [33] Ngarambe, J., Irakoze, A., Yun, G.Y., et al. Comparative performance of machine learning algorithms in the prediction of indoor daylight illuminances. *Sustainability*, 2020.
  - [34] Arbab, M., Rahbar, M., & Arbab, M. A Comparative Study of Artificial Intelligence Models for Predicting Interior Illuminance. *Applied Artificial Intelligence*, 2021, 35, 373 - 392.
  - [35] İlkin Canlı, Orçun koral Işeri, Ipek Gursel Dino, Comparison of Different Data-Driven Models on Prediction of Useful Daylight Illuminance (UDI). 2021.
  - [36] Xie, J., & Sawyer, A.O. Simulation-assisted data-driven method for glare control with automated shading systems in office buildings. *Building and Environment*, 2021, 107801.
  - [37] Lin, C., & Tsay, Y. A metamodel based on intermediary features for daylight performance prediction of façade design. *Building and Environment*, 2021, 206, 108371.
  - [38] Kristiansen, T., Jamil, F., Hameed, I.A., & Hamdy, M. Predicting annual illuminance and operative temperature in residential buildings using artificial neural networks. *Building and Environment*, 2022, 217, 109031.
  - [39] Nault, E., Moonen, P., Rey, E., & Andersen, M. Predictive models for assessing the passive solar and daylight potential of neighborhood designs: A comparative proof-of-concept study. *Building and Environment*, 2017, 116, 1-16.
  - [40] Ngarambe, J., Adilkhanova, I., Uwiragiye, B., & Yun, G.Y. A review on the current usage of machine learning tools for daylighting design and control. *Building and Environment*, 2022, 223, 109507.
  - [41] Page, M.J., McKenzie, J.E., Bossuyt, P.M., et al. The PRISMA 2020 statement: An updated guideline for reporting systematic reviews. *International journal of surgery*, 2020, 105906.
  - [42] Jain, A.K., Mao, J., & Mohiuddin, K.M. Artificial Neural Networks: A Tutorial. *Computer*, 1996, 29, 31-44.
  - [43] Haykin, S.S. *Neural Networks: A Comprehensive Foundation*. 1994.
  - [44] Windhorst, U. On the role of recurrent inhibitory feedback in motor control. *Progress in Neurobiology*, 1996, 49, 517-587.
  - [45] Cortes, C., & Vapnik, V.N. Support-Vector Networks. *Machine Learning*, 1995, 20, 273-297.
  - [46] Quinlan, J.R. *Induction of Decision Trees*. *Machine Learning*, 1986, 1, 81-106.
  - [47] Geva, S., & Sitte, J. Adaptive nearest neighbor pattern classification. *IEEE transactions on neural networks*, 1991, 2 (2), 318-22 .

## ACKNOWLEDGEMENTS

This work was supported by the National Natural Science Foundation of China (52008347), the Project of the Aging Industry Research Center of the Sichuan Key Research Base of Social Sciences (XJLL2022023).

Corresponding Author Name: yaodong Chen

Affiliation: School of Architecture, Southwest JiaoTong University, Chengdu, China

e-mail: 971558522@qq.com

# **EFFECT OF DESKTOP TO BLACKBOARD ILLUMINATION RATIO ON STUDENTS' VISUAL FATIGUE IN A MULTIMEDIA CLASSROOM LIGHT ENVIRONMENT**

Ji Weng, Wenshu Bai, Siyi Ke, Jiayi Zhang

(School of Architecture and Urban Planning, Chongqing University, Chongqing, China)

## **ABSTRACT**

The electronic display devices in multimedia classrooms are self-luminous and have a high color temperature and luminance compared to desktop and paper viewing surfaces. When studying in the multimedia classroom light environment, students' eyes are switched between different viewing surfaces, resulting in frequent adjustments of the pupils and photoreceptor cells, which leads to visual fatigue. Visual fatigue is classified as eye muscle fatigue and mental fatigue, and the repeated accumulation of visual fatigue can easily lead to eye diseases and decreased work efficiency. The study aims to investigate the effects of different desktop to blackboard illumination ratios on the subjects' eye muscle fatigue and mental fatigue under the same color temperature light environment in multimedia classrooms in order to reduce the prevalence of eye diseases and improve the work efficiency of students. The experiment assessed the increase in eye muscle fatigue and mental fatigue of thirteen subjects by using eye movement parameters (EMP) and the index of mental capability (IMC) of visual tasks under different illumination ratios on the blackboard and desktop. The results demonstrated that increasing the illumination level of the blackboard helped to reduce the students' eye muscle fatigue and decrease the level of mental fatigue by keeping the desktop illumination level constant. This research has a positive effect on the alleviation of students' visual fatigue and the improvement of work efficiency in the light environment of multimedia classrooms.

Keywords: multimedia classroom light environment, visual fatigue, illumination ratio, visual task, eye movement parameters

## **1. INTRODUCTION**

The popularity and usage rate of multimedia classrooms has increased significantly in recent years. During class, the visual surfaces of the blackboard, desktop, and electronic whiteboard endure repeated transformations in front of the student's eyes. As a self-illuminating body, the visual surface of the electronic display device typically has a high color temperature and high brightness, resulting in a significant change in the lighting environment of the multimedia classroom. To constantly adapt to the new visual object, the difference between the visual surface will cause the human pupil and photoreceptor cells to adjust frequently, causing visual fatigue and vision loss.

Scott et al. investigated the causes of visual fatigue by analyzing the division of labour in the extraocular muscles of humans and concluded that fatigue is associated with decreased muscle performance and cerebral performance. Harezlak et al.[1] studied oculomotor dynamics from the standpoint of chaotic behavior and self-similarity assessment, concluding that visual fatigue could be evaluated using oculomotor parameters to evaluate eye muscle fatigue. Kim et al.[2] proposed a visual fatigue monitoring system based on eye movement and blink detection; the experimental results demonstrated a significant correlation between visual fatigue and the saccade parameter of the oculomotor parameters. Liang et al. [3] discovered that as the degree of visual fatigue increased, it led to a decrease in visual efficacy, and the magnitude of the change was reflected in changes in work productivity, learning ability, and homework performance.

Li et al.[4] evaluated the illumination elements of desktop illumination, blackboard illumination, and projection curtain brightness in multimedia classrooms in colleges and universities, and discovered that the illumination of the projection curtain frequently affects the illumination of the blackboard due to their proximity. The illumination of the desktop and blackboard in the classroom significantly impacts the environment's lighting quality, and choosing the appropriate illumination

for both of them will benefit students who struggle with visual fatigue. Consequently, it is essential to identify appropriate illumination ratios for the desktop and blackboard for the light source that match the high luminance and high color temperature of the electronic whiteboard.

Therefore, a simulation experiment based on the visual process of learning in a multimedia classroom with an electronic whiteboard was carried out in the laboratory. Through the evaluation of eye movement parameters (EMP) and the index of mental capability (IMC) of visual tasks, the study was conducted to examine the effects of various blackboard to desktop illumination ratios on students' eye muscle fatigue and mental fatigue.

## 2. MATERIALS AND METHODS

### 2.1. Environmental Settings

The experimental scene was set up in the optical laboratory of Chongqing University as depicted in Figure 1. To prevent natural light interference, blackout curtains and sliding blackout panels were installed around the windows and lighting simulation area of the laboratory. The illumination simulation area was furnished with tables and chairs; a monitor was installed in front to simulate a whiteboard, and a printing paperboard was hung next to it to simulate a blackboard. Five males and eight females between the ages of 12 and 25 were enrolled in this study.



Figure 1. Environmental settings.

### 2.2. Subjects

All subjects had a normal color vision, no eye diseases, no refractive errors such as astigmatism and hyperopia, and a visual acuity of 5.0 with correction. To prevent excessive experimental errors caused by the consumption of stimulating substances, the subjects were instructed to abstain from coffee, tea, and other beverages containing central nervous system stimulants for 12 hours before the experiment.

### 2.3. Light source conditions

The illumination distribution between the classroom desk and the blackboard informed the design of the light source conditions. In the Architectural Lighting Design Standards, the desktop illumination level included 300 lx and an increased illumination level of 500 lx, while the blackboard illumination levels were 500 lx and 750 lx. The experiments were set up with 3300K, 4000K, and 4700K corresponding to warm, medium, and cold three color temperatures as a control in order to account for the impact of light source color temperature on the experimental outcomes. The parameters of the specific operating conditions are provided in Table 1.

Table 1. Physical parameters of the experimental environment.

	Illumination Ratio			
CCT	300 lx × 500 lx	300 lx × 750 lx	500 lx × 500 lx	500 lx × 750 lx
3300K	3300×300×500	3300×300×750	3300×500×500	3300×500×750
4000K	4000×300×500	4000×300×750	4000×500×500	4000×500×750
4700K	4700×300×500	4700×300×750	4700×500×500	4700×500×750



## 2.4. Equipment

The Tobii Pro Glasses 2 eye-tracking device (Figure 2) was used for the experiment. During the experiment, eye movement parameters were obtained from the Tobii Pro Glasses 2, which recorded the entire visualization process of the subjects in real time and obtained the corresponding eye movement parameters through the corresponding data processing software.



**Figure 2.** Equipment.

## 2.5. Experimental Procedure

Each experimental subject took part in a total of three major groups of experiments (each major group included four small groups of experiments), with a 10-minute break between every two small groups of experiments and a 20-minute break between every two major groups of experiments, allowing the subjects to get enough rest and effectively avoid the interference of the previous experiment's fatigue level. The specific experimental process is as follows:

Step 1: The experimental procedure and the method for filling out the experimental scale were explained to the subjects, who then completed the scale once for each category.

Step 2: The subjects put on the eye-tracking Tobii Pro Glasses 2, turned on the controller, and calibrated the visual points.

Step 3: The experimenters specified the direction of the opening of the Randall's ring visual scale to be reported. And then the subjects looked at the Randall's ring checklist on the printed paper board and reported the coordinate position of the Randall's ring visual scale in the specified opening direction for 1 min.

Step 4: The experimenters distributed the word lookup table and timed the word lookup. The subjects looked up the words on the VDT, found the corresponding serial number on the printed paperboard, and filled in the serial number on the desk record sheet until all 40 words were found in sequence.

Step 5: The subjects repeated Step 4 for the of Randall's ring recognition.

Step 6: The first small group experiment was completed, and each small group experiment was followed by a 5 min break for the subjects.

Step 7: Repeat steps 3 through 6 three times until the first major group of experiments is completed. After each major group of experiments, the subjects would take a break for 20 min.

Step 8: Subjects repeated steps 2 through 7 twice more until all three major groups of experiments were completed.

The experimental process is depicted in Figure 3.

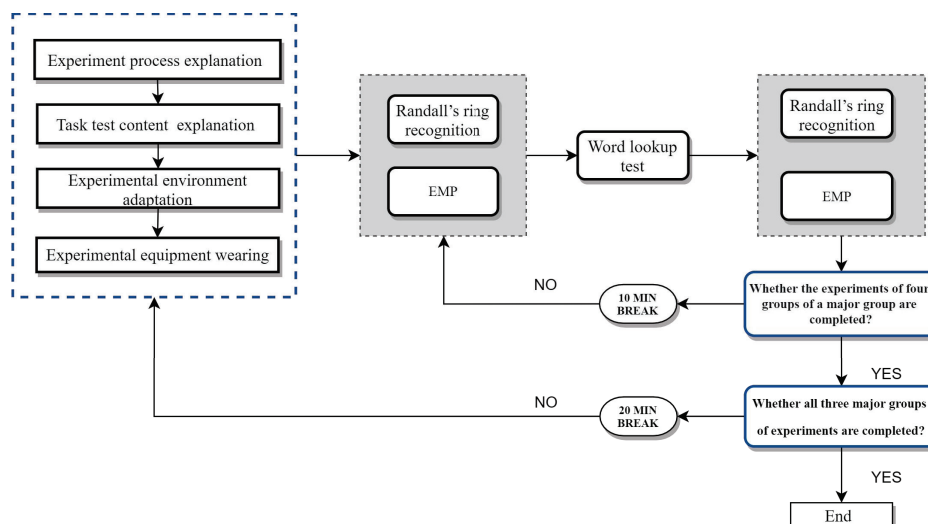


Figure 3. Experimental procedure.

### 3. RESULTS

Two types of evaluation index data were obtained, including eye movement parameters and index of mental capability. The data were put through three tests: a normality test, a homogeneity test of variance, and an independent test. Then, we used one-way or multi-way ANOVA to determine whether the sample data were statistically significant using the data that satisfied the aforementioned conditions. When the result was at the  $P < 0.05$  level, there was a significant difference between the sample data, allowing the data mean to be used for comparative analysis. The above steps were collectively referred to as the basic test.

#### 3.1. Eye Movement Parameters

The Tobii I-VT Fixtation was selected to filter the initial eye movement parameters collected by the oculomotor. Visual fatigue can be evaluated using the fixation frequency, total duration of fixation, average duration of fixation, number of saccades, average amplitude of saccades, and average peak velocity of saccades. The fixation frequency, total duration of fixation, average duration of fixation, and number of saccades are positively correlated with visual fatigue, whereas the average amplitude of saccades and average peak velocity of saccades are negatively correlated with visual fatigue[5, 14]. In the Tobii Pro Lab software, the Max gap length was set to 75 ms, the I-VT fixation classification threshold was 30 %/s, the minimum fixation duration was restricted to 60 ms, and the Tobii I-VT Fixtation filter appropriate for relatively stationary experimental scenes was chosen. The event marker points were chosen as the beginning and ending time points for the two Randall's ring recognition preceding and following the event.

The data on the value of the change in the fixation frequencies in Randall's ring recognition satisfied the basic test, and multiple comparisons between the groups based on the Least-Significant Difference (LSD) were conducted independently. As shown in the Table 2, the results indicated that there were significant differences between the experimental data under the conditions of illumination ratios of 300 lx:500 lx and 300 lx:750 lx ( $P < 0.05$ ), 300 lx:500 lx and 500 lx:750 lx ( $P < 0.05$ ), 500 lx:500 lx and 300 lx:750 lx ( $P < 0.05$ ), and 500 lx:500 lx and 500 lx:750 lx ( $P < 0.05$ ).

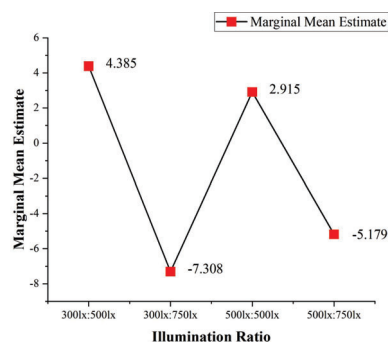
**Table 2.** Multiple comparisons between groups for eye movement parameters based on LSD.

Dependent variable	Illumination ratio	Illumination ratio	Mean difference	significance	95% confidence interval	
					Lower limit	Upper limit
The fixation frequency of Randall's ring recognition	300:500	300:750	11.6923*	.002	4.3459	19.0388
		500:500	1.4692	.693	-5.8772	8.8157
	300:750	500:500	-10.2231*	.007	-17.5695	-2.8766
		500:750	-2.1282	.568	-9.4747	5.2182
	500:500	500:750	8.0949*	.031	.7484	15.4413
	500:750	300:500	-9.5641*	.011	-16.9105	-2.2177

Note: \*. The significance level of the mean difference is 0.05.

Further analysis of the comparison of the eye movement parameters (Figure 4) revealed that the mean value of the difference in the fixation frequencies in the experimental condition with an illumination ratio of 300 lx:500 lx was greater than the mean value of the difference in the fixation frequencies in the experimental conditions with an illumination ratio of 300 lx:750 lx and 500 lx:750 lx; the mean value of the difference in the fixation frequencies in the experimental condition with an illuminance ratio of 500 lx:500 lx was greater than the mean value of the difference in the fixation frequencies in the experimental conditions with an illumination ratio of 300 lx:750 lx and 500 lx:750 lx. There was a negative correlation between the increase in visual fatigue and the brightness of the blackboard when VDT work was performed under identical conditions of color temperature and desktop illumination. Therefore, increasing the blackboard's illumination reduced visual fatigue. However, when the blackboard's illumination level was fixed, the change in the desktop's illumination level had no significant effect on visual fatigue.

Compared with the other groups, the illumination ratios of 300 lx:750 lx and 500 lx:750 lx on the desktop and blackboard had a smaller impact on the increase in visual fatigue among students, so they can be used as the recommended values of illumination in the VDT multimedia classroom.

**Figure. 4** Mean change values of the fixation frequency of Randall's ring recognition.

### 3.2 . Index of Mental Capability

Visual fatigue causes a reduction in visual efficacy, which in turn reduces working efficiency [15]. Consequently, the index of mental capability (IMC), which reflects working efficiency, is also an essential index for evaluating visual fatigue. The index of mental capability is inversely proportional to mental fatigue and directly proportional to working efficiency.

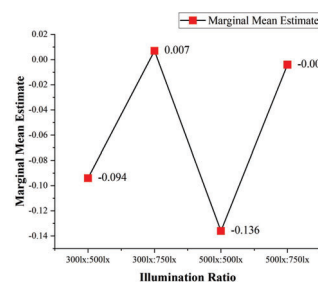
The IMC of Randall's ring recognition passed the basic test. The data were subjected to multiple comparisons based on LSD between groups concerning Section 3.1. As shown in the Table 3, the test results revealed a highly significant difference between the illumination ratios of 00 lx:750 lx and 500 lx:500 lx ( $P<0.001$ ), a significant difference between 300 lx:500 lx and 300 lx:750 lx ( $P<0.05$ ), and a significant difference between 300 lx:500 lx and 500 lx:750 lx ( $P<0.05$ ), as well as between 500 lx:500 lx and 500 lx:500 lx ( $P<0.05$ ).

**Table 3.** Multiple comparisons between groups for index of mental capability based on LSD.

Dependent variable	Illumination ratio	Illumination ratio	Mean difference	significance	95% confidence interval	
					Lower limit	Upper limit
The fixation frequency of Randall's ring recognition	300:500	300:750	-.10092*	.019	-.18501	-.01684
		500:500	.04207	.324	-.04202	.12616
	300:750	500:500	.14300*	.001	.05891	.22708
		500:750	.01059	.804	-.07350	.09468
	500:500	500:750	-.13240*	.002	-.21649	-.04831
	500:750	300:500	.09033*	.035	.00624	.17442

Note: \*. The significance level of the mean difference is 0.05.

Figure 5 depicts a comparative analysis of the change values of the IMC of Randall's ring recognition before and after the experiment, comparing the change in fatigue at each illumination ratio. In an environment where the VDT and the surrounding environment were used as a visual work surface, the results showed that an increase in the blackboard's illumination level slowed the decrease in the subjects' IMC under identical conditions of color temperature and desktop illumination. This indicates that the decrease in the subjects' working efficiency was slowed within a certain range. However, when the blackboard's illumination level was held constant, the change in the table's illumination level did not affect the subjects' working efficiency. When the ratio of desktop to blackboard illuminance was 350 lx:750 lx, the subjects had the highest value of change in mental work index, the highest work efficiency, and the lowest mental fatigue. This value can be used as the recommended value for illuminance selection in the multimedia classroom.



**Figure. 5** Mean values of the index of mental capability of Randall's ring recognition.

#### 4. CONCLUSIONS

This study investigates the effect of the illumination ratio between the desktop and the blackboard on the visual fatigue of students in a multimedia classroom with an electronic whiteboard and the same color temperature. When the illumination level of the desktop was kept constant, the results indicated that increasing the illumination level of the blackboard reduced eye muscle fatigue in the students. When the illumination level of the blackboard was increased while

the illumination level of the desktop remained unchanged, increasing the illumination level of the blackboard could reduce the decrease in mental fatigue and the decline in work productivity. When the blackboard's illumination level is fixed, the change in the desktop's illumination level has no significant effect on the degree of visual fatigue. Concurrently, it is suggested that the illumination ratios of 300 lx:750 lx and 500 lx:750 lx for the desktop and the blackboard be utilized as the illumination of choice in the whiteboard multimedia classroom. In future studies, the sample size will be increased, as will the level of illumination thresholds, in order to gain a deeper understanding of the effects of multimedia classroom lighting on students' visual fatigue.

## REFERENCES

- [1] Harezlak, K.; Kasprowski, P. J. S., Understanding eye movement signal characteristics based on their dynamical and fractal features. 2019, 19, (3), 626.
- [2] Kim, D.; Choi, S.; Choi, J.; Shin, H.; Sohn, K. In Visual fatigue monitoring system based on eye-movement and eye-blink detection, Stereoscopic Displays and Applications XXII, 2011; SPIE: 2011; pp 35-42.
- [3] Shuyin, L.; Chunyu, Y.; Juanjie, L., Experimental Scheme Exploration on Visual Fatigue in
- [4] Multimedia Classroom Light Environment. China Illuminating Engineering Journal 2019, 30, (3), 43-47.
- [5] Tianxing, L. Z. S., An Investigation on Luminous Environment of Multimedia Classroom. China Illuminating Engineering Journal 2009, 20, (02), 46-50.
- [6] Xin, C. Study on Optimization of Lighting Environment of Multimedia Classrooms in Primary and Secondary Shools Using Electronic WhiteBoard. Master's thesis, Chongqin University, 2021.
- [7] Rechichi, C.; Scullica, L., [Asthenopia and monitor characteristics]. Journal francais d'ophtalmologie 1990, 13, (8-9), 456-460.
- [8] Scott, A. B.; Collins, C. C., DIVISION OF LABOR IN HUMAN EXTRAOCULAR MUSCLE. Archives Of Ophthalmology 1973, 90, (4), 319-322.
- [9] Harezlak, K.; Kasprowski, P. J. S., Understanding eye movement signal characteristics based on their dynamical and fractal features. 2019, 19, (3), 626.
- [10] Kim, D.; Choi, S.; Choi, J.; Shin, H.; Sohn, K. In Visual fatigue monitoring system based on eye-movement and eye-blink detection, Stereoscopic Displays and Applications XXII, 2011; SPIE: 2011; pp 35-42.
- [11] Shuyin, L.; Chunyu, Y.; Juanjie, L., Experimental Scheme Exploration on Visual Fatigue in Multimedia Classroom Light Environment. China Illuminating Engineering Journal 2019, 30, (3), 43-47.
- [12] Wei, H.; Chunyu, Y.; Shuying, L., Investigation and Research on Brightness Contrast Value and Suhjective Evaluation of Multimedia Classroom. China Illuminating Engineering Journal 2021, 32, (4), 39-42.
- [13] Schleicher, R.; Galley, N.; Briest, S.; Galley, L. J. E., Blinks and saccades as indicators of fatigue in sleepiness warnings: looking tired? 2008, 51, (7), 982-1010.
- [14] Cazzoli, D.; Antoniadis, C. A.; Kennard, C.; Nyffeler, T.; Bassetti, C. L.; Müri, R. M. J. P. o., Eye movements discriminate fatigue due to chronotypical factors and time spent on task—a double dissociation. 2014, 9, (1), e87146.
- [15] App, E.; Debus, G. J. E., Saccadic velocity and activation: development of a diagnostic tool for assessing energy regulation. 1998, 41, (5), 689-697.

-----

## ACKNOWLEDGEMENTS

Corresponding Author: Ji Weng

Affiliation: School of Architecture and Urban Planning, Chongqing University

e-mail: wengji@cqu.edu.cn



# GRAYSCALE-LUMINANCE CONVERTING POLYNOMIAL FUNCTION FOR EVALUATING INDICATORS OF SPATIAL LUMINANCE DISTRIBUTION VIA DIGITAL IMAGES: A PILOT STUDY IN LOW-CONTRAST LIT SPACE

Peng Chen<sup>1,2</sup>, Lixiong Wang<sup>1,2</sup>, Aiyong Wang<sup>1,2,\*</sup>, Juan Yu<sup>1,2</sup>, Yuting Wu<sup>1,2</sup>

<sup>1</sup> School of Architecture, Tianjin University, Tianjin, China;

<sup>2</sup> Tianjin Key Laboratory of Architectural Physics and Environmental Technology, Tianjin, China

## ABSTRACT

Spatial luminance coefficient ( $Feu$ ) and average luminance ( $L_{av}$ ) can help improve the quality of lighting design by regulating the spatial luminance distribution from subjective and objective perspectives respectively. However, existing methods do not support the evaluation of  $Feu$  and  $L_{av}$  during the design survey due to the difficulty of carrying professional equipment or the time-consuming calibration process. This paper proposes a grayscale-luminance converting polynomial function to measure or calculate the two indicators via digital images obtained from mobile devices or lighting simulation software. By creating a new parameter  $N_{allow}$  to control the polynomial order, the number of measurement points required for calibration is minimised to nine, significantly reducing the workload. Three different categories of low-contrast working conditions with luminance ratios less than 100 and luminance less than 1000 cd/m<sup>2</sup> were set, namely an actual scene, simulated scenes, and experimental scenes. A piecewise function of  $N_{allow}$  values determined by the luminance ratio was constructed, then validated and calibrated with data from 20 working conditions. The piecewise function was determined by the criterion that the error of  $Feu$  or  $L_{av}$  obtained from the polynomial function fitting should be less than 10%. A test scene was set to verify the accuracy of the polynomial function, and the results show that the calculation error for  $Feu$  is 1.1% and for  $L_{av}$  is 0.2%, with lower errors than conventional exponential function fitting results. The proposed polynomial function provides designers with a simple but accurate path for evaluating spatial luminance distribution and supports diverse needs for on-site measurement and simulation calculation.

Keywords: luminance distribution; spatial luminance coefficient  $Feu$ ; polynomial function

## 1. INTRODUCTION

The luminance distribution is closely related to peoples' perception of indoor environments, such as their sense of space and distance.[1, 2] An appropriate luminance distribution can make space more interesting, highlight visual focus, and reduce unnecessary light distribution to save energy. Compared to evaluation via illuminance, the evaluation of indoor lighting design via the luminance distribution is more conducive to improving the design quality.

### 1.1 Indicators of spatial luminance distribution

The average luminance,  $L_{av}$ , is an objective indicator by which to evaluate the overall luminance of a space, but it does not reflect the perceived brightness.

Iwai *et al.*[3] proposed the spatial luminance coefficient,  $Feu$ , which evaluates spatial luminance based on the geometric mean luminance of discrete measurement points in space and expresses peoples' subjective perceptions of luminance via a single value.  $Feu$  has been applied by Panasonic Corporation in the lighting design of residential buildings, public buildings, roads, etc., [3, 4].  $Feu$  is defined as shown in Equation (1):

$$\begin{cases} Feu = 1.5 \times Lg^{0.7} \\ Lg = \sqrt[mn]{\prod_{i=1}^m \prod_{j=1}^n L_{ij}} \end{cases} \quad (1)$$

where  $Lg$  is the geometric mean luminance of grid points within the visual field of 85° vertical and 100° horizontal. A zone with a luminance greater than 1000 cd/m<sup>2</sup> is treated as a light source that contributes little to brightness perception, so it is excluded from the calculation.

## 1.2 Calculation and measurement method of $Feu$ and $L_{av}$

Iguchi *et al.*[5] proposed that in real space,  $Feu$  can be measured via a calibrated camera or imaging luminance meter. In virtual space,  $Feu$  can be calculated by the radiosity algorithm. However, shortcomings of this method are the cumbersome work of the collection of luminance via measurement points, as well as the high cost and poor portability of the equipment. In addition, lighting software familiar to designers (e.g. DIALux evo) does not support  $Feu$  calculation.

By fitting the grayscale-luminance function via the grayscale-luminance data of a small number of pixels on a digital image, the actual luminance,  $L$ , of each point in space can be extracted from the pixel grayscale  $D$ . This is a relatively convenient way to calculate or measure  $Feu$  and  $L_{av}$ . Under ideal conditions,  $D$  and  $L$  have an exponential relationship[6], as shown in Equation (2):

$$L = a_1 \times a_2^D \quad (2)$$

where  $a_1$  and  $a_2$  are parameters related to digital imaging equipment and are obtained through calibration.

In practice, the grayscale-luminance curve of a digital image may not be well fitted to an exponential function due to the limitations of the response range of the digital imaging equipment. A variety of grayscale-luminance functions have been proposed, such as linear model[7], polynomial model[8, 9], and hybrid model[10]. These studies prove the applicability of digital images in the luminance distribution analysis within low contrast (<100) lit space. A relationship between luminance range and model form can also be observed. However, this method still cannot support the evaluation of  $Feu$  and  $L_{av}$  in the design stage well. This is because the mathematical model is linked to specific devices, and a large amount of measurement point data is still needed in calibration, which results in the inconvenience of on-site surveys.

This paper proposes a new grayscale-luminance polynomial function model to obtain accurate values of  $Feu$  and  $L_{av}$  from digital images. The key parameter  $N_{allow}$  and the piecewise function of  $N_{allow}$  determined by the luminance ratio also be proposed. Based on the grayscale-luminance data of at least nine measurement points, the model maintains the errors of  $Feu$  and  $L_{av}$  within 10%. The proposed method reduces equipment requirements and does not require the calibration of equipment in advance, thereby making it easier to evaluate the luminance distribution in indoor lighting design.

## 2. METHODS

### 2.1 Grayscale-luminance polynomial function

The pixel grayscale,  $D$ , and actual luminance,  $L$ , are extracted from measurement points on a digital image. Excluding measurement points with luminance greater than 1000 cd/m<sup>2</sup>, the luminance and grayscale data set of the remaining measurement points are respectively recorded as  $L = \{L_1, L_2, \dots, L_k\}$  and  $D = \{D_1, D_2, \dots, D_k\}$ . The grayscale-luminance data set is recorded as  $S = \{L, D\}$ , and participates in the polynomial function fitting. Considering the greater the number of polynomial function terms, the more measurement points are required, the acceptability index  $N_{allow}$  is proposed to control the number of polynomial terms within two or three and the number of measurement points to nine. The function can be expressed as Equation (3). In the function,  $a_1 \times D$  fits the linear component of the grayscale-luminance relationship, while  $(a_2 \times D)^N$  fits the non-linear component.

$$\begin{cases} L = a_0 + a_1 \times D & (N = 1) \\ L = a_0 + a_1 \times D + (a_2 \times D)^N & (N > 1) \\ N = N_{allow} = f_{exp}(S) \end{cases} \quad (3)$$

Parameters  $a_0$ ,  $a_1$ , and  $a_2$  are positive numbers to be fitted.  $N_{allow}$  was defined as a positive integer, which is the minimum value of the degree of the polynomial function that can ensure both errors of  $Feu$  and  $L_{av}$  are less than 10%.  $N_{allow}$  is determined by luminance distribution in  $S$ .

## 2.2 Value function of $N_{allow}$

### 2.2.1 Case scenes

Twenty working conditions were selected to determine  $f_{exp}(S)$ . Each working condition had a different distribution of  $S = \{L, D\}$ , which can be described by the following indicators.

- Linear correlation  $R$ : This determines whether the grayscale and the luminance have a linear relationship. It is numerically equal to Pearson's correlation coefficient between  $D$  and  $L$ .
- Maximum luminance,  $L_{max}$ , and minimum luminance,  $L_{min}$ : The maximum and minimum values of  $L$  describe the absolute severity of the luminance change in space.
- Average luminance,  $L_{av}$ : The average  $L$ , which describes the overall luminance level.
- Luminance ratio,  $C$ : This is the ratio of  $L_{max}$  to  $L_{min}$ , which reflects the relative severity of the luminance change in space.

According to previous research, the luminance ratio in the field of view of the lighting space that satisfies the comfort standard generally does not exceed 50:1, and the maximum ratio does not exceed 100:1.[11] To cover a variety of luminance distribution possibilities in lighting design, within the luminance ratio range limited by visual comfort, the working conditions were set as the following three categories: actual scene, simulated scenes, and experimental scenes, as shown in Figure 1. The actual scene was in a shopping mall, which represents a typical high-illuminance and high-luminance lighting environment. For the simulated scenes, DIALux evo was used to simulate various possible lighting conditions in conventional office spaces. The experimental scenes were characterised by working surface lighting.

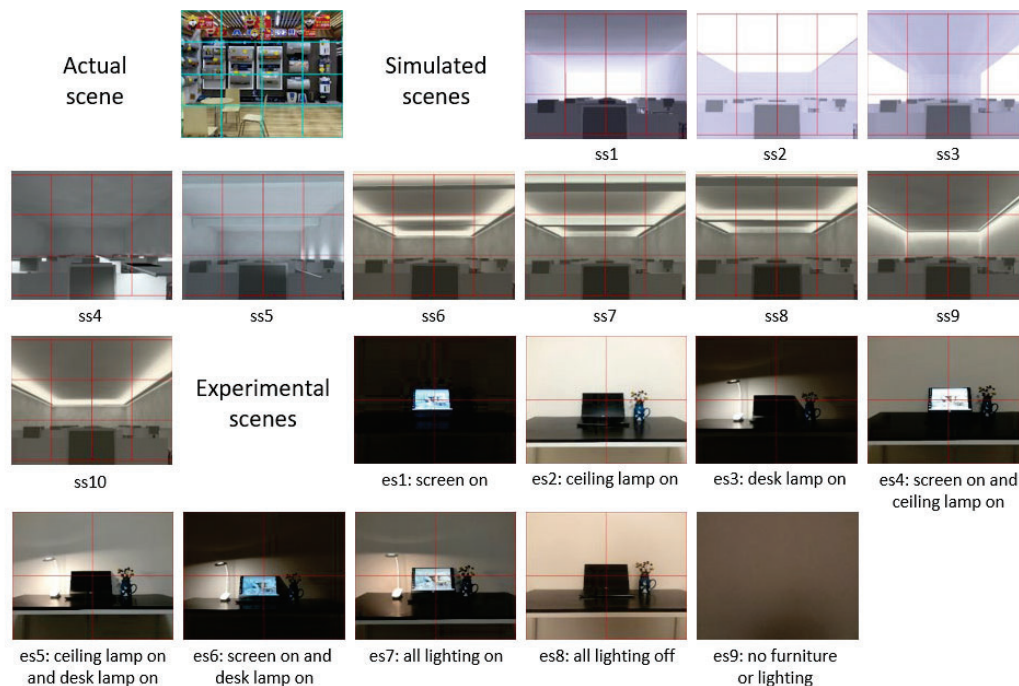


Figure 1. Images, names, and grid divisions of 20 working conditions.

### 2.2.2 Analysis procedure

To determine  $f_{exp}(S)$ , the following steps were applied in the 20 working conditions.

(1) Image acquisition. Photos of real spaces or rendered images of digital models were taken, and the field of view was extracted according to the measurement requirement of *Feu*. iPhone 7 Plus was used in this study in real spaces.

(2) Grayscale sampling. A uniform rectangular grid was overlaid on the image via Photoshop, and the intersection points of the grid were recorded as measurement points. For actual scenes, the dimension of grid was  $4 \times 4$ , the simulated scenes were  $3 \times 4$ , and the experimental scenes were  $2 \times 2$ , according to the actual areas of the fields of view (Figure 1). The straw tool ( $11 \times 11$  average) in Photoshop was used to absorb the RGB value of the measurement points, after which

the grayscale  $D$  of each point was calculated by the conversion algorithm recommended by the BT.601 standard[12] ( $Grayscale = R \times 0.299 + G \times 0.587 + B \times 0.114$ ).

(3) Luminance sampling. A handheld luminance meter (Konica Minolta LS-100 in this study) was used to measure the luminance,  $L$ , of each measurement point in real space. The luminance values at the positions of the measurement points in DIALux evo were also read.

(4) Model fitting. To determine the value function  $f_{exp}(S)$ , Equation (3) was fitted under  $N = 1$  to 15 in 20 working conditions. Then, the variations of the errors of  $Feu$  and  $L_{av}$  with  $N$  for each scene were analysed.

The fitting was conducted by the *scipy* Python module. When  $N > 1$ , the function should be fitted by *scipy.optimize.curve\_fit*, and the *bounds* parameter is as described in Equation (4):

$$\begin{cases} 0 < a_0 \leq L_{\min} \\ 0 \leq a_1 \leq L_{\max} / D_{\arg \max(L)} \\ 0 \leq a_2 \leq \sqrt[N]{L_{\max}} / D_{\arg \max(L)} \end{cases} \quad (4)$$

where  $L_{\min}$  is the lowest value of  $L$ ,  $L_{\max}$  is the highest value of  $L$ , and  $D_{\arg \max(L)}$  is the grayscale value of the measurement point corresponding to  $L_{\max}$ .

When  $N = 1$ , the function should be fitted by *scipy.optimize.leastsq*, and the residual function should be set as the relative error.

The errors of  $Feu$  and  $L_{av}$  were analysed separately to determine the accuracy and feasibility of the polynomial function when fitting was completed. The value function of  $N_{allow}$  was obtained via the analysis of the relationship between the grayscale-luminance distributions in  $S$  and  $N_{allow}$ .

### 2.3 Feasibility validation of the polynomial function

To test whether this model satisfies the need for the accurate calculation of  $Feu$  and  $L_{av}$ , a test scene with a relatively severe luminance distribution gradient was constructed based on an experimental scene.

The test scene included a working condition in which only the desk lamp was turned on (the maximum value of  $C$  in the experimental scene). An 8×8 grid was arranged, and the luminance distribution of the 81 grid intersections is presented in Figure 2. After excluding the point with luminance greater than 1000 cd/m<sup>2</sup> (the origin), the reference values of  $Feu$  and  $L_{av}$  were measured from the luminance values of the remaining 80 grid intersections, which were considered as the true values in the test scene.

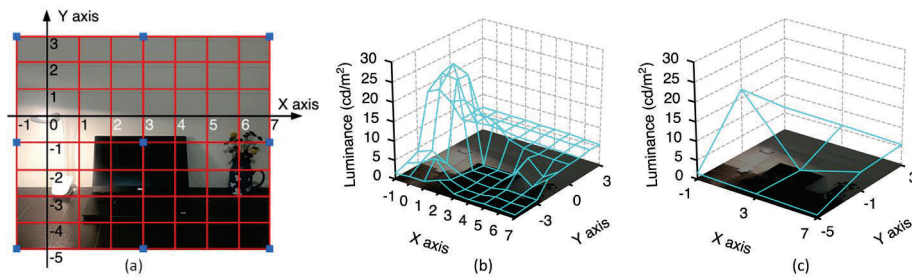


Figure 2. (a) Field of view, 8×8 grid (red lines), and measurement points (blue squares) for fitting, (b) luminance distribution at grid intersections after excluding luminance >1000 cd/m<sup>2</sup>, and (c) luminance distribution of 9 points for fitting of test scene.

The  $\{L, D\}$  values of 2×2 grid intersections (marked by blue squares in Figure 2) were fitted in Python to find the values of  $N_{allow}$ ,  $a_0$ ,  $a_1$ ,  $a_2$ , and the polynomial function. Then  $Feu$  and  $L_{av}$  values were measured by the grayscale values of the 80 intersections (luminance >1000 cd/m<sup>2</sup> excluded) and the polynomial function, which is referred to as the fitted value. The relative error between the fitted value and the reference value was used to verify the feasibility of the polynomial function (the exponential function in Equation (2) was used for parallel comparison).

The  $L_{\max}$  value of the measurement points used for fitting was 17.33 cd/m<sup>2</sup>, the  $L_{\min}$  value was 0.48 cd/m<sup>2</sup>,  $C$  was 36.03,  $L_{av}$  was 4.92 cd/m<sup>2</sup>, and  $R$  was 0.9514.

### 3. RESULTS

#### 3.1 Changing rules and Influencing factors of $N_{allow}$

Fifteen polynomial functions ( $N = 1$  to  $15$ ) were fitted for each working condition. Eighteen working conditions were fitted finally, except for ss1 and es4. The inspection of the data revealed that the edge measurement point of the former and the central measurement point of the latter were placed at a boundary between light and shade, resulting in high errors of luminance and grayscale, as well as the failure of polynomial function fitting. For further analysis, the  $N$  when  $Feu$  reaches the minimum error is defined as  $N_{Feu}$ , and the  $N$  when  $L_{av}$  reaches the minimum error is defined as  $N_{Lav}$ . The minimum errors of  $Feu$  and  $L_{av}$  are respectively defined as  $e_{Feu}$  and  $e_{Lav}$ .

The  $R$  for 18 working conditions was  $\geq 0.7940$ . When the polynomial function was determined by  $N = N_{Feu}$ , the  $e_{Feu}$  was between 0.01% and 2.08%. when the polynomial function was determined by  $N_{Lav}$ , the  $e_{Lav}$  was between 0.00% and 1.14%, and the error of 67% of the working conditions was less than 0.01%.

Figure 3 exhibits the relationships among  $N_{Feu}$ ,  $N_{Lav}$ , and  $N_{allow}$  in the 18 working conditions. There were 6 cases each where  $N_{Feu}$  was greater than, less than, or equal to  $N_{Lav}$ . Although an optimal  $N$  existed, an  $N$  satisfying the minimum errors of both  $Feu$  and  $L_{av}$  could not be found. This demonstrates why  $N_{allow}$  is needed to maintain the errors of  $Feu$  and  $L_{av}$  within an acceptable range. In 12 cases, the value of  $N_{allow}$  was between those of  $N_{Feu}$  and  $N_{Lav}$ , and in 6 cases, the value of  $N_{allow}$  was lower than those of  $N_{Feu}$  and  $N_{Lav}$ . Except for ss8 and es9,  $N_{allow}$  exhibited a similar change pattern as  $N_{Feu}$  and  $N_{Lav}$ , indicating that the uniform fitting of  $Feu$  and  $L_{av}$  with  $N_{allow}$  can achieve high accuracy.

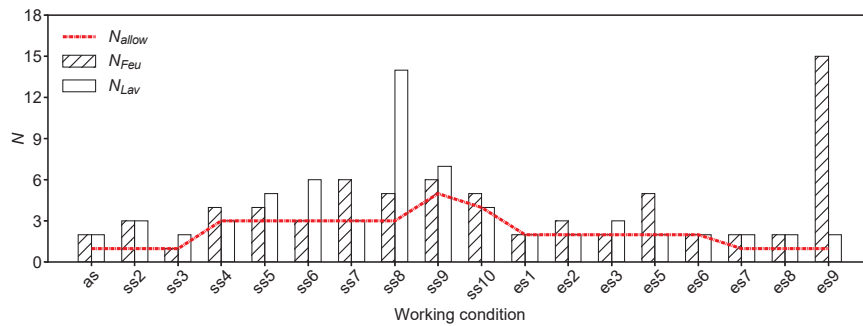


Figure 3. The values of  $N_{Feu}$ ,  $N_{Lav}$ , and  $N_{allow}$  in the 18 working conditions.

Table 1 reports the relationships between  $N_{allow}$ ,  $N_{Feu}$ ,  $N_{Lav}$ ,  $e_{Feu}$ , and the distribution indicators of  $S = \{L, D\}$ , including  $L_{max}$ ,  $C$ , and  $R$ . Because it was unknown whether  $N_{allow}$  has a linear or nonlinear relationship with other parameters, both Spearman and Pearson correlation analyses were conducted.

Table 1. The correlation analysis results of  $N$ , errors, and the distribution indicators of  $S = \{L, D\}$ . Only statistically significant coefficients are reported.

		Spearman analysis				Pearson analysis			
		$N_{allow}$	$e_{Feu}$	$N_{Feu}$	$N_{Lav}$	$N_{allow}$	$e_{Feu}$	$N_{Feu}$	$N_{Lav}$
$L_{max}$	Correlation	.563*	-	-	.774**	.562*	-	-	.563*
	Sig. (2-tailed)	0.015	-	-	0.000	0.015	-	-	0.015
$C$	Correlation	.826**	.724**	-	.722**	.864**	.697**	-	.617**
	Sig. (2-tailed)	0.000	0.001	-	0.001	0.000	0.001	-	0.006
$R$	Correlation	-.650**	-	-.713**	-.572*	-.789**	-	-	-
	Sig. (2-tailed)	0.003	-	0.001	0.013	0.000	-	-	-

The Pearson analysis results reveal the following:

- $N_{allow}$  was significantly related to  $L_{max}$ ,  $C$ , and  $R$ ;
- $e_{Feu}$  was significantly related to  $C$ ;
- $N_{Lav}$  was significantly related to  $L_{max}$  and  $C$ .

In addition, the Spearman analysis results demonstrated that  $N_{Feu}$  and  $N_{Lav}$  were significantly related to  $R$ .



### 3.2 Piecewise function of $N_{allow}$

The correlation analysis results revealed that  $N_{allow}$  had the strongest relationships with  $C$  and  $R$ . Therefore, the  $N_{allow}$  value function was obtained by multiple linear regression in SPSS:

$$N_{allow} = 8.632 + 0.03 \times C - 7.916 \times R \quad (5)$$

where  $C$  is the luminance ratio and  $R$  is the linear correlation of  $\{L, D\}$ .

Because  $R$  is always less than 1, and because the range of  $R$  in this paper is 0.8 to 1.0, Equation (5) can be simplified as Equation (6):

$$N_{allow} = 0.03 \times C + b \quad (6)$$

where  $b$  is a constant in the range of 0.716 to 2.299.

$N_{allow}$  is defined as an integer, so it is necessary to modify the linear function to a piecewise function. Considering that there was no case in which  $N_{allow}$  was higher than  $N_{Feu}$  and  $N_{Lav}$ , the increase of  $N_{allow}$  by 1 or 2 can still satisfy the errors of both  $Feu$  and  $L_{av}$  being maintained as less than 10%. Therefore, a piecewise function was produced by drawing an envelope curve on the  $N_{allow}$ - $C$  figure.

Based on the minimum difference between the piecewise function and the actual  $N_{allow}$ , multiple envelope lines were compared and selected within the range of  $b=0.716$  to  $b=2.299$ . Then the envelope curve produced by the actual  $N_{allow}$  value was determined as the piecewise function, as shown in Figure 4. After the exclusion of measurement points with luminance  $>1000$   $\text{cd/m}^2$ , the luminance ratio in the scene was generally  $<100$ . Therefore, the independent variable range of the piecewise function was set to 1 to 100. However, due to the limit of the experimental conditions, there was only one case in which  $C$  was in the range of 60 to 100 ( $C = 87.1$ ). When  $C$  was in the interval  $(87.1-100]$ ,  $N_{allow}$  was temporarily estimated to be 5. Moreover, the piecewise function for the case in which  $C > 87.1$  requires determination in further research.

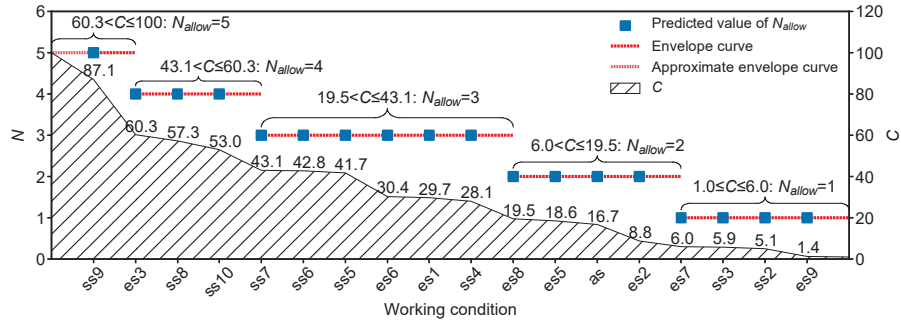


Figure 4. The piecewise function of  $N_{allow}$  and  $C$ .

### 3.3 Feasibility of the polynomial function

The luminance ratio of the test scene was  $C = 36.0$ , so the value of  $N_{allow}$  was 3 according to Figure 4. The polynomial function was then fitted by Equation (3), and the result was as follows in Equation (7):

$$L = 0.1233 + 0.3044 \times D + (0.009974 \times D)^3 \quad (7)$$

Moreover, the exponential function fitted by Equation (2) was as follows in Equation (8):

$$L = 0.6097 \times 1.017^D \quad (8)$$

According to the grayscale  $D$  of the 80 grid intersections,  $Feu$  and  $L_{av}$  were respectively measured by Equations (7) and (8), and the results were as follows:

- The reference values were  $Feu = 3.54$  and  $L_{av} = 5.50$ ;
- The values measured by Equation (7) were  $Feu = 3.58$  and  $L_{av} = 5.49$ ;
- The values measured by Equation (8) were  $Feu = 3.49$  and  $L_{av} = 6.12$ ;

Furthermore, the error of  $L_{av} = 0.2\%$  (polynomial function)  $< 10\%$  (acceptable error)  $< 11.3\%$  (exponential function); the error of  $Feu = 1.1\%$  (polynomial function)  $< 1.4\%$  (exponential function)  $< 10\%$  (acceptable error).

In summary, when the luminance ratio is less than 100 and high-luminance light sources above 1000 cd/m<sup>2</sup> are excluded, the grayscale-luminance polynomial function fitted by 9 measurement points can produce values of  $F_{eu}$  and  $L_{av}$  whose errors are within 10%, which meets the requirements for engineering application. Compared with the error of the exponential function, the error of  $F_{eu}$  determined by the polynomial function was roughly the same, while the error of  $L_{av}$  was significantly lower.

## 4. DISCUSSION

### 4.1 Accuracy of the fitting method

In this paper, 9, 20, or 25 points were used for fitting. The increase in the number of measurement points may have the following two effects on the fitting: the coverage of the luminance range becomes more comprehensive, which can reduce the error; moreover, the possibility of over-fitting increases, which may reduce the predictive ability of the function and increase the error. For the polynomial function,  $L_{av}$  error may decrease and  $F_{eu}$  error may increase when more points are sampled. As a result, considering both convenience and accuracy, the calibration of nine measurement points is the best choice, and setting the dynamic residual function according to the luminance distribution may be an effective way to further improve the accuracy of the polynomial function.

### 4.2 Error sources and correction methods of calibration

The design of the calibration process avoids errors as much as possible, including effects of aperture and shutter, the vignetting effect, noise and misalignment mentioned by Wüller *et al.*[13]. However, there remain two working conditions whose data cannot support function fitting. For es4, the luminance at the centre of the grid was found to be abnormally high. For ss1, the location of the abnormal measurement point is not illuminated and is rendered as a black line. The problems of ss1 and es4 indicate that to increase the fitting accuracy, when overlaying a grid on a scene image, the intersection point should be located at a position where the luminance changes gently.

### 4.3 Directions to improve this research

This study provided a new method for the evaluation of  $F_{eu}$  and  $L_{av}$ , which was validated in a narrow luminance range (luminance ratio < 100 and luminance < 1000 cd/m<sup>2</sup>). This range well covers the dynamic range of conventional indoor artificial lighting (50:1) which ensures visual comfort, and is also applicable to the upper ratio (100:1). However, it remains necessary to explore methods by which to expand the application scope from the aspects of luminance and the luminance ratio to meet the new trend of diversified luminance distributions in lighting design. Specifically, it will be necessary to include surface light sources with luminance >1000 cd/m<sup>2</sup> in the brightness perception evaluation. Currently,  $N_{allow}$  is estimated as 5 when the luminance ratio is in the interval [87.1, 100]. In future research, more grayscale-luminance data within this range will be supplemented to complete the value function of  $N_{allow}$ .

The calibration of HDR images is a way to expand the proposed method to more highly dynamic scenes with mixed artificial lighting and daylighting. Though HDR is considered a convenient and accurate technology, there remains a debate about the feasibility of using mobile devices to capture HDR images[14]. In addition, Newsham *et al.*[15] proposed that in common low-dynamic lighting spaces, the realism of HDR is not stronger than that of traditional images. To determine the best technology, the advantages and disadvantages in terms of the accuracy, convenience, and image realism will be compared between HDR captured by a mobile device and traditional image captured by the proposed method.

## 5. CONCLUSION

This paper proposed a grayscale-luminance polynomial function model and method for the production of  $F_{eu}$  and  $L_{av}$  values from digital images. The polynomial function is applicable to lighting scenes with a luminance ratio of less than 100 and a luminance of light sources of less than 1000 cd/m<sup>2</sup>, and maintains the errors within 10%. The key parameter  $N_{allow}$  of the function is significantly related to the luminance ratio and linear correlation. The results of the test scene revealed that the use of nine measurement points can produce an accurate grayscale-luminance

function, the *Feu* error of which is equivalent to that of the exponential function, and the  $L_{av}$  error of which is less than that of the exponential function.

The proposed method uses the grayscale and luminance data of measurement points obtained from a captured or simulated image of a lighting environment to measure or calculate *Feu* and  $L_{av}$ , which does not require prior calibration and reduces the need for professional equipment. This simplifies the operation, and can yield images that are suitable for both the evaluation of the luminance distribution and the user's preference.

In future research, brightness perception evaluation will be expanded to luminance over 1000 cd/m<sup>2</sup>. The piecewise function at the luminance ratio range of 60 to 100 has yet to be completed. And the proposed method will be compared with an HDR luminance map.

## REFERENCES

- [1] von Castell C, Hecht H, Oberfeld D. Bright paint makes interior-space surfaces appear farther away. PLOS ONE, 2018,13(9): e201976.
- [2] Tai N, Inanici M. Space perception and luminance contrast: investigation and design applications through perceptually based computer simulations. In: Proceedings of the 2010 Spring Simulation Multiconference, Orlando, Florida, USA, 11-15 April. 2010: 73-80.
- [3] Iwai W, Iguchi M. New lighting evaluation techniques for comfortable lighting spaces using sensation-of-room-brightness index "Feu". Matsushita technical journal, 2008, 53(2): 132-134.
- [4] Iwai W. Development of Space Brightness Index "Feu" and Application to Lighting Design, Journal of the Illuminating Engineering Institute of Japan, 2009,93(12): 907-912.
- [5] Iguchi M, Iwai W. Method for defining the brightness sensory index of the lighting space, and the method for designing indoor lighting using it: P2007-171055A. Japan, 2007.
- [6] Chuang J. Study on Tunnel Luminance Detection System Based on Image Processing. Xi'an University of Architecture and Technology, 2012.
- [7] Moore T. Approximate field measurement of surface luminance using a digital camera. Lighting Research & Technology, 2000,32(1): 1-11.
- [8] Gu B, Zhan Q, Zhu Z, Research on Measurement of Luminance Distribution Using a Digital Cameras. China Illuminating Engineering Journal, 2003,14(01): 15-18.
- [9] Bellia L, Cesarano A, Minichiello F, Sibilio S. Setting up a CCD photometer for lighting research and design. Building and Environment, 2002,37(11): 1099-1106.
- [10] Chen Z, Weng J, Hu Y, Zhang Q, Huang K, Zhang S, Liu Y. A Study on Measurement of Luminance Distribution by Using a Digital Camera. China Illuminating Engineering Journal, 2005,16(03): 11-14.
- [11] Linney A S. Maximum Luminances and Luminance Ratios and their Impact on Users' Discomfort Glare Perception and Productivity in Daylit Offices. Victoria University of Wellington, 2008.
- [12] ITU-R. BT.601-7 Studio encoding parameters of digital television for standard 4:3 and wide-screen 16:9 aspect ratios. Geneva, Switzerland: International Telecommunication Union, 2011.
- [13] Wüller D, Gabele H. The usage of digital cameras as luminance meters. In: Proceedings of SPIE - The International Society for Optical Engineering 6502, San Jose, California, USA, 2007, p. 65020U.
- [14] Pierson C, Cauwerts C, Bodart M, Wienold J. Tutorial: Luminance Maps for Daylighting Studies from High Dynamic Range Photography, Leukos, 2021,17(2): 140-169.
- [15] Newsham G R, Cetegen D, Veitch J A, Whitehead L. Comparing lighting quality evaluations of real scenes with those from high dynamic range and conventional images, ACM Transactions on Applied Perception, 2010,7(2): 1-26.

## ACKNOWLEDGEMENTS

Funding: This work was supported by the National Natural Science Foundation of China (No. 52278120).

Corresponding Author Name: Aiyang Wang

Affiliation: School of Architecture, Tianjin University

e-mail: [wayway@tju.edu.cn](mailto:wayway@tju.edu.cn)

# **STUDY ON THE IMPROVEMENT STRATEGY OF PEDESTRIAN SPACE LIGHT ENVIRONMENT IN THE OLD MOUNTAIN COMMUNITY: A CASE STUDY OF CHONGQING WHITE ELEPHANT COMMUNITY**

Yulin Shi

(School of Architecture and Urban Planning, Chongqing University, China)

## **ABSTRACT**

China's urban development has entered the stock era. The old urban communities with mountain characteristics carry the history and context of the city to a certain extent. The walking space in the mountain communities is the representative of the mountain characteristics, and the improvement of the light environment of the community walking space is an important part of the community renewal. It is becoming a way to express the value of urban heritage to realize vitality regeneration on the basis of respecting urban heritage.

This paper takes the White Elephant community in Chongqing as the research object, conducts a survey on the current situation of the community walking space light environment, analyzes and compares the survey results, combines the characteristic features of the walking space in the mountain community, proposes the improvement path from the aspects of functionality and landscape according to local conditions, and improves the environmental quality of the walking space in the mountain community by means of community micro-renewal. Protect mountain features and features.

Keywords: mountain community, White Elephant community in Chongqing, light environment, pedestrian space, investigation and study

## **1. INTRODUCTION**

A large number of residential areas built in China at the end of the last century have become more and more unsuitable for the development of the current society, often showing the characteristics of disorderly spatial organization, fragmented distribution and low quality of space environment. Mountain community refers to the community which is obviously different from the flat land in topography and geomorphic structure and has significant mountain characteristics. The research object of this paper is the mountain community in the narrow sense, that is, the physical form of living space built on the high and low terrain, and the residential buildings and their environment centered on living in the mountain environment. The community walking space consists of roads and nodes in the community, including walking paths, intersections and connected public Spaces. With the city entering a new period of inventory development, the renewal and transformation of old communities has gradually become the core focus of promoting urban renewal. There are many walking stairs in mountainous communities in Chongqing, and the elderly account for the majority of residents in such communities. The lighting system of the stairway space cannot meet the needs of elderly people for night travel. This paper focuses on the organic renewal of the light environment of the walking space in the old mountain community, and explores the organic renewal strategy of the walking light environment in the mountain community, so as to ensure social equity and achieve sustainable development.

## **2. ANALYSIS OF CONCEPTS OF OLD COMMUNITY AND LIGHT ENVIRONMENT**

### **2.1 Old community**

The old community is one of the types of urban communities, and its main characteristics are as follows [1] : First, the community lacks property management, poor environmental health, and insufficient maintenance of infrastructure; Second, the construction time was earlier, most of them were built before 2000; Third, most communities are distributed in the

old city and the central area of the city, which are difficult to rebuild due to the cost of demolition. Fourth, the resident population structure is small, the composition of personnel is complex, and the proportion of elderly groups and vulnerable groups is large. To sum up, the old community defined in this paper mainly refers to the residential community built before 2000 and still inhabited by a large number of people. The supporting facilities, construction standards and use functions enjoyed by public services are different from those enjoyed by high-end closed communities, and it is difficult to travel at night and meet people's needs for security and happiness [2].

## **2.2 Stairway light environment**

Generalized stairway includes the stairway system, which includes the ground platform and connecting roads, and the special regional space from the lowest point to the highest point of the stairway [3]. The stairway defined in this paper is mainly a continuous linear spatial form with topographic elevation difference and its surrounding interface. Light environment generally refers to the system environment established by the horizontal and vertical distribution of light and the color temperature and color rendering index of light, and its purpose is to meet the physical, visual, psychological, aesthetic and other requirements [4]. According to the type of light source, they can be divided into artificial light environment and natural light environment [5], indoor light environment and outdoor light environment according to space, and daytime light environment and night light environment according to time [6].

## **3. LIGHTING NEEDS OF PEDESTRIAN SPACE IN MOUNTAINOUS COMMUNITIES**

### **3.1 Problems**

There are still two major problems in the renovation process of lighting facilities in old communities in Chongqing: First, the mountain environment in Chongqing leads to a large number of stairway Spaces in the walking system, and its high risk increases the difficulty and requirements of night lighting design, but it has not received enough attention at present; Second, the renovation funds mainly come from government grants and subsidies, and limited funds are mostly used for elevator installation and building structure maintenance, etc., leaving limited funds for outdoor lighting. Therefore, the light environment of the pedestrian space in the old community to achieve low-cost, high-quality lighting facilities update is the only way.

### **3.2 Characteristics of community residents and demand of light environment**

The research object of this paper is the mountain community residents with differentiation and particularity, most of whom are elderly groups, so the needs can be divided into four aspects: psychological characteristics, psychological needs, physiological characteristics and physiological needs. In Chongqing, the population aged 60 and above is 701.4 million, accounting for 21.87%. And Chongqing is a mountainous city. In the core area of the city, there are a large number of old communities connected by stairs. The degree of aging in these communities is particularly high, and the elderly fall accidents caused by stairs are frequent. These old residential areas dominated by the elderly have varying degrees of deficiency in the lighting of stairways. In recent years, the renewal of pedestrian space in old communities is relatively small, and there is still a lot of room for improvement.

## **4. FIELD INVESTIGATION**

### **4.1 Current situation of white elephant community**

white elephant community is located in the southeast of Yuzhong Peninsula, Chongqing, China. It faces the main city of Yuzhong on the north side, across the Yangtze River Binjiang Road on the south side, and faces the Yangtze River on the southwest side. On the northeast side is Huguang Guild Hall historical complex, among which there is Wanglongmen cable car site, next to the current Yangtze River ropeway is still in operation. Looking around, there are Jiefangbei business district, Huguang Guild Hall, East water Gate Bridge, mountain city style can be seen here. It was designed and built in the 1990s by teachers Zhang Congzheng, Sun Zhijing and Zeng Fanxiang from the Department of Architecture of Chongqing University [7].



The whole site is roughly trapezoidal, adjacent to the ruins of Longmen cable Drive to the northeast and Yangtze River Binjiang Road to the southeast. There are 6 buildings in the community, which are built on the height difference between south and north, which is a typical residential building form in the mountains, and has the characteristics of Chongqing mountains.

There are six main buildings inside the White Elephant Residence, including two tower residences, the White Elephant Hotel on the northwest side, the L-shaped retreat high-rise residence on the south side, and a three-story parking building inside, and the traffic loop is set up around the building inside, making the interior space rich. Among them, the two groups of tower residences on the north side are the most characteristic buildings of the White elephant House. The buildings are point-type unit residential buildings, the color is mainly white, and the facade is Mosaic veneer. The two groups of buildings are connected by a corridor. In addition, the southernmost side is No. 4 commercial residential complex. The building is built along the Yangtze River, and the roof forms layers of receding platforms from south to north, with the highest being 12 layers and the lowest part 4 layers, forming a unique landscape, making the internal sight of the community transparent and open, creating a unique river view surface, and greatly improving the internal sight comfort of the community. The northwest side is the White Elephant Hotel facing the street, and the center of the community is a three-story parking building with split-level layout inside. The overall architectural style is unique, and the architectural groups are scattered.



Figure 1. Current situation of white elephant community

## 4.2 Walking system

The height difference inside the White elephant House site reaches 38m at the highest point, and the designer has made a clever pedestrian traffic system design according to the terrain. First of all, a ring road is set up inside the site, which not only solves the internal fire problem, but also strengthens the connection between Baixiang Street and the residential community. In addition, an entrance and exit is set on the ring road to enter the inner tower on the north side, so that the tower with 24 floors has three external entrances and exits, which greatly facilitates the daily traffic of residential buildings. The southern entrance is located on the side of Changbin Road. Secondly, the central entrance is connected with the added inner ring road, and the northernmost entrance is connected with White Elephant Street. In the absence of an elevator, vertical traffic is also more convenient. In terms of horizontal traffic, the designer boldly set up a "public transport level" connecting the two towers on the north side, and set up an aerial corridor between the two buildings to connect, which can be regarded as a model of pedestrian system design, which is still highly praised today.

By analyzing the transportation system of the residential community, it can be found that the east-west transportation is relatively convenient, the north-south and vertical transportation is not convenient, the north-south traffic relationship of the site is separated, and the connection with the Yangtze River Binjiang Road and Binjiang Walk is poor. The existing north-south corridor only has the mountain trail on the southwest side of the building complex and the site entrance on the northeast side, which is not convenient to travel and has poor accessibility and insufficient barrier-free facilities. Lack of lighting facilities, poor night lighting quality.



Figure 2. Walking system of white elephant community

### 4.3 Research content

There are more than 10 mountain walking stairs in the White Elephant residence, and 8 representative stairs are selected for measurement based on factors such as ladder level, enclosed form, distribution position, human flow and lighting status. The lighting form in the community is mainly street lamp pole lighting, light source is mainly LED, and a small part is fluorescent lamp or high-pressure sodium lamp, which is relatively simple. Night lighting is seriously insufficient, some of the main stairways have not done special night lighting, only rely on the surrounding residential interior or peripheral street lights to provide astigmatism, the night travel of residents can not be guaranteed, need to use flashlights or mobile phones to fill the light, the elderly even need to use the toes to explore the stairways, most of the stairways are double-sided enclosing form, the width is different, most of the stairways in the later added stainless steel handrails. Opens up possibilities for new forms of lighting. Lighting facilities in the community are insufficient and unevenly distributed, and some stairways lack nighttime lighting. Through the measurement of the nighttime light environment of the important steps in the community, it is found that the average illuminance of the tread is 2.28 ~ 3.93 lx, the average illuminance of the kicking surface is 1.01 ~ 3.78 lx, and the uniformity is 0.1 ~ 0.9. Referring to the research conclusion of the indoor staircase, its lighting status is far from meeting the requirements.

Table 1. Typical lighting data of white elephant community

ID	Tread average illuminance/lx	Tread illuminance uniformity	The average illumination of the kick surface	Evenness of kick surface illumination	Kicker tread illuminance ratio	Temperature/K	Color renderin index
1	3.53	0.8	3.73	0.88	1.02	4086	97
2	2.26	0.6	1.03	0.42	0.47	4869	96
3	3.89	0.5	3.41	0.4	0.88	6752	77
4	2.67	0.3	3.69	0.9	1.37	5716	89
5	2.73	0.2	2.75	0.4	1.01	5529	88
6	2.85	0.3	1.22	0.5	0.41	4897	97
7	3.51	0.9	3.61	0.7	1.01	5117	96
8	2.29	0.4	2.13	0.8	0.89	5123	93

## 5. RECONSTRUCTION STRATEGY

### 5.1 Security

The optimal lighting design of pedestrian space in mountain communities should first meet the functional requirements of safe passage of people at night

Especially in older communities where such elderly people predominate. Combined with the existing safety standards, the tread illuminance value is about 40lx [8]. The recommended illumination value of the kicking surface is about 1/2 of the tread, which should not be greater than 20 lx. It is more appropriate for the shadow ratio of the stairway tread to be between 0.25 and 0.5. At the same time, the sharpness, evenness and glare satisfaction should also be taken into consideration based on the survey results of the residential area. At the upper and lower ends of the stairway, functional street lighting is added as the basis to achieve the recommended illumination value. On the right side, a light art installation with functional lighting, human-lamp interaction, and portable lifting functions of heavy objects is set. Through pressure sensing, the lower front steps are illuminated downward to achieve clarity requirements. If only the vertical pole lighting is used, the uniformity is poor, so the handrail lighting is set on the left side of the stairway to improve the uniformity; In order to avoid glare, the three lighting methods strictly control the lamp shading Angle.

## 5.2 Economy

Nightscape lighting should consider economy, and stairway lighting should avoid excessive energy consumption on the basis of meeting functionality. It is suggested to carry out graded control of weekday mode, weekend mode and major festival mode in individual sections that need to increase energy consumption to create landscape effect, so as to achieve sustainable development.

## 5.3 Aesthetic

The lighting strategy of both functionality and artistry is adopted in the ladder section, and the handrail lighting is set on the left side. The light gradually increases and then goes out as people walk by, which has the aesthetic feeling of "breathing". On the right side, there is a light art installation with functional lighting, human light interaction, and heavy objects portable lifting function. At certain times, such as weekends and holidays, three LED monochrome lights are turned on to form a rich light and shadow effect on the wall with passers-by.

## 3. CONCLUSION

With the development of town has entered the stage of strategic adjustment to improve the quality, the state has successively issued a number of important documents on old city transformation and urban renewal in recent years, paying more attention to the connotation of urban development. Urban lighting plays a unique role in the creation of urban vitality in the physical space environment of the city at night. In addition to the radical renewal method of large-scale demolition of shanty towns, urban renewal should also carry out micro-transformation of communities on the basis of preserving the original urban genes. The existing renewal strategies of old communities mainly focus on infrastructure, public space and other levels, and there are relatively few approaches to landscape lighting as the entry point. Urban public lighting design centering on user behavior pattern from various aspects such as lighting mode, level, quality, adaptability and interactive control is conducive to improving the quality of light environment and community vitality. Stairway lighting is an integral part of urban public space lighting, and the quality of its light environment is related to pedestrian safety, especially in the old communities of mountain cities, where there are many stairways and the proportion of the elderly is large, the importance of the light environment is self-evident. At the same time, as a medium, light can have an impact on the performance and quality of urban space environment at night through the form of public art, or can be used as a micro-transformation of old communities new ideas.

## REFERENCE

- [1] 周俊含.老龄化社会背景下城市老旧小区环境改造设计研究[D].华中科技大学,2019.
- [2] 刘翠.社会工作助推居民参与老旧小区治理[D].南京师范大学,2018.
- [3] 姜建军.山地城市“景观梯道”设计理论与实践研究[D].四川农业大学,2008.

- [4] 袁景玉,张莹.建筑光环境的环境行为学分析[C].,2006.
- [5] 田鲁.光环境设计[M].光环境设计,2006.
- [6] 张越.光环境规划与设计[M].光环境规划与设计,2012.
- [7] 魏皓严,郑曦.生猛的白象居——步行基础设施建筑[J].住区,2017(02):28-39.
- [8] Building regulations 2010: Technical Guidance Document : ISBN 978-1-4064-2317-4 [S] .

## **ACKNOWLEDGEMENT**

Corresponding Author: Yulin Shi  
Affiliation: School of Architecture and Urban Planning, Chongqing University  
e-mail : 857359182@qq.com



# INTELLIGENT STREET LIGHTING CONTROL SYSTEM WITH VISIBILITY PREDICTION FUNCTION

Xizhe Li , Nianyu Zou , Zhisheng Wang

(Research Institute of Photonics, Dalian Polytechnic University, Dalian, China)

## ABSTRACT

With the rapid development of technology and the continuous improvement of residents' living standards, the level of intelligence in lighting equipment and systems is becoming increasingly high. In order to improve lighting efficiency and road safety as much as possible, how to use the environment of the road (such as weather) for scientific and effective lighting regulation is a key research content in the current smart lighting industry. Based on the data of Guizhou Meteorological Observatory and pollutant monitoring station from 2020 to 2022, this paper analyzes various factors affecting visibility. Establish a real-time visibility estimation and prediction model using the VMD-DBO-LSTM method. Secondly, the color of streetlights is controlled through the output values of the VMD-DBO-LSTM model, and the effectiveness of the system is verified through experiments.

Keywords: environment , LSTM , streetlights , visibility prediction

## 1. INTRODUCTION

Street lighting is one of the most important aspects of urban life today. In large metropolitan areas with a large number of people living, street lighting systems play a crucial role in ensuring street safety at night. Modern street lighting systems in many cities use gas-discharge lamps or high-pressure sodium lamps. With the advent of low-power ultra-bright LEDs, lighting systems have changed radically. LED lamps have much more efficiency and lower energy consumption (31e60% energy savings) than conventional high-pressure sodium lamps<sup>[1][2]</sup>. However, traditional street lighting systems are less effective. The use of algorithms for automatically changing the brightness of lamps greatly changes the consumption pattern of devices. In Ref. <sup>[3]</sup> authors propose an efficient intelligent controller for smart grid. Presented system shows positive results in distribution and management of energy based on changing environmental conditions. System, proposed in Ref. <sup>[4]</sup>, shows a control unit for street lighting system to optimize energy consumption. Authors in paper <sup>[5]</sup> proposed a smart street lighting system with a decision making module. The decision making module takes data from different sensors and uses fuzzy logic and ANN to reduce energy consumption of the overall system. Intelligent remote control system for street lighting considered in Ref. <sup>[6]</sup> presents an intelligent street lighting system with algorithms for adjusting lamp's brightness depending on traffic. It uses artificial neural networks and multi-agent systems to make better adjustment of energy consumption. The use of solar panels leads to the development of a new approach to the control of street lighting systems<sup>[7-10]</sup>. For this purpose, wireless sensor networks based on various technologies are used. The paper<sup>[11] [12]</sup> considers wireless adaptive systems for street lighting with IoT access. The system measures the ambient conditions and vehicle density on the roads. Reduction of power consumption was achieved mainly by controlling the brightness of LED lamps when it's necessary, using sensors. In Ref. <sup>[12][13]</sup> authors showed a street lighting system with geocast routing algorithm based on wireless network.

This article is based on Xi'an meteorological data and uses the VMD-DBO-LSTM method to establish a real-time visibility estimation and prediction model. Secondly, the output values of the VMD-DBO-LSTM model were used to control the color of the street lights, and the effectiveness of the system was verified through experiments.

-----



## 2. METHODS

### 2.1 VMD

VMD is highly adaptive and effective in denoising signals<sup>[14]</sup>. Its adaptability is demonstrated by the fact that VMD can determine the number of intrinsic mode functions (IMFs) based on the characteristics of any given sequence. It also matches the central frequency and bandwidth of each IMF component during the search for the optimal solution and the decomposition process. Therefore, VMD decomposition is suitable for handling non-stationary sequences like visibility time series, effectively reducing the complexity and nonlinearity of the sequences. Ultimately, VMD is chosen to decompose the original sequence into several components with different frequency scales and relatively stationary properties. The algorithm's process is as follows:

Using the Hilbert transform, the analytic signal and one-sided spectrum  $E(t)$  of each decomposed IMF signal at different orders are calculated. It can be represented as follows:

$$E(t) = \delta(t) + \frac{j}{\pi t} \quad (1)$$

Each mode signal is multiplied by an exponential term to adjust the central frequency band. The adjusted central frequency  $\omega$  can be represented as:

$$\omega = \partial_t [E(t)u_k(t)]e^{-j\omega_k t} \quad (2)$$

Calculate the gradient norm of the demodulated signal and estimate the bandwidth  $d$  for each mode signal. It can be represented as:

$$d = \sum_{k=1}^K \|\omega\|_2^2 \quad (3)$$

The obtained central frequencies and bandwidths from the above equations are subject to conditional constraints, namely, they should satisfy the requirement of minimizing the sum of signal bandwidths for each IMF. Therefore, it is necessary to establish a constrained variational model.

$$\begin{cases} \left\{ \sum_{k=1}^K \left\| \partial_t \left[ \left( \delta(t) + \frac{j}{\pi t} \right) u_k(t) e^{-j\omega_k t} \right] \right\|_2^2 \right\}_{\{u_k\}\{\omega_k\}}^{min} \\ s. t. \sum_{k=1}^K u_k = f \end{cases} \quad (4)$$

Here,  $k$  represents the minimum bandwidth set,  $\delta(t)$  is the Dirac function.  $\omega_k$  represents the center frequency of each IMF,  $u_k$  is the  $k$ th IMF, and  $f$  is the original signal.

### 2.2 Dung Beetle Optimizer (DBO)

In nature, the habit of dung beetles is to knead their feces into a ball and use celestial bodies for navigation, causing the ball to roll in a straight line. However, if there were no light sources at all, the path of dung beetles would no longer be straight. And many natural factors (such as rough terrain) can also cause dung beetles to deviate from their original direction. In addition, dung beetles can reorient themselves through dance. Fecal balls can also serve as a growth site for insect eggs. In addition, there is also theft, where some dung beetles compete for food as their own. In the DBO algorithm, the position changes of the dung beetle responsible for rolling the ball are as follows:

$$\begin{cases} x_i(t+1) = x_i(t) + \alpha \times k \times x_i(t-1) + b \times \Delta x \\ \Delta x = |x_i(y) - X^\omega| \end{cases} \quad (5)$$

Among them,  $t$  represents the current iteration number, and  $x_i$  represents the position information of the  $i$ th dung beetle;  $K$  represents a constant, expressed as the deflection coefficient;  $\alpha \in (0,1)$  is a random number;  $A$  is a natural coefficient of -1 or 1;  $X^\omega$  It is the worst-case global position.

When encountering obstacles, dung beetles will dance and reposition, updating their position as follows:

$$x_i(t+1) = x_i(t) + \tan(\theta)|x_i(t) - x_i(t-1)| \quad (6)$$

In addition, we need to establish the optimal foraging area to guide young dung beetles to forage and simulate their foraging behavior. The optimal foraging area is defined as follows:

$$\begin{cases} Lb^b = \max(X^b \times (1 - R), Lb^b) \\ Ub^b = \min(X^b \times (1 + R), Ub^b) \end{cases} \quad (7)$$

is the global optimal position. As a result, the position of the small dung beetle has been updated as follows:

$$x_i(t+1) = x_i(t) + C_1 \times (x_i(t) - Lb^b) + C_2 \times (x_i(t) - Ub^b) \quad (8)$$

### 2.3 Long Short-Term Memory Neural Network (LSTM)

Recurrent neural network (RNN) is a neural network for processing sequence data, and long short-term memory neural network (LSTM) is a special kind of RNN, mainly used to solve the gradient disappearance and gradient explosion problems in the long sequence training process. Compared to ordinary RNNs, in longer sequence, LSTM has better performance. On the basis of the original RNN, LSTM adds an additional unit that can save the long-term state in the hidden layer, and the internal structure of the LSTM unit. LSTM and GRU are special RNN architectures used to solve the gradient vanishing problem. GRU can be considered a simplified version LSTM. The performances of GRU and LSTM are indistinguishable in many tasks. The fewer GRU parameters make it easier to converge, but LSTM has better expression performance when the dataset is large. After comprehensive consideration, LSTM is selected as the main algorithm for predicting PM2.5 concentration in this paper. At the top of is a long-term memory C line that runs horizontally to achieve the purpose of sequence learning. Three neural network layers represent three doors.

### 3. CONCLUSION

Due to the regular fluctuations and significant noise in the data, the original visibility sequence is first decomposed using variational mode decomposition (VMD), where the penalty factor and convergence stop condition are used  $\epsilon$  Using the default values of 1000 and  $e^{-7}$ , in order to avoid insufficient or excessive decomposition of the ozone sequence, the K value is determined by observing the center frequency ratio method. Take the K value as 5. The decomposition results are shown in Figure 1.

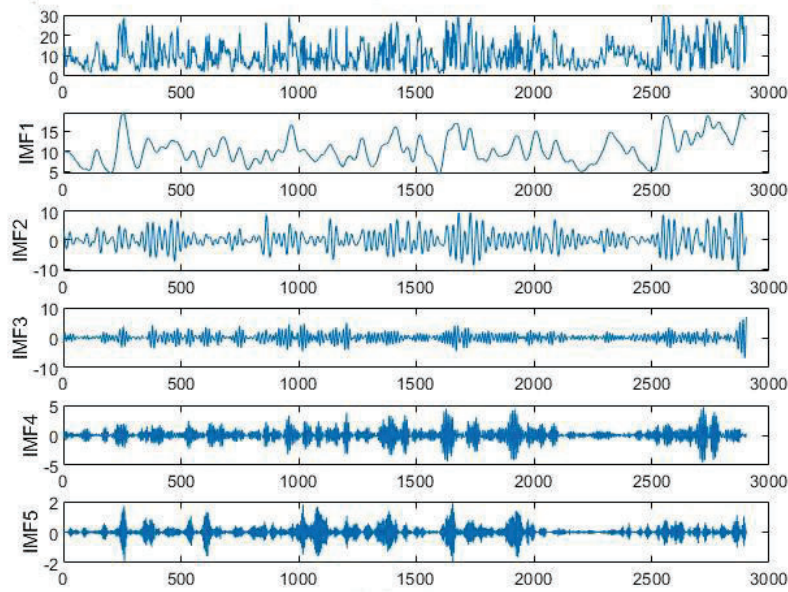


Figure 1 VMD results

In the current visibility model experiment, the VMD-DBO-LSTM model outperforms the VMD-LSTM model and the standalone LSTM model in all three evaluation metrics. The mean absolute error (MAE) for the three models is 0.55, 1.64, and 2.51, respectively. Compared to the highest performing LSTM model, the VMD-DBO-LSTM model has an absolute error increase of 76%. Similarly, the root mean square error (RMSE) for the three models are 0.64, 2.01, and 3.37, respectively. Compared to the LSTM model, the VMD-DBO-LSTM model has an RMSE increase of 81%. The determination coefficients for the VMD-DBO-LSTM model and the LSTM model are 0.98 and 0.64, respectively. The VMD-DBO-LSTM model has a 40% improvement in determination coefficient compared to the LSTM model. As shown in Figure 2, in the experiment of predicting the visibility for the next 5 weeks, the VMD-DBO-LSTM model, VMD-LSTM model, and the standalone LSTM model all outperform each other in various evaluation metrics.

Table 1 The various indicator values of the current visibility model, where 200h and 900h represent 240 hours and 900 hours, respectively

Model	RMSE 240h/900h	MAPE 240h/900h	MAE 240h/900h	R <sup>2</sup> 240h/900h
VMD-DBO-LSTM	0.64/0.79	4.81/4.43	0.55/0.48	0.98/0.98
VMD-LSTM	2.01/2.32	15.13/14.11	1.64/1.52	0.84/0.85
LSTM	3.37/3.69	22.37/24.00	2.51/2.76	0.68/0.70

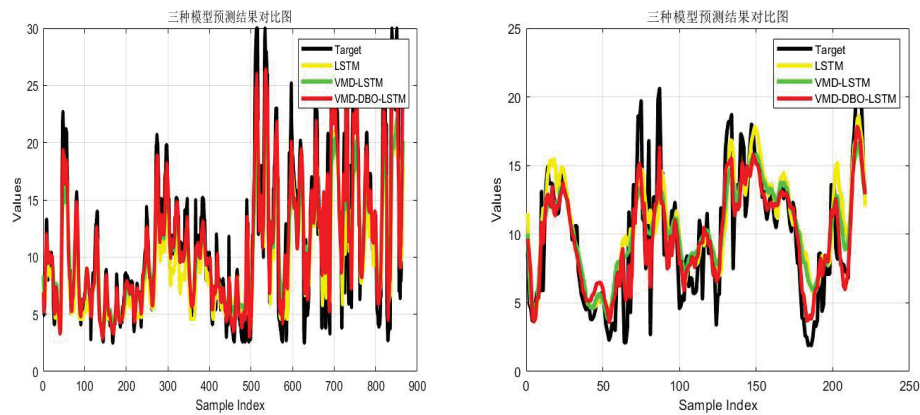


Figure 2 Comparison between predicted and true values of the current visibility model

In order to color through visibility, we store the initial VMD-DBO-LSTM model and combination coefficients in the streetlight centralized controller, use Pycharm software to write the VMD-DBO-LSTM model program, and initialize the weight coefficients to the already trained model. Import data and start updating model parameters. Build a smart street light system platform using PyQt, a third-party software that comes with PyCharm programming software. The interface for implementing self-learning function is shown in Figure 3. The Import Data button represents importing new data into the VMD-DBO-LSTM model. When obtaining the latest month's data from the meteorological station, the data is imported into the model using the Import Data button. Then, the training of the model is started using the Start Training button. After the training is completed, the updated parameters are saved. After the model training is completed, the model parameters are updated and saved, and the model parameters are distributed from the server to the centralized controller.



Figure 3 Functional interface

This system divides the lighting modes of street lights into three types based on the current bead colors, namely white light, yellow light, and yellow white mixed light. Each lighting mode corresponds to different visibility. Due to the lower color temperature of yellow light compared to white light, the corresponding yellow light has stronger penetration than white light. Based on this principle, the lighting modes of street lights can be divided into the following three types. When the visibility is high, i.e. the visibility is at  $VIS > 10\text{km}$ , the street lights will light up with white beads; When the visibility is low, that is, at  $5\text{km} < VIS < 10\text{km}$ , the street lights turn on yellow beads; When the visibility is too low, i.e. the visibility is at  $VIS < 5\text{km}$ , the street lights will light up with white and yellow beads. According to the above analysis, the lighting modes of street lights are shown in Table 2.

Table 2 Street light on mode

VIS	Lighting mode
$VIS > 10$	White

$5 \leq \text{VIS} \leq 10$	yellow
$\text{VIS} < 5$	white yellow

To verify the effectiveness of the model, we simulated different atmospheric environments by changing the temperature, humidity, 2.5 PM, and 10 PM values around the street lamp centralized controller, so that the visibility was within the range of three lighting modes.



Figure 4 Main control street light on mode

From Figure 4, it can be seen that when the visibility is high, the street lights appear in a white light mode. At this time, the white light source of the street lights is brighter, and the lighting effect is the best. When visibility is low, the street lights appear in a yellow light mode. At this time, the yellow light source has better penetration effect and the lighting effect is the best. When visibility is too low, the street lights appear in a mode where both white and yellow beads are lit simultaneously.

## REFERENCE

- [1] Djuretic A, Kostic M. Actual energy savings when replacing high-pressure sodium with LED luminaires in street lighting. *Energy* 2018;157:367-78.
- [2] Beccali M, Bonomolo M, Ciulla G, Galatioto A, Brano VL. Improvement of energy efficiency and quality of street lighting in South Italy as an action of Sustainable Energy Action Plans. The case study of Comiso (RG). *Energy* 2015;92:394e408.
- [3] Kovacs A, Batai R, Csaji BC, Dud as P, Hay B, Pedone G, Revesz T, Vancza J. Intelligent control for energy-positive street lighting. *Energy* 2016;114:40e51.
- [4] Carli R, Dotoli M, Pellegrino R. A decision-making tool for energy efficiency optimization of street lighting. *Comput Oper Res* 2018;96:223e35.
- [5] Mohandas P, Dhanaraj JSA, Gao XZ. Artificial neural network based smart and energy efficient street lighting system: a case study for residential area in Hosur. *Sustain Cities Soc* 2019;48:101499.
- [6] De Paz JF, Bajo J, Rodríguez S, Villarrubia G, Corchado JM. Intelligent system for lighting control in smart cities. *Inf Sci* 2016;372:241e55.
- [7] Kuttybay N, Mekhilef S, Saymbetov A, Nurgaliyev M, Meiirkhanov A, Dosymbetova G, Kopzhan Z. June. An automated intelligent solar tracking control system with adaptive algorithm for different weather conditions. In: 2019 IEEE international conference on automatic control and intelligent systems (I2CACIS). IEEE; 2019. p. 315-9.
- [8] Kuttybay N, Saymbetov A, Mekhilef S, Nurgaliyev M, Tukymbekov D, Dosymbetova G, Meiirkhanov A, Svanbayev Y. Optimized single-Axis schedule solar tracker in different weather conditions. *Energies* 2020;13(19):5226.
- [9] Saymbetov AK, Nurgaliyev MK, Tulkibaiuly Y, Toshmurodov YK, Nalibayev YD, Dosymbetova GB, Kuttybay NB, Gylmzhanova MM, Svanbayev YA. Method for increasing the efficiency of a biaxial solar tracker with exact solar orientation. *Appl Sol Energy* 2018;54(2):126e30.
- [10] Zhang P, Zhou G, Zhu Z, Li W, Cai Z. Numerical study on the properties of an active sun tracker for solar streetlight. *Mechatronics* 2013;23(8):1215e22.
- [11] García-Castellano M, Gonzalez-Romo JM, Gomez-Galan JA, García-Martín JP, Torralba A, Perez-Mira V. ITERL: a wireless adaptive system for efficient road lighting. *Sensors* 2019;19(23):5101.
- [12] Pantoni R, Brand~ao D. A confirmation-based geocast routing algorithm for street lighting



- systems. Comput Electr Eng 2011;37(6):1147e59.
- [13] Sharma V, Parey A. Extraction of weak fault transients using variational mode decomposition for fault diagnosis of gearbox under varying speed[J]. Engineering Failure Analysis, 2020, 107: 104204. (VMD)
- [14] Wang F, Yu L, Wu A. Forecasting the electronic waste quantity with a decomposition-ensemble approach[J]. Waste Management, 2021, 120: 828-838 (VMD)
- 

## ACKNOWLEDGEMENT

Corresponding Author: Nianyu Zou  
Affiliation: Research Institute of Photonics, Dalian Polytechnic University  
e-mail : n\_y\_zou@dlpu.edu.cn

# COMPARATIVE ANALYSIS AND STUDY ON THE EVALUATION OF COLLEGE STUDENTS' MENTAL HEALTH UNDER NATURAL LIGHT AND ARTIFICIAL LIGHT ENVIRONMENT IN UNIVERSITY LIBRARY

Shouyi Wang, Fanpu Meng, Hua Feng

(School of Architecture and Art, Hebei University of Engineering, Handan, China)

## ABSTRACT

As an area for college students to study for a long time, the light environment is the key to affect students' mental health. In this paper through the way of field measurement and subjective evaluation of Hebei university of engineering library reading room natural light, artificial light environment mental health comprehensive evaluation, through weight analysis, multiple index comprehensive evaluation way to determine two kinds of light environment students mental health comprehensive score, and regression analysis, get natural light, artificial light environment best desktop illumination threshold. The study found that the illumination value of natural light environment in the range of 0-3000lx and the mental health evaluation model was  $y = 1.42871 + 0.01612 * x^1 + (-1.73959E-5) * x^2 + (6.99447E-9) * x^3 + (-9.68541E-13) * x^4$ , where y was the comprehensive evaluation score and x was the illumination value of natural light environment, and the optimal illumination threshold was 513.68lx-1101.76lx. The illumination value in artificial light environment in the 0-600lx interval and the mental health evaluation model was  $y = 2.45175 + 0.0148 * x^1 + (-7.07218E-5) * x^2 + (1.90631E-7) * x^3 + (-1.6971E-10) * x^4$ , where y is the comprehensive mental health evaluation score, and x is the desktop illumination value in artificial light environment, and the optimal illumination threshold was 430.56lx-598.65lx. It provides a theoretical basis for the lighting and lighting design of the library reading room in the future.

Key words: reading room luminous environment mental health comprehensive evaluation of multiple indicators

## 1. INTRODUCTION

The 2023 Mental Health Blue Book: Chinese National Health Development Report pointed out that 21.48% of college students are prone to depression, 7.02% of college students have anxiety tendency [1], the mental health of college students should be paid attention to. Light can have an impact on human physical and mental health through visual effects and non-visual effects. On the one hand, through the visual system, inappropriate light environment will affect the visual effect, resulting to visual discomfort, visual fatigue and other [2]. On the other hand, light can influence the circadian rhythm, alertness, cognitive behavior, emotion and others through non-visual channels [3]. Previous studies have found that under the same illumination, the visual efficiency is 5%~20% [4] higher than that under artificial illumination. Wu Zhu [5] analyzed the changes of the pupil size and subjective feeling in the natural light environment in Chongqing. Grunberger et al [6] found that in the afternoon, students' attention was more concentrated in high illumination environment than in low illumination. Cajochen [7] Again confirmed that high illumination environment can improve alertness and reduce drowsiness, and alertness showed a significant positive correlation with the degree of light inhibition on melatonin. Through a literature review, Shilu et al. [8] concluded that high illumination lighting environmental stimuli can enhance alertness. Yan Yonghong [9] studied the effects of T5 fluorescent lamp on learning efficiency, visual fatigue and brain fatigue under different color temperature and illumination levels.

Yang Huanyu [10] evaluates the lighting comfort through the lighting simulation of the library reading room, and uses the multi-objective optimization system to optimize the reading space. Zhang Jingyi [11] concluded the importance of different influencing factors on reading comfort in the general lighting situation of the library. Guo Qi [12] established a prediction model for the subjective evaluation of visual satisfaction and lighting parameters. Feng Zilong [13] proposed a multi-objective optimization method for lighting environment of electronic reading room with illuminance, related color temperature, reflection coefficient and VDT screen brightness as variables.

In the past, the studies on the environment health evaluation of light in library reading rooms were mostly focused on natural light or artificial light alone, but both are important ways

of lighting in reading rooms. This paper comprehensively evaluates and analyzes the natural light environment of the reading room of Hebei University of Engineering from the subjective and objective dimensions, and compares the influence of natural light and artificial light environment in the reading room on students' mental health.

## 2. METHODS

### 2.1 Survey location

The research site is the open reading room of Hebei University of Engineering Library, with the opening time of 8:00-22:00. The space of the reading room is different in size and the depth is large. Only the unilateral window opening is considered. The outdoor environment is open and there are no tall trees. The new campus of Hebei University of Engineering is located in the longitude: 114.603217, latitude: 36.651677, and according to the division of China photolithing Design Standard GB50033-2013 [14], which belongs to the optical climate zone. Most reading rooms are arranged in the east, south and west, and less on the north. The windowsill height is 1 m and the window height is 2.1 m. The wall is large white painting, the reflection ratio is 0.75, the ground is white gray black terrazzo, the reflection ratio is 0.52, the desktop material is wood veneer desktop, and the reflection ratio is 0.7. The lighting fixture is grille type LED lamp, downlight, the height of 3.1 meters, parallel and perpendicular to the desktop layout, horizontal interval of 1-2m, vertical interval of 2-3 meters. Surrounding environment of the library The indoor space environment and light environment are shown in Figure 1.

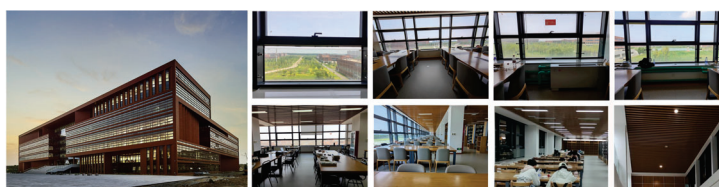


Figure 1. Overview of the library environment

### 2.2 Objective measurement method

The measurement method of the illumination in the reading room according to the characteristics of the operation, combined with the lighting measurement method GB / T5699-2017 [15], the lighting Measurement method GB / T5700-2008 [16], select the desktop illumination measurement method, select the height of the desktop, the measurement point to select the center point of the desktop. The measurement time is selected to measure the desktop illumination value in the natural light environment every one hour in mid-May, 2023, sunny days, 8-20 hours, and when there is no direct sunlight into the room and other artificial light sources. Measure the desktop illumination value in the artificial light environment during the period of 20-22, and extinguish other light sources when measuring. A tape measure and rangefinder are used for dimensional measurement, and a JTG 01 handheld illuminance meter is used for illumination measurement. The illumination value measurement points are shown in Figure 2.

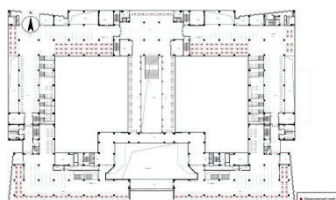


Figure2. Location diagram of the illumination measurement point

### 2.3 Subjective evaluation method

Research object for the students in the reading room, in order to ensure that the results are representative and universality, using personal basic information table to be research students preliminary screening, choose normal mood, no other physiological problems, psychological problems, and daily learning time in 3 hours, learning more than 4 days a week of students to fill in the next step of subjective questionnaire.

Subjective questionnaire content reference the light environment evaluation method (GB / T12454-2017) [17] and guan Yang for Chongqing classroom daytime health lighting study [18],

the introduction of light environment satisfaction evaluation, visual perception evaluation, emotional perception evaluation, cognitive ability evaluation four aspects of natural light, artificial light environment under the mental health level of comprehensive evaluation. The seven-level semantic difference scale was designed, and the corresponding scores of the 7 levels were 1,2,..., 7.

## 2.4 Analysis methods

(1)CRITIC Method, is an objective empowerment method, is through comprehensively considering the contrast intensity of the evaluation index and the conflict between the indicators Sex determines the objective weight of the indicators. It is not that the higher the weight, the more important the index, but the correlation between the variation of the index and the index, and completely uses the objective attributes of the data itself for scientific evaluation. Jiang Minyu [19] used the CRITIC method to analyze the weight of the light environment index of the cruise ship cabin.

(2)The comprehensive evaluation method, also known as the multi-index comprehensive evaluation method, is to establish a statistical index system according to the research purpose, right Several aspects of the development of the phenomenon are described quantitatively, combining the information provided by each index to get a comprehensive evaluation value, and making an overall evaluation of the research object for comparison.Hu Hao [20] studied the computer operation efficiency and fatigue degree of the office personnel under the artificial lighting environment through the method of multi-index comprehensive evaluation.This paper obtains the index data set through the establishment of the evaluation system  $Z = \{Z_1, Z_2, \dots, Z_6\}$ , and the corresponding weight of each index  $W = \{W_1, W_2, \dots, W_6\}$ , Using the weighted average method, the score results of multiple indicators are integrated into a comprehensive evaluation score. The numerical calculation formula of the comprehensive evaluation score is shown as follows:

$$I = \sum_{i=1}^n Z_i \times W_i \quad (1)$$

In the formula,  $0 \leq W_i \leq 1$  and meet  $\sum_{i=1}^n W_i = 1$

## 3. Results

### 3.1 Objective data analysis

#### 3.1.1 Natural light environment

The orientation and the number of floors of the building in the natural light environment will affect the desktop illumination. The average illumination value of the reading room in the reading room is shown in Table 1.

Table 1. Measurement results of desktop illumination in natural light environment all sunny days

time	Average desktop illumination / lux			
	East reading room	South reading room	West reading room	North reading room
8-9	6146	306	235	258
9-10	7482	435	400	383
10-11	811	479	425	380
11-12	699	1035	464	414
12-13	522	8082	395	415
13-14	504	7215	710	356
14-15	439	1089	1333	443
15-16	514	932	4699	439
16-17	357	621	3433	366
17-18	294	334	655	225
18-19	99	202	96	84
19-20	31	46	39	21

During the sunny day, the average of the east reading room from 8-10, the southward reading room from 12-14, and the average of the west reading room from 15-17. In the north reading room, the average illumination of the desktop changes little with time, and the light

environment is relatively stable, but the overall illumination level is low. South, west and north reading rooms in 8,8-10, east, south and north reading rooms in 16-18, east, west, south and north reading rooms in 18-20, the illumination value is lower than the standard value stipulated in GB50033-2013 [14] 450 lx.

### 3.1.2 Artificial light environment

The lowest illumination, highest illumination, average illumination and uniformity of illumination on the desktop from 20-22 in the artificial light environment are shown in Table 2.

Table 2. Measurement results of the desktop illuminance in the lighting environment

Position	Average desktop illumination / lux	The desktop illumination uniformity
East reading room,sixth floor	259	0.93
South reading room,sixth floor	262.5	0.91
West reading room,sixth floor	268.5	0.91
East reading room,fifth floor	266.5	0.95
South reading room,fifth floor	132	0.89
West reading room,fifth floor	239.5	0.88
East reading room, fourth floor	477.5	0.85
Southern reading room,fourth floor	118.5	0.88
Western reading room,fourth floor	550.5	0.90
North reading room,fourth floor	143	0.87
East reading room,third floor	209	0.92
Southern reading room,third floor	143.5	0.92
Western reading room,third floor	125.5	0.89
North reading room,third floor	70	0.94

It is found that the light color of the artificial light environment in the reading room is all white light. The illumination value was generally low, with only 14% of the average desktop illumination area above 300 lx, meeting the requirements of [21], 35.7% between 200 lx and 300 lx, 42.8% between 100 lx and 200 lx, and 7% between 0 and 100 lx. The overall light environment is relatively uniform, and the uniformity of the desktop illumination is basically above 0.8, which is higher than the 0.6 required by the building lighting design standard [21].

### 3.2 Subjective data analysis

Through the preliminary analysis, it is found that students have great differences in their attention to different evaluation indicators of natural light environment and artificial light environment. In order to excavate the students' attention to different indicators, CRITIC weight analysis method is applied to analyze the relative weight of each index.

#### 3.2.1 Natural light environment

The subjective evaluation results of the whole natural light environment in the reading room are shown in Table 3,4.

Table 3. Statistics of the survey results of the natural light environment questionnaire

Classification	Index	Describe	Average value	Standard deviation
Light environment evaluation	Overall satisfaction	Not satisfied / Satisfied	4.930	1.233
	Light color satisfaction	Cold / Warm	5.000	1.700
	No glare evaluation	Dazzling / Not dazzling	3.250	1.274
	Brightness satisfaction	Dark / Bright	4.990	1.679
Visual perception evaluation	Visual comfort	Not comfortable / Comfortable	4.760	1.288
	Visual fatigue	Fatigue / No fatigue	4.370	1.779
	Visual clarity	Fuzzy / Clear	4.630	1.674
	Colour truth	Not real / Real	4.910	1.596
Emotional perception evaluation	Vitality degree	Durbine / Active	4.030	1.636
	Pleasure degree	Frustration / Pleasure	4.220	1.829
	Calm degree	Disturbed / Calm	4.310	1.637
	Relax degree	Nervous / Relax	4.090	1.564
Cognitive appraisal	Cognitive speed	Slow / Fast	4.030	1.636
	Cognitive accuracy	Low accuracy / High accuracy	3.890	1.588

Table 4. Weight analysis of natural light environment evaluation indicators

Classification	Index	Indicator variability	Indicators are conflicting	Quantity of information	Weight
----------------	-------	-----------------------	----------------------------	-------------------------	--------



Classification	Index	Indicator variability	Indicators are conflicting	Quantity of information	Weight
Light environment evaluation	Overall satisfaction	1.233	12.312	15.181	7.77%
	Light color satisfaction	1.700	8.847	15.037	7.70%
	No glare evaluation	1.274	14.573	18.570	9.51%
	Brightness satisfaction	1.679	9.014	15.131	7.75%
Visual perception evaluation	Visual comfort	1.288	10.974	14.134	7.24%
	Visual fatigue	1.779	11.449	20.368	10.43%
	Visual clarity	1.674	8.254	13.815	7.07%
	Colour truth	1.596	10.908	17.409	8.92%
Emotional perception evaluation	Vitality degree	1.636	6.481	10.601	5.43%
	Pleasure degree	1.829	6.864	12.554	6.43%
	Calm degree	1.637	6.801	11.135	5.70%
	Relax degree	1.564	6.594	10.314	5.28%
Cognitive appraisal	Cognitive speed	1.636	6.481	10.601	5.43%
	Cognitive accuracy	1.588	6.560	10.420	5.34%

According to the results of the questionnaire, the students scored more than 4 points on the evaluation indicators of the overall natural light environment under all sunny days, and the overall evaluation is relatively high, indicating that the students are generally satisfied with the natural light environment in the reading room, but the evaluation score of no glare is low.

It can be found from Table 4 that the order of different evaluation indicators in natural light environment is Visual fatigue (10.43%)> No glare evaluation (9.51%)> Colour truth (8.92%)> Overall satisfaction (7.77%)> Brightness satisfaction (7.75%)> Light color satisfaction (7.70%)> Visual comfort (7.24%)> Visual clarity (7.07%)> Pleasure degree (6.43%)> Calm degree (5.70%)> Vitality degree (5.43%) = Cognitive speed (5.43%)> Cognitive accuracy (5.34%)> Relax degree (5.28%).

### 3.2.2 Artificial light environment

The subjective evaluation of the overall artificial light environment in the reading room are shown in Table 5,6.

Table 5. Statistics of the survey results of the artificial light environment questionnaire

Classification	Index	Describe	Average value	Standard deviation
Light environment evaluation	Overall satisfaction	Not satisfied / Satisfied	3.050	1.513
	Light color satisfaction	Cold / Warm	3.900	1.528
	No glare evaluation	Dazzling / Not dazzling	4.980	1.279
	Brightness satisfaction	Dark / Bright	3.060	1.530
Visual perception evaluation	Visual comfort	Not comfortable / Comfortable	2.990	1.367
	Visual fatigue	Fatigue / No fatigue	3.040	1.428
	Visual clarity	Fuzzy / Clear	3.050	1.513
	Colour truth	Not real / Real	3.720	1.102
Emotional perception evaluation	Vitality degree	Durbine / Active	3.140	1.504
	Pleasure degree	Frustration / Pleasure	2.960	1.325
	Calm degree	Disturbed / Calm	3.130	1.587
	Relax degree	Nervous / Relax	3.090	1.491
Cognitive appraisal	Cognitive speed	Slow / Fast	3.070	1.559
	Cognitive accuracy	Low accuracy / High accuracy	2.980	1.497

Table 6. Weight analysis of artificial light environment evaluation indicators

Classification	Index	Indicator variability	Indicators are conflicting	Quantity of information	Weight
Light environment evaluation	Overall satisfaction	1.513	4.373	6.618	4.84%
	Light color satisfaction	1.528	12.291	18.774	13.74%
	No glare evaluation	1.279	23.283	29.780	21.80%
	Brightness satisfaction	1.530	4.349	6.652	4.87%
Visual perception evaluation	Visual comfort	1.367	4.276	5.845	4.28%
	Visual fatigue	1.428	4.639	6.624	4.85%
	Visual clarity	1.513	4.373	6.618	4.84%
	Colour truth	1.102	14.866	16.378	11.99%
Emotional perception evaluation	Vitality degree	1.504	4.333	6.519	4.77%
	Pleasure degree	1.325	4.424	5.862	4.29%
	Calm degree	1.587	4.347	6.898	5.05%
	Relax degree	1.491	4.324	6.448	4.72%
Cognitive appraisal	Cognitive speed	1.559	4.409	6.873	5.03%

Classification	Index	Indicator variability	Indicators are conflicting	Quantity of information	Weight
	Cognitive accuracy	1.497	4.491	6.724	4.92%

According to the results of the questionnaire survey, the score of various evaluation indicators in the overall artificial light environment of the library reading room is basically about 3, indicating that the overall evaluation of the artificial light environment is general, but the evaluation score of non-glare is relatively high.

It can be found from Table 6 that the order of different evaluation indicators in artificial light environment is No glare evaluation (21.80%)> Light color satisfaction (13.74%)> Colour truth(11.99%)> Calm degree(5.05%)> Cognitive speed (5.03%)> Cognitive accuracy (4.92%)> Brightness satisfaction (4.87%)> Visual fatigue (4.85%)> Overall satisfaction (4.84%) = Visual clarity (4.84%)> Vitality degree(4.77%)> Relax degree (4.72%)>Pleasure degree (4.29%)> Visual comfort (4.28%).

### 3.3 Analysis of objective data and subjective data

In order to explore the relationship between subjective data and objective data, the desktop illumination and subjective perception evaluation in natural light and artificial light environment were compared and analyzed, and a regression model of comprehensive score and illumination was established. The preliminary investigation found that there was no student learning in the area where the desktop illumination value of natural light was higher than 3000 lx, so only the illumination measured illumination within 0-3000 lx was considered in the next study. According to the preliminary investigation of the artificial light environment, the measured illumination within 0-600 lx was selected in the next study. In this study, a total of 286 valid questionnaires were collected in the reading room, and SPSS was used to test the validity of the obtained data. The KMO measurements of subjective questionnaire data in natural and artificial light environments were 0.928,0.868, and the Cronbach Alpha coefficient was 0.927,0.931, respectively.

#### 3.3.1 Natural light environment

The change trend of natural light environment illumination value and subjective evaluation index is shown in Figure 3.

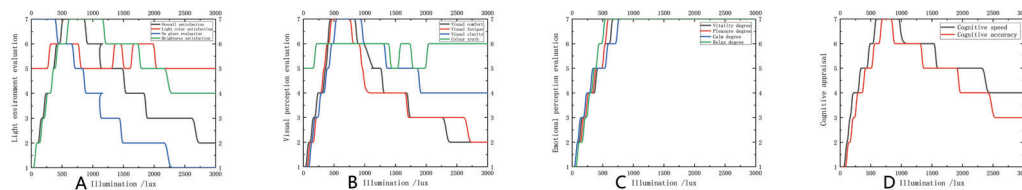


Figure 3. Comparative analysis of illumination and subjective perception evaluation

In the range of mood perception evaluation and illumination is the same change, not glare evaluation and illumination opposite change, light color satisfaction, color reality and illumination value relationship is not obvious, visual comfort, visual fatigue, visual clarity and cognitive evaluation, overall satisfaction, brightness satisfaction with illumination increased after the change.

The regression model fit of the illuminance values in natural light environment and mental health comprehensive evaluation scores is shown in Figure 4.

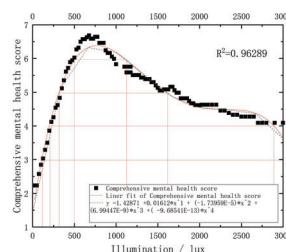


Figure 4. Lance values and mental health composite scores

A function model of 0-3000lx,  $R^2=0.96289$ , F value test,  $P < 0.05$ , whose expression was  $y = 1.42871 + 0.01612 * x^1 + (-1.73959E-5) * x^2 + (6.99447E-9) * x^3 + (-9.68541E-13) * x^4$

$x^4$ , where  $y$  is the comprehensive evaluation score of mental health, and  $x$  is the illumination value of natural light environment. The comprehensive score of mental health first increased and then decreased with increasing illumination, with the highest value of 6.21 and the illumination of 596.95lx, and when the combined score was above 6, the illumination threshold was 513.68lx-1101.76lx. When the combined score is above 5, the illuminance threshold is 316.48-1593.28. When the combined score is above 4, the illuminance threshold is 198.87-2886.12. When the composite score is above 3, the illumination threshold is 109.95-3126.49lx.

### 3.3.2 Artificial light environment

The change trend of the artificial light environment illumination value and the subjective evaluation index is drawn as shown in Figure 5.

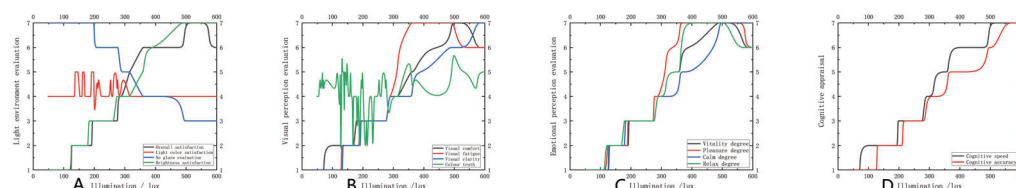


Figure 5. Comparative analysis of illumination and subjective perception evaluation

Under the measured illumination range of the artificial light environment, the overall satisfaction degree, visual comfort degree, visual fatigue degree, activity degree, pleasure degree and relaxation degree all increased first and then decreased with the increase of the illumination degree. Non-glare evaluation gradually decreased with increasing illuminance. Brightness satisfaction, visual clarity, calmness, cognitive speed, and cognitive accuracy all increased with the increasing illuminance. The relationship between light and color satisfaction, color authenticity and illumination value is not obvious.

The regression model fit of the illuminance values in the artificial light environment and the comprehensive evaluation of mental health is shown in Figure 6.

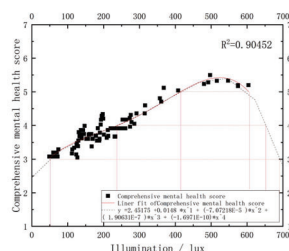


Figure 6. Lance values and mental health composite scores

A function model of 0-600 lx,  $R^2=0.90452$ ,  $F$  value test passed,  $P < 0.05$ , whose expression is  $y = 2.45175 + 0.0148 * x^1 + (-7.07218E-5) * x^2 + (1.90631E-7) * x^3 + (-1.6971E-10) * x^4$ , where  $y$  is the score of comprehensive mental health and  $x$  is the illumination of artificial light environment. When the composite score is above 5, the illumination threshold is 430.56lx-598.65lx. When the composite score is above 4, the illuminance threshold is 239.66-660.68lx. The illumination threshold was 45.93-694.34lx when the composite score was above 3.

## 4. CONCLUSION

The results of the mental health of the students in the natural light and artificial light environment are as follows.

1. The natural light environment changes diverse, which is not easy to control, and is easy to appear problems such as large changes in illumination in the same region in the daytime and large differences in illumination in different regions at the same time. Artificial light environment due to unreasonable lighting layout and partial damage, resulting in lighting quality deviation in some areas.

2. Students' evaluation of natural light environment is higher than that of artificial light environment. Most students are more satisfied with the evaluation of natural light environment, and the evaluation of artificial light environment is more general.

3. Comprehensive evaluation of students' mental health, the best desktop illumination threshold in natural light environment is 513.68lx-1101.76lx, and the best desktop illumination threshold in artificial light environment is 430.56lx-600lx.

## REFERENCE

- [1] Fu Xiaolan, Zhang Kan, Chen Xuefeng, et al. Chinese National Mental Health Development Report 2021-2022 [M]. Beijing: Social Sciences Academic Press, 2023:75-84.
- [2] Jiang Jincai, Wu Wei. Review of evaluation methods for non-visual effects of light and lighting [J]. Journal of Lighting Engineering, 2018,29 (03): 129-136 + 140.
- [3] Peter R. Boyce. The Impact of Light in Buildings on Human Health[J]. Indoor and built environment: Journal of the International Society of the Built Environment,2010,19(1).
- [4] William A. Gosling. To Go or Not to Go? Library as Place[J]. American Libraries,2000,31(11).
- [5] Wu Zhu. Research on natural lighting in office space based on photobiological effect [D]. Chongqing University, 2013.
- [6] Grünberger J.,Linzmayr L.,Dietzel M.,Saletu B.. The effect of biologically-active light on the mood and thymopsychy and on psychophysiological variables in healthy volunteers[J]. International Journal of Psychophysiology,1993,15(1).
- [7] Christian Cajochen,Jamie M Zeitzer,Charles A Czeisler,Derk-Jan Dijk. Dose-response relationship for light intensity and ocular and electroencephalographic correlates of human alertness[J]. Behavioural Brain Research,2000,115(1).
- [8] Stone road. Effect of illumination source color temperature on the physiological function of human CNS [J]. Human ergonomics, 2006(02):59-61+71.
- [9] Yan Yonghong, Guan Yang, Liu Xiangde, etc. The effect of classroom fluorescent light color temperature on student learning efficiency and physiological rhythm [J]. Civil Construction and Environmental Engineering, 2010,32 (04): 85-89.
- [10] Yang Huanyu. Research on light environment of Kunming University Library based on Octopus optimization algorithm [D]. Kunming University of Science and Technology, 2020.
- [11] Zhang Jingyi. Evaluation of coupled reading comfort in library lighting environment [D]. Tianjin University, 2019.
- [12] Guo Qi, Wang Lixiong. Visual satisfaction prediction model of e-reading in a library lighting environment [J]. Journal of Civil and Environmental Engineering (Chinese and English), 2019,41 (01): 144-149.
- [13] Feng Zilong, Wang Lixiong. Multi-objective optimization method for reading comfort lighting in library electronic reading room [J]. Journal of Lighting Engineering, 2022,33 (04): 115-122.
- [14] GB 50033-2013,Design standards for building lighting[S].
- [15] GB / T 5699-2017, Daylighting measurement method [S].
- [16] GB / T 5700-2008, Lighting measurement method [S].
- [17] GB / T 12454-2017, Light environment assessment method [S].
- [18] Guan Yang. Study on daytime health lighting of classrooms in Chongqing area [D]. Chongqing University, 2017.
- [19] Jiang Minyu, Ge Wenjing, Yang Xiu. Comprehensive evaluation of light environment of cruise cabin combining subjective and objective [J]. Journal of Shanghai Maritime University, 2023,44(01):104-110.
- [20] Hu Hao. Research on the computer operation efficiency and fatigue degree in the artificial lighting environment of administrative office space [D]. Chongqing University, 2018.
- [21] GB 50034-2013, Building Lighting Design Standard (attached provision description) [S].

## ACKNOWLEDGEMENT

Corresponding Author: Fanpu Meng

Affiliation: School of Architecture and Art, Hebei University of Engineering

e-mail : 2423078106@qq.com

# RESEARCH ON CROSS-MEDIA PERCEPTION OF CITY NIGHT IMAGE THROUGH A COGNITIVE MODEL

Xiaoxi Liu, Tianke He, Bowen Yang, Yifei Li

(School of Film and Cinematic Arts, Communication University of China, Beijing, China)

## ABSTRACT

"City night image" refers to the impression of a city's characteristics as perceived by a wide audience at night. It is a distinct aspect of the city's overall image and differs greatly from its daytime counterpart. The construction of a city night image relies on both physical nightscape environment and various media environments, resulting in a comprehensive effect. This paper draws on research concepts from user consumption behavior models, such as the AIDMA model (Attention, Interest, Desire, Memory, Action model) and AISAS model (Attention, Interest, Search, Action, Share model), to conduct interviews and questionnaire surveys. Starting from the coupling effect between the physical nightscape environment and media environment in the process of city image construction, this paper analyzes the cognitive model of city night image and how the image generation of physical space and the information reconstruction of media environment influence the construction of city night image from a cross-media perspective. Finally, this paper proposes lighting environment design strategies to enhance the city night image according to the cognitive model.

Keywords: City night image, Cognitive model, Nightscape, Media environments

## 1. INTRODUCTION

In both strategic city planning and city marketing, a fundamental starting point is to evaluate the image of the city itself [1]. Kotler et al. define the image of a place as "the sum of beliefs, ideals, and impressions people have toward a certain place" [2]. In other words, the image of a place is also a complexity of cognitive and affective elements. "City night image" as part of the image of a place, refers to the sum of beliefs and ideals which represent the affective elements, as well as the impressions of the city's characteristics represent the cognitive elements, as formed by the wide audience at night. The night image represents a large pieces of information related to a place at night, and is a cognitive product of the attempt to process large amounts of information, which the contents include on both physical nightscapes environment as well as various media environment.

Lynch, an influential American urban planner and author, maintains [3] there seems to be a public image of any given city which is the overlap of many individual images, or perhaps there is a series of public images each held by some significant number of citizens. Such images, with some content that is rarely or never communicated, limited by the one-way communication mode by the traditional media. As Habib stated [4], the role of time, commence of day and night and its effect on perception and legibility of the environment have not been investigated deeply, although time effects the level and the way of perception and legibility and it should be noted that there is clear difference between human perception and space legibility during day and night, which led study the city night image from a cross-media perspective under the background of the Internet era is meaningful. However, an insufficient capacity to account for the complexity of night image has not hindered the global expansion of the urban nightscapes renewal based on expanding nightlife. By engaging with the cross-media communication as integral to the process of city night image construction, new conceptual trajectories could be proposed that point the way towards a more effective framework for understanding the complexity system of city night image cognitive model.

The purpose of this study is to improve the city night image by enhancing the lighting environment according to the cognitive model of the city night image. This approach provides a vantage point to introspect current approaches to design environmental lighting from the perspective of shaping the city night image.



## 2. SURVEYS

To investigate the impact of city night image construction on both physical and media environments, a combination of interviews and questionnaire surveys were conducted. A total of 42 students from Communication University of China participated in the survey, with 12 of them being selected for follow-up interviews.

Respondents were asked to answer seven questions in the questionnaire, which included two multiple-choice questions: "How familiar are you with the nightscape of Beijing?" and "Have you been to Tokyo before?"; and two fill-in-the-blank questions: "What percentage of the physical nightscape environment contributes to night image of Beijing in your opinion?" and "What percentage of the physical nightscape environment contributes to night image of Tokyo in your opinion?". Additionally, three open-ended questions were included: "In your professional opinion, what are the major approaches and ways for constructing a city night image?", "What are the key descriptive terms for the night image of Beijing in your opinion?", and "What are the key descriptive terms for the night image of Tokyo in your opinion?"

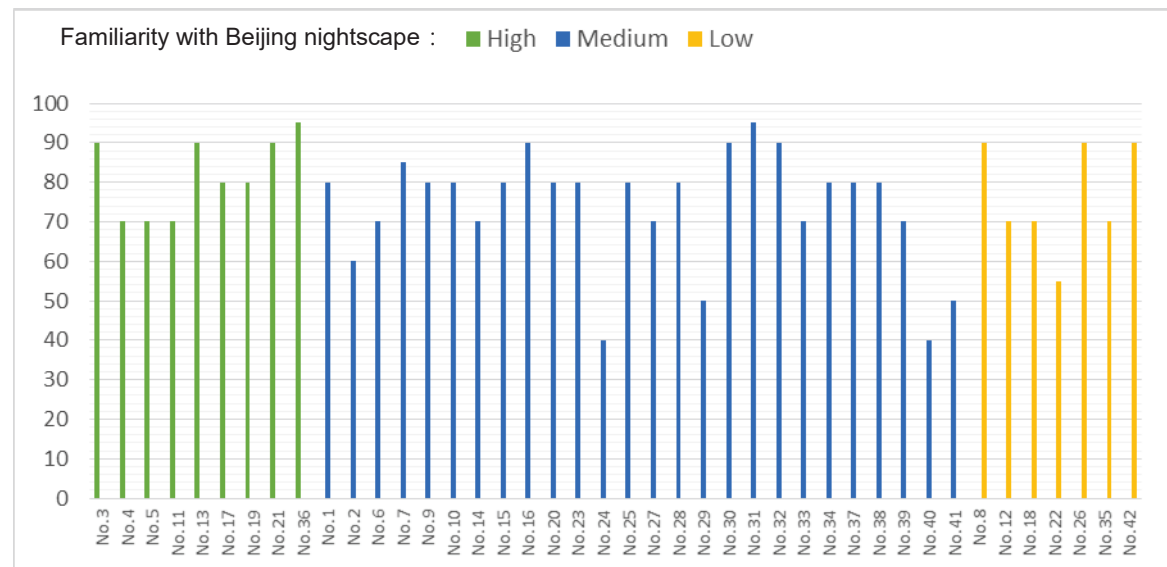


Figure 1. The percentage of physical nightscape environment contribute to the individual night image of Beijing by each participants (author's own drawing)

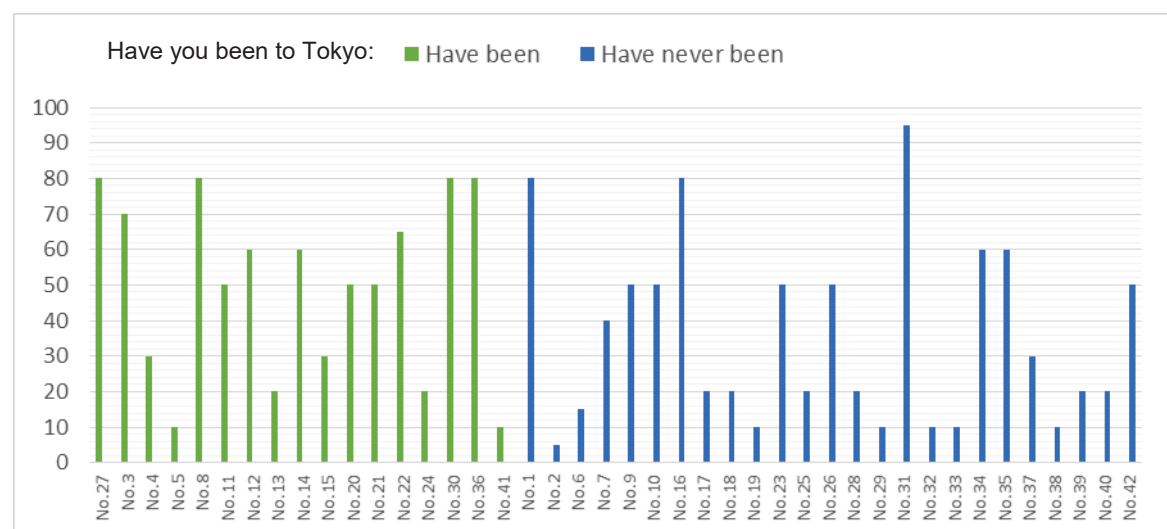


Figure 2. The percentage of physical nightscape environment contribute to the individual night image of Tokyo by each participants (author's own drawing)

The results of the questionnaire regarding the percentage of contribution of the physical nightscape environment to the city night image for each individual were shown in the figures above. The horizontal axis represents the respondent's number, while the vertical axis represents the percentage. In Figure 1, colors represent different levels of familiarity with the Beijing nightscape among the respondents. Green indicates high familiarity, blue indicates medium familiarity, and yellow indicates low familiarity. Respondents who were highly familiar with Beijing nightscape showed relatively high percentage results regarding the physical nightscape environment's contribution to the city night image. Meanwhile, those who belonged to the medium and low familiarity groups showed insignificant differences in their percentage results. However, those who belonged to the low familiarity group had an average value of results even higher than that of the medium group. Figure 2 shows that whether or not respondents had been to Tokyo before did not significantly affect their opinions on the contribution of the physical nightscape environment to the city night image.

After the questionnaire, twelve students of them were interviewed in-depth, with a focus on the following questions: "What roles and trends do media environments play in shaping the city night image?", "What are the differences in the construction of city night images between various media and first-hand experience?", "What images or pictures represent the night image of Beijing and Tokyo in your own impressions?" and "What process do you think is involved in forming city night image?". The interviews were recorded in both text and picture formats, and were summarized and analyzed in the following section of this paper.

### 3. THE CITY NIGHT IMAGE COGNITIVE MODEL

City image is related to two realms of human mentality and objective environment, making it essential to study the content from the objective environment to the psychological cognition. Many views on cognitive processing had coalesced in consumer behavior research before [5]. Drawing upon the theoretical model of the traditional AIDMA model (Attention, Interest, Desire, Memory, Action) proposed by Ronald Hall in 1924 [6] and the AISAS model (Attention, Interest, Search, Action, Share) proposed by Dentsu Group Inc in 2004, which is originally based on the reconstruction of the characteristics of market consumer behavior model in the network age, a conceptual framework of the city night image cognitive model was developed.

According to the summary of interviews and questionnaire surveys, the cognitive process of the city night image was condensed into two models. The dotted line segments in the cognitive models represent the real physical environment created by lighting at night. Meanwhile, the solid line segments represent the key elements in transforming the nightscape into a distinctive night image. The bracketed text on the right indicates how non-first-hand experiences are used to construct the urban night image in different media forms. The cognitive model internalizes reflection and reconstruction of the nightscape in thoughts.

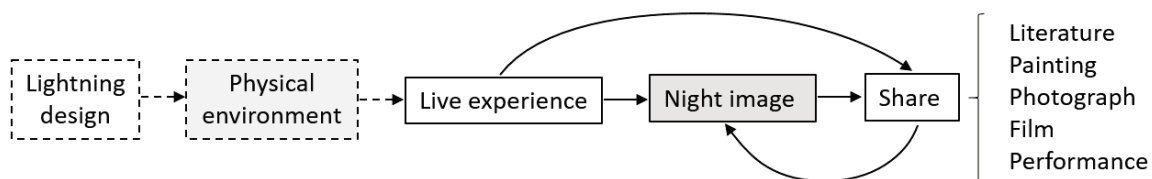


Figure 3. The cognitive model of city night image in the traditional media era (author's own drawing)

Figure 3 illustrates the cognitive model of city night image during the traditional media era. The construction of the city night image was a more linear system with a one-way transmission. Due to the limitations of communication forms during this era, the night image was often constructed indirectly through various media environments, such as literature and paintings, in addition to live experience. In this process, audiences were usually passive receivers of information.

Figure 4 presents a cognitive model of the urban night image in the internet era, based on the theoretical AISAS model. With the development of the internet, more people can now share their experiences and opinions and communicate in various forms, leading to changes in the media environment. This cognitive model emphasizes the processes of search and sharing, which fully reflect the media usage habits of internet generations. It transforms the construction of the urban night image from a linear system to a complex system. The internet and cross-media communication allows the physical nightscape environment to be redeveloped and transmitted at a low threshold, making non-first-hand experiences increasingly influential in shaping the night

image. In these non-first-hand experiences, many live physical environments are shared through live webcasts and Vlogs, which gradually become the main content of media environments constructing the night image. In this process, audiences are no longer just passive receivers of information; they are now actively seeking and sharing it.

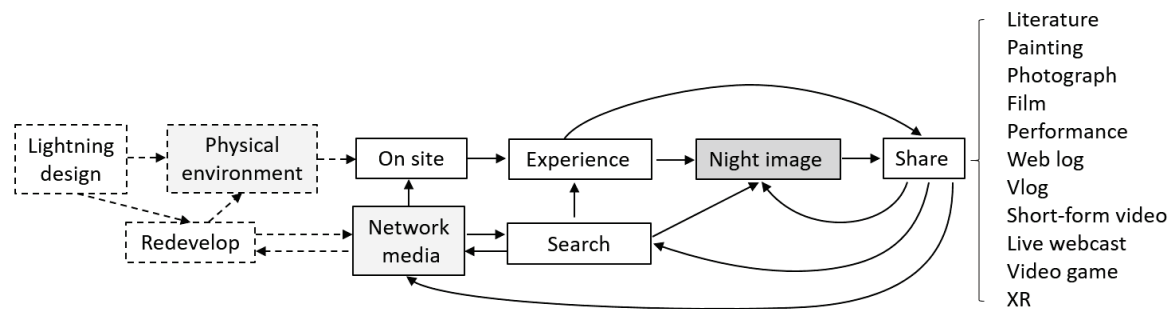


Figure 4. The cognitive model of city night image in the Internet era (author's own drawing).

#### 4. THE LIGHTING ENVIRONMENT DESIGN STRATEGY

Environmental cognition refers to the human ability to comprehend and interpret physical surroundings. The objective of this study is to analyze and summarize the lighting environment design strategy using a cognitive model to promote nightlife. Before discussing the design strategy, the content about physical environment that constitutes the city night image on above interviews and questionnaires survey need to be organized. It is shown that the key descriptive terms regarding the night image of Beijing are solemn, stable, grand, prosperous, modern, cultural and historical, and the key descriptive terms regarding the night image of Tokyo are prosperous, fashion, avant-garde, diverse, neon, cyber and introverted. The pictures that regarding the representations of Beijing's and Tokyo's night image from the interview summaries are shown separately in Figure 5 and 6. Among the images of Beijing (Figure 5), there are numerous landmarks and various roads, architectural clusters in the bird's-eye view and some characteristic public spaces, which are consistent with the survey. Among the images of Tokyo (Figure 6), landmarks, roads, and architectural clusters in medium-to-large sections of the city are the key elements for the urban night image; however, signboards and some characteristic public spaces are also significant elements. That is similar to Habib's [7] study, nightly mental images shows vast difference to the mental images during day, which paths were the first mentioned element of day and landmarks seem more important than the other elements at night. It is worth noting that the perspective and key elements in these pictures, representing the night image, often differ from our live experiences. This leads to the need for a reconsideration of the lighting design strategy.



Figure 5. The examples regarding Beijing night image form interviews summary



Figure 6. The examples regarding Tokyo night image form interviews summary

In traditional lighting design, the first consideration is the parameters that meet the needs of visual functions, such as illuminance and illuminance uniformity. This can be seen in many lighting plan documents and lighting-related standards. Traditional lighting design also emphasizes the integrity and coordination of the lighting environment. Additionally, the visual experience is taken into account, with attention paid to the color rendering index and glare control of the lamps.

According to the two cognitive model of city night image in the traditional media era (Figure 3) and the Internet era (Figure 4), it is not difficult to see that the focus of lighting environment design based on various media and communication forms needs to be adjusted compared to traditional lighting design. Consider the importance of share and search in the cognitive model of the Internet era, the lighting environment design needs to stress the landmarks and highlight the personality. Therefore, the parameters of luminance and luminance contrast, as well as the planning of lighting-related activities and events, become more important. Compared with traditional lighting that emphasizes color rendering index and glare control, lighting design based on the cognitive model of the internet era needs to pay more attention to the choice of color temperature and light color, as well as the control of spill light.

## 5. CONCLUSION

The concept of city image formation is a bilateral process, as Lynch has claimed [8], where the observer and the environment play a crucial role in shaping the image. This process is associated with physical and social stimuli, which are spontaneously linked to the environment. During night, city nightscape also have a significant impact on the nightlife and the night image. To enhance the lighting environment, lighting designers can benefit from studying the cognitive model, which helps to analyze the differences between various environments and the construction of city night images from a cross-media perspective. By doing so, it can provide assistance to create effective lighting environments and construct better city night image.

## REFERENCES

- [1] Luque-Martinez T, Del Barrio-García S, Ibanez-Zapata JA, Molina MA. Modeling a city's image: The case of Granada. *Cities*, 2007, 24(5):335.
- [2] Kotler, P, Haider, D H and Rein, I. *Marketing Places*. Free Press, New York, 1993,141.
- [3] Lynch, Kevin. *The city image and its elements*. The city reader. Routledge, 2015, 99.
- [4] Habib F, Sashourpour M. The Cognition of the City at Night. *International Journal of Architecture and Urban Development*, 2012, 2(3): 5.
- [5] Isada F, Isada Y. An Empirical Study of the International-Tourism Management by a Model of Consumer Behaviour. *International Journal of Business and Management*, 2014, 2(3): 40.
- [6] Hall, S. R., *Retail advertising and selling*. McGraw-Hill, 1924.
- [7] Habib F, Sashourpour M. The Cognition of the City at Night. *International Journal of Architecture and Urban Development*, 2012, 2(3):8.
- [8] Luque-Martinez T, Del Barrio-García S, Ibanez-Zapata JA, Molina MA. Modeling a city's image: The case of Granada. *Cities*, 2007, 24(5):335-338.

## ACKNOWLEDGEMENTS

This paper was funded by the project (22YTC025) of Beijing Social Science Foundation Youth Program : Research on the construction of Beijing city night image from the cross-media perspective

Corresponding Author Name: Xiaoxi Liu

Affiliation: School of Film and Cinematic Arts, Communication University of China

e-mail: lxxcici@163.com

## DEVELOPMENT AND RESEARCH OF HIGH-POWER COB PHASE CHANGE HEAT SINK WITH HIGH THERMAL CONDUCTIVITY

Chaoyue Liu <sup>1</sup>, Long Sun <sup>1</sup>, Cheng Ruan <sup>1</sup>, Yaowei Huang <sup>1</sup>, Yang Wang <sup>1,2</sup>, Yu Cui <sup>1</sup>

*(Changchun Cedar Electronics Technology Co., Ltd., Changchun 130103, China; Changchun Institute of Optics, Fine Mechanics and Physics, Chinese Academy of Sciences, Changchun 130103, China)*

### ABSTRACT

Addressing the heat dissipation predicament stands as a pivotal challenge inhibiting the advancement and utilization of high-power COB light source lighting LEDs. This study proposes the design of a phase change heat sink for high-power COB applications, capable of replacing conventional industry-standard modules, while adhering to specific requirements. The investigation delves into the arrangement of convective heat dissipation fins and the preparation technology concerning multicomponent phase change working fluids. Leveraging existing manufacturing capabilities, the functions of fin spacing, height, and thickness are simulated and computed, leading to the identification of an optimal heat dissipation fin layout plan. By employing a phase change working fluid characterized by excellent chemical inertness, low boiling point, and viscosity under vacuum conditions, efficient heat conduction is achieved, swiftly transferring heat from the heat source to the radiator's surface through variations in the phase change working fluid's state. The resulting heat sink is tailored to meet the COB light sources' 150W heat dissipation requirements while simultaneously maximizing miniaturization and lightweight properties. The optimal heat dissipation structure is simulated, followed by physical production and performance testing. Experimental outcomes manifest a temperature rise of 52.0°C and a thermal resistance of 0.35K/W for a 150W light source, effectively fulfilling the heat dissipation necessities. In comparison to traditional radiators, this design showcases a significant reduction of 24.74°C in temperature rise, a remarkable enhancement in heat dissipation performance, a weight reduction ranging from 30% to 50%, and a wind resistance area reduction of nearly 2/3. The proposed solution aligns with the requirements of major national projects, contributing to the promotion of low-carbon energy-saving technologies in China.

**Keywords :** COB LED lighting, fin arrangement, multicomponent phase transition, miniaturization and lightweight, energy conservation

### 1 INTRODUCTION

Light Emitting Diode (LED), as a semiconductor solid-state lighting device, offers numerous advantages such as low energy consumption, energy efficiency, high luminous intensity, and rapid response[1-5]. Its versatility allows for diverse design possibilities, leading to wide application in the lighting domain. In comparison to Surface Mount Device (SMD) light sources, Chip-on-Board (COB) packages exhibit superior attributes in terms of manufacturing efficiency, thermal resistance, light quality, and cost-effectiveness. Nevertheless, the heat dissipation potential poses a significant challenge for high-power COB lighting devices, as inadequate heat management can result in adverse effects and chip damage[6-10]. Hence, it is imperative to ensure the timely and proper transfer of heat generated by the light source, thereby maintaining a safe operating temperature environment for the LED chip to fully leverage the



benefits of LED lighting[11].

Considering the aforementioned challenges encountered in the design and development of high-power COB LED phase change modules, along with the utilization of industry-standard radiator module dimensions, a comprehensive approach was undertaken. This involved employing Fluent software for simulation calculations and conducting sample-based experiments. Through multiple iterations of design simulations and adjustments, a composite phase change radiator was determined to meet the heat dissipation requirements while also serving as a suitable replacement for the industry standard module. Furthermore, it was ensured that the resulting solution possessed a compact and lightweight form factor, with dimensions measuring 300mm\*74mm\*85mm. The heat sink achieved a net weight of merely 1kg, enabling it to accommodate a power output of 150W. In comparison to equivalent products available domestically and internationally, the weight reduction amounted to 30%-50%, while the wind resistance area experienced a decrease of approximately two-thirds. Additionally, rigorous testing and calculation methodologies were employed to assess parameters such as heat sink temperature rise and thermal resistance, thereby conducting a comprehensive analysis of performance and economic benefits.

## **2 DOMESTIC AND FOREIGN LED MODULE COMPARISON**

The utilization of international renowned Philips LED series modules relies on conventional aluminum profile thermal conductivity design, featuring a single module size measuring 300mm\*70mm\*67mm, applying power outputs ranging from 35W to 84W. Similarly, prominent domestic lighting products predominantly adopt standard module designs. For instance, HPWINNER, holding significant market share, employs a standard module size of 300mm\*75mm\* 52mm, capable of achieving power outputs of 40W to 60W. Moreover, Shanghai SANSE employs ceramic pixel products that utilize a ceramic heat sink body, wherein a single ceramic pixel accommodates 3-5W power, characterized by non-standard module design with a 45W non-standard module size measuring 135mm\*180mm\*40mm. Nevertheless, despite these advancements, the challenge of developing high-power, small-volume heat sinks using standard module sizes persists, representing a technical bottleneck.

In response to market demand, the project team undertook the design and development of a high-power COB LED phase change module. The project encompassed a sequential progression of steps, including experimental scheme design, experimental system design, data acquisition, and data analysis. Throughout this process, valuable process data was gathered, enabling the team to draw the following conclusions.

## **3 EXPERIMENTAL PROTOCOL DESIGN**

Based on the design criteria and adhering to the standard module size of 300mm\*74mm\*85mm, a total of eight structural solutions were devised. Figure 1 illustrates four of these solutions that demonstrate superior characteristics in terms of heat dissipation area, weight, and temperature rise.

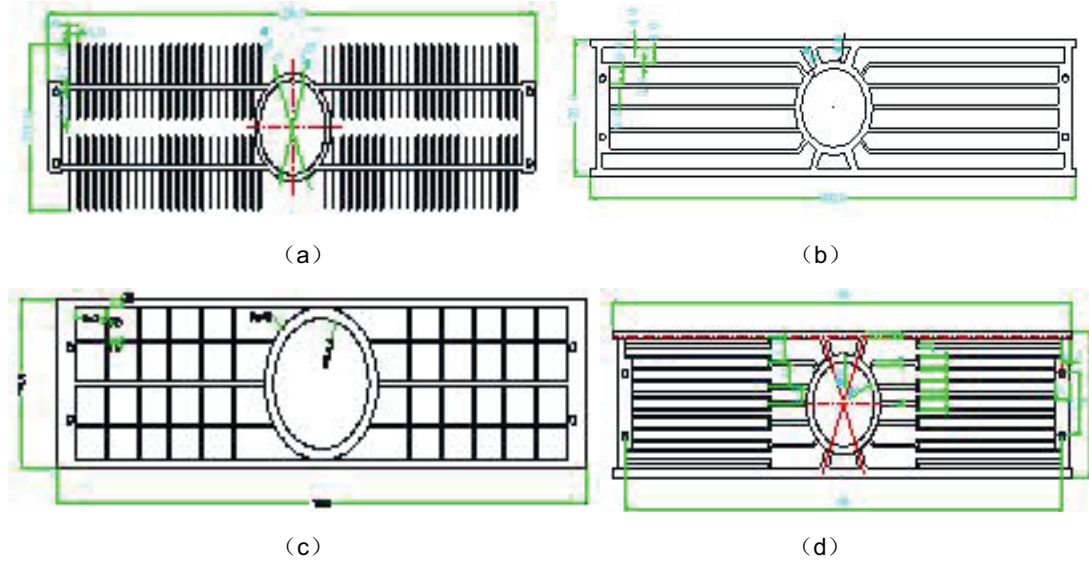


Figure 1 Structure scheme

Table 1 Parameters of each program

Programs		(a)	(b)	(c)	(d)
Heat dissipation area(m <sup>2</sup> )		0.48	0.32	0.37	0.45
Weight(g)		911.80	845.25	984.16	1169.47
Ambient temperature(°C)		50			
Solder joint temperature(°C)	150W	115.3	98.9	105	103.7
	120W	97	90.1	95.2	93.6

Following a comprehensive comparison of the aforementioned four sets of parameters, an evaluation of parameter outputs was conducted. The best-performing solution, denoted as (b), was selected based on its overall effectiveness. Building upon the foundations of solution (b) and incorporating the existing process, further enhancements were made to the heat sink structure. The design improvements focused on optimizing the number and dimensions of the heat sink fins. Consequently, the relationship between fin spacing, height, thickness, and the corresponding requirements can be defined by the following relational equation.

$$N=2 \times (K_2 D) \quad (1)$$

$$13 \leq L/d \leq 15 \quad (2)$$

The relational equation is defined as follows, where  $K_2$  represents the coefficient, constrained within the value range of  $108 \leq K_2 \leq 130$ . Additionally,  $D$  corresponds to the outer diameter of the phase change cavity,  $L$  denotes the length of the edge cooling fins, and  $d$  signifies the spacing between the cooling fins.

The ultimate configuration of the heat sink cross-sectional structure, depicted in Figure 2, yielded a heat sink area measuring 0.2m<sup>2</sup> and a weight of 860g. Subsequently, samples were manufactured to validate and assess the performance of the heat sink, utilizing this structure as the basis for experimental testing.

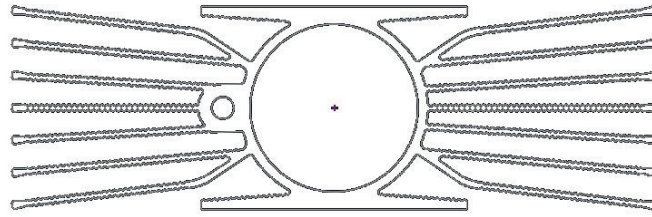


Figure 2 Schematic diagram of fin cross section

Within the heat sink structure, the incorporation of a phase change cavity contributes to the enhancement of heat transfer efficiency. In the selection of an appropriate phase change medium, considerations were given to its prolonged usage, as solutions containing water tend to induce corrosion on the metallic sealed cavity. Such corrosion results in the accumulation of oxides within the miniature straight grooves, consequently impeding the return channel's functionality. Hence, it was crucial to prepare a phase change agent that exhibits high heat transfer efficiency while possessing excellent chemical inertness. The formulated phase change agent, composed of cyclopentane, methyl acetate, and acetone, maintains a low boiling point and viscosity under vacuum conditions, thereby ensuring the device's ability to sustain low temperatures during operation. This prepared phase change agent accelerates the reflux rate of the phase change liquid, thereby augmenting the effectiveness of condensation heat exchange, all while demonstrating non-corrosive properties towards metallic materials.

#### 4 EXPERIMENTAL SYSTEM DESIGN AND DATA ACQUISITION

When the heat sink structure and phase change structure preparation were finalized, a sample of the heat sink was obtained. An experimental system was designed for the heat sink, encompassing an LED chip, the heat sink itself, an HIOKI LR8450 data acquisition instrument, and 6 K-type thermocouples. The HIOKI LR8450 serves as a multi-channel data collector, testing error is only 0.4%. Through direct connection with the thermocouple, temperature measurements are acquired at the radiator's designated measurement point. The experiment employs high-precision K-type thermocouples to measure temperature information at the negative solder joint and the heat sink wall. The temperature measurement range spans from 0 to 1300°C, with a measurement error of  $\pm 0.4^{\circ}\text{C}$ . To ensure the integrity of the experimental data, both the heat sink and the entire experimental process were conducted within a windproof cover, mitigating the influence of wind speed on the acquired data.

To assess the efficacy of the heat sink, temperature measurements were taken at five distinct points, designated as thermocouples 101, 103, 105, 107, and 109. These thermocouples were strategically positioned at the positive and negative solder joints, as well as the upper and lower regions of the fins and the topmost part of the phase change structure. Additionally, thermocouple 111 was employed to record the ambient temperature, thereby minimizing the potential impact of ambient temperature fluctuations on the collected data.

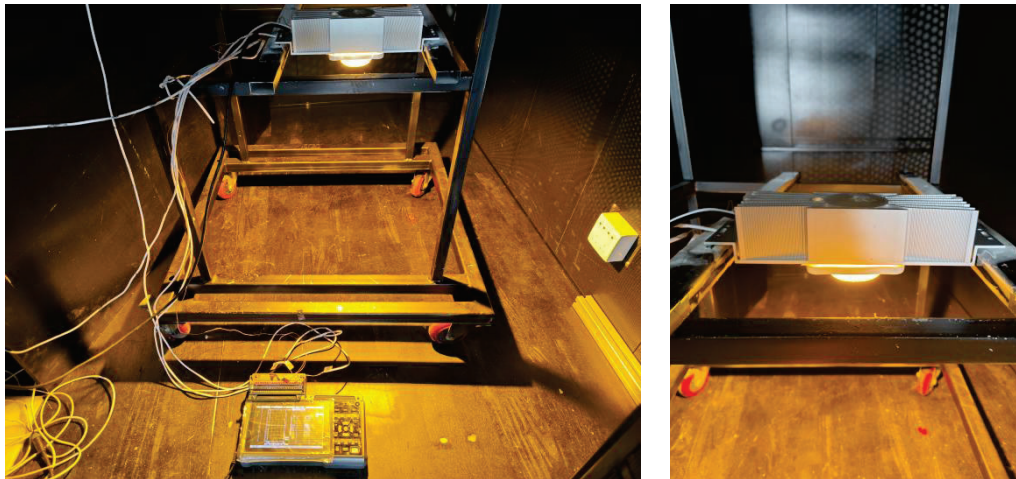


Figure 3 Experimental system and heat sink

In order to maintain precision and accuracy throughout the experimental process, the following procedural steps were strictly executed:

1. Upon establishing the interconnections among the components of the experimental system, the data acquisition system's reliability and accuracy were assessed. This involved sequentially linking the high-power COB light source, LED lighting heat sink, K-type thermocouple, and data acquisition instrument. Initially, the power supply of the data acquisition instrument was activated while keeping the LED power supply deactivated. This facilitated a preliminary assessment to determine whether the thermocouple and data acquisition instrument functioned optimally and could effectively capture data. Furthermore, it allowed for observation of the accuracy and consistency of data acquired from each K-type thermocouple, thereby mitigating potential experimental data discrepancies caused by inherent errors in the thermocouples themselves.
2. In order to ascertain the accuracy of thermocouple data, data collection was initiated. After activating the data acquisition system a 150W light source is quickly connected and the heat sink starts to run. After the temperature of each measurement point is stabilized, the data phone is then continued for more than one hour to ensure the stability and accuracy of the data obtained. Subsequently, data collection was terminated, and the acquired data was saved. To conclude the experiment, the power supply of the LED lighting device was disconnected.

## 5 EXPERIMENTAL DATA ANALYSIS

Based on the experimental data collected from various measurement points, temperature information was obtained for the negative solder joint of the heat sink, the top and bottom of the fin, the top of the phase change cavity, as well as the ambient environment. The collected data was then analyzed to evaluate the heat transfer performance of the high-power COB LED lighting heat sink operating at 150W, with a focus on determining whether it meets the heat dissipation requirements for high-power COB LEDs.

By examining the wall surface temperature data recorded by the thermocouple, a temperature versus time line graph was generated. The horizontal axis represents time, while the vertical axis represents temperature. Figures 4 and 5 show the temperature variation at different measurement points: the negative solder joint maintains a stable temperature of

81.1°C, the top of the phase change cavity remains at 78.2°C, the bottom of the fin stays at 76.3°C, the top of the fin stabilizes at 67.5°C, and the ambient temperature is maintained at 27.5°C.

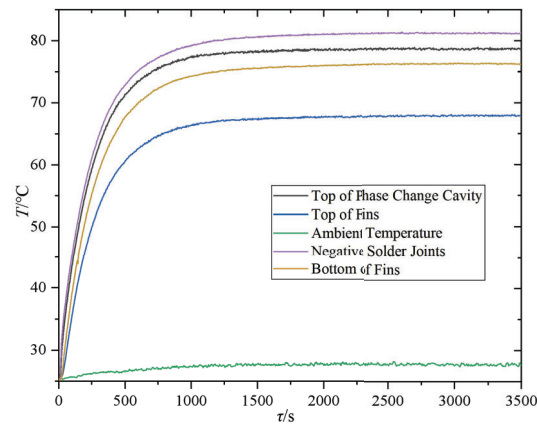


Figure 4 High-power COB LED lighting heat sink temperature of each measurement point

In comparison, the temperature of the negative solder joint in a conventional heat sink remains stable at 101.2°C, while the ambient temperature stabilizes at 24.46°C, as depicted in the figure 5.

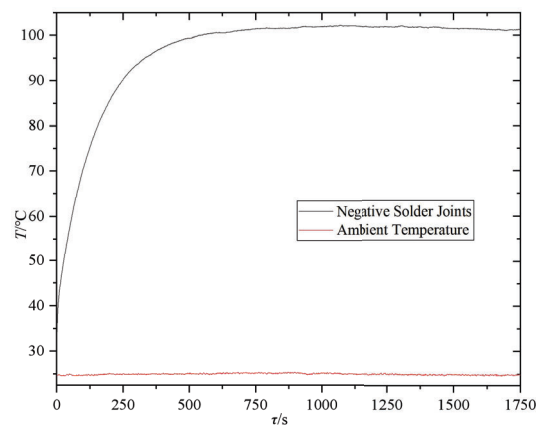


Figure 5 Traditional heat sink temperature of each measurement point

Upon powering the heat source, heat generation gradually occurs, leading to its accumulation. This heat is subsequently transferred to the phase change cavity through a homogeneous plate. Notably, the temperature at the top of the cavity is lower than that at the bottom of the fins, indicating the exceptional thermal conductivity of the phase change cavity. This characteristic enables efficient heat dissipation by rapidly transferring heat to the surroundings, thus preventing heat accumulation and enhancing the overall heat transfer capability of the radiator. The thermal conductivity of the phase change cavity was calculated to be above  $4 \times 10^3 \text{ W/m} \cdot \text{K}$ . Additionally, the arrangement of fins facilitates convective heat transfer. Experimental results demonstrate that under natural convection heat dissipation, the high-power COB LED heat sink experiences a temperature rise of 52°C with a thermal resistance of 0.35K/W when operated at 150W. This performance is ensured through the effective coordination between the phase change structure and fin design.

Comparatively, the high-power COB LED lighting heat sink exhibits a reduction in



temperature rise by 24.74°C when compared to a traditional heat sink, indicating a significant improvement in heat dissipation performance. Moreover, when compared to industry standard modules, the high-power COB LED lighting heat sink has the capability to effectively replace three industry standard modules (each rated at 50W) with a single 150W module. Furthermore, it achieves a weight reduction of 30% to 50% compared to similar power products both domestically and internationally, while also reducing the wind resistance area by nearly two-thirds. These advancements contribute to the realization of a high-power, structurally sound, and lightweight heat sink design.

## **6 CONCLUSIONS**

Through the design and research into the arrangement of convection fins and the preparation techniques for multicomponent phase change agents, we propose an optimized fin arrangement based on the existing manufacturing capabilities. We conduct simulations to analyze the effects of fin spacing, height, and thickness, and select a phase change agent with favorable chemical inertness, low boiling point, and low viscosity under vacuum conditions. Following the rational design and preparation of the fin structure and multicomponent phase change structure for high-power COB LED lighting heat sink, we fabricate samples and perform experimental analysis using the collected data. Additionally, we compare the performance of the heat sink with that of traditional standard module heat sinks.

The designed high-power COB LED lighting heat sink successfully meets the heat dissipation requirements of a 150W light source, exhibiting a temperature rise of 52.0°C and a thermal resistance of 0.35K/W. Compared with the traditional heat sink, the temperature rise of the negative solder joint of the high-power COB LED heat sink is reduced by 24.74°C, and the heat dissipation performance is significantly improved. Furthermore, it achieves a weight reduction of 30% to 50% and diminishes the wind resistance area by nearly two-thirds.

The development of high-power COB LED lighting heat sink plays a pivotal role in promoting the adoption of low-carbon energy-saving technologies in China and aligning with the national strategy of "Carbon peak and carbon neutrality." By fostering scientific and technological innovation and facilitating technology upgrades, we can effectively implement key projects centered on energy conservation and carbon reduction. Moreover, the demonstration and application of advanced green building technologies are encouraged, ultimately promoting comprehensive energy efficiency in urban environments.

## **7 OUTLOOK**

Throughout the design process and sample experiments, it was observed that both the heat sink structure and the multicomponent phase change configuration exhibited remarkable heat dissipation performance. These advancements effectively reduced the temperature of the heat source and facilitated rapid heat transfer, ensuring the safe, stable, and efficient operation of LED lighting devices. Notably, during the experimental investigation, it was discovered that there were directional limitations when rotating the heat sink by 90° for usage. To address this issue, further design studies could be conducted to explore improvements in the cavity wall structure, leveraging capillary force and enhancing hydrophobicity within the phase change cavity.

## REFERENCES

- [1] Simmons J A. Basic Research Needs for Solid State Lighting: LED Science.[J]. 2007.
- [2] Rui Wei, Mengjiao Guo. Application and development of LED light source [J]. Light Source and Lighting,2022(04):1-3.
- [3] Ma Wei. Analysis of the use of LED street lights in road lighting [J]. Electronic World,2017(11):177.
- [4] Xu Zhou. Research on high power COB-LED heat dissipation and heat sink design[D]. Jiangsu University,2018.
- [5] Trevisanello L, De Zuani F, Meneghini M, et al. Thermally activated degradation and package instabilities of low flux LEDs[C]// IEEE International Reliability Physics Symposium. IEEE, 2009:98-103.
- [6] Huazhen Peng, Zuojie Wen, Jianping Liu et al. Simulation of thermal characteristics of 300W-class high-power COB package LEDs [J]. Light Sources and Lighting,2022(05):54-57.
- [7] Xiaofeng Liu. Analysis on high-power LED heat dissipation technology [J]. Electronic World, 2018(10):145-146.
- [8] Zhongliang Shen, Bing Lu, Siwen Li et al. Advances in enhanced heat dissipation technology for high-power LEDs [J]. Light Industry Machinery, 2013, 31(02): 107-112.
- [9] Irvinehalliday D. Solid-state lighting: the only solution for the developing world[J].Proceedings of SPIE-The International Society for Optical Engineering, 2006,5941:59410N-59410N-15.
- [10] Defeng Mao, Weiling Guo, Guo Gao, Guangdi Shen. Analysis of thermal characteristics of power LEDs[J]. Journal of Lighting Engineering,2009,(2): 10-20.
- [11] Rongtian Yan, Wanxia Luo, Dezhao Liang . Thermal management design of a high-power LED module[J]. Electromechanical Engineering Technology,2013,42(11):43-45.

## ACKNOWLEDGEMENT

Corresponding Author: Chaoyue Liu

Affiliation: Changchun Cedar Electronics Technology Co., Ltd., Changchun 130103, China;

e-mail : liucy@ccxida.com

# IMPACT OF URBAN AIR POLLUTANTS ON THE NIGHT SKY BRIGHTNESS AND COLOR IN HOHHOT

Xuran Guo<sup>1</sup>, Yongqing Zhao<sup>1</sup>, Zhen Tian<sup>1,2</sup>, Xiaoming Su<sup>3,4</sup>

(1. School of Architecture and Planning, Hunan University, Changsha, China; 2. Hunan Key Laboratory of Sciences of Urban and Rural Human Settlements at Hilly Areas, Changsha, China; 3. Architecture College, Inner Mongolia University of Technology, Hohhot, China; 4. Inner Mongolia Key Laboratory of Green Building, Hohhot, China)

## ABSTRACT

Urban light pollution reduces the quality of life for all urban inhabitants, including people, animals, and plants. This study investigated the relationship between urban air pollution and urban light pollution. An unmanned aerial vehicle (UAV) was used to assess changes in the night sky's brightness, color, and their spatial distribution before and after the aggravation of air pollution. The results demonstrated that both the brightness and the area of night sky glow increase with higher urban air pollutant concentrations, and the night sky shifted towards red as the urban air pollutants concentration increased. Additionally, the brightness of the night sky decreased with height above ground. Furthermore, the study highlighted the advantages of using UAV observations for analyzing the night sky. Based on the research findings, controlling air pollutant emissions may have a positive impact on reducing the level and area of light pollution. Thus, it may promote sustainable urban environmental development.

Keywords: Light pollution, Night light environment, Air pollution, Particulate matter, Unmanned aerial vehicle

## 1. INTRODUCTION

Air pollution is a severe environmental problem in urban areas in China [1-3]. Air pollutants are known to have direct impacts on human health, as highlighted by several studies [4-7]. Furthermore, urban air pollutants can indirectly cause other types of environmental pollution such as water pollution [8-9] and soil pollution [10-11]. In addition to these effects, air pollution also contributes to light pollution in the night sky [12-14].

Night sky light pollution is caused by the unnatural increase in brightness and change in color of the night sky, which affects normal astronomical observation [15-17], animal physiological and behavioral processes [18-20], plant natural processes [21-22], and human health and mood [23-25]. Urban artificial lighting is the primary driver of night sky light pollution [15]. Still, changes in cloudiness [26-27], moon phase changes [28-29], and changes in aerosol particle composition and concentration can also impact the night sky environment [30-34]. Aerosol particles, produced by the emission of urban air pollutants and chemical reactions of gaseous pollutants in the night sky [35], have a significant impact on night sky light pollution.

Several studies have explored the impact of some urban air pollutants on night sky light pollution [13-14,30,34,36-38]. However, there are different views on whether urban air pollutants affect night sky brightness. Moreover, the effects of urban air pollutants on night sky brightness, color, and their spatial distribution are not fully understood. Therefore, the objectives of the study are:

1. Analyzing the effect of urban air pollutants on the spatial distribution of night sky brightness.
2. Analyzing the effect of urban air pollutants on the spatial distribution of night sky color.
3. Discussing the advantages of using UAVs to observe the night sky.

Through the analysis of the relationship between urban air pollution and urban light pollution, it is expected that the urban air pollution control policies and light pollution control policies can be coordinated to mitigate environmental degradation caused by urbanization.

## 2. METHODOLOGY

### 2.1 Observation site

Our study focuses on Hohhot in the Inner Mongolia Autonomous Region of northern China, which has been reported to have high levels of air pollutants [39-40] and night sky brightness [41]. Therefore, this city serves as an excellent observation site.

### 2.2 Observation process

The DJI MAVIC 3 was used for UAV observations of the night sky. The observation point chosen was Jinchuan Cultural Square, located on the western edge of Hohhot (Figure 1). The observations were conducted from 3:00-3:46 on April 28, 2023 (sunset period: from 21:08 on the 27th to 03:52 on the 28th) and from 3:00-3:46 on April 29, 2023 (sunset period: from 21:09 on the 28th to 03:48 on the 29th). The UAV took off from the square and took images of the night sky every 40 m from the original location towards the east. The camera onboard the UAV was a complementary metal oxide semiconductor (CMOS) sensor, and the camera and image parameters during image shooting are shown in Table 1.

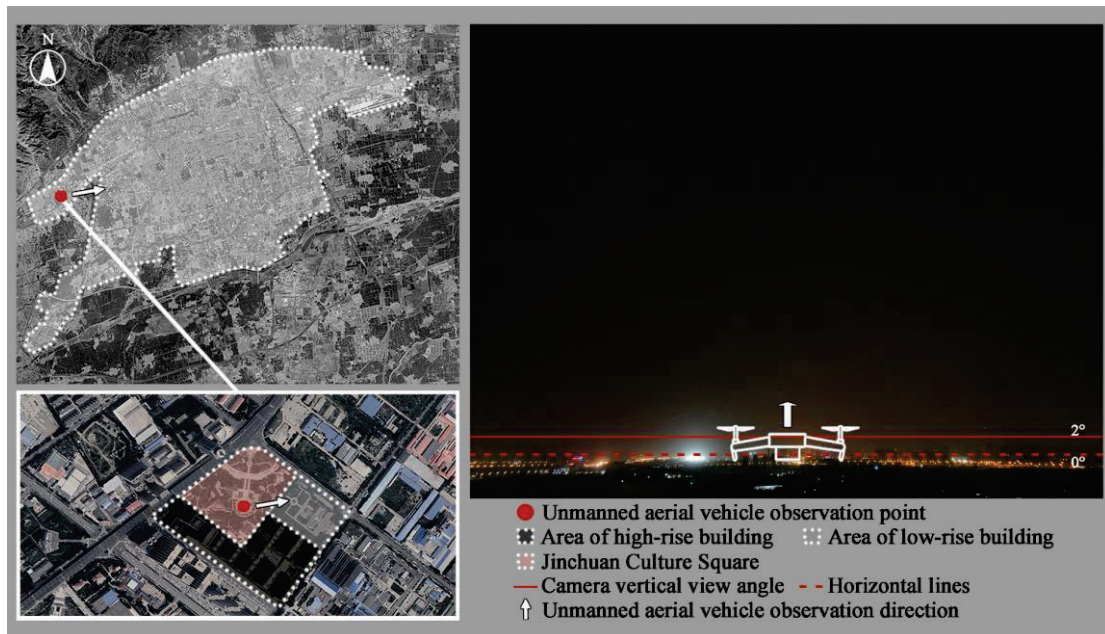


Figure 1. Location and direction of UAV observations and extracted section in UAV images

Table 1. Parameters of the UAV camera and image

Vertical angle	Image format	Image size	Field of view	ISO sensitivity	Lens aperture	Exposure value
+23°	RAW	5280 × 3956	84°	3200	F2.8	0.1s

### 2.3 Observation data

To better present the vertical variations of night sky brightness, the direct urban light component in each UAV image was removed (below the 2° vertical view angle of the UAV camera, as shown in Figure 1). For image analysis, the average digital number (DN) value of each grayscale image was extracted to represent the brightness variation [42-43]. The average DN value represents the average value of DN of each pixel in the image, which is a dimensionless index used to quantitatively describe the brightness magnitude of different bands in the image, ranging from 0 to 255 [44]. Additionally, the average DN values of RGB bands in each image were extracted to represent the color variation.

The concentrations of air pollutants, weather conditions, and moon phases during the observation period are presented in Table 2 and Table 3. The air pollutant concentrations were provided by the Department of Ecology and Environment of Inner Mongolia Autonomous Region (<https://sthjt.nmg.gov.cn/>), weather conditions were sourced from the Weather Channel (<https://weather.com/zh-CN/>), and moon phase data was obtained from the Chinese Astronomical Annual Calendar [45].

Table 2. Pollutant concentrations during observations

Time	AQI	PM <sub>2.5</sub> ( $\mu\text{g}/\text{m}^3$ )	PM <sub>10</sub> ( $\mu\text{g}/\text{m}^3$ )	SO <sub>2</sub> ( $\mu\text{g}/\text{m}^3$ )	CO ( $\text{mg}/\text{m}^3$ )	NO <sub>2</sub> ( $\mu\text{g}/\text{m}^3$ )	O <sub>3</sub> ( $\mu\text{g}/\text{m}^3$ )
2023/04/28 3:00-4:00	100	42	149	10	0.4	36	27
2023/04/29 3:00-4:00	52	20	53	6	0.4	41	13

Table 3. Weather conditions and moon phases during observations

Time	Weather condition	Moon phase
2023/04/28 3:00-3:46	Cloudless	Moonless
2023/04/29 3:00-3:46	Cloudless	Moonless

### 3. RESULTS

#### 3.1 Brightness

The UAV observations of the night sky in Hohhot reveal that when urban air pollutant concentrations increase, the brightness of the night sky at each height increases. Additionally, as the relative height above the ground increased from 40 to 480 meters, the night sky brightness decreased (Figure 2). Moreover, the decay of the night sky brightness accelerated when urban air pollutant concentrations increased. The DN value decay rose from 0.19 to 0.35 per 100 meters in grayscale.

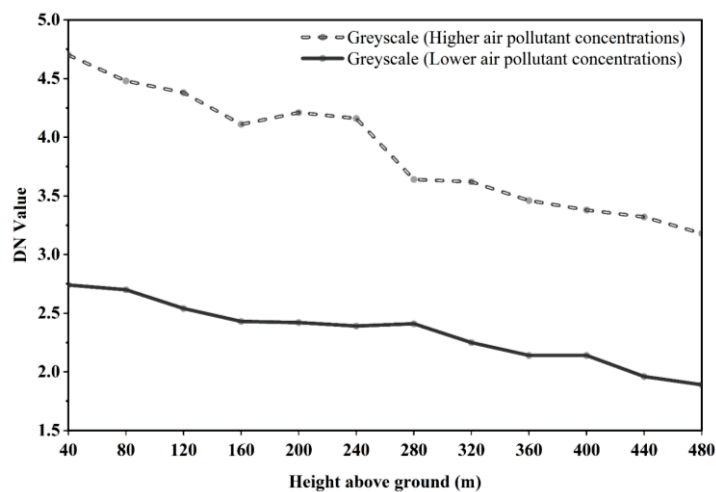


Figure 2. Changes in the vertical distribution of night sky brightness with increasing air pollutant concentrations



Furthermore, two images of the night sky at 480 meters with different air pollutant concentrations were compared, and the comparison showed that the area of the urban sky glow about doubled (Figure 3).

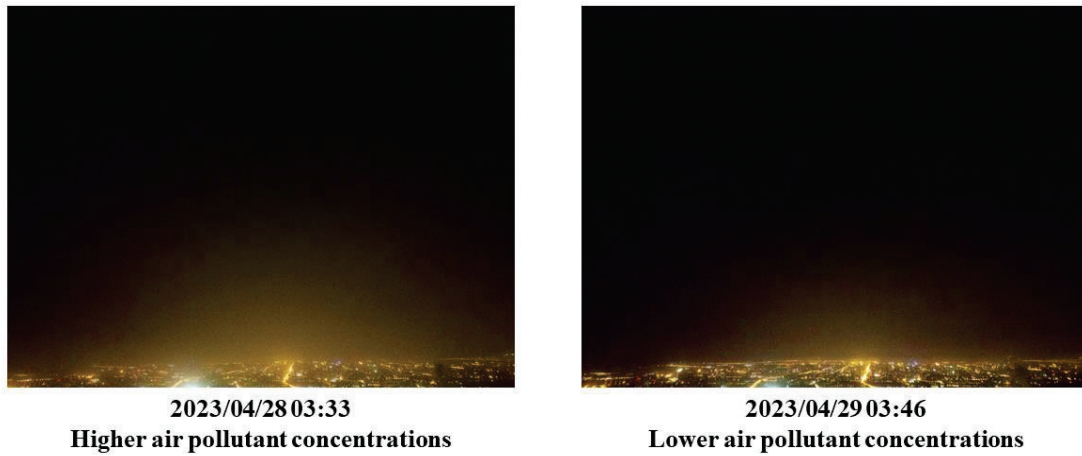


Figure 3. Changes in sky glowing area with increasing air pollutant concentrations (the brightness of images has been adjusted)

### 3.2 Color

Regarding color (Figure 4, Table 4), when air pollutant concentrations increased, the change of DN value in the blue band at each height was relatively weak, while the change of DN value in the green and red bands at each height was more noticeable, with the average DN value for each height increase of 3.74 in the green band and 5.01 in the red band. The color of each height of the night sky shifted towards red.

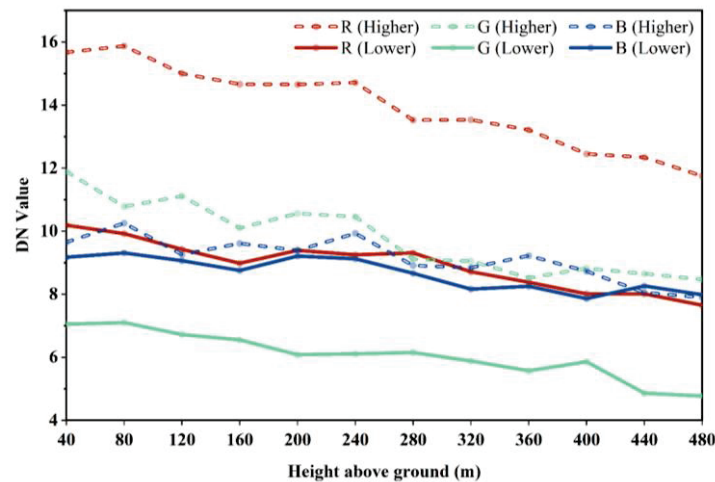


Figure 4. Changes in the vertical distribution of night sky color with increasing air pollutant concentrations

Table 4. Changes in night sky color at different heights with increasing air pollutant concentrations

Height above ground (m)	Changes in DN values		
	Red band	Green band	Blue band
40	5.48	4.84	0.48
80	5.95	3.68	0.94

120	5.58	4.39	0.20
160	5.68	3.55	0.86
200	5.26	4.48	0.18
240	5.46	4.35	0.81
280	4.21	2.96	0.25
320	4.82	3.17	0.68
360	4.83	2.95	0.97
400	4.44	2.96	0.87
440	4.33	3.79	-0.21
480	4.10	3.70	-0.08
Average for each height	5.01	3.74	0.50

### 3. DISCUSSION

#### 3.1 Color change in the night sky

In this study, it was observed that an increase in urban air pollutant concentrations resulted in a redder night sky, and based on the principle of aerosol light scattering [32], two reasons were concluded:

Firstly, in a clean night sky, red light, which has a longer wavelength, can penetrate the sky without being scattered, while the shorter wavelengths of green and blue light are scattered. However, when the atmosphere is polluted, there is more particulate matter (PM) in the night sky, and the red light that was not scattered before is also scattered by the PM, causing the night sky to appear redder than in a clean night sky.

Secondly, the night sky light that observers see is reflected light from artificial lighting into the sky, and this light must scatter multiple times to reach the observers' eyes. When the atmosphere is polluted, there is more PM in the reflective path, resulting in more extinction of shorter wavelength light and more attenuation of its energy. This leads to a shift in the night sky towards red.

Certainly, the scattering of particles in the atmosphere is much more complex than previously thought, and physical models are constantly being refined [46], with deeper principles waiting to be discovered.

#### 3.2 Findings and advantage of night sky observations by UAVs

Observing the night sky through UAVs has revealed two fascinating phenomena. The first is that when the night sky is viewed horizontally, its brightness decreases as the relative height above ground increases. We believe that the reason for this phenomenon is that when the scattering in the atmosphere is dominated by the scattering of PM, the energy of the ground-based artificial light passing through the PM in the atmosphere will gradually decay as the thickness of the atmosphere increases, and the energy of its light scattered by the PM will also gradually decay. Additionally, considering that the concentration of PM may decrease with the increase of atmospheric height [47-48], its ability to scatter ground-based artificial light will also decrease. Combining these two aspects, the brightness of the night sky that we observe gradually decreases as the observation height increases.

The second phenomenon is that the night sky glowing area enlarges with an increase in pollutant concentrations. Our analysis suggests that when air pollutant concentrations rise, higher and more distant areas of the urban night sky are also polluted. This causes urban artificial light to be scattered higher and more distant in the night sky, resulting in a wider glowing area of the night sky.

These phenomena could not have been discovered without the help of UAVs. A new advantage of using UAVs to observe the night sky, as opposed to using UAVs for ground

observations [49-50] and loading a luminance meter to measure the night sky [51], is that UAV images allow for easier analysis of the distribution of night sky brightness and color in space.

#### 4. CONCLUSIONS

This study aimed to investigate the effects of urban pollutants on the brightness and color of the night sky. To achieve this, a comprehensive analysis was conducted, comparing the variations in night sky brightness and color, along with their spatial distribution, before and after the aggravation of air pollution. Notably, the study also shed light on the novel utility of UAVs for observing the night sky. The main conclusions are:

1. When the urban air pollutant concentrations increase, the night sky brightness increases and the color of the night sky shifts towards red.
2. The night sky glowing area increases with the urban air pollutant concentrations, while the night sky brightness decreases with increasing height above ground.
3. UAVs can more easily analyze the distribution of night sky brightness and color in space.

Increased air pollutants may deteriorate the night sky light pollution and may expand its influence in urban environment. The benefits of improving urban air quality are twofold: it not only reduces air pollution but also minimizes light pollution, thereby improving the quality of life for all urban inhabitants, including people, animals, and plants. Therefore, controlling air pollution is essential to mitigate the negative effects of light pollution in urban areas and contribute to a healthier, more sustainable environment.

#### REFERENCE

- [1] Chan, C. K., & Yao, X. (2008). Air pollution in mega cities in China. *Atmospheric Environment*, 42(1), 1-42.
- [2] Huang, R. J., Zhang, Y., Bozzetti, C., Ho, K. F., Cao, J. J., Han, Y., Daellenbach, K. R., Slowik, J. G., Platt, S. M., Canonaco, F., Zotter, P., Wolf, R., Pieber, S. M., Bruns, E. A., Crippa, M., Ciarelli, G., Piazzalunga, A., Schwikowski, M., Abbaszade, G., . . . Prévôt, A. S. H. (2014). High secondary aerosol contribution to particulate pollution during haze events in China. *Nature*, 514(7521), 218-222.
- [3] Shao, M., Tang, X., Zhang, Y., & Li, W. (2006). City clusters in China: air and surface water pollution. *Frontiers in Ecology and the Environment*, 4(7), 353-361.
- [4] Brook, R. D., Rajagopalan, S., Pope III, C. A., Brook, J. R., Bhatnagar, A., Diez-Roux, A. V., Holguin, F., Hong, Y., Luepker, R. V., Mittleman, M. A., Peters, A., Siscovick, D., Smith Jr, S. C., Whitsett, L., & Kaufman, J. D. (2010). Particulate Matter Air Pollution and Cardiovascular Disease. *Circulation*, 121(21), 2331-2378.
- [5] Brunekreef, B., & Holgate, S. T. (2002). Air pollution and health. *The Lancet*, 360(9341), 1233-1242.
- [6] Lim, S. S., Vos, T., Flaxman, A. D., Danaei, G., Shibuya, K., Adair-Rohani, H., AlMazroa, M. A., Amann, M., Anderson, H. R., Andrews, K. G., Aryee, M., Atkinson, C., Bacchus, L. J., Bahalim, A. N., Balakrishnan, K., Balmes, J., Barker-Collo, S., Baxter, A., Bell, M. L., . . . Ezzati, M. (2012). A comparative risk assessment of burden of disease and injury attributable to 67 risk factors and risk factor clusters in 21 regions, 1990-2010: a systematic analysis for the Global Burden of Disease Study 2010. *The Lancet*, 380(9859), 2224-2260.
- [7] Pope III, C. A., Burnett, R. T., Thun, M. J., Calle, E. E., Krewski, D., Ito, K., & Thurston, G. D. (2002). Lung Cancer, Cardiopulmonary Mortality, and Long-term Exposure to Fine Particulate Air Pollution. *JAMA*, 287(9), 1132-1141.
- [8] Shi, M., Geng, B., Zhao, T., & Wang, F. (2021). Influence of atmospheric deposition on surface water quality and DBP formation potential as well as control technology of rainwater DBPs: a review. *Environmental Science: Water Research & Technology*, 7, 2156-2165.
- [9] Souza, I. D. C., Morozeski, M., Mansano, A. S., Mendes, V. A., Azevedo, V. C., Matsumoto, S. T., Elliott, M., Monferrán, M. V., Wunderlin, D. A., & Fernandes, M. N. (2021). Atmospheric particulate matter from an industrial area as a source of metal nanoparticle contamination in aquatic ecosystems. *Science of the Total Environment*, 753, 14976.
- [10] Chen, J. (2007). Rapid urbanization in China: A real challenge to soil protection and food security. *CATENA*, 69(1), 1-15.
- [11] Grantz, D., Garner, J., & Johnson, D. (2003). Ecological effects of particulate matter. *Environment International*, 29(2-3), 213-239.

- [12] Liu, M., Li, W., Zhang, B., Hao, Q., Guo, X., & Liu, Y. (2020). Research on the influence of weather conditions on urban night light environment. *Sustainable Cities and Society*, 54, 101980.
- [13] Liu, M., Liu, X., Zhang, B., Li, Y., Luo, T., & Liu, Q. (2022). Analysis of the evolution of urban nighttime light environment based on time series. *Sustainable Cities and Society*, 78, 103660.
- [14] Posch, T., Binder, F., & Puschnig, J. (2018). Systematic measurements of the night sky brightness at 26 locations in Eastern Austria. *Journal of Quantitative Spectroscopy and Radiative Transfer*, 211, 144-165.
- [15] Falchi, F., Cinzano, P., Duriscoe, D., Kyba, C. C. M., Elvidge, C. D., Baugh, K., Portnov, B. A., Rybnikova, N. A., & Furgoni, R. (2016). The new world atlas of artificial night sky brightness. *Science Advances*, 2(6).
- [16] Falchi, F., Ramos, F., Bará, S., Sanhueza, P., Arancibia, M. J., Damke, G., & Cinzano, P. (2022). Light pollution indicators for all the major astronomical observatories. *Monthly Notices of the Royal Astronomical Society*, 519(1), 26-33.
- [17] Green, R. F., Luginbuhl, C. B., Wainscoat, R. J., & Duriscoe, D. (2022). The growing threat of light pollution to ground-based observatories. *The Astronomy and Astrophysics Review*, 30(1).
- [18] Kyba, C. C. M., Ruhtz, T., Fischer, J., & Hölker, F. (2011). Lunar skylight polarization signal polluted by urban lighting. *Journal of Geophysical Research: Atmospheres*, 116(D24).
- [19] Russart, K. L., & Nelson, R. J. (2018). Artificial light at night alters behavior in laboratory and wild animals. *Journal of Experimental Zoology Part A: Ecological and Integrative Physiology*, 329(8-9), 401-408.
- [20] Shimada, T., Limpus, C. J., FitzSimmons, N. N., Ferguson, J., Limpus, D., & Spinks, R. K. (2023). Sky glow disrupts the orientation of Australian flatback turtles *Natator depressus* on nesting beaches. *Regional Environmental Change*, 23(20).
- [21] Solano-Lamphar, H., & Kocifaj, M. (2018). Numerical research on the effects the skyglow could have in phytochromes and RQE photoreceptors of plants. *Journal of Environmental Management*, 209, 484-494.
- [22] Lian, X., Jiao, L., Zhong, J., Jia, Q., Liu, J., Liu, J., & Liu, Z. (2021). Artificial light pollution inhibits plant phenology advance induced by climate warming. *Environmental Pollution*, 291, 118110.
- [23] Argys, L. M., Averett, S. L., & Yang, M. (2021). Light pollution, sleep deprivation, and infant health at birth. *Southern Economic Journal*, 87(3), 849-888.
- [24] Benfield, J. A., Nutt, R. J., Taff, B. D., Miller, Z. D., Costigan, H., & Newman, P. (2018). A laboratory study of the psychological impact of light pollution in national parks. *Journal of Environmental Psychology*, 57, 67-72.
- [25] Zhong, C., Franklin, M., Wiemels, J., McKean-Cowdin, R., Chung, N. T., Benbow, J., Wang, S. S., Lacey, J. V., & Longcore, T. (2020). Outdoor artificial light at night and risk of non-Hodgkin lymphoma among women in the California Teachers Study cohort. *Cancer Epidemiology*, 69, 101811.
- [26] Kyba, C. C. M., Ruhtz, T., Fischer, J., & Hölker, F. (2012). Red is the new black: how the colour of urban skyglow varies with cloud cover. *Monthly Notices of the Royal Astronomical Society*, 425(1), 701-708.
- [27] Ścieżor, T. (2020). The impact of clouds on the brightness of the night sky. *Journal of Quantitative Spectroscopy and Radiative Transfer*, 247, 106962.
- [28] Krieg, J. (2021). Influence of moon and clouds on night illumination in two different spectral ranges. *Scientific Reports*, 11, 20642.
- [29] Puschnig, J., Schwöpe, A., Posch, T., & Schwarz, R. (2014). The night sky brightness at Potsdam-Babelsberg including overcast and moonlit conditions. *Journal of Quantitative Spectroscopy and Radiative Transfer*, 139, 76-81.
- [30] Bustamante-Calabria, M., Sánchez de Miguel, A., Martín-Ruiz, S., Ortiz, J. L., Vilchez, J. M., Pelegrina, A., García, A., Zamorano, J., Bennie, J., & Gaston, K. J. (2021). Effects of the COVID-19 Lockdown on Urban Light Emissions: Ground and Satellite Comparison. *Remote Sensing*, 13(2), 258.
- [31] Garstang, R. H. (1986). Model for Artificial Night-Sky Illumination. *Publications of the Astronomical Society of the Pacific*, 98(601), 364-375.
- [32] Horvath, H. (2014). Basic optics, aerosol optics, and the role of scattering for sky radiance. *Journal of Quantitative Spectroscopy and Radiative Transfer*, 139, 3-12.
- [33] Kocifaj, M., & Barentine, J. C. (2021). Air pollution mitigation can reduce the brightness of the night sky in and near cities. *Scientific Reports*, 11, 14622.

- [34] Ścieżor, T., & Czaplicka, A. (2020). The impact of atmospheric aerosol particles on the brightness of the night sky. *Journal of Quantitative Spectroscopy and Radiative Transfer*, 254, 107168.
- [35] Jenkin, M. E., & Clemitshaw, K. C. (2000). Ozone and other secondary photochemical pollutants: chemical processes governing their formation in the planetary boundary layer. *Atmospheric Environment*, 34(16), 2499-2527.
- [36] National Institute for Public Health and the Environment. (2010). *Effects of atmospheric conditions on night sky brightness*. Ministry of Health, Welfare and Sport.
- [37] Ścieżor, T., & Kubala, M. (2014). Particulate matter as an amplifier for astronomical light pollution. *Monthly Notices of the Royal Astronomical Society*, 444(3), 2487-2493.
- [38] Pun, C. S. J., & So, C. W. (2012). Night-sky brightness monitoring in Hong Kong. *Environmental Monitoring and Assessment*, 184, 2537-2557.
- [39] Lyu, Y., Liu, L., Guo, L., Yang, Y., Qu, Z., Hu, X., & Zhang, G. (2017). Deposited atmospheric dust as influenced by anthropogenic emissions in northern China. *Environmental Monitoring and Assessment*, 189, 390.
- [40] Zheng, C., Zhao, C., Li, Y., Wu, X., Zhang, K., Gao, J., Qiao, Q., Ren, Y., Zhang, X., & Chai, F. (2018). Spatial and temporal distribution of NO<sub>2</sub> and SO<sub>2</sub> in Inner Mongolia urban agglomeration obtained from satellite remote sensing and ground observations. *Atmospheric Environment*, 188, 50-59.
- [41] Su, X., Hao, Z., & Zhang, M. (2015). Measure of Night-sky Light Pollution in Hohhot. *China Illuminating Engineering Journal*, 26(4), 124-128.
- [42] Niblock, J. H., Peng, J. X., McMenemy, K. R., & Irwin, G. W. (2009). Automated Object Identification and Position Estimation for Airport Lighting Quality Assessment. In Ranchordas, A., Araújo, H.J., Pereira, J.M., Braz, J. (Eds.), *VISIGRAPP 2008: Computer Vision and Computer Graphics. Theory and Applications* (pp. 262-275). Springer.
- [43] Wei, S., Jiao, W., Long, T., Liu, H., Bi, L., Jiang, W., Portnov, B. A., & Liu, M. (2020). A Relative Radiation Normalization Method of ISS Nighttime Light Images Based on Pseudo Invariant Features. *Remote Sensing*, 12(20), 3349.
- [44] Li, X., Levin, N., Xie, J., & Li, D. (2020). Monitoring hourly night-time light by an unmanned aerial vehicle and its implications to satellite remote sensing. *Remote Sensing of Environment*, 247, 111942.
- [45] Purple Mountain Observatory, Chinese Academy of Sciences. (2022). 2023 Chinese astronomical annual calendar. Science Press.
- [46] Kómar, L., & Nečas, A. (2023). Effect of cloud micro-physics on zenith brightness in urban environment. *Journal of Quantitative Spectroscopy & Radiative Transfer*, 302, 108563.
- [47] Dubey, R., Patra, A. K., Joshi, J., Blankenberg, D., & Nazneen. (2022). Evaluation of vertical and horizontal distribution of particulate matter near an urban roadway using an unmanned aerial vehicle. *Science of the Total Environment*, 836, 155600.
- [48] Dubey, R., Patra, A. K., & Nazneen. (2022). Vertical profile of particulate matter: A review of techniques and methods. *Air Quality, Atmosphere & Health*, 15, 979-1010.
- [49] Massetti, L., Paterni, M., & Merlino, S. (2022). Monitoring Light Pollution with an Unmanned Aerial Vehicle: A Case Study Comparing RGB Images and Night Ground Brightness. *Remote Sensing*, 14(9), 2052.
- [50] Podor, A., & Huszar, G. (2022, November 21-22). *Detecting light pollution with UAV, a Hungarian case study* [Paper presentation]. 2022 IEEE 22nd International Symposium on Computational Intelligence and Informatics and 8th IEEE International Conference on Recent Achievements in Mechatronics, Automation, Computer Science and Robotics (CINTI-MACRO), Budapest, Hungary.
- [51] Karpińska, D., & Kunz, M. (2023). Vertical Variability of Night Sky Brightness in Urbanised Areas. *Quaestiones Geographicae*, 42(1), 5-14.

## ACKNOWLEDGEMENT

This work was supported by the National Natural Science Foundation of China (51978429, 51908298), Hunan Provincial Natural Science Foundation (2023JJ30151, 2020JJ4608), Hunan Key Laboratory of Science of Urban and Rural Human Settlements at Hilly Areas (2020TP1009).

Corresponding Author Name: Zhen Tian

Affiliation: School of Architecture and Planning, Hunan University, Changsha, China

e-mail: [zhentian@hnu.edu.cn](mailto:zhentian@hnu.edu.cn)



## STUDY OF LIGHTING METHOD CONSIDERING YOUNG RESIDENTS' CIRCADIAN RHYTHMS

Jingru Shen<sup>1</sup>, Jaeyoung HEO<sup>1</sup>, Youko Inoue<sup>2</sup>

(Nara Women's University<sup>1</sup>, The Open University of Japan<sup>2</sup>, Nara, Japan)

### ABSTRACT

In this paper, design material for appropriate lighting control is provided by comparing results between day and night for lighting impression and heart rate. The final purpose of this research is to propose a lighting method that considers resident's circadian rhythm.

The subjects were 13 young women aged 20-24 with normal vision. The lighting is 6 conditions, a combination of illuminance (50lx, 220lx, 700lx) and correlated colour temperature (3000K, 5300K). Experiments are conducted twice in day and night (8:00 and 20:00) on the same day. Subjects wore Fitbit Charge 5, a device that measures heart rate, and evaluated the lighting environment while sitting in a chair and resting. The lighting conditions were randomly presented to the subjects, and the evaluation was performed three times: immediately after the presentation, 10 minutes later, and 20 minutes later. The elapsed time from immediately after the presentation is called adaptation time. Heart rate was measured at 1-minute intervals. A 7-step semantic differential method was used for lighting evaluation.

This paper reports on the examination results using the average values of all subjects. Comparing the results in day and night, although there were no significant differences. Regarding the result of heart rate, there is little difference between daytime and night except in the case of 50lx3000K and 220lx3000K. In the results of impression evaluation for lighting, the relationship between day and night differs depending on the lighting conditions. At 50lx during steady state, it was shown that the evaluation in the day was higher than in the night. The three perceptions, "Bright - Dark", "Comfortable - Uncomfortable", and "Not Tired - Tired" had the same trend, to decrease as the illuminance increased in three levels of illuminance: 50lx, 220lx, and 700lx. The tendency of evaluation by adaption time is different in day and night. In the case of "Comfortable-Uncomfortable", the longer the adaption time in the day, the higher the value in all conditions.

Keywords : Lighting Method, Impression Evaluation, Circadian Rhythms, Day and Night, Adaption Time

### 1. INTRODUCTION

In recent years, attention has been paid to create a comfortable environment that considers the attributes of residents. In the lighting industry, aiming to create a comfortable and healthy lighting environment, the development of lighting fixtures with a dimming function is progressing. Currently, a system called "Rhythm Support Lighting System" is mainly used in medical and welfare facilities

to maintain and improve the biorhythm function of the elderly<sup>1</sup>. LED lighting fixtures with dimming and colour-tuning functions are being used in ordinary homes as well, however, lighting optimization systems that match the attributes and circadian rhythms of residents have not yet spread.

In past research, we clarified the permissible dimming speed for lighting control methods considering comfort and energy consumption<sup>2</sup>. However, elapsed time and circadian rhythm are not considered. In the report considering the circadian rhythm, it was clarified that the lighting environment with high colour temperature and high illuminance in the morning and low colour temperature and low illuminance at night is preferred<sup>3</sup>. However, the elapsed time has not been explored. It has been reported that illuminance, which is set as brightness suitable for relaxation, is affected by elapsed time and initial adaptation level<sup>4</sup>, but the circadian rhythm was not considered. Although there are many studies on illuminance and heart rate, there are few studies on lighting conditions, heart rate, and day and night.

Therefore, in this paper, design material for appropriate lighting control is provided by comparing results between day and night for lighting impression and heart rate.

## 2. METHODS

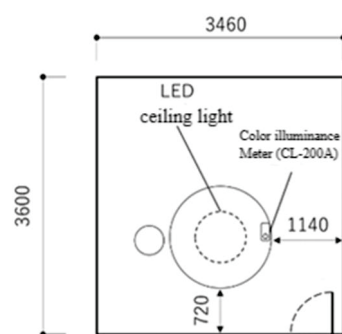


Figure 1. Laboratory layout



Figure 2. Experiment scene

The experiment was conducted from October 17th to November 24th, 2022, at the lighting environment laboratory at Nara Women's University. Figures 1 and 2 show the experimental environment. The dimensions are W3.5m×D3.6m×H2.4m. The interior is completely white, and the lighting equipment is a general diffusion-type LED ceiling light.



Figure 3. Perception questionnaire

The subjects were 13 young women aged 20-24 with normal vision. The lighting is 6 conditions, a combination of illuminance (50lx, 220lx, 700lx) and correlated colour temperature (3000K, 5300K). Experiments are conducted twice in day and night (8:00 and 20:00) on the same day. Subjects wore

Fitbit Charge 5, a device that measures heart rate, and evaluated the lighting environment while sitting in a chair and resting. A 7-step semantic differential method was used for lighting evaluation. Figure 3 shows the Perception questionnaire. “Bright-Dark” and “Warm-Cool” are evaluated for illuminance and correlated colour temperature (CCT), and “Comfortable-Uncomfortable” is examined as comprehensive evaluations and lastly evaluated “Not-tired-Tired”. The lighting conditions were presented randomly to the subjects. The evaluation was performed three times to consider the effect of time: immediately after the presentation, 10 minutes later, and 20 minutes later. The elapsed time from immediately after the presentation is called adaptation time. Heart rate was measured at a 1-minute interval.

### 3. RESULT

This paper reports on the results of the examination using the average values of all subjects.

#### 3.1. CHANGES IN HEART RATE FOR EACH LIGHTING CONDITION

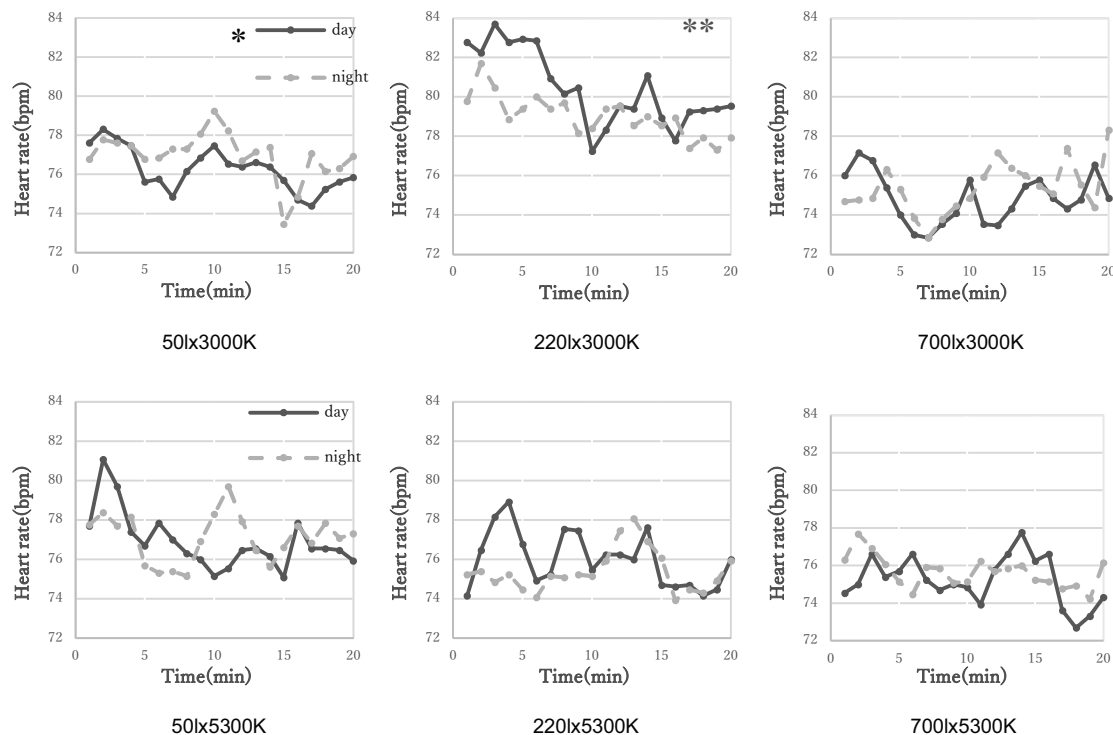


Figure 4. Changes in heart rate for each light condition

Figure 4 shows the average heart rate over time for each lighting condition. \*\* indicates that a significant difference between day and night was obtained with a risk rate of 5% or less, and \* indicates that a significant difference was obtained with a risk rate of  $5\% < p < 10\%$ . Under the condition of 5400K, no difference between day and night was observed, but under the condition of 3000K, a significant difference was obtained at 220lx3000K ( $p = **$ ,  $p < 0.05$ ), and at 50lx3000K ( $p = .06$ ,

0.05<math>p<0.1</math>). It showed a high heart rate under 220lx3000K lighting conditions both day and night. It showed a relatively low heart rate at 700lx regardless of CCT.

### 3.2. RESULTS OF IMPRESSION EVALUATION OF EACH LIGHTING CONDITION

Comparing the results between day and night, although there were no significant differences.

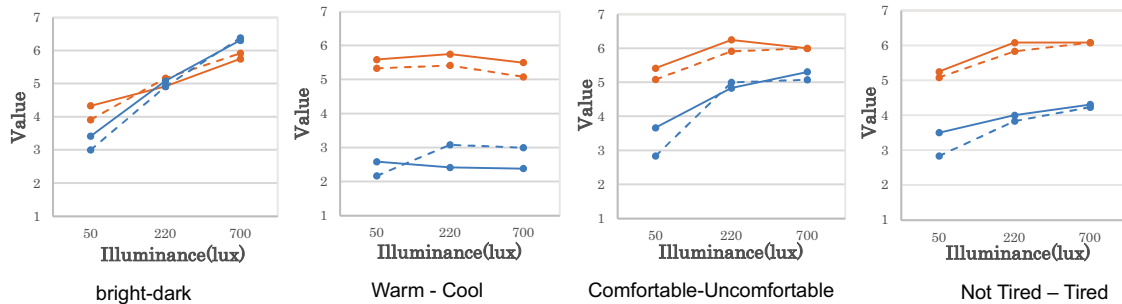


Figure 5. Changes in impression evaluation for each illuminance (Solid line: day, dotted line: night, blue: 5300K, orange: 3000K)

Figure. 5 shows the results of impression evaluation at 20 minutes later (steady state). For the 3 perceptions, "Bright - Dark", "Comfortable - Uncomfortable", and "Not Tired - Tired", the value tended to increase as the illuminance increased. It felt brighter in the daytime at 50lx. As the illuminance increased, the difference became smaller, and at 700lx felt slightly brighter at night. At 5300K, it felt cooler in the day, and at 3000K, it felt warmer in the day. "Comfortable- Uncomfortable" and "Not Tired- Tired" had the same trend, with a slightly more positive impression in day. Regardless of the illuminance, 3000K gave a more positive impression.

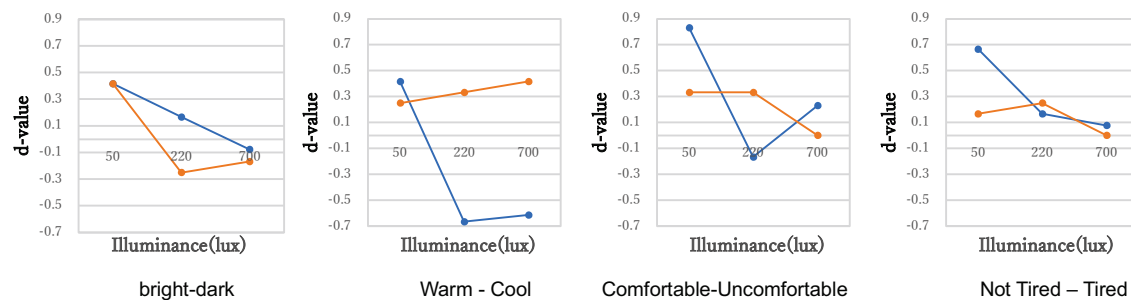


Figure 6. The difference between the day's value and the night's value (Blue: 5300K, orange: 3000K)

Figure. 6 shows the difference in impression evaluation between day and night (= impression evaluation in the day - impression evaluation at night). If the value is a positive number, the evaluation in the day is high, and it is closer to 0, the smaller the difference between day and night. In all conditions, the evaluation at 50lx was higher in the day than at night. The three perceptions, "Bright - Dark", "Comfortable - Uncomfortable", and "Not Tired - Tired" had the same trend, to decrease as the illuminance increased. In "Warm - Cool", the evaluation value in the day is high at 50lx regardless of CCT, but at 220lx and 700lx, the magnitude relationship between day and night differs depending on CCT.

### 3.3. RELATIONSHIP BETWEEN ADAPTATION TIME AND IMPRESSION EVALUATION

The tendency of evaluation by adaption time is different in the day and night. Although there was no significant difference

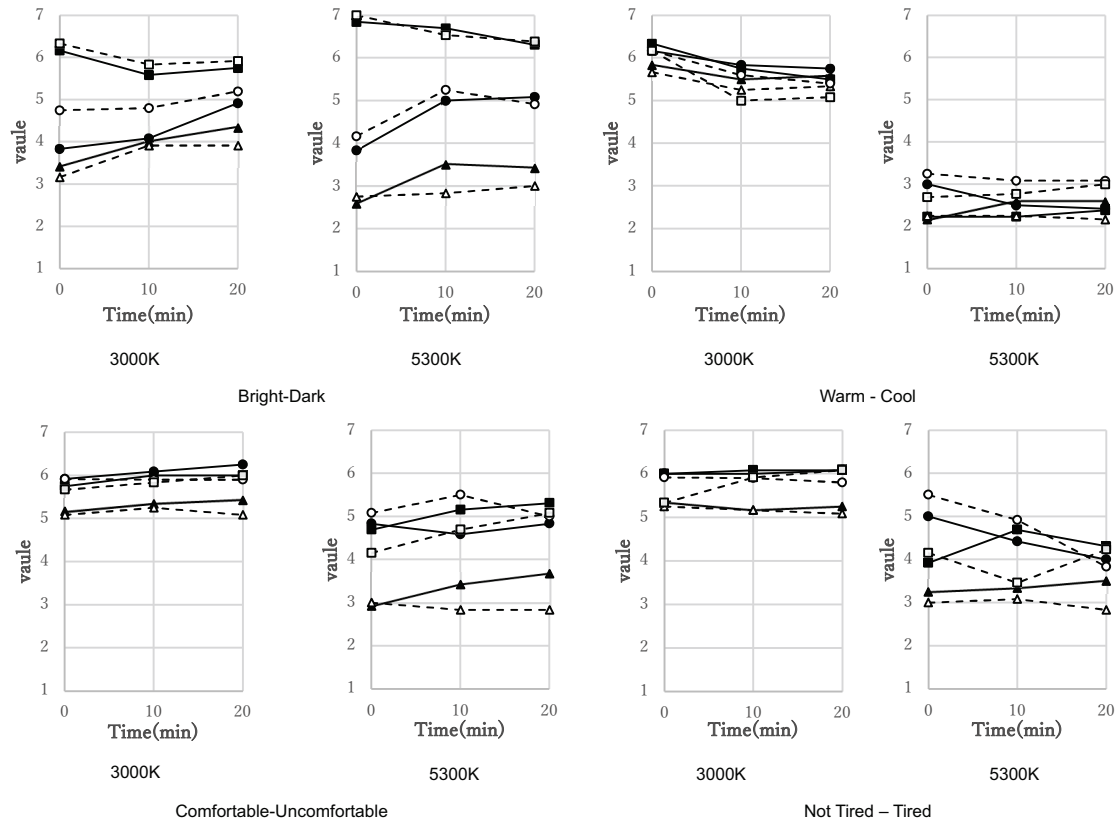


Figure 7. Relationship between adaption time and impression evaluation  
( $\triangle$ : 50lx,  $\circ$ : 220lx,  $\square$ : 700lx, solid line: day, dotted line: night)

Figure. 7 shows the relationship between adaptation time and impression evaluation. At 50lx and 220lx, the longer the adaptation time was, the brighter it felt, regardless of CCT. About the "Warm - Cool", in the case of 3000K, the difference between day and night was small. In the case of 5300K, after 20 minutes of adaptation, the difference between day and night was clearly recognized. About "Comfortable- Uncomfortable ", in the day, the longer the adaptation time was, it had the tendency to be felt more comfortable in every lighting condition. In the case of "Not Tired – Tired", it felt less tired in every illuminance at 3000K. However, at 5300K, there was a tendency to become slightly more fatigued as longer adaption time.



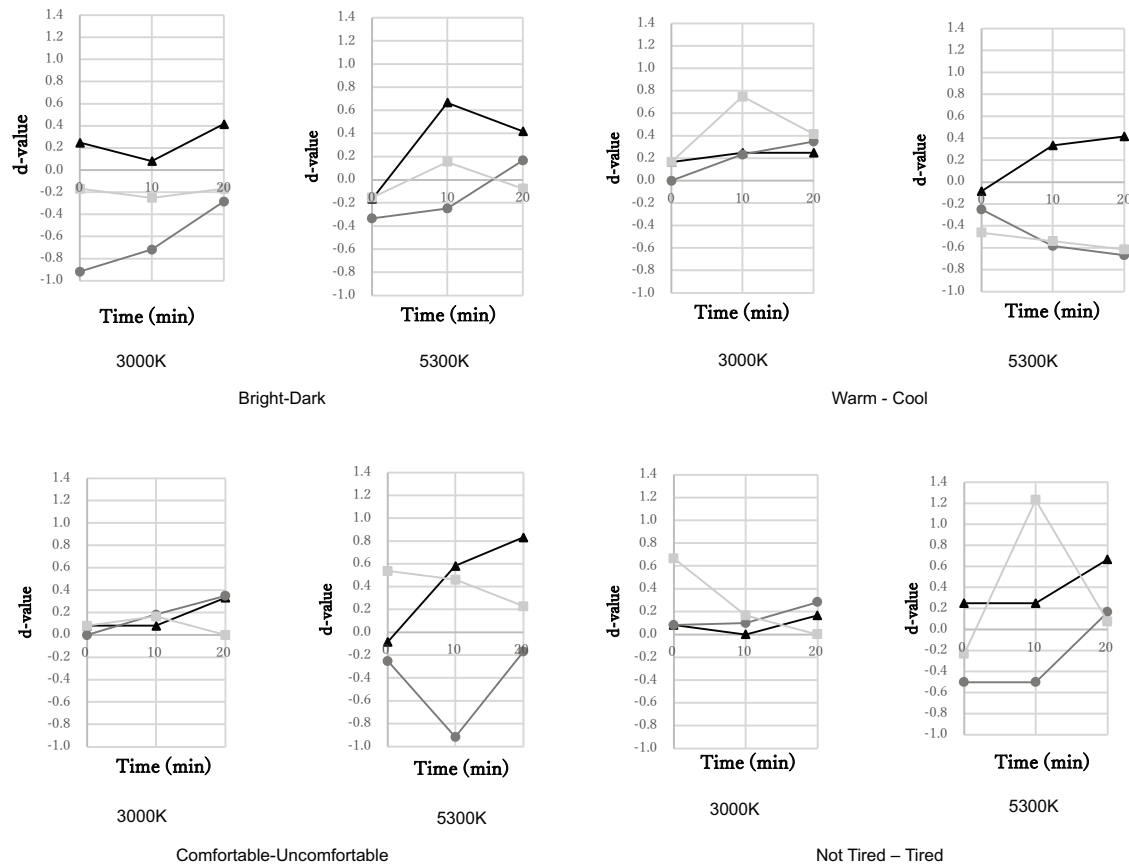


Figure 8. The difference between the day's value and the night's value  
( $\triangle$ : 50lx,  $\circ$ : 220lx,  $\square$ : 700lx)

Figure 8 shows the difference in impression evaluation between day and night (= impression evaluation in the day - impression evaluation at night). If the value is positive-number, the evaluation in the day is high, and it is closer to 0, the smaller the difference between day and night. At 3000K, the values of all conditions were on the positive side in "Warm-Cool", "Comfortable-Uncomfortable" and "Not Tired-Tired", indicating that the evaluation value in the day was high. In the case of 3000K, under the conditions expected 700lx, as the adaption time became longer, it showed an upward trend, and it indicates that the difference between day and night became larger. In " Warm-Cool ", in the case of 5300K, 50lx showed a positive value, 220lx and 700lx showed a negative value, and showed a tendency away from 0 as the adaption time increased. Therefore, it indicates that the day's evaluation is high at 50lx, but the night's evaluation is high at 220lx and 700lx. And the longer the adaption time, the more significant difference between day and night.

#### 4. DISCUSSION AND CONCLUSIONS

In this paper, we used the average values of all subjects to evaluate the illuminance and CCT of the lighting environment in day and night: " Bright-Dark", "Warm-Cool", "Comfortable-Uncomfortable", "Not-tired-Tired". Comparing the results in day and night, although there were no significant differences.

There was little difference in heart rate between day and night, and a significant difference was seen between the conditions of 50lx3000K and 220lx3000K. Next time, instead of heart rate, we will use heart rate variability (HRV) to visualize and analyse stress responses.

In the results of impression evaluation for lighting, the relationship between day and night differs depending on the lighting conditions. At 50lx during steady state, it was shown that the evaluation in the day was higher than in the night. The three perceptions, "Bright - Dark", "Comfortable - Uncomfortable", and "Not Tired - Tired" had the same trend, to decrease as the illuminance increased in three levels of illuminance: 50lx, 220lx, and 700lx. The tendency of evaluation by adaption time is different in day and night. In the case of "Comfortable-Uncomfortable", the longer the adaption time in the day, the higher the value in all lighting conditions.

In the future, individual differences and the relationship between perceptions will continue to be examined.

## REFERENCES

- [1] Masahiro Tezuka: Circadian Rhythm Lighting, J.Illum.Engng.Inst.Jpn., 42 (1), 11-16, 2022
- [2] Tango Mizuki: Study on the lighting adjustment in consideration of age and activities of daily living,-Part.1 Influence of changing ratio and speed for a simultaneous change of illuminance and correlated color temperature in young people-, The illuminating engineering institute of Japan conference, 6-P-13, 2020
- [3] Naohiro Toda: The effect of light exposure on circadian rhythm, Journal of the Illuminating Engineering Institute of Japan 91 (10), 655-658, 2007-10
- [4] Kyoko Ishida: Study on Brightness for Relaxation, - Influence of Initial Adaptation Level and Elapsed Time -, J.Illum.Engng.Inst.Jpn.Vol.89 No.8A,2005
- [5] Jingru Shen: Study of Lighting Method Considering Residents' Circadian Rhythms (Part 1)  
—Morning and evening comparison of young people's impressions of lighting—, AIJ conference, 40213, 2023

## ACKNOWLEDGEMENTS

This work was supported by JSPS KAKENHI Grant Number JP21K02108.

Corresponding Author Name: Jaeyoung HEO

Affiliation: Nara Women's University, Nara, Japan

e-mail: heo@cc.nara-wu.ac.jp

## RESEARCH OF CURRENT BEDROOM LIGHTING SITUATION FOR THE ELDERLY RISING AT NIGHT IN CHINA

Junliang Li<sup>1,2</sup>, Tongyue Wang<sup>1,2</sup>, Rongdi Shao<sup>1,2</sup>, Luoxi Hao<sup>1,2</sup>

(1. School of Architecture and Urban Planning, Tongji University, Shanghai 200092, China;

2. Key Laboratory of Ecology and Energy-saving Study of Dense Habitat (Tongji University), Ministry of Education, Shanghai 200092, China)

### ABSTRACT

As the visual system continues to decline with the increasing age, the elderly usually need higher illumination levels for nighttime activities to ensure their higher alertness and ability to detect and avoid risk factors. However, for rising at night, too much illumination stimulation can affect the rhythm and sleep continuity of the elderly and interfere with the speed of falling back to sleep after lights out. A total of 80 (age=68.71±5.97, 34 males and 46 females) elderly bedrooms were surveyed to analyze the current situation of nighttime lighting and sleep quality of the elderly, and to understand their visual health, nighttime habits and other related factors. The survey involved 5 different types of households (Lilong in Shanghai, 3 rooms and 2 halls, 3 rooms and 1 hall, 2 rooms and 2 halls, and 2 rooms and 1 hall). The horizontal illuminance of the floor and vertical illuminance of the eyes were measured and recorded after the lights for midnight rising were turned on. And the eye diseases, sleep quality (Pittsburgh Sleep Quality Index PSQI), nighttime habits, bedroom and bathroom lighting types and night-time use were also counted. The data showed that: the mean vertical illumination of the eyes of the elderly in the lying position was 75.24lx (SD=46.81), and the mean horizontal illumination of the floor was 25.72lx (SD=14.54). 66.25% of the elderly got up at night using the bedside lamp in the bedroom, and 21.25% did not turn on the light in the bedroom for various reasons. The results of the PSQI showed that the sleep quality score of the elderly people was 8.10±2.463, and the overall sleep quality was poor. Among them, 38.75% scored higher than 8 and had poor sleep quality. 76.25% of the seniors needed to get up at least once a day, and only 6.25% got up less than once a week on average. After their rising, 16.25% of the elderly needed 31 minutes or more to fall asleep, 65% needed 11-30 minutes, and only 18.75% could fall asleep within 10 minutes. The results showed that: the bedside table lamp is the most commonly used by the elderly to get up at night, and there is excessive eye illumination when the lamp is turned on, which has a greater impact on the rhythm and is not conducive to falling back to sleep after getting up at night; insufficient ground illumination makes it difficult for the elderly to notice some safety problems such as the changing height on the ground and the potential clutter. It is recommended that more suitable lighting device and lighting methods be replaced to provide sufficient ground illumination and reduce the degree of eye irritation.

Keywords: Elderly, Vertical Eye Illumination, Sleep Quality, Bedroom Lighting, Number of Wake-ups

### 1. INTRODUCTION

For the elderly, physical factors such as physical decline, related diseases, fatigue, anxiety, emotions, hallucinatory stimuli and other psychological factors, together lead to frequent night waking or night rise of the elderly. At the same time, the aging of the visual system and nervous system, the decline of body coordination and mobility, and the various problems of the lighting environment in the living room at night lead to two major health hazards in the process of rising at night: First, in the process of movement as well as the process of posture changing, such as "lying-standing" and "sitting-standing", there is the possibility of falls and injuries; the other is the loss of sleep continuity at night and the difficulty of falling back to sleep after their rising.

Although the field of residential health lighting and age-appropriate design has developed rapidly in recent years, less research has been conducted specifically on night-time lighting for the elderly rising at midnight. Based on this, the study conducts field research on the current situation of night-time lighting for the elderly, sleep quality, and satisfaction with existing night-time lighting.

## **2. NIGHT LIGHTING FOR THE ELDERLY DESIGNED TO ENSURE SAFETY AND CONTINUITY OF SLEEP AT NIGHT**

### **2.1 Factors affecting the safety of the elderly in getting up at night**

The safety of elderly people at night is mainly affected by their visual ability and mobility. The visual ability includes both aging eye function and eye disease. The aging of the eye is mainly focused on the following aspects: reduction in pupil diameter, which is more pronounced in low light conditions[1]. Decrease in the number of cone and rod cells, with the rod cells being sensitive to low light and playing an important role in dark environments and nighttime situations[2-3]. The decrease in lens transmittance and the increase in lens turbidity and absorption coefficient seriously affect visual clarity[4]. The aging of these ocular functions leads to decreased retinal illumination, decreased visual acuity, decreased contrast sensitivity, and decreased ability to adapt to light and dark, which is exacerbated by the high prevalence of ocular diseases in the elderly[5-10]. Cataracts reduce visual acuity and contrast sensitivity in the visual field, as well as impairing the ability of older adults to discriminate colors and having a higher sensitivity to glare. Macular degeneration causes severe damage to central vision, and studies by Changzheng Chen and Lezheng Wu have shown that this disease also causes a decrease in the number of cone cells and rod cells[11-12]. Glaucoma and diabetic retinal disease can gradually lead to visual blindness.

Mobility declines rapidly with age. Decreased height, reduced strength in the limbs, and decreased ability to balance and maintain homeostasis limit the range, intensity, and willingness of the elderly to move[13].

According to the 2010 U.S. Census, there are 40.3 million senior citizens in the U.S., with 1.3 million of those aged 65 and older in nursing home facilities. More than one in four older adults falls each year, with up to 27 percent of those falls due to environmental influences such as poor lighting[14-15]. The decline in visual and mobility abilities of the elderly increases the likelihood of falls caused by objective and subjective factors in the dark environment, which has a greater impact on nighttime safety.

### **2.2 Factors influencing sleep continuity in the elderly**

The sleep quality of elderly people is a very complex topic, which is highly subjective and varies greatly among individuals. Studies have been conducted to analyze sleep habits and physiological factors, and certain research results have been obtained. Based on a sample of 3272 elderly people in Tianjin, Yan Huang et al. established a regression model ( $R^2=0.65$ ) of sleep quality on seven sleep habit factors, including gender, GHQ score, wake-up time, sleep latency, bed lag time, sleep duration, and sleep regularity, and analyzed each sleep habit[16]. Based on 727 cases of elderly people, Hsiuling Lin et al. found that the sleep quality of respondents differed significantly by age group, gender, education, presence of spouse, and whether they had hypertension and diabetes, and the proportion of light sleep increased with age and the proportion of deep sleep decreased[17]. At the level of physiological factors, endocrine levels of human melatonin and cortisol, pupil contraction changes, core body temperature, EEG and other physiological indicators can be used as monitoring tools. However, no unified evaluation model has been identified for the physiological mechanisms of non-visual effects. Qingyi Zhang and Borong Lin et al. summarized some common evaluation models, and different scholars completed the construction of the model by analyzing relevant action indicators such as melatonin secretion and pupil contraction situation, while the effects of factors related to non-visual effects, including emotional effects and changes in work efficiency, are currently lacking relevant models for quantification[18].

For the elderly with nighttime rising need, the speed of falling back asleep after rising is the dominant factor affecting their nighttime sleep continuity. Among the objective influencing factors: receiving too much light during the night-time action, too bright sleep environment, glare from the lamps, high color temperature light, etc. may lead to difficulty in falling back to sleep for the elderly. According to the results of the study, negative emotions such as anxiety of the subject, psychological stress caused by the standard of living, and frequent thinking caused by the pending schedule may cause the elderly to take more than 15 minutes to fall back asleep after rising, or even unable to fall back asleep. For older adults who share a bedroom with family members, there is a degree of mutual influence on nighttime behavior.

### 3. RESEARCH ON THE STATUS OF NIGHT LIGHTING IN VARIOUS TYPES OF RESIDENTIAL SPACES FOR THE ELDERLY

#### 3.1 Research subjects

This study involved both Shanghai and Nanchang City, Jiangxi Province, and the remaining 80 eligible samples were analyzed after exclusion. In Shanghai, there are 20 elderly households of lane type (including 1 room and 2 room households), 10 elderly households of workers' new village type (including 2 rooms and 2 rooms with 1 hall), and 10 elderly households of residential district type (including 3 rooms with 1 hall and 3 rooms with 2 halls); in Nanchang, there are 10 elderly households of 2 rooms with 1 hall in old houses, 10 elderly households of 2 rooms with 2 halls in old houses, 10 elderly households of 3 rooms with 1 hall in modern style, and 10 elderly households of 3 rooms with 2 halls in modern style.



Figure 1. Field Research

#### 3.2 Methods

The research was conducted through on-site interviews combined with questionnaires, and the content was divided into four parts: the first part was the collection of basic information, including the age and gender of the elderly, and the existence of cataract, macular degeneration and other eye diseases. The second part was the analysis of the sleep quality of the elderly, mainly through the PSQI scale. The third part was the analysis of the use of lighting device both in the bedroom and bathroom of the elderly during their rising at night. This part also include the satisfaction assessment of the current situation, which is done by subjective questionnaire; the fourth part is the illuminance measurement of the elderly's rising. Ground illumination and vertical illumination of the eye are measured by CL-500A spectral illuminance meter and recorded.



Figure 2. Ground illumination and vertical illumination of the eye (left) and the night pot (right)



The elderly usually has a long path to get up and there are high spatial variability and operational complexity existing. These mean a poor uniformity of ground illumination and dynamic changes in vertical illuminance of the eye. In complex situations, illuminance measurement is selected as follows (Figure 2). For more than half of the elderly, the bedside table lamp in the bedroom is the light source that needs to be looked at directly and at the closest distance during the nighttime activities, and the vertical illuminance of the elderly's eyes is the highest at this moment, so the vertical illuminance of the eye is measured when the elderly is in the lying position as well as the bedroom nighttime lamps are turned on. Under normal circumstances, the visual operation related to the ground in the process of the elderly getting up at night is to see the bedside slippers and the possible existence of the night pot/mobile toilet, the ground illuminance measurement point is chosen as the ground illuminance of the location of the bedside slippers of the elderly.

### 3.3 Site

#### 3.3.1 Elderly households in Shanghai Lilong type

The 20 elderly households in the study are located both in the "Yanqing-Xinle" area in Xuhui District and the area near Nanjing Road Pedestrian Street in Huangpu District. The vast majority of the Lilong households do not have a bathroom inside their house, and they need to use the night pot placed inside the house at night. The majority of elderly people choose not to turn on the lights during the night. On the one hand, the limited types of lighting method are not suitable for using when rising at night, especially when sleep together with family members in the same room. On the other hand, the house is susceptible to the influence of street lights in the outdoor lane, and it is easy to see the night pot placed at the bedside normally.

#### 3.3.2 Shanghai workers' new village type elderly households

The 10 elderly households in the Workers' New Village surveyed are located in Tongji New Village, Yangpu District. The elderly need to pass through the dining room or kitchen to get up at night, and most of them choose to go to the bathroom. The lighting device includes table lamps in the bedrooms, line sink lamps and ceiling lamps in the bathrooms.

#### 3.3.3 Shanghai residential community type elderly households

The 10 elderly households in the residential area studied are located in Da'an Garden, Jing'an District, where there are bathrooms in the bedrooms and elderly people go to the bathroom at night, usually using desk lamps, downlights or wall lamps in the bedroom and downlights or nightlights in the bathroom.

#### 3.3.4 Elderly households in Nanchang

The 40 elderly households studied are all located within the family dormitory of Nanchang University in Beijing East Road, Qingshanhu District, and are divided into 20 old low-rise dwellings before 1980 and 20 new multi-storey dwellings after 2000. The former is characterized by a bathroom far away from the bedroom, requiring a walk through the living room and corridor; the latter is characterized by a bathroom at the door of the bedroom, which is closer.

For the former, the majority of elderly residents choose to use the night pot for reasons including distance, no air conditioning outside the room, inconvenience of movement, the fear of falling, and a frequent rising need, etc. For a few elderly people living alone, the reasons also include fear of darkness. For the latter, younger elderly people who have better mobility usually choose to go to the bathroom, while the older elderly people and those who get up too frequently always choose to place a night pot or a portable toilet next to the bed.

As for the use of lamps, the former mainly uses bedside table lamps, while the latter uses bedroom lamps including table lamps, wall lamps, bathroom wall lamps. Some of the latter also use the smart night light.

## 4. ANALYSIS

### 4.1 Analysis of measurement statistics

#### 4.1.1 Vertical illumination of the eye

At present, there is a lack of relevant standards at home and abroad to clearly define the vertical illumination of the eyes during the nighttime rise of the elderly. Excessive ocular

illumination can have a greater inhibitory effect on melatonin levels in the elderly, thus affecting the ability of the elderly to fall back asleep after rising and disrupting the continuity of nighttime sleep. The mean ocular vertical illuminance was 75.24 lx (SD=±46.81) for 80 elderly people in the lying position, of which 16 elderly people did not turn on the bedroom lamps at night, and the mean ocular vertical illuminance was 93.68 lx (SD=±31.91) for the remaining 64 elderly people.

#### 4.1.2 Ground illumination

At present, there is a lack of relevant standards at home and abroad to clearly define the ground illumination level for the elderly in the process of getting up at night. A certain level of ground illuminance is beneficial for the elderly to be fully cognizant of ground objects and ground changes - avoiding possible ground obstacles and clutter, noticing small height differences and ground material changes - and reducing the possibility of falls during the elderly's movement. The measurement results showed that the mean ground illuminance at the bedroom slippers of the elderly was 25.72lx (SD=±14.54), and the illuminance uniformity was poor.

#### 4.2 Questionnaire data analysis

Table 1. Lighting device and whether use or not when rising at night in bedroom

Age group	Number of the elderly	Proportion
55-59	1	1.25%
60-65	30	37.50%
66-70	21	26.25%
71-75	19	23.75%
76-80	4	5.00%
81-85	4	5.00%
86-90	1	1.25%

Table 2. Lighting device and whether use or not when rising at night in bedroom

Lighting device	Number of existences	Number of using when rising at night	Usage rate
Table Lamp	67	43	64.2%
Wall Lamp	12	5	41.6%
Floor Lamp	7	3	42.8%
Ceiling Light	41	1	2.4%
Pendant Light	27	0	0%
Channel Light	9	2	22.2%
Down Light	52	3	5.8%
Smart Night Light	9	7	77.7%

The age composition of the 80 elderly households is shown in the table 1. The types of lighting device used in the bedrooms of the elderly and the usage rate are shown in the table 2. Satisfaction of elderly with lighting device for rising at night is shown in table 3. Color temperature of bedroom and bathroom lighting are shown in table 4. 57 of the elderly reported the need for, or expressed interest in, a night light specifically for rising at night. The use of low color temperature lighting for the elderly from the PSQI score and subjective evaluation are better than high color temperature lighting.

Table 3. Level of satisfaction of the elderly towards their lighting for rising at night

Level of Satisfaction	Number of the elderly	Proportion
Very Satisfied	12	15.00%
Relatively Satisfied	41	51.25%
Relatively Unsatisfied	26	32.50%
Very Unsatisfied	1	1.25%

Table 4. Color temperature of bedroom and bathroom lighting for rising at night

Color temperature	Bedroom	Bathroom
High color temperature(white)	26	26
Low color temperature(yellow)	33	27
No lights on	21	27

The results of the PSQI showed that the sleep quality score of the elderly people was  $8.10 \pm 2.463$ , and the overall sleep quality was poor. Among them, 38.75% scored higher than 8 and had poor sleep quality. However, the evaluation of nighttime lighting among the elderly is relatively very positive. This implies a lack of awareness of the effects of nighttime lighting among the elderly. 76.25% of the elderly needed to get up at least once a day, and only 6.25% got up less than once a week on average. After their rising, 16.25% of the elderly needed 31 minutes or more to fall asleep, 65% needed 11-30 minutes, and only 18.75% could fall asleep within 10 minutes. Overall, the elderly are slower to fall asleep after rising at night.

### 4.3 Common light environment problems and suggestions for the elderly to get up at night

#### 4.3.1 Excessive vertical illumination of the eyes and the glare

The vertical illumination of the eyes is too high in two cases: first, when the side lying switch bedside lamps and lanterns, incorrect light angle, thin light-transmitting shades, light sources close to the eye distance, may lead to a short period of time the elderly eye vertical illumination is too high, accepting too strong light stimulation; second, the use of lamps and lanterns to provide high illumination, not suitable for night activities, such as the use of chandeliers or ceiling lamps and other major lamps and lanterns in the space, this situation for the night elderly also produce direct glare.



Figure 3. Table Lamp used in bedroom at night when rising

It is recommended to use special night lighting, the light source is set in a position away from the eyes of the elderly, to avoid operating the switch while causing strong stimulation, and the light output should be careful to avoid glare.

#### 4.3.2 Insufficient and uneven ground illumination

When the elderly people in the study used table lamps as bedroom night lighting, they were unable to provide sufficient and even illumination on the floor due to the limitation of the lamp's luminous intensity, the blockage of the edge of the bedside table, and the setting of the lamp's light output angle. After receiving strong light stimulation when the lamp is turned on, the lack of illumination on the floor makes it difficult for the elderly to identify slippers and sundries that may cause falls.

It is recommended to set low illumination line lights near the ground to illuminate the ground next to the bed for easy identification of objects, prompting furniture or wall edges, and to provide some guidance for the elderly to get up and move around at night.

#### 4.3.3 Room for improvement in the existing sensor smart night light

Some elderly people set up induction night light on the way, induction means including infrared and acoustic induction. Sensitivity of the light is recognized by the users. The problems reflected include: light duration fixed, suddenly extinguished on the way back because of the duration time; placement limited by the space. As shown in the figure 4, the elderly reported that the smart night light would go out in the middle of using the toilet, and then it would need to be relit in the dark when his activity is sensed.

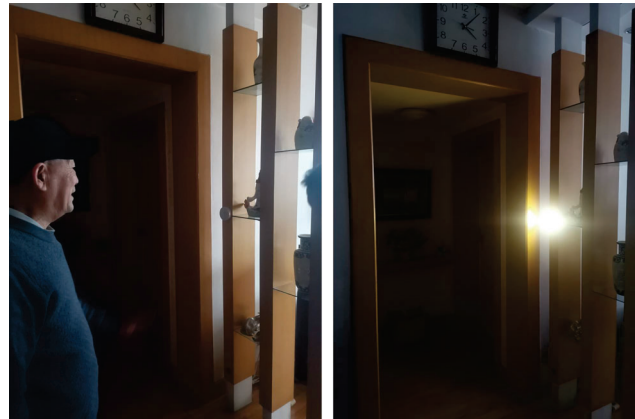


Figure 4. Table Lamp used in bedroom at night when rising

It is recommended that the sensor night light combined with the whole house intelligent control system. The sensor device and the light-emitting device can be separated, by sensing specific actions to control the light on. Or the duration of light can be pre-set by the user during the day, to make sure it can be suitable for different users with different habits.

## 5. CONCLUSION

This paper conducts field research and data analysis from the perspective of household type for the current situation of bedroom night lighting for the elderly in Shanghai and Nanchang. The results show that the most common lighting used by the elderly at night is the bedside table lamp in the bedroom, and in the process of switching on and off the lamp, there is too much eye illumination and a greater degree of rhythmic stimulation, which is not conducive to the continuity of sleep at night; whether using the night pot in the bedroom or going to the bathroom, the common problem is the lack of ground illumination and poor uniformity. There are certain safety hazards for the elderly in the process of moving to the unconscious neglect of ground height difference and potential sundries on the ground. It is recommended to replace more appropriate lighting methods and night lighting to solve the two main problems of ground illumination and the eye illumination of the elderly.

## REFERENCE

- [1] Watson A B, Yellott J I. A unified formula for light-adapted pupil size. *Journal of vision*, 2012, 12(10), 12-12.
- [2] Curcio C A, Millican C L, Allen K A, et al. Aging of the human photoreceptor mosaic: evidence for selective vulnerability of rods in central retina. *Investigative ophthalmology & visual science*, 1993, 34(12): 3278-3296.
- [3] Yingqiao Liu, Research on the effect of light on human physiological rhythm and its application, Hangzhou: Zhejiang University, 2015
- [4] Pokorny J, Smith V C, Lutze M. Aging of the human lens. *Applied optics*, 1987, 26(8): 1437-1440.
- [5] Solley, W. A., & Sternberg Jr, P. (1999). Retinal phototoxicity. *International ophthalmology clinics*, 39(2), 1-12.
- [6] Jackson G R, Owsley C, McGwin Jr G. Aging and dark adaptation. *Vision research*, 1999, 39(23): 3975-3982.
- [7] Gongxia Yang, Xudong Yang. Seniors and Lighting (Continued first). *Light source and lighting*, 2010, 03, 43-45.
- [8] Gongxia Yang, Xudong Yang. Seniors and Lighting (Continued second). *Light source and lighting*, 2010, 04, 44-46.
- [9] Gongxia Yang, Xudong Yang. Seniors and Lighting (Continued third). *Light source and lighting*, 2011, 01, 45-48.
- [10] Gongxia Yang, Xudong Yang. Seniors and Lighting (End). *Light source and lighting*, 2011, 02, 45-47.
- [11] Changzheng Chen, Lezheng Wu, Dezheng Wu. Study of localized cone cell optic rod cell function in the early stages of age-related macular degeneration, *Chinese Journal of Practical Ophthalmology*, 2004, 04, 255-259.
- [12] Changzheng Chen, Lezheng Wu, Dezheng Wu. Early central 25° dark vision sensitivity study of age-related macular degeneration, *Chinese Journal of Practical Ophthalmology*, 2003, 09, 646-648.
- [13] Xiaotong Liu, Research on the design of barrier-free and age-friendly living spaces, *Jiangxi Building Materials*, 2021, 01, 96-98.
- [14] Hegde A L. Environmental Lighting in Nursing Homes: A Comparison of Agency Standards that Regulate Nursing Homes with Industry ANSI/IES RP-28 Lighting Standards. *International Journal of Design in Society*, 2018, 12(1).
- [15] Harris-Kojetin L, Sengupta M, Park-Lee E, et al. Long-term care providers and services users in the United States: data from the National Study of Long-Term Care Providers, 2013-2014. *Vital & health statistics. Series 3, Analytical and epidemiological studies*, 2016 (38): x-xii; 1.
- [16] Yan Huang, Guangming Xu, Huifang Yin, The relationship between sleep habits and subjective sleep quality in community-dwelling older adults, *Chinese Journal of Mental Health*, 2016, 30(12), 901-908.
- [17] Hsiuling Lin, Yan Xu, Jing Yang, Investigation and analysis of sleep quality and influencing factors in 727 cases of elderly people, *The World Journal of Sleep Medicine*, 2023,10(01), 45-47.
- [18] Qinyi Zhang, Borong Lin, Yunyi Zeng, Progress and development of domestic and international research on the non-visual effect of light. *Building Energy Efficiency*, 2020, 48(07), 81-89.

## ACKNOWLEDGEMENT

Corresponding Author: Luoxi Hao  
 Affiliation: Tongji University  
 e-mail : haoluoxi@tongji.edu.cn



## Analysis Of Night Light Pollution Detection Methods and Influencing Factors Based On (Ultra) Low Altitude Perspective

Yezhen Cai<sup>12</sup>, Rongdi Shao<sup>13</sup>, Tongyue Wang<sup>14</sup>, Luoxi Hao<sup>13</sup>

1. School of Architecture and Urban Planning, Tongji University, Shanghai 200092, China;
2. Lumia Lighting Design, Shanghai 200000, China
3. Key Laboratory of Ecology and Energy-saving Study of Dense Habitat (Tongji University).  
Ministry of Education, Shanghai 200092, China)
4. Shanghai Yangzhi Rehabilitation Hospital (Shanghai Sunshine Rehabilitation Center), School of  
Medicine, Tongji University, Shanghai 201619, China;

**Abstract:** Urban light pollution at night has become a global concern with the development of modernization. Currently, countries around the world have set up corresponding restrictions and measurement standards for light pollution, such as CIE 150 2017: Guide on the limitation of the effects of obtrusive light from outdoor lighting installations, 2nd edition, France's Decree on the Prevention, Reduction and Limitation of Light Pollution, 2019 (effective January 2, 2020), China's "Outdoor Lighting Interference Light Limitation Code" (GBT 35626-2017) and "Outdoor Lighting Interference Light Measurement Code" (GB\_T 38439-2019). But the light pollution detection method based on (ultra) low altitude is still inconvenient to operate, and the feedback is not direct. It is difficult to apply in a large area. In this regard, based on the investigation of domestic and foreign light pollution management policies and detection methods, with reference to the current detection technical standards in China, the paper uses imaging luminance meter to detect light pollution at ultra-low altitudes (90M, 60M, 30M and 10M), which compares the detection data under different circumstances by taking the Angle of view, visual distance and weather conditions as influencing parameters. Surveyor can determine the true validity of the test data under certain kind of conditions, that provide scientific basis and technical support for the management department to establish a light pollution evaluation system and improve management detection methods.

**Key words:** light pollution, (ultra) low altitude viewing Angle, detection method, influencing factors

### Introduction

Excessive lighting at night in cities can cause a series of problems. Studies have shown that excessive urban nighttime lighting can have an impact on the nocturnal behavior of animals and the physiological cycle of plants (DM Dominoni et al., 2016) <sup>[1]</sup>: Light pollution can affect anuran calling behavior (Ashley Kobisk et al., 2023) <sup>[2]</sup>, and will affect migrating animals (Carolyn S. Burt et al., 2023) <sup>[3]</sup>, and affect the metabolism of hermit crabs (M. Velasque et al., 2013) <sup>[4]</sup>. In addition, light at night can affect the photosynthesis of street trees in urban environments (Masahiro Takagi et al., 2004) <sup>[5]</sup>. Too bright the sky at night also interferes with astronomical observations (Zoltán Kolláth et al., 2023) <sup>[6]</sup>. Studies have shown that light pollution can also have a negative impact on human health (Tongyu Wang et al., 2023) <sup>[7]</sup>. Light exposure at night suppresses melatonin production, which increases the risk of breast cancer in women and prostate cancer in men (Héctor Lamphar et al., 2022) <sup>[8]</sup>. At the same time, some researchers have confirmed that the brightness of urban night light environment has an increasing trend year by year (Ming Liu et

al.2022 )<sup>[9]</sup>, so the problem will intensify.

At present, the prevention and limitation of light pollution at night has become a global concern. Therefore, the research on the detection, analysis and control strategy of urban night light pollution has gradually become an important content that needs to be solved by urban management. The International Commission on Lighting (CIE) 150 2017 "Guidelines for Limiting the impact of Interfered Light on Outdoor Lighting Facilities"<sup>[10]</sup> provides evaluation indicators for the environmental impact of outdoor lighting, and puts forward recommended limits for related indicators. Chinas "Urban Night scene Lighting Design Code" (JGJ/T 163 -2008)<sup>[11]</sup> related 4 control contents including brightness, average brightness, brightness contrast, brightness uniformity. Chinas "Outdoor Lighting Interference Light Limitation Code" (GBT 35626-2017)<sup>[12]</sup> and "Outdoor Lighting Interference Light Measurement Code" (GB\_T 38439-2019)<sup>[13]</sup> respectively stipulate the urban environment brightness zoning, interference light classification, restriction requirements, measures, measurement requirements and methods. In this paper, based on "Urban nightscape Lighting Design Code" and "Outdoor Lighting Interference light limit Code", the influence of natural environment factors, measuring distance and Angle factors on the detection results is discussed.

The purpose of this study is to collect brightness data of the same object at different apparent heights (90M, 60M, 30M and 10M) at ultra-low altitudes, and to study the influence of natural factors and observation height on brightness data of the measured area combined with meteorological data. The structure and content of this paper are as follows: The first section is the description of the research sites; The second section is data statistics; The third section analyzes the natural and human factors that affect the brightness of the measured area by combing the data, and tries to find out the mechanism of their influence on the measured area. The fourth section is the analysis result. The fifth section is the prospect of follow-up work.

## 1. The Research Site

As shown in Figure 1, the observation point is located in Yangguangcuizhu Garden, Huangpu District, Shanghai, China (as shown by ① in Figure 1), and the geographical location is 31.21°N, 121.50°E. There are two test areas. One is located in Shanghai Tower, Lujiazui, Pudong New Area, Shanghai, China (shown by ② in Figure 1), with a geographical location of 31.22°N and 121.51°E; The other site is located at The Bund One Sino Park , Huangpu District, Shanghai, China (shown by ③ in Figure 1), with a geographical location of 31.21°N, 121.50°E. The measured area ② is 2.33km away from the measuring point ①, and the measured area ③ is 0.5km away from the measuring point ① . The geographic information data comes from Baidu Map (<http://api.map.baidu.com/lbsapi/getpoint/index.html>) . Air quality data is from Chinas air quality monitoring analysis of online platform ( <https://www.aqistudy.cn/> ). Temperature, humidity, cloud cover, the moon and other meteorological data are from Shanghai weather net (<https://m.tianqi.com/lishi/shanghai>).



① observation point, ②test areas 1、6, ③test area 4


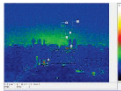

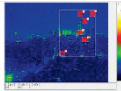
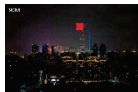
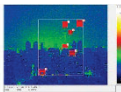

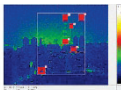
Figure 1: Location of the test areas

## 2. Data Statistics

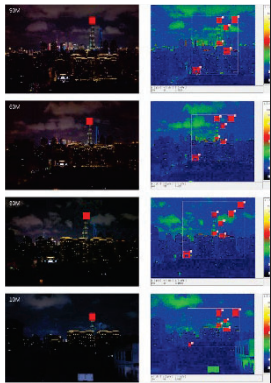
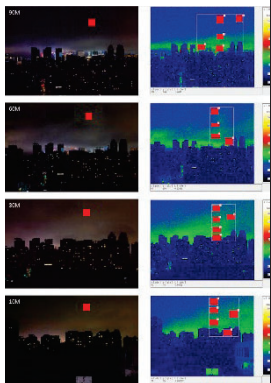
The test brightness data in this study were obtained by using LMK brightness camera (LMK Mobile), and the photo format was JPG+RAW. The analysis software (LMKLABSOFT4) was used to obtain the luminance related data of different observation areas, including the highest luminance, the lowest luminance and the average luminance (the highest luminance and the average luminance were used as the statistical basis). Six test areas were selected: test area 1- crown of Shanghai Center Tower, test area 2- Body of Shanghai Center Tower, test area 3- top of World Financial Center Tower, test area 4- top of residential building of The Bund One Sino Park , test area 5- entrance of The Bund One Sino Park , test area 6- sky near the Shanghai Center. When sorting out the data in the observation areas, it is found that there are data fluctuations in the test area 1, 2 and 3, which are inferred to be caused by the dynamic flashing of the facade light source in Shanghai Center and the World Financial Center. Therefore, the following statistics are only represented by the test area 1 for illustration; The test area 5 is obscured at the height of 10M and only partially visible, resulting in incomplete data, so it is not included in the statistical scope either. Finally, there are three places for analysis and statistics: test areas 1, 4 and 6.

Table 1: Test area 1 record table

Photo (red block in left photo is test area)	Data	Weather	Cloud cover	Air quality	Height of observation point	Maximum brightness (cd/m <sup>2</sup> )	Mean brightness (cd/m <sup>2</sup> )
	2023-06-07	Overcast with light rain	9%	Fine	90M	24.36	24.36
					60M	19.55	16.39

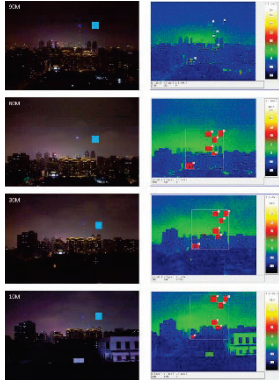
 					30M	2.86	0.84
					10M	3.46	0.77
 	2023-06-14	light rain to cloudy	80%	Fine	90M	165	26.54
					60M	314.4	25.46
					30M	325.9	40.99
					10M	198.5	46.16
 	2023-06-20	Cloudy to overcast	80%	Good	90M	119.2	28.81
					60M	145.9	25.6
					30M	63.23	18.31
					10M	14.58	14.58
 	2023-06-21	Cloudy to overcast	80%	Fine	90M	41.8	16.59
					60M	276.6	21.7
					30M	57.02	17.81
					10M	170.2	22.74
	2023-06-23	Overcast to	80%	Fine	90M	205.3	20.94



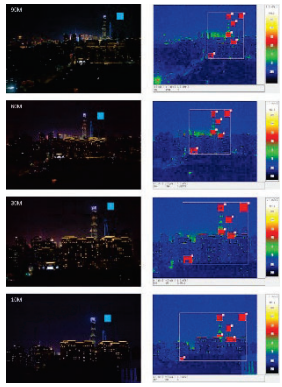
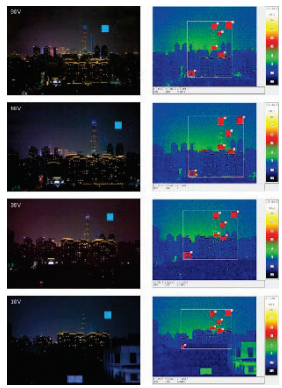
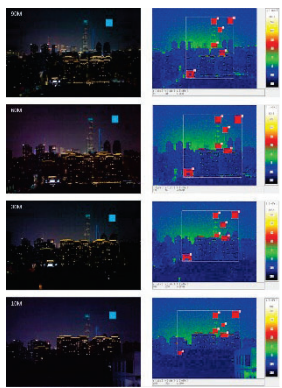
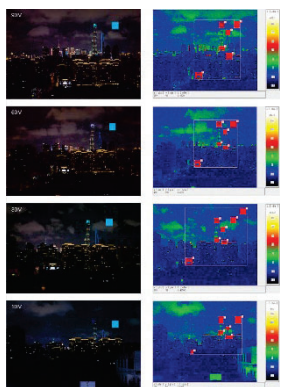
		rainstorm			60M	66.13	25.89
					30M	174.6	27.79
					10M	104.8	31.94
	2023-06-25	Rainstorm to heavy rain	100%	Good	90M	4.32	0.60
					60M	5.48	0.83
					30M	5.03	0.98
					10M	5.19	0.76

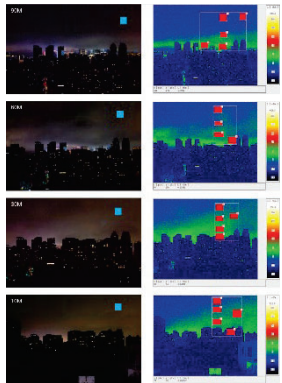
Test area 1 is the top crown of Shanghai Center (LMKLABSOFT4 calculation area 1). As the top crown of Shanghai Center is a dynamic display screen, the captured patterns at different times will be different, and the maximum brightness will be different. On June 25<sup>th</sup>, 2023, the clouds were thick, and the clouds in the rainstorm were also low, so the test area 1 was almost invisible, and the observation data on that day were not included in the subsequent statistical data.

Table 2: Test area 6 record table

Photo (blue block in left photo is test area)	Data	Weather	Cloud cover	Air quality	Height of observation point	Maximum brightness (cd/m <sup>2</sup> )	Mean brightness (cd/m <sup>2</sup> )
	2023-06-07	Overcast with light rain	9%	Fine	90M	4.47	0.76
					60M	3.00	0.99
					30M	3.57	0.79
					10M	2.56	0.69
	2023-06-14	light rain to cloudy	80%	Fine	90M	4.26	0.56

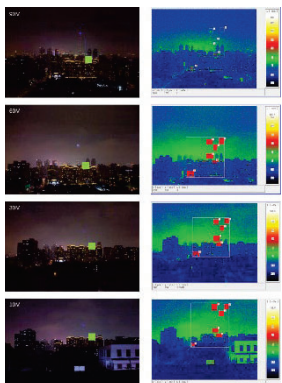
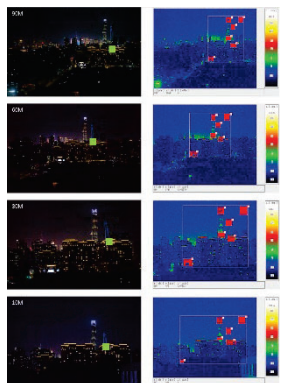


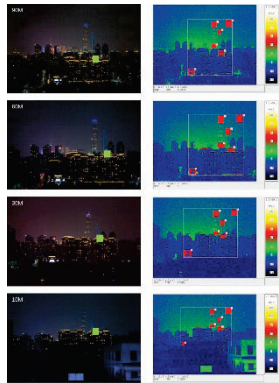
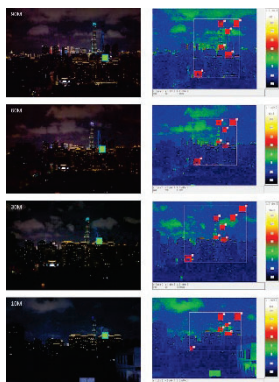
					60M	4.39	0.54
					30M	3.98	0.55
					10M	4.24	0.53
	2023-06-20	Cloudy to overcast	80%	Good	90M	5.16	1.03
					60M	5.37	0.98
					30M	5.27	0.98
					10M	4.28	0.97
	2023-06-21	Cloudy to overcast	80%	Fine	90M	4.57	0.82
					60M	5.00	0.82
					30M	5.24	0.80
					10M	5.18	0.78
	2023-06-23	Overcast to rainstorm	80%	Fine	90M	4.55	1.01
					60M	4.9	0.66
					30M	4.27	0.52
					10M	3.82	0.56
	2023-06-25	Rainstorm to heavy	100%	Good	90M	5.71	0.67

		rain			60M	6.47	1.48
					30M	6.28	0.94
					10M	5.04	1.12

Test area 6 is the sky near Test area 1, which can be used as the sky background brightness data of test area 1.

Table 3: Test area 4 record table

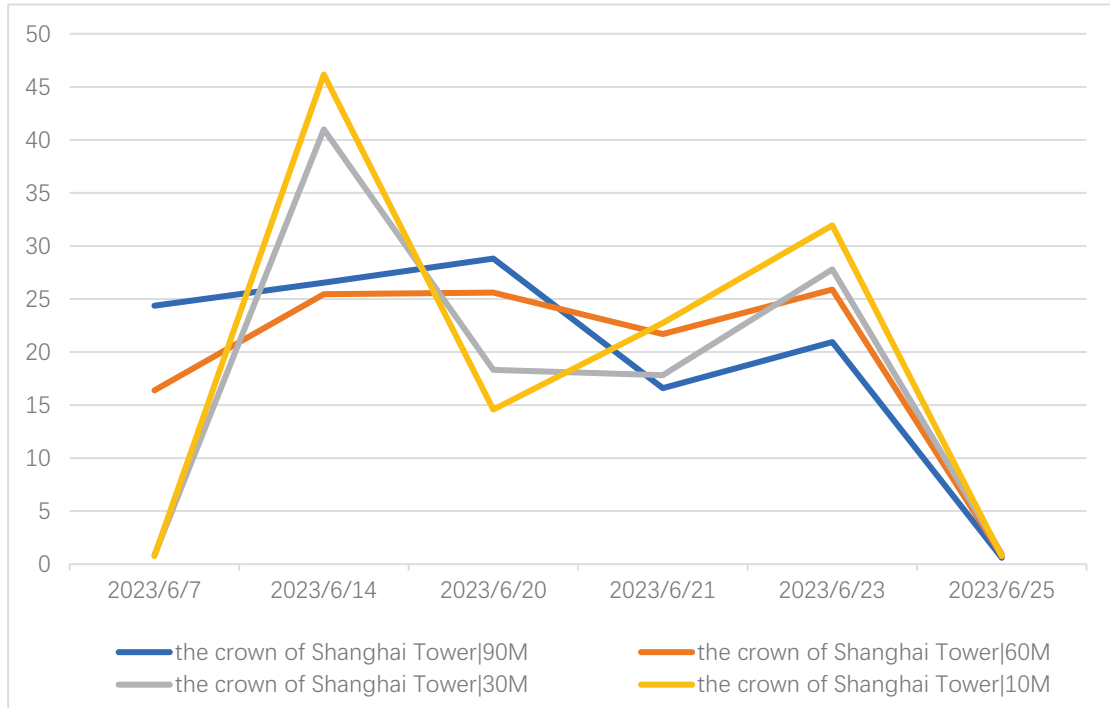
Photo (green block in left photo is test area)	Data	Weather	Cloud cover	Air quality	Height of observation point	Maximum brightness (cd/m <sup>2</sup> )	Mean brightness (cd/m <sup>2</sup> )
	2023-06-07	Overcast with light rain	9%	Fine	90M	158.3	28.09
					60M	340.6	34.54
					30M	336.5	29.05
					10M	344.6	32.07
	2023-06-14	light rain to cloudy	80%	Fine	90M	574.9	34.89
					60M	541.7	31.91
					30M	510	27.26
					10M	542.9	40.84
	2023-06-20	Cloudy to overcast	80%	Good	90M	535	27.22
					60M	546.1	30.46
					30M	529.6	24.08

					10M	529.7	26.18
	2023-06-21	Cloudy to overcast	80%	Fine	90M	541.8	28.4
					60M	551.5	34.02
					30M	532.6	34.54
					10M	524.2	35.15
	2023-06-23	Overcast to rainstorm	80%	Fine	90M	548.8	37.39
					60M	517.4	29.77
					30M	524.5	27.98
					10M	513.6	34.8

Test area 4 is the roof of the house 500M away from the observation point. On June 25<sup>th</sup>, 2023, the top lighting of Sunac Bund One Courtyard residence was not turned on, so there was no measurement data on that day.

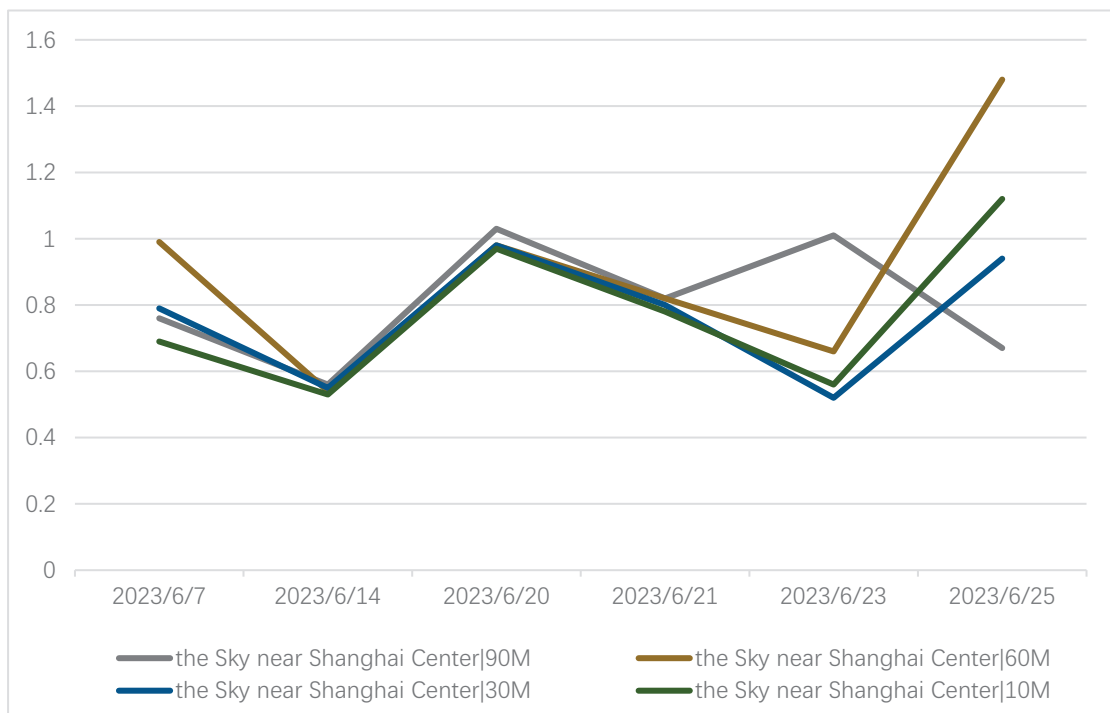
### 3. Data Analysis

#### 3.1 Luminance data of the crown of Shanghai Tower:



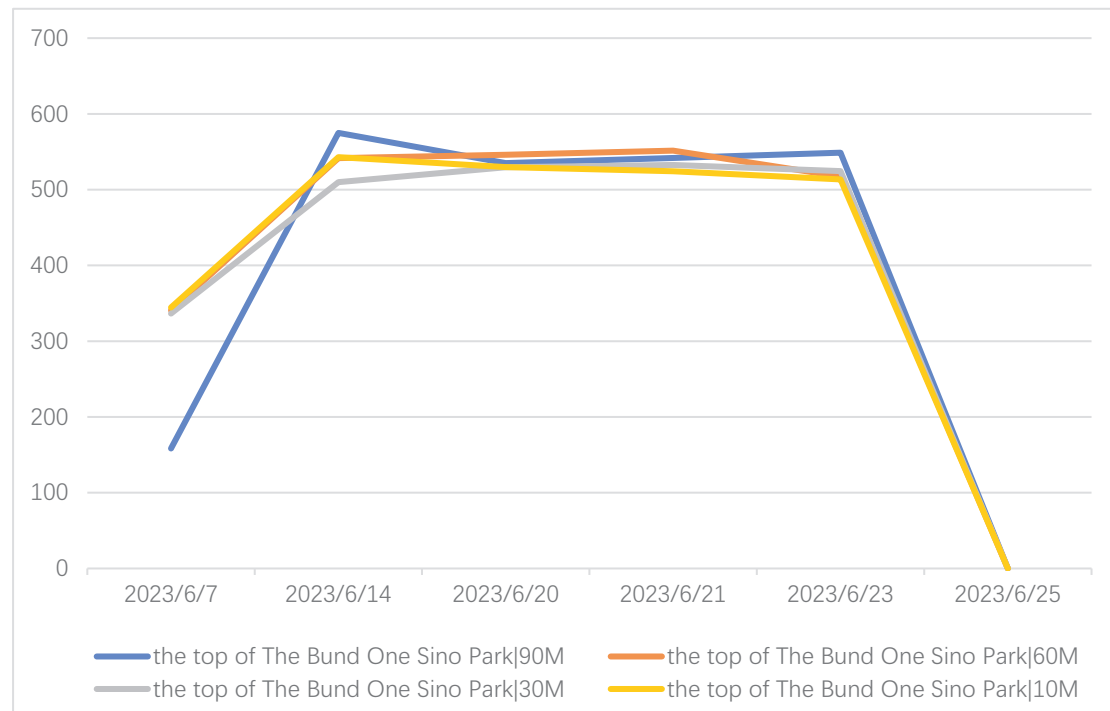
The crown of the Shanghai Tower is a scrolling display screen, and the measurement data is based on the average brightness of the measurement area. On June 7<sup>th</sup>, 2023 and June 25<sup>th</sup>, 2023, the cloud cover was heavy, which had certain impact on the measurement of the crown of the Shanghai Tower. On June 14<sup>th</sup>, 20<sup>th</sup>, 21<sup>st</sup> and 23<sup>rd</sup>, the measurement area was clearly visible, but from the data point of view, the brightness measurement data of the Shanghai Tower crown did not show regularity in terms of height or time. Reason: The dynamic screen causes the brightness measurement value to change constantly.

### 3. 2 Luminance data of the Sky near Shanghai Center



In the sky near the center of Shanghai (test area 6), the measured values of different heights of the measuring point (viewpoints) were relatively stable and almost consistent on June 14<sup>th</sup>, 20<sup>th</sup> and 21<sup>st</sup>, but there are large differences on June 7<sup>th</sup>, 23<sup>rd</sup> and 25<sup>th</sup>. According to the weather conditions and photos, the June 14<sup>th</sup>, 20<sup>th</sup> and 21<sup>st</sup> were cloudy with no obvious clouds in the sky, the 7<sup>th</sup> and 23<sup>rd</sup> were cloudy days, and the 25<sup>th</sup> was a rainstorm day. There were more clouds in these days, which greatly affected the measurement data during the measurement.

### 3. 3 Luminance data of the top of The Bund One Sino Park



The luminance data of the top of The Bund One Sino Park, which was got from different height measuring points, were relatively stable on June 14<sup>th</sup>, 20<sup>th</sup>, 21<sup>st</sup> and 23<sup>rd</sup>. The difference of the luminance data was large on June 7<sup>th</sup> (the lights were not turned-on on June 25<sup>th</sup>, and the data was "0"). The weather condition on June 7<sup>th</sup> was cloudy and rainy, with low cloud cover and high-water vapor in the air, which may be the reason of the large deviation in the measured data.

## 4. Analysis Result

With different observation heights (10M, 30M, 60M, 90M) and weather conditions (cloudy, overcast, rainy), two objects (observation distance 2.33KM, the height of the measured point is about 600M; observation distance 0.5KM, the height of the measured point is about 140M) for brightness detection, the results are as follows:

1 ) Different weather has a great impact on the measurement data, in which cloud cover and cloud height have a more obvious impact. In thunderstorm weather, it is almost impossible to observe the measured object of 2.33KM, and the sky brightness detected at different altitudes change greatly. Therefore, the observation data in thunderstorm weather is not good for use (it is not recommended to test the brightness of buildings in thunderstorm weather). In rainy weather, the data of the measured area 500M fluctuates significantly. Compared with other overcast days, the data fluctuates greatly too. Therefore, the observation data in rainy weather is unavailable (it is not recommended to test the brightness of buildings in rainy weather). In cloudy weather, clouds will



partially block 600M tall buildings, and the measurement data will fluctuate greatly (it is not recommended to test the brightness of super tall buildings in cloudy weather). In all cloudy days, the reliability of the detection data for the brightness of 600M tall buildings needs further experiments. When the observation distance is 500M, the measurement data is more stable at different observation heights. Therefore, the measurement data of 140M high buildings can be adopted on cloudy days.

2) The brightness detection of the same building is carried out at different heights (10M, 30M, 60M, 90M) at (ultra) low altitude. It is found that the measurement data of 500M away from the observation point is stable. Therefore, it can be preliminarily determined that the height of the detection point has little influence on the results of the detection data when the object is detected at (ultra) low altitude.

## 5. The Future Work Prospects

The test group lacks the detection data of sunny days, which will be supplemented in the subsequent work; In this test, the data of the dynamic facade fluctuates greatly, and the subsequent work will carry out continuous detections on the dynamic facades in order to obtain more comprehensive data.

## REFERENCES

- 【1】 Davide M. Dominoni, Jeremy C. Borniger and Randy J. Nelson, Light at night, clocks and health: from humans to wild organisms, *Biology Letters* Volume 12, Issue 2 Feb 2016
- 【2】 Ashley Kobisk, Matthew A. Kwiatkowski, Effects of anthropogenic light on anuran calling site, *Environmental Pollution* Volume 333, 15 September 2023
- 【3】 Carolyn S. Burt, Jeffrey F. Kelly, Grace E. Trankina, Carol L. Silva, Ali Khalighifar, Hank C. Jenkins-Smith, Andrew S. Fox, Kurt M. Fristrup, Kyle G. Horton, The effects of light pollution on migratory animal behavior, *Trends in Ecology & Evolution*, Volume 38, Issue 4, April 2023
- 【4】 M. Velasque, J.A. Denton, M. Briffa, Under the influence of light: How light pollution disrupts personality and metabolism in hermit crabs, *Environmental Pollution*, Volume 316, Part 2, 1 January 2023
- 【5】 Masahiro Takagi, Koichiro Gyokusen, Light and atmospheric pollution affect photosynthesis of street trees in urban environments, *Urban Forestry & Urban Greening*, Volume 2, Issue 3, 2004
- 【6】 Zoltán Kolláth, Andreas Jechow, Natural variation of the colour and spectrum of the night sky observed at a potential european reference site for dark skies, *Journal of Quantitative Spectroscopy and Radiative Transfer*, Volume 303, July 2023
- 【7】 Tongyu Wang, Naoko Kaida, Kosuke Kaida, Effects of outdoor artificial light at night on human health and behavior: A literature review, *Environmental Pollution*, Volume 323, 15 April 2023
- 【8】 Héctor Lamphar, Miroslav Kocifaj, Jorge Limón-Romero, Jorge Paredes-Tavares, Safei Diba Chakameh, Michal Mego, Natalia Jorgelina Prado, Yolanda Angélica Baez-López, Emiliano Raúl Diez, Light pollution as a factor in breast and prostate cancer, *Science of The Total Environment* Volume 806, Part 4, 1 February 2022
- 【9】 Ming Liu, Xiaoshuang Liu, Baogang Zhang, Yiwei Li, Tong Luo, Qingyuan Liu, Analysis of the evolution of urban nighttime light environment based on time series, *Sustainable*

Cities and Society, Volume 78, March 2022

- 【10】 CIE 150:2017. Guide on The Limitation of The Effects of Obtrusive Light from Outdoor Lighting Installations, 2nd Edition, ISBN: 978-3-902842-48-0; DOI: 10.25039/TR.150.2017
- 【11】 Urban nightscape lighting design code: JGJ/T 163-2008[S]. Beijing: Standards Press of China, 2008.
- 【12】 Outdoor Lighting Interference light limit specification: GBT 35626-2017[S] Beijing: Standards Press of China, 2017
- 【13】 Outdoor Lighting interference light measurement specification: GB/T 38439-2019[S] Beijing: Standards Press of China, 2019

This research was funded by the Scientific Research Project of Shanghai Municipal Science and Technology Commission (No. 22dz1202400).

Corresponding Author Name: Luoxi Hao

Affiliation: Tongji University

e-mail: haoluoxi@tongji.edu.cn

# ASSESSMENT OF SPATIAL BRIGHTNESS FOR A VISUAL FIELD IN INTERIOR SPACES BASED ON INDIRECT CORNEAL ILLUMINANCE

Zhiguo Hu<sup>1</sup>, Qi Dai<sup>2,\*</sup>

(<sup>1</sup> Institute of Future Lighting, Academy for Engineering & Technology, Fudan University, Shanghai, China; <sup>2</sup> Institute for Electric Light Sources, Department of Light Sources and Illuminating Engineering, School of Information Science and Technology, Fudan University, Shanghai, China)

## ABSTRACT

With the advance of lighting technology and shift of work style, people pay increased attention to improve the quality of indoor lighting and try to create a bright, comfortable and healthy interior lit environment. Some researchers have proposed to make the switch of the lighting design priority from task illumination to ambient illumination with a focus on spatial brightness, as it is closely related to the visual comfort. Spatial brightness describes a visual sensation related to the magnitude of the ambient illumination level within a space, which encompasses the overall sensation based on the response of a large part of the visual field extending beyond the fovea. However, quantitative evaluation of spatial brightness has been difficult, mainly due to the lack of a metric that is both highly related to subjective evaluation and convenient to measure in the field.

This work investigated the applicability of using indirect corneal illuminance to evaluate spatial brightness for a visual field in interior spaces. Three lighting scenes with different patterns of lighting distribution, which all delivered indirect light to the subjects, were compared against each other in pairs for spatial brightness. The corresponding indirect corneal illuminance required for each test scene to match the spatial brightness of the reference scene with a fixed corneal illuminance was obtained. The results showed that our proposed metric had a high correlation with subjective evaluation of spatial brightness even under very different patterns of lighting distribution. Furthermore, the proposed metric was compared with the prior metrics of MRSE and  $L_{av,B40}$  in spatial brightness evaluation, and the former showed the best correlation with subjective judgments. Since the spatial brightness assessment for various visual fields together compose people's overall impression of an illuminated space, the proposed metric of indirect corneal illuminance, which combines both accuracy and convenience in measurement, could serve as a preferred metric for spatial brightness evaluation.

**Keywords:** Spatial brightness; Indirect corneal illuminance; Spatial distribution of light; Interior luminous environment; Human factor study

## 1. INTRODUCTION

In modern society, indoor space is the place where people spend more than 80% of their daily time. Good lighting design provides people with a comfortable and healthy living and working environment and improves work efficiency. Traditional lighting design mainly focuses on providing sufficient illuminance on horizontal working surfaces, because it is directly related to people's visual task performance [1–3]. However, with the change of work and lifestyles in recent decades, the attention to indoor lighting has gradually expanded from work-plane illuminance to the quality of the overall lit environment [4–6]. Firstly, due to the advance in technology, visual tasks requiring a high

work-plane illuminance are diminishing [7]. For example, paper reading has been largely replaced by reading from self-luminous screens, and difficult manual and visual tasks can usually be completed through automation technology [7]; and secondly, people pay increased attention to the overall lit appearance of indoor spaces (how brightly lit, or dimly lit, the spaces appear) [1–3,7], because that is not only associated with visual satisfaction and comfort, but also related to the quality of visual communication. Thus, some researchers have even proposed to make the switch of the lighting design priority from task illumination to ambient illumination [1–3] with a focus on spatial brightness [7–10]. Spatial brightness describes a visual sensation related to the magnitude of the ambient illumination level within a space, which encompasses the overall sensation based on the response of a large part of the visual field extending beyond the fovea [11,12]. The spectral and spatial distributions of lighting are the two major aspects that affect one's overall impression of spatial brightness [13]: the former is mainly based on the spectral photo-sensitive nature of various types of retinal photoreceptors that distribute across the retina [7–10]; while the latter is related to the pattern and intensity of light distribution within the field of view that affects the quantity (and maybe also the distribution) of the light received at eye-level [1–3].

Even in the same indoor space, the assessment of spatial brightness for a visual field could be very different depending on the observation location and field of view. Therefore, some researchers were committed to finding a general metric to quantify the overall spatial brightness of illuminated interiors [1–3,14–17]. Cuttle [1] proposed to use the concept of mean room surface exitance (MRSE) as a metric to quantify spatial brightness. MRSE is defined as the area-weighted average of surface exitance across the interior room surfaces. Duff et al. [14,15] investigated the suitability of using MRSE as a predictor of spatial brightness, and claimed that there did exist a clear correlation between MRSE and subjective evaluation of spatial brightness, while on the other hand, such a correlation did not exist between horizontal illuminance and spatial brightness. Besides, Loe et al. [16,17] examined the correlation between spatial brightness perception and the average luminance in a horizontal band with a width of  $40^\circ$  within the field of view (denoted as  $L_{av,B40}$ ), and concluded that the values of  $L_{av,B40}$  had a good correlation with the results of subjective spatial brightness assessments. Although these prior studies [1–3,14–17] have verified the correlation between their proposed metrics and spatial brightness perception through subjective evaluation experiments, some limitations prevented these metrics from wide adoption: firstly, the measurement procedures for MRSE and  $L_{av,B40}$  are cumbersome and therefore are not easy to be mastered by lighting designers [18,19]; secondly, some results [14,15] were obtained based on experimental conditions with a relatively uniform lighting distribution, but the real-world scenario can be much more complicated; and lastly, both metrics of MRSE and  $L_{av,B40}$  merely reflect the photometric properties of the illuminated room surfaces, and therefore cannot directly reflect the amount of light received by people's eyes [20], which may be highly relevant to the sensation of spatial brightness.

Compared with MRSE and  $L_{av,B40}$ , indirect corneal illuminance (denoted as  $E_{cor,i}$ ) has the potential to have a better correlation with subjective evaluation of spatial brightness, because it is directly related to the amount of light incident on the eyes and also reflects the spatial distribution of light. Moreover, the  $E_{cor,i}$  metric could be especially useful for scenarios where the perceived spatial brightness at a specific field of view is very important. For example, in the classroom, the most important direction of vision is towards the blackboard, and the lighting design focusing on this direction would be beneficial to students' visual health [21]; in an office space, people's perception of spatial brightness at various locations and viewing directions may be different, and the lighting design focusing on office workers' frequent viewing directions could enhance their visual comfort and work efficiency [22,23]. Thus, it is important to investigate whether there is a high correlation between indirect corneal illuminance and the subjective assessment of spatial brightness for a visual field. Note that the spatial brightness perceptions for various visual fields together can compose one's overall impression of an illuminated space.

In this work, a quantitative method for comparison of spatial brightness within a visual field was

developed. The indirect corneal illuminance required for the test scene to match the spatial brightness of the reference scene with a fixed corneal illuminance was obtained according to subjective assessment. Three lighting scenes with different patterns of spatial lighting distribution were compared against each other in pairs. Based on which, the applicability of using the  $E_{cor,i}$  metric for spatial brightness evaluation was investigated. Furthermore, the performance of the  $E_{cor,i}$  metric was compared with that of the previously proposed metrics including MRSE and  $L_{av,B40}$ .

## 2. METHODS

### 2.1 Experiment setup

The experiment was carried out in a windowless room 4.0 m long, 3.2 m wide and 2.7 m high. The wall and ceiling surfaces were painted white and diffusive for efficient generation and reflection of indirect light. Carefully designed luminaires, which were intensity-, angle- and position- tunable, were located at strip rails hanged 0.2 m under the ceiling. By adjusting the angles of operating luminaires, light goes through at least one reflection in the room before reaching the subjects' eyes. In other words, only indirect light was delivered to the subjects sitting about 1.6 m in front of the long-side wall, as shown in Figure 1(a) and (b). In this work, we intended to investigate the performance of spatial brightness evaluation metrics under different patterns of lighting distribution, therefore a fixed general-lighting spectrum with a typical CCT of about 4400 K and a CRI (Ra) of 81.0 was adopted. The measured spectrum at subjects' eye-level was stable during the experiment, as shown in Figure 1(c).

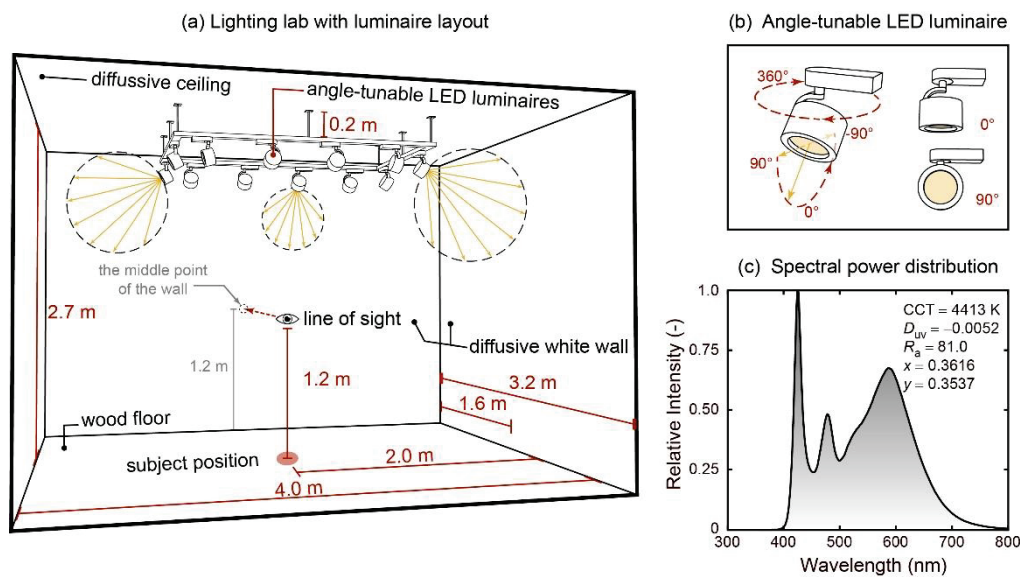


Figure 1. Illustrations of (a) a windowless lighting lab with luminaire layout, (b) an intensity-, angle-, and position- tunable luminaire, and (c) measured spectrum at subjects' eye level.

The observation position was fixed for all subjects during the experiment, and illuminance was measured at the position of the subjects' eyes, which was all contributed by indirect light. The luminance distributions across room surfaces were measured using a luminance meter (JETI SpectraVal 1511, luminance mode with a measuring angle of 2°).

A total of 44 subjects were recruited (24 females and 20 males, mean  $\pm$  SD age: 23.2  $\pm$  2.6; Ethnicity: Chinese). The inclusion criteria were college students, aged between 18 and 30 years old, normal or corrected-to-normal eyesight, and success in passing a color-blind test (Ishihara color vision test). Subjects were naïve (not an expert in lighting technology) and were paid for participation.

Three types of lighting scenes with different patterns of light distribution, named Scenes 1, 2 and



3, were compared against each other in pairs. As shown in Figure 2, the left, middle, and right columns are schematic illustrations of light output from luminaires from the top view, photos taken by a Canon 6D Mark II DSLR camera with an 8 mm fisheye lens, and photos calibrated to luminance distributions taken by an LMK 6 video photometer, respectively. The schematic diagrams and photos of the Scenes 1-3 are shown in Figure 2 (a)-(c), respectively. It can be found that the lighting distribution of Scene 1 is relatively more uniform compared with those of Scenes 2 and 3. Note that each photo in Figure 2 was taken at the condition when corneal illuminance at the observation position was set to 100 lx (the illuminance at the observation position was all indirect).

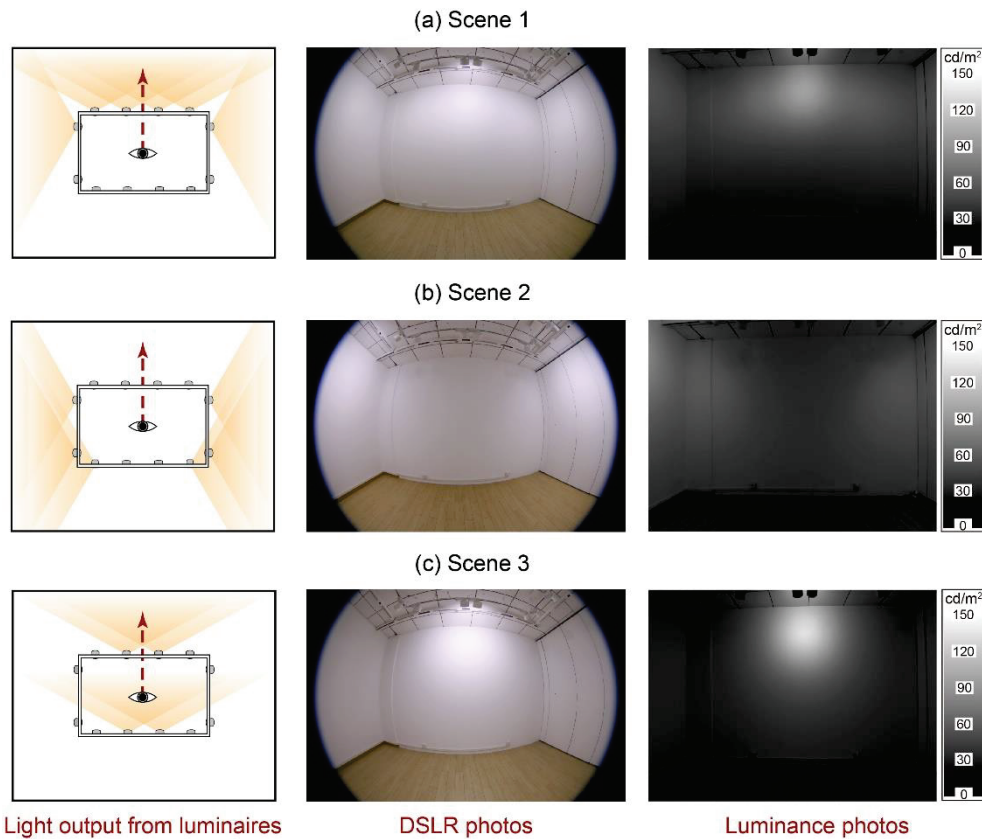


Figure 2. Schematic illustrations and photos of (a) Scene 1, (b) Scene 2 and (c) Scene 3. From left to right, each column represents: the schematic illustrations of the light output from luminaires (top view), photos taken by a DSLR camera with a fisheye lens, and luminance photos.

Spatial brightness comparisons for the fixed visual field (see Figure 2) were performed between the test scenes at different corneal illuminance levels and the reference scene with a fixed corneal illuminance of 100 lx. Among the three lighting scenes, the pattern of lighting distribution is quite different. The lighting intensity of each test scene was tuned to 11 levels of corneal illuminance from 50 to 180 lx (tuned to approximately 50 lx, 60 lx, 70 lx, 80 lx, 90 lx, 100 lx, 110 lx, 120 lx, 140 lx, 160 lx, and 180 lx). It was aimed to find the corresponding corneal illuminance (denoted as  $E_{\text{match}}$ ) that made the subjective spatial brightness assessment of each test scene match that of the reference scene. The  $E_{\text{match}}$  values from all the paired comparisons were then used to investigate the suitability of the  $E_{\text{cor},i}$  metric for spatial brightness evaluation.

## 2.2 Experiment method for spatial brightness comparison

In general, the types of procedures for spatial brightness comparison can be divided into four categories, including adjustment, category rating, discrimination, and matching [8,11]. The first two methods are absolute evaluations without a presented reference: in the adjustment procedure, subjects are directed to tune the light quantity of a space to a preferred level; and in the category rating procedure, subjects use rating scales to describe the spatial brightness appearance of a

visual scene. The last two methods are relative comparisons with the presence of a reference: in the discrimination procedure, subjects are presented with two scenes and instructed to report which one is brighter; while in the matching procedure, subjects are required to adjust the amount of light of the test scene until it matches the reference scene in spatial brightness. In this study, a reference fixed lighting intensity was presented: subjects were instructed to perform comparisons between the reference and test scenes in temporal juxtaposition. However, simply applying one of the two reference-based comparison procedures, discrimination or matching, may not be sufficient to overcome the following limitations: (i) there existed a significant difference in patterns of lighting distribution between the reference and test scenes, which made it difficult for subjects to make a judgement on which one has a higher level of spatial brightness; (ii) it was not easy for subjects to remember the spatial brightness appearance of the first scene when observing the second one; (iii) there existed individual difference among subjects' judgments, and the corneal illuminance of the test scene required for each individual to match the spatial brightness of the reference scene generally follows the Gaussian distribution [13,24–26].

To address these problems, we developed a method of spatial brightness comparison for a visual field that combined the advantages of both discrimination and matching approaches: between the reference scene (fixed at a corneal illuminance of 100 lx) and the test scene (set to various corneal illuminance levels from 50 to 180 lx), subjects were asked to make a forced choice [27] on which scene has a higher level of spatial brightness from their visual field. The percentage of subjects who reported the test scene being brighter (denoted as  $P$ ) versus corneal illuminance of the test scene (denoted as  $E_{\text{cor},i,t}$ ) was obtained. One could imagine that the result should be nearly 0% when the  $E_{\text{cor},i,t}$  value was set to 50 lx and close to 100% when the  $E_{\text{cor},i,t}$  value was set to 180 lx. Assuming that the corneal illuminance values of the test scene required for various individuals to match the spatial brightness of the reference scene generally follow a Gaussian distribution, then the experimental data of  $P$  vs.  $E_{\text{cor},i,t}$  could be fitted by a psychometric function that is derived from the above-mentioned Gaussian function (probability density function) by integral approximate calculation [25]. In this work, the form of the Logistic function was adopted as the psychometric function, and the  $E_{\text{match}}$  value could be quantitatively calculated by fitting the data with the Logistic function [25,26] and finding the point with  $P = 50\%$ .

### 2.3 Procedure

As shown in Figure 3(a), the overall procedure of the study can be divided into three phases: (i) a null-condition trial, (ii) two experimental trials with a fixed reference and (iii) an experimental trial for direct comparison. For the first two phases, each trial was conducted by using one of the three lighting scenes (see Figure 2) as the test scene to compare with a fixed reference scene (Scene 1 with a fixed corneal illuminance of 100.3 lx). First, a null-condition trial was implemented to confirm the removal of systematic biases and verify the accuracy of the experiment method. Scene 1, which shared the same pattern of spatial lighting distribution as the reference scene, was adopted as the test scene. The corneal illuminance of the test scenes was set to one of the eleven levels from 50 to 180 lx, while that of the reference scene was fixed at 100 lx. In the second phase, two experimental trials with the same fixed reference, Scene 2 vs. the reference and Scene 3 vs. the reference, were carried out to investigate the applicability of using the  $E_{\text{cor},i}$  metric to assess spatial brightness by comparing with the performance of previously proposed metrics, including MRSE and  $L_{\text{av},B40}$ , under very different patterns of lighting distribution. The illuminance level of the test scenes was also set to one of the eleven levels and the reference scene was also set to Scene 1 at 100 lx. For the third phase, an experimental trial was conducted to directly compare Scene 2 with Scene 3, which have the biggest difference in the pattern of spatial lighting distribution, to further compare among the metrics of  $E_{\text{cor},i}$ , MRSE and  $L_{\text{av},B40}$  for spatial brightness evaluation. In this experimental trial, Scene 2 at 100 lx was adopted as the new reference scene and Scene 3 at illuminance levels from 50 to 180 lx were adopted as the test scenes.

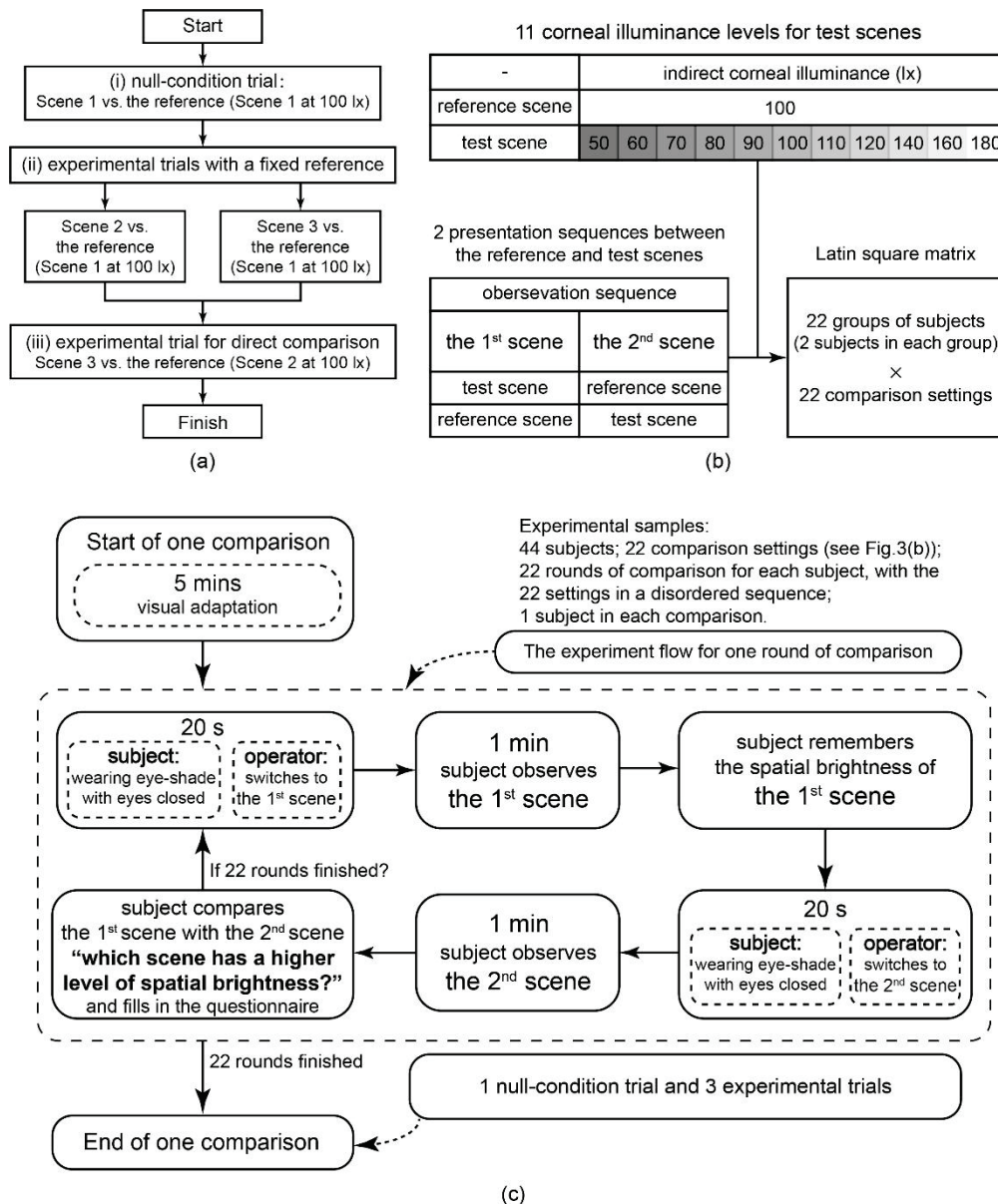
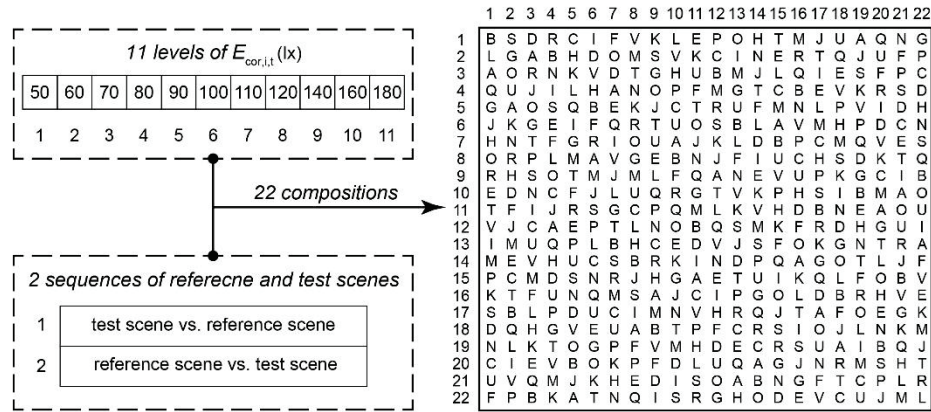


Figure 3. Illustrations of (a) the overall procedure of the experiment, (b) Latin square  $22 \times 22$  disorder matrix for each experiment trial and (c) the detailed comparison procedure.

Each comparison trial includes 11 corneal illuminance levels for the test scenes and 2 presentation sequences between the reference and test scenes, which makes a total of 22 comparison settings for each of the 44 subjects, as shown in Figure 3(b). The corresponding order bias needs to be balanced. Therefore, a  $22 \times 22$  Latin square disorder matrix was constructed for 22 groups of subjects (2 subjects in each group) and 22 comparison settings in different presentation sequences, as shown in Figure 4 (a) and (b). For each group, spatial brightness comparisons were performed following a unique sequence of comparison settings according to the Latin square matrix, as shown in Figure 4(b). Note that the two subjects in each group participated in the comparison experiment separately so that the field of view was identical for all the subjects.



(a) 22 × 22 Latin Square Matrix



(b) Experimental disorder sequence

		test scene vs. reference scene											reference scene vs. test scene										
No. (lx)		A	B	C	D	E	F	G	H	I	J	K	L	M	N	O	P	Q	R	S	T	U	V
		50	60	70	80	90	100	110	120	140	160	180	50	60	70	80	90	100	110	120	140	160	180
1		60	120	80	110	70	140	100	180	180	50	90	90	80	120	140	60	160	160	50	100	70	110
2		50	110	50	60	120	80	80	60	120	180	180	70	140	70	90	110	140	100	160	160	100	90
3		50	80	110	70	180	180	80	140	110	120	160	60	60	160	50	100	140	90	120	100	90	70
4		100	160	160	140	50	120	50	70	80	90	100	60	110	140	70	60	90	180	180	110	120	80
5		110	50	80	120	100	60	90	180	160	70	140	110	160	100	60	70	50	90	180	140	80	120
6		160	180	110	90	140	100	100	110	140	160	80	120	60	50	50	180	60	120	90	80	70	70
7		120	70	140	100	110	110	140	80	160	50	160	180	50	80	60	90	70	60	100	180	90	120
8		80	110	90	50	60	50	180	110	90	60	70	160	100	140	160	70	120	180	80	180	140	100
9		110	120	120	80	140	60	160	80	50	100	100	50	70	90	180	160	90	180	110	70	140	60
10		90	80	70	70	100	160	50	160	100	110	110	140	180	180	90	120	120	140	60	60	50	80
11		140	100	140	160	110	120	110	70	90	100	60	50	180	180	120	80	60	70	90	50	80	160
12		180	160	70	50	90	90	140	50	70	80	60	100	120	60	180	100	110	80	120	110	160	140
13		140	60	160	100	90	50	60	120	70	90	80	180	160	120	100	80	180	110	70	140	110	50
14		60	90	180	120	160	70	120	60	110	180	140	70	80	90	100	50	110	80	140	50	160	100
15		90	70	60	80	120	70	110	160	120	110	50	90	140	160	140	180	100	50	100	80	60	180
16		180	140	100	160	70	100	60	120	50	160	70	140	90	110	80	50	80	60	110	120	180	90
17		120	60	50	90	80	160	70	140	60	70	180	120	110	100	160	140	50	100	80	90	110	180
18		80	100	120	110	180	90	160	50	60	140	90	100	70	110	120	140	80	160	50	70	180	60
19		70	50	180	140	80	110	90	100	180	60	120	80	90	70	110	120	160	50	140	60	100	160
20		70	140	90	180	60	80	180	90	100	80	50	160	100	50	110	160	70	110	60	120	120	140
21		160	180	100	60	160	180	120	90	80	140	120	80	50	60	70	110	100	140	70	90	50	110
22		100	90	60	180	50	140	70	100	140	120	110	110	120	80	80	90	180	70	160	160	60	50
	Round #	1	2	3	4	5	6	7	8	9	10	11	12	13	14	15	16	17	18	19	20	21	22

Figure 4. Illustrations of (a) the overall procedure of the experiment, (b) Latin square 22 × 22 disorder matrix for each experiment trial and (c) the detailed comparison procedure.

The detailed procedure in one round of comparison can be described as follows (also shown in Figure 3(c)):

- One subject sat in the middle of the room and looked forward. The height of the viewing position was 1.2 m from the floor, and a fixed chin rest was used to ensure that the viewing position and the field of view were fixed for all subjects. Before the comparison, lighting was switched to the reference scene to make the subject visually adapt to the light environment for 5 minutes.
- The subject was instructed to close his (her) eyes and put on an eye-shade for 20 seconds. During that period, the lighting mode was switched to the 1st scene and stabilized.
- The subject then took off the eye-shade, opened his (her) eyes, and looked forward for 1 minute, during which he (she) was instructed to memorize the spatial brightness appearance of the 1st scene at the end of the 1-minute period. The 1-minute observation time was chosen

because it takes more than 30 seconds for brightness adaptation [13,24]. As the lighting spectrum was fixed throughout the experiment, the chromatic adaptation does not need to be considered [28].

- The subject closed his (her) eyes and put on the eye-shade again for 20 seconds, and during the same period, the lighting mode was switched to the 2nd scene and stabilized.
- The subject then took off the eye-shade, opened his (her) eyes, and looked forward for 1 minute. Then the subject was instructed to compare the spatial brightness of the 1st scene & 2nd scene, both at the end of the 1-minute period, with the question 'which scene has a higher level of spatial brightness?'. The subject filled in the questionnaire.
- One round of comparison was completed. For each trial, the procedure above was carried out 22 times for each of the 44 subjects with the 22 different comparison settings in a disordered sequence, as shown in Figure 4(b). Note that each subject participated in all trials separately at different times and performed comparisons individually, and they were not allowed to use phones or other electronic devices during the experiment.

### 3. METHODS

#### 3.1 Null-condition trial

First, a null-condition trial was performed, in which both the reference and test scenes shared the same pattern of lighting distribution. For the reference scene, the illuminance at the subject's eye level was fixed at 100 lx, while that of the test scenes was set to one of the eleven levels (from 50 to 180 lx). For each corneal illuminance level of the test scenes ( $E_{cor,i,t}$ ), the percentage of subjects who reported the test scene being brighter than the reference scene ( $P$ ) was obtained, as shown in Figure 5. Note that each data point is an average of 88 comparisons (44 subjects  $\times$  2 sequences) so that the result is statistically representative and the bias caused by comparison sequences and the individual difference can be well balanced.

When the test scene was set to 100 lx, the reference and test scenes were identical, therefore theoretically, the percentage of subjects reporting the test scene being brighter should be 50%. From our null-condition trial, of the 88 comparisons, 52 (59.1%) reported the test scene being brighter (95% confidence interval (CI): 48.6% – 69.6%). It can be found that the expected value of 50% fell into the 95% CI. Moreover, when the test scene was set to 90 lx, 19.3% reported the test scene being brighter (95% CI: 10.9% – 27.7 %), and when the corneal illuminance was set to 110 lx, 76.1% reported the test scene being brighter (95% CI: 67.1% – 85.2%). According to our 50% criteria, the test scenes at 110 lx and 90 lx could be clearly considered as brighter and less bright than the reference scene, respectively. Such results from the null-condition trial proved that our method could effectively balance the potential bias and make the difficult spatial brightness comparison task practical and accurate. Besides, the t-test statistical analysis also showed a significant difference between the experimental data of the test scene at 100 lx and that at all the remaining 10 illuminance levels (from 50 to 180 lx). All the  $p$  values were less than 0.05 ( $p = 0.015$  for corneal illuminance at 110 lx, and  $p < 0.001$  for the other corneal illuminance levels), which indicated that in the null-condition trial, the spatial brightness appearance of the reference scene at 100 lx could be distinguished from that of the test scenes with illuminance levels other than 100 lx. Therefore, the 10 lx interval setting could be considered effective and suitable for this study.



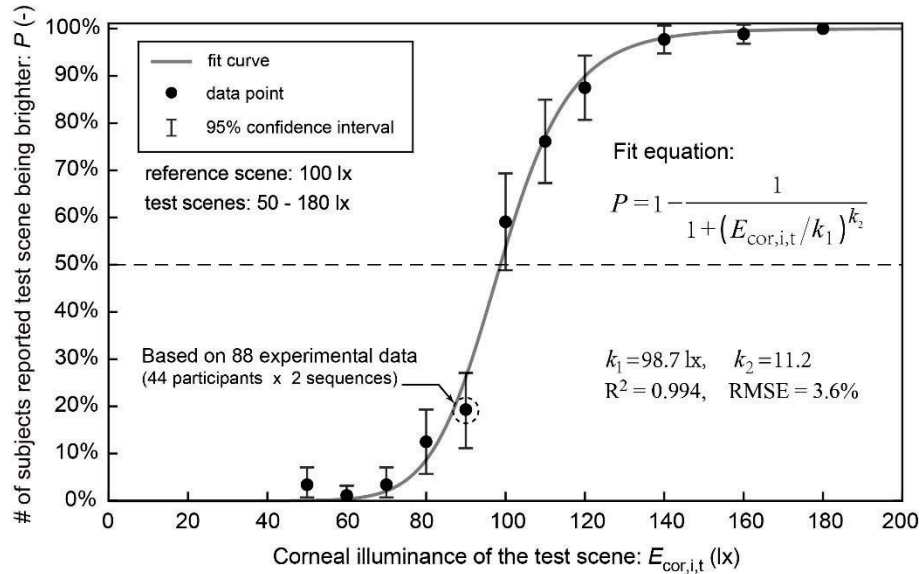


Figure 5. Null-condition trial: the percentage of subjects who reported the test scene being brighter than the reference scene ( $P$ ) vs. corneal illuminance of the test scene ( $E_{cor,i,t}$ ), and the fit curve.

According to the analysis in Section 2.2, the experimental data in Figure 5 can be fit by a 2-parameter logistic equation [7], as follows:

$$P = 1 - \frac{1}{1 + (E_{cor,i,t}/k_1)^{k_2}} \quad (1)$$

where  $P$  represents the percentage of subjects who report the test scene being brighter than the reference scene;  $E_{cor,i,t}$  is the corneal illuminance of the test scene;  $k_1$  is the value of corneal illuminance at which 50% of subjects would rate the test scene being brighter than the reference scene, it is also the illuminance required to match the spatial brightness of the test scene and the reference scene;  $k_2$  is a measure of the steepness of the rising portion of the fit curve, which represents the subjects' sensitivity to the change of spatial brightness caused by increased corneal illuminance and therefore also reflects the degree of difficulty in making the judgments. For this null-condition trial, the fitting result of  $k_1 = 98.7$  lx (95% CI: 96.9 – 100.6 lx) was very close to the expected theoretical  $E_{match}$  value of 100.3 lx, which confirmed the effectiveness and reliability of the experimental method and indicated that by using this method, the potential order bias was well balanced.

### 3.2 Experimental trials with a fixed reference

Next, two experimental trials with a fixed reference (Scene 1 at 100 lx) were carried out, in which Scene 2 and Scene 3 were adopted as test scenes. For each type of test scene, there were 11 corneal illuminance levels ranging from 50 to 180 lx, and the corresponding data of  $P$  vs.  $E_{cor,i,t}$  was obtained, as shown in Figure 6. Fit curves based on Eq. (1) were applied to the experimental data: for Scene 2 vs. the reference, fitting results of  $k_1 = 95.6$  lx (95% CI: 93.7 – 97.5 lx) and  $k_2 = 6.7$  were obtained, with the corresponding fit curve shown in Figure 6 (a); and for Scene 3 vs. the reference, fitting results of  $k_1 = 97.1$  lx (95% CI: 95.2 – 99.1 lx) and  $k_2 = 6.2$  were obtained, with the fit curve shown in Figure 6 (b).

The results of the two experimental trials showed that to match the spatial brightness of the reference scene (Scene 1 with a fixed corneal illuminance of 100.3 lx), corneal illuminances of 95.6 lx and 97.1 lx were needed for Scene 2 and Scene 3, respectively. It indicated that to achieve a certain level of spatial brightness, there existed only a minor difference in required indirect corneal

illuminance among scenes with very different patterns of lighting distribution. In other words, indirect corneal illuminance could serve as a fair candidate for spatial brightness evaluation of lit spaces.

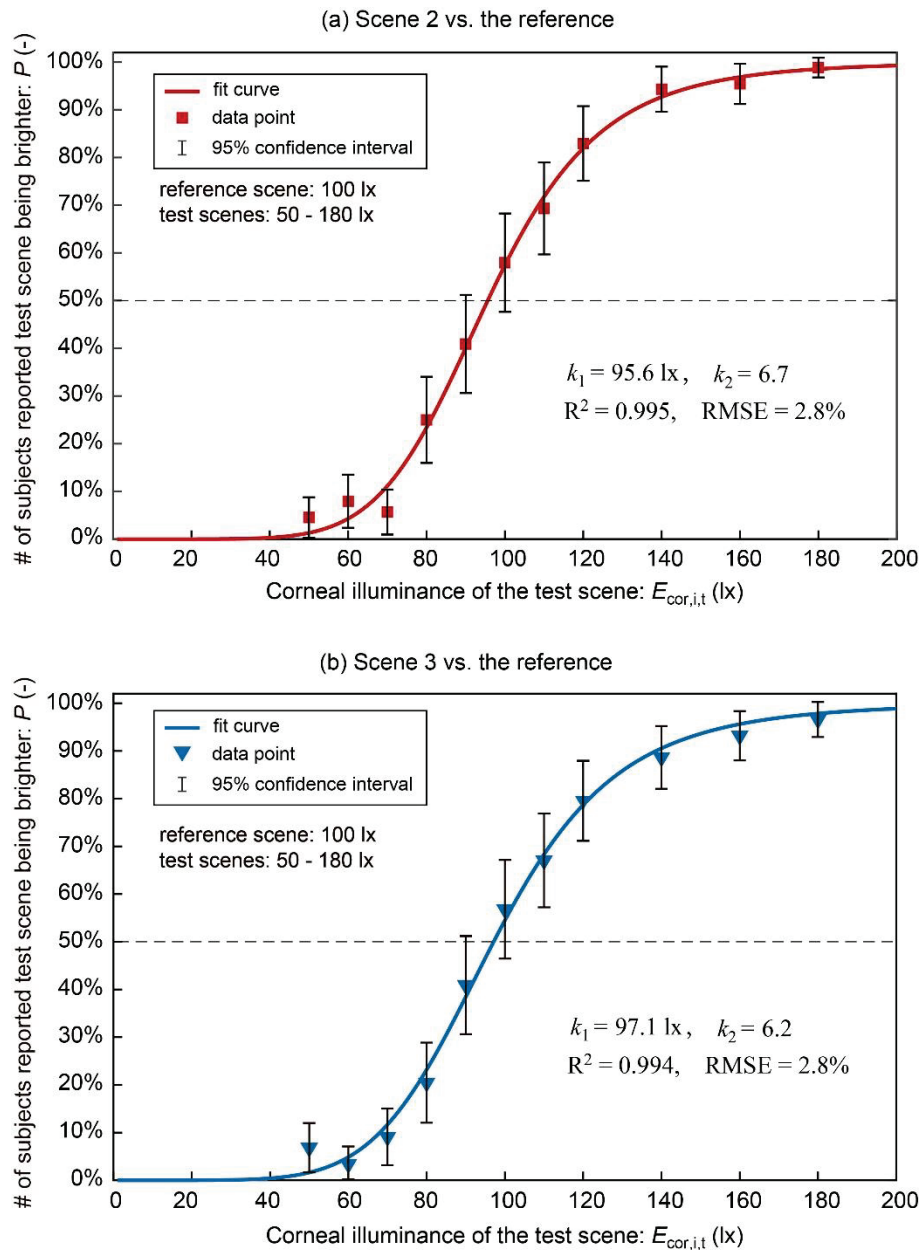


Figure 6. Experimental trials with a fixed reference (Scene 1 at 100 lx): (a) Scene 2 vs. the reference and (b) Scene 3 vs. the reference: the percentage of subjects who reported the test scene being brighter than the reference scene vs. corneal illuminance of the test scene, and the fit curves.

Besides, the  $k_2$  values obtained from both experimental trials were clearly smaller compared with that of the null-condition trial (6.7 & 6.2 for Scenes 2 & 3, respectively vs. 11.2 for Scene 1), which means that it was much more difficult to make a judgement on spatial brightness comparison when the patterns of lighting distribution between the reference and test scenes were different. According to the statistical results of the null-condition trial, it was suggested that the minimum interval of 10 lx was sufficient to distinguish the reference scene at 100 lx from the test scenes under different corneal illuminances other than 100 lx. In the two experimental trials with a fixed reference, the statistical t-test procedure was also applied to compare the data of the test scenes at 100 lx and that at the remaining 10 illuminance levels (from 50 to 180 lx), for Scenes 2 and 3. It was found that for both types of test scenes, there was no significant difference between the data

at 100 lx and that at 110 lx ( $p > 0.05$ , the  $p$  values for Scenes 2 and 3 were 0.068 and 0.118, respectively), while between the data at 100 lx and that at the rest 9 illuminances levels, there were still significant differences, as the corresponding  $p$  values were all less than 0.05. It indicated that when the lighting distribution patterns of the reference and test scenes were different, the judgement on the spatial brightness comparison became a little more difficult, but the influence was limited so that the  $k_1$  values (95.6 lx and 97.1 lx for Scene 2 and -Scene 3, respectively) could still be clearly determined by the same method, and they were found to be close to the ideal value of 100 lx.

### 3.3 Experimental trial for direct comparison

Furthermore, an experimental trial for direct comparison (named as the direct-comparison trial) between Scenes 2 and 3 was conducted by using the Scene 2 at 100 lx as the reference scene and the Scene 3 from 50 to 180 lx as the test scenes. The same experimental procedure in Figure 3(c) was performed and the corresponding data of  $P$  vs.  $E_{\text{cor},i,t}$  was obtained. As shown in Figure 7, fit curve based on Eq. (1) was applied to the experimental data: the fitting results of  $k_1 = 103.0$  lx (95% CI: 100.9 – 105.1 lx) and  $k_2 = 7.6$  were obtained.

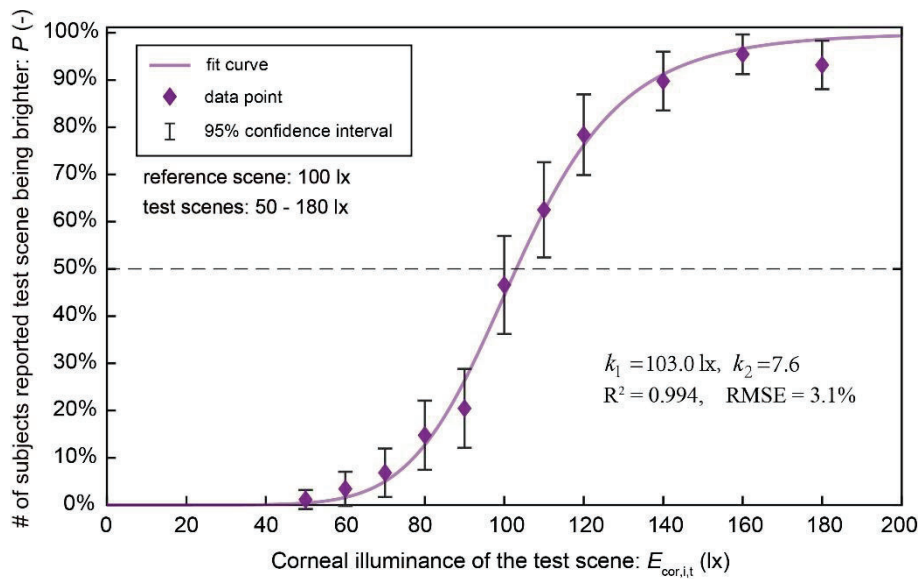


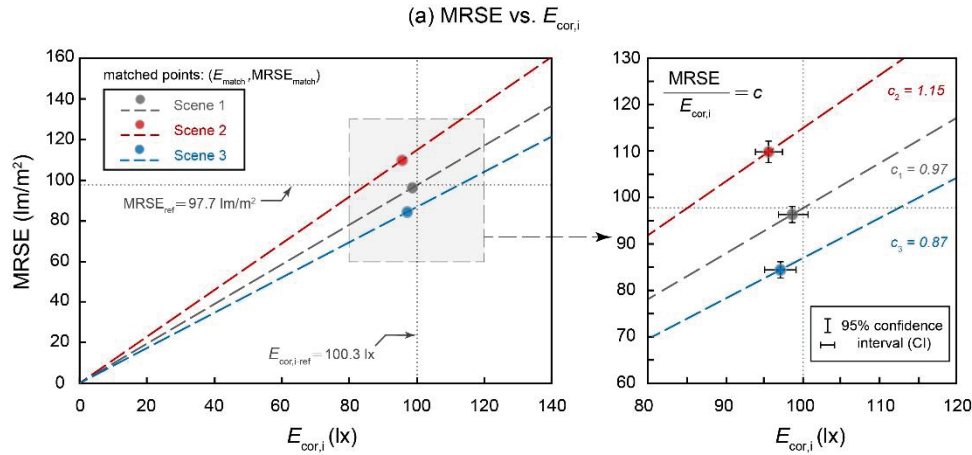
Figure 7. Experimental trial of Scene 3 vs. the reference (Scene 2 at 100 lx): the percentage of subjects who reported the test scene being brighter than the reference scene ( $P$ ) vs. corneal illuminance of the test scene ( $E_{\text{cor},i,t}$ ), and the fit curve.

The result showed that to match the spatial brightness of the reference scene (Scene 2 with a fixed corneal illuminance of 100.1 lx), a corneal illuminance of 103.0 lx was needed for Scene 3, which was also very close to the expected theoretical  $E_{\text{match}}$  value of 100.1 lx. It indicated that the proposed metric is still capable of assessing spatial brightness even when the patterns of lighting distribution for the two scenes are quite different. Besides, the  $k_2$  value obtained was clearly smaller compared with that of the null-condition trial, which means that it was more difficult to make a judgement on spatial brightness comparison when the patterns of lighting distribution between the reference and test scenes were very different.

## 4. Discussion

Based on the experimental results, it can be found that indirect corneal illuminance  $E_{\text{cor},i}$  highly correlates with subjective assessment of spatial brightness, even under very different patterns of lighting distribution. In prior studies, other metrics, including MRSE [1] and  $L_{\text{av},B40}$  [16,17], were also proposed to quantify the spatial brightness of illuminated interiors. To investigate the relative effectiveness among the three metrics, the applicability of the MRSE and  $L_{\text{av},B40}$  metrics were also analyzed by directly comparing with that of the  $E_{\text{cor},i}$  metric based on the same experimental data.

Note that the MRSE values discussed in this section referred to the area-weighted average of room-surface exitance within the subject's field of view, as the distribution of light outside the visual field does not contribute to the subject's perception.

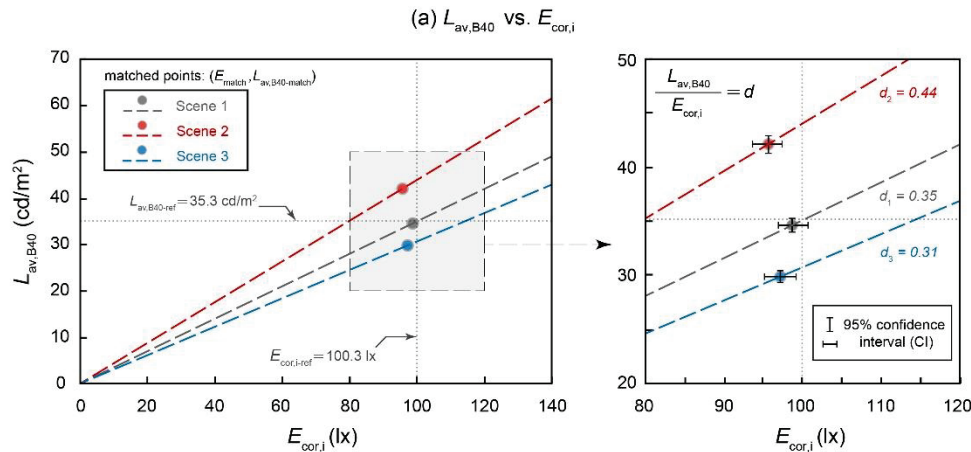


(b) The deviations of the spatial brightness evaluation metrics from the expected values

Matched points ( $E_{\text{match}}$ , $\text{MRSE}_{\text{match}}$ ) for	$E_{\text{match}}$ (lx)	95% CI of $E_{\text{cor},i}$ (lx)	$E_{\text{cor},i\text{-ref}}$ (lx)	deviation	$\text{MRSE}_{\text{match}}$ (lm/m <sup>2</sup> )	95% CI of $\text{MRSE}$ (lm/m <sup>2</sup> )	$\text{MRSE}_{\text{ref}}$ (lm/m <sup>2</sup> )	deviation
Scene 1	98.7	(96.9, 100.6)	100.3	-1.6% ↓	96.2	(94.9, 98.0)	97.7	-1.6% ↓
Scene 2	95.6	(93.7, 97.5)	100.3	-4.7% ↓	109.8	(107.7, 112.0)	97.7	12.4% ↑
Scene 3	97.1	(95.2, 99.1)	100.3	-3.2% ↓	84.3	(82.3, 85.7)	97.7	-13.7% ↓

Figure 8. The first two phases of trials with a fixed reference. (a) MRSE vs.  $E_{\text{cor},i}$ , and (b) the deviations of the  $E_{\text{match}}$  and  $\text{MRSE}_{\text{match}}$  values from the expected values of  $E_{\text{cor},i\text{-ref}}$  and  $\text{MRSE}_{\text{ref}}$ , respectively. The solid dots represent the matched points ( $E_{\text{match}}$ ,  $\text{MRSE}_{\text{match}}$ ) obtained from the experiment.

Under a fixed pattern of lighting distribution, the values of  $E_{\text{cor},i}$ , MRSE and  $L_{\text{av},\text{B40}}$  all increase linearly with the output flux of luminaires. In other words, there exist linear relationships between each of the two prior metrics (MRSE or  $L_{\text{av},\text{B40}}$ ) and our proposed metric of  $E_{\text{cor},i}$ . As shown in Figure 8 and 9, the three dashed lines represent the theoretical relationships between MRSE (or  $L_{\text{av},\text{B40}}$ ) and  $E_{\text{cor},i}$  corresponding to the three lighting scenes, Scenes 1-3. The slope of each line was determined by the specific pattern of lighting distribution. According to the linear relationship between MRSE (or  $L_{\text{av},\text{B40}}$ ) and  $E_{\text{cor},i}$ , once the slope has been determined, the values of MRSE and  $L_{\text{av},\text{B40}}$  required for test scenes to match the spatial brightness of the reference scene, denoted as  $\text{MRSE}_{\text{match}}$  and  $L_{\text{av},\text{B40-match}}$ , can be obtained from the value of  $E_{\text{match}}$ . The solid dots in Figure 8(a) and 9(a), ( $E_{\text{match}}$ ,  $\text{MRSE}_{\text{match}}$ ) and ( $E_{\text{match}}$ ,  $L_{\text{av},\text{B40-match}}$ ), are the “matched points” for equal spatial brightness between a fixed reference and test scenes obtained from the first two phases of trials (a null-condition trial and two experimental trials with a fixed reference). The corresponding values of the reference scene are denoted as  $E_{\text{cor},i\text{-ref}}$ ,  $\text{MRSE}_{\text{ref}}$ , and  $L_{\text{av},\text{B40-ref}}$ , and are marked as the grey dotted lines in Figure 8 and 9.



(b) The deviations of the spatial brightness evaluation metrics from the expected values

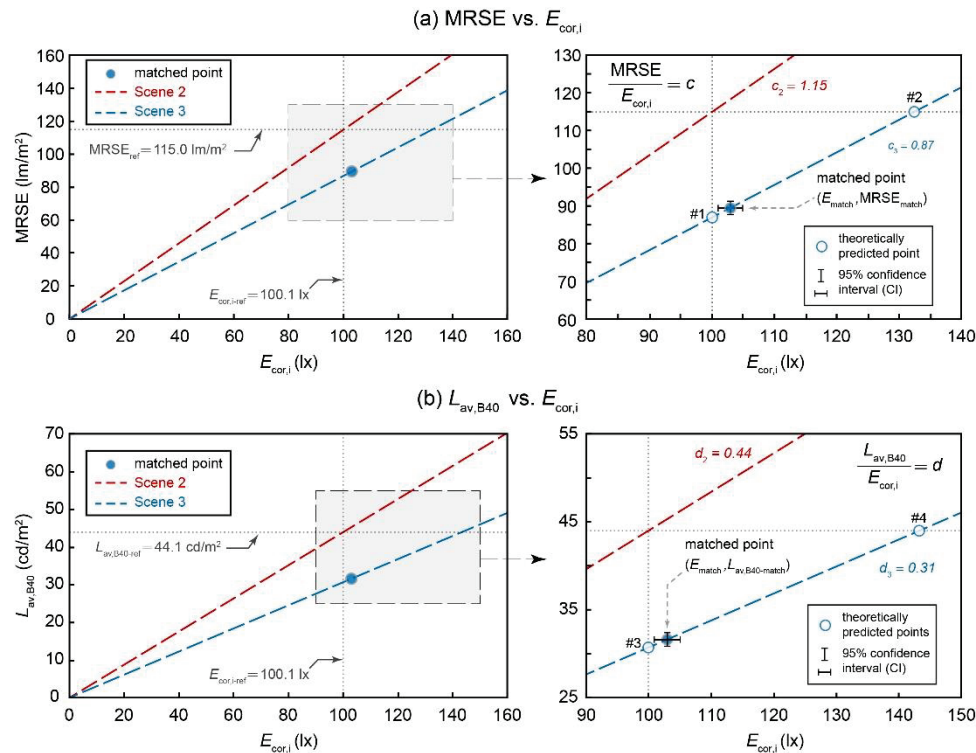
Matched points ( $E_{match}$ , $L_{av,B40-match}$ ) for	$E_{match}$ (lx)	95% CI of $E_{cor,i}$ (lx)	$E_{cor,i-ref}$ (lx)	deviation	$L_{av,B40-match}$ (cd/m <sup>2</sup> )	95% CI of $L_{av,B40}$ (cd/m <sup>2</sup> )	$L_{av,B40-ref}$ (cd/m <sup>2</sup> )	deviation
Scene 1	98.7	(96.9, 100.6)	100.3	-1.6% ↓	34.7	(34.1, 35.4)	35.3	-1.6% ↓
Scene 2	95.6	(93.7, 97.5)	100.3	-4.7% ↓	42.1	(41.2, 42.9)	35.3	19.3% ↑
Scene 3	97.1	(95.2, 99.1)	100.3	-3.2% ↓	29.8	(29.2, 30.5)	35.3	-15.6% ↓

Figure 9. The first two phases of trials with a fixed reference. (a)  $L_{av,B40}$  vs.  $E_{cor,i}$ , and (b) the deviations of the  $E_{match}$  and  $L_{av,B40-match}$  values from the expected values of  $E_{cor,i-ref}$  and  $L_{av,B40-ref}$ , respectively. The solid dots represent the matched points ( $E_{match}$ ,  $L_{av,B40-match}$ ) obtained from the experiment.

As shown in Figure 8 (b) and 9 (b), when the spatial brightness of the test scenes match that of the reference scene (for the reference scene,  $E_{cor,i-ref} = 100.3$  lx,  $MRSE_{ref} = 97.7$  lm/m<sup>2</sup> and  $L_{av,B40-ref} = 35.3$  cd/m<sup>2</sup>), the corresponding values of  $E_{match}$  are 98.7, 95.6 and 97.1 lx, the corresponding values of  $MRSE_{match}$  are 96.2, 109.8 and 84.3 lm/m<sup>2</sup>, and the values of  $L_{av,B40-match}$  are 34.7, 42.1 and 29.8 cd/m<sup>2</sup> for the Scenes 1, 2 and 3, respectively. For the null-condition trial, as the lighting distribution pattern of the Scene 1 and that of the reference scene were identical, the matched point of ( $E_{match}$ ,  $MRSE_{match}$ ) lies in the straight line of  $MRSE$  versus  $E_{cor,i}$  that passes through the origin point and the point of ( $E_{cor,i-ref}$ ,  $MRSE_{ref}$ ) (see the grey dashed line in Figure 8(a)), and the same conclusion holds for the scenario of  $L_{av,B40}$  versus  $E_{cor,i}$  (see the grey dashed line in Figure 9(a)). Therefore, for the null-condition trial, the metrics of  $MRSE$  and  $L_{av,B40}$  have the same deviation (-1.6%) as the metric of  $E_{cor,i}$  from the theoretically ideal values ( $MRSE_{ref}$ ,  $L_{av,B40-ref}$ , and  $E_{cor,i-ref}$ ). For the two experimental trials with a fixed reference, the deviations of  $E_{match}$  from the expected value  $E_{cor,i-ref}$  are still minor: -4.7% and -3.2% based on the comparisons of Scene 2 vs. the reference and Scene 3 vs. the reference, respectively. However, for the metric of  $MRSE$ , much greater deviations of 12.4% and -13.7% could be found from the comparisons of Scene 2 vs. the reference and Scene 3 vs. the reference, respectively, as shown in Figure 8(b). Moreover, even more significant deviations, 19.3% and -15.6%, were found for the metric of  $L_{av,B40}$  based on the comparisons of Scene 2 vs. the reference and Scene 3 vs. the reference, respectively, as shown in Figure 9 (b). In addition, the deviations of the three metrics can also be reflected from the geometric representation: the deviations of the matched points from the grey dotted line of  $E_{cor,i} = E_{cor,i-ref}$  represent the degree of accuracy of the metric  $E_{cor,i}$  (the same conclusion holds for  $MRSE$  and  $L_{av,B40}$ ). As shown in Figure 8(a) and 9(a), the matched points of the three trials in the first two phases are much closer to the line of  $E_{cor,i} = E_{cor,i-ref}$  compared with the lines of  $MRSE = MRSE_{ref}$  and  $L_{av,B40} = L_{av,B40-ref}$ , indicating that the metric of  $E_{cor,i}$  has the highest accuracy among the three metrics in the evaluation of spatial brightness for a visual field when comparing with the subjective assessment. Although a deviation of 10-15% by using the metric of  $MRSE$  may still be considered as acceptable in some lighting design practices, our recommended metric  $E_{cor,i}$  offers not only improved accuracy, but also much



improved convenience in measurement, making it a better metric to quantify spatial brightness for a visual field.



(c) The deviations of the spatial brightness evaluation metrics from the expected values

Scene 2		the values of Matched point for Scene 3		
$E_{\text{cor},i\text{-ref}}$ (lx)		$E_{\text{match}}$ (lx)	95% CI of $E_{\text{cor},i}$ (lx)	deviation
100.1		103.0	(100.9, 105.1)	2.9% ↑
MRSE <sub>ref</sub> (lm/m²)		MRSE <sub>match</sub> (lm/m²)	95% CI of MRSE (lm/m²)	deviation
115.0		89.4	(87.6, 91.2)	-22.3% ↓
$L_{\text{av},B40\text{-ref}}$ (cd/m²)		$L_{\text{av},B40\text{-match}}$ (cd/m²)	95% CI of $L_{\text{av},B40}$ (cd/m²)	deviation
44.1		31.6	(31.0, 32.2)	-28.3% ↓

Figure 10. The direct-comparison trial. (a) MRSE vs.  $E_{\text{cor},i}$ , (b)  $L_{\text{av},B40}$  vs.  $E_{\text{cor},i}$ , and (c) the deviations of the  $E_{\text{match}}$ ,  $\text{MRSE}_{\text{match}}$  and  $L_{\text{av},B40\text{-match}}$  values from the expected values of  $E_{\text{cor},i\text{-ref}}$ ,  $\text{MRSE}_{\text{ref}}$  and  $L_{\text{av},B40\text{-ref}}$ , respectively. The solid dots represent the matched points,  $(E_{\text{match}}, \text{MRSE}_{\text{match}})$  and  $(E_{\text{match}}, L_{\text{av},B40\text{-match}})$ , obtained from the experiment and the hollow dots #1 – #4 represent the theoretical predictions based on the three metrics.

The same analysis procedure is applied to the direct-comparison trial and the result is shown in the Figure 10. The solid dots in Figure 10 (a) and (b),  $(E_{\text{match}}, \text{MRSE}_{\text{match}})$  and  $(E_{\text{match}}, L_{\text{av},B40\text{-match}})$ , are the “matched points” for equal spatial brightness between the reference and test scenes from the experiment, while the hollow dots marked as #1 – #4 are the theoretically predicted points based on the predictions of the three metrics: the points #1 and #3 are based on the  $E_{\text{cor},i}$  metric, the point #2 is based the MRSE metric, and the point #4 is based on the  $L_{\text{av},B40}$  metric. It can be found that when comparing two scenes with very different patterns of spatial lighting distribution, the performance of the three metrics can be significantly different.

The results of the experiment show that the matched points are very close to the theoretically predicted points #1 and #3, which are based on the  $E_{\text{cor},i}$  metric. On the other hand, the theoretically predicted points based on the metrics of MRSE and  $L_{\text{av},B40}$ , the points #2 and #4, respectively, are

far away from the matched points. The geometric representation in Figure 10 (a) and (b) clearly shows that the metric of  $E_{\text{cor},i}$  is much more accurate in quantifying spatial brightness compared with the prior metrics of MRSE and  $L_{\text{av},B40}$ . Besides, a direct data overview of the deviations of the three metrics from the expected values is presented in Figure 10 (c). It can be found that when the spatial brightness of the test scene matches that of the reference scene (for the reference scene,  $E_{\text{cor},i-\text{ref}} = 100.1 \text{ lx}$ ,  $\text{MRSE}_{\text{ref}} = 115.0 \text{ lm/m}^2$  and  $L_{\text{av},B40-\text{ref}} = 44.1 \text{ cd/m}^2$ ), the corresponding values of  $E_{\text{match}}$ ,  $\text{MRSE}_{\text{match}}$  and  $L_{\text{av},B40-\text{match}}$  are  $103.0 \text{ lx}$ ,  $89.4 \text{ lm/m}^2$  and  $31.6 \text{ cd/m}^2$ , respectively. While the deviation of  $E_{\text{match}}$  from the expected value  $E_{\text{cor},i-\text{ref}}$  is still minor (2.9%), the values of  $\text{MRSE}_{\text{match}}$  and  $L_{\text{av},B40-\text{match}}$  show significant deviations of -22.3% and -28.3%, respectively, from the corresponding expected values. The result of the direct-comparison trial reconfirms that the metric of  $E_{\text{cor},i}$  can serve as a better metric with much higher accuracy compared with the prior metrics of MRSE and  $L_{\text{av},B40}$  in assessing the spatial brightness for a visual field.

Therefore, in all possible comparison pairs among the Scenes 1-3, the results all suggest that our proposed metric of  $E_{\text{cor},i}$  has much improved accuracy compared with the prior metrics of MRSE and  $L_{\text{av},B40}$ . Especially, the metric  $E_{\text{cor},i}$  can ensure a deviation within  $\pm 5\%$  in assessing spatial brightness for a visual field. With such a high accuracy and the additional benefit of convenience in measurement, the metric of  $E_{\text{cor},i}$  has much superior performance compared with the prior metrics of MRSE and  $L_{\text{av},B40}$ .

## 5. Limitations

Note that in this work, spatial brightness comparisons were performed with the reference scene fixed at a corneal illuminance of 100 lx. Future work is suggested to investigate the behavior with the reference scene set to other illuminance levels. Also, our proposed method relies on the acquisition of the indirect part of the corneal illuminance value. For those cases where the proportion of direct light is significant for the visual field, we recommend using the method of Duff et al. [18] to obtain the indirect portion of corneal illuminance via a method based on HDR imaging. The involvement of HDR imaging makes the measurement procedure less convenient, but it is still much simpler than the MRSE measurement method [18,19] adopting the same HDR imaging process.

## 6. Conclusion

In this work, a quantitative method was developed for comparisons of spatial brightness within a visual field among three lighting scenes with various patterns of lighting distribution. The indirect corneal illuminance required for each test scene to match the spatial brightness perception of the reference scene with a fixed corneal illuminance was obtained. It was demonstrated that the metric of indirect corneal illuminance,  $E_{\text{cor},i}$ , had a very good correlation with the subjective evaluation of spatial brightness. Furthermore, the performance of the  $E_{\text{cor},i}$  metric was demonstrated to be much better compared with that of the previously proposed metrics of MRSE and  $L_{\text{av},B40}$  in terms of the correlation with the subjective evaluation of spatial brightness. Besides, the  $E_{\text{cor},i}$  metric has a great advantage over the other two alternative metrics in the convenience of measurement, which is also critical for the acceptance of the metric by lighting practitioners. Therefore, we suggest that indirect corneal illuminance could serve as a preferred metric to quantify spatial brightness for a visual field, and the values of this metric at various visual fields together can be used to quantify people's overall impression of an illuminated space. The authors believe that the outcome of this work could provide valuable insights toward the establishment of a widely accepted quantitative evaluation method for the spatial brightness of interior spaces.

## Funding

National Natural Science Foundation of China (51878464); National Natural Science Foundation

of China (52278095).

## Disclosures

The authors declare no conflicts of interest.

## Data availability statement

Data underlying the results presented in this paper are not publicly available at this time but may be obtained from the authors upon reasonable request.

## References

- [1] C. Cuttle. Towards the third stage of the lighting profession. *Lighting Research and Technology*. 2010, 42(1), 73-93.
- [2] C. Cuttle. A new direction for general lighting practice. *Lighting Research and Technology*. 2013, 45(1), 22-39.
- [3] C. Cuttle. Making the switch from task illumination to ambient illumination standards: Principles and practicalities, including energy implication. *Lighting Research and Technology*. 2019, 52(4), 455-471.
- [4] Q. Dai, Y. Huang, L. Hao, Y. Lin, K. Chen, Spatial and spectral illumination design for energy-efficient circadian lighting. *Building and Environment*. 2018, 146, 216-225.
- [5] W. Cai, J. Yue, Q. Dai, L. Hao, Y. Lin, W. Shi, Y. Huang, and M. Wei, The impact of room surface reflectance on corneal illuminance and rule-of-thumb equations for circadian lighting design. *Building and Environment*. 2018, 141, 288-297.
- [6] Q. Yao, W. Cai, M. Li, Z. Hu, P. Xue, and Q. Dai, Efficient circadian daylighting: A proposed equation, experimental validation, and the consequent importance of room surface reflectance. *Energy and Buildings*. 2020, 210, 109784.
- [7] Z. Hu, P. Zhang, Y. Huang, M. Li, Q. Dai, The impact of melanopic and CCT on spatial brightness perception of illuminated interiors and energy-saving implications. *Building and Environment*. 2022, 223, 109524.
- [8] S. Fotios, D. Atli, C. Cheal, K. Houser, A. Logadottir, Lamp spectrum and spatial brightness at photopic levels: A basis for developing a metric. *Lighting Research and Technology*. 2015, 47(1), 80-102.
- [9] S. Fotios, D. Atli, C. Cheal, N. Hara, Lamp spectrum and spatial brightness at photopic levels: Investigating prediction using S/P ratio and gamut area. *Lighting Research and Technology*. 2015, 47(5), 595-612.
- [10] M. S. Rea, X. Mou, J. D. Bullough, Scene brightness of illuminated interiors. *Lighting Research and Technology*. 2016, 48(7), 823-831.
- [11] Commission Internationale de l'Eclairage (CIE), Guidance towards Best Practice in Psychophysical Procedures Used when Measuring Relative Spatial Brightness. CIE 212: 2014.
- [12] S. Fotios, D. Atli, Comparing Judgments of Visual Clarity and Spatial Brightness Through an Analysis of Studies Using the Category Rating Procedure. *Leukos*, 8(4), 261-281.
- [13] W. van Bommel, *Interior Lighting: Fundamentals, Technology and Application*. Springer, 2019.
- [14] J. Duff, K. Kelly, C. Cuttle, Spatial brightness, horizontal illuminance and mean room surface exitance in a lighting booth. *Lighting Research and Technology*. 2017, 49(1), 5-15.
- [15] J. Duff, K. Kelly, C. Cuttle, Perceived adequacy of illumination, spatial brightness, horizontal illuminance and mean room surface exitance in a small office. *Lighting Research and Technology*. 49(2), 133-146.
- [16] D. L. Loe, K. P. Mansfield, E. Rowlands, Appearance of lit environment and its relevance in

- lighting design: experimental study. *Lighting Research and Technology*. 1994, 26(3), 119-133.
- [17] D. L. Loe, K. P. Mansfield, E. Rowlands, A step in quantifying the appearance of a lit scene. *Lighting Research and Technology*. 2000, 32(4), 213-222.
  - [18] J. Duff, G. Antonutto, S. Torres, On the calculation and measurement of mean room surface exitance. *Lighting Research and Technology*. 2016, 48(3), 384-388.
  - [19] P. Zhang, M. Li, Y. Huang, Q. Dai, A practical method for field measurement of mean room surface exitance. *Lighting Research and Technology*. 2022, 54(7), 674-689.
  - [20] S. M. Berman, D. L. Jewett, G. Fein, G. Saika, F. Ashford, Photopic luminance does not always predict perceived room brightness. *Lighting Research and Technology*. 1990, 22, 37-41.
  - [21] W. Hua, J. Jin, X. Wu, J. Yang, X. Jiang, G. Gao, F. Tao, Elevated light levels in schools have a protective effect on myopia. *Ophthalmic and Physiological Optics*. 2015, 35(3), 252-262.
  - [22] A. D. Vries, J. L. Souman, B. D. Ruyter, Lighting up the office: The effect of wall luminance on room appraisal, office workers' performance, and subjective alertness. *Building and Environment*. 2018, 142, 534-543.
  - [23] M. Islam, R. Dangol, M. Hyvarinen, P. Bhusal, M. Puolakka, L. Halonen, User acceptance studies for LED office lighting: lamp spectrum, spatial brightness and illuminance. *Lighting Research and Technology*. 2015, 47(1), 54-79.
  - [24] P. R. Boyce, *Human Factors in Lighting*, 3rd Edition. CRC Press, 2014.
  - [25] S. Grondin, *Psychology of Perception*. Springer, 2016.
  - [26] N. A. Macmillan, C. D. Creelman, *Detection theory: A user's guide*. Cambridge University Press, 1991.
  - [27] S. Fotios, K. Houser, Using Forced Choice Discrimination to Measure the Perceptual Response to Light of Different Characteristics. *Leukos*, 2013, 9(4), 245-259.
  - [28] S. Fotios, Chromatic adaptation and the relationship between lamp spectrum and brightness. *Lighting Research and Technology*. 2006, 38(1), 3-17.

## ACKNOWLEDGEMENT

Corresponding Author: Qi Dai

Affiliation: Institute for Electric Light Sources, Department of Light Sources and Illuminating Engineering,  
School of Information Science and Technology, Fudan University  
e-mail : qidai@fudan.edu.cn

# THE CONTROL OF DAYLIGHT AND ELECTRIC LIGHT COMBINATION MODES IN CLASSROOMS FOR ADOLESCENTS' NON-VISUAL HEALTH: A SIMULATION-BASED APPROACH

Diehong Tong, Junli Xu\*

(School of Architecture, Soochow University, Jiangsu, China)

## ABSTRACT

Improving the classroom's light environment (daylight and electric light) is essential to promote the health of students. When the amount of daylight is insufficient, the use of appropriate electric light to supplement lighting can provide a good visual and non-visual environment for adolescents. The study aimed to develop prediction models for the non-visual environment in classrooms. Firstly, the light environment of a typical classroom was simulated using DIALux evo simulation software, and the vertical illumination of eyes was simulated under different daylight or electronic light condition only. Then, the spectral characteristics of light sources were used to derive and obtain the spatial melanopic EDI distribution rules under these conditions. Secondly, build prediction models that can control the combination modes of daylight and electric light in the classroom from the dataset, which can be used to select the configuration of electric light according to the changes of daylight (different weather conditions, or different seasons). Finally, determine the best combination modes suitable for adolescents' non-visual health. The process and conclusions of the study were helpful to provide methodological and data support for enhancing the design of healthy light environments in classrooms.

Keywords: Classroom, Non-visual effect, Daylight and electric light, Combination modes, Lighting control

## 1. INTRODUCTION

Light (daylight and electric light) is an important part of the building physical environment, which not only has an impact on human vision, but also can trigger non-visual effects, and then affect people's sleep, alertness, mood, work performance, satisfaction, etc. [1]. At the same time, the influence of light on the circadian rhythm system of adolescents is greater than that of adults [2]. Especially in the context of Chinese education, adolescents who stay in the classroom space for a long time tend to suffer from daytime sleepiness, lack of energy, low mood, depression and other problems in the past decade [3]. Therefore, it is very important to improve the quality of the classroom light environment, which will effectively improve the health level of teenagers.

Until now, in order to optimize the availability of light in indoor space, Hertog et al. [4] used a lighting system with adjustable SPD to supplement or increase the amount of light in Spaces with insufficient daylight. It showed that this lighting mode can not only improve lighting quality, but also save significant amounts of energy. Mathew et al. [5] built a daylight-artificial light integrated system based on multi-objective genetic algorithm optimization technology in order to minimize glare and maximize CS in the working space. By collecting light information data, the sensor can automatically adjust electric light parameters according to changes in daylight conditions. Aguilar-Carrasco et al. [6] optimized workspace design both on the electric lighting configurations and windows and indoor distribution to enhance circadian stimulus assuming the integration with daylighting. More and more researchers have begun to pay attention to the control of the combination modes of daylight and electric light [7-9]. Nevertheless, because the calculation of non-visual effects is more complex than that of visual effects, it is more complicated to evaluate the level of rhythmic stimulation in space. So, the novelty of this study lies in developing prediction models for the non-visual environment in classrooms to get results quickly and easily.



## 2. METHODS

### 2.1 Characteristics of the room model

According to the most common classroom design in Suzhou, China, a virtual space 3.4 m high by 7.8 m deep by 9.3 m wide was defined. The reflectance ratio of typical materials used for each surface of the model is 0.70 for the wall, 0.80 for the ceiling, 0.20 for the floor and 0.30 for the desk. DIALux evo simulation software is used to simulate the light environment of the south-facing classroom in the standard level. The virtual classroom and the quantification of its calculation variables are shown in Fig. 1.

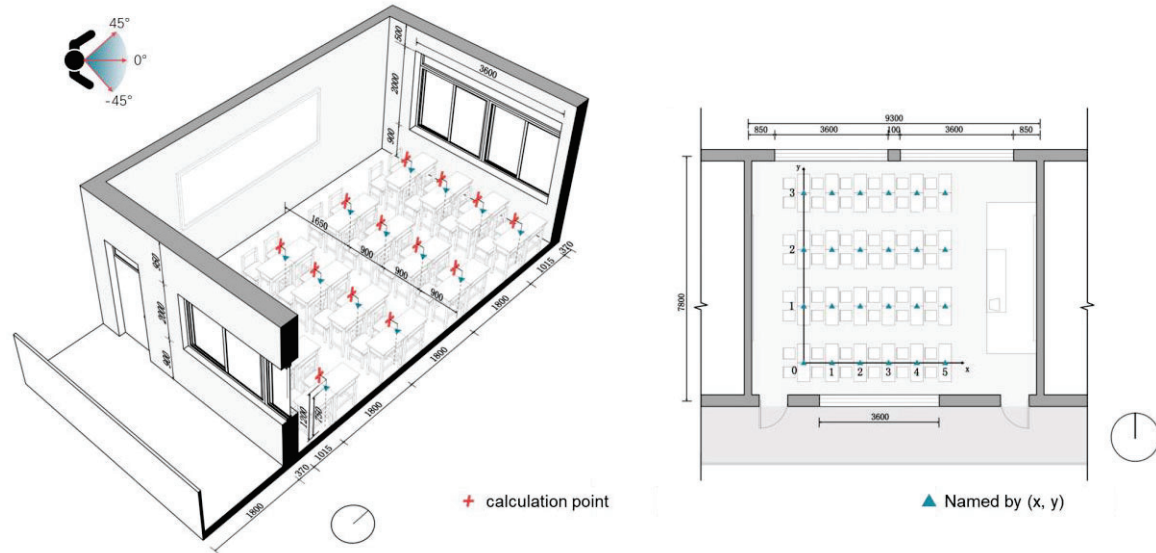


Figure 1. model of the classroom.

### 2.2 Selecting the light conditions

The effect of light on non-visual effects depends on a number of factors, in particular light intensity and SPD. Therefore, taking summer (June 21st) and winter (December 21st) as examples, two typical weather conditions of clear sky (15,000 K) and overcast sky (6500 K) were simulated [10]. Since daylight does not always provide sufficient circadian stimulus [2], electric light plays a vital role in providing human lighting needs and supporting their health, taking 4000K LED as an example, to explore the corresponding luminous fluxes.

### 2.3 Calculation process

DIALux evo simulation software was used to simulate the light environment, and the average vertical eye illumination value of each calculation point was obtained at an interval of 1 h during the period from 9:00 to 13:00. According to the method of Bellia, Aguilar-Carrasco et al. [8,11], as shown in Formula (1)(2), where  $\lambda$  is the wavelength (nm),  $SPD_{eye}(\lambda)$ ,  $SPD_d(\lambda)$ ,  $SPD_e(\lambda)$ ,  $SPD_r(\lambda)$ , are the SPD of the observer's eye, daylight, electric light and average spectral reflectance of the environment,  $E_d$  is the illuminance given by daylight,  $E_e$  is the illuminance given by electric light,  $E_{d\&e}$  is the illuminance given by daylight and electric light,  $S_{mel}(\lambda)$  is the spectral sensitivity function of melanopsin, and  $V(\lambda)$  is the photopic luminous efficiency function.

$$\int_{380}^{780} SPD_{eye}(\lambda) d\lambda = \frac{E_d}{E_{d\&e}} \int_{380}^{780} SPD_d(\lambda) d\lambda \times \int_{380}^{780} SPD_r(\lambda) d\lambda + \frac{E_e}{E_{d\&e}} \int_{380}^{780} SPD_e(\lambda) d\lambda \times \int_{380}^{780} SPD_r(\lambda) d\lambda \quad (1)$$

$$melanopic\ EDI = 1.104 \times \frac{\int_{380}^{780} SPD_{eye}(\lambda) S_{mel}(\lambda) d\lambda}{\int_{380}^{780} SPD_{eye}(\lambda) V(\lambda) d\lambda} \times E_{d\&e} \quad (2)$$

The results were compared with the standard threshold requirement [12] ( $melanopic\ EDI \geq 181\ lx$ ), and the changes of circadian stimulus levels in different areas and their percentage of Effective Circadian Effective Area (CEA) [13] were analysed in the classroom.

### 3. RESULT

#### 3.1 Circadian stimulus promoted by daylight

Fig. 2 shows the melanopic EDI distributions at the eye-level of the basic case during 9:00 to 13:00. For clear sky, due to the high CCT and high illumination of daylight at this time, a high level of circadian stimulus can be achieved under all conditions, and its  $CEA_{4h, 181\text{ lx}}$  is 100 %. However, the melanopic EDI value of each calculation point fluctuates greatly at all times, and its value distribution is relatively discrete, especially in summer (the maximum range is 1308.26 lx from 9:00). For overcast sky, the hourly melanopic EDI value in classroom space increased gradually from 9:00 to 12:00, and decreased slightly from 12:00 to 13:00. Of the four conditions, the level of circadian stimulus on December 21st, overcast sky ( $CEA_{4h, 181\text{ lx}}=25\%$ ) is lower than those of the other conditions.

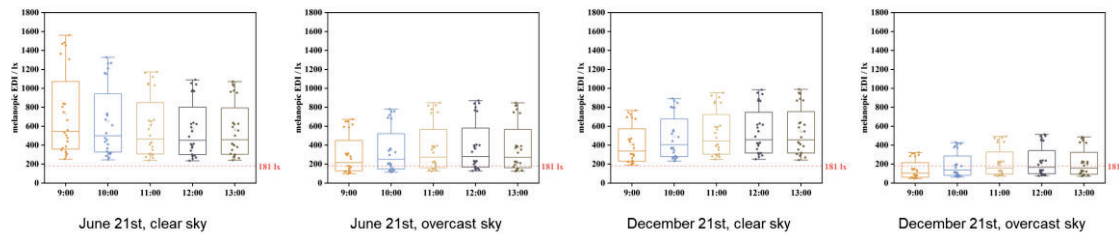


Figure 2. Chronological melanopic EDI distribution of 24 calculation points at the eye-level.

As can be seen in Fig. 3, the distribution of the average melanopic EDI of each calculation point in the classroom space is expressed from a three-dimensional perspective. The red curve represents the distribution position in the space where the melanopic EDI is 250 lx (the recommended minimum threshold for WELL Building Standard grade 2). The black curve indicates the location of the melanopic EDI of 181 lx in space. From the perspective of space as a whole, the level distribution of circadian stimulus in classroom space showed obvious spatial differences, and mostly followed a similar change rule, that is, the melanopic EDI value in the north side was significantly higher than that in the south side. In addition, the west side had better levels of rhythmic stimulation than the east side region, but the amount of difference between the two was smaller. Both the south and middle regions ( $y=0$  or  $1$  or  $2$ ) showed a gradually decreasing trend from west to east showed in Fig. 4, but the trend was more stable than that in the north and south. In the north region ( $y=3$ ), the data fluctuated greatly, and the melanopic EDI increased slightly at the calculation points (3,3) and (3,4), indicating that due to the 100 mm wall between the two windows on the north side, the amount of daylight received by some calculation points decreased. This results in locally abnormal changes in the level of circadian stimulus in this region ( $y=3$ ).

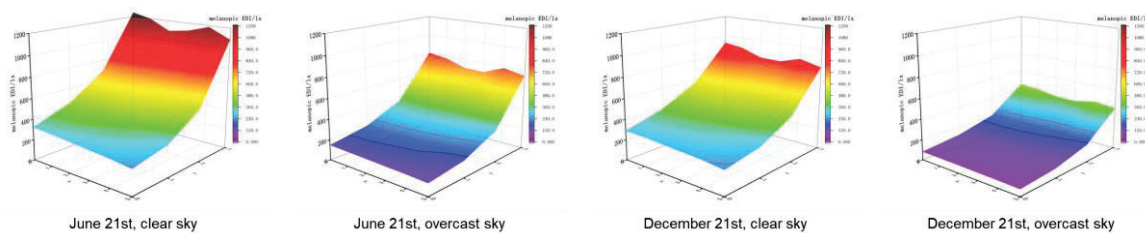


Figure 3. Average circadian stimulus in classroom.

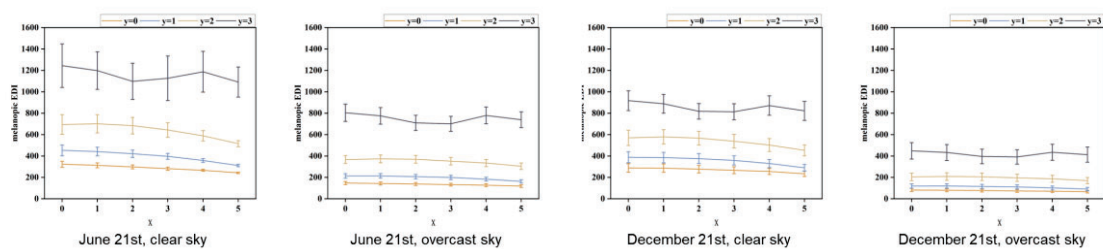


Figure 4. Distribution of mean value and standard deviation of melanopic EDI in each cross section.

### 3.2 Electric light control under different daylight conditions

According to the strength of the influence of daylight on circadian stimulus, the classroom space can be divided into three areas from north to south, namely, the effective use area in the north ( $y=2$  or  $3$ ), the appropriate supplement area in the middle ( $y=1$ ), and the key supplement area in the south ( $y=0$ ).

(1) The effective use area in the north can almost all show a good level of circadian stimulus under the condition of daylight only, but the illumination value in this area is usually too large, which will affect the normal learning behaviour of users. The shading of the north window should be given priority in the design, and the effective use of daylight during the simulation should be achieved by modifying the amount of light entering.

(2) The appropriate supplement area in the middle belongs to the area relative to the middle of the classroom space and is less affected by daylight. In particular, when the winter is overcast sky, it is difficult for the area to meet or exceed the standard threshold requirements. The design can be considered in combination with the other two areas, which also makes it possible to better transition the amount of light in the space.

(3) The key supplementary area in the south is the area in the classroom space in urgent need of reasonable allocation of electric light. Although it is close to the window, compared with the effective utilization area in the north this area is least affected by daylight and needs additional artificial light for supplementary lighting most of the time (except clear sky) to increase the  $CEA_{4h, 181\text{ lx}}$  in this area.

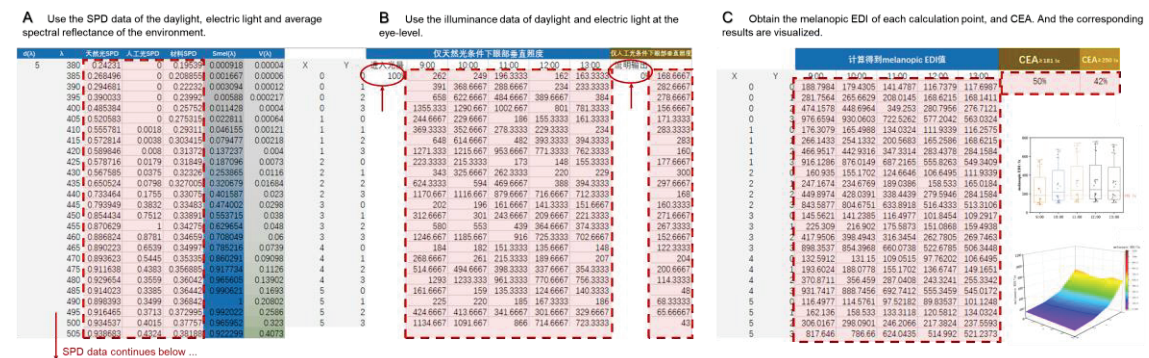


Figure 5. Representations of the toolbox: "Inputs" and "Outputs".

According to the spectral characteristics of light source, Excel software was used to design an evaluation toolbox for calculating the circadian stimulus of classroom showed in Fig. 5, and the corresponding melanopic EDI and CEA under different combination modes of daylight and electric light in the space were calculated, and the results are visualized.

When using the toolbox with the SPD and illuminance data collected for December 21st, overcast sky, the toolbox output sheet gives the following results:

$$CEA_{4h, 181\text{ lx}} = 25\%$$

The results show that the results obtained by the simplified method are similar to those obtained by the toolbox. Therefore, control of electric light can be carried out in the next step. If a electric light with a 4000 K LED, and luminous fluxes of 3091 lm is selected,  $CEA_{4h, \geq 181\text{ lx}}$  can be increased to  $75\% \pm 4\%$ . When the luminous fluxes of electric light continue to increase, the circadian stimulus of the classroom will show a better level. But at this time, it may cause problems such as the increase of the level of illumination of the desk surface and the increase of energy consumption. In the future, we will continue to deepen the toolbox with the goal of integrative lighting. Based on multi-objective optimization, spatial circadian stimulus is optimized.

## 4. CONCLUSION

The classrooms require sufficient melanopic illuminance to entrain the circadian rhythms of their occupants, and the ideal source of that illuminance is daylight. This study briefly introduces the distribution law of different natural light conditions on the classroom rhythm stimulation. It is

important to note that the classrooms can be divided into three areas according to the result of daylight only. Based on this data set, a combined model calculator is designed, which is easy to that control the combination modes of daylight and electric light in the classroom from the dataset, which can be used to select the configuration of electric light according to the changes of daylight. The process and conclusions of the study were helpful to provide methodological and data support for enhancing the design of healthy light environments in classrooms.

## REFERENCE

- [1] Blume C, Garbazza C, Spitschan M. Effects of light on human circadian rhythms, sleep and mood[J]. *Somnologie*, 2019, 23(3): 147-156.
- [2] Acosta I, Campano M Á, Leslie R, et al. Daylighting design for healthy environments: Analysis of educational spaces for optimal circadian stimulus[J]. *Solar Energy*, 2019, 193: 584-596.
- [3] Fu X L, Zhang K, Chen X F, et al. Report on National Mental Health Development in China (2021-2021)[M]. Social Sciences Academic Press (China), 2023.
- [4] Hertog W, Llenas A, Carreras J. Optimizing indoor illumination quality and energy efficiency using a spectrally tunable lighting system to augment natural daylight[J]. *Optics Express*, 2015, 23(24): A1564-A1574.
- [5] Mathew V, Kurian C P, Augustine N. Optimizing daylight glare and circadian entrainment in a Daylight-Artificial Light Integrated scheme[J]. *IEEE Access*, 2022, 10: 38174-38188.
- [6] Campano M Á, Acosta I, Domínguez S, et al. Dynamic analysis of office lighting smart controls management based on user requirements[J]. *Automation in Construction*, 2022, 133: 104021.
- [7] Kaymaz E, Manav B. A Proposal on Residential Lighting Design Considering Visual Requirements, Circadian Factors and Energy Performance of Lighting[J]. *Journal of Asian Architecture and Building Engineering*, 2022 (just-accepted).
- [8] Aguilar-Carrasco M T, Domínguez-Amarillo S, Acosta I, et al. Indoor lighting design for healthier workplaces: natural and electric light assessment for suitable circadian stimulus[J]. *Optics Express*, 2021, 29(19): 29899-29917.
- [9] Zeng Y, Sun H, Lin B. Optimized lighting energy consumption for non-visual effects: A case study in office spaces based on field test and simulation[J]. *Building and Environment*, 2021, 205: 108238.
- [10] Bellia L, Pedace A, Barbato G. Daylighting offices: A first step toward an analysis of photobiological effects for design practice purposes[J]. *Building and Environment*, 2014, 74: 54-64.
- [11] Bellia L, Pedace A, Barbato G. Lighting in educational environments: An example of a complete analysis of the effects of daylight and electric light on occupants[J]. *Building and Environment*, 2013, 68: 50-65.
- [12] Ranking evaluation for classroom lighting quality in primary and middle schools[S]. Beijing: Standards Press of China, 2020.
- [13] Konis K. A novel circadian daylight metric for building design and evaluation[J]. *Building and Environment*, 2017, 113: 22-38.

## ACKNOWLEDGEMENT

This work was supported by the Postgraduate Research & Practice Innovation Program of Jiangsu Province (grant number KYCX23\_3251), the Student Extracurricular Academic Research Fund Project of Soochow University (grant number KY2023229B). National Natural Science Foundation of China (grant number 51808364) and China Scholarship Council (grant number 202106920031)

Corresponding Author: Junli Xu  
 Affiliation: School of Architecture, Soochow University  
 e-mail: xujunlidd@126.com



# RESEARCH ON GUIDING FACTORS OF LIGHTING IN COMPLEX SPACE OF UNDERGROUND RAIL TRANSIT STATION

Lixiong Wang<sup>1</sup>, Bochao Huang<sup>1</sup>, Juan Yu<sup>1</sup>, Chuyao Wang<sup>1</sup>

(1.School of Architecture, Tianjin University, Tianjin, China)

## ABSTRACT

The contradiction between the need for visual order and functional diversity in composite spaces is becoming increasingly prominent. Taking underground rail stations as a typical example, their spatial functions include not only the collection and distribution of people, ticketing, but also commercial retail, with numerous functional facilities intersecting with each other in the traffic flow and interfering with passengers' cognition and recognition of spatial order. The intrinsic guiding characteristics of lighting play an irreplaceable role in regulating and reshaping the order of space. Especially in closed space environments such as underground rail stations, which rely entirely on artificial lighting, the use of lighting to reshape spatial information is an effective means of enhancing the target value of functional composite spaces at low cost. In order to investigate the lighting guiding elements of composite spaces and their influence on the perception of space, and to enhance the orderliness of composite spaces. The lighting elements and typical models of 29 railway station spaces were obtained through field research. The DIALux software was used to simulate the lighting solutions and analyse the simulation data, the number of votes for the solutions and the task completion score. The results show that in addition to the spatial luminosity element which is the basic element influencing the lighting directivity, the spatial layout element and the morphological element of the light source are the key elements influencing the lighting directivity. On this basis, the lighting optimisation strategies proposed in terms of zoned lighting and spatial layout elements of interlaced light sources, and morphological elements of linear light sources extending along the walking direction, can contribute to the efficient enhancement of the orderliness of the architectural composite space.

Keywords: Composite space, Lighting guidance, Influencing factors, Order, Software simulation

## 1. INTRODUCTION

The function of modern public buildings is more diversified and complex, and the contradiction between the spatial visual order demand and the spatial function compound is increasingly prominent. Due to people's phototaxis instinct, the inherent guiding characteristics of lighting play an irreplaceable role in shaping and strengthening space. Using the guidance of lighting can improve the efficiency of space recognition, effectively guide people's searching behavior, reduce people's psychological anxiety, and improve the quality of space design and space experience.

Research has initially demonstrated that lighting influences spatial perception and behavioural performance through interventions in the perception of spatial visual information. Lighting can act as environmental cues to highlight spatial features[1], thereby influencing spatial perception[2] and changing the attractiveness of space to people, thus enabling lighting to guide them at the level of spatial perception[3][4]. Lighting can influence behavioural performance when there is a specific wayfinding task[5], and when there is no specific task[6], lighting can influence walking speed and route choice. Due to the complex relationship between lighting and guidance effects, there is a lack of theoretical research on the factors that influence the guiding effect of lighting in composite spaces, Therefore, it is urgent to explore the influencing factors that produce guiding effect of lighting.

The spatial functions of underground rail transit stations include not only people gathering and distributing, ticket purchasing and checking, but also commercial retail. Traffic flow lines cross each other and many functional facilities are laid out, which interferes with passengers' cognition and discrimination of space order. In the case that the space environment of the station hall is closed and completely dependent on artificial lighting, the use of lighting means to reshape the spatial information is an effective means to improve the target value of functional composite space at low cost.



Therefore, this paper takes the underground rail transit station hall space as an example, with the goal of improving guidance, investigates the lighting data of 29 station halls on the spot, and puts forward a typical model. DIALux software was used to carry out lighting simulation. The analysis results of simulation data, scheme votes and task completion score were integrated. On the basis that the basic environmental lighting parameters such as average illumination, illumination uniformity and glare value of the lighting scheme meet the standard requirements, the influence of spatial layout elements and form elements of the lighting source on the lighting guidance is explored, and the corresponding optimal lighting parameters are obtained. The aim is to improve the lighting design of the composite space and enhance the space order based on the lighting guidance requirements.

## 2. EXPERIMENTAL SIMULATION AND EVALUATION OF GUIDING LIGHTING ELEMENTS OF STATION HALL

Based on the previous questionnaire survey data, the stations with better passenger feedback were selected, the lighting status survey data were extracted, and the lighting design schemes of the stations with higher satisfaction were summarized. Taking each function of the site as the unit, the current situation of light source and the measurement data of lighting parameters were counted, and the lighting scene model required for the experiment was constructed.

### 2.1 Establishment of station hall space model

The 29 rail transit stations are distributed in five cities: Beijing, Shanghai, Hangzhou, Guangzhou and Shenzhen. Among them, Guangzhou Kecun rail transit station is a relatively new construction station, which meets the requirements of typical functional composite space: the hall column network is  $5.8\text{m} \times 8.4\text{m}$ , the columns have a total of 12 spans, the left and right non-paying areas occupy 2-3 spans, and the height is 4m. There are 4 groups of gates and 2 groups of ticket vending machines on the station floor. The interface reflection ratio is set as follows: ceiling 0.7, wall 0.68, floor 0.68, in addition, the reflectivity of the glass in the space is set as 0.08, and the transmittance is 0.8; The reflectance of the stainless steel plate of the brake is 0.72

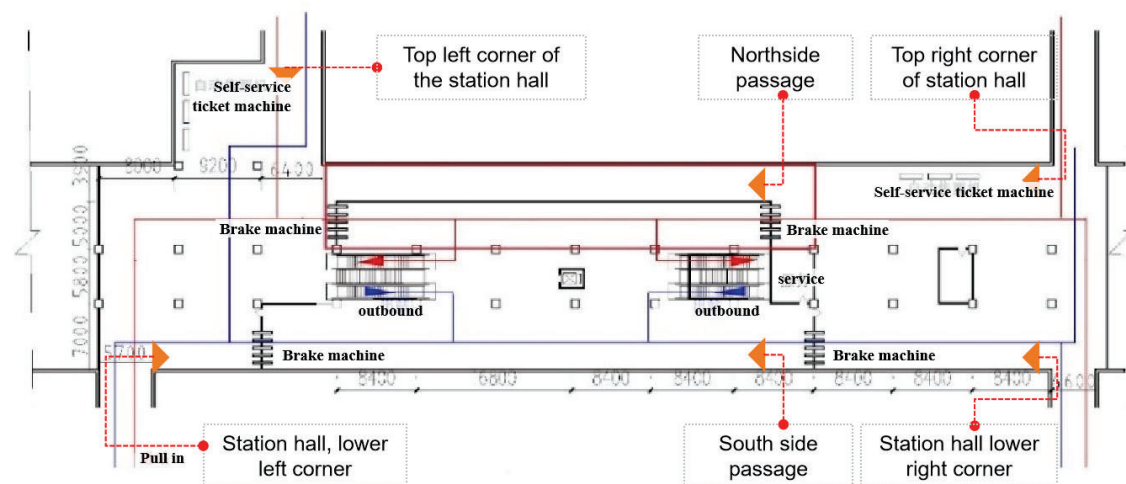


Figure 1 Floor plan of the station hall (Picture source: self-drawn by the author)

### 2.2 Introduction to lighting simulation scheme

Therefore, according to the standard requirements, the average illuminance, uniformity and power density of the horizontal plane of the control station are studied[7]. Starting from the improvement of guidance, this research mainly set up lighting schemes in three typical lighting methods, as shown in Table 1: By changing the installation mode of light source, the category of lamps, the layout direction and arrangement mode of lamps, and other spatial layout elements, as well as the form, size and other morphological elements, the influencing variables of lighting guidance simulation are set up.

According to the specification requirements [8] and survey data statistics, when it is set as A general lighting mode, the spatial layout of the light source is as follows: the installation mode is divided into the more common top-embedded lamps and suspended lamps [9] (respectively

recorded as A and B); The direction of the lighting arrangement is consistent with the direction of the main flow of people as longitudinal, vertical as horizontal; The arrangement of the lamps is transformed, the alignment type is that the central point of the lamps are aligned with each other in the horizontal and vertical directions, the staggered type is aligned every other column or row, and the lamps in the adjacent rows or columns are translated. The shape of the light source: set 3 kinds of LED light source length size; Set point, line, surface 3 light source forms.

Subregional general lighting scheme; The lighting mode of the most middle vertical traffic area in the schemes 1A, 3A, 7A and 9A is transformed. The key lighting is selected to set a cosine type directional projection lamp above the gate and the ticket vending machine, and the solid Angle of the lamp is within  $60^\circ$ .

When set as a zoning lighting method, the general lighting method is used as the basis for the replacement of the lighting method in the area where the most central vertical traffic is located, with the corresponding focus on lighting options above the gates and vending machines with cosine type directional floodlighting fixtures, with a three-dimensional angle of the fixtures within  $60^\circ$ .

Table 1 Station hall lighting simulation scheme setting table

Lighting mode	Station hall general lighting						Station hall subarea general lighting					Emphasis lighting				
	Installation	Light source form and lighting mode	direction	Lamp Size (m)	Arrangement mode	ID	Remaining area		Central area		ID	position	ID			
							lighting mode	Light source form	direction	Lamp Size (m)						
Lighting simulation scheme	A-embedded B-suspension	type linear light source+ Direct illumination	horizontal	1.2	alignment	1A/B	Direct illumination	point	Horizontal	1.2	1A+ point	sidewall	Long A+ indirectly leads the key points			
					interlace	2A/B			longitudinal	1.2	7A+ point	handrail				
				2.4	alignment	3A/B		surface	Horizontal	1.2	1A+ surface	passage way				
					interlace	4A/B			longitudinal	1.2	7A+ surface	Brake machine				
				General length		—		5A	—					Ticket vending machine		
				longitudinal	1.2	alignment		7A/B	Indirect illumination	line	Horizontal	1.2		1A+ indirect	—	
			interlace			8A/B	2.4	3A+ indirect								
			2.4		alignment	9A/B	longitudinal	1.2			7A+ indirect					
					interlace	10A/B		2.4			9A+ indirect					
			General length		—	6A	—									
			Evaluation method		There were 38 people participating in the voting in the common area and the general area respectively						The voting method was divided into three groups with 17 participants					Task completion score

## 2.3 Selection of evaluation method

### 2.3.1 Vote choice method

Based on the scoring method, screenshots were taken of the same location scenarios of the same group of simulation schemes. The schemes considered to be more oriented were selected by comparison and evaluated according to the number of votes selected[10]. In order to avoid the position of pictures in the options interfering with the selection of subjects, the sequence of picture options was randomly arranged.

### 2.3.2 Vote choice method

The optimized scheme of the general lighting of the station hall was transformed into a partitioned general lighting, and guided lighting and local lighting were added. Roaming video recordings were made for these simulated scenes, and 6 pictures were captured from the videos. After watching the videos, the subjects sorted the scene pictures. The image classification task was evaluated with two indexes of completion time and sequence accuracy [11]. If the photo position corresponds to the correct position in the entire sequence, 1 point is awarded; If it is incorrect, but near a photo that follows in chronological order, 0.5 points are awarded; Zero points for a complete misalignment.

### 3. EXPERIMENTAL RESULTS AND ANALYSIS

#### 3.1 Reliability analysis

This experimental data analysis mainly investigated the intrinsic reliability of the questionnaire. The Alpha reliability coefficient method is mainly used to consider the internal reliability of the scale, that is, whether there is a high internal consistency between items. Through the reliability analysis of the voting questionnaire for 18 schemes of general lighting, a total of 38 subjects were tested under 108 working conditions, and the Kronbach coefficient of the obtained experimental data was greater than 0.935, which belongs to a very good degree of reliability, indicating that the reliability of the overall questionnaire is high.

Table 2 Reliability analysis

Kronbach Alpha	Kronbach Alpha based on standardized terms	Number of terms
.935	.945	108

#### 3.2 Experimental result

The 18 scenarios for the general lighting of the station concourse met the standard requirements for average illuminance, uniformity of illuminance in the horizontal reference plane, uniform glare values and power density. Two scenarios for the north-south passing area and four scenarios for the left and right general areas were voted on separately, and a total of 38 valid evaluations were obtained. Taking scenario 3A as an example, the simulated effects of the six scenarios are shown in Table 2 and the voting results are shown in Table 3.

Table 2 Six simulation scenarios -- taking Scheme 3A as an example

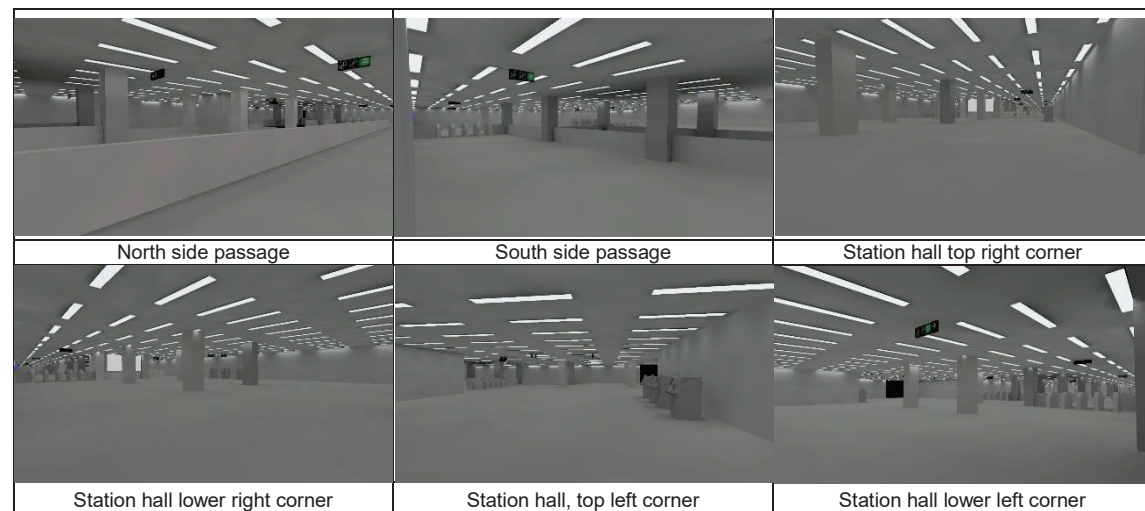


Table 3 General lighting simulation scheme and voting results

Scheme sequence number	8B	7B	9B	10B	1B	4B	2B	10A	3B	2A	8A	1A	7A	4A	6A	9A	3A	5A
Average illumination lux	279	283	227	208	263	293	253	193	296	316	337	318	343	352	207	207	355	261
Illuminance uniformity	0.83	0.87	0.97	0.78	0.78	0.78	0.78	0.79	0.84	0.74	0.82	0.73	0.86	0.8	0.73	0.91	0.82	0.76
Unified Glare Ratin	15.3	15.4	14.1	14.2	11.7	12.3	12.2	12.0	12.0	12.4	14.3	12.2	14.4	11.3	12.0	11.9	11.1	16.4
Voting result	8	12	12	13	15	15	16	18	19	21	22	26	26	28	30	41	54	55

Sub-regional general lighting scheme, the lighting mode of the most middle vertical traffic area in the scheme 1A, 3A, 7A, 9A is transformed, and the voting is divided into three groups. There are 21 votes in each group. The station hall key lighting scheme was compared with the original 5A general lighting scheme, and 17 and 21 people participated in the ranking task assessment respectively in the two scenarios. The voting results are shown in Table 4.

Table 4 Results of simulation scheme for sub-regional lighting and key lighting of station hall

Scheme sequence number	Sub-area lighting - Change the lighting mode of the central area	Emphasis lighting
------------------------	--	-------------------

Emphasis lighting	Vote 1				Vote 2			Vote 3		5A No emphasis lighting	5A+ indirect emphasis
	1A Indirect	3A indirect	7A indirect	9A indirect	1A indirect	1A point	1A Plane	1A point	7A point		
Average illumination (lux)	223.8	296.2	287.1	246.5	223.8	226.1	223.9	226.1	212.7	260.5	248.4
Voting result	6	4	2	5	7	8	2	8	9	3.214	3.911

Based on the above voting results, the normal test and variance homogeneity test were carried out for the voting data of the general lighting scheme. Since the comparison elements between the partition lighting and the key lighting were relatively single, the number of votes and scores could be directly compared and analyzed, so no software statistical analysis was carried out.

The results of the normal test of data are skewed, and the P-value of the results of the homogeneity test of variance is also less than 0.01, that is, the variance is not homogenous. Therefore, Kruskal test (K independent sample test) in non-parametric statistical method was used to analyze the significance of the influence of four variable Settings on the number of guided votes. The results show that the installation mode, size and arrangement of lamps have a significant impact on the guidance, while the arrangement direction of lamps has no significant impact on the guidance. The data analysis results are shown in Table 5.

Table 5 Significance analysis results of influencing factors of general lighting simulation schemes

Test result	Luminaire size	Installation mode	Arrangement mode	Lighting arrangement direction
Kruskal Wallis H	6.453	39.112	5.242	0.120
Asymptotic significance	0.011	<0.001	0.022	0.729

### 3.3 Analysis of spatial layout elements of light source

The simulation results of three types of lighting scenarios general lighting, zoned lighting and accent lighting are analysed comprehensively to explore the influence of the spatial layout elements of the light source on directivity in three aspects: installation method, lighting mode and arrangement.

#### 3.3.1 Installation mode

The significance of the influence on the guided voting is < 0.001, the embedded total vote in the general lighting scheme is 321 points, and the suspended total vote is 110 points, indicating that the embedded guiding evaluation is much higher than the suspended. And the embedded glare value is smaller than that of the suspended type, and the average level illuminance is higher than that of the suspended type, which is speculated to be due to the lack of ceiling as a reflecting surface to reflect the light to the ground.

#### 3.3.2 Lighting mode

According to the results of voting 1 of zoning lighting, it can be seen that indirect lighting is taken as a prerequisite for zoning, and the effect of general areas 1A, 3A, 7A and 9A is compared under the premise of indirect lighting in the central area, and the results show that there is little difference in guidance. According to the voting results of 5A+ indirect key lighting scheme, the average score of task completion of the subjects was significantly improved when the key position was set with indirect lighting.

#### 3.3.3 Arrangement

The significance of influence on guided voting is 0.022. The staggered arrangement in the general lighting scheme has 141 votes, and the normal alignment arrangement has 205 votes. The results show that the staggered arrangement lags behind the normal alignment in the guided vote, and the staggered arrangement has little improvement in uniformity compared with the aligned arrangement. And a wide range of staggered layout is easy to make the visual effect messy, so that the observer appears visual illusion.

### 3.4 Light source form element

The simulation results of the three types of lighting scenarios - general lighting, zoned lighting and accent lighting - are analysed comprehensively, and the influence of the morphological

elements of the light source on directivity is analysed in 2 ways: the form of the light source and the size of the light source.

#### 3.4.1 Light source form

Based on the results of Vote 2 for zoned lighting, it can be seen that the space dominated by line light source, and the space partitioned with point and surface light source received higher votes. According to the results of vote 3 of zoning lighting, taking point lighting as a prerequisite for zoning and comparing the effects of general area 1A and 7A under the premise of point lighting in the central area, the results show that there is a small difference in guiding scores. The results show that the guiding vote value of point lighting in the central area is higher under the premise of embedded installation, lateral alignment of the luminaire and size of 1.2 (m) × 0.3 (m).

#### 3.4.2 Light source size

The significance of the effect on guided voting was 0.011. In the general lighting scheme, 2.4 (m) × 0.3 (m) obtained 134 points, 1.2 (m) × 0.3 (m) obtained 120 points, among which the guiding votes of 3A, 5A and 9A schemes were higher, and the size of 5A lamps was consistent with the length of station. The dimensions of 3A and 9A lamps are 2.4 (m) × 0.3 (m), and the results show that the passenger guidance evaluation of the line light source with longer length is higher than that of the aspect ratio.

### 4. CONCLUSION

Through the station hall space of general lighting, zoning lighting, accent lighting 3 ways a total of 27 lighting programs for software simulation and voting numbers, task completion analysis and comparison can be seen, in the spatial arrangement of light sources: recessed than suspended installation method has better guidance, recommend the use of recessed lighting installation method; alignment arrangement method than staggered arrangement method has better guidance, staggered In improving uniformity is not much, and easy to visual confusion, so can be combined with the ceiling modeling small-scale layout; In addition, in the light source form elements: zoning lighting design, priority change the type of light source to distinguish between different spaces, line light source-based space, point line light source with zoning effect is better; in the station hall pass area according to the actual situation along the walking direction to set the length and width is relatively large, that is, longer Line light sources are set along the actual walking direction to guide passengers forward; the setting of accent lighting helps passengers to perceive the station space, and line light sources can be set along the walls, railings and various access edges. In summary, the lighting optimisation strategy is proposed from the spatial arrangement of light sources and morphological elements, with a view to providing reference for the lighting guidance design of underground rail stations and other architectural composite spaces.

### REFERENCES

- [1] Robert M S, Zygmunt P, Filip J P. Phi is not beta, and why Wertheimer's discovery launched the Gestalt revolution[J]. *Vision Research*, 2000,40(17).
- [2] Minjung, Kim, Laurie, et al. Perceived three-dimensional shape toggles perceived glow.[J]. *Current Biology Cb*, 2016.
- [3] Murray R F. Lightness Perception in Complex Scenes[J]. *Annual Review of Vision Science*, 2021,1(7):417-436.
- [4] Sarah L C, Roland S, Peter B, et al. Non-visual effects of light on melatonin, alertness and cognitive performance: can blue-enriched light keep us alert?[J]. *PLoS ONE*, 2017,6(1).
- [5] Jamshidi S, Pati D. A Narrative Review of Theories of Wayfinding Within the Interior Environment[J]. *HERD*, 2020,14(2):187531221.
- [6] S F, R G. Road lighting research for drivers and pedestrians: The basis of luminance and illuminance recommendations[J]. *Lighting Research & Technology*, 2018,50(1).
- [7] Wang Lixiong, Wang Chuyao, Yu Juan, Chen Tianyi. Investigation and analysis of lighting environment of urban rail transit station [J]. *Journal of Lighting Engineering*, 2022,33(02):169-176.
- [8] GB/T31831-2015, Technical requirements for LED indoor lighting applications [S]
- [9] Jia Hongmei. Current methods and development of indoor environment design for metro stations in China [D]. Jiangsu: Nanjing Forestry University, 2006. .



- [10] Boyce, Peter. Human Factors in Lighting[M]New York: Taylor & Francis Group;Taylor & Francis Group,2003:256-257.
- [11] Giovanni Cosma, Enrico Ronchi, Daniel Nilsson. Way-finding lighting systems for rail tunnel evacuation: A virtual reality experiment with Oculus Rift@[J]. Journal of Transportation Safety & Security,2016,8(sup1).

## **ACKNOWLEDGEMENTS**

The work was supported by the National Natural Science Foundation of China: Study on the Effect of Lighting Guidance on Space Order in Complex Scenes (52278120)

Corresponding Author Name: Juan Yu  
Affiliation: School of Architecture, Tianjin University  
e-mail: 601463949@qq.com

## Ultraviolet Lamp Based on Microwave Stimulated and Application in Photolyzing Volatile Organic Compounds (VOCs)

ZHU Shenghe<sup>1</sup> LYU Jiadong<sup>2</sup>

(1. Gaoyou Gaohe Photoelectricity Equipment Co., Ltd., 225606 Yangzhou, China

2. Southeast University, 210096 Nanjing, China)

**Abstract:** The working principle of UVC and the three kinds of technology to generate UVC were described, and design of microwave stimulated ultraviolet lamp and requirements for material and process were presented. And also in this paper, it was focused on the working principle of microwave, ultraviolet and photocatalyst composite technology used in photocatalytic oxidation for volatile organic compounds (VOCs), the microwave cavity structure and working mechanism were also introduced. Finally, some engineering cases for treating organic waste gas were provided for the reference of environmental protection technology field.

**Key words:** UVC lamp; microwave stimulated; photo catalysis; composite technology; volatile organic compounds (VOCs)

### 1. Introduction

Photons energy of ultraviolet rays in C-waveband (UVC) can be seen in Tab.1, binding energy of the various volatile organic compounds (VOCs) molecules can be seen in Tab.2. By comparing Tab. 1 and Tab. 2, we can see that bond dissociation energy (BDE) of UVC with wavelengths 253.7nm and 185.0 nm is separately 472 kJ/mol and 647 kJ/mol, only part of volatile organic compounds(VOCs) can be dissociated by ultraviolet rays (UVC), photolysis efficiency is not enough.

Tab. 1 Photons energy of UVC

Wavelengths (nm)	Photons energy (kJ/mol)
253.7	472
185.0	647

Tab. 2 Binding energy of VOCs molecules

Binding type	Binding energy (kJ/mol)	Binding type	Binding energy (kJ/mol)
H-H	436.2	C-H	413.6
H-C	347.9	C-F	441.2
C=C	607.0	C-N	291.2
C≡C	828.8	C≡N	791.2
N-N	160.7	C-O	351.6
O-O	139.0	C=O	724.2
O=O	490.6	O-H	463.0

The composite technology of ultraviolet based on microwave stimulated and photo catalyst was used in photocatalytic oxidation for volatile organic compounds (VOCs), the photolysis

efficiency was effectively improved. The volatile organic compounds (VOCs) molecules were dissociated by the electromagnetic field of microwave with ultrahigh frequency (2450 MHz), VOCs macromolecule was dissociated to micromolecule, VOCs micromolecule is easy to be photocatalytic oxidation. When the UVC rays was making the micromolecule photolysis, and be stimulating nano-TiO<sub>2</sub> to generates a large number of hydroxyl-oxidation-group (-OH) and electron hole pairs, its bond dissociation energy (BDE) is more than ten times that of UVC rays, photolysis efficiency is improved.

## 2. Ultraviolet Lamp Based on Microwave stimulated

There are three technical path to excite Penning gas in a glass tube to discharge into a plasma that emits UVC rays. ① The traditional hot-cathode electron discharge has a low operating frequency(50Hz~30 kHz). ② High frequency electromagnetic field induction discharge forms plasma, operating frequency is about 250 kHz. ③ Microwave excite Penning gas discharge to form plasma, operating frequency is 2450 MHz. The hot-cathode UV lamp has mature technology and low cost, but also has big light decay and short life because quartz tube may be polluted with electronic powder sputtering, and also installation and maintenance is not convenient. The discharge lamp based on microwave excitation has no filament, no electron powder, and has low light attenuation, long life, and high cost, it's easy to install and maintain.

UV lamps based on microwave excitation were placed in microwave cavity, Penning gas in the quartz tube is excited by microwave (2450 MHz) to form plasma, emitting wavelength 253.7 nm and 185.0 nm ultraviolet rays ( Fig.1).

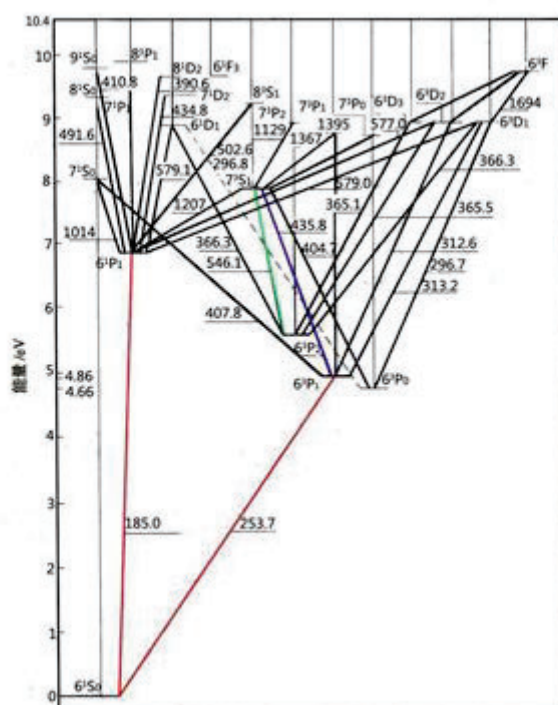


Fig.1 Ultraviolet rays stimulated by Microwave

Microwave-excited UV lamp has a high operating temperature of about 80 °C, far above the optimal temperature of liquid mercury 40 °C, in order to overcome the light decline due to temperature rise and ensure that the lamp is always working in the highest UVC emission state, amalgam and auxiliary amalgam (gold sheet) must be used in UV lamp ( Fig.2). Microwaves also

heat amalgam in the exhaust pipe, causing it to melt away, the optimum operating temperature for amalgam is not achieved. It is necessary to design a stainless steel holder at lamp end, to avoid direct microwaves radiation to gold sheet and amalgam. The support materials in the microwave cavity in contact with the lamp holder must be ceramic, plastic and other insulating materials, such as tetrafluoroidal plate. In order to prevent Hg atoms in plasma from invading the surface lattice of the quartz tube and affecting the transmission of ultraviolet rays, the inner wall of the quartz tube is coated with a protective film of nano-oxide to reduce light decay and to improve lamp quality, the vacuum degree of the tube must be higher  $5 \times 10^{-3}$  Pa ( Fig.3)。



Fig.2 Amalgam and assistant amalgam



Fig. 3 Ultraviolet lamp based on microwave stimulated

### 3. Microwave, ultraviolet, photocatalyst composite technology and mechanism

The ultra-high frequency electromagnetic field in the microwave cavity produces strong magnetic radiation to VOCs molecules, which can cut and split the molecular bonds of benzene, toluene, xylene, ammonia, tri-methylamine, and hydrogen sulfide to form smaller molecules, which is conducive to further photocatalytic oxidation. The microwave-excited ultraviolet lamp can emit ultraviolet rays with wavelengths 253.7 nm and 185.0 nm, UVC rays with wavelength of 253.7 nm is mainly used for sterilization and disinfection, and also can be photolysis of VOCs molecules with molecular bond energy less than 472 kJ/mol. The bond dissociation energy (BDE) of ultraviolet rays with wavelength 185.0 nm reaches 647 kJ/mol, which is mainly used for the oxygen photolysis (bond energy of 490.6 kJ/mol) to produce  $\cdot\text{O}$ , namely ozone, as well as photocatalytic oxidation of VOCs molecules. At the same time, UVC rays excited the oxides on the photocatalyst plate, and produced a large number of hydroxyl oxidation groups( $\cdot\text{OH}$ ) and electron hole pairs, which could

play a stronger role in photocatalytic oxidation ( Fig.4).

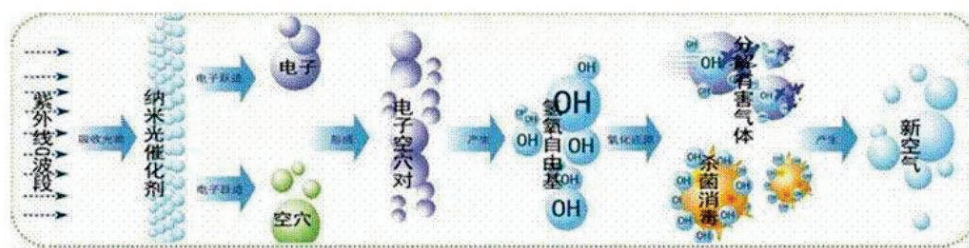


Fig.4 Working principle of nanometer TiO<sub>2</sub> irradiated by UVC

The bond dissociation energy (BDE) of UVC rays, O<sub>3</sub> and -OH are as follows.

The calculation formula of bond dissociation energy (BDE) of ultraviolet rays with wavelength 185.0 nm is as follows.

$$E_{185} = \frac{hc}{\lambda} \times 6.02 \times 10^{23} = 6.626 \times 10^{-34} \times \frac{3 \times 10^8 \text{ m/s}}{185 \times 10^{-9} \text{ m}} \times 6.02 \times 10^{23} \approx 647 \text{ kJ/mol}$$

In formula, h= Planck constant; c= light speed; λ= wavelength; 6.02×10<sup>23</sup>= Avogadro's constant.

Corresponding to 647 kJ/mol, and the bond dissociation energy (BDE) of UVC 185.0 nm is 6.702 eV. According to the report [7] by HGI Industries, the bond dissociation energy (BDE) of ozone (O<sub>3</sub>) is 12.53 eV, and that of hydroxyl oxide group (-HO) is 14.01 eV. The report also pointed out that University of Southern California in United States compared the oxidation potential (namely BDE) differences between ozone and hydroxyl. Compared with ozone (O<sub>3</sub>), the hydroxyl radical's BDE efficiency is 13 times more than that of ozone (O<sub>3</sub>), and the reaction rate is 1 billion times faster than ozone reaction.

The shape of the microwave cavity is usually rectangular or cylindrical, and the air inlet and outlet are made of aluminum base honeycomb photocatalyst net plate which can not only cut off the microwave field but also maintain the ventilation function. Two row of microwave stimulated ultraviolet lamps are installed in the cavity, and the ceramic base photocatalyst net plate is installed between UVC lamps ( Fig.5). A microwave head radiating microwave energy (a combination of magnetron and waveguide) and a switching power providing electrical energy are installed outside the cavity. When the power module is switched on, microwave electromagnetic field, UVC rays, hydroxyl oxide groups(-OH) and electron hole pairs are generated inside the cavity. When VOCs pass through the microwave cavity, these industrial waste gas are subjected to the triple catalytic oxidation of microwave field, UVC rays and hydroxyl oxidation group(-OH), and be decomposed into harmless H<sub>2</sub>O and CO<sub>2</sub>. The photocatalyst device may be consists of several microwave cavities module according to the air volume ( Fig.6).





Fig.5 UVC lamp and ceramic photocatalyst mesh plate in microwave cavity



Fig. 6 Photocatalytic equipment combined with 6 sets of microwave cavities

#### 4. Engineering Case in Treating Volatile Organic Compounds (VOCs)



Fig.7 Application of oil fume purification



Fig.8 Photocatalytic oxidation treatment of industrial waste gas



Fig.9 16 modules combination in photocatalytic treatment of paint and coatings



Fig.10 Application in waste gas treatment equipment



Fig.11 Application of microwave ultraviolet photocatalyst composite technology



Fig.12 Application of waste gas treating in food factory

#### References

- [1] Shenghe ZHU, Application of High Power Electromagnetic Induction UVC Lamp in Photolyzing Volatile Organic Compounds, China Light & Lighting, 1002-6150(2017)01-029-03
- [2] Shenghe ZHU, Development of Microwave Driven Ultraviolet Lamp Used For Photolysis of Organic Waste Gas, China Light & Lighting, 1002-6150(2018)01-023-04
- [3] Shenghe ZHU, chengli WU, Development and Application of Microwave Ultraviolet and Photocatalyst Composite Technology Module and Special Lamp, China Light & Lighting, 1002-6150(2018)11-032-05
- [4] Shenghe ZHU, Anthology of Design and Technology of Amalgam Fluorescent Lamp, China Light Industry Press, 2009
- [5] Hui LIAO, Zhimin FU, Zhiming HE, Application of Ultraviolet Lamp in Organic Waste Gas Treatment, China Light & Lighting, 1002-6150(2015)07-033-03
- [6] Shanduan ZHANG, Qiuqi HAN, Zhong JI, Measurement Methods and Examples of Radiation Flux of Various Ultraviolet Light Sources, Proceedings of the Fifth National HID Light Source Science and Technology Seminar, 2017
- [7] HGI Incorporated Inc., Hydroxyl Efficiency[Z], 2012

# RESEARCH ON THE LIGHTING DESIGN STRATEGY OF SCHOOL FIELD BASED ON VISUAL COMFORT

Yushan Liu<sup>1</sup>, Yue Liu<sup>2</sup> and Zheng Liang<sup>3</sup>

(China Academy of Urban Planning & Design Shenzhen, Shenzhen)

## ABSTRACT

In recent years, with the rapid development of the national economy and the improvement of people's living standards, national fitness and sports events have become an indispensable part of people's daily life. In order to meet people's demand for sports events, various places have invested in the construction of large-scale sports venues and held various sports events. These activities not only promote the development of sports, but also make contributions to the development of society and economy. The sports field in the school is an important place to improve the sports level and physical quality of students and teachers. The quality of the lighting environment in the school sports field has a direct or indirect impact on the visual health of young people, as well as physical and mental health, so the lighting design puts forward higher requirements. Firstly, the lighting standards need to be met to provide clear and bright site conditions; Secondly, it is necessary to meet the requirements of visual comfort, effectively control the glare caused by lighting, and provide a comfortable and safe site environment. Finally, in the context of "carbon peaking and carbon neutrality goals", the construction of smart lighting system and the application of green energy-saving lighting products to ensure the effective use of energy and reduce energy waste is the content that the sports field lighting needs to focus on. By sorting out the problems existing in the current outdoor sports venue lighting design, comparing and analyzing the current lighting standards and the factors that affect the quality of sports lighting, conduct a study of sports field lighting cases, and propose the school outdoor sports field lighting with visual comfort as the design goal. The design strategy is expected to provide direction for the lighting design of the same type of school sports field. Under the guidance of the design strategy, it is applied to a standard football field lighting design in a junior high school in Shenzhen. It is calculated and analyzed by two different high-power LED luminaire layout methods to determine the final lighting strategy. After calculation, the final lighting design can meet the current lighting standard requirements under the premise of meeting the current design conditions, and at the same time control the glare, and create a good outdoor sports field lighting environment for teachers and students.

Keywords: Outdoor sports field; Lighting design; Visual comfort; Glare control

## 1. INTRODUCTION

In recent years, amid the nationwide fitness trend and the hosting of large-scale sports events, participation in sports activities has become an integral part of people's lives. Sports fields serve as crucial venues for physical education in schools, ensuring the orderly conduct of sports teaching, training, competitions, and group activities. They play a significant role in meeting the requirements for activities of varying scales, carrying considerable social significance.

With the development of nightlife and the nighttime economy, there has been a significant increase in the number of people engaging in sports activities at night. To ensure the safety of nighttime public activities, there is a need to improve sports field lighting.

However, existing outdoor sports fields in schools often neglect lighting construction due to lower usage demands and fewer people participating in nighttime activities in the past. Prevalent issues include the absence of lighting infrastructure or poor lighting quality. Insufficient illuminance levels make it difficult to meet the requirements for daily exercise, training, and professional competitions. Severe glare on the field negatively impacts visual perception, and damaged lighting fixtures result in poor lighting effects.

Given that school sports fields cater to young individuals, it is essential to prioritize visual health, as well as physiological and psychological well-being, in lighting construction and design.

The objective is to provide a uniform and comfortable lighting environment while addressing glare and light pollution concerns.

## 2. INTERPRETATION OF LIGHTING STANDARDS

In China, stadium lighting design standards are outlined in *Sports Stadium Lighting Design and Testing Standards* JGJ 153-2016, as well as *Architectural Lighting Design Standards* GB50034-2013. In 2022, the *International Illuminating Engineering Society* (IES) released ANSI/IES RP-6-22, a lighting standard specifically for sports fields and leisure areas. This standard provides control requirements for the lighting of various sports fields and leisure and social activity areas. Given the unique nature of stadium lighting, professional sports organizations at various levels, including FIFA, FIH, NCAA, NFL, UEFA, and the North American and Caribbean Football Association, have established specific requirements for stadium lighting.

### 2.1 Lighting classification

Based on varying usage requirements and specific TV broadcast criteria, sports venue lighting standards are classified. In China, for example, the *Sports Stadium Lighting Design and Testing Standards* JGJ153-2016 categorizes stadium lighting into six levels (Table 1). Similarly, international standards like FIFA and IAAF divide venue lighting into five levels, with "club games" representing amateur games, corresponding to "amateur games and professional training" in our standards. "Domestic and international games" align with the standards for "professional competition" in our country. Different classifications dictate the control of stadium illumination, illumination uniformity, color rendering, color temperature, and glare index. School stadiums typically adopt the first-class lighting standard, primarily catering to the functional needs of teachers and students for fitness and amateur training, with no specific requirements for TV broadcasting (Table 2).

Table 1. Stadium lighting levels

Without TV		With TV	
Grade	Use function	Grade	Use function
I	Fitness and amateur training	IV	TV broadcasting of national competitions and international competitions
II	Amateur competitions, professional training	V	TV broadcast of major national competitions and major international competitions
III	Professional competition	VI	HDTV broadcasting of major national competitions and major international competitions

Note: Levels IV, V and VI in the table are also applicable to other competitions with special requirements.

Table 2. The comparison of stadium lighting requirements

Specification	Class	Horizontal illuminance			Light source		
		Average illuminance	Uniformity of illuminance		Ra	Tcp ( K )	GR
		lx	U1	U2			



<i>Sports Stadium Lighting Design and Testing Standards</i>	I  (Fitness, Amateur Training)	200	—	0.3	65	4000	55
<i>International Football Federation (FIFA) "Soccer Stadium Technical Recommendations and Requirements"</i>		200	—	0.5	≥65	> 4000	≥5 0
<i>International Athletics Federation Athletics Facilities Handbook (FIH) 2008 Edition</i>	II  (Club Competition)	200	0.4	0.6	≥65	> 4000	≥5 0

Note:

- ① The illuminance value in the table is the maintenance illuminance value;
- ② Class I and II stadium lighting has no restrictions on vertical illuminance;
- ③ Maintenance factor should not be less than 0.7;
- ④ It is recommended to use constant lumen technology.

## 2.2. Illumination

Stadium lighting encompasses horizontal illuminance and vertical illuminance. Horizontal illuminance is measured on an imaginary plane located 1 meter above the field's surface in the horizontal direction. Multiple measurements are obtained by using a designated standard grid. For instance, the American Football League specifies a grid spacing of 5 meters. On the other hand, vertical illuminance is measured on an imaginary surface in the vertical direction, originating from a specified position and orientation. Establishing minimum and maximum limits for vertical illuminance is crucial to ensure proper player facial recognition and identification.

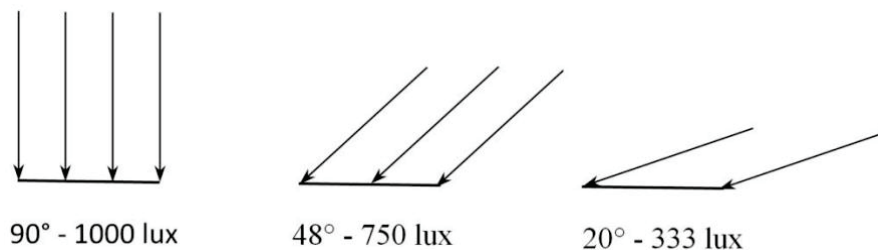


Figure 1. Vertical illuminance with different orientation

## 2.3 Uniformity

To ensure that athletes and spectators can easily follow the action, it is essential to control the uniformity of stadium lighting. Typically, the illuminance uniformity ratio is used to assess the uniformity of horizontal and vertical illuminance in the stadium. Taking the NFL requirements as an example, the horizontal illuminance is denoted as  $E_h$ , and the uniformity ratio is expressed as  $E_{h\max} / E_{h\min}$ . Measurements using a grid spaced 5 meters apart on the playing field must

adhere to a ratio of 1.4:1 or less. Similarly, the vertical illuminance, denoted as  $E_v$ , must also have a uniformity ratio of  $E_{v \max} / E_{v \min}$  that is 1.4:1 or less.

Additionally, the uniformity gradient (UG) can be used to describe the maximum inhomogeneity of the field. UG represents the ratio of illuminance values between adjacent measurement points on the square grid. By controlling the UG, uneven changes in illuminance can be minimized, which is particularly crucial for fast-moving ball games that are sensitive to variations in lighting conditions.

## 2.4 Visual glare

When the luminance of the luminaires within the field of view of the observer (athlete or audience) significantly exceeds the average luminance acceptable to the human eye, visual glare occurs, resulting in visual discomfort for the observer and impairing their ability to perceive object details. The typical evaluation of visual glare involves placing subjects in a laboratory environment and conducting subjective assessments of glare perception in specific lighting scenarios. CIE 112-1994 introduced a glare evaluation system for outdoor sports and area lighting, which assesses the glare level based on key parameters such as the brightness of the luminaire as seen by the observer, the angle range of the luminaire within the observer's field of view, the relative position of the line of sight, the number of luminaires within the observer's field of view, and the average luminance perceived by the observer.

For instance, the JGJ153-2016 *Sports Stadium Lighting Design and Inspection Standard* specifies that the glare value for first-class stadium lighting should be below 55, while for other classes, it should be below 50. Furthermore, there are also regulations concerning the glare value of the primary camera used for video broadcasting. As an example, the NFL requires that the glare value of all primary camera lenses remains below 40.

## 2.5 Color temperature

Professional sports organizations in various countries have established guidelines for stadium lighting, specifying the acceptable correlated color temperature (CCT) and the minimum required color rendering index (CRI). Typically, correlated color temperatures are around 3000K for quartz halogen luminaires and warm white LEDs, 4000K for metal halide luminaires, and 5000K for daylight LED luminaires. In recent years, LED lighting technology has become increasingly popular in stadium lighting design due to its significant advantages, including energy efficiency, high performance, low maintenance costs, and intelligent control capabilities.

Table 3. CCT and CRI requirement for stadium lighting from different sports organizations

Sports Organization	CCT	CRI
FIFA	= 4000K	= 65
FIH	> 4000K	> 65
NCAA	> 3600K	> 65
NFL	5600K ( or 5000K-7000K )	= 90

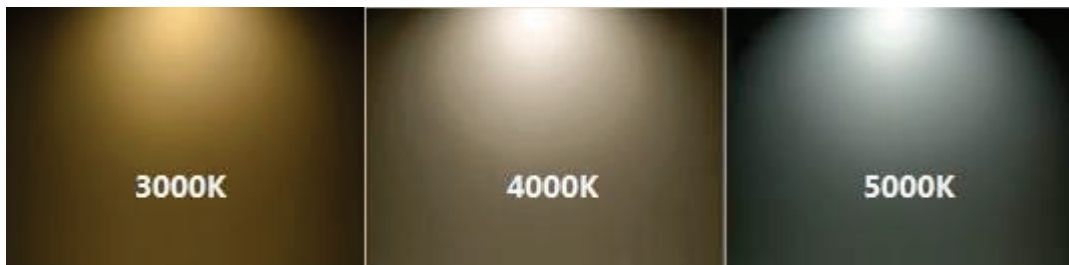


Figure 2. Color temperature

The color rendering index, CRI (Ra), measures the average color shift of various colors observed under a light source compared to the color observed under an incandescent or daylight light source with the same CCT. The minimum requirement for CRI is 65, which represents the performance achievable with high wattage metal halide luminaires. Considering the prevalent use of LED luminaires, those with a color rendering index of 80 or higher offer improved lighting effects, while luminaires with a color rendering index of 90 and above are preferred.

## 2.6 Light pollution

Outdoor lighting serves the purpose of illuminating objects on the ground as well as the sky above. The International Dark Sky Association has highlighted the issue of light pollution caused by excessive lighting construction, which disrupts the ecological balance at night, impacts the circadian rhythm of humans and animals, interferes with astronomical observations, and results in significant energy wastage. Stadium lighting, being a critical source of lighting within a confined space, is particularly susceptible to contributing to light pollution. Therefore, it is essential to effectively shield the upward light and control the lighting duration when selecting lighting fixtures.

## 2.7 Lighting arrangement

The outdoor stadium has a large area and lacks support points, necessitating the arrangement of a combination of high pole lights and centralized lights. This arrangement requires a higher projection angle for the lights. Generally, the outdoor lighting arrangement adopts the four-corner pole type, where concentrated luminaires and high pole lights are arranged at the four corners of the stadium. The height of the light poles is typically between 35 to 60 meters, ensuring that the bottom row of floodlights can reach the center of the stadium and the ground. The included angle should not be less than 25° to ensure proper illuminance distribution throughout the stadium and control glare.

## 3. LIGHTING DESIGN PRACTICE

Taking the lighting design of the outdoor main stadium of a senior high school in Shenzhen as an example, this research is conducted. The senior high school has a compact layout, and the outdoor main stadium is oriented in a north-south direction. It consists of a standard football field, a 400-meter track and field, and spectator stands to cater to the nighttime activities and irregular sports events of teachers and students residing in the school. The outdoor activity area primarily comprises the main stadium, with limited space for other landscape green areas. The close proximity between the main stadium and the teaching building restricts the placement of lighting fixtures. Additionally, due to limited land availability, meeting the lighting requirements of both the football field and track and field simultaneously requires a large number of luminaires and a significant overall area for luminaire heads. Balancing the lighting requirements of the stadium and the aesthetics of the building facade becomes a key aspect of this lighting design. As a result, this lighting design primarily focuses on meeting the lighting standards of the football field, while the track and field is illuminated by overflow light, and accent lighting is not considered for the auditorium.

Referring to the relevant requirements of the *stadium lighting design and testing standard* JGJ153-2016, this stadium lighting complies with the first-level use function requirements, which include fitness and amateur training. Specifically, the average illuminance for track and field fields

and football fields is not less than 200lx, and the illuminance uniformity is U2, which should be less than 0.3. Additionally, the color rendering index (Ra) is not lower than 65, the color temperature is not lower than 4000K, and the glare index should not exceed 55.

Based on lighting design indicators and relevant domestic and international standards, two lighting schemes are proposed for comparative analysis. Scheme 1 adopts the standard four-corner lighting method and utilizes a total of 14 sets of 1430W high-power LED luminaires. The luminaires have a color rendering index of Ra=90 and a color temperature of 5700K. The lighting strobe ratio is  $\leq 1\%$ . The four light poles are positioned within the landscape green space surrounding the playground. The height of light poles P1 and P2 is 30.5 meters, while the height of P3 light pole is 27.5 meters, and P4 light pole is 24.4 meters.

Table 4. Light pole information for option 1

Light pole number	Light pole height (m)	Base level (m)	Number of lamps (pieces)	Single lamp power (w)	Lamp power (kw)
P1、P2	30.5	—	4	1430	5.72
P3	27.5	15.4	3	1430	4.29
P4	24.4	24	3	1430	4.29
4			14		20.02

Table 5. Football field calculation for option 1

Calculation area	Calculation method	Illuminance value				
		Ave	Min	Max	Min /Max	Min / Ave
Football Field	Horizontal Illumination	204lx	148lx	246lx	0.6lx	0.73lx

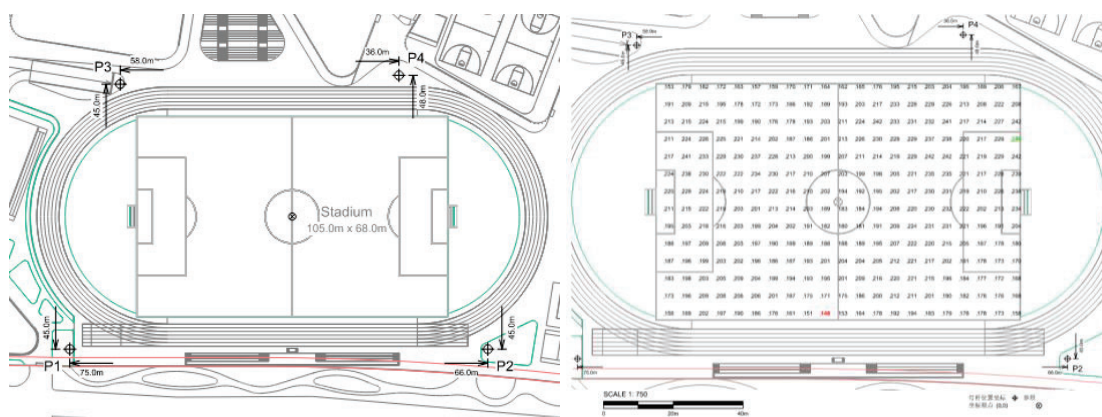


Figure 3. Calculation of football field for option 1

Option 2 takes into account the close proximity between the playground and the teaching building. Erecting traditional light poles would obstruct the visual appeal of the teaching building when looking towards the playground, as well as compromise the overall distant view effect of the west facade of the building. Therefore, the solution considers placing two light poles on the roof of the building near the teaching building. To minimize the impact on the roof structure, a

combination of curtain wall installation brackets or pole installations is employed. This arrangement ensures that the lighting requirements of the football field are met.

The setup includes 15 sets of 1430W high-power LED lamps with a color rendering index of  $Ra=90$  and a color temperature of 5700K. Additionally, the site lighting guarantees a stroboscopic ratio of  $\leq 1\%$ . Among them, the height of light poles P1 and P2 is 30.5 meters, while P3 and P4 are installed on poles combined with the building roof structure, protruding 10 meters from the roof level.

Table 6. Light pole information for option 2

Light pole number	Light pole height (m)	Base level (m)	umber of lamps (pieces)	Single lamp power (w)	Lamp power (kw)
P1、 P2	30.5	—	4	1430	5.72
P3	10.0	15.4	3	1430	4.29
P4	10.0	24	4	1430	5.72
4			15		21.45

Table 7. Football field calculation for option 2

Calculation area	Calculation method	Illuminance value				
		Ave	Min	Max	Min /Max	Min / Ave
Football Field	Horizontal Illumination	207lx	154lx	265lx	0.58lx	0.74lx

After calculating and comparing the illuminance levels, both Scheme 1 and Scheme 2 meet the lighting standard requirements for a first-class football field. Considering architectural aesthetics, load considerations, and lighting effects comprehensively, Scheme 2 is deemed more suitable for meeting the lighting requirements of the outdoor main stadium in senior high schools.

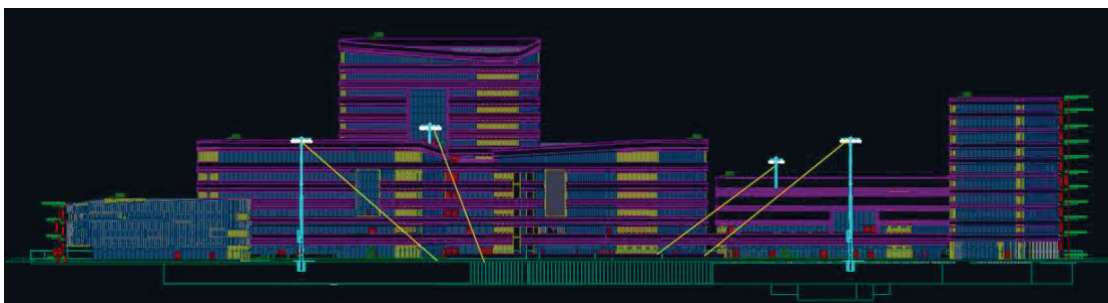


Figure 4. Location of the lamp pole





Figure 5. Rendering of the light pole location on the architecture

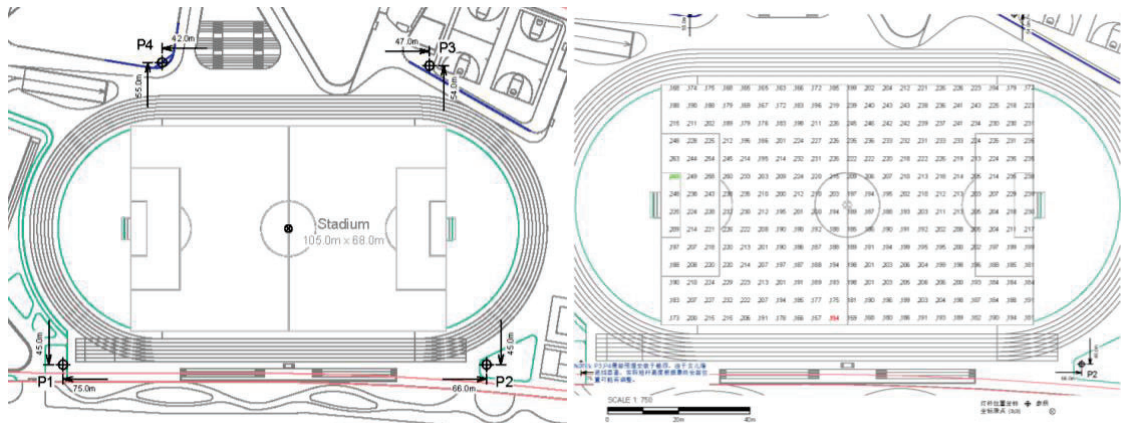


Figure 6. Calculation of football field for option 2

#### 4. CONCLUSION

Drawing from actual cases, this paper elaborates on the issues and solutions that require attention in the lighting design of school stadiums. It aims to ensure that the lighting technical parameters align with the requirements for fitness activities, training, amateur competitions, and more. Moreover, both domestic and international standards are taken into consideration to meet the long-term development needs. By utilizing lamps with appropriate projection angles, the lighting design encompasses the illumination of the stadium runway and surrounding public spaces, while minimizing excessive light spillage. This study provides a valuable reference for the high-quality development of school stadium lighting.

# THE IMPACT AND PREDICTION OF CLASSROOM LIGHTING ENVIRONMENT AND EDUCATIONAL PRESSURE ON THE DEVELOPMENT OF MYOPIA

Yang Wang, Yandan Lin

(School of Information Science and Technology, Fudan University, Shanghai, China)

## ABSTRACT

This article quantified the impact of different schools on educational pressure, investigated classroom lighting, noon outdoor activity duration, educational pressure, and eye usage habits in the Shanghai area based on the designed questionnaire and filed test, and analyzed the impact of four dimensions on the likelihood of myopia and high myopia. Based on correlation analysis, the impact of four dimensions on the likelihood of myopia and high myopia was analyzed. Factors such as classroom lighting condition, noon outdoor activity duration, educational pressure, and eye usage habits were combined with regression analysis, neural networks, or mathematical models to establish a judgment model for myopia, high myopia occurrence, and myopia development in one year. This article discovered that semi-cylindrical illumination has a significant impact on the reading distance of students in the classroom and whether the school gets more policy resources or not has a significant impact on students' myopia and refractive changes, providing a quantitative reference for establishing myopia prediction models in lighting condition and in education.

## 1. INTRODUCTION

In 2000, myopia affected approximately 1.406 billion people, with 163 million suffering from high myopia, accounting for 22.9% and 2.7% of the world population, respectively [1]. These numbers are projected to rise to 4.758 billion and 938 million people by 2050, representing 49.8% and 9.8% of the global population, respectively [1]. By 2050, the prevalence of myopia among the East Asian population is expected to surpass that of other regions, reaching 65.3% [1]. Some studies speculate that the myopia rate among East Asian school-age children and adolescents is as high as 73% [2]. High myopia increases the risk of permanent visual impairments such as glaucoma, cataracts, and retinal detachment, as well as various complications in the macula and optic nerve [3].

Early studies attributed the occurrence of myopia primarily to genetic factors and gender due to limited sample sizes and low myopia rates in the population [4-5]. However, as myopia becomes more prevalent at a younger age, genetic factors are no longer considered the primary influencing factor [4-5]. The role of environmental factors in the development of myopia and high myopia has received attention [6-7].

The light environment plays a significant role in refractive development. Light stimulates the retina, leading to dopamine secretion, which reduces axial elongation of the eye and potentially inhibits the onset of myopia [8]. Specific indicators of the light source, such as related color temperature [9], wavelength [10], and illumination intensity [11], are considered factors

that affect the occurrence of myopia. Animal experiments have demonstrated that high-intensity light exposure during the critical stage of visual development can effectively inhibit myopia, resulting in a faster recovery of normal refractive ability compared to control groups exposed to lower light intensities.

Moreover, outdoor activity duration and educational pressure are independent factors influencing refractive development. Numerous cross-sectional and longitudinal studies have been conducted in China [12-13], Australia [14], Singapore [15], South Korea [16], and other regions. These studies have identified the duration of outdoor activities and educational pressure as independent influencing factors for myopia development, surpassing the influence of race and genetic factors. One study, using eye axis length, diopter, and light intensity measurements, found that the duration of outdoor activities, rather than light intensity, was the primary factor inhibiting myopia during outdoor activities [17]. Another large-scale myopia study (N=19,934) revealed that, among school students, only the duration of outdoor activities at noon significantly correlated with the occurrence of myopia, while the duration of outdoor activities before and after school showed no significant correlation [12].

The impact of eye habits on refractive development remains unclear. Improper eye habits can contribute to eye fatigue, but their significance in relation to myopia has yielded varying results across studies, necessitating further research [12, 17-18]. In addition to testing methods such as axial length and refractive index, the Sydney Myopia Study questionnaire [20] and the Guangzhou Outdoor Activity Longitudinal Study (GOALS) questionnaire [21] are widely used subjective survey tools with validated reliability and validity for assessing myopia.

Previous research indicates that factors such as lighting, outdoor activities, education, and eye habits may impact myopia and its development. However, these studies have primarily analyzed the impact of individual factors on myopia, while lacking exploration of the combined effects of multiple factors on myopia dimensions in large samples. Therefore, this study aims to investigate the occurrence of myopia, high myopia, and the increase in binocular myopia over the past year, focusing on the correlation between multiple factors such as classroom lighting, educational pressure, and duration of outdoor activities. The study aims to establish a composite impact model that incorporates multiple factors and their combined influence on myopia.

## **2. METHOD**

### **2.1 Questionnaire**

A questionnaire survey was conducted among 282 students from selected classes in 8 middle schools and high schools in Shanghai. The questionnaire was designed to collect information on students' vision, classroom lighting, school type, and duration of outdoor activities. The questionnaire used in this study was adapted and simplified from the GOALS (Guangzhou Outdoor Activity Longitudinal Study) English questionnaire, which was originally developed for longitudinal studies [17]. The translated and back-translated questionnaire showed no significant differences compared to the original GOALS questionnaire. Additionally, two experts reviewed the questionnaire content for its validity and relevance.

The questionnaire included the following sections:

- a) basic information: this section collected students' basic demographic information;
- b) lighting conditions: students were asked to provide information about the lighting

- conditions in their classrooms;
- c) outdoor activity duration: students were asked to report the duration of their outdoor activities. Specifically, the questionnaire focused on the duration of outdoor activities during the students' lunch breaks, as this time period has been identified as having a significant impact on myopia [19].
  - d) eye usage habits: this section inquired about students' eye usage habits.
  - e) myopia information: students were asked to provide information about their myopia status, including whether they have been diagnosed with myopia and any changes in their myopia status over the past year.

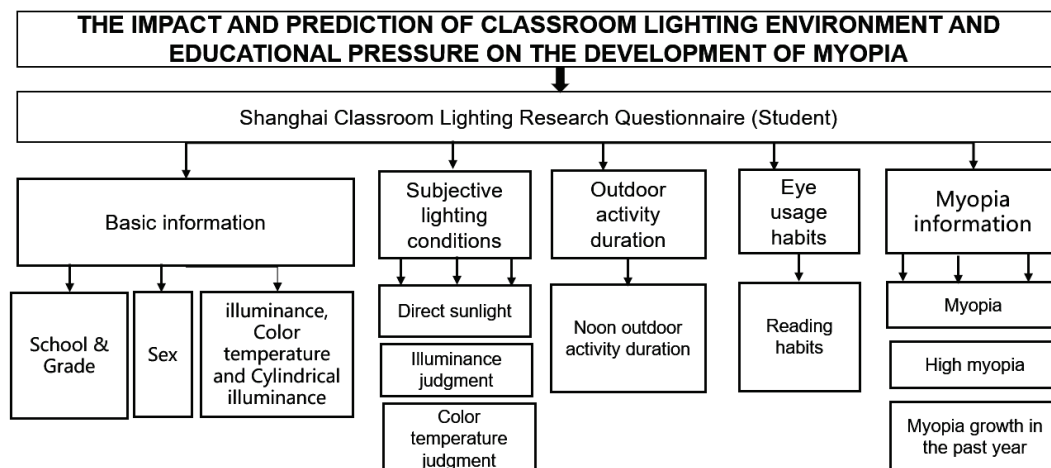


Figure 1. Design of shanghai classroom lighting research questionnaire

## 2.2 Quantification of educational pressure and myopia

Previous research has indicated that areas with high participation in extracurricular tutoring tend to have a higher myopia rate [22]. Additionally, the location (urban or rural) and the classification of schools (key or non-key) have been identified as factors influencing educational pressure [22-23]. However, there is currently a lack of in-depth research on the correlation between policy resource bias and the prevalence of myopia in schools.

In this study, the questionnaire survey included students from eight secondary schools in Shanghai. Based on the policy resource preferences received by urban/suburban areas and schools, the schools were categorized into four groups: urban municipal key middle schools, such as municipal experimental demonstration middle schools, urban district key middle schools, urban general middle schools, and suburban middle schools [24-25]. These categories represent a decreasing order of educational pressure.

The criteria for myopia diagnosis in this study were based on the standard that at least one eye of both the left and right eyes has a refractive error of less than -0.5D. High myopia was defined as a refractive error of at least -5D in at least one eye of both the left and right eyes [26].

By considering the educational pressure categories and applying the myopia criteria, the study aims to quantify the relationship between educational pressure and the prevalence of myopia among the surveyed students.

## 2.3 Data Analysis

The collected data was analyzed using various statistical techniques and modeling approaches. ANOVA analysis was performed to examine the differences and relationships between different variables. Correlation analysis was conducted to explore the associations between classroom lighting, outdoor activity duration, educational pressure, and myopia. Regression analysis was used to establish a predictive model based on the identified factors. Additionally, a neural network model was implemented to further analyze and predict myopia based on the collected data.

Through these analyses and modeling techniques, a myopia prediction model was developed, incorporating the factors of classroom lighting, outdoor activity duration, and educational pressure.

## 3. CONCLUSION

### 3.1 Prediction of the likelihood of myopia and high myopia by single factors

Using the single factor ANOVA method and Kendall's tau-b method (bilateral), analyze the significant correlation between factors and results. The analysis results are shown in Table 1.

The use of natural light in home work has a significant correlation with the occurrence of myopia, suggesting that in the home environment, more direct sunlight or natural light illumination can inhibit the occurrence of myopia; There is a significant correlation ( $p < 0.05$ ) between semi cylindrical illuminance and students' reading and writing distance in class, and semi cylindrical illuminance may affect myopia by affecting students' habit of working close up.

There is a significant correlation between students' subjective perception of color temperature and the occurrence of myopia ( $p = 0.002$ ). It is speculated that the occurrence and development of myopia will have an impact on students' color perception. With the occurrence of myopia, the peak of students' visual spectral sensitivity curve may shift towards lower wavelengths, leading to a higher judgment of color temperature by students.

Under educational pressure, the skewed policy resources obtained by schools have a significant impact on the occurrence of myopia, high myopia, and the increase in right eye myopia in middle school students in the past year. It is speculated that the more policy resources the school obtains, the greater the Psychological stress of education competition, the amount of work, the length of work and other factors that students may face, which will lead to the greater possibility of students' myopia and high myopia, and the greater the growth of myopia in the past year.

In addition, the duration of outdoor activities at noon showed a significant increase in the degree of myopia in the right eye, suggesting that outdoor activities at noon can inhibit the development of myopia. The duration of continuous homework is significantly correlated with the occurrence of myopia, and the frequency of lying down reading is significantly correlated with the development of myopia in the past year.



Table 1. Correlation between illuminance, color temperature, educational stress, outdoor activities at noon, eye habits and myopia

factor \ result	myopia	high myopia	The growth of myopia in the right eye in the past year
Direct sunlight	**	ns	ns
Subjective brightness perception of classroom lighting	ns	ns	ns
Subjective color temperature perception of classroom lighting	**	ns	ns
Educational pressure	*	*	*
Noon outdoor activity duration	ns	ns	**
Lying Reading Frequency	ns	ns	*
Continuous homework duration	*	ns	ns

\*\*p<0.01; \* p<0.05; ns not significant.

### 3.2 Prediction of the likelihood of myopia and high myopia by multiple factors

Based on six factors, including the classification of policy resources obtained by the school, the duration of outdoor activities at noon, grade, the duration of continuous homework writing, the frequency of lying down reading and the use of natural light during homework at home, binomial logistic regression, double-layer BP multi Perceptron neural network and Random forest learning model [27] were used to predict the occurrence of myopia and high myopia. The training set was 70% of the sample set, the test set was 30%, and the neural network was trained five times, Taking the average accuracy of the training results, the comprehensive accuracy of the three methods for predicting the occurrence and nonoccurrence of myopia and high myopia is shown in Table 2. The predictive performance of the double-layer BP neural network for myopia and high myopia is slightly better than the other two methods.

Table 2. Accuracy of three prediction methods

Model \ prediction	Binomial logistic regression	Double layer BP neural network	Random forest
myopia	58.2%	68.1%	68.0%
High myopia	94.3%	95.8%	93.0%

### 3.3 Prediction of myopia development in middle school students based on lighting, educational pressure, duration of outdoor activities at noon, and eye habits

According to the relationship between the factors mentioned in the table 1, set the regression model as shown in formula (1).

$$MDY = a * SL + b * 7.3 * x - c * 6.47 * \ln(y + 1) + d * 0.22 * z + e * LRF \quad (1)$$

Among them, *MDY* is the development of myopia in one year, in D; *x* is the classification of the high school (1: suburban high school; 2: urban ordinary high school; 3: urban district level key high school; 4: urban district level key high school); *y* is the average number of minutes of outdoor activities at noon in the past year, in Min minutes; *z* is the number of consecutive minutes of homework writing, in minutes. *SL* is whether to use direct sunlight or natural light

for homework at home, with values of 0 (no) and 1 (yes); LRF refers to whether one often reads while lying down, with values of 0 (no) and 1 (yes); a, b, c, d, and e are all undetermined parameter coefficients, where b is the proportional coefficient of the impact of educational pressure and outdoor activities on the development of myopia. Characterize the relative degree of the impact of various influencing factors on the development of myopia. Based on the fitting and classification results, the range of undetermined coefficients is  $0 \leq a, e \leq 50$ ,  $0 \leq b, c, d \leq 1$ .

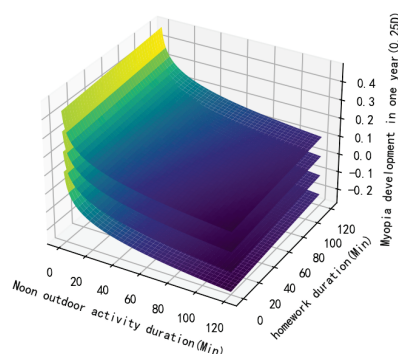
Assuming that the absolute difference between the predicted value and the true value of myopia development is less than 0.125D, the correct prediction is made. Genetic algorithm is used to obtain the optimal undetermined coefficients a, b, c, d, and e. The prediction accuracy of this model is 59.2%, and the prediction model is obtained as formula (2).

$$MDY = -2.68 * SL + 2.71 * x - 1.94 * \ln(y + 1) + 0.01 * z + 46.60 * LRF \quad (2)$$

The meaning represented by variables in this formula is the same as in formula (1). Take *SL* and *LRF* as 0, and *x* as 1, 2, 3, and 4, respectively, to obtain images of MDY, outdoor activity duration *y*, and continuous homework minutes,

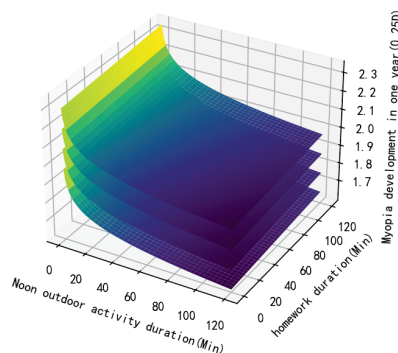
As shown in Figure 2 (a) (b). When MDY is negative, it indicates that according to the fitting formula, the student's myopia has decreased in the past year. For students with myopia growth exceeding 0.25D calculated based on the model, it is recommended to go to a professional institution for visual examination

Fitting curve of myopia growth in the past year (SL=0, LRF=0)



(a)

Fitting curve of myopia growth in the past year (SL=0, LRF=1)



(b)

Figure 2 prediction of myopia development in schools with different school in one year  
(a) SL=0, LRF=0 (not frequently reading while lying down) (b) SL=0, LRF=1 (frequently reading while lying down)

## REFERENCE

- [1] Holden BA, Fricke TR, Wilson DA, Jong M, Naidoo KS, Sankaridurg P, Wong TY, Naduvilath TJ, Resnikoff S. Global Prevalence of Myopia and High Myopia and Temporal Trends from 2000 through 2050[J]. Ophthalmology. 2016 May;123(5):1036-42.
- [2] Morgan IG, Ohno-Matsui K, Saw SM. Myopia. Lancet. 2012 May 5;379(9827):1739-48.
- [3] Ikuno Y. OVERVIEW OF THE COMPLICATIONS OF HIGH MYOPIA[J]. Retina. 2017 Dec;37(12):2347-2351.
- [4] O Pärssinen, A L Lyyra; Myopia and myopic progression among schoolchildren: a three-year follow-up study[J]. Invest. Ophthalmol. Vis. Sci. 1993;34(9):2794-2802.

- [5] Mutti DO, Mitchell GL, Moeschberger ML, Jones LA, Zadnik K. Parental myopia, near work, school achievement, and children's refractive error[J]. *Invest Ophthalmol Vis Sci*. 2002 Dec;43(12):3633-40.
- [6] Morgan, I., Rose, K., How genetic is school myopia[J]? 2005.*Prog. Retin. Eye Res.* 24, 1-38.
- [7] Wojciechowski R. Nature and nurture: the complex genetics of myopia and refractive error[J]. *Clin Genet*. 2011 Apr;79(4):301-20.
- [8] Megaw, P.L., Boelen, M.G., Morgan, I.G., Boelen, M.K. Diurnal patterns of dopamine release in chicken retina[J]. *Neurochem*. 2006; *Int.* 48, 17-23.
- [9] Ying-Zhou Hu, Hua Yang, Hao Li, Long-Bao Lv, Jing Wu, Zhu Zhu, Yu-Hua Zhang, Fang-Fang Yan, Shu-Han Fan, Shu-Xiao Wang, Jian-Ping Zhao, Qiang Qi, Chang-Bing Huang, Xin-Tian Hu. Low color temperature artificial lighting can slow myopia development: Long-term study using juvenile monkeys[J]. *Zoological Research*, 2022, 43(2): 229-233.
- [10] Earl L. Smith, Li-Fang Hung, Baskar Arumugam, Brien A. Holden, Maureen Neitz, Jay Neitz; Effects of Long-Wavelength Lighting on Refractive Development in Infant Rhesus Monkeys. *Invest[J]. Ophthalmol. Vis. Sci.* 2015;56(11):6490-6500.
- [11] Cindy Karouta, Regan Scott Ashby; Correlation Between Light Levels and the Development of Deprivation Myopia. *Invest[J]. Ophthalmol. Vis. Sci.* 2015;56(1):299-309.
- [12] Lin Z, Gao TY, Vasudevan B, Ciuffreda KJ, Liang YB, Jhanji V, Fan SJ, Han W, Wang NL. Near work, outdoor activity, and myopia in children in rural China: the Handan offspring myopia study[J]. *BMC Ophthalmol*. 2017 Nov 17;17(1):203.
- [13] Guan H, Yu NN, Wang H, Boswell M, Shi Y, Rozelle S, Congdon N. Impact of various types of near work and time spent outdoors at different times of day on visual acuity and refractive error among Chinese school-going children[J]. *PLoS One*. 2019 Apr 26;14(4):e0215827.
- [14] Rose KA, Morgan IG, Ip J, Kifley A, Huynh S, Smith W, Mitchell P. Outdoor activity reduces the prevalence of myopia in children[J]. *Ophthalmology*. 2008 Aug;115(8):1279-85.
- [15] Rose KA, Morgan IG, Smith W, Burlutsky G, Mitchell P, Saw S. Myopia, Lifestyle, and Schooling in Students of Chinese Ethnicity in Singapore and Sydney[J]. *Arch Ophthalmol*. 2008;126(4):527–530.
- [16] Jung SK, Lee JH, Kakizaki H, Jee D. Prevalence of myopia and its association with body stature and educational level in 19-year-old male conscripts in seoul, South Korea[J]. *Invest Ophthalmol Vis Sci*. 2012 Aug 15;53(9):5579-83.
- [17] Huang HM, Chang DS, Wu PC. The Association between Near Work Activities and Myopia in Children-A Systematic Review and Meta-Analysis[J]. *PLoS One*. 2015 Oct 20;10(10): e0140419.
- [18] Ian G. Morgan, Pei-Chang Wu, Lisa A. Ostrin, J. Willem L. Tideman, Jason C. Yam, Weizhong Lan, Rigmor C. Baraas, Xiangui He, Padmaja Sankaridurg, Seang-Mei Saw, Amanda N. French, Kathryn A. Rose, Jeremy A. Guggenheim; IMI Risk Factors for Myopia[J]. *Invest. Ophthalmol. Vis. Sci.* 2021;62(5):3.
- [19] Wu PC, Chen CT, Lin KK, Sun CC, Kuo CN, Huang HM, Poon YC, Yang ML, Chen CY, Huang JC, Wu PC, Yang IH, Yu HJ, Fang PC, Tsai CL, Chiou ST, Yang YH. Myopia Prevention and Outdoor Light Intensity in a School-Based Cluster Randomized Trial. *Ophthalmology*. 2018 Aug;125(8):1239-1250.

- [20] Ojaimi E, Rose KA, Smith W, Morgan IG, Martin FJ, Mitchell P. Methods for a population-based study of myopia and other eye conditions in school children: the Sydney Myopia Study[J]. *Ophthalmic Epidemiol.* 2005 Feb;12(1):59-69.
- [21] He M, Xiang F, Zeng Y, Mai J, Chen Q, Zhang J, Smith W, Rose K, Morgan IG. Effect of Time Spent Outdoors at School on the Development of Myopia Among Children in China: A Randomized Clinical Trial[J]. *JAMA.* 2015 Sep 15;314(11):1142-8.
- [22] Morgan IG, Rose KA. Myopia and international educational performance[J]. *Ophthalmic Physiol Opt.* 2013 May;33(3):329-38.
- [23] Xiang Xianming. A Historical Perspective on the Two Education Initiatives of Alleviating Academic Burden in China Since 1949. *Journal of East China Normal University (Educational Sciences)*, 2019, 37(5): 67-79.
- [24] Shanghai Municipal Bureau of Statistics. Main Data Bulletin of the Seventh National Population Census of Shanghai (No. 2) [EB/OL] (2021-5-19) [2023-5-2].  
<https://tjj.sh.gov.cn/7rp-pcyw/20210519/f470438f902f4c88af63be0f84c9808f.html>.
- [25] Shanghai Education Examination Institute. List of High School Enrollment Schools in Shanghai in 2023[EB/OL](2023-5-9)[2023-5-10].  
<https://www.shmeea.edu.cn/download/20230509/117.pdf>.
- [26] Myopia, J.; Mariotti, S.; Kocur, I.; Resnikoff, S.; Mingguang, H.; Naidoo, K.; He, M.; Holden, B.; Salomão, S.; Sankaridurg, P.; et al. The Impact of Myopia and High Myopia. Report of the Joint World Health Organization-Brien Holden Vision Institute Global Scientific Meeting on Myopia[M]; Geneva, Switzerland: World Health Organization, 2015.
- [27] Huang Junjia, Zhang Qi, Zhao Na, Li Rong, Su Yuhua, Zhou Tao. Analysis of myopia influencing factors and myopia prediction based on myopia screening data [J]. *Journal of University of Electronic Science and Technology*, 2021,50 (02): 256-260.

Corresponding Author: Yandan Lin

Affiliation: School of Information Science and Technology, Fudan University

e-mail : ydlin@fudan.edu.cn

# Innovation and Practice of Dark Sky Protection in Urban Lighting Construction

## -- Taking Shenzhen Xichong International Dark Sky Community Declaration as an example

**Abstract:** In April 2023, The Xichong Community (Xichong, Shenzhen, China) was a Dark Sky Community certified by DarkSky International, it is the first Dark Sky Community in China. Taking the Whole process of Xichong International Dark Sky Community declaration as an example, this thesis discusses the urban lighting on the achievement of green and low-carbon development, dark sky and the local nighttime ecological environment protection, value of dark sky economy.

After reviewing the hazards of light pollution, the current situation of dark sky protection, and the concept of Shenzhen's urban lighting planning. Showed that the developments of urban lighting in Shenzhen has always adhered to 'ecology comes first' as the guiding the principle, puts urban light environment protection as a top priority, reduces the impact of artificial light on the natural environment through scientific and moderate urban lighting construction. In the Shenzhen Specialized Urban Lighting (2013-2020), the concept of sensitive urban light environment area was first proposed. The Plan has been released and implemented on 2021, the dark sky protection area was officially demarcated, xichong Community was the key area of dark sky protection, with an aim to pioneer the ecological restoration and protection at night through the construction of the dark sky protection demonstration area.

In vision of building an International Dark Sky Community, "The Management Regulations on Lighting Environment in Xichong Dark Sky Community" was produced, which prescribes measurement indicators of public and private light environment elements. The basic standards are as followed :1, full shielding of all lighting fixtures.2, the correlated color temperature of lamps must not exceed 3000K.3, restrict the total amount of unshielded lighting. 4, restrictions on the luminance、illuminated surface area and extinguish time of illuminated signs.5, improve the lighting arrangement and intelligent control system. Under the guide of Management Regulations, 877 out of 1715 lighting fixtures (51%) successfully meet the IDA's requirements. Sky Quality Meter (SQM-LE) and imaging luminance meter were used to record the sky light data before and after the first round of improvement works, take typical data such as roads for example show that the sky overflow astigmatism was effectively controlled. Now The Xichong International Dark Sky Community's dark sky and ecological environments are now significantly improved.

After the certification, local B&B owners spontaneously transformed the lighting and created star-themed space. The number of overnight tourists for astronomical



observation, science education, research and stargazing camping increased significantly. The tourist peak season was extended from May to October to the whole year, driving the development of local B&B, catering and transportation.

This project has important scientific research and practical value for carrying out Dark Sky protection in the same type of areas, is a milestone in achieving equilibrium between urban lighting development and dark sky protection, and has important reference significance for innovative Dark Sky economic development.

Keywords: International Dark Sky Community, Lighting Plan, Lighting Control, Dark Sky Protection, Dark Sky Economy

## 1. Introduction

With the in-depth advancement of urban construction, the number and scale of urban lighting projects are experiencing explosive growth, playing a vital role in shaping the city's nighttime image. However, excessive and inappropriate lighting in non-core areas and ecological protection zones has led to serious light pollution issues, affecting astronomical observation and physical health. It is crucial to establish a comprehensive framework for urban lighting, regulate the scope and intensity of lighting projects, and protect the nighttime ecological environment.

The International Dark Sky Community, proposed by Dark Sky International in 2001, is one of the five types of dark sky protected areas, with 39 certified areas worldwide. In April 2023, Shenzhen Xichong obtained Dark Sky International certification and became China's first international dark sky community. Under the guidance of the "Xichong Community Light Environment Management Measures," rectification efforts have improved the nighttime lighting environment in the Xichong Community. This serves as a guideline for promoting green and low-carbon development in urban lighting, as well as for dark sky protection and nighttime ecological preservation.

## 2. Definition of International Dark Sky Community

In order to raise global awareness about light pollution control and dark sky protection, the International Dark-Sky Places conservation program (IDSP) was launched by the International Dark-Sky Association (IDA) in 2001. The program aims to promote the preservation of a pristine dark sky worldwide. Organizations such as communities, parks, and protected areas that have favorable conditions or strive for dark sky preservation can protect their local dark skies and develop the dark sky economy by implementing appropriate lighting management policies and promoting scientific education.

International Dark Sky Communities, one of the five categories of dark sky sanctuaries, are towns or communities that develop and enforce high-quality outdoor lighting policies. They actively work towards educating the public on the significance of dark skies. Protecting dark sky conditions involves minimizing or reducing the impact of artificial light on the night sky by implementing eco-friendly lighting control

policies. The International Dark-Sky Association has outlined a series of lighting control requirements for lighting installations in International Dark Sky Communities, and it is essential to ensure that all lighting facilities meet these standards within a specified timeframe.

### 3. International Dark Sky Community Construction

Lighting renovation is a crucial element in establishing an international dark sky community. By adjusting the color temperature, brightness, and shading methods of existing lighting facilities and controlling the overall luminous flux in the area, the overflow of light into the sky can be effectively managed, preventing the negative impact of lighting on the night sky environment.

The Monte Megantic Observatory in Quebec, Canada, undertook lighting renovation and obtained certification as an International Dark Sky Conservation Area (IDSC) in 2007. This initiative aimed to reduce light pollution from surrounding urban developments and mitigate its interference with astronomical observations. By decreasing lighting power and replacing original metal halide and mercury vapor lamps with high-pressure sodium lamps, energy consumption was nearly halved, light spillage was reduced by 40%, and the local night sky environment was significantly improved.

In 2021, Misei Town in Japan partnered with Panasonic to develop lamps that comply with the DarkSky International's full-shade lighting requirements for dark sky protection. The product has successfully obtained certification through the Fixture Seal of Approval program. Through this collaboration, all public outdoor lighting in Bisei Town has been replaced with lighting fixtures that meet the standards set by the DarkSky International.

### 4. Lighting renovation of Xichong dark sky community

#### 4.1 Location

Xichong Community is situated at the southern tip of Shenzhen Dapeng New District, which is recognized as one of the eight most beautiful coastlines in China. Surrounded by mountains on three sides, it is adjacent to Sanmen Island in Huizhou to the east and Saigon in Hong Kong to the south. The region boasts exceptional natural and ecological conditions. Based on the current assessment, the eight natural villages in the area have well-developed accommodation and catering industries, offering comprehensive support services for nighttime stargazing, tourism, and vacations. Xichong Beach, known for its spaciousness and high quality, provides ample space for coastal leisure activities and stargazing at night. The Shenzhen Observatory area is positioned atop a cliff on the eastern side of Xichong Beach, experiencing minimal interference from surrounding lighting installations. The starry sky quality is particularly impressive under sunny conditions. Equipped with professional stargazing facilities and offering popular science explanations, the observatory hosts various activities centered around dark sky stargazing. It is considered the ideal location for

stargazing and event planning.

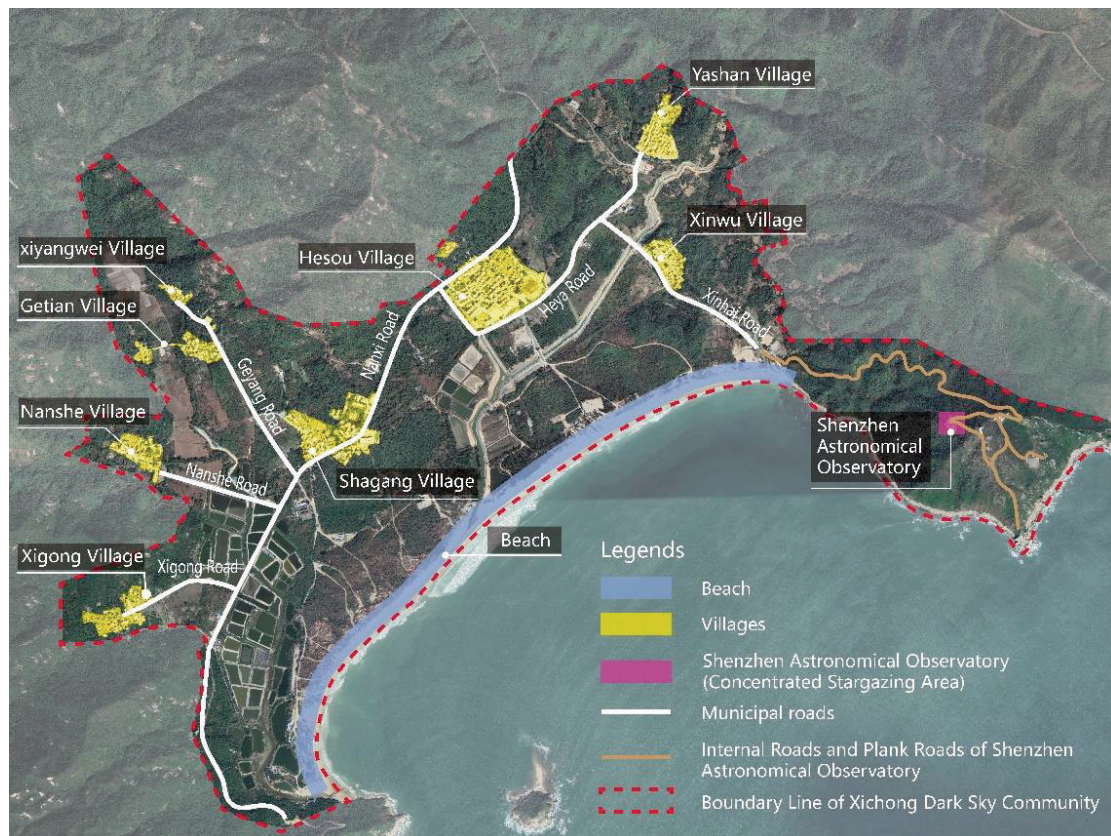


Figure 1 - Area plan of Xichong Dark Sky Community

Based on the application requirements of the International Dark Sky Community, a study was conducted on the lighting conditions of municipal roads, village roads, public spaces within the village, beaches, and outdoor advertising signs in Xichong Community. The types and quantities of lamps were recorded, and data measurements were performed in representative areas. This article focuses on the lighting renovation of municipal roads, village road lighting facilities, and outdoor advertising signboard lighting to showcase the lighting improvement efforts undertaken in Xichong Community.

## 4.2 Municipal road and village road lighting renovation

The municipal road in Xichong Community is an urban secondary road consisting of two-way two-lane lanes. It is illuminated using 60W and 90W single-arm street lamps with a pole height of 7.5 meters. The distance between the poles is 25-30 meters, and LED street lights are used as the light source. Measurements have shown that the uniformity of the lighting on the municipal roads does not meet the required standards, and the color temperature of the lamps exceeds the lighting control requirements of the International Dark Sky Community. The village road is a single-lane road, and it is lit using single-arm street lamps with the same pole height as the municipal road. However, there is inconsistency in the power and type of light source used for the lamps, and in

some cases, street lamps are installed on walls along narrow roads.

Table 1 - Statistics of Municipal Road Lighting fixtures

location	quantity	Lamp overview			H (m)	Street Lighting Arrangement	color temperature (K)	lumens (lx)
		type	power	quantity				
Nanxi road	73	Pole Road light	90W	40	10m	One side, distance 25m	4005k	16.39
			60W	33	7.5m			
Heya road	51		60W	51	7.5m	One side, distance 25-30m	4075k	5.2 lx
Xinhai road	31		60W	31	7.5m	One side, distance 30m	4009k	11.5
Nanshe road	21		60W	21	7.5m	One side, distance 30m	4154k	12.28
Geyang road	44		60W	44	7.5m	One side, distance 25m	3894k	5.8
Xigong road	14		60W	14	7.5m	One side, distance 25m	4579k	6.6
total	234							

In order to enhance the lighting environment in Xichong Community, the first phase of lighting renovation focused on municipal roads and village roads. The street lamp selection for the municipal road renovation involved using 2700K full cut-off lamps while retaining the original height and spacing of the lamp poles. Initially, the plan was to replace lamps with the same power, specifically 60W and 90W lamps. However, after on-site testing, it was found that the average illuminance of the 60W lamps was high. As a result, the lamp power was reduced in the subsequent rectification. Ultimately, 90W lamps were used for municipal road lights with a pole height of 10 meters, while 50W lamps were used for both municipal road and village road lights with a height of 7.5 meters. For street lights that needed to be installed on walls due to the absence of suitable pole installation conditions, 40W floodlights were used as replacements. The average illuminance, calculated through dalux, meets the requirements of the national standard for the reconstructed road lighting. However, the uniformity of illuminance is affected by the wide spacing of the original light poles, resulting in measurements lower than the national standard requirement. This issue will be addressed in the subsequent renovation phase.

Following the reconstruction of the municipal and village roads, a unified color temperature was implemented, establishing a distinct functional lighting framework and effectively controlling scattered light above the water level. The illuminance value after the rectification meets the requirements of the national standard, contributing to an overall improvement in the quality of nighttime scene lighting.

Table 2 - Comparison of renovation and upgrading of lighting fixtures on municipal roads




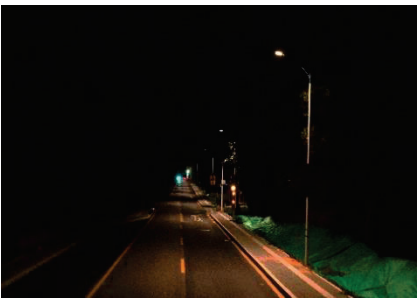






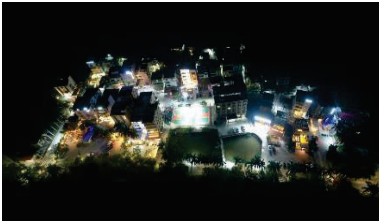
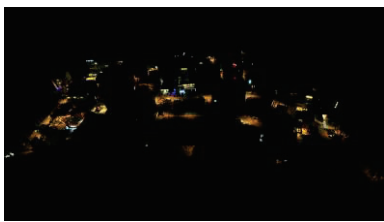
Location	view	Before lighting fixtures replacement	After lighting fixtures replacement
Nanxi Road	car view H1.5m		
	high-altitude view H10m		
	aerial bird view H>80m		

Table 3 - Comparison of renovation and upgrading of lighting fixtures of village roads

Location	view	Before lighting fixtures replacement	After lighting fixtures replacement
Xinwu Village	pedestrian perspective H1.5m		
	aerial perspective H>80m		



### 4.3 Advertising Sign Lighting renovation

Xichong Community has seen the establishment of numerous homestays and restaurants, providing accommodation and catering services for visitors engaging in coastal tourism activities. However, there has been a lack of unified planning regarding the construction of various commercial outdoor advertisements and outdoor signboard lighting. If these advertisements are too bright, they can have a significant impact on the nighttime light environment in Xichong Community. Given the challenges in coordinating various businesses and the large number of advertisements, the first phase of lighting renovation focused on a pilot project in a typical village called Xinwu Village. This village is located near the entrance of No. 4 beach and the observatory. The advertising signs mainly belong to homestays, with some themed around stargazing. The renovation process was not difficult, and the overall lighting environment of the village has greatly improved following the renovation.

Laboratory tests were conducted to ensure that the surface brightness of the advertising signboards is below  $100\text{cd/m}^2$ , the color temperature is below 3000K, and the luminous area is below  $18.6\text{ m}^2$ . Additionally, the signboards are only illuminated during business hours. After the lighting renovation, the advertising signboard lighting now complies with the requirements set by the International Dark Night Community, without compromising the original guiding function they serve.

Table 4 - Comparison of advertising signboards lighting improvement

Location	Before lighting fixtures replacement	After lighting fixtures replacement
Freedom Surf		
Color temperature	5732K	2745K
Luminance	$359\text{ cd/m}^2$	$53\text{cd/m}^2$

After completing the first phase of lighting renovation work, 51% of the lamps in Xichong Community now meet the requirements for applying for the International Dark Night Community certification. To assess the impact of the lighting improvements, a typical space was selected for measurement using a skylight measuring instrument. The measurements were conducted in various locations within the Xichong community, including roads, squares, villages, woodlands, and observatories. By comparing and analyzing the skylight measurement data before and after the rectification, it can be concluded that the lighting quality in the Xichong area has significantly improved. The

rectification efforts have effectively reduced sky spill light caused by improper lighting, resulting in an overall improvement in the quality of the night sky. Under clear and cloudless conditions, it is now possible to observe the Milky Way with the naked eye, enhancing the stargazing experience for the public.



Figure 2 - Skylight measurement sampling points in the Dark Sky community of Xichong

Table 5 - SQM data table for specific data in the Dark Sky community of Xichong		
Date (DD/MM/YYYY)	6-27-2022	8-1-2022
and Time Zone	20:40-21:50	20:50-22:15
weather/moon phase	sunny/waning moon	clear/new moon
Location Name	SQM (mag/arcsec <sup>2</sup> )	
1	19.12	19.36
2	18	18.55
3	18.93	18.98
4	18.44	18.61
5	19.24	19.27
6	19.41	19.44
7	19.23	19.33
8	19.16	19.21
9	19.61	19.61
10	19.57	19.63

### 5. Conclusion

Protecting the dark sky and developing starry sky tourism hold significant environmental, social, and economic value. As China's urbanization rate and urban

population continue to grow, the concept of "dual circulation" and consumption upgrades present new requirements. Driven by the demand for tourism product innovation and high-quality development, as well as the increasing enthusiasm for China's aerospace industry, public recognition and awareness of the importance of protecting the dark night and the starry sky theme are continuously improving. Consequently, the consumption of starry sky-themed experiences is becoming increasingly active, leading to the rapid development of starry sky tourism.

To dispel the public's misconception that protecting the dark night sky restricts development and construction, it is necessary to control the intensity of lighting construction, optimize lighting planning and design, and provide guidance on the selection of appropriate lamps. It is essential to retain necessary functional lighting and elegant-colored landscape lighting while effectively controlling light pollution. By doing so, the impact of lighting construction on the urban ecological environment can be minimized. This approach allows the public to enjoy nighttime activities while creating a harmonious interaction between the dark night environment and starry sky tourism.

# **A LAB EXPERIMENT OF THE LIGHT ENVIRONMENT COMPROMISING READING INTERACTIVELY ON PAPER AND VDT**

Xiaobo Miao, Hang Su, Biao Yang

( iLLab, School of Architecture, Harbin Institute of Technology, Shenzhen, China )

## **ABSTRACT**

With the diversification of meeting space function, the types of visual tasks are growing accordingly. But the demands of interacting between different visual tasks could not be met in one light environment, e.g., the demands of light environment in a meeting room between reading on paper and watching on a projection display terminal at the same time were different significantly. The current paper focuses on the effect of light distribution environment on interactive visual quality between reading on paper and projection display terminal, and optimal light environment solution which compromising multiple visual tasks. In the current study, 20 participants (10 males and 10 females) were recruited in a within-subject experiment in the laboratory under 20 light conditions: 4 types of luminance ratio of the projection screen (1/35, 1/5, 1/2, 1/1.5) with 5 types of desktop illumination (300lx、150lx、75lx、30lx、0lx). The clarity and comfort were assessed by the scales of questionnaires, the performance was measured by the work speed and correct rate of tasks. The results showed that the clarity and comfort was influenced interactively by light environment distribution in general. As the luminance ratio of the projection screen increases, the clarity and comfort of watching the projection screen tends to decrease. As the illuminance of the desktop decreases, the clarity and comfort of reading the paper material tends to decrease. In addition, the results showed that the optimal plan of light environment for multiple visual tasks was not put the plan of light environment for single visual task together simply. The current study would provide some rationale for a promising light environment solution of the multiple visual tasks in one place in future.

Keywords: Multiple visual tasks; VDT, Interactivity, light distribution, meeting scene

## **1. INTRODUCTION**

The light environment plays a vital role in a healthy and comfortable office meeting environment, and is an important physical environment indicator that affects the human perception of space. Although basic lighting can meet the meeting room lighting, with the application of visual terminal display such as monitors, projectors, tablet PCs and LED screens, and the personalized and diverse development of user behavior, multiple visual tasks often exist simultaneously in the meeting scene. If the lighting requirements of paper reading are used as a design guideline, this will lead to glare, blurred target vision, visual fatigue and many other problems. Because the visual display terminal has the characteristics of self-illumination,

its light environment needs and paper reading writing light environment needs are different. Currently, the light environment for a single visual task (e.g. paper print media and visual display terminals) is well researched, but there is a lack of research into the light environment for scenarios where multiple visual tasks exist in the same space.

There has been more research on the lighting requirements for reading and writing on paper alone, and for visual tasks on visual display terminals (VDTs). Huang and Chen [1] investigated the effects of different correlated colour temperature(CCT)s on students' visual comfort and learning efficiency when they are studying, while ensuring basic illumination requirements. The study showed that high CCT fluorescent lighting (4000 K, and 6500 K) had a positive effect on student performance. Yan and Guan [2] further investigated the two-factor effect of CCT and illuminance in classroom light environments. The results showed that the optimal CCT in the classroom was 4000 K and the optimal illuminance value to match was 750 lx. If the CCT was 2700 K, the optimal illuminance value was 300 lx. In addition, Sun[3] suggested an illuminance value of 500-800 lx for non-computer work reading and learning behaviour in an office space in terms of enhancing memory and improving learning performance. kim [4] et al explored the optimal luminance when viewing VDT at different illumination levels. The study showed that when the illumination level of the lighting environment was less than 500 lx, the best visual comfort was achieved when the white field brightness of the screen was between 200 and 500 cd/m<sup>2</sup>. Luo [5] conducted a study on the design of LED office light environments suitable for youth workers when performing VDT visual tasks. The results show that the most suitable light environment parameters for young workers to carry out VDT visual tasks are as follows: CCT of 3800 K, horizontal illuminance of 500 lx and vertical illuminance of 300 lx.

For the light environment requirements in scenarios where multiple visual tasks exist in space, Li et al[6] investigated visual comfort and learning performance when using VDT and paper reading simultaneously under different lighting environments. This study gave lighting design recommendations in terms of visual comfort, operational performance and the relationship between work surface illumination and light source CCT: visual comfort was best evaluated when VDT and paper reading were performed simultaneously in this lighting environment when the lighting environment was 750 lx and 4500 K. Visual comfort and operational learning efficiency were both optimal when the light source correlated color temperature(CCT) was 4500 K and the illumination level was 500 lx. However, most research on VDT light environments has focused on electronic devices such as computers and mobile phones, but there has been less research on projection-based visual display terminals and light environment requirements. Current research in projection-based display endpoints is almost exclusively focused on classroom environments, and rarely addresses conference room scenarios, and multi-visual task light environments in scenarios.

Overall, the requirements of multi-task interaction have been discovered in conference rooms, but the evidences of light environment parameters about multi-task interaction, especially between display terminals and desktop paper materials, were insufficient. Therefore, the current paper investigates the optimal light environment parameters about interaction between the multiple visual tasks :viewing a project display terminal and reading a paper-based medium in a meeting room. The current study can provide some reference and suggestions for the design and optimization of the light environment for multi-visual tasks in meeting rooms



## 2. METHODS

### 2.1 Experimental design

The experiment described in the current paper set up a total of 20 condition of spatial light distribution (4 projection luminance ratios x 5 tabletop illuminance levels), and the subjective perceptions of participants and their task performance were selected as indicators of the quality of the interaction. The experiment was conducted in a closed, windowless dark room, which allowed for complete control of the light environment. Only one white wall was used as a projection wall for projecting the content of the experimental test task, and the rest of the walls were black to avoid multiple reflections of light. Four LED luminaires are installed above the head to control the illumination of the table and two LED sidelights are used to adjust the brightness ratio of the projected contents. The experimental scenario is shown in Figure 1:



Figure1. Experimental scenario environment

### 2.2 independent variables

The experimental independent variables are 20 spatial light distribution scenes (4 projection luminance ratios x 5 desktop illuminance levels). The projection luminance ratio was controlled by the ratio of the projected image to the background luminance, with specific ratios of 1/35, 1/5, 1/2 and 1/1.5. The smaller ratio caused the higher clarity. The different ratio is achieved by two independent infinitely dimmable luminaires illuminating the projected image. The plan is used to simulate the loss of clarity of the projected image due to ambient light in a real scene. 1/35 is the black and white luminance ratio of the projector's image in a no lighting environment. The tabletop illuminance is set to 5 types (300lx, 150lx, 75lx, 30lx, 0lx) and the five parameters are selected from the architectural lighting standard GB 50034-2013 [7] for the grading of standard indoor illuminance values.

### 2.3 Dependent variable

The experiment was evaluated through the subjective perceptions of the subjects and task performance in different light environment scenarios. Clarity and comfort were assessed by subjective questionnaire, which specifically included both clarity and comfort ratings. The questionnaire was based on a Likert eleven-point scale ranging from 0-10, with higher numbers indicating higher levels of reading comfort and clarity in that light environment scenario, with 0 indicating very uncomfortable or very unclear and 10 indicating very comfortable or very clear.

The two measures of task performance were reading speed and accuracy. Three tasks

were set for this experiment: speaking the content of the projected image; writing the content of the paper material on the desktop; and writing the content of the specified area on the projected picture on the paper material. The performance results under the three tasks were used to measure the reading effect of the projection-based visual display terminal; the reading effect of the desktop paper material; and the reading effect when the two visual tasks were interacted. The content of the tasks consisted of Arabic numerals and uppercase and lowercase English letters, and the font of the experimental projection content was in Arial size 24 (some of the tasks are shown in Figure 2).



Figure2. Schematic diagram of the experimental task content ( The first paragraph is the content for speaking and The second paragraph is the content for writing )

## 2.4 Experimental procedure

The expected sample size for this experiment is 40, and 20 participants (10 males and 10 females), aged between 18 and 30 years, have been completed, all of whom have been examined for no visual problems or have normal levels of vision with correction. Before the start of the experiment, a sequence of experimental scenarios generated by a random function will be drawn by the experimenter. The participants will be given a 3-minute adaptation period to the light environment. During this time, the experimenter will explain the procedure of each part of the experiment, the content of the test and the instructions for completing the subjective questionnaire. The participant will read the consent form for the experiment and complete the signature.

At the beginning of the experiment, the participants complete the three tasks in order: reading aloud the projected content, writing the paper content and writing the projected content, as well as completing the questionnaires for each of the three tasks. The experimenter recorded the time of completion of the three tasks. The process is shown in Figure 3. Each light condition took approximately 4 minutes to complete and each participant was required to complete a total of 20 conditions. Each condition required the completion of the corresponding task and subjective questionnaire.

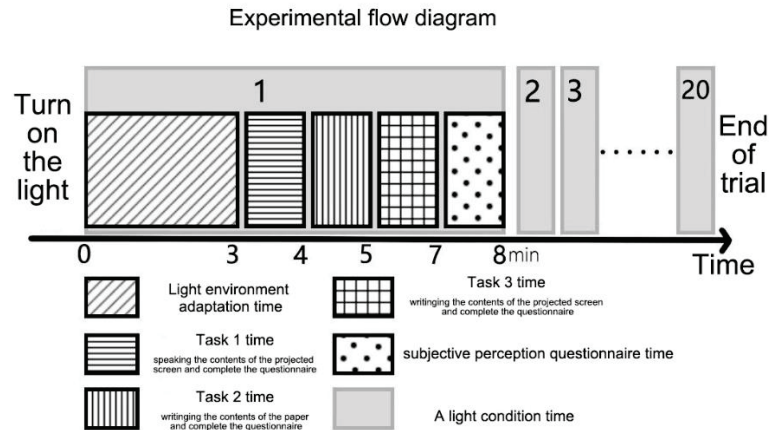


Figure3. Experimental flow diagram

Between the switch of different conditions, the participant is given a one-minute break with the blindfold on, and after the experimenter has finished the next condition, the participant is given 1-2 minutes to adapt to the light environment. The experiment is not completed until all 20 scenarios have been experienced. At the end of the experiment, the participants are paid for the experiment.

### 3. Results

#### 3.1 Projection luminance ratio

In the current paper, the Kruskal-Wallis test was used to analyze the effects of projection luminance ratio on clarity, comfort and task performance (reading speed and accuracy), and the results are shown in Table 1. The results are shown in Table 1. It can be seen that there are significant differences in clarity and comfort for different projection content luminance ratios. Further analysis of the differences by the Nemenyi method showed that there were significant differences ( $p < 0.01$ ) between the two for clarity at different projected content luminance ratios (1/35, 1/5, 1/2, 1/1.5). As shown in Figure 4, as the luminance ratio of the projected screen content increases in sequence, the corresponding projection content clarity score decreases. As shown in Figure 5, for comfort, there was no significant difference between the two projection luminance ratios of 1/35 and 1/5. As the luminance ratio increases from 1/5 to 1/2 and 1/1.5, there is a significant difference ( $p < 0.01$ ) and the comfort score shows a trend of decreasing with increasing luminance ratio. This result indicates that projection luminance ratios 1/35 and 1/5 are better than 1/2 and better than 1/1.5 in terms of comfort on projection reading. In addition, there is no significant difference in task performance across projection luminance ratios, implying that the projection luminance ratio has no effect on task performance.

Table 1 Projected reading clarity and comfort at different projection brightness ratios

projection luminance ratio	Subjective questionnaire scores				Kruskal-Wallis test statistic H value	$p$
	1/35(n=100)	1/5(n=100)	1/2(n=100)	1/1.5(n=100)		
clarity	9.000	8.000	7.000	5.000	174.653	0.000**
comfort	8.000	8.000	7.000	4.000	137.061	0.000**

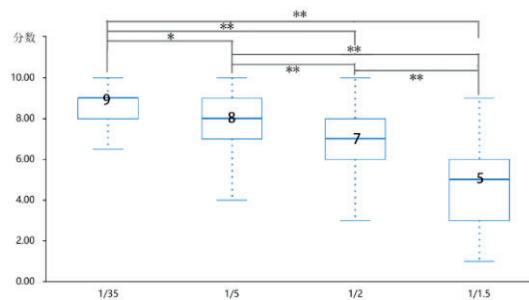
\*  $p < 0.05$  \*\*  $p < 0.01$ 

Figure 4. Clarity scores for projected reading at different projection content luminance ratios

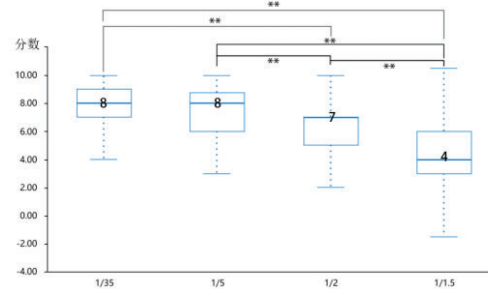


Figure 5. Comfort score for projected reading with different projection content brightness ratios

### 3.2 Horizontal desktop illuminance

Similar to the analysis of the projection luminance ratio in the previous section, the Kruskal-Wallis test of desktop illuminance was used to analyze clarity, comfort and task performance (reading speed and accuracy). As shown in Table 2, different desktop illumination levels showed significant differences on desktop paper reading clarity and comfort.

Table 2 Projected reading clarity and comfort at different desktop illumination levels

Desktop illumination	Subjective questionnaire scores					Kruskal-Wallis test statistic H value	$p$
	300lx(n=80)	150lx(n=80)	75lx(n=80)	30lx(n=80)	0lx(n=80)		
clarity	9.000	9.000	8.000	7.000	6.000	190.537	0.000**
comfort	9.000	8.000	8.000	7.000	5.000	138.697	0.000**

\*  $p < 0.05$  \*\*  $p < 0.01$ 

Further analysis of the differences by the Nemenyi method showed that on paper reading clarity, as shown in Figure 6, there was a significant difference ( $p < 0.01$ ) in reading clarity when

the tabletop illumination was 0 lx compared to 30, 75, 150 and 300 lx. There was a significant difference ( $p<0.01$ ) when the desktop illumination was 30 lx or 75 lx compared to the desktop illumination of 150 lx and 300 lx scenarios, indicating that 300 lx and 150 lx scenes were better than 75 lx and 30 lx and better than 0 lx for reading clarity on paper. as shown in Figure 7, for reading comfort on paper, there was a significant difference ( $p<0.01$ ) when the desktop illumination was 0 lx compared to 30, 75, 150 and 300 lx were significantly different compared to each other ( $p<0.01$ ). There was a significant difference ( $p<0.01$ ) when the desktop illumination was 30 lx compared to a desktop illumination of 150 or 300 lx. This result shows that 300 lx and 150 lx scenes are better than 75 lx and 30 lx and better than 0 lx.

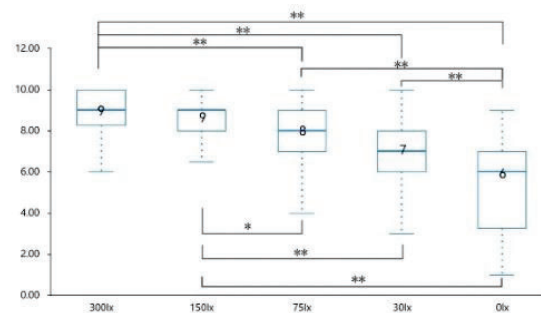


Figure 6 Clarity scores for projected reading at different desktop illumination levels

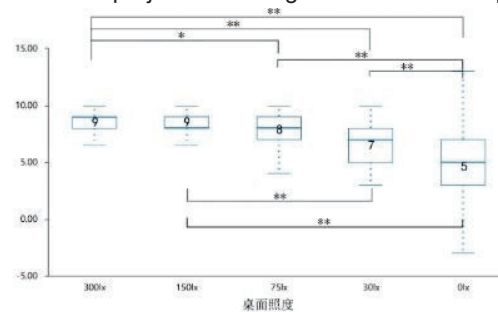


Figure 7 Comfort score for projected reading at different desktop illumination levels

### 3.3 Luminance ratio and desktop illuminance on the alternation between two visual tasks

Two factors, desktop illuminance and projected content luminance ratio, jointly influence the comfort level of alternating between viewing and reading on paper-based visual display terminals. To investigate the effect of these two factors on interaction comfort, a multiple comparison analysis was conducted on 20 data sets using the Least Significant Difference (LSD) method (Table 3).

Table 3 Comfort scores when alternating between multiple visual tasks at different projection luminance ratios and desktop illumination

Projection luminance ratio \ Desktop illumination	Desktop illumination				
	300lx(n=80)	150lx(n=80)	75lx(n=80)	30lx(n=80)	0lx(n=80)
1/35	7.70±1.53	7.25±1.71	7.10±1.48	6.40±2.06	2.85±2.21
1/5	7.45±1.99	<b>7.85±1.31</b>	6.95±1.10	6.60±2.39	3.65±2.25
1/2	7.05±1.28	6.15±1.50	6.65±1.42	5.70±2.05	3.90±2.22
1/1.5	6.00±2.15	6.00±1.69	4.90±1.45	4.00±1.69	3.65±2.35



The alternate reading comfort scores for a given projection luminance ratio are shown in Figure 8 (a). At projection luminance ratios of 1/35 and 1/2, alternate reading comfort is significantly higher at a tabletop illuminance of 300 lx than at a tabletop illuminance of 30 lx. The alternate reading comfort at 300, 150, 75 and 30 lx is significantly higher than the alternate reading comfort at 0 lx. At a projection luminance ratio of 1/5, alternate reading comfort is significantly higher at desktop illuminance levels of 300 and 150 lx than at desktop illuminance levels of 30 lx. The alternate reading comfort at tabletop illumination levels of 300, 150, 75 and 30 lx is significantly higher than the alternate reading comfort at 0 lx. At a projection luminance ratio of 1/1.5, alternate reading comfort is significantly higher at tabletop illuminance levels of 300, 150 and 75 lx than at 0 lx. The alternate reading comfort level at 300 and 150 lx is significantly higher than the alternate reading comfort level at 30 lx.

The alternate reading comfort scores for a given desktop illumination are shown in Figure 8 (b). At a desktop illuminance of 300 lx, the alternate reading comfort at projection content luminance ratios of 1/35 and 1/5 is significantly higher than the alternate reading comfort at a projection luminance ratio of 1/1.5. At a table illumination of 150 lx, the alternate reading comfort at projection content luminance ratios of 1/35 and 1/5 is significantly higher than the alternate reading comfort at a projection luminance ratio of 1/1.5. The alternate reading comfort at a projected content luminance ratio of 1/5 is significantly higher than the alternate reading comfort at a projection luminance ratio of 1/2. At tabletop illumination levels of 75 and 30 lx, alternate reading comfort is significantly higher at projection content luminance ratios of 1/35, 1/5 and 1/2 than at projection luminance ratio of 1/1.5. When the tabletop illuminance was 0 lx, there were no significant differences between the groups, i.e. the different projected content luminance ratios had no effect on interactive comfort.

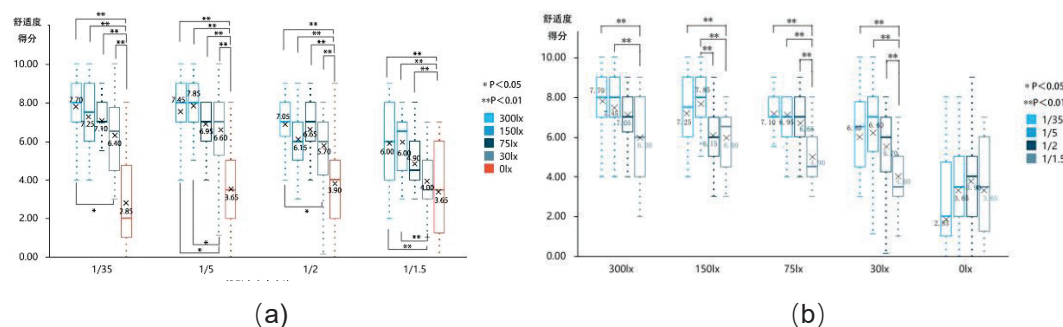


Fig. 8 Display of alternate reading comfort scores for projection display terminal and paper print media

#### 4. Conclusion

The current paper has explored the effects of different light distribution conditions on the comfort, clarity and task performance of reading at projection display terminals, reading on paper print media and alternating between the two. The results show that in single visual task scenarios, the comfort and clarity of reading tasks on projection display terminals tended to decrease when the projection luminance ratio became larger; the reading clarity and comfort of paper print media similarly tended to decrease when the desktop illuminance decreased. In the

multi-visual task scenario, the highest average comfort score for alternate reading was achieved when the desktop illuminance was 150 lx and the projection luminance ratio was 1/5, not a combined condition of the best projection luminance ratio (1/35) for projection reading clarity and the best desktop illuminance (300 lx) for paper print media reading clarity in a single scenario. It can be inferred that the overall optimal light environment for a multi-task interaction scenario is not simply a combination of the optimal light environment for each single visual task, but the statistical analysis of the 20-person sample has not yet shown significance in Statistical methods, and this conclusion will be further verified once the data for the full 40-person sample has been collected.

## REFERENCES

- [1] Huang HJ, Chen ZG. A study of visual efficacy in classroom lighting environments with different light colours[J]. *Light and Lighting*, 2011, 35(4): 14-18.
- [2] Yan YH, Guan Y, Liu XD, et al. Effects of classroom fluorescent light colour temperature on students' learning efficiency and physiological rhythms[J]. *Civil Construction and Environmental Engineering*, 2010, 32(4): 85-89.
- [3] Sun Wenhong. Research on intelligent control system of light environment based on user behavior [D]. Zhejiang University, 2016.
- [4] Konstantzos, Iason & Sadeghi, Seyed Amir & Kim, Michael & Xiong, Jie. (2020). The effect of lighting environment on task performance in buildings – A review. *Energy and Buildings*. 226. 110394. 10.1016
- [5] Luo YJ. Research on LED office light environment with adaptability for young VDT workers [D]. Chongqing University, 2017.
- [6] Li Tiantian, Zhang Jiuxhong, Lv Kunjie. The effect of lighting environment on visual comfort and learning efficiency under different reading media[J]. *China Illuminating Engineering Journal*, 2022, 33(2): 109-116
- [7] Ministry of Housing and Urban-Rural Development of the People's Republic of China. Lighting Design Standards for Buildings GB50034-2013 [s], China Construction Industry Press, 2013.

## ACKNOWLEDGEMENTS

Corresponding Author Name: Biao Yang

Affiliation: School of Architecture, Harbin Institute of Technology, Shenzhen

E-mail: yangbiao@hit.edu.cn

# White LEDs for illumination of polarizing microscope

Man Li, Yahong Li, Nianyu Zou

Research Institute of Photonics, Dalian Polytechnic University, Dalian 116034, China

## Abstract

Polarizing microscope is a high-tech product which combines precision optical microscope technology, advanced photoelectric conversion technology and computer image processing technology perfectly. To obtain white LEDs with high light efficiency and high polarization for illumination of polarizing microscope, an integrated sandwich metal-dielectric structure contained metal-dielectric grating was designed on the base of LED chip. By using FDTD software to simulate and analyze the polarized white LEDs, the results show that the polarization extinction ratio can reach up to 61dB from 475nm-680nm, and the light transmittance up to 0.83 in the whole band. The white LEDs that emit directly polarized light provide a new way for illumination of polarizing microscope instead of the traditional halogen lamp lighting and single wavelength LED. In addition, it can simplify the structure of polarizing microscope device, reduce the light energy loss, and has great application potential in the observation of microstructure morphology and the highlighting of sample characteristics.

Key words: Polarization; White LEDs; Grating; Finite-difference time-domain (FDTD)

## 1. INTRODUCTION

Polarization is one of the fundamental properties of light. As a marker less and non-damaging optical detection technique, polarizing microscope has shown promising applications in the fields of biomedical microstructure, pathological diagnosis, and lesion analysis [1-4]. Among them, polarizing microscopy plays an important role in observing the microstructure of materials such as crystal structure and molecular arrangement [3-4]. Especially, it is sensitive to subwavelength microstructure with the advantages of no need to stain the sample and directly obtain the polarization characteristic parameters of the sample, rich in information and many data dimensions [5-6], which is widely used in accurately distinguishing the types and distribution of different lesion microstructure characteristics.

Polarizing microscope is to use the "anisotropy" of substances to distinguish different structures of substances, in order to make the observation effect clearer and more obvious, the incident light source and the received light need to be adjusted to eliminate or reduce the interference of stray light. Conventional polarizing microscope is to add a polarizer at the illumination end and imaging end of the optical path so that the light emitted from the light source is transformed into linearly polarized light, which is incident on the sample, according to the refractive nature of the sample, produces refraction, reflection and absorption [7-8]. The light emitted from the sample is received by a polarization detector whose polarization direction is orthogonal to the polarizer, and the received image can help us to analyze the characteristics of the sample. This method loses about 50% of the incident light from the non-polarized source and suffers from low light utilization to the surface of the sample [9-11], resulting in the sample features not being highlighted. If the light source can be made to actively emit line polarized light, it can replace the filter structure, which can simplify the microscope device structure, reduce the light energy loss, and increase the beam brightness and viewing angle. Over the past decades, a series of studies on polarized white light have been conducted. For example, Kanamori et al. proposed a polarizing color filter using one-dimensional (1D) silicon subwavelength grating on quartz substrates, achieving transmittances of 0.71, 0.58, and 0.59 for the red, green, and blue filters, respectively [12]. Wang et al. designed a double-layer grating architecture using a hybrid scheme and realized a transmission of ~ 50% and extinction ratio of ~ 60 dB in green [13]. In this paper, a linearly polarized white LEDs structure is designed with a sandwich metal-dielectric gratings structure, which can achieve good polarization performance through optimizing structure parameters in the visible wavelength of 475-680nm. Based on the premise that the grating period is 200nm and the line width is 100nm, the grating height and other parameters are optimized respectively. It can bring savings in preparation, volume and cost, and provides a new design idea for the design about the illumination of polarizing microscope.

## 2. Structural Design and Parameters

When the grating period is much smaller than the incident wavelength, the subwavelength grating will be polarized, resulting in the reflection of the electric field component parallel to the wire gratings and the transmission of the electric field component perpendicular to wire gratings [14-16]. Based on the polarization property of subwavelength grating, this paper designs a sandwich metal-dielectric gratings structure on the LED chip surface to complete polarization performance. Moreover, an anti-reflection film layer is added between the LED chip and the gratings structure to realize the abnormal transmission of light. The structure model is shown in Fig. 1, the LED chip emit 475nm ~ 680nm high quality white light, passes through the anti-reflection film to complete abnormal transmission, and then emits linearly polarized light through the sandwich metal-dielectric gratings. The polarized light with high extinction ratio and transmission can solve the existing problem of low light utilization in polarizing microscope.

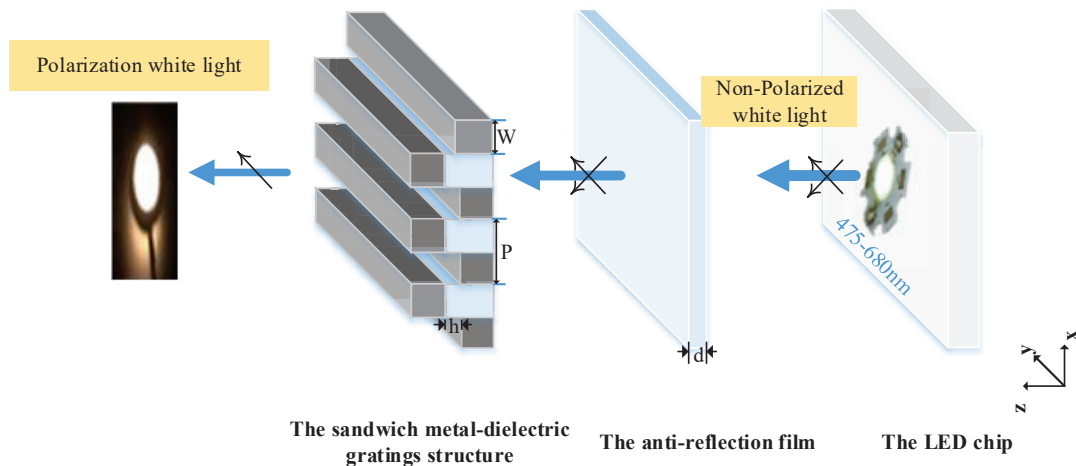


Figure 1. The structural model drawing

As shown in Fig. 1: the sandwich metal-dielectric gratings are composed of metal-dielectric-metal grating mosaic combination in turn, the grating line width is  $W$ , period is  $P$ , duty cycle is  $DC=W/P$ , embedded media grating and metal grating height difference is  $h$ . From the x-y plane to form the light incident surface, along the z-axis direction out of the polarized light. In order to verify the polarization performance of the structure, we apply the finite-difference time-domain method (FDTD) to analyze it [17], and use the higher polarization extinction ratio (ER) and transmittance (T) as the evaluation index of the polarization performance. At present, the grating with a period of 200nm and a line width of 100nm can be processed at the laboratory level. Based on this, the effects of different grating materials and grating heights on the polarization properties of the structure are analyzed and optimized.

## 3. Optimization of Structural materials

The LED chip emits 475 ~ 680nm white light, which is equivalent to passing through a dielectric layer when passing through the anti-reflection film. By changing the thickness and refractive index of the film, the interference can be reduced, thus producing the anti-reflection effect and enhancing the light transmission [18]. In this paper, we choose the transparent medium PMMA ( $n=1.5@ \lambda=580 \text{ nm}$ ) is used for the anti-reflection film. In terms of actual processing and fabrication, this material is easy to make embossed templates, which can reduce the processing process difficulty of the whole structure.

The sandwich metal-dielectric gratings are an important part to realize the non-polarization state conversion of white LEDs, which is combined by metal grating and dielectric grating in turn, and the selection of grating material will affect the polarization performance of the overall structure. Considering the material integration cost and experimental difficulty, PMMA is also selected as the dielectric material of the sandwich metal-dielectric gratings. Since the LED chip emits 475-680nm visible light, we respectively compared the polarization performance of the sandwich gratings structure of gold, silver, copper, aluminum and PMMA. The polarization

transmittance and extinction ratio (ER) of the four metal materials with PMMA grating are shown in Fig. 2(a) and (b). Other structure parameters are period  $P=200\text{nm}$ , duty cycle  $DC=0.5$ , height difference of dielectric and metal grating  $h=20\text{nm}$ , thickness  $d=45\text{nm}$ .

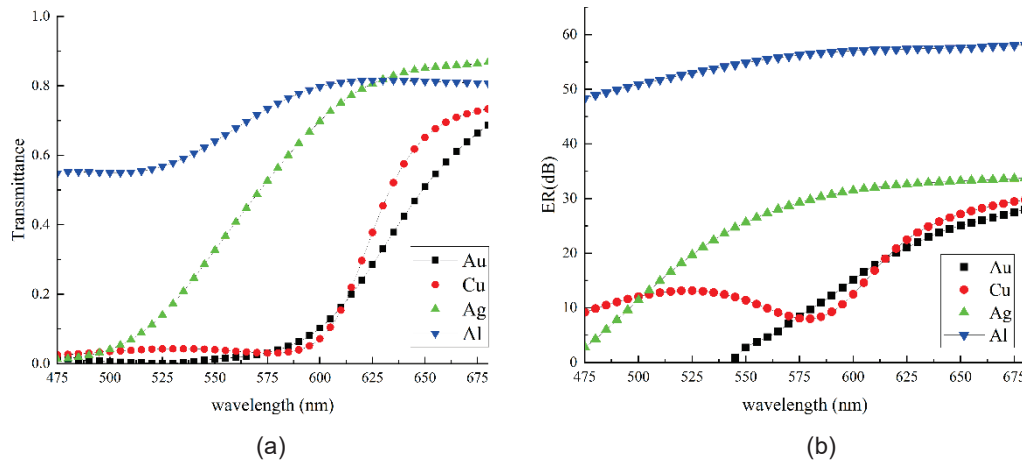


Figure 2. Transmittance and extinction ratio of Al, Ag, Au, Cu gratings at 450-750 nm: (a) transmittance (b) extinction ratio (ER)

As can be seen from Fig. 2(a), the transmittance of metals Cu and Au is less than 0.1, and the transmittance of metal Ag in the blue-green band is improved, but also as low as 0.5 in the 475-600nm band. In contrast, only metal Al maintain transmittance of more than 55% in the visible range and more than 80% at 475-680nm. Fig. 2(b) shows the trend of extinction ratio of four kinds of metal materials in the visible band. The ER of metal Al is greater than 40 dB in the whole band, while the ER of the other three metals can reach up to 30dB. In summary, Al is selected as a suitable metal grating material.

#### 4. Optimization of Structural parameters

##### 4.1 Optimization of the sandwich metal-dielectric gratings structure

Under the condition that the material of the sandwich gratings structure is Al and PMMA, the grating period and linewidth are set to 200nm and 100nm respectively. Fig. 3 shows the effect of height difference  $h$  on the polarization performance of the designed structure in the range of 475 ~ 680nm: (a) transmittance and (b) extinction ratio (ER). It can be clearly seen that at a height difference of about 20 nm, the transmittance can reach a maximum of 0.81, and the ER is generally higher than 47dB. Of course, as can be seen from Fig. 3(a), the height difference  $h = 0 \sim 20$  nm, with the increase of wavelength, the highest value of transmittance shifts to the right; The height difference  $h$  varies in the range of 20 ~ 100 nm, and the smaller the maximum transmittance value, the more left, which can be caused by the resonance enhancement effect of the class F-P cavity at a specific wavelength [19-20]. It can be seen from Fig. 3(b) that ER decreases continuously in the whole band as the height difference  $h$  increases. Therefore, it can be determined that better polarization effect can be obtained when the height difference  $h=20\text{nm}$ .



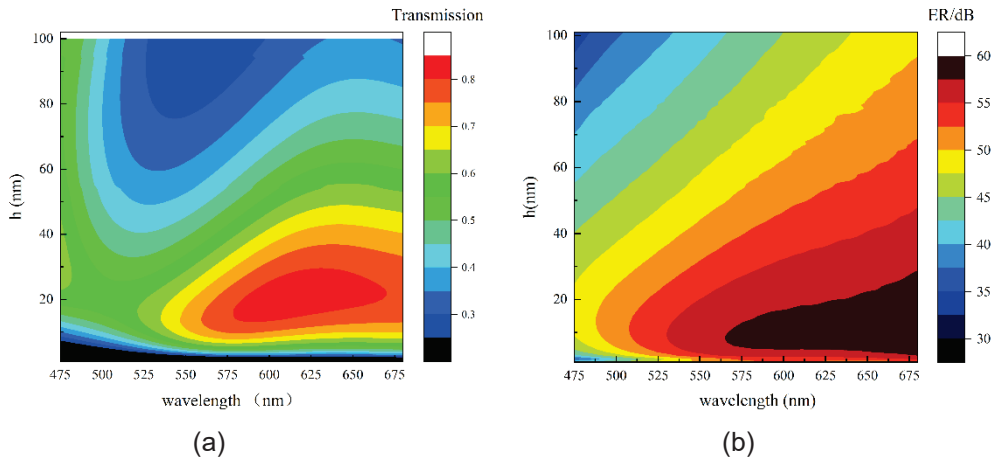


Figure 3. Effect of the height difference ( $h$ ) on the structural transmittance (a) and extinction ratio (b)

#### 4.2 Optimization of the thickness of the anti-reflection film

As can be seen from Section 3, the material of anti-reflection film is PMMA, the thickness of which directly affects the effect of the transmittance in the whole structure. Usually, the thickness of the film is selected based on the principle of thin film interference, so that the light waves reflected on the upper and lower sides of the film are exactly equal to half a wavelength difference, they can cancel each other to reduce the reflection. Fig. 4 show the transmittance of polarized white LEDs from 475 nm to 680nm at different thicknesses ( $d$ ) shown in Figure 2, respectively, with other structural parameters of  $P=200$  nm,  $W=100$  nm, and  $h=20$  nm.

It can be seen from Fig. 4(a) that with the increase of the anti-reflection film layer, the transmittance increases significantly in a certain range. When the thickness ( $d$ ) is from 0 ~ 40 nm, the transmittance increases from the maximum 0.65 to 0.8. While the thickness exceeds 40nm, bands with transmittance below 0.5 gradually increase in the proportion of the whole band. Fig. 4(b) shows the effect of 0 ~ 60 nm thickness  $d$  on extinction ratio in the wavelength range of 475 ~ 680 nm. When the thickness is 0 ~ 40nm, the change trend of ER is not obvious, but when the thickness is greater than 40nm, ER will show a larger band at 625 ~ 680nm. Combined with Fig. 4(a), we choose 40nm as the optimal thickness.

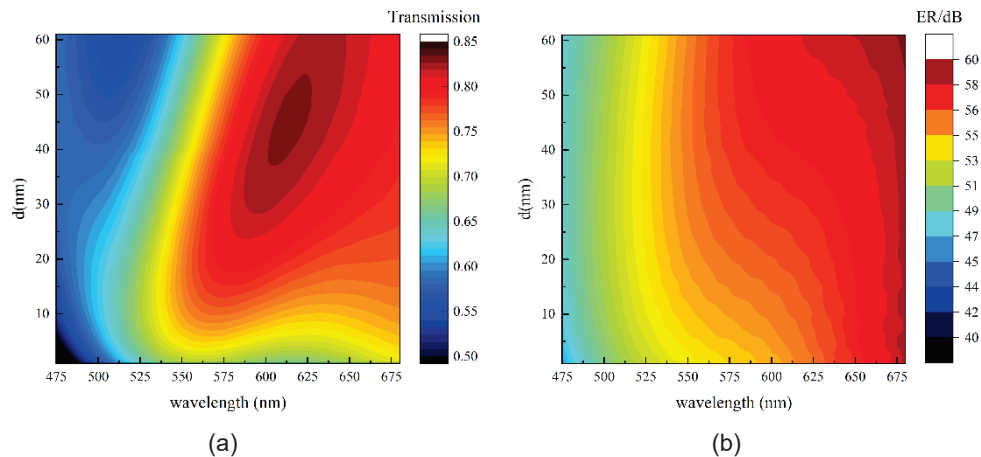


Figure 4. Effect of the thickness of the anti-reflection film on the structural transmittance (a) and extinction ratio (b)

#### 5. Conclusion

Through the above optimization analysis, a sandwich metal-dielectric gratings structure composed of metal Al and PMMA dielectric materials is integrated on the white LED chip, and an anti-reflection film with a thickness of 40nm is inserted between the two, and finally a polarized light transmittance of up to 83% and 61dB can be obtained. This polarized white LEDs not only

has high transmittance, but also has a high extinction ratio, which provides a new design scheme for the illumination of precision instruments such as polarizing microscopes.

## REFERENCE

- [1] Zhou Jialing, He Honghui, Chen Zhenhua, et al. Modulus design multiwavelength polarization microscope for transmission Mueller matrix imaging.[J]. Journal of biomedical optics, 2018, 23(1):1-8.
- [2] Ashraf El-Meanawy, Christopher Mueller, Kenneth A. Iczkowski, et al. Improving sensitivity of amyloid detection by Congo red stain by using polarizing microscope and avoiding pitfalls.[J]. Diagnostic Pathology, 2019, 14(1):1-7.
- [3] Lam Van K, Phan Thuc, Ly Khanh, et al. Dual-modality digital holographic and polarization microscope to quantify phase and birefringence signals in biospecimens with a complex microstructure.[J]. Biomedical optics express, 2022, 13(2):805-823.
- [4] Ivanov Ivan E, Yeh LiHao, PerezBermejo Juan A, et al. Correlative imaging of the spatio-angular dynamics of biological systems with multimodal instant polarization microscope.[J]. Biomedical optics express, 2022, 13(5):3102-3119.
- [5] Chen Yi, Dong Yang, Si Lu, et al. Dual Polarization Modality Fusion Network for Assisting Pathological Diagnosis. [J]. IEEE transactions on medical imaging, 2022.
- [6] Dong Yang, Wan Jiachen, Wang Xingjian, et al. A Polarization-Imaging-Based Machine Learning Framework for Quantitative Pathological Diagnosis of Cervical Precancerous Lesions.[J]. IEEE transactions on medical imaging, 2021.
- [7] J. Chang, H. He, Y. Wang, Y. Huang, X. Li, C. He, R. Liao, N. Zeng, S. Liu, and H. Ma, "Division of focal plane polarimeter-based  $3 \times 4$  Mueller matrix microscope: a potential tool for quick diagnosis of human carcinoma tissues," J. Biomed. Opt. 21, 056002, 2016.
- [8] Sean Thompson, Frank Fueten, David Bockus, et al. Mineral identification using artificial neural networks and the rotating polarizer stage[J]. Computers and Geosciences, 2001, 27(9):1081-1089.
- [9] Srivastava AK, Zhang W, Schneider J, et al. Photoaligned nanorod enhancement films with polarized emission for liquid-crystal-display applications. Adv Mater, 2017, 29: 1701091
- [10] Wang X, Wang Y, Gao W, et al. Polarization-sensitive halide perovskites for polarized luminescence and detection: Recent advances and perspectives. Adv Mater, 2021, 33: 2003615.
- [11] Elkhov VA, Ovechkis YN. Light loss reduction of LCD polarized stereoscopic projection. In: Proc. SPIE 5006, Stereoscopic Displays and Virtual Reality Systems X, Santa Clara, CA, 2003, 45–48.
- [12] Kanamori Y, Shimono M, Hane K. Fabrication of transmission color filters using silicon subwavelength gratings on quartz substrates. IEEE Photon Technol Lett, 2006, 18: 2126–2128.
- [13] J. Wang, Y. Zhao, I. Agha, and A. M. Sarangan, "SU-8 nanoimprint fabrication of wire-grid polarizers using deep-UV interference lithography," Opt. Lett. 2015, 40, 4396–4399.
- [14] Tian Shuoqiu, Liu Tao, Pan Xiaohang, et al. Study of structural effects on the polarization characteristics of subwavelength metallic gratings in short infrared wavelengths.[J]. Optics express, 2022, 30(26):47983-47991.
- [15] Khonina S N, Kazanskiy N L, Butt M A, et al. Spectral characteristics of broad band-rejection filter based on Bragg grating, one-dimensional photonic crystal, and subwavelength grating waveguide[J]. Physica Scripta, 2021, 96(5):055505-.
- [16] A. Liu, F. Fu, Y. Wang, B. Jiang, and W. Zheng, "Polarization insensitive subwavelength grating reflector based on a semiconductor-insulator-metal structure," Opt. Express. 2012, 20, 14991–15000.
- [17] Mohsen Salehi, Nosrat Granpayeh. Numerical solution of the Schrödinger equation in polar coordinates using the finite-difference time-domain method [J]. Journal of Computational Electronics, 2020, 19(1):91-102.
- [18] Shieh, YN. Improve the Properties of Anti-reflective Film by Silica Nano Solution. In: Shen, J., Chang, YC. Su, YS. Ogata, H. (eds) Cognitive Cities. IC3 2019. Communications in Computer and Information Science, 2020, vol 1227.
- [19] Hwang, J., Oh, B., Kim, Y. et al. Fabry-Perot cavity resonance enabling highly polarization-sensitive double-layer gold grating. Sci Rep, 2018, 8, 14787.
- [20] Chang-Lin Wu, Chun-Hway Hsueh, and Jia-Han Li, "Surface plasmons excited by multiple layer grating," Opt. Express 2019, 27, 1660-1671

Corresponding Author Name: Yahong Li, Nianyu Zou

Affiliation: Research Institute of Photonics, Dalian Polytechnic University, Dalian 116034, China

e-mail: liyahong@dlpu.edu.cn, n\_y\_zou@dlpu.edu.cn

## AN ANALISYS OF VERTIPTS LIGHTING TREND IN THE URBAN AIR MOBILITY

Hyunyoung Lee, Jongbin Park, Hojune Bae, Kyeongsik Kim, Jonghyun Han

(Green Energy Division, KIEL Institute, Korea)

### ABSTRACT

Urban Air Mobility (UAM) has recently emerged as a three-dimensional future transportation to solve urban population growth, road traffic congestion and environmental problems. Urban Air Mobility refers to a public transportation system that moves through urban areas using electrically powered vertical take off and landing aircraft (eVTOL). In the past, it remained at the level of aircraft design, but it is increasingly likely to be realized in the near future thanks to the development of eVTOL-based technologies such as distributed electricity propulsion, electric power, and low-noise technology.

Korea has recently announced a "K-UAM" roadmaps and technology roadmaps to prepare strategies. As most PAVs are currently being developed as eVTOLs, it is necessary to establish a Vertiports infrastructure, which is a small take-off and landing space like a heliport of an existing helicopter, rather than a large take-off and landing space like an airport with a runway. Therefore, it is recognized that eVTOL vertiports needs to establish visual information lighting facilities to ensure safety when the aircraft moves to the take-off and landing area in the city center and to move to the airside area. This paper analyzed the development trends, types, and specification of vertiports lighting for the safe establishment of an UAM infrastructure.

Keywords: urban air mobility, approach path indicator, touchdown & lift-off area lighting, system taxiway edge lights

### 1. INTRODUCTION

The size of the UAM market is expected to grow to about \$10.9 billion by 2040. The UAM aircraft market is expected to grow from \$32.92 million in 2025 to about \$1 billion by 2040 and 24% annually, the infrastructure market is expected to grow from \$20.6 million in 2025 to about \$1.7 billion by 2040 and 30% annually, and the service market is expected to grow from \$160 million in 2025 to about \$8.2 billion by 2040, with an average annual growth rate of 27% in Korea.[1]

One of the essential element for spreading the UAM ecosystem is infrastructure construction. As most PAVs are currently being developed as eVTOLs, it is necessary to establish a vertiport infrastructure, which is a small take-off and landing space like a heliport of an existing helicopter, rather than a large take-off and landing space like an airport with a runway. As a result, take-off and landing site infrastructure companies around the world are conducting concept research and design to create a UAM ecosystem, and basic design for Vertiport, like Skyports in the UK, and Hyundai Motor in Korea also proposed a hub concept that forms an integrated mobility ecosystem as shown in figure 1.[2]



Figure 1. Vertiport concept (Skyports\_(L), Hyundai Motor\_(R))


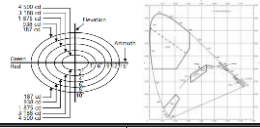


## 2. Experimental & Conclusion

### 2.1 Type of vertiport lighting

Unlike Helipad-based intermittent operation helicopters, which are similar to helicopters, eVTOL requires separate standards due to different infrastructures such as high frequency of take-off and landing use and charging. Lights such as Heliport Approach Path Indicator, Final Approach & Take-off Area Lights [F.A.T.O], Touchdown & Lift-off Area Lighting System [T.L.O.F], etc. shall be installed in the heliport, in accordance with the standards of the Ministry of Land, Infrastructure and Transport Republic of Korea.[3]

It is recognized that eVTOL Vertiport needs to establish visual information lighting facilities to secure safety when the aircraft approaches the take-off and landing site in the city center and moves to the airside area. The types of lights are shown in table 1.[4]

**Table 1. Type of vertiport lighting**

Type of vertiport lighting	Design	Purpose	Optical Characteristics												
Approach Path Indicator		Lights installed to inform the eVTOL to be landing whether the angle of entry is appropriate (green, red)													
Touchdown & Lift- off Area Lighting System		Lights installed to illuminate the landing area (green)	<table><thead><tr><th>angle</th><th>intensity (green)</th></tr></thead><tbody><tr><td>20° ~ 90°</td><td>3 cd</td></tr><tr><td>13° ~ 20°</td><td>8 cd</td></tr><tr><td>10° ~ 13°</td><td>15 cd</td></tr><tr><td>5° ~ 10°</td><td>30 cd</td></tr><tr><td>2° ~ 5°</td><td>15 cd</td></tr></tbody></table>	angle	intensity (green)	20° ~ 90°	3 cd	13° ~ 20°	8 cd	10° ~ 13°	15 cd	5° ~ 10°	30 cd	2° ~ 5°	15 cd
angle	intensity (green)														
20° ~ 90°	3 cd														
13° ~ 20°	8 cd														
10° ~ 13°	15 cd														
5° ~ 10°	30 cd														
2° ~ 5°	15 cd														
Taxiway Edge Lights		Lights installed by eVTOL aircraft running on the ground to inform the edge of taxiway atmospheric areas or moorings (green)	At least 2 cd from the horizontal plane up to 6 °C and 0.2 cd from 6 °C and up to 75 °C												

### 2.2 Vertiport lighting measurement

Vertiport lighting were measured based on ICAO and FAA. The standards for vertiport lights are shown in Table 2. [3]~[5]

**Table 2. Standards of vertiport lighting**

	Standard
MOLIT	Standards for Aeronautical Lights, Signs and Electrical Systems
ICAO	Annex14, Volume I : Aerodromes Design And Operations Annex14, Volume II : Heliports Aerodrome design manual(DOC 9157) : Part 4: Visual Aids, Part 5: Electrical Systems, Part 6: Frangibility
FAA	AC 150/5340-26: Maintenance of Airport Visual Facilities AC 150/5345-30: Design And Installation Details For Airport Visual Aids AC 150/5345 Series: Specification of Airfield Lighting Equipment

### 2.3 CONCLUSION

As a result of the UAM trend analysis, the necessity, type, and related standards of UAM Vertiport lights were found. Based on these results, in the next step, it is necessary to study the establishment of standards for the lights UAM Vertiport lights.

### REFERENCES

- [1] Analysis of Drones Taxi Market, KIAST, 2020
- [2] K-UAM Technology Roadmap, KAIA, 2021.06
- [3] Standards for Aeronautical Lights, Signs and Electrical Systems, MINISTRY OF LAND, INFRASTRUCTURE AND TRANSPORT REPUBLIC OF KOREA
- [4] ICAO (International Civil Aviation Organization)
- [5] FAA (Federal Aviation Administration)

Corresponding Author name: Hyunyoung Lee

Affiliation: KIEL Institute

e-mail : cess517@kiel.re.kr



# A Study on the Standards for Installation Sites of Street Lighting on Expressways

Gi-Hoon, Kim<sup>1</sup>

(<sup>1</sup>Korea Expressway Corporation Research Institute, Gyeonggi-do, Korea )

## ABSTRACT

In this paper, “places where the road width and road alignment change rapidly”, “places with high frequency of traffic accidents”, and “places requiring local lighting in cases other than the above” that have not been clarified and specified in the existing standards. For the first place to be installed was selected. In the future, it will be necessary to examine how much nighttime traffic accidents actually decreased in those places when street lighting was installed by applying these standards.

Keywords: Street Lighting, Installation Sites, Standards, Expressways

## 1. INTRODUCTION

Currently, about 2,000 number of night traffic accidents occur annually, and the fatal accident rate is about 2.4 times higher than the daytime traffic accident rate. The effect of installing road lighting has already been investigated as a reduction rate of night traffic accidents after installing road lighting in a previous study, which was 57% in France and 56% in Japan [1]. In this way, the most effective way to prevent traffic accidents at night is to install road lighting, but it is practically difficult to apply it to all highway sections in various aspects such as budget and manpower. Therefore, in this study, the criteria for the installation location of road lighting were investigated, and other criteria were applied mutatis mutandis for clear and unspecified places to prepare clear criteria.

## 2. BODY

Table 1 below summarizes the current standards for street lamp installation locations. Looking at Table 1, local lighting is divided into mandatory installation places and necessary installation places.

Table 1. Standards for Installation Sites of Street Lighting

Lighting Method	Installation Site	Installation Status
Local Lighting	○ Compulsory installation - Overpass, Toll Booth, Resting Area	- All Installation
	○ Install if necessary - Bridges, Bus stops - Sudden Change in Road Alignment - A Place with a High Frequency of Traffic Accidents - In Addition to the Above, Places Where Local Lighting is Required	- Installation - Not Installed - Not Installed - Not Installed
Continuous Lighting	- Lights Around the Road to Road Traffic Affected Urban Area - Extension Length between IC, Rest Areas, Tunnels, etc. is Section within 1km - Special Needs for Continuous Lighting Situational Section	- All Installation - All Installation - All Installation

Table 2 below shows the place to be installed first for the standards in the existing street light installation place in the current local lighting method, the basis for selecting the place, and the applicable standards.

Table 2. Priority Installation Sites of Street Lighting

Lighting Method	Installation Site (Existing)	Preferred Installation Site Proposal (Draft)
Local Lighting	Road Width, Road Alignment Fast-Changing Place	In the Uphill Section, Annual Average Mixing Rate of Large Cars 25% <sup>1)</sup> More Than One Section
	The Frequency of Traffic Accidents High Place	Accidents at Night in the Last 3 Years 3 Cases/500m <sup>2)</sup> or More, Night/Day Accident Rate 2.0 or Higher <sup>3)</sup> Section
	In Cases Other Than the Above Need Local Lighting Place to Do	Wildlife Accidents in the Last 3 Years 5 cases/km <sup>4)</sup> or more
Mutatis Mutandis Standard	1) "Road Tunnel Disaster Prevention and Ventilation Facility Installation and Management Guidelines" (Ministry of Land, Infrastructure and Transport), Road tunnel disaster prevention rating risk index evaluation criteria → Mixing rate of large vehicles If it is 25% or more, the maximum risk index (2.0) is given 2) "Accident Frequently Improvement Project Handbook" (Ministry of Construction and Transportation), Criteria for selecting places with frequent accidents → In the case of highways, 3 cases are applied 3) US AASHTO street light installation location standard → night/day Installation of streetlights with an accident rate of 2.0 or higher 4) "Establishment of measures to reduce animal road accidents in 2022" (Ministry of Land, Infrastructure and Transport, Ministry of Environment), Criteria for class selection of sections with frequent wild animal road accidents → 5 cases/km (road kill grade 5 or higher) applied	

### 3. CONCLUSION

In this paper, "places where the road width and road alignment change rapidly", "places with high frequency of traffic accidents", and "places requiring local lighting in cases other than the above" that have not been clarified and specified in the existing standards. For the first place to be installed was selected. In the future, it will be necessary to examine how much night time traffic accidents actually decreased in those places when streetlights were installed by applying these standards. In addition, it is judged that night time traffic accidents can be reduced a little by preemptively installing streetlights as a standard for additional installation of streetlights.

### REFERENCE

- (1) Korea Road Traffic Authority, Countermeasures to prevent traffic accidents at night, 2000

### ACKNOWLEDGEMENT

Corresponding Author: Gi-Hoon, Kim  
 Affiliation: Korea Expressway Corporation Research Institute  
 e-mail: gihoonkim@ex.co.kr

# Analysis of the Causes and Facilities of Highway Traffic Accident Multiple Occurrence Section

Gi-Hoon, Kim<sup>1</sup>

(<sup>1</sup>Korea Expressway Corporation Research Institute, Gyeonggi-do, Korea )

## ABSTRACT

In this paper, the correlation with traffic accidents was studied by analyzing the causes of accidents and the statistics of facilities in the section where the majority of highway night traffic accidents occurred. According to the '2021 Traffic Accident Statistical Analysis' report released by the Korea Road Traffic Authority, the number of highway traffic accidents in 2020 was 13,859, accounting for 1.1% of all traffic accidents (1,247,623 cases), but the death rate due to highway traffic accidents is the total number of fatalities. 7.2% of the total, the ratio of fatalities to number of accidents appears to be high. In addition, the fatality rate of traffic accidents occurring at night is 4% during the day and 8% at night, and the fatality rate of traffic accidents at night is more than twice as high. appear large. we tried to derive a correlation with traffic accidents by analyzing the causes of accidents and facility statistics in the section where many night traffic accidents occurred on highways.

Keywords: Traffic Accident, Multiple Occurrence Section, Facilities of Highway

## 1. INTRODUCTION

According to the '2021 Traffic Accident Statistical Analysis' report released by the Korea Road Traffic Authority, the number of highway traffic accidents in 2020 was 13,859, accounting for 1.1% of all traffic accidents (1,247,623 cases), but the death rate due to highway traffic accidents is the total number of fatalities. 7.2% of the total, the ratio of fatalities to number of accidents appears to be high. In addition, the fatality rate of traffic accidents occurring at night is 4% during the day and 8% at night, and the fatality rate of traffic accidents at night is more than twice as high. appear large. In this paper, we tried to derive a correlation with traffic accidents by analysing the causes of accidents and facility statistics in the section where many night traffic accidents occurred on highways.

## 2. BODY

### 2.1 How to derive the section where the majority of highway traffic accidents occur

For accidents that occurred on the highway, the Korea Expressway Corporation converts basic information such as the date and time of the accident, the location of the accident, and data such as the degree and grade of the accident, the cause of the accident, and the details of the accident in 100m increments along the entire highway route. Based on the accident data recorded in the basic 100m section for the last 3 years, the section is extended to 500m and accumulated, and in the case of driver and vehicle factors, it is an accident caused by reduced visibility at night and the influence of road facilities existing at the location of the accident. Because it is difficult to see, the analysis of accident data reflected only accidents (4,375 cases) caused by other factors.

Table 1. Analysis of detailed causes of accidents by other factors

Division	Total	Road Surface rubbish	Road Circumstances	Animal Invasion	Unauthorized Walking	Load Error	Pothole	Cause Unknown
Number of Accidents (cases)	4,375	2,087	165	248	30	235	1,107	503
Rate(%)	100	47.7	3.8	5.7	0.7	5.4	25.3	11.5

## 2.2 Expressway Road Facility Survey

Road facilities existing in the section where many accidents occurred were confirmed through review through Road View, existence of facilities and structures whose current state of facilities is identified in units of miles in the current road construction. If there are two or more overlapping facilities at the point where the accident occurred, such as when a soundproof wall is installed on a bridge or a cut out is located in an IC/JC section, 0.5 points are counted according to the number of overlapping facilities, and 0.33 points when three or more points are overlapped. The number of facilities was applied.

○ Road facility investigation items in the section with the most cumulative accidents

- Existence of streetlights, junction roads (IC/JC, service areas, sleepy shelters), uphill lanes, cuts, over vertical alignment  $\pm 3\%$ , over vertical alignment  $\pm 5\%$ , bridges, tunnels, sound barriers, traffic volume

## 2.3 Analysis of causes of accidents in the upper section of the number of accidents at night and facilities within the section

A total of 59 accidents occurred in 30 sections in order of the number of night accidents per 1,000 vehicles in traffic volume, of which 50 occurred at night. As for the causes of accidents at night, road debris was the highest at 38.0%, and accidents caused by animal intrusion accounted for 30% (15 cases). Accidents caused by road debris and animal intrusion can all be seen as accidents caused by failure to recognize obstacles that suddenly appeared on the road at night on expressways, and it is judged that the possibility of accidents due to these causes is high in sections with low traffic volume. do. In the top 30 sections, there are many sections with low traffic volume, such as the Namhae Line, Gwangju-Daegu Line, and Donghae Line.

As for facilities, the ratio of branch and junction roads with streetlights installed, roads in front and rear of branch and junction roads, and roads in front and rear of tunnels decreased slightly, while the ratios of cut sections and bridge sections with relatively low installation ratios of streetlights increased. The cutting part and the bridge are facilities where the installation of streetlights is not regulated or partially regulated in the current guidelines.

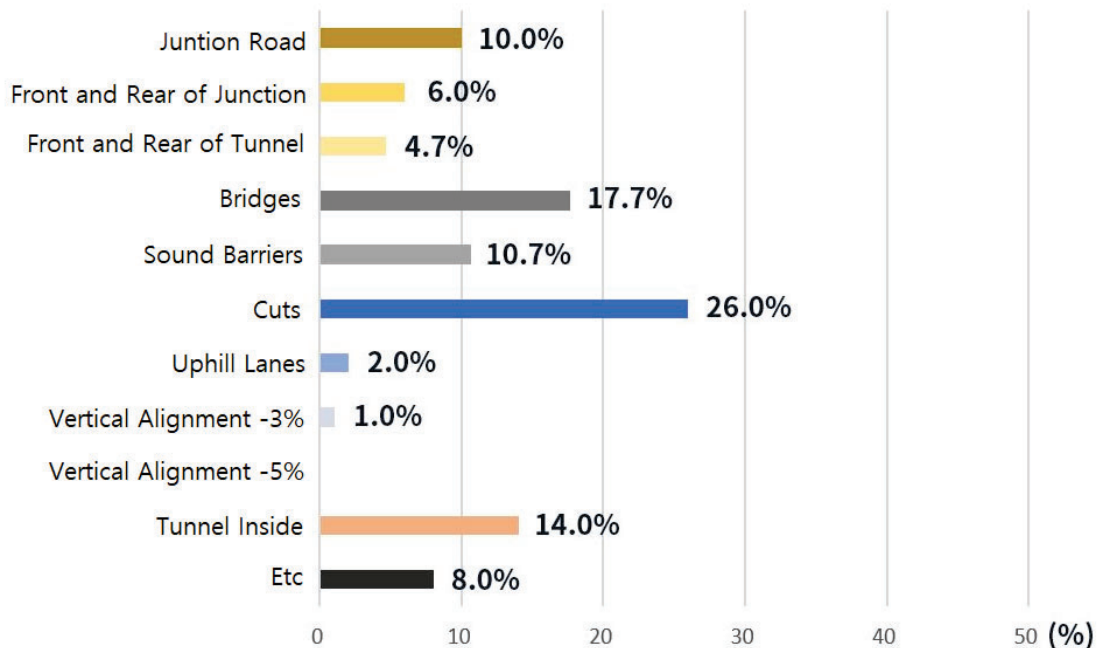


Fig. 1. Distribution of facilities in the top 30 sections

### **3. CONCLUSION**

According to the Ministry of Land, Infrastructure and Transport's Road Safety Facility Installation and Management Guidelines, the accident rate of cuts, sound barriers, and linear deformation sections classified as facilities without street lights is 39.7%. It was higher than the accident rate of 32.7%. Considering that 43% of bridges do not have streetlights installed and that no streetlights are installed in the "no facilities" section classified as other facilities, the difference in traffic accident rates in places where streetlights are not installed at night increases.

### **REFERENCE**

- (1) Road Traffic Authority, 2021 edition (2020 statistics) traffic accident statistical analysis, 2021
- (2) Gi-Hoon Kim, Deduction of risk factors for accidents at night through highway accident data, Proceedings of the Korean Society of Lighting and Electrical Equipment Conference, 2022

### **ACKNOWLEDGEMENT**

Corresponding Author: Gi-Hoon, Kim  
Affiliation: Korea Expressway Corporation Research Institute  
e-mail: gihoonkim@ex.co.kr



# Comparative Study On the Lighting Effect of Tunnel Interior Materials Conditions

Gi-Hoon, Kim<sup>1</sup>

(<sup>1</sup>Korea Expressway Corporation Research Institute, Gyeonggi-do, Korea )

## ABSTRACT

In order to compare the reflection characteristics due to contamination by interior material conditions, the reflection characteristics before contamination using a specimen were compared, and the lighting effect was compared by reflecting the results. the specimen is contaminated step by step to find a change in its reflection characteristics, and the lighting effect is compared by reflecting the results.

Keywords: Lighting Effect, Tunnel, Interior Materials, Conditions

## 1. INTRODUCTION

The tunnel wall requires the same brightness as the road surface to provide a safe visual environment and driving stability. In addition, the optical performance of the tunnel is a very important part for tunnel safety and energy saving. In this study, we try to find a safer and more economical tunnel interior material by finding the reflective characteristics of each type of interior material and comparing and analysing the lighting effect through computer simulation. However, the content of this study presupposes that the results may be limited because only the reflection characteristics of the specimens, not the site of the tunnel, were compared.

## 2. BODY

In order to compare the lighting effect according to the reflective characteristics of each type of interior material installed in the tunnel, samples were provided from the manufacturer for each type of interior material, and first, the reflective characteristics of the type of tunnel interior material were measured, and second, the measured reflective characteristics were reflected to the interior material. I tried to compare and evaluate the lighting effects of each type with computer simulation.

### 2.1 Measurement and analysis of reflective characteristics by type of interior material

Reflection characteristics such as Reflect (total reflectance), Specularity (highlight of reflected light), and Roughness (surface roughness) of BRDF (bidirectional reflectance distribution function) were derived using the specimens provided by each interior material and manufacturer using LightTec's MiniDiff optical characteristics equipment.

Table 1. Measured values of reflection characteristics of interior material specimens

Division		Paint			Tile		
Sample		1	2	3	4	5	6
Adhesive Surface		Iron Plate	Iron Plate	Pseudo-Concrete	-	-	-
Total Reflectivity		72.1	74.2	75.6	64.3	55.1	59.8
Surface Finish	Specularity	0.18	0.19	0.16	0.14	0.23	0.21
	Roughness	0.049	0.049	0.049	0.049	0.049	0.049

Perhaps because it is a specimen, the initial reflection characteristic value of the paint is somewhat higher than that of the tile, and it is expected that there will be some differences from the actual site because the roughness of both the paint and the tile is the same, perhaps because of the limitations of the measurement by the specimen, not the field. . For the reflection characteristics of specimens by interior material condition, only the reflection characteristics of specimen No. 3 painted on a material similar to concrete are reflected as lighting effect data in the case of painting among a total of six specimens, and in the case of tiles, specimen No.4 with the highest reflection characteristics Reflection characteristics were reflected as data

## 2.2 Computer simulation

The evaluation program by computer simulation uses Relux 2016.1.1.0, and based on the Korea Expressway Corporation tunnel standard section, the reflection measurement result value of the provided specimen and the Korea Expressway Corporation standard lighting fixture light distribution are applied to illuminate the basic part of the tunnel The lighting effect was compared with the road surface luminance and wall luminance values.

Table 2. Simulation results reflecting specimen measurement results

Luminance(cd/m <sup>2</sup> )	Luminance Standard	Paint(Sample 3)		Tile(Sample 4)	
Average Road Surface Luminance	9	10.28		10.25	
Wall Luminance	Average Road Surface Luminance 100% or More	Left	Right	Left	Right
		20.02	22.09	17.27	19.07

As shown in Table 2, in the lighting effect by computer simulation, the reflectance of the interior material affected the luminance of the wall, but did not significantly affect the luminance of the road surface. Since the wall luminance of the tunnel lighting is provided at 100% or more of the average road surface luminance, the reflective characteristics of the interior materials are expected to be helpful in energy saving of the tunnel lighting.

## 3. CONCLUSION

In Korea, two types of interior materials, tile and paint, are used as interior materials for tunnel walls. Specimens were provided from the manufacturers of tunnel interior materials, and although there were some differences between manufacturers in terms of reflectance between tiles and painting, overall, the coating was slightly higher. As a result of comparing the lighting effects through computer simulation by reflecting the results, it was confirmed that the effect of the reflection characteristics of the interior materials on the road surface luminance was insignificant, and the wall luminance increased in proportion to the reflectance. However, since this study compared the reflection characteristics of the specimens, it is expected that there will be some differences from the actual field.

Lighting accounts for 60% of maintenance costs in tunnels. Therefore, it is believed that research on interior materials that can increase the lighting effect should be continuously prepared. It is important to develop materials for tunnel interior materials that can increase the lighting effect, but it is also necessary to study tunnel maintenance for 2,742 tunnels currently installed in Korea (as of 2020 by the Ministry of Land, Infrastructure and Transport) [2]. Therefore, in order to find out more about the characteristics of interior materials in the future, the reflection characteristics of interior materials in tunnels before construction or tunnels in operation are searched, and the trend of changes in lighting effects is studied to determine factors that can increase lighting effects. I think there should be an effort to find a way to find it.

## REFERENCE

(1) Molit Statistics System, Road Bridge and Tunnel Statistics, 2020

## ACKNOWLEDGEMENT

Corresponding Author: Gi-Hoon, Kim  
Affiliation: Korea Expressway Corporation Research Institute  
e-mail: gihoonkim@ex.co.kr

# Investigation of the Driving Environment in the Section with Frequent Accidents at Night on Highways

Gi-Hoon, Kim<sup>1</sup>

(<sup>1</sup>Korea Expressway Corporation Research Institute, Gyeonggi-do, Korea )

## ABSTRACT

In this paper, the driving environment was analyzed based on the survey on the risk section of night accidents shown through accident data analysis. As a result of analyzing highway traffic accident data in 2020, night traffic accidents on highways account for a low percentage of all traffic accidents (1.9%), but the ratio of fatalities to the number of accidents is very high (8%). In previous studies, road traffic accident data was analyzed to analyze the risk factors of nighttime traffic accidents. In this study, we tried to analyze the risk factors of the night driving environment through the fact-finding investigation of the risk zone of night accidents that appeared through the analysis of accident data

Keywords: Driving Environment, Frequent Accidents, Night, Highways

## 1. INTRODUCTION

As a result of analysing highway traffic accident data in 2020, night traffic accidents on highways account for a low percentage of all traffic accidents (1.9%), but the ratio of fatalities to the number of accidents is very high (8%). In previous studies, road traffic accident data was analysed to analyse the risk factors of night time traffic accidents. In this study, we tried to analyse the risk factors of the night driving environment through the fact-finding investigation of the risk zone of night accidents that appeared through the analysis of accident data.

## 2. BODY

### 2.1 Highway Night Accident Risk Factors and Night Accident Risk Zone

By analysing highway accident data for 3 years from 2019 to 2021, the rankings were derived: 'sections with a high number of night traffic accidents', 'sections with a high number of night traffic accidents compared to traffic volume', and 'sections with a high rate of night traffic accidents compared to daytime'. Among the sections, 22 locations were selected according to the classification of road facilities (mountain cuts, ICs, JCs, bridges, curves, uphill/downhill, soundproof walls) and presence or absence of street lights.

### 2.2 Investigation Method for Night Accident Risk Zone

The highway night fact-finding survey investigated the road surface and the surrounding environment that affect drivers while driving on the highway. Data were collected by installing a camera for recording the situation in front of the driver's field of vision and a video luminance meter for measuring the luminance of the road surface and surrounding lighting environment inside the vehicle. Road surface recognition and high luminance generation factors (road structure, headlights of opposite vehicles, ambient luminance, etc.)



Fig. 1. Installation of a Camera Inside a Vehicle for a Survey

### 2.3 Night Accident Risk Zone Investigation Characteristics Analysis

Drivers are in a dark adaptation state in sections of the main road where no lighting is installed, and high luminance factors entering the field of vision while driving can act as risk factors that can cause an instantaneous increase in adaptation luminance and inability to glare.

In the highway night driving environment, the measured luminance of the light emitting surface of street lights is distributed as high as  $5,000\text{cd/m}^2$ , but the light emitting area is small, and considering the angle with the line of sight at the point of maximum luminance of the light emitting surface, the effect during driving is expected to be lower than the measured luminance value. judged The surface luminance of advertising lighting and decorative lighting can be significantly higher than the measured luminance value when considering the area occupied within the field of view.

In most cases, the headlights of the opposite vehicle are not exposed to the driver's field of view due to the existence of the median divider. The luminance of the low-beam headlight of the opposite vehicle was measured at  $6,791\text{--}8,886\text{cd/m}^2$ , and the luminance of the high-beam headlamp was measured at  $7,837\text{--}10,800\text{cd/m}^2$ . This luminance distribution can be considered to be very high considering the general distribution ( $500$  to  $2,000\text{cd/m}^2$ ) of luminance exposed to other environmental elements.



Fig. 2. Luminance of the Luminous Surface During Night Driving on Highways

### 3. CONCLUSION

Risk factors in the night driving environment were analysed through a fact-finding survey of highway night danger sections, and characteristics of sections with high traffic accidents at night were derived according to the classification of road facilities. It was found that various factors such as the darkness of the road surface and surroundings due to road facilities and the surrounding environment, and the occurrence of glare due to momentary high luminance in the dark adaptation state affect highway driving at night.



Through the analysis of the driving environment in sections with many traffic accidents at night, sections in which the installation of street lights should be reviewed and sections in which the brightness level of the existing street lights needs to be upgraded were derived in the 'Standards for Installing and Operating Street Lights on Highways.

Table 2. Analysis of Driving Environment on Sections with Highway Night Traffic Accidents

Division	Night Driving Environment Analysis
mountain cut through Road	Due to high terrain features (mountain slopes) on the left and right of the driving direction, there is little light entering the road and the road and surroundings are dark
	It is difficult to secure a stopping distance to prevent collision when obstacles such as road debris, potholes, and animal intrusion are found in low-beam driving conditions.
IC·JC·TG	It is a section with a lot of vehicle traffic, and most of the impact accidents are expected to be caused by traffic congestion.
	Despite the installation of streetlights, collisions with obstacles and poor road surfaces (potholes, road surface damage) continue to occur.
Bridge	Vulnerable to natural environment (fog and wind) compared to flat areas, and degraded driving environment (poor visibility and shaking of vehicles)
	Difficulty recognizing drivers at night due to lack of lights on road safety signs such as accidents and slow driving installed on the right side of the driving direction
Curve Section	Headlights of vehicles on the opposite side are recognized instantaneously in sections where uphill and downhill are mixed along hills while passing through mountainous areas.
Uphill· Downhill	Restriction of vision due to glare from headlights on the opposite side Occurrence of accident risk factors
Sound Barrier	High sound barriers block light, making roads and surroundings dark

## REFERENCE

- (1) Gi-Hoon Kim, Assessment of the necessity of installing streetlights in areas with high risk of night time accidents on highways, Proceedings of the Korean Society of Lighting and Electrical Installations Spring Conference, 2022

## ACKNOWLEDGEMENT

Corresponding Author: Gi-Hoon, Kim  
 Affiliation: Korea Expressway Corporation Research Institute  
 e-mail: gihoonkim@ex.co.kr

# RESEARCH ON KITCHEN WORKING SURFACE LIGHTING CONTROL BASED ON MOTION AMPLITUDE DETECTION

Zhide Wang, Mingyu Zhang, Mengyuan Zhang, Shengdong Li  
(School of Architecture, Tianjin University, Tianjin, China)

## ABSTRACT

In this paper, aiming at the problems of low sensitivity, low intelligence and inability to make control decisions independently of the existing mainstream lighting control methods, a new lighting control method is proposed, that is, to control lights by detecting the amplitude of human body movements. The paper begins with a review of research in related fields, including the development of body motion detection and light control techniques. Secondly, taking cooking activities in the kitchen as an example, the changing rules of body movements in different indoor light environments are obtained through experiments, and the body posture of people working under the recommended working face illuminance value is determined. Finally, the control system software was developed and designed to improve the intellectualization and humanization of lighting control. The user satisfaction of the new light control system increased by 23.72%.

Keywords: Motion detection; Interior lighting; Working face illuminance; Lighting control

## 1. INTRODUCTION

Humanized light environment design has gradually been attached importance [1], lighting energy consumption should be saved, and lighting needs to provide sufficient comfort in the light environment [2]. Traditional artificial lighting control methods result in poor illuminance uniformity and high glare value [3], and common residential interior lighting design results in low indoor illuminance value [4]. This makes it difficult to meet the visual needs of modern complex home activities. Intelligent indoor light environment control can greatly improve traditional artificial lighting design [5]. Intelligence has become the development trend of control systems [6], such as intelligent building lighting energy consumption control system [7], and adaptive public lighting control management system [8]. The degree of intelligence in indoor lighting control is now low [9], and the way lighting interacts needs to become more intelligent.

At present, the intelligent degree of indoor light environment control in the user's life and work is insufficient, and the intelligent control cannot judge the current light environment needs from the user's behaviours. To solve this problem and make the light environment can be adjusted properly without the user's perception, this paper will first study the mutual numerical relationship between different light environment and limb movement amplitude in the kitchen; Secondly, the motion amplitude detection system is developed using the obtained relationship, and the motion amplitude detection system is applied to lighting control. Finally, the accuracy of the lighting control system is verified, and the questionnaire evaluation is carried out.

## 2. METHODS

### 2.1 Relationship between light environment and movement

The experiment site was an ordinary family kitchen, and the experiment time started at 20:00 after sunset. The experimental measuring instrument is the T&D TR74-Ui air temperature and humidity illuminance ultraviolet intensity recorder. There are 4 measuring channels, each channel can record 8000 data, and the test accuracy of illuminance is 0.01lx. The lighting equipment is JZTL005M dimmable LED lamps, and the center illumination can reach 750 lx.

The sample size of the experiment was 12 people. In the experiment, dimming LED table lamp was used to set the illuminance value on the operating table surface, and the illuminance meter was used to calibrate it, which was divided into five levels, 100 lx, 200 lx, 300 lx, 400 lx and 500 lx respectively. The subjects carried out fine operations under different illuminance, and the operation time was 10 minutes. The rest time between switching illuminance was 5 minutes. Human posture was measured in the experiment and recorded as the Angle value of the four angles A, B, C and D, as shown in Figure 1.

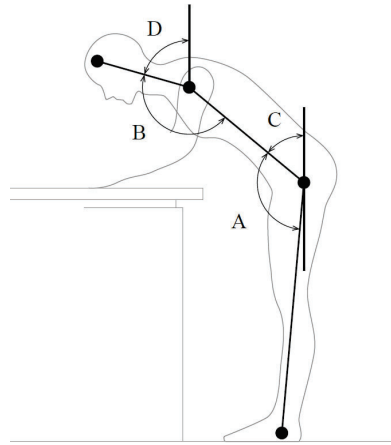


Figure 1. Human movement posture measurement

The curves of the values of each Angle A, B, C and D under different illuminance are shown in Figure 2

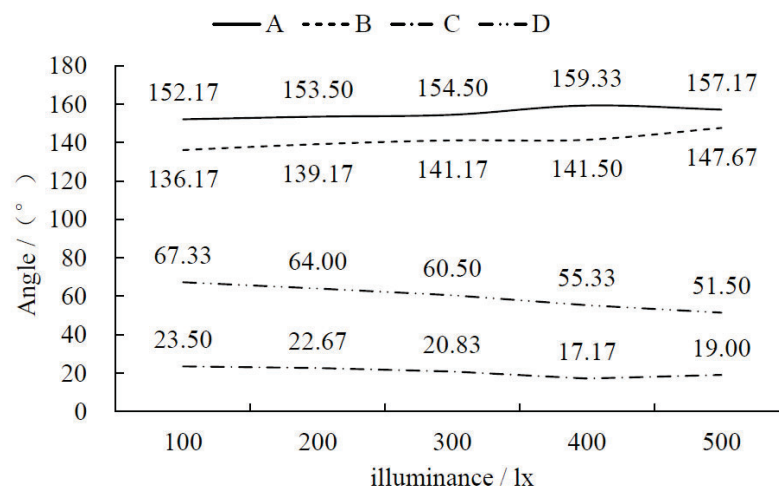


Figure 2. The curves of the values of each Angle A, B, C and D

The relative ranges of the average values of the four angles are 0.21, 0.22, 1.31 and 0.74 respectively, so the values of angles A and B have a smaller range of variation than angles C and D. To establish the numerical relationship between illuminance and action more clearly, the values of Angle C and D are finally selected to represent the amplitude of action.

Thus, an automatic light environment control strategy based on motion changes is obtained: when the upper body tilt Angle is greater than  $20^\circ$ , the illuminance level can be improved, and the head tilt Angle is greater than  $60^\circ$ , the illuminance level needs to be greatly improved. At the same time, set the thresholds of the optical environment adjustment parameters, as shown in Table 1.

Table 1. Parameter threshold of the light environment and scene modes.

Action type	Parameters	Scene modes	Illumination of the working face
Lean forward	$C > 20^\circ$	Working	300 lx
Head down	$D > 60^\circ$	Precision work	500 lx
Squat	$C > 120^\circ$	Finding or pick up	150 lx
Upright	$C < 20^\circ$ & $D < 20^\circ$	Normal	100 lx
Stretch out hands	Distance of hands	Pick up	150 lx

## 2.2 Active intelligent lighting control system

In this paper, the motion amplitude detection system is set up, and the motion data acquisition device uses the Kinect V2 motion sensor designed and manufactured by Microsoft. Kinect uses a depth camera to capture images with depth information. Exemplar artificial intelligence system was used to process these images and output data by frame. The output data set contains 25 joint data of the human body.

Operation process of motion recognition algorithm: Firstly, the human joint data is obtained through the depth image function of Kinect. Then the key joint Angle and the joint movement offset distance are calculated by the program. Finally, the current scene mode is selected according to the preset parameter range values of the action data table.

The flow chart of action recognition and scene mode selection program is shown in Figure 3.

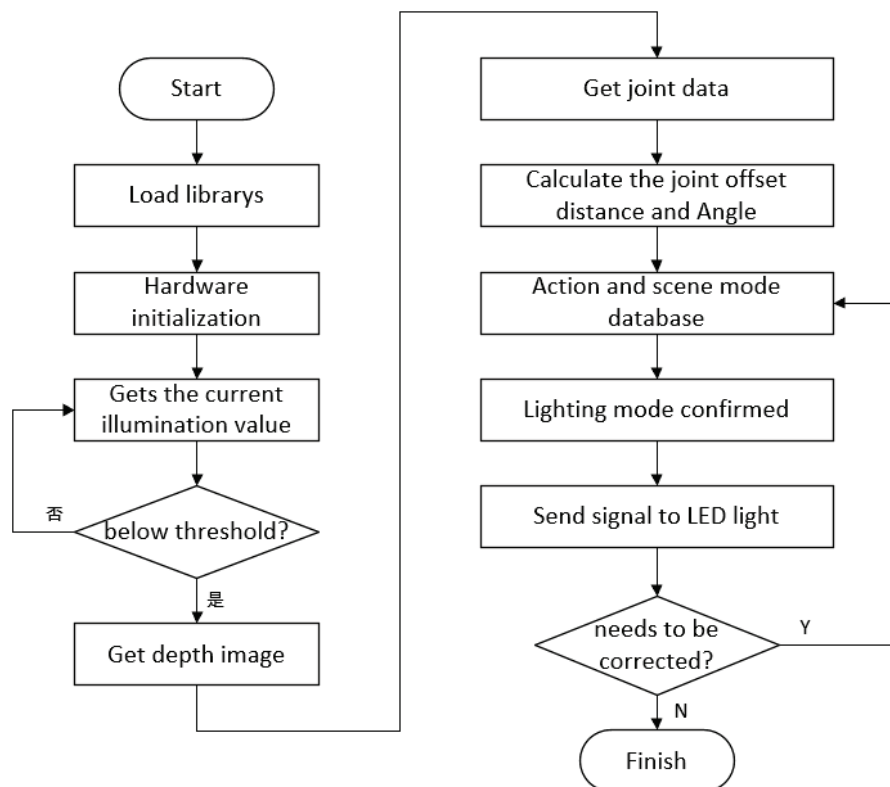


Figure 3. The flow chart of action recognition and scene mode selection program

## 2.3 Prototype lighting control test system

The selected control platform is the Arduino Uno V3. Control program process: First, set the Arduino motherboard LED pin numbers to 5、6 and 3(Corresponding to the RGB); Secondly, set the initial brightness of the LED lamp; Then send a signal to the LED light panel to increase the brightness value of the LED, when the brightness value of the LED light is detected below the target threshold, and the adjustment signal sent by the USB COM serial port is received. The flow chart of lighting control function is shown in Figure 4.

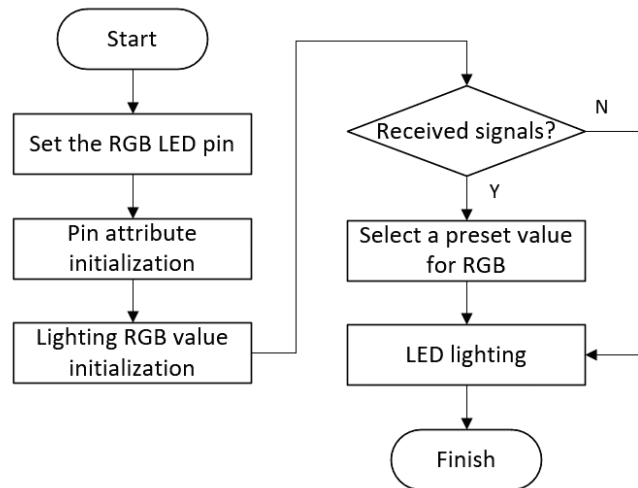


Figure 4. The flow chart of lighting control program

## 2.4 Verified the prototype system

Through the subjective evaluation experiment test, it is concluded that compared with the traditional intelligent lighting control equipment, the autonomous control accuracy of the lighting control system prototype equipment is increased by 82.5%.

After the experiment, the subjects were asked to score and evaluate the ordinary lighting control means and the motion recognition lighting control system respectively. The scoring standard was the convenience of the two lighting control methods, and the scoring rule was 10 points full score system. Compared with the traditional control method, the overall user satisfaction increased by 23.72%. The evaluation results were recorded and sorted by age interval, as shown in Figure 5.

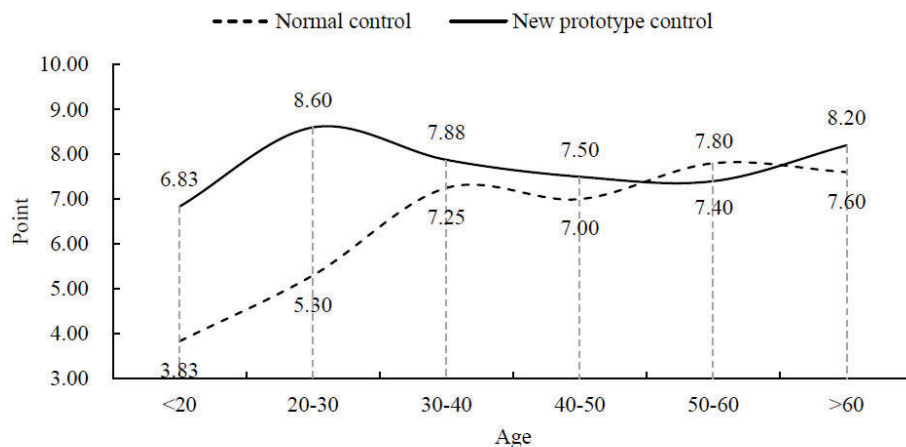


Figure 5. The curve of evaluation results

## 3. CONCLUSION

Residential decoration design in the interior light environment design is usually not fine, the user does not pay attention to the light environment parameters and do not understand aggravated this phenomenon, resulting in the user in the actual living process, the light environment in the house is not ideal. In this paper, the application method of active light environment control strategy is explored, the corresponding algorithm is developed and designed, and an intelligent lighting control system which can replace the user's control decision is proposed. Improved the traditional lighting control must be judged by the user of the quality of the light



environment and control the shortcomings of related lighting equipment, reduce the learning cost of the elderly.

Due to the limited workload and space, the indoor experiment scene of this paper chooses the kitchen where the action scene is more complex and the light environment is more demanding, and the research ideas and principles can be extended to other room scenes in the house.

## REFERENCE

- [1] Qian W. Research on artificial light environment design of residential buildings based on visual perception theory. *Sichuan Building Science Research*, 2013, 39(03), 244-245.
- [2] Ling S, Wang Donglin, Dong Weihua. Green lighting design method based on building light environment. *Building Electric*, 2018, 37(05), 112-117.
- [3] Xiufeng M, Wang Lixiong. Optimization design of an office building lighting based on DIALux Evo software. *Journal of Lighting Engineering*, 2018, 29(03), 37-41
- [4] Jiali J. Research on residential light environment quality evaluation based on China-Japan-South Korea joint survey. *Dalian Polytechnic University*, 2015, 1.
- [5] Song J, Yang Xiaodong. Research and application status of artificial intelligence technology in construction industry at home and abroad. *Value Engineering*, 2018(4), 225-228.
- [6] Xi W. Design and implementation of intelligent wearable lighting equipment control system. *Huazhong University of Science and Technology*, 2019, 1.
- [7] Kandasamy N K, Tseng K J, Soong B. Smart lighting system using ANN-IMC for personalized lighting control and daylight harvesting. *Building & Environment*, 2018, 139.
- [8] Paz J F D, Bajo J, Sara Rodríguez, et al. Intelligent system for lighting control in smart cities. *Information Sciences*, 2016, 372, 241-255.
- [9] Zhe Y. Application of motion recognition and gesture recognition based on Kinect sensor in human-computer interaction. *Yunnan University*, 2018, 1.

## ACKNOWLEDGEMENT

Corresponding Author: Zhide Wang  
Affiliation: School of Architecture, Tianjin University  
e-mail : 436027507@qq.com